

**Posters and Exhibits** 

# Abbreviated MRI (AB-MRI) of the Breast: Case-based Review of the Literature

Sunday, Nov. 27 12:30PM - 1:00PM Room: BR Community, Learning Center Station #6

#### **Participants**

Laura Heacock, MD, MS, New York, NY (*Presenter*) Nothing to Disclose Samantha L. Heller, MD, PhD, New York, NY (*Abstract Co-Author*) Nothing to Disclose Yiming Gao, MD, New York, NY (*Abstract Co-Author*) Nothing to Disclose Linda Moy, MD, New York, NY (*Abstract Co-Author*) Nothing to Disclose

# **TEACHING POINTS**

Abbreviated MRI can accurately diagnose invasive cancers and high-grade DCIS, and allows for a less costly, better-tolerated exam. First post-contrast subtraction images have higher sensitivity than MIPs. Further work needed on protocols, including T2-weighted and diffusion weighted imaging.

## **TABLE OF CONTENTS/OUTLINE**

Introduction Review of MRI in screening high risk women Advantages of MRI over other screening modalities Current MRI screening limitations AB-MRI may allow for sensitive screening test in broader pool (i.e., intermediate risk) Theory behind AB-MRI: exploits fast initial uptake in malignancy Advantages of AB-MRI: decreased cost, less time AB-MRI is experimental, but increasing number of studies **Purpose**: to review literature on AB-MRI, familiarize radiologists with potential AB-MRI protocols, and show case based examples of AB-MRI Literature review Specific AB-MRI protocols and pros/cons Missed cancers on AB-MRI/known pitfalls? Evaluating benign lesions Cases: Invasive cancer MIP vs first post-contrast subtraction imaging Challenging cases: NME with slow initial enhancement Axillary lesion Marked BPE Biopsy clip Role of T2 imaging: Increased reader confidence Benign lesions Additional pearls/pitfalls Future Directions/Summary

# Molecular Biology and "Radiomics": What the Breast Imager Needs to Know

Sunday, Nov. 27 12:30PM - 1:00PM Room: BR Community, Learning Center Station #7

#### **Participants**

Elizabeth S. McDonald, MD, Philadelphia, PA (*Presenter*) Nothing to Disclose Despina Kontos, PhD, Philadelphia, PA (*Abstract Co-Author*) Nothing to Disclose Emily F. Conant, MD, Philadelphia, PA (*Abstract Co-Author*) Consultant, Hologic, Inc; Consultant, Siemens AG

## **TEACHING POINTS**

This exhibit will:1) Review cellular biology of normal breast tissue.2) Discuss molecular classifications of breast cancer.3) Describe the role of "radiomics" in precision medicine.

# TABLE OF CONTENTS/OUTLINE

1. Review of normal breast histology.

# **Tomosynthesis Impact on Screening Patients 40 to 49**

Sunday, Nov. 27 12:30PM - 1:00PM Room: BR Community, Learning Center Station #1

#### **Participants**

Stephen L. Rose, MD, Addison, TX (Presenter) Consultant, Hologic, Inc

## PURPOSE

The benefits versus harms of breast cancer screening for women under the age of 50 has been the subject of intense debate. New guidelines from the American Cancer Society suggest screening should begin at age 45 and women of ages 40-44 should have the opportunity to begin screening. In this study, we investigate if the addition of tomosynthesis to mammography could improve screening performance outcomes for women under the age of 50.

## METHOD AND MATERIALS

Screening performance data was collected from a network of community based screening centers from January 1, 2015 to December 31, 2015. Data for women under 50 years of age from 65,457 screening exams (45,320 mammography exams and 20,137 tomosynthesis plus mammography exams) were evaluated. Women screened with tomosynthesis plus mammography paid an outof-pocket fee. Screening performance parameters including recall rate, cancer detection rate and invasive cancer detection rate were investigated. Chi square test was performed.

# RESULTS

Rates per 1000 women screened are presented. Recall rates were 115 for mammography alone and 108 for tomosynthesis plus mammography; difference 7 (p=0.013). Cancer detection rates were 2.1 for mammography compared to 3.1 with the addition of tomosynthesis; difference 1.0 (p=0.021). Invasive cancer detection rates improved from 1.2 to 1.8 with the addition of tomosynthesis; difference 0.8 (p=0.014). This represented a relative increase in invasive cancer detection of 67%. The positive predictive value for recall increased from 1.8% to 2.8% with the addition of tomosynthesis.

## CONCLUSION

The addition of tomosynthesis to mammography significantly improved recall rates, cancer detection and invasive cancer detection for women under the age of 50. The results confirm that improvements observed with tomosynthesis screening in the general screening population are also observed for the subgroup of women under the age of 50.

## **CLINICAL RELEVANCE/APPLICATION**

For women less than 50 years of age, the addition of tomosynthesis to mammography provides improved screening performance with significantly lower recall rates and higher invasive cancer detection.

Milky Way Sign: A Potential Diagnostic Sign of Breast Cancer on Digital Breast Tomosynthesis

Sunday, Nov. 27 12:30PM - 1:00PM Room: BR Community, Learning Center Station #2

#### **Participants**

Kanae K. Miyake, MD, PhD, Kyoto, Japan (*Presenter*) Fellowship funded, Nihon Medi-Physics Co, Ltd Irene Liu, MD, Stanford, CA (*Abstract Co-Author*) Nothing to Disclose Yingding Xu, MD, Stanford, CA (*Abstract Co-Author*) Nothing to Disclose John R. Downey, Stanford, CA (*Abstract Co-Author*) Nothing to Disclose Jafi A. Lipson, MD, Stanford, CA (*Abstract Co-Author*) Research Grant, Hologic, Inc Kimberly H. Allison, Stanford, CA (*Abstract Co-Author*) Nothing to Disclose Debra M. Ikeda, MD, Stanford, CA (*Abstract Co-Author*) Consultant, F. Hoffmann-La Roche Ltd Consultant, Bracco Group

## PURPOSE

We previously reported a new digital breast tomosynthesis (DBT) finding, "Milky Way sign (MWS)", as microcalcifications overlying non-calcified band-like density. The purpose of this study was to describe frequencies and imaging findings associated with MWS, and to examine the predictive value of MWS for malignancy.

# METHOD AND MATERIALS

We reviewed all stereotactic core biopsies of suspicious calcifications at our institution from 1/1/2015 to 12/31/2015, identifying 124 calcification lesions, including 20 cancers (2 IDC, 5 IDC+DCIS, 13 DCIS) and 104 benign lesions (23 high-risk, 81 benign), in 116 patients undergoing both 2D mammogram and DBT before biopsies. 2 radiologists evaluated images for the presence of MWS, local breast density within 1 cm surrounding the calcifications, calcification morphology and distribution. The predictive value for malignancy was assessed using Chi square test and multivariate logistic analysis.

#### RESULTS

MWS was identified more frequently with DBT (27/124, 22%) than with 2D (13/124, 10%), and more in locally less dense tissue than in locally dense tissue. The calcifications in MWS were fine pleomorphic (13/27, 48%), amorphous (8/27, 30%), fine linear/branching (5/27, 19%), or other (1/27, 4%), with distributions of grouped (20/27, 74%), linear (5/27, 19%) or segmental (2/27, 7%) categories. MWS on DBT was observed in 60% (12/20) malignant lesions and 14% (15/104) benign lesions, and significantly and positively associated with malignant lesions (p < .001). Multivariate analysis demonstrated the MWS on DBT (p < .001) and fine linear/branching calcifications (p < .001) were independent predictors for malignancy.

#### CONCLUSION

MWS, in the context of DBT, may be a predictive sign for malignancy.

#### **CLINICAL RELEVANCE/APPLICATION**

Milky Way sign is more easily identifiable on digital breast tomosynthesis than 2D mammography, and may be a predictive sign for malignancy.

Impact of High Animal Fat Diet on the Development of Mammary Cancers in a Transgenic Mouse Model of Breast Cancer based on Magnetic Resonance Imaging and Histology

Sunday, Nov. 27 12:30PM - 1:00PM Room: BR Community, Learning Center Station #3

**FDA** Discussions may include off-label uses.

## Participants

Devkumar Mustafi, PhD, Chicago, IL (*Presenter*) Nothing to Disclose Sully Fernandez, Chicago, IL (*Abstract Co-Author*) Nothing to Disclose Erica Markiewicz, BA, Chicago, IL (*Abstract Co-Author*) Nothing to Disclose Matthew J Brady, Chicago, IL (*Abstract Co-Author*) Nothing to Disclose Suzanne Conzen, MD, Chicago, IL (*Abstract Co-Author*) Nothing to Disclose Gregory S. Karczmar, PhD, Chicago, IL (*Abstract Co-Author*) Nothing to Disclose Xiaobing Fan, PhD, Chicago, IL (*Abstract Co-Author*) Nothing to Disclose Marta A. Zamora, BS, Chicago, IL (*Abstract Co-Author*) Nothing to Disclose Jeffrey Mueller, MD, Chicago, IL (*Abstract Co-Author*) Nothing to Disclose Brian B. Roman, PhD, Chicago, IL (*Abstract Co-Author*) Nothing to Disclose

#### PURPOSE

Epidemiological studies demonstrate a significant increase in breast and other cancer risk due to effects of the Western diet. More direct information from *in vivo* studies is needed to improve understanding of the influence of the Western diet on pre-neoplastic changes, *in situ* cancers, and invasive breast cancers. Due to lack of spatial resolution and contrast, imaging modalities, e.g., CT or US, have not been adequate to monitor neoplastic changes during early stage breast cancer progression in mouse models. Previous work from this laboratory demonstrated that MRI reliably detects early murine mammary cancers, differentiating *in situ* from invasive cancer. Based on this, we used MRI to evaluate the impact of dietary fat on mammary cancer development in a transgenic mouse model of human breast cancer.

# METHOD AND MATERIALS

Virgin female C3(1)SV40Tag mice (n=16) were weaned at 3 wks of age. At 4 wks of age, mice were assigned to either a control low fat diet (CD) group (n=8, 3.7 kcal/g; 17.2% kcal from fat) or a high animal fat diet (HAFD) group (n=8, 5.3 kcal/g; 60% kcal from pig fat). After 8 wks on the diets, fast spin echo images of inguinal mammary glands were acquired at 9.4T from all 16 mice at 12 wks of age. After *in vivo* MRI, inguinal mammary glands were excised and fixed in formalin for *ex vivo* MRI. 3D volume-rendered MR images were then correlated with histology.

## RESULTS

An average of 1.25±1.16 invasive cancers per mouse (a total of 10) were found in CD, compared to an average of  $3.88\pm1.03$  invasive cancers per mouse (a total of 31) in HAFD; this difference was statistically significant (p<0.007). Average tumor volume was significantly higher in HAFD ( $0.53\pm0.45$  mm<sup>3</sup>) compared to CD ( $0.20\pm0.08$  mm<sup>3</sup>, p<0.02). The volume of the largest tumor was much greater in HAFD compared to CD (2.59 mm<sup>3</sup> vs 0.32 mm<sup>3</sup>). Visual inspection suggested that HAFD mice, compared to CD mice, had denser parenchyma, more irregular and dilated ducts, dilated blood vessels, and increased invasion, indicative of aggressive cancers.

# CONCLUSION

MRI and histological studies of a transgenic mouse model of human triple-negative breast cancer demonstrate that mice on a HAFD develop larger and more invasive cancers.

## **CLINICAL RELEVANCE/APPLICATION**

This work is the first step towards using MRI to improve understanding of the effect of diet on mammary/breast cancer risk and guide development of methods that reduce risk.

Ultrasound in Diagnostic Imaging Evaluation of the Symptomatic Male Breast: Added Value or Added Costs?

Sunday, Nov. 27 12:30PM - 1:00PM Room: BR Community, Learning Center Station #4

#### **Participants**

Eric M. Blaschke, MD, Boston, MA (*Presenter*) Nothing to Disclose Michele Gadd, MD, Boston, MA (*Abstract Co-Author*) Nothing to Disclose Kevin S. Hughes, MD, Boston, MA (*Abstract Co-Author*) Nothing to Disclose Ashley A. Roark, MD, Boston, MA (*Abstract Co-Author*) Nothing to Disclose Michelle C. Specht, MD, Boston, MA (*Abstract Co-Author*) Nothing to Disclose Constance D. Lehman, MD, PhD, Boston, MA (*Abstract Co-Author*) Research Grant, General Electric Company; Medical Advisory Board, General Electric Company Barbara L. Smith, MD, PhD, Boston, MA (*Abstract Co-Author*) Nothing to Disclose

## PURPOSE

The American College of Radiology (ACR) Appropriateness Criteria provide strong support for diagnostic mammography as the initial exam in the symptomatic male > 25 years of age, but are less clear in the role of ultrasound (US) in this clinical setting. We evaluated the impact of US after diagnostic mammography in a large population of symptomatic male patients.

## **METHOD AND MATERIALS**

In this retrospective IRB approved study 399 cases in 360 male patients > 25 years of age, presenting for imaging of an area of focal clinical concern were identified in a large structured reporting breast imaging database from 3/2006 to 3/2015. Each breast with > 1 focal area of clinical concern was designated as a case. Outcomes were determined by imaging, biopsy, or any pathology in our hospital tumor registry within a minimum of 12 months follow up. Performance measures were defined according to the ACR BI-RADS Atlas, Fifth Edition.

#### RESULTS

Of 360 patients (mean age = 52.5, range 25-96), 332 (92.2%) were assessed as BIRADS 1 or 2, 10 (3.8%) as BIRADS 3, and 18 (5.0%) as BIRADS 4 or 5 by mammography. 15 cancers were diagnosed, for a cancer detection rate of 41.7 per 1000 (10 IDC, 1 ILC, 4 DCIS). Performance metrics of mammography were: sensitivity 100%, specificity 99.2%, positive predictive value 83.3%, and negative predictive value 100%. Of the 278/399 (69.7%) cases evaluated with US after mammography, no additional cancers were diagnosed (2 gynecomastia, 1 fat necrosis, 1 angiolipoma, 1 fibrosis, 1 lipoma, 2 foreign body reactions, 1 papilloma).

#### CONCLUSION

Our findings support the ACR guidelines supporting mammography as the primary diagnostic tool in the symptomatic male patient > 25 years of age. Mammography alone identified all cancers and supported clinical follow up rather than biopsy in a large percentage of patients. Our findings do not support the added value of US as an initial examination in this clinical setting. Clinical surveillance rather than biopsy may be a safe alternative in male patients with negative, benign or probably benign imaging findings.

#### **CLINICAL RELEVANCE/APPLICATION**

Mammography is highly accurate in the evaluation of symptomatic male patients, identifying the cancer and avoiding unnecessary biopsy. Ultrasound may be more useful as a method to guide biopsy.

**Breast Cancer Risk Prediction with Density Independent Texture Features** 

Sunday, Nov. 27 12:30PM - 1:00PM Room: BR Community, Learning Center Station #5

#### **Participants**

Michiel Kallenberg, Copenhagen, Denmark (*Abstract Co-Author*) Former Employee, Matakina Technology Limited; Employee, Biomediq A/S; Employee, Screenpoint Medical BV

Mads Nielsen, PhD, Copenhagen, Denmark (*Presenter*) Stockholder, Biomediq A/S Research Grant, Nordic Bioscience A/S Research Grant, SYNARC Inc Research Grant, AstraZeneca PLC

Katharina Holland, Nijmegen, Netherlands (Abstract Co-Author) Nothing to Disclose

Nico Karssemeijer, Nijmegen, Netherlands (Abstract Co-Author) Nothing to Disclose

Martin Lillholm, PhD, Copenhagen, Denmark (Abstract Co-Author) Employee, Biomediq A/S Shareholder, Biomediq A/S

#### PURPOSE

In personalized breast cancer screening stratification is commonly based on breast density. It has been suggested though, that breast density is a too coarse descriptor for breast cancer risk. Several authors have developed texture features that are potentially more predictive of breast cancer. Yet, in several studies, strong correlation between both types of features is an issue. In this work we investigate a method to generate deep learning texture features that are independent of breast density.

#### **METHOD AND MATERIALS**

From the Dutch breast cancer screening program we collected 394 cancers and 1182 age matched healthy controls. To obtain mammograms without signs of cancerous tissue, we took the contralateral mammograms. For each image breast density was computed using automated software. Texture features were automatically learned from the data by means of techniques that are commonly used in deep learning. In the initial matching, breast density was on average higher in the cases than in the controls, as breast density is associated with breast cancer risk. Texture features and scores learned on this set (Td) are determined to be correlated to density. In order to obtain density independent features and scores (Ti) we balanced breast density over the cases and the controls by performing a rematching based on breast density. Non-matching cases and controls were excluded during training; in the testing phase all images were scored. We trained and tested Td and Ti to separate between cancers and controls with 5-fold cross-validation. We compared the performance of Td and Ti in terms of predictive power.

#### RESULTS

Spearman's rank correlation between density and Td was 0.81 (0.79-0.83). The density adjusted odds ratios for breast cancer were 1.15 (0.81-1.65), 1.40 (0.98-2.00), and 1.39 (0.92-2.09) for quartile 2-4 respectively, relative to quartile 1. For Ti the correlation with density was 0.00 (-0.06 - 0.05). The odds ratios were 1.15 (0.82-1.62), 1.33 (0.96-1.86), and 1.45 (1.05-2.01). The AUC for separating cancers from controls was 0.539 (0.506-0.572).

## CONCLUSION

We developed a method for generating density independent texture features and scores. The obtained texture scores were significantly associated with breast cancer risk.

#### **CLINICAL RELEVANCE/APPLICATION**

The obtained density independent texture features may enhance breast cancer risk models beyond breast density, and as such offer opportunities to further optimize personalized breast cancer screening.

Cardiac Lymphomas: Spectrum of Cardiovascular Magnetic Resonance Features with Histological Correlation

Sunday, Nov. 27 12:30PM - 1:00PM Room: CA Community, Learning Center Station #6

# Awards

**Certificate of Merit** 

#### Participants

Monika Arzanauskaite, London, United Kingdom (*Presenter*) Nothing to Disclose Raad Mohiaddin, London, United Kingdom (*Abstract Co-Author*) Nothing to Disclose

## **TEACHING POINTS**

The purpose of this exhibit is:1. To review the pathophysiology of cardiac lymphomas2. To explain the utility of CMR and suggest an protocol for imaging3. To review the CMR appearances of cardiac lymphomas by correlating the cases with the histopathologic features

#### **TABLE OF CONTENTS/OUTLINE**

Cardiac lymphomas are rare tumours that may occur as a primary or secondary malignancy and infiltrate the heart in an ill-defined, diffuse manner. The clinical presentation is non-specific and depends on the site and the size of the tumour, therefore the diagnosis is often late. This and the status of patient's immunocompetence lead to poor prognosis in most cases. On histology, both Hodgkin and non-Hodgkin lymphomas affect the heart. Cardiovascular magnetic resonance imaging is an advanced technique which may show features highly suggestive of cardiac lymphoma and aid to diagnose the disease earlier. This exibit will provide a case-based review of the spectrum of cardiac lymphoma appearances by correlating CMR imaging appearance with histopathologic findings. 1. Pathophysiology of cardiac lymphomas2. Imaging cardiac lymphomas by CMR3. Case-based review of imaging findings4. Differential diagnosis

# Role of Cardiac CT in the Work Up Prior to Percutaneous Pulmonary Valve Implantation

Sunday, Nov. 27 12:30PM - 1:00PM Room: CA Community, Learning Center Station #7

#### Awards Certificate of Merit

#### Participants

Michela Tezza, MD, Verona, Italy (*Presenter*) Nothing to Disclose Maarten Witsenburg, Rotterdam, Netherlands (*Abstract Co-Author*) Nothing to Disclose Koen Nieman, MD, PhD, Rotterdam, Netherlands (*Abstract Co-Author*) Nothing to Disclose Pieter van de Woestijne, Rotterdam, Netherlands (*Abstract Co-Author*) Nothing to Disclose Ricardo P. Budde, MD, PhD, Utrecht, Netherlands (*Abstract Co-Author*) Nothing to Disclose

# **TEACHING POINTS**

Percutaneous pulmonary valve implantation (PPVI) is used to treat pulmonary valve insufficiency or stenosis which often occurs in patients with corrected congenital heart disease. CT has an important role in the work-up prior to PPVI to select suitable patients by evaluating size and shape of the pulmonary trunk (PT) and its relationship to the coronary arteries to assess the risk of coronary compression (CC).

# TABLE OF CONTENTS/OUTLINE

Background of the PPVI procedure and commonly implanted valve types How to perform CT analysis: measurements of pulmonary conduit/right ventricle outflow tract (RVOT) performed with double oblique reconstructed images; measurements of the relationship between coronary arteries and PT and changes after PPVI. Difference in CA-PT relationship between diastole and systole. How to assess CC-risk in candidate patients for PPVI; imaging features that indicate high risk of CC. Case presentations including CT pre and post PPVI and per procedural angiography illustrating different aspects mentioned above.

Quantification of Oxygen Consumption in Heart Failure Using BOLD Effect of T2-star Magnetic Resonance Imaging: Comparison with Cardiopulmonary Exercise Test

Sunday, Nov. 27 12:30PM - 1:00PM Room: CA Community, Learning Center Station #1

# Participants

Michinobu Nagao, MD, Tokyo, Japan (*Presenter*) Nothing to Disclose Satoshi Kawanami, MD, Fukuoka, Japan (*Abstract Co-Author*) Nothing to Disclose Yuzo Yamasaki, MD, Fukuoka, Japan (*Abstract Co-Author*) Nothing to Disclose Takeshi Kamitani, MD, Fukuoka, Japan (*Abstract Co-Author*) Nothing to Disclose Koji Sagiyama, MD, Fukuoka, Japan (*Abstract Co-Author*) Nothing to Disclose Hiroshi Honda, MD, Fukuoka, Japan (*Abstract Co-Author*) Nothing to Disclose Taiki Higo, Fukuoka, Japan (*Abstract Co-Author*) Nothing to Disclose Tomomi Ide, Fukuoka-city, Japan (*Abstract Co-Author*) Nothing to Disclose Yuji Watanabe, MD, Kurashiki, Japan (*Abstract Co-Author*) Nothing to Disclose Satoshi Shimizu, Tokyo, Japan (*Abstract Co-Author*) Nothing to Disclose Umiko Ishizaki, Tokyo, Japan (*Abstract Co-Author*) Nothing to Disclose Kenji Fukushima, Tokyo, Japan (*Abstract Co-Author*) Nothing to Disclose Shuji Sakai, MD, Shinjuku-Ku, Japan (*Abstract Co-Author*) Nothing to Disclose

#### PURPOSE

Oxygen consumption is rate-limiting step of myocardial metabolism, and links to exercise tolerance. In vivo, the imaging technique that can quantify myocardial oxygen consumption is not established. We propose a novel imaging technique to quantify oxygen consumption using the blood-oxygenation-level-dependent (BOLD) effect on T2-star cardiac magnetic resonance (T2\* CMR), and investigate the relation to exercise tolerance on cardiopulmonary exercise test (CPX) in heart failure (HF).

## **METHOD AND MATERIALS**

Thirty non-ischemic refractory HF patients who underwent CMR and CPX for heart transplant were enrolled (mean age, 46 yearold). In addition, 24 patients with suspected cardiomyopathy who had normal left ventricular function (LVEF>50%) on CMR were enrolled as control (mean age, 54 year-old). Myocardial T2\* (M-T2\*) imaging was accomplished using 3-Tesla scanner and multiecho gradient-echo sequence. M-T2\* was calculated by fitting the signal intensity data for the mid-left ventricular septum to a decay curve. During 10 minutes inhalation of oxygen at the flow rate of 10 l/min, M-T2\* was measured under room-air and oxygen inhalation. Oxygen consumption ( $\Delta$ T2\*, ms) was defined as the difference between the two conditions. Changes in T2\* between room-air and O2 inhalation was analyzed by paired t-test. Comparison of  $\Delta$ T2\* between HF and controls was analyzed by Mann-Whitney u-test. Correlations between  $\Delta$ T2\* and CPX (peak VO2, O2 pulse) was analyzed by Pearson coefficient.

## RESULTS

M-T2\* was significantly greater under oxygen inhalation than room-air in HF (29.9 $\pm$ 7.3ms vs. 26.7 $\pm$ 6.0ms, p<0.001), whereas there was no difference in controls (25.5 $\pm$ 4.0ms vs. 25.4 $\pm$ 4.4ms).  $\Delta$ T2\* was significantly greater for HF than controls (3.2 $\pm$ 4.5ms vs. - 0.1 $\pm$ 1.3ms, p<0.001). Significant correlations between  $\Delta$ T2\* and CPX tests (peak VO2, r=-0.46, p<0.05; O2 pulse, r=-0.54, p<0.005) were observed in HF.

#### CONCLUSION

 $\Delta T2^*$  instead of increased M-T2\* at oxygen inhalation is greater in HF patients, demonstrating reduced oxygen consumption.  $\Delta T2^*$  is a candidate for cardiac functional reserve in refractory HF.

## **CLINICAL RELEVANCE/APPLICATION**

Our method allows assessing non-invasively myocardial oxygen metabolism in vivo.  $\Delta T2^*$  could predict the prognosis of refractory HF, and could be used as an indicator for heart transplant.

To Evaluate Stenosis Degree of Coronary Calcified Lesions Using Transluminal Attenuation Gradient: A Preliminary Study of 320-slice Volume CT

Sunday, Nov. 27 12:30PM - 1:00PM Room: CA Community, Learning Center Station #2

## Participants

Yang Fengfeng, Harbin, China (*Abstract Co-Author*) Nothing to Disclose Tong Zhang, MD, Harbin, China (*Presenter*) Nothing to Disclose

## PURPOSE

To evaluate the accuracy of transluminal attenuation gradient (TAG) in diagnosing the stenosis degree of coronary calcified lesions using coronary computed tomography angiography (CCTA)

## METHOD AND MATERIALS

A total of 130 patients consecutively received CCTA and coronary angiography (CAG). For 379 main coronary arteries in the epicardium, the average transluminal Hounsfield units (HU) of the regions of interest were consecutively measured at an interval of 5 mm from the ostium to the distal level where the vessel cross-sectional area fell below 2.0mm2, followed by the calculation of TAG. The effects of different plaque components on TAG were analyzed. The diagnostic performance of CCTA, TAG and CCTA+TAG for the stenosis degree of coronary calcified lesions and their reclassification for stenosis degree were analyzed, especially for calcified lesions.

## RESULTS

Compared with CAG, the TAG in CCTA was consistent with the largest stenosis degree of each blood vessel: 0%-49% stenosis showed a TAG of  $3.49\pm3.23$ HU/10mm and 100% stenosis showed a TAG of  $-24.67\pm18.41$ HU/10mm. TAG improved the accuracy of CCTA in the diagnosis of calcified lesions (c-statistic=0.958 vs.0.866, p<0.0001). When threshold was  $\leq$ -6.9HU/10mm, the sensitivity, specificity, positive predictive value (PPV) and negative predictive value (NPV) of CCTA+TAG in the diagnosis of coronary calcified lesions were 90.26%, 95.45%, 98.58% and 73.68%. In addition, TAG can help to improve the reclassification of CCTA for coronary stenosis degree, especially for calcified lesions (NRI=0.127, P=0.045).

## CONCLUSION

TAG can help to improve the diagnostic performance of CCTA for the stenosis degree of coronary calcified lesions, and it may also help to improve the reclassification of the stenosis degree of calcified lesions.

# **CLINICAL RELEVANCE/APPLICATION**

(dealing with CT angiography)" To evaluate the accuracy of transluminal attenuation gradient (TAG) in diagnosing the stenosis degree of coronary calcified lesions using coronary computed tomography angiography (CCTA) "

## CA203-SD-SUA4

Compressed Sensing Real-time Cine Imaging for Assessment of Ventricular Function, Volumes and Mass in Clinical Practice

Sunday, Nov. 27 12:30PM - 1:00PM Room: CA Community, Learning Center Station #4

# Participants

Benjamin Longere, MD, Lille, France (*Presenter*) Nothing to Disclose Mathilde Vermersch, Lille, France (*Abstract Co-Author*) Nothing to Disclose Julien Pagniez, MD, Lille, France (*Abstract Co-Author*) Nothing to Disclose Hedi Farah, Lille, France (*Abstract Co-Author*) Nothing to Disclose Michaela Schmidt, Erlangen, Germany (*Abstract Co-Author*) Employee, Siemens AG Christoph Forman, Erlangen, Germany (*Abstract Co-Author*) Employee, Siemens AG Aurelien Monnet, Lille, France (*Abstract Co-Author*) Employee, Siemens AG Francois Pontana, MD, PhD, Lille, France (*Abstract Co-Author*) Nothing to Disclose

#### PURPOSE

To evaluate the accuracy of a compressed sensing (CS) real-time prototype cine sequence (Sparse 2D cine, Siemens Healthcare) for quantification of left ventricular (LV) function, volumes and mass and right ventricular (RV) function and volumes in clinical practice.

## **METHOD AND MATERIALS**

50 consecutive adult patients (30 males, 20 females; mean age=  $53 \pm 18.3$  years) referred for cardiac magnetic resonance (CMR) examination were prospectively enrolled. CMR were performed for ischemic heart disease (n= 11), dilated cardiomyopathy (n= 8), valvular disease (n= 8), heart rhythm disorder (n= 7), infiltrative cardiomyopathy (n= 6), hypertrophic cardiomyopathy (n= 5), myocarditis (n= 2) or others (n= 3). Grown-up congenital heart disease patients were excluded. The CMR protocol included short-axis stack, one four-chamber slice and one long-axis slice using (a) a conventional segmented multi-breath-hold steady-state free precession acquisition (bSSFP) as a reference (Group 1) and (b) a CS real-time single-breath-hold sequence (Group 2) providing the same slice number, position and thickness. Two radiologists independently assessed the ejection fraction (LVEF & RVEF), end-diastolic (LVEDV & RVEDV) and end-systolic (LVESV & RVESV) volumes and LV mass (LVM) in both Groups.

#### RESULTS

The CS sequence mean scan time was  $22.2 \pm 5.6$  seconds and for the multi-breath-hold bSSFP sequence it was  $503.7 \pm 94.3$  seconds (p<0.001). There was a high correlation between Group 1 and Group 2 regarding mean LVEF ( $48.8 \pm 15.2 \%$  vs  $48.9 \pm 15.3 \%$ ; r=0.98), mean LVEDV ( $93.8 \pm 33.8 \text{ ml/m2}$  vs  $98.2 \pm 34.2 \text{ ml/m2}$ ; r=0.98), mean LVESV ( $52.5 \pm 32.0 \text{ ml/m2}$  vs  $53.2 \pm 33.3 \text{ ml/m2}$ ; r=0.98) and mean LVM ( $75.5 \pm 21.3 \text{ g/m2}$  vs  $73.3 \pm 19.6 \text{ g/m2}$ ; r=0.92). There was also strong correlation between Group 1 and Group 2 for RV assessment: mean RVEF =  $54.5 \pm 10.8 \%$  vs  $54.7 \pm 11.1 \%$  (r=0.93), mean RVEDV =  $79.2 \pm 20.5 \text{ ml/m2}$  vs  $80.6 \pm 23.1 \text{ ml/m2}$  (r=0.90) and mean RVESV =  $37.4 \pm 15.6 \text{ ml/m2}$  vs  $36.8 \pm 18.3 \text{ ml/m2}$  (r=0.87).

# CONCLUSION

Compressed sensing single-breath-hold cine imaging provides LV function, volumes and mass as well as RV function and volumes, which are comparable to the conventional SSFP multi-breath-hold imaging.

## **CLINICAL RELEVANCE/APPLICATION**

CS real-time cine imaging reduces CMR scan time while providing comparable measurements in patients with cardiac condition that may prevent from iterative breath-holds.

Dynamic CT Myocardial Perfusion Imaging Combined with On-site CT Derived FFR for Detection of Functional Coronary Artery Disease

Sunday, Nov. 27 12:30PM - 1:00PM Room: CA Community, Learning Center Station #5

**FDA** Discussions may include off-label uses.

#### Participants

Adriaan Coenen, MD, Rotterdam, Netherlands (*Presenter*) Nothing to Disclose Alexia Rossi, MD,PhD, London, United Kingdom (*Abstract Co-Author*) Nothing to Disclose Marisa M. Lubbers, MD, Rotterdam, Netherlands (*Abstract Co-Author*) Nothing to Disclose Atsushi K. Kono, MD, PhD, Kobe, Japan (*Abstract Co-Author*) Nothing to Disclose Akira Kurata, PhD, Toon, Japan (*Abstract Co-Author*) Nothing to Disclose Raluca G. Chelu, MD, Rotterdam, Netherlands (*Abstract Co-Author*) Nothing to Disclose Marcel L. Dijkshoorn, RT, Rotterdam, Netherlands (*Abstract Co-Author*) Consultant, Siemens AG Robert J. Van Geuns, MD, Rotterdam, Netherlands (*Abstract Co-Author*) Nothing to Disclose Francesca Pugliese, MD, PhD, London, United Kingdom (*Abstract Co-Author*) Nothing to Disclose Koen Nieman, MD, PhD, Rotterdam, Netherlands (*Abstract Co-Author*) Nothing to Disclose

#### PURPOSE

In the presence of atheroclesrosis CTA tends to overestimate, especially when validated against the current functional standard fractional flow reserve (FFR). Two CT applications to improve specificity are CT myocardial perfusion imaging (CT-MPI) and CTA derived FFR (CTA-FFR). CT-MPI images the distribution of a first pass contrast agent over the left ventricle wall. CTA-FFR applies computational fluid dynamics onto CTA data to simulated the coronary blood flow. In this study both techniques are validated against invasive FFR measurements.

#### **METHOD AND MATERIALS**

Patients with suspect or known CAD, underwent a CTA and dynamic CT-MPI examination  $\leq$  14 days before invasive angiography. An invasive FFR was performed in vessels with a stenosis grade between 30-90%. The dynamic CT-MPI acquisition uses an alternating cranial caudal table position. The myocardial blood flow was computed as index MBF normalizing the ROI suspected perfusion defect for the 75 percentile of the left ventricle myocardial perfusion. CTA-FFR was computed on-site using a hybrid model. (cFFR version 1.4, Siemens Healthcare, Forchheim, Germany; not commercially available).

#### RESULTS

In 74 patients, an invasive FFR was measured in 142 vessels. 67 out of 142 vessels were considered functionally obstructed with an invasive FFR≤0.80. 49 vessels/territories were classified as positive for ischemia with both CTA-FFR and CT-MPI, and 33 vessels as negative with both CTA-FFR and CT-MPI. The sensitivity and specificity for the 82 vessels/territories with concordance between both modalities was 90% (81-99%) and 77% (61-89%) (Figure 1). Overall sensitivity and specificity were 82% (71-90%) and 60% (48-71%) for CTA-FFR and 73% (61-83%) and 68% (56-78%) for CT-MPI. The area under the curve was identical for both CTA-FFR and CT-MPI (0.78).

## CONCLUSION

Dynamic CT-MPI and CT derived FFR are different pathways towards improving the diagnostic accuracy of CT in the detection of functional coronary artery stenosis. In this study shows both dynamic CT-MPI and CT derived FFR perform well in the detection of functional coronary artery stenosis. In the subset of vessels/territories with concordance between CT-MPI and CTA-FFR diagnostic accuracy is increased.

## **CLINICAL RELEVANCE/APPLICATION**

CT derived FFR and dynamic CT myocardial perfusion imaging are different methods for detection of functional coronary artery disease, combination of both modalities could improve diagnostic performance.

## Approach to Pulmonary Hypertension: From Imaging to Clinical Diagnosis

Sunday, Nov. 27 12:30PM - 1:00PM Room: CH Community, Learning Center Station #5

Awards Certificate of Merit Identified for RadioGraphics

#### **Participants**

Felipe Aluja, MD, Bogota, Colombia (*Presenter*) Nothing to Disclose Federico G. Diaz Telli, MD, Pilar, Argentina (*Abstract Co-Author*) Nothing to Disclose Sebastian Yevenes Aravena, MD, Santiago, Chile (*Abstract Co-Author*) Nothing to Disclose Sreevathsan Sridhar, MD, Saint Louis, MO (*Abstract Co-Author*) Nothing to Disclose Fernando R. Gutierrez, MD, Saint Louis, MO (*Abstract Co-Author*) Nothing to Disclose Sanjeev Bhalla, MD, Saint Louis, MO (*Abstract Co-Author*) Nothing to Disclose

## **TEACHING POINTS**

To recognize the different types of pulmonary hypertension, the physiopathology and their clinical presentation. Describe the essential structures that all radiologist should look for in cases of pulmonary hypertension such as: parenchyma, bronchial arteries, pulmonary arteries and heart that may guide to an appropriate diagnosis. Review the key elements in regard to the imaging findings, that the radiologist have to look for in order to do an appropriate clinical approach to the diagnosis based on the imaging findings. Propose a simple check list for the approach to pulmonary hypertension that allows radiologists to classifying pulmonary hypertension disease based on imaging findings and may contribute for the clinical diagnosis of each subtype.

#### TABLE OF CONTENTS/OUTLINE

Introduction Clinical classification with brief but concise clinical presentation and physiopathology Classical signs in pulmonary hypertension in computed tomography, magnetic resonance imaging and echocardiography Essential structures to evaluate: Parenchyma Bronchial arteries Pulmonary arteries Heart Algorithm approach to pulmonary hypertension from the imaging to the clinical diagnosis Conclusion

#### **Honored Educators**

Presenters or authors on this event have been recognized as RSNA Honored Educators for participating in multiple qualifying educational activities. Honored Educators are invested in furthering the profession of radiology by delivering high-quality educational content in their field of study. Learn how you can become an honored educator by visiting the website at: https://www.rsna.org/Honored-Educator-Award/

Sanjeev Bhalla, MD - 2014 Honored Educator Sanjeev Bhalla, MD - 2016 Honored Educator Patterns of Drug-Related Pulmonary Injury: A Pictorial Review

Sunday, Nov. 27 12:30PM - 1:00PM Room: CH Community, Learning Center Station #6

#### **Participants**

Linda DeMello, MD, Warwick, RI (*Presenter*) Nothing to Disclose Saurabh Agarwal, MD, Providence, RI (*Abstract Co-Author*) Nothing to Disclose Michael K. Atalay, MD, PhD, Providence, RI (*Abstract Co-Author*) Nothing to Disclose Thomas K. Egglin, MD, Providence, RI (*Abstract Co-Author*) Nothing to Disclose Terrance T. Healey, MD, Providence, RI (*Abstract Co-Author*) Nothing to Disclose

## **TEACHING POINTS**

The purpose of this exhibit is: To review the pathophysiology of drug-induced pulmonary injury. To briefly discuss the myriads of agents which may cause lung injury (i.e. cardiovascular meds, chemotherapeutics, antibiotics, immunosuppressants and street drugs) To present a series of cases from our institution of various drug-induced pneumonitides and their various manifestations. To discuss the importance of recognizing these patterns and potential causes of injury as the majority are reversible and further exposure may result in death.

# TABLE OF CONTENTS/OUTLINE

Pathophysiology of drug-induced lung injuryVarious medications that may cause lung injury (with emphasis on the most common)Review of cases and imaging findings (predominately radiographs and chest CTs)OutcomesSummary

Comparison of HRCT Appearances and Histopathologic Findings Following Transbronchial Lung Biopsy in Patients with Cryptogenic Organizing Pneumonia

Sunday, Nov. 27 12:30PM - 1:00PM Room: CH Community, Learning Center Station #1

## Participants

Ryoko Egashira, MD, Saga, Japan (*Presenter*) Nothing to Disclose Kazuhiro Tabata, MD, Nagasaki, Japan (*Abstract Co-Author*) Nothing to Disclose Takahiko Nakazono, MD, PhD, Saga, Japan (*Abstract Co-Author*) Nothing to Disclose Ken Yamaguchi, MD, Saga, Japan (*Abstract Co-Author*) Nothing to Disclose Masaki Tominaga, MD,PhD, Kurume, Japan (*Abstract Co-Author*) Nothing to Disclose Hiroyuki Irie, MD, PhD, Saga, Japan (*Abstract Co-Author*) Nothing to Disclose Yuji Ishimatsu, MD,PhD, Nagasaki, Japan (*Abstract Co-Author*) Nothing to Disclose Kazuto Ashizawa, MD, Nagasaki, Japan (*Abstract Co-Author*) Nothing to Disclose Masahiro Takaki, MD, Nagasaki, Japan (*Abstract Co-Author*) Nothing to Disclose

## PURPOSE

To identify features indicative of disease severity or associated with disease relapse in patients with cryptogenic organizing pneumonia (COP). HRCT, clinical and histopathologic findings were retrospectively compared in patients undergoing transbronchial lung biopsy.

## **METHOD AND MATERIALS**

155 consecutive patients diagnosed with organizing pneumonia following TBLB were reviewed. 44 patients had a consensus multidisciplinary diagnosis of COP (male:female= 29:15), median age=68 years (range: 27-87). Pre-biopsy HRCT images were evaluated for the extent of airspace consolidation, ground-glass opacification (GGO), intralobular reticulation and emphysema, HRCT zonal predominance in both the vertical and axial plane and intralesional bronchiolar abnormalities such as irregular/smooth dilatation. The presence or absence of: a perilobular pattern, reversed halo sign, centrilobular nodules and pleural effusions were also documented. Change on serial imaging was classified according to: progression of a parenchymal lesion, residual GGO/parenchymal distortion/traction bronchiectasis, development of honeycomb-like appearances and complete resolution of the abnormality. Histological specimens were quantified for the amount of Masson bodies, airspace fibrin and eosinophils.

#### RESULTS

13 patients relapsed after treatment. Eccentric distribution of the disease in the vertical plane on HRCT was related to disease relapse (38% versus 0%, P<0.05). No other HRCT findings or clinical/histological parameters were significantly associated with disease relapse. Irregular dilatation of bronchi within the lesion on HRCT was significantly related to residual parenchymal distortion/traction bronchiectasis (67% versus 28%, P<0.05). No HRCT or clinical findings were significantly related to histological severity.

# CONCLUSION

HRCT features may help identify those patients with COP that are likely to undergo disease relapse and indicate the subset of patients with COP, in whom parenchymal damage may not resolve.

## **CLINICAL RELEVANCE/APPLICATION**

Patients with COP, where disease is asymmetrically distributed, being more extensive in either the upper or lower zones, may require closer monitoring and/or aggressive steroid therapy as they are more likely to undergo disease relapse.

CT Diagnosis for Thymic Epithelial Tumors: Correlation with the World Health Organization Histologic Classification system Updated in 2015 and New TNM Staging System

Sunday, Nov. 27 12:30PM - 1:00PM Room: CH Community, Learning Center Station #2

## Participants

Akiko Sumi, MD, Kurume, Japan (*Presenter*) Nothing to Disclose Kiminori Fujimoto, MD, PhD, Kurume, Japan (*Abstract Co-Author*) Nothing to Disclose Asako Kuhara, Kurume, Japan (*Abstract Co-Author*) Nothing to Disclose Naoko Ikehara, MD, Kurume, Japan (*Abstract Co-Author*) Nothing to Disclose Ryoji Iwamoto, Kurume, Japan (*Abstract Co-Author*) Nothing to Disclose Shuji Nagata, MD, Kurume, Japan (*Abstract Co-Author*) Nothing to Disclose Toshi Abe, MD, Kurume, Japan (*Abstract Co-Author*) Nothing to Disclose

#### PURPOSE

To evaluate the CT features with histological assessment of thymic epithelial tumors based on the new World Health Organization (WHO) histological classification updated in 2015 and recently proposed TNM staging, and to determine the CT features helpful in differentiating low-risk from high-risk tumors.

#### **METHOD AND MATERIALS**

This retrospective study included 132 patients with thymic epithelial tumor who underwent CT within 2 weeks before surgery. The patients were 74 women and 57 men (median age, 59 years; range, 24-82 years). CT features were classified into 18 categories and were assessed by two independent radiologists. These categories were correlated with the WHO histologic subtypes and the useful findings for predicting tumor invasiveness were assessed.

#### RESULTS

With WHO histologic classification, 132 tumors were regrouped into three categories: 62 low-risk thymomas (10 type A, 22 type AB, and 30 type B1), 39 high-risk thymomas (27 type B2 and 12 type B3), and 31 thymic carcinomas. There was statistically significant relationship between WHO histologic classification and tumor invasiveness (P < .001). There were 93 stage I, 3 stage II, 8 stage IIIa, 3 stage IVa, and 4 stage IVb patients. There was statistically significant difference in size between stage I and stage II-IV tumors (P < .001). Low-risk thymomas were more likely to have smooth contour, homogenous inner character, and homogenous contrast enhancement than high-risk thymomas and thymic carcinomas (all, P < .001). Thymic carcinomas were more likely to have necrotic/cystic component than thymomas (P < .001). The invasiveness of tumors were well-recognized by CT features, such as irregular contour, heterogenous inner component, heterogenous contrast enhancement, and waving boundary with vascular wall and lung surface.

## CONCLUSION

CT characteristics of thymic epithelial tumors correlate with new WHO histologic classification, and it may be helpful in the classification of new TNM staging system.

## **CLINICAL RELEVANCE/APPLICATION**

CT features suggestive of invasiveness in thymic epithelial tumor were irregular contour, heterogenous inner component, heterogenous contrast enhancement, and waving boundary with lung surface, and these features were correlated with new WHO histologic classification.

# Imaging Genotyping for Functional Signaling Pathways in Lung Squamous Cell Lung Carcinoma using Radiomics Approach

Sunday, Nov. 27 12:30PM - 1:00PM Room: CH Community, Learning Center Station #4

## Participants

So Hyeon Bak, MD, Chuncheon-si, Korea, Republic Of (*Presenter*) Nothing to Disclose Ho Yun Lee, MD, Seoul, Korea, Republic Of (*Abstract Co-Author*) Nothing to Disclose Hyunjin Park, Incheon, Korea, Republic Of (*Abstract Co-Author*) Nothing to Disclose Insuk Sohn, Seoul, Korea, Republic Of (*Abstract Co-Author*) Nothing to Disclose Seung-Hak Lee, Suwon, Korea, Republic Of (*Abstract Co-Author*) Nothing to Disclose Keunchil Park, Seoul, Korea, Republic Of (*Abstract Co-Author*) Nothing to Disclose Yoon Ki Cha, MD, Goyang-si, Korea, Republic Of (*Abstract Co-Author*) Nothing to Disclose

## PURPOSE

Imaging features may be useful for identifying distinct genomic difference and may have predictive power for certain phenotypes attributed to genomic mutation. We aimed to identify association between computed tomography (CT) quantitative characteristics and pathway aberration of the lung squamous cell carcinoma (SCCs). We also aimed to find predictive imaging biomarker that underpin genomic signature and clinical outcomes in lung SCCs by means of a radiomics strategy.

# METHOD AND MATERIALS

A total of 57 patients underwent surgical resection and whole-exome sequencing of DNA for lung SCCs were included in this retrospective study. Mutational profiles of core signaling pathways of lung SCCs were classified into five categories such as redox stress, differentiation, apoptosis, cell proliferation, and chromatin remodelers pathway. 65 quantitative imaging features was extracted from CT and 74 clinicoradiological features including 65 image features were classified into 8 categories such as clinical, physical, histogram-based, lung cancer-specific, shape, local, regional, and emphysema features.

## RESULTS

The association between clinicoradiological features and alteration of core signaling pathway or survival was identified. Energy and right lung volume was significantly associated with alternation of redox stress and cell proliferation pathway (p=0.026, AUC=0.681; p=0.030, AUC=0.812). Mass and range was related to the apoptosis pathway (p=0.009, AUC = 0.860). None of the clinicoradiological features showed any significant association with the aberration of differentiation and chromatin remodelers pathway. The minimum value of tumor region was identified as independent prognostic factor (p=0.014).

## CONCLUSION

This study identified that radiomics approaches in lung SCCs have the noninvasively potential to predict clinical outcome and alteration of core signaling pathway.

## **CLINICAL RELEVANCE/APPLICATION**

The clinical benefit of quantitative imaging parameters may allow comprehensive evaluation of the molecular status and targetable pathway of lung SCCs that could be used for specific pathway targeted therapy.

## Dual Energy CT for Abdominal and Pelvic Trauma: A Pictorial Review

Sunday, Nov. 27 12:30PM - 1:00PM Room: ER Community, Learning Center Station #5

Awards Certificate of Merit Identified for RadioGraphics

#### **Participants**

Jeremy R. Wortman, MD, Boston, MA (*Presenter*) Nothing to Disclose Jennifer W. Uyeda, MD, Boston, MA (*Abstract Co-Author*) Nothing to Disclose Urvi P. Fulwadhva, MD, Boston, MA (*Abstract Co-Author*) Nothing to Disclose Aaron D. Sodickson, MD, PhD, Boston, MA (*Abstract Co-Author*) Research Grant, Siemens AG; Consultant, Bayer AG

## **TEACHING POINTS**

1) Dual energy CT enables a number of applications that can be useful in assessing patients with abdominal and pelvic trauma, including creation of iodine overlay and virtual non-contrast (VNC) images, evaluation of bone marrow edema, and creation of virtual monoenergetic images to accentuate differential enhancement or to reduce metal artifact. 2) Dual energy post-processing in trauma patients can be particularly useful in assessment of active contrast extravasation as well as evaluation of decreased enhancement of abdominal and pelvic viscera, which can be crucial in appropriate management of patients with abdominal and pelvic trauma. 3) Routine dual energy CT imaging and post-processing can be performed in trauma patients in the Emergency Department setting, and can be incorporated into clinical workflow.

# TABLE OF CONTENTS/OUTLINE

1) Applications of dual energy CT to patients with abdominal and pelvic trauma: review the variety of post-processing applications available with dual energy CT, and how these can benefit assessment of trauma patients2) Case based review of dual energy CT findings in trauma patients3) Future directions and summary

#### **Honored Educators**

Presenters or authors on this event have been recognized as RSNA Honored Educators for participating in multiple qualifying educational activities. Honored Educators are invested in furthering the profession of radiology by delivering high-quality educational content in their field of study. Learn how you can become an honored educator by visiting the website at: https://www.rsna.org/Honored-Educator-Award/

Aaron D. Sodickson, MD, PhD - 2014 Honored Educator

Trauma - Attenuation of Abdominal and Pelvic Structures on Computed Tomography in the Setting of Shock

Sunday, Nov. 27 12:30PM - 1:00PM Room: ER Community, Learning Center Station #1

#### Awards

#### **Student Travel Stipend Award**

#### **Participants**

Michael Wasserman, MD, Boston, MA (*Presenter*) Nothing to Disclose Michael J. Hsu, MD, Boston, MA (*Abstract Co-Author*) Nothing to Disclose Venkata Satyam, Boston, MA (*Abstract Co-Author*) Nothing to Disclose Tina Shiang, Boston, MA (*Abstract Co-Author*) Nothing to Disclose Jennifer Xiao, MD, Boston, MA (*Abstract Co-Author*) Nothing to Disclose Deepan Paul, Boston, MA (*Abstract Co-Author*) Nothing to Disclose Ahmed Y. El-Araby, MD, West Warwick, RI (*Abstract Co-Author*) Nothing to Disclose Robert Burns, Boston, MA (*Abstract Co-Author*) Nothing to Disclose Robert Burns, Boston, MA (*Abstract Co-Author*) Nothing to Disclose Arthur Baghdanian, MD, Boston, MA (*Abstract Co-Author*) Nothing to Disclose Christina A. LeBedis, MD, Boston, MA (*Abstract Co-Author*) Nothing to Disclose Jorge A. Soto, MD, Boston, MA (*Abstract Co-Author*) Nothing to Disclose Stephan W. Anderson, MD, Boston, MA (*Abstract Co-Author*) Nothing to Disclose

#### PURPOSE

Hypotension is an important marker of a patient's clinical condition in the setting of trauma. Contrast-enhanced computed tomography of the abdomen and pelvis (CTAP) is an invaluable tool in evaluating blunt or penetrating trauma. The purpose of this study is to investigate the effects of hypotension on the enhancement of a patient's abdominopelvic structures in the setting of trauma.

#### **METHOD AND MATERIALS**

This HIPAA-compliant, retrospective study performed at our urban academic teaching hospital was approved by the Institutional Review Board (IRB); informed consent was waived.A database of patients, aged 18 and older, receiving CTAP in the setting of blunt or penetrating trauma during 2014 was assembled using our hospital's EMR. Two cohorts were selected. One cohort comprised of individuals who were hypotensive with a systolic blood pressure of less than 90 on initial presentation to the Emergency Department (ED). The second cohort was comprised of individuals with normal vital signs and lab values on initial presentation to the ED, and without any clinically significant findings on CTAP.Attenuation of the patient's abdominal and pelvic vascular structures and solid organs were measured in Hounsfield Units (HU). Measurements were obtained in the arterial and portal venous phases. 14 hypotensive individuals were evaluated. Mann Whitney U-tests were used in data analysis.

#### RESULTS

In the arterial phase, scanned at 30 seconds, hypotensive individuals demonstrated statistically significant increased attenuation of the aorta, portal vein and renal medulla compared to normotensive individuals. In the portal venous phase, scanned at 70 seconds, hypotensive individuals had significantly decreased attenuation of the renal cortex, spleen, pancreas and liver compared to normotensive individuals.

# CONCLUSION

In the setting of trauma, hypotensive individuals have significant differences in perfusion compared to normotensive individuals, as evidenced by increases in attenuation of the aorta, portal vein and renal medulla in the arterial phase and decreases in attenuation of the renal cortex, spleen, pancreas and liver in the portal venous phase.

#### **CLINICAL RELEVANCE/APPLICATION**

In the setting of trauma, hypotensive individuals have significant differences in perfusion compared to normotensive individuals, which are demonstrated on CTAP. Awareness of these differences may assist in triaging patients and predicting clinical outcomes.

#### **Honored Educators**

Presenters or authors on this event have been recognized as RSNA Honored Educators for participating in multiple qualifying educational activities. Honored Educators are invested in furthering the profession of radiology by delivering high-quality educational content in their field of study. Learn how you can become an honored educator by visiting the website at: https://www.rsna.org/Honored-Educator-Award/

Jorge A. Soto, MD - 2013 Honored Educator Jorge A. Soto, MD - 2014 Honored Educator Jorge A. Soto, MD - 2015 Honored Educator Emergency Ultrasound for Acute Appendicitis: Technical Factors that Influence Follow-up Radiation in Pediatric Patient Populations with Suspected Appendicitis

Sunday, Nov. 27 12:30PM - 1:00PM Room: ER Community, Learning Center Station #2

#### Awards

#### **Student Travel Stipend Award**

#### Participants

Joshua Ewell, DO, Norwalk, CT (*Presenter*) Nothing to Disclose Alicia DeRobertis, MD, Norwalk, CT (*Abstract Co-Author*) Nothing to Disclose Ichiro Ikuta, MD, MMedSc, Norwalk, CT (*Abstract Co-Author*) Nothing to Disclose Steven M. Bernstein, MD, Weston, CT (*Abstract Co-Author*) Nothing to Disclose

## PURPOSE

The purpose of this study is to optimize technical skills to support successful identification of normal and pathologic appendices and to identify technical factors that contribute to non-diagnostic US, with subsequent CT radiation exposure in pediatric patients.

#### **METHOD AND MATERIALS**

All exams were performed by trained radiology residents (RR) or ultrasound technicians (UT). PACS query criteria: date: 01/01-12/31/2015; modality: US; procedure: Appendix. 266 studies met criteria. Data-points: performed by RR or UT; time imaging; visualization/non-visualization; subsequent CT and MRI; ave radiation exposure from subsequent imaging; surgical and pathologic concordance; patient demographics. The primary endpoint of the study is to establish exam optimization/best-practice guidelines for diagnostic identification of the appendix during sonographic evaluation. Secondary endpoints include minimizing radiation dose to pediatric patients and pre-empting more costly follow-up MRI imaging.

#### RESULTS

Preliminary results (17/266) are provided. Sensitivity (visualized) US = 24%. Specificity (surgically proven) = 50%. Ave time scanning 8 min (vis/non-vis). RR = average of 12 min scanning. UT = average of 5.9 min scanning. RR were twice as likely to identify the appendix (33% of the time versus UT 18%). 6/17 US were followed by CT, with 1 surgically proven appendicitis. Total ave effective dose = 2.8 mSv. 11/17 had no followup imaging, with unrelated discharge diagnoses. The remaining 4 were discharged with diagnoses of abdominal pain NOS. 6/17 were followed by CT. 1 went to surgery with surgical and pathologic concordance. The remaining 5 CTs demonstrated normal appendices on CT. The only abnormal appendix in this group was correctly identified on US.

## CONCLUSION

RR are better at identifying the appendix, suggesting multi-modality correlation and anatomic knowledge may improve success. Low suspicion (screening) ultrasounds from the ED were never positive. Average dose to patients = 2.84 mSv, with 1/6 CT positive for acute appendicitis.

## **CLINICAL RELEVANCE/APPLICATION**

Preliminary data suggests use of US as a screening tool for nonspecific abdominal pain in the ED is frequent and inappropriate. UT exams may benefit from anatomic review and landmark identification. Further analysis should identify additional factors that contribute to visualization and non-visualization of the appendix and the associated effective radiation doses of subsequent imaging.

# National Trends in Imaging Suspected Appendicitis: Current Status

Sunday, Nov. 27 12:30PM - 1:00PM Room: ER Community, Learning Center Station #4

#### **Participants**

Victoria F. Tan, MD, Hamilton, ON (*Presenter*) Nothing to Disclose Michael N. Patlas, MD, FRCPC, Hamilton, ON (*Abstract Co-Author*) Nothing to Disclose Douglas S. Katz, MD, Mineola, NY (*Abstract Co-Author*) Nothing to Disclose

#### PURPOSE

To assess the current trends in the imaging of suspected appendicitis in adult patients presenting to emergency departments of academic medical centers across our country.

## METHOD AND MATERIALS

A questionnaire was sent electronically to all 17 academic centers in our country to be completed by Emergency Radiology Section Chiefs. The questionnaires were sent over a period of 3 months staring on October 1, 2015. The survey and analysis of the resulting data was approved by the IRB at our institution.

#### RESULTS

Fifteen centers (88%) responded to the questionnaire. Eleven respondents (73%) used IV contrast - enhanced CT as the imaging modality of choice in imaging of all patients with suspected appendicitis. Twelve respondents (80%) use ultrasound as the initial modality of choice in imaging pregnant patients with suspected appendicitis. Ten respondents (67%) use ultrasound as the modality of choice in patients younger than 40 years of age. When CT is used, 80% use non-focused CT of the abdomen and pelvis, and 47% of centers routinely use oral contrast. Twelve centers (80%) have ultrasound available 24 hours/7 days a week. At twelve centers (80%), the ultrasound examinations are performed by trained ultrasound technologists. Ten centers (67%) have MRI available 24/7. All fifteen centers (100%) use non-enhanced MRI. However, MRI is used as first modality for the imaging of pregnant patients in only three centers (20%) and as first modality for the imaging of patient younger than 40 years in only one center (7%).

#### CONCLUSION

There is heterogeneity in the imaging practice and protocols for patients with suspected appendicitis at our country, which varies depending on patient demographics, resource availability and institutional protocols.

## **CLINICAL RELEVANCE/APPLICATION**

Imaging trends should be considered to develop a national imaging algorithm to permit standardization across our country.

#### **Honored Educators**

Presenters or authors on this event have been recognized as RSNA Honored Educators for participating in multiple qualifying educational activities. Honored Educators are invested in furthering the profession of radiology by delivering high-quality educational content in their field of study. Learn how you can become an honored educator by visiting the website at: https://www.rsna.org/Honored-Educator-Award/

Douglas S. Katz, MD - 2013 Honored Educator Douglas S. Katz, MD - 2015 Honored Educator

## Diagnosis of Gastrogastric Fistula on Computed Tomography: A Quantitative Approach

Sunday, Nov. 27 12:30PM - 1:00PM Room: GI Community, Learning Center Station #2

#### Awards

#### **Student Travel Stipend Award**

#### **Participants**

Guangzu Gao, MD, New Haven, CT (*Presenter*) Nothing to Disclose Nariman Nezami, MD, Baltimore, MD (*Abstract Co-Author*) Nothing to Disclose Mahan Mathur, MD, Boston, MA (*Abstract Co-Author*) Nothing to Disclose Patricia Balcacer, MD, Detroit, MI (*Abstract Co-Author*) Nothing to Disclose Mike Spektor, MD, New Haven, CT (*Abstract Co-Author*) Nothing to Disclose

#### PURPOSE

Logic and observation suggest that after gastric bypass, dense oral contrast in the excluded stomach favors the diagnosis of a gastrogastric fistula, whereas diluted contrast is more likely secondary to reflux. We aim to construct a quantitative method base on this hypothesis.

## **METHOD AND MATERIALS**

After receiving IRB approval with the waiver of informed consent, a retrospective study was performed. A Montage search between 2004 and 2016 identified correlative CTs within 30 days of an upper GI (UGI) exam for patients who had a weight-loss bypass surgery. UGI done on postoperative day 1 was excluded from the search. Imaging review of CTs further selected cases that had oral contrast present in both the excluded stomach and gastric pouch. All CTs showed contrast past the jejunojejunostomy. All charts were reviewed to ensure that there was no surgical intervention between CT and UGI. These cases were randomized and blindly assigned to two radiology attending readers, who recorded their impression of fistula versus reflux for each case, and then computed a relative intensity (RI) ratio (HU in remnant/ HU in pouch). Statistical analysis was performed (SPSS version 20.0) to determine if RI values correlated with UGI findings of gastrogastric fistula.

#### RESULTS

Of 634 cases analyzed, 13 CTs met study criteria. Of these, 46.2% (6/13) were confirmed to have a fistula by UGI. Patients' characteristics (average age 43.2, 84.6% female) and time between CT and UGI (mean 14.2 days, range 3-30 days) were similar for each group. 76.9% (10/13) CTs were performed prior to the UGI.Statistical analysis demonstrated a significant difference in RI ratio (P < 0.05) between the fistula group (RI ratio 1.12, SD 0.29) and the reflux group (RI 0.56, SD 0.19). There was excellent inter-observer reliability (interclass correlation 0.97, p < 0.001). A receiver operating characteristic analysis identified a RI ratio of 0.8 that maximized sensitivity (100%), in expense of specificity (78.6%), for diagnosing gastrogastric fistula. In comparison, the attending radiologists' interpretation yielded a much lower sensitivity (45.8%), and a higher specificity (89.2%).

## CONCLUSION

The relative intensity ratio can be a reliable diagnostic tool for gastrogastric fistula.

## **CLINICAL RELEVANCE/APPLICATION**

We describe a reliable and easy-to-perform quantitative method that markedly improves the sensitivity for diagnosing gastrogastric fistula on computed tomography.

## Development of Cancer in Gall Bladder Polyps Detected on Ultrasound in High Risk Population

Sunday, Nov. 27 12:30PM - 1:00PM Room: GI Community, Learning Center Station #3

#### Awards

#### **Student Travel Stipend Award**

#### **Participants**

Wasey M. Jilani, MBBS, Karachi, Pakistan (*Presenter*) Nothing to Disclose Waseem Akhtar, Karachi, Pakistan (*Abstract Co-Author*) Nothing to Disclose Madiha Jilani, MBBS, Karachi, Pakistan (*Abstract Co-Author*) Nothing to Disclose

### PURPOSE

Management of gall bladder polyps according to the current guideline recommends ultrasound followup for polyps less than 10 mm in size and cholecystectomy for polyps that are greater or equal to 10 mm. While this is helpful for managing patients with large polyps, it does not clearly indicate the size after which follow up is required, the interval and duration of follow-up.

Current literature on this important question is minimal in our region, which is known to have one of the highest risk of developing gall bladder carcinoma. In our study we determined the course of sonographically detected incidental polyps in the gall bladder and on the basis of their size, suggest appropriate management guidelines for these lesions.

#### **METHOD AND MATERIALS**

Radiological data of all "gall bladder polyps" detected on abdominal ultrasounds done between January 2001 and February 2015 were taken at a tertiary care institution. All ultrasound results of included examinations were evaluated to see changes in the size of GB polyps. The medical record files were reviewed to obtain pathologic and clinical follow-up.

## RESULTS

A total of 1226 patients were shortlisted for the reporting engine and One Hundred and fifty five (mean age, 52.6 years; range, 18– 92 years) with GB polyps were included. This included 72 men (46%) and 83 women (54%). US follow-up was performed in a total of 149 patients with minimum follow-up duration of 2 years. Change in size greater or equal to 2 mm was considered relevant. Polyp size was stable in 65 (42%) polyps, decreased in 25 (16 %), increased in 12 (7 %), and resolved in 53 (34%). No neoplastic polyp was found in the 1–6 mm range, one neoplastic polyp was seen in those 7 mm or larger.

#### CONCLUSION

The risk of malignancy of the gall bladder resulting from sonographically detected incidental polyps is very low. GB polyps that are incidentally detected on ultrasound measuring 6 mm or less, may require no additional follow-up. Further studies are required for polyps greater than 7 mm as the available data is inconclusive.

## **CLINICAL RELEVANCE/APPLICATION**

The risk of malignancy of the gall bladder resulting from sonographically detected incidental polyps is very low. GB polyps that are incidentally detected on ultrasound measuring 6 mm or less, may require no additional follow-up.

# GI348-SD-SUA6

Quantification of Hepatic Steatosis in Living Liver Donor Candidates: Comparison Among Automated Twopoint Dixon Reconstruction with Dual-ratio Signal Discrimination Algorithm, Multi-Gradient-Echo Sequence and MR Spectroscopy

Sunday, Nov. 27 12:30PM - 1:00PM Room: GI Community, Learning Center Station #6

## Participants

Hye Young Jang, Seoul, Korea, Republic Of (*Presenter*) Nothing to Disclose So Yeon Kim, MD, Seoul, Korea, Republic Of (*Abstract Co-Author*) Nothing to Disclose Kyoung Won Kim, Seoul, Korea, Republic Of (*Abstract Co-Author*) Nothing to Disclose So Jung Lee, Seoul, Korea, Republic Of (*Abstract Co-Author*) Nothing to Disclose Gi Won Song, Seoul, Korea, Republic Of (*Abstract Co-Author*) Nothing to Disclose Moon-Gyu Lee, MD, Seoul, Korea, Republic Of (*Abstract Co-Author*) Nothing to Disclose Eun Sil Yu, MD, Seoul, Korea, Republic Of (*Abstract Co-Author*) Nothing to Disclose

#### PURPOSE

To compare the diagnostic performance of automated two-point Dixon reconstruction with dual-ratio signal discrimination algorithm ("screening" Dixon), six-point multi-echo 3D gradient-echo (multiple gradient-echo) technique, and high-speed multi-echo 1H MR spectroscopy (MRS) for quantification of hepatic steatosis in living liver donor candidates by using histologic assessment as a reference standard.

#### METHOD AND MATERIALS

This retrospective study included 223 living liver donor candidates who underwent preoperative fat quantification at a 3.0-T MR imaging system and histological evaluation using liver biopsy (mean time between MR imaging and liver biopsy, 3 days). Quantitative MR imaging was performed using the screening Dixon, multiple gradient-echo, and MRS techniques. Results from each technique was correlated with histologic fat fraction. The correlation between the MR techniques was assessed. Receiver operating characteristic (ROC) curve analysis to detect substantial steatosis (macrovesicular fat  $\geq$  10%) was performed.

#### RESULTS

The screening Dixon technique labelled 172 patients as normal, 48 patients as fat and 3 patients as combined, corresponding to the mean values of histological fat fraction of 1.91%, 18.17%, and 0.67%, respectively. The correlation coefficients of multiple gradient-echo and MRS with histologic fat fraction were 0.90 and 0.88, respectively (p<.0001). The fat fraction estimated in the screening Dixon showed a strong correlation with that from the multiple gradient-echo technique (R=0.97, p<.0001) and MRS (R=0.93; p<.0001). The fat fractions between the multiple gradient-echo and MRS were correlated well (R=0.95; p<.0001). The areas under the ROC curve (AUROC) of the screening Dixon, multiple gradient-echo and MRS for the detection of substantial macrovesicular steatosis were 0.921, 0.983, and 0.969; the AUROC of the screening Dixon was significantly lower than the other techniques ( $p \le .018$ ).

## CONCLUSION

Our study validated the capability of the screening Dixon technique in assessing hepatic fat content. Both the six-point multiple gradient-echo technique and MRS showed an excellent diagnostic performance in hepatic fat quantification with a strong correlation between the two techniques.

#### **CLINICAL RELEVANCE/APPLICATION**

The screening sequence using automated two-point Dixon reconstruction and dual-ratio signal discrimination algorithm can be a quick tool for hepatic fat quantification.

Biparametric MRI and Expression of 11 Genes in Apparently Benign Tissue for the Detection of Prostate Cancer: Prospective Registered Clinical Trial

Sunday, Nov. 27 12:30PM - 1:00PM Room: GU/UR Community, Learning Center Station #1

#### Awards

#### **Student Travel Stipend Award**

#### **Participants**

Ivan Jambor, MD, Turku, Finland (*Presenter*) Nothing to Disclose Ileana Montoya Perez, Turku, Finland (*Abstract Co-Author*) Nothing to Disclose Pekka Taimen, Turku, Finland (*Abstract Co-Author*) Nothing to Disclose Saeid Alinezhad, Turku, Finland (*Abstract Co-Author*) Nothing to Disclose Terhi Tallgren, Turku, Finland (*Abstract Co-Author*) Nothing to Disclose Esa Kahkonen, Turku, Finland (*Abstract Co-Author*) Nothing to Disclose Kari Syvanen, Turku, Finland (*Abstract Co-Author*) Nothing to Disclose Matthias Nees, Turku, Finland (*Abstract Co-Author*) Nothing to Disclose Tapio Pahikkala, Turku, Finland (*Abstract Co-Author*) Nothing to Disclose Markku Kallajoki, Turku, Finland (*Abstract Co-Author*) Nothing to Disclose Peter Bostrom, Turku, Finland (*Abstract Co-Author*) Nothing to Disclose Kim Pettersson, Turku, Finland (*Abstract Co-Author*) Nothing to Disclose Hannu J. Aronen, MD, PhD, Kuopio, Finland (*Abstract Co-Author*) Nothing to Disclose

## PURPOSE

To evaluate diagnostic accuracy of biparametric MRI (bpMRI) and expression levels of 11 genes in apparently benign tissue for detection of clinically significantly prostate cancer (SPCa).

#### **METHOD AND MATERIALS**

Eighty patients with an elevated PSA (2.5 - 20.0 ng/ml) and/or abnormal digital rectal examination (DRE) underwent bpMRI examination performed using surface array coils prior to a systematic 12 core biopsy (SB). bpMRI consisted of T2-weighted imaging and three separate diffusion weighted imaging acquisitions (5 b values 0-500 s/mm2, 2 b values 0-1500 s/mm2, 2 b values 0-2000 s/mm2). In addition to SB, two targeted biopsy cores, if a bpMRI target present, and two cores from normal-appearing prostate area, based on bpMRI, were obtained. bpMRI findings were reported using a Likert scoring system (1-5). The RNA transcript levels of ACSM1, AMACR, CACNA1D, DLX1, PCA3, PLA2G7, RHOU, SPINK1, SPON2, TMPRSS2-ERG and TDRD1 were measured with quantitative reverse-transcription PCR. Serum PSA, free PSA (fPSA) were measured and PSA density, prostate volume, age, DRE findings, TRUS findings, use of 5α-reductase inhibitors were included in the analyses as well. A regularized logistic regression classifier was used to evaluate the diagnostic accuracy of individual parameters and their combinations for detection of SPCa. The diagnostic accuracy was estimated using an area under the curve (AUC) values computed from a leave-pair-out cross validation. SPCa was defined as Gleason score 3+4 or higher.

#### RESULTS

SPCa was diagnosed in 36 (45%, 36/80) patients, respectively. Likert score and fPSA were the parameters with the highest AUC values of 0.924, 0.732, respectively. The use all 11 genes resulted in AUC value of 0.645 while the clinical variables, including fPSA, dPSA, demonstrated AUC values of 0.808. The highest AUC value were achieved by the use of Likert score and fPSA (0.930). Predicting SPCa utilizing all features (n=20) resulted in AUC value of 0.900.

# CONCLUSION

The 11 studied genes provided limited added value to bpMRI. bpMRI demonstrated high diagnostic accuracy for detection of SPCa and addition of fPSA resulted in only minor improvement.

## **CLINICAL RELEVANCE/APPLICATION**

The 11 studied genes, fPSA, PSA and clinical parameters provided limited additional value to biparametric MRI for the detection of clinically significantly prostate cancer

## GU201-SD-SUA2

Pelvic Procedures in Gynecologic Oncology Patients: Utilization, Complications, and Impact on Patient Management

Sunday, Nov. 27 12:30PM - 1:00PM Room: GU/UR Community, Learning Center Station #2

#### Awards

**Student Travel Stipend Award** 

#### Participants

Rubina Zahedi, MD, Ann Arbor, MI (*Presenter*) Nothing to Disclose Mishal Mendiratta-Lala, MD, West Bloomfield, MI (*Abstract Co-Author*) Nothing to Disclose Shitanshu Uppal, MBBS, Ann Arbor, MI (*Abstract Co-Author*) Nothing to Disclose Ellen J. Higgins, MS, Ann Arbor, MI (*Abstract Co-Author*) Nothing to Disclose Ashley Nettles, Ann Arbor, MI (*Abstract Co-Author*) Nothing to Disclose Katherine E. Maturen, MD, Ann Arbor, MI (*Abstract Co-Author*) Nothing to Disclose

#### PURPOSE

Image guided percutaneous pelvic procedures often play an important role in the management of gynecologic oncology patients. Although widely considered safe and effective, there is little comprehensive information about interventions among this patient group in the existing literature.

#### **METHOD AND MATERIALS**

IRB-approved retrospective record review of percutaneous pelvic procedures referred from gynecologic oncology, 2005 to 2015. Descriptive statistics and logistic regression were performed.

## RESULTS

392 procedures, including fluid aspiration (n=231 (58.93%)), core biopsy (n=159 (40.6%)), and fine needle aspiration (n=2 (0.5%)), were performed on 225 women, aged 22-91 years. Procedures were performed under sonographic guidance (n=303 (77.3%)), CT guidance (n=87 (22.19%)), or both (n=2 (0.5%)). One patient had self-limited hemorrhage (0.3%), one bladder injury (0.3%), and three had self-limited complaints such as back pain, abdominal pain, and leg tingling (0.8%). One patient developed delayed infection (0.3%). Pathology results included: no specimen sent (n=157 (40.1%)), non-diagnostic (n=6 (1.5%)), new cancer diagnosis (n=55 (14.0%)), recurrence of known primary (n=107 (27.3%)), and benign tissue (n=67 (17.1%)). In terms of management, the procedures led to a new cancer diagnosis (n=46 (11.7%)), surgery (n=15 (3.8%)), chemotherapy (n=88 (22.5%)), radiation therapy (n=9 (2.3%)), cessation of treatment (n=36 (9.2%), treatment of infection (n=10 (2.6%)), or no change in management (n=9 (2.3%)). Many procedures were therapeutic (n=178 (45.4%)) and a minority were performed for genomics (n=1 (0.3%)) or did not impact clinical management (n=9 (2.3%)). Date of service was a significant predictor of a purely therapeutic procedure (OR 1.69 [95% CI 1.44-1.98], p <.0001) and a significant predictor of a malignant diagnosis (OR 0.72 [95% CI 0.64-0.81], p <.0001), for each year later in the 10 year cycle.

## CONCLUSION

At our institution, there has been a trend toward increased utilization of image guided pelvic procedures. The case mix has shifted over the past ten years, with procedures for symptom management constituting a larger proportion and diagnostic procedures constituting a smaller proportion of procedures over time.

#### **CLINICAL RELEVANCE/APPLICATION**

Image guided percutaneous pelvic procedures are safe and impact clinical management in women with gynecologic cancers.

#### **Honored Educators**

Presenters or authors on this event have been recognized as RSNA Honored Educators for participating in multiple qualifying educational activities. Honored Educators are invested in furthering the profession of radiology by delivering high-quality educational content in their field of study. Learn how you can become an honored educator by visiting the website at: https://www.rsna.org/Honored-Educator-Award/

Katherine E. Maturen, MD - 2014 Honored Educator

Discrimination of Clear Cell Renal Cell Carcinoma from Oncocytoma and Fat-Poor Angiomyolipoma on MDCT Using Peak Lesion Enhancement Relative to Uninvolved Renal Parenchyma

Sunday, Nov. 27 12:30PM - 1:00PM Room: GU/UR Community, Learning Center Station #3

## Participants

Heidi Coy, Los Angeles, CA (*Presenter*) Nothing to Disclose Jonathan R. Young, MD, Los Angeles, CA (*Abstract Co-Author*) Nothing to Disclose Michael L. Douek, MD, MBA, Los Angeles, CA (*Abstract Co-Author*) Nothing to Disclose Matthew S. Brown, PhD, Los Angeles, CA (*Abstract Co-Author*) Nothing to Disclose James Sayre, PhD, Los Angeles, CA (*Abstract Co-Author*) Nothing to Disclose Steven S. Raman, MD, Santa Monica, CA (*Abstract Co-Author*) Nothing to Disclose

## PURPOSE

Although a renal mass can have imaging features of a typical clear cell renal cell carcinoma (ccRCC) on MDCT, up to 30% of these are found to be benign after surgery. Most commonly oncocytoma (Onc) and fat-poor angiomyolipoma (fpAML). Discrimination between ccRCC, and Onc or fpAML on imaging would preclude the need for biopsy, and could alter management between surgery and ablation, or active surveillance and no further evaluation. The purpose of our study is to discriminate ccRCC from Onc and fpAML on MDCT using peak lesion enhancement relative to renal cortex.

## **METHOD AND MATERIALS**

With IRB approval for this HIPAA-compliant retrospective study, we queried our clinical databases to obtain a cohort of histologically proven renal masses with preoperative MDCT with four phases (unenhanced, corticomedullary (CM), nephrographic (NP), and excretory (EX)). The entire lesion was segmented in each phase. A CAD algorithm determined a 0.5cm region of interest (ROI) of peak lesion enhancement ≤300HU within the 3D lesion contour. A 0.5cm ROI was placed in enhancing renal cortex. A radiologist approved all lesion contours and ROI placement. Relative enhancement (RE) was calculated as: (lesion ROI-cortex ROI)/ (cortex ROI)\* 100%). A model was derived using logistical regression with RE of ccRCC, Onc, and fpAML as input. Discrimination was evaluated using receiver operator characteristic (ROC) curves.

#### RESULTS

141 patients (61% men, 39% women) with 156 unique renal masses (99 (63%) ccRCC, 43 (28%) Onc, 14 (9%) fpAML) were analyzed. Mean lesion size in ccRCC= 3.1 cm (range 0.8-6.4), Onc=3.0 cm (range 1.0-6.5), and fpAML=2.2 cm (range 0.7-3.6). In discriminating ccRCC from Onc, the model had an AUC of 0.797 (0.726-0.869 95% CI) in the CM phase, 0.598 (0.499-0.697 95% CI) in the NP phase, and 0.672 (0.576-0.768 95% CI) in the EX phase. In discriminating ccRCC from fpAML, the model had an AUC of 0.858 (0.767-0.952 95% CI) in the CM phase, 0.913 (0.837-0.988 95% CI) in the NP phase, and 0.913 (0.836-.0.989 95% CI) in the EX phase.

## CONCLUSION

RE in the CM phase helps discriminate Onc from ccRCC with an AUC of 0.797, while the NP and EX phases help to discriminate fpAML from ccRCC with an AUC of 0.913.

## **CLINICAL RELEVANCE/APPLICATION**

CAD derived RE provides an objective and reproducible measure for the clinician to use when stratifying patients to specific therapeutic pathways, helping to ensure optimal patient outcomes.

2D MRI-based Texture Analysis for Assessment of Lymphovascular Space and Deep Myometrium Invasion of Endometrial Cancer

Sunday, Nov. 27 12:30PM - 1:00PM Room: GU/UR Community, Learning Center Station #4

## Participants

Yoshiko Ueno, MD, PhD, Montreal, QC (*Presenter*) Nothing to Disclose Behzad Forghani, MENG, Cote-saint-Luc, QC (*Abstract Co-Author*) Nothing to Disclose Reza Forghani, MD, PhD, Cote-saint-Luc, QC (*Abstract Co-Author*) Consultant, Real Time Medical, Inc; Shareholder, Real Time Medical, Inc; Committee member, Real Time Medical, Inc; Consultant, General Electric Company; ; Anthony Dohan, MD, Montreal, QC (*Abstract Co-Author*) Nothing to Disclose Benoit P. Gallix, MD, PhD, Montpellier, France (*Abstract Co-Author*) Nothing to Disclose Caroline Reinhold, MD, MSc, Montreal, QC (*Abstract Co-Author*) Consultant, GlaxoSmithKline plc

#### PURPOSE

Lymphovascular space invasion (LVSI) and deep myometrium invasion (MI) are important prognostic factors in patients with endometrial cancer. This study aimed to evaluate the utility of 2D MRI-based texture analysis for the assessment of LVSI and deep MI of endometrial cancer, in comparison with the visual assessment of the depth of myometrial invasion.

#### **METHOD AND MATERIALS**

We retrospectively analyzed the data of 106 patients (mean age, 65.7 years) who underwent 1.5-T MRI scan before hysterectomy for endometrial cancer. Texture analysis using a filtration-histogram technique was performed using a commercial research software (TexRAD®, Somerset, England, United Kingdom) by manually delineating a region of interest (ROI) around the largest diameter of the tumor on MRI images. Texture features of ROIs (mean, standard deviation, entropy, mean of positive pixels, skewness, and kurtosis) were extracted from MR images on 5 different sequences (T2WI, DWI, ADC map, early phase of dynamic contrast-enhanced images, and post contrast-enhanced images). Random forest models using texture features were constructed for diagnosis of LVSI and deep MI. Diagnostic performance of each model was estimated as areas under the receiver-operating characteristic curve (AUC), sensitivity (Sen), specificity (Spe), and accuracy (Acc) and compared with those of independent and blinded visual assessments by two radiologists. The two radiologists included a body MRI fellow and a staff body imager with over 10 years experience with pelvic MR imaging.

#### RESULTS

Forty-eight patients out of 106 (45%) had deep MI and 55 patients (52%) had LVSI. The AUC, Sen, Spe, and Acc of each model were estimated at 0.84, 71.4%, 71.7%, and 71.6% for LVSI; 0.85, 79.2%, 81.0%, and 80.2% for deep MI, respectively. Sen, Spe, and Acc of visual assessment for deep MI were 68.8%, 82.8%, and 76.4% for the less-experienced radiologist, 81.2%, 82.3%, and 82.0% for the more-experienced radiologist.

# CONCLUSION

2D MRI-based texture analysis showed good diagnostic performance for LVSI and deep MI. For deep MI assessment, our model using texture features demonstrated similar diagnostic accuracy to the more experienced radiologist.

# **CLINICAL RELEVANCE/APPLICATION**

2D MRI-based texture analysis has shown promise for the assessment of lymphovascular space and deep myometrium invasion of endometrial cancer. It has the potential to help pre-treatment assessment and treatment planning.

#### **Honored Educators**

Presenters or authors on this event have been recognized as RSNA Honored Educators for participating in multiple qualifying educational activities. Honored Educators are invested in furthering the profession of radiology by delivering high-quality educational content in their field of study. Learn how you can become an honored educator by visiting the website at: https://www.rsna.org/Honored-Educator-Award/

Caroline Reinhold, MD, MSc - 2013 Honored Educator Caroline Reinhold, MD, MSc - 2014 Honored Educator Categorizing Errors in Abdominal Imaging: Lessons Learned from Quality Assurance Conference

Sunday, Nov. 27 12:30PM - 1:00PM Room: HP Community, Learning Center Station #4

#### Awards Cum Laude

### Participants

Thomas E. Pendergrast, MD, Winston-Salem, NC (*Presenter*) Nothing to Disclose Rafel Tappouni, MBBCh, FRCPC, Winston-Salem, NC (*Abstract Co-Author*) Nothing to Disclose

# **TEACHING POINTS**

The purpose of this exhibit is: To discuss categories of errors made in abdominal imaging by individual interpreters: Observation, Interpretation, and Communication. Inadequate Patient Data Gathering will also be included as a category. To demonstrate through example cases the mechanisms by which these errors occur. To share lessons learned through the discussion of errors during adbominal imaging quality assurance conference. These lessons show how categorizing errors can lead to practice modifications that improve quality in radiology.

## **TABLE OF CONTENTS/OUTLINE**

Individual errors as barriers to quality Types of individual errors and contributing mechanisms: Error of Observation Error of Interpretation Error of Communication Inadequate Patient Data Gathering Example cases from abdominal imaging with lessons learned Summary of how categorizing errors helps the individual interpreter avoid such erros in the future

Decision Analysis and Cost-effectiveness Analysis in the Diagnostic Imaging: Practical Tips and Guidance

Sunday, Nov. 27 12:30PM - 1:00PM Room: HP Community, Learning Center Station #5

#### **Participants**

Chong Hyun Suh, MD, Seoul, Korea, Republic Of (*Abstract Co-Author*) Nothing to Disclose Kyung Won Kim, MD, Seoul, Korea, Republic Of (*Presenter*) Nothing to Disclose Seong Ho Park, MD, Seoul, Korea, Republic Of (*Abstract Co-Author*) Research Grant, DONGKOOK Pharmaceutical Co, Ltd Junhee Pyo, Boston, MA (*Abstract Co-Author*) Nothing to Disclose

## **TEACHING POINTS**

1. Understand the importance of diagnostic imaging in medical decision making and its unique feature of cost-effectiveness research2. Understand the overall process of cost-effectiveness analysis

#### **TABLE OF CONTENTS/OUTLINE**

Table of Contents/Outline:1. What is Decision Analysis and Cost-effectiveness assessment (CEA)?2. Unique feature of Decision Analysis and CEA research in the radiology field3. Overall process of CEA research- Framing of the research question- Developing the decision model- Data sources- Interpretation & Reporting4. Issues in the cost-effectiveness analysis in the radiology field-Variation of healthcare between societies- Long process between diagnosis and outcome, increasing uncertainty- Factors influencing medical decision other than cost-effectiveness (e.g., ethical issue, religion, circumference, etc).

## Monitoring Radiology Residency Website Traffic During the Interview Season Including The Match

Sunday, Nov. 27 12:30PM - 1:00PM Room: HP Community, Learning Center Station #1

#### **Participants**

Christopher W. Bailey, DO, Richmond, VA (*Abstract Co-Author*) Nothing to Disclose Mark F. Lisle, MD, Morgantown, WV (*Presenter*) Nothing to Disclose Kenneth A. Veselicky, DDS, MD, Morgantown, WV (*Abstract Co-Author*) Nothing to Disclose Daniel A. Martin, MD, Morgantown, WV (*Abstract Co-Author*) Nothing to Disclose

## PURPOSE

Unfilled Diagnostic Radiology (DR) residency Match spots have varied over time, with the lowest total percent fill rate (86.9%) occurring in the 2015 Match with 152 unfilled positions compared to only 6 unfilled positions in 2010 (99%). Most unfilled positions fill subsequently in the NRMP Supplemental Offer and Acceptance Program (SOAP), known as the Scramble prior to 2012. We predict SOAP applicants utilize institutional website data to gain information about the unfilled programs, as it is well known that medical students view and learn about GME programs via the internet. Google Trends monitors web search traffic over time, and is a useful tool in industry to help analyze product placement.

## METHOD AND MATERIALS

Publicly available NRMP Match data for Match years 2005 to 2016 were reviewed. Google Trends (GT) is a free online application available from parent web browser company Google. GT search terms included: radiology residency and residency in radiology, and data was obtained in weekly quantities throughout annual interview cycles during the study period. Cross reference and analysis of NRMP Match and GT search term data was reviewed.

#### RESULTS

Variation in the number of unfilled DR residency Match spots (Figure 1) during the study period of 2005 to 2016 were found: (average = 52, max = 152 (2015), min = 6 (2010)). GT Search Volume Index (SVI) during Match Week (Figure 2) averaged 43 for "Radiology Residency" and related queries. Internet inquiries peaked during the Scramble/SOAP portion of the NRMP Match week when the total number of unfilled DR positions reached a threshold of 40 (Figure 3).

#### CONCLUSION

Recent NRMP Match results demonstrate an increasing trend of unfilled radiology spots. We predicted and confirmed a peak in internet related search traffic for DR residencies during the NRMP Match week, during which unfilled DR spots are replete via the SOAP/Scramble process. Prior evidence points to residency applicants relying on website data for institutional program information. Thus we encourage that website updates occur before Match week.

#### **CLINICAL RELEVANCE/APPLICATION**

Monitoring radiology residency website traffic via Google Trends application is informative for determining optimal website maintenance scheduling, especially during the interview season.

Effectiveness of Small Group Workshops in Teaching Residents How to Create Educational Radiology Videos

Sunday, Nov. 27 12:30PM - 1:00PM Room: HP Community, Learning Center Station #2

#### **Participants**

Bilal Tahir, MD, Indianapolis, IN (*Abstract Co-Author*) Nothing to Disclose David M. Krause, MD, Indianapolis, IN (*Presenter*) Nothing to Disclose Bharat Kakarala, MD, Indianapolis, IN (*Abstract Co-Author*) Nothing to Disclose Jordan K. Swensson, MD, Indianapolis, IN (*Abstract Co-Author*) Nothing to Disclose Darel E. Heitkamp, MD, Indianapolis, IN (*Abstract Co-Author*) Nothing to Disclose Kulia K. Matsuo, MD, Carmel, IN (*Abstract Co-Author*) Nothing to Disclose

## PURPOSE

The purpose is to evaluate the effectiveness of small group workshops in teaching radiology residents how to create and share educational radiology videos.

## **METHOD AND MATERIALS**

Nine 1st-year and 2nd-year radiology residents, who were Mac computer users, were selected for a 90- minute hands-on workshop performed in small groups of 4-5 participants. The workshop was designed and led by two 4th-year radiology residents and a radiology faculty who were all experienced in creating and publishing radiology educational videos. Participants were expected to complete a pre-participation survey and a 15-minute preparatory computer exercise. Residents were also expected to bring their personal Mac laptops and residency program issued iPads with requisite loaded software (iMovie) to the workshop. One day and three months after the completion of the workshop, participants were resurveyed.

#### RESULTS

On the pre-workshop survey, eight of nine residents indicated that they had no prior experience using Mac products to write movie scripts, record videos or edit videos. When asked what resources could potentially be used to write a script, a variety of free responses were listed such as, but not limited to, Google, StatDx and textbooks to name a few. The remaining questions on the pre-workshop and post-workshop surveys had a five point rating scale (1 = not comfortable at all, 5 = very comfortable). The average resident ratings for various activities prior to, one day after and three months after the workshop are presented, respectively. 1) Writing script: 1.8, 3.6, 4.1; 2) Recording video using iPad: 2.1, 4, 4; 3) Transferring video from iPad to iMovie on Mac: 1.8, 4.2, 4; 4) Video splicing, video order rearrangement, video speed and length adjustment: 1.7, 3.3, 3.2; 5) Recording voice over: 1.6, 4, 3.6; 6) Adding text slides: 1.7, 3.8, 3.9; 7) Adding radiologic images: 2, 4.1, 4.1; 8) Saving video in iMovie: 1.7, 4.2, 3.8; and 9) Uploading video to website: 1.7, 3.7, 3. Subsequently, the nine residents successfully created their own video projects.

## CONCLUSION

Small group workshops are effective teaching tools for improving resident comfort in creating and sharing educational videos.

## **CLINICAL RELEVANCE/APPLICATION**

Small group workshops leading to improve resdient proficiency in creating and sharing educational videos can translate into improved clinical knowledge and procedural proficiency for other residents and radiologists.

# Investigating Quality in Reporting and Clinical Radiology: What the Clinicians Tell Us

Sunday, Nov. 27 12:30PM - 1:00PM Room: HP Community, Learning Center Station #3

#### Participants

Alexander H. Lam, MD, Orange, CA (*Presenter*) Nothing to Disclose Kevin T. Bui, MD, Laguna Hills, CA (*Abstract Co-Author*) Nothing to Disclose Scott C. Goodwin, MD, Los Angeles, CA (*Abstract Co-Author*) Nothing to Disclose David Floriolli, MD, Orange, CA (*Abstract Co-Author*) Nothing to Disclose

## PURPOSE

To better conceptualize quality in both reporting and clinical Radiology through the perspective of the clinician.

## METHOD AND MATERIALS

A 40-question survey (1 = "Strongly Disagree"/"Never"; 5 = "Strongly Agree"/"Always") was distributed to an academic, tertiarycare institution. The survey queried residents, fellows, and attendings from different specialties at varying levels of experience about preferences regarding report formatting, time utilization, and clinical involvement of Radiologists. Differences in response between groups were assessed with Kruskal–Wallis test and Mann-Whitney U.

#### RESULTS

At the time of submission, 138 responses were obtained (80 attendings, 12 fellows, and 46 residents). The respondents were strongly in favor of quality through integration into the healthcare team with formal consultation, interdisciplinary rounds, and conferences (mode 5; IQR 3-5). Clinicians favored direct communication regarding critical findings (mode 5; IQR 4-5). Although respondents tended to neither agree nor disagree with increased patient interaction with Radiology, a small proportion disagreed with direct discussion between the patient and the Radiologist (mode 3; IQR 2-4) and direct referral for interventional services (mode 3; IQR 2-4). Regarding reporting, providing key images with measurements and key findings was viewed favorably (mode 4; IQR 4-5), while allowing flexibility in time constraints for literature references was not favored (mode 2; IQR 2-4).Statistical analysis demonstrated that direct referral for further diagnostic testing from Radiologists was significantly more favorable with residents as compared to fellows or attendings (p=0.043). Integration into the healthcare team was viewed more favorably by fellows and attendings when compared to residents (p=0.047). Detailed discussions of the findings and differential diagnoses was also view more favorably by attendings as compared to residents (p=0.05).

#### CONCLUSION

Clinical integration through established means of direct contact, interdisciplinary rounds, and conferences are highly regarded metrics of quality by clinicians. At this time, direct patient contact can be disagreeable with a minority of clinicians.

#### **CLINICAL RELEVANCE/APPLICATION**

Promoting direct and meaningful contact with the clinician, insightful interdisciplinary rounds, and engaging conferences are valued activities that encourage and maintain quality in Radiology.

# 3D Printing for Endovascular Splenic Artery Aneurysm Repair Planning

Sunday, Nov. 27 12:30PM - 1:00PM Room: IN Community, Learning Center Hardcopy Backboard

#### Participants

Anish Ghodadra, MD, Pittsburgh, PA (*Presenter*) Nothing to Disclose Rakesh K. Varma, MBBS, MD, Monroeville, PA (*Abstract Co-Author*) Nothing to Disclose Ernesto Santos, MD, Madrid, Spain (*Abstract Co-Author*) Nothing to Disclose

## CONCLUSION

Often tortuous in course, the splenic artery is an ideal candidate for 3D printing. Our early experiences illustrate that solid and hollow lumen 3D printed models of splenic artery aneurysms created onsite using consumer grade 3D printers can aid in procedure planning.

## FIGURE

http://abstract.rsna.org/uploads/2016/16002333/16002333\_ure6.jpg

#### Background

First described by Itagaki in 2015, 3D printed models of arterial vasculature can aid in planning the repair of complex splenic artery aneurysms. Here we present our early experience using 3D printed models for the endovascular repair of splenic artery aneurysms.

#### **Evaluation**

First we present a 36 year old male with a 3.2 cm distal splenic artery aneurysm. In addition to a tortuous splenic artery, the inferior spleen blood supply arose from an outflow of the aneurysm and an aberrant accessory artery suppled the superior spleen, arising from the proximal main splenic artery and also feeding the aneurysm. We created a clear, hollow-lumen model of the splenic artery using a Form 1+ stereolithography printer. With the model as a guide, coiling of the distal most aspect of the accessory splenic artery allowed preservation of flow to the superior spleen.Next we present a 69 year old male with a 2.8 cm mid-splenic artery aneurysm. A solid lumen model was created and printed on a Zortrax M200 fused deposition modeling printer. Given the position of the aneurysm, placement of a stent to preserve flow to the spleen was preferred. On CT images, the tortuosity of the splenic artery combined with the moderately steep-appearing angle of the celiac trunk relative to the aorta appeared to prohibit the use of the stent via femoral approach. When working with the model, it became apparent that the steep angle of the celiac trunk would allow passage of a stent via a superior approach. The patient underwent successful axillary-approach stenting of the splenic artery aneurysm.

## Discussion

The above cases illustrate that 3D printed models can aid in endovascular procedure planning. Our first case illustrates the model's ability to maximize preservation of splenic blood flow when treating complex aneurysms with aberrant blood supply, while our second case illustrates a model's role in guiding alternative vascular approaches in treatment.

# Analysis of 3D Printing Accuracy with Geometric and Patient Specific Kidney Phantom

Sunday, Nov. 27 12:30PM - 1:00PM Room: IN Community, Learning Center Hardcopy Backboard

### Participants

Guk Bae Kim, Seoul, Korea, Republic Of (*Presenter*) Nothing to Disclose Hyun Kyung Song, Seoul, Korea, Republic Of (*Abstract Co-Author*) Nothing to Disclose Haekang Kim, Seoul, Korea, Republic Of (*Abstract Co-Author*) Nothing to Disclose Yoon Soo Kyung,, Seoul, Korea, Republic Of (*Abstract Co-Author*) Nothing to Disclose Choung-Soo Kim, Seoul, Korea, Republic Of (*Abstract Co-Author*) Nothing to Disclose Namkug Kim, PhD, Seoul, Korea, Republic Of (*Abstract Co-Author*) Stockholder, Coreline Soft, Inc

# CONCLUSION

3DP methods with multi-materials have been widely used, but their printing accuracies are still not well-known on medical purposes. Sometimes, medical applications may not need higher accuracy. However, in case of a surgical guide, 3DP accuracy is critical to attach the corresponding organ and guide surgical line. This printing error in accuracy would lead to attention of clinicians to use 3DP technology.

## FIGURE

http://abstract.rsna.org/uploads/2016/16015095/16015095\_fvna.jpg

## Background

Three-dimensional printing (3DP) technologies have been applied to various fields of medicine. In partial nephrectomy, our recent 3DP application using patient-specific kidney phantoms with renal cell carcinoma has been used to help surgeons performing more accurate and easier surgery during operations. For a further study developing a surgical guide for partial nephrectomy, however, significant printing discrepancy has been found, caused by 3DP error and instability of materials. In this study, we systemically investigated morphological errors between reconstructed digital models and 3D printed phantoms using patients-specific kidneys and reference artificial geometry models.

## **Evaluation**

EvaluationEight patient-specific kidneys for partial nephrectomy and three reference models of cube, dumbbell and abstracted kidney were evaluated (Fig. 1). All the patient-specific kidney phantoms were manufactured by a 3D printer of PolyJet type with multi-materials of VeroTM color and TangoTM Family. For the comparison study, the reference phantoms were 3D printed by PolyJet type and multi-jet printing (MJP) type. We measured representative lengths of X-axis, Y-axis, Z-axis and volume, and then compared each other.

## Discussion

In the kidney phantoms, there are significant discrepancy from the digital models and to the 3DP phantoms in all the lengths and the volume (Table 1); Y-axis length was elongated (p-value < 0.01), but the length in X-axis and the building-directional length (Z-axis) were shorten (p-value < 0.01). The volume of the 3DP phantom also showed statistically significant increased by 5.15%. The reference phantoms also showed unconformity between the digital model and the phantoms in lengths and volume according to 3DP type and material (Table 2 and 3).

Support Effects of a Similar-image Retrieval System for Image Interpretation of Lung Lesions on Computed Tomography

Sunday, Nov. 27 12:30PM - 1:00PM Room: IN Community, Learning Center Custom Application Computer Demonstration

# Participants

Kotani Tomoya, MD, Moriguchi, Japan (*Presenter*) Research collaboration, Panasonic Corporation Yo Ushijima, Kyoto, Japan (*Abstract Co-Author*) Nothing to Disclose Kenji Kondo, Fukui, Japan (*Abstract Co-Author*) Employee, Panasonic Corporation Kazutoyo Takata, Fukui, Japan (*Abstract Co-Author*) Employee, Panasonic Corporation Toyohiko Sakai, MD, Yoshida-gun, Japan (*Abstract Co-Author*) Nothing to Disclose Hirohiko Kimura, MD, PhD, Fukui, Japan (*Abstract Co-Author*) Nothing to Disclose Takeharu Katoh, Moriguchi, Japan (*Abstract Co-Author*) Nothing to Disclose Daigo Miwa, Moriguchi, Japan (*Abstract Co-Author*) Nothing to Disclose Yoshitomo Nakai, Moriguchi, Japan (*Abstract Co-Author*) Nothing to Disclose Kensuke Wakasugi, Soraku-gun, Japan (*Abstract Co-Author*) Nothing to Disclose Masakai Kiyono, Fukui, Japan (*Abstract Co-Author*) Employee, Panasonic Corporation Masato Tanaka, PhD, Yoshida-gun, Japan (*Abstract Co-Author*) Research Consultant, Panasonic Corporation

# CONCLUSION

Based on our results, reference to similar cases is useful for image interpretation of lung lesions on CT.

## FIGURE

http://abstract.rsna.org/uploads/2016/16005861/16005861\_luq4.jpg

### Background

Daily clinical operations generate a vast amount of medical images, increasing radiologists' workloads. We previously proposed a similar-image retrieval system for supporting image interpretation. Here, we evaluated the effects of this system for image interpretation of lung lesions on computed tomography (CT).

## **Evaluation**

We conducted two experiments. In experiment 1, subjects were nine doctors, of whom five were radiologists. First, each subject wrote an interpretation report for three test cases without references. Second, each subject modified his report with reference to similar cases. In experiment 2, subjects were seven doctors, of whom three were radiologists. First, each subject wrote an interpretation report for six test cases with reference to usual medical texts. Second, each subject modified his report with reference to similar cases. In both experiments, we evaluated number of correct diagnoses and accuracy rate of definite diagnosis. For each test case, approximately 20 similar cases were presented, of which roughly 30% had correct diagnoses. Each similar case contained a key image and definite diagnosis. In experiment 2, similar cases for one-third of the test cases contained no correct diagnosis to investigate the negative influence when the system could not retrieve appropriate similar cases. In experiment 1, number of correct diagnoses increased to 40% with reference to similar cases. The accuracy rate of definite diagnosis improved from 59% to 67%. In experiment 2, the accuracy rate of definite diagnosis improved from 71% to 76%. Further, similar cases containing no appropriate disease had no negative influence on the reports.

### Discussion

In experiment 1, the correlation coefficient between image finding accuracy and the increase in correct diagnosis with reference to similar cases was 0.6. Thus, reference to similar cases is especially suitable for users who can interpret findings correctly. In experiment 2, reference to similar cases improved the precision of definitive diagnosis compared with consulting medical texts.

## Automated Annotation of a Large Scale Radiology Image Database Using Deep Learning

Sunday, Nov. 27 12:30PM - 1:00PM Room: IN Community, Learning Center Station #1

#### Awards

#### **Trainee Research Prize - Fellow**

### **Participants**

Xiaosong Wang, PhD, Bethesda, MD (*Presenter*) Nothing to Disclose Le Lu, PhD, Bethesda, MD (*Abstract Co-Author*) Nothing to Disclose Hoo-Chang Shin, PhD, Bethesda, MD (*Abstract Co-Author*) Nothing to Disclose Lauren M. Kim, MD, Bethesda, MD (*Abstract Co-Author*) Nothing to Disclose Isabella Nogues, BA, Bethesda, MD (*Abstract Co-Author*) Nothing to Disclose Jianhua Yao, PhD, Bethesda, MD (*Abstract Co-Author*) Royalties, iCAD, Inc Ronald M. Summers, MD, PhD, Bethesda, MD (*Abstract Co-Author*) Royalties, iCAD, Inc; ;

## PURPOSE

Obtaining semantic labels on a large scale radiology image database is a prerequisite yet bottleneck to train highly effective deep convolutional neural network (CNN) models for image classification and many Computer Aided Detection tasks. Nevertheless, conventional methods for collecting image labels (e.g., Google search followed by crowd-sourcing) are not applicable due to the limited number of expert observers with the requisite medical training. Here we present an iterative optimization framework for automatic category discovery and labelling of visually coherent and clinically semantic image clusters.

## **METHOD AND MATERIALS**

The framework begins by extracting deep CNN features based on transfer learning from a CNN model pretrained on the ImageNet dataset. Next, the deep feature clustering with k-means is exploited. By evaluating the purity between discovered clusters, the system either terminates the current iteration (which leads to an optimized clustering output) or takes the refined cluster labels as the input to fine-tune the CNN model for the following iteration. Once the visually coherent image clusters are obtained, the system further extracts semantically meaningful text words (by ranking the frequency) for each cluster. All corresponding patient reports per category cluster are adopted for the Nature Language Processing. The image database used in this work contains a total of 216K 2D key-images which are associated with 62K unique patients' radiology reports.

## RESULTS

270 visually coherent image categories are produced with associated clinically semantic key word labels for each category. Sample images and labels from 4 out of 270 categories are shown in the attached Figure. Furthermore, the CNN trained based on the resulting category labels achieves Top-1 classification accuracy of 81.09% and Top-5 accuracy of 94.12% for the testing set respectively.

## CONCLUSION

The proposed framework is capable of generating visually coherent and semantically meaningful text labels for a thematically grouped cluster of radiology images and thereby serves as a potential alternate method of time and cost-intensive task of data labelling.

## **CLINICAL RELEVANCE/APPLICATION**

The labelled image database and the trained CNN model are a potentially valuable addition to the Computer Aided Detection research community.

Software Attributable Dimensional Variability in Threshold Segmentation and Binary Volume Iso-surface Extraction

Sunday, Nov. 27 12:30PM - 1:00PM Room: IN Community, Learning Center Station #2

# Participants

James Shin, MD, MSc, Stony Brook, NY (Presenter) Nothing to Disclose

George L. Shih, MD, MS, New York, NY (*Abstract Co-Author*) Consultant, Image Safely, Inc; Stockholder, Image Safely, Inc; Consultant, MD.ai, Inc; Stockholder, MD.ai, Inc;

Mark E. Schweitzer, MD, Stony Brook, NY (*Abstract Co-Author*) Consultant, MMI Munich Medical International GmbH Data Safety Monitoring Board, Histogenics Corporation

# PURPOSE

To evaluate and quantify differences between open-source and commercial segmentation and binary volume iso-surface extraction algorithms.

# **METHOD AND MATERIALS**

Subsequent to IRB approval, non-contrast CT images of the face (64-slice GE Lightspeed, 1.25mm) and contrast-enhanced cardiac CT images (320-slice Toshiba Aquillon, 1mm) were retrospectively collected and de-identified. Facial bones were segmented by a radiologist using a one-way attenuation threshold in open-source (3D Slicer 4.5) and commercial (Mimics 17) post-processing environments. Cardiac blood pool was similarly segmented. 3D models were generated using maximum settings, without smoothing or mesh decimation. 3D models were co-registered and compared, including comparison with initial segmentation.

# RESULTS

Iso-surface extraction of facial bones resulted in a mesh of 2,325,020 polygons with open-source, and 2,518,652 polygons with commercial (irrespective of interpolation method). Corresponding blood pool counts were 1,069,0350 and 1,060,352; respectively. Dice index for open-source and commercial segmentation by global thresholding was 1, regardless of anatomy. Maximum Hausdorff distances between the models was 14.05mm for facial bones and 0mm/incalculably small for blood pool, with mean distances of 0.081mm and 0mm; respectively. 95% agreement occurred within distances of 0.149mm and 0mm, respectively. Compared to initial facial bone segmentation, Dice indices were 0.9841 for commercial and 0.9940 for open-source. Corresponding blood pool indices were 0.9989 and 0.9989, respectively.

## CONCLUSION

Threshold segmentation is a straightforward means to extract anatomy with characteristic attenuation, and the examined software performed identically. Iso-surface extraction based on marching cube's algorithm performed similarly to derivative commercial algorithms modified for interpolation. Model discrepancies were minimal for facial bones and virtually non-existent for blood pool. Agreement with initial segmentation was high in each case.

# **CLINICAL RELEVANCE/APPLICATION**

In general, the cost to integrate 3D printing into routine patient care has decreased significantly over the past few years. In sharp contradistinction is a potentially dramatic increase in post-processing cost. Demonstrating performative equivalence of open-source software for clinical 3D printing is a key step toward further progress and accessibility, and is demonstrated here with regard to the examined upstream steps.

## Developing an Augmented Virtual Reality Application for Interventional Procedures in Neuroradiology

Sunday, Nov. 27 12:30PM - 1:00PM Room: IN Community, Learning Center Station #3

#### Awards

### **Student Travel Stipend Award**

### Participants

Sergios Gargalas, MD, Oxford, United Kingdom (*Presenter*) Nothing to Disclose Jonathan O. Jones, MBBS, Plymouth, United Kingdom (*Abstract Co-Author*) Nothing to Disclose

## CONCLUSION

Pre-intervention planning using augmented reality approach allows for enhanced 3D visualisation and empowers the interventionist with novels tools for planning the procedure and visualisation of implant placement. We forsee wider future applications in endovascular planning, surgical planning, training and education.

#### Background

Radiology is unique to other medical specialties in it's ability to rapidly absorb technological innovations and set innovation agenda. We strongly believe in the Radiologist's role to drive technological innovation. There is a growing number of 3D visualisation techniques used in surgical specialties and Radiology that are utilised in pre-intervention planning. They tend to be expensive, difficult to use and provide limited functionality. We describe an approach that uses Virtual/ Augmented Reality technology to alleviate many of these issues.

## **Evaluation**

We have developed a virtual reality application on the basis of the Oculus platform and Samsung Gear VR headset, that allows precise and cost-effective planning of interventional procedures. During preparation for aneurysm coiling, the interventionist can access stereoscopic reproduction of CTA-derived vessel geometry, perform measurements and practice behaviour expected during the procedure through added visualisations. The added controls and sensors, such as gyroscope and accelerometer allow for a more natural experience during pre-intervention planning. This technology also allows simultaneous visualisation of several imaging modalities, including DSA at the same time and reduces cumbersome selection between modalities.

#### Discussion

Comparing to other available techniques for 3D planning, our approach is considerably less expensive, easier to set up, more precise and easier to use. We also highlight the potential for other applications, such as intervention simulation for training, vascular anatomy tutorials etc. We are also conducting a study of inter-rater reliability and a questionnaire allowing for quantitative assessment of using this technology. The results of this study will be available by September 2016. From Research to Patient Care: Accelerating Medical Innovation by Creating the World's Largest Open-Indexed Clinical Research Platform

Sunday, Nov. 27 12:30PM - 1:00PM Room: IN Community, Learning Center Station #4

## Participants

Elad Benjamin, Shefayim, Israel (Presenter) CEO, Zebra Medical Vision Ltd

### CONCLUSION

Algorithm development time has decreased significantly by using the Research Platform. Months of data curation turn to minutes, costly storage and computing infrastructure are provided at no cost, and researchers are able to focus purely on development and validation of algorithms and clinical applications, significantly accelerating time to market of clinical innovation.

### Background

Advanced clinical research is fueled by access to data. New techniques, such as Deep Learning, have shown significant improvements over traditional methods, however they require extremely large, annotated data sets to train upon.Unfortunately, accessing hospital data directly is difficult, requiring approvals, integration, anonymization, storage and correct indexing. This process, and the barriers associated with it, make it difficult for most researchers to move forward with meaningful research. It also limits research only to those in academic medical institutions, where some of those barriers are slightly easier to manage.

# **Evaluation**

We have created the largest publically available, anonymized medical research platform globally. The aim is to create a streamlined, web based, hosted, scalable research platform and enable accelerated timelines between research, development and deployment of clinical insights and algorithms. By providing the platform and all ancillary research needs in one place, we believe medical research will be able to take faster, larger leaps forward.

#### Discussion

The Research platform contains over 12M imaging studies, 1M pathology results, 3M lab results, 2M Admission, Transfer and Discharge data points – all correlated across a 4.5M patient population. Data is indexed and searchable through a web based interface, allowing researchers to create specific datasets, including outcomes data, in preparation for research activities. The platform provides built in tagging and annotation tools which are query-able and persistent across data types to allow tailor made data annotation for specific research interests. It is our belief that adoption of this research warehouse by the clinical research community will create improved algorithms and clinical applications that will ultimately improve patient care.

## IN204-SD-SUA5

Analysis of Seven Years of Radiology Resident Errors on Call: Evidence Based Blind Spots to Target Resident Education

Sunday, Nov. 27 12:30PM - 1:00PM Room: IN Community, Learning Center Station #5

### Awards

### **Student Travel Stipend Award**

#### Participants

Jane L. Hur, MD, Philadelphia, PA (*Presenter*) Nothing to Disclose Brendan J. Barnhart, MS,MA, Philadelphia, PA (*Abstract Co-Author*) Nothing to Disclose Richard J. Gorniak, MD, Philadelphia, PA (*Abstract Co-Author*) Nothing to Disclose

#### PURPOSE

Identify trends in errors made on on-call resident preliminary reports which may be useful to target resident education.

### **METHOD AND MATERIALS**

A database of feedback sent from attendings to residents on call at a level 1 trauma center was examined. Feedback sent from 3/1/2008 to 12/31/2015 and categorized as a missed finding was included. Erroneously included cases, feedback with missing information, and duplicate feedback were excluded. Modality, procedure code, and feedback text was examined. Using OpenRefine, a word facet was applied to the feedback text to determine commonly used words within each examination and guide coding. Finally, feedback text, when present, was coded based on finding type and location. Locations of frequently occurring findings were plotted on a representative study.

### RESULTS

There were 1,802 cases of feedback regarding missed findings. Residents received the most feedback on head CTs (339 cases), cervical spine CTs (124), chest radiographs (113), facial CTs (96), and abdominopelvic CTs (70). For head CTs, most of the missed findings concerned a mass, followed by regional hypoattenuation, focal hypoattenuation, fracture, and subdural hemorrhage. A graphic summary of location of missed findings was plotted. On cervical spine CTs, common misses were masses/nodules, fractures, disc herniations, malalignment, and epidural hematomas. For chest XR, commonly missed findings were pneumonias, nodules, fractures, mediastinal abnormalities, and pleural effusions.Common missed findings on facial CT were fracture, mass, and dental disease.Common misses on abdominopelvic CTs were found to be renal stones, enteritis, adnexal masses, colitis, and fractures.The top 5 miss categories in the top 5 studies accounted for 523 cases (30%).

### CONCLUSION

Attending feedback regarding missed findings can be categorized into common categories and locations. This may be useful in selecting high impact training cases. Additionally, a graphic summary of prior miss locations can be generated, illustrating areas where trainees should direct attention.

### **CLINICAL RELEVANCE/APPLICATION**

By targeting the five most common miss types in the five studies most commonly erred on, 30% of on call discrepancies could potentially be avoided.

# MI103-ED-SUA5

Peptide Receptor Radionuclide Therapy (PRRT) of Medullary and Non-Medullary Thyroid Cancer Using Radiolabeled Somatostatin Analogs: A New Paradigm

Sunday, Nov. 27 12:30PM - 1:00PM Room: S503AB Station #5

**FDA** Discussions may include off-label uses.

## Participants

Ali Salavati, MD, MPH, Philadelphia, PA (*Presenter*) Nothing to Disclose Ameya D. Puranik, MBBS, Mumbai, India (*Abstract Co-Author*) Nothing to Disclose Hendra Budiawan, MD, Bad Berka, Germany (*Abstract Co-Author*) Nothing to Disclose Harshad R. Kulkarni, MBBS, MSc, Bad Berka, Germany (*Abstract Co-Author*) Nothing to Disclose Richard P. Baum, MD, PhD, Bad Berka, Germany (*Abstract Co-Author*) Stockholder, OctreoPharm Sciences GmbH; Research Consultant, Novartis AG; Research Consultant, Ipsen SA ; Research Grant, ITG-Medical, Inc

## **TEACHING POINTS**

1) To discuss the role of peptide receptor radionuclide therapy (PRRT) using 177Lu-/90Y-labeled somatostatin analogs in the management of medullary and non-medullary thyroid cancers. 2) To review the application of 68Ga-labeled somatostatin analogs PET/CT imaging in the management of somatostatin receptors (SSTR) expressing thyroid tumors.

## TABLE OF CONTENTS/OUTLINE

Therapeutic options in advanced medullary and non-iodine-avid differentiated (non-medullary) thyroid cancers are limited and associated with significant toxicity. Theranostic (therapy and diagnosis) using radiolabeled somatostatin analogs have proved to be a promising alternative in the management of somatostatin receptors (SSTR) expressing tumors. In this educational exhibit, we will review the molecular basis and clinical application of peptide receptor radionuclide therapy (PRRT) using 177Lu-/90Y-labeled somatostatin analogs in the management of medullary and non-medullary thyroid cancer patients. In addition, the role of 68Ga-labeled somatostatin analogs PET/CT on the management of somatostatin receptors (SSTR) expressing thyroid tumors will be discussed.

## MI201-SD-SUA2

Comparison Analysis of the Tumor Response to Chemotherapy using Diffusion Weighted Imaging and Hyperpolarized 13C MRSI

Sunday, Nov. 27 12:30PM - 1:00PM Room: S503AB Station #2

# Participants

Young-Suk Choi, Seoul, Korea, Republic Of (*Abstract Co-Author*) Nothing to Disclose Eun-Kyung Wang, Seoul, Korea, Republic Of (*Abstract Co-Author*) Nothing to Disclose Han-Sol Lee, Seoul, Korea, Republic Of (*Abstract Co-Author*) Nothing to Disclose Dong-Hyun Kim, PhD, Seoul, Korea, Republic Of (*Abstract Co-Author*) Nothing to Disclose Ho-Taek Song, MD, Seoul, Korea, Republic Of (*Presenter*) Nothing to Disclose

# PURPOSE

To validate the reduction of exchange flux of hyperpolarized [1-13C]pyruvate to lactate after chemotherapy correlated with diffusion weighted imaging technique and hitopatholgy..

## **METHOD AND MATERIALS**

We performed hyperpolarized [1-13C]pyruvate magnetic resonance spectroscopy and imaging after doxorubicin treatment comparison with diffusion weighted MRI (DWI) in orthotropic hepatocellular carcinoma mouse model. 1x10^6 HuH7 cells in PBS were injected into the median liver lobe in Balb/C nude mouse. 6mg/kg of doxorubicin was administrated once by i.p injection. Therapeutic efficacy was evaluate by three imaging techniques: 1) conventional T2W MRI to measure tumor volume, 2) diffusion weighted MR imaging for apparent diffusion coefficient mapping, and 3) hyperpolarized [1-13C]pyruvate MRSI to measure the flux of metabolism. According to the lapse of time, it performed at pre-treatment, post day 3, and post day 6.

### RESULTS

From the ratio analysis of area under the curve of hyperpolarized [1-13C] MRSI, HCC showed remarkably higher conversion ratio from pyruvate to lactate than normal liver tissue. In the early response phase, tumor volumes showed 3.24 fold increases, metabolic flux shows 0.95 fold decreases, and ADC values did not show difference. In the late response phase, tumor volume shows 5.6 fold increases, metabolic flux showed 0.66 fold decrease, and ADC value of tumor showed no significant change. In vehicle treated group, increased in the flux and decreased in the ADC values were significant. In doxorubicin treated group, decrease in the flux was not significant and increase in the ACD was significant.

## CONCLUSION

In this hepatocellular carcinoma model, the decrease of hyperpolarized [1-13C]lactate flux did not correlated with increase in ADC values. hyperpolarized [1-13C]pyruvate MRSI probably quantitate the viable cells in the tumor resistant to chemotherapy.

# **CLINICAL RELEVANCE/APPLICATION**

Although ADC values of diffusion weighted image represent cellularity of tumor or even status of apotosis, the actual tumor viability was not reflected properly. Hyperpolarized [1-13]pyruvate MRSI could be a robust diagnostic metabolic imaging tool to evaluate the tumor viability to evaluate the therapeutic efficacy in clinic.

# [I-123] Ioflupane Study in Parkinsonian Patients: Utility of Putamen to Caudate Ratio

Sunday, Nov. 27 12:30PM - 1:00PM Room: S503AB Station #3

### **Participants**

Manuela C. Matesan, MD, PhD, Seattle, WA (*Presenter*) Nothing to Disclose Santhosh Gaddikeri, MD, Seattle, WA (*Abstract Co-Author*) Nothing to Disclose Katelan H. Longfellow, MD, Seattle, WA (*Abstract Co-Author*) Nothing to Disclose Robert Miyaoka, PhD, Seattle, WA (*Abstract Co-Author*) Nothing to Disclose Saeed Elojeimy, MD, PhD, Seattle, WA (*Abstract Co-Author*) Nothing to Disclose Shana Elman, MD, Seattle, WA (*Abstract Co-Author*) Nothing to Disclose Shu-Ching Hu, Seattle, WA (*Abstract Co-Author*) Nothing to Disclose David H. Lewis, MD, Seattle, WA (*Abstract Co-Author*) Research funded, Eli Lilly and Company Satoshi Minoshima, MD, PhD, Salt Lake City, UT (*Abstract Co-Author*) Royalties, General Electric Company; Research Consultant, Hamamatsu Photonics KK; Research Grant, Hitachi, Ltd; Research Grant, Nihon Medi-Physics Co, Ltd;

### PURPOSE

Value of semi-quantitative analysis of [I-123]ioflupane uptake has been suggested in Parkinsonian patients. We hypothesized that PCR may not be suitable for evaluation of disease progression when both caudate and putamen are involved.

# METHOD AND MATERIALS

We retrospectively reviewed medical records of 32 patients (26 male, average age = 68 yrs) with a clinical diagnosis of Parkinson disease (PD) (n=22) or Parkinson-plus syndrome (PPS) (n=10; including 5 multisystem atrophy, 3 progressive supranuclear palsy, 1 corticobasal degeneration, & 1 non-specified) based on clinical follow- up by a movement disorder specialist. All subjects included in this study had a positive Datscan image by visual interpretation. Brain imaging was performed 4 hours after intravenous injection of 3-5 mCi [I-123]ioflupane using SPECT-CT acquisition. Images were reconstructed using filtered back projection and no attenuation correction was used. Semi-quantitative evaluation using Datquant was performed. We assessed the utility of PCR less than 0.7 as a diagnostic marker of nigrostriatal degeneration in the PD and PPS groups which were further stratified based on their caudate-to-background ratio (CBR) values into mild (CBR>2) and severe disease (CBR <2).

### RESULTS

PCR for both hemispheres ranged from 0.58-0.91, with 24 patients (75%) having PCR above 0.7. In the group with mild disease CBR>2 (n=8; mean 2.65  $\pm$  0.81) mean PCR value was 0.79  $\pm$  0.087 (87.5% patients > 0.7) and in the group with advanced disease CBR <2 (n=24; mean 1.1467  $\pm$  0.353) the mean PCR value was 0.75  $\pm$  0.09 (70.83% patients >0.7). In PD group (mean CBR: 1.5593  $\pm$  0.879), the mean PCR was 0.75  $\pm$  0.09 (72.72 % patients >0.7) and in PSS group (mean CBR: 1.445  $\pm$  0.73) the mean PCR was 0.77  $\pm$  0.10 (80 % patients >0.7).

## CONCLUSION

These findings suggest that PCR ratio may not be a reliable numeric marker in interpretation of [I-123]ioflupane studies, mainly in advanced disease, likely due to decreased both putamen and caudate [I-123]ioflupane uptake.

# **CLINICAL RELEVANCE/APPLICATION**

Although other parameters like caudate to background binding ratio have a role in supporting Datscan visual interpretation, the putamen- to- caudate ratio (PCR) must be interpreted with caution especially in advanced cases of nigrostriatal degeneration when both caudate and putamen have decreased uptake.

Using a Long Circulating Blood Pool Tracer to Perform Multi-patch MPI for Whole Body Imaging of a Mice

Sunday, Nov. 27 12:30PM - 1:00PM Room: S503AB Station #4

#### **Participants**

Caroline Jung, Hamburg, Germany (*Presenter*) Nothing to Disclose Johannes M. Salamon, MD, Hamburg, Germany (*Abstract Co-Author*) Nothing to Disclose Patryk Szwargulski, Hamburg, Germany (*Abstract Co-Author*) Nothing to Disclose Michael G. Kaul, Hamburg, Germany (*Abstract Co-Author*) Nothing to Disclose Gerhard B. Adam, MD, Hamburg, Germany (*Abstract Co-Author*) Nothing to Disclose Tobias Knopp, DIPLENG, Hamburg, Germany (*Abstract Co-Author*) Nothing to Disclose Kannan M. Krishnan, Seattle, WA (*Abstract Co-Author*) Nothing to Disclose Matthew Ferguson, Seattle, WA (*Abstract Co-Author*) Nothing to Disclose Harald Ittrich, MD, Hamburg, Germany (*Abstract Co-Author*) Nothing to Disclose

### PURPOSE

Magnetic particle imaging (MPI) is a new imaging technology that allows the direct quantitative mapping of the spatial distribution of superparamagnetic iron oxide nanoparticles (SPIO). The aim of the study was to perform multi-patch MPI using LS-008 as long circulating blood tracer to achieve mice whole body imaging in a high spatial resolution.

## **METHOD AND MATERIALS**

MPI Scans of FVB mice (n=4) were carried out using a 3D imaging sequence (2.5 T/m gradient strength, 14mT drive-field strength, FoV 22.4x22.4x11.2 mm3). Ten minutes after the injection of 60µl of LS-008 via the tailvein six different drive-field patches (two cranial, two middle and two caudal) each taking 1.5 min were performed. As MPI delivers no anatomic information, MRI scans at 7T ClinScan (Bruker) were performed before MPI examination using a T2-weighted 2D turbo spin echo sequence. Fiducial markers were used to enable MRI/MPI image fusion. Image reconstruction was performed offline using a custom reconstruction framework developed in the programming language Julia using the join formulation.

# RESULTS

The combined MRI/MPI measurements were carried out successfully. The reconstruction of the drive-field patches generated no artifacts at the margins resulting in a whole mice body MP imaging. Compared to previous experiments that we carried out using a gradient strength of 1.5 T/m the multi-patch method with an increased gradient strength of 2.5 T/m resulted in a higher spatial resolution. Therefore we were able not only to visualize the inferior vena cava, the heart and the liver but also the cerebral vessels, liver venes, the thoracic aorta and the kidneys.

## CONCLUSION

In vivo whole body imaging of mice using multi-patch MPI is feasible. The long circulating blood tracer LS-008 enabled us to visualize the whole mice.

## **CLINICAL RELEVANCE/APPLICATION**

The presented technique may offer a strong tool for fast and radiation free whole body angiography.

MRI Appearance of Postoperative Total Hip Arthroplasty 'Pseudotumor': A Review of Terminology (Pseudotumor, ALTR, ALVAL, Metallosis, Particle Disease) and the MR Imaging Similarities and Distinctions between Potential Etiologies

Sunday, Nov. 27 12:30PM - 1:00PM Room: MK Community, Learning Center Hardcopy Backboard

## Participants

Justin Friske, MD, Milwaukee, WI (*Presenter*) Nothing to Disclose Vipul Sharma, MD, Pewaukee, WI (*Abstract Co-Author*) Nothing to Disclose Joseph Davies, MD, Grafton, WI (*Abstract Co-Author*) Nothing to Disclose

## **TEACHING POINTS**

Review the sometimes overlapping terminology ("pseudotumor", adverse local tissue reaction ALTR, aseptic lymphocytic vasculitis associated lesion ALVAL, metallosis, particle disease) and the most current consensus terminology. Review potential etiologies of postoperative THA "pseudotumor" and their MR imaging similarities and distinctions. Review the MRI appearance of periprosthetic infection and the normal expected postoperative THA appearance. Example demonstrating the value of MRI metal suppression sequences for the evaluation of total hip arthroplasty (case of the same patient receiving two separate MRI of the hip, with and without metal suppression, demonstrating a periprosthetic fluid collection obscured by artifact on the non-metal suppression study).

## TABLE OF CONTENTS/OUTLINE

"Pseudotumor": Terminology "Pseudotumor": MR Imaging Findings "Pseudotumor" due to adverse local tissue reaction ALTR/aseptic lymphocytic vasculitis associated lesion ALVAL "Pseudotumor" due to metallosis/particle disease MRI appearance of periprosthetic infection and normal postoperative THA appearance Sample cases Value of MRI metal suppression sequences Sample case of the same patient with a periprosthetic fluid collection not well seen on the initial MRI performed without metal suppression Clinical perspective from the performing surgeon

## MK100-ED-SUA6

Rotator Cuff Injuries: From Imaging to Therapeutic. A Systematic and Structured Approach with Arthroscopic Correlation

Sunday, Nov. 27 12:30PM - 1:00PM Room: MK Community, Learning Center Station #6

# Participants

Alexeys Perez, MD, Caracas, Venezuela (*Presenter*) Nothing to Disclose Luis Cerezal, MD, Santander, Spain (*Abstract Co-Author*) Nothing to Disclose Gustavo Matheus, MSc, Caracas, Venezuela (*Abstract Co-Author*) Nothing to Disclose Eva Llopis, MD, Valencia, Spain (*Abstract Co-Author*) Nothing to Disclose Carolina Pisanti, Caracas, Venezuela (*Abstract Co-Author*) Nothing to Disclose Leonardo E. Garcia, CARACAS, Venezuela (*Abstract Co-Author*) Nothing to Disclose

## **TEACHING POINTS**

Review the anatomy key points in rotator cuff injuries. Illustrate the different types and classifications of rotator cuff injuries. Highlight the importance and surgical implications in each one of the rotator cuff lesions. Suggest a structured radiologic report in order to speak the same language with orthopedic surgeon.

## **TABLE OF CONTENTS/OUTLINE**

Rotator cuff relevant anatomy. Supraspinatus tear classification. Partial tear: Bursal tear: B1, B2, B3. Articular tear classification: PASTA: grade1,2 and 3. STAS: grade 1,2 and 3. Intrasubstance tear. Complete tear: Grade of retraction I, II, III Fatty infiltration (Goutallier 1,2,3,4) Massive tear criteria Massive tear arthropathy. Walch Glenoid morphology (A1,A2,B1,B2,C). Hamada Artrhopathy classitifcation (grade 1,2,3,4,5)Subescapular tear: grade 1,2,3,4 and 5 (Lafosse)Teres minor tear. Miotendinous tears. Cacifyng tendinopathy: Bursal efusion Intramuscular migration Intraosseous migrationRadiologic structured report algorithm for rotator cuff injuries.

# **Ultrasound Assessment of Forefoot Pain: A Pictorial Review**

Sunday, Nov. 27 12:30PM - 1:00PM Room: MK Community, Learning Center Station #7

### **Participants**

Celine Quach, Paris, France (*Presenter*) Nothing to Disclose Anne Miquel, MD, Paris, France (*Abstract Co-Author*) Nothing to Disclose Yves M. Menu, MD, Paris, France (*Abstract Co-Author*) Nothing to Disclose Michel D. Crema, MD, Boston, MA (*Abstract Co-Author*) Shareholder, Boston Imaging Core Lab, LLC

# **TEACHING POINTS**

- To describe the ultrasound technique and to highlight the main anatomical regions of the forefoot usually assessed on ultrasound-To describe the normal anatomy of the main structures of the forefoot, including the plantar plate complex and the metatarsophalangeal joint environment- To illustrate and discuss the specific pathologies potentially diagnosed using ultrasound in selected cases of forefoot pain

## TABLE OF CONTENTS/OUTLINE

1. Ultrasound assessment of forefoot structures: description of the ultrasound technique, including static and dynamic assessment (videos included)2. Review of the main anatomical regions/structures of the forefoot:- metatarsal bone- intermetatarsal spacemetatarsophalangeal joint- plantar plate complex- subcapital space3. Pictorial review of ultrasound-detected pathology in selected cases of forefoot pain (including images and videos):- metatarsal stress fractures - intermetatarsal / subcapital bursitis- interdigital neuromas- turf toe- plantar plate tears and metatarsophalangeal joint instability- metatarsophalangeal arthropathies

# Adult Spinal Deformity: Emphasizing the Sagittal Plane

Sunday, Nov. 27 12:30PM - 1:00PM Room: MK Community, Learning Center Station #8

FDA Discussions may include off-label uses.

## Participants

Thach Huynh, MD, Temple, TX (*Presenter*) Nothing to Disclose Jeffrey D. Stevens, MD, Temple, TX (*Abstract Co-Author*) Nothing to Disclose Ricardo D. Garza-Gongora, MD, Temple, TX (*Abstract Co-Author*) Nothing to Disclose Linda M. Parman, MD, Temple, TX (*Abstract Co-Author*) Nothing to Disclose Connie C. So, MD, Temple, TX (*Abstract Co-Author*) Nothing to Disclose

## **TEACHING POINTS**

1. Understand the radiographic assessment of adult spinal deformity (ASD) and the major causes for morbidity.2. Highlight the concepts behind regional and global spinal alignment.3. Learn the current adult spinal deformity classification system used by surgeons.4. Describe how to assess pelvic parameters and sagittal compensation maneuvers.5. Provide suggested reporting parameters for the radiologist's interpretation of adult scoliosis with an emphasis on the surgical implications.

# TABLE OF CONTENTS/OUTLINE

1. SRS-Schwab ASD Classification Components.2. Technique and examples for measuring coronal curve and sagittal modifier.3. Technique and examples for measuring spinopelvic parameters such as pelvic tilt, pelvic inclination, sagittal vertical axis, and T1 pelvic angle. 4. Discussion and technique for assessing coronal and sagittal imbalance.5. Discussion of sagital imbalance compensation utilizing radiographic samples. 6. Systematic algorithmic approach for analyzing and reporting these findings using a suggested sample report.

## MK290-SD-SUA1

Assessment of Ultrasound versus MRI of the Temporomandibular Joint (TMJ) as a Screening Tool for TMJ Dysfunction

Sunday, Nov. 27 12:30PM - 1:00PM Room: MK Community, Learning Center Station #1

#### Awards

### **Student Travel Stipend Award**

#### Participants

Saul N. Friedman, PhD, MD, Cleveland, OH (*Presenter*) Nothing to Disclose Madhu Rehman, MBBS, Toronto, ON (*Abstract Co-Author*) Nothing to Disclose Hussam K. Beituni, MSc, ARRT, Toronto, ON (*Abstract Co-Author*) Nothing to Disclose Hartley B. Bressler, MD, Toronto, ON (*Abstract Co-Author*) Nothing to Disclose Miriam Grushka, DDS, DPhil, Toronto, ON (*Abstract Co-Author*) Nothing to Disclose Rachel Bressler, Toronto, ON (*Abstract Co-Author*) Nothing to Disclose Masad Markus, Guelph, ON (*Abstract Co-Author*) Nothing to Disclose Lawrence Friedman, FRCPC, MBBCh, Thornhill, ON (*Abstract Co-Author*) Nothing to Disclose

### PURPOSE

Temporomandibular joint (TMJ) dysfunction remains difficult to assess because of factors including complex anatomy and the dynamic nature of pathology. Ultrasound (US) has been proposed as an inexpensive and relatively fast screening tool, enabling realtime evaluation. We assess the sensitivity and specificity of US using MRI as the gold standard. The advantages and disadvantages of the techniques are also explored.

## **METHOD AND MATERIALS**

The patient population consists of 61 patients exhibiting TMJ dysfunction and ranging from 13 to 67 years old with a mean age of 40. Patients were assessed first using US, and then confirmed with MRI as the gold standard. US screening is achieved using a previously-presented technique in which the US probe positions correspond to a clock face at 7 o'clock, 9 o'clock, and 11 o'clock when evaluating the left, with a corresponding mirror image on the right.

### RESULTS

US screening produced no false positive results and only 6 false negative, corresponding to a sensitivity of 100%, specificity of 79%, and estimated positive predictive value of 84% and negative predictive value of 100%. Half of the false negative cases were for medially-displaced disc pathology. Pathology could successfully be seen using US while providing the ability to converse with patients, identify the exact pain locations, and enable real-time identification of crepitus, clicking, motion, locking and unlocking of the jaw, and snapping sensations. Effusions are more easily seen on US compared to MRI. Active inflammation was readily identified using Doppler in all cases; MRI required prior suspicion of inflammatory process and modification of imaging protocol to include gadolinium contrast.

## CONCLUSION

US is a both a sensitive and specific screening tool for TMJ dysfunction. Advantages remain its inexpensive, relatively short scan time, real-time analysis, lack of ionizing radiation, no need for contrast, portability, and adaptably to procedures. Disadvantages are the long learning curve, operator dependence, and difficulty in assessing medially-displaced discs.

## **CLINICAL RELEVANCE/APPLICATION**

Ultrasound is both a sensitive and specific screening tool for temporomandibular joint (TMJ) dysfunction assessment with advantages including real-time analysis and portability.

Magnetic Resonance Angiography with Digital Subtraction and Fusion Images in Assessment of Synovitis in the Hands: Advances in the Assessment of Synovitis

Sunday, Nov. 27 12:30PM - 1:00PM Room: MK Community, Learning Center Station #2

## Participants

Ynyr Hughes-Roberts, MBBS, London, United Kingdom (*Presenter*) Nothing to Disclose Marcela De la Hoz Polo, MD, London, United Kingdom (*Abstract Co-Author*) Nothing to Disclose Yaron J. Berkowitz, MBBChir, MRCS, London, United Kingdom (*Abstract Co-Author*) Nothing to Disclose Anne Kinderlerer, London, United Kingdom (*Abstract Co-Author*) Nothing to Disclose Monica Khanna, MBBS, FRCR, London, United Kingdom (*Abstract Co-Author*) Nothing to Disclose Miny Walker, London, United Kingdom (*Abstract Co-Author*) Nothing to Disclose Dmitri Amiras, MBBS, London, United Kingdom (*Abstract Co-Author*) Nothing to Disclose Anish Raithatha, MBBS, BSC, London, United Kingdom (*Abstract Co-Author*) Nothing to Disclose

### PURPOSE

The inflammatory arthritidies are systemic, inflammatory disorders which have the potential for long term deformity and disability. Early detection of disease and advances in treatment with increasingly effective use of DMARDS (disease modifying anti-rheumatic drugs) and biologic agents has reduced the occurrence of severe long term sequelae in this disease group. We describe our initial experience and evaluate the additional benefit of performing time resolved angiographic imaging in the assessment of synovitis within the hands with the addition of fusion images.

## **METHOD AND MATERIALS**

Retrospective data was collected for patients undergoing imaging to assess for synovitis. Standard MR images including T1, T2 fat saturation and T1 fat saturation with contrast in axial and coronal sequences were reviewed for erosions, bone marrow oedema and synovitis assessed using the OMERACT scoring method. Images were obtained on GE 3T Discovery 750 using Time Resolved Imaging of Contrast KineticS (TRICKS) GE Healthcare. Time resolved MRA images of the same patients obtained during the same data acquisition were scored independently and the imaging finding compared. In addition fusion images of the T1 coronal images with early subtracted MR angiographic sequences were reviewed.

### RESULTS

The fused images were generally good quality and able to identify areas of synovitis demonstrated on the post contrast sequences. Most patients were able to tolerate the scan and able to remain still during the aquisition. Most reviewers felt comfortable reporting the MRA sequences after appropriate training.

## CONCLUSION

Time Resolved Imaging of Contrast KineticS (TRICKS) is a very useful sequence that does not significantly increase scanning time and is technically feasible on current technology. The fusion of these angiographic sequences to the anatomical sequences increases the spatial localisation of the angiographic sequences.

# **CLINICAL RELEVANCE/APPLICATION**

MRA sequences alone of the hands are quick to perform hence performing MRA sequences alone would significantly reduced scanning time for patients and increase the productivity of the scanner. The fusion of the MRA sequences to the anatomical T1 images allows for accurate anantomical localisation of the areas of synovitis with clinicians and patients better able to understand the images.

# **CRMO Revisited: Do MRI Features Correlate with Clinical Response?**

Sunday, Nov. 27 12:30PM - 1:00PM Room: MK Community, Learning Center Station #3

#### Awards

### **Student Travel Stipend Award**

### **Participants**

Jerrin Varghese, MD, Stony Brook, NY (*Presenter*) Nothing to Disclose Marco A. Oriundo Verastegui, MD, Lima, Peru (*Abstract Co-Author*) Nothing to Disclose Julie Cherian, Stony Brook, NY (*Abstract Co-Author*) Nothing to Disclose Mingqian Huang, MD, Syosset, NY (*Abstract Co-Author*) Nothing to Disclose

#### PURPOSE

Chronic recurrent multifocal osteomyelitis (CRMO) is a rare auto-inflammatory disorder that manifests with non-specific bone pain. Diagnosis is challenging and evaluation of clinical improvement after therapy has not been well established. MRI has been shown to be useful at initial evaluation, but data regarding utility of MRI at follow-up is scant. The purpose of this study is to evaluate the correlation between clinical course of CRMO lesions and their changes on follow-up MRI.

## **METHOD AND MATERIALS**

Independent, retrospective chart review was performed of 8 patients with biopsy-proven CRMO who were managed by pediatric rheumatologists. Initial and follow-up MRIs were reviewed by two musculoskeletal fellowship-trained radiologists in regard to changes in marrow edema, periosteal edema, soft tissue edema, and enhancement. Changes in clinical findings were compared to changes on MRI. Statistical analysis of logistic regression was then performed.

## RESULTS

8 patients with diagnosis of CRMO were included with mean age of 14 years (SD  $\pm$ 7.27, range 4-30). There were 5 females and 3 males. Of the 34 total lesions identified, 22 lesions were in the lower extremities, 5 in the upper extremities, and 7 in the axial skeleton. Among the 18 clinically improving lesions, 14 demonstrated decreased bone marrow edema (specificity 100%, p<0.01) and 9 demonstrated decreased periosteal edema (specificity 82%, p=0.059). Since IV contrast was not administered in a majority of the follow up MRI studies, no statistical analysis could be performed for correlation with enhancement. However, if there was improvement in any one of the MRI changes listed above, there was a greater likelihood of clinical improvement when compared to no improvement at all on imaging (p=0.01). Moreover, clinically silent lesions were identified with the help of whole body MRI, including sacral lesions that were then treated and responded well.

## CONCLUSION

Changes in bone marrow edema and periosteal reaction are MRI findings that best correlate with clinical response of CRMO lesions. MRI is also useful in the identification of clinically silent lesions.

## **CLINICAL RELEVANCE/APPLICATION**

Our study demonstrates that MRI is a valuable tool for clinicians in the long term management of CRMO patients.

Diagnostic Performance of Wrist MR Arthrography: Comparison of Three-dimensional Isotropic T1-weighted Fast Spin-Echo MR Arthrography and Two-dimensional MR Arthrography

Sunday, Nov. 27 12:30PM - 1:00PM Room: MK Community, Learning Center Station #4

## Participants

Eunsun Oh, Seoul, Korea, Republic Of (*Presenter*) Nothing to Disclose Young Cheol Yoon, MD, Seoul, Korea, Republic Of (*Abstract Co-Author*) Nothing to Disclose Hyun Su Kim, MD, Seoul, Korea, Republic Of (*Abstract Co-Author*) Nothing to Disclose Ji Hyun Lee, Seoul, Korea, Republic Of (*Abstract Co-Author*) Nothing to Disclose

## PURPOSE

To compare the diagnostic performance of direct wrist MR arthrography (MRA) with 2D T1-weighted FSE sequence and with 3D isotropic T1-weighted FSE sequence for the detection of central perforation of triangular fibrocartilage (TFC), scapholunate ligament (SLL) injury, and lunotriquetral ligament (LTL) injury

## **METHOD AND MATERIALS**

Institutional review board approval was obtained, and the informed consent requirement was waived. Twenty-six patients who had undergone preoperative wrist MRA with the 2D T1-weighted FSE sequence and the 3D isotropic T1-weighted FSE sequence and subsequent arthroscopy were included. Each MR imaging sequence was independently scored by two readers retrospectively for the presence of central perforation of TFC, and tears of SLL and LTL. Sensitivity, specificity, and accuracy of two sequences for diagnosing the injury of each structure were calculated, with arthroscopic finding as a standard reference, and compared each other.

### RESULTS

Arthroscopic surgery revealed 21 central perforation of TFC, 7 SLL tears and 3 LTL tears. Sensitivity, specificity, and accuracy of both sequences for diagnosing the injury of each structure were not statistically significantly different (TFC, 90.5%/80%/88.5% for both readers, both sequences; SLL, 100%/89.5%/92.3% for both readers' 2D and reader 1's 3D, 85.7%/89.5%/88.5% for reader 2's 3D; LTL, 66.7%/100%/96.2% for both readers' 2D, 33.3%/100%/92.3% for both readers' 3D). Interobserver agreements were substantial to excellent (TFC, 0.783, both sequences; SLL, 1.00 for 2D, 0.913 for 3D; LTL, 1.00 for both 2D and 3D).

# CONCLUSION

The diagnostic performance of 3D isotropic T1-weighted FSE wrist MR arthrography is comparable to that of 2D T1-weighted FSE wrist MR arthrography in the diagnosis of central perforation of TFC, and tear of SLL and LTL.

# **CLINICAL RELEVANCE/APPLICATION**

3D isotropic T1-weighted FSE wrist MR arthrography is comparable to 2D T1-weighted FSE wrist MR arthrography in the diagnosis of central perforation of TFC, and tear of SLL and LTL, and 3D isotropic T1-weighted FSE MR arthrography can be alternative.

# 'Who Spoiled the Image - Man or the Machine?': Facts of MRI Artifacts

Sunday, Nov. 27 12:30PM - 1:00PM Room: MS Community, Learning Center Station #1

#### Awards

## **Identified for RadioGraphics**

### **Participants**

Krishnakumari A. Modi, MBBS, Hjorring, Denmark (*Abstract Co-Author*) Nothing to Disclose Nitesh Shekhrajka, Aalborg, Denmark (*Abstract Co-Author*) Nothing to Disclose Victor V. Iyer, MD, Aalborg, Denmark (*Presenter*) Nothing to Disclose Jens Brondum Frokjer, MD, PhD, Aalborg, Denmark (*Abstract Co-Author*) Nothing to Disclose Rune V. Fisker, MD, Aalborg, Denmark (*Abstract Co-Author*) Nothing to Disclose

# **TEACHING POINTS**

The purpose of this exhibit is to summarize the major types of MR artifacts which a radiologist comes across in day to day work, explain the underlying causes/physics and ways to minimise/eliminate the artifacts. Some of the artifacts could mimic pathology while others might make the study suboptimal. So it is important for a radiologist to be familiar with the most common MRI artifacts.

## TABLE OF CONTENTS/OUTLINE

Each type of MRI artifact will be shown in an image accompained by 4 answer options in an interactive multiple choice quiz format and after selecting one of the options, the correct answer will be displayed with the explaination. Each artifact will be discussed in 2 slides (total 15 artifacts = 30 slides + 5 slides for basic physics). **List of artifacts:***MR hardware related:* Herringbone artifact Zipper artifact Central point artifact RF overflow artifact Shading artifact Moire fringes / Zebra stripes *MR software related:* Cross talk artifact *Physiology related:* Ghosting and smearing Entry slice phenomenon *Tissue heterogenicity and Foreign body related:* Black boundary artifact Susceptibility artifact Chemical shift Dielectric effect*Fourier transformation related:* Gibbs/truncation artifact Aliasing/Wrap around artifact

# MS143-ED-SUA2

Successful Integration of Contrast-enhanced Ultrasound (CEUS) into Routine Abdominal Imaging: When and Where Is It Most Useful?

Sunday, Nov. 27 12:30PM - 1:00PM Room: MS Community, Learning Center Station #2



Awards Identified for RadioGraphics

## Participants

Hyun-Jung Jang, MD, Toronto, ON (*Presenter*) Nothing to Disclose Tae Kyoung Kim, MD, PhD, Toronto, ON (*Abstract Co-Author*) Nothing to Disclose Korosh Khalili, MD, Toronto, ON (*Abstract Co-Author*) Nothing to Disclose Mostafa Atri, MD, Toronto, ON (*Abstract Co-Author*) Nothing to Disclose

# **TEACHING POINTS**

Through best illustrative cases over 15-year experience of successful integration of CEUS into routine clinical practice, readers will learn Essential knowledge and requirements for new implementation of CEUS in routine abdominal imaging practice Major differences and unique advantages of CEUS with explanations of mechanisms as compared to CT/MR Proper indications for CEUS to maximize added benefits to CT/MR for the best patient care Cautions in multimodality correlation and correct interpretation of discordant cases

### **TABLE OF CONTENTS/OUTLINE**

Efficient set up and workflow Advantages unique to CEUS and their most relevant clinical applications: purely intravascular properties, real-time imaging, disruption-replenishment, non-nephrotoxicity and easy repeatability Interactive display of CEUS as a problem solver in various representative clinical scenarios Hepatic: Indeterminate nodules on CT/MR FNH versus adenoma Complex cysts Cirrhosis related nodules Tumor vs bland thrombosis Pre- and post-RFA Nodule localization for biopsy Extrahepatic Complex renal cysts Indeterminate renal lesions on CT/MR Post-RFA for RCC Post-EVAR endoleak Incidental splenic mass Complex ovarian cysts Indeterminate pancreatic or gallbladder lesions Pitfalls in interpretation

# NM110-ED-SUA10

Spectrum of PET/CT Findings in Tumors of the Musculoskeletal System: Diagnostic Patterns, Staging, Pearls and Pitfalls

Sunday, Nov. 27 12:30PM - 1:00PM Room: S503AB Station #10

# Awards

Certificate of Merit Identified for RadioGraphics

### Participants

Nilendu C. Purandare, DMRD, Mumbai, India (*Presenter*) Nothing to Disclose Venkatesh Rangarajan, MBBS, Mumbai, India (*Abstract Co-Author*) Nothing to Disclose Sneha A. Shah, Mumbai, India (*Abstract Co-Author*) Nothing to Disclose Archi Agrawal, MBBS, Mumbai, India (*Abstract Co-Author*) Nothing to Disclose

## **TEACHING POINTS**

1)Understand the wide range of metabolic uptake seen in tumors of the bone and soft tissue on FDG PET/CT scans based on their histological type.2)Understand the utility of FDG PET/CT in aiding diagnosis by directing biopsy from the most viable and representative portion of the tumor.3)Understand the role of PET/CT in staging, as a surrogate marker of response to treatment and in predicting malignant transformation in certain benign tumors.4)Understand the pitfalls, false positives and treatment related complications during PET/CT interpretation

## TABLE OF CONTENTS/OUTLINE

1)Patterns of FDG uptake in various benign and malignant tumors of the musculoskeletal system in conjunction with their histopathology and radiological features.2)Clinical utility of FDG PET/CT ina)establishing diagnosis by directing biopsiesb)staging and assessing therapeutic responsec)predicting malignant transformation in benign tumors 3)Diagnostic dilemmas, false positives and pitfalls in PET/CT interpretation.

A Comparative Study of F-18 FDG PET/CT and C-11 Methionine PET/CT for Differentiating Primary CNS Lymphoma from Glioblastoma

Sunday, Nov. 27 12:30PM - 1:00PM Room: S503AB Station #6

## Participants

Yoshihiro Nishiyama, MD, Kagawa, Japan (*Presenter*) Nothing to Disclose Yuka Yamamoto, MD, PhD, Kagawa, Japan (*Abstract Co-Author*) Nothing to Disclose Katsuya Mitamura, Kita-gun, Japan (*Abstract Co-Author*) Nothing to Disclose Takashi Norikane, Kita-gun, Japan (*Abstract Co-Author*) Nothing to Disclose Tetsuhiro Hatakeyama, Kagawa, Japan (*Abstract Co-Author*) Nothing to Disclose

# PURPOSE

The purpose of this study was to compare F-18 FDG (FDG) PET/CT and C-11 methionine (MET) PET/CT for differentiating between primary central nervous system (CNS) lymphoma and glioblastoma.

## **METHOD AND MATERIALS**

A total of 26 patients (6 CNS lymphomas and 20 glioblastomas) with newly diagnosed were examined with both FDG and MET PET/CT. PET emission scanning of the head region with a 15-min acquisition of one bed position was performed at 60 min and 15 min after FDG and MET injection, respectively. The maximum standardized uptake value (SUV), peak SUV, mean SUV, metabolic tumor volume (MTV) and the tumor-to-normal brain tissue (T/N) ratio of tumors were measured.

## RESULTS

All tumors showed positive accumulation on both FDG and MET PET/CT. Using FDG PET/CT, maximum SUV, peak SUV, mean SUV, and T/N ratio in CNS lymphoma were significantly higher than those in glioblastoma. The FDG MTV in glioblastoma was higher than that in CNS lymphoma, although the difference was not statistically significant. In contrast, no significant differences in all PET parameters using MET PET/CT were noted between CNS lymphoma and glioblastoma.

## CONCLUSION

FDG PET/CT is more helpful than MET PET/CT for differentiating between CNS lymphoma and glioblastoma.

## **CLINICAL RELEVANCE/APPLICATION**

FDG PET/CT is more helpful than MET PET/CT for differentiating between CNS lymphoma and glioblastoma.

## Novel CZT-based digital SPECT - Preliminary Results from a Prototype System

Sunday, Nov. 27 12:30PM - 1:00PM Room: S503AB Station #7

#### **Participants**

Simona Ben-Haim, MD, DSc, Ramat Gan, Israel (*Presenter*) Consultant, Spectrum Dynamics Ltd; Consultant, Molecular Dynamics; Spouse, Stockholder, Molecular Dynamics

Ronen Goldkorn, MD, Ramat Gan, Israel (*Abstract Co-Author*) Research support, Molecular Dynamics Elinor Goshen, MD, Ramat Gan, Israel (*Abstract Co-Author*) Nothing to Disclose

## PURPOSE

Cadmium-Zinc-Telluride (CZT)-based digital gamma cameras can provide improved image resolution and greater sensitivity, thereby allowing faster acquisitions and / or reduced administered dose compared to standard scintillator-based analog (Anger) systems. Evaluation of clinical feasibility, image quality, and diagnostic performance of a prototype of a novel CZT-based digital SPECT general purpose camera was performed.

### **METHOD AND MATERIALS**

The digital SPECT system (Valiance X12 prototype, Molecular Dynamics, Hamilton, Bermuda) is equipped with CZT detectors, fitted with a high-sensitivity collimator and mounted on a ring shaped gantry. The detectors are capable of independent motion to acquire data from multiple angular views. The flexible architecture also enables focusing the detection units on a specific region of interest to obtain enhanced images of a specific target. Data are reconstructed using an iterative reconstruction algorithm. Fifteen Tc-99m MDP digital SPECT studies were acquired in 12 patients (7M, age 27-66yrs) immediately following analog SPECT including SPECT of knees (n=7), lumbar spine/pelvis/hips (n=4) and ankles/feet (n=4). Both sets of images were compared by experienced Nuclear Medicine physicians and were graded on a scale of 1 (poor) to 4 (very good) for sharpness, contrast, overall quality and diagnostic confidence.

## RESULTS

Digital SPECT studies were all diagnostic and were of good or very good quality. Mean grades for digital SPECT exceeded those of analog SPECT for sharpness (3.7 vs. 3.1), and contrast (3.9 vs. 3.3). Overall image quality and diagnostic confidence of digital and analog SPECT were comparable (3.7 vs. 3.6 and 3.8 vs. 4.0 respectively).

# CONCLUSION

These preliminary results show improved contrast and sharpness of digital bone SPECT compared to analog SPECT and are encouraging. Further studies in large patient cohorts and other clinical indications are under way.

## **CLINICAL RELEVANCE/APPLICATION**

General purpose digital SPECT with high sensitivity collimators, together with improved resolution, improved sharpness and contrast as compared to analog SPECT technology are expected to have significant clinical impact. Further research will assess other general nuclear medicine applications, as well as the contribution of focused imaging, a unique capability of this CZT-based digital SPECT system.

## Utility of FDG PET-CT in Radiographic Progression of Glioblastoma

Sunday, Nov. 27 12:30PM - 1:00PM Room: S503AB Station #8

#### Awards

### **Student Travel Stipend Award**

### **Participants**

Carlos Leiva-Salinas, MD,PhD, Charlottesville, VA (*Presenter*) Nothing to Disclose David Schiff, MD, Charlottesville, VA (*Abstract Co-Author*) Nothing to Disclose Lucia Flors, MD, Charlottesville, VA (*Abstract Co-Author*) Nothing to Disclose James Patrie, MS, Charlottesville, VA (*Abstract Co-Author*) Nothing to Disclose Patrice K. Rehm, MD, Charlottesville, VA (*Abstract Co-Author*) Nothing to Disclose

## PURPOSE

To determine whether relative SUV measurements at FDG PET can be used to predict survival time in patients with glioblastoma treated with radiation therapy and temozolomide, and suspicion of disease progression on follow-up MRI

# METHOD AND MATERIALS

We retrospectively reviewed 56 patients with glioblastoma treated with surgery followed by radiation and temozolomide, who underwent post therapy FDG PET due to findings of suspected progression on follow-up MRI. We fused the PET and MRI images. Relative SUV measurements were calculated from regions of interest that were placed in the area of highest FDG uptake within the abnormal contrast enhancement as seen on the PET/MRI overlay maps, and in the contralateral normal-appearing white matter. We calculated survival time from initial diagnosis and from post therapy PET; the latter was used as the outcome variable. We used Cox proportional Hazard models to predict survival from PET based on the relative SUV

## RESULTS

Twenty four patients were female (42.9%). Mean age at diagnosis was  $56.8\pm12.2$  years. Overall median survival time from diagnosis was 20.8 months. Overall median survival time from PET was 12.2 months. There was a significant association between survival time from PET and relative SUV (p<0.001). The instantaneous risk of death (hazard) was 1.4 time greater (95% CI: [1.20, 1.62]) for a patient at the 50th percentile of the relative SUV distribution (relative SUV of 2.0) than for a patient at the 25th percentile (relative SUV of 1.7); while it was 2.44 time greater (95% CI: [1.64, 3.64]) for a subject at the 75th percentile (relative SUV of 2.5) than for one at the 25th percentile. Median survival times for patients at the 25th, 50th and 75th percentiles were 15.9 months (95% CI: [12.2, 25.9], 12.6 months (95% CI: [10.3, 17.1]), and 9.7 months (95% CI: [8.7, 12.]), respectively. Predicted probabilities of surviving 10, 20, and 30 months post PET for patients at the 25th, 50th and 75th percentiles were 0.73, 0.37, and 0.25; 0.65, 0.25 and 0.14; and 0.47, 0.09 and 0.03, respectively

## CONCLUSION

Quantitative relative SUV on FDG PET is a biomarker of survival in patients with glioblastoma treated with surgery followed by concurrent radiation therapy and temozolomide, with suspicion of progression on post-therapy MRI

# **CLINICAL RELEVANCE/APPLICATION**

Data is likely to be useful in the patient management and could support the need for further therapeutic actions on selected subjects

# Detection of Unexpected Emergency Diseases by FDG-PET/CT of Oncologic Patients

Sunday, Nov. 27 12:30PM - 1:00PM Room: S503AB Station #9

### **Participants**

Akira Toriihara, Bunkyo-Ku, Japan (*Presenter*) Nothing to Disclose Emi N. Yamaga, MD, Tokyo, Japan (*Abstract Co-Author*) Nothing to Disclose Masashi Nakadate, MD, Asahi, Japan (*Abstract Co-Author*) Nothing to Disclose Ukihide Tateishi, MD, PhD, Tokyo, Japan (*Abstract Co-Author*) Nothing to Disclose

## PURPOSE

To review FDG-PET/CT cases in which unexpected emergency diseases were detected and to establish a checklist for rapid and appropriate management.

## **METHOD AND MATERIALS**

Interpretation reports of 11,663 FDG-PET/CT studies, performed in our hospital from 2012 to 2015, were retrospectively reviewed by consensus of one nuclear medicine physician and two radiologists. Patients with major emergency diseases were extracted according to following exclusion criteria: (1) The findings had been recognized before PET/CT. (2) Any intervention or operation, which can be related to relevant findings, had been undergone within a month prior to PET/CT. (3) Clinical course before or after PET/CT could not be investigated sufficiently, such as patients who were introduced from other hospitals.

## RESULTS

Forty-one patients (0.35%) with unexpected emergency diseases were identified. Most frequent disease was pneumothorax (8 patients), followed by chronic subdural hematoma (CSH) (7 patients), ureteral stone (7 patients), abdominal aortic aneurysm (AAA) with dirty fat sign or high-attenuating crescent sign visualized on CT (4 patients). Nine patients (2 pneumothorax, 3 CSH, 1 cerebral hemorrhage, 1 acute cholecystitis, 1 acute pancreatitis and 1 acute appendicitis) were hospitalized and/or underwent any therapeutic intervention within a week after PET/CT. In two patients with AAA, aneurysm repair was performed prior to therapy of known cancer.

# CONCLUSION

Although rare, unexpected emergency disease which needs urgent management can be detected by FDG-PET/CT, therefore we should check CT, particularly head and thorax, as soon as possible after obtaining PET/CT data.

# **CLINICAL RELEVANCE/APPLICATION**

Based on our results, nuclear medicine physicians, who engage in FDG-PET/CT study, will be able to contribute to life saving and improved prognosis of patients with unexpected emergency diseases.

Don't Blow It: Pre-Operative Evaluation for Functional Endoscopic Sinus Surgery (FESS) - Pearls and Pitfalls

Sunday, Nov. 27 12:30PM - 1:00PM Room: NR Community, Learning Center Station #7

#### Participants

Andrew J. Spain, MD, Detroit, MI (*Presenter*) Nothing to Disclose Brent D. Griffith, MD, Troy, MI (*Abstract Co-Author*) Nothing to Disclose John J. Corrigan, MD, Detroit, MI (*Abstract Co-Author*) Nothing to Disclose Horia L. Marin, MD, Detroit, MI (*Abstract Co-Author*) Nothing to Disclose Suresh C. Patel, MD, Detroit, MI (*Abstract Co-Author*) Nothing to Disclose John Craig, Detroit, MI (*Abstract Co-Author*) Nothing to Disclose

# TEACHING POINTS

Functional endoscopic sinus surgery (FESS) is used to treat chronic sinus conditions by removing causes of functional obstruction to the drainage pathways. The goal of pre-operative imaging is not only to delineate extent of disease, but more importantly, to identify variant or pathologically altered anatomy that might place a patient at increased risk for potentially devastating surgical complications. This exhibit will review: - Surgical approaches utilized in FESS, emphasizing relevant anatomic landmarks and surgical boundaries

- High risk anatomic variants and alterations that must be recognized pre-operatively and potential complications due to failed recognition

## TABLE OF CONTENTS/OUTLINE

Surgical approaches and appearances of the following subtypes: 1) Maxillary Antrostomy, 2) Anterior/Posterior Ethmoidectomy, 3) Sphenoidotomy, 4) Frontal sinusotomy For each surgical approach, case-based discussion will include: Surgical boundaries Key anatomic landmarks in pre-operative evaluation (lamina papyracea, frontal recess, cribriform plate, anterior ethmoidal artery, etc.) High risk anatomic variants/alterations and their imaging appearance (e.g., lateralized uncinate, dehiscence of lamina papyracea and optic canal, Onodi cells, etc.) Potential complications **Broken Bridges - DTI Characterization in Posterior Fossa Malformations** 

Sunday, Nov. 27 12:30PM - 1:00PM Room: NR Community, Learning Center Station #8

## Awards Certificate of Merit

### **Participants**

Lais Fajardo, MD, Sao Paulo, Brazil (*Presenter*) Nothing to Disclose Suely F. Ferraciolli, MD, Sao Paulo, Brazil (*Abstract Co-Author*) Nothing to Disclose Amanda R. Coutinho, Sao Paulo, Brazil (*Abstract Co-Author*) Nothing to Disclose Carolina M. Rimkus, MD, Sao Paulo, Brazil (*Abstract Co-Author*) Nothing to Disclose Maria Martin, MD, PhD, Sao Paulo, Brazil (*Abstract Co-Author*) Nothing to Disclose Leandro T. Lucato, MD, Sao Paulo, Brazil (*Abstract Co-Author*) Nothing to Disclose Claudia D. Leite, MD, PhD, Sao Paulo, Brazil (*Abstract Co-Author*) Nothing to Disclose

# **TEACHING POINTS**

The purpose of this exhibit is to: Discuss the role of Diffusion Tensor Imaging (DTI) and its post-processing tool Fiber Tractography for evaluation of congenital posterior fossa malformations. Show the additional information that DTI provides compared to conventional Magnetic Resonance (MR) sequences to evaluate abnormal fiber course, failure to decussate or ectopic fiber location. Briefly discuss potential future uses for DTI to further understand the pathogenesis of posterior fossa malformations. Show at the beginning the normal DTI findings of the pediatric posterior fossa. Delineate a take home message board, by the analysis of didactic and representative cases with the classic imaging findings of posterior fossa malformations. Neuroimaging plays a key role in the diagnosis of congenital midbrain-hindbrain malformations. DTI is an advanced MR technique that provides qualitative and quantitative information about the microarchitecture of white matter, eventually depicting alterations when conventional structural images didn't show abnormalities.

# TABLE OF CONTENTS/OUTLINE

IntroductionMethodsDTI of the normal pediatric posterior fossaImaging findings Chiari Malformation Dandy-Walker Malformation Joubert Syndrome Tegmental Pontine Cap Dysplasia Medullary Cap DysplasiaDiscussionTake-home message

## NR341-SD-SUA1

## Treatment Effects and Safety of Ethanol Ablation for Thyroglossal Duct Cysts: A Comparison with Surgery

Sunday, Nov. 27 12:30PM - 1:00PM Room: NR Community, Learning Center Station #1

### **Participants**

Mi Sun Chung, MD, Seoul, Korea, Republic Of (*Abstract Co-Author*) Nothing to Disclose Ji Ye Lee, MD, Seoul, Korea, Republic Of (*Presenter*) Nothing to Disclose Jung Hwan Baek, Seoul, Korea, Republic Of (*Abstract Co-Author*) Nothing to Disclose Jeong Hyun Lee, MD, PhD, Seoul, Korea, Republic Of (*Abstract Co-Author*) Nothing to Disclose Young Jun Choi, MD, Seoul, Korea, Republic Of (*Abstract Co-Author*) Nothing to Disclose Jong Ho Yoon, Seoul, Korea, Republic Of (*Abstract Co-Author*) Nothing to Disclose Soon Yuhl Nam, Seoul, Korea, Republic Of (*Abstract Co-Author*) Nothing to Disclose Seong Chul Kim, Seoul, Korea, Republic Of (*Abstract Co-Author*) Nothing to Disclose Jin-Yong Sung, Seoul, Korea, Republic Of (*Abstract Co-Author*) Nothing to Disclose Seon Mi Baek, MD, Pusan, Korea, Republic Of (*Abstract Co-Author*) Nothing to Disclose Dong Gyu Na, MD, Seoul, Korea, Republic Of (*Abstract Co-Author*) Nothing to Disclose

## PURPOSE

We aimed to compare the treatment efficacy and safety of ethanol ablation (EA) for thyroglossal duct cyst (TGDC) against surgery.

### **METHOD AND MATERIALS**

This study included 345 patients (289 of surgery and 56 of EA) treated for TGDC at four institutions between May 2005 and June 2014. The volume reduction rate was calculated using following equation: [initial volume of TGDC – follow-up volume of TGDC]/ initial volume of TGDC  $\times$  100 %. Treatment failure was defined in the EA group as <50% volume reduction at the last visit or regrowth of the lesion during the follow-up period, and in the surgery group as the clinical recurrence of the cosmetic problem because of a visible mass. Complication was defined according to the Society of Interventional Radiology guidelines. Surgery and EA were compared with respect to the treatment failure and complication rates as well as the cost for index treatment incurred. Treatment failure and complications were also compared between EA and Sistrunk operation which is current standard surgical method for TGDC. The Cox regression hazard model and linear regression were used for the adjustment of covariates.

### RESULTS

EA demonstrated higher treatment failures (19.6% vs. 2.4%, p<0.001), but fewer complications (1.8% vs. 10.0%, p=0.04), and lower cost (#423,801 vs. #1,435,707) than surgery. The mean volume reduction rate after EA was 82.3% at the last follow-up and cumulative treatment success rate up to second session of the EA was 85.7% (44/56) in our study. However, the treatment efficacy of EA showed an abrupt decreased in patients who underwent EA more than three times. EA also had more frequent treatment failure than the Sistrunk operation (p=0.004), but fewer complications (p=0.061). After adjustment of covariate, EA and age below 20 years were correlated with treatment failure (p=0.001 and 0.011, respectively).

## CONCLUSION

Both surgery and EA are highly effective in the management of TGDC. Although there is a higher likelihood of treatment failure with EA, it has a better safety profile than surgery. EA could be an alternative treatment for TGDC, however, surgery would be recommended in children and patient who had performed EA more than twice.

## **CLINICAL RELEVANCE/APPLICATION**

Both surgery and EA show acceptable treatment efficacy for TGDC. EA could be an alternative treatment for TGDC in selected patients.

Analysis and Prediction of Claustrophobia During Magnetic Resonance Imaging with the Claustrophobia Questionnaire: An Observational, Prospective, 18-Month, Single-Center Study of 6500 Patients

Sunday, Nov. 27 12:30PM - 1:00PM Room: NR Community, Learning Center Station #2

# Participants

Adriane Napp, Berlin, Germany (*Presenter*) Nothing to Disclose Judith Enders, Berlin, Germany (*Abstract Co-Author*) Nothing to Disclose Robert Rohle, Berlin, Germany (*Abstract Co-Author*) Nothing to Disclose Gerd Diederichs, MD, Berlin, Germany (*Abstract Co-Author*) Nothing to Disclose Matthias Rief, MD, Berlin, Germany (*Abstract Co-Author*) Nothing to Disclose Elke Zimmermann, MD, Berlin, Germany (*Abstract Co-Author*) Nothing to Disclose Peter Martus, PhD, Berlin, Germany (*Abstract Co-Author*) Nothing to Disclose Marc Dewey, MD, Berlin, Germany (*Abstract Co-Author*) Nothing to Disclose Marc Dewey, MD, Berlin, Germany (*Abstract Co-Author*) Research Grant, General Electric Company; Research Grant, Bracco Group; Research Grant, Guerbet SA; Research Grant, Toshiba Corporation; Speakers Bureau, Toshiba Corporation; Speakers Bureau, Guerbet SA; Speakers Bureau, Bayer AG; Consultant, Guerbet SA; Author, Springer Science+Business Media Deutschland GmbH; Editor, Springer Science+Business Media Deutschland GmbH; Institutional research agreement, Siemens AG; Institutional research aqreement, Koninklijke Philips NV; Institutional research agreement, Toshiba Corporation; ; ; ; ; ; ; ; ;

## PURPOSE

To analyze claustrophobia during magnetic resonance (MR) imaging using the 26-item claustrophobia questionnaire (CLQ, range 0– 4) and to explore its potential as a screening tool.

## **METHOD AND MATERIALS**

6520 consecutive patients were included. Overall, 4288 patients were exposed to the CLQ before MR imaging (CLQ cohort) while 2232 patients underwent MR imaging without the CLQ (non-CLQ cohort). Claustrophobic events were recorded by the staff. The study received IRB approval and was registered at ClinicalTrials.gov (NCT BLINDED).

# RESULTS

The overall claustrophobic event rate was 9.8% (95% CI: 9.1%-10.6%). The CLQ did not induce claustrophobic events because the event rate in the CLQ cohort was significantly lower than in the non-CLQ cohort as shown by the adjusted odds ratio of 0.81(95% CI: 0.68-0.96). The CLQ mean score in patients with claustrophobic events ( $1.48\pm0.93$ ) was significantly higher (p<0.01) than in the group without claustrophobic events ( $0.60\pm0.59$ ). CLQ cut-off values for the prediction of claustrophobic events were specified based on the Youden index and ranged from 0.52 for men in the feet-first to 1.14 for women in the head-first position. Due to the low prevalence, negative predictive values of CLQ cut-off values (>0.95) were higher than positive predictive values (<0.27).

# CONCLUSION

The CLQ is a suitable screening tool for the absence of a subsequent claustrophobic event. Furthermore, it is possible to identify patients with a considerable risk of claustrophobia; however, prediction in individual cases is not possible.

# **CLINICAL RELEVANCE/APPLICATION**

The Claustrophobia Questionnaire is a suitable screening tool for ruling out Claustrophobia in patients who undergo MR imaging.

## NR343-SD-SUA3

## Hippocampal Calcification on Brain CT, Prevalence and Risk Factors in a Stroke Population

Sunday, Nov. 27 12:30PM - 1:00PM Room: NR Community, Learning Center Station #3

#### Participants

Remko Kockelkoren, MD, Utrecht, Netherlands (*Presenter*) Nothing to Disclose Mirte Stavenga, BSC, Utrecht, Netherlands (*Abstract Co-Author*) Nothing to Disclose Jill B. De Vis, MD, PhD, Utrecht, Netherlands (*Abstract Co-Author*) Nothing to Disclose Willem P. Mali, MD, PhD, Utrecht, Netherlands (*Abstract Co-Author*) Nothing to Disclose Jeroen Hendrikse, MD, Utrecht, Netherlands (*Abstract Co-Author*) Nothing to Disclose Pim A. De Jong, MD, PhD, Utrecht, Netherlands (*Abstract Co-Author*) Nothing to Disclose Annemieke M. Rozemuller, MD,PhD, Utrecht, Netherlands (*Abstract Co-Author*) Nothing to Disclose Irene van der Schaaf, Utrecht, Netherlands (*Abstract Co-Author*) Nothing to Disclose Birgitta K. Velthuis, MD, Utrecht, Netherlands (*Abstract Co-Author*) Nothing to Disclose Huiberdina L. Koek, MD,PhD, Utrecht, Netherlands (*Abstract Co-Author*) Nothing to Disclose

### PURPOSE

Recently it was discovered that calcification of the hippocampus can be detected on computed tomography (CT) images and were shown to occur in over 30% in people over 65 years of age. Furthermore, in a preliminary study we found a relation between hippocampal calcification (HCC) and cognitive decline. Little is known about potential risk factors for HCC and its prevalence in patients with neurovascular disease.

## METHOD AND MATERIALS

We analyzed 1130 patients (57% male) from a multicenter acute stroke study. All patients underwent a non-contrast enhanced brain CT examination with thin slice reconstruction. HCC was scored bilaterally in all reconstruction planes as absent, mild (one dot), moderate (multiple dots) or severe (confluent). Multivariable logistic regression analysis, adjusting for age and gender as well as adjusting for all CVD risk factors (Age, Gender, CVD history, hyperlipidemia, diabetes mellitus type 2, smoking, BMI, eGFR, family history), was used to determine potential risk factors for HCC.

### RESULTS

Median age was 68.7 years (SD: 13.8). HCC was present in 392 (35%) patients, of which 181 (46%) were mild, 130 (33%) moderate and 81 (21%) severe. Prevalence increased with age. When adjusting for age and gender; age per year (OR:1.03, p<0.01, only adjusted for gender), history of stroke (OR:1.36, p=0.03), DM2 (OR:1.61, p<0.01), hyperlipidemia (OR:1.71, p<0.01), current smoker (OR:1.46, p=0.03) and eGFR (OR:1.49, p=0.03) were significant. When adjusting for all CVD risk factors; age per year (OR:1.04, p<0.01), CVD history (OR:1.44, p=0.01), hyperlipidemia (OR:1.71, p=0.02) and current smoker (OR:1.78, p=0.03) were significant.

## CONCLUSION

HCC was a frequent finding in this cohort of (suspected) stroke patients occurring more frequently with increasing age. HCC appears to be related to classic cardiovascular risk factors like hyperlipidemia and smoking.

## **CLINICAL RELEVANCE/APPLICATION**

HCC is a relatively unknown radiological finding but was found to occur in a large proportion of elderly patients. The relation we found with (modifiable) cardiovascular risk factors could play a role in the prevention (or treatment) of cognitive decline.

## NR346-SD-SUA6

Diagnostic Performance of Arterial Spin Labeling MR Imaging for Detecting Cortical Venous Drainage of Dural Arteriovenous Fistulas

Sunday, Nov. 27 12:30PM - 1:00PM Room: NR Community, Learning Center Station #6

## Participants

Ji Hee Kang, MD, Seoul, Korea, Republic Of (*Presenter*) Nothing to Disclose Tae Jin Yoon, MD, Seoul, Korea, Republic Of (*Abstract Co-Author*) Nothing to Disclose Young Dae Cho, Seoul, Korea, Republic Of (*Abstract Co-Author*) Nothing to Disclose Jong Kook Rhim, Seoul, Korea, Republic Of (*Abstract Co-Author*) Nothing to Disclose Roh-Eul Yoo, MD, Seoul, Korea, Republic Of (*Abstract Co-Author*) Nothing to Disclose Koung Mi Kang, Seoul, Korea, Republic Of (*Abstract Co-Author*) Nothing to Disclose Seung Hong Choi, MD, PhD, Seoul, Korea, Republic Of (*Abstract Co-Author*) Nothing to Disclose Ji-Hoon Kim, MD, Seoul, Korea, Republic Of (*Abstract Co-Author*) Nothing to Disclose Hyun-Seung Kang, MD, Seoul, Korea, Republic Of (*Abstract Co-Author*) Nothing to Disclose Chul-Ho Sohn, MD, Seoul, Korea, Republic Of (*Abstract Co-Author*) Nothing to Disclose Sun-Won Park, MD, Seoul, Korea, Republic Of (*Abstract Co-Author*) Nothing to Disclose Moon Hee Han, MD, Seoul, Korea, Republic Of (*Abstract Co-Author*) Nothing to Disclose

## PURPOSE

The venous drainage pattern in dural arteriovenous fistula (dAVF) determines the severity and provides the basis for its classification schemes. Our aim was to explore whether arterial spin labeling perfusion-weighted imaging (ASL-PWI) can reliably predict the presence of cortical venous drainage (CVD) in dAVFs.

## **METHOD AND MATERIALS**

Among 78 patients with dAVF based on digital subtraction angiography (DSA), 22 patients who underwent ASL-PWI were included. Based on Cognard classification, angiographic features were classified into two groups: "Benign" pattern (types I and IIa) and "Aggressive" pattern (types IIb, IIa+b, III, IV, and V). The following ASL-PWI features were analyzed: 1) presence of bright signal intensity in dural sinuses, 2) presence of bright signal intensity in cortical veins, and 3) presence of bright signal intensity in brain parenchyma. In addition, based on ASL-PWI features, dAVF were classified into two groups: "Benign" pattern with neither finding 2) nor finding 3) and "Aggressive" pattern with finding 2) and/or finding 3). Diagnostic performance of ASL-PWI for differentiating the two groups was assessed, using DSA as the reference standard.

### RESULTS

Based on DSA features, 11 patients (50%) were classified into "Aggressive" pattern. All patients (100%) showed bright signal intensity in dural sinuses on ASL-PWI. Thirteen patients (59%) showed the bright signal intensity in cortical veins and/or brain parenchyma on ASL-PWI and were classified as having "Aggressive" pattern. In those 13 patients, 11 patients were revealed as having "Aggressive" pattern on DSA. Nine patients (41%) among all patients were classified into "Benign" pattern based on ASL-PWI in concordance with the classification based on DSA. The sensitivity, specificity, positive predictive value, and negative predictive value of ASL-PWI for differentiating between "Benign" and "Aggressive" patterns were 100% (95% CI: 72%, 100%), 82% (95% CI: 48%, 98%), 85% (95% CI: 55%, 98%), and 100% (95% CI: 66%, 100%).

## CONCLUSION

ASL-PWI may provide a reliable and noninvasive means of predicting the presence of CVD in patients with dAVFs and thus has a potential to be used as a screening tool for evaluation of dAVF prior to invasive DSA.

## **CLINICAL RELEVANCE/APPLICATION**

ASL-PWI has a potential to be used as a screening tool for evaluation of the presence of CVD in patients with dAVF prior to invasive DSA.

# Abnormal Fourth Trimester Findings: Head to Toe Imaging Manifestations of Postpartum Complications

Sunday, Nov. 27 12:30PM - 1:00PM Room: OB Community, Learning Center Station #1

#### **Participants**

Kerri Vincenti, MD, Philadelphia, PA (*Presenter*) Nothing to Disclose Hima Prabhakar, MD, Philadelphia, PA (*Abstract Co-Author*) Nothing to Disclose Dayna Levin, MD, Philadelphia, PA (*Abstract Co-Author*) Nothing to Disclose

## **TEACHING POINTS**

To review normal postpartum uterine anatomy To discuss typical clinical manifestations and associated imaging findings of common and uncommon complications in postpartum patients To learn the optimal imaging modalities for evaluating various imaging findings

# TABLE OF CONTENTS/OUTLINE

Review of normal uterus in the postpartum period Classic clinical presentation and imaging findings of complications, organized by major affected systems as seen on Ultrasound/MRI/CT/Nuclear Medicine: Nervous System Cardiovascular System Respiratory System Digestive System Reproductive System Urinary System Lymphatic System Endocrine System Musculoskeletal System Integumentary System Common imaging pitfalls and/or mimics to avoid when searching for complications Appropriate imaging modalities for the most common and/or dangerous complications (incorporating ACR criteria when available) Summary

# 3D Ultrasound of the Female Pelvis-Beyond the IUD

Sunday, Nov. 27 12:30PM - 1:00PM Room: OB Community, Learning Center Station #2

### **Participants**

Ghizlane Bouzghar, MD, Philadelphia, PA (*Presenter*) Nothing to Disclose Bryan J. Kang, MD, Philadelphia, PA (*Abstract Co-Author*) Nothing to Disclose Shuchi K. Rodgers, MD, Philadelphia, PA (*Abstract Co-Author*) Nothing to Disclose Peter S. Wang, MD, Philadelphia, PA (*Abstract Co-Author*) Nothing to Disclose Cheryl L. Kirby, MD, Cherry Hill, NJ (*Abstract Co-Author*) Nothing to Disclose

# **TEACHING POINTS**

3D volume ultrasound can produce images of the female pelvis comparable to MRI and CT without radiation, at a lower cost, and in a shorter period of time. Proper acquisition, orientation labeling and post-processing of 3D ultrasound of the female pelvis is important for diagnostic accuracy. A variety of gynecologic conditions (congenital uterine anomalies, endometrial abnormalities, submucosal fibroids) can be evaluated with 3D ultrasound and may obviate need for sonohysterography. Normal and ectopic pregnancy implantation can be accurately characterized with 3D ultrasound, particularly interstitial ectopic pregnancy. 3D ultrasound is useful in evaluation of pregnancy implantation in the presence of a uterine anomaly as well as intrauterine device (IUD).

## TABLE OF CONTENTS/OUTLINE

## 1. Acquisition technique and orientation labeling of female pelvis 3D ultrasound

- 2. Normal 3D ultrasound of the uterus
- 3. Gynecological use
- a. Müllerian duct anomalies
- b. Abnormalities of the endometrium and endometrial cavity
- c. Adenomyosis
- d. Fibroid mapping
- e. Intrauterine device type and position
- f. Assessment of adnexal lesions

# 4. Obstetrical use

- a. Normal pregnancy implantation
- b. Pregnancy implantation in the presence of an IUD or congenital uterine anomaly
- c. Ectopic pregnancy
- i. Cervical
- ii. Cesarean scar
- iii. Interstitial
- d. Angular versus interstitial pregnancy

Maximizing Value of Imaging in Staging and Management of the 'Top 3' Gynecologic Malignancies: Focusing on the Issues that Matter Most in Patient Management

Sunday, Nov. 27 12:30PM - 1:00PM Room: OB Community, Learning Center Station #3

# Participants

Robert Krause, MD, San Antonio, TX (*Presenter*) Nothing to Disclose Eric Bready, San Antonio, TX (*Abstract Co-Author*) Nothing to Disclose Christine O. Menias, MD, Chicago, IL (*Abstract Co-Author*) Nothing to Disclose Kevin L. Hall, San Antonio, TX (*Abstract Co-Author*) Nothing to Disclose Anil K. Dasyam, MD, Pittsburgh, PA (*Abstract Co-Author*) Book contract, Reed Elsevier Venkata S. Katabathina, MD, San Antonio, TX (*Abstract Co-Author*) Nothing to Disclose

## **TEACHING POINTS**

Learning Objectives/Aims Review updated information in origin and pathogenesis of ovarian epithelial cancers Discuss updated changes in FIGO staging of endometrial, cervical, and ovarian cancers that affect management decisions. Describe the role of MR imaging in deciphering these important stages and treatment follow-up. Review potential imaging-related pitfalls that can result in patient mismanagement and suggest possible solutions to the

# TABLE OF CONTENTS/OUTLINE

Role of multiparametric MRI in assessing gynecologic cancers**Ovarian cancer**: Tubal carcinogenesis of high-grade serous cancer & new information in 2014 WHO & FIGO classifications as per this concept. Goal of imaging is to detect metastatic disease, prevent under staging, and provide surgical roadmap.**Endometrial cancer**: MR is useful in distinguishing Stage IA (<50 % myometrial involvement) and IB (>50%). Disruption of the cervical stromal ring upgrades the cancer to Stage II. **Cervical cancer**: MR imaging helps differentiate Stage IB1 (< 4cm) versus IB2 (>4cm), Stage IIIA (invading lower 1/3 of vagina, and IIA (No parametrial invasion) versus IIB (+ parametrial invasion). The above findings are important to identify since their presence precludes surgery.Imaging-related pitfalls & solutionsPost treatment assessment & surveillanceFuture imaging techniques Conclusion

## **Honored Educators**

Presenters or authors on this event have been recognized as RSNA Honored Educators for participating in multiple qualifying educational activities. Honored Educators are invested in furthering the profession of radiology by delivering high-quality educational content in their field of study. Learn how you can become an honored educator by visiting the website at: https://www.rsna.org/Honored-Educator-Award/

Venkata S. Katabathina, MD - 2012 Honored Educator

Christine O. Menias, MD - 2013 Honored Educator

Christine O. Menias, MD - 2014 Honored Educator Christine O. Menias, MD - 2015 Honored Educator

Christine O. Menias, MD - 2015 Honored Educator Christine O. Menias, MD - 2016 Honored Educator

# Primovist/Eovist in Pediatrics: When and How?

Sunday, Nov. 27 12:30PM - 1:00PM Room: PD Community, Learning Center Station #6

FDA Discussions may include off-label uses.

### Awards

**Certificate of Merit** 

## **Participants**

Alaa W. Elmanzalawy, FRCR, Calgary, (Presenter) Nothing to Disclose Xing-Chang Wei, MD, FRCPC, Calgary, AB (Abstract Co-Author) Nothing to Disclose Seemab Haider, MD, Calgary, AB (Abstract Co-Author) Nothing to Disclose Samarjeet K. Bhandal, MBBS, MD, Ludhiana, India (Abstract Co-Author) Nothing to Disclose Ibtisam H. al-Shuaili, MD, Calgary, AB (Abstract Co-Author) Nothing to Disclose Clara L. Ortiz, MD, Red Deer, AB (Abstract Co-Author) Nothing to Disclose

# **TEACHING POINTS**

Describe the mechanism of action of Primovist/Eovist as a hepatocellular selective MRI contrast agent. Recognize the clinical indication of Primovist/Eovist in liver lesions detection and characterization in pediatric population. Discuss key concepts for optimization of MR exam technique to maximize contrast and avoid common pitfalls when using hepatocellular selective contrast agent.

## **TABLE OF CONTENTS/OUTLINE**

Introduction. Characteristics of PRIMOVIST/EOVIST. Role in improving liver tumor detection. Role in improving liver tumor characterization (Emphasis on common hepatic tumors in pediatric population).

Malignant hepatocellular tumors.

- Benign hepatocellular tumors. Role in evaluating bile duct diseases. Challenges for MR imaging using PRIMOVIST/EOVIST. Technique optimization strategies. Conclusion and future directions.

## Voiding Uretrosonography (Ce-US) in Vesical Reflux in Children

Sunday, Nov. 27 12:30PM - 1:00PM Room: PD Community, Learning Center Station #7

**FDA** Discussions may include off-label uses.

#### Awards

**Identified for RadioGraphics** 

#### **Participants**

Carmina Duran, MD, Sabadell, Spain (*Abstract Co-Author*) Nothing to Disclose Carles G. Zaragoza, MD, Sabadell, Spain (*Presenter*) Nothing to Disclose Carlota C. Rodriguez, MD, Sabadell, Spain (*Abstract Co-Author*) Nothing to Disclose Maria Magdalena Serra Salas, MD, Barcelona, Spain (*Abstract Co-Author*) Nothing to Disclose Viviana P. Beltran Salazar, MD, Sabadell, Spain (*Abstract Co-Author*) Nothing to Disclose

### **TEACHING POINTS**

To illustrate the study of the urinary tract, including the urethra, with 2nd generation contrast agents To demonstrate the high quality of the images obtained with this procedure To show that Ce-VUS can diagnose the most prevalent urethral pathologies

### TABLE OF CONTENTS/OUTLINE

Contrast enhanced voiding urethrosonography (Ce-VUS) has proved to be a reliable method for the identification and grading of VUR. It enables high quality morphologic studies of both the upper and lower urinary tract with no ionizing radiation, wich is a great advantage compared to voiding cystourethrography (VCUG). In this review the following examples are shown: Grading of vesicoureteral reflux based on international classification (II to V) Complete and incomplete duplex collecting system Ectopicureter in duplexcollectingsystem Bladder diverticula Posterior urethralvalves (PUV) Congenital urethral stricture Urethral stenosis Anterior urethral valves Diverticulum of the anterior urethra Ventral urethral ectasia Diverticulum of the prostacticutricle Ectopic intravesical ureterocele Obstructive ureterocele in female urethra Spinning top urethra in female urethra Urogenital sinus in female urethra Normal variants such as Cobb's collar or prostatic ducts reflux

### PD182-ED-SUA8

### Congenital Anomalies of the Tracheobronchial Tree: A Comprehensive Review

Sunday, Nov. 27 12:30PM - 1:00PM Room: PD Community, Learning Center Station #8

#### **Participants**

Narendra B. Gutta, MBBS, MD, Little Rock, AR (*Presenter*) Nothing to Disclose Justin White, DO, Little Rock, AR (*Abstract Co-Author*) Nothing to Disclose John C. Faircloth, DO, Sherwood, AR (*Abstract Co-Author*) Nothing to Disclose James Sorensen, MBBCh, MD, Houston, TX (*Abstract Co-Author*) Nothing to Disclose Karen Lyons, MBBCh, FFR(RCSI), Little Rock, AR (*Abstract Co-Author*) Nothing to Disclose

### **TEACHING POINTS**

The purpose of this exhibit is: To review the embryology of the tracheobronchial tree. To illustrate common and uncommon congenital anomalies of the pediatric tracheobronchial tree. To discuss the imaging pitfalls and differential diagnosis. To emphasize the utility of a systematic imaging approach to imaging the airway.

### TABLE OF CONTENTS/OUTLINE

Embryology of the tracheobronchial tree Questions to be addressed at imaging Plain radiography / Fluoroscopy Static crosssectional Imaging (CT/MRI) Dynamic CT and MR Imaging Classification of congenital disorders causing tracheobronchial airway compromise with illustrated case examples. Extrinsic: Vascular rings and slings, bronchopulmonary foregut malformations, vascular malformations. Intrinsic: Bronchopulmonary foregut malformations, bronchial atresia, tracheal stenosis, cartilage hypoplasia, tracheobronchomalacia, tracheobronchial branching anomalies. Common Findings on Head Computed Tomography in Neonates with Confirmed Congenital Zika Syndrome

Sunday, Nov. 27 12:30PM - 1:00PM Room: PD Community, Learning Center Station #1

#### **Participants**

Natacha C. Petribu, MD, Jaboatao Dos Guararapes, Brazil (*Abstract Co-Author*) Nothing to Disclose Marilia D. Abath, MD, Recife, Brazil (*Presenter*) Nothing to Disclose Andrezza C. Vieira Fernandes, MD, Recife, Brazil (*Abstract Co-Author*) Nothing to Disclose Felipe R. Queiroz, BARCH, Recife, Brazil (*Abstract Co-Author*) Nothing to Disclose Jannie D. Araujo, MD, Campina Grande, Brazil (*Abstract Co-Author*) Nothing to Disclose Glauber B. Carvalho, Recife, Brazil (*Abstract Co-Author*) Nothing to Disclose Vanessa van der Linden, Recife, Brazil (*Abstract Co-Author*) Nothing to Disclose

#### PURPOSE

Describe central nervous system (CNS) computed tomography (CT) findings in neonates with congenital microcephaly associated with the presence of Zika virus in cerebral spinal fluid.

### **METHOD AND MATERIALS**

A series of 14 newborns with congenital microcephaly who exhibited abnormality findings on brain CT without contrast as part of the protocol established by the health ministry during outbreak of Zika, from October to December 2015. These infants had negative IgM serology for toxoplasmosis, rubella, cytomegalovirus and syphilis, and IgM negative for dengue virus and positive for ZIKA virus by ELISA in the CSF. All CT scans were performed in multislice CT scanner and analyzed by the same radiologist.

### RESULTS

We reported findings of cranial CT of 14 newborns, 9 male and 5 female. Gestational age ranged from 31 to 40, weight at birth from 810 to 3.840 grams and head circumference from 23 to 33 centimeters. Calcification in the central nervous system (CNS) were seen in all patients, being punctiform in 8 (57.1%) and coarsely in 6 (42.8%). 13 neonates (92.8%) showed calcification in the cortico-medullary junction, 3 (21.4%) in thalamus and 1 (7.1%) in midbrain. The cortico-medullary junction calcifications were located mainly at frontal (92.8%) and parietal lobes (78.5%) and less often at occipital (35.7%) and temporal lobes (28.5%). Global hypogyration of the cerebral cortex was seen in 11 (78.5%) infants. In 13 (92.8%) neonates ventriculomegaly was present. Cerebellar hypoplasia was seen in 4 patients (28.5%). Prominent occipital bone was identified in 9 patients (64.2%), wich can be associated with fetal brain disruption sequence, characterized by severe microcephaly, overlapping sutures, scalp rugae and marked neurological impairment, reflecting important intrauterine brain damage.

### CONCLUSION

There is a pattern of tomographic findings in central nervous system of neonates with microcephaly and Zika virus infection. Although the etiopathogenesis and associated risk factors have not yet been well established these data strongly suggest that Zika virus can cause microcephaly.

### **CLINICAL RELEVANCE/APPLICATION**

There is a pattern of tomographic findings in central nervous system associated with the microcephaly outbreak that suggest a new etiology. In face of the increase of microcephaly cases, and the possibility of global dissemination of Zika virus, its necessary to recognize these radiologic findings.

### **Conquering Cavernous Transformation of the Portal Vein**

Sunday, Nov. 27 12:30PM - 1:00PM Room: PD Community, Learning Center Station #2

#### Awards

#### **Student Travel Stipend Award**

#### **Participants**

Whitney L. Shofner-Michalsky, MD, Seattle, WA (*Presenter*) Nothing to Disclose Eric J. Monroe, MD, Seattle, WA (*Abstract Co-Author*) Nothing to Disclose

#### PURPOSE

To evaluate the efficacy of direct and transjugular intrahepatic portosytemic shunt placement in the treatment of pediatric portal vein thrombosis with cavernous transformation.

### **METHOD AND MATERIALS**

In this retrospective review, a list of patients was generated who underwent direct and trans-jugular intrahepatic portosystemic shunt placement for the treatment of cavernous transformation of the portal vein from 2014-2016. Medical records and imaging were reviewed to assess treatment outcomes and evaluate for any complications. Procedural success was defined by normalization of portosystemic pressures.

### RESULTS

It was determined that three patients underwent TIPS/DIPS for the treatment of portal vein thrombosis with cavernous transformation from 2014-2016. The indication for portosystemic shunt included GI bleeding as a complication related to portal hypertension in all cases. Average portosystemic pressures prior to shunting were 19 compared to 4 after the procedure. One case was complicated by thrombosis of the shunt which resulted in a recurrent gastrointestinal bleed at day 2. This was successfully treated with lysis of the thrombus without further complications at the five month follow up. No recurrent gastrointestinal hemorrhage or other complications were encountered in the two other patients post shunting, and ultrasound follow up confirmed patency of the shunt in each of these cases at 5 months and 22 months respectively. Spleen size decreased in two patients post treatment, and one patient was status post splenectomy.

### CONCLUSION

Direct or transjugular intrahepatic portosystemic shunt placement should be considered in select patients with complications related to portal hypertension in the setting of cavernous transformation of the portal vein to decrease portal pressures and decrease the risk of recurrent GI bleeding.

#### **CLINICAL RELEVANCE/APPLICATION**

These results will allow us to critically review the role of interventional radiology in the management of pediatric portal vein thrombosis with cavernous transformation.

### PD202-SD-SUA3

How to Reduce the Need for Sedation in Pediatric MRI using a Low-Cost Rear-Projection Audiovisual System

Sunday, Nov. 27 12:30PM - 1:00PM Room: PD Community, Learning Center Station #3

#### **Participants**

Angel Sanchez-Montanez, MD, Barcelona, Spain (*Presenter*) Nothing to Disclose Ignacio Delgado, MD, Barcelona, Spain (*Abstract Co-Author*) Nothing to Disclose Luis Riera Soler, MD, Sabadell, Spain (*Abstract Co-Author*) Nothing to Disclose Ana Coma, RT, Barcelona, Spain (*Abstract Co-Author*) Nothing to Disclose Goya Enriquez, MD, Barcelona, Spain (*Abstract Co-Author*) Nothing to Disclose Elida Vazquez, MD, Barcelona, Spain (*Abstract Co-Author*) Nothing to Disclose

### PURPOSE

To show our own made rear-projection audiovisual systemTo divulge the necessity of distractors instruments to achieve children co-operation and immobility

### **METHOD AND MATERIALS**

Two low-cost rear-projection audiovisual systems were settled in a 1,5T and 3T magnets consisting on a DVD player, a projector (both outside the room), a mobile screen with rails (in the room) and a game mirrors (incorporated in the head coil). This simple device does not require special training or complex installation because it uses a commercial material with which both the staff and the children are familiar with.

The patient is placed supine comfortably viewing the film projected from the outside to the screen. The system was used in all of the pediatric population examined to increase comfort and reduce anxiety during the test with special attention to children between 2 and 5 years where whe pursued further in order to avoid sedation.

### RESULTS

The use of our own low-cost rear-projecion audiovisual system (RPAVS) reduced the need for sedation in patients between 2 and 5 years under MRI in more than 30%. This percentage is even higher in females and in older children. The percentage reduction was constant for these more than two years experience. Avoiding sedation in around 400 infants and reducing the scan time has enabled the realization of a 27% more of patients with the consequent reduction of the waiting list.RPAVS has proven to be a useful tool in reducing patient's anxiety to the test, increasing comfort and minimizing the feeling of claustrophobia within the machine. Reducing the amount of sedation also shortens the time of the scan allowing the realization of a greater number of patients in the same time slot which is a real cost saving test.

The simplicity of the system, as well as the price (around thousand euros), make this device suitable for introduction into any environment including developing countries.

### CONCLUSION

The rear-projection audiovisual system applied to the MR has reduced the number of children who require sedcation, has improved patient's safety and satisfaction and, has reduced the emotional impact of the disease on the child and their environment.

### **CLINICAL RELEVANCE/APPLICATION**

Low-cost rear-projection audiovisual system is an easy and cheap tool when performing MRI in children that reduces the number of sedations among other benefits.

### **MR Imaging of Fetal Lymphatic Malformations**

Sunday, Nov. 27 12:30PM - 1:00PM Room: PD Community, Learning Center Station #5

#### **Participants**

Su-Zhen Dong, MD, Shanghai, China (*Presenter*) Nothing to Disclose Ming Zhu, Shanghai, China (*Abstract Co-Author*) Nothing to Disclose Yumin Zhong, MD, Shanghai, China (*Abstract Co-Author*) Nothing to Disclose

#### PURPOSE

To investigate the role of magnetic resonance imaging (MRI) as a complement to ultrasound (US) in the evaluation of fetal lymphatic malformations.

### METHOD AND MATERIALS

The prenatal US and MRI data of 40 fetuses with lymphatic malformations between June 2005 and December 2015 were reviewed. The malformations were confirmed by postnatal imaging or operation. MRI was performed using a 1.5T unit. Imaging sequences included steady-state free-precession (SSFP), single-shot turbo spin echo (SSTSE) and T1-weighted turbo field echo (T1W\_TFE) or T1-weighted fast inversion recovery motion insensitive (FIRM) sequences. MRI evaluation included: number, size and signal intensities of the lesions; thickness of the septa; configuration of the margins; exact expansion of the lesions to the adjacent anatomical structures.

### RESULTS

Twenty-seven cervical, four occipital, four abdominal wall, one axillary, one mediastinal, one antebrachial, one thoraco-abdominal wall and dorsal, and one coxal lymphatic malformations were included. All lesions consisted of multi-septated macrocysts. The diagnostic sensitivity of US for these lymphatic malformations was 67.5% (27/40). Fetal MRI yielded the same diagnosis as postnatal findings in 97.5% (39/40) of patients. The agreement of Fetal MRI with postpartum imaging was excellent.

### CONCLUSION

Prenatal MRI is valuable in the assessment of fetal lymphatic malformations with excellent diagnostic accuracy.

#### **CLINICAL RELEVANCE/APPLICATION**

Prenatal MRI can accurately evaluate the locations, the sizes, the extents, the correlations with peripheral anatomic structures and the tissue characteristics of fetal lymphatic malformations and this exam is recommended after fetal US.

### PH008-EB-SUA

# Development of an Iterative Interior Reconstruction Method for Low Dose CBCT in Proton Therapy Patient Positioning

Sunday, Nov. 27 12:30PM - 1:00PM Room: PH Community, Learning Center Hardcopy Backboard

### Participants

Takashi Yamaguchi, PhD, Yokosuka-Shi, Japan (Presenter) Nothing to Disclose

#### Background

Cone Beam Computed Tomography (CBCT) determining patient position is used before every irradiation, which results in increased radiation exposure for the patient. To reduce the patient exposure, reduction of either X-ray imaging time or X-ray tube current is necessary. However, this leads to increased noise and reduced contrast in images. Furthermore, when the object do not fit to the size of Field of View (FOV), an interior reconstruction is required to reconstruct a part of a tomographic image. To meet these requirements, we have developed an interior image reconstruction method employing an iterative algorithm, which is robust to noise. Our method can achieve high image contrast, and that can visualize a part of a transaxial plane.

#### **Evaluation**

In the iterative image reconstruction process referred to as Ordered Subset Convex, a corresponding system matrix is required for a given measurement geometry. In a gantry-mounted CBCT, the X-ray tube and the detector positions deviate some from their ideal position, resulting in a different geometry at each measurement angle, but full calculation of system matrices requires a large data capacity or significant computation time. To overcome these issues, our method calculates the system matrix for an ideal geometry in advance and performs positional deviation correction on the measured data, also creates a buffer area around a FOV, estimates X-ray attenuations outside of the FOV, and removes the attenuation effect. These techniques allow to obtain an interior image corrected positional deviations.

#### Discussion

We applied the method to positional deviations and Poisson noise-added digital phantom data and verified the method, and were able to obtain noise reduction within the FOV in conditions of low-dose, compared to general iterative reconstruction.

#### CONCLUSION

We have developed an iterative interior reconstruction method for low-dose CBCT in proton therapy patient positioning. The method can perform positional deviation correction and remove the effect of attenuation in the outer of FOV. We expect the method to contribute to reduce radiation exposure to the patient.

### FIGURE

http://abstract.rsna.org/uploads/2016/16011979/16011979\_p3dn.jpg

Accelerated MR Imaging, Its Benefits in Daily Routine, Current Limitations and Future Developments

Sunday, Nov. 27 12:30PM - 1:00PM Room: PH Community, Learning Center Station #7

FDA Discussions may include off-label uses.

#### Awards

**Certificate of Merit** 

#### Participants

Johannes K. Richter, MD, Bern, Switzerland (*Presenter*) Nothing to Disclose Val M. Runge, MD, Bern, Switzerland (*Abstract Co-Author*) Research Grant, Siemens AG Reto D. Merges, Erlangen, Germany (*Abstract Co-Author*) Employee, Siemens AG Markus Klarhofer, Basel, Switzerland (*Abstract Co-Author*) Employee, Siemens AG Johannes T. Heverhagen, MD, PhD, Bern, Switzerland (*Abstract Co-Author*) Research Grant, Bracco Group; Research Grant, Guerbet DA; Research Grant, Siemens AG;

### **TEACHING POINTS**

(1) To present and discuss the clinically relevant accelerated MR techniques currently available, focusing on: (a) improvements in 3D acquisition (CAIPIRINHA and radial VIBE, CAIPI-DIXON-TWIST-VIBE), (b) simultaneous multi-slice imaging (SMS), and (c) sparse imaging. (2) To provide guidance to the radiologist as to the implementation of the above mentioned techniques, with the intent to enable faster and improved clinical scan results.

### **TABLE OF CONTENTS/OUTLINE**

The exhibit will focus on three major areas, using primarily patient images, to convey the benefits of accelerated MR sequences when compared to more conventional scans in day-to-day clinical routine. (1) CAIPIRINHA and radial techniques in 3D imaging - strengths and clinical utility (for example, acquisition of a 6 sec breath hold CAIPI scan at 3 T using a 60 channel body coil in comparison to a non breath hold 21 sec radial scan). (2) SMS - scientific basis and implementation for 2D DWI and T1, T2, and PD FSE/TSE sequences (for example, with DWI, permitting the entire neck to be scanned for lymph node evaluation in 1:54 min:sec, or the whole brain with a 1 mm slice thickness in 4:39 min:sec). (3) Sparse reconstruction techniques - principles, challenges, and current applications (for example in CE-MRA and musculoskeletal imaging, the latter for 3D imaging as well as metal artifact reduction).

A Gradient- and Spin-echo (GRASE) Sequence for Breath-hold Three-dimensional (3D) Magnetic Resonance Cholangiopancreatography (MRCP) at 3.0 T

Sunday, Nov. 27 12:30PM - 1:00PM Room: PH Community, Learning Center Station #2

### Participants

Katsuhiro Kida, Okayama, Japan (*Presenter*) Nothing to Disclose Sachiko Goto, PhD, Okayama, Japan (*Abstract Co-Author*) Nothing to Disclose Ryutaro Matsuura, MSc, Okayama, Japan (*Abstract Co-Author*) Nothing to Disclose Yuka Tanaka, Okayama, Japan (*Abstract Co-Author*) Nothing to Disclose Tsutomu Kajitani, Okayama, Japan (*Abstract Co-Author*) Nothing to Disclose Yoshiharu Azuma, PhD, Okayama, Japan (*Abstract Co-Author*) Nothing to Disclose

### CONCLUSION

These results suggest that the breath-hold 3D GRASE sequence can realize to obtain the MRCP quickly and surely.

#### Background

A respiratory-triggered (RT) three-dimensional (3D) fast spin-echo (FSE) sequence has been used to obtain high-quality magnetic resonance cholangiopancreatography (MRCP). However, this sequence has a long scan time because of using RT. Furthermore, the RT acquisitions are susceptible to motion artifacts and blurring in patients with shallow or irregular respirations, sleep apnea, or significant diaphragmatic drift. In this study, we evaluated a breath-hold (BH) MRCP using 3D gradient- and spin-echo (GRASE) sequence, which could shorten the scan time and be more reliably obtained.

### **Evaluation**

Fifteen patients (10 males and 5 females, aged 40–88 years; mean age 69.5 years) underwent two examinations, one of the BH 3D GRASE sequence and the other of the RT 3D FSE sequence at 3.0 T MR system (Achieva 3.0T TX, Philips). Each MR image was reconstructed into maximum intensity projection (MIP) images. Four radiologists and two radiological technologists performed visual evaluation for overall reader confidence in the diagnosis using a five-point scale (5, excellent; 4, good; 3, moderate; 2, fair; 1, poor). The statistical significance of overall reader confidence of the two sequences were tested using the Wilcoxon signed rank test. Furthermore, we evaluated the images when breath-hold time was not long enough for the acquisition using BH 3D GRASE sequence.

### Discussion

Figure shows the images for the BH 3D GRASE and the RT 3D FSE sequences. While the actual scan time of the RT 3D FSE sequence was about 5-10 min, that of the BH 3D GRASE sequence was only 19 sec. The overall reader confidence had no statistical significance between the sequences (p = 0.67). Though some images of the RT 3D FSE sequence had respiratory motion artifacts and blurring, the images of the BH 3D GRASE sequence had little those. Furthermore, if the breathing stops more than half of scan time, our method can obtain diagnosable image quality. We think the k-space sampling trajectory for the GRASE sequence has an effect of making the signal error related to motion-induced artifact inconspicuous.

### Self-correction of Blood Flow Effect for Fluctuation MRI in Idiopathic Normal Pressure Hydrocephalus

Sunday, Nov. 27 12:30PM - 1:00PM Room: PH Community, Learning Center Station #3

#### **Participants**

Naoki Ohno, PhD, Kanazawa, Japan (*Presenter*) Nothing to Disclose Tosiaki Miyati, PhD, Kanazawa, Japan (*Abstract Co-Author*) Nothing to Disclose Marina Takatsuji, BS, Kanazawa, Japan (*Abstract Co-Author*) Nothing to Disclose Mitsuhito Mase, MD, Nagoya, Japan (*Abstract Co-Author*) Nothing to Disclose Tomoshi Osawa, Nagoya, Japan (*Abstract Co-Author*) Nothing to Disclose Hirohito Kan, Nagoya, Japan (*Abstract Co-Author*) Nothing to Disclose Yuta Shibamoto, MD, PhD, Nagoya, Japan (*Abstract Co-Author*) Nothing to Disclose Toshifumi Gabata, MD, PhD, Kanazawa, Japan (*Abstract Co-Author*) Nothing to Disclose

#### PURPOSE

Arterial inflow into the cranium induces apparent diffusion coefficient (ADC) change of the brain during the cardiac cycle, ie., fluctuation of water molecules. The degree of water fluctuation assists in the diagnosis of idiopathic normal pressure hydrocephalus (iNPH). However, these changes depend on cerebral blood flow (CBF) as a driving force for fluctuating water-molecules. Therefore, we corrected the CBF effect by using the diffusion data itself to evaluate hemodynamic-independent water fluctuation in iNPH.

### **METHOD AND MATERIALS**

On a 1.5 T MRI, we performed ECG-triggered single-shot diffusion echo-planar imaging with the following parameters: repetition time, 2 R-R intervals; echo time, shortest; flip angle, 90°; section thickness, 4 mm; imaging matrix,  $64 \times 64$ ; field of view, 256 mm; number of signals averaged, 2; cardiac phases (different phases acquired by varying the ECG trigger delay), 20; b-values, 0, 500, and 1000 s/mm2; separate measures in the X-, Y-, and Z-axis directions; parallel imaging factor, 2; and half-scan factor, 0.6. Next, we determined the peak ADC with b = 0-500 (ADCpeak: perfusion-related diffusion component) and maximum change in ADC with b = 0-1000 ( $\Delta$ ADC: water fluctuation component) in the cardiac cycle, and divided the  $\Delta$ ADC by the ADCpeak (Corrected- $\Delta$ ADC). Then, we compared those values of the frontal white matter among iNPH (n=17), atrophic ventricular dilatation (atrophic VD group; n=9), and healthy volunteers (control group; n=8).

#### RESULTS

The Corrected- $\Delta$ ADC was significantly higher in the iNPH group compared with the control and atrophic VD groups, whereas no significant difference was observed in the ADCpeak among the groups. These results indicate that hemodynamic-independent water fluctuation, ie., biomechanical property of the brain between the CBF (input) and water fluctuation (output), is increased in iNPH because of low compliance.

### CONCLUSION

Hemodynamically independent analysis for water fluctuation MRI enabled us to obtain more detailed information on biomechanical properties in iNPH.

### **CLINICAL RELEVANCE/APPLICATION**

Corrected- $\Delta$ ADC analysis, as a noninvasive MRI method to assess the degree of fluctuation of the water molecules hemodynamic-independently, makes it possible to obtain more detailed information on biomechanical properties in iNPH.

### MR Fibrography: An Application of Correlation Time Diffusion Synthetic MRI (1.5T and 3.0T)

Sunday, Nov. 27 12:30PM - 1:00PM Room: PH Community, Learning Center Station #4

#### Participants

Hernan Jara, PhD, Belmont, MA (*Presenter*) Patent holder, qMRI algorithms; Research Grant, General Electric Company; Royalties, World Scientific Publishing Co; ; ;

Osamu Sakai, MD, PhD, Boston, MA (*Abstract Co-Author*) Consultant, Guerbet SA Stephan W. Anderson, MD, Boston, MA (*Abstract Co-Author*) Nothing to Disclose Jorge A. Soto, MD, Boston, MA (*Abstract Co-Author*) Royalties, Reed Elsevier

### CONCLUSION

A complete MRI technique for rendering the full white matter fibrogram (Fig. 1) has been developed and tested at 1.5T and 3.0T with standard clinical scanners.

#### Background

Conventional diffusion weighted MRI is based on the pulsed field gradient (PFG) experiment. Alternatively, correlation time diffusion (DCT) MRI is based on T1 relaxometry and therefore probes water diffusion at the very short time scale of the correlation time: ~20ps for brain tissue. The purpose of this technical presentation is to describe a complete multispectral image acquisition technique and image processing pipeline for generating heavily DCT-weighted synthetic MR images starting with the quadraFSE pulse sequence leading to MR Fibrography (MRF), a terminology adopted herein to differentiate it from diffusion tensor imaging based MR Tractography.

#### **Evaluation**

A volunteer (male, 35yo) was scanned at 3.0T (Discovery MR750, GE Healthcare, Waukesha, WI) and a week later at 1.5T (Optima MR450w, GE Healthcare, Waukesha, WI) using the quadraFSE pulse sequence. This is the concatenation of two dual-echo fast spin echo scans differing only in their different repetition time TR.The acquired images were qMRI processed with Mathcad (version 2001i, PTC, Needham, MA) at full spatial resolution (0.47 x 0.47 x 3mm3) to generate coregistered maps of PD, T1, T2, and DCT. These maps were used to generate diffusion-weighted synthetic MR images at arbitrarily large b values: 0-30,000s/mm2. At b values above 3,000s/mm2, an irregular "cobblestone" texture develops in white matter and the acuity of this texture improves as a function of increasing diffusion weighting. The cobblestone texture is observed at 1.5T and 3.0T.

#### Discussion

Developments in ultra-powerful magnetic field gradient technologies have been reported in the context of the of the Human Connectome Project. With a maximum gradient strength of 300mT/m, probing the diffusion of water in tissue with very high b-values and short diffusion times of less than 21ms becomes possible. The technique described herein enables probing motion of water in tissue at the tens of picoseconds time scale and therefore provides complementary information.

### **Honored Educators**

Presenters or authors on this event have been recognized as RSNA Honored Educators for participating in multiple qualifying educational activities. Honored Educators are invested in furthering the profession of radiology by delivering high-quality educational content in their field of study. Learn how you can become an honored educator by visiting the website at: https://www.rsna.org/Honored-Educator-Award/

Hernan Jara, PhD - 2014 Honored Educator Osamu Sakai, MD, PhD - 2013 Honored Educator Osamu Sakai, MD, PhD - 2014 Honored Educator Osamu Sakai, MD, PhD - 2015 Honored Educator Jorge A. Soto, MD - 2013 Honored Educator Jorge A. Soto, MD - 2014 Honored Educator Jorge A. Soto, MD - 2015 Honored Educator MDCT of the Abdomen Using a Wide Volume (WV) Scan Mode with a 320-Detector Row Scanner: Which is the Best Collimation in Terms of Radiation Dose and Image Quality?

Sunday, Nov. 27 12:30PM - 1:00PM Room: PH Community, Learning Center Station #5

### Participants

Catherine Roy, MD, Strasbourg, France (*Presenter*) Nothing to Disclose Raphael Quin, Strasbourg, France (*Abstract Co-Author*) Nothing to Disclose Aissam Labani, MD, Strasbourg, France (*Abstract Co-Author*) Nothing to Disclose Guillaume Alemann, MD, MS, Strasbourg, France (*Abstract Co-Author*) Nothing to Disclose Mickael Ohana, MD, MSc, Strasbourg, France (*Abstract Co-Author*) Nothing to Disclose

### PURPOSE

To optimize a protocol for WV scan mode on a 320 detector CT scanner by means of tests on phantom and CT console analysis of topograms using different collimations in terms of radiation dose and image quality in comparison with the helical mode (HM).

### **METHOD AND MATERIALS**

We recorded the CTDIvol in WV mode with different collimations from 120x0.5mm (6cm) to 320x0.5mm (16cm) using topograms data of medium size patients on a 320-detector CT scanner (Aquilion ONE, Toshiba Medical Systems). A radiosensitive films Gafchromic® were positioned between two homogeneous PMMA (methyl methacrylate) phantom of 10cm in order to realize dose profiles in WV mode (collimation of 200x0.5mm, 0.5s/volume (3 volumes of 8cm) and HM (collimation of 100x0.5mm, 0.5s/turn). Both scans modes were performed at 120kVp with the same FOV, length of coverage and iterative reconstruction. Adaptive blending was used to stitch the wide volumes. Then these films were analyzed with an optical scanner and transcribed in the form of optical density curve.

Ten 100mm<sup>2</sup> ROI were drawn on the Workstation to measure signal to noise ratio (SNR) on each acquisition.

#### RESULTS

At constant parameters, the collimation of 10 cm (200x0.5mm) had the lowest CTDIvol. An increase of CDTIvol by 18% was observed for collimations of 16cm (320x0mm) and 14cm (280x0.5mm). Similarly an increase of CDTIvol by 27% was noted when a smaller collimation of 6cm (120x0.5mm) was used. On radiosensitive films, WV had a higher radiation dose at the site of overlapping volumes, but the overbeaming was clearly shorter compared to HM. In HM, the overranging is visible at both ends of the segment as a large zone. It is completely absent in WV. As we reduce the size of our volumes (from 16 to 4 cm), we increase proportionally the phenomenon of overlapping and overbeaming by repetition of smaller volumes. On the optical density curves, it was found at the ends of the explored segment, a more linear and faster decrease of the dose in WV than in HM. The signal to noise ratio measured on phantoms was not significantly less important in WV than in HM 16.5 +/- 0.7 vs 18.8 +/-1.1, respectively.

### CONCLUSION

In WV mode, the optimal collimation to decrease radiation dose is obtained at 10cm instead of 16cm while keeping a quite similar signal to noise ratio.

### **CLINICAL RELEVANCE/APPLICATION**

A 10cm collimation instead of 16cm in WV mode is the best compromise. This dose reduction is related to various factors.

Conversion of Ultra-low-dose (ULD) to "Virtual" High-dose (VHD) Thin-slice Chest CT by means of 3D Supervised Volume-based Artificial Neural Network (ANN)

Sunday, Nov. 27 12:30PM - 1:00PM Room: PH Community, Learning Center Station #6

### Participants

Nima Tajbakhsh, Chicago, IL (*Abstract Co-Author*) Nothing to Disclose Junchi Liu, MS, Chicago, IL (*Abstract Co-Author*) Nothing to Disclose Toru Higaki, PhD, Hiroshima, Japan (*Abstract Co-Author*) Nothing to Disclose Wataru Fukumoto, Hiroshima, Japan (*Abstract Co-Author*) Nothing to Disclose Kazuo Awai, MD, Hiroshima, Japan (*Abstract Co-Author*) Research Grant, Toshiba Corporation; Research Grant, Hitachi, Ltd; Research Grant, Bayer AG; Research Grant, Eisai Co, Ltd; Medical Advisor, General Electric Company; ; ; ; ; Kenji Suzuki, PhD, Chicago, IL (*Presenter*) Royalties, General Electric Company; Royalties, Hologic, Inc; Royalties, MEDIAN Technologies; Royalties, Riverain Technologies; Royalties, Toshiba Medical Systems Corporation; Royalties, Mitsubishi Corporation; Stockholder, Alara, Inc; Stockholder, AlgoMedica, Inc.; ; ; ; ; ; ; ;

### PURPOSE

Since current radiation dose in chest CT is still very high for lung cancer screening, radiation dose reduction is highly demanded. Our purpose was to develop a volume-processing technique to convert thin-slice ULDCT to VHDCT where noise and artifact are substantially reduced.

### **METHOD AND MATERIALS**

We developed a VHDCT technology based on 3D volume-based massive-training ANNs to convert thin-slice ULDCT into VHDCT. Our technology relies on a new data sampling scheme to collect a representative set of training samples and a set of organ-specific models to achieve higher noise reduction capability. Our technology was trained with a large number of patches (or subvolumes) extracted from input ULDCT volumes and corresponding single voxels in "teaching" HDCT volumes. Through training, our technology learned the relationship between them to convert ULDCT into HDCT. We trained our technology with ULDCT (10 mAs, 120 kVp, 0.24 mSv, 0.5 mm slice thickness) and corresponding "teaching" HDCT (550 mAs, 120 kVp, 13.2 mSv, 0.5 mm) of an anthropomorphic chest phantom (Kyoto Kagaku, Kyoto, Japan). Once trained, our technology no longer requires HDCT, and it provides VHDCT where noise and artifact are substantially reduced. To test our technique, we acquired 4 more sets of CT scans of the same phantom at 4 different radiation doses (0.96, 1.92, 3.84, and 6.6 mSv) by changing tube currents (40, 80, 160, and 275 mAs). We used the structural similarity (SSIM) index for measuring the similarity between our VHDCT and "gold-standard" HDCT.

#### RESULTS

Our VHDCT technology reduced noise and artifacts in ULDCT substantially, while maintaining anatomic structures and pathologies such as vessels, bones, and nodules. With our technology, the average SSIM of ULDCT was improved by 0.62 (from  $0.15\pm.07$  to  $0.77\pm.08$ ) (two-tailed t-test; P<.05), which was equivalent to 96.7% dose reduction (from 7.34 to 0.24 mSv) without compromising image quality. The processing time for a CT scan was 4.8 min on a PC (Intel Core i7, 4.6GHz).

### CONCLUSION

Our technology converted thin-slice ULDCT (0.24 mSv) to "virtual" HDCT with substantially less noise or artifact, which was equivalent to 7.34 mSv CT; and thus, radiation dose reduction in CT by up to 96.7% could be possible.

### **CLINICAL RELEVANCE/APPLICATION**

Substantial reduction in radiation dose in CT by our technology would be beneficial to screening population. Short processing time is an advantage of our technology over iterative reconstruction.

### Implementing Pediatric CT Protocols throughout a Large, Diverse Multihospital Healthcare System

Sunday, Nov. 27 12:30PM - 1:00PM Room: QS Community, Learning Center Hardcopy Backboard

#### Awards

#### **Quality Storyboard Award**

#### **Participants**

James R. Duncan, MD, PhD, Saint Louis, MO (*Presenter*) Stock options, Proteon Therapeutics, Inc; Scientific Advisory Board, Metactive Medical Inc; Scientific Advisory Board, Flow Forward Medical Inc Sumita Markan-Aurora, MD, St Louis, MO (*Abstract Co-Author*) Nothing to Disclose Timothy Street, Saint Louis, MO (*Abstract Co-Author*) Nothing to Disclose Mandie Street, ARRT, Saint Louis, MO (*Abstract Co-Author*) Employee, Bayer AG Sonia Gor, MPH, St. Louis, MO (*Abstract Co-Author*) Nothing to Disclose

### PURPOSE

While the Image Gently campaign has long promoted adjusting CT protocols for pediatric patients, requirements from accreditation agencies have created a pressing need for implementation and monitoring. Local culture together with preexisting practices, diversity, and variations in work flow creates substantial barriers for large scale change. We describe early success with implementing improvement throughout a large, diverse, multihospital healthcare system.

#### **METHODS**

Improvement efforts in radiation dose management expanded in 2011. It began with review and testing of radiation dose monitoring systems. A system was selected and installed throughout the 12 hospital system by late 2014. Concurrently, a Radiology Clinical Expert Committee (CEC) was created as a multidisciplinary governance and oversight body. The CEC includes over 50 members, comprised of physicians, lead technologists, technical directors and improvement leaders who represent each hospital and serve as trusted agents for the system. The Radiology CEC provided a forum to share best practices and implement data-driven improvement projects. Under the guidance of the CEC, CT protocol names were standardized throughout the system. This included adding a "\_PEDS" suffix to every pediatric CT protocol's name. This allowed identification of pediatric protocols within the dose monitoring system was then used to identify what fraction of patients <18 years old were imaged using pediatric CT protocol. The process for investigating and reporting cases where the metric exceeded the expected range was also standardized. These results as well as progress with other improvement efforts are reported at the CEC's quarterly meetings. When early results showed performance gaps with utilization of pediatric CT protocols, the lead CT technologist from the system's pediatric specialty hospital and an enterprise CT application expert traveled to each hospital in the system. They provided on-site education and worked to remove barriers for full implementation.

### RESULTS

The Radiology CEC was convened in May 2014 and has since met each quarter. It oversaw the implementation of a standard radiation dose monitoring system that spanned the entire enterprise. Once all 12 sites began reporting data, it was found that the enterprise had more than 3200 unique CT protocol names. The CEC agreed to develop and adopt a standardized naming convention. A working group was created that reduced the list to 550 approved protocol names. While every site attested they routinely used pediatric protocols, the data in the accompanying figure showed substantial opportunity for improvement. For example, DLP varied more than 3-fold for newborn head CTs. Such data along with monthly tracking displays of pediatric CT protocol utilization was distributed to all Radiology CEC members beginning in June 2015. Enterprise experts began traveling to each hospital in July 2015 to help local teams develop their implementation solutions.As shown in the accompanying figure, between July 2015 and March 2016, pediatric CT protocol utilization at the adult-focused sites has increased from 5% to 48%. One facility increased their pediatric CT protocol usage from 0% to over 90%.

### CONCLUSION

Fifteen years after the Institute of Medicine reported that "The U.S. health care delivery system does not provide consistent, high quality medical care to all people", reliable and widespread implementation of best practices remains elusive. Our baseline data clearly demonstrated that awareness and monitoring were insufficient at fostering routine use of pediatric CT protocols throughout the enterprise. Our improvement efforts reaffirm the change management principles described by Kotter. New accreditation requirements provided a burning platform for change. A guiding coalition was created through the formation of a Radiology CEC that included widespread representation of frontline teams. The CEC also provided a venue for repeated communication and collaboration. A guiding vision for the entire enterprise was agreed upon where every child, no matter where their CT scan was performed, deserved a Pediatric protocol A series of small wins were celebrated starting with connecting CT scanners to the dose monitoring system, standardizing protocol nomenclature, defining the expected range of dose metrics for each CT protocols. This enterprise-wide radiology improvement infrastructure has been a success despite the potential conflicts that exist between academic radiologists vs. private practice groups, community vs. tertiary care centers and adult vs. pediatric focused facilities. Still, substantial work remains.

A Comprehensive CT Radiation Dose Reduction and Protocol Standardization Program in a Complex, Tertiary Hospital System Using Iterative Phantom and Clinical Testing and a Novel Web-based Information Distribution System

Sunday, Nov. 27 12:30PM - 1:00PM Room: QS Community, Learning Center Station #1

### Participants

Prabhakar Rajiah, MD, FRCR, Dallas, TX (*Presenter*) Institutional Research Grant, Koninklijke Philips NV; Speaker, Koninklijke Philips NV Jeffrey B. Guild, PhD, Dallas, TX (*Abstract Co-Author*) Nothing to Disclose Travis Browning, MD, Dallas, TX (*Abstract Co-Author*) Advisor, McKesson Corporation Seth Toomay, MD, Dallas, TX (*Abstract Co-Author*) Nothing to Disclose Viswanathan Venkataraman, MS, MENG, Dallas, TX (*Abstract Co-Author*) Nothing to Disclose Suhny Abbara, MD, Dallas, TX (*Abstract Co-Author*) Author, Reed Elsevier; Editor, Reed Elsevier; Institutional research agreement, Koninklijke Philips NV; Institutional research agreement, Siemens AG Orhan K. Oz, MD, PhD, Dallas, TX (*Abstract Co-Author*) Nothing to Disclose Anthony R. Whittemore, MD, Dallas, TX (*Abstract Co-Author*) Nothing to Disclose Lakshmi Ananthakrishnan, MD, Dallas, TX (*Abstract Co-Author*) Nothing to Disclose Avneesh Chhabra, MD, Dallas, TX (*Abstract Co-Author*) Nothing to Disclose Avneesh Chhabra, MD, Dallas, TX (*Abstract Co-Author*) Consultant, ICON plc; Author with royalties, Wolters Kluwer nv; Author with royalties, Jaypee Brothers Medical Publishers Ltd Sanjeeva P. Kalva, MD, Dallas, TX (*Abstract Co-Author*) Consultant, CeloNova BioSciences, Inc **PURPOSE** 

The radiation doses of CT scans are expected to be maintained As Low As Reasonably Achievable and the revised TJC requires the radiation dose of every CT exam to be recorded with investigation of cases where radiation dose exceeded established reference levels. Instituting a radiation dose reduction program in a large complex health system is not widely reported. We present our experience in a tertiary care health system, comprising of two different health entities, four large hospitals, five outpatient clinics, several remote locations, two PACS systems and 18 CT systems from 4 major manufacturers, with equipment up to 10 years old, ranging from six slice hybrid CT scanners to 320 slice diagnostic scanners. We utilized of a novel web-based information distribution system and iterative process of lowest common denominator using phantom and clinical test cases prior to implementation.

### METHODS

Initial analysis of the radiation doses and the CT protocols across the system identified the following problems: extensive heterogeneity of protocols and radiation doses; no established parameters; lack of training and reliable dissemination; no robust radiation dose tracking process; and lack of uniform data storage. A CT radiation task force was created to coordinate the stakeholders, including physicians, physicists, technologists and hospital administrations through weekly meetings. The aims of the taskforce were to: optimize patient radiation dose across scanners; standardize and homogenize the scan protocols; maintain or improve image quality; establish mechanisms to continually track the dose; establish reliable training and dissemination processes; and establish process of backing up and restoring protocols. All existing protocols were reviewed on a divisional basis. 3-5 studies were retrospectively selected from the PACS for each CT scanner on each protocol by a technologist/administrator, which were the radiation dose (DLP, CTDIvol) and image quality (Contrast to noise ratio) for each protocol using anthropomorphic phantoms. If the image quality was maintained at the lowest dose, that protocol was programed in the scanner. If the image quality was not iterative reconstruction levels based on CNR metrics and other previously optimized CT scanner protocols. The review process was repeated with the proposed protocol. The lowest dose which did not compromise image quality was selected. Redundant protocols were also eliminated, avoiding duplicated studies.

#### RESULTS

The project was started in May 2014, with review of 1500 protocols, and optimization proceeding from division to division. Cardiothoracic, as the first division, imaging protocol optimization was complete in 2 months and the entire optimization process was completed in 9 months. Compared to baseline, the scan protocols were homogenous and the radiation dose was also near homogeneous after almost a year. Radiation doses were tracked consistently and stored in a database. Radimetrics was utilized to store, retrieve and analyze the radiation dose programs Standard operating procedures and protocols were established, especially for maintaining and changing protocols. For any new or updated protocol, information was disseminated to the imaging sites and technologists were trained proper implementation. An intranet site called RADpoint was created, powered by SharePoint, which included a repository of all the protocols Evaluation of radiation doses for each optimized protocol over a period of one year before and one year after implementation was done using geometric mean to measure differences in dose. There were significant improvements in radiation doses and protocol homogeneity. Improvements in radiation doses ranged from 23-58 % dose reduction. This includes 23 % improvement for a routine CT abdomen and pelvis, 27 % for renal stone protocol, 38 % for CT chest pulmonary embolism protocol; 44 % for routine CT chest; 48 % for CT lumbar spine and 58 % for CT bony pelvis.

#### CONCLUSION

We demonstrate that the complex process of homogenizing CT protocols and optimizing radiation doses without compromising image quality can be achieved successfully by establishing a multi-disciplinary comprehensive CT operations program, with collaboration of radiologists, physicists and technologists. We highlight the use of a novel web-based information distribution system and iterative process of lowest common denominator using phantom and clinical test cases prior to implementation.

### **Honored Educators**

Presenters or authors on this event have been recognized as RSNA Honored Educators for participating in multiple qualifying educational activities. Honored Educators are invested in furthering the profession of radiology by delivering high-quality educational content in their field of study. Learn how you can become an honored educator by visiting the website at: https://www.rsna.org/Honored-Educator-Award/

Prabhakar Rajiah, MD, FRCR - 2014 Honored Educator Suhny Abbara, MD - 2014 Honored Educator

### **Improving Telephone Access In Radiology**

Sunday, Nov. 27 12:30PM - 1:00PM Room: QS Community, Learning Center Station #3

#### **Participants**

Hakan Sahin, MD, San Diego, CA (*Presenter*) Nothing to Disclose Emmily Poole, MD, San Diego, CA (*Abstract Co-Author*) Nothing to Disclose Amicare Gentili, San Diego, CA (*Abstract Co-Author*) Nothing to Disclose

#### PURPOSE

Patients are not able to reach the Radiology Department by phone, leave a message or receive follow up phone calls. The aim of this project was to improve telephone access in the Radiology department.

### METHODS

The workload of the Radiology department was categorized as MRI, CT, US, IR, Mammography, X-Rays and CT-Corrected and analyzed from 2001 to 2012. Incoming calls were analyzed from September 2012 to October 2012 and categorized as MRI scheduling, Radiology scheduling, cancelling appointment, reception, disconnect and abandons. The factors surrounding the Radiology procedure scheduling include: policies, people, processes and products were reviewed to determine their potential contribution to the problem. The policy review revealed added new services including mammography, breast biopsy, breast ultrasound, a second CT scanner, a second MR scanner and week-end Compensation & Pension Clinic simultaneously increasing gap in clerical FTEE required (reception and scheduling) and clerical FTEE on board. The process review showed increasing complexity and difficulty in managing phone calls and scheduling walk in patients simultaneously for schedulers especially when VISTA (EMR) is not designed to schedule radiology procedures and the complexity of manually filled protocols forms have been increasing. The people review demonstrated misuse of a scheduler's available time. This time is misused because the provider is not contributing enough information to the ordering process. Specifically, by not informing the patients of data needs, not entering collected data into CPRS, placing incorrect or incomplete orders and by not responding to pagers in order to clarify. The scheduler's time is usurped by trying to correct these deficiencies. The people review also revealed a lack of patient compliance. Patients did not do needed prep work for procedures because they did not know or were not reminded to do so. This was due to messages being left without any contact information that prevented any follow up communication. The review of products associated with phone scheduling revealed lack of a functional ACD system. Calls data was not monitored, voicemail service at the front desk did not exist and due to the high call volume there was not enough time to return calls. The monitoring of call-data and the review process led to discovery of multiple opportunities for improvement. The Radiology department started to implement immediate temporary and gradual permanent solutions simultaneously from January to August of 2013. Phone monitoring was implemented to collect call-data (telephone access performance measures including abandonment rate and delay time). The telephone system was improved with the use of ACD phones; that captures call demand and better manages incoming calls. Creating an electronic protocol process led to improving functionality and efficiency of staff. Staffing numbers were improved by: hiring new NTE positions to answer phone calls and by Training Specialty Care Schedulers that deal with radiology (CT, MR, US, Mammography, C-Ray etc.) specifically. Call volume was handled by training other specialties to answer all calls for scheduling. Using a secretary who is trained in MSA to train new MSA staff and provide scheduling expertise to the System Redesign Process. Shifting scanning responsibilities of MR paperwork to health techs. Requiring preparation of cover sheets for CT orders. By mandating protocol orders prior to scheduling, this allows the correct time slot to be filled and frees the trained MSA for scheduling. The creation of template letters to contact patients regarding future desired date appointments helps prevent incorrect provider orders (correcting unclear CT quick orders in CPRS regarding need for BUN/Creatinine/eGFR, premedication for allergies).

#### RESULTS

Following implementation of the measures mainly including people, process and products surrounding the phone access, the Radiology telephone abandonment percent dramatically decreased from 21.99% in February 2013 to 13.03% in October 2013, the call delay has dramatically decreased from 6:15 (minutes: seconds) in February 2013 to 1:30 in October 2013. The call performance improvements have sustained and are performing well; with a total abandonment rate of 7.75% (target was <10%) and total call delay of 49 seconds (target was <1minute) in July 2015 with no complaints.

#### CONCLUSION

Monitoring and analysis of incoming phone calls for scheduling Radiology procedures as well as review of associated policy, people, process, and products with revision where it is needed results in sustainable improvements in telephone access of patients to radiology services.

Implementing a Structured Reporting Initiative Using a Collaborative and Iterative Approach and Phased Template Rollout

Sunday, Nov. 27 12:30PM - 1:00PM Room: QS Community, Learning Center Station #4

### Participants

Shlomit Goldberg-Stein, MD, Bronx, NY (*Presenter*) Nothing to Disclose William Walter, MD, Bronx, NY (*Abstract Co-Author*) Nothing to Disclose E. Stephen Amis Jr, MD, Bronx, NY (*Abstract Co-Author*) Nothing to Disclose Meir H. Scheinfeld, MD, PhD, Bronx, NY (*Abstract Co-Author*) Nothing to Disclose

#### PURPOSE

To describe the implementation of a structured reporting initiative at a large multi-site, academic medical center radiology department using an iterative approach.

#### **METHODS**

Setting: Our urban tertiary care medical center performs >600,000 radiology exams per year. The department has 82 faculty, 36 residents and 13 fellows. Both adult and pediatric patients are cared for in three hospitals and five outpatient imaging facilities. The department (except for breast imaging, which already utilizes structured reporting) uses Powerscribe 360 (Nuance, Burlington, MA) and a single PACS and RIS system (Centricity, GE healthcare, Chicago, IL).1. Educate Formally presented concepts of structured reporting to staff and trainees Publicized clear goals of the structured reporting initiative and distributed relevant publications Directly addressed specific concerns from skeptical radiologists No financial incentives offered2. Survey Users: Collected data on dictation and user navigation preferences to inform global decisions3. Create Teams Formed subcommittees of stakeholders for specific template categories Teams encouraged to use the tools of structured reporting to adopt templates that conform to national guidelines (e.g. LungRads for screening Chest CT)4. Template Creation: an iterative processStep 1: Template drafting Initial template drafted by sub-specialty physician champion(s) Committee co-chairs edited the draft to meet defined criteria and standardized formStep 2: Limited trial and voting Limited-user two-week template trial for high-frequency subspecialty readers Templates trialed within typical radiologist workflow, with template auto-population Simple mechanism for template feedback during trial period was established Forum for voting on template details was createdStep 3: Department-wide trial Two week trial open to all radiologists (attendings and residents) Written feedback solicited by email, compiled, formally distributed, and voted upon Step 4: Template finalization Final template draft revised by committee co-chairs Optimized and standardized voice command fields, created template pick-list options Feedback and voting results shared with subcommittee members Written responses provided as to why suggestions were adopted or deferred5. Implementation Collaboration with radiology department billing/coding Educate technical staff for standardized exam tracking Collaboration with the IT department to ensure template autopopulation and overall integrity of multi-phase template trials Committee co-chair and IT availability during and immediately following the rollout to ensure a smooth rollout and address any problems in real-time, minimizing workflow interruption6. EvaluationA. Implementation Goal was >90% structured template availability by department exam volume within 2 years The Montage™ database search tool was used to search for monthly exam volume for all exams with finalized templates; monthly departmental crosssectional (CT, MR, and US) imaging volume was also calculated and % by volume of exams with available templates was calculated (see Figure)B. Template compliance audit Following institutional IRB exemption, an audit of radiologist compliance with the use of the finalized standardized structured reporting templates was performed Twelve exam types representing a cross-section of subspecialty divisions, were selected for review A search was conducted for 100 consecutive cases beginning at least one month from the time the template was introduced, to allow for adequate dissemination and learning of the templates Reports from each exam type were reviewed manualy to determine whether the standardized template was utilized Template compliance rates were calculated. Fisher's Exact test was used to determine if there was significant association between involvement of a trainee and template compliance among specific exam types

#### RESULTS

*Implementation:* Structured reporting templates were developed for 95% of total departmental cross-sectional study volume within two years*Compliance:* Overall compliance rate - 94% 100% compliance for knee MR, non-contrast head CT, non-contrast and PE Protocol Chest CT >95% compliance for shoulder MRI, ABDP CT, pediatric abdomen US Lowest rate of compliance seen with renal/bladder US (83%) *Actionable reporting developed, in adherence with national guidelines:* Lung-RADS Li-RADS Pi-RADS Rectal Cancer MR Staging

### CONCLUSION

Implementing Structured Reporting at our large multi-site Radiology Department required consensus building, education, and technical optimization for success. A collaborative and iterative approach achieved an overall compliance rate of 94%. Our experiences will serve as a model to other institutions attempting to improve the quality and actionability of their reports by implementing structured reporting.

### RO107-ED-SUA5

Radiology Collaboration-ECG Gated CT and Radiation Therapy; Saving Coronary Arteries One Heart Beat at a Time

Sunday, Nov. 27 12:30PM - 1:00PM Room: RO Community, Learning Center Station #5

#### Awards

**Certificate of Merit** 

#### **Participants**

Nikkole Weber, Rochester, MN (*Presenter*) Nothing to Disclose Shuai Leng, PhD, Rochester, MN (*Abstract Co-Author*) Nothing to Disclose Eric E. Williamson, MD, Rochester, MN (*Abstract Co-Author*) Research Grant, General Electric Company Emily Sheedy, Rochester, MN (*Abstract Co-Author*) Nothing to Disclose Cynthia Walfoort, Rochester, MN (*Abstract Co-Author*) Nothing to Disclose Katie Halda, Rochester, MN (*Abstract Co-Author*) Nothing to Disclose Alexandria Tasson, Rochester, MN (*Abstract Co-Author*) Nothing to Disclose Rebecca Keller, Rochester, MN (*Abstract Co-Author*) Nothing to Disclose

### **TEACHING POINTS**

Share information about the damaging, long term effects of radiation therapy on coronary structures including, but not limited to the arteries and valves. Identify which patients will benefit from the use of this collaborative approach to radiation therapy Learn about the protocol used to generate detailed imaging of the location of these important structures of the heart and other vulnerable structures of the body and how they are used to design a radiation therapy treatment plan.

### TABLE OF CONTENTS/OUTLINE

Background Widespread use of radiation therapy (lymphoma, breast CA, etc) Danger to cardiac structures (coronary arteries, aortic valve, etc) Cardiac CTA can identify these structures and help design a radiation therapy plan to avoid themWorkflow Identification of patients (RT) CT protocol (CT) Radiation therapy map (RT)Benefits Radiation plans Average radiation dose to radiosensitive structures – without & with "planning" Coronary arteries: left main, left anterior descending, circumflex, RCA Aortic valve Mitral valve Conclusion Radiation therapy planning using ECG-gated CT angiography has the potential to significantly reduce radiation dose to sensitive cardiac structures in patients referred for radiation therapy of the chest and mediastinum.

Design and Implementation of a Radiation Oncology Quality of Life and Outcomes Database for Improving Documentation and Care for Head and Neck Cancer Patients

Sunday, Nov. 27 12:30PM - 1:00PM Room: RO Community, Learning Center Station #3

#### Awards

#### **Student Travel Stipend Award**

#### Participants

Cato Chan, BS , Los Angeles, CA (*Presenter*) Nothing to Disclose Sukhjeet S. Batth, MD, MS, Los Angeles, CA (*Abstract Co-Author*) Nothing to Disclose Nicholas Trakul, MD, PhD, Stanford, CA (*Abstract Co-Author*) Nothing to Disclose

#### ABSTRACT

Purpose/Objective(s): Electronic medical records (EMRs) are widely used to capture un-structured clinical patient information. Analyzing patient outcomes using EMRs is limited by its retrospective nature and the significant resources it requires. We have designed and implemented a web-based, electronic data capture (EDC) system for head and neck cancer patients receiving radiation therapy in order to analyze outcomes prospectively, enhance the quality of clinical information recorded, and to generate regular Quality Improvement and patient safety reports. Materials/Methods: Our institution uses two different implementations of the same EMR at two separate hospitals, one a private NCCN Comprehensive Cancer Center, and the other a safety net hospital. Prior to implementation of the EDC, documentation was performed by both dictation and transcription services as well as direct entry into the EMR. A separate radiation oncology-specific record and verify system maintains all radiation therapy information, including the radiation prescription and treatment plan. The EDC was designed to record patient demographics, history, cancer and treatment characteristics, and to be used for on-treatment visit (OTV) and follow-up visit documentation and reporting. Generated OTV and follow-up visit forms are exported to the EMR. Patient-reported quality of life outcomes were collected prior to treatment, end of treatment, and at each follow-up. Common Toxicity Criteria for Adverse Events version 4.0 is used for observer rated toxicity scoring at all encounters. Results: The EDC system was implemented in February 2016 after an orientation for providers and nurses. It has been used by four providers and three nurses in two clinics for 35 patient encounters. Compliant data was recorded for 2 of 3 new patients, 18 of 20 follow-up patients, and 15 of 15 OTV encounters (total compliance of 92%). Preliminary feedback suggests that the EDC has streamlined OTV and follow-up documentation for providers. Only 10 of 21 (48%) quality of life questionnaires were successfully completed. Low computer literacy rates seen in the safety net hospital setting pose a significant challenge to compliance for patient reported outcomes. Conclusion: Designing and implementing a radiation oncology quality of life and outcomes database is feasible for head and neck cancer patients. Providers and nurses demonstrated compliance with its use. This has the potential to significantly reduce the resources required to analyze patient outcomes, and for enhancing patient safety and Quality Improvement initiatives. We aim to further evaluate user experience, improve the EDC, make it available to share with other institutions, and adapt it to other disease sites.

### Decongesting the Renal Sinus: MR Imaging Approach to Renal Sinus Lesions with Pathologic Correlation

Sunday, Nov. 27 12:30PM - 1:00PM Room: GU/UR Community, Learning Center Hardcopy Backboard

#### Participants

Satheesh Krishna, MD, Ottawa, ON (*Presenter*) Nothing to Disclose Nicola Schieda, MD, Ottawa, ON (*Abstract Co-Author*) Nothing to Disclose Krishna Prasad Shanbhogue, MD, New York, NY (*Abstract Co-Author*) Nothing to Disclose Robert Lim, MD, Ottawa, ON (*Abstract Co-Author*) Nothing to Disclose Trevor A. Flood, MD, FRCPC, Ottawa, ON (*Abstract Co-Author*) Nothing to Disclose Subramaniyan Ramanathan, MD, MBBS, Doha, Qatar (*Abstract Co-Author*) Nothing to Disclose Evan S. Siegelman, MD, Philadelphia, PA (*Abstract Co-Author*) Consultant, BioClinica, Inc Consultant, ICON plc Consultant, ACR Image Metrix

### **TEACHING POINTS**

1. Renal sinus cystic lesions include mainly parapelvic/peripelvic cysts but also less commonly: calyceal diverticula, multilocular cystic nephroma, cystic renal cell carcinoma (RCC), renal sinus urinomas, abscesses and lymphangectasia. Diagnosis can be suggested in most cases.2. Renal sinus solid lesions include mainly upper tract urothelial cell carcinoma (UCC) and hilar RCC which may be potentially differentiated by growth and enhancement pattern and diffusion weighted imaging appearance.3. Uncommon mesenchymal neoplasms (neurofibroma, hemangioma, leiomyoma/fibroma) and rarely ectopic cortical parenchyma should be considered when small well circumscribed non-invasive renal sinus neoplasms are identified.4. Other miscelaneous processes may involve the renal sinus including: lipomatosis, xanthogranulomatous pyleonephritis and vascular conditions.

### TABLE OF CONTENTS/OUTLINE

1. Anatomy and histology of the renal sinus.2. MR technique for imaging the renal sinus including urography.3. Approach to cystic renal sinus diseases.4. Approach to solid renal sinus neoplasms including differentiation of infiltrative RCC from upper tract UCC.5. Approach to renal sinus mesenchymal neoplasms.6. Description of miscelaneous renal sinus pathologies.

### **Honored Educators**

Presenters or authors on this event have been recognized as RSNA Honored Educators for participating in multiple qualifying educational activities. Honored Educators are invested in furthering the profession of radiology by delivering high-quality educational content in their field of study. Learn how you can become an honored educator by visiting the website at: https://www.rsna.org/Honored-Educator-Award/

Evan S. Siegelman, MD - 2013 Honored Educator Krishna Prasad Shanbhogue, MD - 2012 Honored Educator Krishna Prasad Shanbhogue, MD - 2013 Honored Educator

### VI194-ED-SUA8

Advanced Interventional Techniques in the Removal of Non-retrievable and Complex Retrievable Inferior Vena Cava (IVC) Filters

Sunday, Nov. 27 12:30PM - 1:00PM Room: VI Community, Learning Center Station #8

### Participants

Ansar Z. Vance, MD, Philadelphia, PA (*Presenter*) Nothing to Disclose Assaf Graif, MD, Newark, DE (*Abstract Co-Author*) Nothing to Disclose Omar Z. Chohan, DO, Newark, DE (*Abstract Co-Author*) Nothing to Disclose Aaron L. Reposar, MD, Newark, DE (*Abstract Co-Author*) Nothing to Disclose Mark J. Garcia, MD, Chadds Ford, PA (*Abstract Co-Author*) Boston Scientific Merit Medical Daniel A. Leung, MD, Newark, DE (*Abstract Co-Author*) Nothing to Disclose Kevin Lie, MD, Cleveland, OH (*Abstract Co-Author*) Nothing to Disclose George Kimbiris, MD, Narberth, PA (*Abstract Co-Author*) Nothing to Disclose Christopher J. Grilli, DO, Wilmington, DE (*Abstract Co-Author*) Nothing to Disclose

### **TEACHING POINTS**

1. To review the history of and indications for IVC Filter Placement.2. Discuss the various types of IVC Filters available.3. Discuss the various interventional techniques available for the removal of non-retrievable and complex retrievable IVC Filters.4. Case-based pictorial description of the advanced endovascular maneuvers available for the removal non-retrievable and complex retrievable IVC Filters.

### TABLE OF CONTENTS/OUTLINE

A. Background and Clinical Indications for IVC Filter Placement 1. History & Background 2. Clinical IndicationsB. Types of IVC Filters 1. Non-retrievable Filters 2. Retrievable FiltersC. Interventional Techniques 1. Dual Access a. Strategic b. Safety balloon 2. Sheath Options 3. Centering Techniques a. Snare-over-guidewire b. Snare-over-loop guidewire 3. Hangman Technique 4. Coaxial Double-Sheath Dissection 5. Laser-Assisted Double-Sheath Dissection 6. Endobronchial ForcepsD. Clinical Cases 1. Non-retrievable Greenfield IVC Filter Removal, placed 24 years prior 2. Non-retrievable TrapEase Filter Removal from right common iliac vein 3. Complex Celect Platinum IVC Filter Removal a. Complication of leg fracture embolized to the lung 4. Complex Gunther Tuplip IVC Filter Removal 5. Complex Optease IVC Filter RemovalE. Follow-up Protocols

### VI218-SD-SUA1

Interventional and Functional Outcome after Irreversible Electroporation for Surgical Renal Masses in Solitary Kidneys

Sunday, Nov. 27 12:30PM - 1:00PM Room: VI Community, Learning Center Station #1

### Participants

Steffen J. Diehl, MD, Mannheim, Germany (*Abstract Co-Author*) Nothing to Disclose
Nils Rathmann, MD, Mannheim, Germany (*Presenter*) Nothing to Disclose
Michael Kostrzewa, MD, Mannheim, Germany (*Abstract Co-Author*) Institutional research agreement, Siemens AG
Arman Smakic, MD, Mannheim, Germany (*Abstract Co-Author*) Nothing to Disclose
Stefan O. Schoenberg, MD, PhD, Mannheim, Germany (*Abstract Co-Author*) Institutional research agreement, Siemens AG
Maximilian C. Kriegmair, Mannheim, Germany (*Abstract Co-Author*) Nothing to Disclose

### PURPOSE

To examine outcome and complications in patients with a history of RCC and a solitary kidney who were treated with irreversible electroporation (IRE) for a surgical renal mass.

### METHOD AND MATERIALS

In this retrospective study 8 lesions were reviewed (5 patients: 2 female, 3 male; mean age 65 y) who underwent IRE for renal tumors in a solitary kidney with a mean follow-up period of 8.9 months (range 2 to 18). Changes of signal intensity (SI) of the treated lesions were evaluated in contrast-enhanced MRI: increase of SI > 10% was regarded as progressive disease (PD); an SI increase <10% or SI decrease was considered as tumor control (TC). To evaluate functional outcome, creatinine values and estimated glomerular filtration rate (eGFR) were compared to baseline after 1 day, 2-7 days, 3-6 weeks, and 6-12 weeks after the intervention.

### RESULTS

Mean tumor diameter was 25mm (range 15-38) with an average RENAL score of 6.6 (range 4-9). There was a progressive, significant drop in treated tumor SI on subsequent follow-up imaging (mean 56-73%) suggesting an initial TC of 100%. Only one lesion (lesion #6) showed PD after 7 months of follow-up and was ablated again. Two months after additional IRE this lesion (lesion #8) again showed a significant decrease of SI (75%). Two minor acute complications occurred (SIR grade A): transient gross hematuria and stage I acute kidney failure. Overall there was no significant drop in eGFR (mean -1.88ml/min +/-5.99) after 3 months.

### CONCLUSION

The data suggest that percutaneous IRE for renal mass in patients with a solitary kidney is safe and feasible. It may help to preserve renal function and offers promising oncological results in the short-/mid-term follow-up.

#### **CLINICAL RELEVANCE/APPLICATION**

Since IRE seems to be save and does not limit functional outcome in patients with a single kidney and possible malignant renal mass, IRE is a possible alternative ablation technique for patients at risk of dialysis.

Repeated Transarterial Chemoembolization with Degradable Starch Microspheres (DSMs-TACE) of Unresectable Hepatocellular Carcinoma: Preliminary Experience of a Single Center

Sunday, Nov. 27 12:30PM - 1:00PM Room: VI Community, Learning Center Station #2

### Participants

Fabrizio Chegai, MD, Rome, Italy (*Presenter*) Nothing to Disclose Stefano Merolla, Rome, Italy (*Abstract Co-Author*) Nothing to Disclose Laura Greco, Roma, Italy (*Abstract Co-Author*) Nothing to Disclose Antonio Orlacchio, MD, Rome, Italy (*Abstract Co-Author*) Nothing to Disclose

#### PURPOSE

To evaluate Trans-arterial Chemo-embolization (TACE) using Degradable-Starch-Microspheres (DSMs) in term of: Efficacy:

tumor response rates using modified-Response-evaluation-criteria-in-solid-tumors (mRecist) criteria.
 hepatic arterial tree patency after repeated procedures
 Safety :

•Intra- and post-procedural complications according to the classification of the International Society of Radiology (SIR)

#### **METHOD AND MATERIALS**

From November 2013 to Decembe 2015 we enrolled 72 HCC cirrhotic patients (52/20 M/F, mean age 66.3 years) to be treated with three repeated DSMs-TACE procedures, performed at 4-6 week intervals on the basis of patients tolerance. Clinical and biochemical evaluation were performed before and after each procedure. Treatment response was also assessed by computed-tomography (CT) or magnetic-resonance-imaging (MRI)-scan 4-6 weeks following each procedure. The lobar technique was used in case of multiple (>3) HCC in the same lobe or when the superselective catheterization of the feeding artery was not technically feasible. Segmental or sub-segmental approach was performed using microcatheter case by case basis. We used different amount of DSM: 225 – 450 mg EmboCept® S with different concentration of Doxorubicin on the basis of body surface (75 mg/m2) DSMs and Doxorubicin were injected until a complete blockage of the tumor feeding branch was achieved.

### RESULTS

A total of 168 DSMs-TACE procedures were performed. Complete response (CR) was observed in 20.8%, 37.5% and 58.3% patients after the first, second and third procedure, respectively. At the end of each treatment all patients experienced at least a partial response. At the end of the repeated procedures, no differences between mono or bi-lobar disease were observed in CR (64.2% vs 50%; p=ns). Patients with monolobar disease (58.3%) showed higher CR rates after the first procedure compared to those with bilobar HCC (p=0.017). In most cases treatment discontinuation was due to worsening liver function. We observed only 6 cases with vessel occlusion after 2 DSMsTACE cycle.

we observede 1 case of cholecystitis and 1 case of multiple hepatic abscess. PES was observed in 9 patients

### CONCLUSION

DSMs TACE is both a safe and an effective therapy for HCC patients with BCLC A and BCLC B

### **CLINICAL RELEVANCE/APPLICATION**

DSM TACE was Easy and fast procedure with related good downstaging rates and an overall good response to therapy, with low general toxicity and complications

### VI220-SD-SUA3

Analysis of Patient Controlled Analgesia to Define the Time Course of Pain Following Uterine Artery Embolization

Sunday, Nov. 27 12:30PM - 1:00PM Room: VI Community, Learning Center Station #3

### Participants

Shahriar Islam, MBBS, London, United Kingdom (*Presenter*) Nothing to Disclose Seyed Ameli-Renani, MBBS, FRCR, London, United Kingdom (*Abstract Co-Author*) Nothing to Disclose Lakshmi A. Ratnam, MBChB, London, United Kingdom (*Abstract Co-Author*) Nothing to Disclose Leto Mailli, PhD, Athens, Greece (*Abstract Co-Author*) Nothing to Disclose Anna M. Belli, MBBS, London, United Kingdom (*Abstract Co-Author*) Nothing to Disclose Raj Das, MBBS, FRCR, London, United Kingdom (*Abstract Co-Author*) Nothing to Disclose

### PURPOSE

Effective management of the post-procedure pelvic pain after uterine artery embolisation (UAE) remains challenging and is the primary reason for overnight admission. The aim of this study is to evaluate the time course of pain in the 24 hours following UAE.

### METHOD AND MATERIALS

In this single centre retrospective study, the records of patient controlled analgesia (PCA) usage and pain scores after UAE in 34 patients were reviewed and analyzed. All PCA protocols were standardized using Morphine at a concentration of 1mg/ml. PCA delivered morphine usage and pain score documented in the PCA chart using a verbal numerical rating score (1-4) were used as objective pain measurements.

### RESULTS

The peak mean pain score was observed 2 hours post-procedure at 1.74 (SD+/- 1.4, Range 0-4), but gradually reduced after this time, with mean pain scores of 1.26, 1.08 and 0.71 at 3, 4 and 9 hours respectively. The mean peak morphine usage was 10.28 mg/hr (SD +/- 1.9 Range 0-9) at 45 minutes and subsequently reduced to 6.18 mg/hr, 3.85 mg/hr, 3.2 mg/hr and 1.36 mg/hr at 2, 3, 4 and 9 hours respectively. 86% of patients used less than 3mg/hr of morphine PCA by 9 hours, with 16% requiring no further morphine PCA after this time.

### CONCLUSION

These results show the peak pain experienced following UAE is at 2 hours and the pain levels and morphine requirements reduce significantly following this. These results allow us to counsel patients' periprocedurally with regards to expectations of post procedure pain. They also serve as a baseline to compare more novel methods of pain control targeted at the periprocedural 1st 8 to 10 hours.

### **CLINICAL RELEVANCE/APPLICATION**

The results allow us to focus pain control within the first 8 to 10 hours with the potential for patients to be discharged the same day, preventing unnecessary overnight hospital admissions.

### VI222-SD-SUA5

Hepatocellular Carcinoma near Large Vessel: Comparison of Microwaves, Multibipolar and Monopolar Radiofrequency Ablation

Sunday, Nov. 27 12:30PM - 1:00PM Room: VI Community, Learning Center Station #5

### Participants

Amelie Loriaud, Pessac, France (*Presenter*) Nothing to Disclose Herve Trillaud, MD, Bordeaux, France (*Abstract Co-Author*) Nothing to Disclose Pantelis Papadopoulos, Pessac, France (*Abstract Co-Author*) Nothing to Disclose Nora Frulio, Bordeaux, France (*Abstract Co-Author*) Nothing to Disclose Cecile Salut, Bordeaux, France (*Abstract Co-Author*) Nothing to Disclose Mounir Bouzgarrou, MD, Merignac, France (*Abstract Co-Author*) Nothing to Disclose Arnaud Hocquelet, Pessac, France (*Abstract Co-Author*) Nothing to Disclose

### PURPOSE

To compare percutaneous ablation failure (primary ablation failure or local tumor recurrence) between micro waves (MWA), NoTouch mulitibipolar radiofrequency (NTmbpRF) and Monopolar radiofrequency ablation (MonoRF) treating HCC<5cm near large vessels.

### **METHOD AND MATERIALS**

we conducted a single center, retrospective and consecutive per-nodules study from 2011 to 2015. All HCC near large vessel treated either by MWA or NTmbpRF or MonoRF were included. The Radiofrequency Ablation Failure rates were compared with log-rank test.

#### RESULTS

No difference was observed for tumor size between the three groups (P=0.806). 144 nodules were analysed, 44 MWA; 42 NTmnpRF and 58 MonoRF.MWA, NTmbpRFA and MonoRF 2-years LTP rates were respectively, 13.7%, 13.7% and 35.9%. MWA and NTmbpRF were both superior to MonoRF (P<0.02) without significant difference between them (P=0.88). One tumour seeding and 3 aggressive intra-segmental recurrences occurred in MWA versus none in NTmbpRF group.

### CONCLUSION

Although MWA and NTmbpRF provided both better sustained local tumor control than MonoRF for HCC≤5cm near large vessel, NTmbpRF should be preferred to MWA due to the lower risk of tumor seeding and intra-segmental aggressive recurrences.

### **CLINICAL RELEVANCE/APPLICATION**

NoTouch MultiBipolar RFA provide similar sustained local tumor control than Microwaves for hepatocellular carcinoma <5cm near large vessel with lower risk of tumor seeding or agressive recurrence.

### Analyzing Factors Affecting the Hepatic Vein Pressure Gradient in Patients with Chronic Liver Disease

Sunday, Nov. 27 12:30PM - 1:00PM Room: VI Community, Learning Center Station #6

#### Participants

Yasutaka Baba, MD, Hiroshima, Japan (*Presenter*) Nothing to Disclose Tomoyo Fuji, Hiroshima, Japan (*Abstract Co-Author*) Nothing to Disclose Minoru Ishifuro, Hiroshima, Japan (*Abstract Co-Author*) Nothing to Disclose Kenji Kajiwara, Hiroshima, Japan (*Abstract Co-Author*) Nothing to Disclose Masaki Ishikawa, MD, Hiroshima, Japan (*Abstract Co-Author*) Nothing to Disclose Kazuo Awai, MD, Hiroshima, Japan (*Abstract Co-Author*) Nothing to Disclose Kazuo Awai, MD, Hiroshima, Japan (*Abstract Co-Author*) Research Grant, Toshiba Corporation; Research Grant, Hitachi, Ltd; Research Grant, Bayer AG; Research Grant, Eisai Co, Ltd; Medical Advisor, General Electric Company; ; ; ; ; Wataru Fukumoto, Hiroshima, Japan (*Abstract Co-Author*) Nothing to Disclose

### PURPOSE

To investigate factors affecting the hepatic vein pressure gradient (HVPG) in patients with chronic liver disease.

### **METHOD AND MATERIALS**

From September 2011 to September 2015, 134 patients (91 males, 43 females, average age 65) with chronic liver disease underwent HVPG to check their portal vein pressure. Chronic liver disease was due to hepatitis B virus (HBV) (n=26), hepatitis C virus (HCV) (n=47), non-B non-C hepatitis (NBNC) (n=19), nonalcoholic steatohepatitis (NASH) (n=4), alcoholism (n=27), and other factors (n=11). The HVPG was correlated with prognostic factors including patient the background, blood test results, the Child-Pugh (CP)- and the MELD score, and CT splenic volumetry. Correlations were assessed with the Spearman correlation coefficient for continuous- and the Mann-Whitney test for categorical variables. The predictive power of HVPG > 10 mmHg was evaluated with receiver operating characteristic (ROC) curves. Multivariate analysis was with the logistic regression method.

#### RESULTS

There was a statistically significant correlation with albumin (p=0.0097), choline esterase (ChE, p=0.0001), the CP score (p=0.0009), hemoglobin (p=0.0195), ICG15 (p<0.0001), the international normalized ratio of prothrombin time (PT-INR, (p=0.0301), the platelet count (p=0.009), prothrombin time (p=0.0102), red blood cell count (RBC, p=0.0006), T-bilirubin (p=0.0001), white blood cell count (WBC, p=0.0112), NH3 (p=0.007), and splenic volume (p=0.0017). By ROC analysis for predicting a HVPG > 10 mmHg, relevant values were albumin (AUC: 0.636, p=0.004), ChE (AUC: 0.659, p=0.0007), the CP score (AUC: 0.633, p=0.0046), albumin (AUC: 0.636, p=0.004), ICG15 (AUC: 0.680, p=0.001), the platelet count (AUC: 0.614, p=0.0242), RBC (AUC: 0.657, p=0.001), and splenic volume (AUC: 0.675, p=0.0018). By multivariate analysis, albumin (OR: 0.32, 95% CI: 0.12-0.83) and the platelet count (OR: 0.99, 95% CI: 0.98-0.99) were the best factors for predicting HVPG > 10 mmHg.

### CONCLUSION

Our results indicate that albumin and the platelet count are the factors best correlated with HVPG. They can be used to predict HVPG > 10 mmHg.

### **CLINICAL RELEVANCE/APPLICATION**

An HVPG > 10 mmHg is a poor prognostic marker in patients with chronic liver disease; it is correlated with albumin and the platelet count.

### Lesion Localization Using the Scroll Bar on Tomosynthesis: Why Doesn't It Always Work?

Sunday, Nov. 27 1:00PM - 1:30PM Room: BR Community, Learning Center Station #6

Awards Cum Laude Identified for RadioGraphics

### Participants

Sarah M. Friedewald, MD, Chicago, IL (*Abstract Co-Author*) Consultant, Hologic, Inc; Research Grant, Hologic, Inc; Consultant, C. R. Bard, Inc

Victoria A. Young, MD, Chicago, IL (*Presenter*) Nothing to Disclose Dipti Gupta, MD, Chicago, IL (*Abstract Co-Author*) Nothing to Disclose

### **TEACHING POINTS**

The scroll bar on Digital Breast Tomosynthesis (DBT) is an important tool that facilitates localization of a lesion on the orthogonal view and helps target ultrasound evaluation. While this works well most of the time, occasionally the location of the lesion as directed by the scroll bar is not accurate. The purpose of this presentation is to understand the specific scenarios when the location of the lesion on the scroll bar will not accurately predict the true location of the lesion and why.

### TABLE OF CONTENTS/OUTLINE

Review the techniques for lesion localization using digital mammography. Review of the role of the scroll bar in lesion localization on DBT. Four reasons why the lesion location on the scroll bar in DBT may not be precisely where the lesion is truly located. Not orthogonal views Paddle flex Superficial lesions more susceptible to moving during breast repositioning for different views Nipple position not always in the center of the scroll bar 4. Sample cases

Strengths and Shortcomings of Synthetic Mammography (SM): Review of C-View Physics, Artifacts, and Comparison with Full Field Digital Mammography (FFDM)

Sunday, Nov. 27 1:00PM - 1:30PM Room: BR Community, Learning Center Station #7

### Awards

#### Certificate of Merit Identified for RadioGraphics

#### Participants

Linda Ratanaprasatporn, MD, Boston , MA (*Presenter*) Nothing to Disclose Sona A. Chikarmane, MD, Boston, MA (*Abstract Co-Author*) Nothing to Disclose Catherine S. Giess, MD, Wellesley, MA (*Abstract Co-Author*) Nothing to Disclose

### **TEACHING POINTS**

Synthesized 2D mammography (SM) images are two-dimensional images reconstructed from digital breast tomosynthesis. Unlike standard mammography, synthetic images do not require additional radiation exposure and have the potential to replace dose-requiring FFDM without any loss in performance and cancer detection. Studies have demonstrated synthetic images are comparable to standard mammography for the detection of cancer, particularly calcifications. Artifacts of SM include blurring of subcutaneous tissue, loss of resolution in the axilla on MLO views and pseudo-calcifications. Given the increasing focus on radiation exposure in a screening population, the objectives of this exhibit are to review the physics, artifacts, strengths and weaknesses of SM compared to FFDM.

### TABLE OF CONTENTS/OUTLINE

1. To review synthetic mammography image acquisition and physics

2. To highlight synthetic mammography strengths: potential of reducing total radiation dose, increased conspicuity of certain cancers such as calcifications

3. To review synthetic mammography artifacts: Subcutaneous tissue blurring, loss of resolution in axilla, etc.

4. To explore synthetic mammography weaknesses: Appearance of images compared to FFDM, images with foreign objects such as pacemakers

5. To evaluate cancer conspicuity of screen detected cancers seen only or better on C-view vs. FFDM

### **Honored Educators**

Presenters or authors on this event have been recognized as RSNA Honored Educators for participating in multiple qualifying educational activities. Honored Educators are invested in furthering the profession of radiology by delivering high-quality educational content in their field of study. Learn how you can become an honored educator by visiting the website at: https://www.rsna.org/Honored-Educator-Award/

Catherine S. Giess, MD - 2015 Honored Educator

### Morphology of Breast Cancer Uptake on Dedicated Breast PET versus Conventional Whole Body PET

Sunday, Nov. 27 1:00PM - 1:30PM Room: BR Community, Learning Center Station #1

#### Participants

Kanae K. Miyake, MD, PhD, Kyoto, Japan (Presenter) Fellowship funded, Nihon Medi-Physics Co, Ltd Debra M. Ikeda, MD, Stanford, CA (Abstract Co-Author) Consultant, F. Hoffmann-La Roche Ltd Consultant, Bracco Group Andrei Iagaru, MD, Stanford, CA (Abstract Co-Author) Research Grant, General Electric Company; Research Grant, Bayer AG; Research Grant, The Piramal Group Andrew Quon, MD, Los Angeles, CA (Abstract Co-Author) Nothing to Disclose Bruce L. Daniel, MD, Stanford, CA (Abstract Co-Author) Research Grant, General Electric Company Jafi A. Lipson, MD, Stanford, CA (Abstract Co-Author) Research Grant, Hologic, Inc Sunita Pal, MD, Stanford, CA (Abstract Co-Author) Nothing to Disclose Erik S. Mittra, MD, PhD, Stanford, CA (Abstract Co-Author) Nothing to Disclose Henry Guo, Stanford, CA (Abstract Co-Author) Nothing to Disclose Yuji Nakamoto, MD, PhD, Kyoto, Japan (Abstract Co-Author) Nothing to Disclose Shotaro Kanao, MD, Kyoto, Japan (Abstract Co-Author) Nothing to Disclose Masako Y. Kataoka, MD, PhD, Kyoto, Japan (Abstract Co-Author) Nothing to Disclose Kaori Togashi, MD, PhD, Kyoto, Japan (Abstract Co-Author) Research Grant, Bayer AG Research Grant, DAIICHI SANKYO Group Research Grant, Eisai Co, Ltd Research Grant, FUJIFILM Holdings Corporation Research Grant, Nihon Medi-Physics Co, Ltd Research Grant, Shimadzu Corporation Research Grant, Toshiba Corporation Research Grant, Covidien AG PURPOSE

To evaluate differences between high-resolution dedicated breast PET (dbPET) and conventional whole body PET (WB-PET) in tumor uptake morphology and image quality, with comparison to dynamic contrast enhanced breast MRI (CE-MRI).

#### **METHOD AND MATERIALS**

We performed a retrospective study of 35 patients with invasive breast cancer undergoing 18F-fluorodeoxyglucose (FDG) dbPET, FDG WB-PET/CT, and CE- MRI before treatment. Four readers (2 breast radiologists and 2 nuclear medicine physicians) independently evaluated dbPET, WB-PET, and CE-MRI images of unilateral affected breasts, classifying index tumor appearance and scoring image quality. All data were treated as bivariate data for analysis (oval/round or irregular shape, smooth or not-smooth margin, heterogeneous or homogeneous internal pattern, presence or absence of similarity to CE-MRI, sharp or blurry image, positive or negative for artifacts/noise, and high or low signal to noise [S/N]). Final categories were determined on all readers' judgements by majority rule. McNemar test was performed to compare the results between dbPET and WB-PET.

### RESULTS

Tumors more frequently had irregular shapes (51% vs. 6%, p<0.01), not-smooth margins (66% vs. 3%, p<0.01), and heterogeneous internal uptake (77% vs. 6%, p<0.01) on dbPET than on WB-PET. There was rim uptake in 29% cases on dbPET, but in no cases on WB-PET (p<0.01). A similar tumor appearance to CE-MRI was observed more frequently on dbPET than on WB-PET in shape (94% vs. 46%, p<0.01), margin (86% vs. 3%, p<0.01), and internal pattern (80% vs. 6%, p<0.01). Intratumoral distribution of uptake was similar to intratumoral distribution of CE-MRI signal enhancement ratio in 83% on dbPET and in 31% on WB-PET (p<0.01). There was a significant difference between dbPET and WB-PET in image sharpness (94% vs. 20%, p<0.01), but not in artifacts/noise (none to limited in 100% vs. 94%, p=0.48) and in S/N (high in all on both).

#### CONCLUSION

dbPET may visualize more detailed morphology of tumor uptake with almost equivalent image quality compared to WB-PET, which potentially allows deeper understanding of tumoral functional structures and a detailed multimodality approach comparing with MRI.

### **CLINICAL RELEVANCE/APPLICATION**

High-resolution dedicated breast PET can visualize detailed morphology of tumor uptake, and potentially allows deeper understanding of tumoral functional structures and a detailed multimodality approach comparing with MRI.

### BR222-SD-SUB2

#### Changes in Microcalcifications Associated with Breast Cancer after Neoadjuvant Chemotherapy

Sunday, Nov. 27 1:00PM - 1:30PM Room: BR Community, Learning Center Station #2

#### **Participants**

Kazuaki Nakashima, MD, Nagaizumi, Japan (*Presenter*) Nothing to Disclose Takayoshi Uematsu, MD, PhD, Nagaizumi, Japan (*Abstract Co-Author*) Nothing to Disclose kaoru Takahashi, MD, Nagaizumi, Japan (*Abstract Co-Author*) Nothing to Disclose Takashi Sugino, MD, Nagaizumi, Japan (*Abstract Co-Author*) Nothing to Disclose Seiichirou Nishimura, MD, Nagaizumi, Japan (*Abstract Co-Author*) Nothing to Disclose

#### PURPOSE

To evaluate the correlation between changes in mammographic microcalcifications associated with breast cancer and tumor response after neoadjuvant chemotherapy (NAC).

### **METHOD AND MATERIALS**

This retrospective study included 218 breast cancer patients who received NAC from July 2011 to November 2015 and underwent mammography and MRI before and after NAC. One hundred and seven patients with microcalcifications associated with breast cancer on mammogram (group A) were compared with 111 patients without microcalcifications (group B). Changes in tumor size and microcalcifications after NAC were compared with MRI and histopathological findings. Decreased and increased calcifications were defined as any reduction and increase in number of calcifications, respectively, on mammogram after NAC. Pathologic complete response (pCR) was defined as no residual invasive or noninvasive tumor cells in the resected specimen. Trastuzumab was combined with chemotherapy in patients with human epidermal growth factor receptor 2 (HER2) positive breast cancer.

#### RESULTS

Tumor size reduction rate of group A and B measured by MRI were 48% and 63%, respectively (p < 0.001). Nine (8%) patients in group A and 20 (18%) patients in group B achieved pCR (p < 0.05). Microcalcifications on post-NAC mammogram decreased in 23 patients (21%), remained stable in 64 (60%), and increased in 20 (19%). Eight (35%) patients with decreased calcifications and 10 (16%) with stable calcifications achieved disappearance of invasive tumor cells (DIT). Even in patients with increased calcifications, HER2-positive tumor achieved DIT in 3 patients (50%). No patients with hormone receptor positive and HER2-negative tumor and one patient (25%) with triple-negative tumor achieved DIT when calcifications increased.

#### CONCLUSION

Breast cancers without associated microcalcifications showed a higher response rate to NAC. The number of microcalcifications remained stable after NAC in the majority of patients. Although increased calcifications indicate a poor therapeutic response in hormone receptor positive and HER2-negative tumors, it may predict a good response in HER2-positive tumors.

#### **CLINICAL RELEVANCE/APPLICATION**

Breast cancers with associated calcifications are more chemoresistant than those without calcifications. Changes in calcifications can be useful for estimating residual tumor by taking tumor subtypes and MRI findings into account.

### Quantitative MRI in Determining Mechanisms of Action of Taxol and Anthracyclines in Breast Cancer

Sunday, Nov. 27 1:00PM - 1:30PM Room: BR Community, Learning Center Station #3

#### Participants

Reem Bedair, MBChB,MSc, Cambridge, United Kingdom (*Abstract Co-Author*) Nothing to Disclose Andrew Patterson, PhD, Cambridge, United Kingdom (*Abstract Co-Author*) Nothing to Disclose Mary A. McLean, PhD, Cambridge, United Kingdom (*Abstract Co-Author*) Nothing to Disclose Martin J. Graves, PhD, Cambridge, United Kingdom (*Abstract Co-Author*) Nothing to Disclose John R. Griffiths, DPhil, Cambridge, United Kingdom (*Abstract Co-Author*) Nothing to Disclose Fiona J. Gilbert, MD, Cambridge, United Kingdom (*Presenter*) Research Grant, GlaxoSmithKline plc; Research Grant, General Electric Company; Research Grant, Hologic, Inc

#### PURPOSE

Taxanes and anthracycline-based chemotherapy regimens have commonly been used for the treatment of breast cancer in the adjuvant and neoadjuvant settings. In this work, we investigate the effects of anti-cancer drug regimens (taxane vs. anthracycline) on the pharmacokinetic (PK) parameter Ktrans after one cycle of chemotherapy.

#### **METHOD AND MATERIALS**

Thirty female patients (median age 51; range, 36-73) were prospectively enrolled for a 3T MRI in this IRB-approved study prior to the start, after one cycle and at the end of chemotherapy. All patients received 6 cycles of chemotherapy. Sixteen patients were started on taxanes while 14 received anthracyclines first. T1 mapping using the variable flip angle method and B1 mapping using the phase-based Bloch-Seigert method were performed. This enabled the calculation of native tissue T1 and correction for the transmit non-uniformity at 3T. Dynamic contrast-enhanced (DCE) images were acquired at a temporal resolution of 10 seconds using a 3D multi-slice fast SPGR sequence. Regions of interest (ROIs) encompassing the whole tumour were drawn on all slices of enhancing tumour. ROIs were placed at similar locations on the pre- and follow-up MRIs. PK parameters were calculated using the Toft's model. Mean percentage changes in Ktrans were compared after one cycle of treatment and correlated with histopathological response after final surgery.

#### RESULTS

Twelve patients showed complete pathological response while 18 showed partial response. The percentage decrease in size after one cycle did not significantly differentiate between treatment regimens (anthracyclines;  $-16.1 \pm 8.0\%$  vs. taxanes;  $-18.4 \pm 12.3\%$ , p=0.691). Interestingly, the percentage change in Ktrans was significantly different between the regimens after one cycle (Taxanes;  $-21.0 \pm 17.4\%$  vs. Anthracycline;  $15.2 \pm 9.7\%$ , p=0.03). There was no substantial difference between response groups after cycle 1 with regards to mean tumour size or Ktrans (p=0.47, p=0.054).

### CONCLUSION

The large decrease in Ktrans after one cycle of docetaxel reflects the likelihood of normalisation of the immature tumour vessels with decrease in the vascular permeability/perfusion in eventual responders.

### **CLINICAL RELEVANCE/APPLICATION**

Ktrans offers a surrogate biomarker for the underlying physiological processes in breast cancer. Largely influenced by the type of treatment administered, Ktrans can be used for the quantitative assessment of therapy in vivo.

Automated Breast Ultrasound in Breast Cancer Screening in Asian women: Comparison on the Diagnostic Performance between Two-view and Three-view Scan Method

Sunday, Nov. 27 1:00PM - 1:30PM Room: BR Community, Learning Center Station #4

### Participants

Soo-Yeon Kim, MD, Seoul, Korea, Republic Of (*Abstract Co-Author*) Nothing to Disclose Jung Min Chang, MD, Seoul, Korea, Republic Of (*Presenter*) Nothing to Disclose Nariya Cho, MD, PhD, Seoul, Korea, Republic Of (*Abstract Co-Author*) Nothing to Disclose Woo Kyung Moon, Seoul, Korea, Republic Of (*Abstract Co-Author*) Nothing to Disclose

#### PURPOSE

To evaluate and compare the detection performance of benign and malignant breast lesions using 3D volume data obtained by two or three view scans of automated breast ultrasound (ABUS) in Asian women.

### METHOD AND MATERIALS

This study was approved by the institutional review board and informed consent was obtained. Between March and April 2016, bilateral whole breast ultrasound examination were performed with ABUS and handheld breast US (HHUS) for 32 consecutive women with known breast cancer (mean age, 50.5years; range, 35-78). Two-view or three- view scans of ABUS for each breasts were randomly assigned for the women who had less than 20cm of breast width on mammography. Two breast radiologists who were unaware of the results of HHUS and the clinical information reviewed the ABUS data. Sensitivity and specificity in detecting malignant lesions and consistency with HHUS data for benign lesions were calculated and compared in each scans of ABUS.

#### RESULTS

Thirty-seven malignancy (mean size,  $1.9\pm1.1$ cm) in 33 breasts, 26 benign lesions (mean size,  $0.8\pm0.4$ cm) in 16 breasts and 24 normal breasts were included. Average width on mammography and depth in ultrasound (US) were 18.3cm and 2.3cm in the two-view scan group, and 18.2cm and 2.2cm in the three-view scan group (p>0.05). The sensitivities for cancer detection was 93.3% (14/15) in the two-view scan group, and 90.9% (20/22) in the three-view scan group (p>0.05). Specificity was higher for three-view scans (92.9%, 26/28) than two-view scans (66.7%, 16/24) (p<0.05), and higher consistency with HHUS findings were noted for three-view scans 47.1% (8/17) than two-view scans 22.2% (2/9) of ABUS (p=0.39). In three cases of false-negative, all cancers were included in the scans, but 2 DCIS was missed due to non-mass finding, and 1 invasive ductal carcinoma was obscured by the heterogeneous background echotexture on ABUS.

#### CONCLUSION

In detection of malignant breast lesions, there was no difference in sensitivity between two-view scans and three-view scans of ABUS. Specificity was higher for three-view scans than two-view scans, with better visualization of benign lesions.

#### **CLINICAL RELEVANCE/APPLICATION**

For supplemental screening for breast cancer, automated technique with 2 scans of ABUS is feasible to detect breast cancers in Asian women with small breasts, although specificity loss is observed.

### Has the California Breast Density Law changed Provider-ordering Practices?

Sunday, Nov. 27 1:00PM - 1:30PM Room: BR Community, Learning Center Station #5

#### **Participants**

Shruthi Ram, MD, Sacramento, CA (*Presenter*) Nothing to Disclose Shadi Aminololama-Shakeri, MD, Sacramento, CA (*Abstract Co-Author*) Nothing to Disclose

### PURPOSE

To assess the impact of California's breast density legislation (BDL) on physician ordering of screening breast MRI.

### **METHOD AND MATERIALS**

We performed an IRB approved retrospective analysis of contrast-enhanced breast MRI studies done for screening in a 30 month period before and after the California breast density law (BDL) went into effect on 4/1/13. Screening breast MRIs were subcategorized into those with breast density mentioned as an exam indication. Patients were further classified into three levels of risk - (1) defined high risk (eg. calculated lifetime risk>20%, presence of a genetic mutation, radiation at young age for lymphoma or presence of syndromes), (2) above average risk, however not quantified or calculated as <20% lifetime risk, or (3) completely undefined/ average risk. Chi test statistical analysis was performed, using the 2-tailed Fisher exact test to compare overall MR utilization, use of breast density as an indication, patient demographics and ordering provider characteristics.

### RESULTS

Screening breast MRI exams with breast density as clinical indication increased from 8.5% (32/376) to 20.9% (136/650, p<0.001) after the California BDL went into effect. When patients with known or defined high risk were excluded, the increase was from 7.7% to 16.3% (p<0.001). Prior to BDL, 60.9% of the ordering providers were specialists and 37.8% were from primary care compared to 61.1% and 36.9% after the law went into effect, respectively. The majority of exams were ordered female providers, 80.3% before and 75.7% after BDL. When considering only the MRIs ordered with density as indication, 53.1% were requested by specialists and 43.8% by primary providers before BDL compared to 63.2% and 34.6% respectively, after the law went into effect.

### CONCLUSION

Screening breast MRI utilization more than doubled after the California BDL went into effect using breast density as the ordering indication in non-high risk women. The majority of screening breast MRI exams were ordered by specialists and female providers. This has not been affected by breast density legislation in California.

### **CLINICAL RELEVANCE/APPLICATION**

Breast density is of great concern to patients and their providers. Breast density legislation has had an important impact on breast MRI utilization and deserves further study.

### A Winding Road: The Spectrum of Coronary Artery Anomalies

Sunday, Nov. 27 1:00PM - 1:30PM Room: CA Community, Learning Center Station #6

#### Awards Certificate of Merit

#### **Participants**

Lea Azour, MD, New York, NY (*Presenter*) Nothing to Disclose Adam Jacobi, MD, New York, NY (*Abstract Co-Author*) Nothing to Disclose Javier Sanz, MD, New York, NY (*Abstract Co-Author*) Nothing to Disclose Gina Larocca, New York, NY (*Abstract Co-Author*) Nothing to Disclose Rebecca Chang, MD, New York, NY (*Abstract Co-Author*) Nothing to Disclose Matthew D. Cham, MD, New York, NY (*Abstract Co-Author*) Nothing to Disclose

### **TEACHING POINTS**

-To understand normal coronary arterial anatomy and vascular territory.-To identify congenital and acquired coronary artery anomalies.-To distinguish between benign anomalies and those requiring intervention.

### TABLE OF CONTENTS/OUTLINE

Overview of the incidence of coronary artery anomalies.2. Typical coronary arterial anatomy: a. Right dominant 1. system; b. Left dominant system; c. Co-dominant system.3. Congenital coronary artery anomalies (Cine Images will be included): Absence of a coronary artery i. Absent left main a. b. Anomalous Origin trunk ii. Absent RCA i. Anomalous left coronary artery from the pulmonary artery (ALCAPA) ii. Anomalous right coronary artery from the pulmonary artery (ARCAPA) iii. Anomalous coronary artery from opposite sinus (ACAOS) iv. Anomalous coronary artery from non-coronary sinus c. Anomalous course Benign i. 1. Pre-pulmonary 2. Retro-aortic 3. Myocardial bridging 4. Intramuscular septal course 5. Intra-atrial RCA ii. Malignant 1. Inter-arterial iii. Controversies in Management4. Acquired coronary artery anomalies: a. Fistula b. Aneurysm

CT Imaging after the Bentall Procedure: An Updated and Comprehensive Guide

Sunday, Nov. 27 1:00PM - 1:30PM Room: CA Community, Learning Center Station #7

#### Awards Certificate of Merit

#### Participants

Sara Boccalini, MD, Genova, Italy (*Presenter*) Nothing to Disclose Laurens E. Swart, MD, Rotterdam, Netherlands (*Abstract Co-Author*) Nothing to Disclose Jos A. Bekkers, Rotterdam, Netherlands (*Abstract Co-Author*) Nothing to Disclose Koen Nieman, MD, PhD, Rotterdam, Netherlands (*Abstract Co-Author*) Nothing to Disclose Gabriel P. Krestin, MD, PhD, Rotterdam, Netherlands (*Abstract Co-Author*) Research Grant, General Electric Company; Research Grant, Bayer AG; Research Grant, Siemens AG; Consultant, Bracco Group; Scientific Advisor, Zebra Medical Vision Ltd; Advisory Board, Quantib BV Ad J. Bogers, MD, PhD, Rotterdam, Netherlands (*Abstract Co-Author*) Nothing to Disclose

Ad J. Bogers, MD, PhD, Rotterdam, Netherlands (*Abstract Co-Author*) Nothing to Disclose Ricardo P. Budde, MD, PhD, Utrecht, Netherlands (*Abstract Co-Author*) Nothing to Disclose

### **TEACHING POINTS**

To review the indications and surgical technique of the Bentall and associated procedures To illustrate normal postoperative changes and complications and their respective CT appearance To highlight differences between normal postoperative features and complications and raise awareness of the gray zones. To present a series of challenging and previously undetectable complications

### **TABLE OF CONTENTS/OUTLINE**

Clinical indications for the Bentall procedure in emergency and elective settings The Bentall procedure The classic Bentall and its modifications Surgical and/or interventional associated or subsequent procedures (including the Ross procedure, aortic debranching, elephant trunk, TEVAR) CT imaging after the procedure CT exam technical considerations The normal postoperative anatomy and its uncomplicated variations The CT appearance of surgical material (including aortic valves, aortic prosthesis, suture lines, Amplatzer devices) CT appearance of complications Classical findings Findings of previously undetectable complications that are now assessable due to the recent improvements in CT scanners technology How to distinguish complications from normal postoperative changes: the known and the unknown Challenging cases

# CA205-SD-SUB1

Prevalence of Coronary Artery Disease in Adults Under 30 Presenting with Acute Chest Pain - A Retrospective Study

Sunday, Nov. 27 1:00PM - 1:30PM Room: CA Community, Learning Center Station #1

#### Awards

#### **Student Travel Stipend Award**

#### Participants

Bo Liu, MD, Maitland, FL (Presenter) Nothing to Disclose Matthew C. Odell, MD, MPH, Orlando, FL (Abstract Co-Author) Nothing to Disclose Dzmitry Fursevich, MD, Orlando, FL (Abstract Co-Author) Nothing to Disclose Kimberly Beavers, MD, Orlando, FL (Abstract Co-Author) Nothing to Disclose Michael Valente, Orlando, FL (Abstract Co-Author) Nothing to Disclose Ashley Ramirez, Orlando, FL (Abstract Co-Author) Nothing to Disclose Melissa Kendall, Orlando, FL (Abstract Co-Author) Nothing to Disclose Reem Abdalla, Orlando, FL (Abstract Co-Author) Nothing to Disclose Carole Coyne, Orlando, FL (Abstract Co-Author) Nothing to Disclose William F. Sensakovic, PhD, Orlando, FL (Abstract Co-Author) Officer, YellowDot Innovations, LLC Manuel A. Hernandez, MD, Orlando, FL (Abstract Co-Author) Nothing to Disclose Michael Sacerdote, MD, Tampa, FL (Abstract Co-Author) Nothing to Disclose Antonio Gonzalez, MD, Orlando, FL (Abstract Co-Author) Nothing to Disclose Thomas J. Ward, MD, New York, NY (Abstract Co-Author) Nothing to Disclose Nicholas C. Feranec, MD, Winter Park, FL (Abstract Co-Author) Nothing to Disclose Jeremy R. Burt, MD, Windermere, FL (Abstract Co-Author) Nothing to Disclose

# PURPOSE

To evaluate the prevalence of coronary artery disease in the young adult population (age 18-30) presenting to the emergency department for evaluation of acute chest pain as determined by coronary computed tomgraphy angiography (CCTA).

## **METHOD AND MATERIALS**

This retrospective study was granted a waiver of the informed consent as required by HIPAA. A Montage search was performed for CCTAs performed on young adults age 18-30 from January 1, 2013 to October 1, 2015, yielding 914 studies. 30 patients were excluded on the basis of preexisting congenital heart disease, previous cardiac surgery or study performed for reason other than chest pain (e.g. mass), the final study population consisted of 884 patients (age range 18-30, average age 26). Each study was reviewed by 1 of 5 fellowship trained cardiac radiologists. The study was deemed abnormal if any atherosclerotic plaque, coronary artery stenosis or coronary artery anomaly was identified.

#### RESULTS

Of the 884 patients, 28 (3.2%) had abnormal coronary findings. 9 (1.0%) had stenosis caused by myocardial bridging, 9 (1.0%) had coronary artery anomalies, and 11 (1.2%) had stenosis caused by atherosclerotic disease. 1 patient (0.1%) had stenosis caused by both atherosclerosis and myocardial bridging. Of the 9 patients with myocardial bridging, 2 (0.2%) had moderate to severe stenosis. Of the 9 patients with coronary artery anomalies, 3 (0.3%) were malignant and 6 (0.7%) were benign. Of the 11 patients with atherosclerotic disease, 1 (0.1%) had moderate to severe stenosis.

#### CONCLUSION

This single institution retrospective study provides evidence for low prevalence of coronary artery disease in the young adult population (age 18-30). Only 6 (0.7%) patients were identified as having moderate to severe stenosis caused by atherosclerosis, myocardial bridge or a malignant coronary artery anomaly.

# **CLINICAL RELEVANCE/APPLICATION**

This study provides evidence for more restricted use of CCTAs in young adults age 18-30 presenting with acute chest pain. The cost versus benefit of CCTA in this young population requires further research.

Radiation Dose Reduction for Coronary Artery Calcium Scoring at 256-detector CT with an Iterative Reconstruction Technique

Sunday, Nov. 27 1:00PM - 1:30PM Room: CA Community, Learning Center Station #3

# Participants

Chikako Fujioka, RT, Hiroshima, Japan (*Presenter*) Nothing to Disclose Kazushi Yokomachi, RT, Hiroshima, Japan (*Abstract Co-Author*) Nothing to Disclose Nobuo Kitera, RT, Hiroshima, Japan (*Abstract Co-Author*) Nothing to Disclose Eiji Nishimaru, RT, Hiroshima, Japan (*Abstract Co-Author*) Nothing to Disclose Masao Kiguchi, RT, Hiroshima, Japan (*Abstract Co-Author*) Nothing to Disclose Kazuo Awai, MD, Hiroshima, Japan (*Abstract Co-Author*) Research Grant, Toshiba Corporation; Research Grant, Hitachi, Ltd; Research Grant, Bayer AG; Research Grant, Eisai Co, Ltd; Medical Advisor, General Electric Company; ; ; ; ;

## PURPOSE

In previous reports the coronary artery calcium score were lower on image reconstructed with iterative reconstruction (IR) than filtered back projection (FBP) images. An iterative reconstruction (adaptive statistical iterative reconstruction V: ASiR-V) includes object, noise and X-ray physics models and reduces both noise and low signal induced artifacts. The purpose of our study was to assess the possibility of reducing the radiation dose for coronary artery calcium (CAC) scoring by using ASiR-V on a 256-detector CT scanner.

## **METHOD AND MATERIALS**

We scanned a cardiac CT calibration phantom (QRM, Germany) that featured different calcium hydroxyapatite concentrations on a 256-detector CT scanner (Revolution CT, GE) with prospective ECG-triggering. We scanned the phantom 5 times. We reduced dose applied ten IR strength levels (0-100%, 10% step) The tube current was 198-,177-,157-,139-,122-,105-,91-,77-,65-,54-,49 mA. Calcification scoring was compared after calculating the Agatston, volume and mass scores.

# RESULTS

The average Agatston score with ASiR-V (0-100%, step10%) were 639, 644, 641, 639, 636, 641, 645, 636, 639, 627 and 629, respectively. The average volume score with ASiR-V (0-100%, step10%) were 546-, 545-, 546-, 543-, 543-, 539-, 542-, 530- and 531 mm3(true value: 358.2 mm3), respectively. The average mass score with ASiR-V (0-100%, 10% step) were 181-, 180-, 180-, 180-, 180-, 180-, 180-, 180-, 180-, 180-, 180-, 178-, 174- and 174 mgHA(true value: 167.1 mgHA), respectively. There was no significant difference in the Agatston, volume and mass scores among images with various degrees of ASiR-V. Regarding the mean Agatston, volume and mass scores, the difference values obtained at 198- and 49 mA with ASiR-V 100% were very small. The use of ASiR-V made it possible to reduce the radiation dose. The use of ASiR-V (10-100%, 10% step) could reduce the radiation dose was 11, 21, 30, 38, 47, 54, 61, 67, 73 and 75%.

# CONCLUSION

The use of ASiR-V made it possible to reduce the radiation dose by 75% for CAC scoring without impairing quantification of coronary calcification.

# **CLINICAL RELEVANCE/APPLICATION**

The use of ASiR-V can reduced radiation dose in CAC scoring at CT.

High-pitch Versus Sequential Mode in Coronary Calcium Scanning in High Heart Rates: Potential for Dose Reduction

Sunday, Nov. 27 1:00PM - 1:30PM Room: CA Community, Learning Center Station #5

#### Awards

#### **Student Travel Stipend Award**

#### **Participants**

Marleen Vonder, MSc , Groningen, Netherlands (*Presenter*) Nothing to Disclose Rozemarijn Vliegenthart, MD, PhD, Groningen, Netherlands (*Abstract Co-Author*) Nothing to Disclose Marieke van Aerde, MSc, Rotterdam, Netherlands (*Abstract Co-Author*) Nothing to Disclose Carlijn Van Der Aalst, PhD, Rotterdam, Netherlands (*Abstract Co-Author*) Nothing to Disclose Harry De Koning, Rotterdam, Netherlands (*Abstract Co-Author*) Nothing to Disclose Harry De Koning, Rotterdam, Netherlands (*Abstract Co-Author*) Research Grant, F. Hoffmann-La Roche Ltd Equipment support, Siemens AG Medical Advisory Board, F. Hoffmann-La Roche Ltd Matthijs Oudkerk, MD, PhD, Groningen, Netherlands (*Abstract Co-Author*) Nothing to Disclose Peter M. Van Ooijen, MSc, PhD, Groningen, Netherlands (*Abstract Co-Author*) Nothing to Disclose Jan Willem C. Gratama, MD, Apeldoorn, Netherlands (*Abstract Co-Author*) Nothing to Disclose Dirkjan Kuijpers, MD, Den Haag, Netherlands (*Abstract Co-Author*) Nothing to Disclose

#### PURPOSE

To determine the impact of high-pitch spiral mode on dose and risk stratification in coronary calcium scanning in participants with a high heart rate.

# METHOD AND MATERIALS

In total 1978 participants of the cardiovascular screening trial Robinsca were included, whom had average heart rate higher than 65 beats per minute. A coronary calcium scan was acquired with dual-source CT (Definition Flash, Siemens, Germany) at 120 kV, 80 ref mAs in high pitch spiral mode and in the reference sequential mode. The dose parameter CTDIvol was logged and the Agatston score was determined with dedicated software to calculate number of positive scores and to stratify the participants into risk categories: 0, 1-99, 100-399 and 400+. Paired sampled T-testing and McNemar testing was used to analyze differences in dose and positive scores between high-pitch spiral and sequential mode for high heart rates.

## RESULTS

The dose of high-pitch spiral scan (1.75 mGy) was significant lower than of sequential mode (3.38 mGy), p < 0.001. No difference was found for the number of positive (or negative) calcium scores between high-pitch spiral (57.8%) and sequential mode (57.2%), p=0.074. Categorization of participants was for 0.1-99: 34.3%, for 100-399: 15.8% and for 400+: 7.1% at sequential mode. For the high-pitch spiral mode participants were shifted to lower or higher categories in 4.9% of all cases in the four risk categories.

# CONCLUSION

The high-pitch spiral mode has discrete impact on cardiovascular risk stratification in participants with a high heart rate and leads to dose reduction of 48%.

# **CLINICAL RELEVANCE/APPLICATION**

High-pitch spiral mode might be used for coronary calcium scanning irrespective of the heart rate, depending on impact on risk stratification.

Non Thrombotic Pulmonary Arterial Filling Defects And Occlusion-A Differential Every Radiologist Should Know

Sunday, Nov. 27 1:00PM - 1:30PM Room: CH Community, Learning Center Station #5

#### **Participants**

Thomas Capobres, MD, Detroit, MI (*Presenter*) Nothing to Disclose David L. Spizarny, MD, Detroit, MI (*Abstract Co-Author*) Nothing to Disclose Chad Klochko, MD, Farmington Hills, MI (*Abstract Co-Author*) Nothing to Disclose

# **TEACHING POINTS**

To review the differential for non-thrombotic causes of pulmonary arterial emboli and occlusion, highlighting characteristic imaging features as well as historical and clinical manifestations. To understand potential treatment approaches for different types of non-thrombotic pulmonary artery emboli/occlusion. To recognize potential complications related to different types of non-thrombotic pulmonary artery emboli/occlusion.

# TABLE OF CONTENTS/OUTLINE

CT imaging of the pulmonary arteries and normal anatomy Nonthrombotic causes of pulmonary arterial filling defects and occlusion: characteristic imaging features, patient history and clinical manifestations, treatment approach/outcome, potential complications Extrinsic compression Mediastinal fibrosis Tumor Bronchogenic carcinoma Lymphadenopathy/metastatic Intrinsic filling defects Tumors Pulmonary artery sarcoma Intravascular metastases Endogenous emboli Septic Fat Amniotic fluid Exogenous emboli Vertebroplasty cement/barium IVC filter strut Prostate seeds Metallic Mercury Talc Catheter/Wire Buckshot Iatrogenic air Pseudo Emboli Bronchial artery to pulmonary artery fistula Summary

# An Algorithm to Occupational Lung Disease: A Way to Make it Easy

Sunday, Nov. 27 1:00PM - 1:30PM Room: CH Community, Learning Center Station #6

#### **Participants**

Felipe Aluja, MD, Bogota, Colombia (*Presenter*) Nothing to Disclose Federico G. Diaz Telli, MD, Pilar, Argentina (*Abstract Co-Author*) Nothing to Disclose Sebastian Yevenes Aravena, MD, Santiago, Chile (*Abstract Co-Author*) Nothing to Disclose Fernando R. Gutierrez, MD, Saint Louis, MO (*Abstract Co-Author*) Nothing to Disclose Sanjeev Bhalla, MD, Saint Louis, MO (*Abstract Co-Author*) Nothing to Disclose

#### **TEACHING POINTS**

To recognize the different types of occupational lung disease, their clinical presentation, causes and possible treatment. Describe the imaging findings associated with occupational lung disease, their appearance in conventional radiology and computed tomography. Review the key elements in regard to the imaging diagnosis, focusing on their characteristics, distribution, associated findings and some others needed for an adequate diagnosis. Propose a simple algorithm for the occupational lung disease based on imaging findings.

# TABLE OF CONTENTS/OUTLINE

Introduction Clinical characteristics of occupational lung disease Silicosis Classic silicosis Simple form and complicated form Acute silicosis Coal worker pneumoconiosis Siderosis Berylliosis Talcosis Hard metal pneumoconiosis Arc welder lung Asbestos related disease Parenchymal Pleural Asbestosis Hypersensitivity pneumonitis Flavor's worker lung Algorithm approach to occupational lung disease Conclusion

# **Honored Educators**

Presenters or authors on this event have been recognized as RSNA Honored Educators for participating in multiple qualifying educational activities. Honored Educators are invested in furthering the profession of radiology by delivering high-quality educational content in their field of study. Learn how you can become an honored educator by visiting the website at: https://www.rsna.org/Honored-Educator-Award/

Sanjeev Bhalla, MD - 2014 Honored Educator Sanjeev Bhalla, MD - 2016 Honored Educator

# **Diabetes and Mortality in the National Lung Screening Trial**

Sunday, Nov. 27 1:00PM - 1:30PM Room: CH Community, Learning Center Station #1

#### **Participants**

Janet Snell-Bergeon, PhD, Aurora, CO (*Abstract Co-Author*) Nothing to Disclose Kavita Garg, MD, Denver, CO (*Presenter*) Nothing to Disclose Samuel Chang, MD, Aurora, CO (*Abstract Co-Author*) Nothing to Disclose Nayana U. Patel, MD, Aurora, CO (*Abstract Co-Author*) Nothing to Disclose Satish K. Garg, MD, Aurora, CO (*Abstract Co-Author*) Nothing to Disclose

#### PURPOSE

Presence of diabetes increases mortality, but extent to which diabetes increases lung and other cancer mortality among heavy smokers is unclear. We examined the risk for all-cause, lung cancer and non-lung cancer mortality among people with vs without diabetes followed in the National Lung Screening Trial (NLST) cohort.

#### **METHOD AND MATERIALS**

There were 53,212 participants enrolled in the NLST trial, and 5,174 reported having diabetes at screening. Over the course of the study, there were 3,936 total deaths, 1021 from lung cancer and 826 non-lung cancer. Cox proportional hazards regression models were used to examine the relative risk for overall, lung cancer and non-lung cancer mortality associated with diabetes, adjusted for age, gender, randomization group and covariates of interest (body mass index [BMI] and pack-years of smoking).

#### RESULTS

Subjects with diabetes were older ( $62\pm5$  vs.  $61\pm5$  years, p<0.0001), reported more pack-years of smoking ( $62\pm29$  vs.  $55\pm23$ , p<0.0001, and had higher BMI ( $31.1\pm5.8$  vs  $27.6\pm4.9$ , p<0.0001) than people without diabetes at screening. There were 650 deaths (12.6%) among participants with diabetes, vs 3,286 deaths (6.8%) among non-diabetic subjects (p<0.0001). In cox proportional hazards models, diabetes was associated with an increased risk for all-cause mortality (RR=2.2, 95% CI 1.8-2.6, p<0.0001), lung cancer mortality (RR=1.8, 95% CI 1.3-2.5, p=0.0008) and non-lung cancer mortality (RR 1.6, 95% CI 1.04- 2.3, p=0.03) in women. Among men, diabetes increased the risk only for all-cause (RR=1.7, 95% CI 1.5-1.9, p<0.0001) and non-lung cancer mortality (RR=1.68 (95% CI 1.3-2.0, p<0.0001), but not lung cancer (RR=1.1, 95% CI 0.8-1.4, p=0.63).

# CONCLUSION

Diabetes increases the risk of death from all causes and non-lung cancer deaths among heavy smokers, and increases the risk for lung cancer mortality in women.

#### **CLINICAL RELEVANCE/APPLICATION**

Heavy smokers with diabetes are at increased risk for mortality from cancer at sites other than the lung in men and both lung and non-lung cancers in women compared to non-diabetic subjects.

# CH242-SD-SUB2

#### Thoracic Aortic Size by Race and Sex in a Community Dwelling Cohort: Results from the CARDIA Study

Sunday, Nov. 27 1:00PM - 1:30PM Room: CH Community, Learning Center Station #2

#### **Participants**

Andrew E. Kott, MD, Nashville, TN (*Presenter*) Nothing to Disclose Edmond K. Kabagambe, DVM,PhD, Nashville, TN (*Abstract Co-Author*) Nothing to Disclose David R. Jacobs Jr, PhD, Minneapolis, MN (*Abstract Co-Author*) Nothing to Disclose Joseph Yeboah, MD, Winston-Salem, NC (*Abstract Co-Author*) Nothing to Disclose James G. Terry, MS, Winston-Salem, NC (*Abstract Co-Author*) Nothing to Disclose John J. Carr, MD, MS, Nashville, TN (*Abstract Co-Author*) Nothing to Disclose Norrina B. Allen, PhD, Nashville, TN (*Abstract Co-Author*) Nothing to Disclose Yaorong Ge, PhD, Winston Salem, NC (*Abstract Co-Author*) Nothing to Disclose Steve Sidney, MD, MPH, Oakland, CA (*Abstract Co-Author*) Nothing to Disclose David C. Goff, MD,PhD, Aurora, CO (*Abstract Co-Author*) Nothing to Disclose

#### PURPOSE

Limited data on the size distribution of the thoracic aorta (Ao) in middle adult life is available; however, thoracic Ao aneurysm and dissection are a major cause of clinical disease. Non-contrasted, gated cardiac computed tomography (CCT) can be used to provide information about Ao size. In this study, we measured thoracic Ao size with CCT in community-dwelling black and white participants in the CARDIA study.

# **METHOD AND MATERIALS**

1,287 participants who completed thin-slice (<1 mm) CCT of the thoracic Ao during the CARDIA year 25 exam (Y25, 2010-11) were included. A 3D modeling program was used to provide measures of Ao cross-sectional area (mm2) and average diameter (mm) perpendicular to the vessel centerline at 14 locations in 4 Ao segments [root (3), ascending (3), arch (3), and descending (5)]. Demographics and clinical data were obtained at the same exam. The associations of various parameters with Ao size were assessed using multivariable linear models that accounted for potential confounders and mediating risk factors. Hypertension (HTN) was defined by medication use or BP $\geq$ 140/90.

#### RESULTS

Mean(SD) age for participants was 49.9(3.7) years, 54.5% were female, and 53.5% were black. Mean(SD) BMI was 30.5(7.2) kg/m2, 19.3% were current smokers, 13.7% had diabetes, 27.9% were treated for HTN, and 16.2% were treated for dyslipidemia. Male Ao were larger than those of females (Table). When comparing white and black race, whites had a larger Ao root and ascending Ao, and blacks had a larger Ao arch and descending Ao (Table). Participants with HTN compared with those without HTN had larger ascending [33.9(0.7) vs. 32.8(0.7)mm], arch [29.7(0.5) vs. 28.9(0.5)mm] and descending thoracic Ao [24.4(0.4) vs. 23.9(0.4)mm] diameters with all comparisons p<0.001. There was no difference in Ao root size (p=0.75) in participants with and without HTN.

#### CONCLUSION

Sex, race and HTN were associated with differences in mean Ao size. Compared to sex differences, race and HTN differences were relatively small ( $\leq$ 1.0mm). Ao imaging with CCT can be performed with a high degree of precision evidenced by our narrow standard errors in the study.

## **CLINICAL RELEVANCE/APPLICATION**

Thoracic Ao site-specific sex and race differences were demonstrated in this study. The association between HTN and Ao size was most prominent in sites not well visualized by trans-thoracic echocardiography.

Histogram Analysis of Apparent Diffusion Coefficient for Non-Small Cell Lung Cancer: Prediction of Tumor Grade, Lymphovascular Invasion, and Pleural Invasion

Sunday, Nov. 27 1:00PM - 1:30PM Room: CH Community, Learning Center Station #3

# Participants

Naoko Tsuchiya, Kahoku, Japan (*Presenter*) Nothing to Disclose Mariko Doai, Ishikawa, Japan (*Abstract Co-Author*) Nothing to Disclose Hisao Tonami, MD, Kahoku, Japan (*Abstract Co-Author*) Nothing to Disclose Katsuo Usuda, Kahoku, Japan (*Abstract Co-Author*) Nothing to Disclose

## PURPOSE

To investigate the application of histogram analysis of apparent diffusion coefficient (ADC) value in determining tumor grade, lymphovascular invasion, and pleural invasion of non-small cell lung cancer (NSCLC).

# METHOD AND MATERIALS

The study included sixty patients with surgically diagnosed NSCLC. Diffusion-weighted MR imaging (DWI) was performed in the axial plane using a spin-echo, echo-planar imaging sequence with respiratory triggering by navigator-echo method (b=0 and 800 sec/mm<sup>2</sup>). Calculated ADC maps were generated, and placed a 3-D volume-of-interest (VOI) on the tumor superimposing low b-value DWI. All ADC values within the VOI were used to compute the average ADC of the tumor. The ADC values were binned to construct the histogram. Using the histogram, mean, minimum, maximum, skewness, kurtosis, and percentiles (5th- 95th) of ADC of the entire tumor were computed. Histogram parameters were correlated with tumor grade, lymphovascular invasion, and pleural invasion. Receiver operating characteristic (ROC) analysis was performed for assessing diagnostic performance of histogram parameters in distinguishing different pathologic features.

#### RESULTS

The mean, maximum, 10th, 25th, 50th, 75th, 90th, and 95th percentiles of ADC showed significant differences among the pathological tumor grades. The 95th percentile of ADC achieved the highest area under curve (AUC), with a cut-off value of 0.001634mm<sup>2</sup>/sec and sensitivity and specificity of 0.846 and 0.667, respectively. The mean, skewness, kurtosis, 50th, 75th, 90th, and 95th percentiles of ADC showed significant difference between lymphovascular invasion subgroup. Kurtosis achieved the highest AUC, with a cut-off value of 1.081 and sensitivity and specificity of 0.612 and 0.909, respectively. The skewness showed significant difference between pleural invasion subgroup. For skewness, a cut-off value of 0.824 was associated with pleural invasion with sensitivity of 0.600 and specificity of 0.733.

#### CONCLUSION

ADC histogram analysis on the basis of the entire tumor volume is useful for predicting tumor grade, lymphovascular invasion, and pleural invasion of NSCLC.

# **CLINICAL RELEVANCE/APPLICATION**

ADC histogram analysis on the basis of the entire tumor volume is useful for predicting tumor grade and aggressiveness of non-small cell lung cancer.

Imaging of the Perineum in the Emergency Setting: A Pictorial Review

Sunday, Nov. 27 1:00PM - 1:30PM Room: ER Community, Learning Center Station #5

Awards Certificate of Merit Identified for RadioGraphics

#### **Participants**

Jihee Choe, MD, Boston, MA (*Presenter*) Nothing to Disclose Jeremy R. Wortman, MD, Boston, MA (*Abstract Co-Author*) Nothing to Disclose Aaron D. Sodickson, MD, PhD, Boston, MA (*Abstract Co-Author*) Research Grant, Siemens AG; Consultant, Bayer AG Bharti Khurana, MD, Boston, MA (*Abstract Co-Author*) Nothing to Disclose Jennifer W. Uyeda, MD, Boston, MA (*Abstract Co-Author*) Nothing to Disclose

## **TEACHING POINTS**

1) The perineal area can be easily overlooked by radiologists as pathologies are relatively infrequent and potentially complicated. 2) The anatomy of the perineum is complex. It is important for radiologists to be familiar with relevant anatomy of the perineum for accurate identification of origin and extent of the disease. 3) Various imaging modalities can be used to evaluate the perineum; however, CT is most commonly utilized in the acute setting. The widespread availability and rapid acquisition afforded by CT allows for the evaluation of acute perineal pathologies such as traumatic injury, infectious/inflammatory process, neoplastic process, and foreign body.

# TABLE OF CONTENTS/OUTLINE

1) Review anatomy of the perineum 2) Discuss role of the imaging modalities in evaluating the perineum3) Illustrate characteristic imaging features of common traumatic perineal injuries encountered in the emergency setting 4) Demonstrate various cases and imaging features of nontraumatic pathologies including infectious/inflammatory processes, neoplasms, and foreign bodies

#### **Honored Educators**

Presenters or authors on this event have been recognized as RSNA Honored Educators for participating in multiple qualifying educational activities. Honored Educators are invested in furthering the profession of radiology by delivering high-quality educational content in their field of study. Learn how you can become an honored educator by visiting the website at: https://www.rsna.org/Honored-Educator-Award/

Aaron D. Sodickson, MD, PhD - 2014 Honored Educator Bharti Khurana, MD - 2014 Honored Educator

# ER205-SD-SUB2

An Unusual Complication of a Common Finding: Acute Epiploic Appendagitis within Abdominal Wall Hernias -Frequency and Subtypes

Sunday, Nov. 27 1:00PM - 1:30PM Room: ER Community, Learning Center Station #2

#### Awards

#### **Student Travel Stipend Award**

#### Participants

Renata R. Almeida, boston, MA (*Presenter*) Nothing to Disclose Mohammad Mansouri, MD, MPH, Boston, MA (*Abstract Co-Author*) Nothing to Disclose Ajay K. Singh, MD, Boston, MA (*Abstract Co-Author*) Nothing to Disclose Bernardo C. Bizzo, MD, Boston, MA (*Abstract Co-Author*) Nothing to Disclose Michael H. Lev, MD, Boston, MA (*Abstract Co-Author*) Consulant, General Electric Company; Institutional Research Support, General Electric Company; Stockholder, General Electric Company; Consultant, MedyMatch Technology, Ltd; Consultant, Takeda Pharmaceutical Company Limited; Consultant, D-Pharm Ltd

#### PURPOSE

Acute Epiploic Appendagitis (AEA) as a complication of abdominal wall hernias is poorly studied in the literature. Our aim was to assess the prevalence of AEA within abdominal wall hernias, stratified by hernia subtype.

#### **METHOD AND MATERIALS**

This was an IRB approved HIPAA-compliant retrospective study. Our medical data base was searched for Computed Tomography (CT) cases of abdominal wall hernias occurring between 2003 and 2015, to assess the prevalence of AEA within hernia sacs. Imaging findings on CT were analyzed in the positive cases. Medical records were searched for clinical features and treatment.

## RESULTS

Among 4352 abdominal wall hernias from 4069 patients, 44% (1952/4352) were inguinal, 4.1% (185/4352) Spigelian, 1.5% (64/4352) femoral and 49.4% (2151/4352) ventral hernias. Nine patients had AEA within hernia sacs (Mean age: 70.7 years; 66.7% males). The prevalence of AEA was 0.2% (9/4352) within all abdominal wall hernias, 2.2% within Spigelian (4/185), 0.25% (5/1952) within inguinal, and 0% within femoral and ventral hernias. 77.8% (7/9) of the patients had previous history of anterior abdominal wall surgery. Imaging features included fat stranding (88.9%;8/9), central dot (44.5%;4/9), two inflamed epiploic appendages (33.3%;3/9) and fluid inside the hernia sac (33.3%;3/9). In 66.7% (6/9) only the inflamed appendage was herniated. All the cases presented with local pain. Hernia sacs were incarcerated in 4 cases; strangulated in 1 case, and non-palpable in 4 cases. Hernia treatment was conservative in 55.5% (5/9) and surgical in 44.5% (4/9).

# CONCLUSION

AEA within hernia sacs is rare. This complication is exceedingly unlikely (0%) among ventral or femoral hernias, very unusual in inguinal hernias (0.25%), and most likely to occur within Spigelian hernias (2.2%). Patients were most commonly elderly males with a history of previous abdominal wall surgery.

## **CLINICAL RELEVANCE/APPLICATION**

Emergency radiologists should be aware that AEA as a complication of abdominal wall hernia is very rare, but when it does occur is most likely within Spigelian hernias.

Performance of an Ultrasound-First ED Consensus Imaging Algorithm for Suspected Acute Appendicitis Above and Below an Alvarado Score of 3

Sunday, Nov. 27 1:00PM - 1:30PM Room: ER Community, Learning Center Station #3

# Participants

Urvi P. Fulwadhva, MD, Boston, MA (*Presenter*) Nothing to Disclose Sarah Frasure, MD, Boston, MA (*Abstract Co-Author*) Nothing to Disclose Wendy B. Landman, MD, Boston, MA (*Abstract Co-Author*) Nothing to Disclose Jeremy R. Wortman, MD, Boston, MA (*Abstract Co-Author*) Nothing to Disclose Amy Hildreth, Boston, MA (*Abstract Co-Author*) Nothing to Disclose Naomi Schimizu, Boston, MA (*Abstract Co-Author*) Nothing to Disclose Micheal Stone, Boston, MA (*Abstract Co-Author*) Nothing to Disclose Aaron D. Sodickson, MD, PhD, Boston, MA (*Abstract Co-Author*) Research Grant, Siemens AG; Consultant, Bayer AG

#### PURPOSE

We recently implemented an US-first consensus-imaging algorithm for suspected acute appendicitis in non-obese patients younger than 40 years old. The purpose of this study was to evaluate algorithm performance stratified by Alvarado scores above and below a threshold of 3.

## **METHOD AND MATERIALS**

Methods and Materials: This HIPAA compliant, IRB approved retrospective study included 277 consecutive ER patients who underwent appendix ultrasound from May 2015 to Feb 2016 based on a new interdepartmental US-first consensus algorithm with CT following inconclusive US. The Alvarado score for all patients was calculated, and patients stratified into scores 3. The patients were then divided based on results of US (normal appendix, appendix not seen no secondary, equivocal US and acute appendicitis). Sensitivity and specificity was calculated.

## RESULTS

Of 111 patients with Alvarado =/<3, US reported a normal appendix in 4, appendix not seen in 92, equivocal findings in 13, and suspected appendicitis in 2. 53 (47.7%) proceeded to CT, 2 (1.8%) to the OR, and none ultimately proved to have appendicitis. 17 (15.3%) had alternative diagnoses explaining symptoms by US, 13 (24%) by CT. The specificity is 98% with NPV of 100%.Of 165 patients with Alvarado >3, US reported a normal appendix in 3, appendix not seen in 99, equivocal findings in 41, and suspected appendicitis in 22. 101 (60%) proceeded to CT, 49 (29%) to the OR, and 44 had pathology proven appendicitis. 27 (16%) had alternative diagnoses explaining symptoms by US, 23 (22%) by CT. Sensitivity and specificity is 44% and 98% with NPV of 82%.

# CONCLUSION

Ultrasound has a higher negative predictive value and should be used as a first tool for evaluation of non-obese young patients with suspected appendicitis with Alvarado score less than 3. Percentage of patients with alternative diagnosis on either CT or US was similar between the two groups.

# **CLINICAL RELEVANCE/APPLICATION**

Appendix US has higher negative predictive value and should be used as first tool for evaluation of non-obese young patients age less than 40 years with Alvarado score less than 3.

#### **Honored Educators**

Presenters or authors on this event have been recognized as RSNA Honored Educators for participating in multiple qualifying educational activities. Honored Educators are invested in furthering the profession of radiology by delivering high-quality educational content in their field of study. Learn how you can become an honored educator by visiting the website at: https://www.rsna.org/Honored-Educator-Award/

Aaron D. Sodickson, MD, PhD - 2014 Honored Educator

Inadequate Clinical Information in Emergency Radiology Consultations - Does It Really Affect the Error Rate or Is It Merely a Bugbear?

Sunday, Nov. 27 1:00PM - 1:30PM Room: ER Community, Learning Center Station #4

# Participants

Anjali Agrawal, MD, Delhi, India (*Presenter*) Nothing to Disclose Arjun Kalyanpur, MD, Bangalore, India (*Abstract Co-Author*) CEO, Teleradiology Solutions Pvt Ltd

## PURPOSE

The frustration of receiving inadequate clinical information during a referral is well known to any practicing radiologist. We sought to determine if there was any correlation between the quality of clinical information and the types of errors in our emergency teleradiology practice.

# METHOD AND MATERIALS

We maintain a record of cases sent for quality assurance (QA) review by our client radiology practices. These comprise less than 1% of all cases and are scored as per ACR RADPEER guidelines, ranging from 1 (no error) to 4 (obvious miss), further denoted as "a" (clinically insignificant) or "b" (clinically significant). In 831 cases flagged for QA review, we additionally scored the quality of clinical information – category 1 (inadequate), 2 (adequate), 3 (detailed), for the study type ordered, and without knowledge of the missed findings or the QA grade. Similarly, we also scored 304 cases where no QA was flagged. Chi-square tests and regression models were used to determine the associations between quality of clinical information and radiologic error.

## RESULTS

Surprisingly, detailed histories (Category 3) were less frequent in the cases without QA than those with QA or error (p < 0.01). There was no significant influence of clinical information score upon QA category. More history did not reduce the rates of obvious errors or any errors. Stronger effects were seen for the type of study, with MR studies being significantly associated with increased rates of clinically significant (ACR "b") errors (p=0.008). The level of clinical information was not associated with any reduction in the proportion of significant error (ACR2b, 3b, 4b), when compared to no error.

# CONCLUSION

It is likely that experienced radiologists do not require much clinical information to reach an accurate radiological diagnosis in the emergent setting with a relatively well defined mix of cases. Whether this is also true for radiologists-in-training or those in the early years of practice needs to be tested.

# **CLINICAL RELEVANCE/APPLICATION**

Perceived inadequate clinical information by radiologists does not translate to increased rates of radiologic error, at least in an emergency radiology setting with experienced radiologists.

Liver Iron Quantification with MRI: A Primer for Radiologists

Sunday, Nov. 27 1:00PM - 1:30PM Room: GI Community, Learning Center Station #7

#### Awards Certificate of Merit Identified for RadioGraphics

#### **Participants**

Roxanne Labranche, MD, Montreal, QC (*Presenter*) Nothing to Disclose Kim-Nhien Vu, MD, Montreal, QC (*Abstract Co-Author*) Nothing to Disclose Denis Soulieres, MD, MSc, Montreal, QC (*Abstract Co-Author*) Nothing to Disclose Guillaume Gilbert, PhD, Montreal, QC (*Abstract Co-Author*) Employee, Koninklijke Philips NV Leonie Petitclerc, MSc, Montreal, QC (*Abstract Co-Author*) Nothing to Disclose Jean-Sebastien S. Billiard, MD, Montreal, QC (*Abstract Co-Author*) Nothing to Disclose Milena Cerny, MD, Montreal, QC (*Abstract Co-Author*) Nothing to Disclose Damien Olivie, MD, MS, Montreal, QC (*Abstract Co-Author*) Nothing to Disclose An Tang, MD, Montreal, QC (*Abstract Co-Author*) Advisory Board, Imagia Cybernetics Inc

## **TEACHING POINTS**

This educational exhibit will: 1) review the pathophysiology of iron overload, 2) review MRI-based iron quantification techniques, and 3) illustrate these techniques with clinical vignettes.

# TABLE OF CONTENTS/OUTLINE

1) Introduction: clinical indications for liver iron quantification (detection, quantification and assessment of treatment response). 2) Overview of etiology and pathophysiology of iron overload:a. Summary of clinical conditions associated with iron overload.b. Anatomical diagrams of iron overload distribution in hemochromatosis and hemosiderosis.3) Review of MRI-based iron quantification techniques: a. Diagrams illustrating the tissue contrast mechanisms for each technique.i. Concepts of R2\* and T2\* mapping.ii. Concepts of R2 and T2 mapping.iii. Quantitative susceptibility mapping.iv. Liver-muscle signal ratio.b. Summary of MRI protocols with sequences and acquisition parameters.c. Comparison of advantages and limitations of each technique.4) Clinical application:a. Summary table with clinical thresholds for different levels of iron overload severity and associated complications.b. Clinical vignettes.5) Technical pitfalls: severe iron overload.6) Future directions: simultaneous iron and fat quantification; pancreatic iron quantification.7) Summary of key teaching points.

# Technical Best Practices for Contrast-enhanced Ultrasound of Focal Liver Lesions

Sunday, Nov. 27 1:00PM - 1:30PM Room: GI Community, Learning Center Station #8

FDA Discussions may include off-label uses.

#### **Participants**

Alexander M. Vezeridis, MD, PhD, La Jolla, CA (Presenter) Nothing to Disclose

Yuko Kono, MD, PhD, San Diego, CA (Abstract Co-Author) Nothing to Disclose

David O. Cosgrove, MBBCh, FRCR, London, United Kingdom (*Abstract Co-Author*) Research Consultant, SuperSonic Imagine Research Consultant, Bracco Group Speakers Bureau, Toshiba Corporation

Christoph F. Dietrich, MD, Frankfurt Am Main, Germany (Abstract Co-Author) Nothing to Disclose

Hyun-Jung Jang, MD, Toronto, ON (Abstract Co-Author) Nothing to Disclose

Avinash R. Kambadakone, MD, Boston, MA (Abstract Co-Author) Nothing to Disclose

Tae Kyoung Kim, MD, PhD, Toronto, ON (Abstract Co-Author) Nothing to Disclose

Andrej Lyshchik, MD, PhD, Philadelphia, PA (Abstract Co-Author) Nothing to Disclose

Donald G. Mitchell, MD, Philadelphia, PA (Abstract Co-Author) Consultant, CMC Contrast AB

Fabio Piscaglia, Bologna, Italy (Abstract Co-Author) Research support, Bracco Group Speaker, Bayer AG Advisory Board, Bayer AG Speaker, Siemens AG

Cynthia S. Santillan, MD, San Diego, CA (Abstract Co-Author) Consultant, Robarts Clinical Trials, Inc

Claude B. Sirlin, MD, San Diego, CA (Abstract Co-Author) Research Grant, General Electric Company; Research Grant, Siemens AG; Research Grant, Guerbet SA; ;

Juergen K. Willmann, MD, Stanford, CA (*Abstract Co-Author*) Research Consultant, Bracco Group; Research Grant, Siemens AG; Research Grant, Bracco Group; Research Grant, Koninklijke Philips NV; Research Grant, General Electric Company; Advisory Board, Lantheus Medical Imaging, Inc; Advisory Board, Bracco Group

Stephanie R. Wilson, MD, Calgary, AB (*Abstract Co-Author*) Equipment support, Siemens AG; Equipment support, Koninklijke Philips NV

# **TEACHING POINTS**

1. Understand indications for, benefits and limitations of, and common referral patterns for CEUS of focal liver observations2. Review commonly used ultrasound contrast agents for evaluation of focal liver observations3. Understand technical considerations and resources for liver CEUS as a first step towards bringing liver CEUS to the learner's institution

## TABLE OF CONTENTS/OUTLINE

1. Indications for, benefits and limitations of, and common referral patterns for CEUS of focal liver observations.2. Ultrasound contrast agents a. Lumason -- the first ultrasound contrast agent approved by the FDA for evaluation of focal liver lesions b. Definity -- an 'off-label' agent3. Preparation and essential equipment a. Ultrasound machines and transducers b. c. Data storage and PACS transfer d. Equipment for contrast agent preparation Contrast-specific harmonic imaging modes and injection4. Step-by-step approach of a CEUS examination to evaluate focal liver lesions a. Non-contrast examination b. c. Contrast agent preparation and injection d. Multiphase CEUS imaging -- including arterial, portal venous, Vascular access and late phases. Reviewed topics include timing, documentation methods, and troubleshooting tips e. General qualitative and quantitative analysis of ultrasound contrast enhancement

# Pain Management in Cancer Patient: Palliative Care using High Intensity Focused Ultrasound

Sunday, Nov. 27 1:00PM - 1:30PM Room: GI Community, Learning Center Station #9

#### Awards

#### **Identified for RadioGraphics**

#### **Participants**

Susan Dababou, Rome, Italy (*Abstract Co-Author*) Nothing to Disclose Roberto Scipione, Terracina, Italy (*Abstract Co-Author*) Nothing to Disclose Hans Peter Erasmus, Rome, Italy (*Presenter*) Nothing to Disclose Cristina Marrocchio, rome, Italy (*Abstract Co-Author*) Nothing to Disclose Carlo Catalano, MD, Rome, Italy (*Abstract Co-Author*) Nothing to Disclose Alessandro Napoli, MD, Rome, Italy (*Abstract Co-Author*) Nothing to Disclose

#### **TEACHING POINTS**

1. According to BMJ clinical evidence, up to 80% of cancer patients experience pain requiring opioids analgesics. 2. The management of pain in cancer patient is crucial to improve the quality of life and the survival, with oral morphine as the standard opioid used for the management of moderate to severe cancer-related pain. The major benefit of HIFU is the immediate reduction in analgesic consumption with an improvement of the quality of life. 3. High Intensity focused ultrasound (HIFU) is a non-invasive ablation method that induces coagulative necrosis through thermal tissue stimulation. In a single session, pain resolution is achieved by using MRI sequences for accurate targeting, real time monitoring and control of energy deposition. 4. The thermal effect of high intensity US beam on the tissue improve the drug delivery, improving the outcome of targeted therapy.

#### **TABLE OF CONTENTS/OUTLINE**

1) Cancer-related pain:a) Aetiology and clinical presentation 2) Conventional therapies: a) Pharmacological treatment and other invasive treatments (e.g. nerve blocks)c) Limitations and Side effects 3) MRgFUS:a) Basics b) Pain palliation: comparison with conventional and invasive therapiesc) A multi-pronged approach with HIFUd) CASE REPORTS4) Discussion: a) Future of MRgFUS, its potential in the management of cancer patient.

The Utility of LI-RADS v2014 to Characterize the Nodules Detected during Hepatocarcinogenesis in HBVrelated Liver Cirrhosis: A Comparative Study of MR Imaging and Pathology

Sunday, Nov. 27 1:00PM - 1:30PM Room: GI Community, Learning Center Station #1

# Participants

Zhang Qi, Beijing, China (*Presenter*) Nothing to Disclose Hongjun Li, Beijing, China (*Abstract Co-Author*) Nothing to Disclose

# PURPOSE

To study the correlationship between the Liver Imaging and Reporting Data System(LI-RADS)v2014 with magnetic resonance(MR)imaging and hisological grade of nodules in HBV-related liver cirrhosis.

# METHOD AND MATERIALS

Between Decemember 2012 to February 2016, 178 patients with HBV-related liver cirrhosis who had nodules 30mm or smaller detected at MRI were included and all patients provided written informed consent before the study . A LI-RADS category was retrospectively assigned to each nodule on MRI. Final diagnosis was assessed using pathologic diagnosis only (operation or biopsy). We calculate the percentage of the nodules in each LI-RADS category, and analyze with the Chi-square test(P<0.001).The diagnostic accuracy for each LI-RADS category was described by sensitivity, specificity, and positive and negative predictive values .

#### RESULTS

we finally analyzed 192 nodules ,8 regenerative nodules(RNs),16 low grade dysplastic nodules(LGDNs),30 high grade dysplastic nodules(HGDNs),35 early HCCs(eHCCs),103 progressed HCCs(pHCCs).None (0%) of five LI-RADS category 1 lesions,1(9.9%)nodules had a LR-2 assement,consisting of 7 (36.8%)RNs and 12(63.2%)LGDNs;23(12%),a LR-3 assement,consisting of 1(4.3%) RNs,4 (17.4%)LGDNs,12(52.2%)HGDNs,4 (17.4%) eHCCs and 2(8.7%) pHCCs;62(32.3%) a LR-4 assement, including 16(25.8%) HGDNs, 25(40.3%)eHCCs and 21 (33.9%)pHCCs;88(45.8%) a LR-5 assement, including 2(,2.3%) HGDNs, 6(6.7%) eHCCs and 80(90.9%) pHCCs(P<0.001).PPV,sensitivity of HCC diagnosis for LR-5 were higher than that for LR-4(97.7%,65.2% VS 74.2%,34.8%).PPV,sensitivity of LR-3 for HCC+HGDN diagnosis were higher than that for HCC diagnosis only (78.3%,11%vs 26.1%,4.9%).

# CONCLUSION

There is no dirrect correlationship between the LI-RADS with magnetic resonance(MR)imaging and hisological grade of nodules in HBV-related liver cirrhosis, whereas LR-5 criteria had excellent PPV for diagnosing HCC, LR-4 and LR-3 criteria were useful in estimating the probability of malignancy.

# **CLINICAL RELEVANCE/APPLICATION**

LI-RADS is recommended for patients with liver cirrhosis to assess the likelihood of malignancy for MR imaging detected nodules. In particular, a relevant proportion of HGDNs (known as the precancerous lesions) were categorized as LI-RADS category 3 or 4, LI-RADS may help to determin the correct diagnostic workup during further clinical practice.

Ultrasonographic Changes at 12 Weeks of Anti-TNF Drugs Predict 1-year Sonographic Response and Clinical Outcome in Crohn Disease: A Multicenter Study

Sunday, Nov. 27 1:00PM - 1:30PM Room: GI Community, Learning Center Station #3

# Participants

Tomas Ripolles, MD, Valencia, Spain (*Abstract Co-Author*) Nothing to Disclose Gregorio Martin, MD, Valencia, Spain (*Presenter*) Nothing to Disclose Mj Martinez-Perez, MD, Valencia, Spain (*Abstract Co-Author*) Nothing to Disclose Jose M. Paredes, MD, PhD, Valencia, Spain (*Abstract Co-Author*) Nothing to Disclose Jordi Rimola, MD, Barcelona, Spain (*Abstract Co-Author*) Nothing to Disclose Jordi Rimola, MD, Barcelona, Spain (*Abstract Co-Author*) Consultant, Robarts Clinical Trials Arantza Jauregui-Amezaga, Barcelona, Spain (*Abstract Co-Author*) Nothing to Disclose Jose Vizuete, Valencia, Spain (*Abstract Co-Author*) Nothing to Disclose Fructuoso Delgado, MD, Valencia, Spain (*Abstract Co-Author*) Nothing to Disclose

#### PURPOSE

to assess the long-term effect of biological treatment on transmural lesions of Crohn's Disease (CD) evaluated with ultrasound, including contrast-enhanced US (CEUS).

## METHOD AND MATERIALS

51 patients with active CD were included in a prospective multicenter longitudinal study. All patients underwent a clinical assessment and sonographic examination at baseline, 12 weeks after treatment initiation and after 1-year of treatment. Patients were clinically followed at least 2 years from inclusion until the end of the study. Ultrasonographic evaluation included bowel wall thickness, color Doppler grade, parietal enhancement and presence of transmural complications or stenosis. Sonographic changes after treatment were classified as normalization, improvement or lack of response.

#### RESULTS

improvement at 52 weeks was more frequent in patients with improvement at final of induction (12 weeks) compared with patients who did not improve (85% versus 28%; p < 0.0001). 1-year sonographic evolution correlated with clinical response; 28 out of 29 (96,5%) patients with sonographic improvement at 52 weeks showed clinical remission or response. Patients without sonographic improvement at 52 weeks of treatment were more likely to have a change or intensification in medication or surgery (13/20, 65%) during the next year of follow-up than patients with improvement on the sonography (3/28, 11%). Stricturing behavior was the only sonographic feature associated to a negative predictive value of response (p=0.0001).

#### CONCLUSION

sonographic response after 12 weeks of therapy is more pronounced and predicts 1-year sonographic response. Sonographic response at 1-year examination correlates with 1-year clinical response and is a predictor of further treatment's efficacy, 1-year or longer period of follow-up.

#### **CLINICAL RELEVANCE/APPLICATION**

Clinical assessment of CD has low accuracy to predict active disease or remission. Therapeutic responses should be monitored objectively -not only based on symptom control-Monitoring the disease through the use of cross-sectional imaging is gaining increased acceptance as it has advantages over endoscopy. Achievement transmural healing or improvement on sonographic examination after anti-TNF therapy is associated with better outcomes. Imaging monitoring allows medical optimization and individualization of treatment

# GI352-SD-SUB4

Comparison of Measured and Estimated Organ Doses from Two Radiation Dose Tracking Software at Different kV

Sunday, Nov. 27 1:00PM - 1:30PM Room: GI Community, Learning Center Station #4

# Participants

Atul Padole, MD, Boston, MA (*Presenter*) Nothing to Disclose
Yiming Gao, Troy, NY (*Abstract Co-Author*) Employee, Virtual Phantoms, Inc
Alexi Otrakji, MD, Boston, MA (*Abstract Co-Author*) Nothing to Disclose
Bob Liu, PhD, Boston, MA (*Abstract Co-Author*) Nothing to Disclose
George Xu, PhD, Troy, NY (*Abstract Co-Author*) Nothing to Disclose
Mannudeep K. Kalra, MD, Boston, MA (*Abstract Co-Author*) Technical support, Siemens AG; Technical support, Medical Vision

## PURPOSE

To compare the measured and estimated CT organ doses from two radiation dose tracking (RDT) software at different tube voltage (kV) using fixed tube current (mAs) and automatic exposure control (AEC) techniques in a human cadaver.

# METHOD AND MATERIALS

In an IRB approved study, ionization chambers (Radcal) were surgically implanted in an adult male human cadaver (88 yrs, male, 68 kg) in six locations including the liver, stomach, small intestine, left kidney, colon, and urinary bladder. The cadaver was scanned with routine abdomenopelvis CT protocol on a 128-slice dual-source MDCT scanner (Siemens Definition FLASH) at 8 different settings – 4 with AEC (at constant CTDIvol 2.5mGy) & 4 with fixed mAs (at constant CTDIvol 4mGy). Scans were performed at 80, 100, 120 and 140 kV with mA values changed to achieve the abovementioned CTDIvol for each kV. All other scanning parameter were held constant including pitch of 0.9:1, rotation time of 0.5 second, and detector configuration of 128\*0.6 mm. Scanning was repeated three times for each setting and organ doses were recorded for each acquisition (total series = 4\*3\*2=24). All CT image series were exported to the web-based RDT software: eXposure (Bayer, Germany) and VirtualDose (Albany, NY) to obtain estimated organ doses.

# RESULTS

At constant CTDIvol, there was a variation (not statistically significant) in measured organ doses at different kV (both fixed mAs and AEC); lower kV was associated with lower organ doses (p=0.7). However, there were significant variation in estimated organ doses from both RDT software at different kV (p<0.02). The estimated organ doses from both RDT software were lowest at 80 kV compared to 140 kV (p<0.02). The estimated organ doses from VirtualDose were significantly lower than measured (except for 80 kV) and estimated organ doses from eXposure for both fixed mAs and AEC (p<0.02). The estimated organ doses from eXposure were significantly lower than measured (except for 80 kV) and estimated organ doses from eXposure for both fixed mAs and AEC (p<0.02). The estimated organ doses from eXposure were significant (p=0.9).

# CONCLUSION

At constant CTDIvol, both measured and estimated organ doses fluctuate with different kV; lower kV settings are associated with lower dose for both fixed mAs and AEC. The estimated organ doses from VirtualDose were substantially lower than measured and estimated organ doses from eXposure.

#### **CLINICAL RELEVANCE/APPLICATION**

CT at lower kV settings is associated with lower organ doses even at constant CTDIvol.

Intravoxel Incoherent Motion Diffusion-weighted Imaging: Measurement Repeatability of Quantitative Parameters in Rectal Cancer with Different b Values

Sunday, Nov. 27 1:00PM - 1:30PM Room: GI Community, Learning Center Station #5

# Participants

Hongliang Sun, MD, Beijing, China (*Presenter*) Nothing to Disclose Yanyan Xu, Beijing, China (*Abstract Co-Author*) Nothing to Disclose Kaining Shi, PhD, Beijing, China (*Abstract Co-Author*) Nothing to Disclose Wu Wang, MD, PhD, Beijing, China (*Abstract Co-Author*) Nothing to Disclose

## PURPOSE

To verify the possible influence of different b values on intravoxel incoherent motion imaging (IVIM) parameters in rectal cancer.

# METHOD AND MATERIALS

Twenty-six patients with rectal cancer were included in this retrospective study. All diffusion-weighted imaging (DWI) scanning was completed in a 3.0T MR with 16 b-values (0-2000s/mm2). IVIM parameters [D (diffusion coefficient), f (perfusion fraction) and D\* (pseudodiffusion coefficient)] quantification and image analysis were all conducted by IDL 6.3 software with the whole range of adopted b values(0, 10,20,30,40,60,80,100,150,200,400,800,1000,1200,1500 and 2000s/mm2) and 8 of adopted b values(0, 40, 80, 100, 150, 400, 800 and 1000s/mm2), respectively. Quantitative analysis was performed by two observers with manually defined regions of interest (ROI) along the outline of tumor maximal dimension. The IVIM parameters values calculated with 16 b-values and 8 b-values, as well as the corresponding inter-observer variation values, were compared by using paired samples t test or Wilcoxon signed ranks test, respectively. The inter-observer variation of the IVIM parameters were assessed based on the repeatability coefficient and Bland-Altman limits of agreement.

## RESULTS

No significant differences were demonstrated in the values of these three parameters with different b-values (p = 0.111 for D, p = 0.517 for f, and p = 0.657 for D\*), as well as in the inter-observer variation of the IVIM parameters(p = 0.230 for D, p = 0.050 for f, and p = 0.304 for D\*). However, the repeatability coefficient and Bland-Altman bias of eight b-values relevant IVIM parameters (35.2%, 126.3%, and 197.4% for D, f, and D\* respectively; 6.6%, -21.6%, and -20.7% for D, f, and D\* respectively) were greater than that of 16 b-values relevant IVIM parameters (14.6%, 50.8%, and 55.2% for D, f, and D\* respectively; -0.3%, -7.6%, and 3.6% for D, f, and D\* respectively).

## CONCLUSION

Although no significant differences were established between 8 and 16 b-values IVIM parameters, the latter ones showed less repeatability coefficient and Bland-Altman bias, indicating better measurement repeatability.

#### **CLINICAL RELEVANCE/APPLICATION**

Rectal IVIM with more b values may provide accurate parameters for assessing diffusion and perfusion , which is helpful for longitudinal evaluation of therapy response.

# MRI Liver Surface Nodularity Score as a New Noninvasive Biomarker for Chronic Viral Hepatitis

Sunday, Nov. 27 1:00PM - 1:30PM Room: GI Community, Learning Center Station #6

#### **Participants**

Kelly L. Cox, DO, Atlanta, GA (*Presenter*) Nothing to Disclose Sadhna Nandwana, MD, Atlanta, GA (*Abstract Co-Author*) Nothing to Disclose Babatunde Olaiya, MD, Atlanta, GA (*Abstract Co-Author*) Nothing to Disclose Pardeep K. Mittal, MD, Atlanta, GA (*Abstract Co-Author*) Nothing to Disclose Oluwayemisi Ibraheem, MD, Atlanta, GA (*Abstract Co-Author*) Nothing to Disclose Zhengjia Chen, PhD, Atlanta, GA (*Abstract Co-Author*) Nothing to Disclose Chao Zhang, Atlanta, GA (*Abstract Co-Author*) Nothing to Disclose Andrew D. Smith, MD, PhD, Jackson, MS (*Abstract Co-Author*) Research Grant, Pfizer Inc; President, Radiostics LLC; President, Liver Nodularity LLC; President, Color Enhanced Detection LLC; President, eMASS LLC; Pending patent, Liver Nodularity LLC; Pending patent, Color Enhanced Detection LLC; Pending patent, eMASS LLC;

#### PURPOSE

Evaluate the accuracy of liver surface nodularity (LSN) score on magnetic resonance imaging (MRI) as a quantitative imaging biomarker for diagnosing cirrhosis in patients with viral chronic liver disease (vCLD) alone and in combination with fibrosis-4 (FIB-4) index.

#### **METHOD AND MATERIALS**

IRB approved, HIPAA compliant database search identified patients with vCLD who underwent liver MRI during 2005-2015, had a liver biopsy within 6 months of MRI or any prior biopsy with cirrhosis, and laboratory data to calculate FIB-4 index within 3 months of MRI. 10 LSN scores per patient were measured utilizing Liver Surface Nodularity Software on all cases by reviewer 1 and 50 cases by reviewer 2. LSN score mean, median (mdn) and standard deviation (SD) were calculated. Intra-class correlation between reviewers was estimated with Cronbach's alpha. Wilcoxon rank-sum test explored associations between LSN scores, FIB-4 index and Scheuer staging. Receiver operator characteristic (ROC) curve analysis assessed accuracy of LSN score alone and in combination with FIB-4 index.

#### RESULTS

152 cases (54 F: 98 M) of which 45 were non-cirrhotic and 107 were cirrhotic. Mean and mdn LSN scores were 3.85 and 3.68 (SD=0.91) with high inter-observer agreement between reviewers (Cronbach's alpha=0.950, p<0.001). LSN scores were higher for cirrhotic (mdn 4.00, range 2.01-7.68) than for non-cirrhotic cases (mdn 3.31, range 1.76-5.43), p<0.0001. FIB-4 index scores were also higher for cirrhotic (mdn 7.75, range 1.44-30.89) than for non-cirrhotic cases (mdn 1.77, range 0.68-9.80), p<0.001. LSN scores had high accuracy for differentiating cirrhotic from non-cirrhotic cases (AUC=0.774, p<0.001). Accuracy increased when LSN scores were combined with FIB-4 index (AUC=0.923, p<0.001).

# CONCLUSION

While MRI LSN score alone can be used as a quantitative imaging biomarker for the diagnosis of cirrhosis, the combination of both imaging and clinical biomarkers (LSN score and FIB-4 index) has substantial increased diagnostic accuracy for cirrhosis.

#### **CLINICAL RELEVANCE/APPLICATION**

Utilizing MRI LSN score as an imaging biomarker in conjunction with FIB-4 index has high diagnostic accuracy for cirrhosis and could serve as an alternative to liver biopsy in the setting of vCLD.

## **Honored Educators**

Presenters or authors on this event have been recognized as RSNA Honored Educators for participating in multiple qualifying educational activities. Honored Educators are invested in furthering the profession of radiology by delivering high-quality educational content in their field of study. Learn how you can become an honored educator by visiting the website at: https://www.rsna.org/Honored-Educator-Award/

Pardeep K. Mittal, MD - 2016 Honored Educator

# Can Quantitative Contour Analysis be a Marker for Biologic Behavior of T1 Clear Cell Renal Cell Carcinomas?

Sunday, Nov. 27 1:00PM - 1:30PM Room: GU/UR Community, Learning Center Station #2

#### **Participants**

Felix Y. Yap, MD, Los Angeles, CA (*Presenter*) Nothing to Disclose Chidubem G. Ugwueze, MS, Los Angeles, CA (*Abstract Co-Author*) Nothing to Disclose Megha N. Gupta, MD, Los Angeles, CA (*Abstract Co-Author*) Nothing to Disclose Mike Kwon, BS,MS, Los Angeles, CA (*Abstract Co-Author*) Nothing to Disclose Darryl Hwang, PhD, Los Angeles, CA (*Abstract Co-Author*) Nothing to Disclose Bino Varghese, Los Angeles, CA (*Abstract Co-Author*) Nothing to Disclose Steven Cen, PhD, Los Angeles, CA (*Abstract Co-Author*) Nothing to Disclose Mihir Desai, Los Angeles, CA (*Abstract Co-Author*) Nothing to Disclose Inderbir Gill, MD, Los Angeles, CA (*Abstract Co-Author*) Nothing to Disclose Vinay A. Duddalwar, MD, FRCR, Los Angeles, CA (*Abstract Co-Author*) Nothing to Disclose

#### PURPOSE

Clear cell renal cell carcinomas (ccRCC) smaller than 7 cm may be upstaged to pT3 based on imaging or histopathological evidence of vascular invasion. We investigated whether these pT3 tumors demonstrated greater morphologic irregularity on imaging in retrospect that could have portended their more aggressive behavior than pT1 tumors.

#### **METHOD AND MATERIALS**

Computerized tomography (CT) images of patients with cT1 renal masses, including 21 patients with pT1 ccRCC and 11 patients with pT3 ccRCC, between 2011 and 2014 were manually segmented using Synapse 3D (Fujifilm, Stamford, CT). Tessellated 3D models of the tumor were created from the segmented voxels using custom MATLAB code. Eleven shape descriptors were then calculated per tumor: compactness, mean radial distance (RD), RD standard deviation (RDSD), RD area ratio (RDAR), zero crossings, entropy, Feret ratio (FR), convex hull area (CHA) and perimeter (CHP) ratios, elliptic compactness (EC), and sphericity (SPH). The morphometric parameters of pT3 and pT1 RCCs were compared using the Wilcoxon rank-sum test to test the hypothesis that pT3 RCC tumors demonstrate more morphologic irregularity than pT1 RCC.

#### RESULTS

Quantitative contour analysis was technically successful in all cases. pT3 RCCs were less spherical than pT1 RCCs (0.89 vs 0.93, p < 0.01). There were also significant differences between pT1 and pT3 RCCs in 2 parameters when analyzed in the transverse, coronal, and sagittal orientations: CHP (0.92 vs 0.95, p = 0.01; 0.89 vs 0.94, p < 0.01; 0.89 vs 0.95, p < 0.01) and EC (0.88 vs 0.92, p = 0.04; 0.84 vs 0.90, p = 0.01, 0.85 vs 0.90, p < 0.01). Some shape metrics (compactness, RDM, RDAR, RDSD, entropy) were statistically significant in the transverse orientation but showed nonsignificant differences in the coronal and sagittal orientations.

# CONCLUSION

Computerized renal tumor image analysis using shape descriptors is technically feasible and efficient. 3 shape metrics may help distinguish between cT1 and cT3 ccRCCs, and may be additional quantifiable parameters that can help in differentiating between subtypes of other renal tumors.

# **CLINICAL RELEVANCE/APPLICATION**

True objective and quantitative metrics can distinguish between cT1 and cT3 RCCs on imaging and potentially may be able to identify aggressive biologic behavior.

Bubble Over Sign on Computed Tomography Helps Differentiate Fat-poor Angiomyolipoma from Renal Cell Carcinoma: Retrospective Analysis of Consecutive 602 Subjects

Sunday, Nov. 27 1:00PM - 1:30PM Room: GU/UR Community, Learning Center Station #3

# Participants

Yong Hee Kim, MD, Seoul, Korea, Republic Of (*Presenter*) Nothing to Disclose Sung Yoon Park, Seoul, Korea, Republic Of (*Abstract Co-Author*) Nothing to Disclose Young Taik Oh, MD, Seoul, Korea, Republic Of (*Abstract Co-Author*) Nothing to Disclose Dae Chul Jung, MD, Seoul, Korea, Republic Of (*Abstract Co-Author*) Nothing to Disclose Nam Hoon Cho, Seoul, Korea, Republic Of (*Abstract Co-Author*) Nothing to Disclose Minsu Lee, MD, Seoul, Korea, Republic Of (*Abstract Co-Author*) Nothing to Disclose

## PURPOSE

To assess whether morphologic analysis using computed tomography (CT) can help differentiate fat-poor angiomyolipoma (AML) from renal cell carcinoma (RCC).

# METHOD AND MATERIALS

Consecutive 602 patients with a histologically confirmed fat-poor AML (n= 49) or renal cell carcinoma (n= 553) were found between January 2006 and May 2015. Lesion size was less than 4cm on contrast-enhanced CT. For morphologic analysis, the bubble over sign and angular interface were evaluated. The bubble over sign was defined when the length of contact between bulging out portion of a mass and adjacent renal capsule is 3mm or greater. The angular interface was defined when the angle of parenchymal portion of a mass is 90° or less. The sensitivity, specificity, positive predictive value (PPV), negative predictive value (NPV), and accuracy were assessed. Logistic regression was conducted to determine which variable is predictive of fat-poor AML.

## RESULTS

For the diagnosis of fat-poor AML, sensitivity, specificity, PPV, NPV, accuracy, and AUC were 61.2% (30/49), 97.1% (537/553), 65.2% (30/46), 96.5% (537/556), and 94.2% (567/602) with bubble over sign, while they were 55.1% (27/49), 81.9% (453/553), 21.3% (27/127), 95.3% (453/475), and 79.7% (480/602) with angular interface, respectively. Both CT variables were predictive of fat-poor AML (bubble over sign, odds ratio= 39.632, p< 0.001; angular interface, odds ratio= 2.703, p= 0.010).

# CONCLUSION

Angular interface on CT may be seen in some RCCs (18.1% in our study), resulting in low PPV for fat-poor AML. The morphologic analysis of bulging out portion may help the differentiation.

# **CLINICAL RELEVANCE/APPLICATION**

The findings of angular interface seems to have limitation in the exclusion of RCC because some RCCs can show similar morphologic feature and the incidence rate of RCC is much higher than that of fat-poor AML. Our results (e.g. bubble over sign) may help reduce the misdiagnosis of small renal masses.

The Crenulated Rim Sign of a Collapsing Renal Cyst: Appearance of the Wall of a Cystic Renal Lesion Allows Differentiation between Malignant and Benign Renal Lesions

Sunday, Nov. 27 1:00PM - 1:30PM Room: GU/UR Community, Learning Center Station #4

# Participants

Sonam Jaglan, MD, New York, NY (*Presenter*) Nothing to Disclose Justin M. Ream, MD, Ann Arbor, MI (*Abstract Co-Author*) Nothing to Disclose Nicole M. Hindman, MD, New York, NY (*Abstract Co-Author*) Nothing to Disclose

#### PURPOSE

To retrospectively determine whether benign renal cystic lesions can be differentiated from malignant on the basis of a crenulated thickened rim.

# **METHOD AND MATERIALS**

Rad database was retrospectively searched from 1/1/05-5/1/15 for all C+ CT/MRs with cystic renal lesions with priors/follow-up exams or surgical pathology. This yielded 567 exams; 31 with collapsed renal cysts (defined as a cystic lesion with a prior exam demonstrating a larger, simple cyst, with dec in size on follow-up exams). 93 lesions (31 collapsed, 29 benign 33 malignant; avg 3.2 cm) in 93 pts (59:34 M:F, avg age 62.8, age range 23-85) were included. 2 radiologists independently evaluated the lesions for the presence of a crenulated rim (undulating border), internal soft tissue and Bosniak category. Fisher's exact test was used. Sens, spec, PPV, and NPV of the crenulated margin for diagnosing benign masses was calculated. Reader agreement was assessed with kappa.

# RESULTS

Of the 93 lesions, 60 were benign (31/60 collapsed cysts) 33 malignant. Crenulated rim seen in 17/43 benign cysts (15/31 in collapsed) and 1/33 malignant (p=0.0024); a crenulated rim without internal soft tissue was only seen in benign cysts (p=0.0004). A crenulated rim was significant for diagnosis of a collapsed cyst (p=0.0004). Excellent agreement noted for the crenulated rim (k=0.795). The sens, spec, PPV, NPV, for the crenulated rim sign for a collapsed renal cyst were 49%, 97%, 94%, 67%, respectively. In the absence of internal soft tissue, spec and PPV were 100%. Of collapsed cysts with a crenulated rim sign, additional follow-up imaging (0.5-106 months) showed decr in size and complexity in 19/31(61%) of collapsed cysts. None of the collapsed cysts had growth, progression or metastatic disease. Bosniak category for benign lesions ranged from 1-3. For collapsed cysts: Bosniak 2F was most common (21/31).

## CONCLUSION

The presence of a crenulated rim in a renal cystic lesion is a strong predictor of benignity. The presence of this sign highly suggests the diagnosis of a collapsing renal cyst. When this sign is seen, even if the Bosniak category is a 3, consider conservative management instead of surgical resection.

# **CLINICAL RELEVANCE/APPLICATION**

The presence of a crenulated thickened rim in a renal cystic lesion is a strong predictor of a benign collapsing renal cyst. When this sign is seen, even if the Bosniak category of the lesion is a 3, consider conservative management instead of surgical resection.

# Did You Miss Me? Bias in Radiology: The How & Why of Misses and Misinterpretations

Sunday, Nov. 27 1:00PM - 1:30PM Room: HP Community, Learning Center Station #4

#### Awards

# **Identified for RadioGraphics**

#### **Participants**

Lindsay P. Busby, MD, MPH, San Francisco, CA (*Presenter*) Nothing to Disclose Jesse L. Courtier, MD, San Francisco, CA (*Abstract Co-Author*) Nothing to Disclose Christine M. Glastonbury, MBBS, San Francisco, CA (*Abstract Co-Author*) Author with royalties, Reed Elsevier

## **TEACHING POINTS**

The purpose of this exhibit is to: 1. Introduce the cognitive processes used when interpreting radiologic cases.2. Explain the different types of bias that can lead to error.3. Demonstrate instructive case examples of misses due to different types of bias.4. Review strategies for overcoming bias.5. Identify improvements that can be made to reduce systemic errors and personal errors.

## **TABLE OF CONTENTS/OUTLINE**

Introduction: The rates and types of diagnostic radiologic errors Misses vs. misperceptions Approaching a case: Type I and Type II thinking: Relies on heuristics and intuition Type II thinking: Involves logic and reasoning Types of bias that can lead to error Anchoring Attribution Availability Confirmation Satisfaction of search Premature closure Hindsight Instructive case examples of radiologic misses and the bias to which they can be attributed How to reduce systemic errors in your practice Understanding your cognitive process Identify useful strategies for reducing personal errors and minimizing bias Review quiz

Knowledge of the Costs of Diagnostic Imaging: A Survey of Trainees at a Large Academic Medical Center

Sunday, Nov. 27 1:00PM - 1:30PM Room: HP Community, Learning Center Station #1

#### Awards

#### **Student Travel Stipend Award**

#### Participants

Arvind Vijayasarathi, MD, Atlanta, GA (*Presenter*) Nothing to Disclose Richard Duszak JR, MD, Atlanta, GA (*Abstract Co-Author*) Nothing to Disclose Rondi Gelbard, MD, Atlanta, GA (*Abstract Co-Author*) Nothing to Disclose Mark E. Mullins, MD, PhD, Atlanta, GA (*Abstract Co-Author*) Nothing to Disclose

#### PURPOSE

To study the knowledge of trainees across a variety of specialties regarding the costs of common imaging services.

#### **METHOD AND MATERIALS**

During early 2016, we conducted an online survey of all 1,238 trainees enrolled in internships, residencies and fellowships at a large academic medical center. Respondents were asked to estimate Medicare national average total allowable fees for 5 commonly performed imaging examinations: two view chest radiograph, contrast-enhanced CT abdomen and pelvis, unenhanced MRI lumbar spine, complete abdominal ultrasound, and unenhanced CT Brain. Responses within ±25% of the published amount were deemed correct. Respondents were also asked about: training program, postgraduate year of training (PGY status), previous relevant radiology education, and estimated number of imaging studies ordered per week.

#### RESULTS

A total 381 of 1,238 trainees returned complete surveys (30.8%). Across all five examinations, only 5.7% (109/1,905) of responses were within the correct  $\pm 25\%$  range. 76.4% (291/381) of all respondents incorrectly estimated every examination's cost. The vast majority of cost estimates were overestimates (86.8%) with mean absolute percentage estimation errors ranging from 137% for two view chest radiograph to 2852% for unenhanced MRI lumbar spine. Overall, cost estimation accuracy was not associated with number of imaging studies ordered per week or advancing years of training. There was no significant difference in cost estimation accuracy between those who participated in medical school radiology electives vs. those who did not (p=0.14). Only 17.5% of all trainees considered their imaging cost knowledge adequate. 75.3% of respondents would like to see integration of basic cost data into their clinical decision support (CDS) and/or computerized physician order entry systems (CPOE).

## CONCLUSION

Post graduate physician trainees across all disciplines demonstrate limited knowledge of the costs of commonly performed imaging studies. Since trainees regularly order imaging studies, they have a unique opportunity to be lifelong stewards of high value care. Targeted medical school education as well as integration of imaging cost information into CDS/CPOE appear indicated.

## **CLINICAL RELEVANCE/APPLICATION**

Improving referring clinicians' knowledge of costs of common imaging studies could help them provide patient's with higher value care.

## IN023-EC-SUB

Data-driven Imaging Biomarker: Uncovering Diagnostic Features from Large-scale Medical Images Using Deep Learning

Sunday, Nov. 27 1:00PM - 1:30PM Room: IN Community, Learning Center Custom Application Computer Demonstration

# Participants

Anthony S. Paek, PhD, Seoul, Korea, Republic Of (*Presenter*) CEO, Lunit Inc Hyo-Eun Kim, Seoul, Korea, Republic Of (*Abstract Co-Author*) Employee, Lunit Inc Sangheum Hwang, Seoul, Korea, Republic Of (*Abstract Co-Author*) Employee, Lunit Inc Meejin Cho, MD,JD, Seoul, Korea, Republic Of (*Abstract Co-Author*) Employee, Lunit Inc Minhong Jang, Seoul, Korea, Republic Of (*Abstract Co-Author*) Officer, Lunit Inc Kyunghyun Paeng, Seoul, Korea, Republic Of (*Abstract Co-Author*) Co-founder, Lunit Inc Jungin Lee, Seoul, Korea, Republic Of (*Abstract Co-Author*) Officer, Lunit Inc Jihoon Jeong, MD,PhD, Seoul, Korea, Republic Of (*Abstract Co-Author*) Nothing to Disclose

## CONCLUSION

We present the potential use of data-driven imaging features as novel imaging biomarkers. Unlike the conventional CAD designs, DIB learns radiologic features from large-scale medical images without any human annotation. This approach gives a possibility to discover latent imaging features that are hard to be categorized by human visual system. Well-trained DIBs will play an important role in advancing computer-aided diagnosis as well as quantitative imaging.

# FIGURE

http://abstract.rsna.org/uploads/2016/16019376/16019376\_17if.jpg

## Background

Deep learning has been gaining more attention as it shows outstanding performances in various cognitive tasks. Given a large number of training data, deep convolutional neural network can learn a set of multi-layered imaging features that is obtained in a fully data-driven manner. This feature learning capability has a great potential to be used in a development of novel imaging biomarkers, namely data-driven imaging biomarker(DIB).

#### **Evaluation**

We developed a training system of DIB that consists of two parts: deep convolutional neural network and feature activation map generator. We intentionally avoided the use of lesion-annotation to maximize the chance of novel feature discovery. The DIB is visually represented in the feature activation map that provides user experience similar to that of molecular/functional imaging. We evaluated this method in abnormality screening tasks with two datasets: 9,757 digital mammograms and 102,885 chest radiographs.

# Discussion

The DIBs achieved AUC of 0.814 and 0.948 for each task respectively and showed reasonable lesion localization agreement with human readers. Quantitative evaluation of lesion localization performance is required. Extended experimentation with additional data is expected to show more improvements in screening performance.

# A Shiny New World: Creating Your Own Radiology Decision Support Webapps Using R

Sunday, Nov. 27 1:00PM - 1:30PM Room: IN Community, Learning Center Station #6

#### Participants

Jennifer J. Wan, MD, San Francisco, CA (*Presenter*) Nothing to Disclose John Mongan, MD, PhD, San Francisco, CA (*Abstract Co-Author*) Spouse, Employee, Thermo Fisher Scientific Inc Devin Incerti, PhD, Oakland, CA (*Abstract Co-Author*) Nothing to Disclose Jesse L. Courtier, MD, San Francisco, CA (*Abstract Co-Author*) Nothing to Disclose

# **TEACHING POINTS**

1. Existing radiology-related applications and websites are currently in the format of interactive encyclopedias or cases. Creating an interactive web application to help generate a differential diagnosis is a fun and easy way to help radiologists provide value to their clinical colleagues.

R is a free open-source programming language and environment traditionally used for statistical computing, data analysis, and graphic output. As a simple and effective programming language, its function can be expanded with the use of add-on packages.
 Shiny is an open source R package for making interactive web applications. Unlike most web apps, R shiny apps can be deployed with no knowledge of HyperText Markup Language (HTML), Cascading Style Sheets (CSS), or JavaScript while still allowing more advanced developers the added flexibility of writing in these languages. This is a potential method for creating decision support applications to help radiologists identify appropriate differential diagnoses.

## TABLE OF CONTENTS/OUTLINE

Introduce current use of web/mobile apps in radiology Introduce R and Shiny What and how is it used? Basic concept of R and Shiny package Available platforms Basic terms/commands Step-by-step example and explanation for creating decision support app How to deploy the app and host on server

# IN205-SD-SUB1

## Lung Pattern Classification for Interstitial Lung Diseases Using a Deep Convolutional Neural Network

Sunday, Nov. 27 1:00PM - 1:30PM Room: IN Community, Learning Center Station #1

#### Participants

Andreas Christe, Bern, Switzerland (*Presenter*) Nothing to Disclose Stavroula Mougiakakou, Bern, Switzerland (*Abstract Co-Author*) Nothing to Disclose Marios Anthimopoulos, Bern, Switzerland (*Abstract Co-Author*) Nothing to Disclose Stergios Christodoulidis, Bern, Switzerland (*Abstract Co-Author*) Nothing to Disclose Lukas Ebner, MD, Durham, NC (*Abstract Co-Author*) Nothing to Disclose

#### PURPOSE

Deep learning techniques have recently achieved impressive results in a variety of computer vision problems, raising expectations that they might be applied in other domains, such as medical image analysis. We propose and evaluate a convolutional neural network (CNN), designed for the classification of interstitial lung disease (ILD) patterns.

# METHOD AND MATERIALS

The proposed network consists of 5 convolutional layers with  $2\times 2$  kernels and LeakyReLU activations, followed by average pooling with size equal to the size of the final feature maps and three dense layers. The last dense layer has 7 outputs, equivalent to the classes considered: healthy, ground glass opacity (GGO), micronodules, consolidation, reticulation, honeycombing and a combination of GGO/reticulation. To train and evaluate the CNN, we used a dataset of 14696 image patches, derived by 120 CT scans from different scanners and hospitals. A comparative analysis proved the effectiveness of the proposed CNN against previous methods in a challenging dataset.

## RESULTS

The classification performance (~85.5%) demonstrated the potential of CNNs in analyzing lung patterns. Pattern-sensitivities reached from 99% (consolidation) to 69% (honeycombing). The individual "true positive" and "false negative" results for each pattern is demonstrated in the Figure.

# CONCLUSION

The CNN showed very promising results in lung pattern recognition outperforming many state-of-the-art methods. Future work includes, extending the CNN to three-dimensional data provided by CT volume scans.

# **CLINICAL RELEVANCE/APPLICATION**

Integrating the proposed method into a CAD system helps providing a differential diagnosis for ILDs as a supportive tool for radiologists.

# Detection of Liver Fibrosis from MRI Using Histogram of Peak Strains

Sunday, Nov. 27 1:00PM - 1:30PM Room: IN Community, Learning Center Station #2

FDA Discussions may include off-label uses.

# Participants

Yasmine A. Safwat, BSC,BSC, Giza, Egypt (*Abstract Co-Author*) Nothing to Disclose Rasha S. Hussein, MD, Cairo, Egypt (*Presenter*) Nothing to Disclose Ahmed S. Fahmy, Giza, Egypt (*Abstract Co-Author*) Nothing to Disclose Ayman Khalifa, Helwan, Egypt (*Abstract Co-Author*) Nothing to Disclose Heba Abdallah, Cairo, Egypt (*Abstract Co-Author*) Nothing to Disclose Ahmed S. Ibrahim, MD, Cairo, Egypt (*Abstract Co-Author*) Nothing to Disclose Ahmed Samir, Cairo, Egypt (*Abstract Co-Author*) Nothing to Disclose

## PURPOSE

A method is presented to detect liver fibrosis using tagged MR images. The method is based on extracting a set of features representing the liver deformations induced by the heart motion. These features are then used to classify normal from patients with liver fibrosis. Results from data of 34 subjects (15 normal, 19 patients) showed sensitivity and specificity of 89%, and 80% respectively.

# **METHOD AND MATERIALS**

ECG-gated tagged MRI was performed on 15 volunteers and 19 patients (with fibrosis stage from F1 to F3 diagnosed by Fibroscan and/or liver biopsy). Sagittal cross-sections (1-3 slices) were acquired with tag spacing=7mm, voxel size =1.18×1.18×8mm, 11-20 frame/cardiac cycle.Lagrangian strain tensors of all the points within the liver were calculated using phase-based tracking methods [1].Then, at each timeframe, the strain in the superior-inferior direction (major direction of motion), P1(t), and the strain in the perpendicular direction, P2(t), were computed. At each liver point, the peak tissue strain throughout the cardiac cycle is calculated to yield PP1 and PP2. The histogram of the peak strains within the liver is calculated for both directions to yield two feature vectors HOPS1 and HOPS2. Both vectors are also concatenated to form one feature vector, HOPS. Support Vector Machines classifier was used to classify the feature vectors. A leave-one-out cross-validation is used, by leaving one case as testing set and the remaining cases as training set. The process is repeated until testing all datasets.Ref 1 Osman, et al.Cardiac motion tracking using Cine HARP MRI

# RESULTS

Figures 1 and 2 show the peak strain maps (PP1 and PP2) in a volunteer and a patient. Not only the peak strain value differs but also the distribution of the strain values. Table 1 summarizes the performance of the classifier when using the histogram of only one strain direction (HOPS1 or HOPS2) or both directions (HOPS) as feature vectors. The table, shows that the proposed method results in an accuracy of 85% when HOPS2 is used as a feature vector.

# CONCLUSION

A new method for detecting liver fibrosis using tagged MRI images was presented. The results show accuracy of 85% for patients with moderate fibrosis (stages from F1 to F3).

# **CLINICAL RELEVANCE/APPLICATION**

Based only on the inherent heart motion, with no need for external source of mechanical force, tagged MRI can be used to accurately detect liver fibrosis in early and moderate stages .

# IN207-SD-SUB3

# Simulation of Patient-specific Kidney Model Fabricated by a 3D Printer with Volumetric CT for Partial Nephrectomy

Sunday, Nov. 27 1:00PM - 1:30PM Room: IN Community, Learning Center Station #3

# Participants

Haekang Kim, Seoul, Korea, Republic Of (*Presenter*) Nothing to Disclose Namkug Kim, PhD, Seoul, Korea, Republic Of (*Abstract Co-Author*) Stockholder, Coreline Soft, Inc Guk Bae Kim, Seoul, Korea, Republic Of (*Abstract Co-Author*) Nothing to Disclose Yoon Soo Kyung,, Seoul, Korea, Republic Of (*Abstract Co-Author*) Nothing to Disclose Choung-Soo Kim, Seoul, Korea, Republic Of (*Abstract Co-Author*) Nothing to Disclose

# PURPOSE

The goal of partial nephrectomy is to remove renal cell carcinoma completely with preserving normal renal parenchyma maximally within 20 minutes. Because surgeons depend on anatomical information of a patient specific kidney from pre-operative CT image, it is sometimes difficult to localize tumor location and incision line, especially for tumor size < 2cm. Therefore, in this study, patient-specific 3D printed models have been developed and applied to partial nephrectomy to prove the clinical applicability.

### **METHOD AND MATERIALS**

Nine patients successfully underwent partial nephrectomy with complete excision of the suspicious renal cell carcinoma by open (N=7) or robotic assisted laparoscopic (N=2) approach. Volumetric CT scan were performed to evaluate renal mass. All renal units with renal mass were modelled to 3D images and measured each volume using A-view software (Asan Medical Center, Seoul, South Korea). The virtual resection simulation followed a safety margin with 5 mm offset from the renal mass. 3D printed kidney model was fabricated with Objet 500 CONNEX3 (Stratasys, CO, USA). Kidney model composed of parenchyma, artery, vein, ureter, tumor and safety margin, which were discriminated by color coding (Fig. 1). This 3D printed kidney model was used for self-training for patients specific anatomy variation, patient explanation, paramedic discussion, pre-surgical planning, etc.

## RESULTS

The renal mass could be visualized and differentiated from blood vessels and renal collecting system in this model. (Fig. 1) The mean tumor size 2.2 cm, mean tumor volume 7.65 cm<sup>3</sup> and the renal nephrometry score ranges 5-9. 3D printed kidney model has an advantage in the discussion with operating room staff to obtain an incision line and depth of dissection. Additionally, it could measure tumor volume and predict remain renal parenchymal volume after operation. Therefore, these models could be useful for predicting renal function after nephrectomy.

#### CONCLUSION

The use of a patient-specific 3D printed kidney model simplified partial nephrectomy for both the surgeon and patients, because it facilitated better preoperative planning and understanding of the intra-operative orientation of risk structure.

## **CLINICAL RELEVANCE/APPLICATION**

(dealing with partial nephrectomy) "The application of patient-specific 3D printed kidney model which facilitates better recognition of renal tumor is recommendable for planning and operating the partial nephrectomy."

Decoding Neural Circuits: A Color-Coded 3D Printed Atlas of Top Ten Clinically Relevant White Matter Tracts from MR Diffusion Tensor Fiber Tractography

Sunday, Nov. 27 1:00PM - 1:30PM Room: IN Community, Learning Center Station #4

# Participants

Ramin Javan, MD, Washington, DC (*Abstract Co-Author*) Nothing to Disclose Gaurav V. Watane, MBBS, MD, Amravati, India (*Presenter*) Nothing to Disclose Ahmad Shafiei, Washington, DC (*Abstract Co-Author*) Nothing to Disclose Erli Mingomataj, BS, Washington, DC (*Abstract Co-Author*) Nothing to Disclose Alexander Cho, Washington, DC (*Abstract Co-Author*) Nothing to Disclose Paul J. Albertine, MD, Washington, DC (*Abstract Co-Author*) Nothing to Disclose

# CONCLUSION

A modular design was developed for the physical 3D printed models of fiber tractography, which may add a new dimension to the increasing applications of diffusion tensor imaging in neurosurgical procedures, research and education.

#### Background

The use of MR diffusion tensor fiber tracking, which allows for delineation of multiple interconnecting white matter fiber tracts in the brain, has expanded in the clinical realm especially for pre surgical planning. Proper interpretation of this information requires understanding complex 3D relationships, beyond that required for conventional cross-sectional neuroimaging. With the recent surge in rapid prototyping technologies, new opportunities have emerged for discovering innovative applications through low-cost 3D printers, which use virtual 3D datasets to construct solid forms in a layer-by-layer technique. We propose that this technology may offer additional advantages in the visualization of white matter tracts, in settings such as neurosurgical planning, patient counseling and resident training.

#### **Evaluation**

The ten clinically important fiber tracts chosen include the corpus callosum, corticospinal tract, temporal and parietal optic radiations, superior longitudinal fascicles (part of which is the Arcuate fasciculus), inferior longitudinal fasciculus, uncinate fascicles as well as the anterior and posterior thalamic radiations.

## Discussion

The challenge in the case of tractography lies in the fact that the tracts are derived from tensor data, represented as eigenvalues and eigenvectors. This results in splines, directional lines in 3D space describing a curve, as opposed to 3D meshes, that is, a collection of surface triangles created through reconstruction of data from voxel based cross-sectional imaging. Methods for converting splines into 3D meshes for 3D printing purposes were investigated. Successful conversion was achieved by utilizing Amira software, which allows export of tractography splines as DXF (AutoCAD Drawing Exchange Format), which was imported into advanced graphic design software Autodesk 3DStudio Max. Subsequently, multicolor 3D printing was performed through a commercial website using gypsum based material with cyanoacrylate finish.

# IN209-SD-SUB5

#### Efficacy of an Automatic Decision Support System in Facilitating Diagnosis of the Thyroid Diseases

Sunday, Nov. 27 1:00PM - 1:30PM Room: IN Community, Learning Center Station #5

#### **Participants**

Sharbell Y. Hashoul, MD,MBA, Haifa, Israel (*Abstract Co-Author*) Employee, IBM Corporation Sameer Kassem, MD,MPH, Haifa, Israel (*Abstract Co-Author*) Nothing to Disclose Afif Nakhleh, MD, Haifa, Israel (*Abstract Co-Author*) Nothing to Disclose Algit Walach, Haifa, Israel (*Abstract Co-Author*) Employee, IBM Corporation Pavel Kisilev, Haifa, Israel (*Abstract Co-Author*) Researcher, IBM Corporation Ella Barkan, Haifa, Israel (*Abstract Co-Author*) Researcher, IBM Corporation Guy Amit, PhD, Haifa, Israel (*Abstract Co-Author*) Researcher, IBM Corporation Rami Ben-Ari, PhD, Haifa, Israel (*Abstract Co-Author*) Employee, IBM Corporation Vadim Ratner, PhD, Haifa, Israel (*Abstract Co-Author*) Employee, IBM Corporation Flora Gilboa, Haifa, Israel (*Abstract Co-Author*) Employee, IBM Corporation Eugene Walach, PhD, Haifa, Israel (*Presenter*) Employee, IBM Corporation

## PURPOSE

This paper explores the clinical applicability of a novel Decision Support System (DSS) developed for the domain of nuclear imaging of thyroid.

#### **METHOD AND MATERIALS**

The input to the DSS combines both clinical data and radiology semantic descriptions of nuclear thyroid images. Clinical inputs include history of the present illness (shortness of breath, palpitations, etc.), laboratory tests (TSH levels, FT3 levels, etc.) and more. Radiological descriptor inputs include image characteristics derived from the standard radiology report (diffused/focal/multifocal, increased/decreased uptake of radioactive iodine). The system's output includes the diagnosis and the differential diagnosis. In order to test the clinical applicability of this system, we have used an independent benchmark of 36 thyroid disease cases. We have covered a relatively wide gamut of diseases including Hashimoto, Graves, Silent Thyroiditis, etc. We have administered this benchmark to the automatic DSS, and to the two senior endocrinologists working in two different hospitals. The number of successes were counted in two manners: a) TOP: agreement with the correct diagnosis, b) DIF: agreement with the differential diagnosis. Cochran's Q test was used to assess the statistical significance of the results.

#### RESULTS

Success rates of both endocrinologists and DSS are shown below. Note that, in both measurement modes, DSS outperformed expert physicians. However, only for the correct diagnosis mode, the difference was statistically significant (p=0.01).

#### CONCLUSION

The automatic DSS outperforms experienced senior endocrinologists with a significant statistical margin.

# **CLINICAL RELEVANCE/APPLICATION**

The practical use of our system would be in assisting radiologists in adding clinical considerations to their radiological reports. Another potential use case would be in assisting endocrinologists in patient management and treatment decisions.

Evolution in Functional Imaging of Prostate Cancer-Role of PSMA PET/CT: The Pathophysiology, Normal Distribution and Clinical Utility of 68Ga-PSMA PET/CT in Prostate Cancer

Sunday, Nov. 27 1:00PM - 1:30PM Room: S503AB Station #5

**FDA** Discussions may include off-label uses.

Awards Certificate of Merit

# Participants

Venkatesh Rangarajan, MBBS, Mumbai, India (*Presenter*) Nothing to Disclose Archi Agrawal, MBBS, Mumbai, India (*Abstract Co-Author*) Nothing to Disclose Nilendu C. Purandare, DMRD, Mumbai, India (*Abstract Co-Author*) Nothing to Disclose Sneha A. Shah, Mumbai, India (*Abstract Co-Author*) Nothing to Disclose Nilesh Sable, Mumbai, India (*Abstract Co-Author*) Nothing to Disclose

# **TEACHING POINTS**

PSMA PET/CT is a useful imaging tool for identification of the primary tumor, nodal and skeletal metastases in prostate cancer. It has higher sensitivity for nodal disease as it can detect metastases in tiny sub centimetre sized nodes. It helps in assessment of response in skeletal metastases unlike bone scintigraphy.

It helps in detection of tiny recurrences at the primary site and nodal metastases in patients with biochemical relapse.

It is a one-stop-shop imaging for staging and restaging of prostate cancer.

## TABLE OF CONTENTS/OUTLINE

Advantages of 68Ga-PSMA PET/CT in evaluation of prostate cancer over conventional imaging modalities. Pathophysiology and imaging findings in diagnosis, staging, restaging and in response assessment will be discussed. The spectrum of imaging findings for detection of primary, nodal, visceral and skeletal metastases will be described. The potential pitfalls of 68Ga-PSMA PET/CT imaging.

## MI204-SD-SUB1

The Synthesis of avß3 and EGFR Targeted SPECT/MRI Probe and its Application in the Diagnosis of Lung Cancer

Sunday, Nov. 27 1:00PM - 1:30PM Room: S503AB Station #1

# Participants

Jiali Cai, Shanghai, China (*Presenter*) Nothing to Disclose Zhetao Liu, Shanghai, China (*Abstract Co-Author*) Nothing to Disclose Shiyuan Liu, PhD, Shanghai, China (*Abstract Co-Author*) Nothing to Disclose

## PURPOSE

In this study, we constructed three dual-modality SPECT/MRI iron oxide nanoparticles probe which simultaneously target to  $\alpha\nu\beta3$  receptors in tumor angiogenesis and EGFR on non-small cell lung cancer.

# **METHOD AND MATERIALS**

The PEG coated USPIO surface was directly conjugated with peptide c(RGDfK) and GE11.We demonstrated the specificity of the probe to  $\alpha\nu\beta3$  integrin and EGFR with Prussian blue staining and quantitative analysis of Fe contents in vitro. In vitro cytotoxicity testing was performed with three probes for 12, 24 and 48 hour with three concentrations. Blood clearance and biodistribution of these probes show excellent biocompatibility. T2-weighted MR and small-animal SPECT/CT imaging were acquired in a H1299 cell xenografted lung cancer model.

#### RESULTS

USPIOs were synthesized via the polyol method. The resulting 4.8 nm nanoparticles have low r2/r1 of 3.88 (r1 =15.2 mM-1·s-1, r2 = 59.09 mM-1·s-1). On this basis, USPIOs were used as carrier and were applied to conjugate targeting peptide RGD, GE11 and label 99mTc nuclide. The radiochemical purity of 99mTc labeled nanoparticle > 92%, radioactive stability > 95%. The results of Prussian blue staining indicated that three probes can target to H1299 cells, while the dual-targeting probe RGD-GE11@USPIO had better targeting performance than those of the single-targeting probes. The same results were verified in the Fe contents in each cell.MRI showed three probes can specifically target to tumor and decreased the MR signal intensity. SPECT images showed particles mainly gathered in liver and kidney indicated that the particles were metabolized by urine and faeces. The qualitative and quantitative analysis of SPECT/MRI images kept in good concordance, and suggested that tumor accumulation of dual-targeting probe was more efficient and the most accumulation culminated at 6 hour post injection. Histological studies revealed that  $\alpha\nu\beta3$  integrin and EGFR were expressed on H1299 tumor cells.

## CONCLUSION

In this study, 99mTc-RGD-GE11@USPIO has higher specificity and sensitivity for detectingav $\beta$ 3 integrin and EGFR-expressing H1299 lung cancer cells and xenografted tumor models. The dual-modal probe can be diagnosis for the specific imaging of lung cancer.

#### **CLINICAL RELEVANCE/APPLICATION**

Animal procedures were carried out according to a protocol approved by the Institutional Animal Care and Use Committee at Second Military Medical University, Shanghai, China.

Molecular BLI/CT-imaging Reveals Local IFN- $\!\beta$  induction in the Heart in a Murine Model of Acute Viral Myocarditis

Sunday, Nov. 27 1:00PM - 1:30PM Room: S503AB Station #2

# Participants

Wolfgang Koestner, Hannover, Germany (*Presenter*) Nothing to Disclose
Vanessa Herder, Hannover, Germany (*Abstract Co-Author*) Nothing to Disclose
Claudia N. Detje, Hannover, Germany (*Abstract Co-Author*) Nothing to Disclose
Martijn Langereis, UTRECHT, Netherlands (*Abstract Co-Author*) Nothing to Disclose
Stefan Lienenklaus, Hanover, Germany (*Abstract Co-Author*) Nothing to Disclose
Wolfgang Baumgartner, Hannover, Germany (*Abstract Co-Author*) Nothing to Disclose
Wolfgang Baumgartner, Hannover, Germany (*Abstract Co-Author*) Nothing to Disclose
Frank K. Wacker, MD, Hannover, Germany (*Abstract Co-Author*) Research Grant, Siemens AG; Research Grant, Pro Medicus Limited;
Research Grant, Delcath Systems, Inc;
Ulrich Kalinke, Hannover, Germany (*Abstract Co-Author*) Nothing to Disclose

#### PURPOSE

The differentiation of acute, chronic, viral and autoimmune etiology of myocarditis is essential for the choice of treatment. However, non-invasive diagnostics are lacking. We hypothesized that molecular imaging of IFN- $\beta$  induction can be used as a biomarker to determine etiology of myocarditis. Furthermore, the impact of host- and virus-associated factors on pathogenesis was investigated.

# METHOD AND MATERIALS

To preferentially direct Coxsackie-virus B3 (CVB-3) infection to the heart muscle, mice with a myocyte-specific IFNAR-ablation were generated ( $\alpha$ -MHC*cre/wt*-IFNARf//fl). IFNAR-/-, IFN- $\beta$ -/- and WT-C57BL/6 mice were used as controls. Spatio temporal distribution of IFN- $\beta$  induction p.i. was assessed by BLI/CT in IFN- $\beta$  luciferase reporter mice (IFN- $\beta \Delta \beta$ -luc). To investigate the impact of host-associated factors, reporter mice on two different backgrounds, C57BL/6 and BALB/C, as well as male versus female mice were analyzed. For virus-associated factors different infection doses and different viral variants were studied. Furthermore, IFNAR-/-IFN- $\beta \Delta \beta$ -luc mice and  $\alpha$ -MHC*cre/wt*-IFNARf//fl-IFN- $\beta \Delta \beta$ -luc mice were evaluated.

#### RESULTS

Following CVB-3 infection IFNAR-/-IFN- $\beta \Delta \beta$ -luc mice succumbed within 2 to 3 days. Prior to death, a significant BLI signal was detected in the liver of these mice. Signal strength was reduced in IFNARwt/wt-IFN- $\beta \Delta \beta$ -luc-C57BL/6 mice. Other significant BLI-signals were observed in cervical and abdominal lymph nodes. In the heart, a weak BLI signal was observed at d7 p.i.. Signal strength was enhanced in a-MHCcre/wt-IFN- $\beta \Delta \beta$ -luc mice. In addition, these mice developed severe myocarditis and died upon CVB-3 infection within 7 days, whereas C57BL/6 mice showed mild myocarditis and survived. In contrast, IFN- $\beta$ -/- mice died around day 40 post infection and displayed interstitial fibrosis within the myocardium. Thus, BLI-signal distribution and strength varied depending on host- and virus-associated factors.

# CONCLUSION

BLI/CT imaging was used to visualize IFN- $\beta$  induction in liver, lymph nodes and heart *in vivo* after CVB-3 infection. Signal strength and spatiotemporal distribution of BLI-signals were identified as relevant biomarkers. BLI/CT-imaging revealed local IFN- $\beta$  induction in the heart during acute viral myocarditis.

## **CLINICAL RELEVANCE/APPLICATION**

In patients with myocarditis molecular imaging might help to define more homogeneous patient cohorts for the initiation of clinical studies.

Diffusion Kurtosis Imaging of Human Nasopharyngeal Carcinoma Xenografts: Initial Experience with Pathological Correlation

Sunday, Nov. 27 1:00PM - 1:30PM Room: S503AB Station #3

# Participants

Jing Zhong, Fuzhou, China (*Presenter*) Nothing to Disclose Chen Yunbin, MD, Fuzhou, China (*Abstract Co-Author*) Nothing to Disclose Peng Shi, Fuzhou, China (*Abstract Co-Author*) Nothing to Disclose Dechun Zheng, MS, Fuzhou, China (*Abstract Co-Author*) Nothing to Disclose Xiang Zheng, MS, Fuzhou, China (*Abstract Co-Author*) Nothing to Disclose

# PURPOSE

The aim of this study was to investigate the relationship between the diffusion kurtosis imaging (DKI) related parameters and pathological measures using human nasopharyngeal carcinoma (NPC) xenografts in nude mice model.

## **METHOD AND MATERIALS**

24 BALB/c-nu nude mice were divided into two groups which were injected with two different nasopharyngeal squamous cell carcinoma cell lines (CNE1 and CNE2). Mice were sacrificed when the tumor max diameter exceed 1.5cm after MR scanning. The DK MR imaging was performed on a 3 Tesla MR scanner. DKI related parameters-mean diffusivity (MD) and mean kurtosis (MK) were measured. Tumors were then processed for Hematoaylin and Eosin staining. The pathological images were analyzed using computer-aided pixel-wise clustering method to evaluate tumor cellularity, extracellular space portion, cytoplasm portion and ratio of nuclei to cytoplasm (N/C ratio). The relationship between DKI related parameters and pathological features were analyzed statistically.

#### RESULTS

The mean MD of CNE1 xenograft (2.19 $\pm$ 0.39) was higher than CNE2 group (1.76 $\pm$ 0.48, p<0.05), but the mean MK between the two groups has no significant difference (CNE1 0.55 $\pm$ 0.14 and CNE2 0.47 $\pm$ 0.23, p>0.05). The spearmen test showed that the MD values were significantly correlated with cell cytoplasm portion and extracellular space portion (rs=0.370, p<0.05, rs=-0.435, p<0.05). The MK values were significantly correlated with cell cytoplasm portion and N/C ratio (rs=0,528, p<0.01, rs=0.627, p<0.001). Both MD and MK values were not significantly correlated with tumor cellularity.

# CONCLUSION

In the xenografted NPC model, the MD values were significantly correlated with cell cytoplasm portion and extracellular space portion, when the MK value were correlated with cell cytoplasm portion and N/C ratio. The DKI imaging might be utilized as surrogate biomarker for noninvasive assessment of tumor micro-structure.

# **CLINICAL RELEVANCE/APPLICATION**

The preliminary animal results suggest that DKI findings could provide valuable information for NPC micro-characterization.

Bio-Imaging of Unstable Plaques Using Thrombus Targeted Nano-polymers in Severe Hypercholesterolemia

Sunday, Nov. 27 1:00PM - 1:30PM Room: S503AB Station #4

#### **Participants**

Kye S. Kim, MD, Boston, MA (*Presenter*) Nothing to Disclose Peter Kang, MD, Boston, MA (*Abstract Co-Author*) Nothing to Disclose

## PURPOSE

Atheromatous plaques are prone to rupture, resulting in plaque hemorrhage. This can result in recurrent ischemic events, such as myocardial infarction and stroke that have been recognized as the top culprits associated with the highest mortality and morbidity, respectively in U.S. This improving strategies to deal with these conditions are important. In this study, we developed a novel polymer based delivery system to effectively image these unstable plaques by thrombus targeted approach.

## **METHOD AND MATERIALS**

For animal model of unstable plaques, the mice having homozygous knock-in mutations of the HDL receptor (scavenger receptor, class B, type I(SRBI)) and the mice having homozygous null mutations in the apolipoprotein E(ApoE) gene were mated to create SRBI/ApoE double KI/KO mice that exhibited severe hypercholesterolemia and cardinal features of ischemic disease. The polymer-based micelles were generated through hydrophilic-hydrophobic interacting lipid polymers and pluronic F-127. A pentapeptide, CREKA(H-Cys-Arg-Glu-Lys-Ala-OH), shown a high affinity to fibrinogen-fibrin complex, was covalently bonded to the micelle. For thrombus targeted imaging, we loaded the micelles with indocyanine green(ICG), a near-infrared fluorophore with peak absorption at ~800 nm.

## RESULTS

We found that the SRBI/ApoE double KI/KO mice exhibited significantly increased atherosclerosis and plaque hemorrhage compared to WT, single ApoEKO or single SRBI KI mice throughout the vascular system, including aorta, carotid and coronary arteries. Cardiac output was significantly decreased in double KI/KO mice( $\sim$ 29% SRBI/ApoEKI/KO compared to ApoE only, p<0.01). Double KI/KO mice also exhibited histologic evidences of early myocardial infarction at 6-7 weeks. These mice started to die within 7 weeks of age and by 12-13 weeks, there were over 90% mortality due to infarctions and heart failure.

## CONCLUSION

The novel polymer micelle-based bio-imaging system using thrombus targeting may be used for non-invasive targeted imaging of unstable plaques.

# **CLINICAL RELEVANCE/APPLICATION**

This research could be useful in developing thrombus targeted theranostic system to diagnose and treat unstable plaques in myocardial infarction and stroke.

# Diagnosis and Management of Carpal Trauma and Instability: An Illustrated Guide!

Sunday, Nov. 27 1:00PM - 1:30PM Room: MK Community, Learning Center Station #6

#### **Participants**

Matthew R. Skalski, DC, Whittier, CA (*Abstract Co-Author*) Nothing to Disclose George R. Matcuk Jr, MD, Los Angeles, CA (*Abstract Co-Author*) Nothing to Disclose Dakshesh B. Patel, MD, Porter Ranch, CA (*Presenter*) Nothing to Disclose Aaron Schein, MD, Los Angeles, CA (*Abstract Co-Author*) Nothing to Disclose Eric A. White, MD, Santa Monica, CA (*Abstract Co-Author*) Nothing to Disclose Anderanik Tomasian, MD, Saint Louis, MO (*Abstract Co-Author*) Nothing to Disclose

# **TEACHING POINTS**

This exhibit will use multimodality imaging and original high-quality medical illustrations, presented in an engaging comic book style format, to teach the following: Spectrum of carpal fractures Ligamentous anatomy of the carpus Spectrum of carpal dislocations The various instability patterns in the wrist Common management strategies and potential complications for all of the above

#### **TABLE OF CONTENTS/OUTLINE**

Detailed review of carpal fracture assessment, relevant classifications, management strategies, and complications with illustravive cases and diagrams. Interactive review of the intrinsic and extrinsic ligamentous anatomy of the carpus on MR. The spectrum of carpal dislocations, their discriminating features, and associated ligamentous injuries specific to each with illustravive cases and diagrams. Overview of the vast array of instability patterns in the wrist, how to evaluate them, and common management strategies with illustravive cases and diagrams.

# Ultrasound Evaluation of the Hand Joints in Inflammatory Diseases

Sunday, Nov. 27 1:00PM - 1:30PM Room: MK Community, Learning Center Station #8

#### **Participants**

Luis G. Tellez Martinez, MD, Monterrey, Mexico (*Presenter*) Nothing to Disclose Ignacio Cano-Munoz, MD, Guadeloupe, Mexico (*Abstract Co-Author*) Nothing to Disclose Jesus R. Quintana, MD, Monterrey, Mexico (*Abstract Co-Author*) Nothing to Disclose Alejandra Salcedo Gonzalez, Monterrey, Mexico (*Abstract Co-Author*) Nothing to Disclose

## **TEACHING POINTS**

Review the most common ultrasonographic findings in comon hand joint arthripathyThe role of ultrasound in diagnosis and management of different hand joint arthropaties

## **TABLE OF CONTENTS/OUTLINE**

IntroductionObjectiveMaterial and MethodsRheumatoid Arthritispsoriatic arthritisOsteoarthritisSystemic lupus erythematosus arthritisGeneral arthropathyDiscussionBibliography

Show Me the Money! A "Slot-Machine Approach" to MRI Interpretation of Pathologic Conditions Involving the Femoral Head and Neck

Sunday, Nov. 27 1:00PM - 1:30PM Room: MK Community, Learning Center Station #9

# Participants

Brett W. Cerniglia, MD, MPH, Philadelphia, PA (*Presenter*) Nothing to Disclose Micah Cohen, MD, Philadelphia, PA (*Abstract Co-Author*) Nothing to Disclose Tetyana A. Gorbachova, MD, Huntingdon Vy, PA (*Abstract Co-Author*) Nothing to Disclose

## **TEACHING POINTS**

Demonstrate key MR imaging features and ancillary findings of common pathologic conditions involving femoral head and neck. Apply algorithmic approach to evaluation of femoral head bone marrow edema to arrive at specific diagnosis on MRI. Review differential diagnosis of look-alike conditions in a systematic manner.

## **TABLE OF CONTENTS/OUTLINE**

Review of MR imaging sequences, morphologic findings and ancillary signs to evaluate femoral head/neck pathology: T1-W sequences: criteria for marrow edema and marrow replacement, identify fracture lines Fluid sensitive sequences: distribution and extent of marrow edema Subchondral changes: subchondral fracture, cleft, contour deformity, cysts Acetabular involvement Additional, "bonus" features: cartilage loss, periarticular soft tissue involvement, history Application of MRI diagnostic algorithm using clinical case examples: Conditions commonly presenting with bone marrow edema pattern: transient osteoporosis of the hip/bone marrow edema syndrome, subchondral insufficiency fracture, femoral head AVN Etiology-based hip pathology: Traumatic: acute vs stress fracture Degenerative: osteoarthritis and rapidly destructive osteoarthritis Infectious: septic hip Neoplastic: benign (fibrous dysplasia, LSMFT) vs malignant (metastases, lymphoma, clear cell chondrosarcoma)

Modic 1 Signal Evolution after Intradiscal Glucocorticoid Injection (versus sham-procedure) for Patients with Chronic Low Back Pain

Sunday, Nov. 27 1:00PM - 1:30PM Room: MK Community, Learning Center Station #1

## Participants

Aurelien Buisson, MD, PARIS, France (*Presenter*) Nothing to Disclose Nor-Eddine Regnard, MMed, Paris, France (*Abstract Co-Author*) Nothing to Disclose Christelle Nguyen, MD, PARIS, France (*Abstract Co-Author*) Nothing to Disclose Serge Poiraudeau, MD, PhD, Paris, France (*Abstract Co-Author*) Nothing to Disclose Jean-Luc Drape, MD, PhD, Paris, France (*Abstract Co-Author*) Nothing to Disclose Antoine A. Feydy, MD, Paris, France (*Abstract Co-Author*) Nothing to Disclose

#### PURPOSE

Assessment of the Modic signal evolution after intradiscal steroid injection versus sham-procedure for patients with chronic low back pain associated with active discopathy (defined by a Modic 1 MRI pattern).

# METHOD AND MATERIALS

Ninety chronic low back pain patients with active discopathy on MRI (Modic 1) and failure of first line treatments were included in a double-blinded, multicentric trial.Patients were randomized for an intradiscal injection of glucocorticoid (25 mg of prednisolone acetate) during a discography (group 1) or for a sham-procedure (group 2).MRI before and twelve months after discography were assessed for evolution of the Modic type, the Modic extension (volume, maximal height and antero-posterior diameter), the Modic signal intensity and the disc space narrowing, blinded to the procedure.

#### RESULTS

At the 12 months evaluation, no significant difference were observed on MRI about the Modic signal changes between the 45 patients treated with an intradiscal glucocorticoid injection and the 45 patients who had a single discography. The rate of persisting Modic 1 was similar in both groups (80% in group 1 vs 73% in groupe 2, p = 0,62). The extent of endplate oedema did not change differently between the two groups, neither in volume (increase of 830 mm3 in group 1 versus decrease of 99 mm3 in group 2, p=0,60), nor in maximal height (-5% in group 1 vs -1,7% in group 2, p=0,43), nor in maximal antero-posterior diameter (-6,1% in group 1 vs -6,4% in group 2, p=0,95). The signal intensity changes after discography did not differ between the 2 groups. The disc space narrowing at 12 months was similar in both groups (5% in group 1 vs 3,9% in group 2, p=0,61).

## CONCLUSION

Evolution of the vertebral body endplate oedema was similar between patients treated with intradiscal injection of corticosteroids and patients having a sham-procedure.Considering the significant decrease of low back pain in patients treated with intradiscal injection of corticosteroids in this cohort, MRI should not be used as a preditive tool in the follow-up of patients with active discopathy.

## **CLINICAL RELEVANCE/APPLICATION**

MRI should not been used as a pronostic tool in the follow-up of patients with low back pain associated with an active discopathy.

## MK296-SD-SUB2

Hip Aspiration for Pre-operative Management of Peri-prosthetic Infection: Ultrasound vs Fluoroscopic Guidance

Sunday, Nov. 27 1:00PM - 1:30PM Room: MK Community, Learning Center Station #2

#### Awards

#### **Student Travel Stipend Award**

#### Participants

Silvana Sdao, MD, Milano, Italy (*Presenter*) Nothing to Disclose Marco Brioschi, Milan, Italy (*Abstract Co-Author*) Nothing to Disclose Santi Rapisarda, MD, Rome, Italy (*Abstract Co-Author*) Nothing to Disclose Sandro Magnani, Milan, Italy (*Abstract Co-Author*) Nothing to Disclose Filippo Randelli, MD, San Donato Milanese, Italy (*Abstract Co-Author*) Nothing to Disclose Alberto Aliprandi, MD, San Donato Milanese, Italy (*Abstract Co-Author*) Nothing to Disclose

#### PURPOSE

Management of peri-prosthetic hip infection is still a challenge for orthopedic surgeons. To date there is no "gold standard" for the diagnosis of septic implant failure. In this setting, hip aspiration can play a central role in the management of septic implant loosening being able to prove the causative microbiological agent of the infection, possibly modifying treatment and prognosis. Hip aspiration can be performed under fluoroscopic, ultrasound or computed tomography guidance. The aim of our retrospective study was to compare sensitivity, specificity, positive predictive value (PPV), negative predictive value (NPV) and diagnostic accuracy of pre-operative hip aspiration performed with fluoroscopic guidance (FG) vs ultrasound guidance (UG).

#### **METHOD AND MATERIALS**

Between 2013 and 2015, 40 pre-operative hip aspirations (n=19 EG; n=21 FG) were performed at our Institution on 39 patients who underwent revision surgery for implant loosening. Musculoskeletal Infection Society (MSIS) criteria were used as the "gold standard" for the evaluation of hip infection.

#### RESULTS

Aspirations performed under UG revealed better sensitivity (83% vs 50%), specificity (100% vs 85%), PPV (100% vs 60%), NPV (93% vs 80%) and accuracy (95% vs. 75%) compared with FG aspirations.

#### CONCLUSION

UG should be considered as a valid alternative for hip aspiration compared with FG in the diagnosis of peri-prosthetic infections, showing better clinical results.

#### **CLINICAL RELEVANCE/APPLICATION**

Hip aspiration performed under UG can be a valid option to detect peri-prosthetic infections compared to FG. UG aspiration has the advantage of being easier to perform, do not use ionizing radiations and shows good clinical results with lower costs.

Presence of MRI-defined Intra-articular Inflammatory Markers Two Years after Anterior Cruciate Ligament Injury Increases Risk for Tibio-femroal Osteoarthritis at Five Years

Sunday, Nov. 27 1:00PM - 1:30PM Room: MK Community, Learning Center Station #3

## Participants

Frank W. Roemer, MD, Boston, MA (*Presenter*) Chief Medical Officer, Boston Imaging Core Lab LLC; Research Director, Boston Imaging Core Lab LLC; Shareholder, Boston Imaging Core Lab LLC; ;

Ali Guermazi, MD, PhD, Boston, MA (*Abstract Co-Author*) President, Boston Imaging Core Lab, LLC Research Consultant, Merck KgaA Research Consultant, Sanofi-Aventis Group Research Consultant, TissueGene, Inc Research Consultant, OrthoTrophic Research Consultant, AstraZeneca PLC

Stefan Lohmander, Lund, Sweden (Abstract Co-Author) Nothing to Disclose

Jingbo Niu, Boston, MA (Abstract Co-Author) Nothing to Disclose

Richard Frobell, Lund, Sweden (Abstract Co-Author) Nothing to Disclose

#### PURPOSE

The aim of this study was to compare risk of radiographically-defined and MRI-defined patello-femoral (PF) and tibiofemoral (TF) osteoarthritis (OA) at 5 years after anterior cruciate ligament (ACL) injury for knees that have persistent MRI-detected signs of Hoffa-synovitis and effusion-synovitis at 2 years vs. those that do not show inflammation.

#### **METHOD AND MATERIALS**

The KANON study includes 121 subjects with an acute ACL injury in a previously un-injured knee. Subjects were randomly assigned to structured rehabilitation plus early ACL reconstruction or to structured rehabilitation plus optional delayed ACL reconstruction. The current analysis focuses on baseline (BL), 2 year and 5 year MRI regardless of treatment arm.MRI was performed using a 1.5 T system. All available MRIs were read with the semi-quantitative ACLOAS scoring system by one musculoskeletal radiologist. Logistic regression was performed to assess the associations of presence of any inflammatory MRI markers (Hoffa-synovitis and joint effusion-synovitis) with risk of radiographic and MRI-defined PFand TF OA at 5 years. Adjustment was performed for age, sex, body mass index (BMI) and 3-level treatment group (early ACL reconstruction, delayed ACL reconstruction, rehabilitation).

#### RESULTS

111 patients were included that had MRIs available for all three time points. Mean age was  $26.3 \pm 5.1$  years and 12 (19%) were female. Mean body mass index was  $24.4 \pm 3.2$ .Patients with positive inflammatory markers at 2 years (i.e. any Hoffa-synovitis or effusion synovitis  $\geq$  grade 1) did not show increased risk for radiographically defined TF or PF OA at 5 years. However, patients with positive inflammatory markers did have an increased risk of MRI-defined TF OA (Hoffa-synovitis OR 5.44, 95% CI [1.10, 26.95] and effusion-synovitis OR 9.40 95% CI [1.14, 77.48]). No statistically significant association were observed for risk of PFJ OA.

## CONCLUSION

Inflammatory changes observed distant to the initial trauma seem to play a role in OA development at 5 years. While no increased risk was observed for development of radiographically defined PF or TF OA, the risk of MRI-defined TF OA was markedly increased in patients with signs of Hoffa- and effusion synovitis at 2 years.

#### **CLINICAL RELEVANCE/APPLICATION**

While X-ray defined OA shows structural changes only in late disease stages the MRI definition of OA may be helpful in diagnosing patients with unfavorable outcomes more early.

#### **Honored Educators**

Presenters or authors on this event have been recognized as RSNA Honored Educators for participating in multiple qualifying educational activities. Honored Educators are invested in furthering the profession of radiology by delivering high-quality educational content in their field of study. Learn how you can become an honored educator by visiting the website at: https://www.rsna.org/Honored-Educator-Award/

Ali Guermazi, MD, PhD - 2012 Honored Educator

## Progressive Depletion of Skeletal Muscle and of Muscle Quality Predicts Survival of Colorectal Cancer Patients

Sunday, Nov. 27 1:00PM - 1:30PM Room: MK Community, Learning Center Station #4

#### Participants

Colm J. McMahon, MBBCh, Boston, MA (*Abstract Co-Author*) Nothing to Disclose Yu-Ching Lin, MD, Tao Yuan, Taiwan (*Abstract Co-Author*) Nothing to Disclose ChihYing Deng, Tao Yuan, Taiwan (*Presenter*) Nothing to Disclose Kun-Yun Yeh, Keelung, Taiwan (*Abstract Co-Author*) Nothing to Disclose Yun-Chung Cheung, MD, Kwei Shan, Taiwan (*Abstract Co-Author*) Nothing to Disclose Jim S. Wu, MD, Boston, MA (*Abstract Co-Author*) Research Grant, Kaneka Corporation

# PURPOSE

Sarcopenia (low skeletal muscle mass) is associated with poorer prognosis of colorectal cancer patients. The goal of this study was to evaluate the effect on survival of progressive loss of muscle mass at 1 year follow up after diagnosis.

## **METHOD AND MATERIALS**

Patients diagnosed with colorectal cancer between 2007 and 2011 were included and were followed for at least 5 years. CT at baseline and 1 year after diagnosis were analyzed. Skeletal Muscle Index (SMI) of psoas and paraspinal muscles, and mean Hounsfield Units (HU) were measured at baseline, and at 1 year. Interval change in parameters between baseline and 1 year were calculated. Measurements were taken at L4 level. Univariate Cox proportional hazard regression was used to evaluate relationship to overall and progression-free survival.

## RESULTS

\*=p<0.05148 patients were included, mean (+/-SD) age 65.1 (+/-13.5) years, 51 females. Overall survival: Hazard Ratio (HR) of psoas SMI was 0.60, 0.41\*, 7.51\* for baseline, 1 year, interval change respectively. HR for psoas HU was 0.98, 0.93\*, 1.14\* for baseline, 1 year, interval change respectively. HR for paraspinal SMI was 0.67\*, 0.58\*, 2.19\* for baseline, 1 year, interval change respectively. HR for paraspinal HU was 1.00, 0.99, 1.18\* for baseline, 1 year, interval change respectively. Progression-free survival: HR for psoas SMI was 0.67, 0.59\*, 2.45 for baseline, 1 year, interval change respectively. HR for paraspinal SMI was 0.88, 0.79, 1.92 for baseline, 1 year, interval change respectively. HR for paraspinal HU was 1.00, 0.99, 1.20\* for baseline, 1 year, interval change respectively.

#### CONCLUSION

Progressive depletion of muscle mass and of muscle quality at 1 year compared to baseline at diagnosis of colorectal cancer is predictive of poorer overall and progression free survival.

# **CLINICAL RELEVANCE/APPLICATION**

This study identifies the importance of changes in skeletal muscle index and muscle density as a biomarker for colorectal cancer prognosis.

## Role of MRI to Assess Skeletal Age in Pediatric Celiac Disease

Sunday, Nov. 27 1:00PM - 1:30PM Room: MK Community, Learning Center Station #5

#### **Participants**

Silvia Bernardo, MD, Rome, Italy (*Presenter*) Nothing to Disclose Ernesto Tomei, MD, Rome, Italy (*Abstract Co-Author*) Nothing to Disclose Milvia Martino, MS, Rome, Italy (*Abstract Co-Author*) Nothing to Disclose Corrado Tagliati, Rome, Italy (*Abstract Co-Author*) Nothing to Disclose Andrea Laghi, MD, Rome, Italy (*Abstract Co-Author*) Speaker, Bracco Group Speaker, Bayer AG Speaker, General Electric Company Speaker, Koninklijke Philips NV

# PURPOSE

Coeliac children are often subject to weight loss and lower somatic growth rate, compared to healthy children of the same age. The purpose of this study was to asses the feasibility of magnetic resonance imaging (MRI) of the hand and the wrist to assess skeletal age and growth delay.

## **METHOD AND MATERIALS**

We enrolled in our study 39 coeliac children (13 males and 26 females) affected by histological proven coeliac disease, with a chronological age ranged between 5 years and 1 month and 16 years and 4 months (mean age of 10years, +/- 3 years and 8 months standard deviation). A single MRI sequence (T13D SE, acquisition time: 1 minute 31 seconds) of the hand and wrist in coronal plane was performed of each patient to estimate the skeletal age. Patients' data were compared with a population of normal subjects.

#### RESULTS

The preliminary results showed a delay in skeletal age in children affected by coeliac disease in 85,7% of the simple study, with a delay of maturity of 0.83 years (+/-2,2 years of SD). Only 3 children showed advance MRI skeletal age when compared to normal subjects.

# CONCLUSION

MRI of hand/wrist to assess skeletal age may be considered as a reliable indicator of somatic growth. MRI, without radiation exposure, can be an used as a diagnostic tool in skeletal delay. It could play an important role in the follow up of coeliac children, after gluten-free diet.

# **CLINICAL RELEVANCE/APPLICATION**

MRI of hand/wrist skeletal age is a powerful, radiation-free, tool for the evaluation of bone age and follow-up in coeliac children.

# Whole-Body MRI in Multiple Myeloma

Sunday, Nov. 27 1:00PM - 1:30PM Room: MS Community, Learning Center Station #1

#### Awards Certificate of Merit

#### **Participants**

Francesco Mungai, MD, Florence, Italy (*Presenter*) Nothing to Disclose Catia Dini, Firenze, Italy (*Abstract Co-Author*) Nothing to Disclose Stefano Chiti, Firenze, Italy (*Abstract Co-Author*) Nothing to Disclose Chiara Nozzoli, Firenze, Italy (*Abstract Co-Author*) Nothing to Disclose Michela Staderini, Firenze, Italy (*Abstract Co-Author*) Nothing to Disclose Valentina Berti, MD, Florence, Italy (*Abstract Co-Author*) Nothing to Disclose Maurizio Bartolucci, Firenze, Italy (*Abstract Co-Author*) Nothing to Disclose

## **TEACHING POINTS**

In 2014 the International Myeloma Working Group updated the diagnostic criteria for multiple myeloma (MM) and smoldering multiple myeloma (SMM), including MRI findings as possible biomarkers of malignancy. Several works demonstrated the superiority of wholebody (WB) respect to axial skeleton-only MRI in correctly identify the involvement of disease, however implementation and interpretation of WB imaging in MM is often controversial. The aim of this exhibit is: to illustrate the strategies in implementing WB-MR images in clinical practice, including practical tips and tricks to optimize image quality and reduce artifacts; to illustrate the different MRI patterns of involvement of disease and to correlate them with clinical results and other imaging techniques (such as radiographs, CT and FDG-PET); to provide hints for the interpretations of images, showing pitfalls and potential challenges.

# TABLE OF CONTENTS/OUTLINE

1. Introduction2. Criteria for diagnosis of myeloma3. Implementation of WB-MR imaging4. MRI patterns of disease and correlation with other imaging techniques5. MR images processing and interpretation6. Pitfalls and potential challenges

# Imaging and Clinical Features of the Common Endocrine Disorders within the Abdomen

Sunday, Nov. 27 1:00PM - 1:30PM Room: MS Community, Learning Center Station #2

#### **Participants**

Stephen Cole, MD, Atlanta, GA (*Presenter*) Nothing to Disclose Peter J. Park, MD, Atlanta, GA (*Abstract Co-Author*) Nothing to Disclose Pardeep K. Mittal, MD, Atlanta, GA (*Abstract Co-Author*) Nothing to Disclose Fred B. Murphy, MD, Decatur, GA (*Abstract Co-Author*) Nothing to Disclose

# **TEACHING POINTS**

1. The learner will review the most common intra-abdominal endocrine tumor disorders.2. The learner will review each disorders unique clinical presentation, pathophysiology, and individual imaging features (primarily CT and MRI) to accurately distinguish each of these entities.3. The learner will review the Radiologist's role in characterizing functional and non-functional endocrine tumors.4. The learner will brielfly review the common genetic syndromes associated with these endocrine abnormalities.

## TABLE OF CONTENTS/OUTLINE

#### **Honored Educators**

Presenters or authors on this event have been recognized as RSNA Honored Educators for participating in multiple qualifying educational activities. Honored Educators are invested in furthering the profession of radiology by delivering high-quality educational content in their field of study. Learn how you can become an honored educator by visiting the website at: https://www.rsna.org/Honored-Educator-Award/

Pardeep K. Mittal, MD - 2016 Honored Educator

# Lymphoscintigraphy and Its Role in the Management of Pediatric Sarcoma

Sunday, Nov. 27 1:00PM - 1:30PM Room: S503AB Station #10

#### **Participants**

Bret P. Martell, MD, Aurora, CO (Presenter) Nothing to Disclose Brian M. Bagrosky, MD, MS, Castle Pines, CO (Abstract Co-Author) Nothing to Disclose Jennifer J. Kwak, MD, Denver, CO (Abstract Co-Author) Nothing to Disclose

# **TEACHING POINTS**

The purpose of this exhibit is to:1. Learn the roles that lymphoscintigraphy and sentinel lymph node biopsy play in the management of pediatric sarcoma.2. Demonstrate that PET/CT alone is not sufficient to determine if metastatic lymph nodes are present.3. Illustrate how to perform a lymphoscintigraphy procedure in children with sarcoma to identify sentinel lymph nodes.

## **TABLE OF CONTENTS/OUTLINE**

Discuss the roles that lymphoscintigraphy and sentinel lymph node biopsy have in the management of pediatric soft tissue sarcomas.

Learn how SPECT/CT can be helpful in localizing sentinel nodes in areas with complex anatomy such as the head and neck. Discuss how positive lymph nodes status on biopsy doesn't necessarily correlate with positive findings on PET/CT. Review cases of lymphoscintigraphy performed in children with soft tissue sarcomas and how the pathology correlates with PET/CT imaging.

Learn how to perform a lymphoscintigraphy in pediatric patients with soft tissue sarcomas.

Quantification of Thalamic Metabolism on FDG-PET in Patients with Mesial Temporal Sclerosis: Correlation of Thalamic Dysfunction and Seizure Type and Epilepsy Duration

Sunday, Nov. 27 1:00PM - 1:30PM Room: S503AB Station #6

## Participants

Carlos Leiva-Salinas, MD,PhD, Charlottesville, VA (*Presenter*) Nothing to Disclose Nathan Fountain, Charlottesville, VA (*Abstract Co-Author*) Nothing to Disclose Mark Quigg, Charlottesville, VA (*Abstract Co-Author*) Nothing to Disclose W Jeffrey Elias, Charlottesville, VA (*Abstract Co-Author*) Nothing to Disclose James Patrie, MS, Charlottesville, VA (*Abstract Co-Author*) Nothing to Disclose Patrice K. Rehm, MD, Charlottesville, VA (*Abstract Co-Author*) Nothing to Disclose

#### PURPOSE

To correlate the degree of ipsilateral thalamic metabolism on FDG PET with total epilepsy duration and seizure type in patients with intractable epilepsy and mesial temporal sclerosis (MTS) who were seizure-free for at least two years after surgery. To assess the accuracy of thalamic hypometabolism to lateralize the epileptic focus on FDG PET scans

#### **METHOD AND MATERIALS**

We retrospectively reviewed the pre-surgical brain FDG PET of 18 patients with intractable temporal lobe epilepsy and MRI findings of MTS, and who were seizure-free for at least two years after anterior temporal lobectomy. We automatically segmented the thalami and calculated the mean SUV for the ipsilateral and contralateral to the MRI abnormality. We compared the SUV values in the bilateral thalami using the paired t test. We correlated the metabolic activity in the thalami with the total epilepsy duration (years from onset) by means of the Spearman correlation coefficient.

## RESULTS

Fourteen patients were female (77.8%). Twelve subjects had left MTS (66.67%). Eight patients had simple/complex partial seizures, 10 patients had both partial and secondary generalized seizures. Mean age was  $37.2\pm12.91$  years. Mean SUV in the thalamus ipsilateral to the MTS ( $6.36\pm2.31$ ) was significantly lower than the contralateral ( $6.52\pm2.43$ ) (p=0.02). The ipsilateral thalamus was more hypometabolic than the contralateral in 15 of the 18 patients (83.3%). In patients with secondary generalized seizures, the mean SUV in the ipsilateral thalamus ( $6.74\pm2.27$ ) was significantly lower than in the contralateral ( $6.94\pm2.42$ ) (p=0.02). In patients with simple/complex partial seizures, the mean SUV in the ipsilateral thalamus ( $6.74\pm2.27$ ) was significantly lower than in the contralateral ( $6.94\pm2.42$ ) (p=0.02). In patients with simple/complex partial seizures, the mean SUV in the ipsilateral thalamus was  $5.89\pm2.42$  as opposed to  $6\pm2.51$  in the contralateral, p=0.29. There was a significant (p=0.037) strong, negative (rs=-0.66) correlation between the SUV in the ipsilateral thalamus and epilepsy duration in patients with generalized seizures.

# CONCLUSION

In patients with confirmed MTS, the thalamus ipsilateral to the temporal lobe abnormality was significantly hypometabolic compared to the contralateral. The degree of hypometabolism was greater in patients with longstanding epilepsy and in subjects with secondary generalized seizures compared to patients with partial seizures

# **CLINICAL RELEVANCE/APPLICATION**

Semi-quantitative analysis of FDG PET may be used as a biomarker of thalamic impairment and can contribute to lateralizing the epileptic foci in patients with MTS

# PET/CT Neuroimaging of Nanoparticle Intranasal Drug Delivery

Sunday, Nov. 27 1:00PM - 1:30PM Room: S503AB Station #7

#### Awards

#### **Student Travel Stipend Award**

#### Participants

Michael C. Veronesi, MD, PhD, Chicago, IL (*Presenter*) Nothing to Disclose Shih-Hsun Cheng, PhD, Chicago, IL (*Abstract Co-Author*) Nothing to Disclose Marta A. Zamora, BS, Chicago, IL (*Abstract Co-Author*) Nothing to Disclose Hsiu-Ming Tsai, PhD, Chicago, IL (*Abstract Co-Author*) Nothing to Disclose Chin-Tu Chen, PhD, Chicago, IL (*Abstract Co-Author*) Stockholder, EVO Worldwide , IncStockholder, Medical Simulation Corporation Stockholder, EDDA Technology, Inc Stockholder, EnDepth Vision Systems, LLC Research Consultant, DxRay, Inc Advisor, RefleXion Medical Inc

Michael W. Vannier, MD, Chicago, IL (Abstract Co-Author) Nothing to Disclose

## PURPOSE

The fate of radiolabeled nanoparticles administered intranasally was determined with microPET/CT in a rat model to assess the feasibility of CNS drug delivery across the blood-brain barrier via this route.

## **METHOD AND MATERIALS**

100 nm-sized polymer-micellar nanoparticles (NPs) tagged with Zirconium 89 were delivered intranasally (INDD, N=3) or IV (N=3) to adult rats. PET/CT images were obtained over 2 hr in vivo. PET activity was quantitated in brain subregions and SUVs were derived from atlas-based regions-of-interest (ROIs). The olfactory region, brainstem and forebrain regions of several brains were isolated for independent verification of nanoparticle localization using gamma well counting at 1 hr (N=3), 2 hr (N=6), 4 hr (N=3), 6 hr (N=3) and 24 hr (N=3) following INDD or IV administration. Autoradiography studies of three animal brains were performed at 1 and 2 hr following INDD or IV administration and compared to the PET/CT and gamma well counting studies.

#### RESULTS

In vivo PET/CT imaging demonstrated uptake of NPs into the brain as much as 35-fold higher after INDD as compared to IV administration. Brain subregional activity was validated ex vivo by observing the highest activity in the olfactory region and brain stem as observed with in vivo imaging. In a similar pattern, to the PET results, the gamma well counting studies and autoradiography studies demonstrated increased uptake in the olfactory regions and brainstem to a much greater degree than the forebrain structures at early time points.

# CONCLUSION

The temporal and spatial distribution of nanoparticles can be determined after intranasal delivery using microPET/CT. There is a critical and immediate need for better evaluation of drug delivery to the central nervous system, especially through the intranasal route. INDD of radio-nanoparticle drug delivery systems evaluated using in vivo microimaging and validated ex vivo using PET/CT, gamma well counting and autoradiography may significantly impact the emerging field of radio-nanotheranostics.

# **CLINICAL RELEVANCE/APPLICATION**

INDD of radio-nanoparticle drug delivery systems evaluated using in vivo microimaging and validated ex vivo using PET/CT, gamma well counting and autoradiography may significantly impact the emerging field of radio-nanotheranostics.

#### **Honored Educators**

Presenters or authors on this event have been recognized as RSNA Honored Educators for participating in multiple qualifying educational activities. Honored Educators are invested in furthering the profession of radiology by delivering high-quality educational content in their field of study. Learn how you can become an honored educator by visiting the website at: https://www.rsna.org/Honored-Educator-Award/

Michael W. Vannier, MD - 2015 Honored Educator

External Validation of Therapy Response Interpretation Criteria (Hopkins Criteria) with Inter-reader Reliability, Accuracy and Progression Free Survival Outcomes

Sunday, Nov. 27 1:00PM - 1:30PM Room: S503AB Station #8

## Participants

Ayse T. Karagulle Kendi, MD, Rochester, MN (*Abstract Co-Author*) Nothing to Disclose David C. Brandon, MD, Decatur, GA (*Abstract Co-Author*) Nothing to Disclose Jeffrey Switchenko, PhD, Atlanta, GA (*Abstract Co-Author*) Nothing to Disclose J T. Wadsworth, Atlanta, GA (*Abstract Co-Author*) Nothing to Disclose Mark El-Deiry, Atlanta, GA (*Abstract Co-Author*) Nothing to Disclose Nabil F. Saba, Atlanta, GA (*Abstract Co-Author*) Nothing to Disclose David M. Schuster, MD, Atlanta, GA (*Presenter*) Institutional Research Grant, Nihon Medi-Physics Co, Ltd; Institutional Research Grant, Blue Earth Diagnostics Ltd; Consultant, WellPoint, Inc; ; Rathan M. Subramaniam, MD, PhD, Dallas, TX (*Abstract Co-Author*) Nothing to Disclose

#### PURPOSE

Qualitative assessment of post therapy PET/CT results is important to provide reproducible and a systemic reporting. A recently introduced response criteria, known as Hopkins Criteria showed promising results in the assessment of head and neck cancer. In this study our aim is to re-validate the Hopkins interpretation system to assess therapy response and progression free survival in head and neck squamous cell cancer patients (HNSCC).

# METHOD AND MATERIALS

The study included 69 biopsy proven HNSCC patients who underwent post therapy PET/CT between 5-24 weeks after completion of therapy. PET/CT images were interpreted by one nuclear medicine physician and one nuclear radiologist independently. The studies were scored according to Hopkins Criteria for right neck, left neck, primary tumor site, and overall assessment. Scores 1, 2, 3 were considered as negative and scores 4 and 5 were considered positive for persistent tumors. Inter-reader variability was assessed using percent agreement and Kappa statistics. Progression-free survival (PFS) was analyzed by Kaplan-Meier plots.

#### RESULTS

Of the 69 patients in the study, 59 (85.5%) were male, 10 (14.5%) were female. The mean age was 62.8 years. There was 91.3%, 97.6%, 97.6%, 91.3% between the readers for overall, right neck, left neck, and primary tumor site response scores, respectively. The corresponding k coefficients were, 0.57, 0.84, 0.78, 0.65 for overall, right neck, left neck, and primary tumor site, respectively Cox multivariate regression analysis showed positive primary tumor site scores and overall scores were associated with a higher risk of progression (p<0.05).

## CONCLUSION

External validation of Hopkins Criteria showed excellent inter-reader agreement and prediction of PFS in this cohort of HNSCC patients.

# **CLINICAL RELEVANCE/APPLICATION**

Systemic and reproducible interpretation system, called Hopkins criteria better classifies post therapy PET/CT of head and neck carcinoma patients compared to semi-quantitative methods, including SUVmax.

Evaluation of Practical Interpretation Hurdles in 68Ga-PSMA-PET/CT in 55 Patients: Physiologic Tracer Distribution, Non-prostate-cancer Malignancies and Incidentalomas

Sunday, Nov. 27 1:00PM - 1:30PM Room: S503AB Station #9

## Participants

Julian Kirchner, Dusseldorf, Germany (*Presenter*) Nothing to Disclose Benedikt M. Schaarschmidt, MD, Dusseldorf, Germany (*Abstract Co-Author*) Nothing to Disclose Lino Sawicki, MD, Dusseldorf, Germany (*Abstract Co-Author*) Nothing to Disclose Christian Buchbender, Duesseldorf, Germany (*Abstract Co-Author*) Nothing to Disclose Gerald Antoch, MD, Duesseldorf, Germany (*Abstract Co-Author*) Nothing to Disclose Philipp Heusch, MD, Duesseldorf, Germany (*Abstract Co-Author*) Nothing to Disclose

#### PURPOSE

68Ga-labelled prostate-specific mebrane antigen (PSMA) ligand is a novel and promising tracer for positron emission tomography / computed tomography (PET/CT) especially in recurrent prostate cancer. The aim of this study was to investigate the physiologic tracer distribution and evaluate focal or diffuse 68Ga-PSMA uptake in non-prostate-cancer malignancies and incidental findings.

#### **METHOD AND MATERIALS**

68Ga PSMA-PET/CT scans in 55 men (mean age  $66 \pm 9.07$ y; mean activity: 188MBq) performed for staging of prostate cancer (49) or renal cell carcinoma (6) were analysed retrospectively. By two independent readers incidental tracer uptake was analyzed and evaluated on a syngo.via workstation (Siemens Healthcare GmbH, Erlangen, Germany). Maximum standardized uptake value (SUVmax) was measured using an isocontour volume of interest. Metastatic tracer uptake was excluded by follow-up or clinical examinations.

## RESULTS

As expected a mostly homogenous PSMA uptake was found in lacrimal gland (SUVmax 15.7), parotid gland (SUVmax 24.4), submandibular gland (SUVmax 26.6), vocal cords (SUVmax 8.4), waldeyer's ring (SUVmax 10.3), liver (SUVmax 8.5), spleen (SUVmax 10.8), kidneys (SUVmax 66.4) and pars descendens duodeni (SUVmax 17.6).In 13 patients a fokal PSMA uptake of the thyreoid (SUVmax 4.3) was found. In 31 patients a fokal PSMA uptake of knees synovia (SUVmax 2,0) was found. Here, additional 3 patients showed a PSMA uptake of the tibial plateau (SUVmax 2.7), 2 of them with correlating signal irregularities in also performed MRI. The primary renal cell carcinomas in 5 patients had a mean SUVmax of 9.9. Further PSMA uptake was found in one patient due to fibrous dysplasia of right Os ilium (SUVmax 7.7) and in the gluteal fatty tissue of another patient due to a liposarcoma (SUVmax 1.5).

#### CONCLUSION

Biodistribution of the novel 68Ga-PSMA tracer was analysed. Among prostate cancer lesions and healthy organs various other benign findings and malignant neoplasms may also express PSMA and show tracer uptake on 68Ga PSMA-PET/CT.

## **CLINICAL RELEVANCE/APPLICATION**

It is important to be aware of the possibility of non metastatic PSMA uptake to avoid interpretation errors. Biopsy of atypical or clinically unexpected tracer uptake might be advisory in some cases.

Primary Progressive Aphasia: Clinical Variants and FDG-PET Findings

Sunday, Nov. 27 1:00PM - 1:30PM Room: NR Community, Learning Center Station #7

#### **Participants**

Mohammed S. Bermo, MD, FRCR, Seattle , WA (*Presenter*) Nothing to Disclose Malak Itani, MD, Seattle, WA (*Abstract Co-Author*) Nothing to Disclose Megan M. Zare, MD, Seattle, WA (*Abstract Co-Author*) Nothing to Disclose Manuela C. Matesan, MD, PhD, Seattle, WA (*Abstract Co-Author*) Nothing to Disclose

# **TEACHING POINTS**

1-Primary progressive aphasia (PPA) is an uncommon clinical syndrome characterized by progressive deterioration of certain language functions with relative sparing of other cognitive skills. It typically results from neurodegenerative disorder affecting primarily the language areas. Brain tumors and stroke might have similar clinical presentation and have to be ruled out.2-There are three clinical variants of PPA that correlate with the affected region of the brain: Nonfluent/agrammatic, semantic, and logopenic variants.3-Combination of FDG-PET, MRI and fMRI is useful in localizing language function, confirming hypometabolism in the affected language area of the dominant hemisphere and excluding unexpected pathology.

## TABLE OF CONTENTS/OUTLINE

1-Language models: Broca-Wernicke model Dual stream model2-Classification of Primary progressive aphasia: Nonfluent/agrammatic variant Semantic variant Logopenic variant3-Diagnostic tools FDG-PET Other PET tracers MRI fMRIOther techniques

## NR291-ED-SUB8

Navigating the Cavernous Sinus: Clinical and Radiologic Correlation of Pathology at the Crossroad of the Skullbase

Sunday, Nov. 27 1:00PM - 1:30PM Room: NR Community, Learning Center Station #8

# Participants

Michael Wasserman, MD, Boston, MA (*Abstract Co-Author*) Nothing to Disclose Margaret N. Chapman, MD, Boston , MA (*Presenter*) Nothing to Disclose Hirofumi Kuno, MD, PhD, boston, MA (*Abstract Co-Author*) Nothing to Disclose Osamu Sakai, MD, PhD, Boston, MA (*Abstract Co-Author*) Consultant, Guerbet SA

## **TEACHING POINTS**

The cavernous sinus is a busy crossroad at the junction of the skull base and intracranial compartment. Many important structures are located within this region, including arterial/venous structures and cranial nerves. Pathology results in multiple clinical presentations, including cavernous sinus syndrome. The aim of this exhibit is to: 1. Review anatomy and multiple entry and exit points of the cavernous sinus and paracavernous regions2. Review the clinical presentation of cavernous sinus syndrome3. With clinical case presentations, review CT, MR and angiographic imaging features of various pathologies that affect this region and how they may present clinically

## TABLE OF CONTENTS/OUTLINE

1. Discuss anatomy of the cavernous sinus including a. Vascular anatomyb. Cranial nerve anatomyc. Sellad. Review skull base "entry and exit" points that lead to the cavernous region 2. Review clinical presentations of cavernous sinus syndrome and other cavernous sinus pathologies and discuss clinical implications of early recognition3. Case based review of pathologya. Vascular: CCF, cavernous sinus thrombosis, aneurysmsb. Infectious: thrombophlebitis, extension of infection from head and neck and intracranial regionsc. Inflammatory: pseudotumor, Tolosa-Hunt, IgG4 disease, sarcoidosisd. Neoplastic: primary and metastatic

#### **Honored Educators**

Presenters or authors on this event have been recognized as RSNA Honored Educators for participating in multiple qualifying educational activities. Honored Educators are invested in furthering the profession of radiology by delivering high-quality educational content in their field of study. Learn how you can become an honored educator by visiting the website at: https://www.rsna.org/Honored-Educator-Award/

Osamu Sakai, MD, PhD - 2013 Honored Educator Osamu Sakai, MD, PhD - 2014 Honored Educator Osamu Sakai, MD, PhD - 2015 Honored Educator

# Paraspinal Muscle Abnormalities on MRI in Intravenous Drug Users

Sunday, Nov. 27 1:00PM - 1:30PM Room: NR Community, Learning Center Station #1

#### Awards

#### **Student Travel Stipend Award**

#### Participants

Maria Khalid, MD, Boston, MA (*Presenter*) Nothing to Disclose Vanesa C. Andreu, MD, Madrid, Spain (*Abstract Co-Author*) Nothing to Disclose Charles G. Colip, MD, Boston, MA (*Abstract Co-Author*) Nothing to Disclose Mina Lotfi, MD, Boston, MA (*Abstract Co-Author*) Nothing to Disclose Nagaraj-Setty Holalkere, MD, Boston, MA (*Abstract Co-Author*) Owner, Imaginglink, LLC Bindu Setty, MD, Boston, MA (*Abstract Co-Author*) Nothing to Disclose

#### PURPOSE

Spinal infections are a common entity in intravenous drug users (IVDU). MRI findings related to spinal infections, including osteomyelitis, discitis, and epidural abscesses have been reported previously. The significance of findings in the paraspinal musculature, especially isolated paraspinal muscle findings has not been explored previously. The purpose of this study is to determine the incidence and significance of paraspinal muscle findings on MRI in a cohort of IVDU.

## **METHOD AND MATERIALS**

This was a retrospective IRB-approved review of 167 patients with reported IV drug use (M:F = 96:71, mean age= 40 years). From 2010-2014, patients were evaluated with 255 spinal MRIs performed on a 1.5 T magnet in the ER. Medical records and MRI images were retrospectively reviewed. Findings in the paraspinal muscles including T2 signal, post-contrast enhancement, abscess, extent of musculature involved, and uni- or bilateral involvement were evaluated. Findings were correlated with additional findings of spinal infection on MRI as well as medical records, microbiology, and surgical reports.

#### RESULTS

A total of 50/167 patients (29%) showed some paraspinal abnormality. Of these, 5/50 (10%) were not mentioned in the MRI report. 44/50 (88%) patients had abnormal T2 signal , 46/50 (92%) demonstrated post-contrast enhancement, an abscess was seen in 7/48 (15%), while 7/48 (15%) had positive blood cultures. 5/7 (71%) patients with a paraspinal muscle abscess demonstrated positive blood cultures. Of the 50 patients with paraspinal findings, 23 (46%) had isolated paraspinal muscle abnormalities. Surgical intervention was done in just 1 of the 23 (0.04%), while blood cultures were positive in 5 (22%).

## CONCLUSION

While paraspinal muscle abnormalities, particularly abnormal T2 signal and enhancement, are commonly seen in the setting of IVDU, when isolated, these findings are not commonly associated with positive blood cultures or surgical intervention.

## **CLINICAL RELEVANCE/APPLICATION**

Paraspinal muscle abnormalities are often noted on MRI in patients with a history of IV drug use. When isolated, the relevance of these findings has not been previously explored.

Interhemispheric Morphology of Diffusion Properties in the Brainstem Provides New Insight to Clinical Assessment of Chronic Ischemic Stroke Patients with Upper Limb Impairment

Sunday, Nov. 27 1:00PM - 1:30PM Room: NR Community, Learning Center Station #2

# Participants

Meriel Owen, MSc, Chicago, IL (*Presenter*) Nothing to Disclose Carson Ingo, Chicago, IL (*Abstract Co-Author*) Nothing to Disclose Julius P. Dewald, PhD, Chicago, IL (*Abstract Co-Author*) Nothing to Disclose

## PURPOSE

Ischemic damage from stroke causes disruption of neural pathways; however, less is known about the resulting changes in normal appearing white matter in individuals that experience upper limb impairment. In this study, we used Diffusion Tensor Imaging to quantify microstructural integrity changes in sub-cortical regions contralateral to the lesion and in the brainstem in stroke subjects when compared to healthy controls. Additionally, we used these imaging measurements to predict impairment by Fugl-Meyer assessment (FMA), 0 (severely impaired) – 66 (not impaired).

# METHOD AND MATERIALS

MPRAGE (1.0mm<sup>3</sup> isotropic) and spin-echo echo-planar (SE-EPI) DTI (1.5mm<sup>3</sup> isotropic, b=1000 s/mm<sup>2</sup>, 60 directions, 9 b=0 s/mm<sup>2</sup> averages) were performed on 12 moderately to severely impaired stroke individuals (FMA 11-33) and 14 healthy age-matched controls. For stroke participants, FMA was taken to quantify upper extremity impairment. Tract-based spatial statistical (TBSS) analysis was performed using fractional anisotropy (FA), radial diffusivity (RD), and axial diffusivity (AD) measures.

## RESULTS

We demonstrate widespread decreased FA and increased AD and RD in sub-cortical regions contralateral to the lesion in stroke when compared to control; however, we observed the opposite trend in the midbrain. Surprisingly, for the stroke subjects, increased FA in the midbrain significantly correlated with FMA (r=.64, p=.032). Corticospinal tract AD also negatively correlated with FMA (r=-.69, p=.02), suggesting that corticospinal tract and brainstem microstructural properties may be important factors for clinical outcome.

# CONCLUSION

Our results describe the widespread structural changes that occur post-stroke, but highlight the importance of the diffusion properties within the corticospinal tract and midbrain in predicting an individual's clinical impairment level in chronic stroke.

## **CLINICAL RELEVANCE/APPLICATION**

It is important to better understand the structural changes that occur post-stroke and how they relate to impairment. Doing so will help design better treatments and interventions for acute stroke.

Comparison of MR-permeability Imaging from C-11 Methionine PET in Differentiating Radiation Necrosis from Recurrent Metastatic Tumors of the Brain after Gamma Knife Radiosurgery

Sunday, Nov. 27 1:00PM - 1:30PM Room: NR Community, Learning Center Station #3

# Participants

Noriaki Tomura, MD,PhD, Koriyama, Japan (*Presenter*) Nothing to Disclose Toshiyuki Saginoya, MD, PhD, Koriyama, Japan (*Abstract Co-Author*) Nothing to Disclose Yasuhiro Kikuchi, MD, Koriyama, Japan (*Abstract Co-Author*) Nothing to Disclose

#### PURPOSE

MR-permeability imaging was compared with PET using C-11 methionine (MET) in differentiating radiation necrosis from recurrent tumors in patients with metastatic brain tumors after gamma knife radiosurgery (GK).

## **METHOD AND MATERIALS**

The study was performed for 18 lesions from 15 patients with metastatic brain tumors who underwent GK. Ten lesions were identified as recurrent tumors by surgery after the study. Eight lesions were diagnosed as radiation necrosis because of a lack of change or a decrease in size after GK. Both MET-PET and F-18 fluorodeoxyglucose (FDG-PET) were performed on the same day. MR-permeability imaging and diffusion-weighted imaging (DWI) were performed within 1 week before or after PET. Using dynamic contrast-enhanced (DCE)-MRI, the transfer constant between intra- and extravascular and extracellular spaces (Ktrans) (/min.), the extravascular extracellular space (Ve), the transfer constant from the extracellular extravascular space to plasma (Kep), initial area under the signal intensity-time curve (IAUGC), and contrast enhancement ratio (CER), and the minimum apparent diffusion coefficient (ADCmin)(×0.001 mm2/s) were calculated of the lesion. On PET images, the ratio of the maximum standard uptake value (SUVmax) of the lesion divided by the SUVmax of the symmetrical normal site was measured (MET-ratio and FDG ratio, respectively). ROC analysis was performed to evaluate the utility of those parameters for differentiating radiation necrosis from recurrent tumors.

## RESULTS

Area under the ROC curve for differentiating radiation necrosis from recurrent tumors was highest for MET-ratio (0.90) followed by CER (0.81), IAUGC (0.78), Ktrans (0.74), Ve (0.65), ADCmin (0.60), Kep (0.55), and FDG ratio (0.53). The cutoff value was 1.42 with MET ratio, 0.61 with CER, 0.2 with IAUGC, 0.05 with Ktrans, 0.27 with Ve, 0.73 with ADCmin, 0.32 with Kep, and 0.97 with FDG ratio. Significant difference (p<0.05 each) in MET ratio, CER, and IAUGC were evident between radiation necrosis and recurrent tumor.

#### CONCLUSION

MET-PET is superior to MR-permeability imaging, ADC, and FDG-PET in differentiating radiation necrosis from recurrent tumors after GK. In MR-permeability imaging, CER and IAUGC are superior to other parameters.

# **CLINICAL RELEVANCE/APPLICATION**

MET-PET is superior to MR-permeability imaging, ADC, and FDG-PET in differentiating radiation necrosis from recurrent tumors after GK. CER and IAUGC followed MET-PET.

## NR350-SD-SUB4

To Evaluate the Differential Role of PET-CT and Post Contrast MRI in Head and Neck Tumours with Local Metastases

Sunday, Nov. 27 1:00PM - 1:30PM Room: NR Community, Learning Center Station #4

## Participants

Sikandar M. Shaikh, DMRD, Hyderabad, India (Presenter) Nothing to Disclose

#### PURPOSE

To evaluate significant differences between the results of 18F-FDG-PET/CT and MRI in their ability to detect primary head-andneck cancer and local metastatic spread.

#### **METHOD AND MATERIALS**

The test results of 21 patients with suspected primary head-and-neck cancer which were examined with dedicated examination of the neck at simultaneous 18-F-FDG-PET/CT and immediately there after a simultaneous post contrast MRI were analysed. A nuclear medicine physician and a radiologist evaluated the data of both examinations in consensus in a blinded manner with a 6-week gap between evaluation of the two examinations. Thereafter the results were compared with the gold standard of histopathological report, follow-up imaging or a consensus interpretation of all available data. Sensitivity, specificity, positive (PPV) and negative predictive value (NPV) were calculated for both methods.

## RESULTS

Altogether 45 lesions were detected in PET/CT and 63 lesions in MRI. By use of gold standard 25 malignant lesions were found, 8 primary tumours and 30 lymph node metastases. PET/CT presented a sensitivity of 69.6%, a specificity of 97.4%, a PPV of 92.9% and a NPV of 87.0%. PET/MRI presented a sensitivity of 80.4%, a specificity of 90.8%, a PPV of 78.3% and a NPV of 91.8%.

## CONCLUSION

MRI shows a higher sensitivity but a lower specificity in detection of primary head-and-neck cancer and local metastases in comparison to 18F-FDG-PET/CT.

#### **CLINICAL RELEVANCE/APPLICATION**

MR is superior as it has very Good soft tissue sensitivity compared with PET-CT

## NR352-SD-SUB6

# Novel CT Blend Sign Highly Correlates with CTA Spot Sign and Reliably Predicts Poor Outcome after Intracerebral Hemorrhage

Sunday, Nov. 27 1:00PM - 1:30PM Room: NR Community, Learning Center Station #6

# Participants

Uta Hanning, MD, Muenster, Germany (*Presenter*) Nothing to Disclose Thomas Niederstadt, MD, Munster, Germany (*Abstract Co-Author*) Nothing to Disclose Andre Kemmling, MD, Luebeck, Germany (*Abstract Co-Author*) Nothing to Disclose Heindel Walter, Muenster, Germany (*Abstract Co-Author*) Nothing to Disclose Wolfram Schwindt, MD, Muenster, Germany (*Abstract Co-Author*) Nothing to Disclose Christian Cnyrim, Muenster, Germany (*Abstract Co-Author*) Nothing to Disclose Tarek Zoubi, Muenster, Germany (*Abstract Co-Author*) Nothing to Disclose Michael Schwake, Muenster, Germany (*Abstract Co-Author*) Nothing to Disclose Peter Sporns, MD, Munster, Germany (*Abstract Co-Author*) Nothing to Disclose

#### PURPOSE

Significant early hematoma growth in patients with intracerebral hemorrhage (ICH) occurs in approximately one third of the cases and is an independent predictor of poor functional outcome. Recently the novel blend sign (BS) has been introduced as a new imaging sign for predicting hematoma growth in non-enhanced computed tomography (NCCT). Another parameter predicting increasing hematoma size is the well-established spot sign (SS) visible in computed tomography angiography (CTA). We therefore conducted a research that aimed to clarify the association between established SS and novel BS and their values predicting the eventual outcome.

#### **METHOD AND MATERIALS**

Retrospective study of our database for patients with ICH aged > 18 years between January 2010 and August 2015. As inclusion criteria we defined: 1) spontaneous ICH confirmed on NCCT and 2) NCCT and CTA performed on admission within 6 hours after onset of symptoms. We defined a binary outcome (poor and good outcome). As poor outcome we defined 1) early hemicraniectomy within the first 48 hours after symptom onset under standardized criteria or 2) secondary decrease of Glasgow Come Scale of more than 3 points. The predictive value of BS and SS was assessed in univariate and multivariable logistic regression models.

#### RESULTS

Of 182 patients with spontaneous ICH 37 (20.3%) presented with BS and 39 (21.4%) with SS on initial imaging. Of the 81 patients with poor outcome, 38.3% had BS and SS on admission. Of these 30 patients 30 (88.2%) had a poor outcome. In the univariate logistic analysis baseline hematoma volume (p=<0.001), intraventricular hemorrhage (p=0.002) and the presence of BS and SS (both p=<0.001) on admission CT scan were associated with poor outcome. Multivariate logistic regression analysis demonstrated that the baseline hematoma volume (OR 1.06; p=<0.001), intraventricular hemorrhage (OR 3.08 p=0.008) and the presence of BS (OR 11.47; p=<0.001) scan to be independent predictors of poor outcome.

# CONCLUSION

The novel CT blend sign shows a very high correlation with CTA spot sign and is a reliable predictor of poor outcome after spontaneous ICH.

# **CLINICAL RELEVANCE/APPLICATION**

Especially in a setting where CTA is not readily available or with strong contraindications for contrast application (distinct allergy, far progressed renal dysfunction) sole acquisition of NCCT and evaluation of BS is a reliable option for detection of hematoma growth associated with poor outcome.

What Every Radiologist Should Know about Adnexal Torsion: A Pictorial Review and Pitfalls in Imaging

Sunday, Nov. 27 1:00PM - 1:30PM Room: OB Community, Learning Center Station #1

#### Awards

## **Identified for RadioGraphics**

#### **Participants**

Guillaume Ssi-Yan-Kai, Clamart, France (*Presenter*) Nothing to Disclose Anne-Laure Rivain, Clamart, France (*Abstract Co-Author*) Nothing to Disclose Caroline Trichot, Clamart, France (*Abstract Co-Author*) Nothing to Disclose Marie-Chantal Morcelet, Clamart, France (*Abstract Co-Author*) Nothing to Disclose Sophie Prevot, Clamart, France (*Abstract Co-Author*) Nothing to Disclose Xavier Deffieux, Clamart, France (*Abstract Co-Author*) Nothing to Disclose Jocelyne De Laveaucoupet, MD, Clamart, France (*Abstract Co-Author*) Nothing to Disclose

## **TEACHING POINTS**

1. To review anatomical considerations of the female pelvis and describe the types of adnexal torsions2. To highlight the imaging features of adnexal torsions on ultrasonography, doppler, CT and MRI3. To identify the main mimickers of adnexal torsions

# TABLE OF CONTENTS/OUTLINE

The goal of this review is to raise radiologists' awareness of adnexal torsions' pathophysiology, clinical presentation and radiological features. The differentiation of malignant ovarian tumors from chronic adnexal torsion can be challenging. A. Anatomy of the female pelvis and adnexa B. Pathophysiology1. (Tubo-) Ovarian torsion2. Isolated fallopian tube torsion3. Chronic adnexal torsionC. Imaging features of torsion on Ultrasonography, Doppler, CT, MRI1. Representative cases2. Special cases of torsions: in pregnancy, in childhood, in elderlyD. Mimics1. Haemorrhagic corpus luteal cyst2. Appendicitis3. Ovarian hyper stimulation syndrome4. Tubo-ovarian abscess / Pyosalpinx

# The Morbidly Adherent Placenta: A Practical Approach to the MR Imaging and Diagnosis of Placenta Accreta

Sunday, Nov. 27 1:00PM - 1:30PM Room: OB Community, Learning Center Station #2

#### **Participants**

Courtney A. Woodfield, MD, Newtown, PA (*Presenter*) Consultant, Siemens AG Philip S. Lim, MD, Abington, PA (*Abstract Co-Author*) Consultant, BioClinica, Inc ; Consultant, ICON plc ; Consultant, Siemens AG; ;

## **TEACHING POINTS**

1. Placenta accreta occurs along a spectrum of disease and accurate diagnosis of the presence and type of accreta is critical to directing correct patient management.2. Multiple MR imaging signs of placenta accreta have been described and in combination increase the diagnostic accuracy of MR imaging.3. An efficient comprehensive MR imaging protocol and familiarity with both the normal and abnormal appearance of the placenta can improve the performance of MR imaging for placenta accreta.

## TABLE OF CONTENTS/OUTLINE

1. Review the risk factors for and the various types of placenta accreta.2. Provide indications for MR imaging and a comprehensive MR imaging protocol for evaluation of placenta accreta.3. Describe the MR imaging features of the normal placenta.4. Illustrate the MR imaging signs of placenta accreta including extrauterine invasion, intraplacental T2 dark bands, abnormal vascularity, heterogeneous signal, placental bulge, focal myometrial thinning/interruption, urinary bladder tenting, and placental protrusion into the cervix.5. Summarize a stepwise approach to evaluating the placenta for signs of accreta.6. Discuss the MR imaging pearls and pitfalls of diagnosing placenta accreta.7. Review the current management options for patients diagnosed with placenta accreta.

Appendicitis and Beyond: A Case-based Review of Gastrointestinal Pathology in Pediatric Patients Undergoing Ultrasound Evaluation of Acute Abdominal Pain

Sunday, Nov. 27 1:00PM - 1:30PM Room: PD Community, Learning Center Station #6

#### Awards

**Certificate of Merit** 

#### **Participants**

Hailey Allen, MD, Madison, WI (*Presenter*) Nothing to Disclose Brian Y. Chan, MD, Madison, WI (*Abstract Co-Author*) Nothing to Disclose Erica Riedesel, MD, Boston, MA (*Abstract Co-Author*) Nothing to Disclose Kara Gill, MD, Madison, WI (*Abstract Co-Author*) Nothing to Disclose

# **TEACHING POINTS**

1. Discuss ultrasound protocol optimization for evaluation of gastrointestinal pathology in pediatric patients presenting to the emergency department with acute abdominal pain.2. Provide technical and practical tips for radiologists interpreting and often performing such examinations in real time.3. Review in a case-based format the ultrasound findings of various etiologies that can present as right lower quadrant pain.4. Delineate for the learner when findings on ultrasound alone can be diagnostic and when additional studies such as CT or MRI may be indicated.

# TABLE OF CONTENTS/OUTLINE

Introduction Review of the technical features of a sample pediatric abdominal ultrasound protocol in regards to evaluation of the gastrointestinal tract. Practical tips for US scanning the pediatric abdomen in real time. Case-based review of pediatric intraabdominal pathology with important US findings. Complicated and uncomplicated appendicitis Crohn's disease Mesenteric adenitis Enteritis Omental infarct Ischemic bowel Meckel's diverticulitis Henoch-Schonlein purpura Intussusception Hemolytic uremia syndrome

# **Omental Disease: An Often Forgotten Cause of Acute Abdomen in Children**

Sunday, Nov. 27 1:00PM - 1:30PM Room: PD Community, Learning Center Station #7

#### **Participants**

Carles G. Zaragoza, MD, Sabadell, Spain (*Presenter*) Nothing to Disclose Carmina Duran, MD, Sabadell, Spain (*Abstract Co-Author*) Nothing to Disclose Maria Magdalena Serra Salas, MD, Barcelona, Spain (*Abstract Co-Author*) Nothing to Disclose Carlota C. Rodriguez, MD, Sabadell, Spain (*Abstract Co-Author*) Nothing to Disclose

## **TEACHING POINTS**

To call attention to an underrecognized cause of acute abdomen in children To describe and illustrate the main findings for omental disease on US and CT To show different ways omental disease can present

## **TABLE OF CONTENTS/OUTLINE**

US is the initial imaging study in pediatric patients with acute abdominal pain. Omental disease is a rare cause of acute abdominal pain. The differential diagnosis centers on the most prevalent causes (appendicitis and intussusception) but includes less common entities (e.g., cholecystitis and ovarian torsion). The omentum serves to contain inflammatory and traumatic processes in the abdomen. Since in normal conditions imaging techniques cannot distinguish this organ from other abdominal structures and omental disease is uncommon, it is often omitted from the differential diagnosis. Primary and secondary causes have been described. In our experience, primary causes are more common than reported. In this review we have included the following cases: Primary omental infarction/torsion Primary epiploic appendagitis Omental involvement in appendicular phlegmon Omental involvement in cholecystitis Omental and renal infarction secondary to septic emboli Omental involvement in lymphoma

# Current and Future Directions in Pediatric PET/MRI

Sunday, Nov. 27 1:00PM - 1:30PM Room: PD Community, Learning Center Station #8

#### Awards Cum Laude

## Participants

Maria R. Ponisio, MD, St. Louis, MO (Presenter) Nothing to Disclose

Jonathan E. McConathy, MD, PhD, Birmingham, AL (*Abstract Co-Author*) Research Consultant, Eli Lilly and Company; Research Consultant, Blue Earth Diagnostics Ltd; Research Consultant, Siemens AG; Research Consultant, General Electric Company; Geetika Khanna, MD, MS, Iowa City, IA (*Abstract Co-Author*) Nothing to Disclose

## **TEACHING POINTS**

1. Combination of functional PET data with anatomic and functional information from MRI allows for improved local and distant staging in pediatric solid tumors.

2. Preliminary data shows good correlation between standardized uptake value estimated by PET/CT and PET/MRI

3. PET/MRI provides significant reduction in radiation dose in pediatric patients undergoing serial examinations.

4. For pediatric patients who require both PET and MR imaging but need sedation/anesthesia for imaging, simultaneous PET/MRI helps decrease the duration and number of sedation sessions.

5. Advanced MRI techniques combined with new PET tracers and multiparametric analysis have great potential to increase the diagnostic utility of this hybrid imaging modality.

# TABLE OF CONTENTS/OUTLINE

Overview of PET/MRI for pediatric applications Examples of pediatric PET/MRI including:- Lymphoma

- Pediatric solid tumors (Ewing Sarcoma, Neuroblastoma) (Figure 1-2)

-Neuro-oncology [F-18]FDOPA-PET/MRI in recurrent brain tumors (Figure 5) Pharyngeal Rhabdomyosarcoma (Figure 3)-Epilepsy interictal FDG-PET/MRI detection (Figure 4) Summary and future directions

Breast Masses in Adolescents: Keep Calm & Ultrasound

Sunday, Nov. 27 1:00PM - 1:30PM Room: PD Community, Learning Center Station #4

#### Awards

#### **Student Travel Stipend Award**

#### **Participants**

Carlota C. Rodriguez, MD, Sabadell, Spain (*Presenter*) Nothing to Disclose Carmina Duran, MD, Sabadell, Spain (*Abstract Co-Author*) Nothing to Disclose Sergi Ganau, MD, Sabadell, Spain (*Abstract Co-Author*) Nothing to Disclose Melcior Sentis, Sabadell, Spain (*Abstract Co-Author*) Nothing to Disclose Maria Magdalena Serra Salas, MD, Barcelona, Spain (*Abstract Co-Author*) Nothing to Disclose Carles G. Zaragoza, MD, Sabadell, Spain (*Abstract Co-Author*) Nothing to Disclose Viviana P. Beltran Salazar, MD, Sabadell, Spain (*Abstract Co-Author*) Nothing to Disclose

#### PURPOSE

To describe and illustrate the imaging features of the most common solid breast masses in pediatrics. To familiarize general and pediatric radiologists with these lesions, because their management differs from that of breast masses in adults.

## **METHOD AND MATERIALS**

We retrospectively studied the patients aged 11 to 16 years who underwent breast ultrasonography in the radiology department between January 2005 and September 2015. Of these patients, we included those in whom ultrasonography detected a solid mass.We analyzed the location, multiplicity, size, and ultrasonographic appearance of each lesion.Moreover, we analyzed the treatment of these lesions and their outcome.

#### RESULTS

We studied 230 patients and we included those in whom ultrasonography detected a solid mass: 40 patients. Of the 40 patients studied, 31 had a single lesion and 9 had multiple lesions, of which 4 were bilateral. A total of 51 lesions were studied. The typical ultrasound findings were a single nodule (n= 31), hypo or isoechoic (n=50), homogeneous (n=50) and well defined margins (n=51). Of the 51 nodules, 37 had the typical characteristics of fibroadenomas and required only periodic clinical and radiological follow-up. In the 14 remaining lesions, patients were referred to the breast imaging department for biopsy because they had large (>3cm), fastgrowing, and/or atypical appearing lesions; 13 lesions underwent core biopsy and 1 fineneedle aspiration cytology. Two lesions was also studied with elastography. Histological study found 12 fibroadenomas, 1 low grade borderline phyllodes tumor (in the youngest girl) and 1 hamartoma.10 patients underwent tumorectomy; the rest were followed up periodically (mean, 13 months).

## CONCLUSION

Breast masses in pediatric patients are uncommon and generally benign.Ultrasound is the firstchoice imaging technique.Most of these lesions can be managed conservatively, and biopsy is unnecessary in most cases.

## **CLINICAL RELEVANCE/APPLICATION**

In pediatrics, US is the first choice imaging technique for breast masses, and their management is fundamentally conservative with close follow-up. We should not extrapolate the BI-RADS classification to pediatric patients.

# MRI in Pregnancies at Risk for Joubert Syndrome: A Series of 34 Cases

Sunday, Nov. 27 1:00PM - 1:30PM Room: PD Community, Learning Center Station #5

#### **Participants**

Sahar Saleem, MD, Cairo, Egypt (*Presenter*) Nothing to Disclose Maha S. Zaki, MD, Cairo, Egypt (*Abstract Co-Author*) Nothing to Disclose Ahmed Hesham M. Saeed, Bany Swaif, Egypt (*Abstract Co-Author*) Nothing to Disclose

### PURPOSE

Joubert syndrome is a rare recessive disorder characterized by a posterior fossa malformation (Molar tooth sign MTS). Presence of other cranial and extra-cranial features led to the broader classification: Joubert syndrome and related disorders (JSRD). Prenatal genetic testing and ultrasound may not be conclusive in JSRD. Fetal MRI identified MTS in few case reports. In this study we aim to evaluate the role of MRI as a potential adjunct to early prenatal diagnosis of pregnancies at risk of JSRD.

## **METHOD AND MATERIALS**

In this institutional ethics approved study between 2003 and 2016, we prospectively performed cranial and body MRI for 34 pregnancies (average GA 21 weeks; SD 2.7) at recurrence risk for JSRD. Family diagnoses were: classic Joubert Syndrome (n=31), Joubert syndrome with renal disease (n=2), and Joubert Syndrome with hepatic fibrosis (n=1). We correlated fetal MR findings with prenatal counselling, and outcome measures including pathology, postnatal imaging and clinical outcome.

#### RESULTS

Outcome measures identified 15 cases as JSRD-affected and 19 as normal. MRI confidently reached the correct diagnosis in 29 pregnancies (85.2%) at 21w SD3 and missed a JSRD-affected fetus at 17w. In the 4 remaining fetuses, initial MRI study (at average 22w SD3) was inconclusive for JSRD; follow up MRI after 2 weeks correctly suggested 3 JSRD-affected fetuses and 1 normal. The most common MRI findings in JSRD-affected fetuses were reduced transverse cerebellar diameter at 50th percentile or less (n=15), vermian hypopasia (buttock sign) (n=13), (MTS) (n=10), and enlarged cisterna magna (n=9). Associated abnormalities included cerebral ventriculomegaly (n=2), posterior encephalocele (n=1), kinked brainstem (n=1), and bilateral cystic kidneys (n=3). MRI identified MTS between 16-24 weeks of gestation at an average 19w SD 2. Fetal MRI findings supported prenatal counseling and pregnancy management.

# CONCLUSION

MRI is a valuable tool for early prenatal diagnosis of JSRD in pregnancies at high risk of recurrence.

# **CLINICAL RELEVANCE/APPLICATION**

Fetal MRI helps in prenatal counseling for families at high risk for JSRD recurrence through accurate early prenatal confirmation or exclusion of JSRD affection.

Potential Exposure Dose Reductions in Digital Breast Tomosynthesis and Synthetically Reconstructed Digital Mammogram: Selection of Appropriate Reconstruction Technique

Sunday, Nov. 27 1:00PM - 1:30PM Room: PH Community, Learning Center Station #7

# Participants

Tsutomu Gomi, PhD, Sagamihara, Japan (*Presenter*) Nothing to Disclose Katsuya Fujita, BSc, Takasaki, Japan (*Abstract Co-Author*) Nothing to Disclose Masami Goto, Tokyo, Japan (*Abstract Co-Author*) Nothing to Disclose Yusuke Watanabe, MSc, Sagamihara, Japan (*Abstract Co-Author*) Nothing to Disclose Tokuo Umeda, PhD, Sagamihara, Japan (*Abstract Co-Author*) Nothing to Disclose Akiko Okawa, MD, RN, Nagoya, Japan (*Abstract Co-Author*) Nothing to Disclose Tohoru Takeda, MD, PhD, Sagamihara-Shi, Japan (*Abstract Co-Author*) Nothing to Disclose

## **TEACHING POINTS**

1) To use reconstruction techniques [filtered back projection (FBP) and iterative reconstruction (IR)] and processing of synthetically reconstructed digital mammogram (SDM, C-View; Hologic) to identify indications of digital breast tomosynthesis (DBT) at various exposure doses. 2) To compare FBP, IR, SDM, and radiography. 3) To select an appropriate reconstruction technique and exposure dose for breast microcalcifications and lesion detection.

## TABLE OF CONTENTS/OUTLINE

1. Overview of FBP, IR [simultaneous iterative reconstruction techniques (SIRT), maximum likelihood expectation maximization (MLEM)], and SDM for DBT and radiography2. Diagnostic imaging properties Efficacy with respect to normal structure and lesion detection3. Parameter review Full width at half-maximum Signal difference-to-noise ratio Average glandular dose4. Clinical relevanceOutline:DBT (IR) and SDM provides improved visibility for superimposed structures and can improve resolution and contrast visibility after appropriate selection for reduced exposure dose. Hence, DBT (IR) and SDM, rather than FBP, should be further evaluated. The exposure dose could possibly be decreased by half with DBT (IR) and SDM. Understanding the potential of DBT and SDM for exposure dose selection may improve the diagnostic accuracy of this technique in clinical applications.

Spiral-based 3D MR Thermometry for Brain Applications of MR-guided Focused Ultrasound in a Porcine Model

Sunday, Nov. 27 1:00PM - 1:30PM Room: PH Community, Learning Center Station #1

#### Awards

#### **Student Travel Stipend Award**

#### Participants

Matthew G. Geeslin, MD, MS, Charlottesville, VA (*Presenter*) Nothing to Disclose Sam Fielden, Charlottesville, VA (*Abstract Co-Author*) Nothing to Disclose Xue Feng, Charlottesville, VA (*Abstract Co-Author*) Nothing to Disclose Max Wintermark, MD, Lausanne, Switzerland (*Abstract Co-Author*) Advisory Board, General Electric Company; Jason Druzgal, MD, PhD, Charlottesville, VA (*Abstract Co-Author*) Nothing to Disclose Craig Meyer, Charlottesville, VA (*Abstract Co-Author*) Research Grant, Siemens AG

#### PURPOSE

Perform an in vivo evaluation of a newly developed, spiral-based 3D MR thermometry sequence, in preparation for clinical translation.

## **METHOD AND MATERIALS**

MR-guided focused ultrasound (MRgFUS) was used in a porcine model to anatomically target and prescribe a range of temperature elevations in the thalamus, bilaterally. The temperature of sonications was monitored with two different MR-thermometry sequences: a 2D Cartesian based (clinical standard), and a 3D spiral based (experimental) acquisition. The 2D method employs a gradient echo sequence with Cartesian sampling of k-space, and the 3D method implements spiral in/out sampling of in-plane k-space with Cartesian phase encoding of the third dimension. To evaluate for hot-spot position shift between the 2D Cartesian and 3D spiral techniques, identical non-ablative power settings were used to produce sublethal temperature rises at identical thalamic sites. The in-plane position of the hottest voxel was then compared between the 2D Cartesian and 3D spiral methods. Spatial and temporal resolution were also compared between the 2D and 3D techniques.

#### RESULTS

Position-shift of the hot spot due to off-resonance from magnetic inhomogeneity is a known pitfall of Cartesian acquisitions. The consequence of such an artifact can be the ablation of an unintended target. The benefit of spiral in/out k-space sampling for this application, is that off-resonance manifests as image-blur, rather than position shift. Of 12 comparative in vivo sonications, each monitored with both 3D spiral and 2D Cartesian MR-thermometry, 6 Cartesian acquisitions demonstrated a position shift of the hottest voxel of greater than 1 mm, within the in-plane dimension. The spiral-based 3D MR thermometry sequence was able to monitor temperature in real-time, with a temporal resolution of 8.7 seconds and a spatial resolution of 1.5 mm2 (in-plane) by 2 mm (through-plane). By comparison, the 2D sequence has a temporal resolution of 3.5 seconds and a spatial resolution of 1.1 x 2.2 mm.

# CONCLUSION

Spiral in/out acquisitions have demonstrated the ability, in vivo, to produce 3D temperature maps, in real-time, without suffering from position shift due to off-resonance.

## **CLINICAL RELEVANCE/APPLICATION**

Real-time 3D temperature mapping without hot-spot position shift has significant efficiency and safety advantages, when compared with the Cartesian-based 2D MR thermometry presently in use.

## The Effect of Continuous CT Dose Surveys and Feedback on Dose Optimization

Sunday, Nov. 27 1:00PM - 1:30PM Room: PH Community, Learning Center Station #2

#### **Participants**

Yasuhiro Fukushima, RT, Maebashi, Japan (*Presenter*) Nothing to Disclose Akiko Iriuchijima, Maebashi, Japan (*Abstract Co-Author*) Nothing to Disclose Ayako Taketomi-Takahashi, MD, Maebashi, Japan (*Abstract Co-Author*) Nothing to Disclose Takayuki Suto, Gunma-Ken, Japan (*Abstract Co-Author*) Nothing to Disclose Yoshito Tsushima, MD, Maebashi, Japan (*Abstract Co-Author*) Institutional Research Grant, Bayer AG ; Institutional Research Grant, DAIICHI SANKYO Group; Institutional Research Grant, Eisai Co, Ltd; Institutional Research Grant, Nihon Medi-Physics Co, Ltd; Institutional Research Grant, FUJIFILM Holdings Corporation ; Institutional Research Grant, Fuji Pharma Co, Ltd; Institutional Research Grant, Siemens AG ; Institutional Research Grant, OncoTherapy Science, Inc; Institutional Research Grant, Becton, Dickinson and Company; Speaker, Bayer AG ; Speaker, DAIICHI SANKYO Group; Speaker, Eisai Co, Ltd; Speaker, Fuji Pharma Co, Ltd; Speaker, Guerbet SA; .;

#### PURPOSE

To evaluate the effect of continuous CT dose surveys and their feedback on dose optimization.

## **METHOD AND MATERIALS**

From 2011 to 2015, we surveyed all institutions in our prefecture with CT units. The survey period varied between years and was either two weeks or one month. We collected and analyzed data from all CT units during the survey period. The data analyzed were for scans of patients 16 years of age or older, scans of the head, chest, abdomen, abdomen to pelvis, chest to pelvis, and coronary artery. The 25th percentile and 75th percentile of the dose distribution for each year were set as the diagnostic reference level. Each year, the diagnostic reference level was fed back to each institution, along with the dose distribution of the units used in that institution and the suggestion to reconsider imaging parameters. We evaluated the dose-length product (DLP) and compared data for 2011 and 2015 using the Mann-Whitney U test, and used a P-value of .05 to evaluate for significant difference.

## RESULTS

The mean number of CT dose data per survey was 17,793 from 71.8 hospitals/clinics (84.6 CT scanners) for five surveys. The median DLP for chest, abdomen to pelvis, chest to pelvis and coronary arteries decreased during the survey period of 2011 to 2015. The differences between 2011 and 2015 were 20 mGy cm (5%, P = .005) for chest scans, 65 mGy cm (11.2%, P = 0.000) for abdomen to pelvis scans, 138 mGy cm (14.5%, P = .000) for chest to abdomen scans, and 347 mGy cm (44.8%, P = .000) for coronary artery scans. The interquartile range of DLP in all scan areas decreased during the survey period. The differences in DLP interquartile range between 2011 and 2015 were 114 mGy cm (22.0%) for brain scans, 38 mGy cm (13.7%) for chest scans, 116 mGy cm (25.9%) for abdomen scans, 141 mGy cm (24%) for abdomen to pelvis scans, 184 mGy cm (23.4%) for chest to pelvis scans, and 297 mGy cm (32.1%) for coronary artery scans.

# CONCLUSION

Our method consists simply of continuous CT dose surveys and feedback of collected data. This leads to not only dose reduction, but also narrowing of dose distribution, which means dose optimization.

## **CLINICAL RELEVANCE/APPLICATION**

We have shown the efficacy of a strategy for CT dose optimization that is low-cost, minimal effort, and does not involve largescale training sessions. Radiation Exposure of Contrast-enhanced Spectral Mammography Compared with Full-field Digital Mammography and 3D Tomosynthesis

Sunday, Nov. 27 1:00PM - 1:30PM Room: PH Community, Learning Center Station #3

## Participants

Bhavika K. Patel, MD, Phoenix, AZ (*Presenter*) Nothing to Disclose William Pavlicek, PhD, Scottsdale, AZ (*Abstract Co-Author*) Nothing to Disclose James Hanson, BS, Glendale, AZ (*Abstract Co-Author*) Nothing to Disclose Thomas F. Boltz II, PhD, Scottsdale, AZ (*Abstract Co-Author*) Nothing to Disclose Judy R. James, PhD, Scottsdale, AZ (*Abstract Co-Author*) Nothing to Disclose

# PURPOSE

Contrast-enhanced spectral mammography (CESM) demonstrated favorable initial results with accuracy and sensitivity, however the incremental increased dose compared with 2D-FFDM) and 3D-tomo is a consideration. We aim to assess the dose increase of CESM in comparison to FFDM and 3D tomo with phantoms and clinical patients.

# METHOD AND MATERIALS

A single LCC projection determined the breast dose for patients (6,214 FFDM, 3,662 3D-tomo and 173 CESM) in this IRB-approved study using Hologic Selenia-Dimension. Radiation dose data (compressed breast thickness and average glandular dose (AGD)) were obtained. Experiments were also conducted on regular (50/50) and dense (70/30) breast tissue phantoms. Descriptive statistics of the phantom and patient data were generated using Excel and SAS-JMP statistical software packages.

## RESULTS

Patient mean AGD was 1.7 mGy for 2D-FFDM, 2.2 mGy for 3D-Tomo and 3 mGy for CESM exposures. CESM was ~72% higher than 2D-FFDM and ~34% higher than 3D-Tomo. The 50/50 phantom gave a mean AGD of ~1 mGy for 2D-FFDM, 1.3 mGy for 3D tomo and 1.6 mGy for CESM. the 70/30 phantom gave a mean AGD of ~1.3 mGy for 2D-FFDM exposure, 1.4 mGy for 3D tomo exposure and 2.1 mGy for CESM. Phantom CESM is ~ 25 % more in a 70/30 breast phantom compared to a 50/50 at 4.5cm. CESM was ~42% higher for a 6 cm phantom.

## CONCLUSION

Compared to FFDM and 3D tomo, mean AGD with CESM increased by 1.25 mGy and 0.76 mGy, depending upon breast size. Of note, CESM provides the reader with both a low energy image (similar to 2D FFDM) and a contrast-enhanced image that highlights areas of angiogenesis. Initial clinical studies demonstrate a clinical benefit with CESM due to added physiologic information that is provided. CESM shown was found below the MQSA constraints for routine breast dose. However, further studies must be performed, particularly to quantify CESM radiation dose as a function of varying breast density and the sub-populations of patients appropriate for this exam.

# **CLINICAL RELEVANCE/APPLICATION**

CESM provided added physiologic information at doses that meets MQSA requirements. Compared to FFDM and 3D tomo, CESM breast dose increased by  $\sim$ 72% and  $\sim$ 34%, respectively.

#### **Honored Educators**

Presenters or authors on this event have been recognized as RSNA Honored Educators for participating in multiple qualifying educational activities. Honored Educators are invested in furthering the profession of radiology by delivering high-quality educational content in their field of study. Learn how you can become an honored educator by visiting the website at: https://www.rsna.org/Honored-Educator-Award/

William Pavlicek, PhD - 2012 Honored Educator

Low and Consistent Noise Across the Energy Spectrum of Virtual Monoenergetic Images in a Novel Detector Based Spectral CT Scanner

Sunday, Nov. 27 1:00PM - 1:30PM Room: PH Community, Learning Center Station #4

## Participants

Kevin R. Kalisz, MD, Cleveland, OH (*Presenter*) Nothing to Disclose Negin Rassouli, MD, Cleveland, OH (*Abstract Co-Author*) Institutional Grant support, Koninklijke Philips NV Amar Dhanantwari, PhD, Highland Heights, OH (*Abstract Co-Author*) Employee, Koninklijke Philips NV David W. Jordan, PhD, Cleveland, OH (*Abstract Co-Author*) Consultant, Petrone Associates, LLC; Consultant, Applied Medical Physics in Radiology, Inc; Advisory Board, Medical Technology Management Institute; Director, Medical Technology Management Institute; Speaker, Medical Technology Management Institute; Travel support, Sectra AB; Prabhakar Rajiah, MD, FRCR, Dallas, TX (*Abstract Co-Author*) Institutional Research Grant, Koninklijke Philips NV; Speaker, Koninklijke Philips NV

#### PURPOSE

Virtual monoenergetic images (VMI) from dual-energy scanners are utilized for amplifying contrast signal, improving lesion visualization and decreasing artifacts. VMI from currently available dual energy technologies is limited by noise at high and low energies. The recently introduced detector based spectral CT (SCT) system accounts for and removes the anti-correlated noise in VMIs. We sought to evaluate VMI noise obtained from the novel SCT in both phantom and patients.

## METHOD AND MATERIALS

A Catphan® 600 abdomen phantom was scanned on the SCT. Image noise, SNR and CNR were measured at VMI from 40-200 keV. 100 consecutive patients who had an abdominal scan on the SCT were retrospectively selected. VMI were generated from 40-200 keV at 10 keV intervals (Fig 1A). Two radiologists evaluated the image noise, SNR and CNR within the liver, pancreas, spleen, kidney, aorta, portal vein, muscle, bone, and fat. These were also compared to the standard polyenergetic (120 kVp) study. Paired t-test was used for analysis.

## RESULTS

Phantom noise (Fig 1B) was low across all energies, highest at 40 keV (5.31 HU), gradually decreased until 70 keV, after which remained constant until 200 keV (3.45 HU). In the patient cohort, noise showed a similar low, consistent trend for all organs analyzed (Fig 1C). For example, liver noise was greatest at 40 keV (13.2 HU), steadily decreased and then remained constant until 200 keV (11.6 HU). Liver noise at all VMI energies was less than that of the 120 kVp scan (p<.01). Even at the lowest energy of 40 keV, all organs demonstrated noise less than 18 HU except bone (48.9 HU) and kidney (21.4 HU). Similarly, for all organs, SNR and CNR were highest at 40 keV (6.8-34.9; 18.3-44.9, respectively) after which they gradually decreased till 120 keV (3.4-8.7; 9.5-13.9) and remained constant until 200 keV (2.6-8.3; 8.5-12.5). SNR was greater for VMI at 40-70 keV than at 120 kVp for all organs (p<.05), and CNR was greater for VMI at 40-80 keV than at 120 kVp for all organs (p<.01).

# CONCLUSION

VMI obtained from a novel detector based SCT has low and consistent noise across the entire spectrum of energies with significant SNR and CNR improvements compared to those of conventional images.

# **CLINICAL RELEVANCE/APPLICATION**

The low and consistent noise in VMI from detector-based spectral CT scanner enables the use of VMI both at low and high energy levels, for increasing contrast signal and decreasing artifacts respectively.

# **Honored Educators**

Presenters or authors on this event have been recognized as RSNA Honored Educators for participating in multiple qualifying educational activities. Honored Educators are invested in furthering the profession of radiology by delivering high-quality educational content in their field of study. Learn how you can become an honored educator by visiting the website at: https://www.rsna.org/Honored-Educator-Award/

Prabhakar Rajiah, MD, FRCR - 2014 Honored Educator

## Revisiting Dynamic Volume Perfusion CT from a Dose Perspective: A Comparison to Routine Protocols

Sunday, Nov. 27 1:00PM - 1:30PM Room: PH Community, Learning Center Station #6

#### **Participants**

Joshua F. Gawlitza, Mannheim, Germany (*Presenter*) Nothing to Disclose Thomas Henzler, MD, Mannheim, Germany (*Abstract Co-Author*) Research support, Siemens AG; Speaker, Siemens AG Mathias Meyer, Mannheim, Germany (*Abstract Co-Author*) Speaker, Siemens AG Speaker, Bracco Group Nils Vogler, MD, Mannheim, Germany (*Abstract Co-Author*) Nothing to Disclose Sonja Sudarski, MD, Mannheim, Germany (*Abstract Co-Author*) Nothing to Disclose Stefan O. Schoenberg, MD, PhD, Mannheim, Germany (*Abstract Co-Author*) Speaker, Siemens AG Speaker, Bayer AG

## PURPOSE

Reevaluating the concerns over high radiation doses in perfusion CT imaging by comparing the organ-specific-radiation-dose of a dose-optimized abdominal dynamic volume perfusion CT protocol (dVPCT) with three standard triphasic CT (sCT) protocols, performed on three scanners in patients with suspected hepatocellular carcinoma (HCC) using a Monte Carlo Simulation.

#### **METHOD AND MATERIALS**

50 patients with suspected HCC that underwent dVPCT examinations on a 3rd generation dual-source CT(DSCT) (Somatom Force, Siemens) with a dose optimized tube voltage of 70 kV were matched, using the calculated water-equivalent-diameter, with 3 reference groups of sCT examinations, which were performed on a clinical routine scanner (Somatom Emotion 16, Siemens), as well as a 2nd and 3rd generation DSCT. Examination data was exported to an server based analysis platform (Radimetrics, Bayer). This Monte Carlo Simulation based tool was used for the calculation of the organ-specific effective dose (ED) as well as global radiation-dose parameters (e.g. ICRP103).

#### RESULTS

The ED of the dVPCT-liver-protocol was lower compared to the sCT on our routine scanner in 13 of 18, and non-inferior in a total of 16 of 18 metrics (all p < 0.05) - especially in dose sensitive organs such as the red marrow (17.3mSv vs 24.6mSv, p=<0.0001) and the liver (33.3mSv vs 46.9mSv, p=0.0003). Compared to the sCT on the 2nd gen. DSCT, there was no significant difference in the ED in 14 of 18 metrics. All ED in the sCT performed on the 3rd gen. DSCT were lower than the dVPCT doses.

#### CONCLUSION

Our results suggest that the dVPCT compares favourably to the standard CT, performed on the widely spread routine scanner with regard to effective organ dose, especially in dose sensitive organs. Although tri-phasic protocols performed on newer scanners allow an even further dose reduction, the dVPCT provides additional, valuable information with a reasonable level of radiation.

#### **CLINICAL RELEVANCE/APPLICATION**

Dynamic volume perfusion CT on modern CT systems can be performed at lower dose levels than standard triphasic protocols on widespread routine CT systems, thus potentially providing more clinically relevant information for a similar radiation dose cost.

### QS010-EB-SUB

# **Reduce Retained Foreign Object Radiology Report Turnaround Times**

Sunday, Nov. 27 1:00PM - 1:30PM Room: QS Community, Learning Center Hardcopy Backboard

#### Participants

Ranganath Iyer, Houston, TX (*Presenter*) Nothing to Disclose Tara L. Sagebiel, MD, Houston, TX (*Abstract Co-Author*) Nothing to Disclose

### PURPOSE

The study was undertaken by modality Radiography / Fluoroscopy (Rad/Fluoro) in the Division of Diagnostic Imaging (DI). A true Retained Foreign Object (RFO) is defined as surgical tools and objects that are unintentionally left in a patient after an operation. These events are infrequent but potentially life threatening and every precaution is taken to avoid it. Fluoroscopy is one of the common ways to detect these objects. DI-Rad/Fluoro department wants to responds to these calls in a more consistent/timely manner by improving this process. This project is to study about Report Turnaround Time (TAT) that is the amount of time between RFO exam completion and radiology report availability. DI-Rad/Fluoro department wants to responds to these calls in a more consistent/timely manner by improving this process. Team members included Radiologists, staff including Technologists and an Industrial Engineer. The benefits of the project is to reduce anesthesia time for affected patient and reduce OR time for affected surgeons and staffThe study aligns with the institutional goal of "People We Serve".

#### **METHODS**

Aim Statement and Measure of Success for the project were defined and quality tools used to solve the problem. Aim Statement: Achieve an average monthly report turnaround time of 10 minutes or less for retained foreign objects (RFOs) by September 1, 2015Measures of Success: Percentage of months in a calendar year Rad/Fluoro department achieved the average of 10 minutes or less for RFO report Turn Around Time (TAT). Several quality tools were used to solve the problem. Tools included: Process Flow Chart: to understand the current process flow when the RFO or incorrect surgical object count is discovered to when radiology report availability Fishbone: to analyze various factors that causing delays in the process. Benchmarking: to use as a guide for understanding claims and incident reports of RFOs Pareto analysis: to the factors and understand the reasons for delay. Control chart: to measure the pass rate of 10 minute -TAT inthe current calendar yearExamples inlcuded with the abstract include current process flow of RFOs, fishbone diagram, a pareto chart and contol chart to show baseline measure.

#### RESULTS

Improvement Plan were developed for different rolesDI coordinator: *Improvement in communication* DI coordinators are sent weekly RFO faculty coverage schedules Daytime radiologist (7:00 am-5:00 pm) checks in with DISC and provides extension/phone number On-call radiologist's pager and home phone number are given to DI coordinatorsRadiologists*Radiologist coverage* Daytime RFO coverage moved to less busy service Backup radiologist placed on daytime schedule Reminders about 10-minute TAT Reminders about RFO coverage assignments*Communication* Radiologist received RFO notifications via e-mail, phone call, page*Education* Radiologist received an RFO lecture with common RFO example images uploaded to SharePoint for reference

# CONCLUSION

Team achieved the goal of 10-minute TAT (May and June) from radiologist page to OR report (in minutes) after implementation. Diagnostic Imaging is providing a great service to OR. Approximately, ten (10) True RFOs are identified each year saving thousand in legals fees. Implementation of a Weekly Academic Day for the Improvement of Resident Didactic Education: Our Experience at a Hybrid Academic/Private Practice Diagnostic Radiology Residency Program

Sunday, Nov. 27 1:00PM - 1:30PM Room: QS Community, Learning Center Hardcopy Backboard

### Participants

Timothy E. Fahey, MD, Peoria, IL (*Presenter*) Nothing to Disclose Elton Mustafaraj, DO, Peoria, IL (*Abstract Co-Author*) Nothing to Disclose Kevin M. Fahey, MD, Peoria, IL (*Abstract Co-Author*) Nothing to Disclose Bradley A. Johnson, MD, Morton, IL (*Abstract Co-Author*) Nothing to Disclose Sean Meagher, MD, Peoria, IL (*Abstract Co-Author*) Nothing to Disclose Terry M. Brady, MD, FACR, Dunlap, IL (*Abstract Co-Author*) Nothing to Disclose

### PURPOSE

The basis of this project was the creation and implementation of a weekly resident conference day in our diagnostic radiology residency program in lieu of daily noon conferences. Our aim was to provide high-quality lectures while minimizing conference cancellation in an environment where the clinical and value-added demands on faculty apart from resident education have been steadily increasing over the past several years.

### METHODS

Seven core faculty members and two diagnostic radiology residents comprised a subcommittee tasked with exploring ideas to decrease the rate of conference cancellation in our program, which had reached up to 40%. The committee decided to designate each Wednesday as a resident academic day, supplanting the previous daily conference schedule. Additionally, the department hired two part-time image librarians to aid faculty members in the development of presentations. The conference day consists of seven 50-minute lecture slots as well as one hour of designated research time for residents. Assigned presenters were scheduled up to eight weeks in advance, providing ample time for lecture preparation. ACGME annual survey data was reviewed to gauge resident satisfaction with educational content.

### RESULTS

Lecture data was tabulated from November 19, 2014 to March 9, 2016 (68 weeks) and included date, lecture title, subspecialty section, and faculty presenter. During this period, a total of fifty-nine conference days took place (conference hiatuses took place during the weeks of Thanksgiving, RSNA, Christmas, New Year's, and Independence Day). During this period, 391 conferences were presented out of a possible 413 lecture slots (94.7%). Twenty-two lecture slots went unfilled, nineteen of which were scheduled hiatuses and three were due to extenuating circumstances. Conferences included both didactic and case conference methods. After the implementation of the weekly academic day, the ACGME survey data for 2015 showed a significant improvement in satisfaction with educational content, scoring 4.7 out of 5, compared to a score of 3.9 on the 2014 survey (national mean: 4.3).

### CONCLUSION

The transition from daily resident conferences to weekly resident academic days in our program has decreased conference cancellation from up to 40% to approximately 5%. As a result, both resident satisfaction and the quality of didactic lectures have improved significantly. Based on the success of our project, other residency programs that are experiencing a higher than desirable rate of conference cancellation may wish to consider adopting a similar schedule at their programs.

Improving Pediatric Breast Ultrasound Reporting and Recommendations: A Quality Improvement Initiative

Sunday, Nov. 27 1:00PM - 1:30PM Room: QS Community, Learning Center Station #1

#### **Participants**

Aarti Luhar, MD, Los Angeles, CA (*Presenter*) Nothing to Disclose Esha A. Gupta, MD, Los Angeles, CA (*Abstract Co-Author*) Nothing to Disclose Fariba Goodarzian, MD, Los Angeles, CA (*Abstract Co-Author*) Nothing to Disclose Amit Sura, MD, Valley Village, CA (*Abstract Co-Author*) Nothing to Disclose

## PURPOSE

Unlike adult breast imaging, there are no formal guidelines, consensus, or recommendations for management of imaging findings on diagnostic pediatric breast ultrasound. Variable recommendations can lead to confusion for clinicians, inconsistent follow-up, and unnecessary further imaging. At our academic children's hospital, breast ultrasound is reviewed by pediatric radiologists who make individual recommendations. These recommendations are generally based on individual experience and practice, rather than on a literature based or standardized system of reporting. We describe a quality improvement initiative to improve the appropriateness and consistency of recommendations given for pediatric breast ultrasound imaging findings at our institution.

### METHODS

To build evidence for the initiative, we first performed a literature search to investigate best practices in pediatric ultrasound. We specifically queried the appropriateness of applying the standardized BI-RADS reporting system to a pediatric population. Our search of the literature showed two recent articles from Pediatric Radiology (Valeur et al., 2015) and the European Journal of Radiology (Gao et al., 2015) which offered consistent recommendations for common ultrasound findings specific to the pediatric population. An additional article from the Journal of Pediatric Surgery (Koning et al., 2015) concluded that BI-RADS reporting system should not be applied to the pediatric population due to its markelymarkedly lower prevalence of malignancy.Following the literature search, we turned our focus to the educational portion of the intervention. Based on our literature search, we created a standardized algorithm of recommendations for common breast ultrasound findings in the pediatric population. The algorithm was refined following review by the radiology leadership, a fellowship trained breast-imaging radiologist, and a pediatric surgeon. With their approval, the algorithm was established as department guidelines.We introduced the algorithm to the entire radiology staff for personal reference. We then began work on the organizational portion of the intervention which established multi-disciplinary conferences that bring together radiology, surgery and pathology to review imaging findings, follow up recommendations and final pathology.

## RESULTS

Our retrospective analysis of pre-and post- intervention breast ultrasound recommendations showed a dramatic improvement in consistent, literature-based recommendations.For the pre-intervention analysis, we reviewed the 76 diagnostic breast ultrasounds performed from 2013-2015. Nine of the examinations were discarded, because the algorithm was not applicable to the ultrasound findings. The recommendation algorithm was applied to the remaining 67 pre-intervention ultrasounds, and 32 (48%) of the examinations were found to have discordant recommendations.For the post-intervention analysis, we reviewed the 17 ultrasounds performed from 1/2016-4/2016. One examination was discarded, because the algorithm was not applicable to the ultrasound findings. The recommendation algorithm was applied to the remaining 16 post-intervention ultrasounds, and only one examination was found to have a discordant recommendation (6%). The remaining 15 examinations (94%) had recommendations concordant with the literature-based algorithm.Additional retrospective review will be performed at 6 months and 1 year post-intervention. Following review and consultation with the radiology staff, further modification of the standards will be considered based on the practice feedback.

# CONCLUSION

Diagnostic pediatric breast ultrasounds performed at an academic children's hospital demonstrated a lack of consistent, evidence based recommendations for imaging findings. We coordinated a multidisciplinary quality improvement initiative to improve quality and consistency of recommendations for diagnostic pediatric breast ultrasound by 1) developing a straightforward, literature-based algorithm specific to common breast ultrasound findings in the pediatric population 2) adopting the algorithm as a department-wide standard, and, 3) establishing a multi-disciplinary conference with surgery and pathology to ensure imaging follow-up and feedback.Following the introduction of a literature-based, algorithmic approach to common imaging findings, we have seen a dramatic improvement in the appropriateness and consistency of recommendations on diagnostic pediatric breast ultrasounds at our institution.

## Decreasing Patient Wait Times and Optimizing Flow at a Breast Imaging Clinic

Sunday, Nov. 27 1:00PM - 1:30PM Room: QS Community, Learning Center Station #2

#### **Participants**

Patricia L. Cowart, ARRT, Palo Alto , CA (Presenter) Nothing to Disclose

### PURPOSE

Breast imaging is a very time challenged field. Procedures and diagnostic exams tend to run over the allotted appointment times and scheduling the appropriate type of exam has increased in complexity. This consequently leads to long wait times for our patients. A large number of breast imaging patients are cancer patients and the long wait times cause unnecessary anxiety. The impact of reducing wait times for our patients will not only help alleviate this anxiety, but also create a more seamless flow for patient care. Staff satisfaction increases because the patients are more comfortable and happy during their visit and team confidence overall in our workflows is enhanced.Our specific goal was to decrease the average wait time for breast imaging patients from appointment scheduled time to exam begin time from 30 minutes to 10 minutes.

#### **METHODS**

A multidisciplinary team was formed, including a medical assistant, mammography technologist, radiologist, marketing specialist, and a patient advisor who was a breast cancer survivor and had experiences with our long wait times. We reviewed our daily wait times and performed a root-cause analysis using a cause and effect diagram to visualize the contributing factors to long wait times. This was used in order to identify the areas that would make the most impact. It was identified that for procedures, there were many redundant steps in the consent process and for the diagnostic exams, that there were a large number of miss scheduled exams. The cause and effect diagram showed that the key items that would need to be addressed in order for the project to be successful were: Long consent times Unclear role between the MD, nurse, MA and technologist Complex exams not scheduled correctly Process for same day add-on patients Visual tools for communicating for patients and staffWe addressed these key areas through a number of interventions, the most impactful being 1)streamlining the patient consent process and eliminating unnecessary steps, 2)creating new visuals for communicating with patients and staff, 3) protocoling exams before they were processed by scheduling, 4)protecting same day add on slots for only same day exams,In order to measure the impact of interventions and countermeasures, average wait times were tracked daily from June 2015 to October 2015 using a run chart.

#### RESULTS

These interventions decreased average wait times for procedure patients from 30 minutes to 14 minutes and average wait times for diagnostic patients from 30 minutes to 12 minutes. This has been sustained for 6 months now, with our current average wait time being 10 minutes. Figure 1 shows these results for the duration of the improvement project with annotations showing when key interventions were implemented. The results of streamlining and placing roles to the consent process alone was enough to hit our goal of 10 min with slight variation. This was seen in the shift on the run chart with the new mean of 14 min. The RN, MA, MD and technologist were all educated in their role of consenting. It has turned the consenting process into a seamless workflow.By protocolling the diagnostic exams before they were scheduled, we are not only making sure to have the correct order for when the patient arrives, but the mammography technologist will know exactly what to do on that particular patient. This makes for a smooth flow for the patient and technologist. This was seen in the shift on the run chart with a new mean just over 10 minutes. Implementation of a new visual wait time board for patients has increase awareness for patients on current wait times and facilitated communication between the front desk and breast imaging staff.

# CONCLUSION

In reducing patient wait times for mammography we not only are utilizing wasted time but alleviating unnecessary patient anxiety. In making a few small changes, we were able to impact the entire workflow. These small changes were hard to identify, yet instrumental in our change process. The overall feeling in the department is much happier, because we have confidence in our workflows, and the data continues to show the impact.

Pediatric Radiation Dose Reduction during Direct Radiography Exams

Sunday, Nov. 27 1:00PM - 1:30PM Room: QS Community, Learning Center Station #3

#### Participants

Keith J. Strauss, FAAPM, FACR, Cincinnati, OH (*Abstract Co-Author*) Research Consultant, Koninklijke Philips NV; Speakers Bureau, Koninklijke Philips NV

Emily Fiehrer, BS, RT, Cincinnati, OH (*Abstract Co-Author*) Nothing to Disclose Wendy Bankes, Cincinnati, OH (*Presenter*) Nothing to Disclose Rachel Smith, Cincinnati, OH (*Abstract Co-Author*) Nothing to Disclose

#### PURPOSE

A large pediatric radiology department could not accurately estimate radiation dose to the patient from Direct Radiography exams due to lack of standardization of radiographic techniques used by the radiologic technologists (RT). The variation was due to differences in patient size assessment by the RT and their estimated radiographic technique. With over 30 RTs in the radiography department at our main hospital, the wide variation in techniques eliminated the possibility of estimating our patients' overall radiation dose. The department's clinical imaging physicist partnered with the radiology quality improvement team with a goal of establishing appropriate technique ranges for radiographic studies based on measured patient thickness which would ultimately reduce the radiation dose to the patient.

### **METHODS**

The project began with the radiology clinical imaging physicist reviewing historical patient data to understand the techniques being used by the RTs. and the process for setting equipment parameters. A review of one patient's past radiographic studies revealed that the patient had 12 abdominal studies over a period of six months. The highest and lowest radiation dose to the image receptor depended on which RTs performed the cases and varied by a factor of eight. A radiologist reviewed the case with the lowest image receptor dose and confirmed that the image quality was sufficient and diagnostic. The clinical imaging physicist verified that that this lowest image receptor dose was a reasonable starting point for technique standardization. Abdomen techniques were the initial focus of the project. The technique was based on the thickness of the patient's body part being imaged which then determined several scanner parameters. The console of the radiographic equipment was programmed with the new radiographic techniques and the copper filters were activated. Then, a QI lead RT received training from the clinical imaging physicist using the new techniques and how to measure the patient thickness using calipers. Based on the measurement of the patient's body part to be imaged, a size based option was chosen from the pre-programmed technique in the console. The technique was preset with the exact high voltage, tube current, exposure time, filter thickness, focal spot size, manual or AEC mode, and if a grid was to be used. Then, the new technique was tested on patients of various sizes while the image receptor dose was collected in a dose monitoring system along with the patient's measurement that was recorded by the RT in the Radiology Information System. This data allowed for analysis of detector dose and RT compliance using the new standard technique. Every image using the new technique was verified with a radiologist to ensure quality. From there, an iterative process was developed to tweak the technique as needed, copy programmed techniques onto remaining consoles, and train RTs on measuring thickness and the standardized technique. A weekly project review was held to review the technique and dose monitoring dashboard in order to measure the RT's compliance to the techniques, investigate outliers, and identify issues. The team also measured and reviewed the QI Coach RT training progress and tasks on the project plan in order to meet the project timeline. The project took approximately 1 year to roll out radiographic techniques for all body parts and train 78 RTs at the main hospital and 7 locations satellite locations how to manage the paradigm shift in operating protocols. Over the course of the next three years after the initial rollout, this project was expanded to include standardized techniques for specialty exams such as skeletal surveys of infants and toddlers, airway, spine, and long leg exams, exams completed with mobile DR equipment, and fluoroscopy. The measures were the dose to detector, image quality and distribution of patient dose, and RT compliance.Project resources required: Medical Physicist, Radiologists, QI RTs, QI RT coaches, QI Manager, Project Manager and a Data Analyst to create database with interfaces to dose database and Epic and for the programming of an automated visual dashboard.

#### RESULTS

Radiology was able to achieve dose reductions ranging from 28%-100% of published standard dose values based on image quality requirements by implementing standardized techniques. The radiography department now has standard techniques for 100% of the exams performed. To date, the team has achieved 80% of radiographic studies using the appropriate technique range.

### CONCLUSION

Standardized techniques allow estimates of patient dose at significant reductions. The department continues their efforts to increase compliance with standard technique use among the RTs.

### QS107-ED-SUB4

Improving Access to Pediatric MR performed under General Anesthesia- Benefits of a Rapid Improvement Event (RIE)

Sunday, Nov. 27 1:00PM - 1:30PM Room: QS Community, Learning Center Station #4

#### Awards

#### **Quality Storyboard Award**

#### Participants

Nabeel I. Sarwani, MD, Hummelstown, PA (*Presenter*) Nothing to Disclose Michael A. Bruno, MD, Hershey, PA (*Abstract Co-Author*) Nothing to Disclose Steve Mrozowski, Hershey, PA (*Abstract Co-Author*) Nothing to Disclose

#### PURPOSE

Timely access to imaging services for our most vulnerable patient population – children – is a vital aspect of radiology care. For small children, MR imaging must often be performed under general anesthesia (GA) to allow diagnostic quality images to be obtained. Organizing a combined service to provide MRI under GA requires a complex interplay between the referring physician and the departments of anesthesiology and radiology, and scheduling backlogs will result when demand exceeds supply. In December 2014, at our teritary academic medical center, the backlog for the 1st, 2nd and 3rd available MRI appointment to be performed under GA was > 87 days. This resulted in significant "downstream" delays in patient's clinic appointments, especially for Pediatric Neurology and Neurosurgery, as MRI results are required at the time of clinic visit. In addition, as additional time was being given to address the backlog of GA cases, there was less availability for routine MRI studies, creating a broader patient access problem. Accordingly, our 3 SMART goals were as follows, 1) Increase throughput of pediatric, out-patient, GA cases through the MRI scanner, 2) Reduce both the average time and the variability of patient contact times for each appointment slot, and 3) Reduce the GA MRI waiting list to < 30 days.

#### **METHODS**

A Rapid-Improvement Event (RIE), also known as a kaizen event, was co-sponsored by the departments of Radiology and Anesthesiology and coordinated by the institutional process improvement team utilizing Lean methodology. Key stakeholders in attendance included radiologists, anesthesiologist, technologists, radiology nursing, radiology schedulers and image management (IT) personnel. The DMAIC process was used as follows: Define = Process mapping, ID pain points, value analysis, Measure = Gemba walks, Takt-time analysis, waste inventory, Analyze = Brainstorming and root cause identification, B&E, Improve = Finalize action items, future state map, develop implementation and roll-out plan, pilot solutions and Control = Create 30 day action list, development of control plan. Additionally, a representative from radiology met individually with all stakeholders to further understand their processes, clarify available resources, explore options for improvement and coordinate efforts.Availability of services from the department of anesthesia was found to not be limiting. We discovered that the throughput of patients was reduced, in part, by the presence of "blocks" in the radiology scheduling template, which served to limit the availability of the dedicated GA MR scanner. The MRI scheduling template was modified to remove these restrictions. We addressed the high number of "no shows" by making changes to the content of the pre-procedure phone calls and by requiring radiology nursing to speak directly to the patient or relative and not merely leave a message. Frequent failure of parents to follow dietary instructions leading to delayed/rescheduled cases was addressed by a re-design of written dietary instructions that are mailed to the patient. These interventions were all implemented simultaneously in May of 2015.

## RESULTS

The average wait time for the 1st and 3rd available MR exam to be performed under GA in December 2014 was 87 and 107 days, respectively. After implementation of our intervention regimen, the average wait time for the 1st and 3rd available MR exam to be performed under GA fell precipitously, ultimately reaching the current level of < 7 days, exceeding our target.

#### CONCLUSION

RIEs are a useful tool to bring together stakeholders to review complex healthcare delivery processes such as MR exams performed under GA. Identifying sources of inefficiencies as well as scheduling template errors led to a marked decrease in wait times for pediatric MR exams performed at our institution.Shared buy-in from stakeholders allowed us to maintain our gains by development of a novel scheduling technique for these cases, resulting in increased patient throughput on the MRI scanner by decreasing "wasted" scanner downtime, as well as decreased "no show" and last-minute cancellations. Delays and rescheduled cases due to patients not following dietary restrictions also decreased. To date, the improvement has been long-lasting and sustained, with current data showing a wait of 2-3 days for a GA MRI.

## RO204-SD-SUB1

Nanoparticle Imaging and Treatment of Primary and Metastasized Tumor through Immunogenic Cell Death and Abscopal Effect, Respectively, by Targeted Dendritic-cell-mediated T-cell Priming and Immune Checkpoint Blockade via Radiotherapy

Sunday, Nov. 27 1:00PM - 1:30PM Room: RO Community, Learning Center Station #1

FDA

Discussions may include off-label uses.

#### Participants

Satoshi G. Harada, MD, Morioka, Japan (*Presenter*) Nothing to Disclose Shigeru Ehara, MD, Morioka, Japan (*Abstract Co-Author*) Nothing to Disclose Takahiro Satoh, DSc, Takasaki, Japan (*Abstract Co-Author*) Nothing to Disclose Koichiro Sera, Takizawa, Japan (*Abstract Co-Author*) Nothing to Disclose

### PURPOSE

We aimed to image and treat primary tumors and metastasized tumors in vivo through immunogenic cell death (ICD) and abscopal effect, respectively, using microcapsules that release liposome-protamine-hyaluronic acid nanoparticles (LPH-NPs) in three radiation sessions under blockade of CTLA-4 and PD-1.

## METHOD AND MATERIALS

Six hours before session one, 6 mg of anti-CTLA-4 antibody (Ab) was injected intraperitoneally into BALB/c mice with primary LM17 tumor in the left hind leg and lung metastases. For session one, LPH-NPs containing 5% iopamiron and 400  $\mu$ g anti-PD-1 Ab were mixed with 1 mL 4.0% alginate, 3.0% hyaluronate, and 1  $\mu$ g/mL P-selectin solution and added to 0.5 mM FeCl2 with 1  $\mu$ g/mL a4 $\beta$ 1 Ab. The microcapsules (ten billion) were injected intravenously (IV). After 9 h, primary tumors were exposed to 10 or 20 Gy 60Co  $\gamma$ -rays. In session two, dendritic cell (DC)-associated cross-priming of CD8+T cells was intensified for treatment of lung metastases by the abscopal effect. To this end, LPH-NPs containing 250 nmol anti-CD47 siRNA, 40 ng HMGB1, and 10  $\mu$ mol ATP were mixed with the above cocktail and added to 0.5 mM FeCl2 with 1  $\mu$ g/mL anti-P-selectin Ab. Microcapsules (ten billion) were injected IV, which interacted with P-selectin. After 9 h, tumors were irradiated as before. For session three, 4 cGy 60Co whole-body  $\gamma$ -rays were administered at 24 h intervals for 5 days.

#### RESULTS

CTLA-4 was blocked before the first session. In session one, anti- $\alpha$ 4 $\beta$ 1 microcapsules accumulated around the primary tumor and metastases, which was detected by CT. Microcapsules released P-selectin-Ag and anti-PD-1 Ab with LPH-NPs after first irradiation. In session two, microcapsules accumulated around the primary tumor through P-selectin Ag-Ab reaction and released LPH-NPs containing anti-CD47 siRNA, HMGB1, and ATP, which intensified ICD in the primary tumor and CD8+ T-cell priming under CTLA-4 blockade. In session three, primed CD8+ T cells were activated by low dose whole body irradiation and targeted metastases whose PD-1 was blocked in session one. These treatments reduced the size of primary tumors and metastases by 92.4%.

# CONCLUSION

Our targeted radioimunotherapy system has the potential to improve tumor diagnosis and treatment.

#### **CLINICAL RELEVANCE/APPLICATION**

Targeted dendritic-cell-mediated T-cell priming and immune checkpoint blockade through CTLA-4 and PD-1 enhanced the effects of radiotherapy on primary tumors and metastases.

# UR112-ED-SUB6

Penile Ultrasound and Spectral Doppler Ultrasound: Pictorial Review of the Most Common Pathologies Affecting the Penis

Sunday, Nov. 27 1:00PM - 1:30PM Room: GU/UR Community, Learning Center Station #6

## Participants

Eduardo Scortegagna JR, MD, Worcester, MA (*Presenter*) Nothing to Disclose Anna Luisa Kuhn, MD, PhD, Worcester, MA (*Abstract Co-Author*) Nothing to Disclose Larry Z. Zheng, MD, Worcester, MA (*Abstract Co-Author*) Nothing to Disclose Young Hwan Kim, MD, Worcester, MA (*Abstract Co-Author*) Nothing to Disclose

## **TEACHING POINTS**

1. To review normal ultrasonographic penile anatomy and the most common pathologies affecting the penis2. To review Color and Spectral Doppler ultrasonographic technique and findings in the evaluation of erectile dysfunction

# TABLE OF CONTENTS/OUTLINE

- Review the penile anatomy and the most common pathologies affecting the penis- Review the Color and Spectral Doppler ultrasonographic technique for proper evaluation of erectile dysfunction- Samples cases from our institution, correlating penile pathologies and ultrasonographic findings- Summary

### The Many Faces of Pediatric Renovascular Hypertension

Sunday, Nov. 27 1:00PM - 1:30PM Room: VI Community, Learning Center Station #8

#### **Participants**

Arkadiy Palvanov, MD, New Hyde Park, NY (*Presenter*) Nothing to Disclose Jacqueline Siegel, New Hyde Park, NY (*Abstract Co-Author*) Nothing to Disclose David N. Siegel, MD, Woodmere, NY (*Abstract Co-Author*) Consultant, St. Jude Medical, Inc

### **TEACHING POINTS**

Renovascular hyptertension (RVH) accounts for up to 10% of children with secondary hypertension (HTN). Unlike adults, in whom the most common cause of RVH is atherosclerotic disease, the most common cause of pediatric RVH is fibromuscular dysplasia (FMD), with less common causes including congenital vascular malformations, arteritis and neurofibromatosis type I (NF-I). Renal vein renin sampling and digital subtraction angiography (DSA) are performed when renovascular disease is suspected as the etiology of HTN in a child. IR procedures such angioplasty, stent placement, embolization, and alcohol ablation are potential curative therapy options for a child with RVH.

#### **TABLE OF CONTENTS/OUTLINE**

Discuss the definition and background information of RVH, including the causes, risk factors, pathophysiology, presentation, natural history and prognosis. Present various etiologies for RVH, including FMD, renal arterial venous malformation (AVM), and NF-I. Discuss renal vein renin sampling, which in conjunction with DSA can accurately and definitively diagnose and localize this condition.

Use a variety of cases of RVH to demonstrate different types of renal vascular abnormalities. Discusss different treatment approaches and present cases to demonstrate successful interventions, resulting in cure or improvement of RVH in this patient population. Summary

## VI224-SD-SUB1

Comparison of Microwave Absorption of [18F]-FDG and Spherical Nanocarbon to Assist in Thermal Ablation for Cancer Therapy

Sunday, Nov. 27 1:00PM - 1:30PM Room: VI Community, Learning Center Station #1

**FDA** Discussions may include off-label uses.

### Participants

Ana M. Franceschi, MD, New York, NY (*Presenter*) Nothing to Disclose Mark DeSantis, DO, MS, Northport, NY (*Abstract Co-Author*) Nothing to Disclose Thomas Dalessandro, MD, Northport, NY (*Abstract Co-Author*) Nothing to Disclose Caitlin Dolan, Stony Brook, NY (*Abstract Co-Author*) Nothing to Disclose

### PURPOSE

Evaluation of hydrogen free spherical nanocarbon (Graphonyx) injected into human breast and prostate carcinoma animal models has been discussed by Desantis et al 2014. It is known that Graphonyx spherical nanocarbon increases the absorption of microwave energy specifically into tumor cells. This study evaluated the use of [18F]-FDG vs spherical nanocarbon as primary ablation time sequence in egg whites.

#### **METHOD AND MATERIALS**

Microwave antenna ablation time sequence in liquid egg whites was evaluated using 3 parameters: plain egg whites, egg whites with [18 F]-FDG additive and egg whites with spherical nanocarbon. In the 'treatment' group: FDG, nanocarbon and viscous carrier were introduced into egg whites. Medwaves Avecure generators with MRI safe microwave probes were used for thermal ablation with short cycle power using 15 watts at up to 300 sec as baseline settings. Target temperature within the egg white was 60IC.

#### RESULTS

To achieve an adequate ablation zone, the liquid egg whites take at least 300 seconds for significant denaturing of proteins. With introduction of [18 F]-FDG, the ablation time was reduced to 270 seconds, however, with spherical nanocarbon this time was reduced to 40 seconds.

### CONCLUSION

Spherical Nanocarbon maximizes energy transfer with conversion of microwave energy causing thermal ablation. Some shortening of protein denaturing time was also noted with [F18]-labeled FDG. By using shorter treatment times and lower power output of the microwave generator spherical nanocarbon reduce the heat sink effect and surrounding tissue damage further.

## **CLINICAL RELEVANCE/APPLICATION**

Nanocarbon-assisted microwave therapy using MRI safe microwave probes displays significant thermal energy transfer in comparison to [F18]-FDG. Shorter treatment times may be beneficial in cancer therapy.

## Remote Ischemic Conditioning Temporarily Improves heart and Brain Antioxidant Defense

Sunday, Nov. 27 1:00PM - 1:30PM Room: VI Community, Learning Center Station #2

**FDA** Discussions may include off-label uses.

#### Awards

**Student Travel Stipend Award** 

#### **Participants**

Felipe L. Costa, MD, Sao Paulo, Brazil (*Presenter*) Nothing to Disclose Abdallah de Paula Houat, MD, Sao Paulo, Brazil (*Abstract Co-Author*) Nothing to Disclose Pedro Panizza, Sao Paulo, Brazil (*Abstract Co-Author*) Nothing to Disclose Claudia D. Leite, MD, PhD, Sao Paulo, Brazil (*Abstract Co-Author*) Research Grant, General Electric Company Giovanni G. Cerri, MD, PhD, Sao Paulo, Brazil (*Abstract Co-Author*) Nothing to Disclose Marcos R. Menezes, MD, Sao Paulo, Brazil (*Abstract Co-Author*) Nothing to Disclose

### PURPOSE

The syndrome of ischemia and reperfusion (IR) is the main contributor to the mortality and morbidity after a revascularization procedure. In addition to early reperfusion, tissue conditioning by alternating intervals of brief IR episodes is currently the best approach to limit tissue damage. Tissue conditioning is currently being clinically applied locally, through direct intermittent artery clamping. This technique can also be applied in other tissues but those under ischemic distress, what has been called remote ischemic conditioning (RIC), where brief IR cycles in the leg can attenuate a remote IR injury. RIC does not require direct intermittent clamping of an artery, so it could be easily applied during endovascular procedures. RIC induced-protection mechanisms are barely understood, so we evaluated if it works in the heart and brain, through the enhancement of cells antioxidant defense.

#### **METHOD AND MATERIALS**

21 Wistar rats were assigned into 3 groups: SHAM: same procedure as in the remaining groups was performed, but no remote ischemic conditioning was carried out. RIC 10: RIC protocol was carried out. 10 minutes after the end of RIC protocol, heart and brain were harvested. RIC 60: Similar procedure as performed in RIC 10, but the heart and brain were harvested 60 min after the end of RIC protocol. RIC protocol consisted of 3 cycles of 5 min left hind limb ischemia followed by 5 min left hind limb perfusion, lasting 30 min in total. Heart and brain samples were used to measure the tissue Antioxidant Capacity.

### RESULTS

RIC increased heart and brain antioxidant capacity after 10 minutes  $(0.746 \pm 0.160 / 0.801 \pm 0.227 \text{ mM/L})$  when compared to SHAM  $(0.523 \pm 0.078 / 0.404 \pm 0.124 \text{ mM/L})$ . 60 minutes after RIC, no enhancement on heart or brain antioxidant capacity was detected  $(0.551 \pm 0.073 / 0.455 \pm 0.107 \text{ mM/L})$ .

#### CONCLUSION

This is the first demonstration that remote ischemic conditioning enhances heart and brain antioxidant defenses, creating a short window of protection against IR injury. Proper timing and better understand of its mechanisms can turn RIC into an important tool to attenuate IR injury in endovascular procedures.

### **CLINICAL RELEVANCE/APPLICATION**

Remote ischemic conditioning temporarily increases heart and brain antioxidant capacity and might helpful during endovascular procedures to attenuate ischemia and reperfusion injury.

## VI226-SD-SUB3

Three Dimensional Magnetic Resonance Black-Blood Thrombus Imaging for the Diagnosis of Deep Vein Thrombosis: Initial Experience

Sunday, Nov. 27 1:00PM - 1:30PM Room: VI Community, Learning Center Station #3

# Participants

Hanwei Chen, Guangzhou, China (*Abstract Co-Author*) Nothing to Disclose Li Wang, MD, Guangzhou, China (*Abstract Co-Author*) Nothing to Disclose Chen Huang, Guangzhou, China (*Presenter*) Nothing to Disclose Guoxi Xie, Shenzhen, China (*Abstract Co-Author*) Nothing to Disclose Jianke Liang, Guangzhou, China (*Abstract Co-Author*) Nothing to Disclose Wei Deng, Guangzhou, China (*Abstract Co-Author*) Nothing to Disclose Zhuonan He, Guangzhou, China (*Abstract Co-Author*) Nothing to Disclose Yufeng Ye, Guangzhou, China (*Abstract Co-Author*) Nothing to Disclose Xueping He, Guangzhou, China (*Abstract Co-Author*) Nothing to Disclose Zhuonan He, Guangzhou, China (*Abstract Co-Author*) Nothing to Disclose Yufeng Ye, Guangzhou, China (*Abstract Co-Author*) Nothing to Disclose Zhaog, MD, Los Angeles, CA (*Abstract Co-Author*) Nothing to Disclose Zhaoyang Fan, Los Angeles, CA (*Abstract Co-Author*) Nothing to Disclose

## PURPOSE

To evaluate a three dimensional (3D) magnetic resonance (MR) black-blood thrombus imaging (BTI) technique for the diagnosis of deep vein thrombosis (DVT).

### **METHOD AND MATERIALS**

This IRB-approved study was performed on a 3T system (Siemens Tim Trio) with two standard 6-channel body coils and an integrated spine coil. Informed consent was obtained from all subjects. The BTI was conducted in 18 DVT patients (from subacute to chronic stage) to evaluate its diagnostic performance through a comparison with two clinically used MR techniques, contrast-enhanced MR venography (CE-MRV) and 3D gradient-echo with magnetization preparation (MPRAGE). Scan parameters of BTI included: 3D coronal scan with a 352-mm craniocaudal coverage, spatial resolution of  $1.1 \times 1.1 \times (1.1-1.3)$  mm3, scan time < 5 min. Two radiologists blinded to patients' clinical information and imaging protocols independently made diagnosis of DVT (presence or absence) and provided diagnosis confidence scores (1-poor, 4-excellent) on a per-segment basis for BTI, MPRAGE, and CE-MRV, respectively. Using the consensus diagnosis of CE-MRV as the reference, the sensitivity (SE), specificity (SP), positive and negative predictive values (PPV and NPV), and accuracy (ACC) of BTI and MPRAGE were calculated. Diagnostic agreement with the reference and interreader agreements for each technique were determined using Cohen  $\kappa$  test.

# RESULTS

BTI allowed for direct visualization of the entire thrombus within the black-blood lumen regardless of the thrombus stage. In contrast, MPRAGE was sensitive only to part of the thrombus that presumably was at a subacute stage and contained high-T1-signal met-hemoglobin. Higher SE (90.4% vs. 67.6%), SP (99.0% vs. 97.4%), PPV (95.4% vs. 85.6%), NPV (97.8% vs. 92.9%) and ACC (97.4% vs. 91.8%) were obtained by BTI in comparison with MPRAGE. Good diagnostic confidence and excellent diagnostic and interreader agreements were achieved by BTI ( $3.42\pm0.73$ ,  $\kappa=0.92$  &  $\kappa=0.89$ , respectively), which were considerably higher to MPRAGE ( $2.31\pm0.62$ ,  $\kappa=0.71$  &  $\kappa=0.64$ , respectively).

### CONCLUSION

BTI allows direct visualization of DVT within dark venous lumen and has the potential to be a reliable screening tool for the assessment of DVT without the use of contrast medium.

## **CLINICAL RELEVANCE/APPLICATION**

BTI has the potential to be a reliable screening tool for detecting DVT without the need for contrast medium.

## VI227-SD-SUB4

The Maximum Diameter of the Pancreaticoduodenal Arcade on CT Angiograms Can Predict the Blood Flow from the Superior Mesenteric- To the Proper Hepatic Artery in Patients with Median Arcuate Ligament Syndrome

Sunday, Nov. 27 1:00PM - 1:30PM Room: VI Community, Learning Center Station #4

### Participants

Wataru Fukumoto, Hiroshima, Japan (*Abstract Co-Author*) Nothing to Disclose
Nobuo Kitera, RT, Hiroshima, Japan (*Abstract Co-Author*) Nothing to Disclose
Kenji Kajiwara, Hiroshima, Japan (*Abstract Co-Author*) Nothing to Disclose
Masaki Ishikawa, MD, Hiroshima, Japan (*Abstract Co-Author*) Nothing to Disclose
Yasutaka Baba, MD, Hiroshima, Japan (*Abstract Co-Author*) Nothing to Disclose
Kazuo Awai, MD, Hiroshima, Japan (*Abstract Co-Author*) Nothing to Disclose
Kazuo Awai, MD, Hiroshima, Japan (*Abstract Co-Author*) Nothing to Disclose
Kazuo Awai, MD, Hiroshima, Japan (*Abstract Co-Author*) Research Grant, Toshiba Corporation; Research Grant, Hitachi, Ltd;
Research Grant, Bayer AG; Research Grant, Eisai Co, Ltd; Medical Advisor, General Electric Company; ;; ;;
Hidenori Mitani, Hiroshima, Japan (*Presenter*) Nothing to Disclose

### PURPOSE

When the median arcuate ligament compresses the celiac axis it is known as median arcuate ligament syndrome (MALs). CT angiography (CTA) is useful for diagnosing MALs; its reported incidence is 1-4% in patients undergoing CT studies. Although most patients with MALs are asymptomatic, it can lead to abdominal pain, pancreaticoduodenal artery aneurysms, and hepatic ischemia after pancreaticoduodenectomy. Under the hypothesis that MALs is symptomatic in patients with physiological blood flow from the superior mesenteric- to the proper hepatic artery (SMA, PHA) we assessed whether CTA findings can predict the degree of blood flow from the SMA to the PHA.

#### **METHOD AND MATERIALS**

We retrospectively reviewed superior mesenteric arteriograms (SMAGs) from 1013 patients and identified 23 with physiological blood flow from SMA to the PHA due to MALs (20 men, 3 women; median age 69 years, range 47-90 years). They were classified as type A (scant flow from the SMA to the PHA, n=8) and type B (visible flow from the SMA to the PHA, n=15). We recorded the maximum and minimum diameter of the celiac axis and calculated its stenosis ratio (maximum / minimum diameter) on CTA images. We also measured the maximum diameter of the pancreaticoduodenal arcade (PDA).

#### RESULTS

The stenosis ratio of the celiac axis was 2.66 (SD 1.04) for type A and 1.86 (SD 1.62) for type B (p=0.16, t-test). The maximum diameter of the PDA was 2.1 (SD 1.0)- and 4.6 (SD 1.4) mm in type A and B, respectively (p<0.01). When the maximum diameter of the PDA exceeded 4 mm, sensitivity was 80% and specificity was 88% for type B.

#### CONCLUSION

The maximum diameter of the PDA on CTA images can predict blood flow from the SMA to the PHA.

#### **CLINICAL RELEVANCE/APPLICATION**

The maximum diameter of the PDA on CTA images may correlate with symptomatic MALs.

Technical Development: MRI-TRUS Fusion for Electrode Positioning during Irreversible Electroporation for Treatment of Localized Prostate Cancer

Sunday, Nov. 27 1:00PM - 1:30PM Room: VI Community, Learning Center Station #7

**FDA** Discussions may include off-label uses.

### Participants

Alexander D. Baur, MD, Berlin, Germany (Presenter) Speaker, Bayer AG

Federico Collettini, MD, Berlin, Germany (Abstract Co-Author) Nothing to Disclose

Judith Enders, Berlin, Germany (Abstract Co-Author) Nothing to Disclose

Carsten Stephan, MD, PhD, Berlin, Germany (Abstract Co-Author) Nothing to Disclose

Bernhard Gebauer, MD, Berlin, Germany (*Abstract Co-Author*) Research Consultant, C. R. Bard, Inc; Research Consultant, Sirtex Medical Ltd; Research Grant, C. R. Bard, Inc; Research Consultant, PAREXEL International Corporation; Travel support, AngioDynamics, Inc

Bernd K. Hamm III, MD, Berlin, Germany (*Abstract Co-Author*) Research Consultant, Toshiba Corporation Stockholder, Siemens AG Stockholder, General Electric Company Research Grant, Toshiba Corporation Research Grant, Koninklijke Philips NV Research Grant, Siemens AG Research Grant, General Electric Company Research Grant, Elbit Imaging Ltd Research Grant, Bayer AG Research Grant, Guerbet SA Research Grant, Bracco Group Research Grant, B. Braun Melsungen AG Research Grant, KRAUTH medical KG Research Grant, Boston Scientific Corporation Equipment support, Elbit Imaging Ltd Investigator, CMC Contrast AB

Thomas Fischer, MD, Berlin, Germany (Abstract Co-Author) Speaker, Toshiba Corporation; Advisory Board, Toshiba Corporation

## PURPOSE

To introduce a new technical approach for image-guided positioning of needle-like electrodes for irreversible electroporation (IRE) in patients with localized prostate cancer (PCa) using a magnetic resonance imaging (MRI) transrectal ultrasound (TRUS) fusion technique.

## METHOD AND MATERIALS

Patients undergoing IRE of the prostate for treatment of biopsy-proven localized PCa between October 2014 and November 2015 participating in a prospective study were included. Three to 4 needle-like monopolar 19 G electrodes were inserted into the prostate through a brachytherapy grid using a transperineal approach. Multiparametric MRI of the prostate acquired before IRE was fused with TRUS images acquired during IRE using a rigid image fusion algorithm. On MRI the target volume was delineated; the exact position of the electrodes was visualized in real-time on ultrasound images. Goal was to enclose the target volume in its maximal extension within the electrodes and therefore within the estimated ablation zone. The distance between electrodes was measured on ultrasound imaging. Based on these measurements the proprietary software installed on the IRE unit was able to calculate the voltage necessary to generate the electric field for ablation.

### RESULTS

In 10 consecutive patients with localized prostate cancer undergoing IRE using the described technical approach satisfactory positioning of the electrodes around the target volume was achieved. The target lesion as well as a safety margin was covered within the estimated ablation zone whilst critical structures (e.g. neurovascular bundle, urethra, rectum) were excluded to the greatest possible extent. In all patients a loss of tissue perfusion within the ablation zone was documented by contrast-enhanced TRUS one day after IRE. The extension of the ablation zone corresponded well with the estimated ablation zone in all patients.

### CONCLUSION

In patients with localized prostate cancer MRI-TRUS fusion allows exact positioning of the electrodes under real-time image guidance. This technical approach combines the advantages of optimal visualization of the target lesion on MRI with the ability of TRUS to acquire imaging in real-time with a mobile device.

### **CLINICAL RELEVANCE/APPLICATION**

MRI-TRUS fusion allows improved positioning of the electrodes used for IRE under real-time image guidance and thereby improved control of the shape and extensions of the ablation zone in the prostate.

Andreas Maxeiner, Berlin, Germany (Abstract Co-Author) Nothing to Disclose

## Spectrum of Axillary Hyperdense Masses and Foci

Monday, Nov. 28 12:15PM - 12:45PM Room: BR Community, Learning Center Station #7

#### **Participants**

Jaclyn Thiessen, MD, Portland, OR (*Presenter*) Nothing to Disclose Phillip A. Setran, MD, Portland, OR (*Abstract Co-Author*) Nothing to Disclose Karen Y. Oh, MD, Portland, OR (*Abstract Co-Author*) Nothing to Disclose Mark D. Kettler, MD, Portland, OR (*Abstract Co-Author*) Nothing to Disclose

## **TEACHING POINTS**

Axillary hyperdense foci visible on mammography are caused by a variety of malignant, benign and iatrogenic conditions. In the setting of breast cancer, calcifications in axillary lymph nodes may, but do not necessarily reflect metastatic disease. Knowledge of benign and iatrogenic patterns of axillary hyperdense foci can obviate unnecessary additional imaging and biopsies.

### **TABLE OF CONTENTS/OUTLINE**

Definition: Axillary hyperdense foci include calcifications and/or metallic densities within axillary lymph nodes or masses/foci denser than normal axillary tissue. Axillary lymph node calcifications caused by metastatic disease Invasive breast cancer and DCIS metastases Psammomatous calcifications associated with metastatic thyroid and ovarian cancer Axillary lymph node calcifications caused by systemic disease Sarcoidosis Granulomatous diseases Axillary lymph nodes containing metal opacities Gold salt therapy for rheumatoid arthritis Tattoo pigment Hyperdense axillary lymph nodes associated with hematologic disorders such as leukemia and lymphoma Other/Iatrogenic causes of axillary hyperdensities Dermatomyositis Talc emboli Calcified oil cyst Catheter fragment Free silicone/silicone granuloma Surgical clip Deodorant artifact Breast Imaging in the Transgender Patient: Traversing New Terrain

Monday, Nov. 28 12:15PM - 12:45PM Room: BR Community, Learning Center Station #8

#### Awards Certificate of Merit

#### **Participants**

Bianca M. Carpentier, MD, San Francisco, CA (*Presenter*) Nothing to Disclose Jessica H. Hayward, MD, San Francisco, CA (*Abstract Co-Author*) Nothing to Disclose Katharine D. Maglione, MD, New York, NY (*Abstract Co-Author*) Nothing to Disclose Loretta M. Strachowski, MD, San Francisco, CA (*Abstract Co-Author*) Nothing to Disclose

#### **TEACHING POINTS**

The purpose of this exhibit is to provide the reader with an approach to breast imaging in the transgender patient. After viewing this presentation, the reader will gain a better understanding of the appropriate terminology to use with transgender patients who may present for screening or diagnostic breast evaluation. Surgical and hormonal treatments most commonly used in gender reassignment, including both male-to-female (MTF) and female-to-male (FTM) patients, will be reviewed, as well as the resultant expected imaging features on mammography, ultrasound and MRI. This exhibit will also cover the known breast cancer risk in the transgender population with examples of malignancy. The reader will be provided with current screening recommendations of this population, as well as the current screening controversies.

## TABLE OF CONTENTS/OUTLINE

-Terminology to use with transgender patients-Current therapy and resultant physiological changes-Imaging features post therapy-Breast cancer risk with gender reassigned patients-Current screening recommendations and controversies-Reimbursement in the US for the asymptomatic transgender screening patient-How to create a sensitive, welcoming environment in your practice-Our institution's approach for both screening and diagnostic evaluation in transgender patients Value of Preoperative Axillary US for Preventing Unnecessary axillary Lymph Node Dissection in a Large Series of Patients with Early-Stage Breast Cancers

Monday, Nov. 28 12:15PM - 12:45PM Room: BR Community, Learning Center Station #1

## Participants

Ga Ram Kim, MD, Incheon, Korea, Republic Of (*Abstract Co-Author*) Nothing to Disclose Ji Soo Choi, MD, PhD, Seoul, Korea, Republic Of (*Presenter*) Nothing to Disclose Boo-Kyung Han, MD, PhD, Seoul, Korea, Republic Of (*Abstract Co-Author*) Nothing to Disclose Eun Young Ko, MD, PhD, Seoul, Korea, Republic Of (*Abstract Co-Author*) Nothing to Disclose Eun Sook Ko, MD, Seoul, Korea, Republic Of (*Abstract Co-Author*) Nothing to Disclose

# PURPOSE

To investigate value of preoperative axillary ultrasound (US) for preventing unnecessary axillary lymph node dissection (ALND) in a large series of patients with early-stage breast cancers.

### **METHOD AND MATERIALS**

From March 2009 to February 2013, 1929 patients who had undergone preoperative axillary US and subsequent breast conserving surgery for clinically node negative T1/T2 breast cancers were included as follows: 1475 (76.5%) with negative sentinel lymph node biopsy (SLNB) and stability on follow-up for more than 2 years, 327 (17.0%) with positive SLNB and subsequent ALND, 127 (6.6%) with positive US-guided fine-needle aspiration result of axillary LN and subsequent ALND. Preoperative axillary US results (positive or negative) and clinicopathologic features (age, clinical T stage, histologic type, nuclear grade, lymphvascular innvasion, and molecular subtypes) were compared according to the presence of non-SLN metastasis. Multivariate logistic regression was performed to find independent factors for non-SLN metastasis.

### RESULTS

Of 1929, 203 (10.5%) patients had non-SLN metastasis in their ALNDs. Patients with ultrasonographically positive axilla showed non-SLN metastasis more frequently than patients with ultrasonographically negative axilla (53.8% versus 3.6%, P <0.001). At multivariate analysis, the independent factors associated with non-SLN metastasis were ultrasonographically positive axilla (odds ratio [OR], 30.163; 95% confidential interval [CI], 19.970-45.558), clinical T2 stage (OR, 1.733; CI, 1.156-2.598) and lymphovascular invasion (OR, 5.922; CI, 3.971-8.832). In our 1284 patients who had clinical T1 cancers and ultrasonographically negative axilla, 185 (14.4%, 184 of 1284) underwent ALND, and non-SLN metastasis was confirmed in 30 patients (2.3%, 30 of 1284).

#### CONCLUSION

In early-stage breast cancer patients, positive axilla and clinical T2 stage determined by preoperative staging US were significantly associated with non-SLN metastasis. This study suggests that ALND can be avoided for patients with ultrasonographically negative axilla and clinical T1 stage cancers with a minimal risk of non-SLN metastasis.

### **CLINICAL RELEVANCE/APPLICATION**

Axillar lymph node dissection might be avoided for patients with negative axilla and clinical T1 stage determined by preoperative US with a minimal risk of non-sentinel lymph node metastasis.

## BR227-SD-MOA2

#### Follow-up of Patients Undergoing Oncoplastic Surgery- More Palpable Masses and Benign Biopsies

Monday, Nov. 28 12:15PM - 12:45PM Room: BR Community, Learning Center Station #2

#### **Participants**

Yoav Amitai, MD, Tel Aviv, Israel (*Presenter*) Nothing to Disclose Orit Golan, MD, PHD, Tel-Aviv, Israel (*Abstract Co-Author*) Nothing to Disclose Yoav Barnea, Tel Aviv, Israel (*Abstract Co-Author*) Nothing to Disclose Tehillah Menes, MD, Tel Aviv, Israel (*Abstract Co-Author*) Nothing to Disclose

## PURPOSE

Oncoplastic surgery is increasingly being used in the management of women undergoing breast conserving surgery. Data on the impact of oncoplastic surgery on the follow-up of these women is lacking. We hypothesized that the combined surgery may make post-operative surveillance more difficult, mainly due to breast parenchymal rearrangement. The goal of this study was to compare the post-operative follow up of patients who underwent breast conserving surgery with and without plastic reconstruction.

### **METHOD AND MATERIALS**

All patients undergoing breast conserving surgery with oncoplastic reconstruction in our institution between 2009-2014 were included in the study. For each patient in the oncoplastic reconstruction group, the first 4 patients who underwent lumpectomy alone in the same week were selected and included in the control arm. The two groups were compared regarding demographics, tumor characteristics, details of the surgery, post-operative patient complaints, breast exam, imaging findings and subsequent biopsies done during follow-up.

### RESULTS

The study group included 72 women who had oncoplastict surgery and 291 who underwent breast conserving surgery without oncoplastic surgery. Mean follow up was similar (888 vs. 932; p=0.5).Patients undergoing oncoplastic surgery were younger (49 vs. 57 years; P=0.015), had more advance disease (Average tumor size 1.9 vs. 1.6 cm; p=0.02, Involved lymph nodes 41% vs. 17%; P<0.001)) and more often had undergone neoadjuvant treatment (35% vs. 8%; P<0.001). Larger volumes of tissue were removed in the oncoplastic group (388 cm3 vs. 123 cm3, P<0.001).New lumps on physical examination were more frequently found in patients after oncoplastic surgery (22% vs. 5%; P<0.001). Patients after oncoplastic surgery had more biopsies during follow-up (30% vs.14%; P<0.001). This finding remained significant after controlling for age, use of neoadjuvant treatment and volume of tissue removed. Ninety percent of biopsies in the oncoplastic group were benign, most commonly-fat necrosis ( 63%).

#### CONCLUSION

Oncoplastic surgery is followed by higher rates of palpable findings and subsequent breast biopsies compared to lumpectomy alone. Most biopsies are benign, most commonly fat necrosis.

#### **CLINICAL RELEVANCE/APPLICATION**

Women and their physicians should be aware of the higher rate of palpable abnormalities and breast biopsies after oncoplastic surgery, and more importantly of its benign nature.

### BR228-SD-MOA3

Impact of Imaging Features and Neoadjuvant Chemotherapy on Breast Intraoperative Specimen Interpretation

Monday, Nov. 28 12:15PM - 12:45PM Room: BR Community, Learning Center Station #3

#### Awards

#### **Student Travel Stipend Award**

#### Participants

Bryan Jordan, MD, Houston, TX (*Presenter*) Nothing to Disclose Wei Wei, Houston, TX (*Abstract Co-Author*) Nothing to Disclose Mark J. Dryden, MD, Houston, TX (*Abstract Co-Author*) Nothing to Disclose Alejandro Contreras, MD, Houston, TX (*Abstract Co-Author*) Nothing to Disclose Kelly K. Hunt, MD, Houston, TX (*Abstract Co-Author*) Nothing to Disclose Basak E. Dogan, MD, Houston, TX (*Abstract Co-Author*) Nothing to Disclose

### PURPOSE

To investigate the influence of imaging features and history of neoadjuvant therapy (NAC) on the accuracy of intraoperative specimen radiography (IOSR) evaluation of histopathological margin status in breast cancer patients.

### **METHOD AND MATERIALS**

We retrospectively reviewed electronic health records of consecutive patients with invasive carcinoma who underwent specimen radiography at the time of their definitive surgery from July 2014-February 2015 at our institution in an IRB approved study. Patient demographics, type of surgery, and tumor histopathological type (with or without associated DCIS), history of NAC and clinical NAC response, initial IOSR assessment, need for intraoperative additional tissue, re-excision surgery and mastectomy rates were recorded. History of NAC prior to surgical excision were compared with IOSR interpretation findings and final pathological margin [close or positive margins (CPM) versus negative margins (NM)] status.

#### RESULTS

Our eligibility criteria was met by 625 patients. Median patient age was 56 (range 28-87) years. At presentation, 223(52.5%) patients had pure invasive, 271(46%) had invasive and in situ cancer, and 131(3%) were of other subtypes. 514(82.2%) cancers were unifocal, 106(17.8%) were multifocal or centric. 300(48%) underwent mastectomy and 325(52%) segmental mastectomy. A total of 226 (36%) patients underwent NAC and 399 (63%) upfront surgery. IOSR indicated CPM in 232 (37.1%), prompting excision of additional tissue, while final pathology showed CPM in 29.7%. Sensitivity, specificity, PPV, and NPV, and accuracy of IOSR in predicting CPM were, 94%, 86.8%, 75.4%, 97.1%, 89%, respectively (95% CI: 86-91%). CPM was significantly lower in the NAC group (21%) than non NAC group (35%)(p = 0.0002). While sensitivity (93.6 vs 94.1%), specificity (86.4 vs 87.6%) and NPV (98.0 vs 96.4%) of IOSR were similar in NAC vs non NAC groups, false positive rate was higher in NAC (35%) vs non NAC(19.5%) and PPV was lower in the NAC (64.7%) compared to non NAC(80.5%) group.

## CONCLUSION

IOSR is a highly accurate method of intraoperative specimen margin evaluation. While preoperative NAC increases the rate of negative surgical margins, it increase false positive rate and decreases PPV of IOSR.

#### **CLINICAL RELEVANCE/APPLICATION**

While NAC history decreases the probability of CPM, it influences IOSR evaluation of surgical margins and may contribute to an increase in excision volume.

### BR229-SD-MOA4

Long-term Survival Outcomes of Primary Breast Cancer in Women with or without Preoperative MR Imaging: A Matched Cohort Study

Monday, Nov. 28 12:15PM - 12:45PM Room: BR Community, Learning Center Station #4

### Participants

Ga Young Yoon, Seoul, Korea, Republic Of (*Presenter*) Nothing to Disclose Woo Jung Choi, MD, Seoul, Korea, Republic Of (*Abstract Co-Author*) Nothing to Disclose Joo Hee Cha, MD, Seoul, Korea, Republic Of (*Abstract Co-Author*) Nothing to Disclose Hwa Jung Kim, Seoul, Korea, Republic Of (*Abstract Co-Author*) Nothing to Disclose Hak Hee Kim, MD, Seoul, Korea, Republic Of (*Abstract Co-Author*) Nothing to Disclose Hee Jung Shin, MD, Seoul, Korea, Republic Of (*Abstract Co-Author*) Nothing to Disclose Eun Young Chae, Seoul, Korea, Republic Of (*Abstract Co-Author*) Nothing to Disclose

## PURPOSE

To investigate whether preoperative magnetic resonance (MR) imaging use in patients with primary breast cancer are predictive of disease-free (DFS) and overall (OS) survival.

### **METHOD AND MATERIALS**

From 2009 to 2010, 875 women with primary breast cancer who undergone preoperative MR imaging were matched with 1635 women without preoperative MR imaging. The patients were matched with regard to age at diagnosis, address, job, parenchymal pattern of mammography, operation date, hormone receptor status, Ki-67 status and molecular subtype. Cox proportional hazards model was used to investigate time to recurrence and to estimate the hazard ratio (HR) for preoperative MR imaging.

#### RESULTS

A total of 759 matched-pairs were available for survival analysis. There were 143 recurrence; 65 locoregional recurrence, 23 contralateral breast cancer, and 55 distant recurrence. There were 40 deaths. The MR imaging group had a tendency toward better distant recurrence DFS (HR, 0.67; 95% confidence interval; 0.39, 1.14; P = .138) than did the no MR imaging group. However, no difference was found for locoregional recurrence (P = .893), contralateral breast cancer (P = .839) DFS or OS (P = .504).

#### CONCLUSION

Preoperative breast MR imaging for primary breast cancer was associated with a reduced risk of distant recurrence; however, no observed reduction in risk of locoregional, contralateral breast cancer or overall survival was shown.

### **CLINICAL RELEVANCE/APPLICATION**

The use of a breast MR imaging at the time of initial diagnosis and evaluation of primary breast cancer may help reduce risk of distant recurrence.

### BR230-SD-MOA5

Computer-aided Detection (CAD) for Synthesized Mammography: Does it Perform the Same as CAD for Full-field Digital Mammography?

Monday, Nov. 28 12:15PM - 12:45PM Room: BR Community, Learning Center Station #5

## Participants

Rosalind P. Candelaria, MD, Houston, TX (*Presenter*) Nothing to Disclose William R. Geiser, MS, Houston, TX (*Abstract Co-Author*) Nothing to Disclose Monica L. Huang, MD, Houston, TX (*Abstract Co-Author*) Nothing to Disclose Roland Bassett Jr, Houston, TX (*Abstract Co-Author*) Research Grant, Lantheus Medical Imaging, Inc Deanna L. Lane, MD, Houston, TX (*Abstract Co-Author*) Nothing to Disclose Lumarie Santiago, MD, Houston, TX (*Abstract Co-Author*) Nothing to Disclose Marion E. Scoggins, MD, Houston, TX (*Abstract Co-Author*) Nothing to Disclose Elsa M. Arribas, MD, Houston, TX (*Abstract Co-Author*) Nothing to Disclose Beatriz E. Adrada, MD, Houston, TX (*Abstract Co-Author*) Nothing to Disclose

#### PURPOSE

To compare the performance of computer-aided detection (CAD) in synthesized mammography (SM) to CAD in full-field digital mammogram (FFDM) in the same screening patients

## METHOD AND MATERIALS

An IRB-approved retrospective review of all screening mammograms performed during a two-month period from 12/2015 through 2/2016 at one academic institution was completed. Patients were included if their screening examination was comprised of FFDM, digital breast tomosynthesis (DBT) and SM. All studies were acquired with a Selenia Dimensions platform (Hologic). The synthesized 2D images were obtained using C-view, the 2D image reconstruction algorithm developed by Hologic. ImageChecker CAD settings (Hologic Cenova platform) were optimized in accordance with manufacturer recommendations. The number and types of lesions detected by SM CAD and FFDM CAD were recorded and compared. Paired differences between modalities were made using the Wilcoxon signed-rank test. All statistical tests used a significance level of 5%.

#### RESULTS

380 out of 1453 patients who had screening mammograms performed during the study timeframe met inclusion criteria. Median patient age was 59 years, range 31-90 years. A significantly greater number of masses were detected by SM CAD than by FFDM CAD (p<0.0001). There was no significant difference in the number of calcifications detected by SM CAD and FFDM CAD (p=0.4408). There was a greater number of MALCs (masses plus calcifications) detected by SM CAD than by FFDM CAD (p=0.0168). Overall, a greater total number of lesions was detected by SM CAD than by FFDM CAD (p=0.0117).

### CONCLUSION

There is a statistically significant difference in the performance of CAD in identifying masses and MALCs on SM compared to FFDM. However, CAD performance was not significantly different in identifying calcifications between the two modalities.

### **CLINICAL RELEVANCE/APPLICATION**

Radiologists who utilize CAD, which is intended to reduce false negatives by marking suspicious areas on mammograms for consideration, should judiciously recognize the differential performance of CAD between SD and FFDM.

## BR231-SD-MOA6

### Pilot Reader Study of Concurrent CAD for Digital Breast Tomosynthesis

Monday, Nov. 28 12:15PM - 12:45PM Room: BR Community, Learning Center Station #6

**FDA** Discussions may include off-label uses.

#### **Participants**

Corinne Balleyguier, MD, PhD, Villejuif, France (*Presenter*) Nothing to Disclose Julia Arfi Rouche, Maisons-Alfort, France (*Abstract Co-Author*) Nothing to Disclose Laurent Levy, MD, Paris, France (*Abstract Co-Author*) Nothing to Disclose Patrick R. Toubiana, MD, Paris, France (*Abstract Co-Author*) Nothing to Disclose Franck Cohen-Scali, MD, Neuilly Sur Siene, France (*Abstract Co-Author*) Nothing to Disclose Alicia Toledano, DSc, Kensington, MD (*Abstract Co-Author*) Consultant, iCAD, Inc Senthil Periaswamy, PhD, Nashua, NH (*Abstract Co-Author*) Director of Research, iCAD, Inc Jonathan Go, Nashua, NH (*Abstract Co-Author*) Sr. Vice President, iCAD, Inc Jeffrey W. Hoffmeister, MD, Nashua, NH (*Abstract Co-Author*) Employee, iCAD, Inc; Stockholder, iCAD, Inc

### PURPOSE

To evaluate the concurrent use of a Computer-Aided Detection (CAD) system with Digital Breast Tomosynthesis (DBT). To obtain performance estimate information for use in designing and computing the sample size (number of readers and cases) to adequately power a pivotal reader study.

## METHOD AND MATERIALS

6 radiologists read an enriched sample of 80 DBT cases, with 21 cancer cases and 23 malignant lesions with a crossover design with and without CAD. All readers reviewed all cases in 2 visits separated by a period of at least 4 weeks. The CAD system detects and extracts suspicious masses, architectural distortions and asymmetries from 3D DBT planes and blends them into the corresponding 2D synthetic image. With CAD, the radiologist views the lesion on 2D projection then navigates directly to the tomosynthesis plane for characterization. Area Under the Receiver Operating Characteristic (ROC) Curve (AUC) was used to compare the two readings in terms of cancer detection. Sensitivity, specificity, recall rate and reading time were also assessed. The magnitude, direction of differences between AUCs and reading time for with and without CAD and correlations that influence sample sizes for the pivotal study were obtained from the pilot study.

### RESULTS

Average AUC across readers without CAD was 0.854 and 0.850 with CAD (-0.046, 0.039, 95% CI). Time reduction of reading time with CAD was statistically significant with average improvement in reading time of 23.5% (7.0 to 37.0%, 95% CI). No statistically significant differences in radiologist sensitivity, specificity or recall rate for non-cancers when reading concurrently with CAD vs. without CAD was found. Using parameter estimates obtained from the pilot study, sample size calculation determined that a pivotal reader study with 20 readers, 60 cancers, and 180 non-cancers provides estimated power of 90% for demonstrating non-inferior AUC and estimated power of 93% for demonstrating superior radiologist reading time.

#### CONCLUSION

Concurrent use of CAD results in a 23.5% faster reading time with non-inferiority of radiologist performance compared to reading without CAD. A pivotal reader study with 20 readers, 60 cancers, and 180 non-cancers is planned to more robustly evaluate these endpoints.

#### **CLINICAL RELEVANCE/APPLICATION**

Concurrent use of CAD maintains high performance of DBT with a significant reduction in reading time thus improving workflow even for very experienced radiologists.

## Non-congenital Ventricular Septal Defects: A Pictorial Review

Monday, Nov. 28 12:15PM - 12:45PM Room: CA Community, Learning Center Hardcopy Backboard

#### **Participants**

Christopher M. DeClue, MD, Tampa, FL (*Presenter*) Nothing to Disclose Jonathan M. Ford, PhD, Tampa, FL (*Abstract Co-Author*) Nothing to Disclose John Donatelli, MD, Tampa, FL (*Abstract Co-Author*) Nothing to Disclose Summer J. Decker, PhD, Tampa, FL (*Abstract Co-Author*) Nothing to Disclose Carlos Andres Rojas, MD, Tampa, FL (*Abstract Co-Author*) Nothing to Disclose

#### **TEACHING POINTS**

The purpose of this exhibit is to:I. Examine the etiology and pathophysiology of non-congenital ventricular septal defects (VSDs)II. Describe the imaging features of traumatic and ischemic VSDs on echocardiography, CT, and MRI III. Review imaging pitfalls and differential considerationsIV. Discuss the role of surgical and endovascular repair

### **TABLE OF CONTENTS/OUTLINE**

I. Incidence of acquired VSDsII. Etiologies of non-congenital VSDs A. Traumatic: Blunt and penetrating injuries B. Ischemic C. IatrogenicIII. Acute clinical presentation A. Physical exam B. Hemodynamic compromiseIV. Pathophysiology of traumatic and ischemic VSDs A. Vascular territories involved in ischemic VSDs B. Blunt injury to the heart and pathophysiology of VSD formationV. Review of imaging findings A. Imaging characteristics of ischemic and traumatic VSDs B. Role of different imaging modalities 1. Chest radiograph 2. CTA 3. Cardiac MRI 4. EchocardiographyVI. Treatment options A. Factors determining treatment 1. Size of the defect 2. Symptoms 3. Pulmonary to systemic flow ratio (Qp:Qs) B. Surgical repair 1. Cardiopulmonary bypass, ventriculotomy, and patching of the VSD C. Percutaneous repair with closure device

## CA131-ED-MOA8

## How to Take Full Advantage of Dual Source CT for Daily Clinical Cardiovascular Imaging

Monday, Nov. 28 12:15PM - 12:45PM Room: CA Community, Learning Center Station #8

#### Participants

Tatsuya Nishii, MD, PhD, Kobe, Japan (*Presenter*) Nothing to Disclose Shinsuke Shimoyama, MD, Kobe, Japan (*Abstract Co-Author*) Nothing to Disclose Erina Suehiro, RT, Kobe, Japan (*Abstract Co-Author*) Nothing to Disclose Wakiko Tani, RT, Kobe, Japan (*Abstract Co-Author*) Nothing to Disclose Toshinori Sekitani, MS, Kobe, Japan (*Abstract Co-Author*) Nothing to Disclose Yoshiaki Watanabe, MD, Kobe, Japan (*Abstract Co-Author*) Nothing to Disclose Atsushi K. Kono, MD, PhD, Kobe, Japan (*Abstract Co-Author*) Nothing to Disclose Shumpei Mori, Kobe, Japan (*Abstract Co-Author*) Nothing to Disclose Satoru Takahashi, MD, Suita, Japan (*Abstract Co-Author*) Nothing to Disclose Kazuro Sugimura, MD, PhD, Kobe, Japan (*Abstract Co-Author*) Nothing to Disclose Philips NV Research Grant, Bayer AG Research Grant, Eisai Co, Ltd Research Grant, DAIICHI SANKYO Group

### **TEACHING POINTS**

In dual source CT (DSCT), two x-ray source/detector simultaneously rotate acquiring the image data. Two systems are oriented with 90 degree offset in the gantry contributing unique advantages. The advantage of DSCT has been well investigated for the coronary examination; however, the applicability of DSCT is not sufficiently utilized in daily clinical routine examination. This exhibit shows both basic and detailed tips for using DSCT in daily clinical cardiovascular examination. The aims of this exhibit are: (1) To review each scanning mode that can use only in dual source system, and (2) To share the clinical impacts of each scanning mode with representative cases.

## TABLE OF CONTENTS/OUTLINE

1.Brief review of what is DSCT

- 2. The concepts and advantages of scanning modes with dual source system
- 2-1. Cardiac scanning
- 2-2. High-pitch dual-spiral scanning
- 2-3. Dual energy scanning
- 2-3. Dual power scanning3. Sharing the clinical impacts of DSCT
- 3-1. High temporal resolution
- 3-2. Fast and wide volume coverage
- 3-3. Sedation free and breath-hold free
- 3-4. Radiation dose reduction
- 3-5. Contrast material amount reduction
- 3-6. Iodine uptake analysis with material decomposition method
- 3-7. Maximization of iodine enhancement

# CA138-ED-MOA9

MSCT Imaging of Various Shunts and Grafts in Post Operative Cases of Congenital Heart Diseases

Monday, Nov. 28 12:15PM - 12:45PM Room: CA Community, Learning Center Station #9

#### **Participants**

Yashpal Rana, MD, MBBS, Ahmedabad, India (*Abstract Co-Author*) Nothing to Disclose Megha Sheth, Ahedabad, India (*Abstract Co-Author*) Nothing to Disclose Dinesh Patel, MD, DMRE, Ahmedabad, India (*Abstract Co-Author*) Nothing to Disclose Zalak Patel, MD, Ahmedabad, India (*Presenter*) Nothing to Disclose S. Patel, Ahmedabad, India (*Abstract Co-Author*) Nothing to Disclose Milin Garachh, Ahmedabad, India (*Abstract Co-Author*) Nothing to Disclose

# **TEACHING POINTS**

Understanding various shunts and grafts in congenital heart diseases Normal & abnormal post-operative findings on MSCT

## TABLE OF CONTENTS/OUTLINE

Details of various shunts and grafts used in congenital heart diseases correction MSCT technique and imaging appearances MSCT imaging appearances of abnormal post-operative findings Summary

### CA210-SD-MOA1

Distensibility Characteristics of Ascending Aorta, Descending Aorta and Pulmonary Artery without Coronary Artery Disease

Monday, Nov. 28 12:15PM - 12:45PM Room: CA Community, Learning Center Station #1

## Participants

Fei Yang, Zhangjiakou, China (*Presenter*) Nothing to Disclose Dawei Wang, Zhang Jiakou, China (*Abstract Co-Author*) Nothing to Disclose Shujun Cui, Zhang Jiakou, China (*Abstract Co-Author*) Nothing to Disclose Yuexiang Zhu, Zhang Jiakou, China (*Abstract Co-Author*) Nothing to Disclose Huaijun Liu, PhD, Shijiazhuang, China (*Abstract Co-Author*) Nothing to Disclose Zhenshun Hu, Zhang Jiakou, China (*Abstract Co-Author*) Nothing to Disclose Jing Wen, Shenyang, China (*Abstract Co-Author*) Nothing to Disclose Xiaocan Wang, Zhangjiakou, China (*Abstract Co-Author*) Nothing to Disclose Xiaohong Yang, Zhang Jiakou, China (*Abstract Co-Author*) Nothing to Disclose

#### PURPOSE

As the prevalence of coronary computed tomographic angiography (CCTA), it is meaningful that CCTA can provide not only the structural details of aorta and pulmonary artery, but also functional information of vessel elasticity. Our aim was to study the distensibility characteristics of ascending aorta (AA), descending aorta (DA), main pulmonary artery (MPA), left pulmonary artery (LPA) and right pulmonary artery (RPA), their relationship between each other ,and relations with age using 640 slice-volume CT.

## METHOD AND MATERIALS

42 subjects who underwent CCTA on 640 slice-volume CT without cardiovascular disease, high blood pressure, diabetes and hyperlipidemia were enrolled in this study. CT data were reconstructed in 10% step throughout the RR interval. The maximal, minimal area and changes in area of AA, DA, MPA, LPA and RPA were measured, and the aortic distensibility (AD) was calculated. Then the subjects divided into 2 groups, Group 1 age<46, Group 2 age≥46.The AD of AA, DA, MPA of each group was calculated and compared.

#### RESULTS

The AD of AA, DA, MPA,LPA and RPA was  $(4.02\pm2.16)$ ,  $(3.16\pm1.49)$ ,  $(7.94\pm3.04)$ ,  $(5.89\pm3.61)$ and  $(7.37\pm2.77)$ . The correlation coefficient of AA and DA, r=0.661,p=0.000. The correlation coefficient of AA and MPA, r=0.520,p=0.000. The correlation coefficient of DA and MPA, r=0.303,p=0.051. Group 1 the mean AD of AA was5.21±2.32,Group 2 the mean AD of AA was 2.71±0.85, there was statistically significant difference(t=4.546,p=0.000). Group 1 the mean AD of DA was3.75±1.70,Group 2 the mean AD of DA was2.50±0.85, there was statistically significant difference (t=3.055,p=0.005). Group 1 the mean AD of MPA was8.98±3.02.Group 2 the mean AD of DA was6.80±2.69, there was statistically significant difference(t=2.454,p=0.019).

### CONCLUSION

The distensibility of AA, DA, MPA, LPA and RPA could be well shown by ECG-gated 640 slice-volume CT. The distensibility relativity was observed between AA and DA, AA and MPA. A obvious age-related decrease in vascular distensibility was found in AA, DA and MPA, which should be taken into account in clinical trials and treatments for the distensibility related cardiovascular diseases.

## **CLINICAL RELEVANCE/APPLICATION**

The correlation relationship of distensibility between AA and DA , AA and MPA was positive correlation. The distensibility of AA, DA and MPA was age-related decreased.

Multi-parametric Approach to Myocarditis at 3-Tesla Including T1 Relaxation Times, T2 Imaging, and Myocardial Strain Analysis Assessed by Cardiac Magnetic Resonance Feature Tracking

Monday, Nov. 28 12:15PM - 12:45PM Room: CA Community, Learning Center Station #2

#### **Participants**

Jonas Doerner, MD, Cologne, Germany (*Presenter*) Nothing to Disclose Julian A. Luetkens, MD, Bonn, Germany (*Abstract Co-Author*) Nothing to Disclose Daniel K. Thomas, MD, PhD, Bonn, Germany (*Abstract Co-Author*) Nothing to Disclose Daniel Kuetting, MD, Bonn, Germany (*Abstract Co-Author*) Nothing to Disclose Darius Dabir, Bonn, Germany (*Abstract Co-Author*) Nothing to Disclose Hans H. Schild, MD, Bonn, Germany (*Abstract Co-Author*) Nothing to Disclose Claas P. Naehle, MD, Bonn, Germany (*Abstract Co-Author*) Consultant, Medtronic, Inc

### PURPOSE

In a clinical setting, acute myocarditis is frequently observed and is associated with a high morbidity and mortality in its acute phase and the long-term. We aimed to evaluate cardiac magnetic resonance feature tracking analysis as a post-processing tool for detection of strain alterations as an ad on tool in a multi-parametric protocol for the diagnosis of myocarditis.

#### **METHOD AND MATERIALS**

Cardiac magnetic resonance (CMR) was performed on a 3-Tesla whole body scanner (Ingenia, Philips Healthcare). A multiparametric protocol was applied which comprised balanced-SSFP cine imaging in common orientations (SAX, HLA, VLA, LVOT), T1mapping, T2 imaging. A total of 17 patients who were admitted with acute myocarditis were included in this study and 10 patients who were examined for other indications served as healthy controls. In addition to T1 relaxation times and T2 ratio, circumferential and longitudinal strain as well as global radial displacement was assessed using the feature tracking technique.

#### RESULTS

No between group differences were observed for baseline characteristics. Global native T1 relaxation times were significantly prolonged in patients with myocarditis (1181±43ms vs. 1098±40ms, P<0.0001). T2 imaging revealed an increased T2 ratio in patients with myocarditis (1.8±0.3SI vs. 1.5±0.3SI, p=0.01). Furthermore, ejection fraction (EF) (57±9% vs. 65±6%, p<0.05), global longitudinal strain (17.2±2.7% vs. 19.9±2.6%, p<0.05) and global circumferential strain (-22.7±3.2% vs. -26.2±4.1%, p<0.05) as well as global radial displacement (4.9±0.7mm vs. 5.9±0.8mm, p<0.01) were significantly reduced in such patients.

### CONCLUSION

Patients with acute myocarditis show signs of myocardial dysfunction which can be detected and quantitatively assessed using feature tracking analysis. This approach gives further insights in regional myocardial function without the need of additional dedicated tagging sequences and should therefore considered as an ad on tool in the wide variety of CMR features for the diagnosis of acute myocarditis. Nevertheless, further studies need to evaluate the clinical value of segmental analysis especially in patients with myocarditis and preserved EF.

### **CLINICAL RELEVANCE/APPLICATION**

Feature tracking derived strain analysis may be a useful ad on tool for the diagnosis of myocarditis in a multi-parametric protocol, without the need of additional tagging sequences.

## CA212-SD-MOA3

Cardiovascular Risk Stratification in Diabetic Patients with Maturity Onset Diabetes of the Young (MODY) Using Coronary Artery Calcium Score

Monday, Nov. 28 12:15PM - 12:45PM Room: CA Community, Learning Center Station #3

## Participants

Gilberto Szarf, MD, Sao Paulo, Brazil (*Presenter*) Nothing to Disclose Luciana F. Franco, Sao Paulo, Brazil (*Abstract Co-Author*) Nothing to Disclose Fernando M. Giuffrida, MD, Sao Paulo, Brazil (*Abstract Co-Author*) Nothing to Disclose Carlos G. Verrastro, MD, Sao Paulo, Brazil (*Abstract Co-Author*) Nothing to Disclose Alfredo A. Rodrigues, MD, Sao Paulo, Brazil (*Abstract Co-Author*) Nothing to Disclose Andre F. Reis, MD, PhD, Sao Paulo, Brazil (*Abstract Co-Author*) Nothing to Disclose

### PURPOSE

Monogenic diabetes due to glucokinase mutations (GCK-Maturity Onset Diabetes of the Young - MODY) is characterized by mild nonprogressive hyperglycemia. This condition can be potentially associated with lower cardiovascular (CV) risk compared to Type 2 diabetes, but solid data are lacking in literature. It was shown that coronary artery calcium (CAC) score provides incremental predictive value over the Framingham risk score when used in asymptomatic patients. It also outperformed other cardiovascular risk stratification tools, as C-reactive protein and carotid intima media thickness. The aim of this study is to compare the CAC score between type 2 diabetes patients, individuals with GCK-MODY diabetes and controls.

### **METHOD AND MATERIALS**

Forty individuals without CAD have been assessed for coronary artery calcium score using non-contrast multi-slice computed tomography of the heart (Agatston score). Twenty of those were type 2 diabetes patients, 12 were individuals with GCK-MODY from 7 families (diagnosed by Sanger sequencing), and 8 were controls (age- and BMI-matched spouses or non-affected relatives of MODY patients).

### RESULTS

Seventy percent of the type 2 diabetes patients were female compared to 12.5% in the control group and 91.7% among the GCK-MODY individuals. Mean age was 54.7+6.7, 44.9+5.5 and 37.8+10.8 years for the type 2 diabetes patients, the control group and the GCK-MODY patients respectively. Body mass index was different (statistically significant) between type 2 diabetes (30.5+5.4 kg/m2) versus GCK-MODY patients (23.9+2.0 kg/m2). 84.2% of patients with type 2 diabetes had low Framingham risk score and 15.9% were in the intermediate risk group. All GCK-MODY individuals and controls had low risk. Glycated hemoglobin was significantly higher in type 2 diabetes patients compared to GCK-MODY and control groups. Coronary calcium score was significantly lower in GCK-MODY individuals 0 [0-0] and in the control group 0 [0- 4.41] compared to Type 2 diabetes patients 6.2 [0- 161.4] (median[interquartile range]).

### CONCLUSION

Our data suggest that GCK-MODY patients to bear a low long term risk for CAD, despite having lifelong hyperglycemia.

### **CLINICAL RELEVANCE/APPLICATION**

These data could have potential implications in the clinical management of GCK-MODY diabetes patients as they probably have a lower cardiovascular risk compared to Type 2 diabetes patients. Prospective large studies are necessary to further clarify this point.

### CA214-SD-MOA5

Characterization of Left Ventricular Remodeling in Professional Soccer Players: Can We Prevent Sudden Cardiac Death Using CMR?

Monday, Nov. 28 12:15PM - 12:45PM Room: CA Community, Learning Center Station #5

## Participants

Enver G. Tahir, MD, Hamburg, Germany (*Presenter*) Nothing to Disclose Jacob Schmidt-Holz, Hamburg, Germany (*Abstract Co-Author*) Nothing to Disclose Gunnar K. Lund, MD, Hamburg, Germany (*Abstract Co-Author*) Nothing to Disclose Kai Muellerleile, Hamburg, Germany (*Abstract Co-Author*) Nothing to Disclose Gerhard B. Adam, MD, Hamburg, Germany (*Abstract Co-Author*) Nothing to Disclose Jitka Starekova, Hamburg, Germany (*Abstract Co-Author*) Nothing to Disclose Jitka Starekova, Hamburg, Germany (*Abstract Co-Author*) Nothing to Disclose Jin Yamamura, MD, Hamburg, Germany (*Abstract Co-Author*) Nothing to Disclose Dennis Saring, Wedel, Germany (*Abstract Co-Author*) Nothing to Disclose Cyrus Behzadi, Hamburg, Germany (*Abstract Co-Author*) Nothing to Disclose Marc Regier, Hamburg, Germany (*Abstract Co-Author*) Nothing to Disclose

#### PURPOSE

Regular physical activity over a long time period leads to a cardiac adaptation described as "athlete's heart". The purpose of this study was to determine the effects of intensive daily training in a specific type of sports- professional soccer, in regard to morphological and functional left ventricular parameters assessed by cardiac magnetic resonance imaging (CMR) and to compare these with non-athletic healthy volunteers.

#### **METHOD AND MATERIALS**

CMR was performed in 21 male professional soccer players from the German Bundesliga team squad of the Hamburger SV and 15 age-, sex- and weight-matched untrained controls at 1.5 T (Achieva, Philips) during the active season. For quantitative CMRI, an electrocardiographically triggered steady-state free precession (SSFP) cine sequence (TR/TE, 3.2/1.6ms; pixel-size, 1.7mm×1.7mm) was performed in short- and long-axis views. Quantitative analysis included end-diastolic (EDV) and end-systolic volumes (ESV), stroke volume (SV), left ventricular ejection-fraction (EF) as well as end-diastolic (EDMM) and end-systolic myocardial mass (ESMM). CMRI data were analyzed by two independent observers using the HeAT-Software. Data are given as the mean of both observers.

### RESULTS

In professional soccer players a significant increase of the following parameters was determined compared to non-athletes: EDV (229 ±24 ml vs. 196 ±30 ml, P< 0.04), ESV (96 ±16 ml vs. 82 ±11 ml, P< 0.04) and LV mass (189 ±34 g vs. 143 ±19 g, P= 0.001). Stroke volume (133 ±19 ml vs. 115 ±23 ml, P= ns) and LV ejection fraction (0.58% vs. 0.58%, P= ns) were similar in both groups. The professional soccer players had a significantly lower resting heart rate than non-athletes (50 beat/min vs. 64 beat/min, P= 0.01).

## CONCLUSION

Long-term training in professional soccer players is characterised by left ventricular adaptation leading to an increase in functional parameters and myocardial mass. CMRI allows an objective quantitative assessment and might help to differentiate physiologic cardiac adaptations from inherited hypertrophic cardiomyopathy.

#### **CLINICAL RELEVANCE/APPLICATION**

CMR imaging enables studies to the mechanisms of LV adaptation in professional soccer players and may help to differentiate physiological changes to high-level exercise from inherited cardiomyopathy.

The Effect of New Generation Motion Correction Algorithms on Diagnostic Image Quality and Reproducibility in Aortic Annular Computed Tomography Evaluation Pre Transcatheter Aortic Valve Replacement (TAVR)

Monday, Nov. 28 12:15PM - 12:45PM Room: CA Community, Learning Center Station #6

#### Awards

#### **Student Travel Stipend Award**

#### Participants

Jeanette V. Soon, MBBS, Vancouver, BC (*Presenter*) Nothing to Disclose Nada Sulaiman, Madinah, Saudi Arabia (*Abstract Co-Author*) Nothing to Disclose Jong Kwan Park, Vancouver, BC (*Abstract Co-Author*) Nothing to Disclose Philipp Blanke, MD, Freiburg, Germany (*Abstract Co-Author*) Consultant, Edwards Lifesciences Corporation; Consultant, Neovasc Inc ; Consultant, Tendyne Holdings, Inc; Consultant, Circle Cardiovascular Imaging Inc Jennifer D. Ellis, MD, Vancouver, BC (*Abstract Co-Author*) Nothing to Disclose Cameron J. Hague, MD, Vancouver, BC (*Abstract Co-Author*) Nothing to Disclose Darra T. Murphy, MD, FRCPC, Vancouver, BC (*Abstract Co-Author*) Nothing to Disclose Jonathon A. Leipsic, MD, Vancouver, BC (*Abstract Co-Author*) Nothing to Disclose Jonathon A. Leipsic, Consultant, Heartflow, Inc; Consultant, Circle Cardiovascular Imaging Inc; Consultant, Edwards Lifesciences Corporation; Consultant, Heartflow, Inc; Consultant, Circle Cardiovascular Imaging Inc; Consultant, Edwards Lifesciences Corporation; Consultant, Neovasc Inc; Consultant, Samsung Electronics Co, Ltd; Consultant, Koninklijke Philips NV; Consultant, Arineta Ltd; Consultant, Pi-Cardia Ltd;

#### PURPOSE

Vendor specific motion correction algorithms (SnapShot Freeze, GE Health care, Milwaukee, WI) have shown to improve image quality, interpretability and diagnostic accuracy with regard to coronary assessment in CCTA. We aim to determine if a new generation motion correction algorithm, extended to the whole heart, demonstrates similar improved image quality and reproducibility of annular measurements in pre TAVR CT.

### **METHOD AND MATERIALS**

Thirty consecutive prospective, ECG triggered pre TAVR CT's without rate control were retrospectively identified. Standard (STD) 35% and 75% R-R interval phases were constructed, from which new motion corrected (MC) data sets were generated offline. Four data sets sets (2 MC, 2 STD) per patient were analyzed by 2 independent, blinded readers for aortic annular size, short and long axis, perimeter and average diameter. Image quality was graded using a 5 point Likert score (1 = poor, 2 = fair, 3 = good, 4 = very good, 5 = excellent). Statistical analysis was performed using paired Student t tests and Bland Atlman plots.

### RESULTS

120 data sets were analysed (60 STD, 60 MC). 8 data sets (3,5) were excluded due to post TAVR status abnormal valve morphology. At 35%, a significant improvement in Likert score image quality was present after motion correction was applied (mean $\pm$ STDEV 3.318 $\pm$ 0.883 vs. 3.931 $\pm$ 0.661, p < 0.001). Bland Altman plots also demonstrated a narrower agreement interval with regard to short and long axis, average diameter, aortic annular area (bias 0.033mm2, 95% limits of agreement -0.323 to 0.388mm2 vs -0.504 to 0.545mm2), and perimeter (bias 0.292 mm, 95% limits of agreement -3.171 to 3.755mm vs -4.845 to 5.237mm). At 75%, there was a trend toward improved image quality (3.318 $\pm$ 0.883 vs. 3.477 $\pm$ 0.762 (p =0.302)), and narrower limits of agreement for annular measurement, however, this did not reach statistical significance.

## CONCLUSION

Application of a vendor specific motion correction algorithm yields improvement in image quality, as well as higher interobserver reproducibility of aortic annular measurements at 35% of the R-R cycle. While no difference was observed at 75%, this may reflect improved baseline image quality with little margin for incremental gain.

## **CLINICAL RELEVANCE/APPLICATION**

Accurate CT measurement of the aortic annulus and evaluation of morphology is intergral to device and size selection, and is recommended pre transcatheter aortic valve replacement.

### **Honored Educators**

Presenters or authors on this event have been recognized as RSNA Honored Educators for participating in multiple qualifying educational activities. Honored Educators are invested in furthering the profession of radiology by delivering high-quality educational content in their field of study. Learn how you can become an honored educator by visiting the website at: https://www.rsna.org/Honored-Educator-Award/

Jonathon A. Leipsic, MD - 2015 Honored Educator

### CA216-SD-MOA7

### Monochromatic Evaluation versus Iodine Maps for Myocardial Perfusion Assessment Using Dual Energy CT

Monday, Nov. 28 12:15PM - 12:45PM Room: CA Community, Learning Center Station #7

#### Participants

Patricia M. Carrascosa, MD, Buenos Aires, Argentina (*Presenter*) Research Consultant, General Electric Company Carlos Capunay, MD, Buenos Aires, Argentina (*Abstract Co-Author*) Nothing to Disclose Alejandro Deviggiano, MD, Vicente Lopez, Argentina (*Abstract Co-Author*) Nothing to Disclose Macarena De Zan, Vicente Lopez, Argentina (*Abstract Co-Author*) Nothing to Disclose Gaston Rodriguez Granillo, Vicente Lopez, Argentina (*Abstract Co-Author*) Nothing to Disclose Roxana Campisi, Vicente Lopez, Argentina (*Abstract Co-Author*) Nothing to Disclose

# PURPOSE

Dual energy CT has the potential to evaluate myocardial perfusion (CTP) using different approaches such as virtual monochromatic evaluation or material decomposition using "iodine maps". We sought to explore the diagnostic performance of monochromatic evaluations versus iodine maps for the identification of perfusion defects in stress-rest CTP.

## METHOD AND MATERIALS

We prospectively included patients with suspected CAD who had a clinical indication of a stress-rest SPECT. In all patients, a stress-rest CTP was performed. The same pharmacolocical agent was used in both studies (dipyridamole). Single-source dual energy CTP was performed, allowing the generation of monochromatic image reconstructions with 10 keV increments from 40 to 140 keV. Stress-CTP was performed first using prospective scan at 60% phase with 150 -200 msec of padding was employed so as to cover from 40 to 80% of the R-R interval. A second prospective scan at 75% of the R-R interval with 100 milisec of padding was complemented 30 minutes later after the administration of aminophylline to revert the effect of the dipyridamole. For monochromatic evaluation, a perfusion defect was defined if present at 40, 60 and 80 kev; whereas if the defect was only present at 40 keV, reduced at 60 keV, and faded away at 80 keV it was considered a BHA. For both iodine maps and monochromatic evaluation, perfusion defects were initially identified in a qualitative manner, and subsequently complemented with a semiquantitative analysis that defined defects as myocardium having a signal density/amount of iodine two standard deviations below the mean myocardium.

#### RESULTS

A total of 28 patients were included. The mean effective radiation dose associated to stress-rest CTP was  $8.1\pm2.0$ mSv. Both at stress and rest, the diagnostic performance of the monochromatic evaluation was significant higher than the iodine map evaluation (p< 0.0001) and the combination of both for myocardial perfusion evaluation (p<0.0001).

### CONCLUSION

In the present study, CTP analysis using virtual monochromatic analysis derived from dual energy CT showed an improved diagnostic performance compared to iodine maps for the detection of perfusion defects. Furthermore, the addition of iodine maps to the monochromatic assessments failed to provide any incremental diagnostic value in this subset of patients.

### **CLINICAL RELEVANCE/APPLICATION**

Dual energy CT has the potential to evaluate myocardial perfusion using different approaches.

## CA220-SD-MOA4

#### Diagnostic Additive Value of MDCT-scan in Case of Suspected Left-sided Prosthetic Heart Valve Dysfunction

Monday, Nov. 28 12:15PM - 12:45PM Room: CA Community, Learning Center Station #4

#### Participants

Giacomo Agliata, MD, Saint-Denis, France (*Presenter*) Nothing to Disclose Laurent Macron, Saint Denis, France (*Abstract Co-Author*) Nothing to Disclose Jean-Louis Sablayrolles, Saint Denis, France (*Abstract Co-Author*) Nothing to Disclose

### PURPOSE

To define diagnostic performances and contribution of MDCT in the follow-up of left-sided prosthetic heart valve (PHV)

#### **METHOD AND MATERIALS**

We retrospectively enrolled 64 patients (33 patients referred for PHV dysfunction and 31 with left-sided PHV as the control group, 44 mechanical and 20 bioprothesis) who underwent an ECG-gated 256-MDCT scan. The acquisition (axial, one beat scanning, 280 msec/rot, multi-phase, 120 kV, 600 mA, 3.9 mSv of mean radiation dose) was performed after IV administration of iodinated contrast media (75 ml; three-phase injection). MDCT findings were blindly reviewed and compared to echocardiographic data, surgical reports (n=11, surgical group) and follow-up.

#### RESULTS

Sensitivity and specificity of MDCT for the diagnosis of PHV dysfunction were 96.9% (32/33) and 100% (31/31) respectively, resulting in a diagnostic accuracy of 98.2% Only one small paravalvular leakage on a mechanical aortic prosthesis was not visualised by MDCT. Among the 33 patients with PHV dysfunction (20 cases of obstructive pathology, 12 regurgitations and 1 endocarditis) MDCT demonstrated a 100% concordance with echocardiographic diagnosis in assessing the kind of dysfunction. More importantly, MDCT identified among the patients with obstructive pathology 9 valve degenerations, 4 pannus, 3 thrombosis and 2 cases of mixed pannus+thrombus, with confirmation by surgical findings (n=9) and follow-up data in 100% of the cases. Also of note, MDCT findings were confirmed in all patients among the surgical group.

### CONCLUSION

256 MDCT-scan enables with high accuracy the discrimination between normal and pathological PHV and the characterization of PHV dysfunction. In obstructive PHV, MDCT is also able to correctly establish etiology, suggesting potential therapeutic impact.

#### **CLINICAL RELEVANCE/APPLICATION**

MDCT-scan assesses Prosthetic Heart Valve conditions as well as the gold standard echocardiography, adding the possibility to evaluate also etiology in obstructive dysfunctions, suggesting therapy

## CH142-ED-MOA6

### How Does Smoking Tobacco Affect the Lungs? Radiopathologic Correlation

Monday, Nov. 28 12:15PM - 12:45PM Room: CH Community, Learning Center Station #6

#### **Participants**

Maria Magdalena Serra Salas, MD, Barcelona, Spain (*Presenter*) Nothing to Disclose Xavier Gallardo, MD, Sabadell, Spain (*Abstract Co-Author*) Nothing to Disclose Marta Andreu, MD, Sabadell, Spain (*Abstract Co-Author*) Nothing to Disclose Eva Castaner, MD, Sabadell, Spain (*Abstract Co-Author*) Nothing to Disclose Maria R. Escoda, Sabadell, Spain (*Abstract Co-Author*) Nothing to Disclose Joseph M. Mata, MD, PhD, Sabadell, Spain (*Abstract Co-Author*) Nothing to Disclose Carles G. Zaragoza, MD, Sabadell, Spain (*Abstract Co-Author*) Nothing to Disclose Carlota C. Rodriguez, MD, Sabadell, Spain (*Abstract Co-Author*) Nothing to Disclose

## **TEACHING POINTS**

To describe and illustrate the radiologic findings in the different types of interstitial lung diseases related to smoking. To point out the most important radiologic criteria for the diagnosis of the different types of interstitial lung diseases and to relate these criteria to the histologic findings.

### **TABLE OF CONTENTS/OUTLINE**

**INTRODUCTION:** Cigarette smoking is recognized as a risk factor for interstitial lung disease. HRCT is sensitive in detecting interstitial lung disease and characterizing it into distinct individual entities. However, the clinic, radiologic, and histologic features of these entities overlap, and mixed patterns can coexist in the same patient. **REVIEW OF IMAGING FINDINGS:** Respiratory bronchiolitis - interstitial lung disease. Pulmonary Langerhans cell histiocytosis Desquamative interstitial pneumonia. Interstitial pneumonia combined with emphysema. Overlap and relationship between different interstitial smoking-related diseases. **SUMMARY:** The variety of interstitial diseases associated with cigarette smoking is wider than generally appreciated. HRCT allows us to evaluate the type, degree, extension, possible overlap, and evolution of these diseases. An integrated clinical, radiologic, and pathologic approach is necessary for accurate diagnosis of smoking-related interstitial disease.

# Lung Resection Surgery: A Primer for Radiologists

Monday, Nov. 28 12:15PM - 12:45PM Room: CH Community, Learning Center Station #7

#### **Participants**

Divya Kumari, MD, Cleveland, OH (*Abstract Co-Author*) Nothing to Disclose Michael B. Shvarts, MD, Cleveland, OH (*Abstract Co-Author*) Nothing to Disclose Jonathan H. Chung, MD, Chicago, IL (*Abstract Co-Author*) Royalties, Reed Elsevier; Consultant, F. Hoffmann-La Roche Ltd; Consultant, Boehringer Ingelheim GmbH; Consultant, Veracyte, Inc Luis A. Landeras, MD, Cleveland, OH (*Presenter*) Institutional Grant support, Koninklijke Philips NV

### **TEACHING POINTS**

To understand the most common surgical approaches to lung surgery To familiarize with normal postoperative appearance in plain film radiography and computed tomography To review the most common complications

### TABLE OF CONTENTS/OUTLINE

IntroductionTypes of Lung Resection Wedge Resection Segmentectomy Lobectomy Sleeve lobectomy PneumonectomyFlaps and Chest Wall ReconstructionComplications Pulmonary edema/ARDS Pneumonia Hemorrhage/hematoma Bronchopleural fistula Empyema Lobar torsion Gossypiboma Lung hernia Pulmonary artery stump thrombosis Postpneumonectomy Syndrome

## **Honored Educators**

Presenters or authors on this event have been recognized as RSNA Honored Educators for participating in multiple qualifying educational activities. Honored Educators are invested in furthering the profession of radiology by delivering high-quality educational content in their field of study. Learn how you can become an honored educator by visiting the website at: https://www.rsna.org/Honored-Educator-Award/

Jonathan H. Chung, MD - 2013 Honored Educator

## CH245-SD-MOA1

Quantitative Shape Analysis of CT Images in Thymic Epithelial Tumors: Correlation with World Health Organization Classification

Monday, Nov. 28 12:15PM - 12:45PM Room: CH Community, Learning Center Station #1

## Participants

Motohiko Yamazaki, MD, Niigata, Japan (*Presenter*) Nothing to Disclose Kanako Yamana, Niigata, Japan (*Abstract Co-Author*) Nothing to Disclose Takuya Yagi, Niigata City, Niigata Prefecture, Japan (*Abstract Co-Author*) Nothing to Disclose Hiroyuki Ishikawa, MD, Niigata, Japan (*Abstract Co-Author*) Nothing to Disclose Hidefumi Aoyama, MD, PhD, Niigata, Japan (*Abstract Co-Author*) Nothing to Disclose

# PURPOSE

In diagnostic imaging, shape evaluation plays an important role in predicting tumor aggressiveness. This study aimed to differentiate CT features of low- and high-risk thymic epithelial tumors using quantitative shape analysis derived from a computer software.

### **METHOD AND MATERIALS**

This retrospective study included 46 consecutive patients with 47 thymomas or thymic cancers. Tumor segmentation on CT images was manually performed on each axial section with a thickness of less than or equal to 3 mm. Subsequently, whole tumor volume, surface area, and quantitative shape parameters including circularity, sphericity, solidity, and convexity were calculated using a computer software. These quantitative shape parameters reflect the complexity, and a low value indicates that a tumor shape is complex. Furthermore, as conventional CT findings, the presence of lobulation, irregular contour, internal heterogeneity, and cystic or necrotic change was visually evaluated. Differences between low- and high-risk thymic epithelial tumors were statistically assessed by the Student's t-test or Fisher's exact test, and factors with P < 0.10 underwent multivariate logistic regression analysis. Discriminating performance was calculated by area under the receiver operating characteristic curves (AUC).

#### RESULTS

Based on the World Health Organization classification, 21 were low-risk tumors (4 type A, 9 type AB, and 8 type B1 thymomas) and 26 were high-risk tumors (12 type B2 and 7 type B3 thymomas and 7 thymic cancers). Compared to low-risk tumors, high-risk tumors had significantly lower values of circularity, sphericity, solidity, and convexity (P < 0.05). For conventional CT findings, only the presence of heterogeneity was significantly associated with high-risk tumors (P < 0.05). Multivariate analysis revealed that lower solidity at the maximum cross-section of the tumor (2D solidity) was an independent factor to predict high-risk tumors (odds ratio, 0.061; P = 0.011). Discriminating performance of 2D solidity was significantly higher than that of the whole tumor volume (AUC = 0.80 vs. 0.57; P = 0.02).

### CONCLUSION

Quantitative shape analysis using a computer software can help differentiate low- and high-risk thymic epithelial tumors.

#### **CLINICAL RELEVANCE/APPLICATION**

Compared with visual CT evaluation, quantitative shape analysis using a computer software is a more objective method and may more accurately predict the aggressiveness of thymic epithelial tumors.

Intravoxel Incoherent Motion and Diffusion Kurtosis Diffusion Weighted Imaging in Lung: Capability for Quantitative Differentiation of Small-cell Lung Cancer from Non-small-cell Lung Cancer and Correlations with Lung Cancer Markers

Monday, Nov. 28 12:15PM - 12:45PM Room: CH Community, Learning Center Station #2

## Awards

### **Student Travel Stipend Award**

#### Participants

Yaru Tian, MBBCh, Beijing, China (*Presenter*) Nothing to Disclose Tao Jiang, MD, Beijing, China (*Abstract Co-Author*) Nothing to Disclose Hui Li, Beijing, China (*Abstract Co-Author*) Nothing to Disclose Lu Liang, MD, Beijing, China (*Abstract Co-Author*) Nothing to Disclose Xin Ye, Beijing, China (*Abstract Co-Author*) Nothing to Disclose Peng Peng, Beijing, China (*Abstract Co-Author*) Nothing to Disclose Yang Yu, Beijing, China (*Abstract Co-Author*) Nothing to Disclose Qinglei Shi, Beijing, China (*Abstract Co-Author*) Nothing to Disclose

## PURPOSE

Study the value of intravoxel incoherent motion (IVIM) diffusion weighted imaging (DWI) and diffusion kurtosis imaging (DKI) in differentiation of small-cell lung cancer (SCLC) from non-SCLC (NSCLC), and evaluate the relationship between IVIM and DKI-derived parameters and lung cancer markers at 3.0T.

### **METHOD AND MATERIALS**

Thirty-six patients with NSCLC (21 males and 9 females; mean age, 66.8 years) and 6 patients with SCLC (4 males and 2 females; mean age, 68.6 years) confirmed by hispathology were enrolled and underwent lung diffusion-weighted imaging MR exam. The protocol included routine MR exam and IVIM and DKI-DWI sequences before surgery or biopsy in a 10-month period (table 1). The IVIM-derived parameters were obtained by using prototype software provided by the manufacturer (Siemens Healthcare) and DKI-derived parameters were obtained by using an in-house developed software program based on a computing language and interactive environment (MATLAB; Mathworks, Natick, Mass). ADC maps were calculated automatically on machine. Independent-Samples T test was used to compare the difference between SCLC and NSCLC group. The relationship between IVIM and DKI-derived parameters and lung cancer markers was assessed by using the Pearson correlation test. Receiver operating characteristic (ROC) analysis of discrimination between SCLC and NSCLC was performed for K, Dkur, Divim and ADC values.

### RESULTS

Dkur, Divim and ADC values all were significantly lower in SCLC group than NSCLC group (P<0.05). The positive correlation seems existed between Dkur and CYFRA211 (r=0.360, P=0.026), D\* and proGRF (r=0.329,P=0.041) and negative correlation seems existed between ADC and NSE (r=-0.301, P=0.032). ROC analysis demonstrated a higher AUC for Dkur [ $0.956\pm0.031$ ,(0.842 to 0.996)] and D [ $0.867\pm0.0691$ ,(0.725 to 0.953)] than for ADC [ $0.848\pm0.0601$ ,(0.702 to 0.941)] (P>0.05), the AUC of K was [ $0.777\pm0.071$ , (0.619 to 0.891)].

### CONCLUSION

IVIM and DKI-derived parameters of lung showed better diagnostic performance than ADC values in differentiating SCLC from NSCLC, and significant correlation was observed between quantitative parameters and some lung cancer markers.

## **CLINICAL RELEVANCE/APPLICATION**

Intravoxel incoherent motion (IVIM) diffusion weighted imaging (DWI) and diffusion kurtosis imaging (DKI) may differentiate smallcell lung cancer (SCLC) from non-SCLC (NSCLC) which may provide vital information in making therapy strategy of lung cancer.

# Imaging Trends in Acute Venous Thromboembolic Disease: 2000-2015

Monday, Nov. 28 12:15PM - 12:45PM Room: CH Community, Learning Center Station #3

#### Awards

#### **Student Travel Stipend Award**

#### **Participants**

Isaac Wang, MD, Ann Arbor, MI (*Presenter*) Nothing to Disclose Matthew S. Davenport, MD, Cincinnati, OH (*Abstract Co-Author*) Royalties, Wolters Kluwer nv; ; Ella A. Kazerooni, MD, Ann Arbor, MI (*Abstract Co-Author*) Nothing to Disclose

### PURPOSE

To correlate imaging utilization for suspected acute venous thromboembolism (VTE) in inpatients and emergency department (ED) patients with landmark publications and institutional care guidelines.

#### METHOD AND MATERIALS

Between 2000 and 2015, the number of CT pulmonary angiograms (CTPA) alone, CTPA combined with indirect CT venography (CTV) of the pelvis and lower extremities, ventilation/perfusion (V/Q) scans, and lower extremity venous Doppler examinations (US) were obtained from the hospital and radiology information systems for each calendar month for inpatients and ED patients, and correlated with landmark publications and release of institutional care guidelines.

### RESULTS

Annual V/Q volume peaked in 2004-2005 (n=373 inpatient, n=1049 ED) and has decreased since. US volume steadily increased in both populations since 2002, and was higher than CT volume throughout the study period for inpatients (annual mean volume: n=4210 [US]; n=1196 [CT]), but not ED patients (annual mean volume: n=1082 [US]; n=1902 [CT]). Use of CTV with CTPA peaked at 51% of examinations in 2006. For ED patients, overall CTPA volume peaked in 2008, declined through 2012, then rose annually since, predominantly without CTV (8-28% rate 2012-2015). For inpatients, CTPA volume also peaked in 2008, but declined steadily since (n=1941 in 2008 vs. n=843 in 2015). PIOPED II was released in 2006, Brenner et al's landmark NEJM publication on CT-related radiation exposure was published in 2007, and an institutional inpatient VTE prophylaxis guideline was implemented with a hard-stop best-practice alert in 2008. While there was a sustained decline in CTPA utilization following 2008 for inpatients, the decline was temporary for ED patients.

### CONCLUSION

Following the PIOPED II and Brenner et al. publications, there was a transient 4-year decline in CTPA utilization for ED patients that reversed course in 2012. This decline was sustained through the end of the study period (2015) in the inpatient setting, where a hard-stop best-practice alert was incorporated into the electronic medical record system.

#### **CLINICAL RELEVANCE/APPLICATION**

A best-practice alert incorporated into an electronic medical record system can more successfully sustain imaging best practices than the influence of major landmark publications.

#### **Honored Educators**

Presenters or authors on this event have been recognized as RSNA Honored Educators for participating in multiple qualifying educational activities. Honored Educators are invested in furthering the profession of radiology by delivering high-quality educational content in their field of study. Learn how you can become an honored educator by visiting the website at: https://www.rsna.org/Honored-Educator-Award/

Ella A. Kazerooni, MD - 2014 Honored Educator

Airway Dimensions in Current and Former Smokers: An Independent Predictor of Airflow Obstruction and **Respiratory Quality of Life in Chronic Obstructed Pulmonary Disease** 

Monday, Nov. 28 12:15PM - 12:45PM Room: CH Community, Learning Center Station #5

# Participants

Jean-Paul Charbonnier, Nijmegen, Netherlands (Presenter) Employee, Thirona BV Esther Pompe, MD, Utrecht, Netherlands (Abstract Co-Author) Nothing to Disclose Camille Moore, Denver, CO (Abstract Co-Author) Nothing to Disclose Stephen Humphries, Denver, CO (Abstract Co-Author) Research Consultant, PAREXEL International Corporation Bram Van Ginneken, PhD, Nijmegen, Netherlands (Abstract Co-Author) Stockholder, Thirona BV; Co-founder, Thirona BV; Research Grant, MeVis Medical Solutions AG; Research Grant, Delft Imaging Systems; Research Grant, Toshiba Corporation; David A. Lynch, MBBCh, Denver, CO (Abstract Co-Author) Research support, Siemens AG Scientific Advisor, PAREXEL International Corporation Consultant, Boehringer Ingelheim GmbH Consultant, Gilead Sciences, Inc Consultant, F. Hoffmann-La Roche Ltd Consultant, Veracyte, Inc

Barry J. Make, Denver, CO (Abstract Co-Author) Nothing to Disclose

Eva M. Van Rikxoort, PhD, Nijmegen, Netherlands (Abstract Co-Author) Stockholder, Thirona BV; Co-founder, Thirona BV

#### PURPOSE

We investigated the relationship between airway dimensions and airflow obstruction and respiratory quality of life in current and former cigarette smokers.

# METHOD AND MATERIALS

Cigarette smokers were studied that enrolled in the COPDGene study. Spirometry assessment included forced expiratory volume in 1 sec (FEV1), forced vital capacity (FVC), % predicted FEV1 (FEV1%-p), % predicted FVC (FVC%-p), and peak expiratory flow (PEF). Respiratory quality of life was assessed by the St George's Respiratory Questionnaire (SGRQ) score and 6 Minute Walking Distance (SMWD).Inspiratory CT was available to extract the airways, the amount of emphysema, and the total lung capacity (TLC). Lumen perimeters and airway wall areas were automatically extracted perpendicular to the airways. Linear regression was performed on these measurements to calculate an index score of airway wall thickness, expressed as the square root of wall area at airways with a perimeter of 10mm (Pi10). Emphysema was defined as the percentage of low-attenuation area below -950 HU (LAA%-950). Multiple linear regression was used to determine the predictive value of Pi10 and smoking status on airflow obstruction and respiratory quality of life. An interaction was included in the model to investigate if the effect of Pi10 differed by smoking status. All models were adjusted for age, gender, body mass index, pack years, bronchodilator responsiveness, TLC, and LAA%-950.

## RESULTS

1544 cigarette smokers (894 former smokers) were included, with a mean age of  $60.7 \pm 8.9$  years and a mean Pi10 of  $2.23 \pm$ 0.57mm. Pi10 was significantly associated with all airflow obstruction and respiratory quality of life measures (all p<0.001). The interaction between Pi10 and smoking status was significant for all measures except FVC%-p (p=0.30) and SGRQ score (p=0.064). This indicates that the effect of Pi10 on FEV1%-p, PEF, FEV1/FVC and SMWD was significantly reduced in current smokers compared to former smokers.

# CONCLUSION

Pi10 independently contributes to airflow obstruction and respiratory quality of life. This effect is stronger in former smokers as compared to current smokers.

### **CLINICAL RELEVANCE/APPLICATION**

Pi10 is an independent marker for airflow obstruction and respiratory quality of life and may be more strongly associated with these outcomes in former smokers than current smokers.

## ER166-ED-MOA6

MDCT of Midfacial Fractures: Classification Systems, Principles of Reduction, and Common Complications

Monday, Nov. 28 12:15PM - 12:45PM Room: ER Community, Learning Center Station #6

## Awards Certificate of Merit Identified for RadioGraphics

#### **Participants**

David Dreizin, MD, Baltimore, MD (*Presenter*) Nothing to Disclose Silviu Diaconu, Baltimore, MD (*Abstract Co-Author*) Nothing to Disclose Uttam Bodanapally, MD, Baltimore, MD (*Abstract Co-Author*) Nothing to Disclose Arthur Nam, MD, MS, Baltimore, MD (*Abstract Co-Author*) Nothing to Disclose Michael N. Patlas, MD, FRCPC, Hamilton, ON (*Abstract Co-Author*) Nothing to Disclose Felipe Munera, MD, Miami, FL (*Abstract Co-Author*) Nothing to Disclose

### **TEACHING POINTS**

After completing this exhibit, viewers will be able to...

Understand the dependent nature of midfacial fractures and importance of sagittal buttresses for restoring facial projection.2.
 Explain why Le Fort fracture **level** is the most important aspect of these fractures to plastic and reconstructive surgeons.
 Describe common fracture classifications of the palatoalveolar, naso-orbito-ethmoid, zygomatic (malar), and orbital regions, and how they influence operative decision making.4. Deduce the surgeon's reasoning for operative approach, mandibulo-maxillary fixation, choice of plate-fixation points, use of bone grafting, trans-nasal canthal wiring and other techniques based on post-operative MDCT.

# TABLE OF CONTENTS/OUTLINE

Beyond buttresses: "stability" in midface fractures. Know your sutures. Palatoalveolar fractures: classifactions Le Fort fractures: Le Fort I/II/III - review/limitations. Level is key. coexisting ZMC and NOE fractures. Orbital fractures: herniated fat, orbital volume, and enophthalmos; Blow in and blow out; Defect size mattersNOE fractures: NOE I/II/III; Know your anatomy; post-op findingsZMC fractures: Grading ZMCs- the zygomaticosphenoid suture; How many plates are enough? A note on zygomatic archLooking to the future: 3D printing and intra-operative CBCT

Multi Detector CT Angiography (CTA): Influence of Its Findings in Therapeutic Decision-making in Patients with Acute Lower Gastrointestinal Bleeding in the Emergency Service

Monday, Nov. 28 12:15PM - 12:45PM Room: ER Community, Learning Center Station #1

# Participants

Alfonso Martin Diaz, BMedSc, San Sebastian De Los Reyes, Spain (*Presenter*) Nothing to Disclose Lucia Fernandez Rodriguez, BMBS, Madrid, Spain (*Abstract Co-Author*) Nothing to Disclose Lorena F. Rodriguez-Gijon, MD, Madrid, Spain (*Abstract Co-Author*) Nothing to Disclose Milagros Marti De Gracia, MD, Madrid, Spain (*Abstract Co-Author*) Nothing to Disclose Alberto Borobia, Madrid, Spain (*Abstract Co-Author*) Nothing to Disclose Aurea Diez Tascon, MD, Madrid, Spain (*Abstract Co-Author*) Nothing to Disclose Jose Maria Artigas, Zaragoza, Spain (*Abstract Co-Author*) Nothing to Disclose

#### PURPOSE

To evaluate the influence of multidetector CTA findings in therapeutic management of patients with ALIB.

# METHOD AND MATERIALS

Retrospective observational study that includes patients with ALIB signs in the Emergency Service of a tertiary Hospital, from October 2009 to October 2013. Adults with rectal bleeding/ hematochezia (anorectal source excluded) or patients with melena and negative upper endoscopy are included. A triphasic CT examination was performed.Studied variables: demographics, nature, source and etiology of bleeding, and therapeutic procedure.Descriptive results are expressed as absolute frequencies and percentages. Univariate analysis (chi-square and student-T, or their non parametric equivalent) was performed to evaluate differences in variables between patients with and without active bleeding. Statistic software IBM SPSS Statistic v.20 was used.This study has been approved by Etical Comitee of Clinical Investigation from La Paz Universitary Hospital.

# RESULTS

In this period of time 173 CTA were performed in patients with ALIB signs. 30 of them were excluded because of insufficient information. Final analysis was made over 143 patients (68 women; 75 men), mean age 72,6 years (SD 19,6). CTA indicated bleeding lesion in 121 patients (84,6%) and showed active bleeding in 48 (33,6%), 43 arterial and 5 venous source.32 patients (66,7%) from the group with active bleeding required immediate therapeutic procedure (8 angiography, 17 endoscopy and 7 surgery) versus 5,3% in patients without demonstrated active bleeding(p<0,001).

#### CONCLUSION

Presence of active bleeding on CTA is an independent factor in the therapeutic decision-making.

## **CLINICAL RELEVANCE/APPLICATION**

CT angiography has become the image modality of chice for the management of patients with acute lower gastrointestinal bleeding in Emergency Service.

Variability in Emergency Department Utilization of Lumbar spine MRI for Evaluation of Low Back Pain: How Much Inappropriate Imaging is Being Done, and for What Reasons

Monday, Nov. 28 12:15PM - 12:45PM Room: ER Community, Learning Center Station #2

# Participants

Travis Smith, BS,MS, Hershey, PA (*Presenter*) Nothing to Disclose Michael A. Bruno, MD, Hershey, PA (*Abstract Co-Author*) Nothing to Disclose Timothy J. Mosher, MD, Hershey, PA (*Abstract Co-Author*) Research Consultant, Medical Metrics, Inc Stockholder, Johnson & Johnson

#### PURPOSE

Managing the appropriate use of advanced medical imaging is both an essential element and a significant challenge for radiologists seeking to optimizing value in imaging. The high value for patients of appropriately utilized imaging services is readily apparent; however no value is added when imaging is chosen inappropriately. Determining appropriate uses of Magnetic Resonance Imaging (MRI) for evaluation of patients with low back pain is under review by several agencies, based on evidence of comparative effectiveness and as an opportunity to increase value of clinical care. The National Quality Forum (NQF) currently has two quality measures under consideration addressing imaging of patients with low back pain; NQF measure number 0052 "Use of Imaging Studies for Low Back Pain", and NQF measure number 0514 MRI Lumbar Spine for Low Back Pain.

#### **METHOD AND MATERIALS**

A total of 233 MRI examinations of the lumbar spine were performed on patients seen in our ED in CY 2014, of which 63 were requested for evaluation of low back pain and another 76 were listed as "other." We scored these studies via a detailed manual audit of the EMR in order to assess the level of appropriate utilization based on the National Quality Forum (QPS) Measure 0514. Secondarily, we have attempted to identify factors that drive inappropriate ED utilization of lumbar spine MRI for patients with low back pain, testing the hypotheses that (1) there is inappropriate use of the ED specifically for the purpose of circumventing outpatient MRI utilization controls and (2) that there is significant self-referral of patients to ED in order to expedite their care, i.e., to "jump the queue."

#### RESULTS

Of the 233 examinations, 41 (17.6%) were considered to be inappropriate based on our standard. A significant fraction of these appear to represent misuse of the Emergency Department either to circumvent outpatient utilization controls or to expedite a scheduled outpatient study .

#### CONCLUSION

While most utilization of MRI in the Emergency Setting was appropriate, a significant fraction of patients appear to be misusing the ED to circumvent utilization controls or wait times for routine outpatient care.

### **CLINICAL RELEVANCE/APPLICATION**

This study is clinically relevant in that it evaluates the use of evidence-based medicine vs. other factors in the utilization of advanced medical imaging in the ED setting.

Very Affordable Immersion Pump for Post Mortem CT Angiography in Forensic Pathology: First 10 Cases. The Results Were Comparable, In That No Notable Differences Remained

Monday, Nov. 28 12:15PM - 12:45PM Room: ER Community, Learning Center Station #3

# Participants

Wolf Schweitzer, MD, Zuerich, Switzerland (*Presenter*) Nothing to Disclose Patricia M. Flach, MD, Zurich, Switzerland (*Abstract Co-Author*) Nothing to Disclose Michael J. Thali, MD, Zurich, Switzerland (*Abstract Co-Author*) Nothing to Disclose Dominic Gascho, Zurich, Switzerland (*Abstract Co-Author*) Nothing to Disclose Stamatios Stamou, MD, Zurich, Switzerland (*Abstract Co-Author*) Nothing to Disclose

# PURPOSE

About ten years after the usage of roller pumps for post mortem CT angiography was introduced into forensic pathology, it remains an open question why that relatively expensive pump mechanism (costing around 1000 USD for a used old heart lung machine to 80 000 USD for dedicated top of the line post mortem equipment) is actually necessary for post mortem CT angiography (PMCTA).Roller pumps make sense for non-Newtonian fluids like blood, where also mechanical hemolysis is a factor. In PMCTA, however watery or oily liquid is pumped into the vascular system of a body.After we established in a feasibility study that a simple immersion pump (priced around 15-20 USD) can be calibrated to obtain a linear voltage - flowrate relationship for the contrast agent solution used, and that vascular filling compared to a roller pump is basically the same, we present the results of the first ten cases in this talk.

# METHOD AND MATERIALS

Cantonal ethics review board waived responsibility (retrospective anonymized data usage).10 cases from forensic pathology caseload were selected where PMCT angiography (PMCTA) was seen as relevant to the case. 10 control cases examined with a conventional heart lung machine roller pump were used as comparison. Both arterial and venous sides were filled from a femoral access.Immersion pump: a Barwig model 0444 pump (max. 10L/min) was used (required PMCTA flow rate 0,2 - 0,8L/min).Roller pump: Stoeckert Shiley heart lung machine (max. 10L/min) was employed.PMCT / PMCTA: Dual source / energy CT scanner (Somatom Flash Definition, Siemens, Germany) was used (100 kVp tube voltage, automatic dose modulation).

#### RESULTS

Vascular filling was compared related to large vessels, coronary arteries, neck and head arteries, extremity arteries and on the same level, veins. Figure (IP: immersion pump: HLM: heart lung machine).

#### CONCLUSION

With a very low fraction of the cost, forensic pathology may be supplemented with high quality PMCTA when using a cheap immersion pump.

### **CLINICAL RELEVANCE/APPLICATION**

To be able to perform a post mortem CT angiography with very affordable equipment means that a parametrized method can be validated and employed in far more institutes than when very expensive equipment is used.

# ER211-SD-MOA4

## Absent Secondary Signs of Appendicitis When the Appendix is Not Visualized

Monday, Nov. 28 12:15PM - 12:45PM Room: ER Community, Learning Center Station #4

#### **Participants**

Vivek Patel, MD, New Haven, CT (*Abstract Co-Author*) Nothing to Disclose Aditi Vyas, MD, Norwalk, CT (*Abstract Co-Author*) Nothing to Disclose Saad Hussain, MD, New Haven, CT (*Presenter*) Nothing to Disclose Mahan Mathur, MD, Boston, MA (*Abstract Co-Author*) Nothing to Disclose Mike Spektor, MD, New Haven, CT (*Abstract Co-Author*) Nothing to Disclose

#### PURPOSE

The purpose of this study is to determine the negative predictive value (NPV) of the sonographic secondary signs of appendicitis when the appendix is not visualized. The secondary signs of appendicitis seen on ultrasound (US) include free fluid, hyperemia, lymphadenopathy, and phlegmon formation.

### **METHOD AND MATERIALS**

A retrospective review was completed looking for ultrasound images and reports that did not visualize the appendix in its entirety and also specifically stated that no secondary signs of appendicitis were visualized. The review spans 2013-2015. 130 studies were found meeting the inclusion criteria.

### RESULTS

Of the 130 total studies, 95 did not have imaging follow up or surgery for appendicitis. Either the ultrasound revealed an alternate diagnosis (example: mesenteric adenitis) or the patient was discharged with an alternate clinical diagnosis (example: constipation). 35 studies had follow up imaging with CT (31), MRI (2) or US (2). Of the 31 follow up CTs, 4 did not visualize the appendix (and the patients were discharged) and the remaining 27 revealed normal appendices. The 2 MRI examinations showed normal appendices and the patients were discharged. One repeat ultrasound was negative and the patient was discharged. The other repeat ultrasound was positive and the patient was taken to surgery and had pathology proven appendicitis. The negative predictive value for absent secondary signs of appendicitis when the appendix is not visualized is 97%. CT, MRI, and repeat US that visualized a negative appendix were considered true negatives.

# CONCLUSION

When the appendix is not visualized clinicians are often left to make a decision on whether or not to subject the patient (often pediatric) to ionizing radiation (CT), a lengthy MRI or a repeat US. It is important that radiologists and technologists look for the secondary signs of appendicitis when the appendix is not visualized. The radiologist should specifically mention the lack of secondary signs when appropriate. Based on the findings of this study, such a statement carries a high NPV. Armed with such information, the clinicians will be better suited in making the difficult decision in regards to further imaging or intervention.

#### **CLINICAL RELEVANCE/APPLICATION**

Secondary signs of appendicitis carry a high negative predictive value and should be evaluated for when the appendix is not visualized on ultrasound.

# ER212-SD-MOA5

## Epiploic Appendagitis is Associated with Peritoneal Inflammation and Visceral Obesity

Monday, Nov. 28 12:15PM - 12:45PM Room: ER Community, Learning Center Station #5

#### **Participants**

James P. Nugent, Vancouver, BC (*Presenter*) Nothing to Disclose Hugue A. Ouellette, MD, Vancouver, BC (*Abstract Co-Author*) Nothing to Disclose D. P. O'Leary, PhD, Limerick, Ireland (*Abstract Co-Author*) Nothing to Disclose Savvas Nicolaou, MD, Vancouver, BC (*Abstract Co-Author*) Institutional research agreement, Siemens AG Patrick D. McLaughlin, FFRRCSI, Vancouver, BC (*Abstract Co-Author*) Speaker, Siemens AG

#### PURPOSE

The location, size and coexisting local inflammatory findings in acute epiploic appendagitis have not been reported outside of isolated case reports. The association between EA and increased body mass index is controversial and disputed in the radiological and surgical literature. Our aim is to investigate if abdominal adipose volume (AAV), visceral adipose area (VAA) and subcutaneous adipose area (SAA) quantified by CT scans is higher in EA patients than matched controls. We also report the location, size and frequency of coexisting local inflammatory findings in a series of patients with acute epiploic appendagitis.

#### **METHOD AND MATERIALS**

Consecutive patients with an imaging diagnosis of EA scanned between January 2009 and June 2014 were selected for inclusion (n = 100). 100 consecutive patients imaged with abdominal CT for non-EA related acute abdominal pain were selected as controls. OsiriX v.5.5.2 (Pixmeo, Geneva, Switzerland) was used to retrospectively quantify abdominal adipose tissue volume and crosssectional area using Hounsfield unit threshold based semi-automated segmentation between -50 HU and -180 HU. The site, size and severity of inflammation of the involved appendage was also recorded.

#### RESULTS

EA had a male sex predilection, with 67% of EA versus 41% of acute abdominal cases (p = 0.0002). EA patients had 34% greater AAV, 197% greater VAA, and 135% greater SAA than the control subjects (p < 0.0001). The inflamed appendage was found in the sigmoid colon in 49% of cases, descending colon in 23% and right colon in 19%. Peritoneal thickening was a frequently reported associated sign of inflammation found in 76% of cases. Bowel wall thickening was common (47%) and diverticulosis co-existed incidentally in 28% of cases.

### CONCLUSION

VAA was almost 200% larger in patients with EA as compared with control subjects. Peritoneal thickening was a frequently reported associated sign of inflammation found in 76% of cases. Inflammation of the parietal peritoneum may contribute to the clinical presentation with acute pain.

#### **CLINICAL RELEVANCE/APPLICATION**

The association between EA and increased body mass index is controversial and disputed in radiological and surgical literature. Our study finds that visceral adipose area is almost 200% higher in EA.

# GI108-ED-MOA9

Cross-Sectional Imaging in Celiac Disease: Uncomplicated, Refractory, Enteropathy-Associated Lymphoma and Adenocarcinoma

Monday, Nov. 28 12:15PM - 12:45PM Room: GI Community, Learning Center Station #9

#### Awards

#### **Identified for RadioGraphics**

#### **Participants**

Badr Al-Bawardy, MD, Rochester, MN (*Presenter*) Nothing to Disclose John M. Barlow, MD, Rochester, MN (*Abstract Co-Author*) Nothing to Disclose Rogerio Vasconcelos, MD, Rochester, MN (*Abstract Co-Author*) Nothing to Disclose Sarasa T. Kim, Rochester, MN (*Abstract Co-Author*) Nothing to Disclose David Bruining, MD, Rochester, MN (*Abstract Co-Author*) Research Grant, Given Imaging Ltd Consultant, Bracco Group Stephanie Hansel, MD, Rochester, MN (*Abstract Co-Author*) Research support, Given Imaging Ltd Advisory Board, Medtronic, Inc Shannon P. Sheedy, MD, Rochester, MN (*Abstract Co-Author*) Nothing to Disclose Jeff L. Fidler, MD, Rochester, MN (*Abstract Co-Author*) Nothing to Disclose Joel G. Fletcher, MD, Rochester, MN (*Abstract Co-Author*) Grant, Siemens AG; ;

# **TEACHING POINTS**

1.Celiac disease (CD) affects 1% of the US population, and diagnosis is often delayed.2.CT/MR enterography (CT/MRE) of CD show distinctive intestinal and extra-intestinal features that facilitate diagnosis.3.CT/MRE are used to detect complications such as type I/type II refractory celiac disease (RCD), ulcerative jejunitis, enteropathy-associated lymphoma (EATL) and small bowel adenocarcinoma (SBA).

# TABLE OF CONTENTS/OUTLINE

Diagnosis: Non-specific sx: GI (diarrhea, bloating, weight loss) and extraintestinal (neuropsychiatric sx, arthritis, Fe deficiency, metabolic bone dz, infertility) Implications/limitations of TTG IgA and permissive genes (HLA DQ2/DQ8) Endoscopy - fold flattening, fissuring, scalloping and mosaic appearance. Histology: partial-total villous atrophy, intraepithelial lymphocytosis, and crypt hyperplasia.CT/MRE findings (examples): Intestinal - decreased number of duodenal and jejunal folds, duodenal edema, increased number of ileal folds, excessive fluid, intussusception Extraintestinal - Hyposplenism, mesenteric vascular engorgement, and lymph node enlargement.CD complications on CTE/MRE: Ulcerative jejunitis; small bowel dilation and increased small bowel thickness in RCD Refractory CD: EATL > SBA, but rare EATL patterns – aneurysmal, infiltrative, annular, gastricCase study quiz

**Pseudocirrhosis: Pathogenesis and Imaging Features** 

Monday, Nov. 28 12:15PM - 12:45PM Room: GI Community, Learning Center Station #10

#### Participants

Christopher Czaplicki, Phoenix, AZ (*Abstract Co-Author*) Nothing to Disclose Christine O. Menias, MD, Chicago, IL (*Presenter*) Nothing to Disclose Venkata S. Katabathina, MD, San Antonio, TX (*Abstract Co-Author*) Nothing to Disclose Anil K. Dasyam, MD, Pittsburgh, PA (*Abstract Co-Author*) Book contract, Reed Elsevier Akram M. Shaaban, MBBCh, Salt Lake City, UT (*Abstract Co-Author*) Nothing to Disclose Antonio Luna, MD, Jaen, Spain (*Abstract Co-Author*) Nothing to Disclose Khaled M. Elsayes, MD, Ann Arbor, MI (*Abstract Co-Author*) Nothing to Disclose Nina Karlin, MD, Phoenix, AZ (*Abstract Co-Author*) Nothing to Disclose Abimbola Adike, MD, Phoenix, AZ (*Abstract Co-Author*) Nothing to Disclose Elizabeth Carey, MD, Phoenix, AZ (*Abstract Co-Author*) Nothing to Disclose

#### **TEACHING POINTS**

1) Discuss the pathophysiology of Pseudocirrhosis- Due to the regression and response to chemotherapy of hepatic metastasis and as the progression with fibrosis surrounding the infiltrating hepatic tumorsA) Response of hepatic tumors to chemotherapy resulting in scarring and capsular retractionB) Fibrosis surrounding infiltrating hepatic metastatic massesC) Nodular regenerative hyperplasia in response to ischemia from chemotherapy-induced hepatic injuryD) Sinusoidal obstruction with venous obstruction as a result of chemotherapy 2) Review the imaging Features of Pseudocirrhosis on CT and MR

# TABLE OF CONTENTS/OUTLINE

Pseudocirrhosis is an imaging diagnosis used to describe the development of diffuse hepatic nodularity in the setting of hepatic metastases successfully treated with chemotherapy. While it has been described in multiple types of cancer, it is most common in patients with breast cancer. It is important to recognize pseudocirrhosis early as it can be associated with complications of portal hypertension, rapid progression to liver failure and increased morbidity in patients with metastatic cancer. This review will discuss the imaging features of this important but under recognized entity on CT and MR.

#### **Honored Educators**

Presenters or authors on this event have been recognized as RSNA Honored Educators for participating in multiple qualifying educational activities. Honored Educators are invested in furthering the profession of radiology by delivering high-quality educational content in their field of study. Learn how you can become an honored educator by visiting the website at: https://www.rsna.org/Honored-Educator-Award/

Christine O. Menias, MD - 2013 Honored Educator Christine O. Menias, MD - 2014 Honored Educator Christine O. Menias, MD - 2015 Honored Educator Christine O. Menias, MD - 2016 Honored Educator Venkata S. Katabathina, MD - 2012 Honored Educator Khaled M. Elsayes, MD - 2014 Honored Educator Akram M. Shaaban, MBBCh - 2015 Honored Educator Akram M. Shaaban, MBBCh - 2016 Honored Educator

### GI355-SD-MOA1

Usefulness of Double Frequency MR Elastography for Assessment of the Necroinflammation on Liver Stiffness Measurements

Monday, Nov. 28 12:15PM - 12:45PM Room: GI Community, Learning Center Station #1

# Participants

Minori Onoda, PhD,RT, Kanazawa, Japan (*Presenter*) Nothing to Disclose Tomoko Hyodo, MD, Osaka-Sayama, Japan (*Abstract Co-Author*) Nothing to Disclose Takamichi Murakami, MD, PhD, Osakasayama, Japan (*Abstract Co-Author*) Nothing to Disclose Masakatsu Tsurusaki, MD, PhD, Osaka, Japan (*Abstract Co-Author*) Nothing to Disclose Takahiro Sakamoto, Osakasayama, Japan (*Abstract Co-Author*) Nothing to Disclose Tosiaki Miyati, PhD, Kanazawa, Japan (*Abstract Co-Author*) Nothing to Disclose

#### PURPOSE

The measurement of liver stiffness with magnetic resonance elastography (MRE) is affected by the liver viscosity which can be found by testing different vibration frequency settings. We aimed to evaluate the utility of double vibration frequency MRE method in estimation of liver fibrosis and necroinflammation.

### **METHOD AND MATERIALS**

Thirty patients underwent MRE with a 1.5-T MR system and liver biopsy for liver investigation. We performed MRE with two different driver frequencies of 60 and 80 Hz to measure the liver stiffness. The frequencies of motion encoding gradient were set as the same as driver frequencies (60, 80 Hz) to optimize MR pulse sequences for MRE. We defined the difference of liver stiffness values as  $\Delta G$  (G80Hz - G60Hz) to compare with pathological findings of liver fibrosis (stages F0-4) and necroinflammation (grades A0-3). Statistical analysis included Spearman's rank correlation test, followed by ROC analysis and AUC calculation when significant correlation exists. A P value <.05 was considered statistical significant.

#### RESULTS

The mean liver stiffness values with both 60 Hz and 80 Hz increased as fibrosis stages and necroinflammation grades progressed. For all patients, the measurements of liver stiffness by using vibration frequency of 80 Hz showed higher values than those of 60 Hz.  $\Delta$ G showed moderate positive correlation with liver necroinflammation grades (r=0.68, P<0.01). No significant correlation was observed between  $\Delta$ G and pathological fibrosis stages (r=0.30, P=0.11). In ROC analyses, the optimal cutoff values of  $\Delta$ G were 0.36 for  $\geq$ A1 (AUC 0.80, sensitivity 79%, specificity 100%), 0.90 for  $\geq$ A2 (AUC 0.81, sensitivity 55%, specificity 100%), and 1.58 for  $\geq$ A3 (AUC 0.96, sensitivity 100%, specificity 83 %).

#### CONCLUSION

 $\Delta G$  increased as necroinflammation grades progressed, but not as fibrosis stages.  $\Delta G$  may be useful index for evaluating the liver necroinflammation on liver stiffness measurements by MRE.

### **CLINICAL RELEVANCE/APPLICATION**

The double vibration frequency MRE method has a potential to evaluate the liver necroinflammation without biopsy, and may be useful to avoid the overestimation of liver fibrosis using MRE.

# GI356-SD-MOA2

Amide Proton Transfer Imaging to Predict Tumor Response after Preoperative Chemotherapy in Locally Advanced Rectal Cancer

Monday, Nov. 28 12:15PM - 12:45PM Room: GI Community, Learning Center Station #2

# Participants

Akihiro Nishie, MD, Fukuoka, Japan (*Presenter*) Nothing to Disclose Yoshiki Asayama, MD, Fukuoka, Japan (*Abstract Co-Author*) Nothing to Disclose Kousei Ishigami, MD, Iowa City, IA (*Abstract Co-Author*) Nothing to Disclose Yasuhiro Ushijima, MD, Fukuoka, Japan (*Abstract Co-Author*) Nothing to Disclose Yukihisa Takayama, MD, Fukuoka, Japan (*Abstract Co-Author*) Nothing to Disclose Yukihisa Takayama, MD, Fukuoka, Japan (*Abstract Co-Author*) Research Grant, FUJIFILM Holdings Corporation Hiroshi Honda, MD, Fukuoka, Japan (*Abstract Co-Author*) Nothing to Disclose Daisuke Okamoto, MD, Fukuoka City, Japan (*Abstract Co-Author*) Nothing to Disclose Nobuhiro Fujita, MD, PhD, Fukuoka, Japan (*Abstract Co-Author*) Nothing to Disclose Osamu Togao, MD, PhD, Fukuoka, Japan (*Abstract Co-Author*) Nothing to Disclose Koji Sagiyama, MD, Fukuoka, Japan (*Abstract Co-Author*) Nothing to Disclose Daisuke Tsurumaru, MD, Fukuoka, Japan (*Abstract Co-Author*) Nothing to Disclose Eiji Oki, Fukuoka, Japan (*Abstract Co-Author*) Nothing to Disclose Eiji Oki, Fukuoka, Japan (*Abstract Co-Author*) Nothing to Disclose Eiji Oki, Fukuoka, Japan (*Abstract Co-Author*) Nothing to Disclose Tatsuya Manabe, Fukuoka, Japan (*Abstract Co-Author*) Nothing to Disclose Jochen Keupp, PhD, Hamburg, Germany (*Abstract Co-Author*) Employee, Koninklijke Philips NV

#### PURPOSE

To elucidate if amide proton transfer (APT) imaging can predict tumor response after preoperative chemotherapy in locally advanced rectal cancer

### **METHOD AND MATERIALS**

A total of 17 patients with locally advanced rectal cancer who underwent MR examination including APT imaging and preoperative chemotherapy (at least two courses) were enrolled. APT imaging was scanned with single-shot 2D TSE-DRIVE on a 3T clinical scanner using a 32-channel coil and 2-channel parallel transmission. APT signal was defined as MTR asymmetry (MTRasym) at the offset of 3.5 ppm: {Ssat(-3.5 ppm)-Ssat(+3.5 ppm)}/S0(control). APT map was generated and a region-of-interest was carefully placed in each rectal cancer to measure APT signal (%). Each tumor resected was histologically evaluated for the degree of degeneration and necrosis and was divided into the five Grades (0, none; 1a, less than 1/3; 1b, 1/3 to 2/3; 2, more than 2/3; 3, all). The mean APT signal was compared between Grade 0/1a (Low response group) and Grade 1b/2/3 (High response group) using a Student's t-test. Diagnostic performance of APT signal, as well as apparent diffusion coefficient (ADC) obtained in diffusion-weighted imaging, for predicting tumor response was evaluated using receiver operating characteristics curve.

## RESULTS

The mean APT signal of Low response group (n=12; 3.05+/-1.61%) was significantly higher than that of High response group (n=5; 1.14+/-1.13%)(p=0.029). There was no significant difference in ADC between Low and High response groups. The area under curve for predicting tumor response using APT signal was 0.867. When 2.75% or less was an indicator of high tumor response, sensitivity, specificity and accuracy of APT signal were 100%, 75% and 82.4%, respectively.

# CONCLUSION

APT imaging can predict tumor response after preoperative chemotherapy in locally advanced rectal cancer. For predicting tumor response APT signal is superior to ADC.

# **CLINICAL RELEVANCE/APPLICATION**

APT imaging contributes to the selection of a therapeutic strategy in locally advanced rectal cancer.

Comparison Study on the Accuracy of Detecting Colorectal Cancer Lymph Nodes Metastasis with Arterial Phase Dual-energy CT Spectral Curve and the Morphological Findings

Monday, Nov. 28 12:15PM - 12:45PM Room: GI Community, Learning Center Station #4

## Participants

Xuejun Yang, kunming, China (*Abstract Co-Author*) Nothing to Disclose Wei Zhao, Kunming, China (*Abstract Co-Author*) Nothing to Disclose Jing Lei, Kunming, China (*Abstract Co-Author*) Nothing to Disclose Han Dan, PhD, MD, Kunming, China (*Abstract Co-Author*) Nothing to Disclose Yaying Yang, Kunming, China (*Presenter*) Nothing to Disclose

# PURPOSE

To explore the accuracy of arterial phase dual-energy CT spectral curve and the morphological findings in detecting the metastatic lymph nodes in colorectal cancer .

### **METHOD AND MATERIALS**

22 patients with pathologically confirmed colorectal cancer had a total of 40 enlarged lymph nodes in the pelvic region underwent dual energy CT scan, We measured the size of the lymph nodes on CT images, and the CT value in non-enhanced and arterial phase CT scan; We also computed short-long diameter ratio and enhancement value of lymph node (lymph node CT value in arterial phase - CT value in plain scan). We observed the change trend of the spectrum curve and compared the diagnostic accuracy in detecting colorectal cancer lymph nodes metastasis.

### RESULTS

In the 40 lymph nodes, 17 lymph nodes were metastatic, while reactive hyperplasia was seen in 23 lymph nodes. Short-long diameter ratio and the enhancement CT value in the diagnosis of lymph node metastasis had weak consistency with the pathological results (Kappa value=0.100 and 0.016, repsectively). The sensitivity of 64.7%, 35.3%, the specificity of 64.7%, 68.2%, the area under the ROC curve were 0.434, 0.501 for short-long diameter ratio and the enhancement CT value in the diagnosis of lymph node metastasis, respectively. Dual-energy CT spectral curve had strong consistency with the pathological results (Kappa value=0.899) and higher sensitivity of 94.1%, the specificity of 95.5%, and area under the ROC curve (0.949) compared with morphological findings.

# CONCLUSION

The spectrum curve of dual-energy CT had higher sensitivity and specificity than the conventional morphology findings in diagnosis of colorectal cancer lymph nodes metastasis.

## **CLINICAL RELEVANCE/APPLICATION**

The arterial phase dual-energy CT spectral curve had higher accuracy than the morphological findings in detecting the metastatic lymph nodes in colorectal cancer .

## Imaging Evaluation of Common Duct Size: Comparison between CT and US Measurements

Monday, Nov. 28 12:15PM - 12:45PM Room: GI Community, Learning Center Station #5

#### **Participants**

Tatum A. Mcarthur, MD, Aurora, CO (*Presenter*) Nothing to Disclose Desmin Milner, MD, Birmingham, AL (*Abstract Co-Author*) Nothing to Disclose Argha Chatterjee, MBBS, MD, Chicago, IL (*Abstract Co-Author*) Nothing to Disclose Bradford Jackson, Birmingham, AL (*Abstract Co-Author*) Nothing to Disclose Mark E. Lockhart, MD, Birmingham, AL (*Abstract Co-Author*) Author, Oxford University Press

# PURPOSE

To compare the common duct (CD) diameter by CT and ultrasound (US) in patients undergoing both studies within 48 hours of each other.

## METHOD AND MATERIALS

This IRB-approved, HIPAA-compliant retrospective study compared the CD diameter measured by both CT and US performed within a 48-hour period in 342 patients (ages 24 - 88) from 1/1/2004 - 4/1/2015. 132 patients were excluded secondary to complex biliary surgery, acute cholecystectomy, liver transplant, CD stent, hepatobiliary malignancy, interval papillotomy, irretrievable images, and/or nonvisualization of the CD. In the remaining 210 patients, the CD was measured at the porta hepatis on US and CT in randomized order by a blinded board-certified radiologist. CT readings were performed 6 months after US readings to limit recall bias. Presence of CD wall thickening was also recorded. 79% (n=166) of the CT exams were contrast-enhanced. Distributional characteristics are presented as mean and standard deviation (SD). Bland-Altman analysis was used to estimate the bias and 95% limits of agreement between modalities. Paired T-tests were used to assess the statistical significance of the difference between modalities.

# RESULTS

The study population consisted of 113 women and 97 men with a mean age of 53.8 (+/-15.3) years. Mean CD diameter by CT measures  $1.01\pm2.2$ mm more than US [p<0.0001]. The 95% confidence limit of agreement between the two modalities suggests CT measurements were 3.39 mm less to 5.42 mm more than that of US.

# CONCLUSION

In our study, CT overestimated the CD diameter compared to US, and we observed a fixed bias of 1.01 mm.

# **CLINICAL RELEVANCE/APPLICATION**

US is considered the reference standard to evaluate CD size. In our study, CT does overestimate the CD diameter when compared to US, but not enough to typically change management, and US is not necessary to confirm duct size.

# GI360-SD-MOA6

Texture based Classification and Correlation of Non-alcoholic Fatty Liver Disease Activity Score (NAS) using Gabor Wavelet Filters

Monday, Nov. 28 12:15PM - 12:45PM Room: GI Community, Learning Center Station #6

# Participants

Rohit Badida, MS,BEng, Tempe, AZ (*Abstract Co-Author*) Nothing to Disclose Christine M. Zwart, PhD, Scottsdale, AZ (*Abstract Co-Author*) Nothing to Disclose Alvin C. Silva, MD, Scottsdale, AZ (*Presenter*) Nothing to Disclose

### PURPOSE

Our main objective was to analyze texture features extracted from CT images of NAFLD patients and correlate with NAS score. Current non-invasive methods have limitations and cannot replace/assist liver biopsy for classifying Non-Alcoholic SteatoHepatitis (NASH) from fatty liver not diagnostic of NASH (steatosis). NAS scores of 0-3 occurred in cases largely considered not diagnostic of NASH, whereas scores of 5-8 were largely considered diagnostic of NASH (PMID:15915461).

#### **METHOD AND MATERIALS**

37 histologically diagnosed patients with NAFLD and their respective NAS scores were considered for the study (20 patients with NAS 5-8 and 17 with NAS 0-3). For extracting and analyzing textures, venous phase slices of contrast enhanced CT images with the largest cross-sectional areas were selected followed by manual segmentation of region of interest (ROI). A MATLAB-based tool was developed and utilized for extracting ROI, specifically avoiding larger blood vessels. This was followed by applying Gabor wavelet filters for feature extraction. Support Vector Machine was used to classify the extracted Gabor features and receiver operating characteristics curve (AUROC) was used to calculate the performance of the classifier along with k-fold cross validation.

#### RESULTS

An AUC (Area under curve) of 0.88 was obtained for separating NASH versus fatty liver without NASH. A 5-fold cross validation on 37 images (single ROI per patient) yielded a misclassification rate of 0.25 indicating excellent performance of the classifier.

## CONCLUSION

Currently, there is no robustly validated CT technique for discriminating the spectrum of NAFLD. However, our results indicate that Gabor filters have the ability to classify fatty liver texture patterns for replacing/assisting NAS score. This also demonstrates that texture features can be correlated to NAS score interpretation of NASH disease for a score of 5-8 and fatty liver without NASH for a score of 0-3.

# **CLINICAL RELEVANCE/APPLICATION**

A noninvasive application applied to routine CT images that can differentiate steatosis from NASH in lieu or as a complement to biopsy can have meaningful impact on the screening & management of this increasingly prevalent disease.

Quantitative Prediction of Treatment Effect of Transarterial Chemoembolization using Drug-eluting Bead for Hepatocellular Carcinoma with use of Preoperative Dual-phase Contrast-enhanced CT

Monday, Nov. 28 12:15PM - 12:45PM Room: GI Community, Learning Center Station #7

# Participants

Keisuke Todoroki, Matsumoto, Japan (*Presenter*) Nothing to Disclose Akira Yamada, MD, Matsumoto, Japan (*Abstract Co-Author*) Nothing to Disclose Takanori Aonuma, Nagano, Japan (*Abstract Co-Author*) Nothing to Disclose Fumihito Ichinohe, Matsumoto, Japan (*Abstract Co-Author*) Nothing to Disclose Kazuki Oyama, matsumoto-shi, Japan (*Abstract Co-Author*) Nothing to Disclose Mana Nakamura, Matsumoto, Japan (*Abstract Co-Author*) Nothing to Disclose Yasunari Fujinaga, MD, Matsumoto, Japan (*Abstract Co-Author*) Nothing to Disclose Masumi Kadoya, MD, Matsumoto, Japan (*Abstract Co-Author*) Nothing to Disclose

#### PURPOSE

To clarify the possibility predicting treatment effect of transarterial chemoembolization using drug-eluting bead (DEB-TACE) for hepatocellular carcinoma (HCC) with use of quantitative perfusion parameters obtained from preoperative dual-phase contrast-enhanced CT (DPCE-CT).

### METHOD AND MATERIALS

Consecutive 16 patients with radiologically diagnosed HCC by DPCE-CT who underwent DEB-TACE were included in this retrospective study. Arterial and portal venous input functions were estimated from CT values of 7 vessels (left atrium, abdominal aorta, right renal vein, superior mesenteric vein, inferior vena cava, splenic vein, and portal vein) using newly proposed dynamic phase index (DPI) technique. Perfusion parameters of the liver and HCC such as arterial and portal venous inflow velocity constant [K1a and K1p], arterial flow fraction [AF = K1a/(K1a + K1p)] were determined by compartment model analysis. Treatment effect was evaluated within 8 weeks after DEB-TACE using contrast-enhanced CT or MRI. Predictive performance to classify complete necrosis group and the others using these perfusion parameters and Naïve Bayes classifier was statistically analyzed.

#### RESULTS

In univariate analysis, significant differences between complete necrosis group and the others were seen in AF (P = 0.032) and K1p (P = 0.036) of the liver, difference of K1p (P = 0.045) and AF (P = 0.046) of HCC against the liver. The area under the receiver operating characteristic curve (AUROC) and its 95% confidence interval (95%CI) to classify complete necrosis group and the others using variable number of perfusion parameters and NBA were 0.850 (0.831, 0.868) using 1 parameter (AF of the liver), 0.931 (0.919, 0.943) using 2 features (K1a of the liver and difference of AF of HCC against the liver), respectively. No significant increase in AUROC was observed even if more than 2 parameters were used.

# CONCLUSION

Treatment effect of DEB-TACE for HCC can be predicted with use of quantitative perfusion parameters obtained from preoperative DPCE-CT using DPI technique and compartment model analysis.

# **CLINICAL RELEVANCE/APPLICATION**

Quantitative perfusion analysis of DPCE-CT using DPI technique will help determine the management of patients with HCC.

Diagnostic Value of Preoperative Abdominal CT Examination in Assessment of Quantitative Body Composition Analysis to Predict and Stratify Risk of Severe Pancreatic Fistula after Pancreatoduodenectomy

Monday, Nov. 28 12:15PM - 12:45PM Room: GI Community, Learning Center Station #8

# Participants

Cammillo R. Talei Franzesi, Milan, Italy (*Presenter*) Nothing to Disclose Davide Ippolito, MD, Monza, Italy (*Abstract Co-Author*) Nothing to Disclose Luca Riva, MD, Missaglia, Italy (*Abstract Co-Author*) Nothing to Disclose Davide Fior, MD, Monza, Italy (*Abstract Co-Author*) Nothing to Disclose Marta Sandini, MD, Monza, Italy (*Abstract Co-Author*) Nothing to Disclose Luca V. Gianotti, MD, Monza, Italy (*Abstract Co-Author*) Nothing to Disclose Sandro Sironi, MD, Monza, Italy (*Abstract Co-Author*) Nothing to Disclose

## PURPOSE

To assess whether measures of abdominal fat distribution, visceral density, and antropometric parameters obtained from computed tomography (CT) may predict postoperative pancreatic fistula (POPF) occurrence in patient who undergo to pancreatodudenectomy surgery.

## **METHOD AND MATERIALS**

We analyzed 117 patients who underwent pancreatoduodenectomy (PD) and had a preoperative CT scan staging. CT images were obtained either with 16- or 256- MDCT (Brilliance iCT; Philips), applying a multiphase acquisition protocol (unenhanced, arterial, portal venous and equilibrium phase). CT reconstruction of unenhanced upper abdomen were used to obtain measures of total fat volume (TFV), visceral fat volume (VFV), thickness of retro-renal fat, diameter of pancreatic duct and the density ratio of spleen and pancreas. The predictive ability of each parameter was investigated by receiver-operating characteristic (ROC) curves methodology and assessing optimal cutoff thresholds.

# RESULTS

The overall rate of clinically relevant (grades B and C of ISGPF classification) POPF was 20.5% (24/117 patients). Areas under ROCcurves showed that none of the parameters was per se significantly predictive. Patient with grade A or no POPF had lower median value of each CT parameters analyzed than the patients with grades B-C (i.e. VFV median value of 1800 cm3 vs 2702 cm3; TFV 4100 cm3 vs 5432 cm3; Wirsung diameter 4 mm vs 2 mm). Moreover the multivariate analysis revealed that a VFV>2334 cm3, TFV>4408 cm3, pancreas/spleen density ratio <0.707, and pancreatic duct diameter <5 mm were predictive of POPF. The risk of POPF progressively increased with the number of the CT parameters involved and age.

# CONCLUSION

The risk of occurrence of clinically relevant POPF may be predicted with relative accuracy by combining specific information obtained from preoperative CT such as TFV and VFV, pancreas/spleen density, pancreatic duct diameter, in combination with patient age. Even if it has been already suggested that obesity might be a handy predictor of complications after PD, the distribution of fat is more important than obesity and probably the amount and specific organ deposition of visceral fat plays a central role in this process.

### **CLINICAL RELEVANCE/APPLICATION**

The organ fat distribution analysis, obtained at preoperative abdominal CT scan examination, may offer important information on the risk of post-surgical pancreatic fistula occurrence.

# Evaluating the Performance of PI-RADS v2 in the Non-Academic Setting

Monday, Nov. 28 12:15PM - 12:45PM Room: GU/UR Community, Learning Center Station #1

#### **Participants**

Eric J. Jordan, MD, San Francisco, CA (*Abstract Co-Author*) Nothing to Disclose Charles E. Fiske, MD, Moraga, CA (*Abstract Co-Author*) Nothing to Disclose Spencer T. Lake, MD, San Francisco, CA (*Presenter*) Nothing to Disclose Ronald J. Zagoria, MD, San Francisco, CA (*Abstract Co-Author*) Nothing to Disclose Antonio C. Westphalen, MD, Mill Valley, CA (*Abstract Co-Author*) Scientific Advisory Board, 3DBiopsy LLC ; Research Grant, Verily Life Sciences LLC

# PURPOSE

To evaluate the utility of PI-RADS v2 to diagnose clinically significant prostate cancer (CS-PCa) with magnetic resonance ultrasound (MR/US) fusion guided prostate biopsies in the non-academic setting.

# METHOD AND MATERIALS

IRB approved retrospective analysis of men whom underwent prostate multiparametric MRI and subsequent MR/US fusion biopsies at a single non-academic center from 11/2014 - 3/2016. Indications for prostate MRI included elevated PSA, abnormal digital rectal exam and/or negative transrectal ultrasound biopsy. Prostate MRIs were performed on a 3-Tesla scanner with a surface body coil including T2, diffusion-weighted (b-values:10, 400, 800, 1200) and dynamic contrast enhancement sequences. The Prostate Imaging Reporting and Data System (PI-RADS) v2 scoring algorithm was utilized on all patients. MR/US fusion biopsies were performed in all cases with a suspicious lesion. Mixed effect logistic regression analyses were used to determine the ability of PIRADS v2 alone and combined with PSA density (PSAD) to predict CS-PCa (defined as Gleason score ≥7 per PIRADS v2 guidelines). Performances of PIRADS v2 and combined with PSA density (PSAD) were compared utilizing receiver-operating characteristic (ROC) curves derived from the logistic models.

## RESULTS

170 patients underwent prostate MRI with a total of 282 PI-RADS lesions. MR/US fusion diagnosed 71 CS-PCa. Of the remaining lesions, 168 were negative and 33 were Gleason score 3+3 prostate cancer. The overall PIRADS v2 score is a statistically significant predictor of CS-PCa (p<0.001). For each one-point increase in the overall PIRADS v2 score, the odds of having CS-PCa increases by 4.2 (95%CI=2.2-8.3). The area under the ROC curve for PI-RADS v2 to discriminate CS-PCa positive patients was 0.69 (95%CI = 0.63-0.76). PSAD was an independent predictor on the multivariate model (p=0.03), and the model that included PIRADS and PSAD revealed an area under the ROC of 0.76 (95%CI=0.69-0.82), statistically higher than that of PI-RADS v2 alone (p<0.001). The rate of CS-PCa was about twice higher in men with high PSAD ( $\geq 0.15$ ) compared to men with low PSAD (<0.15) when a PI-RADS 4 or 5 lesion was detected (p=0.005).

## CONCLUSION

PI-RADS v2 is a strong predictor of CS-PCa in the non-academic setting and can be further strengthened when utilized with PSAD.

## **CLINICAL RELEVANCE/APPLICATION**

PI-RADS v2 is a new scoring algorithm which appears applicable and fairly accurate in a non-academic center.

## GU211-SD-MOA2

Identifying a Large-Scale Radiomic Profiling Imaging Signature for non-Invasive, Computational Model Training Based Discrimination of Prostate Cancer Aggressiveness

Monday, Nov. 28 12:15PM - 12:45PM Room: GU/UR Community, Learning Center Station #2

# Participants

Philipp Kickingereder, Heidelberg, Germany (*Abstract Co-Author*) Nothing to Disclose Boris Hadaschik, Heidelberg, Germany (*Abstract Co-Author*) Nothing to Disclose Jan P. Radtke, Heidelberg, Germany (*Abstract Co-Author*) Nothing to Disclose Michael Gotz, Heidelberg, Germany (*Abstract Co-Author*) Nothing to Disclose Kathrin Wieczorek, Heidelberg, Germany (*Abstract Co-Author*) Nothing to Disclose Klaus Maier-Hein, Heidelberg, Germany (*Abstract Co-Author*) Nothing to Disclose Martin Bendszus, Heidelberg, Germany (*Abstract Co-Author*) Nothing to Disclose Matthias Roethke, MD, Heidelberg, Germany (*Abstract Co-Author*) Nothing to Disclose Matthias Roethke, MD, Heidelberg, Germany (*Abstract Co-Author*) Nothing to Disclose Heinz-Peter W. Schlemmer, MD, Heidelberg, Germany (*Abstract Co-Author*) Nothing to Disclose David Bonekamp, MD, PhD, Heidelberg, Germany (*Presenter*) Nothing to Disclose

#### PURPOSE

Prostate cancer (PC) is a leading cause of cancer-related morbidity and mortality in men, but its management hampered by diagnostic uncertainty leading to over- and undertreatment of disease. We study the potential of a large-scale radiomic approach to distinguish low- to intermediate risk PC (IrPC) (Gleason score (GS) $\leq$ 3+4 and pathological T-stage (pT) $\leq$ 2c) from clinically significant aggressive (aPC) PC ((GS) $\geq$ 4+3 and pT $\geq$ 3a).

### METHOD AND MATERIALS

Index lesions of 137 patients with with radical prostatectomy (RPE) – proven PCa were manually segmented on T2-weighted images and ADC maps. After intensity normalization, a total of 6095 quantitative radiomics features [including first-order, volume and shape features, texture features and features based on undecimated (UWT) and discrete (DWT) wavelet transforms] were automatically extracted and z-score transformed. We performed feature selection and model training with a penalized logistic regression (PLR) procedure to generate a sparse model with good prediction accuracy, while simultaneously promoting the grouping of strongly correlated predictors. The model prediction was compared to ADC metrics and PI-RADS (V1 and V2) scoring in its ability to predict the pathological assessment.

#### RESULTS

The final classifier incorporated 25 features and achieved differentiation of IrPC from aPC with ROC AUC of 95.9% and accuracy of 91.2% (sensitivity: 96.7%; specificity: 80.0%, PPV: 90.8% NPV: 92.3%), which was significantly better than ROC AUC of mean ADC (92.8%, p=0.049), median ADC (92.6%, p=0.040), 10th percentile of ADC (90.2%, p=0.010), PI-RADS version 1 (71.0%, p<0.001) and PI-RADS version 2 (70.0%, p<0.001).

# CONCLUSION

Good imaging-based discrimination accuracy between IrPC and aPC was achieved using a large scale radiomic signature in RPE proven PC, which performed significantly better than imaging assessment using classical ADC metrics or clinical assessment using PIRADS.

# **CLINICAL RELEVANCE/APPLICATION**

A trained computational model training based classifier may be able to support clinical assessment of PCa aggressiveness in the future.

## GU212-SD-MOA3

Hyperpolarized MRS/PET/Ultrasound Molecular Image Fusion for Improved Diagnosis and Guided Biopsy of Prostate Cancer

Monday, Nov. 28 12:15PM - 12:45PM Room: GU/UR Community, Learning Center Station #3

# Participants

Keerthi S. Valluru, MS, Stanford, CA (*Presenter*) Nothing to Disclose Jae Mo Park, PhD, Stanford, CA (*Abstract Co-Author*) Nothing to Disclose Sunitha Bachawal, PhD, Stanford, CA (*Abstract Co-Author*) Nothing to Disclose Changhao Liu, Stanford, CA (*Abstract Co-Author*) Nothing to Disclose Valentina Taviani, PhD, Stanford, CA (*Abstract Co-Author*) Nothing to Disclose Praveen Gulaka, PhD, Stanford, CA (*Abstract Co-Author*) Nothing to Disclose Yamil Saenz, Stanford, CA (*Abstract Co-Author*) Nothing to Disclose Stephen A. Felt, DVM, MPH, Stanford, CA (*Abstract Co-Author*) Nothing to Disclose Jose G. Vilches-Moure, DVM, PhD, Stanford, CA (*Abstract Co-Author*) Nothing to Disclose Bruce L. Daniel, MD, Stanford, CA (*Abstract Co-Author*) Research Grant, General Electric Company Zhen Cheng, PhD, Stanford, CA (*Abstract Co-Author*) Nothing to Disclose Daniel M. Spielman, PhD, Stanford, CA (*Abstract Co-Author*) Nothing to Disclose Juergen K. Willmann, MD, Stanford, CA (*Abstract Co-Author*) Nothing to Disclose Juergen K. Willmann, MD, Stanford, CA (*Abstract Co-Author*) Nothing to Disclose Juergen K. Willmann, MD, Stanford, CA (*Abstract Co-Author*) Nothing to Disclose Juergen K. Willmann, MD, Stanford, CA (*Abstract Co-Author*) Nothing to Disclose Juergen K. Willmann, MD, Stanford, CA (*Abstract Co-Author*) Nothing to Disclose Juergen K. Willmann, MD, Stanford, CA (*Abstract Co-Author*) Nothing to Disclose Juergen K. Willmann, MD, Stanford, CA (*Abstract Co-Author*) Research Consultant, Bracco Group; Research Grant, Siemens AG; Research Grant, Bracco Group; Research Grant, Koninklijke Philips NV; Research Grant, General Electric Company; Advisory Board, Lantheus Medical Imaging, Inc; Advisory Board, Bracco Group

#### PURPOSE

Blinded transrectal ultrasound (TRUS) biopsy can fail to identify prostate cancer (PCa) in 10-25% of patients [1]. Novel molecular imaging techniques such as Hyperpolarized 13C Magnetic Resonance Spectroscopy (HMRS) with pyruvate [2], PET imaging with 68Ga-NODAGA-RM1 [3], and ultrasound molecular imaging (USMI) with vascular endothelial growth factor receptor type-2 (VEGFR-2) targeted microbubbles (BR55, Bracco Suisse SA) [4] can facilitate improved cancer detection. In this study, we investigated the feasibility of real-time HMRS/PET/USMI fusion and TRUS biopsy in canine PCa in vivo.

## **METHOD AND MATERIALS**

60e6 Ace-1 cells [5] were orthotopically-transplanted in the prostate of immunosuppressed dogs (n=3, 10-12Kg). Two weeks later, simultaneous prostatic HMRS/PET/MRI was performed with 68Ga-NODAGA-RM1 (~1mCi) dynamic PET scan in all the dogs and an additional 18F-FDG (~2mCi) scan in dogs 2 and 3. 1H-MRI and HMRS (250mM pyruvate, 0.8mL/Kg) images were acquired using 13C/1H dual-tuned endorectal receive and 13C clamshell transmit coils. Subsequently, USMI (BR55, 0.05mL/Kg) and real-time fusion with TRUS (dog 1:HMRS/MRI, dog 2:HMRS/PET/MRI, dog 3:HMRS/PET/MRI+Biopsy) was implemented followed by histological analysis (H&E) of the resected prostate and biopsy samples.

## RESULTS

In all dogs, Ace-1 tumors were seen on TRUS and T2-weighted MRI, while USMI revealed peripheral binding in tumors, associated with rapid clearance (~3 minutes), possibly due to low affinity of BR55 for canine VEGFR-2. In dog 1, 68Ga PET showed no specific uptake but HMRS showed increased 13C-lactate production in tumor (lactate/pyruvate=0.5). H&E confirmed PCa with ~1 mm heterogenic nests surrounded by inflammatory cells. In dog 2, FDG-PET and HMRS showed elevated metabolic activity with lactate/pyruvate=0.64 in tumor, with no 68Ga-tracer uptake. On H&E, extracapsular growth of PCa was confirmed. In dog 3, 18F-FDG and 68Ga showed uptake in tumor with little signal observed on HMRS. Overall, in each dog the tumors were confirmed to be viable at least by one physiological imaging modality showing the benefit of multimodality imaging in improving the diagnosis of PCa.

#### CONCLUSION

Real-time HMRS/PET/MR fusion guided TRUS biopsy of focal PCa is feasible.

### **CLINICAL RELEVANCE/APPLICATION**

Our study lays the foundation for clinical translation of a multimodality imaging approach for improved guided biopsy results in patients with prostate cancer.

### GU213-SD-MOA4

#### Acute Non-Hemorrhagic Adrenal Infarction in Pregnancy: Incidence, MRI Features, and Outcome

Monday, Nov. 28 12:15PM - 12:45PM Room: GU/UR Community, Learning Center Station #4

#### **Participants**

Sha-har Admoni, MD, Boston, MA (*Presenter*) Nothing to Disclose Jeffrey P. Guenette, MD, Boston, MA (*Abstract Co-Author*) Nothing to Disclose Wendy B. Landman, MD, Boston, MA (*Abstract Co-Author*) Nothing to Disclose Servet Tatli, MD, Boston, MA (*Abstract Co-Author*) Nothing to Disclose

# PURPOSE

Non-hemorrhagic adrenal infarction is a rare cause of acute abdominal or back pain in pregnancy. The diagnosis is often overlooked, as pregnant women do not typically undergo CT or MRI with gadolinium-based contrast material due to potential fetal toxicity. Recently, case reports have described non-hemorrhagic adrenal infarction on unenhanced MRI. This study aims to measure the incidence of non-hemorrhagic adrenal infarction in pregnant women presenting with acute symptoms, describe the MRI features, and evaluate outcomes.

#### **METHOD AND MATERIALS**

All 444 consecutive MRI scans performed on pregnant women from May 2005 to April 2015 were reviewed. Studies with an indication other than acute pain (n=30) and those not fully including the adrenals (n=35) were excluded. The remaining MRI examinations were retrospectively evaluated by two radiologists, and abnormal morphological and signal characteristics were recorded. Patient demographics and outcomes were gathered from the medical record.

# RESULTS

In 5 (1.3%) of 379 studies in 4 patients (ranging 16-35 weeks gestational age), findings were suggestive of non-hemorrhagic adrenal infarction. MRI features included unilateral adrenal gland enlargement and retroperitoneal edema centered at the adrenal. No additional imaging findings were found to explain the patients' symptoms. The patients presented with severe acute abdominal/flank pain with nausea and/or vomiting. All patients had tenderness to palpation without peritoneal signs on exam, leukocytosis (11.4-20.0 thousand cells/uL), and a bland urinalysis. None had a personal or family history of thrombophilia. Patients were treated with IV fluids, analgesia, antiemetics, bowel regimen, and, in two cases, anticoagulation. Symptoms eventually resolved, and all women delivered healthy babies.

#### CONCLUSION

Non-hemorrhagic adrenal infarction was identified in 1.3% of non-contrast abdominal MRI examinations performed in pregnant women with acute abdominal/back pain. Imaging features included unilateral adrenal gland enlargement and surrounding edema. This diagnosis is often overlooked in pregnant women, as CT and gadolinium-based contrast are typically avoided. Therefore, it must be recognized by its unenhanced MRI characteristics.

### **CLINICAL RELEVANCE/APPLICATION**

Due to avoidance of CT and gadolinium in pregnancy, diagnosis of non-hemorrhagic adrenal infarction must be made on unenhanced MRI by recognizing edema surrounding an enlarged adrenal gland.

## GU214-SD-MOA5

# Ultrasound (US) of Indeterminate Adnexal Cysts: Incidence of Ovarian Cancer

Monday, Nov. 28 12:15PM - 12:45PM Room: GU/UR Community, Learning Center Station #5

#### Awards

#### **Student Travel Stipend Award**

#### **Participants**

Elizabeth B. Maddox, Madison, WI (*Presenter*) Nothing to Disclose Elizabeth A. Sadowski, MD, Madison, WI (*Abstract Co-Author*) Nothing to Disclose Krupa Patel-Lippman, MD, Madison, WI (*Abstract Co-Author*) Nothing to Disclose Ashish P. Wasnik, MD, Ann Arbor, MI (*Abstract Co-Author*) Nothing to Disclose Viktoriya Paroder, MD,PhD, Bronx, NY (*Abstract Co-Author*) Nothing to Disclose Sarah Averill, Madison, WI (*Abstract Co-Author*) Nothing to Disclose Lisa Barroilhet, MD, Madison, WI (*Abstract Co-Author*) Nothing to Disclose Laura Huffman, MD, Madison, WI (*Abstract Co-Author*) Nothing to Disclose Katherine E. Maturen, MD, Ann Arbor, MI (*Abstract Co-Author*) Nothing to Disclose Alexander D. Blaty, BS, Ann Arbor, MI (*Abstract Co-Author*) Nothing to Disclose Jessica B. Robbins, MD, Madison, WI (*Abstract Co-Author*) Nothing to Disclose

#### PURPOSE

Most ovarian lesions can be characterized on ultrasound (US) as benign appearing or worrisome for malignancy, and appropriately triaged. However, when cystic lesions have avascular septations and/or solid components or are larger than 5cm they are incompletely characterized by US and considered sonographically indeterminate (Ekerhovd E et al. Am J Obstet Gynecol 2001). The rate of ovarian cancer development in ovarian lesions characterized as benign or potentially malignant is well documented; however there is a paucity of data on the incidence of ovarian cancer in US indeterminate ovarian lesions. The goal of our study was to determine the incidence of ovarian cancer in sonographically indeterminate lesions.

#### **METHOD AND MATERIALS**

This is an IRB approved retrospective review of transvaginal US studies performed consecutively at 3 institutions from January to June 2011. Adnexal cystic lesions were considered indeterminate if they met one of the following criteria: presence of septations or soft tissue elements without Doppler vascularity, or cyst size >5 cm. Surgical pathology or resolution on follow-up were the inclusion criteria end-points. The incidence of benign and malignant ovarian neoplasms was calculated.

### RESULTS

166 cystic adnexal lesions in 158 women (mean age 43  $\pm$  14 years) met the inclusion criteria. 71.7% (119/166) of US indeterminate lesions resolved on follow up or were physiologic cysts on pathology. 24.1% (40/166) were benign ovarian neoplasms (cystadenomas; dermoids). 3.0% (5/166) were borderline or low-grade ovarian neoplasms. 1.2% (2/166) were clear cell or high-grade serous/endometroid carcinomas.

# CONCLUSION

In our cohort of sonographically indeterminate lesions, 71.7% were non-neoplastic, 24.1 % were benign ovarian neoplasms, and 4.2% were either borderline tumors or carcinomas. Study accrual is ongoing to increase the number of indeterminate lesions. Continued analysis will be important to accurately access the incidence of ovarian cancer in sonographically indeterminate lesions, which may help guide management of women with indeterminate adnexal lesions in the future.

## **CLINICAL RELEVANCE/APPLICATION**

Determining the incidence of ovarian cancer in sonographically indeterminate adnexal lesions is an important step in the formulation of appropriate recommendations for follow up of these lesions.

## **Honored Educators**

Presenters or authors on this event have been recognized as RSNA Honored Educators for participating in multiple qualifying educational activities. Honored Educators are invested in furthering the profession of radiology by delivering high-quality educational content in their field of study. Learn how you can become an honored educator by visiting the website at: https://www.rsna.org/Honored-Educator-Award/

Katherine E. Maturen, MD - 2014 Honored Educator

# GU215-SD-MOA6

# Role of 64 Slice MDCT Urethrography In Evaluation Of Male Urethral Pathologies

Monday, Nov. 28 12:15PM - 12:45PM Room: GU/UR Community, Learning Center Station #6

#### **Participants**

Shuchi Bhatt, MD, Delhi, India (*Presenter*) Nothing to Disclose Avinaba Banerjee, MBBS, New Delhi, India (*Abstract Co-Author*) Nothing to Disclose Anupama Tandon, MBBS, MD, Delhi, India (*Abstract Co-Author*) Nothing to Disclose Arun Gupta, MBBS, MS, Delhi, India (*Abstract Co-Author*) Nothing to Disclose

# PURPOSE

Urethral pathologies are traditionally imaged on retrograde urethrography for anterior and micturating cystourethrography for posterior urethra, but have limitations which can be overcome by Multi-Detector CT Urethrography (MDCTU); the role of which is assessed in this study.

## METHOD AND MATERIALS

After institutional ethical approval and informed consent 50 males with urethral complaints underwent Conventional Urethrography (CU) and MDCTU on 64 slice CT. Visualization of urethra, presence, level, cause and extent of urethral pathology were assessed by two radiologists independently and compared with surgery/ cystoscopy or IOU. Wilcoxon signed rank test, intraclass correlation coefficients (for length and severity) and Kappa for interobserver agreement was used for statistical analysis.

#### RESULTS

Visualization of anterior urethra was adequate 96% on CU, 98% on MDCTU with substantial (kappa=0.66) & perfect agreement (kappa=1.0) respectively. Posterior urethra seen in 98% (MDCTU) Vs 48% (CU) (p value<0.05) & perfect (kappa=0.932) and substantial (kappa=0.658) agreement for MDCTU & CU respectively. For assessment anterior urethral pathologies perfect agreement was noted for CU & MDCTU (kappa=0.93 and 0.949 respectively). Visualization of posterior urethra was not possible in 52% on CU and 2% on MDCTU (p value<0.05). Interobserver agreement was perfect (CU & MDCTU kappa=0.917& 0.916 respectively).48 strictured urethral segments were present in 83.8% patients. The specificity (97.8%) and PPV (97.5% - CU Vs 97.9%-MDCTU) for both CU & MDCTU was comparable but sensitivity & NPV was higher for MDCTU (Sensitivity: 97.9% Vs 83.3% & NPV: 97.8% Vs 84.9%). Level of stricture was determined in 37 on CU Vs 48 on MDCTU. The mean stenosis was 72.76% on CU Vs 73.16% on MDCTU, with excellent ICC of 0.962. Mean length was 16.40 mm on CU Vs 18.66 mm on MDCTU, with ICC of 0.978 & perfect agreement. MDCTU was superior to CU in detecting PUDDs, false tracts & urethral calculus also.The mean effective dose was 2.61±0.898 mSv on CU & 3.63±2.416 mSv on MDCTU.

## CONCLUSION

MDCTU was superior to CU, in visualization and pathology detection of the urethra, especially posterior urethra.

#### **CLINICAL RELEVANCE/APPLICATION**

MDCTU is a reliable and superior in visualization and pathology detection especially of posterior urethra and has the potential to replace CU as gold standard investigation for urethral evaluation.

Radiation Safety in the Fluoroscopy Suite: History, Current Devices, Future Developments, and Controversies

Monday, Nov. 28 12:15PM - 12:45PM Room: HP Community, Learning Center Station #6

#### Awards Certificate of Merit

#### Participants

Diane Szaflarski, MD, Mineola, NY (*Presenter*) Nothing to Disclose Esther E. Coronel, MD, Mineola, NY (*Abstract Co-Author*) Nothing to Disclose Faraz Khan, Pittsford, NY (*Abstract Co-Author*) Nothing to Disclose Amandeep Ahluwalia, BA, Glen Cove, NY (*Abstract Co-Author*) Nothing to Disclose David Gregorius, MS, Mineola, NY (*Abstract Co-Author*) Nothing to Disclose Jason C. Hoffmann, MD, Mineola, NY (*Abstract Co-Author*) Consultant, Merit Medical Systems, Inc; Speakers Bureau, Merit Medical Systems, Inc

## **TEACHING POINTS**

1. Many radiation protection devices, such as newer lightweight aprons and slim fitted leaded glasses, may fit and look better, but may not offer the same degree of protection as some of their counterparts.2. As new data emerges regarding how much radiation exposure is too much, radiologists must be aware of risks to eyes, brain, and other critical structures so that they can take appropriate measures to maximize safety and mitigate risks.

# TABLE OF CONTENTS/OUTLINE

-Review current guidelines for radiation exposure to workers in the fluoro suite-Detail the function and use of radiation badges, including appropriate use and interpreting their results-Review history of radiation safety in the fluoro suite, including original, current, and future products-Thoroughly review current devices -Specific topics discussed include (but are not limited to):-Time, distance, and shielding-Dose reduction in the IR suite, including last image hold, changing frame rate, and road mapping-Shielding built into the fluoro suite-Lead aprons, glasses, face shields, and caps-Leaded gloves-Detailed discussion about current radiation safety controversies, including possible changes to exposure limits, cataracts and brain tumors in fluoroscopy suite workers, and debates over various types of personal protective devices (lightweight lead, leaded caps, etc)

# HP206-SD-MOA1

## Incidental Findings Detected during Research MRI: Analysis in Healthy Volunteers

Monday, Nov. 28 12:15PM - 12:45PM Room: HP Community, Learning Center Station #1

#### Participants

Alexandra Ljimani, MD, Duesseldorf, Germany (*Presenter*) Nothing to Disclose Hans-Joerg Wittsack, PhD, Duesseldorf, Germany (*Abstract Co-Author*) Nothing to Disclose Joel Aissa, Duesseldorf, Germany (*Abstract Co-Author*) Nothing to Disclose Gerald Antoch, MD, Duesseldorf, Germany (*Abstract Co-Author*) Nothing to Disclose Rotem S. Lanzman, MD, Duesseldorf, Germany (*Abstract Co-Author*) Nothing to Disclose

#### PURPOSE

Magnetic resonance imaging (MRI) research is frequently performed in healthy volunteers in order to evaluate or optimize new pulse sequences. The purpose of this study was to assess the frequency and clinical significance of incidental findings (IFs) in healthy volunteers undergoing research MRI scans.

## METHOD AND MATERIALS

Research MRI scans of 218 healthy subjects (119 male, 95 female, mean age  $33.1 \pm 10.6$  years) performed in our department over a one year period were considered for this analysis. Research scans of the brain (n=65), spinal cord (n=100), kidneys (n=3), liver (n=3), hands (n=13) and hips (n=34) were reviewed systematically by board certified radiologists for incidental findings. Incidental findings were documented and reported directly to the subjects and further. The type of recommended follow-up examinations and their findings were analysed.

# RESULTS

Incidental findings were reported in 17 of 218 (7.8%) subjects. 3 ovarial cyst, 1 expanded ductus choledochus and 3 subject with increased number of lymph nodes inguinal. 6 subjects were identified to have disc prolaps in the spinal cord and needed further orthopedic threatment. 1 subject needed further treatment in neurosurgery course of a clivuschonrome and 1 subject needed further treatment by the dermatologist as the IF was identified as a melanoma. 2 subjects didn't need any further treatment. The most IFs were found in the spinal cord scans (n=14). 3 IFs were identified in the brain scans. No IFs were found in the hand, renal, hepatic or hip scans.

# CONCLUSION

Incidental findings that required further medical examination may occur in up to 8% of healthy volunteers undergoing research MRI scans. Therefore, subject should be informed about the possibility of an incidental findings and the research scans should be revised by a board certified radiologist.

#### **CLINICAL RELEVANCE/APPLICATION**

MRI research scans should be systematically evaluated for incidental findings.

## HP207-SD-MOA2

A Study of the Clinical Significance of Short-Term Repeat Computed Tomography Examination on Same Anatomic Region

Monday, Nov. 28 12:15PM - 12:45PM Room: HP Community, Learning Center Station #2

# Participants

Hyunji Kim, Bucheon City, Korea, Republic Of (*Presenter*) Nothing to Disclose Sang Hyun Paik, MD, Bucheon, Korea, Republic Of (*Abstract Co-Author*) Nothing to Disclose Joonseok Hwang, MD, Bucheon, Korea, Republic Of (*Abstract Co-Author*) Nothing to Disclose Jai Soung Park, Bucheon, Korea, Republic Of (*Abstract Co-Author*) Nothing to Disclose Heon Lee, MD, PhD, Seoul, Korea, Republic Of (*Abstract Co-Author*) Nothing to Disclose Yousun Won, MD, Bucheon, Korea, Republic Of (*Abstract Co-Author*) Nothing to Disclose

#### PURPOSE

To evaluate the clinical significance of repeat computed tomography (CT) examination on the same anatomical region within 1 month for the diagnosis and management of the patient.

# METHOD AND MATERIALS

Our retrospective cohort enrolled the 182 patients whose outside CT scans were registered in our picture archiving and communicating system (PACS) and who underwent repeat CT examination on same anatomical region within 1 month from October to December of 2013. The reasons for repeat CT examinations were classified four categories; unrelated, follow-up, duplicative, and supplementary examinations. And then, we classified clinical significance of repeat CT examination based on the changes of clinical symptoms, management, and CT findings.

#### RESULTS

In total of 182 patients, unrelated, follow-up, duplicative, and supplementary examinations were 4 (2.2%), 114 (62.7%), 20 (11%), and 44 (24.1%) cases, respectively. Among them, appropriate examinations were 155 (85.2%) and inappropriate examinations were 27 (14.8%) cases. Each of appropriate-unhelpful and inappropriate-helpful examinations were 4 cases (2.2%). Consequently, there were 8 cases (4.4%) of cause-clinical significance discordance (CCSD).

## CONCLUSION

Most of the repeat CT examinations were helpful and beneficial to clinical practices. The guideline for repeat CT examinations needs to be widely spread and used to train the physicians to reduce the CCSD and unhelpful repeat CT examinations.

# **CLINICAL RELEVANCE/APPLICATION**

In 2011, repeat computed tomography examinations on the same anatomical region within 1 month were reported as up to 20% in Korea. For this reason, Korean society of radiology published 'The guideline for CT examination and repeat CT examination' for reducing unnecessary repeat CT examination. In our study based on this guideline, most of the repeat CT examinations were appropriate and helpful for the diagnosis and management of the patient, but there were some unhelpful repeat CT examinations. And there were a few unhelpful examinations, which were classified to appropriate and a few helpful examinations, which were classified to inappropriate examinations according to the guideline, showing CCSD. Therefore, we think that modification of the guideline and training of clinicians about the guideline will helpful to reduce the CCSD and unhelpful repeat CT examination.

# Trends in Cardiac Magnetic Resonance Imaging within the Medicare Population from 2002-2014

Monday, Nov. 28 12:15PM - 12:45PM Room: HP Community, Learning Center Station #3

#### Participants

Jesse K. Sinanan, MD, Philadelphia, PA (*Presenter*) Nothing to Disclose David C. Levin, MD, Philadelphia, PA (*Abstract Co-Author*) Consultant, HealthHelp, LLC; Board of Directors, Outpatient Imaging Affiliates, LLC Laurence Parker, PhD, Philadelphia, PA (*Abstract Co-Author*) Nothing to Disclose Baskaran Sundaram, MRCP, FRCR, Philadelphia, PA (*Abstract Co-Author*) Nothing to Disclose

#### PURPOSE

To study trends in the use of cardiac magnetic resonance imaging (CMR) in the Medicare population from 2002-2014.

### **METHOD AND MATERIALS**

The nationwide Medicare Part B Physician/Supplier Procedure Summary Master Files for 2002 through 2014 were the data source. All primary CPT-4 codes for CMR were selected and grouped together. The add-on codes for velocity flow mapping were analyzed separately. Procedure volumes for the codes were provided by the databases each year. Medicare's specialty codes were used to indicate how many exams were performed by radiologists, cardiologists, and other physicians. Trends were analyzed over the course of the study.

### RESULTS

In 2002, 3019 CMR exams were performed in the Medicare population. Volume increased to 12,210 in 2007 (+304%). Over the next 2 years, volume declined ,but then increased to 14,227 in 2010. From 2010 to 2014, there were steady increases each year, reaching 18,925 in the latter year (+33% compared with 2010). In 2002, radiologists had performed 70% of all CMR exams, while cardiologists had performed 24%. Thereafter, participation by cardiologists increased much more rapidly than it did by radiologists. By 2005, cardiologists were doing more than radiologists, but both specialties continued to increase their participation at the approximately the same rates in subsequent years. In 2014, radiologists performed 8902 cases (47%) while cardiologists performed 9196 (49%). The add-on velocity flow mapping exams were rarely done clinically until 2010, when 3515 were done. By 2014, 5460 were done, of which 40% were by radiologists and 56% by cardiologists.

# CONCLUSION

The use of CMR in the Medicare population grew rapidly from 2002 to 2007, then more slowly thereafter. However, overall volume of primary CMR exams is low, compared with other cardiac imaging modalities. Participation by radiologists and cardiologists in 2014 was approximately equal.

## **CLINICAL RELEVANCE/APPLICATION**

N/A

ICD-10 Implementation: Initial Report of Its Impact on Radiology A Large Multi-Hospital Radiology Practice

Monday, Nov. 28 12:15PM - 12:45PM Room: HP Community, Learning Center Station #4

#### Awards

#### **Student Travel Stipend Award**

#### **Participants**

Margaret Fleming, MD, Atlanta, GA (*Presenter*) Nothing to Disclose Richard Duszak JR, MD, Atlanta, GA (*Abstract Co-Author*) Nothing to Disclose Dan MacFarlane, Atlanta, GA (*Abstract Co-Author*) Nothing to Disclose

### PURPOSE

Last year's conversion of the nation's International Classification of Diseases (ICD) coding system from 14,025 ICD-9 to 69,823 ICD-10 codes was projected to result in a 6-fold increase in codes used by radiology practices. We aimed to determine the actual code conversion magnitude and the revenue impact of ICD-10 on a large multi-hospital practice that diligently prepared for this transition.

#### **METHOD AND MATERIALS**

Using billing data stripped of all patient identification, we studied all 232,798 professional claims for 118 radiologists at a large health system for the first 5 months after ICD-10 implementation on October 1, 2015. Primary ICD-10 codes for the top 90th percentile of all radiology examinations were identified, both overall and by subspecialty division. Using ICD-9 codes for the entirety of 2014 and previously described methodology, we calculated code conversion impact factors (number of applicable ICD-10 codes  $\div$  number of applicable ICD-9 codes). To assess the impact of the ICD-10 implementation on cash flow, average monthly claims days in accounts receivable status both before and after October 1, 2015 were compared.

#### RESULTS

For all 232,798 radiology service claims, 5,135 ICD-10 codes were used as primary diagnoses, but only 540 codes (11% of all) comprised the top 90% of all claims. By comparison, 348 ICD-9 codes accounted for the top 90% of all claims in 2014. This translates to a code conversion impact factor of 1.6 for the department as a whole, far less than the literature predicted 6-fold increase. The code conversion impact for individual divisions ranged from 0.5 (breast) to 3.3 (musculoskeletal). All other divisions saw impact factors in the 1.5-2.0 range. The average monthly number of days claims were in accounts receivable status ranged from 33 to 39 days both before and after ICD-10 implementation. Monthly averages for the 7 months prior to and the 5 months after ICD-10 conversion were similar (35.0 vs. 35.2, p=0.86).

## CONCLUSION

For large radiology groups adhering to "best practice" ICD-10 implementation planning guidelines, the impact of last year's widely feared ICD-10 transition, both with regard to code conversion magnitude and delays in cash flow, was negligible.

## **CLINICAL RELEVANCE/APPLICATION**

For well-prepared radiology practices, the coding and revenue impact of last year's widely feared national ICD-10 transition was minimal.

Natural History of Intraductal Papillary Mucinous Neoplasm Regarding Development of Pancreatic Cancer: A Systematic Review and Meta-analysis

Monday, Nov. 28 12:15PM - 12:45PM Room: HP Community, Learning Center Station #5

# Participants

Sang Hyun Choi, Seoul, Korea, Republic Of (*Presenter*) Nothing to Disclose Seong Ho Park, MD, Seoul, Korea, Republic Of (*Abstract Co-Author*) Research Grant, DONGKOOK Pharmaceutical Co, Ltd Kyung Won Kim, MD, Seoul, Korea, Republic Of (*Abstract Co-Author*) Nothing to Disclose Ja Youn Lee, Seoul, Korea, Republic Of (*Abstract Co-Author*) Nothing to Disclose Jae Ho Byun, MD, Seoul, Korea, Republic Of (*Abstract Co-Author*) Nothing to Disclose

# PURPOSE

Current management guidelines for intraductal papillary mucinous neoplasm (IPMN) of the pancreas largely consider the association between morphologic features and odds of harboring malignancy at a cross-sectional time. Knowledge of natural history of the disease will help guide even more proper patient management. This study was to create a systematic evidence synthesis on cumulative incidence of pancreatic cancer in IPMNs during follow-up.

#### **METHOD AND MATERIALS**

Original research studies that investigated cumulative incidence of pancreatic cancer, including both noninvasive and invasive cancers, in unresected IPMNs or presented data detailed enough for the cumulative incidence to be drawn were identified with thorough systematic search of PubMed MEDLINE and EMBASE (until December 31, 2015). We calculated meta-analytic estimates of the cumulative incidence at 1-, 3-, 5- and 10-year follow-up separately for low-risk patients, defined as lack of mural nodule/solid component and main pancreatic ductal dilatation, and non-low-risk patients. Studies containing a small fraction (<10%) of non-low-risk patients were pooled together with low-risk group. Study heterogeneity was analyzed using Higgins' *I*<sup>2</sup> and Cochrane Q test.

#### RESULTS

Of 1304 papers screened, we found 9 studies for low-risk group, also including 3 studies containing a small fraction (1.8–9%) of non-low-risk patients, for a total of 2388 patients and 10 studies for non-low-risk group for a total of 879 patients. Meta-analytic pooled cumulative incidence at 1-, 3-, 5- and 10-year follow-up was 0.25% (95% CI, 0.03–0.58%;  $I^2$ =0.0%), 1.51% (0.68–2.60%;  $I^2$ =64.3%), 3.55% (1.20–6.97%;  $I^2$ =91.9%) and 8.28% (5.18–11.98%;  $I^2$ =80.4%) for low-risk group; and 1.78% (0.01–5.29%;  $I^2$ =82.3%), 6.37% (1.65–13.29%;  $I^2$ =86.9%), 12.17% (5.00–21.59%;  $I^2$ =88.0%) and 24.32% (14.42–35.71%;  $I^2$ =75.2%) for non-low-risk group.

#### CONCLUSION

Despite some ambiguity related to large study heterogeneity, the natural history of unresected IPMNs also supports the current risk stratification for management. Potentially fairly high long-term incidence of cancer in low-risk IPMNs may indicate a need for long-term follow-up while large study heterogeneity requires further data accumulation.

## **CLINICAL RELEVANCE/APPLICATION**

Knowledge of natural history of IPMN regarding cancer development in addition to known morphologic risk factors for harboring cancer facilitates more precise patient management.

# Methods of Advanced 3D Printing from Medical Scans Using Freeware and Low-Cost Printers

Monday, Nov. 28 12:15PM - 12:45PM Room: IN Community, Learning Center Hardcopy Backboard

#### **Participants**

Michael W. Itagaki, MD, MBA, Seattle, WA (Presenter) Owner, Embodi3D, LLC

#### **TEACHING POINTS**

1) Understand how free and open-source software can be used to design complex anatomic models for 3D printing.2) Understand how low-cost consumer 3D printers can be used to create large anatomic models with fine detail.

# TABLE OF CONTENTS/OUTLINE

3D printing from medical imaging scans is increasingly used for medical education, device testing/development, and presurgical planning. Use of large, expensive 3D printers and high-cost proprietary design software are major barriers to more widespread adoption of 3D printing in hospitals. Large and expensive printers are required to manufacture parts equivalent in size to those found in the human body. We have developed a robust workflow that allows the creation and design of complex anatomic models using free open-source software. Furthermore, large models can be made on small, low-cost consumer 3D printers. Unrestricted by requirements for proprietary software and physically large printers, the cost of starting an in-hospital 3D printing lab can be greatly reduced, with an initial outlay of approximately \$5000. This vastly expands the number of institutions that can offer 3D printing services.A) Conversion of DICOM data sets to STL filesB) Editing and modification of STL filesC) 3D printing of STL files on consumer 3D printersD) Postprocessing of 3D prints and fusion to create large models

## IN211-SD-MOA2

Reading Chest X-Rays Using Deep Learning: Recurrent Neural Cascade Model for Automated Image Annotation

Monday, Nov. 28 12:15PM - 12:45PM Room: IN Community, Learning Center Station #2

## Participants

Hoo-Chang Shin, PhD, Bethesda, MD (*Presenter*) Nothing to Disclose Kirk Roberts, Richardson, TX (*Abstract Co-Author*) Nothing to Disclose Le Lu, PhD, Bethesda, MD (*Abstract Co-Author*) Nothing to Disclose Dina Demner-Fushman, Bethesda, MD (*Abstract Co-Author*) Nothing to Disclose Jianhua Yao, PhD, Bethesda, MD (*Abstract Co-Author*) Royalties, iCAD, Inc Ronald M. Summers, MD, PhD, Bethesda, MD (*Abstract Co-Author*) Royalties, iCAD, Inc; ;

### PURPOSE

Automated medical image annotation has a great potential to make the radiology big data in hospital databases more accessible. A vast amount of images can be retrieved by searching for the keywords describing the images. Additionally, it can be useful for large-scale patient screening. We propose an approach to automatically learn to annotate images from a dataset of radiology images and reports.

## **METHOD AND MATERIALS**

A publicly available dataset of chest x-rays and reports were used in order to promote community efforts in solving this challenging problem. The anonymized data consist of 3955 radiology reports and 7283 associated chest x-rays. Moreover, the radiology reports were labeled using Medical Subject Headings (MeSH) according to pre-defined grammar to annotate the images. Summarizing radiology reports to the standardized MeSH terms with pre-defined grammar rules helps remove the ambiguity found in radiology reports. Convolutional neural networks and recurrent neural networks were then trained on the chest x-ray and MeSH annotation pairs, to generate "human-like" text diagnosis on new chest x-ray cases. Given a patient image, not only can the presence/absence of a disease be detected but also its context can be automatically generated, such as the location, size, and severity.

#### RESULTS

A total of 217 MeSH terms were used, where the number of terms (N) describing a disease ranges from 1 to 8, with a mean of 2.56 and standard deviation of 1.36. The number of images used for training/validation/testing was 6316/545/422. The rate of predicting the words matching the true annotation words in training/validation/testing were 0.90/0.62/0.79, and the rate of two- and three-consecutive predicted words matching the true annotation words were 0.62/0.30/0.14 and 0.79/0.14/0.05, respectively. This is a promising first step towards more comprehensive automated medical image understanding using radiology images and reports.

#### CONCLUSION

We present an effective framework to learn, detect disease, and describe their contexts from patient chest x-rays and their accompanying radiology reports with MeSH annotations. To the best of our knowledge, this is the first system to generate "human-like" annotation from radiology images.

### **CLINICAL RELEVANCE/APPLICATION**

This work has a greater potential to be developed into a clinically useful system, e.g. as a pre-screening tool in developing countries where limited clinical resources are available.

Preliminary Results Using Deep Learning Artificial Intelligence to Estimate Bone Mineral Density on Abdominal CT Exams for Screening Osteoporosis

Monday, Nov. 28 12:15PM - 12:45PM Room: IN Community, Learning Center Station #3

# Participants

Michael Y. Park, MD, Seoul, Korea, Republic Of (*Presenter*) Nothing to Disclose Seung Eun Jung, MD, Seoul, Korea, Republic Of (*Abstract Co-Author*) Nothing to Disclose Sangki Kim, PhD, Seoul, Korea, Republic Of (*Abstract Co-Author*) Nothing to Disclose Moon Hyung Choi, MD, Seoul, Korea, Republic Of (*Abstract Co-Author*) Nothing to Disclose Joon-II Choi, Seoul, Korea, Republic Of (*Abstract Co-Author*) Nothing to Disclose Soon Nam Oh, MD, Seoul, Korea, Republic Of (*Abstract Co-Author*) Nothing to Disclose Sung Eun Rha, MD, Seoul, Korea, Republic Of (*Abstract Co-Author*) Nothing to Disclose Jae Young Byun, MD, Seoul, Korea, Republic Of (*Abstract Co-Author*) Nothing to Disclose

#### PURPOSE

To determine whether deep learning artificial intelligence can be used to automatically estimate and screen for osteoporosis on abdominal CT exams.

# METHOD AND MATERIALS

A total 4,203 pairs of lumbar spine dual-energy X-ray absorptiometry (DXA) exams and abdominal CT exams taken within 60 days of the same patient were included in this study. The median age of patients was 54 (IQR: 48-60), and the 3,973 (94.5%) of the cases had the DXA and CT exams on the same day (mean 0.4 days). The L1-L4 mean bone mineral density (BMD) values were used as a reference standard, and 3,783 (90%) randomly selected cases were used for deep learning artificial intelligence training using a convolutional neural network model (VunoNet, Seoul, Korea). The other 420 (10%) of cases were excluded from training and used to evaluate the deep learning results. Cutoff values for using deep learning estimated BMD to screen osteoporosis were analyzed. Osteoporosis for determining cutoff values in this study was defined as cases with BMD T-scores of less than or equal to -2.5, with T-scores calculated only using lumbar spine DXA BMD results using reference population BMD T-score tables without compensating for weight.

#### RESULTS

The median DXA BMD and median deep learning estimated BMD were 1.159 (IQR: 1.042-1.271) and 1.171 (IQR: 1.055-1.286). A high linear correlation (r2 = 0.714) between deep learning estimated BMD values and DXA BMD values were noted. When using a deep learning estimated BMD cutoff value of less than or equal to 0.929 g/cm2 for screening osteoporosis, a sensitivity of 94.4% and specificity of 97.0% could be achieved when using lumbar spine DXA results as a gold standard, with a high AUC of 0.990.

#### CONCLUSION

Deep learning artificial intelligence for estimating BMD on abdominal CT exams has the potential to be used to automatically screen for osteoporosis in routine abdominal CT exams.

## **CLINICAL RELEVANCE/APPLICATION**

This study shows the potential for using deep learning artificial intelligence to fully automate screening for osteoporosis in routine abdominal CT exams taken for other reasons.

# First Computer-Aided Diagnosis of Neural Foramina Stenosis

Monday, Nov. 28 12:15PM - 12:45PM Room: IN Community, Learning Center Station #4

FDA Discussions may include off-label uses.

#### **Participants**

Xiaoxu He, London, ON (*Presenter*) Nothing to Disclose Jaron Chong, MD, Montreal, QC (*Abstract Co-Author*) Nothing to Disclose Manas Sharma, MBBS, MD, Toronto, ON (*Abstract Co-Author*) Nothing to Disclose Olga Shmuilovich, MD, London, ON (*Abstract Co-Author*) Nothing to Disclose Gary L. Brahm, BMedSc, MD, London, ON (*Abstract Co-Author*) Nothing to Disclose Shuo Li, PhD, London, ON (*Abstract Co-Author*) Nothing to Disclose

# PURPOSE

Neuro Foramina Stenosis (NFS) is a leading cause of lower back pain and has the risk of disability. However, clinical diagnosis of NFS is a highly laborious and time-consuming task for physicians. In this study, a fully automated CAD of NFS was firstly developed and validated in clinic against manual diagnosis.

# METHOD AND MATERIALS

A new label-supervised feature learning algorithm was used to transfer the experts' knowledge to computer, and then neural foramina diagnosis is automatically reported. Following IRB approval, spine magnetic resonance images from 110 subjects (58 women, 52 men, 56±12 yrs) were collected to validate the proposed CAD against manual diagnosis by two expert physicians. The performance was evaluated via the diagnostic accuracy, specificity, and sensitivity, using a leave-one-subject-out strategy.

#### RESULTS

High diagnostic accuracy of the proposed CAD has demonstrated by 98.52% accuracy with specificity as 100.00% and sensitivity as 97.96%.

## CONCLUSION

This study demonstrated that the developed CAD has a comparable accuracy and sensitivity with the expert physicians. These findings provide an effective way to relieve the heavy burden of physicians, pay more attention to high-level clinical tasks, and offer an efficient clinical tool for neural foramina stenosis.

# **CLINICAL RELEVANCE/APPLICATION**

Computer-aided diagnosis based on supervised feature learning offers an automated and accurate clinical tool for aiding physicians in providing efficient clinical diagnosis and timely treatment.

A Feasibility Study of Deep Learning Technique in Distinguishing Normal Lungs, Pulmonary Tuberculosis and Non-tuberculous Mycobacterial Lung Disease on Chest CT: The 'Alpha Radiologist' is Beginning?

Monday, Nov. 28 12:15PM - 12:45PM Room: IN Community, Learning Center Station #5

# Participants

Joon Chul Ra, Seoul, Korea, Republic Of (*Abstract Co-Author*) Nothing to Disclose Semin Chong, MD, Seoul, Korea, Republic Of (*Presenter*) Nothing to Disclose Myungjoo Kang, Seoul, Korea, Republic Of (*Abstract Co-Author*) Nothing to Disclose Kyungmin Song, Seoul, Korea, Republic Of (*Abstract Co-Author*) Nothing to Disclose Sangyeon Kim, Seoul, Korea, Republic Of (*Abstract Co-Author*) Nothing to Disclose Min Jae Cha, Seoul, Korea, Republic Of (*Abstract Co-Author*) Nothing to Disclose Yang Soo Kim, MD, Seoul, Korea, Republic Of (*Abstract Co-Author*) Nothing to Disclose

### CONCLUSION

The computer-assisted CT image classification using a deep learning technique might be a complimentary or problem solving tool for characterization and discrimination of the pulmonary TB and NTM lung disease as well as normal lungs in the future.

#### Background

Our purpose is to evaluate the diagnostic performance of deep learning technique in distinguishing normal lungs, pulmonary tuberculosis (TB) and non-tuberculous mycobacterial (NTM) lung disease on chest CT.

#### **Evaluation**

All CT data were obtained in 329 patients with normal lungs (n = 113), pulmonary TB (n = 115) and NTM lung disease (n = 101). From these CT data, we included 11641 CT images of normal lungs, 5851 CT images of pulmonary TB and 5963 CT images of NTM lung disease in the training and test sets. We used the VGG (visual geometry group)-16 network, which is one of the most popular networks currently for classifying images and won the second place on the ILSVRC (ImageNet Large Scale Visual Recognition Challenge) 2014 competition. It has enough layers and parameters for finding features in large complex images. We used the pre-trained parameters trained on the ILSVRC classification task before fully connected layers and got feature vectors for each image. Each image turn into 4096 length feature vectors and passed through one hidden layer and output layer for classifying the image belongs to normal, TB and NTM groups. We trained with 17255 CT images consist of 6917 normal images, 5393 TB images and 4945 NTM images. After training, we tested 6200 CT images which were not included in the training set. We also trained and tested for normal group versus abnormal group consisting of TB and NTM.

#### Discussion

The test result showed an overall accuracy of 68.3% in the three groups (75.9% in normal, 60.0% in TB and 36.8% in NTM); whereas 80.6% in the two groups (79.6% in normal group and 83.8% in abnormal group). Our study revealed that the deep learning technique may have potential and good feasibility for distinguishing normal lung images with abnormal lung images. However, we think that many more sample sizes should be tested and the improvement of deep learning technique may be required in order to enhance its diagnostic performance.

Intra- and Interobserver Reliability on a Quantitative CT Analysis of Ground-glass Opacity Nodules: Manual versus Automated Segmentation

Monday, Nov. 28 12:15PM - 12:45PM Room: IN Community, Learning Center Station #6

# Participants

Hyein Kang, Seoul, Korea, Republic Of (*Presenter*) Nothing to Disclose Semin Chong, MD, Seoul, Korea, Republic Of (*Abstract Co-Author*) Nothing to Disclose Min Jae Cha, Seoul, Korea, Republic Of (*Abstract Co-Author*) Nothing to Disclose Joon Chul Ra, Seoul, Korea, Republic Of (*Abstract Co-Author*) Nothing to Disclose Yang Soo Kim, MD, Seoul, Korea, Republic Of (*Abstract Co-Author*) Nothing to Disclose

# PURPOSE

To evaluate the intra- and inter-observer reliability on quantitative CT parameters of ground-glass opacity nodules (GGN) estimated by manual and automated segmentation

### **METHOD AND MATERIALS**

Fifty GGNs were segmented manually by two observers (Obs 1 and 2) on image analysis software, which were repeated two times. All GGNs were also segmented twice repeatedly using by our house software, which we called "Isocontour" based on a modified Marching Squares algorithm. The quantitative CT characteristics of GGNs were estimated by the following 12 parameters: mean HU (Mean), median HU (Median), maximum HU (Max), minimum HU (Min), standard deviation (SD), skewness and kurtosis; area, perimeter, Feret's diameter (Feret), circularity and aspect ratio (AR). On the manual and automated segmentation, the inter- and intra-observer reliability on the quantitative CT parameters was assessed by the intraclass correlation coefficient (ICC) with two-way fixed model with absolute agreement. The ICC values were interpreted as  $excellent(\geq 0.75)$ , good(0.60-0.74), fair(0.40-0.59), and poor(<0.40).

#### RESULTS

On the manual segmentation, the intra- and interobserver reliability were excellent in 7 parameters such as Mean, Median, Max, SD, skewness, Feret, perimeter and area; whereas fair to good in kurtosis and poor to good in Min, circularity, AR. Regarding the automated segmentation using the Isocontour software, intra-observer reliability on all 12 parameters was excellent in Obs 1 and good to excellent in Obs 2. Inter-observer reliability was excellent for all 12 quantitative CT parameters. Comparing manual and automated segmentation, Obs 1 had excellent agreement in 5 parameters such as Mean, Median, Max, perimeter and area; whereas poor to good agreement in other parameters. Obs 2 had excellent agreement only in 3 parameters such as Mean, Median, and Area; whereas fair to good agreement in others parameters.

# CONCLUSION

The automated segmentation of GGN showed more stable intra- and interobserver reliability of quantitative CT characteristics than the manual segmentation in both observers. Particularly, the reliability of Mean, Median, Max and area were constantly good to excellent in every settings.

## **CLINICAL RELEVANCE/APPLICATION**

When a GGN will be segmented by either manual or automated methods, the highly reproducible parameters should be selected and analyzed by the practiced radiologist in the segmentation.

# Structural Considerations for 3D Printing the Skeletally Immature Craniocervical Junction

Monday, Nov. 28 12:15PM - 12:45PM Room: IN Community, Learning Center Station #7

#### Participants

James Shin, MD, MSc, Stony Brook, NY (*Presenter*) Nothing to Disclose C. Douglas Phillips, MD, New York, NY (*Abstract Co-Author*) Stockholder, MedSolutions, Inc Consultant, Guerbet SA Mark E. Schweitzer, MD, Stony Brook, NY (*Abstract Co-Author*) Consultant, MMI Munich Medical International GmbH Data Safety Monitoring Board, Histogenics Corporation

# CONCLUSION

Skeletal immaturity can present segmentation and modeling challenges not present for adults. Structural integrity of noncontiguous ossified components can be achieved with basic CAD techniques, however variable ossification patterns must be anticipated and carefully considered in order to apply them appropriately, as areas of inadequate fusion or subtle non-contiguity may be inapparent on a digital model. Familiarity with potential ossification patterns is thus critical to ensuring structural integrity of a 3D printed bone model, especially so at the craniocervical junction.

#### Background

Robust segmentation and iso-surface extraction algorithms have facilitated maturation of 3D printing workflows using CT image data. While these techniques are extensible to the immature skeleton, achieving structural integrity of non-contiguous osseous anatomy requires additional structural geometries. This represents a significant departure from routine post-processing. In addition to familiarity with basic CAD tools, understanding the full range of potential ossification patterns and their variable progression is critical to fabrication of a patient model representative of anatomic position, as imaged.

#### **Evaluation**

De-identified CT images of a skeletally immature skull base were processed in 3D Slicer (4.5) using standard threshold segmentation and iso-surface extraction algorithms. An initial threshold was chosen to ensure contiguity of the segmented skull base. A subsequent lower threshold was chosen to segment the spine more inclusively. Support rods were fused by Boolean addition at a diameter of 3.5mm in Meshmixer (11.0), determined by trial and error with a bias toward minimization.

#### Discussion

Type 3a anterior/type B posterior C1 arches were identified. This represents a non-typical ossification pattern, and could introduce additional structural requirements that may be subtle depending on stage of maturation, though not in this case. 5 ossification centers of C2 were partially fused and structurally adequate by analysis of the digital model, with the exclusion of the chondrum terminale. Midline supports from C2 to C5, and anterior arch C1 to dens, were added. Lateral masses were anchored to the occipital condyles and C2 lateral neural arches.

Fully-Automated Multi-Atlas Lobe Based Lung Segmentation of Lung Perfusion MR Images Using Machine Learning Techniques in COPD Patients

Monday, Nov. 28 12:15PM - 12:45PM Room: IN Community, Learning Center Station #8

# Participants

Hinrich B. Winther, MD, Hannover, Germany (Presenter) Nothing to Disclose Christoph P. Czerner, MD, Hannover, Germany (Abstract Co-Author) Nothing to Disclose Christian Hundt, DIPLPHYS, PhD, Mainz, Germany (Abstract Co-Author) Nothing to Disclose Till F. Kaireit, Hannover, Germany (Abstract Co-Author) Nothing to Disclose Frank K. Wacker, MD, Hannover, Germany (Abstract Co-Author) Research Grant, Siemens AG; Research Grant, Pro Medicus Limited; Research Grant, Delcath Systems, Inc; Hoen-Oh Shin, MD, Hannover, Germany (Abstract Co-Author) Nothing to Disclose Jens Vogel-Claussen, MD, Hannover, Germany (Abstract Co-Author) Nothing to Disclose CONCLUSION

This study illustrates the first practical method for a lobe based lung segmentation of MRI lung perfusion images using machine learning techniques.

#### Background

The World Health Organization lists chronic obstructive pulmonary disease (COPD) as the third most common cause of death. 4D dynamic contrast-enhanced (DCE) MRI can reliably quantify lung parenchymal perfusion, providing clinically relevant information. However, this technique currently requires human interaction, running the risk of high inter-observer variability and binding valuable human resources.

# **Evaluation**

MRI and CT data sets of 11 COPD participants were acquired on the same day. On each CT dataset lobar segmentation was performed by a human expert, yielding the ground truth. The CT images were registered onto the corresponding DCE-MRI of the same patient. The resulting MRI segmentation was accepted as ground truth under the assumption that no significant interval changes have occurred. In machine learning ensemble methods were employed to boost predictive performance. This study uses this concept by performing a multi-atlas image registration of the other MRIs onto the target MRI. Majority label voting was employed as label fusion algorithm Using this technique, a lung overlap of 92.36±2.52 (mean±sd in %) for each lung (right and left) and an overlap of 85.23 $\pm$ 3.79 on a lobar level was achieved by employing 9 atlases. Overlap is defined as (A $\cap$ B)=(A $\cup$ B) where A is the predicted segmentation and B the ground truth.

#### Discussion

Machine learning was successfully applied for fully-automated lobe-based segmentation of DCE-MR images of the lung eliminating the need for human interaction. Previously a study (doi:10.1007/s11548-014-1090-0) has performed total right and left lung segmentation only with an overlap between human experts of 94%. This is comparable to the presented results achieved by the proposed method. This method will drastically reduce the associated costs, making lobe based MRI lung segmentation feasible without the need for CT for large scale research studies and future clinical routine.

Additive Manufacturing Models of Fetuses built from Three-dimensional Ultrasound, Magnetic Resonance Imaging and Computed Tomography Scan Data

Monday, Nov. 28 12:15PM - 12:45PM Room: IN Community, Learning Center Station #1

# Participants

Heron Werner, MD, Rio de Janeiro, Brazil (*Presenter*) Nothing to Disclose Bianca Guedes Ribeiro, MD, Rio de Janeiro, Brazil (*Abstract Co-Author*) Nothing to Disclose Jorge Lopes, Rio de Janeiro, Brazil (*Abstract Co-Author*) Nothing to Disclose Gerson Ribeiro, Rio de Janeiro, Brazil (*Abstract Co-Author*) Nothing to Disclose Tatiana M. Fazecas, MD, Rio de Janeiro, Brazil (*Abstract Co-Author*) Nothing to Disclose Renata A. Nogueira, MD, Rio De Janeiro, Brazil (*Abstract Co-Author*) Nothing to Disclose Pedro Daltro, MD, Rio De Janeiro, Brazil (*Abstract Co-Author*) Nothing to Disclose Leise Rodrigues, Rio De Janeiro, Brazil (*Abstract Co-Author*) Nothing to Disclose

#### PURPOSE

To generate physical fetal models using images obtained by three-dimensional ultrasonography (3DUS), magnetic resonance imaging (MRI) and, in some cases, computed tomography (CT) to guide additive manufacturing technology.

#### **METHOD AND MATERIALS**

Images from 32 pregnant women, including 5 sets of twins, were used. Scans were performed using high-resolution 3DUS. In cases of abnormalities, MRI and CT, were performed on the same day as 3DUS. The images obtained with 3DUS, MRI or CT were exported to a workstation in DICOM format. A single observer performed slice-by-slice manual segmentation using a digital high-definition screen. Software that converts medical images into numerical models was used to construct virtual 3D models, which were physically made using additive manufacturing technologies.

#### RESULTS

Physical models based upon 3DUS, MRI and CT were successfully generated. They were similar to the postnatal appearance of the aborted fetus or newborns, especially in cases with pathology.

# CONCLUSION

The use of 3DUS, MRI and CT may improve our understanding of fetal anatomical characteristics, and these technologies can be used for educational purposes and as a method for parents to visualize their unborn baby. The images can be segmented and applied separately or combined to construct 3D virtual and physical models.

# **CLINICAL RELEVANCE/APPLICATION**

The techniques described in this study can be applied at different stages of pregnancy and constitute an innovative contribution to research on fetal abnormalities. We believe that physical models will help in the tactile and interactive study of complex abnormalities in multiple disciplines. They may also be useful for prospective parents because a 3D physical model with the characteristics of the fetus should allow a more direct emotional connection to their unborn child.

# Beyond VQ Scan-Nuclear Medicine and Molecular Imaging in the Chest

Monday, Nov. 28 12:15PM - 12:45PM Room: S503AB Station #4

#### **Participants**

Joanna E. Kusmirek, MD, Richmond, VA (Presenter) Nothing to Disclose

Jeffrey P. Kanne, MD, Madison, WI (*Abstract Co-Author*) Research Consultant, PAREXEL International Corporation; Advisory Board, F. Hoffmann-La Roche Ltd

Cristopher A. Meyer, MD, Madison, WI (Abstract Co-Author) Stockholder, Cellectar Biosciences, Inc Investor, NeuWave, Inc

## **TEACHING POINTS**

The exhibit will:- review commonly used nuclear medicine applications in chest imaging- provide helpful tips in interpretationhighlight technical and interpretative pitfalls- describe rare and evolving techniques to include molecular imaging Familiarity with nuclear medicine thoracic imaging applications is crucial for radiologists serving as consultants to referring clinicians, especially in unusual and challenging cases, when routine imaging tests fail to establish the diagnosis.

## **TABLE OF CONTENTS/OUTLINE**

Major topics:VQ scintigraphy in the era of CTA and MRA: imaging during pregnancy (dose reduction options), chronic thromboembolic disease and preoperative quantitative scans, tips for interpretation, examples of non-embolic abnormalities, right-to-left shunt quantification. Oncologic imaging: gallium and thallium scintigraphy, neuroendocrine imaging (MIBG, Octreotide, DOTA-TATE), and newer PET tracers in cancer imaging (F18-FMISO, F18-FLT, C11-thymidine). Inflammation/infection imaging: sarcoidosis (gallium, FDG PET/CT, and cardiac PET), labeled WBC imaging, FDG PET/CT for relapsing polychondritis and vasculitis, radiolabeled antibodies and peptides. in vascular graft infection. Pleura and miscellaneous: FDG PET/CT for pleural pathology, scintigraphic evaluation of abdominal-pleural fistulas, hepatic hydrothorax, splenosis.

#### **Honored Educators**

Presenters or authors on this event have been recognized as RSNA Honored Educators for participating in multiple qualifying educational activities. Honored Educators are invested in furthering the profession of radiology by delivering high-quality educational content in their field of study. Learn how you can become an honored educator by visiting the website at: https://www.rsna.org/Honored-Educator-Award/

Jeffrey P. Kanne, MD - 2012 Honored Educator Jeffrey P. Kanne, MD - 2013 Honored Educator

# MI209-SD-MOA2

Dual-Modal Positron-Emission Tomography (PET)/near Infrared Fluorescent Imaging-based in Vivo T Cell Tracking Platform

Monday, Nov. 28 12:15PM - 12:45PM Room: S503AB Station #2

# Participants

Stefan Harmsen, PhD, New York, NY (*Presenter*) Nothing to Disclose Ilker Medine, New York, NY (*Abstract Co-Author*) Nothing to Disclose Fuat Nurili, New York, NY (*Abstract Co-Author*) Nothing to Disclose Jose Lobo, New York, NY (*Abstract Co-Author*) Nothing to Disclose Maxim A. Moroz, MD, New York, NY (*Abstract Co-Author*) Nothing to Disclose Richard Ting, PhD, New York, NY (*Abstract Co-Author*) Nothing to Disclose Nagavarakishore Pillarsetty, New York, NY (*Abstract Co-Author*) Nothing to Disclose Vladimir Ponomarev, MD, New York, NY (*Abstract Co-Author*) Nothing to Disclose Oguz Akin, MD, New York, NY (*Abstract Co-Author*) Nothing to Disclose Omer Aras, MD, New York, NY (*Abstract Co-Author*) Nothing to Disclose

## PURPOSE

We explored the feasibility of labeling human T cells with a 89Zr-PET/NIRF imaging agent to enable in vivo T cell tracking over a range of scales.

## **METHOD AND MATERIALS**

Human T cells were labeled with a dual-modal 89Zr-labeled NIRF nanoparticle using protamine sulfate (PS) and heparin (H). The effects of the labeling on cell viability were examined by Trypan blue staining. In vivo trafficking of 89Zr-PET/NIRF-labeled T cells were performed using a small animal PET and NIRF imager.

#### RESULTS

A high level of cell labeling was achieved after incubating T cells with the 89Zr/NIRF imaging agent for 30 min in the presence of the PS-H serum-free mixture. In vitro microPET imaging and gamma counting as well as optical imaging of the labeled T cells demonstrated that the PS-H labeling procedure resulted in improved labeling relative to other methods without affecting cell viability and functionality. Upon i.v. administration, we successfully tracked the dual-modal 89Zr/NIRF nanoparticle labeled T cells by small animal PET and end-point NIRF imaging. The labeled T cells were initially distributed to the lungs, and then migrated to the liver and spleen over longer periods of time.

#### CONCLUSION

We developed intrinsically 89Zr-labeled NIRF nanoparticles that can be used to introduce dual-modal PET/NIRF imaging capabilities to T cells using a protamine/heparin cell labeling procedure. Our results indicate that T cells can be safely and efficiently labeled with these dual-modal imaging probes without compromising their viability function to enable T cell tracking over long-periods of time and over a range of scales.

# **CLINICAL RELEVANCE/APPLICATION**

Our method could be applied to various cell types and provides a new tool for sensitive in vivo cell tracking in a preclinical as well as clinical setting to monitor the fate of these cells.

Chemical Exchange Saturation Transfer (CEST) Imaging vs. Diffusion-Weighted MR Imaging vs. FDG-PET/CT: Capability of Molecular Information for Differentiation of Malignant from Benign Pulmonary Lesions

Monday, Nov. 28 12:15PM - 12:45PM Room: S503AB Station #3

# Participants

Yoshiharu Ohno, MD, PhD, Kobe, Japan (*Presenter*) Research Grant, Toshiba Corporation; Research Grant, Koninklijke Philips NV; Research Grant, Bayer AG; Research Grant, DAIICHI SANKYO Group; Research Grant, Eisai Co, Ltd; Research Grant, Fuji Pharma Co, Ltd; Research Grant, FUJIFILM RI Pharma Co, Ltd; Research Grant, Guerbet SA; Masao Yui, Otawara, Japan (*Abstract Co-Author*) Employee, Toshiba Corporation Yuji Kishida, MD, Kobe, Japan (*Abstract Co-Author*) Nothing to Disclose Shinichiro Seki, Kobe, Japan (*Abstract Co-Author*) Nothing to Disclose Hisanobu Koyama, MD, PhD, Kobe, Japan (*Abstract Co-Author*) Nothing to Disclose Takeshi Yoshikawa, MD, Kobe, Japan (*Abstract Co-Author*) Research Grant, Toshiba Corporation Yoshiko Ueno, MD, PhD, Montreal, QC (*Abstract Co-Author*) Nothing to Disclose Kouya Nishiyama, Kobe, Japan (*Abstract Co-Author*) Nothing to Disclose Katsusuke Kyotani, RT, Kobe, Japan (*Abstract Co-Author*) Nothing to Disclose Mitsue Miyazaki, PhD, Otawara, Japan (*Abstract Co-Author*) Nothing to Disclose Mitsue Miyazaki, PhD, Kobe, Japan (*Abstract Co-Author*) Research Grant, Toshiba Corporation Kazuro Sugimura, MD, PhD, Kobe, Japan (*Abstract Co-Author*) Research Grant, Toshiba Corporation Kazuro Sugimura, MD, PhD, Kobe, Japan (*Abstract Co-Author*) Research Grant, Toshiba Corporation

# PURPOSE

To directly and prospectively compare the capability for differentiation of malignant from benign pulmonary nodules and/ or masses among chemical exchange saturation transfer (CEST) imaging targeted to amide (-NH)groups, diffusion-weighted MR imaging (DWI) and FDG-PET/CT.

## **METHOD AND MATERIALS**

Eighty-eight consecutive patients (54 men and 34 women; mean age 70 years) with pulmonary nodules and/ or masses underwent CEST imaging and DWI at a 3T MR system, FDG-PET/CT and pathological and/or follow-up examinations. According to final diagnoses, all lesions were divided into malignant (n=49) and benign (n=39) groups. To obtain CEST imaging data in each subject, respiratory-synchronized fast advanced spin-echo images were conducted following a series of magnetization transfer (MT) pulses. Then, magnetization transfer ratio asymmetry (MTRasym) was calculated from z-spectra at 3.5ppm in each pixel, and MTRasym map was computationally generated. To evaluate the capability for differentiation between two groups at each lesion, MTRasym, apparent diffusion coefficient (ADC) and SUVmax were assessed by ROI measurements. To compare each index between two groups, Student's t-test was performed. Then, ROC analysis was performed to determine each feasible threshold value for differentiation of two groups. Finally, sensitivity, specificity and accuracy were compared each other by McNemar's test.

## RESULTS

Mean MTRasym (1.97±6.38%), ADC (1.17±0.25×10-3mm2/sec) and SUVmax (3.19±1.60) of malignant group had significant difference with those of benign group (MTRasym: -2.9±4.9%, p=0.0002; ADC:  $1.33\pm0.18\times10-3mm2/sec$ , p=0.0024, SUVmax: 2.27±0.48, p=0.0008). Results of ROC analysis showed that there were no significant differences of area under the curve (Az) among all indexes (MTRasym: Az=0.72, ADC: Az=0.67, SUVmax: Az=0.72) (p>0.05). When applied each feasible threshold value, there were no significant differences of diagnostic performance among all indexes (p>0.05).

#### CONCLUSION

CEST imaging is considered at least as valuable as DWI and FDG-PET/CT for differentiation of malignant from benign pulmonary lesions.

# **CLINICAL RELEVANCE/APPLICATION**

CEST imaging is considered at least as valuable as DWI and FDG-PET/CT for differentiation of malignant from benign pulmonary nodules and/ or masses.

Necrotizing Fasciitis: A Review of Pathophysiology, Early and Late Radiographic and Cross-sectional Imaging Features, and Clinical Management

Monday, Nov. 28 12:15PM - 12:45PM Room: MK Community, Learning Center Station #8

## Participants

Andrew M. Petraszko, MD, Detroit, MI (*Presenter*) Nothing to Disclose Matthew C. Rheinboldt, MD, Detroit, MI (*Abstract Co-Author*) Nothing to Disclose

# **TEACHING POINTS**

the purpose of this review is to: review the pathophysiology underlying types I and II necrotizing fasciitis, potential comorbidities, the three stages of clinical presentation and strategms for management describe the radiographic, sonographic, CT and MR imaging findings of necrotizing fasciitis with an emphasis on detecting potential early findings on cross-sectional imaging prior to the formation of frank soft tissue emphysema discuss potential clinical and imaging differential diagnostic considerations

# TABLE OF CONTENTS/OUTLINE

introduction pathophysiology, clinical staging and potential comorbidities type I necrotizing fasciitis Fournier's gangrene type II necrotizing fasciitis radiographic features cross-sectional features early signs: deep fascial exudative thickening, hyperemia and non-enhancement, multicompartmental involvement soft tissue emphysema differential diagnostic considerations cellulitis, paraneoplastic and eosinophilic fasciitis, dermatomyositis, lupus myofasciitis, compartment syndrome and myonecrosis, clinical management summary

# MK208-ED-MOA10

Dynamic Ultrasound in the Shoulder Impingement: Easy and Useful

Monday, Nov. 28 12:15PM - 12:45PM Room: MK Community, Learning Center Station #10

#### **Participants**

Montserrat C. del Amo, Barcelona, Spain (*Presenter*) Nothing to Disclose Jaume Pomes, MD, Barcelona, Spain (*Abstract Co-Author*) Nothing to Disclose Xavier Tomas-Batlle, MD, Barcelona, Spain (*Abstract Co-Author*) Nothing to Disclose Ana Isabel Garcia, MD, Barcelona, Spain (*Abstract Co-Author*) Nothing to Disclose Isaac Pomes, Barcelona, Spain (*Abstract Co-Author*) Nothing to Disclose Jose Bonilla, Barcelona, Spain (*Abstract Co-Author*) Nothing to Disclose

# **TEACHING POINTS**

. To show the importance to adding a dynamic study in the routine ultrasound exam of the shoulder. To describe and expose the dynamic maneuvers for evaluating impingement with images and videos of ultrasound findings

# TABLE OF CONTENTS/OUTLINE

Impingement syndrome is produced by dynamic changes or compression. The supraspinatus tendon and subacromial bursa are "impinged" between: humeral head, acromion and coracoacromial ligament (CAL). MRI and basal US cannot easily prove conflict in the subacromial space. After routine US using high frequency linear-array transducers, dynamic assessment of the shoulder will be performed. In the dynamic study, the arm should be positioned at 60-degree forward flexion, 60-degree abduction and with internal rotation of the shoulder. The ultrasound probe is positioned in the coronal plane along the long axis of the supraspinatus tendon, between the acromion and the greater tuberosity. The explorer moves few times the arm in this position. The motion of the bursa, supraspinatus tendon, humeral head and CAL is seen well and furthermore allows us better diagnosis of lesions in the supraspinatus tendon. Also, with the arm lifted 45 degrees, we can show changes in the subacromial space. Dynamic US shows these structures in motion, check their involvement in the impingement and the consequences in the tendon and bursa.

Capsuloligamentous Plane of the Knee: Illustrative Review of Anatomy and Component Injuries with Biomechanical Approach of the Knee Trauma

Monday, Nov. 28 12:15PM - 12:45PM Room: MK Community, Learning Center Station #11

# Participants

Yun Hee Cho, MD, Seongnam, Korea, Republic Of (*Presenter*) Nothing to Disclose Yusuhn Kang, MD, Seoul, Korea, Republic Of (*Abstract Co-Author*) Nothing to Disclose Eugene Lee, Seongnam-Si, Korea, Republic Of (*Abstract Co-Author*) Nothing to Disclose Joon Woo Lee, MD, PhD, Sungnamsi, Korea, Republic Of (*Abstract Co-Author*) Nothing to Disclose Joong Mo Ahn, MD, PhD, Pittsburgh, PA (*Abstract Co-Author*) Nothing to Disclose Heung Sik Kang, Gyeonggi-Do, Korea, Republic Of (*Abstract Co-Author*) Nothing to Disclose

## **TEACHING POINTS**

The complex anatomy of the knee is due largely to the controversies about anatomical description of capsules and ligaments of the knee. The injured capsuloligamentous components reflect the mechanism of injury. Understanding of the capsuloligamentous plane of the knee will enhance the detection and extent evaluation of the knee injury. The goal of this exhibit is to present in detail the complex anatomy and imaging findings of the capsuloligamentous plane and associated traumatic abnormality.

## **TABLE OF CONTENTS/OUTLINE**

1. Introduction. a. Illustrative review of anatomy with schematic drawings and MR imaging.

- b. Review of the controversies about anatomical description of capsules and ligaments of the knee.2. Anatomy and mechanism based approach of the knee injury. a. Review of imaging findings about the capsuloligamentous injuries of the knee.
- b. Associated lesions including bone and cartilage injury.3. Summary.

4. References.

# MK300-SD-MOA1

# Prevalence of Vertebral Compression Fractures at Abdominal CT According to Trabecular Attenuation

Monday, Nov. 28 12:15PM - 12:45PM Room: MK Community, Learning Center Station #1

#### Participants

Peter Graffy, Madison, WI (*Presenter*) Nothing to Disclose Timothy J. Ziemlewicz, MD, Madison, WI (*Abstract Co-Author*) Consultant, NeuWave Medical, Inc Perry J. Pickhardt, MD, Madison, WI (*Abstract Co-Author*) Co-founder, VirtuoCTC, LLC; Stockholder, Cellectar Biosciences, Inc; Stockholder, SHINE Medical Technologies, Inc; Research Grant, Koninklijke Philips NV

# PURPOSE

Abdominal CT scans contain robust bone data that are often underutilized, but opportunistic osteoporosis screening is now gaining traction. The purpose of this study was to correlate L1 trabecular HU measurements with prevalent vertebral body fractures in older adults undergoing abdominal CT for other indications.

## **METHOD AND MATERIALS**

ROI mean HU measurement of the anterior trabecular space of the L1 vertebral body was retrospectively performed on the axial CT images in 214 consecutive adults over the age of 65 years (Mean age 74.3  $\pm$  6.2 years; 93 men, 121 women), regardless of study indication. Sagittal CT scout view and sagittal reconstructions were analyzed for prevalent moderate (grade 2) or severe (grade 3) thoracolumbar vertebral compression fractures, according to the Genant semi-quantitative assessment method. All potential fractures were verified by a second experienced radiologist. Diagnostic performance of L1 HU alone for predicting prevalent vertebral fractures was performed, including ROC analysis.

## RESULTS

A total of 37 (17%) individuals (mean age, 76.5 years; 19 men, 18 women) had at least one moderate-severe vertebral fracture, and 13 patients had multiple fractures. Mean L1 attenuation was 74.0 HU among patients with a prevalent fracture, compared with 123.5 HU among patients without a fracture (p<0.001). Fracture prevalence increased to 49% (32/66) at or below L1 attenuation of 90 HU. Sensitivity and specificity for fracture was 70% and 87% at a threshold of 80 HU, 86% and 81% at a 90 HU threshold, and 92% and 69% at a 100 HU threshold, respectively. The corresponding area under the ROC curve (ROC AUC) was 0.893.

## CONCLUSION

L1 vertebral trabecular attenuation is highly predictive of prevalent vertebral fractures. When L1 attenuation measures 90-100 HU or less on the axial images at routine abdominal CT, the sagittal reconstruction should be scrutinized for vertebral compression fractures.

# **CLINICAL RELEVANCE/APPLICATION**

Early incidental/opportunistic detection of osteoporosis via abdominal CT is easy to incorporate into routine practice and provides added value to our practice.

# **Honored Educators**

Presenters or authors on this event have been recognized as RSNA Honored Educators for participating in multiple qualifying educational activities. Honored Educators are invested in furthering the profession of radiology by delivering high-quality educational content in their field of study. Learn how you can become an honored educator by visiting the website at: https://www.rsna.org/Honored-Educator-Award/

Perry J. Pickhardt, MD - 2014 Honored Educator

Feasibility of Volumetric ADC Mapping to Tumor Habitats Derived from Dynamic Contrast Enhanced MRI in Soft Tissue Sarcomas

Monday, Nov. 28 12:15PM - 12:45PM Room: MK Community, Learning Center Station #2

# Participants

Jared S. Mahan, MD, Miami, FL (*Presenter*) Nothing to Disclose Ty K. Subhawong, MD, Miami, FL (*Abstract Co-Author*) Nothing to Disclose Yu-Cherng C. Chang, Miami, FL (*Abstract Co-Author*) Nothing to Disclose Raphael Yechieli, MD, Detroit, MI (*Abstract Co-Author*) Nothing to Disclose Radka S. Stoyanova, MS, Philadelphia, PA (*Abstract Co-Author*) Nothing to Disclose

# PURPOSE

To determine feasibility of semi-automated volumetric delineation of soft tissue sarcoma habitats from Dynamic Contrast Enhanced (DCE) MRI data, and compare volumetric ADC measurements among those habitats.

# **METHOD AND MATERIALS**

Eight patients with soft tissue sarcomas underwent MRI with DWI (b-values 50 and 600 s/mm2) and DCE with 10 sec temporal resolution. Tumors were manually segmented in 3D using T1 post-contrast. Tumor habitats were delignated using previously developed technique that automatically identifies three unique temporal patterns from DCE-MRI datasets corresponding to well-perfused, hypoxic, and necrotic tumor environments. ADC maps were co-registered with T1 MRI and ADC mean values were derived for each habitat. ADC were compared across tumor environments.

### RESULTS

The DCE-MRI dataset allowed identification of three habitats 7 patients, and 2 habitats in one patient with a small residual subcutaneous tumor. Mean tumor volume was 151 cc. Mean ADC of hypoxic, well-perfused, and necrotic tumor compartments were 1.25, 1.33, and 1.33 x 10–3 mm2/sec, respectively; although there was a slight increase in ADC values in the necrotic habitat, this small 0.08 x 10–3 mm2/sec within-subject difference between well-perfused and necrotic compartments was not statistically significant (p = 0.27, paired t-test). The volumetric % necrosis correlated with % histologic necrosis in 5 patients where available (r = 0.91). Ktrans values in hypoxic, well-perfused, and necrotic tumor compartments were 0.16, 0.097, and 0.049 min-1, respectively; there was little correlation with tumor habitat mean ADC (Pearson r range -0.0.19 to 0.047).

# CONCLUSION

Volumetric mean ADC values showed little correlation with automatically delineated tumor habitats in soft tissue sarcoma regardless of treatment response; the non-overlapping nature of these results suggests they may serve complementary roles in assessing tumor viability in different sarcoma microenvironments.

#### **CLINICAL RELEVANCE/APPLICATION**

Combining volumetric ADC data and DCE sequences with automated identification of tumor habitats is feasible in soft tissue sarcoma and could improve quantitative multiparametric tumor response assessment.

Accelerated Onset of Knee Osteoarthritis - Role of MRI-Defined Risk Factors One Year Prior Osteoarthritis Incidence

Monday, Nov. 28 12:15PM - 12:45PM Room: MK Community, Learning Center Station #3

# Participants

Frank W. Roemer, MD, Boston, MA (*Presenter*) Chief Medical Officer, Boston Imaging Core Lab LLC; Research Director, Boston Imaging Core Lab LLC; Shareholder, Boston Imaging Core Lab LLC; ; Kent C. Kwoh, MD, Pittsburgh, PA (*Abstract Co-Author*) Advisory Panel, Pfizer Inc Data Safety Monitoring Board, Novartis AG Erin Ashbeck, Tucson, AZ (*Abstract Co-Author*) Nothing to Disclose Charles Ratzlaff, PhD, Boston, MA (*Abstract Co-Author*) Nothing to Disclose Michael Hannon, Oakland, PA (*Abstract Co-Author*) Nothing to Disclose Ali Guermazi, MD, PhD, Boston, MA (*Abstract Co-Author*) President, Boston Imaging Core Lab, LLC Research Consultant, Merck KgaA Research Consultant, Sanofi-Aventis Group Research Consultant, TissueGene, Inc Research Consultant, OrthoTrophic Research Consultant, AstraZeneca PLC

#### PURPOSE

To identify structural features on MRI that distinguish knees with accelerated incident radiographic osteoarthritis ROA) from those with slow development of OA.

## METHOD AND MATERIALS

Participants were drawn from the Osteoarthritis Initiative (OAI) study. Incident cases of ROA were identified, defined as Kellgren and Lawrence (KL) grade  $\geq 2$ , through 48 months of follow-up. Structural features in the two years prior to incident ROA were assessed using the semi-quantitative MOAKS instrument. Two radiographic definitions of the development of accelerated incident OA over two annual OAI visits were considered as outcomes in the analyses, i.e. accelerated KL grade (i.e., from KL 0 or 1 to  $\geq 3$ ) and accelerated OARSI medial joint space narrowing (i.e., OARSI JSN; 0 to  $\geq 2$  or 1 to 3). The association between structural damage one year prior to incident ROA and accelerated incident ROA compared to those with slow development of incident ROA (i.e., from KL 0 or 1 to 2 or OARSI JSN from 0 to 1 or 1 to 2) was estimated using logistic regression with generalized estimating equations with knees showing slow incident ROA as the referent group.

#### RESULTS

Altogether 328 knees were included for the KL grade definition and 329 knees for the JSN definition. 20.4% and 9.1% showed accelerated incident ROA according to the different definitions. One year prior to incident ROA, only presence of effusion-synovitis was associated with increased odds of accelerated early OA based on KL Grade (OR=1.97, 95%CI[1.10, 3.51], p=0.0223). None of the other analyzed structural risk factors was more commonly associated with accelerated incident ROA compared to those knees that with slow development of incident ROA.

## CONCLUSION

Presence of effusion-synovitis one year prior incident ROA is associated with accelerated incident ROA based on the K-L grade definition supporting a role of joint inflammation in accelerated disease onset. The fact that presence of none of the other structural parameters could distinguish knees with accelerated from those with slow incidence of ROA suggests that factors may play a role in radiographically defined accelerated disease onset.

# **CLINICAL RELEVANCE/APPLICATION**

A subgroup of patients with early knee OA shows accelerated disease onset with inflammation being a strong risk factor for this phenotype. Further work is needed to understand whether targeting inflammation early in the disease course may prevent knees from an accelerated disease course.

# **Honored Educators**

Presenters or authors on this event have been recognized as RSNA Honored Educators for participating in multiple qualifying educational activities. Honored Educators are invested in furthering the profession of radiology by delivering high-quality educational content in their field of study. Learn how you can become an honored educator by visiting the website at: https://www.rsna.org/Honored-Educator-Award/

Ali Guermazi, MD, PhD - 2012 Honored Educator

Early MRI of Occult Hip Fracture in Symptomatic Patients with Normal Hip Radiographs: A Cost-Effectiveness Study from a Health-Services Prospective

Monday, Nov. 28 12:15PM - 12:45PM Room: MK Community, Learning Center Station #5

# Participants

Eman Alqahtani, MD, MPH, La jolla, CA (*Presenter*) Nothing to Disclose Evelyne Fliszar, MD, Mount Royal, QC (*Abstract Co-Author*) Nothing to Disclose Donald L. Resnick, MD, San Diego, CA (*Abstract Co-Author*) Nothing to Disclose Brady K. Huang, MD, San Diego, CA (*Abstract Co-Author*) Nothing to Disclose

## PURPOSE

Hip fractures are common cause of morbidity and mortality in elderly patients, and is expected to double or triple due to an aging population. Approximately 5% of patients will have normal hip radiographs despite having an occult fracture. MRI can detect up to 90% of those occult fractures; however, it needs to be performed shortly after the trauma for optimal survival benefit. Our study compares lifetime health outcomes, healthcare costs, and incremental cost-effectiveness of occult hip fractures without and with early MRI

#### **METHOD AND MATERIALS**

A healthcare analytic model was created to compare the lifetime cost and lifetime health outcome of early hip MRI versus no MRI in symptomatic patients with occult hip fractures who had negative hip radiographs. The 2 adverse outcomes considered are: early morbidity and mortality in delayed or no surgical intervention and complications of surgery despite early detection. A Markov Monte Carlo decision model was developed to calculate the lifetime costs and effectiveness, quality-adjusted life-years (QALYs) and incremental cost-effectiveness ratio (ICER). Gross and micro-cost data for procedure, medical and surgical costs, were obtained from published sources. The cost and health outcomes were discounted at %3 to account for future cost increase. A number of variables, and probabilities of surgical complications were evaluated with sensitivity analysis

#### RESULTS

For a 65 years old male patient, early MRI of occult hip fracture followed by early-uncomplicated surgical repair had higher QALYs and lower immediate costs (14.41 QALYs, \$57.992) compared to patients who did not receive early MRI and subsequently had a complicated clinical course (12.88 QALYs, \$71.600). The ICER was -\$8,195 per QALY. As the probability of surgical complications increased, both groups would have similar costs and outcomes. Also, the sensitivity of MRI for the detection of occult fracture influenced the results, while MRI cost had less influence

#### CONCLUSION

Early hip MRI in patients with occult hip fractures can be a cost-effective method to identify patients who are most likely to benefit from early surgery

## **CLINICAL RELEVANCE/APPLICATION**

Hip fractures are an increasing public health burden in an aging population. Failure to identify occult hip fractures can lead to significant morbidity and mortality for elderly patients. Timely performance of MRI can carry survival benefits as well as health services saving

# Sciatic Nerve Anatomical Variants and Piriformis Syndrome: Is It Painful to Be Different

Monday, Nov. 28 12:15PM - 12:45PM Room: MK Community, Learning Center Station #6

#### **Participants**

Adam C. Luce, MD, MS, Stanford, CA (*Presenter*) Nothing to Disclose Praveen Anchala, MD, Saint Louis, MO (*Abstract Co-Author*) Nothing to Disclose Christopher F. Beaulieu, MD, PhD, Stanford, CA (*Abstract Co-Author*) Nothing to Disclose Amelie M. Lutz, MD, Stanford, CA (*Abstract Co-Author*) Nothing to Disclose

# PURPOSE

To investigate the purported relationship between sciatic nerve variant anatomy and piriformis syndrome and radiculopathy, previously related in the literature through surgical case series and cadaver studies, using anatomical data from hip MRI correlated with clinical data from chart review.

## **METHOD AND MATERIALS**

Over 18 months at an academic medical center, 343 hip MRIs were completed for all indications. MRI studies were excluded if they were repeat studies or if the protocol was insufficient to determine anatomical variants. Images were reviewed by MSK radiologists to evaluate for sciatic nerve variants, and patients were categorized into Beaton and Anson anatomical types. Retrospective chart review determined the prevalence of ICD9 diagnoses related to radiculopathy and pain syndromes, as well as explicit diagnosis of piriformis syndrome or buttock pain, which do not have dedicated ICD9 codes. Student's t test was completed for each diagnosis, comparing the prevalence of the diagnosis in the variant anatomy and normal groups.

# RESULTS

263 MR studies were included in the analysis. Sciatic nerve variants were present in 50 hips (19.0%). Piriformis syndrome had a similar prevalence in variant and normal hips (8.0% vs 7.5%, respectively) and there was no significant difference in prevalence (p=0.55). Similarly, there was no significant difference in the prevalence of buttock pain (38.0% vs 31.5%, p=0.81). Additionally, using a 5% significance level, there was no significant difference between the groups for the investigated ICD9 diagnoses (lesion of the sciatic nerve; sciatica; disorder of sacrum; thoracic or lumbosacral neuritis or radiculitis; neuralgia, neuritis, and radiculitis unspecified).

## CONCLUSION

No significant differences in prevalence of piriformis syndrome, buttock pain, and the various investigated pain syndromes existed between the patients with anatomical variants of the sciatic nerve and those with normal anatomy. This first radiologic study into the relationship between sciatic nerve variant anatomy and pain syndromes calls into question this purported relationship.

## **CLINICAL RELEVANCE/APPLICATION**

This first radiologic study into the relationship between sciatic nerve variant anatomy and pain syndromes calls into question this purported relationship.

Image-guided Percutaneous Biopsy of Rib Lesions: A Retrospective Review of Efficacy and Safety in 166 Patients

Monday, Nov. 28 12:15PM - 12:45PM Room: MK Community, Learning Center Station #7

# Participants

Casey Medina, BA, Houston, TX (*Presenter*) Nothing to Disclose Samuel Kusin, Houston, TX (*Abstract Co-Author*) Nothing to Disclose Michael J. Wallace, MD, Houston, TX (*Abstract Co-Author*) Speaker, Siemens AG Research support, Siemens AG Sharjeel Sabir, MD, Houston, TX (*Abstract Co-Author*) Nothing to Disclose

## PURPOSE

To assess the efficacy and safety of percutaneous image-guided biopsy of rib lesions.

## **METHOD AND MATERIALS**

A retrospective review of all percutaneous image-guided rib biopsies performed between 8/2009 and 9/2014 was undertaken. Biopsy was performed with coaxial technique.13-20 gauge core needles and 22 gauge FNA needles were used. Imaging guidance was with CT, US, or MRI. Procedures were performed with moderate sedation or general anesthesia, dependent on patient's clinical status. Patient demographic, lesion imaging, and procedural technique variables were collected. Complications associated with the procedures were noted. The pathologiy reports were reviewed and the results were categorized as malignant, benign, or non-diagnostic. For any patient with a benign diagnosis, follow up imaging or clinic notes were reviewed to confirm benignity of the lesion. In addition, the pathology reports of all patients that had surgical resection were reviewed.

### RESULTS

166 patients underwent 172 procedures. 74 (45%) were women with an average age of 59 years (range 13-84). Nearly all of the lesions were metastases most commonly from lung 24%, breast 20%, and prostate 14%. Of the biopsied lesions, 43% were FDG and 43% were MDP avid on nuclear imaging performed within 6 months prior to biopsy. The lesions biopsied were lytic rib 62%, sclerotic rib 21%, or soft tissue extending from rib 17%. The average long axis size of lesions targeted was 2.7 cm +/-1.8. The procedures were performed under CT 93%, US 5.8%, and MRI 1.2% guidance. 99% of procedures were technically successful. 139 (81%) procedures had core biopsy of which 94% were diagnostic and 150 (87%) procedures had FNA of which 89% were diagnostic. 2 (1%) complications occurred: 1 pneumothorax needing chest tube, 1 hematoma requiring pressure. 6 patients had repeat procedures: 2 for treatment assessment, 2 showed new malignancy, 1 true negative, and 1 false negative. 5 patients had post-biopsy surgical resection of the rib lesion: 3 cases were concordant and 2 cases were discordant with biopsy. The sensitivity of rib biopsy was 95%, specificity was 100%, positive predictive value was 100%, negative predictive value was 93%.

# CONCLUSION

Image-guided percutaneous rib biopsy is both effective and safe in the diagnosis of rib lesions.

## **CLINICAL RELEVANCE/APPLICATION**

We show rib biopsies to be highly sensitive and specific as well as safe in a larger cohort of patients than previously reported.

Diagnostic Accuracy of MRI and Diffusion-weighted MR Neurography in Comparison with Clinical and Surgical Findings in Traumatic Brachial Plexus Injuries

Monday, Nov. 28 12:15PM - 12:45PM Room: MK Community, Learning Center Station #4

# Participants

Marcelo Bordalo-Rodrigues, MD,PhD, Sao Paulo, Brazil (*Presenter*) Nothing to Disclose Marcelo R. Rezende, PhD, MD, Sao Paulo, Brazil (*Abstract Co-Author*) Nothing to Disclose Hugo P. Costa, MD, Sao Paulo, Brazil (*Abstract Co-Author*) Nothing to Disclose Joao Carlos Rodrigues, MD, Sao Paulo, Brazil (*Abstract Co-Author*) Nothing to Disclose Alvaro Baik Cho Lee, MD,PhD, Sao Paulo, Brazil (*Abstract Co-Author*) Nothing to Disclose Giovanni G. Cerri, MD, PhD, Sao Paulo, Brazil (*Abstract Co-Author*) Nothing to Disclose

## PURPOSE

To evaluate the diagnostic accuracy of MRI in the diagnosis of traumatic brachial plexus injuries in adults, using surgical findings as the gold standard method. We also evaluated the accuracy of diffusion weighted image neurography (DW neurography) compared to conventional MRI and the ability to differentiate the three types of brachial plexus nerve injuries by MRI: avulsion, rupture and lesion-in-continuity.

## **METHOD AND MATERIALS**

Thirty-two patients with history and clinical diagnosis of traumatic brachial plexus injury were prospectively evaluated by a 1.5T MR magnet. MRI findings (obtained with and without the use of DW neurography) and clinical examination were compared with intraoperative findings. Sensitivities, specificities, accuracies, PPV and NPV were calculated. Interobserver agreement was performed by Spearman's rank correlation coefficient. Statistical analysis was performed with 5% significance association.

#### RESULTS

We found a high correlation between DW neurography and surgery (r=0.79) and a low correlation between conventional MRI and surgery (r=0.41). The interobserver correlation was higher for MRI with DW neurography (r=0.94) than for conventional MRI (r=0.75). The sensitivites, accuracies and positive predictive values obtained were above 90% for MRI, with no statistically significant difference (p>0.05). The specificities were generally higher for DW neurography (p<0.05). MRI demonstrated high sensitivity in the diagnosis of avulsion / rupture (94,1%) and low sensitivity in the diagnosis of lesion-in-continuity (42.8%). MRI accuracy (93.9%) was significantly higher than clinical examination (76.5%) in diagnosis of brachial plexus traumatic lesions (p <0.05).

#### CONCLUSION

MRI presents high accuracy and low specificities in the diagnosis of traumatic brachial plexus injuries. DW neurography provides a higher correlation with surgical results and higher interobserver correlations compared to conventional MRI. Also, MRI is useful in the diagnosis of avulsion and rupture, however it needs improvement for the diagnosis of lesion-in-continuity. MRI accuracy is significantly higher than clinical examination in diagnosis of the traumatic brachial plexus injuries.

# **CLINICAL RELEVANCE/APPLICATION**

MRI with the use of DW neurography is an accurate tool and may provide topographic diagnosis for the surgeon. However, MRI still needs improvement in the diagnosis of partial nerve lesions (lesions-in-continuity).

# MS109-ED-MOA1

Listening to Stiffness: A Comprehensive Review of Ultrasound Elastography Methods and Clinical Applications

Monday, Nov. 28 12:15PM - 12:45PM Room: MS Community, Learning Center Station #1

#### **Participants**

Rosa Maria Silveira Sigrist, MD, Palo Alto, CA (*Presenter*) Nothing to Disclose Joy Liau, MD, PhD, Palo Alto, CA (*Abstract Co-Author*) Nothing to Disclose Ahmed El Kaffas, PhD, Palo Alto, CA (*Abstract Co-Author*) Co-founder, Oncoustics Maria Cristina Chammas, MD, Sao Paulo, Brazil (*Abstract Co-Author*) Nothing to Disclose Juergen K. Willmann, MD, Stanford, CA (*Abstract Co-Author*) Research Consultant, Bracco Group; Research Grant, Siemens AG; Research Grant, Bracco Group; Research Grant, Koninklijke Philips NV; Research Grant, General Electric Company; Advisory Board, Lantheus Medical Imaging, Inc; Advisory Board, Bracco Group

## **TEACHING POINTS**

Review principles and concepts of Ultrasound Elastography (USE), a technique recently cleared by the FDA; Describe different USE techniques offered by various vendors and their limitations; Discuss current and future clinical applications of USE in liver, breast, thyroid, kidney, prostate and lymph nodes.

#### **TABLE OF CONTENTS/OUTLINE**

Introduction; Principles and Concepts of USE; Elastography Physics; USE Techniques: Strain Imaging (Strain Elastography and Acoustic Radiation Force Impulse Strain Imaging) and Shear Wave Imaging (1D Transient Elastography, Point Shear Wave Elastography and 2D Shear Wave Elastography); Technical Limitations; Clinical Applications: Liver (Diffuse Liver Disease, Portal Hypertension, Focal Liver Lesions); Breast; Thyroid; Kidney (Renal Fibrosis, Renal Focal Masses); Prostate; Lymph Nodes.For each clinical application mentioned, different USE techniques will be discussed as well as their limitations, current and future applications. Conclusion 'When Lost in Darkness He who Lights the Way, Marks Himself as Easy Prey': Lighting the Infection/Inflammation on Hybrid Imaging- Review of Literature

Monday, Nov. 28 12:15PM - 12:45PM Room: S503AB Station #11

#### Awards

**Certificate of Merit** 

#### **Participants**

Nitesh Shekhrajka, Aalborg, Denmark (*Abstract Co-Author*) Nothing to Disclose Krishnakumari A. Modi, MBBS, Hjorring, Denmark (*Abstract Co-Author*) Nothing to Disclose Rune V. Fisker, MD, Aalborg, Denmark (*Abstract Co-Author*) Nothing to Disclose Victor V. Iyer, MD, Aalborg, Denmark (*Abstract Co-Author*) Nothing to Disclose Ramune Aleksyniene, MD, PhD, Aalborg, Denmark (*Presenter*) Nothing to Disclose

# **TEACHING POINTS**

Diagnosis and characterization of the infectious or inflammatory processes is often challenging for clinicians as these are heterogeneous class of diseases. The diagnostics is most often performed with conventional radiology and biochemical tests. Nuclear medicine (NM) hybrid imaging techniques provides additional information about biological and biochemical changes in specific infectious and inflammatory processes. Our aim is to review and highlight the up-to-date literature recommendations and to establish our local regional guidelines for the best NM imaging modality choice for a given/suspected infection/inflammation in order to improve patient care.

# TABLE OF CONTENTS/OUTLINE

Each type of infection will be accompanied by a relevant first choice nuclear medicine image, supplemented by relevant CT/MRI/Xray image with discussion. We plan to discuss the following: Fever of unknown origin Metastatic infection with bacteremia Large vessel vasculitis Spondylodiscitis and vertebral osteomyelitis Peripheral acute osteomyelitis Peripheral chronic osteomyelitis Orthopaedic prosthesis and implant infection Charcot foot Infected diabetic foot Sarcoidosis Prosthetic valve endocarditis and/or metastastic infection UTI, polycystic kidneys & lever Suspected abscess in abdomen Vascular graft infections Infected foreign body

# Development of an Automatic Acquisition Time Control System for Whole-body PET

Monday, Nov. 28 12:15PM - 12:45PM Room: S503AB Station #6

#### **Participants**

Koumei Takauchi, Hiroshima, Japan (*Presenter*) Nothing to Disclose Ayaka Ushio, hiroshima, Japan (*Abstract Co-Author*) Nothing to Disclose Makoto Kobayashi, hiroshima, Japan (*Abstract Co-Author*) Nothing to Disclose Nobukazu Abe, hiroshima, Japan (*Abstract Co-Author*) Nothing to Disclose Makoto Iida, Hiroshima, Japan (*Abstract Co-Author*) Nothing to Disclose Kazuo Awai, MD, Hiroshima, Japan (*Abstract Co-Author*) Nothing to Disclose Kazuo Awai, MD, Hiroshima, Japan (*Abstract Co-Author*) Research Grant, Toshiba Corporation; Research Grant, Hitachi, Ltd; Research Grant, Bayer AG; Research Grant, Eisai Co, Ltd; Medical Advisor, General Electric Company; ; ; ; ;

#### PURPOSE

To develop a system in which the acquisition time is automatically regulated to obtain uniform image quality irrespective of the imaging site on whole-body FDG-PET scans (PET-automatic acquisition time control system: PET-AATC).

## **METHOD AND MATERIALS**

We arranged 3 NEMA image quality phantoms (Model NU-2001, national electrical manufacturers association) in series and set the FDG activity of all hot spheres to 6.6 kBq/ml, and their background activity to 1/4, 3/4, and 1/2 times. First we obtained a PET scout view (3 sec/bed) and then a standard WB-PET scan (300 sec/bed) in the same scan range.Image quality was evaluated using the actually measured contrast-to-noise ratio (aCNR) obtained on the WB-PET images of the NEMA phantoms. We also calculated the CNR (cCNR) obtained by converting the background activity and its standard deviation (SD). Conversion accuracy of cCNR was confirmed with the Pearson correlation coefficient of the cCNR and the aCNR. The cutoff value for CNR was acquired by ROC analysis of the visual score and the CNR. The CNR was the actually measured value of the NEMA phantoms on WB-PET images. The cCNR was obtained from an approximately straight line to acquire a conversion formula. The line was derived from the correlation between the background activity on PET-WB images and the true coincidence rate on a PET scout view, and their SDs. The cCNR was determined by using the converted background activity and the SD. Conversion accuracy was confirmed with the Pearson correlation accuracy activity and the SD. Conversion accuracy was confirmed with the CNR.

#### RESULTS

The correlation coefficient between the background activity and the true coincidence rate, their SD, and the cCNR and the aCNR were 0.99, 0.98, and 0.96, respectively (all: p<0.01). The area under the curve between the visual score and cCNR or aCNR was 0.96 and 0.95, respectively. The CNR cutoff value was 1.73 and 1.54, respectively.

# CONCLUSION

The cCNR and the aCNR were comparable for the evaluation of the image quality. We demonstrate that the CNR on WB-PET scans is an alternative cCNR on PET scout views. Our findings suggest that PET-AATC is feasible.

# **CLINICAL RELEVANCE/APPLICATION**

Automation of the acquisition time improved inhomogeneity of the image quality irrespective of the imaging site and yielded a diagnostic image quality at a short acquisition time.

Assessment of Primary Tumor FDG PET/CT Texture Features for Predicting Tumor Response to Chemoradiotherapy and Prognosis of Patients with Esophageal Cancer

Monday, Nov. 28 12:15PM - 12:45PM Room: S503AB Station #7

# Participants

Masatoyo Nakajo, MD, PhD, Kagoshima, Japan (*Presenter*) Nothing to Disclose Megumi Jinguji, Kagoshima, Japan (*Abstract Co-Author*) Nothing to Disclose Yoshiaki Nakabeppu, Kagoshima, Japan (*Abstract Co-Author*) Nothing to Disclose Ryutaro Higashi, MD, Kagoshima, Japan (*Abstract Co-Author*) Nothing to Disclose Yoshihiko Fukukura, MD, PhD, Kagoshima, Japan (*Abstract Co-Author*) Nothing to Disclose Takashi Yoshiura, MD, PhD, Kagoshima, Japan (*Abstract Co-Author*) Nothing to Disclose

#### PURPOSE

To investigate whether F-18-fluorodeoxyglucose (FDG) PET/CT texture features is useful for predicting outcomes to therapy in patients with esophageal cancer treated by chemoradiotherapy (CRT).

# METHOD AND MATERIALS

Fifty two patients with esophageal cancer were enrolled and underwent FDG PET/CT studies before CRT. In addition to SUVmax, SUVmean, metabolic tumor volume (MTV), total lesion glycolysis (TLG), heterogeneity parameters assessed by texture analysis including the intensity variability (IV) and size-zone variability (SZV) were obtained for primary lesions. IV measures the similarity in pixel intensities throughout the image and SZV measures the similarity in zone sizes. Heterogeneous images tend to have larger IV and SZV. Patients were classified as responders or non-responders according to RECIST. Progression free survival (PFS) and overall survival (OS) were calculated by Kaplan-Meier method. Prognostic significance was assessed by Cox proportional hazards analysis.

## RESULTS

There were 18 responders and 34 non-responders. The following parameters were significantly lower in the responders than in the non-responders; MTV (46.7 cm $3 \pm 33.3$  vs. 93.0 cm $3 \pm 64.3$ , P=.006), TLG (287.7  $\pm 249.6$  vs. 58 $2.2 \pm 434.9$ , P=.007), IV (17.9  $\pm$  10.5 vs. 32.2  $\pm$  18.6, P=.003) and SZV (291.2  $\pm$  201.3 vs. 519.7 $\pm$  319.1, P=.004). In Kaplan-Meier analysis, patients with lower values in the following parameters than those with higher values were significantly associated with longer median PFS and OS; MTV (PFS: 7 months vs. 11 months, P=.018; OS: 8 months vs. median not reached, P=.018), TLG (PFS: 7 months vs. 12 months vs. median not reached, P=.025), IV (PFS: 7 months vs. 13 months, P=.013; OS: 8 months vs. median not reached, P=.010; OS: 8 months vs. median not reached, P=.000; OS: 8 months vs. median not reached, P=.010; OS: 8 months vs. median not reached, P=.000; OS: 8 months vs. median not reached, P=.010; OS: 8 months vs. median not reached, P=.000; OS: 8 months vs. median not reached, P=.010; OS: 8 months vs. median not reached, P=.000; OS: 8 months vs. media

### CONCLUSION

Not only MTV and TLG, but also texture feature IV and SZV in baseline FDG PET/CT scans may predict treatment response and prognosis in patients with esophageal cancer treated by CRT.

# **CLINICAL RELEVANCE/APPLICATION**

The texture feature intensity variability and size-zone variability in baseline FDG PET/CT scans may predict treatment response and prognosis in patients with esophageal cancer treated by CRT.

The Utility of Surrogates for Lung Shunt Fraction in Patients with Hepatocellular Carcinoma being Evaluated for Yttrium-90 Radioembolization

Monday, Nov. 28 12:15PM - 12:45PM Room: S503AB Station #8

#### Awards

#### **Student Travel Stipend Award**

#### **Participants**

Joseph R. Kallini, MD, Detroit, MI (*Presenter*) Nothing to Disclose Ahmed Gabr, MD, MBBCh, Chicago, IL (*Abstract Co-Author*) Nothing to Disclose Ryan Hickey, MD, Chicago, IL (*Abstract Co-Author*) Advisor, BTG International Ltd Kush R. Desai, MD, Chicago, IL (*Abstract Co-Author*) Speakers Bureau, Cook Group Incorporated; Consultant, Cook Group Incorporated Bartley G. Thornburg, MD, Philadelphia, PA (*Abstract Co-Author*) Nothing to Disclose Riad Salem, MD, MBA, Chicago, IL (*Abstract Co-Author*) Research Consultant, BTG International Ltd Research Grant, BTG International Ltd Robert J. Lewandowski, MD, Chicago, IL (*Abstract Co-Author*) Advisory Board, BTG International Ltd; Advisory Board, Boston

Robert J. Lewandowski, MD, Chicago, IL (*Abstract Co-Author*) Advisory Board, BTG International Ltd; Advisory Board, Boston Scientific Corporation; Consultant, Cook Group Incorporated; Consultant, ABK Medical Inc

#### PURPOSE

To investigate the correlation of baseline and imaging characteristics with lung shunt fraction (LSF) as measured by technetium-99m macroaggregated albumin (99mTc-MAA) scan in patients with hepatocellular carcinoma (HCC)

#### **METHOD AND MATERIALS**

A cohort of 428 subjects with HCC from 2004 to 2011 was assessed for lung shunting by MAA scan. LSF measurements were obtained for each patient and categorized into low (LSF<10%), intermediate ( $10\% \le LSF \le 20\%$ ), and high (LSF>20%). Patient characteristics included age, gender, ethnicity, tumor burden (%), maximum dimension, focality, presence of extrahepatic metastases, macrosvascular invasion (hepatic and portal vein), ascites on imaging, baseline laboratory values, alpha-fetoprotein, and multiple staging systems. Correlations were expressed as likelihood ratios (LR+), Pearson correlation coefficients ("r"), and positive predictive values (PPV). Chi square test for categorical variables and nonparametric ANOVA for continuous variables were used for analysis.

## RESULTS

Most characteristics yielded low LR+ and PPV for high LSF, as well as "r" coefficients close to 0 (p<0.05). The absence of macrovascular invasion (PPV 85%), and tumor size  $\leq$ 5cm (LR+ 8.24, PPV 89%) were strongly predicitve of low LSF. ECOG 0 was 91% predictive of low LSF (p<0.05). United Network for Organ Sharing (UNOS) stage T2 (LR+ 13.14, PPV 93%), low GRoupe d'Etude et de Traitement du Carcinoma Hépatocellulaire (GRETCH) stage (PPV 94%), and BCLC Stage A (LR+ 23.67, PPV 96%) were very strongly predictive of low LSF (p<0.05).

## CONCLUSION

Several characteristics are statistically significant but weakly predictive of high LSF: laboratory values, imaging findings, and clinical assessments. The absence of macrovascular tumor invasion, small tumor size, and favorable prognostic stage/score were strongly associated with low LSF. These factors may serve as an adequate predictor of low LSF determined by 99mTc-MAA in clinical practice.

#### **CLINICAL RELEVANCE/APPLICATION**

The clinically and statistically significant predictors of LSF<10% can be used to confidently anticipate full-dose treatment with yttrium-90 (90Y) resin microspheres, planning of same-day MAA-90Y treatment via cross-sectional dosing assumptions, or to promote studies forgoing MAA in low-risk settings.

# A 2-h Delayed FDG PET/CT with Water Ingestion Increases the Detection of Primary Gastric Cancer

Monday, Nov. 28 12:15PM - 12:45PM Room: S503AB Station #9

#### **Participants**

Yoriko Kajiya, Kagoshima, Japan (*Presenter*) Nothing to Disclose Atsushi Tani, MD, PhD, Kagoshima, Japan (*Abstract Co-Author*) Nothing to Disclose Tooru Nandate, Kagoshima, Japan (*Abstract Co-Author*) Nothing to Disclose Keisuke Kariya, Kagoshima, Japan (*Abstract Co-Author*) Nothing to Disclose Masayuki Nakajo, PhD, Kagoshima, Japan (*Abstract Co-Author*) Nothing to Disclose Takashi Yoshiura, MD, PhD, Kagoshima, Japan (*Abstract Co-Author*) Nothing to Disclose

# PURPOSE

To evaluate whether a 2-h delayed FDG PET/CT with water ingestion increases the detection rate of primary gastric cancer.

## **METHOD AND MATERIALS**

The study population of 145 gastric cancer patients had 162 lesions: 89 early gastric cancers (T1, tumor invasion within 0.5 mm of the muscularis mucosa) and 73 advanced cancers (16 T1 lesions with > 0.5 mm penetration of the muscularis mucosa, 15 T2, 7 T3, 31 T4a, and 4 T4b lesions). PET/CT scans were performed 1 h after FDG injection (FS), immediately after the first scan, with 300–400 mL of water intake (SS), and as a 2-h delayed scan, with 300–400 mL of water intake (TS). Primary lesions were assessed as visible or non-visible. The SUVs of the tumors and adjacent nontumor gastric wall were obtained. The tumor-to-nontumor gastric wall SUV ratio was also estimated. Statistical differences in detection rates and SUV values were assessed using a McNemar test, and those in the SUV ratio using a one-way repeated measure ANOVA.

#### RESULTS

Sixty lesions were detected in FS, 69 in SS, and 76 in TS. No positive tumor became negative. SUV ratios were obtained for 57 of the 60 lesions detected; for the three lesions at the boundary of the normal gastric wall, SUVs were not determined. The detection rate was significantly better in TS than in FS and SS. The rates of early gastric cancer detection were 15.7% (14/89), 6.7% (6/89), and 11.2% (10/89) (FS vs. SS; P=0.125, SS vs. TS; P=0.125, FS vs. TS; P=0.008), respectively, and those of advanced gastric cancer 84.9% (62/73), 74.0% (54/73), and 80.8% (59/73) (FS vs. SS: P=0.063, SS vs. TS; P=0.25, FS vs. TS: P=0.008), respectively. SUV values were highest in TS; the  $\Delta$ SUV ratio was larger than the  $\Delta$ SUV. The SUVs of the 57 lesions were 8.0±5.2 (range: 2.2–34.7) for FS, 7.7±5.2 (2.2–34.2) for SS, and 9.4±6.7 (3.0–43.0) for TS (FS vs. SS: P=0.065, SS vs. TS: P<0.001, FS vs. TS: P<0.001), respectively. The corresponding SUV ratios were 3.1 ±2.6 (1.1–14.2), 4.9±3.5 (1.4–22.8), and 6.1±4.6 (1.7-29.7) (FS vs. SS: P<0.001, SS vs. TS: P<0.001, FS vs. TS: P<0.001).

#### CONCLUSION

A 2-h-delayed FDG PET/CT scan with water ingestion increases the detection rate of primary gastric cancers.

## **CLINICAL RELEVANCE/APPLICATION**

A 2-h delayed FDG PET/CT scan with water ingestion is recommended to improve the detection of primary gastric cancer.

# F-18 NaF PET/CT for the Evaluation of Carotid Artery Atherosclerosis

Monday, Nov. 28 12:15PM - 12:45PM Room: S503AB Station #10

#### **Participants**

Takashi Norikane, Kita-gun, Japan (*Presenter*) Nothing to Disclose Yuka Yamamoto, MD, PhD, Kagawa, Japan (*Abstract Co-Author*) Nothing to Disclose Yukito Maeda, Kita-gun, Japan (*Abstract Co-Author*) Nothing to Disclose Tetsuhiro Hatakeyama, Kagawa, Japan (*Abstract Co-Author*) Nothing to Disclose Yoshihiro Nishiyama, MD, Kagawa, Japan (*Abstract Co-Author*) Nothing to Disclose

#### PURPOSE

The purpose of this study was to investigate the feasibility of F-18 NaF (NaF) and F-18 FDG (FDG) on PET/CT for evaluation of carotid artery atherosclerosis.

# **METHOD AND MATERIALS**

A total of 17 patients with carotid artery stenosis of 50% or greater determined by using ultrasonography were examined with NaF PET/CT and FDG PET/CT. PET emission scanning of the neck region with a 15-min acquisition of one bed position was performed at 60 min after each radiotracer injection. CT images were used to draw region of interest (ROI) around area of plaque at the level of carotid bifurcation bilaterally. The maximum attenuation in Hounsfield units (HU) was calculated. The maximum standardized uptake value (SUV) was calculated for each ROI using the coregistered PET data. In one patient, only unilateral carotid artery was used because of indwelling stent.

## RESULTS

In 31 out of the 33 sites, increased NaF uptake was observed in areas overlying and adjacent to plaque. Thirty-one sites with increased NaF uptake had calcified plaque ( $\geq$ 130 HU) and 2 sites without increased NaF uptake had no calcified plaque (<130 HU), on CT images. A significant correlation was observed between NaF SUV and CT HU (r=0.593, p<0.001). There was no significant correlation between FDG SUV and CT HU. There was no significant correlation between NaF SUV and FDG SUV.

#### CONCLUSION

These preliminary results suggest that NaF PET/CT is feasible for evaluation of carotid artery atherosclerosis.

## **CLINICAL RELEVANCE/APPLICATION**

F-18 NaF PET/CT is feasible for evaluation of carotid artery atherosclerosis.

Overview of a Synthetic MRI: Basic, Clinical Applications, and Limitations

Monday, Nov. 28 12:15PM - 12:45PM Room: NR Community, Learning Center Hardcopy Backboard

#### Awards Certificate of Merit

#### Participants

Christina Andica, Tokyo, Japan (*Presenter*) Nothing to Disclose Akifumi Hagiwara, MD, Tokyo, Japan (*Abstract Co-Author*) Nothing to Disclose Masaaki Hori, MD, Tokyo, Japan (*Abstract Co-Author*) Nothing to Disclose Kanako K. Kumamaru, MD, PhD, Tokyo, Japan (*Abstract Co-Author*) Nothing to Disclose Misaki Nakazawa, Tokyo, Japan (*Abstract Co-Author*) Nothing to Disclose Nao Takano, Tokyo, Japan (*Abstract Co-Author*) Nothing to Disclose Koji Kamagata, Tyuuouku, Japan (*Abstract Co-Author*) Nothing to Disclose Mariko Yoshida, Tokyo, Japan (*Abstract Co-Author*) Nothing to Disclose Shigeki Aoki, MD, PhD, Tokyo, Japan (*Abstract Co-Author*) Nothing to Disclose

# **TEACHING POINTS**

Synthetic MRI is a quantification method that measures MR physical parameters by a single scan. From this quantitative data, tailored contrast-weighted image with any combination of TE, TR, and TI can be created and adjusted. Synthetic MRI also allows segmentation of different brain tissue type and automatic calculation of the segmented volume. The latest feature of synthetic MRI is myelin map, which used to estimate the presence of myelin and brain edema. Synthetic MRI shows many advantages in the evaluation of brain disorders; however some limitations were also noted.

## **TABLE OF CONTENTS/OUTLINE**

The purpose of this exhibit is to show: The basic physical principles of synthetic MRI. Clinical settings in our institute. The clinical applications of synthetic MRI in the evaluation of brain disorders, such as: Brain metastases: maximizing contrast between metastases and parenchyma. Meningeal enhancement: DIR to suppress the signals from CSF and fat in the bone marrow. Sturge-Weber syndrome: appropriate parameters and myelin map for showing "Accelerated Myelination". Multiple sclerosis: DIR, PSIR, and myelin map to assess lesions in multiple sclerosis. And many more. Limitation of synthetic MRI: partial volume effect, especially for fluid-attenuated inversion recovery (FLAIR) images and B1 inhomogeneity.

White-matter-attenuated Inversion Recovery (WAIR): A New Sequence for Evaluating Various Neurologic Diseases

Monday, Nov. 28 12:15PM - 12:45PM Room: NR Community, Learning Center Station #9

#### Awards

**Certificate of Merit** 

# Participants

Yoshito Tsushima, MD, Maebashi, Japan (*Presenter*) Institutional Research Grant, Bayer AG ; Institutional Research Grant, DAIICHI SANKYO Group; Institutional Research Grant, Eisai Co, Ltd; Institutional Research Grant, Nihon Medi-Physics Co, Ltd; Institutional Research Grant, FUJIFILM Holdings Corporation ; Institutional Research Grant, Fuji Pharma Co, Ltd; Institutional Research Grant, Siemens AG ; Institutional Research Grant, OncoTherapy Science, Inc; Institutional Research Grant, Becton, Dickinson and Company; Speaker, Bayer AG ; Speaker, DAIICHI SANKYO Group; Speaker, Eisai Co, Ltd; Speaker, Fuji Pharma Co, Ltd; Speaker, Guerbet SA; .;

Syunichi Motegi, Fujioka, Gunma, Japan (*Abstract Co-Author*) Nothing to Disclose Hiroyasu Tomonaga, MD, Maebashi, Japan (*Abstract Co-Author*) Nothing to Disclose Takehiro Shimada, Maebashi, Japan (*Abstract Co-Author*) Nothing to Disclose Norio Hayashi, PhD, Maebashi, Japan (*Abstract Co-Author*) Nothing to Disclose Hiroyuki Nagase, Maebashi, Japan (*Abstract Co-Author*) Nothing to Disclose Kouichi Ujita, Maebashi, Japan (*Abstract Co-Author*) Nothing to Disclose Kenzo Okauchi, MD, Maebashi-Shi, Japan (*Abstract Co-Author*) Nothing to Disclose Takahito Nakajima, MD, Maebashi, Japan (*Abstract Co-Author*) Nothing to Disclose

Ayako Taketomi-Takahashi, MD, Maebashi, Japan (Abstract Co-Author) Nothing to Disclose

#### **TEACHING POINTS**

1. To understand the best method to create an appropriate sequence for White-matter-attenuated inversion recovery (WAIR).2. To understand the usefulness of WAIR sequence in various neurologic diseases, compared to conventional MR sequences.

#### **TABLE OF CONTENTS/OUTLINE**

1. How to create an appropriate WAIR sequence2. Degenerative diseases3. Multiple sclerosis4. Brain tumors5. Seizures6. Congenital anomalies7. Post-inflammatory changes8. Brain infarction9. Intracranial hemorrhage10. Intracranial trauma11. Further research proposals

# NR353-SD-MOA1

Comparison of PET, Diffusion, Perfusion, and MRS in Glioma Grade: Which is the Best Predictor for Glioma Grade and Cell Proliferation?

Monday, Nov. 28 12:15PM - 12:45PM Room: NR Community, Learning Center Station #1

# Participants

Keiichi Kikuchi, MD, Matsuyama, Japan (*Presenter*) Nothing to Disclose Yoshiyasu Hiratsuka, Toon City, Japan (*Abstract Co-Author*) Nothing to Disclose Takeshi Inoue, Matsuyama, Japan (*Abstract Co-Author*) Nothing to Disclose Hitoshi Miki, MD, PhD, Matsuyama, Japan (*Abstract Co-Author*) Nothing to Disclose Shiro Ohue, MD, Matsuyama, Japan (*Abstract Co-Author*) Nothing to Disclose Teruhito Mochizuki, MD, Toon, Japan (*Abstract Co-Author*) Nothing to Disclose Shohei Kohno, Toon City, Japan (*Abstract Co-Author*) Nothing to Disclose

#### PURPOSE

Various imaging modalities are used for preoperative examinations of brain tumors. We investigated the capacity of DWI, MRS, rCBV and PET-CT to predict the WHO glioma grade and identify correlations to the Ki-67 index as a marker of tumor cell proliferation.

#### **METHOD AND MATERIALS**

We retrospectively reviewed 114 glioma patients' data. DWI were obtained from 107 patients, MRS were obtained from 78, rCBV were obtained from 68. MET- and FDG-PET were obtained from all patients. Tumor pathological diagnoses were made via surgical specimens (G-II, 17; G-III, 26; G-IV, 71). The Ki-67 proliferation index was assessed by histochemical staining. To obtain the minimum ADC value of the tumor, several round ROIs were placed on the ADC map to include the area with the lowest ADC value (ADCmin).MRS data was obtained using single-voxel PRESS from the solid components of the tumor and Cho/Cr ratios (Cho/Cr) were recorded.rCBV data was obtained from dynamic susuceptibility contrast technique with bolus injection of Gd contrast medium. rCBV ratio (tumor/normal-appearing contralateral white matter) was used.MET-PET data were acquired for 20 min after the administration of a MET dose of 5 MBq/kg body weight. FDG-PET scan was initiated 90 min after the administration of an FDG dose of 3.5 MBq/kg body weight. The highest SUV was chosen among the ROIs over the tumor as the maximum SUV (SUVmax) on MET-and FDG-PET. The SUV ratios (tumor SUV/SUV of the contralateral normal cortex) were recorded.

#### RESULTS

ADCmin, Cho/Cr, rCBV ratio, MET-SUV, and FDG-SUV of each glioma grades are presented in Table. There were statistically significant deferences in the ADCmin values between each glioma grade. The Spearman rank correlation showed strong correlation between the Ki-67 index and rCBV ratio (p = -0.662, p < 0.0001). An inverse correlation was observed between the Ki-67 index and ADCmin (p = -0.552, p < 0.0001).

# CONCLUSION

The findings of this limited patient series showed that ADCmin was superior to Cho/Cr, rCBV ration, MET-, and FDG-SUV as a preoperative histological predictor of glioma. rCBV ratio was significantly correlated with the Ki-67 index and thus, should be considered as a reliable marker of cellular proliferations.

# **CLINICAL RELEVANCE/APPLICATION**

Minimum ADC was considered the best predictor of the glioma grade and rCBV showed significant correlation with Ki-67 indicating its potential as a reliable marker of cellular proliferation.

# Assessment of Interobserver Variability for the New ACR Thyroid Ultrasound Reporting Lexicon

Monday, Nov. 28 12:15PM - 12:45PM Room: NR Community, Learning Center Station #2

#### Awards

#### **Student Travel Stipend Award**

#### Participants

Malak Itani, MD, Seattle, WA (*Presenter*) Nothing to Disclose Mohammed S. Bermo, MD, FRCR, Seattle , WA (*Abstract Co-Author*) Nothing to Disclose Manjiri K. Dighe, MD, Seattle, WA (*Abstract Co-Author*) Research Grant, General Electric Company

## PURPOSE

To evaluate interobserver variability for the new ACR thyroid ultrasound reporting lexicon in retrospective analysis of thyroid nodules classified as Bethesda 3 on cytopathology

# METHOD AND MATERIALS

The study was approved by the Institutional Review Board. We reviewed all records of thyroid aspirations performed in our department from 7/1/2007 to 6/31/2014. Bethesda 3 nodules with available surgical pathology were reviewed independently by two radiologists who were blinded to the final pathology report, based on the new ACR TIRADS lexicon paper. Percent agreement and Cohen's Kappa ( $\kappa$ ) were analyzed for the sonographic features of the lexicon.

## RESULTS

A total of 61 Bethesda 3 nodules were reviewed. For the four categories of nodule composition, percent agreement was 72.1% and  $\kappa$  was 0.495, for two categories (solid versus cystic) the percent agreement becomes 100%. For nodule echogenicity, percent agreement was 63.9% for four categories, with  $\kappa$  of 0.445, and for two categories (hypoechoic or not hypoechoic) the percent agreement becomes 78.7%. There was 83.6% agreement for normal thyroid background and 73.8% agreement for halo. No nodules had extrathyroid extension. There was a 91.8% agreement for a taller-than-wide shape, but  $\kappa$  was only 0.243 due to low incidence. There was 83.3% agreement for the four categories of margins with  $\kappa$  of 0.455, and with only two categories (smooth vs. suspicious) this becomes 85%, with  $\kappa$  of 0.481. For calcifications, there was high variability with 50.8% agreement for punctate echogenic foci, 85.2% for macrocalcifications, and 88.5% for comet-tail artifacts with respective  $\kappa$  values of 0.028, 0.401 and 0.306. There was 95.1% agreement for peripheral calcifications; this is high due to the very low incidence.

#### CONCLUSION

With the new ACR lexicon for TIRADS, there is good observer agreement regarding nodule composition, echogenicity, shape, and margins, but suboptimal agreement for punctate echogenic foci.

#### **CLINICAL RELEVANCE/APPLICATION**

The new ACR lexicon paper provides guidance for an acceptable interrater variability. Interobserver agreement for evaluating calcifications can be improved, possibly by additional image dictionary and more specific descriptors.

Elasticity Index of Papillary Thyroid Carcinoma on Preoperative Shear-wave Elastography Can Improve the Diagnostic Performance of US for the Prediction of Cervical Lymph Node Metastasis

Monday, Nov. 28 12:15PM - 12:45PM Room: NR Community, Learning Center Station #3

# Participants

Ah Young Park, MD, Ansan , Korea, Republic Of (*Presenter*) Nothing to Disclose Jeong-Ah Kim, MD, PhD, Seoul, Korea, Republic Of (*Abstract Co-Author*) Nothing to Disclose Eun Ju Son, MD, PhD, Seoul, Korea, Republic Of (*Abstract Co-Author*) Nothing to Disclose Ji Hyun Youk, MD, Seoul, Korea, Republic Of (*Abstract Co-Author*) Nothing to Disclose

## PURPOSE

To investigate whether the elasticity index (EI) of shear wave elastography (SWE) can predict cervical lymph node (LN) metastasis of papillary thyroid carcinoma (PTC) preoperatively.

# METHOD AND MATERIALS

This retrospective study included 363 patients who were surgically diagnosed with PTC and underwent preoperative SWE evaluation between April 2011 and December 2013. Elasticity indices of PTC (Emean, Emax, Emin, Eratio-p, Eratio-m) and gray-scale US parameters (extrathyroidal extension, multifocality, and cervical LN metastasis) were correlated with the pathologic staging parameters (extrathyroidal extension, multifocality, and cervical LN metastasis) using independent T-test, Fisher's exact test, and multivariate regression analysis. The optimal cut-off values of elasticity indices were determined for predicting cervical LN metastasis and diagnostic performance was compared between gray-scale US and the combined application of gray-scale US and SWE using ROC curve analysis.

#### RESULTS

Central LN metastasis was associated with all EIs (P<.001 for Emean, Emax, Emin; P=.023 for Eratio-p; P=.046 for Eratio-m). Lateral LN metastasis was associated with Emean, Emax and Emin (P<.001, P=.002, and P=.002, respectively). On multivariate analysis, Emean and Emax were the independent factors for predicting central LN metastasis (P=.037) and Emin for lateral LN metastasis (P=.015). Emean higher than 124 kPa or Emax higher than 138 kPa plus suspicious central LN metastasis on gray-scale US, and Emin higher than 63 kPa plus suspicious lateral LN metastasis improved sensitivity and AUC (for central LN, sensitivity, 45.4% and 44.6% vs 28%, P<.001; AUC, 0.659 and 0.667 vs 0.615; P=.011 and P=.019; for lateral LN, sensitivity, 95.8% vs 75%, P=.025; AUC, 0.924 vs 0.871, P=.047).

#### CONCLUSION

Quantitative EI of PTC on preoperative SWE could predict cervical LN metastasis.

# **CLINICAL RELEVANCE/APPLICATION**

High EIs of PTC are independent predictors of cervical LN metastasis and preoperative SWE evaluation could improve the low sensitivity of gray-scale US for central LN metastasis.

4D Fluoroscopy Reconstruction using Learning Based Device Segmentation in Unsubtracted Projection Images

Monday, Nov. 28 12:15PM - 12:45PM Room: NR Community, Learning Center Station #4

#### Participants

Martin Wagner, Madison, WI (Presenter) Nothing to Disclose

Michael Speidel, PhD, Madison, WI (Abstract Co-Author) Nothing to Disclose

Charles M. Strother, MD, Madison, WI (*Abstract Co-Author*) Research Consultant, Siemens AG Research support, Siemens AG License agreement, Siemens AG

Charles A. Mistretta, PhD, Madison, WI (Abstract Co-Author) Founder, Mistretta Medical Intellectual Property Licensing Activities Research, Siemens AG

# PURPOSE

We recently developed a novel approach for 4D fluoroscopy reconstruction from simultaneous biplane projections, enabling the guidance of interventional procedures using virtual endoscopic and fluoroscopic views. The algorithm was originally developed for neurovascular applications, assuming very little patient motion. The device segmentation relies on subtracted fluoroscopy frames to simplify the process. However, in many applications, patient motion might cause subtraction artifacts, which considerably reduce the quality of the device segmentation. We propose a modification of the 4D fluoroscopy reconstruction using a learning based approach that does not rely on mask subtracted fluoroscopic images.

## **METHOD AND MATERIALS**

The proposed algorithm uses a ridge detection filter based on the local first and second derivatives to find curvilinear structures in the image. The centerlines of all curvilinear structures are then extracted using topology preserving thinning. To separate device structures from segments that represent anatomical structures, features are extracted for each centerline segment. These include the height, width and symmetry of the average profile along the centerline as well as length and curvature of each segment. A support vector machine (SVM) is then trained with these features to classify segments as either part of the device or not. A 2D path search then connects the device segments and a 3D reconstruction is performed based on the original algorithm.

# RESULTS

The method was evaluated using datasets from 12 animal studies and 2 clinical cases. The SVM was able to classify 94.7 % of all segments correctly. In all cases, the subsequent 2D path search was able to filter out the remaining misclassified segments. The extracted 2D device paths were compared to the original method using subtracted fluoroscopy frames. The median error was  $0.55 \pm 0.47$  pixels, which corresponds to  $0.16 \pm 0.14$  mm.

# CONCLUSION

The presented results show that curvilinear segments can be classified with high accuracy using shape and image based features. This allows to segment curvilinear devices robustly without mask subtraction, which can be used in 4D fluoroscopy reconstructions, where patient motion prevents artifact free mask subtraction.

## **CLINICAL RELEVANCE/APPLICATION**

The presented algorithm could open up a new field of clinical applications for 4D fluoroscopy, where more patient motion can be expected, like cardiac and breathing motion.

# NR357-SD-MOA5

Physiological Response Delay may Overestimate the Default Mode Network Changes in Alzheimer's Disease Patients

Monday, Nov. 28 12:15PM - 12:45PM Room: NR Community, Learning Center Station #5

#### Participants

Yi-Tien Li, MSc, New Taipei, Taiwan (Presenter) Nothing to Disclose

#### PURPOSE

We study the impact of spontaneous physiology on characterizing the DMN of AD patients. The goal is to test how the difference in default mode network (DMN) features may change, while physiological response due to spontaneous cardiac and breathing rhythms are appropriately controlled in Alzheimer's Disease (AD) patients.

# METHOD AND MATERIALS

Resting-state functional magnetic resonance imaging (fMRI) scans were acquired by T2\*-weighted echo-planar imaging (EPI) for 400 seconds. Cardiac and respiratory cycles were recorded using a pulse oximeter and a respiration belt, respectively. The total of 32 subjects of AD patients as well as age andgender matched controls were include. We rely on RETROICOR (Gary H. Glover, 2000) to remove phase-locked physiological artifact. The lower frequency physiological effects of the same phase but different amplitudes (for respiration variations) or intervals (for heart rate) were corrected by RVHRCOR (Chang and Glover, 2009).

# RESULTS

While AD patients have different DMN characteristics from the normal controls before physiological noise correction, however, the difference could not be significantly observed after suppressing physiological noise. We found that the RV and HR factors both did not explain as much variance as the healthy subjects in the AD group. The weighted map of beta values estimated in GLM for both RV and HR showed significant differences between the healthy controls and AD patients, especially at DMN regions. Further, the delayed physiological response in AD patients could be observed by comparing the arrival time of respiration and cardiac response function with normal controls.

# CONCLUSION

The impact of the spontaneous physiology in the two groups were not the same, especially dominated by the low frequency physiological factors, RV and HR, especially at the regions near the DMN nodes. The phenomenon was attributed to the different BOLD responses between the AD and control groups supported by the evidence of physiological response functions delay measured in the AD patients.

# **CLINICAL RELEVANCE/APPLICATION**

The evidences that the physiological response changes could alter the DMN features in the AD patients had been revealed in our study. Our results suggest the importance of controlling hemodynamic responses associated with spontaneous physiology in order to achieve sensitivity and specificity of AD patients' features of DMN.

## NR359-SD-MOA7

Comparison of Amide Proton Transfer Imaging and 11-C Methionine PET in Monitoring Recurrence in Posttreatment Gliomas: A Pilot Study

Monday, Nov. 28 12:15PM - 12:45PM Room: NR Community, Learning Center Station #7

# Participants

Ji Eun Park, Seoul, Korea, Republic Of (*Abstract Co-Author*) Nothing to Disclose Kyeong Hwa Ryu, MD, Seoul, Korea, Republic Of (*Presenter*) Nothing to Disclose Ho Sung Kim, Seoul, Korea, Republic Of (*Abstract Co-Author*) Nothing to Disclose Sang Joon Kim, MD, Seoul, Korea, Republic Of (*Abstract Co-Author*) Nothing to Disclose Seung Chai Jung, MD, Seoul, Korea, Republic Of (*Abstract Co-Author*) Nothing to Disclose Woo Hyun Shim, Seoul, Korea, Republic Of (*Abstract Co-Author*) Nothing to Disclose Joo Young Oh, Seoul, Korea, Republic Of (*Abstract Co-Author*) Nothing to Disclose Ha-Kyu Jeong, PhD, Seoul, Korea, Republic Of (*Abstract Co-Author*) Nothing to Disclose

#### PURPOSE

To evaluate the utility of amide proton transfer (APT) imaging in monitoring recurrence in post-treatment gliomas by comparing and correlating APT asymmetry with 11-C Methionine (MET) PET uptake in the tumor.

#### **METHOD AND MATERIALS**

This retrospective study enrolled eleven patients (3 low grade and 8 high grade) with recurrence after treatment, and examined with APT imaging and MET PET. APT and MET PET images were co-registered using SPM software. APT asymmetry on tumor and normal parenchyma and tumor-to-normal count density ratio (TNR) of the cortex from MET PET were measured. The maximum TNR (TNRmax) and maximum APT asymmetry (APTmax) were compared between recurrent low- and high grade gliomas. Voxel-wise correlations between TNR and APT asymmetry were evaluated.

#### RESULTS

APTmax were significantly increased in tumor portion compared to normal parenchyma (mean $\pm$ SD, 2.25 (%)  $\pm$  1.57 vs. 0.48 (%)  $\pm$  0.32, P <.001). TNRmax of recurrent glioma was 1.63  $\pm$  0.36. APTmax in recurrent high-grade glioma was significantly higher than recurrent low-grade gliomas (Mann-Whitney's U test, P=.041), but no significant difference was found for TNRmax between low-and high-grade gliomas. Voxel-wise plotting between APT asymmetry and TNR did not show correlation that regions with high MET uptake did not correspond with regions with high APT asymmetry.

## CONCLUSION

APT imaging showed difference in recurrent high- and low-grade gliomas while MET PET did not. APT asymmetry and MET uptake within a tumor were independent of each other. Thus, APT imaging and MET PET might have a complementary role in characterization of recurrent gliomas.

## **CLINICAL RELEVANCE/APPLICATION**

APT imaging might have a complementary role in characterization of recurrent gliomas by providing additional information to distinguish high grade recurrence while MET PET did not. APT imaging will be useful in terms of providing additional molecular information of viable tumor with less economic burden compared to MET PET.

## Olfactory Functional MRI in Patients with Posttraumatic Anosmia as an Objective Measure of Olfactory Deficit

Monday, Nov. 28 12:15PM - 12:45PM Room: NR Community, Learning Center Station #8

#### **Participants**

Mina Park, MD, Seoul, Korea, Republic Of (*Presenter*) Nothing to Disclose Jin Kook Kim, Seoul, Korea, Republic Of (*Abstract Co-Author*) Nothing to Disclose Won-Jin Moon, MD, Seoul, Korea, Republic Of (*Abstract Co-Author*) Nothing to Disclose

## PURPOSE

Posttraumatic anosmia is the third most common cause of olfactory deficits. Olfactory deficits significantly affect the quality of life for those who affected by it. The olfactory function evaluation, however, has strongly relied on subjective responses given by patients. This study was designed to investigate the difference of the brain activation in the patients with posttraumatic anosmia by using fMRI with two different olfactory stimuli compared to those in normal controls.

# METHOD AND MATERIALS

16 patients (M:F=12:5; mean age, 42.2±10.4 years) with clinically diagnosed traumatic anosmia and 19 healthy control subjects (M:F=11:8; mean age, 29.3±8.5 years) underwent fMRI with olfactory stimuli of Citraval and  $\beta$ -mercaptoethanol (BME), respectively. Olfactory function test (The Korean version of Sniffin' Sticks II Test) and nasal endoscopic exploration were assessed in the all participants. For the group analysis, the two-sample t-test was performed with an age as a covariate in each Citraval and BME stimuli.

#### RESULTS

All of the subjects showed patent olfactory cleft on the nasal endoscopic exploration. The patient group showed marked reduced olfactory function compared to the control group when assessed via the Korean version of Sniffin' Sticks II Test ( $3.2\pm2.9 \text{ vs}$   $48.0\pm0.0$ , respectively, P<0.001). Four of the traumatic anosmia patients had focal tissue loss in the prefrontal cortex, while none of the control subjects had focal tissue loss in the brain (P=0.035).Compared with the control subjects, patients with traumatic anosmia demonstrated markedly decreased activation in the bilateral primary and secondary olfactory cortex and limbic system under BME stimuli (FDR-corrected P <0.05) while decreased activation was only observed in the right prefrontal cortex and left orbitofrontal cortex under Citraval stimuli (uncorrected P <0.05).

# CONCLUSION

Olfactory fMRI enables the objective visualization of the marked impaired brain activation of olfactory cortex and limbic cortex in the patients with traumatic anosmia, especially under BME stimuli and further study is needed to determine its diagnostic role in posttraumatic anosmia.

# **CLINICAL RELEVANCE/APPLICATION**

Our study indicates that fMRI can be an objective tool to measure olfactory deficits in the posttraumatic anosmia patients.

3D/4D Translabial Ultrasound and Dynamic Magnetic Resonance Imaging of the Pelvic Floor: A Comprehensive Approach of the Normal Anatomy and Pelvic Floor Dysfunction

Monday, Nov. 28 12:15PM - 12:45PM Room: OB Community, Learning Center Station #1

#### Awards

**Identified for RadioGraphics** 

#### **Participants**

Luciana P. Chamie, MD, PhD, Sao Paulo, Brazil (*Presenter*) Nothing to Disclose Duarte M. Ribeiro, MD, Sao Paulo, Brazil (*Abstract Co-Author*) Nothing to Disclose Angela H. Caiado, MD, Sao Paulo, Brazil (*Abstract Co-Author*) Nothing to Disclose Gisele Warmbrand, MD, Sao Paulo, Brazil (*Abstract Co-Author*) Nothing to Disclose Paulo C. Serafini, MD, PhD, Sao Paulo, Brazil (*Abstract Co-Author*) Nothing to Disclose

#### **TEACHING POINTS**

To review the protocol and imaging algorithm of the 3D/4D translabial ultrasound and dynamic MRI of the pelvic floorTo review the normal anatomy of the pelvic floor through both methods To demonstrate abnormal findings of the three compartments of the pelvis, such as cistocele, uterine prolapse, rectocele, enterocele, peritoneocele and pelvic floor descent, emphasizing advantages and limitations of each method

# TABLE OF CONTENTS/OUTLINE

A. Clinical and epidemiological aspects of pelvic floor dysfunctionB. PathophysiologyC. Diagnostic Imaging: 3D/4D translabial ultrasound of the pelvic floor- protocol and imaging findings Dynamic pelvic MRI- protocol and imaging findings with emphasis on the importance of the evacuatory phase G. Normal anatomyH. Abnormal findings: cistocele, uterine prolapse, rectocele, enterocele, peritoneocele and pelvic floor descentI. Pitfalls and limitations of each methodJ. Summary

# OB142-ED-MOA2

MRI of Malignant Neoplasms of the Uterine Corpus and Cervix: Staging, Treatment Planning, and Follow-up. How to Make it Easy

Monday, Nov. 28 12:15PM - 12:45PM Room: OB Community, Learning Center Station #2

# Participants

Fatima Matute Teresa, MD, Madrid, Spain (*Presenter*) Nothing to Disclose Mercedes Ruiz Tolon, madrid, Spain (*Abstract Co-Author*) Nothing to Disclose

# **TEACHING POINTS**

A. To demonstrate diagnostic strategy of malignant neoplasms of the uterine corpus and cervix by using MRI techniquesB. Learn how to interpret the MRI findings C. Review the limitations and potential pitfalls of MRI in the malignant neoplasms of the uterine corpus and cervix D. To provide an educational and pictorial review of the MRI findings of malignant neoplasms of the uterine corpus and cervix

# TABLE OF CONTENTS/OUTLINE

A. Normal anatomyB. Imaging technique, MR pulse sequencesC. Diagnostic checklistD. StagingE. Lymphadenopathy evaluationF. Treatment planningG. Follow-up H. Outcomes (include complications) I. Limitations and potential pitfalls of MRI J. Final recommendations

# PD107-ED-MOA6

**Multimodality Imaging of Pediatric Non-malignant Adrenal Lesions** 

Monday, Nov. 28 12:15PM - 12:45PM Room: PD Community, Learning Center Station #6

Awards Certificate of Merit Identified for RadioGraphics

#### **Participants**

Kiran M. Sargar, MBBS, MD, Saint Louis, MO (*Presenter*) Nothing to Disclose Jing Qi, MD, Brentwood, MO (*Abstract Co-Author*) Nothing to Disclose Rebecca L. Hulett, MD, St Louis, MO (*Abstract Co-Author*) Nothing to Disclose Geetika Khanna, MD, MS, Iowa City, IA (*Abstract Co-Author*) Nothing to Disclose

# **TEACHING POINTS**

Ultrasound is preferred initial imaging modality for the evaluation of neonatal adrenal lesions. Horseshoe adrenal is associated with asplenia (most common), neural tube defects and renal anomalies. Discoid adrenal is typically associated with absent kidneys. Adrenal hemorrhage maybe secondary to trauma or renal vein thrombosis (typically in neonate). Follow up is essential to exclude adrenal neuroblastoma. "Cerebriform morphology" characterized by abnormal contour and thickness of adrenal glands is specific for congenital adrenal hyperplasia. It may be difficult to distinguish between ganglioneuroma from neuroblastoma on imaging, in absence of metastatic disease.

# TABLE OF CONTENTS/OUTLINE

1. Classification of pediatric non-malignant adrenal lesions-I. Congenital-a) Epithelial cyst b) horseshoe adrenals c) discoid adrenalsII. Traumatic- Adrenal hemorrhageIII. Infections - granulomatous diseasesIV. Benign neoplasms- a) Ganglioneuroma b) Pheochromocytoma c) Adrenal adenoma d) MyelolipomaV. Enzyme deficiency disorders- a) Congenital adrenal hyperplasia b) Wolman DiseaseVI. Adrenal lesion mimics- a) Extralobar sequestration b) Extramedullary hematopoiesis2. Illustrative cases from the radiology-surgery archives of a tertiary children's hospital will be used to discuss non-malignant adrenal lesions in children.

# PD188-ED-MOA7

# Approach to the Differential Diagnosis of the Cloacal Malformation

Monday, Nov. 28 12:15PM - 12:45PM Room: PD Community, Learning Center Station #7

#### **Participants**

Young Ah Cho, Seoul, Korea, Republic Of (*Presenter*) Nothing to Disclose Jeong Rye Kim, MD, Seoul, Korea, Republic Of (*Abstract Co-Author*) Nothing to Disclose Hee Mang Yoon, MD, Seoul, Korea, Republic Of (*Abstract Co-Author*) Nothing to Disclose Ah Young Jung, MD, Seoul, Korea, Republic Of (*Abstract Co-Author*) Nothing to Disclose Jin Seong Lee, MD, Seoul, Korea, Republic Of (*Abstract Co-Author*) Nothing to Disclose

# **TEACHING POINTS**

1. Recognizing the spectrum of cloacal malformaton in children2. Understanding the characteristic imaging and best way to approach to differentiate types of cloacal malformation.

#### TABLE OF CONTENTS/OUTLINE

- 1. Introduction
- \_ Clinical findings: incidence and symptoms
- \_ Normal Anatomy: embryology
- Classification
- Associated anomalies
- 2. Management of Cloacal Malformation
- \_ Type of malformation
- Imaging techniques
- \_ Management strategies
- \_ Treatment methods
- 3. Various Cases
- A. Long common channel
- B. Short common channel
- C. Urogenital sinus anomaly

SUMMARY

Cloacal malformation is congenital anomaly in pediatric patients that presents various anatomical dysarrangement. The prompt surgical correction is necessary for improving clinical outcome, and the complex anatomy could be well demonstrated by the imaging modalities; voiding cystourethrogram, colostogram, ultrasound, computed tomography and magnetic resonance imaging. Because the management for each lesion is different, the imaging findings of various conditions could be valuable information to make an accurate management. In this presentation, imaging findings and diagnostic strategies for cloacal malformation will be demonstrated.

A Diagnostic Decision Guide to Pediatric Vascular Lesions According to the Current ISSVA Classification-Making it Practical and Simple!

Monday, Nov. 28 12:15PM - 12:45PM Room: PD Community, Learning Center Station #8

# Participants

Fernando D. Tamamoto Sr, MD, Sao Paulo, Brazil (*Abstract Co-Author*) Nothing to Disclose Gustavo P. Rodi, MD, Curitiba, Brazil (*Abstract Co-Author*) Nothing to Disclose Camila Joau, MD, Sao Paulo, Brazil (*Presenter*) Nothing to Disclose Taisa D. Gasparetto, MD, PhD, Sao Paulo, Brazil (*Abstract Co-Author*) Nothing to Disclose Rodrigo Regacini, MD, Sao Paulo, Brazil (*Abstract Co-Author*) Nothing to Disclose

# **TEACHING POINTS**

Given the paucity of research on this field, a diagnostic approach to vascular anomalies may become a challenge for many physicians. Therefore, the aim of this work is to propose a pratical diagnostic decision guide to pediatric vascular anomalies, based on the current ISSVA Classification and by illustrating with clinical cases from our radiology department.

# TABLE OF CONTENTS/OUTLINE

Twenty vascular anomalies clinical cases & differencial diagnosis flow chart.

### PD210-SD-MOA1

Fetal MRI Findings of Congenital Diaphragmatic Hernia Suggestive of a Hernia Sac: Preliminary Observations

Monday, Nov. 28 12:15PM - 12:45PM Room: PD Community, Learning Center Station #1

#### **Participants**

Chihiro Tani, MD, Hiroshima, Japan (*Abstract Co-Author*) Nothing to Disclose Hiroaki Sakane, MD, Hiroshima, Japan (*Presenter*) Nothing to Disclose Yoko Kaichi, Hiroshima, Japan (*Abstract Co-Author*) Nothing to Disclose Fuminari Tatsugami, Hiroshima, Japan (*Abstract Co-Author*) Nothing to Disclose Yasutaka Baba, MD, Hiroshima, Japan (*Abstract Co-Author*) Nothing to Disclose Kazuo Awai, MD, Hiroshima, Japan (*Abstract Co-Author*) Research Grant, Toshiba Corporation; Research Grant, Hitachi, Ltd; Research Grant, Bayer AG; Research Grant, Eisai Co, Ltd; Medical Advisor, General Electric Company; ; ; ; ; Makoto Iida, Hiroshima, Japan (*Abstract Co-Author*) Nothing to Disclose Yukiko Honda, MD, Hiroshima, Japan (*Abstract Co-Author*) Nothing to Disclose

#### PURPOSE

The prognosis for congenital diaphragmatic hernia (CDH) is highly variable; it may be better for CDH with a hernia sac. No diagnostic criteria for the identification of a sac by prenatal MRI have been established. We studied prenatal MR findings suggestive of a hernia sac in fetuses with CDH.

## **METHOD AND MATERIALS**

This study included 14 pregnant women who underwent fetal MRI during the last 4 years because fetal ultrasound suggested CDH. The mean gestational age was 34.8 weeks (range 32 - 40 weeks). Two board-certified radiologists visually evaluated the affected side of the lung on fetal MRI scans and assigned a grade by consensus (grade A = more than 50% of the thoracic cavity is occupied by the lung, grade B = more than 50% of the thoracic cavity is occupied by the hernia, grade C = no lung is identified in the thoracic cavity). They also recorded the boundary line between the affected side of the lung and the hernia as smooth or rough. We recorded the presence of a hernia sac and cranial migration of the liver and of survival and death using postnatal reports.

#### RESULTS

Of 14 fetuses, 2 were with- and 12 without a hernia sac; 8 were with- and 6 without cranial liver migration. Seven survived including both with CDH and hernia sac. The grade was A and the boundary lines were smooth. Five fetuses without a hernia sac survived. The grade was B (n=5) or C (n=7), and the boundary was rough. All fetuses with grade C died (n=7). Of the 8 fetuses with cranial migration of the liver, only one fetus with a hernia sac survived.

### CONCLUSION

In fetuses with MRI findings of CDH with a hernia sac the volume on the affected side of the lung was larger and the boundary between the affected side and the hernia was smooth.

## **CLINICAL RELEVANCE/APPLICATION**

In fetuses with CDH, a large volume on the affected side of the lung and a smooth boundary with the hernia on fetal MRI scans suggests the presence of a hernia sac and a better prognosis.

## PD211-SD-MOA2

Anatomic Classification of Coronary Arteries in Complete Transposition of Great Arteries: Diagnosis and Analysis with Multi-slice CT

Monday, Nov. 28 12:15PM - 12:45PM Room: PD Community, Learning Center Station #2

## Participants

Luo Hai-Ying, Guangzhou, China (*Presenter*) Nothing to Disclose Xiao-Mei Zhong, Guangzhou, China (*Abstract Co-Author*) Nothing to Disclose Meiping Huang, GuangZhou, China (*Abstract Co-Author*) Nothing to Disclose Changhong Liang, Guangzhou, China (*Abstract Co-Author*) Nothing to Disclose

## PURPOSE

To evaluate the diagnostic value of multi-slice spiral CT (MSCT) in classifying coronary arteries of complete transposition of great arteries (D-TGA)

## **METHOD AND MATERIALS**

The clinical and imaging data of 367 patients with D-TGA who had undergone MSCT examination from March 2005 to June 2015 were retrospectively analyzed. The origin and course of the coronary arteries of the patients were classified according to the Marie Lannelongue classification. There were four patterns of courses: normal, looping, intramural and miscellaneous. And the four patterns were subdivided into eleven subgroups. The anatomic classification of coronary arteries in complete transposition of great arteries were recorded, and the ratio of descriptive statistics was used according to categorical variable data

### RESULTS

All the origin and course of the coronary arteries could be clearly displayed on MSCT. Of 367 patients with D-TGA, 209 cases (56.95%) were normal course (type I), 138 cases (37.60%) were looping course (type II), 16 cases (4.36%) were intramural course (type III), and 4 cases (1.09%) were miscellaneous course (type IV). In looping course, the posterior looping (type IIA), anterior looping (type IIB) and double looping (type IIC) were found in 63 cases (17.17%), 30 cases (8.17%) and 45 cases (12.26%), respectively. The ratios of the anatomic classification of looping courses were IIA-1 44(11.99%), IIA-2 19(5.18%), IIB-1 12(3.27%), IIB-2 8(2.18%), IIB-3 10(2.72%), IIC-1 25(6.81%), IIC-2 17(4.63%), IIC-3 3(0.82%)

### CONCLUSION

MSCT is an effective technique to visualize and classify the coronary arteries in patients with D-TGA. And it is helpful for successful transfer of the coronary arteries and reducing the rate of coronary events after operation.

# **CLINICAL RELEVANCE/APPLICATION**

MSCT is an effective technique to visualize and classify the coronary arteries in patients with D-TGA, and it is helpful for successful transfer of the coronary arteries and reducing the rate of coronary events after operation.

## PD212-SD-MOA3

Assessment of Kinetic Energy and Vorticity in the Pulmonary Artery in Pediatric Patients with Repaired Tetralogy of Fallot Using 4D Flow MRI

Monday, Nov. 28 12:15PM - 12:45PM Room: PD Community, Learning Center Station #3

## Participants

Julio Garcia, BEng, PhD, Calgary, AB (*Presenter*) Nothing to Disclose Silvia Hidalgo-Tobon, PhD, Mexico City, Mexico (*Abstract Co-Author*) Nothing to Disclose Benito de Celis Alonso, PhD, Puebla, Mexico (*Abstract Co-Author*) Nothing to Disclose Manuel Obregon, MD, Mexico City, Mexico (*Abstract Co-Author*) Nothing to Disclose Porfirio Ibanez, MD, Mexico City, Mexico (*Abstract Co-Author*) Nothing to Disclose Julio Erdmenger, MD, Mexico City, Mexico (*Abstract Co-Author*) Nothing to Disclose Pilar Dies-Suarez, MD, Mexico City, Mexico (*Abstract Co-Author*) Nothing to Disclose

### PURPOSE

Flow alterations in the pulmonary artery (PA) of patients with repaired tetralogy of Fallot (rTOF) may be linked with the expending of kinetic energy (KE) and vortical flow patterns as measured by 4D flow MRI. The aim was to investigate the impact of flow alterations in the PA and its association with KE and vorticity.

#### **METHOD AND MATERIALS**

15 patients with rTF (age=9±6 yrs, 6 females) underwent thoracic 4D flow MRI. PA was segmented from the 4D flow derived angiogram to mask the velocity field (v) which was used to calculate KE (KE=1/2×rho×v2, rho=1.06 g/mL), and vorticity ( $\omega$ =curl(v)). Maximum intensity projection (MIP) was calculated for flow velocity, KE, and vorticity. Peak velocity (PV), maximal flow (Qmax), and mean flow (Qmean) were extracted from the main (MPA), right (RPA), and left (LPA) PA. Volumetric median of KE was used to divide the cohort into low and elevated KE. The association of KE at MPA, RPA, and LPA with other flow parameters was assessed by Pearson's correlation. Comparison between KE groups was performed by Mann-Whitney test.

## RESULTS

Maximal and mean KE in the PA showed a correlation with PV (r=0.47,p<0.05; r=0.38,p<0.05), Qmax (r=0.49,p<0.05; r=0.45,p<0.05), and Qmean (r=0.49,p<0.05; r=0.44,p<0.05). Both maximal and mean KE were originated from the RPA where associations with PV (r=0.87,p=0.001; r=0.84,p<0.001), Qmax (r=0.77,p<0.001; r=0.75,p<0.001), and Qmean (r=0.69,p<0.05; r=0.69,p<0.05) were more important. Maximal KE was 59% higher in the MPA than in the RPA, as well as mean KE with 33% increment. Velocity, KE, and vorticity MIPs (Fig 1) showed elevated KE and vortical flow at the pulmonary bifurcation. PA mean and median KE were associated with mean vorticity (r=0.78,p<0.001 and r=0.44,p<0.001). Low and elevated KE differences were found for mean KE ( $0.029\pm0.019$  mJ vs.  $0.047\pm0.022$  mJ,p=0.02), median KE ( $0.041\pm0.012$  mJ vs.  $0.07\pm0.02$  mJ,p<0.001), and mean vorticity ( $0.032\pm0.008$  1/s vs.  $0.037\pm0.006$  1/s,p<0.05).

## CONCLUSION

Maximal and mean KE in the RPA were associated with flow hemodynamic parameters, whereas in the MPA and LPA were not. This was explained by flow distribution within the PA and the elevated energy dissipation at PA bifurcation.

## **CLINICAL RELEVANCE/APPLICATION**

The flow distribution in the pulmonary artery of patients with repaired tetralogy of Fallot may be linked with the expend of kinetic energy and vorticity. Alterations in flow, kinetic energy, and vorticity may guide the clinical survey of this population.

## PD213-SD-MOA4

MRI and Clinical Assessment in Juvenile Idiopathic Arthritis: The Discrepancy Explored: Looking into the Confusing Group of Clinically Inactive Patients with Synovitis on MRI

Monday, Nov. 28 12:15PM - 12:45PM Room: PD Community, Learning Center Station #4

## Participants

Charlotte van Gulik, MD,MSc, Amsterdam, Netherlands (*Presenter*) Nothing to Disclose Mendy Welsink-Karssies, Haarlem, Netherlands (*Abstract Co-Author*) Nothing to Disclose Anouk M. Barendregt, BSC, MSc, Amsterdam, Netherlands (*Abstract Co-Author*) Nothing to Disclose Dieneke Schonenberg-Meinema, Amsterdam, Netherlands (*Abstract Co-Author*) Nothing to Disclose Merlijn van den Berg, Amsterdam, Netherlands (*Abstract Co-Author*) Nothing to Disclose Mario Maas, MD, PhD, Utrecht, Netherlands (*Abstract Co-Author*) Nothing to Disclose Taco Kuijpers, MD, PhD, Amsterdam, Netherlands (*Abstract Co-Author*) Nothing to Disclose Robert Hemke, MD,PhD, Amsterdam, Netherlands (*Abstract Co-Author*) Nothing to Disclose

#### PURPOSE

Synovitis, as a sign of active, ongoing disease activity, is seen on MRI in up to 50% of clinically inactive Juvenile Idiopathic Arthritis (JIA) patients. This study evaluates patient characteristics and disease activity parameters in a cohort of clinically inactive JIA patients, both with and without synovitis seen on MRI, in order to get more insight in the observed discrepancy.

#### **METHOD AND MATERIALS**

We prospectively enrolled 52 clinically inactive JIA patients (median age 13.3 years, 63.5% female). Patients were divided into two groups; 1: clinically inactive disease without synovitis on MRI and 2: clinically inactive patients with synovitis on MRI. The Juvenile Arthritis MRI Scoring (JAMRIS) system was used to evaluate synovial thickening. A JAMRIS score of > 0 is interpreted as synovitis. Patient characteristics and disease activity parameters (physical and laboratory examination) were gathered to determine clinical inactivity. Patient characteristics and disease activity parameters were compared between both groups.

### RESULTS

Subclinical synovitis on MRI was present in 18 clinically inactive patients (34.6%). The age was significantly lower for the patients with subclinical synovitis versus patients without subclinical synovitis (p=0.008, median 10.75 versus 14.40). Concerning other patient characteristics and disease activity parameters, no significant differences were observed between both groups.

## CONCLUSION

Subclinical synovitis on MRI was present in nearly 35% of the clinically inactive JIA patients. These patients were significantly younger than patients without subclinical synovitis. To not underestimate this alarming signal of synovitis in young children, younger patients could benefit from frequent monitoring of disease activity using MRI.

### **CLINICAL RELEVANCE/APPLICATION**

In clinically inactive JIA patients synovitis is often seen on MRI, especially in younger patients. To optimize treatment regimens, frequent monitoring of synovitis using MRI is recommended.

## PH110-ED-MOA9

MRI and Cochlear Implants with Magnets: Strategies for Reducing Artifacts Near Highly Inhomogenous Magnetic Fields

Monday, Nov. 28 12:15PM - 12:45PM Room: PH Community, Learning Center Station #9



Awards Identified for RadioGraphics

#### Participants

Heidi A. Edmonson, PhD, Rochester, MN (*Presenter*) Nothing to Disclose Robert E. Watson Jr, MD, PhD, Rochester, MN (*Abstract Co-Author*) Nothing to Disclose Alice C. Patton, MD, Rochester, MN (*Abstract Co-Author*) Nothing to Disclose

# **TEACHING POINTS**

MRI of the head and neck near a cochlear implant can be quite challenging due to conductive wire components and local magnetic field inhomogeneities. Several manufacturers now offer cochlear implant devices containing an internal magnet that are FDA-approved as MR-conditional at 1.5T, and at least one device is also MR-conditional for 3T. Artifacts from magnet-in cochlear implants can extend more than 10 cm from the implant using a spin echo sequence, an imaging technique that is typically robust in the presence of magnetic field inhomogeneities. Artifacts from more advanced imaging techniques, such as parallel imaging or long echo train imaging with modulated flip angles, may mimic pathology and appear in unexpected locations displaced from the main artifact. This exhibit will demonstrate: Common artifacts arising from cochlear implants with typical neuro imaging sequences Performance of metal artifact reduction sequences near cochlear implants Strategies to reduce or shift artifacts from a region of interest

# TABLE OF CONTENTS/OUTLINE

Introduction to cochlear implants, location of components, interactions with the MRI magnetic fields Common diseases and pathology associated with hearing loss Typical MRI protocols and associated Cochlear Implant artifacts Suggested protocol modifications and trouble-shooting

High-resolution Diagnostic Protocol for Cochlear Implants Imaging through Flat-panel Angio CT (FPCT): Measurements of Organ Doses and Comparison with Software Calculations

Monday, Nov. 28 12:15PM - 12:45PM Room: PH Community, Learning Center Station #1

## Participants

Mauro Campoleoni, BS, Milano, Italy (*Presenter*) Nothing to Disclose Roberto Brambilla, PhD, Milan, Italy (*Abstract Co-Author*) Nothing to Disclose Clara Sina, MD, Milan, Italy (*Abstract Co-Author*) Nothing to Disclose Riccardo Biffi, MILANO, Italy (*Abstract Co-Author*) Nothing to Disclose Luca Messaggi, MILANO, Italy (*Abstract Co-Author*) Nothing to Disclose

# PURPOSE

To evaluate the dose to irradiated organs in a recently introduced angioCT procedure for the imaging of the cochlear implants and the middle ear, both with direct measurements and with software calculations.

## **METHOD AND MATERIALS**

At the Neuroradiology Department of our insitution a new high-resolution diagnostic protocol for middle ear acquisition and cochlear implants visualization has been introduced. The technique is based on angio CT with Flat-panel detector and the equipment used is a Philips Allura Xper FD20. This equipment was chosen to lower patient doses and because it allows a better patient positioning compared to other available technologies, like dental cone beam with standing patient. To assess the relevant organ doses a Alderson RANDO anthropomorphic phantom was used; LiF TLD GR-200 were inserted into the cavities of the head according to a suitable and established scheme for the evaluation of the doses to the main organs. The acquisition protocol consists in a 240° rotation, symmetrically with respect to the midline of the head, passing through the back of the skull and saving the front part, with a small FOV of about 15cmx20cm which allows the simultaneous analysis of both ears. The standard protocol employs a pulsed X-ray beam at 80kV, 260mA, 25s acquisition time, 30 fps with a 7 ms pulse. The images are acquired with a 0.14 mm thickness while the reconstructed images are only 0.07 mm thick. The total DAP is about 10500 mGy\*cm2. For comparison, it was also calculated the equivalent doses to the different organs through a simulation software (PCXMC-2.0 - Rotation Mode).

#### RESULTS

The measured doses in the phantom were averaged over 4 thermoluminescent dosimeters, with CV% less than 10%. The measurements have shown dose values to organs in the range 1 - 35 mSv: in particular bone marrow, which has the highest wT received 2.9 mSv, while the most exposed were the salivary glands with 31,7 mSv. For the most exposed organs the doses calculated with the PCXMC-2.0 software are in agreement with the measurements (20%).

### CONCLUSION

The protocol studied has the advantage of using an angio equipment instead of a CT, and allows an optimal visualization of the inner ear. Its HR 0.07 mm thick images can better detail the structure of cochlear implants reducing exposure with respect to CT and saving dose to the eye lens.

# **CLINICAL RELEVANCE/APPLICATION**

Optimal visualization of the inner ear and of cochlear implants with lower doses.

# PH213-SD-MOA2

## The Role of Contrast Media on Absorbed Radiation Dose in Cardiac CT: A Monte Carlo Simulation Study

Monday, Nov. 28 12:15PM - 12:45PM Room: PH Community, Learning Center Station #2

#### **Participants**

Nico Buls, DSc, PhD, Jette, Belgium (*Presenter*) Nothing to Disclose Edilaine Honorio da Silva, Mol, Belgium (*Abstract Co-Author*) Nothing to Disclose Toon Van Cauteren, MSc, Brussels, Belgium (*Abstract Co-Author*) Nothing to Disclose Lara Struelens, Mol, Belgium (*Abstract Co-Author*) Nothing to Disclose Gert Van Gompel, PhD, Brussel, Belgium (*Abstract Co-Author*) Nothing to Disclose Filip Vanhavere, Mol, Belgium (*Abstract Co-Author*) Nothing to Disclose Johan De Mey, Jette, Belgium (*Abstract Co-Author*) Nothing to Disclose

#### PURPOSE

To investigate the impact of iodine concentration levels on absorbed radiation dose in blood for various incident photon energies in a cardiac CT model.

### **METHOD AND MATERIALS**

A representative model for cardiac CT imaging was defined, including a cardiac-chest model and the exposure geometry of a widebeam CT scanner (Revolution CT, GE Healthcare). In the chest model, the heart was represented by a volume filled with blood including six relevant iodine contrast fractions (c = 0-50, step 10 mg I/mL), surrounded by air (lungs) and water (soft tissue). A one-heartbeat CT acquisition was simulated by 8 rotational projections over 360° with 7 types of photon spectra: X-ray CT spectra 70, 80, 100, 120, 140 kVp and gamma spectra 137Cs (662 keV) and 60Co (1250 keV). For each energy-contrast combination, the absorbed dose (D), was calculated using the f6 tally of MCNPX code, with enough particles to maintain the uncertainties below 1%.

## RESULTS

With X-ray energies, the presence of iodine in blood increased D between 70 and 140 kVp by 1.7 (70 kVp, c = 10 mg I/ml) and 2.9 (140 kVp, c = 50 mg I/ml) fold, following an exponential trend.On the other hand, for 662 and 1250 keV gamma energies, a negligible increase of less than 4% and 1% was observed, respectively, even for c = 50 mg I/ml. This underlines the fact that the elevated D with X-ray energies is caused by the photoelectric effect.

# CONCLUSION

Our results indicate that the presence of iodine increases radiation dose in CT due to increased photoelectric effect, and that there is an exponential trend with iodine concentration.

## **CLINICAL RELEVANCE/APPLICATION**

A reduction in iodine contrast administration load also reduces radiation dose to the patient.

Clinical Utility of SSDE vs CTDI as the Radiation Dose Index Used to Comply with the New Joint Commission Element of Performance on CT Dose Monitoring for Exams of the Abdomen and Pelvis

Monday, Nov. 28 12:15PM - 12:45PM Room: PH Community, Learning Center Station #4

## Participants

Mark P. Supanich, PhD, Chicago, IL (*Presenter*) Research agreement, Siemens AG; Advisory Board, Bayer AG Benjamin Bienia, MD, Chicago, IL (*Abstract Co-Author*) Nothing to Disclose Joseph DeBartolo, MD, Chicago, IL (*Abstract Co-Author*) Nothing to Disclose Daniel R. L'Heureux, MD, Chicago, IL (*Abstract Co-Author*) Nothing to Disclose John Raseman, MD, Chicago, IL (*Abstract Co-Author*) Nothing to Disclose

# PURPOSE

A new element of performance for hospitals performing CT scans introduced by the Joint Commission in July 2015 requires that exams with a Radiation Dose Index (RDI) outside a defined range be reviewed. This work aims to determine if there is a difference in the clinical utility (identifying scans with poor image quality or higher than normal radiation dose) of using CTDI or SSDE as the RDI for abdomen and pelvis scans.

# METHOD AND MATERIALS

CT scans performed at the institution are transmitted to a dose monitoring software program, Radimetrics (Bayer Healthcare). Radimetrics calculates the SSDE for each body acquisition in the scan using the WED determined from the localizer radiograph. CTDI and SSDE values were exported from Radimetrics for analysis from single phase scans of the abdomen and pelvis performed on 3 scanners of the same model for a 6 month period. Scans identified as being in the bottom and top 5th percentiles for each RDI were selected for image quality evaluation by a group of 4 Radiology residents. 440 exams were identified of which 173 were in both the SSDE and CTDI sets, giving a total of 267 unique exams. The readers were blinded to the group the scans fell into and were asked to evaluate the image quality on a scale of 1 (non-diagnostic) to 5 (low noise, excellent image quality). Example scans were provided to the readers for each of the categories.

## RESULTS

Inter-reader reliability was evaluated using Fleiss' Kappa and found to be moderate for the non-diagnostic and poor image quality rankings and slight for the other 3 rankings. For the bottom 5th percentile the mean and standard deviation of the average image quality rankings for CTDI and SSDE were 3.27(0.58) and 3.20(0.67). For the top 5th percentile the CTDI and SSDE mean and standard deviation scores were 3.10(0.70) and 3.16(0.77).

### CONCLUSION

The similar average scores for the scans in each of the percentile groups for both RDIs examined suggests that for abdomen and pelvis scans, CTDI and SSDE are of equivalent clinical utility to use as the dose index off which to identify exams exceeding a defined range. This result may not hold for examinations of other body regions, such as the thorax.

## **CLINICAL RELEVANCE/APPLICATION**

CTDI and the existing recommendations on notification levels may continue to be used as a reasonable dose index off which to initiate investigations into exams exceeding a defined range to comply the new Joint Commission element of performance.

# Exploring Iodine Quantification and Attenuation in Wide Detector DECT Technology: A Phantom Study

Monday, Nov. 28 12:15PM - 12:45PM Room: PH Community, Learning Center Station #5

**FDA** Discussions may include off-label uses.

#### **Participants**

Diana Murcia, MD, Boston, MA (*Presenter*) Nothing to Disclose Manuel Patino, MD, Boston, MA (*Abstract Co-Author*) Nothing to Disclose Avinash R. Kambadakone, MD, Boston, MA (*Abstract Co-Author*) Nothing to Disclose Dushyant V. Sahani, MD, Boston, MA (*Abstract Co-Author*) Research support, General Electric Company; Medical Advisory Board, Allena Pharmaceuticals, Inc

### PURPOSE

To compare inter- and intra-scanner variability of iodine concentration, and attenuation values on virtual monochromatic (VMC) images between wide-detector (w) and narrow-detector (n) single-source and dual-source DECT technologies.

#### **METHOD AND MATERIALS**

A head and body CT phantom (Gammex 461A) with 9 cavities was used. Fifteen solutions were prepared with water and iodinated contrast media (ICM) (3 groups): high iodine: 15, 40, 70, 100mgI/ml; low iodine: 0.9, 1.8, 3.75, 7.5 mg/ml, and water; and ultralow iodine: 0.06, 0.12, 0.25, 0.5, 1mgI/ml, and water. Each solution was stored in 50ml tubes and placed the phantom. The phantom was scanned on DECT mode (140/80kVp) on a wide-detector and narrow-detector ssDECT with fast KvP enabled (Revolution CT, GE. Not FDA approved), a narrow-detector ssDECT (Discovery CT 750HD, GE), and a narrow-detector dsDECT (Somatom Definition Flash, Siemens). Iodine images and VMC images of 40-90KeV (10-KeV increments) were obtained. A total of 56 datasets were generated (8 scans, 7 per scan). Five ROIs were placed on each test tube; iodine was recorded in mgI/ml and attenuation in HU. Percentage measurement error were calculated for iodine quantification. Agreement between scanners was assessed with Bland-Altman plots. Inter- and intra-scanner variability and interaction of Iodine and HU measurements was compared with repeated-measures ANOVA and paired t-test.

#### RESULTS

There was a positive correlation for Iodine values, and for HU in MCI (P<0.05). For Iodine <1mgI/ml, there was 55% less overestimation in ssDECT/w compared to ssDECT/n, ssDECT, and dsDECT. For 1-7.5mgIml there was >28% of underestimation in ssDECT/w. For >40mgI/ml, there was similar underestimation in all DECT technologies (12%, 8%, 8%, and 15%). Attenuation values showed lower variability between ssDECT/w and ssDECT/n (15-50 HU), whereas higher variability between ssDECT and dsDECT (10-300 HU) in 40-60 KeV images (P<0.05).

## CONCLUSION

Iodine Quantification with a wide detector ssDECT was more accurate in Iodine concentrations <1mgI/ml compared to other DECT technologies. There is significant intra-scanner variability in HU and Iodine values in VMC images that requires a careful interpretation in clinical practice.

## **CLINICAL RELEVANCE/APPLICATION**

Wide detector DECT systems generate robust data acquisition and processing that may affect quantification parameters. Reliable iodine quantification and HU measurements is warranted for clinical decision-making.

### **Honored Educators**

Presenters or authors on this event have been recognized as RSNA Honored Educators for participating in multiple qualifying educational activities. Honored Educators are invested in furthering the profession of radiology by delivering high-quality educational content in their field of study. Learn how you can become an honored educator by visiting the website at: https://www.rsna.org/Honored-Educator-Award/

Dushyant V. Sahani, MD - 2012 Honored Educator Dushyant V. Sahani, MD - 2015 Honored Educator Dushyant V. Sahani, MD - 2016 Honored Educator First Results of the Quick Project: Accuracy Comparative Evaluation of PET Quantitation Among Multiple PET/CT Systems

Monday, Nov. 28 12:15PM - 12:45PM Room: PH Community, Learning Center Station #6

# Participants

Olivier Caselles, PhD, Toulouse, France (*Presenter*) Grant, General Electric Company Elena Deponti, Monza, Italy (*Abstract Co-Author*) Nothing to Disclose Delphine Vallot, Toulouse, France (*Abstract Co-Author*) Nothing to Disclose Jorge Uribe, PhD, Waukesha, WI (*Abstract Co-Author*) GE Healthcare employee Frederic Courbon, MD,PhD, Toulouse, France (*Abstract Co-Author*) Research Grant, General Electric Company

# PURPOSE

QUICK acronym stands for Quantitation Unified Intercomparison Control Kit (QUICK). The end point of the study is to estimate the global statistical multicenter quantitation accuracy taking into account the discrepancies between PET facilities, using a solid phantom with accurately known activities and volumes.

# METHOD AND MATERIALS

This study was based on NEMA NU-2 2012 Image Quality test without any out-of-field activity. Image analysis was performed using the software available on the operating console. The QUICK phantom was designed to meet the IEC61675/NEMA Body IQ phantom in terms of geometry and activity concentrations (spheres vs background ratio = 3.91:1). Tests were performed with the same phantom on different PET scanners. Acquisition time was adjusted to compensate activity decay.5 iterations of acquisitions were made at different dates to test both reproducibility and accuracy. Each set included 5 acquisitions performed without moving the phantom to evaluate repeatability.2 reconstruction algorithms were used: a Block Sequential Regularized Expectation Maximization (BSREM) algorithm and the standard OSEM reconstruction remaining the reference. Recovery coefficients (RC), background variability (BV) and lung error (LE) were reported and statistically analyzed using a single factor variance analysis.

## RESULTS

The ß noise constraint factor of the BESRM algorithm was set to 25 to match the OSEM (FWHM=2 mm, 12 subsets, 8 iterations). The equality hypothesis H0 was tested. No statistical difference for the RC was observed concerning both the repeatability and the reproducibility tests (p-value>0.99 - F vs F-criteria ratio<3%), meaning that H0 was true. Same results were observed for both BV and LE. Comparing the OSEM reconstruction to the regularized algorithm, H0 was not always verified. In particular, RC were 11% to 38% higher with BSREM while BV remained statistically the same. At last, no statistical difference was observed comparing the first two PET scanners tested in this study, regardless of any analyzed measurement.

## CONCLUSION

These first results of the QUICK project demonstrate that a roaming solid resin phantom may be used to assess quantitation consistency between different PET scanners.

## **CLINICAL RELEVANCE/APPLICATION**

The QUICK test is relevant as a first step in facility accreditation for multicentric clinical trials based on quantitative PET evaluation.

## PH218-SD-MOA7

Validation of Two Methods of Measuring Contact Area for Estimation of Applied Compression Pressure in Mammography

Monday, Nov. 28 12:15PM - 12:45PM Room: PH Community, Learning Center Station #7

FDA Discussions may include off-label uses.

#### **Participants**

Woutjan Branderhorst, PhD, Amsterdam, Netherlands (Presenter) Employee, SigmaScreening BV

Jerry E. De Groot, PhD, Amsterdam, Netherlands (Abstract Co-Author) Employee, SigmaScreening BV

Monique van Lier, MSc, Amsterdam, Netherlands (Abstract Co-Author) Employee, SigmaScreening BV

Ralph P. Highnam, PhD, Wellington, New Zealand (Abstract Co-Author) CEO, Matakina Technology Limited CEO, Volpara Solutions Limited

Cornelis A. Grimbergen, PhD, Amsterdam, Netherlands (*Abstract Co-Author*) Founder, SigmaScreening BV Employee, SigmaScreening BV Board Member, SigmaScreening BV Patent holder, SigmaScreening BV

Gerard J. den Heeten, MD, PhD, Nijmegen, Netherlands (Abstract Co-Author) Founder, SigmaScreening BV

## PURPOSE

In mammographic breast compression, the importance of estimating and controlling pressure rather than force is understood to an increasing degree. Recent publications point out the benefits in terms of reproducibility, pain, radiation dose, image quality and even detectability of breast cancer. The average pressure applied by the paddle can be calculated as the applied force divided by the contact area between the breast and the paddle. In this study, we have assessed the accuracy of two methods of estimating the contact area.

### **METHOD AND MATERIALS**

For a set of 300 breast compressions, we measured the contact areas between breast and paddle capacitively using a transparent indium-tin-oxide (ITO) foil attached to the paddle, and retrospectively from the obtained DICOM images using Volpara software (algorithm version 1.5.2). A gold standard was obtained from video images of the compressed breast captured from above using an optical camera. During each compression, the breast was illuminated from the sides in order to create a dark shadow on the video image where the breast was in contact with the compression paddle. We manually segmented the shadows captured at the time of X-ray exposure and measured their areas.

### RESULTS

We found a strong correlation between the manual segmentations and the capacitive measurements ( $r^2 = 0.979$ ) and between the manual segmentations and the Volpara measurements ( $r^2 = 0.955$ ). The regression lines were both very close to the line of identity (respectively, y = 0.046 + 0.965x and y = 0.022 + 0.985x).

#### CONCLUSION

The contact area between the paddle and the breast can be measured accurately, both in real-time using the capacitive method, and retrospectively using Volpara software. This finding substantiates many present and future studies that depend on one of these two methods for determining the pressure on the breast during mammographic compression.

# **CLINICAL RELEVANCE/APPLICATION**

Recent evidence suggests that using too high pressure reduces the detectability of breast cancer. An accurate method to determine the contact area is essential to accurately estimate applied pressure.

## Backscatter Factors for Computing Skin Dose in Fluoroscopically Guided Interventions (FGIs)

Monday, Nov. 28 12:15PM - 12:45PM Room: PH Community, Learning Center Station #8

#### Participants

David Borrego, PhD,MS, Gainesville, FL (*Presenter*) Nothing to Disclose Emily Marshall, MS, Gainesville, FL (*Abstract Co-Author*) Nothing to Disclose Wesley E. Bolch, PhD, Gainesville, FL (*Abstract Co-Author*) Nothing to Disclose

## PURPOSE

Previously, the authors of this work have quantified a rapid in-clinic peak skin dose (PSD) algorithm. The PSD algorithm makes use of the backscatter factors (BSFs) reported in ICRU Report 74. The goal of this study is to update the BSFs and better understand how they differ from the reported literature values when computed at different intervention sites on computational phantoms that better represent the adult and pediatric populations.

## METHOD AND MATERIALS

The BSFs were computed as the ratio of the energy deposition in air on the surface of a computational phantom, to the energy deposition in air to the same point in space in absence of the phantom. The energy deposition was computed with a Monte Carlo transport code on underweight, healthy, and overweight phantoms covering the reference height for adult and pediatric populations. The pediatric population was considered at the following ages: newborn, 1, 5, 10, and 15 year old. The BSFs were computed posterior to the following three sites: pubic symphisis, pericardium, and opisthocranion. The field size at the site of the BSF computation ranged from 5 x 5 to 25 x 25 cm<sup>2</sup>. The BSFs were computed for monoenergetic beams at 10–120 keV at 10 keV increments to allow for spectral weighting. Polychromatic spectra were also modeled to represent clinical beams with energies ranging from 60-120 kVp with no added filtration and added filtration of 0.1 through 0.9 mm of Cu.

#### RESULTS

In total, over 10k Monte Carlo runs were performed with a computer time of  $2.2 \times 10^3$  minutes per run to achieve a relative error less than 1%. The results of this study are in agreement with the values of ICRU 74 for the sites posterior to the pericardium and public symphisis. The BSFs at the site posterior to the opisthocranion are not in agreement with previous literature values. The maximum BSFs occurred in the energy range of 60-70 keV. The maximum BSFs also occurred at the largest field size. The BSFs decrease with increasing weight.

### CONCLUSION

This work provides a set of BSFs that are energy, field size, and site dependent. Adhering to a BSF computed from a healthy or underweight phantom will provide the most conservative estimate of PSD. Special consideration should be given to neurointerventional procedures when selecting a BSF.

#### **CLINICAL RELEVANCE/APPLICATION**

This work will disseminate BSFs for various energies, field sizes, phantoms, and interventional sites to be used in computing PSDs for FGIs.

## **Manual for Chest Radiograph Dictation**

Monday, Nov. 28 12:15PM - 12:45PM Room: QS Community, Learning Center Hardcopy Backboard

#### Participants

Mark Le, MD, Detroit, MI (*Presenter*) Nothing to Disclose Hiren Rangunwala, MD, Detroit, MI (*Abstract Co-Author*) Nothing to Disclose Vasavi Paidpally, MD, Detroit, MI (*Abstract Co-Author*) Nothing to Disclose Anum Aslam, MD, Detroit, MI (*Abstract Co-Author*) Nothing to Disclose Ronela Hanson, MD, Troy, MI (*Abstract Co-Author*) Nothing to Disclose

#### PURPOSE

The clinical report is an essential part of the service that radiologists provide to patients and referring physicians. It provides the pertinent assessment of the presenting pathology and the interpretation of the progression or resolution of a disease. As such, the written communication in the radiology reports should be uniform, comprehensive, and easily understood. For diagnostic radiology trainees, the learning curve is steep, particularly in chest radiographs as the findings are not always straightforward. The aim of the current study is to provide a systemic method to interpret chest radiographs, describe the essential components of a chest radiology report, and provide descriptive terminologies for common findings on chest radiographs along with their differentials.

#### **METHODS**

Forty commonly encountered chest radiographs were obtained at Detroit Medical Center by four residents. Each resident worked through each case and provided a systematic method to assess and interpret the case via a written step-by-step analysis to include description of the findings, the reasoning for each terminology used, explanation for each essential components in a radiology report, and provide the differentials for each findings. The clarity and accuracy of the case analysis was reviewed and corrected when applicable by four different staff radiologists. A pre- and post-chest rotation survey was given to each first-year radiology resident to assess his or her progression. The case analysis was only provided after the pre-chest rotation survey was obtained. The following areas were scored from a scale of 1 to 5, with 5 indicating outmost confidence: knowledge of essential commonly used terminology; and ability to perform a systematic method to interpret chest radiograph; ability to understand commonly used terminology; and ability to describe abnormal findings and provide common differentials. Additionally, the average evaluation scores at the end of the chest rotation are compared between junior residents who did receive the training manual versus junior residents who did not receive the training manual. Residents were evaluated from a scale of 1 to 4, with 2 indicating a resident who meets expectation.

#### RESULTS

Knowledge of essential components of a radiology report scored 3.57 and 4.71 on pre- and post-chest rotation survey. Ability to perform a systematic method to interpret chest radiograph scored 3.29 and 5.00 on pre- and post-chest rotation survey. Ability to understand commonly used terminology scored 3.00 and 4.00 on pre- and post-chest rotation survey. Ability to describe abnormal findings scored 2.57 and 4.29 on pre- and post-chest rotation survey. Ability to provide common differentials scored 3.00 and 4.00 on pre- and post-chest rotation survey. Summarized scores before the intervention were 3.05, and after the intervention were 4.45 (p < 0.05.) Junior residents who received the intervention scored an average of 2.8 by the end of the chest rotation while junior residents who did not receive the intervention scored an average of 1.9. (p < 0.05.)

## CONCLUSION

Novice radiology trainees show marked improvements in knowledge and communication when a training manual is provided early in their residency training.

# Improving Patient Flow in an Outpatient General Radiology Facility

Monday, Nov. 28 12:15PM - 12:45PM Room: QS Community, Learning Center Hardcopy Backboard

#### Participants

Katy Naumann, Rochester, MN (Presenter) Nothing to Disclose

### PURPOSE

An outpatient general radiology practice was reduced from five imaging rooms to two full function rooms (any general radiology exam can be performed in these two rooms), and one chest-only room due to allocating equipment and staff. Due to these changes, the general radiology team launched a project to look more closely at patient appointment times and the patient flow into and out of the department. New processes and guidelines needed to be established to better coordinate the flow of patients through the practice. The goal of this project was to decrease the average general radiology outpatient's overall lead time (from patient arrival to dismissal) from 26 minutes (May 2015) to 20 minutes by November 20th 2015.

### **METHODS**

A multidisciplinary team was formed between desk operations, radiology technologists, and phlebotomy staff to standardize the practice of patients being brought back for their general radiology examinations. The team performed manual timings and utilized electronic data sources to obtain the appropriate data necessary to assess the process. The baseline measure for the average time a patient spends in the radiology department was 26 minutes from the time the clinical assistant was notified a patient had arrived until the patient left the department, based on a sample of 57 patients. Of those patients, 24.5% of them were brought to general radiology early (over 30 minutes prior to their scheduled appointment) with no communication between staff. The current practice was for the clinical assistants to bring patients back to the department as soon as the patient arrived, rather than by availability of staff or appointment time. Upon analysis of the data, factors contributing to the inefficiencies in the practice included the lack of communication between phlebotomy and the radiology group, the clinical assistants and the patient, and the clinical assistants with the technologists. The team also noticed the lack of adherence to appointment times both from the schedulers and radiology staff. The practice had been operating on a push system instead of a pull system. Based on that analysis, the team selected to focus on improvements to these main concerns in an effort to improve the patient experience: better communication throughout the process, creating a pull system, and better compliance to appointment times. During the improve phase, successive Plan Do Study Act (PDSA) cycles were executed until the group found an improved standard of care that was reached and could be sustained. The team implemented the following interventions to decrease overall patient time in the department: (a) the clinical assistant and lead technologist use symbols in the electronic system to denote when patients can be brought back to the changing booths (pull system); (b) the clinical assistant will be stationed in the sub-wait area to create an environment more conducive to communication with both the phlebotomy group and initial communication with the patient about appointment time, wait time, and for welcoming them to the department; (c) the lead technologist will be stationed in the changing booth area to be more attuned to what exam rooms are available, how many patients are in the department, if patients need assistance, and to be more accessible to employees and patients.

#### RESULTS

After implementing all of these process improvements, the overall patient lead time in the department was reduced from 26 minutes to 18 minutes. The team was also successful in obtaining better control of when patients were brought back for their exam and decreased the percentage of patients being brought back early from 24.5% to 9%. The team accomplished this by using a pull system for the lead technologist to let the clinical assistant know when they were ready for the patient to be brought back to the department.

### CONCLUSION

Overall, this initiative provided improvements to the outpatient general practice and for our patients, allowing us to move forward with minor renovation plans to allow the staff to be stationed in the appropriate areas to sustain these results. These interventions will be fully implemented as routine practice upon completion of those renovations in our outpatient general radiology area. The team will continue to monitor the improvements to ensure the practice is working efficiently throughout these process changes.

## QS017-EB-MOA

## Applying Lean Methodology to Improve Workflow in a Growing Cross Sectional Procedure Service

Monday, Nov. 28 12:15PM - 12:45PM Room: QS Community, Learning Center Hardcopy Backboard

#### **Participants**

Aparna Baheti, MD, Charlottesville, VA (*Presenter*) Nothing to Disclose Arun Krishnaraj, MD, MPH, Charlottesville, VA (*Abstract Co-Author*) Nothing to Disclose Rachita Khot, MD, Charlottesville, VA (*Abstract Co-Author*) Nothing to Disclose Michael Hanley, MD, Charlottesville, VA (*Abstract Co-Author*) Nothing to Disclose Drew L. Lambert, MD, Charlottesville, VA (*Abstract Co-Author*) Nothing to Disclose Sebastian Feuerlein, MD, Charlottesville, VA (*Abstract Co-Author*) Nothing to Disclose

## PURPOSE

The cross sectional procedure team at the University of Virginia provides a wide array of services ranging from superficial fluid aspirations to renal ablations. The demand for these minimally invasive percutaneous interventions has increased. This is due in part to the continued pressure to decrease health care expenditures primarily through decreasing length of stay. The procedure service, as it was historically structured, was not prepared to scale to the increasing demand we were facing. In order to restructure our procedure service and maintain quality, the department embraced lean methodology to reduce waste, increase efficiency, and standardize workflow. The specific goals were as follows:

1)Identify potential areas for improvement by engaging all stakeholders at every level of operations.

2)Create a daily workflow with standardized processes.

3)Complete procedures within a 10 hour work day minimizing overtime, to improve morale among team members.

4)Improve the financial stewardship of scarce resources.

# METHODS

A Value Stream Analysis was created to clarify current problems and define goals. A multidisciplinary team was assembled to develop countermeasures using A3 analyses.

The following countermeasures emerged from the value stream process:

1) Engaging all attending physicians on service (inclusive of diagnostic staff) to be available for procedures in order to maximize use of available procedure rooms and to increase options for scheduling patients.

2) Creation of order sets to enable referring physicians to input all the necessary data required to schedule a patient electronically.3) Implementing a visualized daily schedule that is easily accessed and fluid for changes.

4) Improving coordination and standardization of pre-procedure evaluation to start all procedures by a set time each day.

5) Improving training of residents to allow level-appropriate autonomy.

## RESULTS

The cross-sectional procedure service was able to successfully manage a doubling in volume from approximately 150 to 300 procedures per month, without a concomitant increase in nursing, mid-level or upper level staffing.

## CONCLUSION

Lean continuous improvement methods were applied to our cross sectional procedure service to counter the challenges we were facing to meet the growing demand for our services. The most efficacious change made to our practice was the development of a call order for attending physicians to staff procedures, with reliance on physicians on the diagnostic services to help staff short procedures. Coupling this change with standardizing our processes throughout our intake, procedure, and post-procedure care allowed us to effectively double capacity without any additional capital or human resource expenditures.

# **Communication of Actionable Findings**

Monday, Nov. 28 12:15PM - 12:45PM Room: QS Community, Learning Center Station #1

#### **Participants**

Benjamin Z. Cooper, MD, Teaneck, NJ (*Presenter*) Nothing to Disclose PV Viswanath, PhD, New York, NY (*Abstract Co-Author*) Nothing to Disclose Rajwinder Singh, MD, Easton, PA (*Abstract Co-Author*) Nothing to Disclose

### PURPOSE

While communication of critical test results in radiology departments has improved greatly over the last 2-3 decades, there remains a strong need to improve communication of important but non urgent radiology test results (AF) to referring physicians.At our 220 bed community hospital center located in NE PA we developed a new method (nM) used in conjunction with standard distribution (sM) of final reports. The nM is intended to improve communication between the radiologist and the referring physician of important but non urgent findings (AF).

#### METHODS

This new method (nM) was implemented on January 1, 2015 and was monitored through September 9, 2015. All diagnostic imaging studies performed in our department with the exception of mammograms were considered for the nM.Reports describing Actionable findings (Category 3) as defined by the American College of Radiology Work Group were printed and signed by the reporting radiologist. Sometimes, the radiologist communicated the AF directly to the ordering physician. Mostly, a radiology facilitator faxed a copy of the report to the ordering physician and then called the physician's office to confirm receipt. The facilitator then entered metrics into a spread sheet including patient name, exam date, exam type, name of ordering physician and date of confirmation.Time from report completion to communication initiation (lag time1/LG1) and to communication completion (lag time2/LG2) were computed.

# RESULTS

46,000 diagnostic examinations were reported with sM, of which 514 reports (1.11%) were also communicated with nM.There was a large drop in LG1 and LG2 from the first month (0.80 & 0.80, n=5) to the second month (0.0 & 0.0, n=20). Average values of LG1 and LG2, excluding the first month, were 0.04 & 0.08. Lag times from the second month onwards were modelled using linear regression and were seen to decrease at a steady rate (0.015 & 0.021 per month, p=0.03 and 0.02).

#### CONCLUSION

We have successfully implemented a new method to improve communication of important but non critical radiology test results. Reduction in lag time shows that it can be easily implemented. Each radiology department workflow is unique. Efforts should be made to develop systems appropriate for each department to ensure effective and timely communication of results.

Assessment of Cirrhotic Liver Enhancement with Multiphasic CT using a Faster Injection Rate, Late Arterial Phase, and Weight-based Contrast Dosing

Monday, Nov. 28 12:15PM - 12:45PM Room: QS Community, Learning Center Station #2

## Participants

Kathleen Eddy, MD, Halifax, NS (*Presenter*) Nothing to Disclose Andreu F. Costa, MD, FRCPC, Halifax, NS (*Abstract Co-Author*) Nothing to Disclose

#### PURPOSE

Imaging with multiphasic CT plays a primary role in the diagnosis, staging and surgical planning of cirrhotic patients with hepatocellular carcinoma (HCC). Since HCC is typically hypervascular and displays washout in portal venous or delayed phases, good imaging technique is critical. In our practice we observed several liver CT studies demonstrating poor hepatic parenchymal enhancement. We sought to update our liver CT protocols according to the literature. The aim of this audit was to quantitatively evaluate the effect of our CT liver protocol modifications according to established imaging quality criteria.

#### **METHODS**

As an audit, the need for Research Ethics Board approval was waived. We modified our protocol to employ a faster injection rate (from 3 to 5 mL/s), later arterial phase (from 10 to 20 seconds post bolus triggering) and a weight-based contrast dosing scheme (previously 100 mL for all patients, changed to 1.7 mL/kg to a maximum of 150 mL). Liver and vascular attenuation values were recorded in consecutive CT livers with imaging features of cirrhosis from January to September 2015 (Old Protocol: 100mL Isovue 370, injection rate of 3 mL/s, early arterial phase at 10 seconds, n=49), and October to December 2015 (Modified Protocol: 1.7mL/kg Isovue 370 to maximum of 150mL, injection rate of 5 mL/s, arterial phase at 20 seconds, n=31). Patient weight was obtained from the electronic chart in order to calculate iodine concentration. Mean hepatic enhancement and iodine concentrations were calculated and compared using the student T-test. A study was considered adequate if the liver enhancement exceeded 50 HU (portal venous – unenhanced attenuation difference). If the unenhanced phase was not available, an iodine concentration of at least 500 mg I/kg was used as a surrogate measure for image quality. Other vascular and hepatic enhancement values were calculated and compared to benchmark values proposed in the literature.

#### RESULTS

First Cycle (Old Protocol) – Mean relative liver enhancement was  $51 \pm 16$  HU (38/49 patients) and mean iodine concentration was  $456 \pm 112$  mg I/kg. Fifty seven percent (57%, 28/49) of studies were suboptimal. The mean peak aortic attenuation in the arterial phase (242  $\pm$  92 HU) was also lower than the reference standard of  $\geq$  250 HU.Second Cycle (Modified Protocol) – There was significant improvement in mean relative liver enhancement ( $61 \pm 15$  HU, 17/31 patients, p 0.0282) and mean iodine concentration (595  $\pm$  88 mg I/kg, p<0.0001). There were only 7/31 (23%) suboptimal studies (p 0.01), and in all of these studies the patients weighed greater than 100 kg. There was significant improvement in other measures of image quality including the mean peak aortic attenuation in the arterial phase (317  $\pm$  98 HU vs. 242  $\pm$  92 HU, p 0.0008), mean peak portal vein attenuation in the arterial phase (180  $\pm$  70 HU vs. 112  $\pm$  41 HU, p < 0.0001), and mean peak hepatic vein attenuation in the portal venous phase (149  $\pm$  37 HU vs. 125  $\pm$  32 HU, p 0.003).

## CONCLUSION

A modified protocol with delayed arterial phase, faster injection rate, and weight-based dosing of intravenous contrast significantly improves liver enhancement and iodine concentrations in patients with cirrhosis, with a significant decrease in the number of suboptimal studies. As a result of this audit, the modified protocol has been permanently adopted at our institution for all CT liver studies. The findings of this audit were also presented at a broadcast Grand Rounds, and the modified protocol is now being implemented across the region.

## QS110-ED-MOA3

## Eliminating Lost and Non-reported Imaging Exams in US Air Force Teleradiology Practice

Monday, Nov. 28 12:15PM - 12:45PM Room: QS Community, Learning Center Station #3

#### **Participants**

Robert A. Jesinger, MD, Travis AFB, CA (*Presenter*) Nothing to Disclose Charles A. Tujo, MD, APO, AE (*Abstract Co-Author*) Nothing to Disclose

#### PURPOSE

In the practice of diagnostic radiology, every imaging exam must be viewed and reported by a radiologist; however, in daily practice, acquired images may be lost during transmission to a PACS system, and exams on PACS may go un-reviewed and/or unreported for a variety of reasons. These exams pose a tremendous patient safety and quality problem for any radiology practice, and lack of processes to identify and review these exams in a timely fashion pose an ethical and legal risk to the radiologist.Currently in US Air Force radiology, exams are ordered and processed thru the CHCS (Composite Health Care System) system, which functions as the RIS (radiology information system). Stand-alone imaging equipment (eg. CR, CT, MRI equipment) receives patient/order information from CHCS and transmit acquired images to PACS (AGFA IMPAX) through a secure tele radiology network. Once on PACS, the images are reviewed and dictated/finalized by a military radiologist using an integrated voice dictation system (TalkStation), and reports are electronically routed to the patient's military electronic medical record (EMR, currently AHLTA/Essentris). Unfortunately, not every imaging exam flawlessly appears on PACS. On a daily basis, technologists are expected to validate that all imaging exams on their machines are available on the PACS system for viewing, but errors persistently occur due to human and technical factors. In addition, exams that are on PACS may go unviewed (eg. mistakenly marked in a dictated status) due to radiologist human errors from workday interruptions. Final radiology reports may be lost in transmission to the EMR and/or stuck in the voice dictation system used in modern military teleradiology reporting. The purpose of this radiology QI project is to identify and minimize (i) the frequently of exams being lost between transmission from imaging equipment to PACS and (ii) the frequently of exams on PACS missing final reports in a patient's electronic health record. Our goal has been to identify processes that would ensure that all radiology exams were transmitted, reviewed, and reported in a timely fashion in our military teleradiology practice.

### **METHODS**

RIS (CHCS) exam status includes ordered, arrived (imaging ongoing), examined (imaging completed), and completed (final report in RIS). We use search tools in CHCS and high-reliability techniques to identify all incomplete imaging exams (arrived and examined status) for the 2015 calendar year, starting in September 2015. This list of exams is compared to cases on PACS, and lost exams are retransmitted to PACS by technologists. Exams on PACS without final CHCS reports are sorted into their PACS status (new, dictation started, dictated, finalized), and the reasons for their status are investigated. A daily search for lost and unreported exams are tracked. Weekly "incomplete" exam reports are generated by the technologists and provided to the radiologists and radiology leadership, and reasons for lost and non-reported exams are discussed at the weekly radiology leadership meetings.

#### RESULTS

At the start of our project, we identified 3 imaging exams that had not been transmitted to PACS, one of which (a sinus CT) had to be repeated. We also identified 47 exams that did not have final reports in CHCS, 2 of which had never been reviewed, 15 in "dictation started or dictated" status on PACS with no voice dictation report, and 30 of which had final reports in the voice dictation system that failed to transmit to CHCS. At the end of the 2015 calendar year, of the 100,000+ imaging exams completed, no lost or undictated exams were present. Daily searches began occurring on 1 Jan 2016 and continue thru the current day with continuous effort to keep the number of lost and non-reported exams at zero.

### CONCLUSION

Daily identification of lost and unreported radiology exams with CHCS is necessary in current Air Force teleradiology practice. In spite of an expectation that exams on imaging machines are flawlessly transmitted to PACS, in daily practice this was not seen due to ongoing network errors and in spite of technologist dedication to duty. In addition, exams in PACS can be mistakenly left in "dictation started" status by the radiologist, not allowing other radiologists to identify them for interpretation. Exams can be signed by the radiologist in our voice dictation system, but due to hardware and network issues, the final report may fail to be accepted and posted in CHCS and the EMR. Having a robust, high-reliability process in place to identify lost and incomplete exams using CHCS searches improves patient safety and reduces ethical and legal risks to the radiologist.

### QS111-ED-MOA4

A Quality Improvement Initiative to Decrease Radiation Exposure in Pediatric Patients Suspected to have Acute Appendicitis

Monday, Nov. 28 12:15PM - 12:45PM Room: QS Community, Learning Center Station #4

## Participants

Aderonke Ramos, MD, Mineola, NY (*Presenter*) Nothing to Disclose Patrice Villa, BS, Mineola, NY (*Abstract Co-Author*) Nothing to Disclose Irene Sher, MD, Mineola, NY (*Abstract Co-Author*) Nothing to Disclose

#### PURPOSE

Many children come to the emergency department presenting with right lower quadrant pain, concerning for acute appendicitis. Radiation exposure is a great concern in the pediatric population. Many pediatric patients receive CT examinations during the work-up for acute appendicitis in the emergency department. Analysis of baseline data at our institution from June-August 2014 showed that 79% of pediatric patients aged 4-18 years suspected to have acute appendicitis have received a CT scan of the abdomen as part of diagnostic imaging work-up. Review of the literature showed a utilization pattern closer to 45% at children's hospitals. Further gap analysis identified the availability and reliability of abdominal US to diagnose acute appendicitis in pediatric patients in our institution as a limiting factor. We posed a goal of decreasing the percentage of pediatric patients receiving abdominal CT examinations for suspected appendicitis by 30% at our institution over the course of one year. We formed a multidisciplinary team of pediatric emergency room physicians, radiologists, and pediatric surgeons. Pediatric emergency room physicians and surgeons ordered ultrasounds as the first line diagnostic study and triaged patients based on risk. The radiology department implemented a multi-step approach to improve the accuracy of right lower quadrant ultrasounds.

## **METHODS**

The Pediatric Appendicitis Score (PAS) system was implemented in the pediatric emergency room at our institution for evaluation of patients with suspicion for appendicitis. The PAS algorithm was then used to determine the patient's plan of treatment. PAS <=2 "low" consider imaging with ultrasound, observe or discharge home; PAS>=3 and <=7 "moderate", image with ultrasound; PAS >=8 operate. Therefore ultrasound was utilized as the first line modality in imaging patients with suspected appendicitis. In order to improve the accuracy of ultrasound we have provided didactic and hands on education to the sonographers and radiologists. In addition, as the volume of ultrasounds grew, the exposure and expertise of the sonographers also increased. The ultrasounds were interpreted as the following: normal, abnormal or equivocal (non visualization of the complete appendix or borderline appendix). In equivocal cases, based on the PAS score, the patients were triaged to CT scan or were admitted and observed. Negative cases were discharge and positive cases went to surgery. The ultrasound results and follow-up management such as observation, discharge, CT or surgery and pathology for April 2015 to present were recorded. To monitor the decrease in CT utilization and improvement of ultrasound accuracy, a retrospective review of the ultrasound results and CTs performed during June 2014 to August 2014 was logged.

### RESULTS

The multidisciplinary effort of the departments of Pediatric Surgery, Pediatric Emergency Medicine, and Radiology has resulted in a 50% decrease in the percentage of pediatric patients receiving abdominal CT for suspected appendicitis. Didactic and hands on training for the sonographers and radiologists has increased the

reliability of abdominal ultrasound in pediatric patients with suspected acute appendicitis at our institution up to 46% in the summer of 2015 as compared to 22% in the summer of 2014.

## CONCLUSION

We created a multidisciplinary team which included pediatric surgery, pediatric emergency medicine, and radiology with a goal to reduce radiation exposure in pediatric patients. Our aim was to accomplish a 30% reduction by December 2015 in abdominal CT scans performed for pediatric patients with right lower quadrant pain. Our team superseded that goal achieving a 50% reduction in the number of pediatric abdominal CT scans performed by August 2015. The goal is to continue to build and improve this initiative at our institution.

## RO209-SD-MOA2

Image Based Response Evaluation Of Intracranial Lesions after Cyberknife Robotic Radiosurgery-A Radiological Review

Monday, Nov. 28 12:15PM - 12:45PM Room: RO Community, Learning Center Station #2

**FDA** Discussions may include off-label uses.

#### Awards

**Student Travel Stipend Award** 

#### Participants

Shazia Kadri SR, MBBS, Karachi, Pakistan (*Presenter*) Nothing to Disclose Naveed V. Ahmed, MBBS, FRCR, karachi, Pakistan (*Abstract Co-Author*) Nothing to Disclose kelash kumar Sr, MBBS, Karachi, Pakistan (*Abstract Co-Author*) Nothing to Disclose Aneeta Ghulam Mohammad Sr, MBBS, Karachi, Pakistan (*Abstract Co-Author*) Nothing to Disclose Shumaila Arooj Sr, MBBS, Karachi, Pakistan (*Abstract Co-Author*) Nothing to Disclose Kamran Saeed Sr, MBBS, DMRD, Karachi, Pakistan (*Abstract Co-Author*) Nothing to Disclose tarig mahmood VI, MBBS, DMRD, Karachi, Pakistan (*Abstract Co-Author*) Nothing to Disclose

#### PURPOSE

To study the radiological response of Cyber Knife Robotic Radiosurgery for treating intracranial tumors by tailored MRI sequences in providing maximum details

## **METHOD AND MATERIALS**

653 patients were selected from December 2012 to June 2015 who were referred to the department of cyberknife from different hospitals within and outside Pakistan for the radiosurgery. Tumors with less than 6 cm size, post operative residual/recurrent tumor and surgically unresectable tumor were included. Patient was followed every three months with 3D T1 contrast MRI and added sequences according to need.

#### RESULTS

Out of 653 patients, Overall 35% of benign tumors showed reduction in size and 63% remain stable and 2% were resolved radiologically with clinical improvement in 80% cases where as 47% of malignant tumors were reduced , 31% remain stable and 22% showed progression radiologically but 70% of patients showed clinical improvement. Considering Meningiomas, out of 135 cases 33% were reduced, 65% remained stable and 2% resolved with clinical improvement in 82% of cases. In 109 AVM,82% were reduced,13% remained stable and 5% were resolved with clinical improvement in 84% of cases. Out of 91 cases of gliomas 64% of low grade gliomas and 58% of high grade gliomas were reduced with clinical improvement of 86% and 73% respectively. From 76 cases of Acoustic neuroma 20% reduced and 80% remained stable with clinical improvement in 85%. Out of 71 cases of pituitary adenomas 52% were reduced and 76% clinically improved. From 17 cases of craniopharyngioma 53% were reduced and 88% were clinically improved.

## CONCLUSION

Our results clearly shows that cyberknife is highly effective in controlling benign tumors and a good palliative modality for recurrent malignant and metastatic brain tumors.T1 3D contrast is the sequence of choice for most of the intra cranial lesions after treatment follow up, while in cases of pituitary adenoma, acoustic neuroma, schwannoma we utilized BTFE for cranial nerve definition. Longer follow up with conventional MRI is mandatory.

### **CLINICAL RELEVANCE/APPLICATION**

Cyberknife Robotic Radiosurgery showed promising results in patients with residual /recurrent or surgically unresectable intracranial neoplastic mass lesions.

# **Treatment Outcome for Ependymal Tumors in the United States**

Monday, Nov. 28 12:15PM - 12:45PM Room: RO Community, Learning Center Station #3

#### **Participants**

Kailin Yang, PhD, Cleveland, OH (Presenter) Nothing to Disclose

## ABSTRACT

Purpose/Objective(s): Ependymal tumors are rare CNS neuroectodermal neoplasm with a significant impact on patient mortality and quality of life. This study is to compare the effect of surgery and adjuvant radiation therapy (RT) on survival outcomes for various histological subtypes of ependymal tumors in the United States.Materials/Methods: All patients aged >=18 with ependymal tumors (myxopapillary ependymoma 9394/1, subependymoma 9383/1, ependymoma 9391/3, and anaplastic ependymoma 9392/3) were identified from the Surveillance, Epidemiology, and End Results registry (2000-2009). Patients with unknown status of RT or surgery were excluded. Surgical treatment was categorized into gross total resection (GTR) and no GTR (including no surgery and subtotal resection). Demographic and clinicopathological predictors were analyzed using chi-square test and t-test. Log-rank test and multivariate Cox proportional hazard modeling were used to examine treatment effect on overall survival (OS).Results:The primary analysis totaled 2091 patients, with 424 cases of myxopapillary ependymoma (20.3%), 211 subependymoma (10.1%), 1325 ependymoma (83.4%), and 131 anaplastic ependymoma (6.2%). On univariate analysis, GTR was associated with improved OS for ependymoma (89% vs. 81%, pConclusion: Ependymoma was the most common histological subtype among all ependymal tumors in the United States. Age at diagnosis was found to significantly contribute to patient long term survival for all 4 subtypes. Surgery in the format of GTR provided survival benefit particularly in ependymoma. Adjuvant RT was found to adversely impact on OS of ependymoma, which might reflect a selection bias of preferential offering of RT to patients with worse prognosis. More definitive study incorporating factors including disease severity and chemotherapy would be needed to validate our findings.

## RO212-SD-MOA5

## Phase Ib/II Clinical Trial of Novel Oxygen Therapeutic in Chemoradiation of Glioblastoma

Monday, Nov. 28 12:15PM - 12:45PM Room: RO Community, Learning Center Station #5

#### Participants

Jason Lickliter, MBBS, PhD, Melbourne, Australia (*Abstract Co-Author*) Nothing to Disclose Jeremy Ruben, MBBCh, MD, Melbourne, Australia (*Abstract Co-Author*) Nothing to Disclose David Wilson, Tucson, AZ (*Abstract Co-Author*) Shareholder, NuVox Pharma LLC; Heling Zhou, Dallas, TX (*Abstract Co-Author*) Nothing to Disclose Ralph P. Mason, PhD, Dallas, TX (*Abstract Co-Author*) Nothing to Disclose Evan C. Unger, MD, Tucson, AZ (*Presenter*) Shareholder, NuVOx Pharma LLC; Shareholder, Microvascular Therapeutics

# PURPOSE

Tumor hypoxia limits the response of glioblastoma multiforme (GBM) to radiotherapy (RT). The purpose of this study is to evaluate the use of a novel oxygen therapeutic (OT), dodecafluoropentane emulsion (DDFPe) in chemoradiation treatment of GBM.

## **METHOD AND MATERIALS**

Adult GBM patients with residual tumor post surgery enrolled in an open label Phase Ib/II clinical trial received doses of 0.05 mL/kg, 0.1 mL/kg or 0.17 mL/kg 2% w/vol DDFPe administered via IV infusion prior to each of 30 fractions of RT over a 6-week period. PK samples were obtained in five patients at the recommended dose. Patients were followed with serial MR scans and evaluated as per RANO criteria and also underwent TOLD MRI scans pre and post DDFPe on days 1 and 5 or 10 of dosing. Tumor DNA profiling (with methylation) analysis was performed on all patients.

## RESULTS

Six patients have completed dosing; 3 more patients are presently being treated. There were no acute adverse events associated with administration of DDFPe. At the dose of 0.17 mL/kg a DLT was observed due to Grade III radiation necrosis confirmed by surgery 3 months post RT and 0.1 mL/kg was determined to be the therapeutic dose. One other patient treated at the 0.1mL/kg dose had Grade III radiation necrosis confirmed by surgery at 9 months post RT. The first patient was predicted non responder to temozolomide (negative methylation of MGMT) survived 21-months post diagnosis. At this time all other patients are alive. Survival data will be presented. TOLD MRI showed significant decreases in T1 of tumor tissue with little appreciable change in contralateral brain.

### CONCLUSION

Acute administration of DDFPe is well tolerated in association with chemoradiation but may increase risk of radiation necrosis. TOLD MRI confirms tumor re-oxygenation. Preliminary survival data suggests therapeutic benefit.

### **CLINICAL RELEVANCE/APPLICATION**

DDFPe is the first OT with sufficient safety factor to enable administration during each fraction of RT. A randomized, prospective placebo controlled trial is planned.

# Contrast-enhanced Ultrasound (CEUS) of Cystic and Solid Renal Lesions: Introduction and Imaging Primer

Monday, Nov. 28 12:15PM - 12:45PM Room: GU/UR Community, Learning Center Station #7

**FDA** Discussions may include off-label uses.

#### **Participants**

Mittul Gulati, MD, La Canada Flintridge, CA (*Abstract Co-Author*) Nothing to Disclose Armen S. Aivazi, MD, Los Angeles , CA (*Presenter*) Nothing to Disclose Phillip M. Cheng, MD, MS, Los Angeles, CA (*Abstract Co-Author*) Nothing to Disclose Chidubem G. Ugwueze, MS, Los Angeles, CA (*Abstract Co-Author*) Nothing to Disclose Edward G. Grant, MD, Los Angeles, CA (*Abstract Co-Author*) Research Grant, General Electric Company ; Medical Advisory Board, Nuance Communications, Inc Vinay A. Duddalwar, MD, FRCR, Los Angeles, CA (*Abstract Co-Author*) Nothing to Disclose **TEACHING POINTS** 

1. Background on contrast-enhanced ultrasound (CEUS) of focal renal lesions.

- 2. Differentiating features and examples of cystic and solid renal lesions on both conventional ultrasound and CEUS.
- 3. Brief overview of CEUS derived quantitative imaging of renal lesions.

## TABLE OF CONTENTS/OUTLINE

OUTLINE:1. CEUS technique in evaluation of focal renal lesions.2. Advantages and limitations of renal CEUS.3. Differentiating features of cystic renal lesions on CEUS, with examples and analogues to Bosniak CT classification.4. Differentiating features of solid renal lesions on CEUS, with examples including: -clear cell renal cell carcinoma -papillary renal cell -angiomyolipoma (both typical and lipid-poor) carcinoma - oncocytoma -renal -lymphoma5. Overview of quantitative imaging (time-intensity curves, or TIC) pseudotumor -metastases derived from CEUS, and the utility of TICs in differentiating renal lesions.SUMMARYAfter reviewing this exhibit the participant will:1. Be familiar with technique, advantages, and limitations of CEUS in evaluation of cystic and solid renal lesions.2. Be familiar with the CEUS appearance of a variety of common cystic and solid renal lesions.3. Understand the emerging role of CEUS derived quantitative imaging in differentiating renal lesions.

# Percutaneous Biliary Interventions: What the Radiologist Needs to Know

Monday, Nov. 28 12:15PM - 12:45PM Room: VI Community, Learning Center Station #8

#### Awards Certificate of Merit

## Participants

Maria Khalid, MD, Boston, MA (*Presenter*) Nothing to Disclose Marina C. Bernal Fernandez, MD, Boston, MA (*Abstract Co-Author*) Nothing to Disclose Michael J. Hsu, MD, Boston, MA (*Abstract Co-Author*) Nothing to Disclose Anthony S. Armetta, MD, Boston, MA (*Abstract Co-Author*) Nothing to Disclose Katherine M. Gallagher, MD, Boston, MA (*Abstract Co-Author*) Nothing to Disclose Stephan W. Anderson, MD, Boston, MA (*Abstract Co-Author*) Nothing to Disclose Rajendran Vilvendhan, MD, Newton Lower Falls, MA (*Abstract Co-Author*) Nothing to Disclose Vijay Ramalingam, MD, Boston, MA (*Abstract Co-Author*) Nothing to Disclose

# **TEACHING POINTS**

1. Interventional radiology (IR) plays an important role in management of biliary pathologies, particularly in patients who cannot be treated by an endoscopic approach. IR offers precise anatomic definition of biliary pathology via percutaneous transhepatic cholangiography (PTC), biliary access through percutaneous transhepatic drainage, and other treatment options including balloons, stents, and drain placement.

2. Common biliary interventions occur in the setting of malignant and benign biliary obstructions, percutaneous management of bile leaks, and PTC assisted ERCP.

Biliary drainage is important in the management of biliary obstruction, especially in the setting of cholangitis. PTC-assisted ERCP is a combined approach consisting of PTC biliary drainage and internalizing the drainage tube using an endoscope.
 Biliary leaks can occur as a complication of hepatobiliary surgery. In cases in which surgical repair or endoscopic management are not an option, bile flow can be diverted from the defect through percutaneous transhepatic biliary drainage.

# TABLE OF CONTENTS/OUTLINE

I. Techniques of biliary drainage

- II. Clinical applications with cases:
- a. Malignant and non-malignant biliary obstructions (i.e. choledocholithiasis, strictures, cholangiocarcinoma, pancreatic cancer)
- b. Percutaneous management of bile leaks
- c. Rendezvous procedures with ERCP

Transarterial Chemoembolization (TACE) in Hepatocellular Carcinoma (HCC): Intraprocedural Blood Volume Measurement using Fast Cone-Beam CT for Monitoring the Response

Monday, Nov. 28 12:15PM - 12:45PM Room: VI Community, Learning Center Station #1

## Participants

Thomas J. Vogl, MD, PhD, Frankfurt, Germany (*Presenter*) Nothing to Disclose Stefan Tietz, Frankfurt, Germany (*Abstract Co-Author*) Nothing to Disclose Nour-Eldin A. Nour-Eldin, MD,PhD, Frankfurt Am Main, Germany (*Abstract Co-Author*) Nothing to Disclose Nagy N. Naguib, MD, MSc, Frankfurt Am Main, Germany (*Abstract Co-Author*) Nothing to Disclose

## PURPOSE

To evaluate the response criteria of transarterial chemoembolization (TACE) in hepatocellular carcinoma (HCC) by measuring parenchymal blood volume (PBV) using C-arm cone-beam Dyna CT, monitoring changes in PBV after repeated TACE and correlating these with the changes in tumor diameter in MRI.

## **METHOD AND MATERIALS**

In a retrospective study 39 patients diagnosed with a HCC received 100 sessions of TACE (2-6 sessions/patient, mean: 3) with PBV using fast-protocol and MRI in 4-week intervals. During TACE treatment Dyna CT (Axiom Artis Zeego, Siemens, Healthcare Forchheim Germany) was monitored using fast-protocol for managing timing and infusion of contrast agent as follows: Start of contrast injection at 0s, injector mode with 3.5s X-ray delay. This allowed fill run at exactly 9s. Total scan time was 12s. After examination Dyna CT scans were processed by software (syngo InSpace) on a research workstation (Syngo XWP, Siemens AG Healthcare Sector) and PBV maps were printed. Then MRI was examined for the maximum diameter of the lesion and blood volume was calculated in the overlapping PBV.

## RESULTS

Statistical analysis was realized by software (BiAS, Darmstadt, Germany); survival was analyzed with the Kaplan-Maier-Method and the Log-Rank-Test.

For all patients a coefficient of correlation of r=0.4 was taken into account. This demonstrates a fair correlation between PBV and size in MRI (Landis and Koch: fair) with a power of 1-beta=0.80 and a level of significance of alpha=0.05. First results showed no significant correlation between change of size in MRI and change of PBV (rho= 0.27, p=0.08) using Spearman's rank correlation. Analyzing the relation of initial PBV and change in PBV showed strong significant correlation (rho=0.61, p=0.000029).

#### CONCLUSION

The current preliminary data underline that intraprocedural PBV allows predicting and monitoring treatment response to TACE.

## **CLINICAL RELEVANCE/APPLICATION**

Intraprocedural PBV is a promising predictor for treatment response to TACE.

Application of Casein Particle as a New Embolic Material for Vascular Interventional Radiology: An Experimental Study in a Rabbit Model

Monday, Nov. 28 12:15PM - 12:45PM Room: VI Community, Learning Center Station #2

# Participants

Shobu Watanabe, MD, Otsu, Japan (*Abstract Co-Author*) Nothing to Disclose Norihisa Nitta, MD, Kyoto, Japan (*Presenter*) Nothing to Disclose Shinichi Ota, MD, Otsu, Japan (*Abstract Co-Author*) Nothing to Disclose Yuki Tomozawa, MD, Otsu, Japan (*Abstract Co-Author*) Nothing to Disclose Akinaga Sonoda, MD, PhD, Otsu, Japan (*Abstract Co-Author*) Nothing to Disclose Kiyoshi Murata, MD, Otsu, Japan (*Abstract Co-Author*) Nothing to Disclose

### PURPOSE

Milk casein micelles are a natural nano-delivery system. They are part of the milk transport system in which nutrients are passed from the mother to a suckling offspring as a primary source of amino acids and calcium phosphates for neonates. Many of the structural and physicochemical properties of caseins facilitate their functionality in drug delivery systems and reported that  $\beta$ -casein nanoparticles can entrap and deliver hydrophobic chemotherapeutics such as mitoxantrone, vinblastine, irinotecan, docetaxel, and paclitaxel. In this study, we used casein particles (CPS) as an emboric material and evaluated the embolic effect and pathology of embolized arteries of CPS and gelatin microspheres (GMS) in a rabbit model.

## **METHOD AND MATERIALS**

12 rabbits were divided into 2 groups and the renal artery was embolized using each embolus material (CPS and GMS). Complete embolization of the lobular arteries and filling of the distal parts of the lobar arteries was considered as the end point of the embolization. 3 rabbits in each group were sacrificed 2, and 5 days later and kidneys were extracted.Pathological specimens were constructed in 3-mm interval by a coronal section and changes in arterial walls (wall distension, inflammatory change, and fibrosis) were evaluated.

## RESULTS

In microscopic specimens, wall distension was observed in all cases. The degree of the wall distension, however, was stronger in the casein particle, and the embolic range was relatively extensive. Mold-shaped repletion was also recognized. Inflammatory change was most remarkable after 2 days, and fibrosis was most remarkable after 5 days.

## CONCLUSION

There was no difference in the embolic effects of CPS and GMS. And there was also no significant difference in pathological changes in arterial walls and around the embolization materials (CPS and GMS).

### **CLINICAL RELEVANCE/APPLICATION**

Further studies are necessary, casein particle might become an accepted alternative embolic material to other gelatin materials in the future.

Lower Extremity Ultrasonography in the Evaluation of Hospitalized Patients Suspected of Deep Vein Thrombosis: Developing a Setting-Specific Risk Stratification Model

Monday, Nov. 28 12:15PM - 12:45PM Room: VI Community, Learning Center Station #3

# Participants

Emily C. Alper, BA, Boston, MA (*Presenter*) Nothing to Disclose Ivan Ip, MD, MPH, Brookline, MA (*Abstract Co-Author*) Nothing to Disclose Patricia Balthazar, MD, Framingham, MA (*Abstract Co-Author*) Nothing to Disclose Gregory Piazza, MD, Boston, MA (*Abstract Co-Author*) Nothing to Disclose Samuel Z. Goldhaber, MD, Boston, MA (*Abstract Co-Author*) Nothing to Disclose Carol B. Benson, MD, Boston, MA (*Abstract Co-Author*) Nothing to Disclose Ronilda Lacson, MD, PhD, Brookline, MA (*Abstract Co-Author*) Nothing to Disclose Ramin Khorasani, MD, Boston, MA (*Abstract Co-Author*) Consultant, Medicalis Corp

#### PURPOSE

Although validated in outpatient settings, the Wells score for deep venous thrombosis (DVT) has high failure rate and low efficiency among hospitalized patients. The purpose of this study is to develop an inpatient-specific risk stratification model for pre-test probability of DVT in hospitalized patients.

### **METHOD AND MATERIALS**

This HIPAA-compliant, observational study was conducted at a 793-bed quaternary care, academic hospital. All adult inpatients suspected of having DVT undergoing lower-extremity venous duplex ultrasound studies (LEUS) during the study period were included. Relevant risk factors (e.g. demographics) were collected from the order entry and medical records. Samples were divided into a model derivation cohort and a validation cohort. A prediction rule for DVT was derived using recursive partitioning algorithm. Our primary outcome was presence of proximal DVT; secondary outcome was presence of any DVT (proximal or distal).

### RESULTS

2,960 hospitalized patients underwent LEUS during the study period: 1,135 in the derivation group. 343 (11.6%) had proximal DVT (137 [12.1%] in the derivation group, 206 [11.3%]) in the validation group); 603 (20.3%) had lower extremity DVT regardless of location (241 [21.1%] derivation, 362 [19.8%] validation). Significant predictors were obtained from the most accurate and parsimonious recursive partitioning model and points were empirically assigned for significant predictors and added together to determine a score: history of DVT (4 pt), active cancer (1 pt), hospital stay of >5 days before imaging (1 pt), and age >45 years (1 pt). Patients were considered low risk (score=0), moderate, or high (score >4). In the validation cohort, 2.9% in the low risk group had proximal DVT, 7.8% in the moderate group, and 33.9% in the high risk group (p<0.0001). Negative predictive value (NPV) of the score to predict proximal DVT was 97.1%; sensitivity was 98.1%. By comparison, with Wells criteria, the NPV was 94.1%; sensitivity was 94.2.

# CONCLUSION

In adult hospitalized patients, a scoring system based on specified risk factors can be used to predict risk of DVT and identify those at low risk for DVT.

## **CLINICAL RELEVANCE/APPLICATION**

In assessing patients at risk for developing DVT, a novel inpatient-specific scoring system for hospitalized patients was more accurate than Well's criteria for this patient population.

## VI233-SD-MOA4

Peer Review Designed for Interventional Radiology - Feasibility and Usefulness in Assessing Performance and Practice in Interventional Radiology

Monday, Nov. 28 12:15PM - 12:45PM Room: VI Community, Learning Center Station #4

#### Awards

#### **Student Travel Stipend Award**

#### Participants

Michael Luo, MD, Boston, MA (*Presenter*) Nothing to Disclose Seth J. Berkowitz, MD, Boston, MA (*Abstract Co-Author*) Nothing to Disclose Chun-Shan Yam, PhD, Boston, MA (*Abstract Co-Author*) Nothing to Disclose Jeff L. Weinstein, MD, Philadelphia, PA (*Abstract Co-Author*) Nothing to Disclose Salomao Faintuch, MD, Boston, MA (*Abstract Co-Author*) Nothing to Disclose Salomao Faintuch, MD, Boston, MA (*Abstract Co-Author*) Nothing to Disclose Muneeb Ahmed, MD, Wellesley, MA (*Abstract Co-Author*) Nothing to Disclose Ammar Sarwar, MD, Boston, MA (*Abstract Co-Author*) Stockholder, Agile Devices Jonathan B. Kruskal, MD, PhD, Boston, MA (*Abstract Co-Author*) Author, UpToDate, Inc Olga R. Brook, MD, Boston, MA (*Abstract Co-Author*) Research Grant, Toshiba Medical Systems Corporation

# PURPOSE

Existing radiology peer review systems are designed for diagnostic radiology and are not directly applicable for the assessment of performance in interventional radiology (IR) practice. We evaluated an IR peer review system based on the capture of peer review data during daily board rounds.

# METHOD AND MATERIALS

This was an IRB-approved HIPAA-compliant retrospective review of a prospectively entered web-based peer review system within a multi-physician academic interventional radiology group. During daily board rounds recent cases were discussed between attending physicians and assessed for clinical decision-making and patient care (agree; acceptable alternative; inappropriate) and procedure technique appropriateness (agree; acceptable alternative; inappropriate) with details provided in free-text format. Technical success, short-term complications, learning opportunities and near misses were also noted.

#### RESULTS

665 cases were entered into the IR peer review system in a 21 month period, out of 5906 IR cases performed. The majority of the cases represented advanced procedures: 180/665 (27%) arterial cases, 149/665(22.4%) biliary cases, 67/665(10%) renal cases, 49/665( 7.4%) TIPS cases. Average number of IR attendings present in each case review was 3.38±1.06 with average of 14 cases reviewed by each attending per month. The majority of cases (627/665, 94.3%) were technically successful. There were 9/665(1.4%) major and 35/665(5.3%) minor complications. 40/665(6%) cases were graded as acceptable alternative for technique and 4/665(0.6%) cases were graded as acceptable alternative for clinical management, and there were no cases of inappropriate clinical decision making. 8/665(1.2%) near misses and 66/665(9.9%) learning opportunities were entered. In a comparison period of 11 months prior to implementation of IR peer review, 150 cases were submitted to diagnostic peer review by IR attendings, with only 34 IR cases.

## CONCLUSION

IR specific peer review system effectively captures outcomes and clinical practice variation of image guided procedures. It allows prompt determination and documentation of clinical decision-making process and patient care outcomes, technical appropriateness, near-miss cases and short-term complications.

# **CLINICAL RELEVANCE/APPLICATION**

IR peer review system is feasible and effective means of assessing performance in the practice of interventional radiology.

## **Honored Educators**

Presenters or authors on this event have been recognized as RSNA Honored Educators for participating in multiple qualifying educational activities. Honored Educators are invested in furthering the profession of radiology by delivering high-quality educational content in their field of study. Learn how you can become an honored educator by visiting the website at: https://www.rsna.org/Honored-Educator-Award/

Jonathan B. Kruskal, MD, PhD - 2012 Honored Educator Jonathan B. Kruskal, MD, PhD - 2016 Honored Educator

**Percutaneous Cryoablation for Pelvic Bone Metastases** 

Monday, Nov. 28 12:15PM - 12:45PM Room: VI Community, Learning Center Station #5

#### **Participants**

Takashi Yamanaka, MD, Tsu, Japan (*Presenter*) Nothing to Disclose Atsuhiro Nakatsuka, MD, Tsu, Japan (*Abstract Co-Author*) Nothing to Disclose Masafumi Takafuji, Tsushi Edobashi 2 choume 174, Japan (*Abstract Co-Author*) Nothing to Disclose Yuichi Sugino, MD, Tsu, Japan (*Abstract Co-Author*) Nothing to Disclose Naritaka Matsushita, MD, Tsu, Japan (*Abstract Co-Author*) Nothing to Disclose Masashi Fujimori, MD, Tsu, Japan (*Abstract Co-Author*) Nothing to Disclose Hajime Sakuma, MD, Tsu, Japan (*Abstract Co-Author*) Nothing to Disclose Hajime Sakuma, MD, Tsu, Japan (*Abstract Co-Author*) Departmental Research Grant, Siemens AG; Departmental Research Grant, Bayer AG; Departmental Research Grant, Guerbet SA; Departmental Research Grant, Nihon Medi-Physics Co, Ltd

## PURPOSE

To retrospectively evaluate safety and clinical utility of percutaneous cryoablation for pelvic bone metastases.

## **METHOD AND MATERIALS**

Consecutive 16 patients (9 male and 7 female) with a mean age  $\pm$  standard division of 53.8  $\pm$  12.9 years (range 27–71 years) underwent percutaneous cryoablation under real-time CT fluoroscopy guidance for 17 pelvic bone metastases between January 2012 and December 2015. The mean target tumor diameter was 6.2  $\pm$  3.5 cm (range; 1.5 cm to 15 cm). Feasibility, safety, and clinical outcomes were evaluated. Treatment response was evaluated using a modified-RECIST criteria. Pain was evaluated using a visual analog scale (VAS) score in patients having painful tumors.

#### RESULTS

Total 17 treatment sessions for 17 tumors were performed and planed protocol were completed in all patients. There was no major complication related to procedures. Therapeutic response was complete response in 4 tumors (23.5%, 4/17), partial response in 8 tumors (47.1%, 8/17), and stable disease in 5 tumors (29.4%, 5/17), resulting in response rate of 70.6% (12/17). During a median follow-up periods of 10.9 months, 1- and 2- year overall survival rate were 83.6% (95% confidential interval (CI); 47.9–95.7%) and 66.9% (95% CI; 24.2–89.2%). In all 8 patients having painful tumors, mean VAS score significantly decreased from 4.5  $\pm$  2.6 (range 1.0–8.0) to 2.3  $\pm$  2.6 (range 0–7.0) (p=0.012) at 1-week after.

#### CONCLUSION

Percutaneous cryoablation is a feasible, safe and useful therapeutic option for pelvic bone metastases which leads pain relief in patients having painful tumors and might help to patient's prognosis.

#### **CLINICAL RELEVANCE/APPLICATION**

Percutaneous cryoablation for pelvic bone metastases leads pain relief in patients having painful tumors and might help to patient's prognosis.

Complications Following US-guided Core-needle Biopsy for Thyroid Lesions: A Retrospective Study of 6169 Consecutive Patients with 6687 Thyroid Nodules

Monday, Nov. 28 12:15PM - 12:45PM Room: VI Community, Learning Center Station #6

## Participants

Eun Ju Ha, Suwon, Korea, Republic Of (*Presenter*) Nothing to Disclose Jung Hwan Baek, Seoul, Korea, Republic Of (*Abstract Co-Author*) Nothing to Disclose

### PURPOSE

To present the spectrum of clinical adverse events of ultrasound (US)-guided core needle biopsy (CNB) for thyroid lesions and to illuminate the potential complications with preventive measures.

## METHOD AND MATERIALS

Institutional review board approval was obtained for this retrospective study. From January 2008 to March 2013, 6,169 patients underwent US-guided CNB of 6,687 thyroid nodules at a single institution. We assessed the number and types of major and minor complications, and evaluated the factors associated with complications.

## RESULTS

The authors observed 53 complications in 50 patients (0.81%), including 4 major and 49 minor complications. The major complications were massive hematoma (n = 2), pseudoaneurysm (n = 1), and voice change leading to disability of more than 30 days (n = 1). The minor complications were small to moderate hematoma (n = 42), carotid injury (n = 2), voice change that recovered within 30 days (n = 3), tracheal puncture (n = 1), and dysphagia (n = 1). Edema (n = 12), vertebral puncture (n = 3), and vasovagal reaction (n = 1) were recorded as side effects. There were no patients with permanent problems resulting from complications and procedure-related death. The presence of a co-procedure was the only significant factor associated with complication after thyroid CNB (P = 0.023).

#### CONCLUSION

US-guided CNB for thyroid lesions is a safe procedure with a low complication rate in a large population. However, comprehension of various complications with a management plan is necessary to prevent potential complications or properly manage those that occur.

## **CLINICAL RELEVANCE/APPLICATION**

1.The complication rate after ultrasound (US)-guided core needle biopsy (CNB) for thyroid lesions was 0.81% (50/6,169),<br/>and the major complication rate was 0.06 % (4/6,169).2.Vascular injury was the most common complication (47/6,169;<br/>0.76%).3.0.76%).3.Understanding the various complications, knowledge of techniques and management to prevent complications will<br/>minimize complications and sequelae in patients undergoing CNB of thyroid nodules..

## BR133-ED-MOB7

Tomosynthesis Physics Taught by the Non-physicist: A Simple Explanation Using Demonstrations without Equations

Monday, Nov. 28 12:45PM - 1:15PM Room: BR Community, Learning Center Station #7

## Participants

Ezra Bobo, MD, Philadelphia, PA (*Presenter*) Nothing to Disclose Raymond Acciavatti, Philadelphia, PA (*Abstract Co-Author*) Nothing to Disclose Margaret Nolan, philadelphia, PA (*Abstract Co-Author*) Nothing to Disclose Will Mannherz, philadelphia, PA (*Abstract Co-Author*) Nothing to Disclose Brian S. Englander, MD, Philadelphia, PA (*Abstract Co-Author*) Nothing to Disclose Andrew D. Maidment, PhD, Philadelphia, PA (*Abstract Co-Author*) Nothing to Disclose Research support, Analogic Corporation; Spouse, Employee, Real-Time Tomography, LLC; Scientific Advisory Board, Gamma Medica, Inc

## **TEACHING POINTS**

Graphically illustrate the continuum between CT, tomosynthesis, and radiography. Understand the effect of various acquisition parameters on image quality and dose. Understand why some objects are discernible in tomosynthesis and others are not. Understand the source of common artifacts seen in tomosynthesis. Help the radiologist understand when tomosynthesis is preferred over CT or radiography.

## TABLE OF CONTENTS/OUTLINE

Provide an overview of the geometry of tomosynthesis acquisition. Graphically compare tomosynthesis acquisition to CT and radiography. Graphically compare the information contained within a tomosynthesis scan to the information within a CT scan or radiograph. Using computer simulations, demonstrate the impact of changing different acquisition parameters, including: angular range, number of projections and reconstruction filter. Using experiments based on physical phantoms, demonstrate the impact of an objects location, orientation, and size. Using simple examples, explain the source of common tomosynthesis artifacts. Relate these concepts to the clinically available scanners. Describe the situations in which tomosynthesis is preferable to radiography or CT.

How to Best Utilize T2-weighted MR Images of the Breast: Diagnostic Algorithm of T2-high SI Area Based on Location, Enhancement Pattern, and ADC Value

Monday, Nov. 28 12:45PM - 1:15PM Room: BR Community, Learning Center Station #8

#### Awards

Magna Cum Laude

#### Participants

Natsuko Onishi, MD, Kyoto, Japan (*Presenter*) Nothing to Disclose Masako Y. Kataoka, MD, PhD, Kyoto, Japan (*Abstract Co-Author*) Nothing to Disclose Shotaro Kanao, MD, Kyoto, Japan (*Abstract Co-Author*) Nothing to Disclose Makiko Kawai, MD, Kyoto, Japan (*Abstract Co-Author*) Nothing to Disclose Masakazu Toi, Kyoto, Japan (*Abstract Co-Author*) Nothing to Disclose Kaori Togashi, MD, PhD, Kyoto, Japan (*Abstract Co-Author*) Nothing to Disclose Kaori Togashi, MD, PhD, Kyoto, Japan (*Abstract Co-Author*) Nothing to Disclose Kaori Togashi, MD, PhD, Kyoto, Japan (*Abstract Co-Author*) Research Grant, Bayer AG Research Grant, DAIICHI SANKYO Group Research Grant, Eisai Co, Ltd Research Grant, FUJIFILM Holdings Corporation Research Grant, Nihon Medi-Physics Co, Ltd Research Grant, Shimadzu Corporation Research Grant, Toshiba Corporation Research Grant, Covidien AG Mami Iima, MD, PhD, Kyoto, Japan (*Abstract Co-Author*) Nothing to Disclose Akane Ohashi, Kyoto, Japan (*Abstract Co-Author*) Nothing to Disclose Rena Sakaguchi, MD, Ashiya, Japan (*Abstract Co-Author*) Nothing to Disclose Ayami Ohno Kishimoto, Kyoto, Japan (*Abstract Co-Author*) Nothing to Disclose

#### **TEACHING POINTS**

Although dynamic contrast-enhanced MR images are the pivotal part of breast MRI, routinely scanned T2-weighted images can contain useful information for proper diagnosis. This exhibit focuses on differential diagnosis of high signal intensity areas on T2-weighted images (T2-high SI areas). We will:1. Classify T2-high SI areas identified on breast MRI based on location2. Propose diagnostic algorism of T2-high SI areas based on enhancement pattern and ADC values obtained from diffusion-weighted images, with corresponding pathological findings

## TABLE OF CONTENTS/OUTLINE

1. Location of T2-high SI area: outside/inside a breast mass2. T2-high SI area outside a breast mass: edema, dilated and fluid filled mammary ducts, breast vessels, intramammary lymph nodes, uneven fat suppression.3. T2-high SI area inside a breast mass and its classification based on enhancement patterns: A. Well-enhanced mass: spindle cell lesions, mucinous carcinoma, hemangioma B. Slightly enhanced mass: necrosis, abscess, mucus C. Non-enhanced mass: cyst.4. T2-high SI area inside a breast mass and its classification based on ADC value— breast cancer and cancer mimics: triple negative breast carcinoma with central necrosis, granulomatous mastitis, mucinous carcinoma.

# BR232-SD-MOB1

### Preliminary Result of a Multi-center Study of ABUS for the Diagnosis of Breast Cancer in China

Monday, Nov. 28 12:45PM - 1:15PM Room: BR Community, Learning Center Station #1

#### **Participants**

Xi Lin, Guangzhou, China (*Presenter*) Nothing to Disclose Mengmeng Jia, Beijing, China (*Abstract Co-Author*) Nothing to Disclose Shaoming Wang, Beijing, China (*Abstract Co-Author*) Nothing to Disclose Rui-Mei Feng, Beijing, China (*Abstract Co-Author*) Nothing to Disclose Guoxue Tang, Guangzhou, China (*Abstract Co-Author*) Nothing to Disclose You-Lin Qiao, Beijing, China (*Abstract Co-Author*) Nothing to Disclose Anhua Li, Guangzhou, China (*Abstract Co-Author*) Nothing to Disclose

## PURPOSE

Access to breast cancer screening in China is primarily limited by the shortage of qualified radiologists in primary hospitals. Automated Breast Ultrasound System (ABUS) is a potential method to alleviate current challenges in accessible breast cancer screening. This study aims to evaluate the initial effectiveness of ABUS by comparing it with Hand Held Ultrasound (HHUS) and Mammography (MAM) in a hospital-based multi-center study.

## **METHOD AND MATERIALS**

Women ages of 30 to 69 who visited breast surgeons for the first time without visible, suspicious signs of breast cancer were eligible undergone HHUS and ABUS, and women in the older group (40 to 69 years old) also received MAM. The images of the lesions were interpreted independently by using BI-RADS without knowledge of clinical or other imaging results. 122 women have been enrolled. By taking breast as the unit of analysis, we have acquired 244 results for each exam. The consistency rates and Kappa statistics were calculated to assess the reliability of ABUS compared with HHUS or MAM.

#### RESULTS

The average age was 44.47 in the whole group and 48.52 in the older group. Of all the 244 breasts, HHUS detected 41 suspicious lesions and ABUS detected 32. Among the 41 suspicious lesions detected by HHUS, ABUS detected 31; In the older group, ABUS detected 22 suspicious lesions and MAM detected 21. Among the 21 suspicious lesions detected by MAM, only 3 lesions were undetected by ABUS. Among the 22 lesions detected by ABUS, only 4 were not detected by MAM. The consistency rates between HHUS and ABUS was 95.49%, and that between ABUS and MAM was 95.39%. The Kappa value between ABUS and HHUS was 0.82 and that of ABUS and MAM in the older group was 0.81.

### CONCLUSION

Fairly good reliability was observed in comparisons between ABUS and HHUS or MAM. As ABUS is an automated system, images can be collected by technicians and interpreted later by qualified doctors, it may be an alternative modality in breast cancer screening in remote or low-resource areas. Other clinical performance indicators of ABUS, including sensitivity and sepcificity, need to be further demonstrated in multi-center screening trials.

#### **CLINICAL RELEVANCE/APPLICATION**

Reliability of ABUS was comparable to HHUS and MAM, it may be an alternative modality in breast cancer screening in remote or low-resource areas.

Clinical Utility of Real-time MR-navigated Ultrasound with Supine Breast MRI for Suspicious Enhancing Lesions Not Identified on Second-look Ultrasound

Monday, Nov. 28 12:45PM - 1:15PM Room: BR Community, Learning Center Station #2

# Participants

Pae Sun Suh, Suwon, Korea, Republic Of (*Presenter*) Nothing to Disclose Taeyang Ha, MD, Suwon, Korea, Republic Of (*Abstract Co-Author*) Nothing to Disclose Dong Hyun Lee, MD, SUWON, Korea, Republic Of (*Abstract Co-Author*) Nothing to Disclose Doo Kyoung Kang, MD, Suwon, Korea, Republic Of (*Abstract Co-Author*) Nothing to Disclose Taehee Kim, MD, PhD, Suwon, Korea, Republic Of (*Abstract Co-Author*) Nothing to Disclose

# PURPOSE

This study evaluated the usefulness of MR-navigated US for evaluation of MRI-detected lesions not visible on second-look US and analyzed differences of the lesion to nipple distance between supine and prone position.

## **METHOD AND MATERIALS**

Of the 831 consecutive patients who were diagnosed as breast cancer and examined with breast MRI from June 2013 to September 2015, we included 40 lesions in 37 patients who underwent MR-navigated US for MRI-detected lesions which were not visible on second-look US. First MRI was performed in prone position using a 1.5-T imager and second MRI was performed in a supine position for MR-navigated US.

## RESULTS

Of 40 lesions, 31 (78%) were identified with MR-navigated US, whereas 5 (13%) lesions disappeared on supine MRI and 4 (10%) showed no correlation on MR-navigated US. Of 31 lesions with pathologic confirmation, 7 (23%) were malignant, 2 (6%) were high risk lesions and 22 (71%) were benign lesions. Comparing the US findings of benign and malignant lesions, orientation of the lesion showed significant difference (p=0.045), whereas lesion shape, margin and echo pattern were not significantly different between two groups (p=0.088, p=0.094 and p=0.412, respectively). Median difference of lesion to nipple distance on supine and prone MRI was 8 mm (0-34 mm) in horizontal direction and 5 mm (0-39.5 mm) in vertical direction. Thirteen lesions showed more than 1cm difference in both horizontal and vertical direction.

# CONCLUSION

MR-navigated US is useful for the evaluation of MRI-detected lesions which were not visible on second-look US in breast cancer patients.

## **CLINICAL RELEVANCE/APPLICATION**

MR-navigated US is useful for the evaluation of MRI-detected lesions which were not visible on second-look US in breast cancer patients.

Intravoxel Incoherent Motion Diffusion Weighted Imaging: Does It Correlate with Prognostic Factors and Molecularsubtypes of Breast Cancers?

Monday, Nov. 28 12:45PM - 1:15PM Room: BR Community, Learning Center Station #3

# Participants

Shunan Che, MD, Beijing, China (*Presenter*) Nothing to Disclose Chunwu Zhou, Beijing, China (*Abstract Co-Author*) Nothing to Disclose Xinming Zhao, Beijing, China (*Abstract Co-Author*) Nothing to Disclose Han Ouyang, MD, Bejing, China (*Abstract Co-Author*) Nothing to Disclose Jing Li, MD, PhD, Beijing, China (*Abstract Co-Author*) Nothing to Disclose

# PURPOSE

to investigate whether parameters deriving from intravoxel incoherent motion(IVIM) model correlate with prognostic factors and subtypes of breast cancers

## **METHOD AND MATERIALS**

From March 2014 to May 2015, 110 cases with 114 lesions, histologically confirmed breast invasive ductal cancer, were collected. All of them were examined with multiple-b value DWI(12b from 0-1000s/mm<sup>2</sup>) before surgery or core needle biopsy. GE postproecssing workstation was used to automatically calculate parameters(D, D\* and f) deriving from IVIM model. Correlation between IVIM parameters and prognostic factors (including size, grade, status of vascular invasive and axillary lymph node, and the expression status of ER, PR, HER2 and Ki67) was analyzed using Mann–Whitney U test and spearman's correlation coefficient. IVIM parameters among different molecular subtype was compared with Kruskal–Wallis H test

#### RESULTS

The median D value of the low aggressive group, PR-negative group and HER2-positive group were significantly higher than that of the highly aggressive group, PR-positive group and HER2-negative group(P<0.001; P=0.042; P=0.001, respectively). The median D\* value of HER2-positive lesions was significantly higher than that of HER2-negative ones(P=0.033). The median f value of the low aggressive lesions was significantly lower than that of the highly aggressive ones(P<0.001). The median D value of HER2 enriched subtype tumor  $(1.11 \times 10^{-3} \text{mm}^2/\text{s})$  was significantly higher than that of Luminal and triple-negative subtype one( $0.80 \times 10^{-3} \text{mm}^2/\text{s}$ ;  $0.82 \times 10^{-3} \text{mm}^2/\text{s}$ , respectively), there were statistically significant differences among them(P=0.026, P=0.048; respectively)

### CONCLUSION

D value was negatively correlated with tumor grade and PR status, while positively correlated with HER2 status. D\* value was positively correlated with HER2 status. f value was positively correlated with tumor grade. D value can be used to distinguish the subtype of HER2 enriched tumors from the Luminal and triple-negative ones.

#### **CLINICAL RELEVANCE/APPLICATION**

Parameters of IVIM model may be valuable for predicting the prognosis and distinguishing different molecular subtype of breast cancer

T2 Signal Intensity of Breast Cancer as a Prognostic Indicator of Response to Neoadjuvant Chemotherapy

Monday, Nov. 28 12:45PM - 1:15PM Room: BR Community, Learning Center Station #4

#### Awards

#### **Student Travel Stipend Award**

#### **Participants**

John C. Benson, MD, Saint Paul, MN (*Presenter*) Nothing to Disclose Lei Zhang, MS, Minneapolis, MN (*Abstract Co-Author*) Nothing to Disclose Noelle E. Hoven, MD, Minneapolis, MN (*Abstract Co-Author*) Nothing to Disclose Michael Nelson, MD, Minneapolis, MN (*Abstract Co-Author*) I hold license and patents on a breast marker named VizMark Patrick J. Bolan, PhD, Minneapolis, MN (*Abstract Co-Author*) Research Consultant, Breast-Med, Inc

## PURPOSE

To evaluate quantitative intra-tumoral T2 signal intensity as a prognostic marker in patients receiving neoadjuvant chemotherapy for breast cancer.

## **METHOD AND MATERIALS**

This was an exploratory, retrospective analysis using data from the I-SPY 1 TRIAL (CALGB 150007/ACRIN6657). Patients had a stage 2 or 3 breast tumor measuring  $\geq$ 3 cm; each received neoadjuvant chemotherapy with an anthracycline-cyclophosphamide (AC) regimen with or without a taxane-based regimen. MR imaging was completed  $\leq$ 4 weeks before starting AC (MR1),  $\geq$ 2 weeks after AC cycle #1 and prior to AC cycle #2 (MR2), after AC cycle #2 and before taxane (MR3), and after completing neoadjuvant chemotherapy (MR4). Regions of interest (ROIs) corresponding to tumors on T2-weighted images (T2WI) were obtained by corregistering T2WI to the functional tumor volume (FTV) ROIs, which were calculated using signal enhancement ratio (SER) images and were used in the trial's primary analysis. The median, 5th percentile, 95th percentile, and interquartile range of intra-tumoral T2 signal intensity from MR1 and MR2 images were recorded. Patient outcome was evaluated using change in FTV and presence or absence of complete pathologic response (pCR) following chemotherapy.

#### RESULTS

Of 222 patients, 57 lacked imaging at MR2 or FTV/pCR data, and 56 lacked imaging sequences or had poor image quality. Hence, 109 patients met inclusion criteria (100% female); mean age at time of enrollment was 46.7 $\pm$ 9.2 years. Of all patients, 31/109 (28.4%) had pCR following neoadjuvant chemotherapy. The 5th percentile of intra-tumoral T2 intensity on MR2 was significantly lower in patients that achieved pCR (p=0.0169). The median and 95th percentile signal intensity of tumoral T2 intensity on MR2 were also lower in patients that achieved pCR, though these findings were not statistically significant (p=0.3147 and p=0.2388, respectively). No association was found between MR2 tumoral T2 signal intensity and  $\Delta$ FTV.

## CONCLUSION

Patients that achieved pCR following chemotherapy had low 5th percentile intra-tumoral T2 signal intensity after early neoadjuvant chemotherapy. Further investigation is warranted to assess quantitative T2 signal as a prognostic indicator in breast cancer.

## **CLINICAL RELEVANCE/APPLICATION**

In patients receiving neoadjuvant chemotherapy for breast cancer, intra-tumoral T2 signal intensity may represent a useful prognostic tool on non-contrast MR imaging.

Leveraging "Deep Learning" Methods to Elucidate and Incorporate Novel Breast Parenchymal Complexity Phenotypes to Enhance Breast Cancer Risk Assessment

Monday, Nov. 28 12:45PM - 1:15PM Room: BR Community, Learning Center Station #5

# Participants

Andrew Oustimov, Philadelphia, PA (*Abstract Co-Author*) Nothing to Disclose Aimilia Gastounioti, Philadelphia, PA (*Presenter*) Nothing to Disclose Meng-Kang Hsieh, Philadelphia, PA (*Abstract Co-Author*) Nothing to Disclose Lauren Pantalone, BS, Philadelphia, PA (*Abstract Co-Author*) Nothing to Disclose Emily F. Conant, MD, Philadelphia, PA (*Abstract Co-Author*) Consultant, Hologic, Inc; Consultant, Siemens AG Despina Kontos, PhD, Philadelphia, PA (*Abstract Co-Author*) Nothing to Disclose

#### PURPOSE

To leverage the use of Deep Learning methods for elucidating novel quantitative phenotypes of breast parenchymal complexity and investigate their added value in breast cancer risk assessment.

# METHOD AND MATERIALS

We retrospectively analyzed "For Processing" contralateral mediolateral-oblique (MLO) view digital mammograms from 106 women with unilateral primary invasive breast cancer and 318 age- and side-matched controls, acquired with either a GE Healthcare 2000D or DS FFDM system. We coupled our previously validated lattice-based strategy for mammographic texture analysis with deep convolutional neural networks (ConvNets), which are capable of non-linearly merging input data to hierarchical representations (i.e., meta-features) useful for a particular learning task, here discriminating between cancer cases and controls. The lattice-based strategy was first used to generate feature maps of 29 established texture descriptors, including histogram, co-occurrence, runlength, and fractal dimension features, each capturing a different aspect of the tissue complexity and its distribution within the breast. The extracted feature maps for each woman were then simultaneously fed into a ConvNet, with two convolutional layers, and a fully-connected multilayer perceptron (MLP) layer feeding into a logistic regression classifier. Training and validation was performed using a split-sample approach. Discriminatory capacity was assessed via the area under the curve (AUC) of the receiver operating characteristic (ROC), and compared to the standard approach of feeding the texture features directly into a logistic regression classifier.

#### RESULTS

The deep learning classifier demonstrated high discriminatory capacity, having an AUC=0.90 (95% CI=[0.82-0.98]), outperforming conventional logistic regression classification of the texture features which had a discriminatory capacity of AUC=0.85 on the same case-control dataset. Deep learning classification was based on 5 meta-features efficiently combining subtle discriminative information.

## CONCLUSION

Deep learning methods hold the promise to reveal parenchymal pattern phenotypes that may augment the predictive value of conventional parenchymal pattern measures in risk prediction.

## **CLINICAL RELEVANCE/APPLICATION**

Improving breast cancer risk prediction using deep-learned parenchymal pattern phenotypes could help better guide personalizing breast cancer screening and prevention strategies.

## Trends in Breast Density Assessment Over Time: Patterns Related to Legislation and Patient Age

Monday, Nov. 28 12:45PM - 1:15PM Room: BR Community, Learning Center Station #6

#### **Participants**

Krystal C. Buchanan, MD, New Haven, CT (*Presenter*) Nothing to Disclose Patricia C. Barrett, New Haven, CT (*Abstract Co-Author*) Nothing to Disclose Paul H. Levesque, MD, Madison, CT (*Abstract Co-Author*) Nothing to Disclose Jaime L. Geisel, MD, New Haven, CT (*Abstract Co-Author*) Consultant, QView Medical, Inc Consultant, Siemens AG Regina J. Hooley, MD, New Haven, CT (*Abstract Co-Author*) Consultant, FUJIFILM Holdings Corporation; Consultant, Siemens AG Liane E. Philpotts, MD, New Haven, CT (*Abstract Co-Author*) Nothing to Disclose

## PURPOSE

Breast density notification legislation is being passed in more states every year. Density classification on mammography is primarily achieved by subjective means. With such laws in effect, there is the possibility of radiologists overtly or subconsciously changing density, particularly downgrading such that supplemental tests will not be required. The purpose of this study was to determine the effect of density classification over time and by patient age.

#### **METHOD AND MATERIALS**

A search of the electronic breast imaging database (PenRad, MN) was performed to determine the density classifications (BI-RADS categories a,b,c,d) reported on digital screening mammograms over a 10 year period (2006 – 2015). Our state density notification law went into effect in 2009. Prior to 2011 these were FFDM and after 2011, the majority were tomosynthesis exams (all Hologic, MA). The combined data was assessed and additionally, the data were subdivided by patient age by decade: 40-49, 50-59, 60-69, 70 and up.

## RESULTS

A total of 76,924 screening exams were assessed. For all age groups, there was a small decrease in dense breast categories and corresponding increase in non-dense of 5% in 2009, which returned to usual the following year. However, there has been a consistent trend of increasing percentage of heterogeneously dense since that time, from 23% to 34%. When assessed by age, this trend is found mostly in women in the 50's and 60's decade. No specific pattern change was noted in 2011 with the conversion to tomosynthesis.

## CONCLUSION

The patterns of density reporting appear to be initially affected by state legislation, yet the pattern did not return to previous rates, but actually shows increase towards more women being reported as dense, particularly women in the 50-69.

## **CLINICAL RELEVANCE/APPLICATION**

Density reporting appears to be affected by legislation, but such trends may change over time, with increase towards more women being reported as dense. This may be a reflection of radiologists not downgrading density as women age, or leaning towards allowing more women the possibility of supplemental screening.

# CA115-ED-MOB8

# Advanced MR and CT Imaging Techniques in the Diagnosis of Cardiac Thrombus

Monday, Nov. 28 12:45PM - 1:15PM Room: CA Community, Learning Center Station #8

#### **Participants**

Ana Alvarez Vazquez, Madrid, Spain (*Presenter*) Nothing to Disclose Vicente Martinez, MD, Madrid, Spain (*Abstract Co-Author*) Nothing to Disclose Manuel Recio Rodriguez, Pozuelo de Alarcon, Spain (*Abstract Co-Author*) Nothing to Disclose Gonzalo Pizarro, Madrid, Spain (*Abstract Co-Author*) Nothing to Disclose Chawar Hayoun, Pozuelo De Alarcon, Spain (*Abstract Co-Author*) Nothing to Disclose Julio Fernandez Mata, Madrid, Spain (*Abstract Co-Author*) Nothing to Disclose

# **TEACHING POINTS**

- To know the clinical situations where the presence of cardiac thrombi must be suspected. - To outline an appropriate MR imaging protocol to assess cardiac thrombus for each clinical context. - To use perfusion imaging and delayed-enhancement imaging to check the presence of thrombi.- To learn new CT scanning equipments enable detect trombus in the left atrial appendage- To list the most common congenital abnormalities that simulate a trombus

## **TABLE OF CONTENTS/OUTLINE**

A. Anatomical variantsB. The most common causes of cardiac thrombus.C. Diagnostic Imaging: value of CT angiography D. Diagnostic Imaging: perfusion and delayed-enhancement MRI.E. Diagnostic Imaging: MR imaging oriented parallely to the longitudinal catheter axis.

Demystifying the Mitral Valve: Practical Anatomy for Radiologists

Monday, Nov. 28 12:45PM - 1:15PM Room: CA Community, Learning Center Station #9

## Awards Cum Laude

#### Participants

Dmitry Levin, Seattle, WA (*Presenter*) Nothing to Disclose Mario M. Ramos, Seattle, WA (*Abstract Co-Author*) Nothing to Disclose Elizabeth Perpetua, PhD,RN, Seattle, WA (*Abstract Co-Author*) Nothing to Disclose G. B. Mackensen, MD,PhD, SEATTLE, WA (*Abstract Co-Author*) Nothing to Disclose Mark Reisman, MD, Seattle, WA (*Abstract Co-Author*) Nothing to Disclose Beth A. Ripley, MD, PhD, Seattle, WA (*Abstract Co-Author*) Nothing to Disclose

#### **TEACHING POINTS**

There is an unmet need for catheter-based therapies to treat mitral valvular disease, with 9% of the population over age 75 suffering from mitral valvular disease. The growing number of percutaneous mitral valve replacement and intervention devices requires a detailed understating of 3-dimensional mitral anatomy. Understanding mitral valve anatomy will allow radiologists to report essential information regarding the safety and feasibility of both surgical and catheter-based approaches to repair. The choice of access site and approach for mitral valve intervention is informed by patient-specific anatomy assessed during preprocedural imaging.

# TABLE OF CONTENTS/OUTLINE

Exposure to essential mitral valve anatomical structures including commissures, leaflets, annulus, papillary muscles and chords with radiology-pathology correlation. Imaging approach to mitral valve anatomy, including optimal imaging planes for viewing different components and optimization of imaging parameters. Measurement and documentation of valve shape, annulus size, LV size and annular calcification in anticipation of catheter-based repair. Anatomical considerations relating to catheter approach for mitral repair- including trans-septal versus retrograde approach through the aorta and left ventricular outflow tract. Anomalous mitral apparatus anatomy and imaging pitfalls.

## CA213-SD-MOB4

Reproducibility of Native and Contrast-enhanced CMR Techniques to Measure Lesion Size Following Acute Myocardial Infarction

Monday, Nov. 28 12:45PM - 1:15PM Room: CA Community, Learning Center Station #4

# Participants

Enver G. Tahir, MD, Hamburg, Germany (*Presenter*) Nothing to Disclose Martin Sinn, Hamburg, Germany (*Abstract Co-Author*) Nothing to Disclose Maxim Avanesov, MD, Hamburg, Germany (*Abstract Co-Author*) Nothing to Disclose Joshua Wien, Hamburg, Germany (*Abstract Co-Author*) Nothing to Disclose Dennis Saring, Wedel, Germany (*Abstract Co-Author*) Nothing to Disclose Christian Stehning, Hamburg, Germany (*Abstract Co-Author*) Nothing to Disclose Christian Stehning, Hamburg, Germany (*Abstract Co-Author*) Nothing to Disclose Kai Muellerleile, Hamburg, Germany (*Abstract Co-Author*) Nothing to Disclose Gerhard B. Adam, MD, Hamburg, Germany (*Abstract Co-Author*) Nothing to Disclose Gunnar K. Lund, MD, Hamburg, Germany (*Abstract Co-Author*) Nothing to Disclose

## PURPOSE

The purpose of this study was to analyze the reproducibility of native and contrast-enhanced CMR techniques to measure lesion size after acute myocardial infarction (AMI) using native T1/T2 mapping, T2-weighted (T2w) imaging, late gadolinium enhancement (LGE), post-contrast T1 mapping and extracellular volume (ECV) quantification.  $\Box$ 

# METHOD AND MATERIALS

Lesion size was independently quantified by 2 experienced observers in total of 176 consecutive CMRs obtained in 44 patients within the first 6 months after AMI using native and contrast-enhanced sequences. Lesion sizes were quantified using a threshold method (cutoff >2SD of remote myocardium) on short-axis left ventricular slices. Lesion size is given as the mean of both observers. Bland-Altman analysis was performed to determine the agreement between the two observers. Non-parametric Levene's test was used to compare the variances of the relative differences. Statistical analysis was performed using GraphPad Prism 6.

#### RESULTS

The relative median difference of the native CMR techniques were -1.95% (-12.7% and 9.8%) for T2w, -5.3% (-19.6% and 14.8%) for native T1 and -4.0% (-23.9% and 9.9%) for native T2. Results for contrast-enhanced CMR imaging were: 2.9% (-4.5% and 10.5%) for LGE, 7.5% (-2.4% and 21.5%) for post-contrast T1 and -2.9% (- 11.4% and 9%) for ECV measurement. Bland-Altman analysis revealed a better agreement for all post-contrast sequences indicted by lower limits of agreement compared to native sequences. The increased variability of native imaging was caused by higher interobserver differences in small lesions with sizes between 0-15 %LV compared to lager lesions >15 %LV. This bias was not observed for post-contrast imaging.  $\Box$ 

## CONCLUSION

In general, there was a good agreement between the two observers to measure lesion size after AMI, but all post-contrast sequences had a better agreement compared to the native sequences. The low agreement of native imaging was mainly caused by higher interobserver differences in small lesions with lesion sizes between 0-15 %LV compared to lager lesions >15 %LV.

# **CLINICAL RELEVANCE/APPLICATION**

Accurate ischemic lesion size measurement with non-invasive techniques can help to explore different aspects of the ischemic cardiomyopathy and lead to a better clinical patient management. It has also the potential to improve our understanding of ischaemic cardiomyopathy for research purposes.

## CA217-SD-MOB1

# Utility of Late Iodine Enhancement Computed Tomography with Image Subtraction Technique of Left Ventricular Cavity

Monday, Nov. 28 12:45PM - 1:15PM Room: CA Community, Learning Center Station #1

# Participants

Takanori Kouchi, Toon, Japan (*Presenter*) Nothing to Disclose Yuki Tanabe, Toon, Japan (*Abstract Co-Author*) Nothing to Disclose Teruhito Kido, MD, PhD, Toon, Japan (*Abstract Co-Author*) Nothing to Disclose Tomohisa Okada, Toon, Japan (*Abstract Co-Author*) Nothing to Disclose Takahiro Yokoi, Toon, Japan (*Abstract Co-Author*) Nothing to Disclose Naoki Fukuyama, Toon, Japan (*Abstract Co-Author*) Nothing to Disclose Akira Kurata, PhD, Toon, Japan (*Abstract Co-Author*) Nothing to Disclose Tomoyuki Kido, Toon, Japan (*Abstract Co-Author*) Nothing to Disclose Masao Miyagawa, MD, PhD, Toon, Japan (*Abstract Co-Author*) Nothing to Disclose Teruhito Mochizuki, MD, Toon, Japan (*Abstract Co-Author*) Nothing to Disclose

#### PURPOSE

The purpose of this study was to evaluate utility of late iodine enhancement computed tomography (LIE-CT) with image subtraction of left ventricular (LV) cavity for assessment of myocardial infarction (MI) extent.

## **METHOD AND MATERIALS**

The study group consisted of 21 patients (mean age: 69.0 years) who underwent comprehensive cardiac CT protocol and late gadolinium enhancement magnetic resonance imaging (LGE-MRI) for assessment of coronary artery disease (CAD). Comprehensive cardiac CT scan protocol consisted of stress CT perfusion (CTP), coronary CT angiography (CTA) and LIE-CT using 256-slice CT (Philips Healthcare, Cleveland, OH). LIE-CT data was acquired 10 minutes after CTP and CTA (mean contrast medium (CM) volume: 92 mL, 370 mg iodine/mL) using low tube voltage of 80 kV (mean radiation dose: 0.41 mSv) without additional CM. LIE-CT images were reconstructed with iterative model reconstruction (IMR). Subtracted LIE-CT images were also created by deducting image signal of LV cavity from original images using a dedicated workstation (Ziostation2, Ziosoft Inc., Tokyo, Japan). For global assessment of MI extent, %MI volume in LIE-CT with/without image subtraction was analyzed, and compared with LGE-MRI. For regional assessment of MI extent, transmural extent of LV wall thickness (TME; 0%, 1-24%, 25-49%, 50-74%, and 75-100%) was visually assessed in LIE-CT with/without image subtraction according to the 16-segment model, and the concordance ratio was evaluated between LGE-MRI and LIE-CT with/without image subtraction.

## RESULTS

Of 21 patients, 103 of 336 segments showed MI in LGE-MRI. For global assessment, close correlations for %MI volume were observed between LGE-MRI and LIE-CT with/without image subtraction (r=0.90 / 0.85, p < 0.05 in each). For regional assessment, concordance ratios of TME were 80% / 75% between LGE-MRI and LIE-CT with/without image subtraction. In the assessment of TME  $\geq$ 50% or not, concordance ratios were 91% / 86% between LGE-MRI and LIE-CT with/without image subtraction. Concordance ratios of TME assessed by LGE-MRI was significantly higher in LIE-CT with image subtraction than in original LIE-CT images (p < 0.05).

## CONCLUSION

LIE-CT with image subtraction of LV cavity allowed for accurate assessment of MI extent assessed by LGE-MRI.

## **CLINICAL RELEVANCE/APPLICATION**

LIE-CT with image subtraction of LV cavity has a potential for accurate assessment of myocardial viability in patients with CAD.

## CA219-SD-MOB3

Image Quality of a Novel Motion Correction Algorithm in Coronary CT Angiography for Patients with Atrial Fibrillation

Monday, Nov. 28 12:45PM - 1:15PM Room: CA Community, Learning Center Station #3

# Participants

Hideyuki Sato, Edogawa-ku, Japan (*Presenter*) Nothing to Disclose Maiko Miyamoto, Tokyo, Japan (*Abstract Co-Author*) Nothing to Disclose Aki Iwasa, Tokyo, Japan (*Abstract Co-Author*) Nothing to Disclose Masahiro Uematsu, RT, Tokyo, Japan (*Abstract Co-Author*) Nothing to Disclose

## PURPOSE

Patients with atrial fibrillation cannot undergo conventional motion artifact reduction application in coronary CT angiography (CCTA), since high heart rates lead to motion artifacts. However, a motion-correction algorithm (MCA) can reduce these artifacts. The aim of this study is to evaluate the effect of a novel MCA on the diagnostic image quality of CCTA for patients with atrial fibrillation.

# METHOD AND MATERIALS

A total of 40 patients with atrial fibrillation (age,  $73.0\pm11.6$  years; heart rate,  $69.4\pm12.6$  bpm; range, 36-96 bpm) underwent CCTA with a 64-multidetector-row CT. The diagnostic image quality of their results was then evaluated for images with or without MCA application using a four-step linear measure method (4, excellent; 1, very poor).

## RESULTS

Diagnostic image quality scores obtained with MCA were higher than those obtained without MCA at the average heart rate  $(3.9\pm0.4 \text{ vs}. 3.7\pm0.6, P < 0.01)$ , >70 bpm  $(3.7\pm0.5 \text{ vs}. 3.4\pm0.7, P < 0.01)$ , >80 bpm  $(3.5\pm0.6 \text{ vs}. 3.1\pm0.8, P < 0.01)$ , and >90bpm  $(3.3\pm0.7 \text{ vs}. 2.8\pm0.7, P < 0.01)$ .

## CONCLUSION

Application of this novel MCA improves diagnostic image quality in patients with high heart rates attributable to atrial fibrillation.

#### **CLINICAL RELEVANCE/APPLICATION**

In patients with atrial fibrillation, a clear image of CCTA can be obtained even if the patient has a high heart rate.

## CA221-SD-MOB5

Stress Myocardial Perfusion Computed Tomography Using Different Scanning Techniques: Implications for Dose-Saving Strategies

Monday, Nov. 28 12:45PM - 1:15PM Room: CA Community, Learning Center Station #5

## Participants

Patricia M. Carrascosa, MD, Buenos Aires, Argentina (*Presenter*) Research Consultant, General Electric Company Alejandro Deviggiano, MD, Vicente Lopez, Argentina (*Abstract Co-Author*) Nothing to Disclose Macarena De Zan, Vicente Lopez, Argentina (*Abstract Co-Author*) Nothing to Disclose Carlos Capunay, MD, Buenos Aires, Argentina (*Abstract Co-Author*) Nothing to Disclose Roxana Campisi, Vicente Lopez, Argentina (*Abstract Co-Author*) Nothing to Disclose Gaston Rodriguez Granillo, Vicente Lopez, Argentina (*Abstract Co-Author*) Nothing to Disclose

## PURPOSE

Myocardial computed tomography perfusion (CTP) has gained relevance during the past years. Since the pharmacological agents used for stress-CTP tend to increase the heart rate, both systolic and diastolic acquisition are frequently performed in order attain motion-free images. This can be achieved using either a retrospective scan, or a prospective scan with wide padding. Both strategies demand a higher radiation dose in order to cover systolic and diastolic phases. Accordingly, we sought to explore the diagnostic performance of using a systolic, a diastolic, or a combination of both for the assessment of CTP.

## **METHOD AND MATERIALS**

We prospectively included patients with suspected CAD who had a clinical indication of a stress-rest SPECT. In all patients, a stress-rest CTP was performed. Dipyridamole was used in both studies. Single-source dual energy CTP was performed, allowing the generation of monochromatic image reconstructions with 10 keV increments from 40 to 140 keV. The stress scan was performed using a prospective mode with a wide padding ranging from 40 to 75% of the R-R interval. Images were reconstructed independently in systolic and diastolic phases. Patients were categorized in tertiles according to the heart rate in order to determine the best phase to analyze myocardial perfusion in relation to heart rate.

## RESULTS

A total of 48 patients were included. The mean age was 67.9±5.1 years, and 39 (81%) were male. The mean heart rate during stress was 67.9±5.1 bpm. The mean effective radiation dose associated to stress DE-CTP was 5.1±1.7 mSv. Compared to the diastolic and sisto-diastolic evaluation, the diagnostic performance was lowest at the systolic evaluation independently of the heart rate, but particularly at low heart rates (Table). The best results for CTP evaluation were obtained by the combination of systole an diastole and diastole alone, with no significant differences between them among patients with low (tertile 1) and average (tertile 2) heart rates. In patients with heart rate above 75 bpm, the combined evaluation was the best approach.

## CONCLUSION

In the present study, we found that the scanning technique of stress-CTP can be adapted according to the patient's heart rate, requiring both systolic and diastolic phases only among patients with heart rate above 75 bpm.

# **CLINICAL RELEVANCE/APPLICATION**

Myocardial computed tomography perfusion scans can be adapted according to each patient.

# CA222-SD-MOB6

Cardiac Magnetic Resonance Imaging for Detection of Subclinical Chemotherapy-Induced Cardiac Injury: Feasibility and Initial Findings

Monday, Nov. 28 12:45PM - 1:15PM Room: CA Community, Learning Center Station #6

**FDA** Discussions may include off-label uses.

#### Participants

Jesse Habets, MD, Utrecht, Netherlands (*Abstract Co-Author*) Nothing to Disclose Luuk Vugts, BSC, Utrecht, Netherlands (*Abstract Co-Author*) Nothing to Disclose Arco Teske, MD,PhD, Utrecht, Netherlands (*Abstract Co-Author*) Nothing to Disclose Maarten-Jan M. Cramer, MD, Utrecht, Netherlands (*Abstract Co-Author*) Nothing to Disclose Folkert Asselbergs, MD,PhD, Utrecht, Netherlands (*Abstract Co-Author*) Nothing to Disclose Tim Leiner, MD, PhD, Utrecht, Netherlands (*Presenter*) Speakers Bureau, Koninklijke Philips NV Research Grant, Bayer AG Research Grant, Bracco Group

#### PURPOSE

Cancer mortality in the Western world is slowly decreasing but many patients now suffer from long-term side-effects. One of the most significant long-term complications of chemotherapy (CTx) is cardiotoxicity. The purpose of this work was to investigate to ability of cardiac magnetic resonance (CMR) to detect and quantify CTx-induced cardiac damage.

#### **METHOD AND MATERIALS**

In this retrospective study all patients with a documented history of CTx > 1 year ago who underwent CMR over a 21-month period were identified. All patients underwent a comprehensive CMR protocol including cine steady state free precession imaging for determination of functional parameters and wall-motion abnormalities, delayed gadolinium-enhancement imaging for detection of focal myocardial scarring and T1-mapping for detection of non-focal myocardial abnormalities. Wall-motion abnormalities were assessed with global longitudinal left ventricular strain (LV-GLLS) using commercially available software (Q-mass V7, Medis, The Netherlands). Due to the retrospective nature of the study, the IRB waived the need for informed consent.

#### RESULTS

Patients with causes other than CTx-induced cardiac damage were excluded from analysis. In total, 19 patients were identified (13M/6F; mean age: 56 years). The median indexed left ventricular end-diastolic volume (LV-EDV) was 100 (82-140 ml/m2). Median left ventricular ejection (LV-EF; %) was 39 (28-54) and 13 (68,4%) patients had an ejection fraction of less than 50%. Median T1 values without contrast were 1088 (1045-1132) and 1630 (1526-1673) for the myocardium and bloodpool, respectively. The median T1 values with contrast enhancement were 408 (385-442) in the myocardium and 269 (267-275) in the bloodpool. The median calculated extracellular volume (ECV) was 0,27 (0,25-0,36). The median LV-GLLS value was -12,25 (range: -21,33 - -7,82). 13 (68%) patients had a values under -10, which is considered abnormal. Six patients had ECV and LV-GLLS abnormalities in the absence of decreased LV-EF.

# CONCLUSION

Cardiac magnetic resonance imaging can unmask myocardial abnormalities in patients who received cardiotoxic chemotherapy, even in the presence of normal left ventricular ejection fraction.

# **CLINICAL RELEVANCE/APPLICATION**

Chemotherapy can induce myocardial damage that can be detected with CMR prior to a decline in left ventricular function. This may offer opportunities to institute preventive measures to avoid CTx-induced heart failure.

## CA223-SD-MOB7

Flow Patterns and Peak Velocity in Dilated Ascending Aorta With and Without Aortic Valve Stenosis and Regurgitation

Monday, Nov. 28 12:45PM - 1:15PM Room: CA Community, Learning Center Station #7

#### Awards

#### **Student Travel Stipend Award**

#### **Participants**

Kenichiro Suwa, MD, Chicago, IL (*Presenter*) Nothing to Disclose Ozair A. Rahman, MD, Chicago, IL (*Abstract Co-Author*) Nothing to Disclose Emilie Bollache, Chicago, IL (*Abstract Co-Author*) Nothing to Disclose Michael Rose, Chicago, IL (*Abstract Co-Author*) Nothing to Disclose Amir Ali Rahsepar, MD, Chicago, IL (*Abstract Co-Author*) Nothing to Disclose James C. Carr, MD, Chicago, IL (*Abstract Co-Author*) Nothing to Disclose James C. Carr, MD, Chicago, IL (*Abstract Co-Author*) Nothing to Disclose James AG Advisory Board, Guerbet SA Jeremy D. Collins, MD, Chicago, IL (*Abstract Co-Author*) Nothing to Disclose Alex Barker, Chicago, IL (*Abstract Co-Author*) Nothing to Disclose Michael Markl, PhD, Chicago, IL (*Abstract Co-Author*) Institutional research support, Siemens AG; Consultant, Circle Cardiovascular Imaging Inc;

## PURPOSE

To characterize differences in aortic blood flow patterns and velocity between patients with AAo dilatation and either Aortic valve stenosis (AS), regurgitation (AR), AS and AR (ASR), and neither AS nor AR (no AS/AR), and healthy controls using 4D flow MRI.

#### **METHOD AND MATERIALS**

Five patients with moderate to severe ASR (56±18 years, 4 men, mid ascending aorta diameter [MAAd]: 40.3±3.2mm), 7 patients with moderate to severe AS (72±10 years, 6 men, MAA diameter: 40.5±2.9mm), 20 patients with moderate to severe AR (63±144 years, 16 men, MAAd: 44.9±4.2 mm), 18 patients with no AS/AR (64±10 years, 13 men, MAAd: 41.6±4.6 mm) all with dilated AAo were identified via IRB-approved retrospective chart review. Eleven healthy controls (61±13 years, 8 men, MAAd: 32.4±3.0 mm) were selected from the existing database. All subjects underwent in-vivo 4D flow MRI for the measurement of 3D blood flow velocities. AAo flow patterns were visualized using time resolved pathlines and were semi-quantitatively graded for the presence of vortex and helix flow using a 3-point scale (1, no vortex/mild helix [flow rotation: less than 180°]; 2, 1-2 large vortex/moderate supra-physiologic helix [flow rotation: 180° to 360°]; 3, more than 2 large vortex/prominent supra-physiologic helix [flow rotation: more than 360°]). Further quantification included systolic peak velocities in analysis planes at the aortic root, proximal-, mid- and distal-AAo, proximal-and distal-arch, as well as proximal-, mid- and distal-descending aorta.

## RESULTS

Patients with AR showed significantly elevated vortex flow compared to control subjects  $(2.00\pm0.46 \text{ vs. } 1.45\pm0.52, \text{ p}<0.05)$ . Helix flow was significantly elevated for the patients with ASR, AS, AR, and without AS/AR compared to control subjects  $(3.00\pm0.00, 2.71\pm0.49, 2.40\pm0.82, \text{ and } 2.50\pm0.86, \text{ respectively, vs. } 1.45\pm0.52, \text{ p}<0.05)$ . Peak velocities were significantly greater in the patients with ASR from root to distal arch and AS from root to proximal arch compared to those with AR and without AS/AR, as well as controls.

# CONCLUSION

Patients with ASR and AS demonstrated elevated peak velocity from the root to proximal arch compared to those with AR and without AS/AR. Interestingly blood flow patterns were similar between groups.

# **CLINICAL RELEVANCE/APPLICATION**

The elevated peak flow observed in the dilated AAo in patients with ASR and those with AS may lead to accelerated aneurysm progression; further outcomes studies are warranted.

# Don't Be Nervous: An Overview of the Anatomy and Pathology of the Nerves of the Thorax

Monday, Nov. 28 12:45PM - 1:15PM Room: CH Community, Learning Center Station #6

# Awards

**Certificate of Merit** 

## Participants

Rishi Agrawal, MD, Chicago, IL (*Presenter*) Speakers Bureau, Boehringer Ingelheim GmbH Nishant D. Parekh, MD, Chicago, IL (*Abstract Co-Author*) Nothing to Disclose Hatice Savas, MD, Chicago, IL (*Abstract Co-Author*) Nothing to Disclose Larry Cochard, Chicago, IL (*Abstract Co-Author*) Nothing to Disclose Eric M. Hart, MD, Chicago, IL (*Abstract Co-Author*) Nothing to Disclose

# **TEACHING POINTS**

- After viewing this exhibit, the learner will be able to:
- (1) Identify the course of the major nerves in the thorax
- (2) Recognize imaging characteristics of nerve dysfunction in the thorax
- (3) Recognize pertinent clinical history suggesting nerve dysfunction in the thorax
- (3) Anticipate nerve dysfunction based on anatomic localization of thoracic lesions

# TABLE OF CONTENTS/OUTLINE

- I. Anatomy and function
  - A. Esophageal plexus
  - B. Intercostal nerves
  - C. Long Thoracic nerves
  - D. Phrenic nerves
  - E. (White) Ramus communicans
  - F. Recurrent laryngeal nerves
  - G. Splanchnic nerves
  - H. Sympathetic chain
  - I. Vagus nervesII. Pathology
  - A. Neoplasm and other soft tissue impingement
  - B. Inflammatory lesions
  - C. Injury (trauma and iatrogenic)

The Minimum Lung Area during Tidal Breathing on Magnetic Resonance Imaging (MRI) Correlates with the Prognosis of the Patients with Chronic Obstructive Pulmonary Disease (COPD)

Monday, Nov. 28 12:45PM - 1:15PM Room: CH Community, Learning Center Station #1

## Participants

Tae Iwasawa, MD, PhD, Yokohama, Japan (*Presenter*) Research Consultant, Ono Pharmaceutical Co, Ltd.; Speaker, Shionogi & Co, Ltd

Akimasa Sekine, Yokohama, Japan (*Abstract Co-Author*) Nothing to Disclose Takeshi Shinohara, MD, Yokohama, Japan (*Abstract Co-Author*) Nothing to Disclose Tomohisa Baba, MD, Yokohama, Japan (*Abstract Co-Author*) Nothing to Disclose Takashi Ogura, MD, Yokohama, Japan (*Abstract Co-Author*) Nothing to Disclose Toshiyuki Gotoh, PhD, Yokohama, Japan (*Abstract Co-Author*) Nothing to Disclose

## PURPOSE

We investigated the correlation between the minimum lung area during tidal breathing on MRI and the prognosis of patients with chronic obstructive pulmonary disease (COPD).

## **METHOD AND MATERIALS**

This study was approved by the review board . Written informed consent was obtained from the participants. The subjects were 35 male patients with COPD (age,  $69.7 \pm 6.2$  years). We obtained 80 sagittal images of the right lung during tidal breathing by using MRI with a 1.5T unit and a balanced fast-field echo sequence. The image slice thickness was 10 mm, and acquisition time per image was 0.28 s. We measured lung area on 80 images by using an original system. We determined minimum lung area and divided it by predicted total lung capacity (TLC) to calculate the corrected- minimum lung area (minLA). We compared minLA with the initial pulmonary function tests, the ratio of low attenuation area under -950 HU (LAA%) on computer tomography (CT), and the St. George Respiratory Questionnaire (SGRQ) score by using Spearman's correlations. Cox regression analysis was used to examine the relationships between these parameters and overall survival.

# RESULTS

The mean minLA was 46.2 cm<sup>2</sup>/cm<sup>3</sup>x10-5. This correlated well with forced expiratory volume in 1 s (FEV1, %) (correlation coefficient r=-0.756), residual volume (RV, %)(r=0.509), inspiratory capacity (IC, %)(r=-0.618), LAA% (r=0.559), and SGRQ total score (r=0.491). The median clinical follow-up period was 101 months (range: 7.3-124.4 months). One patient dropped out and six patients died during the follow-up period. Univariate Cox analysis showed the following significant predictors: minLA (p=0.004), IC (p=0.028), RV (p=0.033), LAA% (p=0.016). Multivariate analysis including minLA and LAA% identified minLA as a significant predictor of overall survival (p=0.014, hazard ratio =1.463, 95% confidence interval =1.082–1.979).

#### CONCLUSION

We think minLA will be a simple predictor of COPD patient's survival.

## **CLINICAL RELEVANCE/APPLICATION**

MRI during tidal breathing requires no irradiation or no additional effort, therefore minLA is a gentle and steady measure for COPD patients.

# CH251-SD-MOB2

## Whole-lesion Apparent Diffusion Coefficient Histogram Analysis of Anterior Mediastinal Solid Tumors

Monday, Nov. 28 12:45PM - 1:15PM Room: CH Community, Learning Center Station #2

#### **Participants**

Takahiko Nakazono, MD, PhD, Saga, Japan (*Presenter*) Nothing to Disclose Ken Yamaguchi, MD, Saga, Japan (*Abstract Co-Author*) Nothing to Disclose Ryoko Egashira, MD, Saga, Japan (*Abstract Co-Author*) Nothing to Disclose Takeshi Imaizumi, Saga, Japan (*Abstract Co-Author*) Nothing to Disclose Yukari Takase, Saga, Japan (*Abstract Co-Author*) Nothing to Disclose Masanobu Mizuguchi, MD, Saga City, Japan (*Abstract Co-Author*) Nothing to Disclose Hiroyuki Irie, MD, PhD, Saga, Japan (*Abstract Co-Author*) Nothing to Disclose

#### PURPOSE

To assess the utility of whole-lesion apparent diffusion coefficient (ADC) histogram analysis in the diagnosis of anterior mediastinal solid tumors.

## **METHOD AND MATERIALS**

In this retrospective study, a whole-lesion ADC histogram analysis was performed in 49 consecutive patients with thymomas (n=32), thymic carcinomas (n=8), malignant lymphomas (n=6), or germ cell tumors (n=3). The ADC histogram parameters (mean, 10th, 25th, 50th, 75th, and 90th percentile ADC values, kurtosis, and skewness) were calculated. These parameters were compared between the thymic epithelial tumors (TETs, n=40) and non-thymic epithelial tumors (non-TETs, n=9). In the thymomas that underwent surgical resection (n=29), the parameters were compared between the low-risk (n=15) and high-risk thymomas (n=14) and between the non-invasive (n=14) and invasive thymomas (n=15). The highest diagnostic performance of the parameters was evaluated by a receiver operating characteristic (ROC) analysis, and the area under the curve (AUC), sensitivity, specificity, and accuracy were calculated.

## RESULTS

There were significant differences among the 25th, 50th, 75th and 90th percentile ADC values, and in the skewness between the TETs and non-TETs (p<0.05). The results of the ROC analysis showed that the diagnostic performance of the skewness was the highest for differentiating non-TETs from TETs. When the cutoff of skewness was 0.81, the following values were obtained: AUC 0.79, sensitivity 88.9%, specificity 72.5%, and accuracy 75.5%. There was no significant difference in the ADC histogram parameters between the low-risk and high-risk thymomas (p>0.05). There were significant differences in the mean ADC values and 10th, 25th, 50th, 75th, and 90th percentiles between the non-invasive and invasive thymomas (p<0.05). In the ROC analysis, the diagnostic performance of the 25th percentile ADC values was the highest for differentiating invasive thymomas from non-invasive thymomas. When the cutoff of 25th percentile ADC values was  $1.44 \times 10-3$  mm2/s, the following values were obtained: AUC 0.82, sensitivity 93.3%, specificity 71.4%, and accuracy 82.8%.

## CONCLUSION

The ADC histogram analysis revealed significant differences in parameters between the TETs and non-TETs and between the non-invasive and invasive thymomas.

#### **CLINICAL RELEVANCE/APPLICATION**

An ADC histogram analysis can be used to obtain additional information about the characterization of anterior mediastinal solid tumors.

# CH252-SD-MOB3

Effectiveness of Lead Gloves for Radiation Protection during Percutaneous Transthoracic Lung Biopsy Guided by C-Arm Cone-Beam CT

Monday, Nov. 28 12:45PM - 1:15PM Room: CH Community, Learning Center Station #3

# Participants

Yoon Kyung Kim, MD, Incheon, Korea, Republic Of (*Abstract Co-Author*) Nothing to Disclose Yon Mi Sung, MD, Incheon, Korea, Republic Of (*Abstract Co-Author*) Nothing to Disclose Min Kyoung Lee, MD, Incheon, Korea, Republic Of (*Abstract Co-Author*) Nothing to Disclose Chorong Seo, MD, Incheon, Korea, Republic Of (*Presenter*) Nothing to Disclose Jeong Ho Kim, MD, Incheon, Korea, Republic Of (*Abstract Co-Author*) Nothing to Disclose Hye-Young Choi, MD, PhD, Incheon, Korea, Republic Of (*Abstract Co-Author*) Nothing to Disclose

## PURPOSE

To assess the effectiveness of lead gloves for radiation protection during C-arm cone-beam CT guided percutaneous transthoracic lung biopsy.

# METHOD AND MATERIALS

From February to November 2014, 112 percutaneous transthoracic lung biopsies were performed by two experienced thoracic radiologists under guidance of c-arm cone-beam CT, with using lead gloves (n=57) or without using lead gloves (n=55). Optically-stimulated luminescence dosimeters were attached to the dorsum and ventral side of each hand of operators to measure the hand surface dose during the procedure. The total fluoroscopy time, radiation dose to the patient, lesion characteristics and biopsy results were recorded for each procedure.

#### RESULTS

Mean surface dose was significantly lower in lead glove group (p<0.001, 0.0176±0.0172 mGy vs. 0.0260±0.0131 mGy at the right dorsum; 0.0290±0.0248 mGy vs. 0.0497±0.0353 mGy at the right ventral side; 0.0195±0.0152 mGy vs. 0.0298±0.0171 mGy at the left dorsum; 0.0192±0.0099 mGy vs. 0.0523±0.0429 mGy at the left ventral side). The dose reduction with the gloves was 45.9% in average (32.3% at the right dorsum, 63.2% at the left ventral side). There was no significant difference between lead glove group and control group in the total fluoroscopy time (p=0.208,  $1.57\pm0.76$  minutes vs.  $2.06\pm2.84$  minutes), radiation dose to the patient (p=0.845, 88.9\pm68.6 mGy vs. 92.7±129.4 mGy), lesion size (p=0.080,  $3.9\pm2.5$  cm vs.  $4.6\pm2.1$  cm), lesion depth from the skin (p=0.192,  $4.3\pm1.5$  vs.  $4.8\pm1.9$  cm cm), lesion depth from the pleura (p=0.587,  $2.0\pm1.0$  cm vs.  $1.8\pm1.2$  cm). False negative result was observed in 5 of lead glove group (8.7%) and 12 of control group (21.8%) (p=0.096). Development of pneumothorax (5/57 vs. 3/55, p=0.753) or hemoptysis (1/57 vs. 1/55, p=0.491) was not significantly different between two groups.

# CONCLUSION

Lead gloves have a radiation attenuation effect of 32.3-63.2% during c-arm cone-beam CT guided transthoracic lung biopsy without affecting the accuracy or safety.

#### **CLINICAL RELEVANCE/APPLICATION**

Considering the trend of increasing demand of transthoracic percutaneous lung biopsy, appropriate radiation protection to the hands during procedure is important.

Noise Reduction Filtering Improves Repeatability of Quantitative Lung Density Metrics Between Full and Reduced-dose CT Scans

Monday, Nov. 28 12:45PM - 1:15PM Room: CH Community, Learning Center Station #4

# Participants

Charles Hatt, Delafield, WI (Presenter) Employee, Imbio, LLC

Craig J. Galban, PhD, Ann Arbor, MI (Abstract Co-Author) Nothing to Disclose

Stephen Humphries, Denver, CO (Abstract Co-Author) Research Consultant, PAREXEL International Corporation

David A. Lynch, MBBCh, Denver, CO (*Abstract Co-Author*) Research support, Siemens AG Scientific Advisor, PAREXEL International Corporation Consultant, Boehringer Ingelheim GmbH Consultant, Gilead Sciences, Inc Consultant, F. Hoffmann-La Roche Ltd Consultant, Veracyte, Inc

Meilan K. Han, Ann Arbor, MI (*Abstract Co-Author*) Consultant, Boehringer Ingelheim GmbH; Consultant, GlaxoSmithKline plc; Consultant, Novartis AG; Consultant, AstraZeneca PLC; Royalties, UpToDate, Inc

### PURPOSE

Lung cancer screening offers an additional opportunity to screen for computed tomography (CT) based imaging biomarkers associated with emphysema. It is important to understand how decreasing the radiation dose affects the repeatability of lung densitometry measures compared to those obtained from full-dose scans, and if noise-reduction filtering can help improve repeatability. The aim of this study was to quantify the repeatability of quantitative lung density metrics using full dose (FD) and reduced dose (RD) CT acquisitions of the same patient obtained during the same study. It was hypothesized that 1) RDCT would have a higher average %LAA and a lower Perc15 than the corresponding FDCT scan and 2) noise reduction filtering would decrease this bias as well as the variation between the measurements.

## **METHOD AND MATERIALS**

As part of the COPDGene study, 179 patients were scanned at inspiration using the standard FD protocol (200 mAs, B31f or STD kernel). Next, a repeat scan was obtained with dose modulation at a lower dose (mAs range 40-80, B31f or STD kernel). The lung was segmented from the images using Imbio LDA software. Ventilation differences between scans were corrected using a dry-sponge model method. Each RDCT image was then processed with a 3x3x3 neighborhood median filter. Lung density was quantified as low-attenuation area less than -950 HU (%LAA) and 15th percentile HU (Perc15).

#### RESULTS

Mean and 95% confidence interval (CI95) of differences in biomarker metrics between scans were calculated with and without noise reduction filtering. Bland-Altman analysis was used to examine the effect of baseline %LAA and Perc15 on the measurement difference. The mean  $\pm$  CI95 differences between FDCT and unfiltered RDCT were 5.9% $\pm$ 7.1% for %LAA and -15.2 HU  $\pm$  12.0 HU for Perc15. The differences in %LAA and Perc15 between FDCT and filtered RDCT were significantly lower (0.6% $\pm$ 2.4% and -2.9 HU  $\pm$  11.0 HU, respectively).

# CONCLUSION

Noise reduction filtering improves repeatability of lung density metrics between FDCT and LDCT scans, which is important for determining the reliability of quantitative biomarker measurements associated with emphysema in a lung-cancer screening context.

# **CLINICAL RELEVANCE/APPLICATION**

Noise reduction filtering can be used to correct for differences in measurements between FDCT, the clinical gold standard, and RDCT, which is recommended for patients undergoing yearly lung cancer screening CT exams.

# CH254-SD-MOB5

## Clinical Significance of Indeterminate Pulmonary Nodules in Patients with Melanoma

Monday, Nov. 28 12:45PM - 1:15PM Room: CH Community, Learning Center Station #5

#### **Participants**

Magdy M. Soliman, MBBCh, FRCR, Toronto, ON (*Presenter*) Nothing to Disclose Teresa Petrella, MD,FRCPC, Toronto, ON (*Abstract Co-Author*) Nothing to Disclose Frances Wright, MD, MEd, Toronto, ON (*Abstract Co-Author*) Nothing to Disclose Nicole Look Hong, MD,MSc, Toronto, ON (*Abstract Co-Author*) Nothing to Disclose Laura Jimenez-Juan, MD, Toronto, ON (*Abstract Co-Author*) Nothing to Disclose Anastasia Oikonomou, MD, PhD, Toronto, ON (*Abstract Co-Author*) Nothing to Disclose

## PURPOSE

Followup algorithms for pulmonary nodules in melanoma patients are controversial and largely left to institutional preference. This study aims to determine the clinical significance of indeterminate pulmonary nodules in patients with melanoma.

## **METHOD AND MATERIALS**

This retrospective cohort study included consecutive patients surgically treated with localized melanoma. Patients with definitely benign nodules, definite pulmonary or extrapulmonary metastases and other non-melanoma malignancies were excluded. Nodules were volumetrically measured on sequential follow-up CTs (median interval between CTs: 4 months (3-9)) and a cut-off of 15% difference in volume was considered as increase or decrease in size. Distance from pleura, peripheral versus central location, perifissural location, irregularity, solid density, cavitation were evaluated. Nodules were considered metastases on follow-up CT if they increased in size on 2 sequential CTs, if increase in size was accompanied by development of new pulmonary nodules and/or extrapulmonary metastases or based on histology.

#### RESULTS

Out of 584 melanoma patients surgically managed at our institution between September 2012-2015, 277 had baseline chest CT. 53 patients, (29 female), median age 62 yrs (range: 24-84) with indeterminate pulmonary nodules at baseline CT were identified. 188 nodules - median volume:0.0252 cm3, median distance from pleura: 2 mm, 37 perifissural, 165 peripheral in location and 166 with solid density - were evaluated for a median period of 15 months (range: 6-33). 124 pulmonary nodules remained stable, 10 resolved, 42 decreased in size, 11 increased less than 15%. Only one nodule doubled its size in 3 months and was proven to be metastatic (0.5%). During follow-up 6 newly developed nodules in a median interval period of 7 months (range: 3-26) were confirmed metastatic in a short-term 3 month follow up CT.

## CONCLUSION

Indeterminate pulmonary nodules in melanoma patients at baseline chest CT were extremely rarely metastatic (0.5%) and in this case a 3 month follow-up CT confirmed increase in size. Newly developed nodules during follow up confirmed to be metastatic in a 3 month follow-up CT.

# **CLINICAL RELEVANCE/APPLICATION**

Indeterminate pulmonary nodules at baseline CT in melanoma patients are almost always benign and a 3 month follow-up CT will most likely confirm their metastatic nature otherwise.

# ER172-ED-MOB6

CT Evaluation of Suspected Small Bowel Obstruction and Its Etiology. The Role of CT/CTA with Multiplanar and 3D Imaging in Diagnosis, Determining Cause, Identifying Complications and Guiding Patient Management: An Interactive Quiz

Monday, Nov. 28 12:45PM - 1:15PM Room: ER Community, Learning Center Station #6

## Participants

Christopher R. Bailey, MD, Baltimore, MD (*Presenter*) Nothing to Disclose Pamela T. Johnson, MD, Baltimore, MD (*Abstract Co-Author*) Consultant, National Decision Support Company Elliot K. Fishman, MD, Baltimore, MD (*Abstract Co-Author*) Institutional Grant support, Siemens AG; Institutional Grant support, General Electric Company;

# **TEACHING POINTS**

MDCT has become the primary imaging modality for patients with small bowel obstruction. Evidence in the literature underscores the importance of multiplanar evaluation to optimally interpret these studies. Following review of the exhibit the user will understand the role MPR/3D imaging in detection and differential diagnosis of small bowel obstruction recognize the various CT appearances of small bowel obstruction learn how specific CT findings help define the cause of small bowel obstruction be cognizant of CT findings that define the urgency of surgical management

## TABLE OF CONTENTS/OUTLINE

Critical CT findings for each diagnosis are emphasized and the importance of high value interpretations to guidemanagement of these patients. Case studies (10) in quiz formatwith specific diagnosis include: SBO due to adhesions from prior surgery SBO following robotic prostatectomy andport site hernia incarcerated inguinal hernia internal hernia with midgut volvulus SBO secondary to volvulus with SMA and SMV occlusion as well as bowel infarction obstruction due to intussuception of a primary small bowel tumor obstruction due to intussuception of a metastatic tumor to the small bowel obstruction due to stricture from Crohn's disease SBO due to radiation enteritis SBO due to gallstone ileus

## **Honored Educators**

Presenters or authors on this event have been recognized as RSNA Honored Educators for participating in multiple qualifying educational activities. Honored Educators are invested in furthering the profession of radiology by delivering high-quality educational content in their field of study. Learn how you can become an honored educator by visiting the website at: https://www.rsna.org/Honored-Educator-Award/

Elliot K. Fishman, MD - 2012 Honored Educator Elliot K. Fishman, MD - 2014 Honored Educator Elliot K. Fishman, MD - 2016 Honored Educator Pamela T. Johnson, MD - 2016 Honored Educator

## ER213-SD-MOB1

# Clinical Parameters Predict Subsequent Traumatic Hepatic and Splenic Injury Identified on Computed Tomography

Monday, Nov. 28 12:45PM - 1:15PM Room: ER Community, Learning Center Station #1

# Participants

Michael J. Hsu, MD, Boston, MA (*Presenter*) Nothing to Disclose Michael Wasserman, MD, Boston, MA (*Abstract Co-Author*) Nothing to Disclose Jennifer Xiao, MD, Boston, MA (*Abstract Co-Author*) Nothing to Disclose Venkata Satyam, Boston, MA (*Abstract Co-Author*) Nothing to Disclose Tina Shiang, Boston, MA (*Abstract Co-Author*) Nothing to Disclose Deepan Paul, Boston, MA (*Abstract Co-Author*) Nothing to Disclose Ahmed Y. El-Araby, MD, West Warwick, RI (*Abstract Co-Author*) Nothing to Disclose Robert Burns, Boston, MA (*Abstract Co-Author*) Nothing to Disclose Arthur Baghdanian, MD, Boston, MA (*Abstract Co-Author*) Nothing to Disclose Christina A. LeBedis, MD, Boston, MA (*Abstract Co-Author*) Nothing to Disclose Jorge A. Soto, MD, Boston, MA (*Abstract Co-Author*) Nothing to Disclose

#### PURPOSE

The purpose of this study was to examine commonly collected clinical parameters in the trauma patient, and to determine which parameters predict subsequent traumatic injury to the liver and spleen as identified on computed tomography (CT).

## METHOD AND MATERIALS

This HIPAA-compliant, retrospective study performed at our urban academic teaching hospital was approved by the Institutional Review Board (IRB); informed consent was waived. All adult patients presenting over a two-year period with hepatic or splenic trauma as evidenced by CT imaging were enrolled (n=49). A control group of 50 patients presenting with trauma but with negative CT findings was included for comparison. Admission clinical parameters such as heart rate (HR) and blood pressure (BP) as well the admission lab values hematocrit (Hct), lactate, blood urea nitrogen (BUN) and creatinine (Cr) were collected for each patient. Subsequently, the differences in these clinical parameters between the two groups were analyzed using a t-test with p-value of <0.05 considered statistically significant.

#### RESULTS

The mean Hct was 39.5 for females and 43.4 for males in the control group and 35.0 for females and 40.6 for males in the hepatosplenic injury group. Hematocrit was significantly lower in the hepatosplenic injury group (p = 0.003 for females and p = 0.006 for males). Mean lactate was 1.72 and 3.28 for the control and hepatosplenic injury groups, respectively. While lactate was abnormally elevated for both groups, the hepatosplenic injury group demonstrated a significantly greater degree of lactate elevation (p = 0.0001). Heart rate and blood pressure were similar between the two groups with no statistically significant differences identified. Additional laboratory values which were analyzed, including BUN and Cr, were not predictive of hepatosplenic injury as no statistically significant differences were identified.

## CONCLUSION

The admission clinical parameters of HCT and lactate are predictive of traumatic hepatic and splenic injury identified on CT imaging. Awareness of the potential utility of these clinical parameters may assist in triage and CT protocol considerations during the initial patient evaluation in the trauma setting.

# **CLINICAL RELEVANCE/APPLICATION**

Identifying clinical parameters that predict hepatosplenic injury on CT alerts physicians to possible hepatosplenic injury, which may help CT protocol decision-making and support earlier CT imaging.

## **Honored Educators**

Presenters or authors on this event have been recognized as RSNA Honored Educators for participating in multiple qualifying educational activities. Honored Educators are invested in furthering the profession of radiology by delivering high-quality educational content in their field of study. Learn how you can become an honored educator by visiting the website at: https://www.rsna.org/Honored-Educator-Award/

Jorge A. Soto, MD - 2013 Honored Educator Jorge A. Soto, MD - 2014 Honored Educator Jorge A. Soto, MD - 2015 Honored Educator

# Evaluating the Predictive Value of Risk Factors for Retroperitoneal Hemorrhage

Monday, Nov. 28 12:45PM - 1:15PM Room: ER Community, Learning Center Station #2

#### Participants

Ahmed Fadl, MD, Mineola, NY (*Presenter*) Nothing to Disclose Rishi Chopra, Mineola, NY (*Abstract Co-Author*) Nothing to Disclose Abieyuwa Eweka, MD, Mineola, NY (*Abstract Co-Author*) Nothing to Disclose Amanjit S. Baadh, MD, New York, NY (*Abstract Co-Author*) Nothing to Disclose Douglas S. Katz, MD, Mineola, NY (*Abstract Co-Author*) Nothing to Disclose Jason C. Hoffmann, MD, Mineola, NY (*Abstract Co-Author*) Consultant, Merit Medical Systems, Inc; Speakers Bureau, Merit Medical Systems, Inc Sameer Mittal, MD, Mineola, NY (*Abstract Co-Author*) Nothing to Disclose

#### PURPOSE

Retroperitoneal bleed (RPB) is an uncommon and potentially life threatening condition, often requiring a high index of suspicion to diagnose correctly. Concern for RPB is often raised given physical examination findings and pertinent laboratory values. Non-contrast computed tomography (CT) has proven to be a fast and accurate means to emergently assess these patients. We retrospectively evaluated specific risk factors in a series of patients and determined their predictive values in developing RPB when correlating with CT findings, with the goal of determining which factors are important to consider when determining if emergent imaging is warranted.

## METHOD AND MATERIALS

A single institutional retrospective analysis of 1,000 consecutive patients who underwent a non-contrast CT of the abdomen and pelvis to evaluate specifically for RPB was conducted. Patients were selected from a database of CT imaging requests (June 2008-June 2011). Values including vital signs, recent invasive procedures, coagulation panel, hematologic status, and anticoagulant use were documented. Corresponding CT imaging at the time of evaluation was analyzed by two board-certified radiologists for the presence of a retropertioneal bleed. Findings were subsequently compared between the RPB and non-RPB cohorts.

#### RESULTS

Of the 1,000 patients meeting inclusion criteria, 29 were found to have CT confirmed RPB. A randomly selected equal size cohort with CT confirmed studies negative for RPB was gathered for comparison. Analysis demonstrated that the CT confirmed RPB patients had a statistically significant low mean arterial pressure (MAP), with average MAP 76 mmHg versus 86 mmHg in control group (p=0.0008). Recent invasive procedure was also found to have significance, with 24 of 29 in the RPB group having recent invasive procedures, compared to 3 of 29 in the control group (p=0.0068). Drop in hemoglobin/hematocrit, coagulation panel, and anticoagulant use were not found to have statistical significance.

## CONCLUSION

Although uncommon, RPB warrants a high index of suspicion and prompt evaluation due to associated morbidity and mortality. Low mean arterial pressure and recent invasive procedure have predictive value in determining which patients should be emergently imaged.

#### **CLINICAL RELEVANCE/APPLICATION**

Low mean arterial pressure and history of a recent invasive procedure have predictive value in deciding whether emergent imaging is appropriate to evaluate for RPB.

# **Honored Educators**

Presenters or authors on this event have been recognized as RSNA Honored Educators for participating in multiple qualifying educational activities. Honored Educators are invested in furthering the profession of radiology by delivering high-quality educational content in their field of study. Learn how you can become an honored educator by visiting the website at: https://www.rsna.org/Honored-Educator-Award/

Douglas S. Katz, MD - 2013 Honored Educator Douglas S. Katz, MD - 2015 Honored Educator

# ER215-SD-MOB3

# The Combination of SWI and DTI in Diagnosing Different Severity's Traumatic Brain Injury

Monday, Nov. 28 12:45PM - 1:15PM Room: ER Community, Learning Center Station #3

#### Participants

Chengru Song, Zhengzhou, China (*Presenter*) Nothing to Disclose Jingliang Cheng, MD,PhD, Zhengzhou, China (*Abstract Co-Author*) Nothing to Disclose Yong Zhang, DO, Zhengzhou, China (*Abstract Co-Author*) Nothing to Disclose

## PURPOSE

To explore the diagnostic value of SWI and DTI on different severity's traumatic brain injury(TBI).

#### **METHOD AND MATERIALS**

Totally 60 TBI patients (including 20 mild TBI patients, 20 moderate TBI patients and 20 severe TBI patients) and 20 health volunteer underwent SWI, DTI and conventional MRI examination. The numbers of involving regions, numbers and areas of hemorrhagic lesions detected by SWI, and FA values of 37 brain regions (including knee, body, splenium of corpus callosum, cingulate bundle, et al.) were compared between each two groups. The correlation analysis between GCS scores and the number of involving regions, number of hemorrhagic lesions, areas of hemorrhagic lesions detected by SWI, and FA values of each region were performed.

# RESULTS

The differences of involving regions' number, lesions' number, lesion's areas detected by SWI between each two groups were statistically significant (P<0.05). Severe TBI group got the maximum number of involving regions, lesions, and the largest areas. Followed by moderate group and mild group. Among the 37 regions, totally 30 regions differ in FA values between the four groups (P<0.05). And among these 30 regions, 18 regions' FA values, for example corpus callosum region, gradually reduce as the severity of TBI aggravate. The GCS scores are highly negatively correlated with the number of involving regions, number of lesions, areas of lesions detected by SWI, but are positively correlated with 30 regions' FA values. The descending order of relevance is hemorrhagic lesions' areas(r=-0.932), lesions' number(r=-0.911), involving regions' number(r=-0.900), FA values of right cingulum(r=0.872), right anterior limb of internal capsule(r=0.801), left cingulum (r=0.787), the splenium of corpus callosum (r=0.765), et al.

# CONCLUSION

The clinical applications of SWI and DTI is valuable in diagnosing different severity's TBI.

# **CLINICAL RELEVANCE/APPLICATION**

SWI and DTI can be applied in the diagnosis of different severity's TBI.

Reducing the Use of CT Angiography in Low Risk Patients with Suspected Pulmonary Embolism via Implementation of Decision Points in the Emergency Room Setting

Monday, Nov. 28 12:45PM - 1:15PM Room: ER Community, Learning Center Station #4

#### Awards

#### **Student Travel Stipend Award**

#### Participants

Andrew J. Cantos, MD, East Meadow, NY (*Presenter*) Nothing to Disclose Michael Drabkin, MD, East Meadow, NY (*Abstract Co-Author*) Nothing to Disclose Harold Hunt, MD, East Meadow, NY (*Abstract Co-Author*) Nothing to Disclose Alexander Martynov, MD, East Meadow, NY (*Abstract Co-Author*) Nothing to Disclose Eli Q. Harris, BA, East Meadow, NY (*Abstract Co-Author*) Nothing to Disclose Victor J. Scarmato, MD, East Meadow, NY (*Abstract Co-Author*) Nothing to Disclose

## PURPOSE

To reduce waste in spending, radiation exposure to patients and Radiology Department resources by using accepted criteria and obtaining D-dimers in order to minimize ordering of CT angiography (CTA) for exclusion of pulmonary embolus.

## **METHOD AND MATERIALS**

Following IRB approval, we reviewed 697 consecutive patients who had CTA to exclude PE over an 18-month period. We set out to determine whether the appropriate decision points were being used. We systematically documented patients' presenting symptoms, demographic information, comorbidities and the results of their hospital workup. Risk categories were assigned, including consideration of the Wells Criteria.

## RESULTS

Of the 697 patients reviewed, 319 were considered low risk for PE using Well's criteria. D-dimer was ordered in only 89 of these low risk patients. Overall, 16 of 319 CTAs were positive (5.0%) in the low risk patient group. Of the 89 patients in whom D-dimer was performed, 24 had a negative D-dimer (<0.5  $\mu$ g/mL), all of which yielded negative CTA. Of the 65 patients with positive D-dimers, 5 demonstrated PE on CTA (avg. D-dimer = 7.23  $\mu$ g/mL). Of 230 patients in whom a CTA was performed without D-dimer being ordered, 11 were found to have CT findings suspicious for PE (4.8%).

#### CONCLUSION

Data suggests that we are underutilizing D-dimer, and not effectively using that D-dimer value when it is obtained; for both of these reasons CTAs are not being ordered efficiently. This is evidenced by the low rate of positive CTAs in our selected patient group, (5.0%) and high number needed to treat (20). By being more discerning in pursuing CTA to evaluate for PE, we can reduce costs (\$27 per D-dimer versus \$2,104 per CTA) and patient radiation exposure (7 mSv per CTA), while also allowing our radiologists more time to focus on more strongly indicated studies. We have since proposed to the ED that all patients meeting "low-risk criteria" have a D-dimer. We have begun collecting prospective data on patients in whom PE is considered; documenting Wells score, D-dimer and CTA results.

# **CLINICAL RELEVANCE/APPLICATION**

Excessive ordering of CTA to "rule out" PE results in increased costs, and patient radiation exposure, as well as taking up the time of our radiologists.

# ER217-SD-MOB5

## The Utility of Early CT of Patients with a First Attack of Acute Pancreatitis in Emergency Department

Monday, Nov. 28 12:45PM - 1:15PM Room: ER Community, Learning Center Station #5

#### **Participants**

So Hyun Park, MD, Incheon, Korea, Republic Of (*Abstract Co-Author*) Nothing to Disclose Seung Joon Choi, Incheon, Korea, Republic Of (*Abstract Co-Author*) Nothing to Disclose Young Sup Shim, MD, Incheon, Korea, Republic Of (*Abstract Co-Author*) Nothing to Disclose Sungjin Yoon, Incheon, Korea, Republic Of (*Presenter*) Nothing to Disclose

# PURPOSE

Contrast-enhanced computed tomography (CT) is considered a diagnostic tool of acute pancreatitis (AP) and ideal time is after 72 hours from onset of symptoms. However, in the emergency department (ED), CT has been used in the early stage of AP recently. This study is to investigate whether early CT affects clinical management of AP.

## **METHOD AND MATERIALS**

Of 116 consecutive adults of AP with a first attack in the ED between March 2015 and March 2016, 56 patients (56/116, 48.3%) of AP (M:F, 34:22; 50.3 ±15.6) underwent CT in the ED within 48 hours from onset of symptoms. CT images were retrospectively evaluated for the stage of AP and assessment of complications. Urgent clinical management including endoscopic retrograde cholangiopancreatitis (ERCP), percutaneous drainage (PCD) or percutaneous transhepatic biliary drainage (PTBD) within 24 hours after early CT was assessed in AP patients.

#### RESULTS

Of 56 patients, four patients showed acute necrotizing pancreatitis (3 patients in peripancreatic tissue only, 1 in both pancreas and peripancreatic tissue) and 52 patients had acute interstital pancreatitis. Alcohol abuse (25/56, 44.6%) and biliary obstruction or cholangitis (20/56, 35.7%) were the most common causes of AP. Of 20 biliary pancreatitis, 11 received urgent therapeutic ERCP (mean time interval between CT and ERCP,  $11.4 \pm 5.4$ ). Of 11 patients, 5 received stone removal from the common bile duct (CBD) and endoscopic sphincterotomy (EST), 2 received interposition of biliary stent, 2 underwent EST, 1 underwent removal of pancreatic ductal stones, and 1 underwent CBD stone removal.

## CONCLUSION

In conclusion, early CT is useful when a patient suspected of acute biliary pancreatitis and could be applied in clinical management of AP.

# **CLINICAL RELEVANCE/APPLICATION**

Early CT may be useful in diagnosis and management of suspicious acute biliary pancreatitis.

## Imaging Appearance and Surgical Management of Anovaginal and Rectovaginal Fistulas

Monday, Nov. 28 12:45PM - 1:15PM Room: GI Community, Learning Center Station #10

Awards Certificate of Merit Identified for RadioGraphics

#### **Participants**

Wendaline M. VanBuren, MD, Rochester, MN (*Presenter*) Nothing to Disclose Shannon P. Sheedy, MD, Rochester, MN (*Abstract Co-Author*) Nothing to Disclose Amy L. Lightner, Rochester, IA (*Abstract Co-Author*) Nothing to Disclose Sarasa T. Kim, Rochester, MN (*Abstract Co-Author*) Nothing to Disclose Madeline Miller, Rochester, MN (*Abstract Co-Author*) Nothing to Disclose Joel G. Fletcher, MD, Rochester, MN (*Abstract Co-Author*) Grant, Siemens AG; ; Christine O. Menias, MD, Chicago, IL (*Abstract Co-Author*) Nothing to Disclose

# **TEACHING POINTS**

Anovaginal and rectovaginal fistulas (AVF/RVF's) represent a challenging subset of pelvic fistulas for radiologists and surgeons, and have a wide range of imaging appearances on CT, MR, and fluoroscopy. AVF/RVF may arise from obstetrical trauma, Crohn's disease, malignancy, pelvic radiation/iatrogenic, infection/diverticulitis. The surgical management of AVR/RVF's will change based on size, anatomic classification, etiology, and other factors.

# TABLE OF CONTENTS/OUTLINE

Background of RV/AV fistulas Clinical presentation & non-imaging assessment Normal anatomic appearance Classification: RVF vs. AVF, low/middle/highETIOLOGY-based imaging of AVF/RVF's (protocol, findings) Obstetric Inflammatory: Crohn's disease, diverticulitis Malignancy Radiation IPAA IatrogenicCritical features across etiologies Relationship to dentate line and location within vagina Sphincter involvement Previous sphincter damage or child birth Proctitis and condition of surrounding tissues Associated abscess or undrained fluid collectionIllustrative review of surgical techniques and when/why they are chosen Surgical management prior to definitive repair Fistulotomy Mucosal advancement flap +/- sphincteroplasty Transvaginal repair Tissue transfer procedures (gracilis/sartorius flaps, fad pad) Proctectomy, diversion

## **Honored Educators**

Presenters or authors on this event have been recognized as RSNA Honored Educators for participating in multiple qualifying educational activities. Honored Educators are invested in furthering the profession of radiology by delivering high-quality educational content in their field of study. Learn how you can become an honored educator by visiting the website at: https://www.rsna.org/Honored-Educator-Award/

Christine O. Menias, MD - 2013 Honored Educator Christine O. Menias, MD - 2014 Honored Educator Christine O. Menias, MD - 2015 Honored Educator Christine O. Menias, MD - 2016 Honored Educator

## GI363-SD-MOB1

The Assessment of Radiation Dose and Image Quality by using Different Scan Parameter Selection Methods with for Fast Kilo Voltage Switching Dual-energy CT (ssDECT) with Different Scan Parameter Selection Methods

Monday, Nov. 28 12:45PM - 1:15PM Room: GI Community, Learning Center Station #1

## Participants

Tsuyoshi Kagimoto, hiroshima, Japan (*Presenter*) Nothing to Disclose Chisato Yoritaka, RT, Hiroshima, Japan (*Abstract Co-Author*) Nothing to Disclose Satoshi Inada, hiroshima, Japan (*Abstract Co-Author*) Nothing to Disclose Masashi Takahashi, RT, hiroshima, Japan (*Abstract Co-Author*) Nothing to Disclose Xiao Zhu Lin, MD, Shanghai, China (*Abstract Co-Author*) Nothing to Disclose

## PURPOSE

The comparison of scan dose and image quality between DECT and 120kV helical scan mode (SECT) is important for DECT clinical application. The purpose of this study iwas to assess radiation dose and image quality by using different scan parameter selection methods with for the fast kV switching dual-energy CT (DECT) with different scan parameter selection methods.

#### **METHOD AND MATERIALS**

50th abdomen dynamic scans were performed on 64detector DECT scanner (Revolution GSI, GE) using combination of 120kV helical and fast kV (80/140kV) switching DECT techniques with in different scanning phases using different scan parameters:Plain scan with 120kV and noise index (NI) of 12@5mm slice thickness,Arterial phase:GSI Assist by using automatically DECT scan parameter selection method (NI of 12@5mm), Portal vein phase:manual parameter selection using Max mA of mA table of SECT scan (NI of 12@5mm).The CTDI (mGy),DLP (mGy-cm),ED (mSv) and Noise (SD) of three different scans compared between SECT and two parameter selection methods of DECT.

## RESULTS

The averages of CTDI with different scan mode and DECT parameter selection method were 12.2±4.8mGy at in Plain phase (120kV), 12.8±4.2mGy at in Arterial phase (GSI assist), 14.5±4.8mGy at in Portal vein phase (Max mA GSI). GSI assist produced similar CTDI as the 120kV scan, while the Max mA GSI had statistically higher CTDI than the 120kV scan there was a significant difference between 120kV and two GSI parameter selector methods. The averages of DLP were 374.0±164.2mGy-cm at 120kV, 391.8±149.1mGy-cm at with GSI assist and, 443.6±169.0mGy-cm at with Max mA GSI, there was a no significant difference between 120kV and two GSI parameter selector methods. The averages of ED were 5.6±2.5mSv at 120kV, 5.9±2.2mSv at GSI assist and, 6.7±2.5mSv at Max mA GSI. The averages of Noise (SD) were 18.6±3.9HU at 120kV, 14.5±4.2HU at GSI assist and 14.2±4.6HU at with Max mAs GSI there was a significant difference between 120kV and GSI assist and, between 120kV and Max mA GSI.

# CONCLUSION

From this study, we can conclude that the automatically DECT scan parameter selection method (GSI Assist) has similar scan dose and image quality with as the 120kV helical and manual parameter selection methodscans.

### **CLINICAL RELEVANCE/APPLICATION**

The automatically DECT scan parameter selection method (GSI assist) has similar scan DOSE and image quality with helical scan (SECT) and is very useful for clinicial application and clinical research of DECT.

## The Diagnostic Performance of Shear-wave Elastography in Patients with Autoimmune Liver Disease

Monday, Nov. 28 12:45PM - 1:15PM Room: GI Community, Learning Center Station #2

**FDA** Discussions may include off-label uses.

#### **Participants**

Changtian Li, Beijing, China (*Presenter*) Nothing to Disclose Manish Dhyani, MBBS, Boston, MA (*Abstract Co-Author*) Nothing to Disclose Stephan D. Pratt, Boston, MA (*Abstract Co-Author*) Nothing to Disclose Atul K. Bhan, MD, Boston, MA (*Abstract Co-Author*) Nothing to Disclose Anthony E. Samir, MD, Boston, MA (*Abstract Co-Author*) Nothing to Disclose Anthony E. Samir, MD, Boston, MA (*Abstract Co-Author*) Consultant, Pfizer Inc Consultant, General Electric Company Consultant, PAREXEL International Corporation Research Grant, Koninklijke Philips NV Research Grant, Siemens AG Research Grant, Toshiba Corporation Research Grant, General Electric Company Research Grant, Samsung Electronics Co, Ltd Research Grant, Analogic Corporation Research support, SuperSonic Imagine Research support, Hitachi, Ltd

## PURPOSE

(1) To assess shear wave elastography (SWE) performance for liver fibrosis staging in patients with autoimmune liver disease (ALD) (2) to validate a previously established Young's modulus cut-off value in this new cohort.

## **METHOD AND MATERIALS**

Patients with known or suspected ALD scheduled for ultrasound guided non-focal liver biopsy were included. SWE imaging was performed with the Aixplorer US system quipped with a convex broadband probe. Eight elastograms were obtained intercostally in the right upper liver and the median value of the best 8 measurements was calculated. A single blinded pathologist staged liver fibrosis and calculated steatosis and necroinflammation scores using the METAVIR system. The Spearman correlation test was performed to assess correlation between estimated tissue Young's modulus (eYM) and fibrosis, steatosis, necroinflammatory score, PBC stage and clinical data. The diagnostic performance of SWE for differentiating higher grades of fibrosis ( $F \ge 2$ ) from lower grades(F0, F1) was evaluated using ROC curve analysis.

#### RESULTS

51 subjects were enrolled. Fibrosis stage, necroinflammation score and PBC stage had moderate correlations with eYM, but steatosis did not correlate with eYM. For all patients, AST, ALT and total bilirubin levels were positively correlated with eYM while serum albumin was negatively correlated with eYM; for patients with PBC, AST and ALT had positive correlations with eYM; for patients with AIH, AST, ALT, Alk Phos and total bilirubin had positive correlations with eYM. The AUROC for differentiating  $F \ge 2$  from F0 and F1 was 0.781. Our previously established cut-off value of 7.29 kPa for a heterogenous population of subjects with diffuse liver disease had sensitivity and specificity of 88.9% and 39.4% in this cohort. A cut-off value of 9.15kPa provided a sensitivity of 83.3% and specificity of 72.7%, which also provided a sensitivity of 84.6% and specificity of 75% in the follow-up subgroup and a sensitivity of 80% and specificity of 69.2% in the diagnostic subgroup.

# CONCLUSION

Shear wave elastography is a novel, supplementary adjunct to liver biopsy in the evaluation of histological staging in patients with ALD. A higher cutoff value for diagnosis of advanced fibrosis may yield superior diagnostic performance in these patients.

## **CLINICAL RELEVANCE/APPLICATION**

Shear wave elastography is a supplementary adjunct to liver biopsy in the evaluation of histological staging in patients with ALD.

## GI365-SD-MOB3

Prediction of the Gastrointestinal Stromal Tumor Response to Second-line Sunitinib Therapy with Apparent Diffusion Coefficient

Monday, Nov. 28 12:45PM - 1:15PM Room: GI Community, Learning Center Station #3

# Participants

Zheng Zhong, Chicago, IL (*Presenter*) Nothing to Disclose Lei Tang, MD, Beijing, China (*Abstract Co-Author*) Nothing to Disclose Muge Karaman, PhD, Chicago, IL (*Abstract Co-Author*) Nothing to Disclose Yi Sui, PhD, Chicago, IL (*Abstract Co-Author*) Nothing to Disclose Yingshi Sun, Beijing, China (*Abstract Co-Author*) Nothing to Disclose Xiaohong J. Zhou, PhD, Chicago, IL (*Abstract Co-Author*) Nothing to Disclose

## PURPOSE

To demonstrate the use of apparent diffusion coefficient (ADC) for early prediction of gastrointestinal stromal tumor (GIST) response to second-line sunitinib treatment.

# METHOD AND MATERIALS

With the approval of the institutional review board, a total of 43 patients were enrolled in the study. All the patients underwent sunitinib treatment after imatinib resistance. MRI scans with multi-b-value diffusion-weighted imaging (DWI) were performed prior to treatment (baseline) and two weeks (for prediction of response) after initiating sunitinib treatment. Conventional MRI images at twelve weeks were used to determine the good (GoodR) and poor (PoorR) responders according to the established criteria. The regions of interest (ROIs) were drawn on the b=1000 sec/mm<sup>2</sup> images in the solid tumor regions. Up to two ROIs (the largest ones) were selected from each patient, resulting in 36 GoodR and 27 PoorR ROIs. The ADC values were then calculated for each ROI by using the mono-exponential diffusion model. The changes in the ADC values ( $\Delta$ D) and the longest diameter of the lesion ( $\Delta$ LD) before and after two weeks of treatment were compared between the two groups. A receiver operating characteristic (ROC) analysis was also performed to evaluate the response to sunitinib treatment.

# RESULTS

Significant differences were detected in the change of ADC values ( $\Delta$ D) (62.2% vs. 11.7%, p<0.001) between the two groups.  $\Delta$ D provided a significantly higher predictive power than  $\Delta$ LD, producing higher AUC in the ROC analysis (80% vs. 69%). This performance was further improved (AUC value of 82%) when  $\Delta$ D was combined with  $\Delta$ LD.

## CONCLUSION

The change in ADC values two weeks into the treatment provides a better prediction of GIST response to sunitinib therapy than the change of tumor size.

#### **CLINICAL RELEVANCE/APPLICATION**

The change in ADC values after two weeks of therapy can be a useful marker to predict early response of GIST to sunitinib treatment.

Can the Detection of Peritoneal Metastatic Disease be Improved using Virtual Monenergetic Reconstructions of Contrast-enhanced Dual-energy CT Scans?

Monday, Nov. 28 12:45PM - 1:15PM Room: GI Community, Learning Center Station #4

## Participants

Kathryn Darras, MD, Vancouver, BC (*Presenter*) Nothing to Disclose Sheldon J. Clark, MD, Vancouver, BC (*Abstract Co-Author*) Nothing to Disclose Sarah A. Barrett, MBBCh, Vancouver, BC (*Abstract Co-Author*) Nothing to Disclose Triona M. Walshe, FFR(RCSI), Vancouver, BC (*Abstract Co-Author*) Nothing to Disclose Heejun Kang, MD, Vancouver, BC (*Abstract Co-Author*) Nothing to Disclose Luck J. Louis, MD, Vancouver, BC (*Abstract Co-Author*) Nothing to Disclose Silvia D. Chang, MD, Vancouver, BC (*Abstract Co-Author*) Nothing to Disclose Alison C. Harris, MBChB, Vancouver, BC (*Abstract Co-Author*) Nothing to Disclose Mohammed F. Mohammed, MBBS, Vancouver, BC (*Abstract Co-Author*) Nothing to Disclose Savvas Nicolaou, MD, Vancouver, BC (*Abstract Co-Author*) Institutional research agreement, Siemens AG Patrick D. McLaughlin, FFRRCSI, Vancouver, BC (*Abstract Co-Author*) Speaker, Siemens AG

#### PURPOSE

To evaluate the role of virtual monochromatic imaging (VMI) in the detection of peritoneal metastatic disease in contrast-enhanced computed tomography (CT) of the abdomen and pelvis and to compare this technique to conventional polychromatic imaging (PCI).

## METHOD AND MATERIALS

Institutional review board approval was obtained, with no informed consent required, for this retrospective analysis. 43 consecutive patients with confirmed peritoneal disease were scanned using a standard protocol on a 128-section dual source, dual energy CT system (100/140 keV). Scans were retrospectively reconstructed at VMI energy levels from 40 – 110 keV in 1 keV increments and were analyzed both quantitatively and qualitatively. CNR values for peritoneal metastatic deposits were recorded using region of interest (ROI) analysis at each energy level for all VMI datasets. Subjective analysis was performed by two independent, blinded fellowship-trained readers with greater than 15 years combined experience. Qualitative parameters included diagnostic acceptability, subjective noise, spatial resolution, contrast resolution.

#### RESULTS

The contrast-to-noise ratios (CNRs) for peritoneal metastatic deposits at the different VMI energy levels were compared using a one-way ANOVA with Tukey Post Test and the optimal CNR was observed at 40 keV (p < 0.0001). Qualitative parameters were compared using a Paired T Test. Subjective noise and spatial resolution was significantly better on PCI but contrast resolution was significantly better on VMI at 40 keV (p < 0.0001). Readers reported increased confidence on VMI at 40 keV compared to PCI.

## CONCLUSION

VMI reconstruction of contrast enhanced dual energy CT scans of the abdomen and pelvis at 40 keV maximizes the conspicuity of metastatic peritoneal deposits when compared with PCI.

## **CLINICAL RELEVANCE/APPLICATION**

Improved detection of peritoneal metastases will enable surgeons and oncologists to make more informed decisions regarding operative intervention and chemotherapeutic regimens.

Hepatocellular Carcinoma treated with 90Yttrium Radioembolization: Value of Tumor Stiffness Measured with MR Elastography for Assessment of Treatment Response

Monday, Nov. 28 12:45PM - 1:15PM Room: GI Community, Learning Center Station #5

# Participants

Sonja Gordic, MD, New York, NY (*Presenter*) Nothing to Disclose Jad M. Bou Ayache, MD, New York, NY (*Abstract Co-Author*) Nothing to Disclose Mathilde Wagner, MD, PhD, Paris, France (*Abstract Co-Author*) Consultant Olea Medical Paul Kennedy, MSc,PhD, New York, NY (*Abstract Co-Author*) Nothing to Disclose Cecilia Besa, MD, New York, NY (*Abstract Co-Author*) Nothing to Disclose Richard L. Ehman, MD, Rochester, MN (*Abstract Co-Author*) CEO, Resoundant, Inc; Stockholder, Resoundant, Inc; Edward Kim, MD, New York, NY (*Abstract Co-Author*) Consultant, Koninklijke Philips NV; Advisory Board, Onyx Pharmaceuticals, Inc; Advisory Board, Sterigenics International LLC Bachir Taouli, MD, New York, NY (*Abstract Co-Author*) Consultant, MEDIAN Technologies ; Grant, Guerbet SA

## PURPOSE

To correlate tumor stiffness (TS) measured with MR elastography (MRE) to degree of tumor enhancement and necrosis on contrastenhanced T1-weighted imaging (CE-T1WI) in hepatocellular carcinomas (HCC) treated with 90Yttrium radioembolization (RE).

# METHOD AND MATERIALS

This retrospective study was IRB-approved and the requirement for informed consent was waived. 22 patients (M/F 14/8, mean age 64 y) with HCC who underwent RE and 11 patients (M/F 8/3, mean age 63 y) with newly diagnosed untreated HCC were included. Liver MRI included 2D GRE MRE sequence. Mean TS values were obtained by placing regions of interest (ROIs) over HCCs on stiffness maps. Visual assessment of tumor necrosis and calculation of enhancement ratio by placing ROIs over tumors on CE-T1WI including subtracted images was performed. Data were analyzed using an independent-samples t-test and Pearson correlation.

## RESULTS

33 HCCs (mean size 3.1 cm) were evaluated. Mean TS in treated HCCs was significantly lower compared to untreated tumors ( $3.8\pm1.9$  vs.  $6.9\pm3.4$  kPa, p < 0.05). TS showed a significant negative correlation with percentage of tumor necrosis (r -0.72, p < 0.001) and a positive correlation with the enhancement ratio (r 0.64, p < 0.001).

# CONCLUSION

TS measured with MRE may potentially be used as a marker of HCC response to RE. These results need to be verified in a prospective study.

# **CLINICAL RELEVANCE/APPLICATION**

In patients with HCC, tumor stiffness measured with MRE may potentially be used as a marker of tumor necrosis after RE.

## **Honored Educators**

Presenters or authors on this event have been recognized as RSNA Honored Educators for participating in multiple qualifying educational activities. Honored Educators are invested in furthering the profession of radiology by delivering high-quality educational content in their field of study. Learn how you can become an honored educator by visiting the website at: https://www.rsna.org/Honored-Educator-Award/

Richard L. Ehman, MD - 2016 Honored Educator

## GI368-SD-MOB6

Differentiation of Neoplastic Polyp of Gallbladder from Cholesterol Polyp with High Resolution Gallbladder Ultrasound

Monday, Nov. 28 12:45PM - 1:15PM Room: GI Community, Learning Center Station #6

# Participants

Song-Ee Baek, MD, Seoul, Korea, Republic Of (*Presenter*) Nothing to Disclose Yong Eun Chung, MD, PhD, Seoul, Korea, Republic Of (*Abstract Co-Author*) Nothing to Disclose Sungwon Kim, MD, Seoul, Korea, Republic Of (*Abstract Co-Author*) Nothing to Disclose Ho Kyoung Hwang, Seoul, Korea, Republic Of (*Abstract Co-Author*) Nothing to Disclose Chang Moo Kang, Seoul, Korea, Republic Of (*Abstract Co-Author*) Nothing to Disclose Moon Jae Chung, Seoul, Korea, Republic Of (*Abstract Co-Author*) Nothing to Disclose Myeong-Jin Kim, MD, PhD, Seoul, Korea, Republic Of (*Abstract Co-Author*) Nothing to Disclose

#### PURPOSE

To evaluate the diagnostic performance of high resolution ultrasound (HRUS) of gallbladder (GB) for differentiation of neoplastic polyps from cholesterol polyps

#### **METHOD AND MATERIALS**

Between Nov 2012 and Feb 2016, pathologically confirmed GB polyps (n=108) with HRUS were included (86 cholesterol polyps and 22 neoplastic polyps including 10 adenomas and 12 carcinomas). HRUS is performed with a convex probe (1-6MHz) at first and followed with a linear probe (2-8 MHz). Two radiologists retrospectively determined image findings: multiplicity, size, layer disruption, shape (sessile, polypoid), surface contour (lobulated, smooth), echogenicity of GB wall, echotexture (homogenous, heterogeneous), presence of echogenic foci, hypoechoic internal echo and Doppler flow. To find imaging features suggesting neoplastic polyps, logistic regression and receiver operating characteristic curve analysis were used.

#### RESULTS

Mean size of polyp was  $12.1\pm7.4$  mm and there was a significant difference in size between benign ( $9.8\pm4.2$  mm) and neoplastic polyps ( $21.0\pm10.3$  mm, P<0.001). On univariate logistic regression, single, large size polyp, layer disruption, sessile shape, presence of echogenic internal echo and presence of Doppler flow were significantly associated with neoplastic polyp (P<0.05, respectively). On multivariate logistic regression, only singularity (P=0.014) and size (P=0.005) were significantly associated with neoplastic polyp. On ROC analysis neoplastic polyp could be diagnosed with sensitivity 81.8%, specificity 84.9%, accuracy 84.3%, PPV 58.1% and NPV 94.8%, using cutoff value of 13.4mm. In subgroup analysis which excluded single polyps with more than 13.4mm (n=27, including 4 neoplastic polyps), presence of hypoechoic internal echo showed statistically significance higher in neoplastic polyps at multivariate analysis (p=0.045, sensitivity 75\%, specificity 82.6%, accuracy 81.5%, PPV 42.9% and NPV 95%).

## CONCLUSION

Single, large polyps (>13.4mm) have higher malignancy potential. In the small polyps, presence of hypoechoic internal echo is the feature suggesting possibility of malignancy.

## **CLINICAL RELEVANCE/APPLICATION**

Even at the small GB polyp, if you find sessile shape, layer disruption and presence of hypoechoic internal echo in the polyp, you need to consider cholecystectomy.

## GI369-SD-MOB7

Reliability and Intra-observer Reproducibility of Liver Surface Nodularity Software for the Assessment of Cirrhosis with CT and MRI

Monday, Nov. 28 12:45PM - 1:15PM Room: GI Community, Learning Center Station #7

#### Awards

#### **Student Travel Stipend Award**

#### **Participants**

Grace C. Lo, MD, New York, NY (*Presenter*) Nothing to Disclose Cecilia Besa, MD, New York, NY (*Abstract Co-Author*) Nothing to Disclose Martin Kang, New York, NY (*Abstract Co-Author*) Nothing to Disclose Mathilde Wagner, MD, PhD, Paris, France (*Abstract Co-Author*) Consultant Olea Medical Ashley Stueck, MD, New York, NY (*Abstract Co-Author*) Nothing to Disclose Andrew D. Smith, MD, PhD, Jackson, MS (*Abstract Co-Author*) Research Grant, Pfizer Inc; President, Radiostics LLC; President, Liver Nodularity LLC; President, Color Enhanced Detection LLC; President, eMASS LLC; Pending patent, Liver Nodularity LLC; Pending patent, Color Enhanced Detection LLC; President, MEDIAN Technologies ; Grant, Guerbet SA

# PURPOSE

To assess the repeatability and reproducibility of liver surface nodularity (LSN) measurement using custom software with CT vs. MRI and to evaluate the accuracy of LSN score in diagnosing liver cirrhosis.

# METHOD AND MATERIALS

This IRB-approved retrospective study included adult patients with liver MRI and CT within 6 months of biopsy. Custom software was used to measure LSN on noncontrast CT (NCT), contrast-enhanced CT (CECT), T2-weighted HASTE images (T2 HASTE), and post-contrast T1-weighted delayed hepatobiliary phase images (T1w HBP). Measurements were made along the anterior left lobe on 2D axial images on NCT, CECT, T2 HASTE, and HBP and along the right lobe on 2D coronal images on HBP. Ten unique slices were measured for each series and averaged to generate a LSN score. Technical failure was defined as inability to measure LSN on 10 slices. Intra- and inter-observer agreement were assessed using intraclass correlation coefficient (ICC). For intra-observer assessment, one reader repeated measurements two weeks after the first session. A second independent reader was used to assess inter-observer agreement. Accuracy of LSN score for detection of cirrhosis was assessed using receiver operating characteristic analysis.

# RESULTS

A total of 27 patients (M/F 20/7, mean age 57y) with 30 MRIs, 25 NCTs, 27 CECTs, and pathology were included. 37% (10/27) had cirrhosis on histopathology. Technical failure occurred only on NCT (4%, 1/25) and T2 HASTE (30%, 9/30). Intra-observer agreement was excellent for NCT, CECT, axial T1w HBP, and coronal T1w HBP (ICC=0.982, 0.946, 0.929, 0.914) but moderate for T2W HASTE (ICC=0.451). Inter-observer agreement was good for NCT and axial and coronal T1w HBP (ICC=0.669, 0.73, 0.683), moderate for CECT (ICC=0.517), poor for T2 HASTE (ICC=0.361). On NCT and coronal T1w HBP, there was a significant difference between F0-3 versus F4 (2.9 vs. 3.82, 3.73 vs 4.56; p<0.05) with AUCs of 0.758 (NCT) and 0.804 (T1 HBP) for identifying cirrhosis.

#### CONCLUSION

Liver surface nodularity measurement is reliable with NCT and post-contrast T1w HBP on MRI, with very good intra-observer and good inter-observer reproducibility, and may be helpful in evaluating for liver cirrhosis.

#### **CLINICAL RELEVANCE/APPLICATION**

Liver surface nodularity quantified with software is a potential non-invasive marker of cirrhosis.

Role of Magnetic Resonance Imaging (MRI) in Fistula-in-ano-A MRI-Operation Correlation in 229 Consecutive Patients: Can We Decide the Indications of getting MRI in Fistula-In-Ano Patients?

Monday, Nov. 28 12:45PM - 1:15PM Room: GI Community, Learning Center Station #8

# Participants

Pankaj Garg, MBBS,MS, Mohali, India (*Abstract Co-Author*) Nothing to Disclose Pratiksha Singh, Fort Worth, TX (*Presenter*) Nothing to Disclose Prof Mohinder Kumar Garg, Khanpur Kalan, India (*Abstract Co-Author*) Nothing to Disclose

## PURPOSE

To corroborate MRI findings with operative findings in fistula-in-ano patients and quantify the information added by MRI.

## **METHOD AND MATERIALS**

All consecutive fistula-in-ano patients operated between July 2013- May 2015 were prospectively enrolled. Preoperative MRI was done in every patient. The details of tracts, internal opening and the presence of `complexing features'- additional tract or internal opening, horseshoe tract, associated abscess and supralevator extension -were correlated in MRI and operative notes.

## RESULTS

229 patients (424 tracts) were included. Mean age-  $49.0 \pm 11.3$  years. M/F- 198/31. James hospital classification: Type I-58, II-20, III-49, IV-86, V-16. The sensitivity and specificity of MRI in diagnosing fistula tracts was 98.8% and 99.7% respectively and in identifying internal opening was 97.7% and 98.6% respectively. MRI added significant information in 107 (46.7%) patients which was presence of additional tracts in 71 (66.3%), horseshoe tract in 63 (58.8%), supralevator extension in 16 (14.9%), unsuspected abscess in 11 (10.3%) and multiple internal openings in one patient (1%)[categorized as 'complexing features']. The proportion of simple/complex fistula (based on history and clinical examination alone) was 32.8/67.2% which changed to 21.4/78.6% after the MRI scan. MRI added significant information about unsuspecting 'complexing features' which were missed on history and clinical examination in more than one-third (26/75-34.6%) of simple fistulae and more than half (81/154 -52.5%) of already known complex fistulae.

## CONCLUSION

MRI is highly sensitive and specific. It adds significant information in about one-third of simple and half of complex fistula-in-ano. It should perhaps be done in all fistula-in-ano cases

# **CLINICAL RELEVANCE/APPLICATION**

This is the largest study correlating MRI findings and operation in 229 patients of fistula-in-ano. MRI added significant information (to the information already obtained on history and clinical examination) about unsuspecting 'complexing features' (additional tracts, horseshoe tracts, abscess and supralevator extension) in 46.7% patients [34.6%-simple and 52.5%-complex fistula].

## GU216-SD-MOB1

Texture Analysis as an Image-Based Discriminator between T1 Renal Cell Carcinoma and pT3 Renal Cell Carcinoma

Monday, Nov. 28 12:45PM - 1:15PM Room: GU/UR Community, Learning Center Station #1

# Participants

Chidubem G. Ugwueze, MS, Los Angeles, CA (*Abstract Co-Author*) Nothing to Disclose Megha N. Gupta, MD, Los Angeles, CA (*Abstract Co-Author*) Nothing to Disclose Darryl Hwang, PhD, Los Angeles, CA (*Abstract Co-Author*) Nothing to Disclose Steven Cen, PhD, Los Angeles, CA (*Abstract Co-Author*) Nothing to Disclose Felix Y. Yap, MD, Los Angeles, CA (*Abstract Co-Author*) Nothing to Disclose Bhushan Desai, MBBS, MS, Los Angeles, CA (*Abstract Co-Author*) Nothing to Disclose Vinay A. Duddalwar, MD, FRCR, Los Angeles, CA (*Presenter*) Nothing to Disclose Mike Kwon, BS,MS, Los Angeles, CA (*Abstract Co-Author*) Nothing to Disclose Bino Varghese, Los Angeles, CA (*Abstract Co-Author*) Nothing to Disclose

## PURPOSE

Clear cell renal cell carcinomas (ccRCC) smaller than 7 cm may be upstaged to pT3 based on imaging or histopathological evidence of vascular invasion. This study evaluated if Gray Level Co-occurrence Matrix (GLCM) textures features could differentiate between T1and pT3 tumors.

## METHOD AND MATERIALS

In this retrospective cohort study, Computerized Tomography (CT) images 8 patients with pT3 RCC and 21 patients with T1 RCC tumors were extracted using semi-automated segmentation on Synapse 3D (Fujifilm, Stamford, CT). Two and three dimensional GLCM calculations were performed on each tumor. These calculations, 2D and 3D respectively, extracted thirteen GLCM features: mean gray value (MGV), standard deviation (SD), inverse difference moment (IDM), difference variance (DV), entropy (ENT), contrast (CON), sum of squares variance (SQV), sum entropy (SE), sum average (SA), angular second moment (ASM), Correlation (COR), information measures of correlation1 (IMC1), and IMC2. Descriptive analyses based on ttest or Wilcoxon Rank Sum test, depending on data distribution and with box whisker plot were used to illustrate the difference in imaging parameter between patient categories.

#### RESULTS

GLCM Calculations were technically successful for all cases. Features extracted in 2D found significant differences, p < 0.01, between the two groups: MCC in all four phases (see figure) and ASM (0.02 vs 0.01), HOM (0.43 vs 0.36), CON (7.94 vs 6.05), and uniformity (0.12 vs 0.15) in the nephrographic phase. 3D features did not find significant differences between the two groups on all phases and texture features.

## CONCLUSION

Five image texture features may help distinguish between T1 and pT3 Clear Cell RCC tumors with the nephrographic venous phase being of high importance for the discrimination.

## **CLINICAL RELEVANCE/APPLICATION**

Quantitative texture metrics can distinguish between tumors with different biologic behavior with potential to allow for image-based patients' risk stratification.

## GU217-SD-MOB2

Diagnostic Utility of MR Biomarkers Derived from Fat-suppressed T1-weighted 3D Gradient-echo Imaging in Distinguishing Malignant from Benign Solid Renal Tumors and Subtyping of Renal Cell Carcinoma

Monday, Nov. 28 12:45PM - 1:15PM Room: GU/UR Community, Learning Center Station #2

## Participants

David D. Childs, MD, Clemmons, NC (*Presenter*) Nothing to Disclose Jennings Clingan, MD, Winston Salem, NC (*Abstract Co-Author*) Nothing to Disclose Ronald J. Zagoria, MD, San Francisco, CA (*Abstract Co-Author*) Nothing to Disclose Jose Sirintrapun, MD, New York, NY (*Abstract Co-Author*) Nothing to Disclose Rafel Tappouni, MBBCh, FRCPC, Winston-Salem, NC (*Abstract Co-Author*) Nothing to Disclose Andrea Anderson, MS, Winston Salem, NC (*Abstract Co-Author*) Nothing to Disclose John R. Leyendecker, MD, Dallas, TX (*Abstract Co-Author*) Nothing to Disclose

#### PURPOSE

To assess the ability of MR biomarkers derived from fat-suppressed T1-weighted 3D gradient-echo (3D T1 GRE) imaging to discriminate benign from malignant lesions, as well as subtypes of renal cell carcinoma (RCC) from one other, among a cohort of pathologically confirmed solid renal masses.

## **METHOD AND MATERIALS**

The cohort consisted of 291 renal masses (245 RCC, 5 non-RCC malignant, 41 benign lesions) in 267 patients. For the qualitative portion, 3D T1 GRE sequences were independently reviewed by 2 radiologists who were blinded to additional imaging or patient data. Lesions were visually examined for internal T1 hyperintense foci (defined as discrete nonhomogeneous foci greater in signal than normal renal cortex). For the quantitative portion, a single radiologist measured lesion-to-cortex ratios (T1 ratio) via averaged regions of interest. Univariate logistic regression was used to assess the ability of each variable to predict malignancy and RCC subtype. Odds ratios (OR), AUC statistics, and 95% confidence intervals for each variable were also calculated. For the qualitative variable, inter-observer agreement was measured with the Kappa coefficient.

## RESULTS

Intra-lesion T1 hyperintense foci were significantly predictive of malignancy, with an OR of 5.912 (95% CI, 1.762-19.839, P=0.004) and AUC of 0.6331 (95% CI, 0.5785-0.6878). Inter-observer agreement was good, with a Kappa coefficient of 0.7136. A higher T1 ratio was also significantly predictive of malignancy, with an OR of 10.691 (95% CI, 1.749-65.359, P=0.0103) and AUC of 0.6110 (95% CI, 0.5194-0.7026). While a higher T1 ratio was predictive of papillary RCC (pRCC) over clear cell RCC (ccRCC) (Odds ratio=4.14, 95% CI 1.348-12.717, P=0.0131), T1 hyperintense foci were not helpful in differentiating RCC subtypes.

# CONCLUSION

Both T1 hyperintense intra-lesion foci and a high lesion-to-cortex T1 signal ratio are significantly predictive of malignancy in this cohort of solid renal masses, with good inter-observer agreement. Additionally, a higher T1 signal ratio is also predictive of the pRCC over the ccRCC subtype.

## **CLINICAL RELEVANCE/APPLICATION**

Image features derived from T2-weighted, chemical shift, dynamic post-contrast, and diffusion weighted imaging have been shown to be useful in the characterization of solid renal tumor histology. 2 additional useful biomarkers can also be obtained from fat-suppressed 3D T1 GRE imaging, which is already included in routine clinical protocols.

Clear Cell Renal Cell Carcinoma: Discrimination from Chromophobe RCC and Papillary on MDCT using CAD Derived Peak Lesion Enhancement Relative to Renal Cortex

Monday, Nov. 28 12:45PM - 1:15PM Room: GU/UR Community, Learning Center Station #4

## Participants

Heidi Coy, Los Angeles, CA (*Presenter*) Nothing to Disclose Jonathan R. Young, MD, Los Angeles, CA (*Abstract Co-Author*) Nothing to Disclose Michael L. Douek, MD, MBA, Los Angeles, CA (*Abstract Co-Author*) Nothing to Disclose Matthew S. Brown, PhD, Los Angeles, CA (*Abstract Co-Author*) Nothing to Disclose James Sayre, PhD, Los Angeles, CA (*Abstract Co-Author*) Nothing to Disclose Steven S. Raman, MD, Santa Monica, CA (*Abstract Co-Author*) Nothing to Disclose

## PURPOSE

Currently, all solid enhancing renal lesions without macroscopic fat are treated as malignant. Renal cell carcinoma (RCC) subtypes are a heterogeneous group treated by surgery, ablation or active surveillance with a prognosis based on histology, with clear cell RCC (ccRCC) having the highest incidence and metastatic potential. The purpose of our study is to determine if relative enhancement derived from volumetric 3D lesion contour and a Computer Aided Diagnostic (CAD) algorithm to derive lesion enhancement relative to uninvolved renal cortex can discriminate ccRCC from RCC subtypes (chromophobe RCC (chrRCC) and papillary RCC (pRCC)) on four phase MDCT.

## **METHOD AND MATERIALS**

With IRB approval for this HIPAA-compliant retrospective study, we queried our clinical databases to obtain a cohort of histologically proven renal masses with preoperative MDCT with four phases (unenhanced, corticomedullary (CM), nephrographic (NP), and excretory (EX)). The lesion was segmented in each phase. A CAD algorithm selected a 0.5cm region of interest (ROI) of peak lesion enhancement  $\leq$ 300HU within the 3D lesion contour. A 0.5cm ROI was placed in normal renal cortex. A radiologist approved lesion contours and ROI placement. Relative enhancement (RE) was calculated as: (lesion ROI-cortex ROI)/ (cortex ROI)\* 100%). A model was derived using logistical regression with RE of ccRCC, Onc, and fpAML as input. Discrimination was evaluated using receiver operator characteristic (ROC) curves.

#### RESULTS

165 patients (69% men, 31% women) with 168 unique renal masses (105 (63%) ccRCC, 18 (11%) chRCC, 45 (27%) pPRCC were analyzed. Mean lesion size in ccRCC = 3.1 cm (range 1.8-6.5), chRCC=2.5 cm (range 0.8-6.0, and pRCC=3.1 cm (range 1.1-6.8). In discriminating ccRCC from chRCC, the model had an AUC of 0.846 (0.735-0.957 95% CI) in the CM phase, 0.827 (0.718-0.937 95% CI) in the NP phase, and 0.848 (0.765-0.937 95% CI) in the EX phase. In discriminating ccRCC from pRCC, the model had an AUC of 0.958 (0.929-0.986 95% CI) in the CM phase, 0.844 (0.773-0.914 95% CI) in the NP phase, and 0.805 (0.725-0.884 95% CI) in the EX phase.

## CONCLUSION

RE in the CM phase helps discriminate chRCC from ccRCC with an AUC of 0.846 and pRCC from ccRCC with an AUC of 0.958.

## **CLINICAL RELEVANCE/APPLICATION**

CAD derived RE provides an objective and reproducible measure for the clinician to use when stratifying patients to specific therapeutic pathways, helping to ensure optimal patient outcomes.

A Comparative Study between the use of Transvaginal Ultrasound (TVUS) and Saline Infusion Sonohysterogram (SIS) for Diagnosis of Endometrial Polyps

Monday, Nov. 28 12:45PM - 1:15PM Room: GU/UR Community, Learning Center Station #5

#### Awards

## **Student Travel Stipend Award**

#### Participants

Shaimaa A. Fadl, MD, Seattle, WA (Presenter) Nothing to Disclose

Ahmed S. Sabry, MD, Doha, Qatar (Abstract Co-Author) Nothing to Disclose

Daniel S. Hippe, MS, Seattle, WA (*Abstract Co-Author*) Research Grant, Koninklijke Philips NV; Research Grant, General Electric Company

Amal Al Obadli, Doha, Qatar (Abstract Co-Author) Nothing to Disclose

Theodore J. Dubinsky, MD, Seattle, WA (Abstract Co-Author) Stockholder, Global Cancer Technology; Grant, Toshiba Corporation

# PURPOSE

To determine the level of confidence in detecting endometrial polyps on TVUS in patients with abnormal uterine bleeding or infertility and to determine if SIS is necessary when the level of confidence is high.

## **METHOD AND MATERIALS**

A retrospective study of 152 consecutive patients who underwent both TVUS and SIS for evaluation of abnormal uterine bleeding and infertility. TVUS images were obtained by Philips and GE machines and were reviewed by two independent observers who were blinded to the outcome. For each patient, a grade was given for the diagnosis of endometrial polyp. Grade 0: Negative for polyp, Grade: I when the diagnosis of polyp is equivocal and grade II positive for polyp. SIS was performed within three months using GE, Voluson E8. The imaging criteria included for the diagnosis of polyps are: well circumscribed echogenic lesion, stalk flaw pattern, the presence of cysts in an endometrial echogenic lesion. The results of the TVUS were compared with that of the SIS and then correlated with the hysteroscopy results which were considered the gold standard for the final diagnosis. Statistical analysis was performed. Confidence intervals were computed using generalized estimating equations to account for repeated measurements per patient.

#### RESULTS

152 patients who underwent both TVUS and SIS were selected. Seven patients were excluded for having non-diagnostic TVUS images by at least one reader, leaving 145 for analysis. From the combined assessments of both readers, 47% were negative for polyps by TVUS, 28% equivocal, and 25% positive. Inter-reader agreement was good with Cohen's kappa = 0.67 (95% CI: 0.57-0.77). SIS has greater sensitivity (p<0.001) and specificity (p=0.03) than TVUS when grade II polyp diagnosis was considered, however SIS and TVUS have similar sensitivity in cases when grade I and grade II polyp diagnosis is considered by TVUS.

## CONCLUSION

When confidence is high that a polyp is present or absent on TVUS, SIS is not necessary to confirm their presence. Indeterminate or equivocal cases still benefit from SIS to confirm that a polyp is indeed present or absent.

# **CLINICAL RELEVANCE/APPLICATION**

TVUS is of high enough sensitivity and specificity, equal to that of SIS such that when confidence is high that TVUS is positive or negative, SIS is not necessary to confirm the findings on TVUS prior to hysteroscopy. However when the findings are equivocal, SIS adds to diagnostic confidence significantly.

#### **Honored Educators**

Presenters or authors on this event have been recognized as RSNA Honored Educators for participating in multiple qualifying educational activities. Honored Educators are invested in furthering the profession of radiology by delivering high-quality educational content in their field of study. Learn how you can become an honored educator by visiting the website at: https://www.rsna.org/Honored-Educator-Award/

Theodore J. Dubinsky, MD - 2012 Honored Educator Theodore J. Dubinsky, MD - 2013 Honored Educator

# GU221-SD-MOB6

## Diffusion-weighted Imaging in the Bladder: A Comparison between iShim, Resolve and SS-EPI at 3T

Monday, Nov. 28 12:45PM - 1:15PM Room: GU/UR Community, Learning Center Station #6

#### **Participants**

hongyi li, Changchun, China (*Abstract Co-Author*) Nothing to Disclose Mengchao Zhang, Changchun, China (*Presenter*) Nothing to Disclose Hong Zeng, MD, PhD, Changchun, China (*Abstract Co-Author*) Nothing to Disclose Qinglei Shi, Beijing, China (*Abstract Co-Author*) Nothing to Disclose Tianyi Qian, PhD, Beijing, China (*Abstract Co-Author*) Nothing to Disclose Lin Liu, Changchun, China (*Abstract Co-Author*) Nothing to Disclose

# PURPOSE

To evaluate the image quality of diffusion-weighted imaging in the bladder acquired using a prototype iShim readout segmentation of long variable echo trains (RESOLVE) and conventional single-shot echo-planar-imaging (SS-EPI) sequences at 3T.

## METHOD AND MATERIALS

Twenty patients (17 males age 62±3.52) with focal bladder lesions and ten healthy volunteers (18 males, age 35±4.23) were enrolled and underwent diffusion-weighted imaging MR exam of the bladder. The protocol included routine MR exam and three types of DWI sequences, including: Siemens prototype iShim, RESOLVE and SS-EPI on a 3T MR scanner (MAGNETOM Skyra, Siemens AG, Erlangen, Germany,Table1). The signal-to-noise ratio (SNR), contrast-to-noise ratio (CNR), and ADC values of gluteus maximus muscle were measured. The coefficients of variances of ADC were calculated. To evaluate the distortion of images obtained using different sequences, the distance between the anatomical marker on T2W TSE and b=0 maps were defined as the distorted distance (DD). Finally, the degree of distortion, the efficiency of fat saturation and overall image quality were independently scored by two radiologists with 10+ years experience. All the quantitative and qualitative parameters were analyzed with one-way ANOVA and Kruskal-Wallis techniques. One-way ANOVA was applied for group comparison with Bonferroni correction.

## RESULTS

The SNR and CNR of iShim ( $54.18\pm24.84$ ,  $42.04\pm22.81$ ) were higher than RESOLVE ( $24.14\pm11.93$ , p<0.01;  $28.30\pm11.67$ , p<0.01) and SS-EPI ( $50.36\pm28.30$ , p=0.02;  $39.55\pm26.57$ , p=0.01). The iShim's distortions were larger than RESOLVE but smaller than SS-EPI. The subjective evaluation score of iShim in fat saturation efficiency and overall image quality were higher than RESOLVE and SS-EPI. The coefficient of variation of iShim was the lowest, and significant difference was found between SS-EPI and iShim sequences. No significant difference was found between ADC values measured with the different sequences.

## CONCLUSION

The iShim sequence shows better performances than RESOLVE and SS-EPI in the DWI exam of the bladder. It has the best image quality, fat saturation efficiency, SNR and CNR, and reproducibility of ADC. It could also reduce the susceptibility artifacts and distortions compared to SS-EPI.

# **CLINICAL RELEVANCE/APPLICATION**

The iShim sequence shows better performances in bladder DWI exam and this exam is recommended to make the diagnosis of bladder cancer more accurate.

 $zFij_{2}^{1/2}ij_{2}^{1/2}2ij_{2}^{1/2}gij_{2}^{1/2}$ 

## Reviewing the Reviewers: The Timeliness of Peer Review in Radiology Journals

Monday, Nov. 28 12:45PM - 1:15PM Room: HP Community, Learning Center Station #1

#### Awards

#### **Student Travel Stipend Award**

#### **Participants**

Kip Guja, PhD, Stony Brook University, NY (*Presenter*) Nothing to Disclose Anuradha Janardhanan, MBBS, Ampang, Malaysia (*Abstract Co-Author*) Nothing to Disclose Jann Stavro, Stony Brook, NY (*Abstract Co-Author*) Nothing to Disclose Mauricio Castillo, MD, Chapel Hill, NC (*Abstract Co-Author*) Nothing to Disclose Mark E. Schweitzer, MD, Stony Brook, NY (*Abstract Co-Author*) Consultant, MMI Munich Medical International GmbH Data Safety Monitoring Board, Histogenics Corporation

#### PURPOSE

Timeliness is an important attribute of scholarly peer review because it allows new evidence to become promptly available to readers, and lack thereof is thought to contribute to longer publication cycle times. Hence, we sought to identify patterns among late reviewers.

## **METHOD AND MATERIALS**

We analyzed 17,404 editorial requests for manuscript peer review sent from Radiology (RSNA), JMRI, and AJNR from July 2013 to June 2015. Data were obtained directly from the editorial staff of the journals and analyzed in Scholar One, a web-based peer review tool. Reviewers were classified as on-time or late based on compliance with the 14-day window provided. Each review was quality scored independently, and these scores were correlated with reviewer seniority, geographic location, and reviewer frequency.

## RESULTS

During the two-year period analyzed, 3,251, 4,055, and 10,096 peer reviews were submitted to JMRI, AJNR, and RSNA, respectively. Of those, 36%, 37%, and 26% were submitted late. Nearly half of the late reviews were overdue by 1-3 days (41% in JMRI, 44% in AJNR, and 53% in RSNA). Only 1% of the reviews submitted to RSNA and AJNR were overdue by two weeks or more, but that figure rose to nearly 9% for the JMRI reviews. However, there was no statistically significant difference in score between JMRI reviews that were on-time when compared to those that were two weeks late or more. Interestingly, reviewer scores in RSNA tended to worsen with lateness, such that the on time average was 1.0 vs 1.7 (higher is inferior) for reviews that were two weeks late or more. A similar trend was seen in AJNR, where the on-time average was 2.73 vs 2.53 (lower is inferior) for late reviews. Reviewers from the US or Europe are nearly twice as likely to be late (40%) as compared to reviewers from other parts of the world (25%).

# CONCLUSION

The study shows that over a two-year period, more than 25% of peer reviews were submitted late, and a significant portion of the late submissions were overdue by more than 7 days. Late reviews were associated with worse scores, smaller journals, and reviewers from either the US or Europe.

## **CLINICAL RELEVANCE/APPLICATION**

Rigorous and timely peer review is vitally important, as highlighted by growing concern over the reproducibility of research. Lack of timely peer review is a common problem in radiological journals.

# HP212-SD-MOB2

# Beyond Reading Images: A National Survey of Radiology Residents' Study Habits

Monday, Nov. 28 12:45PM - 1:15PM Room: HP Community, Learning Center Station #2

#### **Participants**

Fadi Toonsi, MBBS,FRCPC, Montreal, QC (*Presenter*) Nothing to Disclose Wid Kattan, MBBS, MA, Montreal, QC (*Abstract Co-Author*) Nothing to Disclose Fahad Essbaiheen, MBBS,FRCPC, Ottawa, ON (*Abstract Co-Author*) Nothing to Disclose Jeffrey Chankowsky, MD, Montreal West, QC (*Abstract Co-Author*) Nothing to Disclose

# PURPOSE

Our goal was to identify study habits of radiology residents across the country's residency training programs and to rank their top reading resources.

#### **METHOD AND MATERIALS**

An online survey investigating various study habits was distributed to residents in 11 university-based radiology programs. The survey was adopted from the literature and designed to measure study habits unique to radiology residency. 263 residents were emailed. 80 responded (30% response rate). Two responses were excluded, one was in the internship year and the other did not specify residency level.

# RESULTS

Outside working hours, the mean number of hours spent studying per week was 11 (min 2 max 50, standard deviation 8.6).Recommended reading lists provided by other/senior residents were considered important in guiding 70 % of respondents' reading, while only 23% of residents depended on lists provided by their departments. None depended on the ACR recommended readings lists.54% of residents had specific reading goals in terms of material to cover during the year. Only 32% of them covered more than 40% of this material.43% of residents decided upon a radiology textbook. Selected textbooks were Fundamentals of Diagnostic Radiology (59%), Primer of Diagnostic Imaging (26%), Diagnostic Imaging series and STATdx (9%) and the Radiology Review Manual (6%).Textbooks were most ranked as the top educative source for radiology reading (39%), followed by case-based books (24%) then the online website STATdx (20%).Radiographics was considered an important study source by 87% of residents, Radiology by 56%, The American Journal of Radiology by 44%, The Journal of American College of Radiology by 10%.83% of residents try to keep daily reading relevant to the rotation they are doing and 88% try to read about pathologies they encounter in daily work.

#### CONCLUSION

Radiology residents tend to follow a pattern of reading habits and focus their readings to specific resources. Most residents follow recommendations from each other on what and where to read from.

#### **CLINICAL RELEVANCE/APPLICATION**

Identifying study habits and most used radiology resources can guide new residents to trusted reading sources, saving them time and money. Our survey could potentially be used for detection and eventual guidance of low-performing residents.

## **Patient-specific Management of Adrenal Incidentalomas**

Monday, Nov. 28 12:45PM - 1:15PM Room: HP Community, Learning Center Station #3

#### Participants

Romy R. de Haan, BSC, Rotterdam, Netherlands (*Abstract Co-Author*) Nothing to Disclose Johannes B. Visser, MSc, Eindhoven, Netherlands (*Abstract Co-Author*) Nothing to Disclose Ewoud Pons, MD, Rotterdam, Netherlands (*Abstract Co-Author*) Nothing to Disclose Richard A. Feelders, MD, PhD, Rotterdam, Netherlands (*Abstract Co-Author*) Nothing to Disclose Ewout W. Steyerberg, Rotterdam, Netherlands (*Abstract Co-Author*) Nothing to Disclose Uzay Kaymak, PhD, Eindhoven, Netherlands (*Abstract Co-Author*) Nothing to Disclose M.G. Myriam Hunink, MD, PhD, Rotterdam, Netherlands (*Abstract Co-Author*) Nothing to Disclose Jacob J. Visser, MD, PhD, Rotterdam, Netherlands (*Presenter*) Nothing to Disclose

# PURPOSE

To develop a clinical prediction model to predict a clinically relevant outcome for patients with adrenal incidentaloma.

## **METHOD AND MATERIALS**

This retrospective study was approved by the institutional review board, with waiver of informed consent. Natural language processing was used for filtering of potential adrenal incidentaloma cases in all thoracic and abdominal CT reports from 2010 till 2012. A total of 635 patients, with initial presentation or follow-up imaging for adrenal incidentaloma during this period, were identified. Demographical data, the radiological characteristics of the lesion, values of biochemical evaluation, and patient outcome were all recorded. Stepwise logistic regression was used to construct the prediction model. The model predicts at the presentation of an adrenal incidentaloma if a patient is at risk for malignancy or hormonal hyperfunction of the adrenal gland, thus generates a predicted probability for every individual patient. The prediction model was evaluated on its usefulness in clinical practice using decision curve analysis based on different threshold probabilities. For patients whose predicted probability is lower than the predetermined threshold probability, treatment can be omitted. Patient outcomes were verified with the nationwide network and registry of histo- and cytopathology in the Netherlands (PALGA).

#### RESULTS

A prediction model was successfully developed, with an area under the curve (AUC) of 0,76 on both the training and validation data. Unnecessary diagnostic work-up was avoided in 7% of patients with an adrenal incidentaloma by using a threshold probability of 1,5% on the validation data. The sensitivity of the decision curve analysis was 100% and specificity was 7%. By increasing the threshold probability to 2%, unnecessary diagnostic work-up was avoided in 23% of the patients, but clinically relevant patients were missed. The sensitivity and specificity were 90% and 24%.

# CONCLUSION

Using a prediction model for predicting a clinically relevant outcome of adrenal incidentalomas is an effective solution for saving patients from unnecessary diagnostics. Hereby, management of this growing patient group can be tailored to the individual patient.

## **CLINICAL RELEVANCE/APPLICATION**

Our predicition model enables both radiologists and referring physicians to reduce unnessary work-up for adrenal incidentaloma.

# Repeat Head CT Imaging in the Emergency Department: Are We Over Utilizing?

Monday, Nov. 28 12:45PM - 1:15PM Room: HP Community, Learning Center Station #4

#### Participants

Gelareh Sadigh, MD, Atlanta, GA (*Presenter*) Nothing to Disclose Nadja Kadom, MD, Boston, MA (*Abstract Co-Author*) Nothing to Disclose Richard Duszak JR, MD, Atlanta, GA (*Abstract Co-Author*) Nothing to Disclose

## PURPOSE

Unnecessary medical services, including the repetition of medical tests, has been estimated to contribute to \$210B healthcare costs annually. The purpose of this study was to quantify repeat head CT imaging rates for repeat patient visits for similar clinical indications.

# METHOD AND MATERIALS

Our clinical data warehouse was retrospectively queried for all patients 18 years or older who underwent a head CT examination within 24 hours (h) of an emergency department (ED) visit at any of our health system's four hospitals during 2014 (index enrollment). All head CT scans performed prior to and after the index enrollment and associated ICD-9 codes were obtained. Our primary outcome measure was the rate of repeat head CT imaging (defined as any head CT obtained on the same patient before or after index enrollment in 2014). We assessed rates of repeat head CT by ICD-9 code category.

## RESULTS

In 2014, 1,259 patients who visited one of our health system ED underwent a head CT examination within 24h of their encounter. These patients underwent a total of 1,673 head CT examination during any encounter before or after index enrollment that year. 27.4% (345/1,259) of patients underwent 414 repeat head CTs in addition to their initial head CTs (total of 759 head CTs) with an overall repeat imaging rate of 24.7% (414/1,673). Repeatedly imaged patients underwent between 2 - 5 scans. In repeatedly imaged patients, the most common ICD codes for initial and repeat head CT scans were head injury (26.7%; 203/759), headache (14.8%; 113/759), altered mental status, dizziness, or syncope (9.7%; 74/759) and convulsion or epilepsy (5.2%; 40/759).

# CONCLUSION

At least a quarter of head CT examinations in the ED setting result in a repeat study during the same year, with the majority being trauma related. In non-trauma patients, headache, altered mental status, and convulsion are the most common ICD-9 codes associated with repeat imaging.

# **CLINICAL RELEVANCE/APPLICATION**

A substantial number of patients in the ED setting undergoing head CT imaging undergo at least one additional examination for a similar indication during another ED visit within one year.

# HP215-SD-MOB5

## Tuberculosis Screening in Asylum Seekers during Germany's Migrant Crisis: A Single Center Experience

Monday, Nov. 28 12:45PM - 1:15PM Room: HP Community, Learning Center Station #5

#### **Participants**

Michael Kostrzewa, MD, Mannheim, Germany (*Presenter*) Institutional research agreement, Siemens AG Anja M. Weidner, MD, Mannheim, Germany (*Abstract Co-Author*) Nothing to Disclose Erika Buchholz, Mannheim, Germany (*Abstract Co-Author*) Nothing to Disclose Thomas Henzler, MD, Mannheim, Germany (*Abstract Co-Author*) Research support, Siemens AG; Speaker, Siemens AG Stefan O. Schoenberg, MD, PhD, Mannheim, Germany (*Abstract Co-Author*) Institutional research agreement, Siemens AG Gerald Weisser, MD, PhD, Mannheim, Germany (*Abstract Co-Author*) Institutional Grant support, Apple Inc

## PURPOSE

Europe's migrant crisis has posed a multitude of challenges, especially to the health care systems. We report on our experiences and outcomes after 15 months of screening for tuberculosis (TB) and present an overview of our adopted workflow and findings.

# METHOD AND MATERIALS

The German law for asylum seekers defines the following screening algorithm: asylum seekers older than 15 years, not pregnant, living in a camp, have to accept a medical investigation for infectious diseases including one x-ray of the chest. From September 2014 until December 2015 all asylum seekers referred to our University Medical Center from two reception camps (Mannheim and Darmstadt) were included in this retrospective study. Screening consisted of a chest x-ray in one plane posterior-anterior. In case of abnormal findings a low dose chest computed tomography (CT) without contrast medium was performed. Patients with suspicious findings for infectious disease on CT were then admitted to our ward for infectious diseases for further diagnostic workup and therapy if necessary.

# RESULTS

In total, 7238 asylum seekers were screened (1043 female, 6195 male, mean age 28y). Most frequent countries of origin were Syria (1577), Gambia (1063) and Iraq (572). It has to be noted that reception camps are assigned asylum seekers of a certain origin, thus our patient cohort is not representative of the whole asylum seeker collective in Germany. In 79 cases (1.1%) findings suspicious of an acute TB infection triggered a chest CT. CT confirmed a suspected acute TB infection in 34 patients (0.47%), which was proven positive by further laboratory tests in 16 patients (0.22%, 2 female, 14 male, mean age 26y). In 28 patients (0.39%) CT findings were compatible with an old TB infection, 9 (0.12%) presented with other findings (e.g. atelectasis, old lobar pneumonia, interstitial lung disease) and 8 CTs (0.11%) showed no appreciable disease.

## CONCLUSION

In our cohort of 7238 asylum seekers the prevalence of acute TB of 0.22% was lower when compared to the current literature. We assume, that the low prevalence is due to preselection of people who flee from their countries (younger, well educated, healthier) and a preselection of countries.

# **CLINICAL RELEVANCE/APPLICATION**

Due to the European migrant crisis TB screening and prevalence among asylum seekers has a high impact on the German health care system.

Exact Mapping of Medical Images Inside a Patient Body Using Three-Dimensional Printing Surgical Guides: Evaluation for Guiding Breast Cancer Margin

Monday, Nov. 28 12:45PM - 1:15PM Room: IN Community, Learning Center Custom Application Computer Demonstration

# Participants

Sang-Wook Lee, BS, Seoul, Korea, Republic Of (*Presenter*) Nothing to Disclose Guk Bae Kim, Seoul, Korea, Republic Of (*Abstract Co-Author*) Nothing to Disclose Beom Seok Ko, Seoul, Korea, Republic Of (*Abstract Co-Author*) Nothing to Disclose Jongwon Lee, MD, Export, PA (*Abstract Co-Author*) Nothing to Disclose Sei Hyun Ahn, Seoul, Korea, Republic Of (*Abstract Co-Author*) Nothing to Disclose Namkug Kim, PhD, Seoul, Korea, Republic Of (*Abstract Co-Author*) Stockholder, Coreline Soft, Inc

## CONCLUSION

The surgical guide for breast cancer resection using 3DP could be used for more exact and conserving surgery. This quantitative mapping of MRI information into a patient body lets surgeons securing tumors' surgical margin, and promises shorter operation time and convenience as well.

#### FIGURE

http://abstract.rsna.org/uploads/2016/16012109/16012109\_elln.jpg

#### Background

Partial resection of breast cancer recently has been achieved even though a tumor size is relatively small. To identify the cancer position, a method of clip or h-wire with ultrasonography has been usually provided, but it causes patient's pain as well as cost. In addition, no exact guidance for cancer margin makes surgeons determine relatively larger surgical exclusion. However, it would be subjective. Therefore, the objective of this study is developing a patient-specific three-dimensional printing (3DP) surgical guide enabling quantitatively to map cancer margin on a patient body and evaluating its clinical usage.

#### **Evaluation**

From MRI images, morphological shapes of breasts and tumors were modelled (Fig. 1A and 1B). The surgical margin including safety area was designed, and then the margin was projected onto the surgical guiding surface, fitting to the breast surface. Here, morphology of breast and nipple became landmarks for tailored guidance. We proposed two types of surgical guides including a skin marking type (Fig. 1C and fig. 2A) to enable drawing a line on skin and a hybrid type (Fig. 2B) providing a guide line on skin and columns for guiding dye-injections into tissue, which had each different lengths for needle targeting on the exact surgical margin indepth. The prepared models was saved in STL format and then exported to a 3D printer. The manufactured surgical guide was used in operation room after the sterilization.

#### Discussion

Four patients enrolled from December 2015 to January 2016. Median age was 46.5 years. After surgery using the developed surgical guide, the distances from the tumor to the margins were measured. Pathological complete remission occurred in two patients. All patients had clear resection margins (Fig 2C). The median distance from the tumor to the margins was 1.2 cm.

Web Browser Based Cloud System for Generating and Sharing 3D Models for 3D Printing with Workflow Management, Hybrid Visualization and Mobile Interfaces in Hospital

Monday, Nov. 28 12:45PM - 1:15PM Room: IN Community, Learning Center Custom Application Computer Demonstration

# Participants

Namkug Kim, PhD, Seoul, Korea, Republic Of (*Abstract Co-Author*) Stockholder, Coreline Soft, Inc Jaeyoun Yi, Seoul, Korea, Republic Of (*Presenter*) Officer, Coreline Soft Inc Semyeong Jang, Seoul, Korea, Republic Of (*Abstract Co-Author*) Nothing to Disclose Guk Bae Kim, Seoul, Korea, Republic Of (*Abstract Co-Author*) Nothing to Disclose Haekang Kim, Seoul, Korea, Republic Of (*Abstract Co-Author*) Nothing to Disclose Sang-Wook Lee, BS, Seoul, Korea, Republic Of (*Abstract Co-Author*) Nothing to Disclose Joon Beom Seo, MD, PhD, Seoul, Korea, Republic Of (*Abstract Co-Author*) Nothing to Disclose

## CONCLUSION

We developed web browser based cloud system for generating and sharing 3D models for 3D printing for collaborations among image processing specialists, radiographer, radiologist, physician, patients, and operation room staffs

## FIGURE

http://abstract.rsna.org/uploads/2016/16015490/16015490\_rsbl.jpg

#### Background

Three dimensional modeling for 3D printing needs very complicated communication workflow and collaborations among image processing specialists, radiographer, radiologist, physician, patients, and operation room staffs. Especially, 3D visualization of models is not easy in conventional communication environment including e-mail, chatting program, etc. Therefore, it is very important to develop web browser based cloud system from production to sharing of 3D models for 3D printing.

#### **Evaluation**

For workflow of 3D modelling and printing, many collaborators with diverse specialties including image processing specialists, radiographer, radiologist, physician, patients, and operation room staffs needs to be involved and collaborated in synchronous and/or asynchronous manner. For effective communication and collaboration in clinical environment, a platform to support and manage the 3D model data workflow is needed with new technical features including web based cloud system, hybrid rendering (surface and volume rendering) and mobile interface. In addition, advanced techniques for semi-automatic image segmentation including graph cut and volume sculpt and mutil-atlas based segmentation. For 3D modelling with different modalities including MRI, multiphase CT, etc, various registrations including level-set based, optical flow based, b-spline based registrations were implemented. Workflow including 3D models generated by image processing specialists and radiographer, confirmed by radiologist and physician, shared with patient and operation room staffs is flexibly defined and managed by this could system. Measurements (x-axis, y-axis, a-axis, volume) of eight patient-specific kidneys by this system are 61.87±4.56mm, 120.64±9.03 mm, 55.38±10.62 mm, 226.45±67.95 cm3, respectively.

## Discussion

For communication and collaborations, there should be a platform to support and manage the 3D model data workflow and collaboration in the real clinical environment in effective manner.

# Deep Learning: A Primer for Radiologists

Monday, Nov. 28 12:45PM - 1:15PM Room: IN Community, Learning Center Station #7

**FDA** Discussions may include off-label uses.

## Awards Cum Laude Identified for RadioGraphics

#### **Participants**

Gabriel Chartrand, BEng, Montreal, QC (*Presenter*) Research intern, Imagia Cybernetics Inc Eugene Vorontsov, Montreal, QC (*Abstract Co-Author*) Intern, Imagia Cybernetics Inc Mathieu Flamand, Montreal, QC (*Abstract Co-Author*) Nothing to Disclose Simon Turcotte, Montreal, QC (*Abstract Co-Author*) Nothing to Disclose Christopher Pal, PhD, Montreal, QC (*Abstract Co-Author*) Nothing to Disclose Samuel Kadoury, Montreal, QC (*Abstract Co-Author*) Nothing to Disclose An Tang, MD, Montreal, QC (*Abstract Co-Author*) Advisory Board, Imagia Cybernetics Inc

#### **TEACHING POINTS**

1. To review the key concepts of deep convolutional neural networks (DCNN), an artificial intelligence technique2. To illustrate applications of deep learning techniques for lesion detection, classification, and monitoring3. To discuss the potential benefits of computer assisted diagnosis with deep learning techniques

## TABLE OF CONTENTS/OUTLINE

-Clinical applications: lesion detection, segmentation, classification, image interpretation, prioritization and monitoring.-Classification of computer vision techniques: deformable models (active contour, level-set, statistical shape models), graph-cut, machine learning (support vector machines, random forest algorithms, deep learning).-Comparison: advantages and limitations of each computer vision technique.-Illustration of key ideas behind neural networks: biological inspiration, artificial neural networks, hidden layers, learning process.-Illustration of key concepts of deep learning: multiple stacked layers, convolution applied to images, pooling, activation functions.-Technical requirements: supervised (labelled), semi-supervised and unsupervised learning; training dataset; hardware (GPU).-Pitfalls: size of training dataset, quality of ground truth, spectrum of disease, architecture of neural network.-Future directions: natural language processing, caption generation.

## IN210-SD-MOB1

Performance Assessment of Data-driven Imaging Biomarker for Screening Pulmonary Tuberculosis on Chest Radiographs

Monday, Nov. 28 12:45PM - 1:15PM Room: IN Community, Learning Center Station #1

# Participants

Hee Jin Kim, MD, Cheongju-si, Korea, Republic Of (*Abstract Co-Author*) Nothing to Disclose Kyunghyun Paeng, Seoul, Korea, Republic Of (*Presenter*) Co-founder, Lunit Inc Sangheum Hwang, Seoul, Korea, Republic Of (*Abstract Co-Author*) Employee, Lunit Inc Hyo-Eun Kim, Seoul, Korea, Republic Of (*Abstract Co-Author*) Employee, Lunit Inc Chul-Bum Lee, Cheongju-si, Korea, Republic Of (*Abstract Co-Author*) Nothing to Disclose Minhong Jang, Seoul, Korea, Republic Of (*Abstract Co-Author*) Officer, Lunit Inc Anthony S. Paek, PhD, Seoul, Korea, Republic Of (*Abstract Co-Author*) CEO, Lunit Inc

#### PURPOSE

The aim of the study was to investigate the performance of screening tuberculosis (TB) lesion based on data-driven imaging biomarker (DIB), which is an imaging biomarker that is derived from large-scale medical image data by using deep learning technology. Especially, we assessed DIB for TB screening in chest radiographs (DIB-TB) in various race groups and different scales of training sets.

# METHOD AND MATERIALS

We constructed experiments on two different datasets which consist of 10,848 (7,020 for normal, 3,828 for TB) and 45,621 (22,202 for normal, 23,419 for TB) cases, respectively. The ground truth diagnosis results only include whether each case is TB or not. DIB-TB was trained based on deep convolutional neural networks. Two independent DIB-TBs trained based on two different datasets were used for demonstrating the impact of the number of training samples. In order to evaluate the performance of DIB-TB, we used three datasets; Shenzhen, Montgomery (public dataset) and in-house validation set (10% of the entire dataset was randomly selected for validation). Especially, two public datasets were used to show the robustness of DIB-TB in various race groups. Shenzhen dataset consists of 326 normal and 336 TB cases, and Montgomery dataset consists of 80 normal and 58 TB cases.

#### RESULTS

DIB-TB trained on the first (small-scale) dataset achieved viable TB screening performance; 0.964, 0.926, 0.884 in terms of AUC and 0.903, 0.837, 0.674 in terms of accuracy for in-house, Shenzhen, and Montgomery datasets, respectively. In DIB-TB trained on the second (large-scale) dataset, screening performance was significantly improved; 0.973, 0.963, 0.931 in AUC and 0.915, 0.894, 0.848 in accuracy for the same order. The best accuracy, sensitivity, specificity were 0.902 (at probability threshold 0.4), 0.863, 0.942 for Shenzhen set, and 0.855 (at probability threshold 0.45), 0.810, 0.863 for Montgomery set, respectively.

## CONCLUSION

The screening performance of DIB-TB can be significantly improved as the number of training samples increases. Additionally, we showed that DIB-TB is robust against the various race groups; DIB-TB trained from the dataset with specific race group can be used for different races with high screening performance.

#### **CLINICAL RELEVANCE/APPLICATION**

DIB-TB based on a large-scale chest radiographs can significantly improve the performance of TB screening. And, it can be applied for other race groups.

A Path to Affordable 3D in Radiology - Applied 3d-printing and Low-cost Virtual Reality in a University Hospital Setting

Monday, Nov. 28 12:45PM - 1:15PM Room: IN Community, Learning Center Station #2

# Participants

Philipp Brantner, MD, Basel, Switzerland (*Presenter*) Nothing to Disclose Florian Thieringer, Basel, Switzerland (*Abstract Co-Author*) Nothing to Disclose Tobias Heye, MD, Basel, Switzerland (*Abstract Co-Author*) Nothing to Disclose

## PURPOSE

While radiologists are used to interpret images "by slice" and to communicate through a written report, it may not be the most powerful method to convey information to non-radiologists including patients. With the advent of new visualization tools, the presentation of medical imagery may return to the third dimension through virtual reality and 3D printing. An outline of a low threshold approach to bring medical imagery back into the true and virtual third dimension is presented.

## **METHOD AND MATERIALS**

The basis of creating a 3d-model is a cross sectional imaging study (CT/MRI). Common radiology post-processing software is used to extract the intended 3D model by thresholding and segmentation. After export as STL-file, post-processing (smoothing, defect-filling and consistency checking) is performed in freely available software e.g. Blender, Meshlab or Meshmixer. 3d-models are then printed on standard commercially available fused filament fabrication (FFM) consumer 3D printers, ranging from 500-4000\$. Virtual visualisation of the model is achieved by utilizing the identical 3D model file on a 3D web platform (sketchfab.com). This allows for a low cost virtual reality setup by using google cardboard, a \$5-10 box housing lenses and a smartphone. The smart phone creates dynamic stereoscopic imagery on screen oriented by its sensors positional information.

## RESULTS

The described workflow proved to be a feasible and robust way to create 3D models in a reasonable time frame with low financial investments of approx. \$3500. The created 3D models were well received by referring physicians in particular pediatric cardiology, cranio-maxillofacial, vascular and cardiac surgery as well as urology. According to the referring physicians, 3D models facilitate surgical planning, understanding of complex pathology, communicating pathological findings to patients and teaching students or residents.

# CONCLUSION

A robust and feasible workflow to bring medical images back into the virtual and true third dimension is demonstrated. The presented approach allows any radiology departement to perform "first steps" in this expanding technology with a low financial and organizational threshold.

#### **CLINICAL RELEVANCE/APPLICATION**

3D printing and virtual reality are becoming important ways to communicate image findings. Radiology needs to master this technology to maintain its leading role as a technology driven specialty.

# IN220-SD-MOB3

## **Developing Multi-resolution Convolutional Neural Networks for Lung Nodule Segmentation**

Monday, Nov. 28 12:45PM - 1:15PM Room: IN Community, Learning Center Station #3

#### **Participants**

Shuo Wang, Beijing, China (*Abstract Co-Author*) Nothing to Disclose Mu Zhou, PhD, Mountain View, CA (*Abstract Co-Author*) Nothing to Disclose Di Dong, Beijing, China (*Abstract Co-Author*) Nothing to Disclose Yali Zang, Beijing, China (*Abstract Co-Author*) Nothing to Disclose Zhenyu Liu, Beijing, China (*Abstract Co-Author*) Nothing to Disclose Olivier Gevaert, PhD, Stanford, CA (*Abstract Co-Author*) Nothing to Disclose Jie Tian, PhD, Beijing, China (*Presenter*) Nothing to Disclose

#### PURPOSE

To develop a data-driven approach for automated lung nodule segmentation in CT images to facilitate computer-aided diagnosis of lung cancer.

#### **METHOD AND MATERIALS**

Lung nodule segmentation in CT images remains challenging due to the fact that nodules can be attached to lung wall or vessel and various nodule sizes pose an additional challenge. We propose a framework utilizing convolutional neural networks (CNN) to distinguish lung nodule and healthy tissues. Our data-driven approach defines multi-resolution lung nodule patches by extracting 0.34 million patches centered on nodules (21x21, 45x45, and 65x65 pixel sizes) from coronal, median sagittal, and axial views. We train three CNN models separately corresponding to the three views to generate probability scores for pixel classification. We achieve the ultimate segmentation by applying a logistic regression to integrate probability outcomes obtained from three trained CNN models. Segmentation performance was evaluated on 893 lung nodule cases (450 for training and 443 for testing) from LIDC-IDRI dataset. We report segmentation accuracy on the testing set by comparing outcomes against ground-truth contours with Average Dice Score (ADS(%)) and Average Hausdorff Distance (AHD).

## RESULTS

The proposed CNN approach achieved encouraging segmentation results (ADS=80.20%, AHD=3.83), outperforming conventional graph cut method (ADS=68.97%, AHD=7.78) on 443 testing nodules. In particular, we reported superior results for segmenting tumors attached to the lung wall (124 cases) with ADS 79.53% and AHD 4.31. We additionally showed outcomes given various tumor diameters (D). For the 350 nodules with D<12 mm, our CNN achieved ADS=79.30% and AHD=3.31. For the remaining 93 nodules with D>=12mm, the ADS is 83.59% and AHD is 5.83. Overall, our results revealed superior outcomes of segmenting nodules given a variety of lung nodule locations and sizes.

## CONCLUSION

Developing computerized segmentation technique is a crucial step in computer-aided lung cancer diagnosis. We presented a datadriven CNN model for lung nodule segmentation that is able to deal with nodules attached to lung wall and nodules with various sizes.

## **CLINICAL RELEVANCE/APPLICATION**

The proposed automated lung nodule segmentation holds promise to accelerate follow-up lung nodule CT diagnosis (e.g., survival, TNM staging) with growing number of lung nodule CT sequences.

# IN221-SD-MOB4

#### A Manufacturer-independent Ultrasound Strain Elastography Module: Phantom and Clinical Study

Monday, Nov. 28 12:45PM - 1:15PM Room: IN Community, Learning Center Station #4

FDA Discussions may include off-label uses.

#### **Participants**

Mohamed Abdelhafez, Giza, Egypt (*Abstract Co-Author*) Nothing to Disclose Mohamed Salaheldien, Giza, Egypt (*Abstract Co-Author*) Nothing to Disclose Ahmed M. Sayed, PhD, Cairo, Egypt (*Abstract Co-Author*) Nothing to Disclose Hanan S. Gewefel, MD, Cairo, Egypt (*Abstract Co-Author*) Nothing to Disclose Ahmed M. Mahmoud, PhD,MSc, Giza, Egypt (*Presenter*) Nothing to Disclose

#### PURPOSE

Ultrasound strain elastography has been widely used to assess tissue mechanical properties. We develop and assess a novel manufacturer-independent elastography ultrasound module that can be integrated with commercially available gray-scale ultrasound machines to introduce strain elastography using freehand quasi-static compression.

## METHOD AND MATERIALS

Conventional grayscale ultrasound images were acquired from, at least, 10 ultrasound machines of 7 manufacturers. Cine-loops (n> 200) of breast elastography phantom were collected while applying freehand compression (1-5%) using the transducer. The phantom included solid masses two times stiffer than background. Video signals were acquired via a high-definition video capture device. Frame-to-frame displacements were calculated using a novel hierarchy recursive displacement tracking technique. Strain was calculated as displacement spatial derivative, and was then superimposed on gray-scale images to provide both anatomical and mechanical information. Under Internal Review Board and consented forms, cine-loops of female breasts (n=27) were acquired while applying freehand compression. 14 women underwent double readings and their BI-RADS was classified.

## RESULTS

Using the module, strain elastography was reconstructed successfully form all machines. The stiffer phantom masses exhibited low strain compared to the background tissue-mimicking material with a strain ratio of  $2.52\pm0.29$  between background and harder masses. A strain signal to noise ratio (SNR) of  $7.50\pm3.01$  and contrast to noise ratio (CNR) of  $5.21\pm1.58$  were measured. Elastograms reconstructed using the module showed good match with those of a commercial machine. Strain images were reconstructed successfully for clinical breast data and masses were observed, however, lower values of SNR and CNR were measured.

# CONCLUSION

This study showed the feasibility of a vendor-independent strain elastography module via both phantom and clinical data. Quantitative strain values measured using the module integrated with 10 different ultrasound machines exhibited good match with known phantom mechanical stiffness. This add-on module may provide a cost-effective and standardized ultrasound strain elastography complementary tool for the diagnosing and monitoring of tumors.

#### **CLINICAL RELEVANCE/APPLICATION**

This vendor-independent elastography add-on module can be integrated with gray-scale ultrasound machines to assess the mechanical tissue changes such as breast and thyroid tumors.

## Open-source and Commercial Software Applications for Clinical 3D Printing

Monday, Nov. 28 12:45PM - 1:15PM Room: IN Community, Learning Center Station #5

#### **Participants**

James Shin, MD, MSc, Stony Brook, NY (Presenter) Nothing to Disclose

George L. Shih, MD, MS, New York, NY (*Abstract Co-Author*) Consultant, Image Safely, Inc; Stockholder, Image Safely, Inc; Consultant, MD.ai, Inc; Stockholder, MD.ai, Inc;

Mark E. Schweitzer, MD, Stony Brook, NY (*Abstract Co-Author*) Consultant, MMI Munich Medical International GmbH Data Safety Monitoring Board, Histogenics Corporation

#### CONCLUSION

Common to all applications related to 3D visualization is the need for post-processing of image data. 3D printing introduces new geometric constraints to existing clinical workflows, and familiarity with available CAD tools is prerequisite to successful integration of this technology into patient care.

#### Background

3D modeling for 3D printing is intrinsically different from clinical post-processing such as surface rendered reconstructions, and introduces new model constraints - most notably the concept of manifold geometry. Other novel and important characteristics include face normals, compactness, and polygon counts. These play a critical role in fabrication of a patient model. Expertise in other fields routinely address these needs with CAD software tools, and we have an opportunity to develop analogous medical imager-specific workflows for 3D printing. As the full library of open-source and commercial options may not be widely known, this work seeks to demonstrate how myriad combinations of such tools may be used to achieve the common aim of translating medical image data into a physical object.

## **Evaluation**

We limit this work to post-processing of CT image data into a printable 3D model. This invariably includes initial review of images, threshold segmentation, and modeling in a CAD environment.

#### Discussion

Several DICOM viewers include tools for post-processing and threshold segmentation. Label maps are generated according to attenuation parameters and/or region seeds, and used to triangulate polygons into a surface mesh. This must satisfy manifold geometric requirements to be represented in physical space. Non-manifold geometries commonly include edges with multiple adjoining faces or result from self-intersecting faces, and are limited to mathematical representation. Models should also satisfy the requirement of compactness, referring to a closed Euclidean space, violations of which commonly include holes or flipped normals. These model characteristics are addressed efficiently in a CAD environment, with automated and semi-automated tools. The final surface mesh representing the anatomy of interest is then translated into printing instructions, often specific to each 3D printing technology and sometimes proprietary.

# PET/CT In Lung Cancer: An Automated Imaging Tool for Decision Support

Monday, Nov. 28 12:45PM - 1:15PM Room: IN Community, Learning Center Station #6

#### **Participants**

Jakub Nalepa, Gliwice, Poland (Presenter) Contract, TexRAD Limited; Contract, Cambridge Computed Imaging Ltd Janusz Szymanek, Bytom, Poland (Abstract Co-Author) Contract, TexRAD Limited; Contract, Cambridge Computed Imaging Ltd Sarah J. McQuaid, PhD, Guildford, United Kingdom (Abstract Co-Author) Nothing to Disclose Raymondo Endozo, London, United Kingdom (Abstract Co-Author) Nothing to Disclose Vineet Prakash, MBBCh, Chertsey, United Kingdom (Abstract Co-Author) Nothing to Disclose Balaji Ganeshan, PhD, London, United Kingdom (Abstract Co-Author) CEO, TexRAD Ltd; Director, Feedback plc; Director, Stone Checker Software Ltd; Director, Prostate Checker Ltd Alex Menys, London, United Kingdom (Abstract Co-Author) Director, Feedback plc; Director, Motilent Ltd; Shareholder, Motilent Ltd Mike Hayball, Cambridge, United Kingdom (Abstract Co-Author) Director, TexRAD Limited; Director, Cambridge Computed Imaging Ltd; Director, Feedback PLC; Shareholder, Feedback PLC; Veni Ezhil, MRCP, FRCR, Guildford, United Kingdom (Abstract Co-Author) Nothing to Disclose Liz Bellamy, Guildford, United Kingdom (Abstract Co-Author) Nothing to Disclose James Crawshaw, MBBS, Surrey, United Kingdom (*Abstract Co-Author*) Nothing to Disclose John Hall, FRCR, London, United Kingdom (*Abstract Co-Author*) Nothing to Disclose Ashley M. Groves, MBBS, Hitchin, United Kingdom (Abstract Co-Author) Investigator, GlaxoSmithKline plc Investigator, General Electric Company Investigator, Siemens AG

Andrew Nisbet, PhD, Guildford, United Kingdom (Abstract Co-Author) Nothing to Disclose

#### PURPOSE

Lung cancer (LC) accounts for 12.7% of the world's total cancer incidence. PET/CT plays a central role in LC diagnosis and staging. Powerful quantitative techniques e.g. CT texture analysis (CTTA) can enhance the diagnostic utility of PET/CT by providing information on tumor aggression & resistance. Such techniques however cannot be used in busy clinics where the analysis remains time-consuming & prone to user error. This preliminary study assesses the performance of an automated PET/CT analysis in lung cancer and compare against experienced imaging reporting.

# METHOD AND MATERIALS

Patients: 44 consecutive patients (age:68.7+/-10.3 years, 32 males) with LC who underwent FDG-PET/CT (GE Discovery) were analyzed retrospectively. Average follow up was 22.7+/-16.1 months. Clinical stage information was available in 42 patients (I:1, II:9, III:28, IV:4). Reader analysis: Two clinically qualified readers analyzed the patients independently; manually segmenting the tumor on the CT slice corresponding to the most avid lesion on PET. Unenhanced CTTA using the filtration-histogram technique (TexRAD Ltd, www.texrad.com, part of Feedback Plc, Cambridge, UK) was employed. Automated analysis: Automated algorithm uses both CT and PET to auto-segment the lung and lesion. Statistics: 1) Inter-user agreement for ROI area was assessed with Bland-Altman (BA) statistics & Intra-class correlation (ICC). 2) Algorithm segmentation accuracy (ROI area) against ground-truth (mean reader area) was assessed with BA statistics. 3) Survival analysis was performed using Kaplan-Meier analysis log-rank test.

## RESULTS

Automated approach was successful in 41/44 (93%). 1) Inter-reader agreement for ROI area revealed a mean difference of 372mm2, 95% limits of agreement (LoA) of 2671mm2 across a data range of 328mm2 to 4735mm2 (ICC=0.32). 2) ROI area of algorithm and ground-truth demonstrated a mean difference of 11mm2, 95% LoA of 1030 mm2 across a data range of 433mm2 to 4426mm2 (ICC=0.85). 3) CTTA from automated analysis predicted survival (Kurtosis,p=0.028).

#### CONCLUSION

The automated approach requires no user intervention and represents a repeatable method for lung identification, lesion segmentation and texture-analysis on PET/CT in lung cancer.

# **CLINICAL RELEVANCE/APPLICATION**

Automated PET/CT lung cancer tool may standardize clinical performance whilst allowing access to quantitative texture analysis to improve prognostication and fit within clinical workflow.

# MI211-SD-MOB1

CT Perfusion Differences between Primary and Secondary Pulmonary Malignancies and Certain Genetic Mutation (KRAS or EGFR)

Monday, Nov. 28 12:45PM - 1:15PM Room: S503AB Station #1

#### Awards

#### **Student Travel Stipend Award**

#### Participants

Shaun M. Nordeck, MS, RRA, Dallas, TX (*Presenter*) Nothing to Disclose Gary Arbique, PhD, Dallas, TX (*Abstract Co-Author*) Research Grant, Toshiba Corporation Yin Xi, Dallas, TX (*Abstract Co-Author*) Nothing to Disclose Monica Patel, BS, Dallas, TX (*Abstract Co-Author*) Nothing to Disclose Lori M. Watumull, MD, Dallas, TX (*Abstract Co-Author*) Research Grant, Toshiba Corporation Cecelia Brewington, MD, Dallas, TX (*Abstract Co-Author*) Research Grant, Toshiba Corporation

#### PURPOSE

To evaluate CT Perfusion differences between primary and metastatic pulmonary malignancies based on histopathology. In addition, those with and without genetic mutations were compared with CT perfusion.

## **METHOD AND MATERIALS**

Retrospective analysis of CT Perfusion (CTP) was performed on 29 participants for an indeterminate pulmonary nodule < 3cm and  $\geq 0.6$ cm with a pathologic diagnosis of malignancy. CTP data was analyzed using commercial perfusion software. Single and dual input CTP assessments were based on defined ROI analysis.

# RESULTS

Of the 29 malignancies, 18 were primary and 11 metastatic. Single and Dual input CTP methods successfully differentiated primary versus metastatic lesions (p=0.01 and p=0.04 with AUC of 0.8 and 0.7 respectively). Sixteen (16) underwent further genetic testing in which 8 were positive for either KRAS or EGFR mutations. Those with mutations had different dual input pulmonary flow values than those without (p=0.03). A dual input pulmonary flow cutoff value of 103 provided a sensitivity of 100% and specificity of 62% for the presence of a gene mutation.

## CONCLUSION

CTP values of pulmonary flow are significantly different between primary and metastatic pulmonary malignancies using single or dual input. Furthermore, dual input CTP pulmonary flow values were significantly different between malignancies with and without gene mutations.

## **CLINICAL RELEVANCE/APPLICATION**

Non-invasive CTP demonstrates differences between primary and secondary lung cancers and offers promise in differentiating between the presence or absence of certain gene mutations.

Contrast Ultrasound Imaging of Tumor Vasculature with Positively Charged Microbubbles

Monday, Nov. 28 12:45PM - 1:15PM Room: S503AB Station #2

#### Participants

Elizabeth Herbst, BS, Charlottesville, VA (*Abstract Co-Author*) Nothing to Disclose Galina Diakova, MS, Charlottesville, VA (*Abstract Co-Author*) Spouse, Co-founder, Targeson, Inc; Spouse, Shareholder, Targeson, Inc

Zhongmin Du, PhD, Charlottesville, VA (Abstract Co-Author) Nothing to Disclose

John A. Hossack, PhD, Charlottesville, VA (Abstract Co-Author) Nothing to Disclose

Alexander L. Klibanov, PhD, Charlottesville, VA (*Presenter*) Co-founder, Targeson, Inc; Minority Shareholder, Targeson, Inc; Institutional research collaboration, AstraZeneca PLC;

## PURPOSE

Molecular ultrasound imaging is usually based on microbubble contrast agents targeted to endothelial markers of disease. A universal method of targeting tumor vasculature independent of specific ligands is desirable. We present enhanced accumulation of positively charged microbubbles in murine tumor vasculature, i.e., tumor-specific ultrasound imaging.

#### **METHOD AND MATERIALS**

Microbubbles were prepared from C4F10, with lipid shell made of DSPC and PEG stearate, with a fraction of positively charged lipids, distearoyl trimethylammoniumpropane (DSTAP) or a biodegradable distearoyl ethyl phospatidylcholine (DSEPC). Bubble size and concentration was assessed by Coulter, zeta potential - by Zetasizer. Murine colon adenocarcinoma model was used (MC38 cells, J. Schlom, NIH, inoculated in the hind leg of C57BL/6 mice). Ultrasound conditions: Sequoia c512, 15L8 probe, CPS, 7 MHz, MI 0.2. We monitored contrast signal of tumor vs contralateral leg muscle up to 30 min following an iv bolus of 2.10^7 microbubbles.

## RESULTS

Without positive lipid, microbubble zeta potential was close to zero; it increased with the fraction of positive lipid. Following iv bolus, neutral bubbles cleared bloodstream and tumor within ~10 min. For bubbles with high DSTAP load, adherent contrast signal in the tumor was high, but its level in normal muscle was also high: at DSTAP:DSPC molar ratio 1:4, at 10 min contrast signal of tumor vs muscle was not different (p>0.3). At 30 min, tumor/muscle signal ratio was 2.1. To reduce normal muscle retention, we reduced bubble charge surface density. For DSTAP:DSPC 1:13, tumor/muscle signal ratio was >3 at 30 min. DSTAP:DSPC ratio 1:22 was optimal for tumor targeting: at 10 min, tumor/muscle ratio was >7 (p=0.00015); at 20 min, >15 (p=0.0034); at 30 min, >16 (p=0.00011), with excellent tumor delineation. Bubbles with DSEPC:DSPC 1:20 ratio also provided excellent delineation of tumor mass (at 10 min, p<0.001), with >5 tumor/muscle signal ratio. We assume that selective targeting is via retention of positively charged microbubbles on the negatively charged endothelium in slow-flow tortuous tumor vasculature.

## CONCLUSION

Positively charged microbubbles selectively accumulate in the tumor vasculature and provide high target-to-muscle contrast; optimized formulations are a universal ultrasound contrast agent for tumor imaging.

## **CLINICAL RELEVANCE/APPLICATION**

This study proposes a translatable ultrasound contrast for tumor vasculature delineation.

# MI213-SD-MOB3

The Comparison of Effects of Varenicline and Nicotine on NMDA Receptors in Animal Model by Using Proton Magnetic Resonance Spectroscopy at 9.4T

Monday, Nov. 28 12:45PM - 1:15PM Room: S503AB Station #3

**FDA** Discussions may include off-label uses.

#### **Participants**

Song-I Lim, BSC,BSC, Seoul, Korea, Republic Of (*Presenter*) Nothing to Disclose Kyu-Ho Song, Seoul, Korea, Republic Of (*Abstract Co-Author*) Nothing to Disclose Chi-Hyeon Yoo, Seoul, Korea, Republic Of (*Abstract Co-Author*) Nothing to Disclose Bo-Young Choe, PhD, Seoul, Korea, Republic Of (*Abstract Co-Author*) Nothing to Disclose

## PURPOSE

Nicotine exerts its effects through the activation of nicotinic acetylcholine receptors (nAChRs) 1. Varenicline, a smoking cessation aid, is a partial agonist acting at the  $\alpha 4\beta 2$  nAChRs. Although nicotine and varenicline contribute to the reward system at the same time, the influence of the substances on hippocampal neurochemical changes has not been investigated yet. We therefore studied the effects of repeated nicotine exposure and varenicline administration on hippocampus of rats by using in vivo proton magnetic resonance spectroscopy (1H MRS) at 9.4T.

#### **METHOD AND MATERIALS**

Eight-week-old male Wistar rats (n = 11; mean body weight,  $304.9 \pm 9.9$  g; range, 290.1-323.21 g) were divided into 3 groups: control rats (control, saline injection, n = 3); nicotine-induced rats (nicotine, subcutaneous injection of nicotine, 0.4 mg/kg/day free base, n = 4); and nicotine- and varenicline-induced rats (varenicline, subcutaneous injection of nicotine, 0.4 mg/kg/day free base, intraperitoneal injection of varenicline 0.3 mg/kg/day free base, n = 4). On day 5, <sup>1</sup>H MRS was performed on 9.4T Agilent MR scanner approximately 1 h after the last injection. After the T2 weighted image acquisition, in vivo <sup>1</sup>H MRS were acquired in the voxel ( $1.5 \times 2.5 \times 3$  mm<sup>3</sup>) using PRESS sequence and T2-weighted images for anatomical guidance with the following parameters: TR = 5000 ms, TE = 13.4 ms, 256 averages. The LC Model software was used to quantify the metabolites in the frequency domain.

#### RESULTS

In this study, the results show the tendency of increased Glu level in nicotine group than in the control and varenicline groups. Moreover, GSH and NAA levels tended to decrease in the nicotine group in comparison with those in the control and varenicline groups.

#### CONCLUSION

In conclusion, the hippocampus is integrally linked to the brain reward sensitization involved in addiction and glutamate release through mobilization of intracellular calcium stores. Further, oxidative stress and toxicity of nicotine on brain would cause the decline of GSH and NAA. Therefore, we suggest that varenicline effectively inhibits the reward cycle.

## **CLINICAL RELEVANCE/APPLICATION**

MRS can evaluate regional cerebral neurochemical levels precisely and is recommended as part of a MR study prior to neurodegenerative disease.

# **Traumatic Acetabular Fractures: Classification Made Easy!**

Monday, Nov. 28 12:45PM - 1:15PM Room: MK Community, Learning Center Station #9

#### **Participants**

Matthew J. Wu, MD, Halifax, NS (Presenter) Nothing to Disclose

## **TEACHING POINTS**

The purpose of this exhibit is to:1. Review the anatomical landmarks of the inominate bone and their correlate on plain film and CT.2. To provide a simplified, systematic aproach to classifying traumatic acetabular fractures. 3. Describe additional features not included in the Letournel classification scheme that the surgeons want to know.

## TABLE OF CONTENTS/OUTLINE

1. Title Slide2. Disclosures and target audience3. Anatomy4. Judet-Letournel Classification5. Additional Imaging Features6. Test Yourself7. Summary8. References and Author Contact

# Lines and Angles of Hip and Proximal Femur

Monday, Nov. 28 12:45PM - 1:15PM Room: MK Community, Learning Center Station #10

#### **Participants**

Sung Moon Kim, MD, Ann Arbor, MI (*Presenter*) Nothing to Disclose Yoav Morag, MD, Ann Arbor, MI (*Abstract Co-Author*) Nothing to Disclose Monica Kalume Brigido, MD, Ann Arbor, MI (*Abstract Co-Author*) Nothing to Disclose Jon A. Jacobson, MD, Ann Arbor, MI (*Abstract Co-Author*) Consultant, BioClinica, Inc; Royalties, Reed Elsevier; ; ; Gandikota Girish, MBBS, FRCR, Ann Arbor, MI (*Abstract Co-Author*) Nothing to Disclose Corrie M. Yablon, MD, Ann Arbor, MI (*Abstract Co-Author*) Nothing to Disclose Qian Dong, MD, Ann Arbor, MI (*Abstract Co-Author*) Nothing to Disclose

## **TEACHING POINTS**

After reviewing this exhibit, the learner will be able to:1. Draw the lines and measure the angles of hip and proximal femur. 2. Understand the meaning of the lines and angles of hip and proximal femur.

3. Correlate the abnormal angles and lines with the diseases of hip and proximal femur.

#### **TABLE OF CONTENTS/OUTLINE**

1. Lines and angles of the hip and proximal femur are frequently used to diagnose developmental dysplasia of the hip, pincer and cam types of femoroacetabular impingement, acetabular and proximal femur fractures, failed total hip arthroplasty, acetabular protrusion, and coxa profunda.2. Iliopubic line, ilioischial line, Hilgenreiner line, Perkin line, Shenton line, anterior, posterior, and medial acetabular wall lines, acetabular angle, acetabular abduction angle, Tonnis angle, lateral and anterior center-edge angles, acetabular version angle, alpha and beta angles of Graf, alpha, beta, and gamma angles, two different delta angles, neck-shaft angle (angle of inclination), femoral calcar line, and femoral anteversion angle will be discussed.3. Plain radiography, CT, or MRI can be used to draw the lines and measure the angles. Ultrasonography can be used in neonates with developmental dysplasia of the hip.

# **Honored Educators**

Presenters or authors on this event have been recognized as RSNA Honored Educators for participating in multiple qualifying educational activities. Honored Educators are invested in furthering the profession of radiology by delivering high-quality educational content in their field of study. Learn how you can become an honored educator by visiting the website at: https://www.rsna.org/Honored-Educator-Award/

Jon A. Jacobson, MD - 2012 Honored Educator

# MR Imaging Findings in Neuromuscular Diseases: A Primer for the Musculoskeletal Radiologist

Monday, Nov. 28 12:45PM - 1:15PM Room: MK Community, Learning Center Station #11

#### Awards

## **Identified for RadioGraphics**

#### **Participants**

Lais U. Aivazoglou, MBBS, Sao Paulo, Brazil (*Presenter*) Nothing to Disclose Andre Y. Aihara, MD, Sao Paulo, Brazil (*Abstract Co-Author*) Nothing to Disclose Artur D. Fernandes, MD, Sao Paulo, Brazil (*Abstract Co-Author*) Nothing to Disclose Carlos H. Longo, MD, Sao Paulo, Brazil (*Abstract Co-Author*) Nothing to Disclose Hamilton Guidorizzi, MD, Sao Paulo, Brazil (*Abstract Co-Author*) Nothing to Disclose Acary S. Oliveira, Sao Paulo, Brazil (*Abstract Co-Author*) Nothing to Disclose Paulo Victor S. Souza, Sao Paulo, Brazil (*Abstract Co-Author*) Nothing to Disclose Wladimir B. Pinto, Sao Paulo, Brazil (*Abstract Co-Author*) Nothing to Disclose Fabiano N. Cardoso, MD, Sao Paulo, Brazil (*Abstract Co-Author*) Nothing to Disclose

# **TEACHING POINTS**

Review the main MR imaging findings in neuromuscular diseases. Highlight specific patterns of distribution in muscular involvement that help making the diagnosis.

# TABLE OF CONTENTS/OUTLINE

Radiologists are not much familiar with neuromuscular diseases, probably because most of them are diagnosed clinically and also because of the prior relative lack of usage of diagnostic imaging in this field. However, during the two past decades, MR imaging has gained critical importance in diagnosing these entities, specially in regard to inherited and inflammatory neuromuscular diseases. Its value lies on adding relevant information about the pattern of muscular involvement and assessing its degree. Besides, although muscle biopsy is still the gold standard for establishing a definitive diagnosis, MR imaging helps in narrowing the range of differential diagnosis and supporting a clinical hypothesis, once we get to know the key features of neuromuscular imaging. Therefore, the main goal of this pictorial review is to provide a general overview of the most common neuromuscular diseases and myopathies that might help the radiologist reaching a diagnosis.

## MK303-SD-MOB4

Accessory Anterolateral Talar Facet Associated with Tarsal Coalition: Prevalence and Cross-sectional Characterization

Monday, Nov. 28 12:45PM - 1:15PM Room: MK Community, Learning Center Station #4

# Participants

Eman Alqahtani, MD, MPH, La jolla, CA (*Presenter*) Nothing to Disclose Evelyne Fliszar, MD, Mount Royal, QC (*Abstract Co-Author*) Nothing to Disclose Donald L. Resnick, MD, San Diego, CA (*Abstract Co-Author*) Nothing to Disclose Brady K. Huang, MD, San Diego, CA (*Abstract Co-Author*) Nothing to Disclose

## PURPOSE

The accessory anterolateral talar facet (AALTF) is a developmental entity recently described as a potential cause for rigid painful flat foot. We hypothesize that there is an association between AALTF and other flat foot etiologies such as tarsal coalitions.

# METHOD AND MATERIALS

We investigated the presence of AALTF on all CT and MRI of patients with possible tarsal coalition or sinus tarsi syndrome (01/01/2010-12/31/2016). Exclusion criteria included acute ankle trauma, recent ankle surgery, motion or metal artifacts. We evaluated the AALTF length and height, and the lateral talocalcaneal structures and sinus tarsi for edema and osseous changes. The presence of tarsal coalitions such as calcaneonavicular (CNC), intra- articular middle facet talocalcaneal (MFTCC), posterior facet talocalcaneal (PFTCC), extra-articular posteromedial talocalcaneal (EATCC) and other rare coalitions were also evaluated.

## RESULTS

187 patients were included in this study (age range 14-91 years; mean  $\pm$  SD age; 50  $\pm$  17 years), 47.1% males and 52.9% females. Overall AALTF prevalence was 31.55% (59/187), 41.91% in men, and 23.23% in women. AALTF average length was 4.5 $\pm$ 1.1mm, and average height was 8.9 $\pm$ 3.4mm. AALTF was found to be significantly associated with lateral talocalcaneal osseous changes such as cortical thickening and cystic changes (34/59 and 24/59 respectively, P< 0.01).At least one type of collation was identified in 37.43% of study population (70/187). The most common type was CNC (52.86%) followed by EATCC (35.71%). Intra-articular MFTCC (12.86%,) was found to be more common than PFTCC (5.71%). Other rare coalitions were present in less than 3%. There was a significant association between AALTF and the presence of EATCC (19/59, P < 0.01) and MFTCC (7/59, P < 0.05). No association was found with CNC, PFTCC or other rare coalitions. AALTF was also found to be significantly associated with sinus tarsi edema on MRI (45 of 59, P < 0.05).

#### CONCLUSION

AALTF is common and significantly associated with tarsal coalitions, specifically EATCC and MFTCC. When a coalition is identified, special attention should be made to evaluate for other associated pathologies. Failure to recognize an AALTF may result in persistent symptoms if only the coalition is treated.

# **CLINICAL RELEVANCE/APPLICATION**

Imaging interpreter must be aware of possible association between AALTF and tarsal coalition to aid appropriate clinical and surgical decisions.

Mucoid Degeneration of the Anterior Cruciate Ligament Preceding Progression of Medial Joint Space Narrowing: A FNIH Biomarkers Consortium Study

Monday, Nov. 28 12:45PM - 1:15PM Room: MK Community, Learning Center Station #2

# Participants

Robert M. Kwee, Heerlen, Netherlands (Presenter) Nothing to Disclose

Nima Hafezi Nejad, MD, MPH, Baltimore, MD (Abstract Co-Author) Nothing to Disclose

Bashir Zikria, Baltimore, MD (Abstract Co-Author) Nothing to Disclose

Ali Guermazi, MD, PhD, Boston, MA (*Abstract Co-Author*) President, Boston Imaging Core Lab, LLC Research Consultant, Merck KgaA Research Consultant, Sanofi-Aventis Group Research Consultant, TissueGene, Inc Research Consultant, OrthoTrophic Research Consultant, AstraZeneca PLC

Shadpour Demehri, MD, Baltimore, MD (*Abstract Co-Author*) Research support, General Electric Company; Researcher, Carestream Health, Inc; Consultant, Toshiba Corporation;

#### PURPOSE

To investigate whether ACL mucoid degeneration at 3T magnetic resonance (MR) imaging is associated with 2-year progression of radiographic medial tibiofemoral compartment (MTFC) joint space narrowing (JSN).

## **METHOD AND MATERIALS**

The study was IRB-approved and HIPAA-compliant. One index knee of six hundred subjects (41% males; median age 61 years, range 45-79) from the Osteoarthritis Biomarkers Consortium FNIH Project were included. The ACL was evaluated at 3T MR imaging at baseline. Minimum joint space width (minJSW) in the MTFC was assessed at knee radiographs at baseline and after 2 years. JSN progression was defined as decrease in minJSW >0.7 mm. Multivariable logistic regression analysis identified the association of ACL mucoid degeneration with JSN progression. Covariate adjustments were performed for age, gender, BMI, baseline WOMAC pain score, and MTFC minJSW (adjusted OR).Stratified data identified whether baseline Kellgren-Lawrence (KL) and Osteoarthritis Research Society International (OARSI) grade are interacting with ACL mucoid degeneration in association with JSN progression.

# RESULTS

Subjects with ACL mucoid degeneration more often showed JSN progression compared to subjects with a normal ACL (64% vs. 47%, P<0.01). In multivariable logistic regression, ACL mucoid degeneration was associated with JSN progression (adjusted OR=1.68, 95% confidence interval= 1.02-1.77, P=0.04). Subjects with baseline KL grade 1 and 2 and OARSI grade 0 were more likely to demonstrate JSN progression compared to subjects with baseline KL grade 3 (P=0.03) and higher OARSI grades (P<0.01), respectively.

# CONCLUSION

ACL mucoid degeneration is associated with 2-year progression of MTFC JSN. It is more likely to be a risk factor for JSN progression among subjects with milder features of radiographic OA at baseline.

## **CLINICAL RELEVANCE/APPLICATION**

Given the association between ACL mucoid degeneration and progression of MTFC JSN, strategies should be developed in order to prevent and slow down MTFC OA in subjects with ACL mucoid degeneration at MR imaging.

#### **Honored Educators**

Presenters or authors on this event have been recognized as RSNA Honored Educators for participating in multiple qualifying educational activities. Honored Educators are invested in furthering the profession of radiology by delivering high-quality educational content in their field of study. Learn how you can become an honored educator by visiting the website at: https://www.rsna.org/Honored-Educator-Award/

Ali Guermazi, MD, PhD - 2012 Honored Educator

Accelerating Knee MR Imaging: Compressed Sensing MRI in Isotropic Three-dimensional Fast Spin-echo Cube Compared with Conventional Cube Sequence

Monday, Nov. 28 12:45PM - 1:15PM Room: MK Community, Learning Center Station #3

# Participants

Seung Hyun Lee, MD, Seoul, Korea, Republic Of (*Presenter*) Nothing to Disclose Jisook Yi, MD, Bucheon-Si, Korea, Republic Of (*Abstract Co-Author*) Nothing to Disclose Young Han Lee, MD, Seoul, Korea, Republic Of (*Abstract Co-Author*) Nothing to Disclose Jin-Suck Suh, MD, Seoul, Korea, Republic Of (*Abstract Co-Author*) Nothing to Disclose

## PURPOSE

To compare image quality between compressed sensing (CS) fat-suppressed isotropic 3D fast spin-echo (FSE) Cube and conventional 3D FSE Cube sequence of knee magnetic resonance (MR) imaging and to evaluate their diagnostic agreements of meniscal lesion.

# METHOD AND MATERIALS

Fifteen knee MR studies consisted of sagittal conventional Cube and CS Cube sequences were reviewed retrospectively. Imaging parameters of 3D FSE Cube were TR/TE=1300/30 ms; echo train length (ETL)=48; matrix=320×320; field-of-view (FOV)=160×160mm; slice thickness=0.5mm. Sagittal MRI scans using CS with an acceleration factor of 1.5 were repeated with identical MR parameters. Overall image quality was assessed by calculating correlation coefficient, root-mean-square error (RMSE), and structural similarity index (SSIM). Regional image quality was evaluated with signal-to-noise ratio (SNR) of cartilage to background noise and contrast-to-noise ratio (CNR) of synovial fluid-cartilage, cartilage-bone, and meniscus-infrapatellar fat. Diagnostic agreements between the two sequences were assessed by evaluating images for lesions of anterior horn, body, and posterior horn of medial/lateral menisci with a three-point scale (0, normal; 1, degeneration; 2, tear). The Wilcoxon signed-rank test and intra-class correlation coefficient (ICC) were used for statistical analysis.

## RESULTS

Fifteen patients (M:F=5:10, mean age 56.8) were enrolled. Scan time was reduced (7min 48sec vs. 5min 12sec) with CS acceleration factor 1.5. Mean correlation coefficient between CS Cube and conventional Cube were 0.88 (P<0.05) while averages of RMSE and SSIM were calculated as 132.15 and 0.99, respectively. SNR was significantly higher in conventional Cube MRI compared to CS Cube MRI (124.6 vs 73.5; P=0.001). CNRs were higher in conventional Cube MRI compared to CS Cube MRI (219.5 vs 131.9, 70.1 vs 41.6, 44.5 vs 37.2; P=0.001, P=0.003, P=0.005, respectively). Diagnostic agreements for evaluating meniscal lesions were excellent with inter-method agreement (ICC=0.994) and inter-observer agreement (ICC=0.981).

# CONCLUSION

Compressed sensing Cube knee MRI sequence demonstrates acceptable image quality while reducing scan time. The CS Cube could replace conventional Cube in knee MR imaging with optimized acceleration factor.

# **CLINICAL RELEVANCE/APPLICATION**

Knee MRI acquisition can be accelerated with the use of compressed sensing technique while maintaining image quality and diagnostic acceptability.

# MK311-SD-MOB5

## Sagittal Balance Evaluation of Total Ankle Arthroplasty Implants: SEMAC MRI versus Radiography

Monday, Nov. 28 12:45PM - 1:15PM Room: MK Community, Learning Center Station #5

#### **Participants**

Cesar de Cesar Netto, Baltimore, MD (Abstract Co-Author) Nothing to Disclose Lucas Fonseca, Baltimore, MD (Abstract Co-Author) Nothing to Disclose Apisan Chinanuvathana, Baltimore, MD (Abstract Co-Author) Nothing to Disclose Mathias Nittka, PhD, Erlangen, Germany (Abstract Co-Author) Employee, Siemens AG Lew Schon, MD, Baltimore, MD (Abstract Co-Author) Royalties, DJO, LLC Royalties, Arthrex, Inc Royalties, DARCO International, Inc Royalties, Gerson Lehrman Group, Inc Royalties, Zimmer Biomet Holdings, Inc, Inc Royalties, Reed Elsevier Speakers Bureau, Tornier, Inc Speakers Bureau, Zimmer Biomet Holdings, IncSpeakers Bureau, BioMimetic Therapeutics, Inc Consultant, Zimmer Biomet Holdings, Inc Consultant, BioMimetic Therapeutics, Inc Consultant, Guidepoint Global, LLC Consultant, Gerson Lehrman Group, Inc Consultant, Tornier, Inc Consultant, Wright Medical Technology, Inc Consultant, Royer Medical, Inc Consultant, Carestream Health, Inc Stockholder, Tornier, Inc Stockholder, Royer Medical, Inc Stockholder, Bioactive Surgical, Inc Stockholder, HealthpointCapital Research support, Royer Medical, Inc Research support, Zimmer Biomet Holdings, IncResearch support, Tornier, Inc Research support, Arthrex, Inc Research support, SpineSmith LP Research support, BioMimetic Therapeutics, Inc Support, Bioactive Surgical, Inc Support, Educational Concepts in Medicine, LLC Support, Smith & Nephew plc Support, OrthoHelix Surgical Designs, Inc Support, Chesapeake Surgical Biocomposites Support, Olympus Corporation Support, Omega Surgical Instruments Ltd Jan Fritz, MD, Baltimore, MD (Presenter) Research Grant, Siemens AG; Scientific Advisor, Siemens AG; Scientific Advisor, Alexion Pharmaceuticals, Inc; Speaker, Siemens AG

#### PURPOSE

Radiographs are commonly used for sagittal balance alignment measurements of total ankle arthroplasty implants (TAA), but are prone to rotation misalignment. In contrast, MRI allows for alignment with the true sagittal plane of the talar implant and anatomically correct measurements. Therefore, we compared sagittal balance alignment measurements on metal artifact reduction MRI and radiographs in patients following TAA.

## **METHOD AND MATERIALS**

Following prospective IRB approval, 23 subjects [10 men/13 women, age 60(41-73) years] with TAA underwent SEMAC MRI and standard radiography of the ankle. Sagittal SEMAC MR images were aligned with the sagittal talar component axis. Maximum-intensity-projection MR images were created to bring anatomic landmarks into one single image. Three experienced, board-certified physicians performed sagittal balance alignment measurements twice in an independent, randomized, and blinded fashion, including lateral talar station (LTS), tibial axis-to-talus (T-T) ratio, and normalized tibial axis-to-lateral-process (T-L) distance. Pearson correlation coefficient (r), Concordance-Correlation-Coefficient (CCC) and Intraclass-Correlation-Coefficient (ICC) were calculated. Bonferroni-corrected p-values  $\leq 0.01$  were considered significant.

#### RESULTS

The intra-observer agreements were excellent for radiography (CCC=0.93-0.97) and MRI (CCC=0.90-0.97). The inter-observer agreements were good-to-excellent with overall higher agreements for MRI (ICC=0.76-0.93) than for radiography (ICC=0.58-0.95). There was statistically significant inter-method correlation between radiographic and MRI measurements including LTS (r=0.83, p<0.001), T-T ratio (r=0.86, p<0.001) and normalized T-L distance (r=0.72, p<0.001). The T-T ratios of radiographs and MRI were statistically not different (p=0.36), whereas LTS and normalized T-L distance were significantly lower on MR images when compared with radiographs (p<0.001).

## CONCLUSION

Sagittal balance measurements performed on standardized radiographs and SEMAC MRI demonstrate substantial correlation and similarity. Given its high inter-observer agreement, SEMAC MRI may be helpful for the evaluation of sagittal balance following TAA.

# **CLINICAL RELEVANCE/APPLICATION**

SEMAC MRI allows for anatomically accurate sagittal balance measurements of total ankle arthroplasty, which demonstrate a higher inter-observer agreement and may therefore be more accurate than measurements of standardized radiographs.

#### MK312-SD-MOB6

Subchondroplasty: Pre-operative MR Imaging Findings and Outcomes

Monday, Nov. 28 12:45PM - 1:15PM Room: MK Community, Learning Center Station #6

#### **Participants**

Ashima Lall, MD, Newtown Square, PA (*Abstract Co-Author*) Nothing to Disclose Peter R. Wahba, MD, Philadelphia, PA (*Abstract Co-Author*) Nothing to Disclose William B. Morrison, MD, Philadelphia, PA (*Presenter*) Consultant, General Electric Company Consultant, AprioMed AB Patent agreement, AprioMed AB Consultant, Zimmer Holdings, Inc Adam C. Zoga, MD, Philadelphia, PA (*Abstract Co-Author*) Nothing to Disclose Johannes B. Roedl, MD, PhD, Philadelphia, PA (*Abstract Co-Author*) Nothing to Disclose Peter Sharkey, MD, Philadelphia, PA (*Abstract Co-Author*) Nothing to Disclose Peter Sharkey, MD, Philadelphia, PA (*Abstract Co-Author*) Royalties, Corentec Co, Ltd; Royalties, StelKast; Royalties, Zimmer Biomet Holdings, Inc; Speaker, ConvaTec Inc; Speaker, Corentec Co, Ltd; Speaker, Zimmer Biomet Holdings, Inc; Consultant, Corentec Co, Ltd; Consultant, Zimmer Biomet Holdings, Inc; Stockholder, CrossCurrent, Inc; Stockholder, Force PT; Stockholder, Universal Research Solutions, LLC; Stockhoder, Physician Recommended Nutriceuticals Steven C. Cohen, MD, Philadelphia, PA (*Abstract Co-Author*) Consultant, Smith & Nephew plc ; Consultant, Zimmer Biomet Holdings, Inc

## PURPOSE

Subchondroplasty (SCP) is an emerging minimally invasive orthopedic procedure for patients with osteoarthritis of the knee in which a calcium phosphate bone substitute is injected into the subchondral bone; it is intended as an alternative pain-reducing treatment between conservative therapy and joint replacement. We sought to investigate pre-operative MR imaging features resulting in improved outcomes.

# METHOD AND MATERIALS

Pre-operative MRI exams of 35 knees in 34 patients (age range 42-81, average 60; 19 males, 15 females) who subsequently underwent SCP were reviewed. Clinical charts and surgical notes were reviewed for location of SCP as well as knee pain (scale 0-10) before and after the procedure. MR exams were reviewed for extent of cartilage damage in compartment undergoing SCP; extent of subchondral edema as a percentage of articular surface in the compartment; presence of subchondral fracture; and intensity of bone marrow edema, as a percentage signal relative to joint fluid. Comparison was made between pain scores and pre-operative imaging findings.

## RESULTS

Of 35 knees, 33 (94%) had improvement in pain. Numerical scores for pain were available for 20 knees, with an overall change from an average pain score of 6.8 to 2.7. Most common sites for SCP were the medial femoral condyle (N=9) and medial tibial plateau (N=11). Multiple sites were injected in 5 knees. Subchondral fracture was present in 9 of the 20 knees with numerical pain scores, without difference in outcome compared to non-fractures (6.7 to 3.0 vs 6.8 to 2.4). There was also no difference in pain improvement related to extent of chondrosis, nor extent / intensity of bone marrow edema. Data collection is ongoing.

# CONCLUSION

A decrease in pain related to knee osteoarthritis is seen in patients undergoing subchondroplasty. As yet, there is no evidence of an MR imaging predictor for improved outcomes.

# **CLINICAL RELEVANCE/APPLICATION**

Pre-procedure MR imaging is essential for planning of the subchondroplasty procedure. Calcium phosphate injection is targeted in areas of bone marrow edema. However, no apparent MR imaging sub-features have been identified to stratify patients into those who might have improved outcomes.

Low Dose Tin-filter High-kVp Computed Tomography of the Lumbar Spine - Feasibility and Comparison to Standard Techniques

Monday, Nov. 28 12:45PM - 1:15PM Room: MK Community, Learning Center Station #7

# Participants

Moritz Kaup, Frankfurt, Germany (*Presenter*) Nothing to Disclose Ralf W. Bauer, MD, Frankfurt, Germany (*Abstract Co-Author*) Speakers Bureau, Siemens Healthcare GmbH; Speakers Bureau, Bayer Healthcare; Speakers Bureau, GE Healthcare Katrin Eichler, MD, Frankfurt Am Main, Germany (*Abstract Co-Author*) Nothing to Disclose Andreas Bucher, MD, Frankfurt, Germany (*Abstract Co-Author*) Nothing to Disclose Christoph Polkowski, MD, Frankfurt, Germany (*Abstract Co-Author*) Nothing to Disclose Thomas J. Vogl, MD, PhD, Frankfurt, Germany (*Abstract Co-Author*) Nothing to Disclose Jan-Erik Scholtz, MD, Boston, MA (*Abstract Co-Author*) Nothing to Disclose

#### PURPOSE

To evaluate tin-filtered 150-kVp high tube voltage low tube current computed tomography of the lumbar spine in comparison to standard unenhanced dual-energy CT with regards to objective and subjective image quality and radiation dose exposure.

## **METHOD AND MATERIALS**

100 patients were included in this IRB-approved retrospective study with a waiver for written consent. Patients underwent low dose (LD; 150 kVp with tin filter, 60 mAs) or standard dose (SD; dual-energy 140/80-kVp, 260/620 mAs) unenhanced lumbar spine CT on a 3rd-generation 192-slice dual-source CT. Attenuation and noise in various anatomic landmarks (bone, fat, musclem) was measured and Signal-to-noise ratio (SNR) was calculated. Subjective image quality was rated by three independent reviewers (5-9 years of experience in CT diagnostic) using 5-point grading scales with regards to image sharpness of trabecular and cortical bone structure, visualization of intervertebral joints, delineation of neuroforamina and intervertebral discs in both axial and sagittal reconstructions. Radiation dose was assessed as CTDIvol. Interobserver agreement was calculated using intraclass correlation coefficient (ICC).

#### RESULTS

Radiation exposure was reduced by 85% in LD compared to SD settings (CTDIvol,  $2.12 \pm 0.56$  vs.  $14.25 \pm 5.64$  mGy). SNR was significantly lower in LD ( $1.1 \pm 0.2$  vs.  $3.4 \pm 0.6$ ; p<0.05). Subjective ratings of bone structures were good to excellent with no case of non-diagnostic for both protocols. Sharpness of trabecular and cortical bone structures were rated significantly better for SD compared to LD (LD: 4.20/3.31; SD: 4.74/4.42; both p<0.05) with substantial interrater agreement (ICC > 0.72). Delineation of intervertebral joints (LD: 4.83; SD: 4.91) and neuroforamina (LD: 4.98; SD: 5.0) were rated excellent for both protocols without significant differences (both p>0.05). Visualization of vertebral discs were rated sufficient in both image series with no significant difference (LD: 3.61; SD: 3.79; p = 0.17). Global interrater reliability was almost perfect (ICC: 0.839).

# CONCLUSION

Low dose tin-filter high-kVp CT of the lumbar spine provides good to excellent visualization of bone structures, while radiation exposure is reduced by 85 % compared to SD with radiation doses close to conventional two-plain x-ray examinations.

# **CLINICAL RELEVANCE/APPLICATION**

Low dose tin-filter high-kVp lumbar spine CT allows substantial radiation dose reduction while image quality maintains good.

# MS110-ED-MOB1

# Renal Sparing CT: How to Dramatically Reduce Iodinated Contrast Dose When Needed

Monday, Nov. 28 12:45PM - 1:15PM Room: MS Community, Learning Center Station #1

#### **Participants**

Nikkole Weber, Rochester, MN (*Presenter*) Nothing to Disclose Terri J. Vrtiska, MD, Rochester, MN (*Abstract Co-Author*) Nothing to Disclose Michael L. Wells, MD, Rochester, MN (*Abstract Co-Author*) Nothing to Disclose Ahmed Halaweish, PhD, Rochester, MN (*Abstract Co-Author*) Employee, Siemens AG Roy Marcus, MD, Rochester, MN (*Abstract Co-Author*) Institutional research agreement, Siemens AG; Research support, Siemens AG Cynthia H. McCollough, PhD, Rochester, MN (*Abstract Co-Author*) Research Grant, Siemens AG Joel G. Fletcher, MD, Rochester, MN (*Abstract Co-Author*) Grant, Siemens AG; ; Eric E. Williamson, MD, Rochester, MN (*Abstract Co-Author*) Research Grant, General Electric Company

# **TEACHING POINTS**

Substantial reduction ( $\geq$  50%) of iodinated contrast dose without altering radiologic diagnosis is important for multiple patient groups and clinical indications Acquisition options that facilitate diagnostic imaging with reduced IV contrast generally work to increase iodine signal, reduce image noise, and individualize timing of image acquisition to the contrast bolus Methods for enhancing iodine signal include low kV imaging, dual energy(DE) monoenergetic images, multiphase low-dose scanning, and ultrafast imaging Techniques employed for IV contrast reduction should depend on the patient, diagnostic task, and CT system

#### **TABLE OF CONTENTS/OUTLINE**

Patient-specific barriers to routine iodine dose Common approach (and rationale) for all methods: improved iodine signal (many methods) + iterative reconstruction + bolus-tracking + saline flush CT angiography- iodine dose reduction ( $\leq$  50mL) Low kV & DE virtual monoenergetic images Low-dose multiphase acquisition (adaptive 4D spiral) and novel display methods Dual source FLASH mode Solid organ cross-sectional imaging Low kV or DE acquisition Organ-specific bolus tracking delays Comparison to full iodine dose exams in same patients Task and scanner-specific considerations Future directions - injector (multi dose injector technology) and improved multi-energy detectors

#### **Honored Educators**

Presenters or authors on this event have been recognized as RSNA Honored Educators for participating in multiple qualifying educational activities. Honored Educators are invested in furthering the profession of radiology by delivering high-quality educational content in their field of study. Learn how you can become an honored educator by visiting the website at: https://www.rsna.org/Honored-Educator-Award/

Terri J. Vrtiska, MD - 2016 Honored Educator

Tumors in Von Hippel Lindau Syndrome from Head to Toe: A Comprehensive State-of-the-Art Review

Monday, Nov. 28 12:45PM - 1:15PM Room: MS Community, Learning Center Station #2

## Awards Certificate of Merit Identified for RadioGraphics

#### **Participants**

Dhakshina M. Ganeshan, MBBS, FRCR, Houston, TX (*Presenter*) Nothing to Disclose Sanjeev Bhalla, MD, Saint Louis, MO (*Abstract Co-Author*) Nothing to Disclose Kumaresan Sandrasegaran, MD, Carmel, IN (*Abstract Co-Author*) Nothing to Disclose Perry J. Pickhardt, MD, Madison, WI (*Abstract Co-Author*) Co-founder, VirtuoCTC, LLC; Stockholder, Cellectar Biosciences, Inc; Stockholder, SHINE Medical Technologies, Inc; Research Grant, Koninklijke Philips NV Meghan G. Lubner, MD, Madison, WI (*Abstract Co-Author*) Grant, Koninklijke Philips NV; Grant, Johnson & Johnson; Christine O. Menias, MD, Chicago, IL (*Abstract Co-Author*) Nothing to Disclose

## **TEACHING POINTS**

To review the epidemiology, molecular cytogenetics, histopathology and clinical presentation of Von Hippel Lindau (VHL) Syndrome To illustrate characteristic multimodality imaging features of tumors in VHL Syndrome affecting multiple organ systems, from head to toe To review the latest advances in management of VHL Syndrome and discuss current recommendations for surveillance and screening

## TABLE OF CONTENTS/OUTLINE

- Introduction - Epidemiology - Molecular Cytogenetics- Histopathology - Clinical Features- Illustrate imaging findings of tumors in Von Hippel Lindau Syndrome in multiple organ systems - Potential pitfalls in diagnosis – Management of VHL Syndrome.Summary: Von Hippel Lindau Syndrome is an autosomal dominant inherited disorder resulting from germline mutations in the VHL tumor suppressor gene. A wide range of benign and malignant tumors can occur in VHL including retinal & CNS hemangioblastomas, renal cell carcinoma, pheochromocytoma, pancreatic neuroendocrine tumors, endolymphatic sac tumors and papillary cystadenomas of epididymis. Broadly, VHL can be divided into 2 clinical subtypes based on the absence (Type 1) or presence of pheochromocytoma (Type 2). Given the wide spectrum of multi-system involvement, a multidisciplinary team approach to diagnosis, screening and treatment is needed.

#### **Honored Educators**

Presenters or authors on this event have been recognized as RSNA Honored Educators for participating in multiple qualifying educational activities. Honored Educators are invested in furthering the profession of radiology by delivering high-quality educational content in their field of study. Learn how you can become an honored educator by visiting the website at: https://www.rsna.org/Honored-Educator-Award/

Christine O. Menias, MD - 2013 Honored Educator Christine O. Menias, MD - 2014 Honored Educator Christine O. Menias, MD - 2015 Honored Educator Christine O. Menias, MD - 2016 Honored Educator Sanjeev Bhalla, MD - 2014 Honored Educator Sanjeev Bhalla, MD - 2016 Honored Educator Kumaresan Sandrasegaran, MD - 2013 Honored Educator Kumaresan Sandrasegaran, MD - 2014 Honored Educator Furmaresan Sandrasegaran, MD - 2016 Honored Educator Mumaresan Sandrasegaran, MD - 2016 Honored Educator Mumaresan Sandrasegaran, MD - 2014 Honored Educator Meghan G. Lubner, MD - 2014 Honored Educator Meghan G. Lubner, MD - 2015 Honored Educator PET/CT for Primary Staging of Rectal Cancer Patients with and without Extramural Vascular Invasion Detected by MR (EMVI-MR): Preliminary Findings

Monday, Nov. 28 12:45PM - 1:15PM Room: S503AB Station #6

# Participants

Marcelo A. Queiroz, MD, Sao Paulo, Brazil (*Presenter*) Nothing to Disclose Cinthia D. Ortega, MD, Sao Paulo, Brazil (*Abstract Co-Author*) Nothing to Disclose Tiago O. Morita, MD, Sao Paulo, Brazil (*Abstract Co-Author*) Nothing to Disclose Publio C. Viana, MD, Sao Paulo, Brazil (*Abstract Co-Author*) Nothing to Disclose Marcelo F. Zagatti, MD, Sao Paulo, Brazil (*Abstract Co-Author*) Nothing to Disclose Roberto Blasbalg, MD, Sao Paulo, Brazil (*Abstract Co-Author*) Nothing to Disclose Marcos R. Menezes, MD, Sao Paulo, Brazil (*Abstract Co-Author*) Nothing to Disclose Carlos A. Buchpiguel, MD, Sao Paulo, Brazil (*Abstract Co-Author*) Nothing to Disclose

## PURPOSE

To evaluate the use of PET/CT for primary staging of rectal cancer according to EMVI-MR status.

# METHOD AND MATERIALS

Twenty-two patients with rectal cancer before neoadjuvant radio and chemotherapy were enrolled in this prospective study. All patients underwent contrast-enhanced CT of thorax and abdomen, pelvic MR, whole-body PET/CT and liver MR with DWI and Primovist®. Imaging analysis consisted on evaluation of the primary tumor on MR concerning T- and N-staging, mesorectal involvement and EMVI status. PET/CT, ceCT and liver MR were analyzed for the presence of distant metastases. Biopsy of rectal tumor was obtained in all patients before treatment. The patients were divided based on the presence of EMVI-MR and the detection rate of metastatic disease was compared between ceCT, PET/CT and liver MR. Additionally, quantitative analysis of the primary tumor was done using DWI (ADC) and PET parameters (SUV, TLG, MTV) and compared to histology.

## RESULTS

Metastatic disease was found in 4/22 patients (18%) accounting for 28 lesions. There were 13/22 (59%) patients without EMVI-RM and 9/22 (41%) patients with EMVI-RM, which 4/9 (44%) presented distant metastases. PET/CT detected two more lesions than ceCT, which had high clinical impact, changing the patient management from curative to palliative intention. Liver MR did not identify any additional lesion to PET/CT or ceCT. Quantitative analysis showed an inverse correlation of TLG and grade of histological differentiation of the primary rectal tumor.

## CONCLUSION

Positive EMVI-MR can be used to select patients that would benefit from whole-body staging with PET/CT. Quantitative data of PET/CT aid on the characterization of tumor aggressiveness.

# **CLINICAL RELEVANCE/APPLICATION**

PET/CT might be preferred to stage rectal cancer with EMVI-MR due to higher detection rate of distant metastases and potential clinical impact on patient management.

## NM214-SD-MOB7

# Using DAT-SPECT, MIBG Myocardial Scintigraphy and the Combined Index for the Efficient Diagnosis of Parkinson Syndrome

Monday, Nov. 28 12:45PM - 1:15PM Room: S503AB Station #7

# Participants

Noriko Tsuda, Kumamoto, Japan (*Presenter*) Nothing to Disclose Fumi Sakamoto, Kumamoto, Japan (*Abstract Co-Author*) Nothing to Disclose Shinya Shiraishi, Kumamoto, Japan (*Abstract Co-Author*) Nothing to Disclose Masataka Nakagawa, Kumamoto, Japan (*Abstract Co-Author*) Nothing to Disclose Hideaki Yuki, MD, Kumamoto, Japan (*Abstract Co-Author*) Nothing to Disclose Mamoru Hashimoto, Kumamoto, Japan (*Abstract Co-Author*) Nothing to Disclose Seiji Tomiguchi, MD, Kumamoto, Japan (*Abstract Co-Author*) Nothing to Disclose Seiji Tomiguchi, MD, Kumamoto, Japan (*Abstract Co-Author*) Nothing to Disclose Manabu Ikeda, Kumamoto, Japan (*Abstract Co-Author*) Nothing to Disclose Yasuyuki Yamashita, MD, Kumamoto, Japan (*Abstract Co-Author*) Nothing to Disclose

#### PURPOSE

In a diagnosis of the Parkinson syndrome (PS), 123I-MIBG myocardial scintigraphy (MIBG) has been used for determining the possible occurrence of Lewy body disease (LBD). Whereas, many reports have demonstrated the usefulness of 123I-FP-CIT dopamine transporter single photon emission computed tomography (DAT-SPECT) for the accurate diagnosis of Parkinson's disease (PD). The aim of this study was to evaluate the effectiveness of using DAT-SPECT and 123I-MIBG myocardial scintigraphy separately, as well as a Combined index for obtaining an accurate diagnosis in the Parkinson syndrome.

#### **METHOD AND MATERIALS**

In this retrospective study, 58 patients with the Parkinson syndrome who had undergone DAT-SPECT assessment followed by MIBG myocardial scintigraphy were evaluated. The delayed heart-to-mediastinum (H/M) ratio of the MIBG scintigraphy, and the specific binding ratio (SBR) of the DAT-SPECT imaging were used as semi-quantitative measures. In groups with (DLB, PD, PSP, CBS, MSA) or other disorders, the diagnostic performance of each procedure when used independently as well as the combined utilization of DAT-SPECT and MIBG were evaluated. The cut off value for each index was determined by ROC analysis. The sensitivity, specificity, and accuracy of each imaging technique were calculated separately.

#### RESULTS

In DAT-positive diagnosis of (DLB/PD/CBS/MSA/PSP) disorders, the best parameters for the AUC were provided by the Combined index. For MIBG-positive (DLB/PD) diagnosis, the highest index for the AUC was obtained with the MIBG scintigraphy.For differentiating sensitivity, specificity, and accuracy in DAT-SPECT-positive groups (DLB/PD/CBS/MSA/PSP) from the negative cases the rates were 76.6, 90.9, and 79.3% with the Combined index.As for differentiating sensitivity, specificity, and accuracy in the MIBG-positive groups (DLB/PD) from the negative group, the rates were 84.6, 93.8, and 89.7% by the delayed H/M ratio of MIBG.

# CONCLUSION

For diagnosis of DAT-SPECT positive groups such as DLB, PD, CBS, MSA and PSP, the combined index proved useful, while in the diagnosis of MIBG positive groups such as DLB and PD, the MIBG scintigraphy achieved the best performance. Thus, when the occurrence of Lewy body disease is suspected, MIBG scintigraphy should be performed initially.

## **CLINICAL RELEVANCE/APPLICATION**

When Lewy body disease is suspected, performing MIBG first is considered to be the more desirable approach to adopt.

Effects of New Block Sequential Regularized Expectation Maximization (BSREM) Reconstruction Algorithm on SUV and MTV of Thoracic and Abdominal Malignancies in FDG PET-CT Examinations

Monday, Nov. 28 12:45PM - 1:15PM Room: S503AB Station #8

# Participants

Mitsuaki Tatsumi, MD, PhD, Suita, Japan (*Presenter*) Nothing to Disclose Takashi Kamiya, Suita, Japan (*Abstract Co-Author*) Nothing to Disclose Kayako Isohashi, Suita, Japan (*Abstract Co-Author*) Nothing to Disclose Hiroki Kato, Suita Osaka, Japan (*Abstract Co-Author*) Nothing to Disclose Noriyuki Tomiyama, MD, PhD, Suita, Japan (*Abstract Co-Author*) Nothing to Disclose Jun Hatazawa, MD, PhD, Osaka, Japan (*Abstract Co-Author*) Nothing to Disclose

## PURPOSE

BSREM reconstruction algorithm, or so called "Q. Clear", was recently introduced by GE Healthcare to improve image quality and quantification in PET examinations. The purpose of this study was to evaluate the effects of this new algorithm on SUV and metabolic tumor volume(MTV) of thoracic and abdominal malignancies in FDG PET-CT examinations, comparing the results to those by an ordered subset expectation maximization(OSEM) reconstruction algorithm.

# METHOD AND MATERIALS

This study included 13 thoracic(lung ca.) and 17 abdominal(liver and pancreatic ca.) malignant lesions >2cm as well as 22 pulmonary and 11 hepatic lesions <1cm. Oncologic FDG PET-CT images were acquired with a GE Discovery 710 scanner equipped with a time-of-flight system. Images were reconstructed using BSREM beta 700 and OSEM(subset 8, iteration 3, and Gaussian filter 4mm; regular setting in our hospital) algorithms. SUVmax, -mean, and MTV were compared between BSREM and OSEM images in all 30 lesions >2cm and in thoracic or abdominal lesions separately. SUVmax was also compared in all 33 lesions <1cm and in pulmonary or hepatic lesions separately. Tumor margin was delineated with SUVmax 2.5 threshold. Statistical analysis was performed with a Wilcoxon signed-rank test and a Spearman's correlation method.

# RESULTS

In 30 lesions >2cm(49+/-19mm), SUVmean was 4.3+/-1.2(mean+/-SD), SUVmax 9.2+/-3.9, and MTV 32.8+/-39.5ml in OSEM. BSREM increased SUVmean by 2.9%, but decreased SUVmax by 0.8% with statistical significances(p<0.001) as compared to OSEM. MTV showed no significant difference between OSEM and BSREM. BSREM also increased SUVmean and decreased SUVmax of thoracic or abdominal lesions in the subgroup analysis. A moderate negative correlation was observed between changes of SUVmax and lesion size, SUVmax, or MTV in OSEM(|Rho|=0.50-0.56, p<0.001). In 33 small lesions <1cm, BSREM increased SUVmax by 8.8% with a statistical significance(p<0.001). This increase was also observed on small pulmonary or hepatic lesions in the subgroup analysis.

# CONCLUSION

This study demonstrated that BSREM had a similar effect on SUV depending on the lesion size both in thoracic and abdominal malignancies. Further studies are required regarding an association of the decrease of SUVmax in larger lesions and noise reduction in BSREM.

# **CLINICAL RELEVANCE/APPLICATION**

BSREM increased SUVmax in small lesions <1cm, but decreased SUVmax in lesions >2cm both in the thoracic and abdominal malignancies.

Hepatic 18F-FDG Uptake Measurements on PET/MR: Impact of Volume of Interest Location on Repeatability

Monday, Nov. 28 12:45PM - 1:15PM Room: S503AB Station #9

#### **Participants**

Liran Domachevsky, MD, Tel Aviv, Israel (*Presenter*) Nothing to Disclose Hanna Bernstine, MD, Petah Tikva, Israel (*Abstract Co-Author*) Nothing to Disclose Meital Nidam, Tel Aviv, Israel (*Abstract Co-Author*) Nothing to Disclose Dan Stein, Tel Aviv, Israel (*Abstract Co-Author*) Nothing to Disclose Natalia Goldberg, MD, Petah Tiqwa, Israel (*Abstract Co-Author*) Nothing to Disclose Dorit Stern, MD, Tel-Aviv, Israel (*Abstract Co-Author*) Nothing to Disclose Ifat Abadi-Korek, PhD, Tel Aviv, Israel (*Abstract Co-Author*) Nothing to Disclose David Groshar, MD, Tel Aviv, Israel (*Abstract Co-Author*) Nothing to Disclose

### PURPOSE

To investigate same day 18F-FDG (fluoro-deoxyglucose) PET/MR test-retest repeatability of Standardized Uptake Value measurements normalized for body weight (SUV) and lean body mass (SUL) in different locations in the liver.

## **METHOD AND MATERIALS**

This prospective study was IRB approved and written informed consent was obtained from all patients. Between September 2015 and January 2016, patients that performed a whole-body non-enhanced 18F-FDG PET/MR followed by contrast-enhanced 18F-FDG PET/MR centered at the liver were included. 19 patients (11 women and 8 men, mean age 59±10.7 years) were enrolled. All patients performed PET/CT prior to the PET/MR. Maximal, peak and mean uptake (SUV/L max, mean and peak, respectively) were measured inferior, superior, and at the level of the right portal vein as well as in the left lobe of the liver. Mean differences of the various SUV/L's between test and retest were measured. The coefficient of variation (CV) and intraclass correlation coefficient (ICC) were calculated to estimate the absolute agreement among measurements.

# RESULTS

Very good agreement between test-retest measurements was found only for SULmean, SUVmean, SUVpeak and SUVmax measured in the region inferior to the portal vein. The CV for SUV/L's measurements were lowest inferior to the portal vein (<11%) followed by measurements performed at the level of the portal vein (<18%). The highest CV was found superior to the portal vein and at the level of the left lobe.

#### CONCLUSION

The area inferior to the portal vein is the most reliable location for hepatic 18F-FDG uptake measurements on PET/MR.

## **CLINICAL RELEVANCE/APPLICATION**

The least variability of SUV/L measurements in the liver was demonstrated inferior to the portal vein, suggesting this location as the preferred area for background comparison on follow-up studies.

Myocardial Perfusion Imaging: A Community Hospital System's Perspective on Improving Accuracy of 99mTc-Tetrofosmin Studies with SPECT-CT with Cardiac Catheterization Correlate

Monday, Nov. 28 12:45PM - 1:15PM Room: S503AB Station #10

#### Awards

#### **Student Travel Stipend Award**

#### **Participants**

Jonathan C. Lee, MD, BS, Milwaukee, WI (*Presenter*) Nothing to Disclose Alexandre L. Da Silva, MD, Milwaukee, WI (*Abstract Co-Author*) Nothing to Disclose Uma Suriyanarayanan, MD, BROOKFIELD, WI (*Abstract Co-Author*) Nothing to Disclose Paresh B. Desai, MD, Colgate, WI (*Abstract Co-Author*) Nothing to Disclose Eric M. Jakubowski, MD, Whitefish Bay, WI (*Abstract Co-Author*) Nothing to Disclose Orlin Hadjiev, MD, Elgin, IL (*Abstract Co-Author*) Nothing to Disclose

## PURPOSE

Single photon emission computed tomography (SPECT) and SPECT combined with conventional computed tomography for localization and attenuation correction (SPECT/CT) are well established tools utilized to assess clinically significant cardiac ischemia. However, the application of these techniques can vary across hospital systems and even within hospital systems. This study aims to identify the positive predictive values of SPECT alone versus SPECT/CT at our institution in order to improve diagnostic accuracy.

## RESULTS

85/186 (46%) of patients determined to have a positive myocardial perfusion scan had been scanned utilizing SPECT alone, and 57/85 (67%) of these patients underwent cardiac catheterization. 23/57 (40%) had positive cardiac catheterization results while 34/57 (60%) did not. Thus, the positive predictive value for a positive myocardial perfusion scan utilizing SPECT alone was 0.40. 101/186 (54%) of patients determined to have a positive myocardial perfusion scan had been scanned utilizing combined SPECT/CT, and 61/101 (60%) of these patients underwent cardiac catheterization. 40/61 (66%) had positive cardiac catheterization results while 21/61 (34%) did not. Thus, the positive predictive value for a positive myocardial perfusion scan utilizing combined SPECT/CT was 0.66.

# CONCLUSION

Myocardial perfusion imaging utilizing combined SPECT/CT had a higher positive predictive value than utilizing SPECT alone at this institution. While this data suggests SPECT/CT has superior diagnostic capability than SPECT alone in identifying clinically significant cardiac ischemia, factors such as cost, radiation dose, and other emerging technologies have not been considered in this analysis. Further study of these and other variables should be performed prior to making changes to this institution's myocardial perfusion imaging protocols.

## METHODS

We conducted a retrospective analysis of 186 consecutive patients over a period of a year (11/10/2014 to 11/10/2015) from two separate patient groups who were determined to have positive myocardial perfusion studies as interpreted by five qualified radiologists within a local radiology practice. One patient group (n=85/186, 46%) underwent myocardial perfusion scan at a facility without SPECT/CT capability, while the other group (n=101/186, 54%) underwent myocardial perfusion scan with SPECT/CT capabilities at a different facility. A positive myocardial perfusion scan was defined as any reversible perfusion defect that was not due to artifact. The corresponding patient charts from these positive myocardial perfusion scans were then reviewed to determine whether these patients underwent cardiac catheterization and the result of that cardiac catheterization. A positive myocardial perfusion scans were then correlated to the findings from the cardiac catheterization to assess the institutional diagnostic accuracy of myocardial perfusion scan utilizing SPECT/CT versus SPECT alone.

## PDF UPLOAD

http://abstract.rsna.org/uploads/2016/16018290/16018290\_w4c5.pdf

# Standing Cone Beam CT Myelography of the Spine

Monday, Nov. 28 12:45PM - 1:15PM Room: NR Community, Learning Center Station #9

#### Awards Certificate of Merit

#### **Participants**

Norbert G. Campeau, MD, Rochester, MN (*Presenter*) Nothing to Disclose Gary M. Miller, MD, Rochester, MN (*Abstract Co-Author*) Nothing to Disclose Alice C. Patton, MD, Rochester, MN (*Abstract Co-Author*) Nothing to Disclose Kent R. Thielen, MD, Rochester, MN (*Abstract Co-Author*) Nothing to Disclose

#### **TEACHING POINTS**

1. To illustrate the technique for performing standing cone beam CT myelography.2. Standing cone beam CT myelography can demonstrate posturally dependent changes not seen using conventional technique and is an excellent adjunct to conventional CT myelography.3. Standing myelography is inherently more physiologic than using compression devices in the recumbent position or even upright MRI which is often typically performed in sitting position; not standing.

# TABLE OF CONTENTS/OUTLINE

A. Overview of Weight Bearing Imaging of the Spine.B. Method for Performing Standing Cone Beam CT MyelographyC. Clinical Findings in 100 Patients Undergoing Standing Cone Beam CT MyelographyD. Imaging Examples: Spinal Canal Stenosis; Lateral Recess Stenosis, Foraminal Narrowing, Changes in Spine AlignmentE. Artifacts and Pitfalls of Standing Cone Beam CT MyelographyH. Outcomes (include complications)

# Arterial Spin Labeling Based MR Perfusion in Symptomatic Epilepsy: Delineating the Epileptogenic Zone

Monday, Nov. 28 12:45PM - 1:15PM Room: NR Community, Learning Center Station #10

## Awards Certificate of Merit

## Participants

Chinmay Nagesh, MBBS, MD, Trivandrum, India (*Presenter*) Nothing to Disclose Savith Kumar, MBBS, MD, Trivandrum, India (*Abstract Co-Author*) Nothing to Disclose B M Krishna Vadana, Trivandrum, India (*Abstract Co-Author*) Nothing to Disclose Aneesh Mohimen, Trivandrum, India (*Abstract Co-Author*) Nothing to Disclose Ramshekhar N. Menon, Trivandrum, India (*Abstract Co-Author*) Nothing to Disclose Bejoy Thomas, Trivandrum, India (*Abstract Co-Author*) Nothing to Disclose Chandrasekharan Kesavadas, Trivandrum, India (*Abstract Co-Author*) Nothing to Disclose

# **TEACHING POINTS**

Overview of ASL and the recommended sequence of pseudo-continuous ASL.

Define Symptomatic Epilepsy as an epilepsy of acquired or genetic cause, associated with anatomic-pathologic abnormalities, and/or clinical features indicating an underlying disease or condition.

Describe the contrasting methods by which ASL and PET imaging delineate the epileptogenic focus and to review the principle of Neurovascular coupling.

Demonstrate the advantages of fusion imaging of Structural MRI and ASL in demonstrating the ictal focus.

Describe the aberrations in perfusion is present in specific disease entities with case examples and the additional insight that can be gained with ASL.

# TABLE OF CONTENTS/OUTLINE

Neurovascular coupling and the importance of peri-ictal and inter-ictal periods.

Definition of Symptomatic Epilepsy with an etiologic classification.

Pictorial Essay of ASL in Symptomatic EpilepsyGenetic / Developmental-Developmental anomalies, Childhood & Progressive myoclonic epilepsies

-Neurocutaneous, genetic & Chromosomal disordersAcquired-Hippocampal Sclerosis

-Perinatal & infantile causes

-Trauma, Tumors

-Cerebrovascular, Immunologic & Degenerative conditionsIn conclusion ASL helps in delineating the epileptogenic zone and is an advantageous addition to the existing armamentarium of imaging in epilepsy

Thyroid Atypia and Follicular Lesions of Undetermined Significance (AUS and FLUS): Can Imaging Features Help Classify Risk and Direct Further Management?

Monday, Nov. 28 12:45PM - 1:15PM Room: NR Community, Learning Center Station #1

# Participants

Malak Itani, MD, Seattle, WA (*Presenter*) Nothing to Disclose Mohammed S. Bermo, MD, FRCR, Seattle , WA (*Abstract Co-Author*) Nothing to Disclose Tracy Tylee, Seattle, WA (*Abstract Co-Author*) Nothing to Disclose Emily E. Waner, MD, Seattle, WA (*Abstract Co-Author*) Nothing to Disclose Iram Ahmad, Seattle, WA (*Abstract Co-Author*) Nothing to Disclose Georgios Deftereos, Seattle, WA (*Abstract Co-Author*) Nothing to Disclose Stephen Schmechel, Seattle, WA (*Abstract Co-Author*) Nothing to Disclose Manjiri K. Dighe, MD, Seattle, WA (*Abstract Co-Author*) Research Grant, General Electric Company

## PURPOSE

To evaluate TIRADS score utility in classification of indeterminate thyroid nodules (Bethesda 3).

#### **METHOD AND MATERIALS**

The study was approved by the Institutional Review Board. We reviewed all records of thyroid aspirations performed in the radiology department between 7/1/2007 and 6/31/2014. All indeterminate pathology results were reviewed by a cytopathology fellow who assigned a Bethesda score to each nodule. The records of patients who had nodules with Bethesda scores of 3, atypia of undetermined significance (AUS) and follicular lesion of undetermined significance (FLUS), were reviewed. Ultrasound images of Bethesda 3 nodules with available surgical pathology were then reviewed by two radiologists. TIRADS score were given based on the classification by Kwak et al, and compared to the final pathology of nodules.

#### RESULTS

A total of 1810 thyroid aspirations on 1476 patients were performed during the study period. Initial pathology screening revealed 407 indeterminate nodules. Follow-up screen by pathology fellow showed that a total of 190 patients had Bethesda 3 nodules. Of these, 56 patients with 61 nodules had surgical pathology, 26 AUS and 35 FLUS. There is potential selection bias as more aggressive or rapidly growing lesions may have been preferentially referred to surgery. Final pathology for the 26 AUS nodules was benign in 15 nodules and for 35 FLUS nodules was benign in 26 nodules. Using Kwak TIRADS score, analysis was performed for each reviewer separately. Our reference was the calculated risk of malignancy by Kwak et al in TIRADS 3 nodules as 1.9%, 4A as 4.2%, 4B as 12.9%, 4C as 49.8%, and 5 as 92.3%. Per reviewer 1, the malignancy risk was 0% in 2 TIRADS3 nodules, 30.4% in 23 TIRADS4A nodules, 27.3% in 22 TIRADS4B nodules, and 64.3% in 14 TIRADS4C nodules, with no TIRADS5 nodules. Per reviewer 2, the malignancy risk was 0% in 2 TIRADS3 nodules, 33.3% in 15 TIRADS4A nodules, 40.1% in 22 TIRADS4B nodules, and 23.8% in 21 TIRADS4C nodules, in addition to a single malignant TIRADS5 nodule.

# CONCLUSION

Thyroid nodules that are Bethesda 3 on aspiration may harbor a higher risk for malignancy than other thyroid nodules with similar TIRADS classification, especially TIRADS4A and 4B.

# **CLINICAL RELEVANCE/APPLICATION**

Management in Bethesda 3 thyroid nodules is still controversial. Bethesda 3 nodules with at least 1 suspicious feature on ultrasound (TIRADS4A and above) may warrant more aggressive management.

Radiomics Model from 3D Volumetric MRI High Order Texture Analysis for Pre-treatment Stratification of Patients with Nasopharyngeal Carcinoma

Monday, Nov. 28 12:45PM - 1:15PM Room: NR Community, Learning Center Station #2

#### Awards

#### **Student Travel Stipend Award**

#### Participants

Jaykumar R. Nair, MD, Montreal, QC (*Presenter*) Nothing to Disclose Jeffrey Chankowsky, MD, Montreal West, QC (*Abstract Co-Author*) Nothing to Disclose Martin Vallieres, Montreal, QC (*Abstract Co-Author*) Nothing to Disclose Marco Mascarella, MD, Montreal, QC (*Abstract Co-Author*) Nothing to Disclose Carl Frederic Duchatellier, MD, Montreal, QC (*Abstract Co-Author*) Nothing to Disclose Nagi El Sabbagh, MD, Montreal, QC (*Abstract Co-Author*) Nothing to Disclose George Shenouda, MD, PhD, Montreal, QC (*Abstract Co-Author*) Nothing to Disclose Anthony Zeitouni, MD, Montreal, QC (*Abstract Co-Author*) Nothing to Disclose

## PURPOSE

To develop a risk assessment, multi-variate model, for nasopharyngeal cancer, based on 3D Volumetric MRI high order texture analysis for pre-treatment estimation of possible treatment failure, loco-regional recurrence and distant metastasis.

# METHOD AND MATERIALS

35 patients with histologically proven primary nasopharyngeal carcinoma and minimum follow-up of 24 months were retrospectively evaluated following research ethics board (REB) approval.Forty-two textures (3 global and 39 high order features) were extracted at 4 different resolutions (0.5 mm,1 mm, 2 mm, 3 mm), using 4 different number of gray-levels (8, 16, 32, 64) from contoured tumor region of the MRI images.The construction of prediction models for prediction of failure to treatment, loco-regional recurrence and distant metastasis from the combination of different textural features was performed using 100 bootstrap samples (100 training and testing sets) and logistic regression with feature set reduction, forward feature selection and correction for small sample size effect.

### RESULTS

Multivariable model for each outcome (failure to treatment, loco-regional recurrence and distant metastasis) separated the patients into either a positive (no event: red dot)or negative outcome(event: blue dot). The error bars represented the standard deviation of the multivariable model response for each patient over all 100 bootstrap samples, on a 95% confidence interval. (Figure:1). The estimated AUC, Sensitivity and Specificity of each prediction of model has been tabulated in Table 1. Finally, the "Prediction confidence" metric calculated the average prediction probabilities for positive and negative outcomes in all patients. This metric was meant to show strength of the predictions, considering all patients (e.g., in Figure 1: Distant metastasis is strong while loco-regional recurrence is medium)

## CONCLUSION

Multivariate models based on 3D Volumetric MRI texture promises to be an important tool in work-up of patients with nasopharyngeal cancer, especially in predicting treatment response and estimating risk for loco-regional recurrence and distant metastasis.

### **CLINICAL RELEVANCE/APPLICATION**

Based on" Radiomics Model" it is possible to predict response to treatment, locoregional or distant metastasis, which can help the physician to personalise treatment protocol in newly daignosed cases of nasopharyngeal cancer.

# NR363-SD-MOB3

Evaluation of Malignant and Benign Lesions Using Real-time Elastography and Strain Ratio in Patients with Parotid Mass

Monday, Nov. 28 12:45PM - 1:15PM Room: NR Community, Learning Center Station #3

# Participants

Leyla Karaca, Erzurum, Turkey (*Abstract Co-Author*) Nothing to Disclose Suat Eren, MD, Erzurum, Turkey (*Abstract Co-Author*) Nothing to Disclose Mecit Kantarci, MD, PhD, Erzurum, Turkey (*Presenter*) Nothing to Disclose Recep Sade, MD, Erzurum, Turkey (*Abstract Co-Author*) Nothing to Disclose Hayri Ogul, Erzurum, Turkey (*Abstract Co-Author*) Nothing to Disclose Ummugulsum Bayraktutan, Erzurum, Turkey (*Abstract Co-Author*) Nothing to Disclose Ihsan Yuce, Erzurum, Turkey (*Abstract Co-Author*) Nothing to Disclose

### PURPOSE

The elastography is a new visualization modality that has been commonly used in the recent years. This study aimed to investigate the contribution of real-time elastography and strain ratio in evaluating malignant and benign lesions in patients having a solid mass in their parotid gland.

#### **METHOD AND MATERIALS**

A total of 26 prospective patients who had parotid mass were evaluated using elastosonography. The elasticity score and strain ratio of the patients were evaluated. Both the elasticity score and the strain ratio for benign and malignant masses were evaluated statistically.

#### RESULTS

Mann–Whitney U test evaluation showed a statistically significant difference in the elasticity scores of two groups that were diagnosed as benign and malignant. The elasticity score of the patients with malignant and benign masses was found to be 3–4 and 1–2, respectively. The strain ratios of the malignant masses were also found to be higher than the strain ratios of the benign masses. A positive and strong correlation between the elasticity score and the strain ratio values of benign and malignant pathologies was detected using Spearman-'s rho correlation test (rs: 0.83; P < 0.0001). A significant difference was found between the average values of elasticity score and strain ratio of benign and malignant lesions (P < 0.0001). Also, a statistically significant difference was observed between the strain ratio values of pleomorphic adenoma and both benign and malignant lesions.

## CONCLUSION

Both elasticity score and strain ratio are convenient parameters for characterizing malignant and benign parotid lesions and hence contribute to diagnosis. In combination with gray-scale and color Doppler findings, they may either increase the diagnosis of malignancy or decrease the possibility of unnecessary biopsy and false-negative histopathological diagnosis. Future large-scale studies will highlight the significance of the strain ratio value.

# **CLINICAL RELEVANCE/APPLICATION**

Both elasticity score and strain ratio are convenient parameters for characterizing malignant and benign parotid lesions and hence contribute to diagnosis

# Quantitative Flow and Velocity Measurements with 4D-DSA Using Fourier Analysis

Monday, Nov. 28 12:45PM - 1:15PM Room: NR Community, Learning Center Station #4

#### Participants

Gabe Shaughnessy, PhD, Madison, WI (*Presenter*) Nothing to Disclose Jimmy Xu, BS, Madison, WI (*Abstract Co-Author*) Nothing to Disclose

Carson Hoffman, Madison, WI (Abstract Co-Author) Nothing to Disclose

Sebastian Schafer, BA, Madison, WI (Abstract Co-Author) Consultant, Siemens AG Employee, Siemens AG

Charles A. Mistretta, PhD, Madison, WI (Abstract Co-Author) Founder, Mistretta Medical Intellectual Property Licensing Activities Research, Siemens AG

Charles M. Strother, MD, Madison, WI (*Abstract Co-Author*) Research Consultant, Siemens AG Research support, Siemens AG License agreement, Siemens AG

### PURPOSE

Recently 4D DSA has provided time-resolved 3D C-Arm CT angiography data sets with 30/sec temporal resolution. Using these data it is possible to examine signal time curves along complex vessel centerlines. The method described here exploits the pulsatility of the signal waveform. The spatial variation in phase of the principal Fourier component provides a measure of the velocity. Coupled with area measurements, flow can also be calculated. The ultimate aim is to automatically provide a color display of velocity or flow to guide the planning and evaluation of interventional procedures.

### METHOD AND MATERIALS

Spatial distances and cross-sectional areas are found via the conventional 3D DSA static volume. Temporal measurements for each voxel are used to determine the FFT phase of the waveform at peak pulsatility. Velocity is determined by fitting the phase versus position along the centerline. Validation datasets include MR PCVIPR measurements of both clinical and canine cases and utilizing flow probe measurements on a head phantom. Artifact rejection techniques are implemented to improve reliability of measurements.

## RESULTS

The proposed method is less susceptible to transient artifacts such as vessel overlap or than other methods including mean transit time and cross correlation. However, its utility in distal vessels is diminished due to pulsatility damping. Flow conservation is verified to be within 6% and we find an accuracy of the 4D-DSA flow measurements to be within 15% and 16% RMSE of PCVIPR and flow probe measurements, respectively.

### CONCLUSION

4D-DSA allows a fast and unique spatial 3D and temporal view of vasculature. This information can be obtained quickly using traditional C-Arm angiographic methods. Contrast pulsatility can lead to a robust map of blood flow and velocity that rivals US and MR velocity measurements.

## **CLINICAL RELEVANCE/APPLICATION**

The availability of velocity and flow information could provide a more quantitative approach to treatment planning and evaluation in interventional radiology.

## NR365-SD-MOB5

QSM Texture Analyses to Differentiate Alzheimer's Disease from Cognitive Normal and Mild Cognitive Impairment

Monday, Nov. 28 12:45PM - 1:15PM Room: NR Community, Learning Center Station #5

# Participants

Jung Min Lee, MD, Seoul, Korea, Republic Of (*Presenter*) Nothing to Disclose Ye Na Son, Seoul, Korea, Republic Of (*Abstract Co-Author*) Nothing to Disclose Eo Jin Hwang, Seoul, Korea, Republic Of (*Abstract Co-Author*) Nothing to Disclose Hak Young Rhee, Seoul, Korea, Republic Of (*Abstract Co-Author*) Nothing to Disclose Chang-Woo Ryu, MD, Seoul, Korea, Republic Of (*Abstract Co-Author*) Nothing to Disclose Geon-Ho Jahng, PhD, Seoul, Korea, Republic Of (*Abstract Co-Author*) Nothing to Disclose Hyug-Gi Kim, Suwon, Korea, Republic Of (*Abstract Co-Author*) Nothing to Disclose Tian Liu, PhD, New York, NY (*Abstract Co-Author*) Nothing to Disclose Yi Wang, PhD, New York, NY (*Abstract Co-Author*) Nothing to Disclose

### PURPOSE

Although a number of studies have focused on finding anatomical regions in which iron concentrations are high, no study has been conducted to examine the overall variations in susceptibility maps of Alzheimer's disease (AD). The objective of this study, therefore, was to differentiate AD from cognitive normal (CN) and mild cognitive impairment (MCI) using a texture analysis of quantitative susceptibility maps (QSMs).

# METHOD AND MATERIALS

The study was approved by the local institutional review board, and informed consent was obtained from all subjects. The participants were 18 elderly CN, MCI and AD subjects. A fully first-order flow-compensated three-dimensional (3D) gradient-echo (GE) sequence was run to obtain axial magnitudes and phase images and to produce QSM data. Sagittal structural 3D T1-weighted (3DT1W) images were also obtained with the magnetization-prepared rapid acquisition of gradient echo sequence to obtain brain tissue images. The first- and second-ordered texture parameters of the QSMs and 3DT1W images were obtained to evaluate group differences using a one-way analysis of covariance.

#### RESULTS

For the first-order QSM analysis, mean, standard deviation and covariance of signal intensity separated the subject groups (F = 5.191, p = 0.009). For the second-order analysis, angular second moment, contrast, and correlation separated the subject groups (F = 6.896, p = 0.002). Finally, a receiver operating characteristic curve analysis differentiated MCI from CN in the white matter on the QSMs (z = 3.092, p = 0.0020).

### CONCLUSION

This was the first and the only study to evaluate the textures of QSMs in AD, which overcame the limitations of voxel-based analyses. The QSM texture analysis successfully distinguished both AD and MCI from CN.

# **CLINICAL RELEVANCE/APPLICATION**

Using the QSM texture analysis, MCI and AD can be differentiated from CN. Therefore QSM texture analysis using a few useful parameters is recommended in early detection of AD.

Correlation Analysis between Protein-based Amide Proton Transfer (APT) Imaging and Message RNA Expression: A Preliminary Study of Radiogenomics in Glioblastoma

Monday, Nov. 28 12:45PM - 1:15PM Room: NR Community, Learning Center Station #6

# Participants

Shanshan Jiang, MD, Baltimore, MD (*Presenter*) Nothing to Disclose Zhibo Wen, Guangzhou, China (*Abstract Co-Author*) Nothing to Disclose Jinyuan Zhou, PhD, Baltimore, MD (*Abstract Co-Author*) License agreement, Koninklijke Philips NV Hao Yu, Guangzhou, China (*Abstract Co-Author*) Nothing to Disclose Xianlong Wang, Guangzhou, China (*Abstract Co-Author*) Nothing to Disclose Lu Shilong, Guangzhou, China (*Abstract Co-Author*) Nothing to Disclose Jiandong Xi, Guangzhou, China (*Abstract Co-Author*) Nothing to Disclose Tianyu Zou, Guangzhou, China (*Abstract Co-Author*) Nothing to Disclose

### PURPOSE

Glioblastoma is the most common and deadly primary brain tumor. New biological understanding helped to perfect targeted, molecular based therapies that are individualized on particular biological or genomic modifications in each unique patient. Amide proton transfer (APT) imaging is a novel MRI technique in which amide protons of endogenous cellular proteins are detected. This research was designed to explore the differentially expressed genes (DEGs) and enriched pathways related to the protein-based APTw imaging phenotype of GBM.

### **METHOD AND MATERIALS**

16 patients with GBM were recruited and underwent T1w, T2w, FLAIR, APTw, and Gd contrast-enhanced T1w (T1C) sequences. Descriptors based on APTw imaging or conversional MR imaging morphologic features were evaluated by two experienced neuroradiologists, and the computational segmentations were assessed by imaging software semi automatically. Paired tumor and adjacent normal tissues were obtained intraoperatively for each patient. Global gene expression and genomic DNA measurements (RNA-seq) from the matched specimens with use of research identifiers were performed. Gene Set Enrichment Analysis (GSEA) enrichment analyses were performed for DEGs in Kyoto Encyclopedia of Genes and Genomes (KEGG), Gene Ontology (GO).

#### RESULTS

A total of 29 curated pathway gene sets were found to be significantly associated with two binary matrixes (APT/T1C area index > or  $\leq$  1.3, w/wo liquefactive necrosis) and three continuous MR values (APTmax, APTrange, APT/FLAIR area ratio), including four APTw features and one conventional MR trait. Vitamin B6 Metabolism Pathway (GSEA) was significantly negatively correlated with APTmax and APTrange. The presence of liquefactive necrosis was associated with the immune system process (GO\_Biological process). APTrange was correlated to the largest number of pathways (n=13), including human leukocyte antigen (HLA) system and TNF receptor superfamily.

# CONCLUSION

Our initial findings demonstrated a novel correlation between molecular imaging and gene characteristics of gliomas, and revealed the potential genetic and biologic significance of non-invasive protein-based APTw imaging features, which may facilitate the GBM precision medicine that depends on genomics.

# CONCLUSION

Our initial findings demonstrated a novel correlation in molecular imaging and gene characteristics of gliomas, and revealed the potential genetic and biologic significance of the non-invasive protein-based APTw imaging features, which may facilitate the GBM precision medicine that depends on genomics.

# CONCLUSION

Our initial findings demonstrated a novel correlation in molecular imaging and gene characteristics of gliomas, and revealed the potential genetic and biologic significance of the non-invasive protein-based APTw imaging features, which may facilitate the GBM precision medicine that depends on genomics.

## **CLINICAL RELEVANCE/APPLICATION**

APTw imaging signal has the potential to unveiling some special genomic changes in GBMs that may eventually provide insight into their genetic and molecular properties non-invasively.

## NR367-SD-MOB7

Permeability of the Blood-brain Barrier to Differentiate Multiple Sclerosis from Neuromyelitis Optica Spectrum Disorders

Monday, Nov. 28 12:45PM - 1:15PM Room: NR Community, Learning Center Station #7

# Participants

Xiaoxiao Ma, Beijing, China (*Presenter*) Nothing to Disclose Jinhao Lyu, Beijing, China (*Abstract Co-Author*) Nothing to Disclose Zihua Su, Beijing, China (*Abstract Co-Author*) Employee, General Electric Company Dehui Huang, Beijing, China (*Abstract Co-Author*) Nothing to Disclose Lin Ma, MD, Beijing, China (*Abstract Co-Author*) Nothing to Disclose Xin Lou, MD, PhD, Beijing, China (*Abstract Co-Author*) Nothing to Disclose

## PURPOSE

In our study, we quantitatively measured Ktrans of both normal appearing white matter (NAWM) and lesions in multiple sclerosis (MS) and neuromyelitis optica spectrum disorders (NMOSD) patients to compare the permeability characteristics of blood-brain barrier (BBB) in the two diseases using dynamic contrast-enhanced magnetic resonance imaging (DCE-MRI), thus to explore whether permeability could be a novel and reliable parameter to differentiate the pathphysiological differences between MS and NMOSD.

## METHOD AND MATERIALS

We prospectively enrolled 24 consecutive patients with NMOSD (according to the 2015 revised diagnostic criteria) and 19 consecutive patients with MS (according to the 2010 revised Mcdonald criteria) from September to December, 2015. They had performed magnetic resonance imaging (MRI) including axial T2-weighted images (T2WI) and DCE-MRI. T2WI and Ktrans map post-processed using in house software Omini-Kenetics (GE Healthcare, China) were co-registered slice by slice by SPM 8. MS and NMOSD lesions, NAWM, thalamic grey matter were manually outlined on T2WI as regions of interest (ROIs) by software MIPAV. ROIs were duplicated to Ktrans map (Figure 1) and Ktrans value of each ROI was obtained. Mann-Whitney U-tests was conducted to test the permeability differences between MS and NMOSD lesions and each corresponding location.

#### RESULTS

There were no significant differences in age between MS ( $39\pm9$  years; 13 women) and NMOSD ( $36\pm12$  years; 24 women). We totally studied 77 lesions in NMOSD and 176 lesions in MS, NAWM and thalamic grey matter of each patient. Ktrans of MS lesions were significantly higher compared to NMOSD lesions ( $0.0063\pm0.0078$  vs  $0.0025\pm0.0028$ , p=0.000). In the NAWM and thalamic grey matter, no significant differences were detected between MS and NMOSD ( $0.0063\pm0.0083$  vs  $0.0036\pm0.0019$ , p=0.058 and  $0.0018\pm0.0019$  vs  $0.0011\pm0.0009$ , p=0.145).

### CONCLUSION

Our present study manifests the permeability of BBB varied in MS and NMOSD lesions but no marked differences in NAWM and thalamic grey matter. The different pathophysiological changes lead to different permeability results. This research may provide novel insights into the potential pathophysiological differences in MS and NMOSD.

# **CLINICAL RELEVANCE/APPLICATION**

The permeability of blood-brain barrier may be a new imaging biomarker to differentiate the pathphysiological differences between multiple sclerosis and neuromyelitis optica spectrum disorders.

### NR368-SD-MOB8

# Standardized Brain Function Test: Making Functional MRI Standardized, Fast, and Physician Friendly

Monday, Nov. 28 12:45PM - 1:15PM Room: NR Community, Learning Center Station #8

FDA Discussions may include off-label uses.

#### Participants

Conrad C. Gibby, MD, Houston, (*Presenter*) Nothing to Disclose Steve T. Cvetko, PhD, American Fork, UT (*Abstract Co-Author*) Vice President, Novarad Corporation Long Nguyen, BS, American Fork, UT (*Abstract Co-Author*) Stockholder, Novarad Corporation Dennis H. Tolley, Provo, UT (*Abstract Co-Author*) Nothing to Disclose Wendell A. Gibby, MD, Provo, UT (*Abstract Co-Author*) Nothing to Disclose

### PURPOSE

Major brain dysfunction can exist, even if the brain looks structurally normal. Functional magnetic resonance imaging (fMRI) can detect subtle abnormalities that range from conditions such as traumatic brain injury, autism, ADD, psychiatric illnesses, and senile dementia. Despite its potential, few applications exist outside of pre-surgical planning.Widespread use of (fMRI) is hampered by lack of standards and poor control data. Technical challenges like noise and complex multi-step processing are other challenges. Good results have required immense physician time commitments.

### **METHOD AND MATERIALS**

Well developed, standard neuropsychological tests such as the Matrix Reasoning (part of WAIS); Trail Making; Boston Naming; Facial and Verbal Memory; and Verbal Fluency tests were used in a 1.5T MRI scanner. Statistical analyses included the usual random field theory for functional imaging, with the addition of restricted maximum likelihood (REML), cubic spline interpolation, and on-the-fly thresholding of t-maps. Software was developed to run the statistics on a 2GB gaming GPU (approximately 1000x improvement in speed). Scalp stripping and motion-reduction techniques were used.

### RESULTS

fMRI tests with t-test activation at 1.5T were applied on 23 patients in an attempt to form a control population. Patient data then underwent auto segmentation of the brain into a high resolution brain atlas to standardize the activation anatomy onto which the data was mapped. This data was then used to create high-resolution images to qualitatively assess brain activation. Average values and standard deviation (SD) were calculated using the 23 patients. Picture Naming tests as an example: average activation of the fusiform gyrus 1.75 with a standard deviation (SD) of 1.24; primary visual cortex activation 1.92 with a SD of 1.31; visual association cortex 3.04 with SD 1.07; medial frontal gyrus 0.84 with SD of 0.85, and inferior frontal gyrus 1.33 with SD of 1.18.

## CONCLUSION

A standardized battery of brain function tests will help clinicians to assess individual patients and researchers to study abnormal brain function with useful and objective control data.

# **CLINICAL RELEVANCE/APPLICATION**

A streamlined, standardized battery of fully integrated fMRI neuropsychological tests, combined with up-to-date fMRI techniques, helps to decrease the time of each fMRI test to about 2 min/test.

# Atypical Sites of Deeply Infiltrative Endometriosis: Clinical Characteristics and Imaging Findings

Monday, Nov. 28 12:45PM - 1:15PM Room: OB Community, Learning Center Station #1

#### Awards

# **Identified for RadioGraphics**

#### **Participants**

Luciana P. Chamie, MD, PhD, Sao Paulo, Brazil (*Presenter*) Nothing to Disclose Duarte M. Ribeiro, MD, Sao Paulo, Brazil (*Abstract Co-Author*) Nothing to Disclose Dario A. Tiferes, MD, Sao Paulo, Brazil (*Abstract Co-Author*) Nothing to Disclose Augusto C. Macedo Neto, Sao Paulo, Brazil (*Abstract Co-Author*) Nothing to Disclose Paulo C. Serafini, MD, PhD, Sao Paulo, Brazil (*Abstract Co-Author*) Nothing to Disclose

# **TEACHING POINTS**

The purpose of this exhibit is:1. To demonstrate atypical sites of deeply infiltrative endometriosis such as small bowel, lungs, pleura, diaphragm, pelvic nerves, pelvic floor, umbilicus, abdominal wall incisions and episiotomy scars 2. To discuss the phatogenesis, clinical suspicion and imaging characteristics of each atypical site3. To explain the utility and importance of imaging methods in the diagnosis and clinical counseling

# TABLE OF CONTENTS/OUTLINE

Possible mechanisms and pathogenesis of atypical endometriotic sitesAtypical sites- small bowel: jejunal and ileal loops- thoracic: lungs, pleura, diaphragm- pelvic nerves: inferior lumbosacral plexus, sciatic nerve, presacral nerves, obturator nerve- pelvic floor: puborectalis muscle, piriformis muscle, endopelvic fascia - abdominal wall incisions: cesarean scars, laparoscopic scars- umbilicusepisiotomy scars Relationship between atypical sites and pelvic diseaseClinical presentationDemonstration of imaging findings –US, CT and MRI with surgical correlationDiscuss the imaging role and therapeutic optionsSummary

# OB143-ED-MOB2

## The Pathways and Risk of Lymphatic Metastasis in Female Genital Pelvic Malignancies

Monday, Nov. 28 12:45PM - 1:15PM Room: OB Community, Learning Center Station #2

#### **Participants**

Yusaku Moribata, MD, Kyoto, Japan (*Presenter*) Nothing to Disclose Aki Kido, MD, Kyoto, Japan (*Abstract Co-Author*) Nothing to Disclose Fuki Shitano, MD,PhD, New York, NY (*Abstract Co-Author*) Nothing to Disclose Kayo Kiguchi, Kyoto, Japan (*Abstract Co-Author*) Nothing to Disclose Yasuhisa Kurata, Kyoto, Japan (*Abstract Co-Author*) Nothing to Disclose Kyoko Kameyama, Kyoto, Japan (*Abstract Co-Author*) Nothing to Disclose Noriomi Matsumura, Kyoto, Japan (*Abstract Co-Author*) Nothing to Disclose Kaori Togashi, MD, PhD, Kyoto, Japan (*Abstract Co-Author*) Nothing to Disclose Kaori Togashi, MD, PhD, Kyoto, Japan (*Abstract Co-Author*) Research Grant, Bayer AG Research Grant, DAIICHI SANKYO Group Research Grant, Eisai Co, Ltd Research Grant, FUJIFILM Holdings Corporation Research Grant, Nihon Medi-Physics Co, Ltd Research Grant, Shimadzu Corporation Research Grant, Toshiba Corporation Research Grant, Covidien AG

#### **TEACHING POINTS**

Lymph node status is an important factor for making treatment strategy and estimation of prognosis in addition to the FIGO stage in female pelvic cancers. Recognizing the lymphatic pathways and risk factors of metastasis in each tumor will facilitate to depict the nodal metastases and lead to successful surgery. These knowledge will teach where diagnostic radiologists should attend the image of CT or MRI and also important to discuss with gynecological oncologists.Teaching points are:1. To understand anatomical considerations of normal lymph node groups and pathways visualized in CT and MRI imaging with the sample cases 2. The pathways of nodal metastasis of female pelvic malignancies including cervical cancer, endometrial cancer and ovarian cancers3, Risk factors of nodal metastasis in each disease

# TABLE OF CONTENTS/OUTLINE

1. Normal anatomyA. Normal lymph node groupsB. Normal lymphatic pathways2. Female pelvic malignancies: cervical cancer, endometrial cancer and ovarian cancersA. The pathways of nodal metastasis B. The frequent and infrequent location of lymph node metastases in each tumorC. Risk factors of nodal metastasis in each disease

Pediatric Liver Transplantation-Techniques and Complications

Monday, Nov. 28 12:45PM - 1:15PM Room: PD Community, Learning Center Station #6

#### Awards

# **Identified for RadioGraphics**

#### **Participants**

Natally d. Horvat, MD, Sao Paulo, Brazil (*Presenter*) Nothing to Disclose Antonio S. Marcelino, MD, Sao Paulo, Brazil (*Abstract Co-Author*) Nothing to Disclose Tassia R. Yamanari, MD, Sao Paulo, Brazil (*Abstract Co-Author*) Nothing to Disclose Jose de Arimateia B. Araujo Filho, Sao Paulo, Brazil (*Abstract Co-Author*) Nothing to Disclose Joao Seda-Neto, Sao Paulo, Brazil (*Abstract Co-Author*) Nothing to Disclose Eduardo Antunes da Fonseca, Sao Paulo, Brazil (*Abstract Co-Author*) Nothing to Disclose Francisco C. Carnevale, Sao Paulo, Brazil (*Abstract Co-Author*) Nothing to Disclose Paulo Chapchap, MD, Sao Paulo, Brazil (*Abstract Co-Author*) Nothing to Disclose Luciana Cerri, MD, PhD, Sao Paulo, Brazil (*Abstract Co-Author*) Nothing to Disclose Giovanni G. Cerri, MD, PhD, Sao Paulo, Brazil (*Abstract Co-Author*) Nothing to Disclose

## **TEACHING POINTS**

- To review the main techniques used in liver transplantation- To discuss the role of radiologists in the pre- and postoperative evaluation- To discuss the imaging features of the various early and late complications after liver transplantation illustrated by sample cases from our hospital

# TABLE OF CONTENTS/OUTLINE

- Epidemiology of the pediatric liver transplantation- Techniques of liver transplantation- Normal appearance of the liver parenchyma and of the vascular and biliary anastomosis after liver transplantation on US, CT and MRI- Vascular, biliary and parenchymal complications after liver transplantation- Posttransplantation lymphoproliferative disorder

# Congenital Adrenal Hyperplasia: Fetal and Pediatric Imaging Findings and Management

Monday, Nov. 28 12:45PM - 1:15PM Room: PD Community, Learning Center Station #7

#### Awards Certificate of Merit

#### **Participants**

Petra Vajtai, MD, Portland, OR (*Presenter*) Nothing to Disclose Kyle Jensen, MD, Portland, OR (*Abstract Co-Author*) Nothing to Disclose Chelsea Pyle, MD, Portland, OR (*Abstract Co-Author*) Nothing to Disclose Roya Sohaey, MD, Portland, OR (*Abstract Co-Author*) Nothing to Disclose Karen Y. Oh, MD, Portland, OR (*Abstract Co-Author*) Nothing to Disclose

# **TEACHING POINTS**

1. The learner will understand the pathogenesis of congenital adrenal hyperplasia, including genetic and hormonal contributions.2. The learner will become familiar with the characteristic prenatal imaging findings in CAH in both male and female fetuses, as well as those in the growing child and adolescent.3. CAH is a chronic disease with life-long sequelae and variable effects on fertility, morbidity (including physical and psychosocial) in both male and female patients.

# TABLE OF CONTENTS/OUTLINE

1. Definition of CAH: autosomal recessive disorder of cortisol production; two subtypes a) virilizing b) salt-wasting.2. Fetal imaging findings in a) female patients: virilization of genitalia including clitoromegaly and enlarged/fused labia; b) male patients: normal genitalia; c) both sexes: adrenal glands can be enlarged, sometimes asymmetrically.3. Imaging recommendations: in cases where sex is unclear, ultrasound the genital ridge sagitally or use 3D US. Use MRI for better resolution of suprarenal "mass"/enlarged adrenal gland.4. Differential diagnosis: other disorders of sexual development and other etiologies for suprarenal masses.5. Pathology: 95% from mutation in CYP21A2 gene.6. Presentation and demographics.7. Natural history, prognosis and treatment including imaging follow-up.

# The CNS Intrauterine Zika Virus Infection Manual: Perinatal US, MR an CT Imaging Findings

Monday, Nov. 28 12:45PM - 1:15PM Room: PD Community, Learning Center Station #8

## Awards Magna Cum Laude Identified for RadioGraphics

#### **Participants**

Bianca Guedes Ribeiro, MD, Rio de Janeiro, Brazil (*Presenter*) Nothing to Disclose Heron Werner, MD, Rio de Janeiro, Brazil (*Abstract Co-Author*) Nothing to Disclose Luiz Celso H. Da Cruz, MD, Rio De Janeiro, Brazil (*Abstract Co-Author*) Nothing to Disclose Tatiana M. Fazecas, MD, Rio de Janeiro, Brazil (*Abstract Co-Author*) Nothing to Disclose Pedro Daltro, MD, Rio De Janeiro, Brazil (*Abstract Co-Author*) Nothing to Disclose Renata A. Nogueira, MD, Rio De Janeiro, Brazil (*Abstract Co-Author*) Nothing to Disclose Leise Rodrigues, Rio De Janeiro, Brazil (*Abstract Co-Author*) Nothing to Disclose Taisa D. Gasparetto, MD, PhD, Sao Paulo, Brazil (*Abstract Co-Author*) Nothing to Disclose Arine S. Pecanha, MD, Rio de Janeiro, Brazil (*Abstract Co-Author*) Nothing to Disclose

# **TEACHING POINTS**

Congenital infections involving the brain are caused by relatively few agents, but Zika virus (ZIKV) infection is relatively increasing around the world, particularly in South America and it is related with common findings to congenital infections on CNS and the severely increased rate of microcephaly. Ultrasound remains the method of choice to the fetal evaluation of congenital infection and should be complemented by magnetic resonance (MR) imaging for a better evaluation of lesions extent.Postnatal CT and MRI can also add many extra findings of the CNS involvement, such as microcephaly with almost complete agyria, hydrocephalus, and multifocal dystrophic calcifications in the cortex and subcortical white matter, with associated cortical displacement. The calcifications have cortical distribution and mainly subcortical, an aspect that has been repeated in all of our cases with microcephaly associated with Zika virus antenatal infection.Small anterior fontanel with premature closure sutures are also seen on ZIKV infection.

## TABLE OF CONTENTS/OUTLINE

1. Etiology and pathophysiology of ZIKV infection2. Manifestations / Clinical Presentation 3. Fetal US and MRI Findings 4. Postnatal Brain CT and MRI Findings5. Differential Diagnosis of Imaging Findings - CMV, Toxoplasmosis, Rubella 6. Follow-up and Prognosis

# PD215-SD-MOB1

Intra-venous and Intra-cavitary Contrast-enhanced Ultrasound (CEUS): How Can It Help in Complicated Pediatric Pneumonia?

Monday, Nov. 28 12:45PM - 1:15PM Room: PD Community, Learning Center Station #1

FDA Discussions may include off-label uses.

### Participants

Annamaria Deganello, MD, London, United Kingdom (*Abstract Co-Author*) Speaker, Bracco Group Vasileios Rafailidis, MD, Thessaloniki, Greece (*Presenter*) Nothing to Disclose Maria E. Sellars, MD, FRCR, London, United Kingdom (*Abstract Co-Author*) Nothing to Disclose Aikaterini Ntoulia, MD, PhD, Ioannina, Greece (*Abstract Co-Author*) Nothing to Disclose Kleanthi Kalogerakou, MD, MSc, Athens, Greece (*Abstract Co-Author*) Nothing to Disclose Gary Ruiz, MD,FRCR, London, United Kingdom (*Abstract Co-Author*) Nothing to Disclose Paul S. Sidhu, MRCP, FRCR, London, United Kingdom (*Abstract Co-Author*) Speaker, Koninklijke Philips NV; Speaker, Bracco Group; Speaker, Hitachi, Ltd; Speaker, Siemens AG

## PURPOSE

The purpose of this work-in-progress report is to investigate the application of contrastenhanced Ultrasound (CEUS) in the diagnosis and management of complicated pediatricpneumonia.

# **METHOD AND MATERIALS**

Ten children (mean age 4.1 years, range 1-12 years) with complicated pneumonia were initially evaluated with chest x-ray and grey-scale ultasonography (US). CEUS (intravenous, intra-cavitary) was then performed for further evaluation addressing specific management demands. Kappa coefficient was used to investigate the inter-observer agreement of US and CEUS for the diagnosis of necrotizing pneumonia. Chi-squared test was used to evaluate whether CEUS clearly demarcated the lung border more often than US; the Mann-Whitney test was used for comparison of US and CEUS diagnostic confidence for the diagnosis of necrotizing pneumonia.

#### RESULTS

US identified consolidation in 5/10 patients, empyema in 6/10 and pleural effusion in 2/10. In 7/10 patients, US could not address management demands related to the presence of lung necrosis (2/7), differentiation of empyema and necrotizing pneumonia (2/7), position of chest drainage catheter (2/7) and identification of residual empyema (1/7). Intra-cavitary CEUS (2/10) could identify the chest drainage catheter, facilitating use of fibrinolytic therapy. The inter-observer agreement for the diagnosis of necrotizing pneumonia was better with CEUS than US (kappa 0.8 vs 0.048, proportion of agreement 0.9 vs 0.7), CEUS more often clearly demarcated the lung border (p=0.001) and provided greater diagnostic confidence for the diagnosis of necrotizing pneumonia (p<0.001).

# CONCLUSION

Intravenous use of CEUS provides significantly better delineation of the pleural space and consolidated lung providing increased diagnostic confidence for necrotizing pneumonia and clearly demonstrates pleural fluid extent. Intracavitary CEUS helps identify the chest drainage catheter and highlights the need for fibrinolytic therapy, guiding patient management.

# **CLINICAL RELEVANCE/APPLICATION**

CEUS can be used in children with complicated pneumonia for necrotizing pneumonia diagnosis, clear delineation of lung border and pleural effusion and guiding treatment with fibrinolytic therapy.

## PD218-SD-MOB4

## Reduced FOV Diffusion Tensor MR Imaging and Fiber Tractography of the Pediatric Cervical Spinal Cord

Monday, Nov. 28 12:45PM - 1:15PM Room: PD Community, Learning Center Station #4

#### Participants

Mahdi Alizadeh, Philadelphia, PA (*Presenter*) Nothing to Disclose Alani Intintolo, Philadelphia, PA (*Abstract Co-Author*) Nothing to Disclose Devon M. Middleton, Philadelphia, PA (*Abstract Co-Author*) Nothing to Disclose Chris Conklin, Philadelphia, PA (*Abstract Co-Author*) Nothing to Disclose Scott H. Faro, MD, Haddonfield, NJ (*Abstract Co-Author*) Nothing to Disclose M. J Mulcahey, Philadelphia, PA (*Abstract Co-Author*) Nothing to Disclose Feroze B. Mohamed, PhD, Philadelphia, PA (*Abstract Co-Author*) Nothing to Disclose

## PURPOSE

(a) evaluate the feasibility of generating diffusion tensor tractography (DTT) images of the cervical spinal cord in children using a deterministic method, (b) to measure the DTI indices as well as tract specific information using regions of interest (ROIs) generated at every axial slice location along the entire cervical spinal cord based on DTT images, and (c) to investigate if there are differences in these values between the typically development (TD) subjects and patient group with SCI.

# METHOD AND MATERIALS

A total of 20 pediatric subjects included 10 healthy subjects (with the age of  $15.13\pm3.51$  (mean ±standard deviation) and age range of 11-21) and 10 subjects with SCI in the cervical area (with the age of  $13.8\pm3.26$  (mean ±standard deviation) and age range of 8-20) were recruited and scanned using 3.0T Siemens Verio MR scanner with 4-channel neck matrix and 8-channel spine matrix coils. The DTI parameters used were: number of directions=20, b=1000s/mm2, voxel size= $1.2 \times 1.2 \times 3.0$ mm3, matrix size= $36\times208$ , axial slices=35-45, TR=6100-8000ms, TE=115ms, number of averages=3 and acquisition time=7min.The fiber tracks generated based on pre-defined upper and lower FA thresholds (0.30 and 0.15 for all TD and SCI patients, respectively) were constrained within the limits of these thresholds as well as when the fiber track turns by more than a particular angle threshold in this case 70 degrees. Also, a lower track length threshold of 4.8mm was set to eliminate fiber fragments caused by noise within the tract reconstruction.

#### RESULTS

The mean FA values in the controls and patients were  $0.6\pm0.13$  and  $0.45\pm0.14$ , respectively. FA values were significantly decreased in the patients with SCI (p=0.0238). ADC values in the controls and patients were  $7.38\pm1.81\times10-4$ mm2/sec and  $7.67\pm2.37\times10-4$ mm2/sec, respectively. However they were not statistically significant. The mean number of fiber tracks in the controls and patients were  $1157\pm156.1$  and  $750\pm259.4$ , respectively and was significantly decreased in the SCI group (p=0.0005). However, the mean length of fiber tracks (24.30±15.85mm and 23.06±15.11mm in the controls and patients, respectively) did not show significant differences.

# CONCLUSION

DTI and DTT could be used a surrogate marker for quantification and visualization of the injured spinal cord.

# **CLINICAL RELEVANCE/APPLICATION**

DTT can be used to demonstrate three dimensional structures of white matter tracts in the brain and spinal cord.

### PD219-SD-MOB5

Body Composition Predictors of Trabecular and Cortical Microarchitecture in Adolescents with Morbid Obesity

Monday, Nov. 28 12:45PM - 1:15PM Room: PD Community, Learning Center Station #5

#### Participants

Fatima C. Stanford, Boston, MA (*Abstract Co-Author*) Nothing to Disclose
Vibha Singhal, Boston, MA (*Abstract Co-Author*) Nothing to Disclose
Stijn A. Bos, Boston, MA (*Abstract Co-Author*) Nothing to Disclose
Ryan Woolley, Boston, MA (*Abstract Co-Author*) Nothing to Disclose
Alexander Toth, Boston, MA (*Abstract Co-Author*) Nothing to Disclose
Madhusmita Misra, MD, MPH, Boston, MA (*Abstract Co-Author*) Research Grant, F. Hoffmann-La Roche Ltd Consultant, Advance
Medical Author, UpToDate, Inc Speaker, JCR Pharmaceuticals Co, Ltd
Miriam A. Bredella, MD, Boston, MA (*Presenter*) Nothing to Disclose

### PURPOSE

Obesity was believed to be protective for bone health; however, recent studies have shown that childhood obesity is associated with a higher incidence of forearm fractures. The purpose of our study was to determine predictors of trabecular and cortical microarchitecture of the distal radius in adolescents with morbid obesity. We hypothesized that lean mass would be positively, and visceral adiposity negatively, associated with bone microarchitecture in this population.

# METHOD AND MATERIALS

Our study was IRB approved and HIPAA compliant. Written informed consent was obtained. We recruited 11 adolescents (mean age:  $16\pm2$  yrs, 9 f, 2 m - recruitment is ongoing) with morbid obesity (mean BMI: $42\pm6$  kg/m2). 3D HR- pQCT of the distal radius was performed with an isotropic voxel size of 82 µm (Xtreme CT, Scanco Medical, Basserdorf, Switzerland) to assess cortical and trabecular microarchitecture, including individual trabecular segmentation (ITS), which models the trabecular region as a lattice of individual plates and rods. Body composition, including estimated visceral adipose tissue (VAT) mass was determined by DXA (Discovery A; Hologic, Bedford, MA, USA). Non-parametric linear regression analysis was performed to determine body composition predictors of bone microarchitecture.

#### RESULTS

Two subjects were unable to undergo HR-pQCT due to body size. BMI was positively associated with cortical thickness (r=0.82, p=0.007) and cortical area (r=0.68, p=0.04). Lean mass was positively associated with trabecular density and volume (r=0.77, p=0.02 for both correlations), and measures of trabecular integrity by ITS (r=0.72 to 0.83, p=0.04 to 0.003). VAT mass was positively associated with cortical porosity (r=0.73, p=0.02).

## CONCLUSION

Lean mass is a positive predictor of measures of trabecular integrity, whereas VAT is a negative predictor of cortical integrity in adolescents with morbid obesity.

## **CLINICAL RELEVANCE/APPLICATION**

High VAT mass and low lean mass are risk factors for skeletal dysregulation in adolescents with morbid obesity.

Machine-Learning-Based Delineation Approach for Gross Tumor Volume Region of Three Types of Lung Tumors using Planning CT and PET/CT Datasets

Monday, Nov. 28 12:45PM - 1:15PM Room: PH Community, Learning Center Custom Application Computer Demonstration

# Participants

Koujiro Ikushima, BS, Fukuoka, Japan (*Presenter*) Nothing to Disclose Hidetaka Arimura, PhD, Fukuoka, Japan (*Abstract Co-Author*) Nothing to Disclose Ze Jin, Fukuoka, Japan (*Abstract Co-Author*) Nothing to Disclose Hidetake Yabuuchi, MD, Fukuoka, Japan (*Abstract Co-Author*) Nothing to Disclose Jyunpei Kuwazuru, BS, Fukuoka, Japan (*Abstract Co-Author*) Nothing to Disclose Yoshiyuki Shioyama, Fukuoka, Japan (*Abstract Co-Author*) Nothing to Disclose Tomonari Sasaki, MD, Fukuoka, Japan (*Abstract Co-Author*) Nothing to Disclose Hiroshi Honda, MD, Fukuoka, Japan (*Abstract Co-Author*) Nothing to Disclose Masayuki Sasaki, Fukuoka, Japan (*Abstract Co-Author*) Nothing to Disclose

### Background

We have developed a computer-assisted delineation system for gross tumor volume (GTV) region of three types of lung tumors with a machine learning classifier based on the planning computed tomography (CT) and positron emission tomography (PET)/CT datasets. Our software consisted of an image registration step, a machine learning step, and the segmentation step for the GTV region. At the image registration step, PET and diagnostic CT images were registered with a planning CT image based on the centroid of lung regions with bronchus. The next machine learning step contained our key idea, which was to feed voxel-based image features around GTV contours determined based on the knowledge of radiation oncologists into a machine learning classifier during the training step, after which the classifier produced the "degree of GTV" for each voxel in the testing step. At the segmentation step, the final GTV regions were estimated using the optimum contour selection (OSC) method that can be used to select global optimum object contours based on multiple active delineations with a level set method around the GTV.

### **Evaluation**

Our proposed framework was applied to fourteen lung cancer patients (age range: 65-86 years, mean: 76, solid: 6, ground glass opacity (GGO): 4, mixed GGO: 4), who had undergone stereotactic body radiotherapy. Our proposed framework achieved average three-dimensional Dice similarity coefficients (DSCs) of 0.836, 0.763, and 0.701 for solid, GGO, and mixed GGO types, respectively. On the other hand, the conventional approach, in which 80% of the maximum standardized uptake value region was used as initial region for the OCS method, produced average DSCs of 0.776, 0.110, and 0.500 for solid, GGO, and mixed GGO types, respectively.

#### Discussion

The GTV regions were segmented by our proposed approach even if the tumor type of lung tumor was the GGO. The segmented GTV region can be modified in our software if the segmented GTV region is inadequate.

# CONCLUSION

Our results suggested that the software based on our proposed approach may be useful as a tool to assist radiation oncologists for delineation of various types of GTV regions.

# FIGURE

http://abstract.rsna.org/uploads/2016/16016920/16016920\_mjc4.jpg

How to Perform a Contrast-enhanced Ultrasound in 10 Lessons?

Monday, Nov. 28 12:45PM - 1:15PM Room: PH Community, Learning Center Station #9

#### **Participants**

Salma Moalla, MD, Paris, France (*Presenter*) Nothing to Disclose Benedicte Coiffier, Vilejuif, France (*Abstract Co-Author*) Nothing to Disclose Samy Ammari, Villejuif, France (*Abstract Co-Author*) Nothing to Disclose Baya Benatsou, Villejuif, France (*Abstract Co-Author*) Nothing to Disclose Stephanie Pitre-Champagnat, Villejuif, France (*Abstract Co-Author*) Nothing to Disclose Nathalie B. Lassau, MD, PhD, Villejuif, France (*Abstract Co-Author*) Speaker, Toshiba Corporation; Speaker, Bracco Group

## **TEACHING POINTS**

Focus on the basics of Contrast-enhanced ultrasound's tehnique and learn how to analyse images and information provided by contrast ultrasound

## **TABLE OF CONTENTS/OUTLINE**

Contrast-enhanced ultrasound (CEUS) consists in performing a "classical" ultrasound associated with the administration of intravenous contrast agents containing microbubbles approuved in Europe, China, Korea for several years and recently in USA in 2016. The intra-vascular bubbles with a diameter around 3 micrometers increase the detection of vascularization as intravenous contrast agents used in CT and MRI. This review describes CEUS techniques, indications, non and contraindications. It summarizes usefulness of CEUS in detection and characterization of lesions but also of dynamic contast-enhanced ultrasound (DCE-US) in quantification of the effect of anti-angiogenic treatments through selected teaching cases. CEUS is a cheap, seducing, alternative technique, that have the advantage over contrast-enhanced MRI and CT in patients with contraindications such as renal failure or contrast allergy. It allows repeated examinations. With DCE-US, new softwares allows the quantification of blood flow and blood volume using the automatic dynamic aquisition during 3 minutes with a high temporal resolution (4 images per second using raw linear data).

## PH220-SD-MOB1

Accurate Measurement of Modulation Transfer Function of CT from Extremely Low-contrast Non-zoomed Wire Images

Monday, Nov. 28 12:45PM - 1:15PM Room: PH Community, Learning Center Station #1

# Participants

Chiaki Tominaga, BSc, Sendai, Japan (*Presenter*) Nothing to Disclose Hiroki Azumi, BSc, Sendai, Japan (*Abstract Co-Author*) Nothing to Disclose Mitsunori Goto, MMedSc, RT, Natori, Japan (*Abstract Co-Author*) Nothing to Disclose Masaaki Taura, BMedSc, RT, Sendai, Japan (*Abstract Co-Author*) Nothing to Disclose Noriyasu Homma, PhD, Sendai, Japan (*Abstract Co-Author*) Nothing to Disclose Issei Mori, PhD, Sendai, Japan (*Abstract Co-Author*) Nothing to Disclose

## CONCLUSION

By use of tilted-wires for PSF method, MTF measurement at extremely low-CNR conditions is possible. This should be useful to elucidate the resolution behavior of nonlinear CT images.

#### Background

Measurement of low contrast modulation transfer function (MTF) is becoming common for non-linear CT images reconstructed by iterative method.Present mainstream is the edge method that observes edge response of plastic rod. But, it still requires some level of contrast-to-noise ratio (CNR) which is not low-enough to represent soft-tissue images.The point-spread function (PSF) method that uses wire image is the basic way of MTF measurement. But it requires very high CNR and zooming reconstruction both of which lose touch with clinical conditions, and can't be applied to non-linear images.We show that the PSF method can be made applicable to non-zoomed extremely low-CNR wire images.

#### **Evaluation**

In our method, a wire is not parallel to rotation axis (or z), but tilted with a small angle. By scanning certain range of z, an array of images is obtained. Wire positions, each different for each slice, are detected by multi-dimensional regression. All images are combined, with exact alignment, to form a PSF image that is finely-sampled and noise-tolerant by the aid of many images. For further noise tolerance, we take average of plural wires. Using a variety of thickness and material for tilted wires, we constructed multi-wire multi-contrast phantom to measure MTFs of several CNRs at once. This phantom was immersed in water. Using Toshiba's Aquilion64, z-range of 50mm was scanned helically. A hundred images of 0.5mm pitch were reconstructed by FBP with standard body kernel and 320mm reconstruction FOV.All MTFs obtained from various wires, including the wire of lowest peak-CNR 3.4 (peak height=60HU, SD=17.5) matched well with the ground truth.

#### Discussion

The concept of tilted-wire method is proven. Zooming reconstruction is unnecessary. Regarding noise, the wire of peak-CNR 3.4, which gave accurate MTF, is obliterated by noise and almost invisible. This CNR is far lower than that has been attainable by any other methods.

### PH221-SD-MOB2

### Super-hybrid Quantitative MRI using Displacement and Recovery-based Water-lipid Separation Imaging

Monday, Nov. 28 12:45PM - 1:15PM Room: PH Community, Learning Center Station #2

#### Participants

Shuto Suzuki, BS,RT, Kanazawa, Japan (*Presenter*) Nothing to Disclose Tosiaki Miyati, PhD, Kanazawa, Japan (*Abstract Co-Author*) Nothing to Disclose Naoki Ohno, PhD, Kanazawa, Japan (*Abstract Co-Author*) Nothing to Disclose Hirohito Kan, Nagoya, Japan (*Abstract Co-Author*) Nothing to Disclose Toshitaka Aoki, Nagoya, Japan (*Abstract Co-Author*) Nothing to Disclose Yuki Hiramatsu, RT, Kanazawa, Japan (*Abstract Co-Author*) Nothing to Disclose Yoshitaka Nakamura, RT, Kanazawa, Japan (*Abstract Co-Author*) Nothing to Disclose Toshifumi Gabata, MD, PhD, Kanazawa, Japan (*Abstract Co-Author*) Nothing to Disclose

### PURPOSE

Functional information on water and lipid tissues (e.g., diffusion, perfusion, relaxation time, lipid fraction) obtained with magnetic resonance imaging (MRI) is useful to assess the physiological conditions, physical properties, and tissue metabolism. However, it is difficult to obtain all of them at a time. Therefore, to simultaneously acquire those functional information, we developed displacement and recovery-based SeParation of Lipid Tissue (SPLIT) imaging with different inversion time (TI), echo time (TE), and b-values.

#### **METHOD AND MATERIALS**

On a 3.0-T MRI, the SPLIT imaging was used with single-shot diffusion echo-planar imaging (SSD-EPI), and optimized scan parameters to eliminate overlap between water and lipid images in the phase-encoding direction, ie., 524 µs echo spacing, 250 kHz receiver bandwidth, 430 mm field of view, 87.7 ms TE, and 0 - 3000 s/mm2 b-values (7 points). Moreover, inversion pulse (292 ms TI) was added to the SSD-EPI to remove olefinic signals. Consecutively, the SSD-EPI (0 s/mm2 b-value) was performed using 31.8 ms TE and 0 ms TI, respectively. We obtained transverse SPLIT images of the lower leg in six healthy subjects, and calculated T1 and T2 from different TE or TI images in muscle, bone marrow, and subcutaneous fat. We also calculated the monoexponential diffusion coefficient (DC), and biexponential perfusion-related and restricted diffusion coefficients (DCp, DCr). Furthermore, we obtained lipid fraction of the muscle after the T1 and T2 corrections.

#### RESULTS

Water and lipid images of the lower leg were completely separated, and olefinic signals were effectively suppressed. DC of the bone marrow and subcutaneous fat calculated from the lipid images were  $0.02\pm0.02$  and  $0.04\pm0.02 \times 10-3$ mm2/s, and DCp, DCr, T1, T2, and lipid fraction of the muscle calculated from the water images were  $20.1\pm10.6 \times 10-3$ mm2/s,  $1.60\pm0.07 \times 10-3$ mm2/s,  $837.0\pm30.8$  ms,  $27.3\pm0.7$  ms, and  $3.3\pm2.2\%$ , respectively. All values were consistent with previous studies.

# CONCLUSION

Our method makes it possible to simultaneously obtain quantitative values concerning diffusion, perfusion, relaxation time, and lipid fraction, thereby increasing the functional information on the water and lipid tissues.

# **CLINICAL RELEVANCE/APPLICATION**

Our method enables one to simultaneously obtain quantitative diffusion, perfusion, relaxation time, and lipid fraction values of the water and lipid tissues without special pulse sequence.

### PH223-SD-MOB4

## A Framework for Organ-based Dose Monitoring System for Body CT Examinations

Monday, Nov. 28 12:45PM - 1:15PM Room: PH Community, Learning Center Station #4

#### **Participants**

Xiaoyu Tian, durham, NC (*Abstract Co-Author*) Nothing to Disclose Joshua Wilson, PhD, Durham, NC (*Presenter*) Nothing to Disclose William P. Segars, PhD, Durham, NC (*Abstract Co-Author*) Nothing to Disclose Federica Zanca, PhD, Leuven, Belgium (*Abstract Co-Author*) Employee, General Electric Company Pierre Guntzer, MSc, Strasbourg, France (*Abstract Co-Author*) Nothing to Disclose David E. Miller, PhD, Kirkland, WA (*Abstract Co-Author*) Employee, General Electric Company Ehsan Samei, PhD, Durham, NC (*Abstract Co-Author*) Research Grant, General Electric Company; Research Grant, Siemens AG

## PURPOSE

Quantifying and monitoring computed tomography (CT) radiation dose for an individual patient has become an unavoidable requirement to practice medical imaging. Among various dose metrics, organ dose is generally regarded as one of the best metrics for characterizing patient radiation burden. The purpose of this work was to develop a patient-specific radiation dose monitoring system capable of tracking individual patient organ dose for clinical CT exams.

## **METHOD AND MATERIALS**

The dose-monitoring program was developed based on a commercial software (DoseWatch research version, GE Healthcare, Waukesha, WI). The exam CTDIvol, DLP, TCM profiles, scanning parameters, outline of patient contour image, and anatomical landmarks were extracted as bases to estimate organ dose. In the first phase of the study, 30 patients who underwent six unique protocols were selected from the database. A library of 60 adult computational phantoms (age range: 18–70 y.o., weight range: 60–180 kg) were included in the study. Based on the outline of the anatomical landmarks, a clinical patient was optimally matched to a computational phantom to obtain a representation of organ location/distribution. Each of the computational models were previously associated with CTDIvol-normalized-organ dose coefficients as function of size. The organ doses were computed via the h factors, adjusted by size, CTDIvol, and a regional dose convolution factor accommodating the tube current modulation field at the organ location.

#### RESULTS

Organ doses demonstrated varied distributions across patients and protocols. Across the pilot 30 clinical patients evaluated, the organs that received the highest dose were thyroid for chest CT examinations (average 9.4 mGy), bladder for pelvic CT examinations (average 14.1 mGy), and liver for abdominal examinations (average 21.4 mGy).

### CONCLUSION

We extended a dose-monitoring program to include organ dose for individual patients. This tool improves the patient exposure record by incorporating patient-specific information as well as facilitating quality assurance and standardization of CT protocols.

## **CLINICAL RELEVANCE/APPLICATION**

The organ-based dose monitorting system may enable dose tracking pertaining patient-specific information and also aid in the design of individulized CT protocols.

# Comprehensive Study of Spectrum Optimization for Split-Filter Dual-Energy CT

Monday, Nov. 28 12:45PM - 1:15PM Room: PH Community, Learning Center Station #5

#### Participants

George S. Fung, PhD, Baltimore, MD (Presenter) Research support, Siemens AG

Karl Stierstorfer, PhD, Forchheim, Germany (Abstract Co-Author) Employee, Siemens AG

Matthew K. Fuld, PhD, Iowa City, IA (Abstract Co-Author) Researcher, Siemens AG

Satomi Kawamoto, MD, Laurel, MD (Abstract Co-Author) Nothing to Disclose

Elliot K. Fishman, MD, Baltimore, MD (*Abstract Co-Author*) Institutional Grant support, Siemens AG; Institutional Grant support, General Electric Company;

Benjamin M. Tsui, PhD, Baltimore, MD (Abstract Co-Author) Researcher, Koninklijke Philips NV; License agreement, General Electric Company;

Katsuyuki Taguchi, PhD, Baltimore, MD (Abstract Co-Author) Research Grant, Siemens AG

### PURPOSE

To investigate multiple parameters for shaping the x-ray spectrum of split-filter dual-energy computed tomography (DE-CT) and determine the optimal spectrum for the iodine quantification (IQ) and virtual-non-contrast (VNC) imaging.

## **METHOD AND MATERIALS**

The spectrum of LE and HE beams is the most important factor affecting the performance of DE-CT. In clinical split-filter DE-CT system, gold and tin prefilters are employed to split the cone beams into low-energy (LE) and high-energy (HE) beams, respectively. A comprehensive study of multiple spectrum shaping parameters, including 16 feasible prefilter materials, the prefilter thickness ranging from 0mm to 0.5mm in step of 0.025mm, and the tube potential ranging from 100kVp to 150kVp in step of 10kVp, were performed through simulation with the HE prefilter being fixed to 0.6mm tin. A cylindrical phantom with multiple iodine inserts and a 3D anthropomorphic phantom with hyperdense hepatic lesion were used in the study. An analytical physics-based CT projection simulation tool was employed to generate the LE and HE noisy projection data with the corresponding prefilter and tube potential settings. Projection data were beam-hardening corrected before filtered backprojection image reconstruction. The IQ and VNC images were obtained by applying image-based two-material decomposition method to the reconstructed DE-CT images. The figure-of-merit (FOM) used for optimization was the normalized inverse of the noise-dose product obtained from the IQ and VNC images and a Monte-Carlo CT simulation tool.

### RESULTS

Tungsten, tantalum, and gold LE prefilters, with k-edges of 70 to 80keV, achieved significant higher FOM than other candidate materials  $(2.08\pm0.20 \text{ vs } 1.03\pm0.07, \text{ p}<0.01)$ . With the optimal gold prefilter thickness, operating tube potential at 120kVp achieved significantly higher FOM than other suboptimal settings  $(1.88\pm0.07 \text{ vs } 1.77\pm0.05 (110kVp), \text{ p}<0.01)$ .

# CONCLUSION

Significant improvement in noise levels of IQ and VNC images under minimal patient dose could be achieved by employing the optimal prefilter material and thickness, and tube potential settings. Practical constraints, such as tube power reserve, and targeted applications might affect the optimal settings.

## **CLINICAL RELEVANCE/APPLICATION**

Operating the clinical split-filter DE-CT system at the optimal spectrum settings would not only reduce noise in the IQ and VNC images but also potentially reduce the radiation dose to patients.

# **Honored Educators**

Presenters or authors on this event have been recognized as RSNA Honored Educators for participating in multiple qualifying educational activities. Honored Educators are invested in furthering the profession of radiology by delivering high-quality educational content in their field of study. Learn how you can become an honored educator by visiting the website at: https://www.rsna.org/Honored-Educator-Award/

Elliot K. Fishman, MD - 2012 Honored Educator Elliot K. Fishman, MD - 2014 Honored Educator Elliot K. Fishman, MD - 2016 Honored Educator

# Revisiting FLT PET Dosing: A Clinical Trial List Mode Based Determination to Guide Dose Reduction

Monday, Nov. 28 12:45PM - 1:15PM Room: PH Community, Learning Center Station #6

#### Participants

Katherine Binzel, PhD, Columbus, OH (*Presenter*) Nothing to Disclose Preethi Subramanian, MS, BEng, Columbus, OH (*Abstract Co-Author*) Nothing to Disclose Xiaoli Liu, Columbus, OH (*Abstract Co-Author*) Nothing to Disclose Bhuvaneswari Ramaswamy, Columbus, OH (*Abstract Co-Author*) Nothing to Disclose Jun Zhang, PhD, Columbus, OH (*Abstract Co-Author*) Nothing to Disclose Michael V. Knopp, MD, PhD, Columbus, OH (*Abstract Co-Author*) Nothing to Disclose

# PURPOSE

In order to assess proliferation with PET/CT imaging, 18F-Fluorothymidine (FLT) has been developed as an alternative to 18F-FDG. However, current standard dosing protocols can make such studies costly in addition to having a large radiation burden. We used acquired and archived listmode FLT data to simulate low dose acquisitions in order to assess potential for FLT dose reduction and to evaluate quantitative impacts.

# **METHOD AND MATERIALS**

20 breast cancer patients underwent whole body FLT scans on a Philips Gemini TF 64 PET/CT using a standard dose of 10mCi (370 MBq) with a time of 90 seconds per acquisition volume. Following prior validation of the relationship between decreased acquisition times used for image reconstruction and radiopharmaceutical dose, listmode data were reconstructed using 2/3, 1/2, 1/3 and 1/6 of the original coincident event data, equating to a range of 33 to 83% dose/count reductions. Regions of interest were placed on 53 target tumor lesions as well as a variety of reference background areas. PET images were quantitatively evaluated using the 90s per frame SUVmax as a reference value, calculating SUVmax changes for the dose reduction simulations.

### RESULTS

The average SUVmax of all tumor lesions was within 12% of the reference values for even the 5/6 dose reduction. Those images exhibited the greatest noise, yet all but 2 lesions had a SUVmax variability no greater than 15% at 50% dose reduction. Background tissues showed similar quantitative results. Low uptake tissues, such as the muscle and lungs, showed greater variation at larger dose reductions, yet all tissues had SUVmax changes below 20% at a 50% dose reduction. A multi-reader review for image quality is ongoing, however all lesions identified on 90s images were visible at each of the simulated dose reduction levels.

#### CONCLUSION

FLT dosing can be substantially reduced when using current technology time of flight PET/CT systems. A dose reduction by 50% to 5 mCi (185 MBq) can be achieved even at a 90s acquisition time per bed position, further dose reductions can be achieved by simultaneously increasing the time per bed position making a 2.5 mCi (87 MBq) FLT PET feasible when a 3min bed position acquisition is used.

## **CLINICAL RELEVANCE/APPLICATION**

18F-FLT PET/CT dosing using current generation time of flight PET/CT can be substantially reduced to a 5mCi / 90 s bed acquisition that can be further reduced scans with increasing acquisition time.

Radiation Dose Reduction in Digital Breast Tomosynthesis (DBT) by Means of Patch-based Trainable Nonlinear Regression (PTNR)

Monday, Nov. 28 12:45PM - 1:15PM Room: PH Community, Learning Center Station #7

# Participants

Junchi Liu, MS, Chicago, IL (Presenter) Nothing to Disclose

Amin Zarshenas, MSc, Chicago, IL (Abstract Co-Author) Nothing to Disclose

Laurie L. Fajardo, MD, MBA, Park City, UT (*Abstract Co-Author*) Consultant, Hologic, Inc; Scientific Advisory Board, Hologic, Inc; Consultant, Koninklijke Philips NV; Advisory Board, Koninklijke Philips NV; Consultant, Siemens AG; Consultant, FUJIFILM Holdings Corporation; Advisory Board, Galena Biopharma, Inc

Kenji Suzuki, PhD, Chicago, IL (*Abstract Co-Author*) Royalties, General Electric Company; Royalties, Hologic, Inc; Royalties, MEDIAN Technologies; Royalties, Riverain Technologies; Royalties, Toshiba Medical Systems Corporation; Royalties, Mitsubishi Corporation; Stockholder, Alara, Inc; Stockholder, AlgoMedica, Inc.; ; ; ; ; ; ; ;

## PURPOSE

To reduce cumulative radiation exposure and lifetime attributable risks for radiation-induced cancer from mammographic and tomographic screening, we developed PTNR for radiation dose reduction.

## **METHOD AND MATERIALS**

Our dose reduction technology based on PTNR was trained with input images and corresponding teaching images to convert the pixel values in patches in a given image to desired pixel values and obtain the entire image by a convolutional operation with the model. PTNR learns the relationship between low-dose (LD) and higher-dose (HD) images to convert new LD images to "virtual" higher-dose (VHD) images. We trained our technology with quarter-dose (25% of standard dose: 12 mAs at 32 kVp) tomosynthesis raw projection (RP) images and corresponding "teaching" HDRP (higher-dose raw projection) images (200% of standard dose: 99 mAs at 32 kVp) of a breast cadaver phantom acquired with a DBT system (Selenia Dimensions, Hologic, CA, U.S.). Once trained, our technique no longer requires HD images. It provides the images that look like HD images; thus term VHD. To determine a dose reduction rate, we acquired 4 sets of RP images of the phantom at 4 different radiation doses (1.35, 2.7, 4.04, and 5.39 mGy entrance dose). Structural SIMilarity (SSIM) index was used to evaluate the image quality. For testing, we collected half-dose (50% of standard dose: 30±10 mAs at 35±5 kVp) and full-dose (standard dose: 70±15 mAs at 35±5 kvp) images of 51 patients with the DBT system at Univ of Iowa Hospitals.

### RESULTS

Our PTNR technology was able to convert quarter-dose images (1.35 mGy; SSIM: 0.9911) of the breast cadaver to VHD images with the image quality (SSIM: 0.9972) equivalent to 90% dose images (4.8 mGy); thus, it achieved 72% dose reduction. The image quality of our VHD images of clinical cases was nearly equivalent to full-dose images. Our technology was able to reduce noise in half-dose images, while preserving microcalcifications and breast-tissue structures. The processing time for each breast was 5.1 sec. on a PC (Intel i7-4790K CPU, 4GHz).

# CONCLUSION

Our PTNR technology converted LD DBT images to VHD DBT images which were nearly equivalent to full-dose DBT images. Our phantom experiment demonstrated a potential 72% dose reduction.

# **CLINICAL RELEVANCE/APPLICATION**

Substantial radiation dose reduction would benefit patients by reducing the risk of radiation-induced cancer from DBT screening.

Value of Phantom Dosimetry to Estimate Patient Dose in Contrast-Enhanced Spectral Mammography (CESM)

Monday, Nov. 28 12:45PM - 1:15PM Room: PH Community, Learning Center Station #8

#### Participants

Jordana Phillips, MD, Boston, MA (*Presenter*) Nothing to Disclose Georgeta Mihai, PhD, Boston, MA (*Abstract Co-Author*) Nothing to Disclose Alexander Brook, PhD, Boston, MA (*Abstract Co-Author*) Nothing to Disclose Matthew R. Palmer, PhD, Boston, MA (*Abstract Co-Author*) Nothing to Disclose Da Zhang, PhD, Boston, MA (*Abstract Co-Author*) Investigator, Toshiba Medical Systems Corporation

#### PURPOSE

CESM is increasingly being used in clinical practice. As with all mammography systems, a reliable quality control program using phantom dosimetry is vital to successful implementation. However, it is currently unknown how phantom dosimetric measures compare with patient data for CESM. The purpose of this study is to compare average glandular dose (AGD) measured with phantoms with those in patients.

### **METHOD AND MATERIALS**

A phantom study using different simulated breast thicknesses on each of 3 different x-ray systems (GE 2D, GE CESM, and Hologic 2D +3D) was performed to measure the entrance skin exposure (ESE) and compare with reported ESE to calibrate the systems. Sixteen patients undergoing 4 view mammograms using each of the 3 systems between 2012-2016 were then identified. Reported ESE was recorded for each image. Phantom data was used to calibrate the reported ESE for patient images. As different vendors use different algorithms for AGD reporting, our study used the Dance model for calculating both phantom and patient AGD using the equation  $AGD = K^*g^*c^*s^*t$  (K is measured ESE [for phantom calculations], calibrated ESE [for patient calculations], and g, c, s and T are conversion factors determined from Monte Carlo simulation). Calibrated patient AGD (cAGD) and phantom measured AGD (pAGD) for CESM were compared to the other systems using a paired t-test.

## RESULTS

The mean ratio of differences between cAGD and pAGD for GE 2D and Hologic 2D and 3D are: is 1.01 + -.15, 1.25 + -.28, and 1.05 + -.17. The mean ratio is not significantly different from recently published data. For CESM, the mean ratio is 0.98 + -.27 (low energy) and 1.11 + -.23 (high energy). Figure 1 presents the mean ratios for all systems separated by breast thickness. Phantom dosimetry for low energy CESM was comparable to GE 2D but more accurate compared with Hologic 2D and Hologic 3D (p<.05). Phantom dosimetry for high energy CESM was comparable to Hologic 3D but was more accurate compared with GE 2D and Hologic 2D (p<.05). Phantoms did not correlate well with patient dose in thicknesses >80cm.

#### CONCLUSION

Phantom dosimetry may be useful for approximating patient dose for CESM as part of a quality control program.

## **CLINICAL RELEVANCE/APPLICATION**

Phantom dosimetry may be useful for approximating patient dose for CESM as part of a quality control program.

# What is the Influence of a 50% Dose Reduction on Mammographic Image Quality?

Monday, Nov. 28 12:45PM - 1:15PM Room: QS Community, Learning Center Hardcopy Backboard

### Participants

Wiesje Prins, MD, Arnhem, Netherlands (*Presenter*) Nothing to Disclose Hester van Hall, Arnhem, Netherlands (*Abstract Co-Author*) Nothing to Disclose Marijn P. Rolf, PhD, Arnhem, Netherlands (*Abstract Co-Author*) Nothing to Disclose Carla Meeuwis, Arnhem, Netherlands (*Abstract Co-Author*) Nothing to Disclose

# PURPOSE

Most women have to undergo frequent mammography's provided under the national breast cancer screening program. In The Netherlands all women between 50 and 75 years are called for a mammography every two years. The mean glandular dose varies between 0.7-1.6 mGy, depending on breast thickness, amount of glandular tissue and the mammographer system used. Estimated lifetime risk on developing lethal radiation-induced breast carcinoma, for women participating in the screening program is 1.6 of 100.000 women. This risk is higher in younger women and BRCA-mutation carriers.

The system used for screening mammography's in the Dutch breast cancer screening program is an Hologic Digital Mammographer. The system used in our hospital was a Philips MammoDiagnost DR.

The introduction of a new mammographer, the Philips MicroDose based on photon counting technology, was the background of this evaluation study. "What is the influence of the 50% dose reduction on image quality?"

## METHODS

Institutional review board of our center approved the research.

From May 2014 until February 2015 all women with previous mammography's made on the MammoDiagnost of the Hologic were asked to participate. Indications for diagnostic mammography were breast cancer follow-up, referral from the screening program and screening high-risk patients. The technical evaluation has been performed according to the Dutch Guidelines for the breast cancer screening program, which is basically identical to the European guidelines (EUREF).

Both, radiographers and radiologist filled in an evaluation form and scored the following items: 1) positioning of the breast for the MicroDose only, 2) visibility of skin contour and microcalcifications, breast composition categories (according to the new ACR-guidlines) for all three systems and overall impression compared with the MammoDiagnost/Hologic.

All women were asked about their experience with the MicroDose, in comparison with their previous experience with the MammoDiagnost/Hologic.

Also the doses (mGy) and breast thickness as reported in the header of both systems were reported.

# RESULTS

A total of 454 women were included, of these 218 women had previous breast surgery. The previous mammography was made with the MammoDiagnost in 422 women, the remaining 32 with Hologic.

Positioning of the breast was scored insufficient in 19, sufficient in 334 and good in 101 women. Reported problems in positioning of the breasts were mostly because of difficulties with positioning of large or operated breasts, but did not differ from the MammoDiagnost or Hologic.

Visibility of skin contour was rated as excellent 359, good/sufficient in 94 women and insufficient in one woman. Visibility of microcalcifications was excellent in 181 and good in 46 women. The remaining 227 women showed no microcalcifications at all. The average breast composition is 1.96 in MicroDose, 2.02 in MammoDiagnost (NS) and 2.41 in Hologic (NS).

Overall impression of the radiologists considering MicroDose in comparison to either MammoDiagnost or Hologic was better in 401 and comparable in 51 women. In two women the MicroDose was scored negatively, due to breast prosthesis. Not all breast prosthesis were scored negatively.

The experience of the women with the MicroDose was better than MammoDiagnost/Hologic in 71, worse in 41 and the remaining 342 women experienced no difference at all.

The mean glandular dose received with MicroDose was 0.84 mGy, comparing to 1.61-1.69 and 1.61 mGy in MammoDiagnost and Hologic respectively.

One year after the first visit 234 women had a follow-up mammography. In three women a recurrent breast carcinoma was found, all of these were not visible on both previous and current

mammography. Two women developed microcalcifications, both showed to be benign.

# CONCLUSION

The MicroDose system realizes a dose reduction of 50% compared to both the MammoDiagnost and Hologic systems, while retaining sufficient image quality.

In the Dutch breast cancer screening program the MicroDose system could be a replacement of the current Hologic mammographer, achieving significant dose reduction during the 25 years of screening.

Further more, in BRCA-mutation carriers and young women with positive family history who need frequent screening mammography's, the effect of the dose reduction is even more profound.

# Would You Pay To Wait? Our General Radiology Department's Journey to Direct Rooming of Patients

Monday, Nov. 28 12:45PM - 1:15PM Room: QS Community, Learning Center Hardcopy Backboard

#### Participants

Michelle Nordland, Rochester, MN (*Presenter*) Nothing to Disclose Shelly R. Champa, RT, Rochester, MN (*Abstract Co-Author*) Nothing to Disclose

## PURPOSE

To enhance our patient's experince by establishing a process for calling inpatients patients from thier rooms directly to radiology exam rooms Monday-Friday 7:00a.m. – 5:00 p.m. by November 1, 2015. In the process assisting Desk Operations with staffing concerns by reallocating 2 desk staff to a Radiology Command Center for use by other radiology modalities.

#### **METHODS**

Using our inpatient value stream map (VSM) to measure steps in the process, baseline data was collected by manually timing 25 inpatient visits to General Radiology the week of April 6-10, 2015. In addition to the quantitative data gleaned from the VSM, we also gathered qualitative data by surveying both our inpatients and the members of the units caring for those patients. After reviewing the quantitative and qualitative data during our weekly workgroup meeting, our team proceeded with a 6-3-5 brainstorming activity. We developed an affinity diagram with the ideas generated from the 6-3-5 to categorize our opportunities for improvement. From the affinity diagram an impact versus effort grid was completed to help the team prioritize ideas based on their impact to the process and effort to develop and put in place. The group identified the following factors contributing to the gap in our process: main desk was closing and there was no area to hold patients while the exam room was being prepped, delay in transporting patient back to their room after the exam, and an inability to track the patients electronically once General Radiology was ready for the patient. To assist the group in determining where to start each member of the team choose their top three ideas off of the affinity diagram and placed them on the impact vs. effort grid such as: utilizing the 'round trip' feature in our patient transport system, surveying high volume floors for preferred transport time, develop a radiology based transportation system, assign 1-2 exam rooms to provide 'quick' turn around, utilize a work flow coordinator, develop an on-line General Radiology inpatient schedule, and develop a new patient tracking and room utilization system

#### RESULTS

During the Improvement Phase, successive PDSA cycles were executed until a final recommendation for transporting patients directly to the exam was achieved. Due to the changes in the process, the group was able to reduce the average patient's total time in General Radiology from 13 minutes to 3 minutes. We were also able to completely eliminate an additional 7 minutes of patient wait time on the front end and 7 minutes on the back end of their visit by bypassing the Main Mary Brigh desk E and transporting the patients directly to the exam room. Through the successes of these multiple PDSAs a cohesive and working relationship was built between Desk Operations, General Service, and General Radiology team members. Utilization of a Lead work flow coordinator in collaboration with a centrally situated clinical assistant ensured open dialogue and orchestration of inpatients throughout the day. As a result of the efforts by this team, the process for calling patients directly to the exam room was spread to our secondary inpatient practice as well.

# CONCLUSION

On November 9th the process of transporting patients directly to the General Radiology exam rooms was made standard operating procedure for the General Radiology practice. In addition, the Lead work flow coordinator role and assigning technologists to our two high volume chest exams rooms were also implemented. The Lead technologist will be responsible for coordinating patient transport and technologist work flow on a day-to-day basis. The project resulted in a 23 minute reduction in patient's overall time in the General Radiology department.

Improving Breast MRI Wait Times: A Model for Transitioning Newly Implemented Diagnostic Imaging Procedures into Routine Clinical Operation

Monday, Nov. 28 12:45PM - 1:15PM Room: QS Community, Learning Center Station #1

# Participants

Colleen H. Neal, MD, Ann Arbor, MI (*Presenter*) Nothing to Disclose Glenn E. Houck Jr, MS, ARRT, Ann Arbor, MI (*Abstract Co-Author*) Nothing to Disclose Mitra Noroozian, MD, Ann Arbor, MI (*Abstract Co-Author*) Nothing to Disclose Ella A. Kazerooni, MD, Ann Arbor, MI (*Abstract Co-Author*) Nothing to Disclose Matthew S. Davenport, MD, Cincinnati, OH (*Abstract Co-Author*) Royalties, Wolters Kluwer nv; ;

# PURPOSE

Breast MRI for the detection of breast cancer has increased in use over the last decade. In our department, demand and volume for screening and diagnostic breast MRI had increased beyond available access resulting in prohibitively long wait times. We embarked on a quality improvement effort to increase patient access to breast MRI while maintaining image quality.

# METHODS

Institutional review board approval was waived for this HIPAA-compliant quality improvement (QI) initiative. This prospective longitudinal QI project was conducted from December 2014 through March 2016. A team comprised of a breast imaging radiologist, the health system MR manager, an MR supervisor, and the lead breast MR technologist was formed for this initiative. Breast MRI patient wait times, scheduling grids, and the radiologist and technologist staffing models were reviewed to identify root causes. Breast MRI wait times were tracked on a bi-weekly basis before and during the QI project as root causes were identified and action plans put in place. Bi-weekly wait times were tracked before and after implementation of action plans. Patient recall rates for additional MR imaging were tracked. In accordance with our institution's standards, wait time was defined as the length of time from order placement to the third available examination date.

# RESULTS

The root causes identified were: 1) small number of MRI technologists trained to perform breast MR examinations, and 2) required radiologist physical availability for monitoring breast MR examinations. The root causes prevented adding appointments after routine weekday hours of operation (e.g., evenings, weekends). We developed a plan to train additional MRI technologists in breast MRI across afternoon/evening and weekend shifts, and eliminated the requirement for physical presence by a breast imaging radiologist. Four breast MRI technologist trainees were selected by the MRI manager.A 17-item proficiency checklist was developed by the MRI supervisor and the breast imaging radiologist that included the following domains: 1) pre-scan assessment of the patient's last menstrual period, 2) proper external marking of areas of clinical concern, 3) proper positioning of the patient in the breast coil, 4) proper sequence and saturation technique, and 5) correct documentation following the scan. Technologist training to be completed before independent scanning was permitted included: 1) reviewing the breast MR protocol with the lead technologist and MR supervisor, 2) reviewing the expected proficiencies on the checklist, 3) scanning ≥10 breast MRI examinations under the direct supervision of an experienced breast MRI technologist, and 4) demonstrating proficiency to the MRI supervisor by independent completion of the items on the checklist. Additional training was conducted as needed. One month after the training began, the scheduling grid was expanded to weekend appointments; eight months later, the scheduling grid was expanded to weekday evenings.798 breast MRI examinations were performed during the study period, and monthly volume increased from 36 in December 2014 to 50 in March 2016 (range: 36-64). Wait time for a routine breast MRI fell from 101 days before implementation to 11 days at study completion (Figure 1; range: 5-101 days). Only one patient was recalled for repeat imaging during the study period, due to incorrect protocol assignment by the radiologist. The recall rate was 0.13% (1/798); no recall was performed for a technologistrelated error or scan quality concern.

## CONCLUSION

A new specialized MRI examination was transitioned into routine clinical operation while maintaining image quality, engaging employees, and developing imaging technologists and radiology leadership. A structured training plan with a proficiency checklist coupled with side-by-side scanning with an experienced technologist allowed us to offer breast MRI through the weekdays, evenings and weekends, improving patient access and decreasing wait times. This model may be useful for transitioning other newly implemented advanced diagnostic imaging examinations into routine clinical operation.

## **Honored Educators**

Presenters or authors on this event have been recognized as RSNA Honored Educators for participating in multiple qualifying educational activities. Honored Educators are invested in furthering the profession of radiology by delivering high-quality educational content in their field of study. Learn how you can become an honored educator by visiting the website at: https://www.rsna.org/Honored-Educator-Award/

Ella A. Kazerooni, MD - 2014 Honored Educator

## QS113-ED-MOB2

## Pay it forward- Improving Radiology Trainee Orientation through Feedback Driven Change

Monday, Nov. 28 12:45PM - 1:15PM Room: QS Community, Learning Center Station #2

#### **Participants**

Ankaj Khosla, MD, Dallas, TX (*Presenter*) Nothing to Disclose Jason W. Wachsmann, MD, Dallas, TX (*Abstract Co-Author*) Nothing to Disclose Viswanathan Venkataraman, MS, MENG, Dallas, TX (*Abstract Co-Author*) Nothing to Disclose Seth Toomay, MD, Dallas, TX (*Abstract Co-Author*) Nothing to Disclose Travis Browning, MD, Dallas, TX (*Abstract Co-Author*) Advisor, McKesson Corporation

#### PURPOSE

One of the greatest barriers to success in the early career of a radiologist is learning the information technology associated with radiology. Medical students are rarely exposed to the terms Picture Archive and Communication System (PACS), voice-recognition dictation, 3rd party imaging reconstruction application, and Radiology Information System (RIS); but are expected to understand these terms and proficiently utilize the associated technologies shortly upon entering radiology residency. Given the difficulties in transitioning to radiology and learning the associated radiology information technology, the technical orientation at our institution was restructured to give a more functional and useful experience.

### METHODS

Originally, radiology information technology orientation at our institution consisted of lectures. Didactic information was given regarding PACS, using the dictation software and accessing the electronic medical record. Additional didactics covering add-on applications (i.e. reconstruction tools) were included in the orientation as well. Following these presentations, residents participated in a 'hands on' tutorial proctored by designated 'superusers' with the aim of completing certain predetermined tasks with the superuser demonstrating to multiple residents on one workstation. An initiative was introduced to improve the orientation for incoming radiology residents. Residents involved in the orientation were surveyed on their opinions about the orientation (13 incoming residents) 1-2 months post orientation. Survey questions asked the residents about the effectiveness and usefulness of the orientation, and their level of preparedness for clinical rotations with questions on a 1-5 Likert scale. Open-ended questions were included asking for comments on improvement and which application orientations needed attention. The results of the survey were tabulated and individual comments assessed. From the results and comments, changes were made to subsequent orientations and subsequent trainees were resurveyed on their opinions about the orientations subsequently, for a total of 3 orientations.

### RESULTS

In the first iteration of the survey, 12 residents responded. The responses varied on the Likert scale, but the majority of the residents did not find didactic portion of the orientation helpful (2.4 average, with 1 being not helpful at all and 5 being extremely helpful). Additionally, a majority of residents did find the hands on portion beneficial (3.2, with 1 being not helpful and 5 being extremely helpful) but were neutral about how well prepared they were for the first day of work (2.9 average, with 1 not at all prepared and 5 as very well prepared). As a result of these responses, a number of changes were made to the orientation process. The didactic portion of the orientation, previously taking up half of the time, was shortened by half. Additionally, respondents had identified certain software applications that needed increased attention while others needing less. Adjustments were made in the didactic portion to accommodate these suggestions. Finally the hands on portion was given freer reign and residents were given more time to complete all of the suggested tasks on dedicated PACS workstation for each resident. A repeat survey was conducted after the second orientation. Respondents stated that the didactic presentations were more beneficial (average 2.9) and the changes in the hands on portion of the orientation received a positive response (average 4.5). Trainees felt better prepared for clinical service (average 3.1). Additionally, a number of trainees suggested that having a refresher course 1-2 months into training would be beneficial. A second overhaul of the orientation was performed including a change in the orientation room where trainees had access to their own individual computers. Didactic sessions were performed where trainees could follow along. The hands-onportion was changed to a follow along session on an individual PC, where a task would be performed and trainees would be given time to accomplish the task demonstrated. Superusers were available to assist the trainees as they underwent orientation. Finally, a refresher course 1 month following the training was given. Trainees responded positively to these changes with a large majority finding didactics beneficial (average 3.8) and the hands on portion helpful (4.3). Trainees felt more prepared for clinical service (average 3.4) and also found benefit from the refresher course (average 3.2).

# CONCLUSION

Radiology information technology can pose a challenge to a trainee's success initially in radiology residency. Utilizing hands on tools and involving trainees in feedback can create a more beneficial orientation session that allows for trainees to be well prepared for clinical service.

### QS114-ED-MOB3

Frequency of Recurrent CT Examinations among Patients with High Cumulative Dose and/or High Number of CT examinations

Monday, Nov. 28 12:45PM - 1:15PM Room: QS Community, Learning Center Station #3

# Participants

Maryam Bostani, PhD, Los Angeles, CA (*Presenter*) Research support, Siemens AG Katrina R. Beckett, MD, Pittsburgh, PA (*Abstract Co-Author*) Nothing to Disclose Banafsheh Salehi, MD, Los Angeles, CA (*Abstract Co-Author*) Nothing to Disclose Ali R. Sepahdari, MD, Los Angeles, CA (*Abstract Co-Author*) Nothing to Disclose Thomas Oshiro, PhD, Los Angeles, CA (*Abstract Co-Author*) Nothing to Disclose Christopher H. Cagnon, PhD, Los Angeles, CA (*Abstract Co-Author*) Nothing to Disclose Michael F. McNitt-Gray, PhD, Los Angeles, CA (*Abstract Co-Author*) Institutional research agreement, Siemens AG Research support, Siemens AG

### PURPOSE

The Joint Commission requires institutions to consider a patient's imaging history when determining the appropriateness of an imaging exam to avoid unnecessary duplication of studies. Radiation dose management software offers new opportunities to retrospectively identify patients who have undergone a large number of studies or who may have accumulated a large value of effective dose and review their imaging history to determine if recurrent CT exams occurred. Therefore, the purpose of this work was to use a radiation dose management system to retrospectively identify patients with high cumulative dose and/or large number of CT exams as a cohort in whom a detailed review of their imaging history was performed to identify recurrent CT Exams.

### METHODS

Using Radimetrics a total of 72073 CT examinations performed from Jan 2015 to Jan 2016 were studied to categorize patients with a cumulative effective dose of 100 mSv and above as well as highest number of CT examinations. Imaging histories of 20 patients (10 in each category) with highest cumulative dose and highest number of exams were further investigated by three radiologists for appropriateness of recurrent studies and potential opportunities for reducing the number of imaging studies and doses. The review process for each patient's imaging history was timed to assess the feasibility of a larger scale review study.

#### RESULTS

Out of 34762 patients, 2.7% were identified with a cumulative dose of 100 mSv and above. The 10 patients with the cumulative dose had values that ranged from 376 to 842 mSv, while the 10 patients with the largest number of CT examinations ranged from 25 to 55 CT exams. Most patients in the highest cumulative dose category were oncology patients who had undergone ablation procedures, while most patients in the largest number of examinations group were head trauma patients. An imaging history review of these patients only identified two possible CT scan that could have been avoided. As per radiologist's review, one of the scan was performed to assess liver transplant vessel patency, which may be more appropriately assessed with ultrasound as the initial imaging modality. Additionally, a technical factor analysis identified certain CT guided interventional protocols where dose reduction could be achieved by simply using lower mAs values for repeated scans that can tolerate lower image quality. Radiologists reported an average of 20 min per patient for their review process.

### CONCLUSION

With the introduction of dose management software, institutions now have access to heretofore untapped patient dose data that can be analyzed for opportunities to improve clinical practice. Retrospective review of all exams for appropriateness can be challenging, is time consuming and presents a difficult, ongoing problem for the institution. Analysis of the root causes of large numbers of scans or a large number of high dose scans can be very complicated and difficult to discern given clinical practices. During our Investigation we learned valuable lessons that are not necessarily obvious or not openly discussed and worth sharing with others. In our analysis, we investigated patients with the highest cumulative dose and highest number of examinations. Usually these patients are critically ill patients who cannot be evaluated by just knowing their history and performing physical exams due to being intubated and sedated; others are patients with advanced staged cancer who need periodic restaging scans and in some cases frequent CT guided ablation procedures to improve guality of life. The probability of coming across any scans that could have been avoided among these kinds of patients is very low, not only because of their physical status, but also because transporting these patients to the radiology department can be challenging. Such scans are therefore not usually ordered unless absolutely necessary. Future studies should carefully select patient populations to be reviewed separate from the population of severely ill patients and oncologic patients. Future studies may focus on a specific CT procedure, or a specific patient population. There are still lessons learned in this study that can be implemented to reduce radiation dose. Although most of reviewed patients were extremely ill patients, scans performed to check for positioning of tubes and devices can be performed at lower mAs values. Reducing radiation dose should be a common practice regardless of patient's prognosis. Additionally, the review process itself has suggested areas for potential improvement in patient care, including improved documentation and Radiologist involvement in patient management. Under ideal circumstances radiologists would protocol all ordered studies and decide on the most appropriate type of imaging exam, but in many current practices the volume and workflow demands are such that occasionally indications that may have been better assessed by a different modality slip through and are inadvertently performed.

# QS115-ED-MOB4

# Designing Imaging for Primary Care: Serving the Needs of Our Community Partners

Monday, Nov. 28 12:45PM - 1:15PM Room: QS Community, Learning Center Station #4

#### **Participants**

Karen Weiser, MBA, Toronto, ON (*Presenter*) Nothing to Disclose Corwin Burton, Toronto, ON (*Abstract Co-Author*) Nothing to Disclose Jennifer Catton, Toronto, ON (*Abstract Co-Author*) Nothing to Disclose Christina Ciapanna, MBA, Toronto, ON (*Abstract Co-Author*) Nothing to Disclose Paul Cornacchione, BSC, Toronto, ON (*Abstract Co-Author*) Nothing to Disclose Ravi Menezes, PhD, Toronto, ON (*Abstract Co-Author*) Nothing to Disclose Heidi C. Schmidt, MD, Toronto, ON (*Abstract Co-Author*) Nothing to Disclose Catherine Wang, BSC, Toronto, ON (*Abstract Co-Author*) Nothing to Disclose

### PURPOSE

Hospital-based imaging has traditionally been designed to serve inpatients and specialist physicians, often overlooking the needs of patients in the community and their primary care providers (PCP). This has resulted in challenges for PCPs to effectively navigate the system and select the most appropriate imaging intervention required to manage their complex, diverse patient populations. In response to these challenges, the "Designing Imaging for Primary Care" project was launched to redesign a sub-specialized imaging department to better serve the unique requirements of primary care through improved integration with radiology. Through focused discussions, education sessions, and surveys, PCPs identified barriers to hospital-based imaging which have led them to refer patients to emergency departments or private imaging providers to expedite imaging. To address common challenges, services were collaboratively redesigned based on the following goals: Streamline referral process, removing barriers to entry Provide convenient high quality imaging Create bi-directional communication between community primary care providers and sub-specialized radiologists Ensure appropriate care by providing integrated support for primary care

#### **METHODS**

The medical imaging department partnered with two PCP groups:i) 120 solo-practicing PCPs who were enrolled in an existing program that provides navigational and consultation support through a virtual interprofessional hubii) 15 PCPs who belong to a group practice. A team of clinical and administrative staff from the imaging department engaged these PCPs to better understand the challenges they experienced with hospital-based imaging. Emphasis on the provision of convenient and timely imaging resulted in the phased implementation of the following services: **Medical Imaging Call Centre:** Staffed during business hours by clerical staff and an on-call radiologist to enable real-time support in selecting the most appropriate imaging, providing a second opinion on images and reports, and general navigation. A database was used to collect data including caller and service accessed through the call centre. **Same Day Imaging/Walk-Ins:** Patients with completed requisitions could access imaging without appointments for ultrasound, x-ray, and nuclear medicine. Data was captured in the department's Radiology Information System. Weekly reports tracked volumes and trends to trigger operational changes required to accommodate changing demand. **MRI Standby List:** Patients who wanted to be contacted on short notice (as few as 4 hours), were given the option of being placed on an MRI standby list. These patients were called for appointments when MRI slots became available due to last minute cancellations. Data was captured in the department's Radiology Information System, and monthly reports allowed tracking of volumes and wait times for imaging.

# RESULTS

1. Medical Imaging Call Centre (April 1, 2015 – March 31, 2016) (See Figure 1)353 calls (monthly median: 31 calls) 35% requests for information/other 32% urgent imaging 18% radiology consultations 8% appropriateness consultations 7% expedited reports2. Same Day Imaging (June 1, 2015 – February 29, 2016)(See Figure 2)618 Ultrasounds (monthly median: 84) Min: 28 per month Max: 104 per month812 X-rays (monthly median: 83) Min: 55 Max: 1215 Nuclear Medicine exams (monthly median: 0) Min: 0 per month Max: 3 per month3. MRI Standby List (December 1, 2015 – January 31, 2016)n= 38 patientsWait time - ordered to performed (90th percentile): 42 daysBaseline wait time (90th percentile): 71 days

# CONCLUSION

In the past, many initiatives aiming to improve the PCP experience were developed without primary care input. By creating an ongoing partnership that regularly engaged PCPs and responded directly to their feedback, this project enhanced services for the community. By offering a value proposition that resonated with the PCPs, the imaging department achieved a 165% increase in referrals from these partners over the course of one year (cumulatively across all modalities) (See Figure 3).Bi-directional communication and ability to trial and modify solutions have proven to be invaluable in this partnership. When uptake of the same day nuclear medicine was minimal, the imaging team sought to understand why. Feedback from PCPs revealed that they required additional information regarding indications and appropriate referrals. In response, the imaging department began to offer a lecture series on advanced imaging. Other communication tools such as guidelines for special preparation have been created. The department continues to gather feedback from the community to identify future opportunities for further integration. As services expand, evaluation of both patient and referring PCP experience will be crucial to measure impact and sustainability

# RO216-SD-MOB2

Patterns of Failure in Glioblastoma Multiforme Following Standard (60 Gy) or Short-course (40 Gy) Radiation and Concurrent Temozolomide

Monday, Nov. 28 12:45PM - 1:15PM Room: RO Community, Learning Center Station #2

# Participants

Miyu Mizuhata, MD, Kanazawa city, Japan (*Presenter*) Nothing to Disclose Shigeyuki Takamatsu, MD, PhD, Kanazawa city, Japan (*Abstract Co-Author*) Nothing to Disclose Tomoyasu Kumano, Ishikawa, Japan (*Abstract Co-Author*) Nothing to Disclose Shinji Fujita, MD, kanazawa city, Japan (*Abstract Co-Author*) Nothing to Disclose Yoko Taima, MD, Kanazawa city, Japan (*Abstract Co-Author*) Nothing to Disclose Mikoto Nakagawa, MD, Kanazawa city, Japan (*Abstract Co-Author*) Nothing to Disclose Toshifumi Gabata, MD, PhD, Kanazawa, Japan (*Abstract Co-Author*) Nothing to Disclose

# PURPOSE

To analyze the patterns of failure in patients with glioblastoma multiforme (GBM) that were treated with standard (St; 60 Gy/30 fractions) or short-course (Sc; 40 Gy/15 fractions) radiation therapy and concurrent temozolomide.

# METHOD AND MATERIALS

Thirty-one consecutive patients with newly diagnosed glioblastoma that were treated at our hospital between 2007 and 2015, were included. All patients underwent complete surgical resection followed by St (n=15) or Sc (n=16) with concurrent temozolomide. We analyzed the failure pattern in 31 patients who underwent a radical course of radiotherapy and chemotherapy with gadolinium-enhanced post-operative magnetic resonance imaging. The chi-square test was used to analyze the associations between the tumor recurrence pattern and the type of treatment.

## RESULTS

We found that after St recurrences occurred at the resection margin alone in 11 of 15 (73%) patients, only at distant sites in 1 of 15 (7%) patients, and at both the resection margin and distant sites in 3 of 15 (20%) cases. After Sc, recurrences occurred at the resection margin alone in 12 of 16 (75%) patients, only at distant sites in 1 of 16 (6%) patients, and at both the resection margin and distant sites in 1 of 16 (6%) patients, and at both the resection margin and distant sites in 1 of 16 (6%) patients, and at both the resection margin and distant sites in 3 of 16 (19%) cases.

### CONCLUSION

There was no differences in the tumor recurrence pattern between the two protocols.

### **CLINICAL RELEVANCE/APPLICATION**

Patterns of failure in glioblastoma multiforme following standard (60 Gy) or short-course (40 Gy) radiation is not different with concurrent temozolomide.

# Analysis of Risk Factors and Treatment Outcome in Adult Patients with Brainstem Glioma

Monday, Nov. 28 12:45PM - 1:15PM Room: RO Community, Learning Center Station #4

#### Awards

#### **Student Travel Stipend Award**

#### Participants

Kailin Yang, PhD, Cleveland, OH (Presenter) Nothing to Disclose

# ABSTRACT

Purpose/Objective(s): Brainstem glioma (BSG) is much more rare and heterogeneous in adults compared to pediatric population. The maturation of MRI-guided biopsy has enabled more definitive diagnosis of BSG. Clinical outcome of this type of brain tumor remains poor despite aggressive treatment. We aim to analyze the effect of radiation therapy (RT) and surgery on survival outcome of BSG in an adult population. Materials/Methods: Adult patients of age 19 or older with the diagnosis of BSG were identified from the NCI Surveillance, Epidemiology, and End Results (SEER) database (1973-2012). Information for the status of radiation therapy was obtained. Surgical treatment was categorized into no surgery, subtotal resection (STR), and gross total resection (GTR). Demographic and clinicopathological predictors were analyzed using chi-square test, t-test, and logistic regression modeling. Kaplan-Meier analysis and multivariate Cox proportional hazard modeling were used to assess the impact of treatment on overall survival (OS).Results:1667 adult patients with BSG were identified. 54.6% were males, and 83.1% were Caucasian. The median age was 45.5 years. 67.5% of patients received RT. Surgery was only performed in a small subset of patients with 7.4% receiving STR and 6.4% receiving GTR. 12.1%, 13.3%, 10.3%, and 18.1% were diagnosed with WHO grade I, II, III, and IV glioma respectively, with the rest of unknown grade status. OS at 10 years was 26.8%, with a median follow-up time of 9.7 years. Advanced age and high WHO grade were associated with poor OS, with 8.9% for age 75+ and 10.3% for grade IV at 10 years respectively. There was no significant OS benefit with RT for grade III (18.9% with RT vs. 18.4% without RT, p=0.94), but improved OS with RT for grade IV (12.1% with RT vs. 3.39% without RT, p=0.03). However, worse OS was observed with RT for grade I (50.0% with RT vs. 77.3% without RT, pConclusion: The overall outcome of high-grade adult BSG remains poor though RT provides benefit on OS for grade IV tumors, keeping in mind possible bias in offering RT to patients with worse prognosis. GTR is associated with improved survival in a subset of patients. More definitive diagnosis and grading of adult BSG would guide improved management strategy. Given the unfavorable survival of high-grade BSG, more specific therapeutic regimen targeting the underlying genetic aberration is needed to improve patient outcome.

## Cervical Cancer Treatment Outcomes in a Public Safety Net Hospital and Association with Race

Monday, Nov. 28 12:45PM - 1:15PM Room: RO Community, Learning Center Station #6

#### Participants

Suisui Song, MD, Elgin, IL (Presenter) Nothing to Disclose

# ABSTRACT

Purpose/Objective(s): Race and socioeconomic status (SES) are both independently associated with cervical cancer survival, with Hispanics and African Americans patients and patients in lower SES showing worse survival. This study aims to explore association between race and treatment outcomes among patients with cervical cancer treated in a public safety net hospital setting, where non-white patients comprises the majority. Materials/Methods: We retrospectively reviewed 49 patients with locally advanced cervical cancer treated consecutively from April 2013 to December 2014 in a public safety net hospital. All patients received concurrent chemoradiation followed by high dose rate brachytherapy boost as a curative treatment. Median follow up was 10 months. The primary study outcome measures were locoregional failure (LF), distant failure (DF), and failure-free survival (RFS), which were calculated using Kaplan-meier method. Results: Median age was 51. 71% were squamous cell histology. Median tumor size was 6cm. Stage distribution were 16 patients with stage IB (33%); 19 patients with stage II (39%); 11 patients with stage III (22%), and 3 patients with stage IV (6%). 49% of patients had node positive disease. Racial distribution for the entire cohort were 3 black (6%), 30 Hispanics (61%), 15 Asians (31%), and 1 white (2%). There was no significant differences in stage distribution, node positivity, tumor histology, or tumor size among the different races. LF, DM, and any failure rates for the entire cohort were 18%, 20%, and 30%, respectively. There was more LF in Asians vs. Hispanics patients (33% v 10%, p=0.04). 1y LF free survival, DF free survival, and RFS for the entire cohort were 83%, 80%, and 70%, respectively. Asians vs Hispanics patients had a significantly worse 1y LF free survival and RFS: 72% v 91% (pConclusion: Our study shows that in our public safety net hospital, the Asian patients with locally advanced cervical cancer had a significantly higher LF and worse 1y LF free survival than Hispanic patients, despite a similar stage distribution and tumor characteristics. Longer follow up will be needed to see if this result would hold.

# UR119-ED-MOB7

# Penile Ultrasound, Is It Useful?

Monday, Nov. 28 12:45PM - 1:15PM Room: GU/UR Community, Learning Center Station #7

#### **Participants**

Paula Gallego Ferrero, MD, Santander, Spain (*Presenter*) Nothing to Disclose Alejandro Fernandez Florez, MD, Santander, Spain (*Abstract Co-Author*) Nothing to Disclose Beatriz Garcia Martinez, BDS, Santander, Spain (*Abstract Co-Author*) Nothing to Disclose Victor Fernandez Lobo, Santander, Spain (*Abstract Co-Author*) Nothing to Disclose Marta Drake Perez, MD, Santander, Spain (*Abstract Co-Author*) Nothing to Disclose Elena Yllera Contreras, MD, Santander, Spain (*Abstract Co-Author*) Nothing to Disclose Gerardo Lopez Rasines, MD, Santander, Spain (*Abstract Co-Author*) Nothing to Disclose

## **TEACHING POINTS**

To revise the anatomical characteristics of the penis and its normal ultrasound (US) appearance. To recognize and illustrate the sonographic features of penile pathologies and their differential diagnosis.

### **TABLE OF CONTENTS/OUTLINE**

Ultrasound normal anatomy of the penis. Penile pathologies and their sonographic findings: Inflammatory diseases: Peyronie's disease, infection. Vascular diseases: Mondor's disease, sclerosing lymphangitis. Neoplastic diseases: primary and metastatic penile and urethral tumors. Erectile dysfunction treatment (intracavernosal injections of vasoactive agents) evaluation. Penile trauma: penile fractures, hematomas. Main teaching point: sonography is a basic tool in the evaluation of penile pathologies, beacause of its 24/7 availability, non invasive character and great diagnosis ability.

# Hepatic Imaging Following Intra-arterial Embolotherapy

Monday, Nov. 28 12:45PM - 1:15PM Room: VI Community, Learning Center Station #7

#### Participants

Joseph R. Kallini, MD, Detroit, MI (Presenter) Nothing to Disclose

Frank H. Miller, MD, Chicago, IL (Abstract Co-Author) Research Grant, Siemens AG

Ahmed Gabr, MD, MBBCh, Chicago, IL (Abstract Co-Author) Nothing to Disclose

Riad Salem, MD, MBA, Chicago, IL (Abstract Co-Author) Research Consultant, BTG International Ltd Research Grant, BTG International Ltd

Robert J. Lewandowski, MD, Chicago, IL (*Abstract Co-Author*) Advisory Board, BTG International Ltd; Advisory Board, Boston Scientific Corporation; Consultant, Cook Group Incorporated; Consultant, ABK Medical Inc

## **TEACHING POINTS**

(1) To discuss salient findings on cross-sectional imaging of hepatocellular carcinoma treated with different forms of intra-arterial embolotherapy (e.g. chemoembolization and ytrrium-90 radioembolization).(2) To discuss size-based tumor response criteria (WHO and RECIST), necrosis/enhancement criteria (EASL and mRECIST), and the limitations of each.

## TABLE OF CONTENTS/OUTLINE

OVERVIEW OF INTRA-ARTERIAL PROCEDURES Bland embolization and trans-arterial chemoembolization Trans-arterial radioembolization POST-PROCEDURAL IMAGING MODALITIES General Considerations Computed Tomography Magnetic Resonance Imaging and Diffusion Weighted Imaging Fluorodeoxyglucose-Positron Emission Tomography (FDG-PET) Contrast-Enhanced Ultrasonography MEASURES OF TREATMENT RESPONSE Limitations of current tumor response criteria European Association for the Study of the Liver Guidelines (EASL) Modified RECIST criteria (mRECIST) Three-dimensional volumetric methods Primary Index Lesion Tumor markers IMAGING FINDINGS AFTER INTRA-ARTERIAL THERAPY Trans-arterial embolization and chemoembolization Trans-arterial radioembolization CONCLUSION

# **Honored Educators**

Presenters or authors on this event have been recognized as RSNA Honored Educators for participating in multiple qualifying educational activities. Honored Educators are invested in furthering the profession of radiology by delivering high-quality educational content in their field of study. Learn how you can become an honored educator by visiting the website at: https://www.rsna.org/Honored-Educator-Award/

Frank H. Miller, MD - 2012 Honored Educator Frank H. Miller, MD - 2014 Honored Educator Does Preserved Peripheral Portal Vein Patency have an Impact on Survival in Patients with Advanced-stage HCC and Portal Vein Thrombosis treated with TACE?

Monday, Nov. 28 12:45PM - 1:15PM Room: VI Community, Learning Center Station #1

#### Awards

### **Student Travel Stipend Award**

#### **Participants**

Boris Gorodetski, MD, Berlin, Germany (Presenter) Nothing to Disclose

Julius Chapiro, MD, New Haven, CT (Abstract Co-Author) Research Grant, Koninklijke Philips NV

Ming De Lin, PhD, Cambridge, MA (Abstract Co-Author) Employee, Koninklijke Philips NV

Bernhard Gebauer, MD, Berlin, Germany (*Abstract Co-Author*) Research Consultant, C. R. Bard, Inc; Research Consultant, Sirtex Medical Ltd; Research Grant, C. R. Bard, Inc; Research Consultant, PAREXEL International Corporation; Travel support, AngioDynamics, Inc

Jean-Francois H. Geschwind, MD, Westport, CT (*Abstract Co-Author*) Consultant, BTG International Ltd; Consultant, Bayer AG; Consultant, Guerbet SA; Consultant, Sterigenics International LLC; Consultant, Koninklijke Philips NV; Consultant, Jennerex Biotherapeutics, Inc; Grant, BTG International Ltd; Grant, Bayer AG; Grant, Koninklijke Philips NV; Grant, Sterigenics International LLC; Grant, Threshold Pharmaceuticals, Inc; Grant, Guerbet SA; Founder and CEO, PreScience Labs, LLC

### PURPOSE

Our study sought to evaluate the impact of preserved peripheral portal vein patency (PVP) on the outcome of patients with hepatocellular carcinoma (HCC) and portal vein thrombosis (PVT) treated with trans-arterial chemoembolization (TACE).

### **METHOD AND MATERIALS**

This retrospective analysis included a total of 74 HCC patients with PVT who were treated either with conventional (N=50) or drugeluting beads (N=24) TACE. Patients with a Child-Pugh score (CP) of C, a tumor burden >50% and extrahepatic metastasis were excluded. PVP was defined as patent (N=10) if the portal vein on segmental level was opacified on both lobes on baseline contrastenhanced MR or CT imaging and non-patent (N=64) if at least one segmental vein was not opacified. The extent of PVT has been categorized as a) 2. order only (N=8), b) 1. order only (N=7), c) main + 1. order (N=44), d) main + hepatic vein (N=9) and e) 1. order + hepatic vein (N=6). A Kaplan-Meier survival analysis for PVP was performed. A Cox proportional hazard regression model for time to death and PVP was adjusted for other covariates as potential confounders.

### RESULTS

The demographics were as follows: CP A [N=37 (50%)], Eastern Cooperative Oncology Group performance status [ECOG PS 0,1-2,>2; N=21 (28.4%), N=49 (66.2%), N=4 (5.4%), respectively] infiltrative tumor type [N=43 (58.1%)], bilobar tumor infiltration [N=59 (79.7%)] and tumor diameter >5cm [N=61 (82.4%)]. The median overall survival was 13.1 (95% CI, 9.7-n/a) and 6.1 (95% CI, 4.0-12.7) months for patent and non-patent PVP, respectively. In the Cox hazard regression analysis PVP (patent vs. non-patent; HR, 0.15; p=0.014), ECOG PS (>2 vs. 0-2; HR, 6.4, p=0.017) and PVT localization (main + hepatic artery vs. rest; HR, 2.6; p=0.047) were identified as independent predictive factors.

## CONCLUSION

In patients with CP A/B, tumor burden  $\leq$ 50% and without extrahepatic metastasis patent PVP is a prognostic factor for prolonged survival. An ECOG PS >2 and the simultaneous invasion of the main portal and hepatic vein are poor prognostic factors for survival.

## **CLINICAL RELEVANCE/APPLICATION**

Preserved peripheral portal vein patency has a beneficial impact on survival in patients with HCC and PVT treated with TACE.

The Development of Double Balloon Catheter for Bleeding Control in Patients with Placenta Accreta during Cesarean Hysterectomy, in a Swine Model

Monday, Nov. 28 12:45PM - 1:15PM Room: VI Community, Learning Center Station #2

# Participants

Hiroshi Kondo, MD, Tokyo, Japan (*Abstract Co-Author*) Nothing to Disclose Masayoshi Yamamoto, MD, Tokorozawa, Japan (*Presenter*) Nothing to Disclose Yukichi Tanahashi, MD, Tokyo, Japan (*Abstract Co-Author*) Nothing to Disclose Marie Osawa, Tokyo, Japan (*Abstract Co-Author*) Nothing to Disclose Takahiro Yamamoto, Tokyo, Japan (*Abstract Co-Author*) Nothing to Disclose Shigeru Furui, MD, Itabashi-Ku, Japan (*Abstract Co-Author*) Nothing to Disclose

# PURPOSE

Life-threatening hemorrhage often occurs in cases of placenta percreta during cesarean section. Temporary balloon occlusion of the iliac artery is one potential therapy to control bleeding during cesarean delivery in patients with placenta accreta. However, it is controversial where the balloon catheter should be positioned, especially, common iliac artery (CIA) or internal iliac artery (IIA). To resolve this matter, we have developed a double balloon catheter which can occlude CIA, IIA or both.

### **METHOD AND MATERIALS**

A 6Fr diameter double balloon prototype catheter was developed. The balloons were located 30mm and 70mm from the tip of catheter. The experiment was performed on a swine. The balloon catheters were inserted and placed in the branch of external iliac artery. The distal and proximal balloons were located in the branch of external iliac artery and the external iliac artery, respectively. The pressure of the tip of catheter, side hole located between double balloons, and systemic blood pressure were monitored before and after the inflation of each balloon and both.

#### RESULTS

No balloon rupture, catheter migration and embolism of the lower extremities were experienced. The arterial pressure of the tip of catheter was decreased 37.1%, 31.2% and 30.9% with the inflation of both, proximal and distal balloon, respectively. That of side hole was decreased 39.6%, 32.7% and 1.9% with the inflation of both, proximal and distal balloon, respectively.

## CONCLUSION

The double balloon occlusion might be more efficient to decrease the blood flow of the branch of external iliac artery than previous balloon occlusion procedure.

## **CLINICAL RELEVANCE/APPLICATION**

The double balloon catheter is safe and can occlude the iliac artery more consistently and efficiently, compared with conventional single balloon catheter.

Ultrasound for DVT - is a Repeat Examination Necessary? Data from 9623 Examinations at a Single Institution

Monday, Nov. 28 12:45PM - 1:15PM Room: VI Community, Learning Center Station #3

#### Awards

### **Student Travel Stipend Award**

#### Participants

Flora C. Daley, BMBS, Cambridge, United Kingdom (*Presenter*) Nothing to Disclose Janette Smith, MBBChir, Cambridge, United Kingdom (*Abstract Co-Author*) Nothing to Disclose Annie Davenport, Cambridge, United Kingdom (*Abstract Co-Author*) Nothing to Disclose Caroline Lewis, Cambridge, United Kingdom (*Abstract Co-Author*) Nothing to Disclose Ann Taylor, Cambridge, United Kingdom (*Abstract Co-Author*) Nothing to Disclose Gillian O'Brien, Cambridge, United Kingdom (*Abstract Co-Author*) Nothing to Disclose Edmund M. Godfrey, MBBCh, FRCR, Cambridge, United Kingdom (*Abstract Co-Author*) Nothing to Disclose

### PURPOSE

Patients with suspected deep venous thrombosis (DVT) are imaged with ultrasound (US). If the exam is negative, patients are imaged again after a short interval to exclude a missed or propagating thrombus. The aim of this study was to assess the incidence of DVT at the primary and secondary US and evaluate if these rates vary across different "at risk" groups.

### **METHOD AND MATERIALS**

A database of patients referred to an ambulatory thrombosis service at a large tertiary center was interrogated to identify patients presenting with suspected DVT between January 2008 and November 2015. Demographics, symptoms, risk factors (recent surgery or trauma, current infection, pregnancy or recent delivery, malignancy, history of DVT or intravenous drug use (IVDU)) and the US results were recorded. US comprised of compression ultrasonography of the proximal lower limb veins. Patients were selected for a repeat US on the basis of a raised d-dimer, strong clinical suspicion of DVT or a high Wells' score. The incidence, odds ratio (OR), 95% confidence interval and P-value for each group was calculated for each ultrasound.

#### RESULTS

7314 patients underwent an initial US. A DVT was detected in 14.4% (Male 52%, mean age 67 yrs). The highest incidence of DVT found at initial US was in the IVDU group (63.9%, OR 13.17; 95% c.i. 26.14 to 6.63, p<0.001) followed by patients with malignancy (36.2%, OR 4.22; 95% c.i. 5.82 to 3.06, p<0.001). Patients with current infection had the lowest incidence (3.7%, OR 0.28; 95% c.i. 0.48 to 0.17, p<0.001). 2309 patients had a repeat US with a 2.3% incidence of DVT. The highest incidence was observed in patients with malignancy (8.8%, OR 5.63; 95% c.i.19.51 to 1.63, p=0.006) and in those with a past history of DVT (6.1%, OR 3.75; 95% c.i. 6.88 to 2.05, p<0.001).

# CONCLUSION

Patients with clinical signs or symptoms of DVT should be referred for US. In selected patients, a repeat US after 7-14 days should be used to exclude missed or propagating thrombus. The overall incidence of DVT at repeat US was 2.3%, but in patients with a history of previous DVT or malignancy, it was 6.1% and 8.8% respectively.

# **CLINICAL RELEVANCE/APPLICATION**

This data confirms the importance of a repeat US in selected patients with suspected DVT. Further research to improve selection of patients who would benefit most from a repeat ultrasound is required.

Combined Effect of GNRH Agonist Therapy and Uterine Artery Embolization in Symptomatic Uterine Fibroids: MRI Evaluation of the Necrotic Area Reabsorption Time and Clinical Outcome after 2 Years

Monday, Nov. 28 12:45PM - 1:15PM Room: VI Community, Learning Center Station #4

# Participants

Fernando Smaldone, MD, L'Aquila, Italy (*Presenter*) Nothing to Disclose Francesco Arrigoni, Coppito, Italy (*Abstract Co-Author*) Nothing to Disclose Fabiana Ferrari, MD, LAquila, Italy (*Abstract Co-Author*) Nothing to Disclose Sonia Iafrate, LAquila, Italy (*Abstract Co-Author*) Nothing to Disclose Carlo Masciocchi, MD, L'Aquila, Italy (*Abstract Co-Author*) Nothing to Disclose Ilaria Capretti, L Aquila, Italy (*Abstract Co-Author*) Nothing to Disclose

### PURPOSE

To evaluate the combined effects of gonadotropin-releasing hormone (GnRH) agonists therapy and UAE for a faster reabsorption time in women affected by symptomatic uterine fibroids

# METHOD AND MATERIALS

We treated 42 women (mean age, 41 years) affected by symptomatic uterine fibroids. We divided our patients into two groups: 17/42 women were submitted to GnRH-agonists therapy after 1 month from the treatment (Group A); 25/42 did not receive any therapy after UAE (Group B).All patients were submitted to c.e. MRI to evaluate the necrotic area extension after 1 month and 2 years to assess the different reabsorption time of the necrotic area. The variation of symptomatology was assessed using the SSS-Questionnaire after 2 years

### RESULTS

The mean value of necrotic area extension was 94.5%. After 2 years from UAE, in the group A, 11/17 patients (64.7%) showed faster necrotic area reabsorption with a mean value of 85%; in six out of 17 women (35.3%) reabsorption of 65% was observed. After 2 years, in the group B, 17/25 (68%) showed a mean value of necrotic area reabsorption of 60%; only 8/25 patients (32%) showed a reabsorption of the necrotic area of 85%. All patients did not complain of significant complications and presented a similar improvement of symptomatology after 2 years.

# CONCLUSION

GnRH-agonists after UAE treatment can be a useful therapy to promote a faster reabsorption of necrotic area with a consequent recovery of the uterine wall.

# **CLINICAL RELEVANCE/APPLICATION**

The use of GnRH agonists in association to UAE treatment seems to reduce the reabsorption time of the necrotic area with good improvement of symptomatology

# Percutaneous Image-Guided Cryoablation of T1 Renal Cell Carcinoma: Outcomes in 285 Patients

Monday, Nov. 28 12:45PM - 1:15PM Room: VI Community, Learning Center Station #5

#### Awards

### **Student Travel Stipend Award**

### **Participants**

Farzad Sedaghat, MD, Boston, MA (*Presenter*) Nothing to Disclose Kemal Tuncali, MD, Boston, MA (*Abstract Co-Author*) Nothing to Disclose Paul B. Shyn, MD, Boston, MA (*Abstract Co-Author*) Research Consultant, Galil Medical Ltd; Research Grant, Siemens AG Servet Tatli, MD, Boston, MA (*Abstract Co-Author*) Nothing to Disclose Vincent M. Levesque, MA, Boston, MA (*Abstract Co-Author*) Nothing to Disclose Stuart G. Silverman, MD, Brookline, MA (*Abstract Co-Author*) Author, Wolters Kluwer nv

## PURPOSE

To describe our 13-year experience and outcome of image-guided percutaneous cryoablation of T1 renal cell carcinomas.

## **METHOD AND MATERIALS**

285 patients, 180 (65%) males, 105 (37%) females, 38-92 yrs, (mean 66.8 yrs) with solitary renal cell carcinomas were treated with percutaneous image-guided cryoablation from August 1, 2000 through December 31, 2013. Lesions (260 T1a , 25 T1b, median size 2.5 cm, range, 0.6 - 6.5 cm), were ablated using one to seven (median three) cryoprobes. CT (n=155) or MRI (n=130) was utilized for imaging-guidance and iceball monitoring. In selected cases, adjacent normal structures were displaced from the treatment site by percutaneous instillation of saline and/or manual displacement of bowel. MRI was obtained at 24 hrs to assess for early complications. In addition to a review of the medical record, MRIs were repeated at 3 to 6 month intervals for the first year, and every 6 to 12 months thereafter (median 26 mos; range 3-143 mos) to assess for treatment efficacy and additional complications.

### RESULTS

Primary efficacy was 97.8%; all recurrences were successfully treated. Overall complication rate was 14%, including 9 CTCAE grade 1 (e.g., pain, perinephric hematoma), 17 grade 2 (e.g., myoglobinemia, urinary retention), 11 grade 3 (e.g., UTI, anemia, pneumonia), and 3 grade 4 complications (CVA, aspiration pneumonia, hypertensive emergency).

### CONCLUSION

Percutaneous image guided cryoablation of T1 renal cell carcinoma resulted in highly successful intermediate to long term outcomes.

### **CLINICAL RELEVANCE/APPLICATION**

Image-guided cryoablation is clinically efficacious and a viable alternative to partial nephrectomy.

Digital Breast Tomosynthesis Guided Biopsy Procedures: Why Now and How

Tuesday, Nov. 29 12:15PM - 12:45PM Room: BR Community, Learning Center Station #8

#### Awards

# **Identified for RadioGraphics**

### **Participants**

Helen Anne D'Alessandro, MD, Boston, MA (*Presenter*) Nothing to Disclose Dorothy A. Sippo, MD, Boston, MA (*Abstract Co-Author*) Nothing to Disclose Leslie Lamb, MD, MSc, Boston, MA (*Abstract Co-Author*) Nothing to Disclose Eric M. Blaschke, MD, Boston, MA (*Abstract Co-Author*) Nothing to Disclose Constance D. Lehman, MD, PhD, Boston, MA (*Abstract Co-Author*) Research Grant, General Electric Company; Medical Advisory Board, General Electric Company

# **TEACHING POINTS**

The use of digital breast tomosynthesis (DBT) is increasing given its benefits of improved sensitivity and specificity for lesion detection. Suspicious lesions seen only on DBT without a 2D mammographic, sonographic or MRI correlate require intervention. New methods of DBT guided intervention offer two distinct benefits: 1) The option of minimally invasive needle biopsy for lesions seen only on DBT and 2) An efficient, safe alternative to 2D mammographic-guided needle/wire localization. The goal of this educational exhibit is to review why and how to perform histologic tissue sampling of breast lesions seen on DBT and to review the indications, imaging workup and techniques required to perform DBT guided needle/wire localization for surgical excisional biopsies and DBT guided vacuum assisted biopsies. Imaging pearls, pitfalls and practicalities with relevant teaching cases from these two DBT tissue sampling techniques will be discussed and reviewed.

# TABLE OF CONTENTS/OUTLINE

Reasons for DBT needle/wire localization and DBT vacuum assisted biopsy:Indications/Literature review/Advantages/ Diagnostic workup and principles of lesion localization/ Imaging techniques and access/Sampling methods/Surgical and core tissue specimen pathology evaluation/Comparison with prone stereotactic VAB/Patient care implications/Teaching cases

# Enhancing Foci on Dynamic Breast MRI: What Should be our Diagnostic Strategy?

Tuesday, Nov. 29 12:15PM - 12:45PM Room: BR Community, Learning Center Station #9

# Awards

**Certificate of Merit** 

### Participants

Mariko Goto, MD, Kyoto, Japan (Presenter) Nothing to Disclose

Maki Kiba, Kyoto-Shi, Japan (Abstract Co-Author) Nothing to Disclose

Koji Sakai, Kyoto, Japan (Abstract Co-Author) Research funded, Siemens AG; Speaker, Terumo Corporation; Author, Medical View Co, Ltd

Mariko Yoshida, Kyoto, Japan (Abstract Co-Author) Nothing to Disclose

Kei Yamada, MD, Kyoto, Japan (*Abstract Co-Author*) Research funded, DAIICHI SANKYO Group Research funded, Eisai Co, Ltd Research funded, FUJIFILM Holdings Corporation Research funded, Nihon Medi-Physics Co, Ltd Research funded, Koninklijke Philips NV Consultant, H. Lundbeck A/S Consultant, Olea Medical Speaker, Bayer AG Speaker, DAIICHI SANKYO Group Speaker, Eisai Co, Ltd Speaker, Mitsubishi Corporation Speaker, Nihon Medi-Physics Co, Ltd Speaker, Otsuka Holdings Co, Ltd Speaker, Koninklijke Philips NV Speaker, Siemens AG Speaker, sanofi-aventis Group Speaker, Takeda Pharmaceutical Company Limited Speaker, Terumo Corporation

### **TEACHING POINTS**

The Breast Imaging Reporting and Data System (BI-RADS) lexicon is now used worldwide for assessing breast lesions on dynamic MRI, and it demonstrates good correlation with the likelihood of malignancy in both mass and non-mass enhancement. According to BI-RADS MRI, "focus" is another enhancing lesion type, which is defined as tiny enhancing spots without specific findings on dynamic MRI. Currently, there are few reports about the diagnostic strategy of these foci. Thus, we do not yet have a solid idea as to how we should be managing these lesions. The aims of this exhibit are: To review which enhancing lesion should be defined as focus on MRI To learn how we should manage these foci

### TABLE OF CONTENTS/OUTLINE

 1. Focus which should be detected as abnormal enhancement on MRI Differentiation from background parenchymal enhancement

 - Solitary, unique tiny enhancing spot
 - Stronger enhancement than other foci in early phase2. Key findings to

 differentiate malignant from benign focus Kinetic analysis: washout or persistent enhancement Signal intensity on T2WI: hyper-,

 hypo-intensity, or indistinct Interval change: size or kinetic pattern3. Suggestion of adequate MR category classification in focus

# BR238-SD-TUA1

Breast MR Spectroscopy at 3T in Biopsy Proved Breast Cancers: Does Choline Peak Correlate with Prognostic Factors?

Tuesday, Nov. 29 12:15PM - 12:45PM Room: BR Community, Learning Center Station #1

#### Awards

### **Student Travel Stipend Award**

#### Participants

Costanza Cavallini, MD, Rome, Italy (*Presenter*) Nothing to Disclose Maria L. Luciani, MD, Rome, Italy (*Abstract Co-Author*) Nothing to Disclose Federica Pediconi, MD, Rome, Italy (*Abstract Co-Author*) Nothing to Disclose Carlo Catalano, MD, Rome, Italy (*Abstract Co-Author*) Nothing to Disclose

# PURPOSE

To evaluate the correlation between the presence of Choline peak on MR spectroscopy at 3T and prognostic factors in patients with biopsy proved breast cancer.

### **METHOD AND MATERIALS**

Breast MR spectroscopy was performed at 3T in patients with biopsy proved malignant lesions measuring 8 mm or larger at MR imaging.Single-voxel MR spectroscopy data were collected from a single volume of interest that encompassed the lesion.Findings were considered positive in case of signal/noise ratio of Choline peak greater or equal to 2 and negative in all other cases.MR spectroscopy findings were then compared with histologic findings, lesion size, histotype, nuclear grade, receptor status (ER, PgR), Ki67 and HER2 expression were evaluated.

# RESULTS

102 patients with BI-RADS 6 lesions (94/102 IDC; 8/102 ILC) were evaluated. Choline peak was detectable in 48/102 cases. The average dimension of the lesions was 26.29mm (8-60mm). There was a statistically significant association between the choline peak (p=0.005) and the lesions size and between Choline peak with Ki-67 (p=0.003). We observed a statistically significant association between choline peak and grade 3 (p=0.001) and between choline peak and HER2 (p=0.04). No statistically significant association of choline peak with receptor status (ER, PgR) and Luminal A, B1 and B2 was detected, as well as, between choline peak and triple negative.

### CONCLUSION

3T breast MR spectroscopy, can be a tool to predict tumour aggressiveness and the correlation between choline peak and prognostic factors such as Ki67, HER2 and grading 3, may have a clinical relevance.

### **CLINICAL RELEVANCE/APPLICATION**

To evaluate the role of Choline peak as a prognostic factors in biopsy proved breast cancers using MR Spectroscopy at 3T .

Impact of Background Parenchymal Enhancement on Diagnostic Performance in Screening Breast MRI

Tuesday, Nov. 29 12:15PM - 12:45PM Room: BR Community, Learning Center Station #2

#### **Participants**

Geoffrey M. Rutledge, MD, Boston, MA (*Abstract Co-Author*) Nothing to Disclose Dorothy A. Sippo, MD, Boston, MA (*Presenter*) Nothing to Disclose Pragya A. Dang, MD, Boston, MA (*Abstract Co-Author*) Nothing to Disclose Ashley A. Roark, MD, Boston, MA (*Abstract Co-Author*) Nothing to Disclose Elkan F. Halpern, PhD, Boston, MA (*Abstract Co-Author*) Research Consultant, Hologic, Inc; Research Consultant, Real Imaging Ltd; Research Consultant, Gamma Medica, Inc; Research Consultant, K2M Group Holdings, Inc Constance D. Lehman, MD, PhD, Boston, MA (*Abstract Co-Author*) Research Grant, General Electric Company; Medical Advisory Board, General Electric Company

## PURPOSE

To evaluate the impact of background parenchymal enhancement (BPE) on diagnostic performance in screening breast magnetic resonance imaging (MRI).

# **METHOD AND MATERIALS**

Consecutive screening breast MRIs performed between February 7, 2011 and February 6, 2015 were reviewed with IRB approval. Clinical indication, BI-RADS assessment, and qualitative BPE assessment (minimal, mild, moderate, or marked) were extracted from radiology reports. Exams were excluded if there was a cancer diagnosis or biopsy in the previous six months, non-diagnostic study, or missing BPE assessment. Exams were grouped by BPE into minimal, mild, or moderate/marked. Cancer diagnosis was defined as a tissue diagnosis of invasive or in situ carcinoma within twelve months of the MRI or before the next screening MRI, whichever occurred first. Performance measures were defined according to the ACR BI-RADS Atlas, Fifth Edition. BPE impact on sensitivity was compared with a Fisher's exact test, on specificity with a chi-square test.

# RESULTS

The study cohort included 4935 screening MRIs performed in 2581 women, grouped by BPE into minimal (1850/4935, 37.5%), mild (2308/4935, 46.8%), or moderate/marked (777/4935, 15.7%). Eighty cancers were diagnosed overall (rate of 16.2 per 1000); BPE was assessed in these cases as minimal (20/80, 25%), mild (40/80, 50%), or moderate/marked (20/80, 25%). Descriptive performance measures across the three groups (minimal, mild, moderate/marked) were as follows: abnormal interpretation rate (5.6%, 9.8%, 13.4%), biopsy rate (2.7%, 4.2%, 5.9%), cancer detection rate per 1000 exams (9.7, 14.3, 19.3), PPV2 (26.0%, 29.9%, 28.3%), PPV3 (30.2%, 35.8%, 30.2%). Across the three groups (minimal vs. mild vs. moderate/marked), there was no statistically significant difference in sensitivity [90.0% (exact confidence interval 68.2-98.8) vs. 82.5% (67.2-92.7) vs. 75.0% (50.9-91.3), p=0.48], but there was a statistically significant decrease in specificity [95.4% (94.3-96.3) vs. 91.4% (90.2-92.6) vs. 88.2% (87.0-91.5), p<0.001].

# CONCLUSION

Increased BPE does not impact the sensitivity of screening MRI to detect breast cancer, but does decrease specificity, with trends toward increased abnormal interpretation and biopsy rates.

### **CLINICAL RELEVANCE/APPLICATION**

With increased BPE, sensitivity of screening MRI to detect cancer remains high, but specificity is decreased. Methods to help distinguish BPE from suspicious lesions may reduce false positive exams.

# Breast-Specific Gamma Imaging (BSGI)-guided biopsy for the Diagnosis of Breast Cancer

Tuesday, Nov. 29 12:15PM - 12:45PM Room: BR Community, Learning Center Station #3

#### **Participants**

Jialu L. Yang, Washington, DC, DC (Abstract Co-Author) Nothing to Disclose

Jocelyn A. Rapelyea, MD, Washington, DC (*Abstract Co-Author*) Speakers Bureau, General Electric Healthcare Company; Research consultant, Q-view LLC.; Research consultant, QTUS

Christel Velasco, Washington, DC, DC (Abstract Co-Author) Nothing to Disclose

Rachel F. Brem, MD, Washington, DC (*Presenter*) Board of Directors, iCAD, Inc; Board of Directors, Dilon Technologies LLC; Stock options, iCAD, Inc; Stockholder, Dilon Technologies LLC; Consultant, U-Systems, Inc; Consultant, Dilon Technologies LLC; Consultant, Dune Medical Devices Ltd

### PURPOSE

The purpose of this study was to evaluate the outcomes of BSGI-guided biopsy in women with abnormal BSGI findings and to determine the cancer detection rate.

## **METHOD AND MATERIALS**

All patients who underwent BSGI-guided biopsy between April 2011 and October 2015 were retrospectively reviewed. 113 women (ages 32 to 78) had 116 BSGI-guided biopsies, 103 of which were successful. Patients with abnormal BSGI findings underwent BSGI-guided biopsy.

### RESULTS

Of the 116 attempted biopsies, 103 were successful, and 13 were canceled. Of the canceled biopsies, 12 were canceled because the lesion was less conspicuous or no longer visible, and 1 because of a vasovagal reaction. The 13 canceled biopsies were followed for one year, and no cancers were found within that time frame. Of the 103 successful biopsies, 32 had abnormal findings: 8/32 invasive ductal carcinoma (25.0%), 1/32 invasive mammary carcinoma (3.13%), and 6/32 DCIS (18.8%). High risk lesions included 3/32 LCIS (9.38%), 5/32 ADH (15.6%), 2/32 ALH (6.25%), 1/32 flat epithelial atypia (3.13%), and 6/32 papillomas (18.8%). Of these 17 high-risk lesions, 2 cases of ADH were upgraded to DCIS at surgery, for an upgrade rate of 11.8% (2/17). The overall cancer detection rate for BSGI-guided biopsy was found to be 16.5% (17/103: 8 IDC and 9 DCIS). In this study, BSGIguided biopsy was found to have a sensitivity of 100%, a specificity of 82.6%, a PPV1 (PPV of total positive BSGI exams) of 53.1%, a PPV3 (PPV of total successful biopsies) of 16.5%, and an NPV of 100%.

### CONCLUSION

Of the 103 BSGI-guided biopsies performed for lesions not visible by mammography or ultrasound, biopsy demonstrated 17 cancers (16.5%), or a combined 32 cancers and high-risk lesions (31.1%) out of 103 successful biopsies.

### **CLINICAL RELEVANCE/APPLICATION**

BSGI-guided biopsy is a reasonable and accurate approach to biopsy BSGI-detected lesions. Our results compare favorably to those reported for MRI guided biopsy.

The Role of Strain Elastography in the Characterization of Lesions Detected during Second Look Ultrasound

Tuesday, Nov. 29 12:15PM - 12:45PM Room: BR Community, Learning Center Station #5

#### Awards

### **Student Travel Stipend Award**

#### Participants

Iulia Filip, MD, Montreal, QC (*Presenter*) Nothing to Disclose Romuald Ferre, MD, Montreal, QC (*Abstract Co-Author*) Nothing to Disclose Benoit D. Mesurolle, MD, Clermont-Ferrand, France (*Abstract Co-Author*) Nothing to Disclose

### PURPOSE

Evaluate strain elastography (SE) as a complementary tool for characterization of lesions during second look ultrasound (SLUS) after breast dynamic contrast material-enhanced (DCE) magnetic resonance imaging (MRI).

# METHOD AND MATERIALS

This retrospective single center study received approval from the Institutional Research Ethics Board. We identified 75 patients with 83 lesions characterized by MRI, SLUS and strain elastography between November 2012 and June 2014. Two patients had three distinct lesions and five patients each had two lesions that were characterized separately. An ultrasound-guided biopsy was performed in all cases. Two breast radiologists reviewed the MRI and ultrasound characteristics of the lesions, as well as the elastography specific measurements: the elasticity score (ES) and the fat-to-lesion strain ration (FLR).

# RESULTS

Mean patient age was 56 (range 33-85). At MRI, 40 (48.2%) lesions were described as masses (6-22mm), 30 (36.1%) as non mass-like enhancement (NMLE) and 13 (15.7%) as focus of enhancement. At SLUS, 56 (67.5%) lesions were defined as masses (5-25mm) and 27 (32.5%) as non-masses. After histo-pathology review, 43 lesions (51.8%) were benign, 36 lesions (43.4%) were malignant and 4 (4.8%) were high-risk lesions. Amongst the 40 malignant and high-risk lesions, 23 (57.5%) had elasticity scores of 3 and higher, whereas 35 (81.4%) of the 43 benign lesions had elasticity scores of 1 and 2 (p=0.01). The mean FLR for benign lesions was  $4.13\pm5.66$  and  $9.78\pm14.77$  for malignant and high-risk lesions. The sensitivity and specificity for FLR was 0.35 and 0.86 (p=0.02) with 14 true positive (TP) cases and 26 false negative (FN). The sensitivity and specificity for ES was 0.58 and 0.81 (p=0) with 23 TP and 17 FN. For BI-RADS 4A lesions at MRI, both FLR and ES had a sensitivity of 0.263 and a specificity of 0.923 with 11 TP and 29 FN.

## CONCLUSION

The results of this study show that the addition of strain elastography offers limited benefit in the characterization of lesions at SLUS after MRI. The elasticity score appears to perform better than FLR, however both tests have a low sensitivity with a large number of false negative results.

# **CLINICAL RELEVANCE/APPLICATION**

The evaluation of MRI detected lesions with second look ultrasound can be challenging. Strain elastography could be a potentially helpful tool that can aid radiologists to characterize and guide management for these lesions.

# BR243-SD-TUA6

Improving Lesion Conspicuity in Women with Dense Breasts using Computed High b-value Diffusion Weighted MR Imaging

Tuesday, Nov. 29 12:15PM - 12:45PM Room: BR Community, Learning Center Station #6

# Participants

Averi Kitsch, BS, Seattle, WA (*Abstract Co-Author*) Nothing to Disclose Habib Rahbar, MD, Seattle, WA (*Abstract Co-Author*) Research Grant, General Electric Company Savannah C. Partridge, PhD, Seattle, WA (*Presenter*) Nothing to Disclose

### PURPOSE

Higher b-values on diffusion weighted imaging (DWI) can improve visibility of breast malignancies, but acquiring these b-values lengthens the scan time of this rapid non-contrast technique and degrades signal-to-noise. This study investigates the potential of a computed high b-value DWI approach for maximizing distinguishability of breast cancer in women with dense breasts.

## METHOD AND MATERIALS

In this IRB-approved study, we retrospectively identified women with heterogeneously or extremely dense breasts on mammography that had a DCE-MRI detected invasive cancer between 1/2014 and 8/2015. MRI was performed on a 3T scanner and included DWI with multiple acquired b-values (0, 100, 600, 800, 1000 s/mm2). High b-value (1000, 1500, 2000, 2500, 3000 s/mm2) DW images were computed by fitting the acquired DWI signal to an IVIM model by a linear least-square technique and extrapolating values. Regions of interest (ROIs) were measured for lesion and contralateral tissue to calculate relative intensity (RI), a metric of conspicuity, as follows: RI=( $\mu$ I- $\mu$ t)/ $\mu$ t;  $\mu$  = mean of signal intensity values within the ROI. RI was compared between b-values by Wilcoxon signed-rank test. The effects of lesion characteristics (size, histology, and morphology) on lesion conspicuity also were explored by Wilcoxon rank sum test.

### RESULTS

The study included 25 invasive lesions (22 ductal; 3 lobular) detected on MRI in 23 women (median age, 58 yrs) with dense breasts. Lesion sizes ranged from 4-83mm (median, 12mm) with 18 masses and 6 non-mass enhancements. RI increased consistently with b-value up to the maximal value investigated of b=3000 s/mm2 (p<0.05) and was observed to be reflective of qualitative visibility of the lesions. No significant differences in lesion RI were observed based on histology, morphology, or size (p>0.05).

# CONCLUSION

Computed high b-value DW images generated with IVIM modeling can increase the contrast between tumor and normal tissue on DWI, which could save scan time, improve image quality, and facilitate a non-contrast screening method for women with dense breasts. Further validation in a larger clinical cohort is needed to better determine factors influencing conspicuity and optimal b-values.

# **CLINICAL RELEVANCE/APPLICATION**

Computed high b-value DWI can extend the range of b-values without incurring scan time penalties and holds promise to improve conspicuity of invasive cancers.

# Lobular Carcinomas in the Era of Digital Breast Tomosynthesis: Are Imaging Findings Changing?

Tuesday, Nov. 29 12:15PM - 12:45PM Room: BR Community, Learning Center Station #7

#### Awards

### **Student Travel Stipend Award**

#### **Participants**

Tisha M. Singer, MD, Providence, RI (*Presenter*) Nothing to Disclose Ana P. Lourenco, MD, Providence, RI (*Abstract Co-Author*) Nothing to Disclose Grayson L. Baird, PhD, Providence, RI (*Abstract Co-Author*) Nothing to Disclose Hai Wang, Providence, RI (*Abstract Co-Author*) Nothing to Disclose Yihong Wang, MD, Providence, RI (*Abstract Co-Author*) Nothing to Disclose Martha B. Mainiero, MD, Providence, RI (*Abstract Co-Author*) Nothing to Disclose

### PURPOSE

To compare presenting imaging findings for invasive lobular carcinomas (ILC) in patients imaged by digital breast tomosynthesis (DBT) vs digital mammography (DM).

# METHOD AND MATERIALS

IRB approved, HIPAA compliant retrospective search of pathology databases of 2 tertiary breast centers identified 191 ILCs from 1/1/09 to 12/31/14. Patient identifiers, imaging modality and findings (architectural distortion (AD), focal asymmetry (FA), asymmetry (A), mass (M), calcification (CALC), negative (NEG)) and pathology results were recorded. Imaging findings for patients undergoing DBT vs DM were compared. Generalized linear modeling assuming a binomial distribution using least squares estimation were used to examine rates over time. Significance is .05 and all interval estimates are calculated for 95% confidence.

### RESULTS

There were 191 ILCs in 189 women; 54 imaged with DBT and 135 with DM. Mean age for DBT was 60.8 and DM was 61.7. With DBT, AD rates were significantly higher than DM (36% [14-23] vs. 18% [9-19]) initially and later (53% [20-32] vs. 0), all p<.05. No differences were observed for FA (p=.3441) or M (p=.35). False negatives were lower for DBT (0%) than DM (7% [2-26]), p<.0001. Asymmetry was higher for DBT (15% [4-55]) than DM (10%[3-29]) initially and later (7% [1-44] vs. 0%), p<.001. CALC were higher for DBT (8% [1-50]) than DM (7% [2-25]), p<.001.

#### CONCLUSION

ILC presented more commonly as architectural distortion and asymmetry at DBT compared with DM. There were also fewer false negatives with DBT than DM.

#### **CLINICAL RELEVANCE/APPLICATION**

ILCs often present with subtle imaging findings. Awareness of how the presenting imaging findings may differ at DBT and DM may be helpful to breast radiologists.

# CA116-ED-TUA8

Evaluation of Myocardial Late Iodine Enhancement in the Era of Dual-Energy CT: Correlation of CT and MRI Findings

Tuesday, Nov. 29 12:15PM - 12:45PM Room: CA Community, Learning Center Station #8

# Participants

Yasutoshi Ohta, MD, Yonago, Japan (*Presenter*) Nothing to Disclose Yoshitake Yamada, MD, PhD, Boston, MA (*Abstract Co-Author*) Nothing to Disclose Haruhiko Machida, MD, Tokyo, Japan (*Abstract Co-Author*) Nothing to Disclose Yoshiro Hori, MD, Kanagawa, Japan (*Abstract Co-Author*) Nothing to Disclose Shinichiro Kitao, Yonago, Japan (*Abstract Co-Author*) Nothing to Disclose Toshihide Ogawa, MD, Yonago, Japan (*Abstract Co-Author*) Nothing to Disclose

### **TEACHING POINTS**

1.To learn the basic principles of myocardial late iodine enhancement (LIE) using dual-energy CT. 2.To learn how to acquire good LIE images for interpretation of various ischemic and non-ischemic cardiomyopathies.3.To review the image features of LIE in various ischemic and non-ischemic by comparison with gadolinium delayed enhancement MRI.

### **TABLE OF CONTENTS/OUTLINE**

For tissue characterization of the myocardium, late gadolinium enhancement with cardiac magnetic resonance (CMR) imaging is widely used, whereas late enhancement by single energy CT is not widely used for its limited image contrast for tissue characterization. Recently, dual-energy CT has been introduced that makes it possible to depict the spread of iodinated contrast agent using iodine density image or monochromatic image with higher contrast as well as CMR. 1. Limitations of LIE in single energy CT. 2. Basic principles of DECT in LIE imaging.3. Image acquisition and post-processing of LIE images in DECT for good interpretation.4. Reviewing the imaging features of LIE in various ischemic and non-ischemic cardiomyopathies (e.g. myocardial infarction, dilated cardiomyopathy, hypertrophic cardiomyopathy, cardiac sarcoidosis, Anderson-Fabry disease) by comparison with gadolinium enhancement with CMR.

Radiation Dose Reduction for Coronary Artery Calcium Scoring at 320-detector CT with Full Iterative Reconstruction: Study using a Cardiac CT Calibration Phantom

Tuesday, Nov. 29 12:15PM - 12:45PM Room: CA Community, Learning Center Station #1

# Participants

Kazushi Yokomachi, RT, Hiroshima, Japan (*Presenter*) Nothing to Disclose
Fuminari Tatsugami, Hiroshima, Japan (*Abstract Co-Author*) Nothing to Disclose
Yoshinori Funama, PhD, Kumamoto, Japan (*Abstract Co-Author*) Nothing to Disclose
Chikako Fujioka, RT, Hiroshima, Japan (*Abstract Co-Author*) Nothing to Disclose
Eiji Nishimaru, RT, Hiroshima, Japan (*Abstract Co-Author*) Nothing to Disclose
Kazuo Awai, MD, Hiroshima, Japan (*Abstract Co-Author*) Nothing to Disclose
Kazuo Awai, MD, Hiroshima, Japan (*Abstract Co-Author*) Research Grant, Toshiba Corporation; Research Grant, Hitachi, Ltd;
Research Grant, Bayer AG; Research Grant, Eisai Co, Ltd; Medical Advisor, General Electric Company; ;; ;
Masao Kiguchi, RT, Hiroshima, Japan (*Abstract Co-Author*) Nothing to Disclose
Toru Higaki, PhD, Hiroshima, Japan (*Abstract Co-Author*) Nothing to Disclose
Nobuo Kitera, RT, Hiroshima, Japan (*Abstract Co-Author*) Nothing to Disclose

### PURPOSE

The coronary artery calcium (CAC) score measured on computed tomography (CT) scanners is an unequivocal marker of coronary atherosclerosis. It has been reported that the use of hybrid IR (AIDR 3D) made it possible to reduce the radiation dose for CAC measurements without impairing the quantification of coronary calcification. However, on low-dose CT studies, blooming artifacts are not reduced by AIDR 3D and the CAC score may be overestimated. The forward-projected model-based iterative reconstruction solution (FIRST) is a new reconstruction algorithm that repeats both back and forward projections in the image-reconstruction process. The advantages of FIRST include higher spatial resolution, lower image noise, and the reduction of artifacts. We assessed the possibility of reducing the radiation dose for CAC scoring by using the FIRST- rather than the AIDR 3D algorithm or FBP.

### **METHOD AND MATERIALS**

We quantitatively evaluated the CAC score using the QRM-Cardio-Phantom and a 320-detector row CT scanner. The tube current was set at 150-, 100-, 70-, 50-, 40-, and 20 mA; the standard deviation (SD) of the CT values on images reconstructed with FBP corresponds to 20-, 25-, 30-, 35-, 40-, and 50 HU. Reconstruction was performed using FBP, AIDR 3D (strength level: standard), and FIRST. CAC scoring was compared after calculating the Agatston-, volume- and mass scores.

## RESULTS

The Agatston scores for the FBP, AIDR 3D, and FIRST at 150 mA were 771, 756, and 717, respectively; at 20 mA, they were 948, 808, and 714, respectively. The volume scores for FBP, AIDR 3D, and FIRST at 150 mA were 627, 621, and 589, respectively; at 20 mA, they were 742, 661, and 597, respectively (true value of 361 mm3). The mass scores for the FBP, AIDR 3D, and FIRST at 150 mA were 172, 170, and 174, respectively and at 20 mA, they were 191, 167, and 166, respectively (true value of 168 mg). The Agatston-, volume- and mass scores obtained at 150 mA and reconstructed with FIRST were comparable to those at 20 mA.

# CONCLUSION

The use of FIRST made it possible to reduce the radiation dose by 87% for CAC measurements without impairing the quantification of coronary calcification.

# **CLINICAL RELEVANCE/APPLICATION**

FIRST can reduce the radiation exposure of patients undergoing CAC scoring by 87% compared with the dose currently applied with FBP.

# CA226-SD-TUA3

Assessment of Contrast Enhanced MRA Volumetry to Detect Growth of the Ascending Aorta in Patients with Bicuspid Aortic Valves

Tuesday, Nov. 29 12:15PM - 12:45PM Room: CA Community, Learning Center Station #3

#### Awards

### **Student Travel Stipend Award**

#### **Participants**

Brian Trinh, Chicago, IL (*Presenter*) Nothing to Disclose Iram Dubin, MD, Chicago, IL (*Abstract Co-Author*) Nothing to Disclose Ozair A. Rahman, MD, Chicago, IL (*Abstract Co-Author*) Nothing to Disclose Marcos P. Ferreira Botelho, MD, Houston, TX (*Abstract Co-Author*) Nothing to Disclose Nicholas Naro, MD, Chicago, IL (*Abstract Co-Author*) Nothing to Disclose James C. Carr, MD, Chicago, IL (*Abstract Co-Author*) Research Grant, Astellas Group Research support, Siemens AG Speaker, Siemens AG Advisory Board, Guerbet SA Jeremy D. Collins, MD, Chicago, IL (*Abstract Co-Author*) Nothing to Disclose Alex Barker, Chicago, IL (*Abstract Co-Author*) Nothing to Disclose

# PURPOSE

Patients with BAV have an increased risk for developing thoracic aortic aneurysms (TAA) and require serial imaging to monitor aortic growth. Aortic diameter measurements, the clinical standard, may be insensitive to focal aneurysmal changes. This study assesses the reliability of CEMRA volumetry compared to two-dimensional diameter measurements to identify TAA growth in BAV patients with significant power.

## **METHOD AND MATERIALS**

A retrospective, IRB approved and HIPAA compliant study was conducted on 20 BAV patients (45±8.9 years old, 80% males) who underwent serial CEMRA with a minimum imaging follow-up of 11 months. MRI was performed at 1.5 T with ECG-gated time-resolved CEMRA. Two independent analysts (MB, BT) measured diameters at the sinuses of valsalva (SOV) and mid-ascending aorta (MAA). Two other independent analysts (IA, OR) measured volume between the aortic annulus and innominate branch using Mimics. Growth rates were calculated via baseline and follow-up exam and differences assessed by two-sided, paired Student's t-test; p<0.05 considered statistically significant. Intra/inter-observer error was computed. Intraclass correlation coefficient (ICC) was calculated for reliability. The power to detect growth for diameter and volume was computed.

# RESULTS

The mean time of follow-up was 2.6 $\pm$ 0.82 years. Average aortic measurements at baseline (follow-up) were 4.2 $\pm$ 0.3 cm (4.2 $\pm$ 0.3 cm, p=0.074) at SOV, 4.6 $\pm$ 0.4 cm (4.7 $\pm$ 0.4 cm, p<0.05) at MAA, and 130 $\pm$ 23 mL (144 $\pm$ 24 mL, p<0.05) with volumetry. Average growth was 0.07 $\pm$ 0.06 cm/y (2% $\pm$ 1%) at MAA and 6 $\pm$ 3 mL/y (4% $\pm$ 2%) with volumetry. Inter-observer mean error was 0.2 $\pm$ 0.1 cm (3% $\pm$ 3%) at SOV, 0.2 $\pm$ 0.1 cm (4% $\pm$ 3%) at MAA, and 6 $\pm$ 5 mL (5% $\pm$ 3%) with volume measurements. ICC was 0.89 for diameter and 0.95 for volume. Based on aortic growth rate reported in the literature, the power for detecting a significant change was 10.0% for MAA and 99.5% for volume.

# CONCLUSION

3D CEMRA volumetric analysis exhibited a larger percentage growth, better ICC, and higher power to detect size changes. Thus, volumetric analysis is more sensitive to size changes and less affected by inter-observer error than diameter, providing a promising method to detect ascending aortic growth to guide future research investigating BAV outcomes.

# **CLINICAL RELEVANCE/APPLICATION**

3D CEMRA volumetric analysis has potential to detect TAA size changes on serial imaging with better reliability and less error for patients with BAV.

# Change in Coronary Artery Calcium Scores over 10 years: Results from the CARDIA Study

Tuesday, Nov. 29 12:15PM - 12:45PM Room: CA Community, Learning Center Station #4

#### **Participants**

Alexandra Ritts, MD, Nashville, TN (*Presenter*) Nothing to Disclose James G. Terry, MS, Winston-Salem, NC (*Abstract Co-Author*) Nothing to Disclose David R. Jacobs Jr, PhD, Minneapolis, MN (*Abstract Co-Author*) Nothing to Disclose Pamela Schreiner Schreiner, PhD, Minneapolis, MN (*Abstract Co-Author*) Nothing to Disclose Donald Lloyd-Jones, MD, Chicago, IL (*Abstract Co-Author*) Nothing to Disclose Steve Sidney, MD, MPH, Oakland, CA (*Abstract Co-Author*) Nothing to Disclose Edmond K. Kabagambe, DVM,PhD, Nashville, TN (*Abstract Co-Author*) Nothing to Disclose Cora E. Lewis, MD, Birmingham, AL (*Abstract Co-Author*) Institutional Research Grant, Novo Nordisk AS John J. Carr, MD, MS, Nashville, TN (*Abstract Co-Author*) Nothing to Disclose

#### PURPOSE

Coronary artery calcium (CAC) is a measure of the presence and extent of coronary atherosclerosis. The incidence of cardiovascular events increases with CAC score. Improved understanding of change in the CAC score in an individual may help inform clinical decision-making. We analyzed increases and decreases in CAC score in a subset of participants of the CARDIA study.

## **METHOD AND MATERIALS**

Participants (n=2,158) included those with CAC scores at the exam in 2000-01 (ages 33-45 years) and at follow-up 10 years later, in 2010-11. CAC was measured blinded to clinical information and reported as Agatston scores (AU) with paired CT scans in 2000-2001 and single scan at follow-up. Blinded adjudications were performed within and across the CT exams and technical errors, coronary stents, and coronary grafts identified and resolved.

### RESULTS

CAC prevalence in 2000-01 was 9.9% (213/2,158) and 29.1% (627/2,158) had measurable CAC 10 years later. CAC was not detected in 70.9% (1,531/2,158) at both exams. Focusing on those with non-zero CAC in 2000-1, 13 of 2,158 (0.6%) had a decreased score at follow-up. Their median score in 2000-01 was 1.6 AU (range 0.5-12) with a median change of -2.9 AU noted at follow-up (interquartile range -4.5 to -2.0). Using the criterion of any, 1 or 5 AU/year change in score to categorize results as stable, increased or decreased, the percentage of people with any CAC in 2000-01 that decreased at follow-up was 6.1%, 0.5%, and 0%, respectively (Table).

# CONCLUSION

CAC was observed to increase almost exclusively over 10 years in adults initially ages 33-45 years. 10-year decreases in score were small in magnitude and indistinguishable from the expected magnitude of measurement error in this highly quality-controlled longitudinal study. Findings do not support measurable regression of calcified plaque. Criteria of 1 AU/year or 5 AU/year are reasonable for categorizing change in CAC when there is careful reading to avoid false positives and negatives.

### **CLINICAL RELEVANCE/APPLICATION**

We evaluated 10-year change in coronary artery calcium (CAC) by cardiac CT in 2,158 participants to determine how many increased, decreased or were stable to help inform clinical decision-making.

Cardiac-Gated-CT Angiography for Evaluation of The Proximity of Left Atrial Appendage and Pulmonary Artery in Patients with Atrial Fibrillation

Tuesday, Nov. 29 12:15PM - 12:45PM Room: CA Community, Learning Center Station #5

# Participants

Clara Cohen, Tel Aviv, Israel (*Presenter*) Nothing to Disclose Raphael Rosso, Tel Aviv, Israel (*Abstract Co-Author*) Nothing to Disclose Haim Shmilovich, Tel-Aviv, Israel (*Abstract Co-Author*) Nothing to Disclose Ehud Chorin, Tel Aviv, Israel (*Abstract Co-Author*) Nothing to Disclose Dotan Cohen, MD, Mevaseret Zion, Israel (*Abstract Co-Author*) Nothing to Disclose Amir Halkin, Tel Aviv, Israel (*Abstract Co-Author*) Nothing to Disclose Galit Aviram, MD, Tel-Aviv, Israel (*Abstract Co-Author*) Institutional Research Grant, Koninklijke Philips NV

## PURPOSE

Left atrial appendage closure (LAAC) has emerged as an alternative to oral anticoagulation for stroke prevention in patients with nonvalvular atrial fibrillation (AF). Although this procedure is very safe in experienced hands, delayed pulmonary artery (PA) perforation by LAAC device is a rare complication. The prevalence of the anatomic variant which might be susceptible to PA perforation is unknown. Transesophageal echocardiography (TEE) is commonly used pre and during LAAC, but provides limited visualization of the anatomic relationship between the landing zone of the device in the proximal LAA and the PA. Cardiac-gated CT angiography (CCTA) offers 2D and 3D imaging of the heart and the great vessels. This may allow accurate anatomical evaluation of the relations between the LAA and the PA (R-LAA-PA). Using CCTA, we aimed to describe the R-LAA-PA among patients with AF and determine the incidence of patients who are at risk of PA perforation due to close contact of their proximal LAA and the PA.

# **METHOD AND MATERIALS**

The study includes 100 consecutive patients diagnosed with paroxysmal atrial fibrillation who underwent CCTA. Mean age was 59,7±10, 66% were male. This cohort was used as our model for patients who are candidates for treatment of atrial fibrillation; however, they eventually underwent treatment by pulmonary vein isolation. Using 2D and 3D reconstructions of the CTA data along the central line created within the LAA, the various R-LAA-PA variants were analyzed and classified into 3 types, based on the location, length, and width of the LAA-PA segment of contact. Type I: proximal LAA-PA contact, defined as a contact within first 15mm of the LAA ostium into the LAA and the PA; Type II: distal LAA-PA contact, defined as contact within the distal end of the LAA (> 15mm of the ostium) and the PA; and Type III: no LAA-PA contact.

## RESULTS

Types I, II, and III anatomic subsets were present in 25 (25%), 68 (68%), and 7 (7%) patients, respectively. Among Type I patients, mean contact width was 0.6 mm $\pm$ 0.3 and mean contact length was 18.1mm $\pm$ 10.6.

# CONCLUSION

In this series, the proximal LAA, serving as the landing zone for most commercially available LAAC devices, came in direct contact with the PA in one quarter of cases.

# **CLINICAL RELEVANCE/APPLICATION**

The LAA-PA anatomical relationship described by CCTA may contribute to patients' safety during LAA closure.

Non-binary Myocardial Infarct Quantification Technique Accounting for Partial Volume Averaging Predicts Segmental Left Ventricular Myocardial Contraction

Tuesday, Nov. 29 12:15PM - 12:45PM Room: CA Community, Learning Center Station #6

**FDA** Discussions may include off-label uses.

### Participants

Balazs Ruzsics, MD, PhD, Charleston, SC (*Presenter*) Nothing to Disclose
Pal Suranyi, MD, PhD, Charleston, SC (*Abstract Co-Author*) Nothing to Disclose
Rob J. van der Geest, PhD, Leiden, Netherlands (*Abstract Co-Author*) Nothing to Disclose
Carlo N. De Cecco, MD, PhD, Charleston, SC (*Abstract Co-Author*) Nothing to Disclose
Moritz H. Albrecht, MD, Charleston, SC (*Abstract Co-Author*) Nothing to Disclose
U. Joseph Schoepf, MD, Charleston, SC (*Abstract Co-Author*) Research Grant, Astellas Group; Research Grant, Bayer AG; Research Grant, General Electric Company; Research Grant, Siemens AG; Research support, Bayer AG; Consultant, Guerbet SA; ; ;
Taylor M. Duguay, Charleston, SC (*Abstract Co-Author*) Nothing to Disclose
Gabriel A. Elgavish, PhD, Birmingham, AL (*Abstract Co-Author*) Owner, Elgavish Paramagnetics, Inc; Consultant, Elgavish Paramagnetics, Inc
Akos Varga-Szemes, MD, PhD, Charleston, SC (*Abstract Co-Author*) Consultant, Guerbet SA

#### PURPOSE

Binary myocardial infarct (MI) quantification techniques do not take partial volume averaging into consideration, resulting in an overestimation in MI size. Non-binary approaches, such as Percent Infarct Mapping (PIM), are able to address these shortcomings. The aim of this study was to investigate the influence of true MI content determined by PIM on segmental myocardial contraction.

# **METHOD AND MATERIALS**

Twenty patients (57±11 years, 16 males) with prior MI underwent 1.5T MRI (Avanto, Siemens). Short-axis balanced steady-state free-precession (bSSFP) cine imaging, post-contrast (0.1mmol/kg gadobenate-dimeglumine) T1-mapping (modified Look-Locker inversion recovery (IR), scheme 4(1)3(1)2), and late gadolinium enhancement (LGE) imaging (bSSFP with IR pulse) were performed. Myocardial contraction was quantified as radial wall thickening (RWT) using the centerline method according to the 17-segment model. Segmental MI content was calculated based on both T1 and LGE images applying the previously described PIM algorithm (PIMT1 and PIMLGE, respectively) using an in-house developed application. MI was also quantified based on LGE images using a binary approach (full-width at half-maximum, FWHM). Relationship between MI percentage (MI%) and RWT was tested using a linear regression.

## RESULTS

Sixteen segments were excluded due to image artifacts. MI was observed in 69 of the remaining 324 segments. The FWHM method measured significantly higher global MI% compared to PIMT1 and PIMLGE  $(13.3\pm3.1\%, 8.3\pm2.9\%, and 8.7\pm3.5\%, respectively, P=0.0024)$ , as well as higher segmental MI% (66.1±26.1%, 47.4±18.0%, and 44.9±16.7%, respectively, P=0.0009). Average RWT in the normal and MI segments was 149.6±47.3% and 43.1±46.4%, respectively (P<0.0001). Strong correlation between MI% and RWT was observed using PIMT1 (r=-0.605, P=0.0012) and PIMLGE (r=-0.757, P<0.0001) methods, while the correlation was weaker using the binary FWHM threshold (r=-0.399, P=0.0319).

# CONCLUSION

Both PIMT1 and PIMLGE showed good correlation with segmental myocardial contraction. The PIM-based methods measured lower MI% due to their ability to account for partial volume averaging. Non-binary approaches may become preferred techniques for quantitative LGE evaluation.

# **CLINICAL RELEVANCE/APPLICATION**

Non-binary MI quantification is able to account for partial volume averaging thus provides more reliable MI measurement and better prediction of segmental myocardial contraction.

# CA230-SD-TUA7

Contrast-enhanced T1 Mapping-based Extracellular Volume Fraction Independently Predicts Clinical Outcome in Patients with Non-Ischemic Dilated Cardiomyopathy

Tuesday, Nov. 29 12:15PM - 12:45PM Room: CA Community, Learning Center Station #7

# Participants

Yoo Jin Hong, MD, Seoul, Korea, Republic Of (*Presenter*) Nothing to Disclose Chul Hwan Park, MD, Seoul, Korea, Republic Of (*Abstract Co-Author*) Nothing to Disclose Donghyun Hong, MS, Essen, Germany (*Abstract Co-Author*) Nothing to Disclose Byoung Wook Choi, MD, Seoul, Korea, Republic Of (*Abstract Co-Author*) Nothing to Disclose Hye-Jeong Lee, MD, Seoul, Korea, Republic Of (*Abstract Co-Author*) Nothing to Disclose Joshua Jinhan Kim, Seoul, Korea, Republic Of (*Abstract Co-Author*) Nothing to Disclose Jin Young Kim, MD, Seoul, Korea, Republic Of (*Abstract Co-Author*) Nothing to Disclose

# PURPOSE

We aimed to evaluate the prognostic role of contrast-enhanced T1 mapping-based extracellular volume fraction (ECV) in patients with non-ischemic dilated cardiomyopathy (NIDCM) and compare this parameter with conventional late gadolinium enhancement (LGE) parameters.

# METHOD AND MATERIALS

We examined 117 NIDCM patients (71 men; age, 51.9±16.7 years) who underwent cardiac magnetic resonance imaging, including pre- and post-contrast T1 mapping, and cine and late gadolinium enhancement (LGE) imaging with a clinical 3T magnetic resonance scanner. Myocardial ECV was calculated from the pre- and post-contrast T1 values of the myocardium (16 segments) and hematocrit value. LGE was quantified using the 5-SD threshold method, and the presence of midwall LGE was also detected. Nineteen healthy volunteers served as controls. Patients were followed for a median duration of 11.2 months (25–75 percentile, 7.8–21.9 months), and survival analyses were performed. The primary end-points were cardiovascular death, re-hospitalization due to heart failure, and heart transplantation.

# RESULTS

The mean ECV and native T1 values were higher in NIDCM patients  $(32.0\pm5.7\%$  and  $1326.3\pm91.1$  ms) than in controls  $(25.8\pm2.2\%$  and  $1213.9\pm37.4$  ms; p<0.001). During the follow-up period, a certain outcome was noted in 19 patients (16.2%). A 3% increase and 1% increase in ECV was associated with a hazard ratio (HR) of 1.80 and 1.22 (95% confidence interval (CI): 1.48–2.20, 1.14–1.30; p<0.001) for the clinical outcome. Native T1, LGE quantification values, and midwall LGE could predict the clinical outcome with an HR of 1.01 (95% CI, 1–1.01; p=0.03), 1.04 (95% CI, 1.01–1.08; p=0.01), and 4.89 (95% CI: 1.43–16.80; p=0.01), respectively. Multivariate analysis also indicated that ECV was still an independent prognostic factor (3% increase: HR=1.97, 95% CI=1.53–2.52, p<0.001; 1% increase: HR=1.25, 95% CI=1.15–1.36, p<0.001), and had a higher prognostic value (Harrell's c statistic, 0.89) than LGE quantification values (0.76) or midwall LGE (0.80).

# CONCLUSION

Contrast-enhanced T1 mapping based-myocardial ECV independently predicts the clinical outcome in patients with NIDCM. We determined a noninvasive measure of risk stratification among these patients.

# **CLINICAL RELEVANCE/APPLICATION**

The quantification of diffuse myocardial disease by T1 mapping cardiac magnetic resonance imaging may have prognostic value in patients with non-ischemic dilated cardiomyopathy.

# CA232-SD-TUA2

Diagnostic Performance of Peak Enhancement Ratio of Myocardium to Aorta for Detecting Myocardial Ischemia in Dynamic Myocardial Computed Tomography Perfusion Imaging

Tuesday, Nov. 29 12:15PM - 12:45PM Room: CA Community, Learning Center Station #2

# Participants

Yuki Tanabe, Toon, Japan (*Presenter*) Nothing to Disclose Teruhito Kido, MD, PhD, Toon, Japan (*Abstract Co-Author*) Nothing to Disclose Takahiro Yokoi, Toon, Japan (*Abstract Co-Author*) Nothing to Disclose Naoki Fukuyama, Toon, Japan (*Abstract Co-Author*) Nothing to Disclose Akira Kurata, PhD, Toon, Japan (*Abstract Co-Author*) Nothing to Disclose Ryo Ogawa, MD, Toon, Japan (*Abstract Co-Author*) Nothing to Disclose Masashi Nakamura, Toon, Japan (*Abstract Co-Author*) Nothing to Disclose Tomoyuki Kido, Toon, Japan (*Abstract Co-Author*) Nothing to Disclose Masao Miyagawa, MD, PhD, Toon, Japan (*Abstract Co-Author*) Nothing to Disclose Teruhito Mochizuki, MD, Toon, Japan (*Abstract Co-Author*) Nothing to Disclose

## PURPOSE

Myocardial CT perfusion (CTP) imaging with pharmacological stress has emerged as a useful method for the assessment of hemodynamic significance of coronary artery disease. The purpose was to evaluate the diagnostic performance of peak enhancement ratio of myocardium to aorta (PER) for detecting myocardial ischemia.

# METHOD AND MATERIALS

The study population consisted of 39 patients (mean age 68.6±10.3 years), who underwent pharmacological stress dynamic myocardial CTP, and magnetic resonance myocardial perfusion imaging (MR-MPI) for assessment of coronary artery disease. Stress dynamic CTP (whole-heart datasets over 30 time points at every cardiac cycle, tube voltage of 100 kV, tube current of 80mAs) was acquired with prospective ECG gating (mean radiation dose: 10.6 mSv). Per segment-based analysis using the 16-segment model, peak enhancement (PE) [Hounsfield units (HU)] of the ascending aorta and myocardium was measured by analyzing the time attenuation curves. PE of myocardium was divided by that of the aorta to obtain PER. All myocardial segments were classified as normal and ischemic segments assessed by MR-MPI. The relations for PE values between the aorta and myocardium were assessed by Spearman test. Diagnostic performance of PER and PE for detecting myocardial ischemia were evaluated by the receiver operating characteristics curve analysis, and compared.

#### RESULTS

Of 39 patients, a total of 242/624 (39%) segments were diagnosed as ischemic segments. The close correlation for PE was observed between the aorta and myocardium (r= 0.79 for normal segments and r= 0.53 for ischemic segments, p <0.05, in each). PE and PER in the ischemic segments were significantly lower than those of normal segments (p <0.05, in each). Sensitivity and specificity for detecting ischemic segments were 64% (95%CI: 58-70) and 81% (95%CI: 77-85) for PE, and 74% (95%CI: 68-79) and 85% (95%CI: 81-88) for PER, respectively. The area under the curve of PER was significantly higher than that of PE [0.86 (0.82-0.89) vs. 0.77 (0.73-0.81), p<0.05].

## CONCLUSION

For the assessment of myocardial perfusion, PER is a feasible quantitative method for detecting myocardial ischemia with high diagnostic performance.

### **CLINICAL RELEVANCE/APPLICATION**

PER is a simple quantitative method for the assessment of myocardial perfusion, and it has a potential for establishing a standardized cut-off independently of substantial individual variations in myocardial perfusion.

A Look at Lung Function Beyond FEV1 with Hyperpolarized 129Xenon MRI: Guide to Building a Clinical Imaging Routine -How We Do It and Why We Need It!

Tuesday, Nov. 29 12:15PM - 12:45PM Room: CH Community, Learning Center Hardcopy Backboard

**FDA** Discussions may include off-label uses.

#### Participants

Lukas Ebner, MD, Durham, NC (*Presenter*) Nothing to Disclose Rohan Virgincar, Durham, NC (*Abstract Co-Author*) Nothing to Disclose Mu He, Durham, NC (*Abstract Co-Author*) Nothing to Disclose Scott H. Robertson, Durham, NC (*Abstract Co-Author*) Nothing to Disclose Jennifer Wang, Durham, NC (*Abstract Co-Author*) Nothing to Disclose Kamran Mahmood, Durham, NC (*Abstract Co-Author*) Nothing to Disclose H. Page McAdams, MD, Durham, NC (*Abstract Co-Author*) Nothing to Disclose H. Page McAdams, MD, Durham, NC (*Abstract Co-Author*) Research Grant, General Electric Company; Consultant, MedQIA Imaging Core Laboratory ; Author, Reed Elsevier; Author, UpToDate, Inc; Research Consultant, F. Hoffmann-La Roche Ltd; Research Consultant, Boehringer-Ingelheim GmbH Justus E. Roos, MD, Durham, NC (*Abstract Co-Author*) Nothing to Disclose

Bastiaan Driehuys, PhD, Durham, NC (Abstract Co-Author) Research support, General Electric Company; Royalties, General Electric Company; Stockholder, Polarean, Inc

### **TEACHING POINTS**

The role of hyperpolarized (HP) 129Xe MRI will be elucidated in the context of current standards in lung function assessment and imaging. The audience will learn about the unique contrast mechanisms of HP129Xe MR imaging. A structured review of the technical requirements for noble gas imaging will be provided. We introduce a point-by-point directive for how to build a comprehensive imaging strategy for evaluating patients with various pulmonary conditions. An overview of the current clinical applications of HP129Xe MRI will be provided. We will present a pictorial review of different clinical applications of HP129Xe MRI.

## TABLE OF CONTENTS/OUTLINE

Introduction of standards in pulmonary function assessment and pulmonary MRI. Identify the inherent shortcomings hampering traditional pulmonary function tests and imaging. Revisit the technical prerequisites for noble gas MRI (scanner, coils, gas and polarizer). Summary of an image protocol consisting of anatomical and functional sequences. Safety considerations. Clinical applications and appropriate interpretation of results. Pictorial review of sample cases from our institution comprising cases of asthma, IPF and bronchial stenosis quantification. Elaborate the incremental clinical value of HP129Xe MRI. Outlook.

# **Honored Educators**

Presenters or authors on this event have been recognized as RSNA Honored Educators for participating in multiple qualifying educational activities. Honored Educators are invested in furthering the profession of radiology by delivering high-quality educational content in their field of study. Learn how you can become an honored educator by visiting the website at: https://www.rsna.org/Honored-Educator-Award/

H. Page McAdams, MD - 2012 Honored Educator

# Multi-Vendor Spectral CT Lung Perfusion: What Is Real and What Is Not?

Tuesday, Nov. 29 12:15PM - 12:45PM Room: CH Community, Learning Center Station #6

#### Participants

Michael D. Collard, MD, Dallas, TX (*Presenter*) Nothing to Disclose Asha Kandathil, MD, Dallas, TX (*Abstract Co-Author*) Nothing to Disclose Prabhakar Rajiah, MD, FRCR, Dallas, TX (*Abstract Co-Author*) Institutional Research Grant, Koninklijke Philips NV; Speaker, Koninklijke Philips NV Sachin S. Saboo, MD, FRCR, Dallas, TX (*Abstract Co-Author*) Nothing to Disclose Suhny Abbara, MD, Dallas, TX (*Abstract Co-Author*) Author, Reed Elsevier; Editor, Reed Elsevier; Institutional research agreement, Koninklijke Philips NV; Institutional research agreement, Siemens AG Kiran Batra, MD, Coppell, TX (*Abstract Co-Author*) Nothing to Disclose

# **TEACHING POINTS**

1. Review similarities and differences between the different spectral CT techniques and their implementations2. Discuss the principles and techniques of spectral CT lung perfusion and its clinical utility3. Explain artifacts encountered in iodine perfusion maps and techniques to decrease/eliminate artifacts4. Compare artifacts encountered in different techniques, such as dual-source and detector-based spectral CT5. Provide guidelines on distinguishing artifacts from pulmonary embolism

# TABLE OF CONTENTS/OUTLINE

Spectral CT - basic physicsSpectral CT techniques Dual source Rapid kV switching Dual spin Detector-based spectral CT Split beam Photon countingBenefits of spectral CT in thoracic imaging Lung perfusion Decreased artificats (beam hardening) Improved vascular contrast (salvage of suboptimal studies, low contrast dose) Virtual noncontrast imagesSpectral CT lung perfusion Physical processing Image interpretationCase illustration of CT lung perfusion benefits (acute and chronic pulmonary embolism, infarct, pulmonary hypertension, small vessel disease)Artifacts and pitfalls with spectral CT lung perfusion Beam hardening Lung disease Airsoft tissue interface Cardiac and diaphragm movement Atelectasis Field of view (seen only in dual source)QuizSummary

#### **Honored Educators**

Presenters or authors on this event have been recognized as RSNA Honored Educators for participating in multiple qualifying educational activities. Honored Educators are invested in furthering the profession of radiology by delivering high-quality educational content in their field of study. Learn how you can become an honored educator by visiting the website at: https://www.rsna.org/Honored-Educator-Award/

Suhny Abbara, MD - 2014 Honored Educator Prabhakar Rajiah, MD, FRCR - 2014 Honored Educator

# CH255-SD-TUA1

Quantitative CT Texture Analysis for Predicting Recurrence in Lung Adenocarcinoma with a Solid Component Larger than 5 mm

Tuesday, Nov. 29 12:15PM - 12:45PM Room: CH Community, Learning Center Station #1

# Participants

Motohiko Yamazaki, MD, Niigata, Japan (*Presenter*) Nothing to Disclose Takuya Yagi, Niigata City, Niigata Prefecture, Japan (*Abstract Co-Author*) Nothing to Disclose Hiroyuki Ishikawa, MD, Niigata, Japan (*Abstract Co-Author*) Nothing to Disclose Hidefumi Aoyama, MD, PhD, Niigata, Japan (*Abstract Co-Author*) Nothing to Disclose

## PURPOSE

Lung adenocarcinoma with a pathological invasive focus  $\leq$ 5 mm shows excellent prognoses, whereas an invasive focus >5 mm has shown to increase the possibility of recurrence. This study aimed to evaluate the utility of quantitative CT texture analysis for predicting the recurrence of adenocarcinoma exhibiting a solid component >5 mm on thin-section CT.

## **METHOD AND MATERIALS**

This retrospective study consisted of 149 consecutive patients with 149 surgically resected stage I adenocarcinomas with the largest diameter of  $\leq$ 3 cm and a solid component on the mediastinal window settings of >5 mm on preoperative CT examination. Tumor segmentation was manually carried out on each axial section with a thickness of 1 or 1.25 mm. Subsequently, CT histogram features (kurtosis, skewness, entropy, and 10th to 90th percentile CT values) and quantitative morphologic features (whole tumor volume, mass, surface area, circularity, and sphericity) were computed using an image analysis software. Univariate and multivariate Cox regression analysis were performed to determine the factors associated with recurrence-free survival (RFS), defined as the time from surgery to recurrence. Survival curves were compared using the Log-rank test.

### RESULTS

During the follow-up period, 21 patients showed a recurrence of adenocarcinoma. In the univariate analysis, the recurrence rate was significantly higher in patients with lower entropy (P = 0.02), higher 50th/75th/90th percentile CT values (P = 0.014-0.027), higher circularity (P < 0.01), and higher sphericity (P = 0.011). There was a trend towards increased recurrence rate in patients with lower skewness (P = 0.053) and higher 25th percentile CT values (P = 0.05). Multivariate analysis revealed that 75th percentile CT values (hazard ratio, 1.04; P = 0.03) and circularity (hazard ratio, 1.76; P = 0.024) remained significant factors. Patients with greater than average values for 75th percentile CT values (>-107 Hounsfield units) and circularity (>0.68) had significantly lower 5-year RFS rate compared with the other patients (69.5% vs. 92.0%; P < 0.01).

### CONCLUSION

Quantitative CT texture parameters have a potential for predicting recurrence of lung adenocarcinoma with a solid component >5 mm.

## **CLINICAL RELEVANCE/APPLICATION**

Quantitative CT texture analysis is a more objective method than visual evaluation and may provide more accurate prognostic information for lung adenocarcinoma patients.

# CH256-SD-TUA2

Improving the Patient Experience by Reducing Overnight Interruptions Related to the Performance of Portable Chest X-rays

Tuesday, Nov. 29 12:15PM - 12:45PM Room: CH Community, Learning Center Station #2

# Participants

Michael S. Kelleher Jr, MD, New Haven, CT (*Abstract Co-Author*) Nothing to Disclose Robert DeVito, New Haven, CT (*Abstract Co-Author*) Nothing to Disclose Cheryl Granucci, Hamden, CT (*Abstract Co-Author*) Nothing to Disclose Michael Bennick, New Haven, CT (*Abstract Co-Author*) Nothing to Disclose Irena Tocino, MD, Branford, CT (*Presenter*) Nothing to Disclose

# PURPOSE

The purpose of this study was to evaluate the effect of a patient centered hospital wide intervention focused on reducing the number of routine portable chest x-rays (CXR) performed overnight.

## **METHOD AND MATERIALS**

In response to patient surveys, during the spring of 2015, our institution embarked on a hospital wide initiative aimed at decreasing the number of sleep interruptions related to non-urgent tests. In the case of radiology, the "Quiet Nights" initiative concerned mainly the non-urgent Portable Chest x-rays. Based on feedback at meetings with directors of all ICU and in-patient floors, a decision was made to stop performing routine and daily portable CXRs between the hours of 10 pm and 5 am. For 6 months prior and 6 months after the intervention, we recorded the number of routine, stat, and total portable CXRs performed during the hours of 10pm-5am. We also recorded the monthly in-patient census, and total number of portable CXRs performed each month. Statistical significance between the pre-intervention and post-intervention periods was determined using a 2 sample T test. A p-value of less than 0.05 was deemed to be statistically significant.

#### RESULTS

From February 2015 through July 2015, an average of 470 overnight portable chest x-rays were performed per month. The average number decreased to 91 per month after the intervention (p<0.0001). The number of stat overnight portable x-rays did not change significantly (average of 353 per month prior to intervention, 372 per month after intervention, p=0.14). No significant change (p=0.59) in the total number of portable x-rays performed before the intervention (4042) compared to after the intervention (4129). Inpatient census before and after the intervention remained relatively constant (778 per month before intervention, 764 per month after intervention, p=0.3).

### CONCLUSION

The introduction of a patient centered initiative succeeded in decreasing the number of overnight sleep interruptions by not performing routine portable CXRs between the hours of 10:00PM and 5:00AM while maintaining the number of stat portable CXRs.

### **CLINICAL RELEVANCE/APPLICATION**

By collaborating with our clinical colleagues, we were able to significantly reduce the number of overnight portable x-rays, and, as a result, the number of overnight interruptions.

Assessment of Selection Criteria for Low-dose Lung Screening CT among Asian Ethnic Groups in Taiwan -From Mass Screening to Specific Risk-based Screening for Non-smoker Lung Cancer

Tuesday, Nov. 29 12:15PM - 12:45PM Room: CH Community, Learning Center Station #3

# Participants

Fu-Zong Wu, Kaohsiung, Taiwan (*Presenter*) Nothing to Disclose Ming-Ting Wu, MD, Kaohsiung, Taiwan (*Abstract Co-Author*) Nothing to Disclose

# PURPOSE

The National Lung Screening Trial (NLST) showed low-dose screening chest CT reduced lung cancer mortality rate up to 20% in high risk patients in the United States. We aim to investigate the impact of applying the NLST eligibility criteria to the population in Taiwan, and to identify additional risk factors to select subjects at risk of lung cancer.

# METHOD AND MATERIALS

We retrospectively review the medical record of 1763 asymptomatic healthy subjects (40~80 year old) who voluntarily underwent low-dose chest CT (1029 male, 734 female) from August 2013 to August 2014. Clinical information and nodule characteristics were recorded. Results of subsequent follow-up and outcome were also recorded.

# RESULTS

8.4% (148/1763) of subjects would have been eligible for lung cancer screening based on the NLST criteria. However, only one of these eligible subjects would have a lung cancer detected at baseline. Among the 1615 subjects who did not meet the NLST criteria, the detection rates of lung cancer was 2.6% in women and 0.56% in men. Logistic regression showed that female gender and a family history of lung cancer were the two most important predictor of lung cancer in Taiwan (odds ratio of 6.367, P value = 0.003; odds ratio of 3.017, P value = 0.016, respectively).

# CONCLUSION

In conclusion, NLST eligibility criteria may not be effective in screening lung cancer in Taiwan. Risk-based prediction model based on the family history of lung cancer and female gender can potentially improve efficiency of lung cancer screening programs in Taiwan.

# **CLINICAL RELEVANCE/APPLICATION**

1. To clarify the impact of applying the NLST eligibility criteria for lung cancer screening in Taiwan

2. Female gender and family history of lung cancer were two important predictors of lung cancer3. The significantly higher prevalence of pure GGNs and subsolid nodules in subjects with family history of lung cancer

4. High-risk nodules may be more efficiently identified with specific risk factors

5. From mass screening to selective high-risk screening for non-smoker lung cancer

**3D** Computer-Aided Diagnosis System for Thin-Section CT: Utility for Pulmonary Functional Loss and Treatment Response Assessments in Connective Tissue Disease Patients

Tuesday, Nov. 29 12:15PM - 12:45PM Room: CH Community, Learning Center Station #4

# Participants

Yoshiharu Ohno, MD, PhD, Kobe, Japan (Presenter) Research Grant, Toshiba Corporation; Research Grant, Koninklijke Philips NV; Research Grant, Bayer AG; Research Grant, DAIICHI SANKYO Group; Research Grant, Eisai Co, Ltd; Research Grant, Fuji Pharma Co, Ltd; Research Grant, FUJIFILM RI Pharma Co, Ltd; Research Grant, Guerbet SA; Atsushi Yaguchi, MENG, Kawasaki, Japan (Abstract Co-Author) Employee, Toshiba Corporation Tomoya Okazaki, MS, Kawasaki, Japan (Abstract Co-Author) Employee, Toshiba Corporation Kota Aoyagi, Otawara, Japan (Abstract Co-Author) Employee, Toshiba Corporation Shigeo Kaminaga, Otawara-shi, Japan (Abstract Co-Author) Employee, Toshiba Corporation Takeshi Yoshikawa, MD, Kobe, Japan (Abstract Co-Author) Research Grant, Toshiba Corporation Wakiko Tani, RT, Kobe, Japan (Abstract Co-Author) Nothing to Disclose Erina Suehiro, RT, Kobe, Japan (Abstract Co-Author) Nothing to Disclose Noriyuki Negi, RT, Kobe, Japan (Abstract Co-Author) Nothing to Disclose Yuji Kishida, MD, Kobe, Japan (Abstract Co-Author) Nothing to Disclose Shinichiro Seki, Kobe, Japan (Abstract Co-Author) Nothing to Disclose Hisanobu Koyama, MD, PhD, Kobe, Japan (Abstract Co-Author) Nothing to Disclose Hitoshi Yamagata, PhD, Otawara, Japan (Abstract Co-Author) Employee, Toshiba Corporation Kazuro Sugimura, MD, PhD, Kobe, Japan (Abstract Co-Author) Research Grant, Toshiba Corporation Research Grant, Koninklijke Philips NV Research Grant, Bayer AG Research Grant, Eisai Co, Ltd Research Grant, DAIICHI SANKYO Group

# PURPOSE

To evaluate the capability of a newly developed 3D computer-aided diagnosis (CAD) system for quantitative pulmonary functional loss and treatment response assessment in connective tissue disease (CTD) patients.

## **METHOD AND MATERIALS**

Thirty-seven consecutive CTD patients (12 male, 25 female; mean age, 59 year old) underwent initial and follow-up thin-section CTs and pulmonary function tests. In this study, total 135 follow-up examinations were performed, and divided as following three groups at each time point: stable (n=103), acute exacerbation (n=16) and after treatment (n=16) phase scans. In this study, all CT data were analyzed by a newly developed our proprietary CAD software, and percentages of following six volume extents to total lung volume were automatically calculated in each CTD patient: normal lung, ground-glass opacity (GGO) and reticulation (GGO/reticular), honeycombing, consolidation, nodular and emphysema. Then, differences of each volume between two serial CT examinations were also calculated in each patient. To determine the capability of pulmonary functional loss assessments, stepwise regression analyses were performed. To evaluate the capability for treatment response assessment, each volume and pulmonary functional changes were compared among three groups by Tukey's HSD test.

### RESULTS

In the step-wise regression test, VC change was significantly affected by the following two factor changes: the first-step factor was GGO/reticulation, and the second-step factor was honey comb (r=0.39, p<0.05). On comparison of each volume change, stable and after treatment phase scan groups had significant differences with acute exacerbation phase scan group (normal lung: p<0.0001, GGO/reticulation: p<0.0001, honeycombing: p<0.0001, and consolidation: p<0.0001). In addition, consolidation volume change had significant difference between stable and after treatment phase scan groups (p=0.0002).

## CONCLUSION

The newly developed 3D CAD system for thin-section CT has a potential for pulmonary functional loss and treatment response assessments in CTD patients.

# **CLINICAL RELEVANCE/APPLICATION**

The newly developed 3D CAD system for thin-section CT has a potential for pulmonary functional loss and treatment response assessments in CTD patients.

Diagnostic Performance of Fourier Decomposition based Self-gated Functional Lung MRI for Detection of Thromboembolic Lung Perfusion Defects

Tuesday, Nov. 29 12:15PM - 12:45PM Room: CH Community, Learning Center Station #5

# Participants

Andreas Kunz, MD, Wurzburg, Germany (*Presenter*) Nothing to Disclose Andreas M. Weng, Wurzburg, Germany (*Abstract Co-Author*) Nothing to Disclose Janine Knapp, Wurzburg, Germany (*Abstract Co-Author*) Nothing to Disclose Daniel Stab, St Lucia, Australia (*Abstract Co-Author*) Nothing to Disclose Christian Kestler, Wurzburg, Germany (*Abstract Co-Author*) Nothing to Disclose Bernhard Petritsch, Wurzburg, Germany (*Abstract Co-Author*) Nothing to Disclose Constantin Lapa, Wurzburg, Germany (*Abstract Co-Author*) Nothing to Disclose Matthias Held, Wurzburg, Germany (*Abstract Co-Author*) Nothing to Disclose Herbert Kostler, Wurzburg, Germany (*Abstract Co-Author*) Nothing to Disclose Horsten A. Bley, MD, Hamburg, Germany (*Abstract Co-Author*) Nothing to Disclose Simon Veldhoen, MD, Wurzburg, Germany (*Abstract Co-Author*) Nothing to Disclose

#### PURPOSE

To assess the diagnostic performance of Fourier transform based functional lung MRI (SENCEFUL-MRI: SEIf-gated Non-Contrast-Enhanced FUnctional Lung imaging) for detection of thromboembolic lung perfusion defects.

# METHOD AND MATERIALS

10 patients with either acute or chronic thromboembolic perfusion defects as assessed by standard lung scintigraphy were included in the prospective study. They underwent Fourier decomposition-based MRI on a 1.5T scanner using the SENCEFUL approach (2D-FLASH sequence with quasi-random sampling for data acquisition). The lungs were segmented from the perfusion-weighted images and the perfusion information depicted in color-coded perfusion maps. Coronal lung scintigraphy images were anatomically matched with coronal SENCEFUL-maps and individually rated for perfusion deficits. The analysis was performed for 4 lung quadrants in each coronal image (right upper & lower; left upper & lower quadrant). As slice positioning, thickness and thus registered parts of the lung parenchyma per specific slice can vary between both techniques, a 3D analysis of the entire lung was added (4 lung quadrants per patient: right upper & lower; left upper & lower).

### RESULTS

Slice-by-slice analysis revealed agreement between SENCEFUL-MRI and scintigraphy ratings in 88.3% of quadrants (427 quadrants, agreement in 377; ICC 0.77, p<0.05). 41 quadrants were falsely rated positive with SENCEFUL. We found sensitivity to be 0.97 and specificity to be 0.63 (PPV 0.90; NPV 0.86). Using the 3D quadrant analysis, overall rating agreement was 95%. SENCEFUL-MRI correctly identified all quadrants affected in scintigraphy (i.e. 30 of 40 quadrants; ICC 0.93, p<0.05). Only two quadrants were falsely rated positive. Here, SENCEFUL-MRI achieved a diagnostic sensitivity of 1.0 and specificity of 0.8 (PPV 0.9; NPV 1.0).

## CONCLUSION

SENCEFUL-MRI and scintigraphy showed strong agreement levels for identification of pulmonary thromboembolic perfusion defects. SENCEFUL-MRI provided high sensitivity and specificity, especially for 3D quadrant analysis. Differences between 3D and slice-byslice analyses are most probably related to varying slice thickness and positioning between MRI and scintigraphy.

### **CLINICAL RELEVANCE/APPLICATION**

SENCEFUL-MRI bears the potential as viable alternative to lung scintigraphy for detection of thromboembolic lung diseases without disadvantages like radiation, need for i.v.-contrast or breath-holds.

# Blunt Traumatic Vascular Injuries of the Neck in the ED: What the Radiologist Must Know

Tuesday, Nov. 29 12:15PM - 12:45PM Room: ER Community, Learning Center Station #6

#### Awards

### **Identified for RadioGraphics**

### **Participants**

Elizabeth George, MD, Boston, MA (*Presenter*) Nothing to Disclose Ashish R. Khandelwal, MD, Boston, MA (*Abstract Co-Author*) Nothing to Disclose Christopher A. Potter, MD, Boston, MA (*Abstract Co-Author*) Nothing to Disclose Aaron D. Sodickson, MD, PhD, Boston, MA (*Abstract Co-Author*) Research Grant, Siemens AG; Consultant, Bayer AG Srinivasan Mukundan, MD, PhD, Boston, MA (*Abstract Co-Author*) Institutional research support, Siemens AG Institutional research support, Toshiba Corporation Consultant, Toshiba Corporation Bharti Khurana, MD, Boston, MA (*Abstract Co-Author*) Nothing to Disclose Diego B. Nunez JR, MD, MPH, Boston, MA (*Abstract Co-Author*) Nothing to Disclose

## **TEACHING POINTS**

1. Blunt trauma to the neck is associated with distinct patterns of vascular injuries. These include intramural hematoma, dissection, pseudoaneurysm, occlusion, transection and fistula.2. The mechanism of trauma, associated fractures and soft tissue injuries can be indicative of the likelihood and nature of vascular injury.3. Increased use of screening CTA in high-risk trauma patients has resulted in increased detection of these injuries. It is essential that radiologists are cognizant of the evidence for the screening criteria for CTA and understand the imaging features, grading, and management of such vascular injuries.

### TABLE OF CONTENTS/OUTLINE

1. Evidence for screening criteria for the initial evaluation of patients with suspected cerebrovascular injury.2. Systematic approach to CTA interpretation in trauma patients.3. Imaging features of vascular injuries of the neck, including the vertebral and carotid arterial system and the grades of blunt cerebrovascular injury.4. Review the mechanism of injury by analyzing the associated fractures and soft tissue injuries. The basic mechanisms, such as shearing from flexion/extension/rotational injury and direct trauma from fracture fragments will be discussed.5. Describe current management strategies, specifically anticoagulation and the limited indications for intervention.

# **Honored Educators**

Presenters or authors on this event have been recognized as RSNA Honored Educators for participating in multiple qualifying educational activities. Honored Educators are invested in furthering the profession of radiology by delivering high-quality educational content in their field of study. Learn how you can become an honored educator by visiting the website at: https://www.rsna.org/Honored-Educator-Award/

Aaron D. Sodickson, MD, PhD - 2014 Honored Educator Bharti Khurana, MD - 2014 Honored Educator

# ER218-SD-TUA1

Potentially Important Unreported Incidental Findings in Urgent Nonenhanced Abdominal CT Performed for Renal Colic

Tuesday, Nov. 29 12:15PM - 12:45PM Room: ER Community, Learning Center Station #1

# Participants

Elena Belloni, MD, Castel San Giovanni, Italy (*Abstract Co-Author*) Nothing to Disclose Paola Scagnelli, Castel san Giovanni, Italy (*Abstract Co-Author*) Nothing to Disclose Ilaria Fiorina, Pavia, Italy (*Presenter*) Travel support, Shenzhen Mindray Bio-Medical Electronics Co, Ltd; Consultant, Esaote SpA; Consultant, Shenzhen Mindray Bio-Medical Electronics Co, Ltd; Consultant, SuperSonic Imagine; Consultant, Hitachi, Ltd; Consultant, Toshiba Corporation

# PURPOSE

To retrospectively evaluate the prevalence of potentially important unreported incidental findings in consecutive nonenhanced abdominal CTs performed specifically for renal colic in the urgent setting.

## **METHOD AND MATERIALS**

One radiologist with eight years of experience in CT (two as resident and six as specialist) retrospectively evaluated 156 consecutive nonenhanced abdominal CTs performed specifically for renal colic in 156 patients from the Emergency Department. The incidental findings, both urinary and extraurinary, were classified as potentially important if they required further imaging and/or clinical workup. The radiologist was blinded to the potentially important incidental findings highlighted in the finalized reports performed in the urgent setting, but was aware of the reports of previous radiological examinations, if any. It was evaluated if the CTs were performed, and the report generated, in the morning shift (hrs 8-14), in the afternoon shift (hrs 14-20) or in the night shift (hrs 20-8).

# RESULTS

The 156 patients in the study were 104 males and 52 females, aged 51  $\pm$  15 years (range 24-89 years). 98 CTs were performed and reported in the morning shift, 49 in the afternoon shift, 9 in the night shift. In the finalized reports, 19 potentially important incidental findings in 19 different CTs were highlighted (12.2%), 10 in the morning, 8 in the afternoon and 1 at night. The blinded retrospective evaluation confirmed all the 19 reported findings and added 24 unreported potentially important incidental findings in 24 different CTs (13 in the morning, 8 in the afternoon, 3 at night) (total of 43 findings in 156 CTs, 27.6%) (p<0.01).

# CONCLUSION

A fair amount of potentially important additional findings was present in urgent nonenhanced abdominal CTs performed for renal colic. Even in the urgent setting, when the radiologist is under pressure, care should be taken to avoid underreporting (that in our series was particularly frequent in the night shift) and its possible consequences.

### **CLINICAL RELEVANCE/APPLICATION**

CT is a pan-exploratory radiologic technique. For this reason, the radiologist should evaluate every body part included in the fieldof-view, in order to avoid underreporting, even in the urgent setting.

# ER220-SD-TUA3

Retrospective Study of the Clinical Predictors of a Positive Abdominal Renal CT Scan in Patients Suspected to Nephro-ureteral Obstruction

Tuesday, Nov. 29 12:15PM - 12:45PM Room: ER Community, Learning Center Station #3

#### Awards

### **Student Travel Stipend Award**

#### **Participants**

Francisco E. Valles, MD, Bridgeport, CT (*Presenter*) Nothing to Disclose Nisarg A. Parikh, MD, MBBS, Bridgeport, CT (*Abstract Co-Author*) Nothing to Disclose Yogesh Kumar, MD, Bridgeport, CT (*Abstract Co-Author*) Nothing to Disclose Stephen Stein, MD, Westport, CT (*Abstract Co-Author*) Nothing to Disclose Scott C. Williams, MD, Westport, CT (*Abstract Co-Author*) Nothing to Disclose

#### PURPOSE

Renal CT scans are often used to evaluate patients suspected of having renal colic, which are often negative despite best clinical judgement. The purpose of this retrospective study is to aid clinicians to more selectively order renal CT scans, thereby minimizing radiation risk to those with a low likelihood of a positive result.

## **METHOD AND MATERIALS**

A retrospective study of 200 consecutive patients who arrived at a Level I trauma center and subsequently underwent a renal CT scan. Indications for renal CT scan were analyzed statistically using univariate and multivariate models.

#### RESULTS

Univariate chi-square tests showed pyuria (OR=2.41; 95% CI; P=0.02) was a predictor of positive renal CT scan. Unilateral flank pain (OR=2.00; 95% CI; P=0.06) and male sex (OR=1.81; 95% CI; P=0.05) had a tendency towards predicting a positive renal CT scan. Multivariate logistic regression demonstrated that males with unilateral pain (OR=2.14; 95% CI; P=0.02), males with hematuria (OR=3.01; 95% CI; P=0.01), and males with pyuria (OR=3.17; 95% CI; P=0.01) were significant predictors of positive renal CT scan. Males with unilateral flank pain and hematuria (OR=4.09; 95% CI; P=0.02), and males with unilateral flank pain, pyuria and hematuria (OR=4.52; 95% CI; P=0.01) yielded the highest likelihood of predicting a positive renal CT scan. Women with non-lateral pain were statistically more likely to have a negative CT scan (P<0.0001).

#### CONCLUSION

Our data suggests that pyuria is a significant risk factor for a positive renal CT scan in both men and women. Males with unilateral flank pain, hematuria and/or pyuria have a statistically significant risk for a positive renal CT scan due to nephro-ureteral obstruction. Conversely, women with non-lateralizing abdominal or back pain have a statistically significant likelihood of negative renal CT scan.

### **CLINICAL RELEVANCE/APPLICATION**

Clinical predictors for positive renal CT scans would aid clinicians to more selectively order a renal CT scan minimizing radiation risk to those that have a low likelihood of a positive result.

Image Quality and Dose Reduction of CT Pulmonary Angiogram with 100 kVp and Iterative Reconstruction to Detect Pulmonary Embolism in Emergency Room Patients

Tuesday, Nov. 29 12:15PM - 12:45PM Room: ER Community, Learning Center Station #4

#### Awards

### **Trainee Research Prize - Resident**

#### Participants

Edward Kuoy, MD, Orange, CA (*Presenter*) Nothing to Disclose Jeanie C. Zhang, MD, Orange, CA (*Abstract Co-Author*) Nothing to Disclose Phillip Reich, MD, Orange, CA (*Abstract Co-Author*) Nothing to Disclose Thangavijayan Bosemani, MBBS, MD, Orange, CA (*Abstract Co-Author*) Nothing to Disclose Pablo J. Abbona, MD, Orange, CA (*Abstract Co-Author*) Nothing to Disclose Mayil S. Krishnam, MBBS, MRCP, Orange, CA (*Abstract Co-Author*) Nothing to Disclose

### PURPOSE

To assess image quality (IQ) and dose savings of CTPA for detecting pulmonary embolism (PE) in patients with 100kVp and iterative reconstruction(IR) and to compare results with 120kVp and filtered back projection(FBP).

# **METHOD AND MATERIALS**

CTPA performed on 256-slice scanner for 96 consecutive ER patients with suspected PE using 100kVp protocol with adaptive IR (iDose3) (Group A), and 28 consecutive patients previously imaged for PE with 120kVp and FBP (Group B), stratified by BMI of 25, were evaluated for dose length product (DLP), volume CT dose index (CTDIv) and effective dose(ED). Arterial contrast density (Hounsfield Units,HU), contrast-to-noise ratio (CNR) and signal-to-noise ratio (SNR) of 27 pulmonary artery(PA) segments were calculated per patient. Two experienced radiologists independently assessed PA segments for IQ, noise, motion artifacts (MA) and PE.

#### RESULTS

The median CTDIv in Group A vs B with BMI<25: 6(IQR 5-7) and 10(IQR 9-13) mGy, respectively, and BMI>25: 9(IQR 7-13) and 17(IQR 13-20) mGy, respectively. Median DLP in Group A vs B with BMI<25: 227(IQR 178-283) and 366(IQR 303-486) mGy•cm, respectively, and BMI>25: 320(IQR 271-448) and 685(IQR 520-824) mGy•cm, respectively. ED in Group A vs B with BMI<25: 3(IQR 2-4) & 5(IQR 4-7) mSv, respectively (40% reduction), and BMI>25: 4(IQR 4-6) & 10(IQR 7-12) mSv, respectively (60% reduction). CNR and SNR were lower in Group A than B across BMI (p<0.01). Median arterial HU in Group A vs B with BMI<25: 438(IQR 320-519) & 310(IQR 249-451) HU, respectively, and BMI>25: 359(IQR 301-447) & 285(IQR 230-348) HU, respectively (both p<0.01). Overall IQ was statistically better in Group A than B with BMI<25, but vice versa for BMI>25 (p<0.01) with good inter-observer agreement (K>0.6). Minimal subjective noise without affecting diagnostic contents was more in Group A than B across BMI (p<0.01, K>0.6). There was no difference in MA between groups (p>0.05, moderate K>0.5). Acute segmental and subsegmental PEs (3) and findings of pulmonary infarcts, nodules and adenopathy were noted in Group A.

## CONCLUSION

CTPA with 100kVp and IR results in significant dose reduction and provides improved arterial attenuation with sufficient CNR and SNR to reliably detect PE in patients with BMI<25.

## **CLINICAL RELEVANCE/APPLICATION**

CTPA with 100kVp and IR can be employed in patients with BMI<25 to achieve significant dose reduction, while also preserving diagnostic ability for assessment of PE.

An Approach to the Diagnosis of Focal Liver Masses with CEUS

Tuesday, Nov. 29 12:15PM - 12:45PM Room: GI Community, Learning Center Station #9

FDA Discussions may include off-label uses.

Awards Magna Cum Laude Identified for RadioGraphics

### **Participants**

David P. Burrowes, MD, Calgary, AB (*Presenter*) Nothing to Disclose Alexandra Medellin-Kowalewski, MD, Calgary, AB (*Abstract Co-Author*) Nothing to Disclose Alison C. Harris, MBChB, Vancouver, BC (*Abstract Co-Author*) Nothing to Disclose Laurent Milot, MD, MSc, Toronto, ON (*Abstract Co-Author*) Nothing to Disclose Stephanie R. Wilson, MD, Calgary, AB (*Abstract Co-Author*) Equipment support, Siemens AG; Equipment support, Koninklijke Philips NV

# **TEACHING POINTS**

Diagnosis of focal liver masses with CEUS has similar algorithms to those for CT and MR based on enhancement in the arterial, portal, and delayed phases of contrast enhancement.Differentiation of benign and malignant disease is initially achieved by assessing enhancement in the portal venous phase.Malignant tumors are characterized by washout, a reduction of the enhancement of a region of interest to less than the adjacent liver parenchyma, following initial enhancement. Washout raises the possibility of malignant disease. Timing and intensity of washout differentiate malignant disease as hepatocellular or nonhepatocellular in origin. Sustained enhancement in the portal venous and delayed phase is supportive of benignancy.Benign tumors, hemangioma, focal nodular hyperplasia, and adenoma have specific and suggestive arterial phase vascular morphology, well shown with the high temporal resolution of dynamic real-time CEUS.Malignant tumors have more variable arterial phase enhancement on CEUS, making it less helpful for specific diagnoses..

### **TABLE OF CONTENTS/OUTLINE**

An Approach to diagnosis with CEUSWashout – its significance.Washout – variations of intensity and timingSpecific AP enhancement morphology of benign liver tumorsMalignant enhancement characteristics on CEUS

When Size Matters: Achieving Better Interreader Agreement with a Modified LIRADS Algorithm in the Diagnosis of Hepatocellular Carcinoma

Tuesday, Nov. 29 12:15PM - 12:45PM Room: GI Community, Learning Center Station #1

# Participants

Anton S. Becker, Zurich, Switzerland (*Presenter*) Nothing to Disclose Borna Barth, Zurich, Switzerland (*Abstract Co-Author*) Nothing to Disclose Olivio Donati, MD, Zurich, Switzerland (*Abstract Co-Author*) Nothing to Disclose Erika J. Ulbrich, MD, Zurich, Switzerland (*Abstract Co-Author*) Nothing to Disclose Christoph A. Karlo, MD, New York, NY (*Abstract Co-Author*) Nothing to Disclose Caecilia S. Reiner, MD, Durham, NC (*Abstract Co-Author*) Nothing to Disclose Michael A. Fischer, MD, Stockholm, Sweden (*Abstract Co-Author*) Nothing to Disclose

#### PURPOSE

LiRads is a standardized reporting system for liver lesions. Although providing excellent diagnostic performance, interreader agreement is only moderate at best. We propose a simplified LiRads decision tree for indeterminate or likely malignant lesions to improve interreader agreement while maintaining diagnostic performance for HCC.

### **METHOD AND MATERIALS**

MRI scans of 104 liver lesions were retrospectively selected and stratified for LiRads grades (LR1-5). Histopathology and imaging follow up served as standard of reference. Previous exams were provided to readers if available. Four independent and blinded radiologists categorized all lesions as benign (LR1-2) or potentially malignant (LR3-5), determined the primary LiRads based imaging features lesion size, arterial enhancement, wash-out, capsule-like enhancement and threshold growth for LR3-5 lesions and timed their readouts. LR3-5 lesions were classified according to LiRads v.2014-C and to a modified LiRads (mLiRads) algorithm. Diagnostic performance and Interreader agreement were determined for LiRads and mLiRads using receiver operating characteristics (ROC) and Fleiss' and Cohen's Kappa analysis respectively.

# RESULTS

Diagnostic performance for LiRads and mLiRads was equal with an area under the receiver-operator curve of 0.91. Feature-wise interreader agreement was better for lesions  $\leq 2 \text{ cm}$  for arterial enhancement (0.61  $\pm$  0.13 vs. 0.37  $\pm$  0.18), washout (0.48  $\pm$  0.13 vs. 0.33  $\pm$  0.18), and threshold growth (0.44  $\pm$  0.13 vs. 0.13  $\pm$  0.18). Interreader agreement was higher using mLiRads as compared to current LiRads showing an improved overall ( $\kappa = 0.53\pm0.04$  vs. 0.45 $\pm$ 0.04), and pair-wise agreement between most readers ( $\kappa$  range 0.42-0.67 vs. 0.35-0.60) at a reduced evaluation time (median 44 vs. 62 sec/lesion, p<0.0001).

## CONCLUSION

Giving lesion size and washout-behaviour more weight in a simplified, stepwise LiRads algorithm for LR3-5 lesions results in higher interobserver reliability and faster classification while maintaining diagnostic accuracy.

### **CLINICAL RELEVANCE/APPLICATION**

Evaluation of HCC-suspect liver lesions using LiRads may be simplified for higher interreader agreement at preserved diagnostic performance.

Can Extra-Mural Vascular Invasion on MRI Rectum Predict Development of Liver Metastases in Rectal Cancer?

Tuesday, Nov. 29 12:15PM - 12:45PM Room: GI Community, Learning Center Station #3

#### Awards

### **Student Travel Stipend Award**

#### Participants

Barry Hutchinson, MBBCh, MRCS, Galway, Ireland (*Presenter*) Nothing to Disclose Jeeban-Paul Das, MBBS, MRCPI, Galway, Ireland (*Abstract Co-Author*) Nothing to Disclose Declan G. Sheppard, MD, Galway, Ireland (*Abstract Co-Author*) Nothing to Disclose

# PURPOSE

The MRI features of extramural vascular invasion (EMVI) in rectal cancer have been well-described and are an independent predictor of poor prognosis and synchronous hepatic metastases. The correlation between EMVI and development of hepatic/distant metastases in patients who were M0 at initial staging has not been well-described. The purpose of this study was to review the MRI findings of a large cohort of patients with rectal cancer for EMVI to look for an association between those who do and don't go on to develop hepatic/distant metastases.

# **METHOD AND MATERIALS**

The pre-operative MRI rectum studies of 150 patients with histologically-proven adenocarcinoma of rectum, <15 cm from the anus were reviewed. Studies were assessed for the presence of EMVI, as evidenced by the presence of: Increased vessel caliber, increased signal within the lumen, mural thickening/irregularity or visible extension of tumor into an adjacent vessel. The T staging, overall tumor length, enlarged lymph nodes and involvement of the circumferential resection margin (CRM) were also recorded. All staging studies were reviewed for the presence of hepatic and distal solid organ metastases. Measure of correlation was assessed using a Chi-square test.

## RESULTS

16 patients were excluded as they had no follow-up staging. Mean age was 66 +/- 11 years and median tumor length was 50 mm. The radiological T staging was T1 in 8 patients, T2 in 43, T3 in 73 and T4 in 10 patients. 44/134 (32.8%) demonstrated MRI features of EMVI. Enlarged or abnormal lymph nodes were reported in 109 (81.3%) and involvement of the CRM in 26/134 (19.4%). 20 patients (14.9%) were diagnosed with synchronous metastases and a further 23 patients (17.2%) developed hepatic/distant metastases on follow-up CT staging (median follow-up time of 26 months). EMVI was demonstrated in 9/11 (45%) with synchronous metastases, 12/23 (52.2%) of those who subsequently developed metastases and 21/43 (48.8%) of all patients with metastases (p=0.007, 0.08, 0.01). Involvement of the CRM was found to be significant for presence of synchronous metastases (p=0.04). Age, tumor length and MRI nodal status showed no correlation with metastases.

### CONCLUSION

The presence of EMVI was found to be the only significant independent predictor of interval development of metastatic disease in patients with rectal cancer in this study.

# **CLINICAL RELEVANCE/APPLICATION**

EMVI detected on MRI in rectal cancer can be a predictor of metastases.

# Diagnostic Accuracy of R2\* as a Noninvasive Biomarker for Hepatic Iron Concentration

Tuesday, Nov. 29 12:15PM - 12:45PM Room: GI Community, Learning Center Station #4

#### **Participants**

Adrija Mamidipalli, MBBS, San Diego, CA (*Presenter*) Nothing to Disclose Jonathan C. Hooker, BS, San Diego, CA (*Abstract Co-Author*) Nothing to Disclose Gavin Hamilton, PhD, San Diego, CA (*Abstract Co-Author*) Nothing to Disclose Tanya Wolfson, MS, San Diego, CA (*Abstract Co-Author*) Nothing to Disclose Curtis N. Wiens, PhD, Madison, WI (*Abstract Co-Author*) Nothing to Disclose Nathan Artz, Madison, WI (*Abstract Co-Author*) Nothing to Disclose Alan B. McMillan, PhD, Madison, WI (*Abstract Co-Author*) Nothing to Disclose Santiago Horgan, MD, San Diego, CA (*Abstract Co-Author*) Nothing to Disclose Michael S. Middleton, MD, PhD, San Diego, CA (*Abstract Co-Author*) Nothing to Disclose AG Institutional research contract, sanofi-aventis Group Institutional research contract, Isis Pharmaceuticals, Inc Institutional research contract, Johnson & Johnson Institutional research contract, Synageva BioPharma Corporation Institutional research contract, Pfizer Inc Scott B. Reeder, MD, PhD, Madison, WI (*Abstract Co-Author*) Institutional research support, General Electric Company Institutional research support, Bracco Group

Claude B. Sirlin, MD, San Diego, CA (Abstract Co-Author) Research Grant, General Electric Company; Research Grant, Siemens AG; Research Grant, Guerbet SA; ;

### PURPOSE

The purpose of this study was to estimate the accuracy and identify the diagnostic cutoff of  $R2^*$  to diagnose hepatic iron overload in adults with nonalcoholic fatty liver disease (NAFLD), using contemporaneous percutaneous liver biopsy as the reference standard

## **METHOD AND MATERIALS**

In this prospective, cross-sectional study, fifty-three adults with NAFLD, without suspicion for hepatic iron overload, and undergoing standard-of-care percutaneous liver biopsy had 3T MR exams within three days of biopsy. Each exam included low-flip-angle, multi-echo magnitude (M)- and complex (C)-based MRI with spectral modeling of fat to generate hepatic R2\* parametric maps. For each method (M- and C-MRI), regions of interest (ROIs) were placed on the R2\* maps in each of the nine Couinaud liver segments, and average whole-liver R2\* values were calculated. Demographics (BMI, age, sex) were collected. Biopsy was the reference standard for the presence and degree of iron overload, scored using a standard hepatic iron grading system. Receiver operating characteristics (ROC) analyses were performed and diagnostic parameters at the Youden-index-based cutoffs computed for each method

### RESULTS

Nine subjects had biopsy-proven iron overload with iron grades of 1 or 2; R2\* values ranged from 44 to 112 s-1 (mean 76 s-1) for M-MRI and 39 to 129 s-1 (mean 75 sec-1) for C-MRI. Forty-four subjects had biopsy-proven absence of iron overload; R2\* ranged from 27 to 96 s-1 (mean 49 s-1) for M-MRI and 25 to 119 s-1 (mean 44 s-1) for C-MRI. Areas under ROC curves were 0.82 and 0.85 for M-MRI and C-MRI, respectively. Youden-based cutoffs and their corresponding sensitivities/specificities were 59.5 s-1 and 67%/80% for M-MRI, and 57 s-1 and 78%/84% for C-MRI

### CONCLUSION

R2\* estimated by M- and C-MRI provides reasonable accuracy to diagnose unsuspected iron overload in NAFLD. At 3T, R2\* values greater than 43 s-1 for M-MRI, and greater than 38 s-1 for C-MRI suggest the diagnosis. These cutoffs are lower than reported previously using non-histology reference standards

# **CLINICAL RELEVANCE/APPLICATION**

Our findings support that R2\* estimated at 3T by M-MRI and C-MRI can diagnose unsuspected iron overload in adults with NAFLD; C-MRI had a slightly higher accuracy than M-MRI

# GI377-SD-TUA7

## Quantification of Dual-Energy CT Iodine Uptake in Hepatic Metastases Using a Novel Volumetric Segmentation

Tuesday, Nov. 29 12:15PM - 12:45PM Room: GI Community, Learning Center Station #7

#### **Participants**

Katharina Stella Winter, Munich, Germany (*Presenter*) Nothing to Disclose Julian Holch, Munich, Germany (*Abstract Co-Author*) Nothing to Disclose Markus Haindl, BS, Muenchen, Germany (*Abstract Co-Author*) Nothing to Disclose Martin U. Sedlmair, MS, Forchheim, Germany (*Abstract Co-Author*) Employee, Siemens AG Melvin D'Anastasi, MD, New York, NY (*Abstract Co-Author*) Nothing to Disclose Florian Schwarz, MD, Munich, Germany (*Abstract Co-Author*) Nothing to Disclose Thorsten R. Johnson, MD, Munich, Germany (*Abstract Co-Author*) Nothing to Disclose Christoph G. Trumm, MD, Munich, Germany (*Abstract Co-Author*) Speaker, Siemens AG Maximilian F. Reiser, MD, Munich, Germany (*Abstract Co-Author*) Nothing to Disclose Wieland H. Sommer, MD, Munich, Germany (*Abstract Co-Author*) Founder, QMedify GmbH

#### PURPOSE

With its unique capability to quantify absolute iodine uptake, dual-energy CT has the potential to reveal considerable diagnostic information about vascularity and viability of hepatic metastases – however, there currently is no consensus on how to measure absolute iodine uptake within metastatic tissue. Our aim was to compare interobserver agreement of a novel tool for 3D-segmentation to quantify iodine uptake in hepatic colorectal metastases with conventional 2D-measurements.

## METHOD AND MATERIALS

Seventy-five consecutive patients with a total of 222 hepatic metastases from colorectal cancer who had undergone Dual-Energy CT of the abdomen (140kVp plus Tin-Filter at 155mAs and 100kVp at 200mAs) were included. For semiautomatic segmentation and VOI-based quantification of specific iodine uptake (mgl/cm<sup>3</sup>) of all hepatic metastases, a novel software prototype was used by two independent observers. At an interval of four weeks, both observers also used manual 2D-ROI-measurements on 3.0mm slices to quantify specific iodine uptake on a representative slice for each metastasis. To account for the clustering of metastases within patients, linear regression with random effects was used for calculating correlations. Intra-class-correlation coefficient was compared between the two methods.

### RESULTS

The two methods showed high correlation in iodine uptake of metastases (r=0.85, p<0.01). However, 3D VOI-based quantification of iodine uptake yielded systematically higher values than 2D ROI-based assessment ( $1.2\pm0.48$  mgI/cm<sup>3</sup> vs.  $1.05\pm0.51$  mgI/cm<sup>3</sup>, p<0.05). Interobserver agreement for the 3D-VOI-based approach was significantly higher than for 2D ROI-based measurements (r=0.99 vs. r=0.88, p<0.01).

# CONCLUSION

For the assessment of specific iodine uptake in hepatic metastases, 3D VOI-based shows a significantly higher interobserver agreement than the conventional 2D-approach. Assuming that the 3D VOI-based quantification is more accurate, our results indicate that conventional 2D-approaches underestimate iodine uptake.

## **CLINICAL RELEVANCE/APPLICATION**

In patients with colorectal liver metastases, the novel 3D VOI-based method produces more reliable results and might therefore become a valuable tool for an improved therapy response evaluation.

Validation of Clinical Scoring System SNACOR (Tumor Size and Number, Baseline Alpha-fetoprotein, Child-Pugh and Objective Radiological Response) after TACE of HCC

Tuesday, Nov. 29 12:15PM - 12:45PM Room: GI Community, Learning Center Station #8

# Participants

Roman Kloeckner, MD, Mainz, Germany (*Presenter*) Nothing to Disclose Aline Maehringer-Kunz, MD, Mainz, Germany (*Abstract Co-Author*) Nothing to Disclose Michael B. Pitton, MD, Mainz, Germany (*Abstract Co-Author*) Nothing to Disclose Christoph Dueber, MD, Mainz, Germany (*Abstract Co-Author*) Nothing to Disclose Irene Schmidtmann, Mainz, Germany (*Abstract Co-Author*) Nothing to Disclose Arndt Weinmann, Mainz, Germany (*Abstract Co-Author*) Nothing to Disclose

## PURPOSE

Transarterial Chemoembolization (TACE) is the standard of care for intermediate stage hepatocellular carcinoma (HCC). Deciding to what extent treatment should be repeated remains challenging. Therefore, we performed an external validation of the recently published SNACOR risk prediction model.

## **METHOD AND MATERIALS**

933 patients with HCC underwent TACE at our institution from 01/2000 to 09/2015. All variables needed to calculate the SNACOR (at baseline: tumor Size and Number, baseline Alpha-fetoprotein, Child-Pugh and after the first TACE Objective radiological Response) were determined. The score could range from 0 - 10 points. Overall survival was calculated for a low (0-2 points), intermediate (3-6 points), and high risk (7-10 points) group. Furthermore, Harrell's C-index and the integrated Brier score (IBS) were calculated. Cox regression was performed in order to identify independent predictors of survival.

# RESULTS

256 patients were finally included. The final evaluation date was the 31st of December 2015, by then 216 patients had been deceased and 40 were censored. Low, intermediate, and high SNACOR scores predicted median survivals of 24.9, 17.3, and 8.1 months, respectively. Harrell's C-index was 0.562 and IBS was 0.130. Baseline Child-Pugh and Alpha-fetoprotein as well as objective radiological response after the first TACE were independent predictors of survival (all p<0.05). Tumor size and tumor number were no additional independent predictors for survival.

# CONCLUSION

The SNACOR risk prediction model is able, after the first TACE, to identify patients with a dismal prognosis which are unlikely to benefit from further TACE. Nonetheless, Harrell's C-index showed only a moderate performance.

# **CLINICAL RELEVANCE/APPLICATION**

This risk prediction model tends to overly simplify clinical decision-making as this is usually based on a greater number of variables. Accordingly, this risk prediction model can only serve as one of several components in forming the decision whether the treatment should be repeated. Further research is needed to more reliably identify patients who may benefit from further TACE sessions. Volumetric Prostate Cancer Lesion Correlation on 3-Tesla Multiparametric MRI and Whole Mount Histopathology with Use of 3D-printed Custom-designed Molds

Tuesday, Nov. 29 12:15PM - 12:45PM Room: GU/UR Community, Learning Center Station #1

#### Awards

## **Student Travel Stipend Award**

#### **Participants**

Pooria Khoshnoodi, MD, Los Angeles, CA (*Presenter*) Nothing to Disclose Alan Priester, MS, Los Angeles, CA (*Abstract Co-Author*) Nothing to Disclose Hector E. Alcala, MPH,PhD, Charlotteville, VA (*Abstract Co-Author*) Nothing to Disclose Nazanin H. Asvadi, MD, Los Angeles, CA (*Abstract Co-Author*) Nothing to Disclose Shyam Natarajan, Los Angeles, CA (*Abstract Co-Author*) Nothing to Disclose Daniel J. Margolis, MD, Los Angeles, CA (*Abstract Co-Author*) Nothing to Disclose Jiaoti Huang, Los Angeles, CA (*Abstract Co-Author*) Nothing to Disclose Leonard S. Marks, MD, Los Angeles, CA (*Abstract Co-Author*) Nothing to Disclose Leonard S. Marks, MD, Los Angeles, CA (*Abstract Co-Author*) Speaker, Avero Diagnostics Investigator, Actavis, Inc Investigator, Indevus Pharmaceuticals Inc Investigator, Light Sciences Corporation Investigator, Hologic, Inc Investigator, Danaher Corporation Investigator, GlaxoSmithKline plc Investigator, Allergan, Inc Investigator, GTx, Inc Advisor, Indevus Pharmaceuticals Inc Advisor, Robert E. Reiter, MD, Los Angeles, CA (*Abstract Co-Author*) Nothing to Disclose Steven S. Raman, MD, Santa Monica, CA (*Abstract Co-Author*) Nothing to Disclose

# PURPOSE

To evaluate correlation of Prostate Cancer (CaP) tumor volume (TV) of regions of interest (ROI) on prostate multiparametric (MP) magnetic resonance imaging MRI (TVm) with concordant foci TV on whole mount histopathology (WMHP) (TVh), and assess accuracy of MRI in estimating CaP TV stratified by Gleason score (GS) and MP-MRI overall suspicion assessment (OA).

## **METHOD AND MATERIALS**

A HIPAA-compliant, IRB-approved study of 114 men who underwent 3T prostate MP-MRI before robotic radical prostatectomy from August 2013 to November 2015 was performed. Prostate and suspicious regions of interest (ROIs) were segmented on MRI and OA was determined using standardized criteria on a 1-5 scale. TVm was calculated by radiologist delineation of ROIs. A 3D patient-specific mold was printed to precisely fit the excised prostate based on MRI prostate segmentation. A pathologist contoured each tumor on all WMHP slides. Custom software automatically imported the annotated contoured WMHP slides, reconstructed the tumors in 3D, and calculated the TVh. A radiologist and pathologist reviewed each case to match each ROI to the concordant focus on WMHP. Pearson correlation coefficients (p) were calculated to determine strength of association between volumes of concordant lesion foci on MRI and WMHP. Accuracy (A) of MRI in estimating CaP tumor volume (A=TVm/TVh) was calculated. Analyses were conducted using Stata 14.1. P-values<.05 were considered significant.

# RESULTS

114 patients had 118 CaP foci (94 index tumors) on WMHP matched with MRI ROIs concordantly. Of 118 CaP foci GS was  $\leq 6(3+3)$  in 26 (22%), 7(3+4) in 59 (50%),  $\geq 7(4+3)$  in 33 (28%). OA was 2 in 3 (3%), 3 in 37 (31%), 4 in 45 (38%), and 5 in 33 (28%). The median TVh and TVm were 1.12cc and 0.41cc respectively. The  $\rho$  between TVh and TVm was 0.55 overall ( $\rho<0.001$ ), 0.27 in GS=6 ( $\rho=0.18$ ), 0.52 in GS=3+4 ( $\rho<0.001$ ) and 0.57 in GS $\geq$ 4+3 ( $\rho<0.001$ ) tumors. The  $\rho$  was 0.55,0.48 and 0.65 for tumors with OA of 3,4 and 5 respectively. The A was 0.28, 0.43 and 0.55 for OA 3,4 and 5 respectively ( $\rho<0.001$ ).

# CONCLUSION

On 3T MP-MRI, TVm has overall moderate correlation with TVh and true volume is consistently underestimated on MR. The best correlation is achieved for higher grade lesions and lesions with higher overall assessments.

# CLINICAL RELEVANCE/APPLICATION

3T MP-MRI consistently underestimates tumor size estimation, and its accuracy is important for targeted biopsy or focal therapy.

## GU223-SD-TUA2

Image Texture Analysis as an Image-Based Discriminator between Chromophobe Renal Cell Carcinoma and Oncocytoma

Tuesday, Nov. 29 12:15PM - 12:45PM Room: GU/UR Community, Learning Center Station #2

# Participants

Chidubem G. Ugwueze, MS, Los Angeles, CA (*Abstract Co-Author*) Nothing to Disclose Megha N. Gupta, MD, Los Angeles, CA (*Abstract Co-Author*) Nothing to Disclose Mike Kwon, BS,MS, Los Angeles, CA (*Abstract Co-Author*) Nothing to Disclose Felix Y. Yap, MD, Los Angeles, CA (*Abstract Co-Author*) Nothing to Disclose Darryl Hwang, PhD, Los Angeles, CA (*Abstract Co-Author*) Nothing to Disclose Steven Cen, PhD, Los Angeles, CA (*Abstract Co-Author*) Nothing to Disclose Bhushan Desai, MBBS, MS, Los Angeles, CA (*Abstract Co-Author*) Nothing to Disclose Vinay A. Duddalwar, MD, FRCR, Los Angeles, CA (*Presenter*) Nothing to Disclose Bino Varghese, Los Angeles, CA (*Abstract Co-Author*) Nothing to Disclose Mittul Gulati, MD, La Canada Flintridge, CA (*Abstract Co-Author*) Nothing to Disclose

## PURPOSE

It is difficult on imaging and even biopsy to differentiate between benign (oncocytomas) and malignant (chromophobe renal cell carcinomas) oncocytic tumors. We evaluated if texture metrics such as Gray Level Co-occurrence Matrix (GLCM) texture features could differentiate between Chromophobe RCC and Oncocytoma.

# METHOD AND MATERIALS

In this retrospective cohort study, Computerized Tomography (CT) images of tumors for 14 patients with Chromophobe RCC and 20 patients with Oncocytoma were extracted using semi-automated segmentation on Synapse 3D (Fujifilm, Stamford, CT). Two and three dimensional GLCM calculations were performed on each tumor. These calculations, 2D and 3D respectively, extracted thirteen GLCM features: mean gray value (MGV), standard deviation (SD), inverse difference moment (IDM), difference variance (DV), entropy (ENT), contrast (CON), sum of squares variance (SQV), sum entropy (SE), sum average (SA), angular second moment (ASM), Correlation (COR), information measures of correlation1 (IMC1), and IMC2. Descriptive analyses based on ttest or Wilcoxon Rank Sum test, depending on data distribution and with box whisker plot were used to illustrate the difference in imaging parameter between patient categories.

## RESULTS

GLCM Calculations were technically successful for all cases. Chromophobe and Oncocytoma 3D features (ASM, ENT, DIS, IDM, HOM, IMC1, SQV, SD, SA, and Uniformity) were significant significantly different, p < 0.1, in all four phases (see figure for ASM boxplot). 2D features were significantly different, p < 0.1, mainly in the arterial phase (ASM, ENT, DIS, IDM, HOM and SE). No significant difference was seen between study groups in the nephrographic phase.

# CONCLUSION

Ten 3D texture features may help distinguish between Oncocytoma and chRCCs in all phases. 2D features may also a role with the corticomedullary phase being of high importance for the discrimination.

# **CLINICAL RELEVANCE/APPLICATION**

Quantitative texture metrics can distinguish between oncocytic tumors with different biologic behavior with potential to allow for image-based patients' risk stratification.

## Utility of Multi-parametric MRI to Predict Pathological Stage and Surgical Margins in Anterior Prostate Cancers

Tuesday, Nov. 29 12:15PM - 12:45PM Room: GU/UR Community, Learning Center Station #4

#### **Participants**

Muhammad Idris, MBBS, Ottawa, ON (*Presenter*) Nothing to Disclose Nicola Schieda, MD, Ottawa, ON (*Abstract Co-Author*) Nothing to Disclose Christopher Lim, MD, Ottawa, ON (*Abstract Co-Author*) Nothing to Disclose Robert Lim, MD, Ottawa, ON (*Abstract Co-Author*) Nothing to Disclose Wael M. Shabana, MD, Ottawa, ON (*Abstract Co-Author*) Nothing to Disclose Satheesh Krishna, MD, Ottawa, ON (*Abstract Co-Author*) Nothing to Disclose Trevor A. Flood, MD, FRCPC, Ottawa, ON (*Abstract Co-Author*) Nothing to Disclose Rodney H. Breau, MD, Ottawa, ON (*Abstract Co-Author*) Nothing to Disclose Christopher Morash, MD, Ottawa, ON (*Abstract Co-Author*) Nothing to Disclose Matthew D. McInnes, MD, FRCPC, Ottawa, ON (*Abstract Co-Author*) Nothing to Disclose

#### PURPOSE

Clinical staging of anterior prostate cancer (APC) is limited and studies evaluating MRI for staging of APC are lacking. Moreover, there are higher rates of positive surgical margins (PSM) after radical prostatectomy (RP) in APC. This study evaluates subjective and quantitative MRI, to predict extraprostatic extension (EPE) and PSM in APC.

## **METHOD AND MATERIALS**

With IRB approval, 25 patients underwent RP with APC (>2/3 of tumor anterior to urethra; 21 transition zone, 4 anterior peripheral zone tumors) and MRI between 2012-2015. Two blinded radiologists assessed MRI for: tumor size (mm), invsion of anterior fibromuscular stroma (AFMS), whether tumor crosses midline and EPE. Radiologists measured leading edge of tumor (relative to prostate capsule) on b>1000 mm2/sec EPI fused onto T2W. Comparisons were performed using chi-square, regression and ROC.

## RESULTS

Age and PSA were 65.2  $\pm$  5.9 years and 9.91  $\pm$  7.62 ng/mL with no difference by EPE or PSM (p>0.05). Rates of EPE and PSM were 52% (13/25) and 40% (10/25). Gleason scores were: 3+3=6 (N=1), 3+4=7 (N=12), 4+3=7 (N=9), 4+4=8 (N=1) and 4+5=9 (N=2).Tumor size was 19.0  $\pm$  8.3 (7-33) mm overall; larger tumors were associated with EPE and PSM (p=0.009 and 0.011). AUC for size prediciting EPE/PSM were 0.79 (SE=0.09, CI0.62-0.97) and 0.77 (0.11, 0.55-0.99) with size  $\geq$ 16mm yielding sensitivity/specificity (SENS/SPEC) of 76.9/66.7% and 80/60% respectively.52% (13/25) of tumors crossed the midline, this was associated with EPE and PSM (p=0.009 and 0.002). 72% (18/25) tumors invaded AFMS, this was not associated with EPE or PSM (p>0.05). Radiologist impression of EPE had SENS/SPEC of 61.5/75.0%. Leading edge of tumor was 1.3  $\pm$  3.7 (-7 - 10) mm overall and was associated with both EPE and PSM (p=0.011 and 0.013). AUC for leading edge predicting EPE/PSM were 0.79 (SE=0.09, CI0.61-0.98) and 0.77 (0.09, 0.59-0.96) with  $\geq$ 2mm extension yielding SENS/SPEC of 76.9/75% and 70/73.3% respectively.

# CONCLUSION

In anterior prostate cancers, size of tumor, extension accross midline and the leading edge of tumor are findings associated with extraprostatic extension and positive surgical margins after RP.

## **CLINICAL RELEVANCE/APPLICATION**

Diagnosis of extraprostatic spread of tumor in anterior prostate cancers is possible with MRI. These findings correlate with positive surgical margin rates after radical prostatectomy and may alter surgical approach or management.

# GU226-SD-TUA5

Predictive Value of Diffusion Weighted MR Imaging in Therapeutic Outcome of Uterine Fibroids Following High Intensity Focused Ultrasound (HIFU)

Tuesday, Nov. 29 12:15PM - 12:45PM Room: GU/UR Community, Learning Center Station #5

#### Participants

Kueian Chen, Taoyuan, Taiwan (*Presenter*) Nothing to Disclose Chien-Min Han, Taoyuan, Taiwan (*Abstract Co-Author*) Nothing to Disclose Gigin Lin, MD, Guishan, Taiwan (*Abstract Co-Author*) Nothing to Disclose Yun-Chung Cheung, MD, Kwei Shan, Taiwan (*Abstract Co-Author*) Nothing to Disclose Yu-Ting Huang, Guishan, Taiwan (*Abstract Co-Author*) Nothing to Disclose Koon-Kwan Ng, Guishan, Taiwan (*Abstract Co-Author*) Nothing to Disclose

## PURPOSE

To evaluate the predictive value of diffusion weighted (DW) MR imaging in therapeutic outcome of uterine fibroids following high intensity focused ultrasound (HIFU).

#### METHOD AND MATERIALS

This single center retrospective analysis included 90 uterine fibroids from 37 symptomatic women treated with ultrasound (US)- guided HIFU. Pre- treatment and post- treatment MR images within 1 month were obtained by using DWI (b=0, 1000 s/mm2) on a 1.5- T MR unit.Two- dimensional (2D) and volumetric (3D) datasets from each fibroid on pre- treatment and post- treatment MR images were recorded respectively. Two readers measured diameter/volume. Apparent diffusion coefficient (ADC) values of each fibroid with manually drawn ROI on the largest tumor plane/whole tumor volume were recorded. Nonprefusion area/volume (NPA/NPV) ratio for post- treatment fibroids, defined as NPV diameter/volume divided by the post- treatment fibroid diameter/volume, with responder group defined as NPA/NPV > 95%. Mann- Whitney test and logistic regression was used to evaluate the predictive value of pretreatment ADC values of fibroids. Differences with P < .05 were considered statistically significant.

#### RESULTS

Volumetric ADC value significantly correlated with 2D ADC value (r = 0.83, P < .0001). 2D analysis revealed a significantly lower pre- treatment ADC value ( $1.14 \pm 0.19 \vee 1.23 \pm 0.17 \times 10^{-3} mm2/s$ , P = .027) and higher post- treatment ADC value ( $1.45 \pm 0.21 \vee 1.32 \pm 0.27 \times 10^{-3} mm2/s$ , P = .012) in responder group, as compared with non- responder group. Pre- and post- treatment ADC values predicted the successful treatment for fibroids (P = .025 and P = .009 respectively). Post- treatment volumetric ADC value was significantly increased in responder group ( $1.46 \pm 0.21 \vee 1.35 \pm 0.27 \times 10^{-3} mm2/s$ , P = .004), which could predicted the successful HIFU treatment (P = .035). Pre- treatment volumetric ADC value was lower in responder group ( $1.17 \pm 0.24 \vee 1.23 \pm 0.69 \times 10^{-3} mm2/s$ ), albeit not statistically significant (P = .084).

#### CONCLUSION

DW MR imaging has potential to be surrogate biomarkers in prediction of therapeutic outcome of uterine fibroids following HIFU. Both 2D and volumetric ADC measurements

## **CLINICAL RELEVANCE/APPLICATION**

DW MR imaging has potential to be surrogate biomarkers in prediction of therapeutic outcome of uterine fibroids following HIFU.

# GU227-SD-TUA6

How Low Can We Go? Dose Saving Through Low-dose Examination for Urolithiasis via Modern Computer Tomography with Tin-Filter

Tuesday, Nov. 29 12:15PM - 12:45PM Room: GU/UR Community, Learning Center Station #6

# Participants

Youssef Erfanian, MD, Essen, Germany (*Presenter*) Nothing to Disclose Nika Guberina, MD, Essen, Germany (*Abstract Co-Author*) Nothing to Disclose Lino Sawicki, MD, Dusseldorf, Germany (*Abstract Co-Author*) Nothing to Disclose Saravanabavaan Suntharalingam, Essen, Germany (*Abstract Co-Author*) Nothing to Disclose Axel Wetter, Essen, Germany (*Abstract Co-Author*) Nothing to Disclose Jens M. Theysohn, MD, Essen, Germany (*Abstract Co-Author*) Nothing to Disclose

# PURPOSE

Modern high-performance computer tomography (CT) devices provide high resolution images with lower radiation exposure. Such CT scanners offer more and yet better diagnostic possibilities. Radiation dose saving is particularly important in young patients since the cumulative dose during lifetime can increase the risk of cancer. Examinations are often performed in order to diagnose kidney stones. The aim of this study was to compare radiation exposure doses and image quality of two older CT devices to a tin-filter CT in patients with suspected urolithiasis.

#### **METHOD AND MATERIALS**

We compared low-dose CT examinations of 139 patients on two standard CTs (Siemens AS+, Siemens Flash) to a tin-filter CT (Siemens Force) regarding dose-length product (DLP) and Computed Tomography Dose Index volume (CTDIvol). Furthermore, image quality of each CT scan was assessed using a five-point Likert scale (0= major blurring, 4= excellent depiction). All imaging datasets were independently analyzed by two radiologists. Bonferroni-corrected Mann-Whitney U tests for post-hoc comparisons after Kruskal-Wallis analysis of variance were performed to test for significant subgroup differences in DLP, CTDIvol and image quality. Inter-rater agreement was evaluated in terms of image quality using Cohen's kappa.

# RESULTS

DLP of tin-filter CTs was 51% lower in comparison to CTs without tin-filter, respectively (81 vs. 163 mGycm; p<0.001). Moreover, CTDIvol of with tin-filter showed 55% lower values (1.5 vs. 3.4 mGy; p<0.001). Mean image quality of tin-filter CTs was comparable (3.67 vs. 3.59; p>0.05). Inter-rater agreement regarding image quality was substantial for all CTs ( $\kappa$ =0.74, n=139).

## CONCLUSION

Modern CTs with tin-filter are able to significantly reduce radiation exposure in young patients suspected to have kidney stones without sacrificing image quality.

## **CLINICAL RELEVANCE/APPLICATION**

Especially young patients should receive low-dose examinations on modern tin-filter CT scanners if available, since these can cut radiation exposure to half even when using low-dose protocols.

## Photon Counting CT versus Dual-energy CT for Measurement of Urinary Stone Size and Composition

Tuesday, Nov. 29 12:15PM - 12:45PM Room: GU/UR Community, Learning Center Station #3

#### Participants

Juan Montoya, Rochester, MN (*Presenter*) Nothing to Disclose Roy Marcus, MD, Rochester, MN (*Abstract Co-Author*) Institutional research agreement, Siemens AG; Research support, Siemens AG Ahmed Halaweish, PhD, Rochester, MN (*Abstract Co-Author*) Employee, Siemens AG Shuai Leng, PhD, Rochester, MN (*Abstract Co-Author*) Nothing to Disclose Cynthia H. McCollough, PhD, Rochester, MN (*Abstract Co-Author*) Research Grant, Siemens AG

#### PURPOSE

To assess the accuracy with which the size and composition of small urinary stones could be measured using photon counting computed tomography (PCCT) and to compare to dual-energy CT (DECT).

## **METHOD AND MATERIALS**

Seventy stone fragments (from 35 patients) of different size and composition were included in the study. Composition was determined using infrared spectroscopy and only stones with >90% of a single material were used. Size was determined using digital calipers and only stones <5mm long were used. Stones were embedded in gelatin and placed in a 35-cm-wide torso-shaped water phantom. Dose-matched acquisitions were performed using a 2nd generation DECT (Definition Flash, Siemens Healthcare) at 80/Sn140 kV and a research whole body PCCT (Somatom CounT, Siemens) at 140 kV (25 and 75 keV energy thresholds). Images were reconstructed using a medium-soft kernel (D30), 15 cm field of view, 1.0 mm slice thickness and 0.8 mm increment. Stone detection and segmentation were performed on the 80kV DECT and 25-75 keV PCCT images and CT number ratio (CTR) and size calculations were performed for each stone using in-house Matlab-based software. The bias and precision of stone size measurement was assessed using Bland-Altman analysis and CTR data were summarized using box and whisker plots. ROC analysis was used to determine the accuracy of stone composition.

# RESULTS

16 uric acid (UA), 12 cystine (CYS), 24 calcium oxalate monohydrate (COM), 8 brushite (BRU) and 10 apatite (APA) stones were included. Mean ( $\pm$  SD) stone size was 2.63  $\pm$  0.92 mm for all stones (range 1.34 – 5.02 mm). Four stones (1 COM and 3 UA) were not detected in DECT and 2 stones (UA) were not detected in PCCT. Mean differences in stone size measurements (CT vs caliper) were -0.02  $\pm$  0.61 mm and -0.18  $\pm$  0.51 mm for DECT and PCCT, respectively. Area under the ROC curve (AUC) was higher for the detection of small UA stones using PCCT, however the increased spectral separation of DECT allowed better classification of non-UA stones.

# CONCLUSION

PCCT allows similar accuracy and higher precision for the measurement of small stones. Improved detection and classification of small UA stones was observed using PCCT compared to DECT.

## **CLINICAL RELEVANCE/APPLICATION**

PCCT demonstrated superior performance for small stone detection and similar stone composition characterization compared to DECT. PCCT might allow the diagnosis of stone precursor lesions.

# Morphological and Functional Tumor Response Assessment Criteria: A Primer for Radiologists

Tuesday, Nov. 29 12:15PM - 12:45PM Room: HP Community, Learning Center Station #6

## Awards Magna Cum Laude

#### **Participants**

Bhanusupriya Somarouthu, MD, Boston, MA (*Presenter*) Nothing to Disclose Hamed Kordbacheh, MD, Boston, MA (*Abstract Co-Author*) Nothing to Disclose Trinity Urban, Boston, MA (*Abstract Co-Author*) Nothing to Disclose Gordon J. Harris, PhD, Boston, MA (*Abstract Co-Author*) Medical Advisory Board, Fovia, Inc; Stockholder, IQ Medical Imaging LLC; Dushyant V. Sahani, MD, Boston, MA (*Abstract Co-Author*) Research support, General Electric Company; Medical Advisory Board, Allena Pharmaceuticals, Inc

Avinash R. Kambadakone, MD, Boston, MA (Abstract Co-Author) Nothing to Disclose

# **TEACHING POINTS**

The purpose of this exhibit is to Review various morphological and functional criteria available for tumor response assessment to various therapies Discuss limitations and challenges encountered while applying criteria Discuss with case based examples for each of the response assessment criteria

## **TABLE OF CONTENTS/OUTLINE**

Discuss various morphological response assessment criteria including RECIST (Response Evaluation Criteria in Solid Tumors), Cheson, immune related RECIST etc Discuss functional criteria including EORTC (European Organization for Research and Treatment of Cancer guideline), PERCIST (PET Response Criteria in Solid Tumors) Discuss 3D imaging based criteria such as tumor volumes for brain lesions Rationale for appropriate technique and rules for assessment while using standardized response assessment criteria Case based examples highlighting the various criteria Discussion of pitfalls including pseudo-progression Summary and Conclusion

#### **Honored Educators**

Presenters or authors on this event have been recognized as RSNA Honored Educators for participating in multiple qualifying educational activities. Honored Educators are invested in furthering the profession of radiology by delivering high-quality educational content in their field of study. Learn how you can become an honored educator by visiting the website at: https://www.rsna.org/Honored-Educator-Award/

Dushyant V. Sahani, MD - 2012 Honored Educator Dushyant V. Sahani, MD - 2015 Honored Educator Dushyant V. Sahani, MD - 2016 Honored Educator

# Has the Objective Quality of Imaging Papers Changed Over the Last 20 Years?

Tuesday, Nov. 29 12:15PM - 12:45PM Room: HP Community, Learning Center Station #1

#### Awards

## **Student Travel Stipend Award**

## **Participants**

Danielle Kruse, BA, Stony Brook, NY (*Presenter*) Nothing to Disclose Renee Cattell, BA, Stony Brook, NY (*Abstract Co-Author*) Nothing to Disclose Franco Momoli, MSc,PhD, Ottawa, ON (*Abstract Co-Author*) Nothing to Disclose Mark E. Schweitzer, MD, Stony Brook, NY (*Abstract Co-Author*) Consultant, MMI Munich Medical International GmbH Data Safety Monitoring Board, Histogenics Corporation

# PURPOSE

Government bodies and insurance companies are requiring higher evidence and technical efficacy levels in order to provide reimbursements for medical and imaging procedures. Hence we sought to determine if both the evidence levels as well as the technical efficacy levels of imaging manuscripts have changed over the last twenty years.

# **METHOD AND MATERIALS**

Using Web of Science (2014) we determined the 10 highest impact factor imaging journals. For each journal the 10 most cited and 10 average cited papers were compared, for each of the following years: 1994, 1998, 2002, 2006, 2010 and 2014. Evidence level (EL) was graded on a scale of 1-5, with 1 being prospective randomized trials, and hence the highest level, and 5 being "expert opinions", considered the lowest evidence level. Technical efficacy (TE) was graded on a scale of 1-6, with 1 being the lowest, focused on image quality, and 6 as the highest, based on the criteria of Thornbury and Fryback [1]. Statistical software R and package lme4 were used to fit mixed regression models with fixed effects for group (average vs. top cited) and year, and a random effect for journal. 1. Fryback, D. G., & Thornbury, J. R. (1991). The Efficacy of Diagnostic Imaging. Medical Decision Making, 11(2), 88-94. doi:10.1177/0272989x9101100203

#### RESULTS

The evidence level of manuscripts has improved over time, -0.03 every year on average (p <0.001). In 1994 the average EL was 3.81, and in 2014, it was 2.99. Furthermore, the more cited papers also had better evidence levels (group effect = -0.23, SE 0.09, p = 0.011). Interestingly, the levels of technical efficacy were lower in top cited as compared to average cited articles, although the difference was not significant (group effect = -0.14, SE = 0.09, p = 0.16). However, technical efficacy level did increase modestly over this 20 year time period, with an average score of 1.57 in 1994 to 2.83 in 2014 (0.06 per year, SE = 0.007, p <0.001).

# CONCLUSION

Compared to average cited papers, top cited papers have better evidence levels, with no difference in technical efficacy level. Over the last 20 years, imaging journal articles have improved modestly in quality, as measured by evidence level and technical development.

# **CLINICAL RELEVANCE/APPLICATION**

The quality of top impact factor imaging journal articles has improved over time, which may impact clinical knowledge base.

# HP217-SD-TUA2

Clinical Impact of Second-Opinion Musculoskeletal Interpretations in an Orthopedic Oncology Patient Population

Tuesday, Nov. 29 12:15PM - 12:45PM Room: HP Community, Learning Center Station #2

#### Awards

**Student Travel Stipend Award** 

#### Participants

Aleksandr Rozenberg, MD, Philadelphia, PA (*Presenter*) Nothing to Disclose Barry Kenneally, Philadelphia, PA (*Abstract Co-Author*) Nothing to Disclose John Abraham, Philadelphia, PA (*Abstract Co-Author*) Nothing to Disclose Kristin Strogus, Philadelphia, PA (*Abstract Co-Author*) Nothing to Disclose Johannes B. Roedl, MD, PhD, Philadelphia, PA (*Abstract Co-Author*) Nothing to Disclose William B. Morrison, MD, Philadelphia, PA (*Abstract Co-Author*) Consultant, General Electric Company Consultant, AprioMed AB Patent agreement, AprioMed AB Consultant, Zimmer Holdings, Inc Adam C. Zoga, MD, Philadelphia, PA (*Abstract Co-Author*) Nothing to Disclose

### PURPOSE

To analyze the impact on clinical management when subspecialty musculoskeletal radiologists render second opinion consultation interpretations on outside imaging examinations of orthopedic oncology patients.

## **METHOD AND MATERIALS**

An institutional PACS database was searched for secondary interpretations placed on outside imaging studies as requested by an orthopedic oncology service from January 2014 to February 2016. The MSK consultation reports were compared to the original interpretations, when available. Reports were categorized using a seven-point scale: I (no discrepancy), II (failure to detect a clinically insignificant abnormality), III (clinically insignificant difference in interpretation), IV (difference in imaging follow up recommendation), V (equivocal initial interpretation with subsequent definitive subspecialty interpretation), VI (clinically significant difference in interpretation), VI (clinically significant abnormality). Clinical significance was defined by whether a discrepant interpretation resulted in a change in diagnosis or treatment.

## RESULTS

214 patients met inclusion criteria, with an average age of 47.0  $\pm$ 19.2 years. The most common indication for initial imaging was "pain" (76%). There were 49 (22.9%) instances of discrepant interpretations resulting in clinically significant differences in management; 36 (16.8%) were category VI and 13 (6.1%) were category VII. An additional 42 subjects (19.6%) were identified as category IV and another 11 (5.1%) as category V, yielding at total of 102 (47%) clinically relevant discrepancies. When definitive diagnosis was available from pathology reports, the secondary consultations were determined to be correct in 23 of 29 cases (79%) and the outside interpretations were determined to be correct in 15 of 29 cases (52%, p<0.05).

# CONCLUSION

A 22.9% rate of clinically significant difference in interpretations was observed between primary reads and secondary musculoskeletal consultations in an orthopedic oncology patient population. Consistent with published literature, most discrepancies were interpretational as opposed to observational.

#### **CLINICAL RELEVANCE/APPLICATION**

The substantial rate of clinically relevant discrepant interpretations suggests that subspecialty expertise is likely to improve patient outcomes. The findings represent a tremendous opportunity for subspecialty radiologists to demonstrate their value in the accountable healthcare paradigm.

# Readability of Online Patient Education Material in Breast Imaging: Where Do We Stand?

Tuesday, Nov. 29 12:15PM - 12:45PM Room: HP Community, Learning Center Station #3

#### Awards

## **Student Travel Stipend Award**

## **Participants**

Sadia Choudhery, MD, Boston, MA (*Presenter*) Nothing to Disclose Nader Aboul-Fettouh, Dallas, TX (*Abstract Co-Author*) Nothing to Disclose YPaul GoldenMerry, Dallas, TX (*Abstract Co-Author*) Nothing to Disclose Charles Ho, Dallas, TX (*Abstract Co-Author*) Nothing to Disclose Hannah Viroslav, Dallas, TX (*Abstract Co-Author*) Nothing to Disclose Chelsea Zhang, Dallas, TX (*Abstract Co-Author*) Nothing to Disclose Alex Bass, College Station, TX (*Abstract Co-Author*) Nothing to Disclose Stephen J. Seiler, MD, Dallas, TX (*Abstract Co-Author*) Nothing to Disclose Sally Goudreau, MD, Dallas, TX (*Abstract Co-Author*) Nothing to Disclose

## PURPOSE

Due to the constantly evolving nature of information regarding breast cancer screening, mammography, tomosynthesis, and breast density, there is a clear need for radiologists to convey the appropriate information to patients via the Internet. It is also crucial for the readibility of this information to be at around the seventh grade level, which is considered the average readibility level of Americans. The purpose of this study is to evaluate 1) if websites of American College of Radiology (ACR) designated Breast Imaging Centers of Excellence (BICOE) have patient information regarding mammography, tomosynthesis, and high breast density and 2) what the readability level of this information is.

## **METHOD AND MATERIALS**

Websites of all ACR-accredited breast imaging centers in the United States with a designation of Breast Imaging Center of Excellence (BICOE) were searched for information regarding screening mammography, tomosynthesis, and breast density by five graduate students. Any material on these websites that provided patient education regarding risks and benefits of 2D mammography or tomosynthesis, the actual mammography/tomosynthesis procedure, patient preparation tips, and screening issues in high density breasts was then analyzed for well-known readibility variables.

# RESULTS

1482 breast centers were analyzed out of which 1451 (98%) had websites. 79% of these websites had information regarding mammography whereas only 45% and 16% had information regarding tomosynthesis and breast density respectively. Readibility analysis showed that the average grade level of patient information was 12.38 +/- 2.43. Additional average readibility scores, which all mark the level of education needed to understand the text, were: Flesch Kincaid Grade Level of 11.46 +/- 2.74, Gunning Fog Score of 14.05 +/- 2.49, Coleman Liau Index of 14.07 +/- 2.24, and SMOG Index of 10.9 +/- 2.08. The average Flesch Kincaid Reading Ease score was 45.01 +/- 14.05, which corresponds to a high school to college education level.

## CONCLUSION

Although most breast centers have websites and information regarding mammography, there is overall scarcity of information regarding tomosynthesis and breast density. Additionally, this patient education material has readibility scores much higher than the 7th grade level at which an average American reads.

## **CLINICAL RELEVANCE/APPLICATION**

In breast imaging, there is a need to provide better online patient information in more simplistic terms.

# HP219-SD-TUA4

High-Risk Medical Device Innovation from 2000-2015: Benchmarking the Performance of Radiology with Other Medical Specialties

Tuesday, Nov. 29 12:15PM - 12:45PM Room: HP Community, Learning Center Station #4

#### Awards

## **Student Travel Stipend Award**

#### **Participants**

Comeron W. Ghobadi, MD, BEng, Chicago, IL (*Presenter*) Nothing to Disclose Emily H. Ghobadi, MD, Chicago, IL (*Abstract Co-Author*) Nothing to Disclose Pritesh Patel, MD, Chicago, IL (*Abstract Co-Author*) Nothing to Disclose Shuai Xu, MD, MSc, Chicago, IL (*Abstract Co-Author*) Nothing to Disclose

# PURPOSE

To assess high-risk radiological device innovation via the pre-market approval (PMA) pathway and compare innovation activity to other specialties.

#### **METHOD AND MATERIALS**

Class III approvals were mined from the Food and Drug Administration (FDA) Center for Devices and Radiological Health (CDRH) public online database across a recent period of 15 years (September 1, 2000 to August 31, 2015). The number of approvals in radiology was determined by using the parameters of Advisory Committee: "Radiology" and Supplement Type: "Originals Only". The number of approvals from other medical specialties was also determined based on existing FDA advisory committee designations. For each radiological device the following data was extracted: device modality, manufacturer, and indication.

# RESULTS

Twenty-one distinct medical and surgical specialties were identified. In assessing high-risk device approvals of specific specialties within the corresponding period of time (Figure 1), cardiology ranked highest with 161 approvals. 23 unique radiological device approvals were identified. Molecular genetics, hematology, and toxicology medical device fields did not have any approvals and were excluded from the figure. The most represented modality was mammography, which accounted for 16 (70%) of the approvals. Computer aided detection (CAD) software packages accounted for 9 (39%) of the approvals. 22 (96%) of the approvals were for diagnostic indications.

# CONCLUSION

In comparison to other specialties, radiology ranked 7th out of 20 in the number of PMA approvals from September 1, 2000 to August 31, 2015 based on FDA advisory committee designation. Radiology devices accounted for approximately 5% of PMA approvals across all specialties with mammography and CAD software packages being most represented. Although high-risk device innovation represents one important metric of a robust research and development environment, many substantial components of radiological innovation do not fall into the category of Class III devices. Direct comparison of innovation activity among specialties is difficult. High-risk approvals provide a limited yet important perspective and serve as a single benchmark to improve upon.

# **CLINICAL RELEVANCE/APPLICATION**

High-risk radiological device innovation increases the utility of radiology in medicine and enhances patient care. Efforts should be made to spur impactful device innovation in the field.

## HP220-SD-TUA5

Do Patients Get What They Pay For? Relationship between Imaging Examination Cost and Imaging Center Yelp Ratings

Tuesday, Nov. 29 12:15PM - 12:45PM Room: HP Community, Learning Center Station #5

# Participants

Ankur Doshi, MD, New York, NY (*Presenter*) Nothing to Disclose Luke A. Ginocchio, MD, New York, NY (*Abstract Co-Author*) Nothing to Disclose Andrew B. Rosenkrantz, MD, New York, NY (*Abstract Co-Author*) Nothing to Disclose

## PURPOSE

To identify associations between the cost of radiology examinations and imaging center Yelp ratings.

## **METHOD AND MATERIALS**

OKcopay.com, a publically available website that provides the costs of medical services, was searched to identify the self-pay costs of brain MRI, abdominopelvic CT, and pelvic ultrasound exams within the 16 U.S. cities represented on the website at the time of the study. Yelp.com was searched to identify overall satisfaction scores from patient reviews for the corresponding imaging centers. Imaging centers were included if: a non-hospital based center, cost information on OKcopay.com included both professional and technical fees, and  $\geq$  3 patient reviews available on Yelp.com. Spearman's correlation coefficients were computed between imaging examination price and imaging center rating for the three exams.

#### RESULTS

98 imaging centers were included, providing data for 87 brain MRI, 72 abdominopelvic CT, and 65 pelvic ultrasound exams. These three exams had costs of [listed as mean (range)]: \$725 (\$250 - \$3129), \$467 (\$190 - \$3117) and \$256 (\$80 - \$1000), respectively. The mean number of Yelp reviews per imaging center was 13.2 ±11.9 range (3 - 59). The mean Yelp rating (1-5 scale; 5=highest score) was 2.97±0.97. For all three imaging exams, price and Yelp scores exhibited weak, albeit statistically significant, positive correlations: brain MRI, r=0.224 (p=0.037); abdominopelvic CT, r=0.248 (p=0.036); and pelvic ultrasound, r=0.376 (p=0.002).

## CONCLUSION

Imaging exam prices and Yelp scores exhibited weak positive correlations. Thus, an imaging center selected based on a low price may be associated with poorer patient satisfaction.

# **CLINICAL RELEVANCE/APPLICATION**

Patients must be cautious when "shopping" for radiology services using price alone, as price variation may be associated with additional variation in patient experience.

# Pixar Meets CT: Cinematic Rendering-A Novel, Life-Like Three-dimensional Visualization Technique

Tuesday, Nov. 29 12:15PM - 12:45PM Room: IN Community, Learning Center Station #9

**FDA** Discussions may include off-label uses.

## **Participants**

Marwen Eid, MD, Charleston, SC (*Presenter*) Nothing to Disclose Carlo N. De Cecco, MD, PhD, Charleston, SC (*Abstract Co-Author*) Nothing to Disclose Damiano Caruso, MD, Rome, Italy (*Abstract Co-Author*) Nothing to Disclose Moritz H. Albrecht, MD, Charleston, SC (*Abstract Co-Author*) Nothing to Disclose Akos Varga-Szemes, MD, PhD, Charleston, SC (*Abstract Co-Author*) Consultant, Guerbet SA Adam Spandorfer, Charleston, SC (*Abstract Co-Author*) Nothing to Disclose U. Joseph Schoepf, MD, Charleston, SC (*Abstract Co-Author*) Research Grant, Astellas Group; Research Grant, Bayer AG; Research Grant, General Electric Company; Research Grant, Siemens AG; Research support, Bayer AG; Consultant, Guerbet SA; ; ;

## **TEACHING POINTS**

Present an overview of the advanced Cinematic Rendering algorithm. Discuss the potential applications of Cinematic Rendering in clinical practice. Illustrate the realistic appearance and accuracy of 3D images with Cinematic Rendering compared with traditional Volume Rendering.

# TABLE OF CONTENTS/OUTLINE

Volume-Rendering technique (VRT) reconstruction is increasingly used in routine clinical radiology, and allows for calculation of accurate 3D reconstructions from the original data set. Since the impact of imaging in modern medicine is constantly growing, these VRT images are widely used in radiological routine both by referring clinicians and radiologists.Cinematic Rendering is a new prototype 3D rendering algorithm. This algorithm simulates the propagation of light rays, each with different paths, through the volumetric data as well as the interaction of light with the data, thus modelling real life physical conditions of light propagation. The resulting images provide a photorealistic and more accurate 3D representation of the acquired images compared with standard VRT.The aim of this pictorial essay is to give an overview of the Cinematic Rendering technique illustrating its potential advantages and applications in the medical field of future 3D imaging.

# IN224-SD-TUA1

# **Clinical Validation of Direct Volume Estimation for Left Atrial Aneurysm**

Tuesday, Nov. 29 12:15PM - 12:45PM Room: IN Community, Learning Center Station #1

**FDA** Discussions may include off-label uses.

### **Participants**

Liansheng Wang, Xiamen, China (*Presenter*) Nothing to Disclose Shusheng Li, Xiamen, China (*Abstract Co-Author*) Nothing to Disclose Xiantong Zhen, PhD, London, ON (*Abstract Co-Author*) Nothing to Disclose Changhua Liu, Xiamen, China (*Abstract Co-Author*) Nothing to Disclose Mousumi Bhaduri, MD, Toronto, ON (*Abstract Co-Author*) Nothing to Disclose Ashley J. Mercado, MD, London, ON (*Abstract Co-Author*) Nothing to Disclose Shuo Li, PhD, London, ON (*Abstract Co-Author*) Nothing to Disclose

# CONCLUSION

Our proposed method for the first time enables automatic volume estimation of left atrial aneurysm without segmentation and experimental results demonstrate our method achieves high estimation accuracy with a CC of 0.91 with those obtained manually by experienced doctors, which is clinically significant, indicating its potential use in the clinical diagnosis.

## Background

The left atrial aneurysm is a severe heart disease, which can produce compression symptoms with diverticulum oppressing neighboring atrium and ventricle leading to arrhythmias, embolic manifestations and heart failure. Accurate volume estimation of left atrial aneurysm plays an essential role in the early diagnosis and therapy planning.

#### **Evaluation**

To handle the high variabilities and variations, we propose a new multi-view semi-supervised manifold learning (MSML) algorithm, which fuses multiple complementary features to generate compact, informative and discriminative aneurysm image representation by leveraging both labeled and unlabeled data. Based on the obtained image representation by the MSML, we adopt random regression forests to conduct direct and efficient volume estimation without segmentation. Experiments are conducted on a clinical dataset of 67 subjects with a total of 1220 images. Three evaluation metrics, correlation coefficient (CC), mean deviation (MD), and standard deviation (SD), were computed based on our direct volume estimation and ground truth manually labelled by clinical experts.

## Discussion

The proposed direct estimation method achieves MD of 158.172, SD of 24.448, and a high CC of 0.91 with ground truth and largely outperforms other methods. It demonstrates the effectiveness for aneurysm volume estimation and reveals its clinical application of the proposed method. This study opens a new direction on automatic analysis of the left atrial aneurysm by providing a large annotated clinical dataset.

## IN225-SD-TUA2

## Experimental Reproduction of Skeletal Erosion Pattern Caused By Chronic Lymphocytic Leukemia

Tuesday, Nov. 29 12:15PM - 12:45PM Room: IN Community, Learning Center Station #2

#### **Participants**

Carlo Emanuele Neumaier, Genoa, Italy (Presenter) Nothing to Disclose Alberto Nieri, Genoa, Italy (Abstract Co-Author) Nothing to Disclose Francesco Fiz, Tubingen, Germany (Abstract Co-Author) Nothing to Disclose Giorgio Ricca, Genoa, Italy (Abstract Co-Author) Nothing to Disclose Francesca Rosa, MD, Genova, Italy (Abstract Co-Author) Nothing to Disclose Serena Matis, Genoa, Italy (Abstract Co-Author) Nothing to Disclose Giulia Ferrarazzo, Genoa, Italy (Abstract Co-Author) Nothing to Disclose Annalisa Bozano, Genoa, Italy (Abstract Co-Author) Nothing to Disclose Roberta Piva, Genoa, Italy (Abstract Co-Author) Nothing to Disclose Silvia Bruno, Genoa, Italy (Abstract Co-Author) Nothing to Disclose Paolo Giannoni, Genoa, Italy (Abstract Co-Author) Nothing to Disclose Daniela De Totero, Genoa, Italy (Abstract Co-Author) Nothing to Disclose Giovanna Cutrona, Genoa, Italy (Abstract Co-Author) Nothing to Disclose Anna Maria Massone, Genoa, Italy (Abstract Co-Author) Nothing to Disclose Franco Fais, Genoa, Italy (Abstract Co-Author) Nothing to Disclose Cristina Campi, Genoa, Italy (Abstract Co-Author) Nothing to Disclose Michele Piana, Genoa, Italy (Abstract Co-Author) Nothing to Disclose Gianmario Sambuceti, Genoa, Italy (Abstract Co-Author) Nothing to Disclose Laura Emionite, Genoa, Italy (Abstract Co-Author) Nothing to Disclose Anna Maria Orengo, Genoa, Italy (Abstract Co-Author) Nothing to Disclose Cecilia Marini, Genoa, Italy (Abstract Co-Author) Nothing to Disclose

## PURPOSE

Chronic Lymphocytic Leukemia (CLL) is a heterogeneous disease characterized by low-grade proliferation of immature B-cell clone. Recently, we reported that estimation of compact bone volume (CBV) by a computational analysis of CT images can predict death rate in these patients suggesting a possible role for intraosseous microenvironment in disease progression. This study aimed to verify whether neoplastic clone is able to alter bone structure in healthy mice.

## **METHOD AND MATERIALS**

CT slices of 40 prospectively enrolled CLL patients were submitted to our validated computational analysis to define the degree of bone alterations. Twenty NOD-SCID IL-2R  $\gamma$  chain null (NSG) mice were intravenously inoculated with 8x107 CLL cells sampled from the patient with the highest (10 mice, group A) or the lowest (10 mice, group B) bone erosion, respectively. Two serial high-resolution CT scan (GE Lightspeed pro32) were performed at week #3 and #6 post-xenograft according to the following parameters: 40 mA, 140 kV, DFOV 9. 6 cm, SFOV 32 cm, thickness of slices 0.625 mm. Reoriented slices of both femurs were analyzed with a computational algorithm to define their whole bone (WBV) and intraosseous (IBV volumes) as well as CBV. Ten sham NSG mice served as controls.

# RESULTS

WBV was similar in all three groups at both time points. At week #3, IBV/WBV ratio was highest in group A (7.2% $\pm$ 1.1%) with respect to both group B (5.7% $\pm$ 1.1%, p<0.01 vs both) B and controls (4.2 $\pm$ 1.3%, p<0.001 vs both), indicating skeletal erosion with cortical bone loss. Blood sampling documented an accelerated CLL progression only in group B. In agreement with this finding, IBV/WBV ratio increased only in these animals up to 8% $\pm$ 1% at week #6 (p<0.01 vs week#3). By contrast, femur structure remained unchanged both in group A and in control mice.

## CONCLUSION

CLL induces skeletal alterations that parallel disease progression. Computational analysis of CT images is able to tell apart different B-Cell CLL grades.

## **CLINICAL RELEVANCE/APPLICATION**

CT-based computational analysis of skeletal structure is a potential new tool to study disease progression and to test response to experimental treatments in the preclinical setting.

Conjugate Gaze Adjusted Length (CGAL):Can Evaluation of Eye Deviation in Three Dimensions Convey Critical Clinical Information in the Setting of Acute Stroke?

Tuesday, Nov. 29 12:15PM - 12:45PM Room: IN Community, Learning Center Station #3

#### Awards

## **Student Travel Stipend Award**

#### Participants

Hillel S. Maresky Jr, MD, Zeriffin, Israel (*Presenter*) Nothing to Disclose Paul Gottlieb, MD, Zerifin, Israel (*Abstract Co-Author*) Nothing to Disclose Max Levitt, Ramat Aviv, Israel (*Abstract Co-Author*) Nothing to Disclose Sigal Tal, MD, Tel Aviv, Israel (*Abstract Co-Author*) Nothing to Disclose

# PURPOSE

Conjugate eye deviation (CED) has been accepted for over a century as a clinical sign of acute stroke; however, two-dimensional limitations of cross-sectional imaging have kept this tool in the real of the clinician. Our purpose is to evaluate the use of threedimensional imaging as an adjunct to diagnose acute stroke in the emergency setting, using MDCT post-processing software.

## **METHOD AND MATERIALS**

All non-contrast CT scans of patients who presented to the emergency department with single-vessel acute ischemic stroke during the year 2013 were analyzed. Volumetric reconstruction was performed of the patient's eyes, and analyzed for CED. CGAL was calculated by dividing the vector of deviation from the centre of the globe by the diameter of the globe, and was compared to the clinical vascular territory. Kappa agreements were ascertained for right-right and left-left CED and MCA territory. CGAL was compared with NIH stroke scale on presentation. Short interval ollow-up scans (CT/ MRI) were compared with original scans for sensitivity and specificity.

#### RESULTS

One hundred and three patients' eyes were reconstructed. Horizontal deviation was noted in 86% of the patients (48% right, 42% left). CGAL > 0.35 was noted in 89% of the patients;48% right, 45% left. Substantial Kappa agreements were observed, with right-sided gaze and clinical right MCA territory K=0.85; left-sided gaze and clinical left MCA territory K=0.72 Follow-up CT scans for 39 patients were obtained and reconstructed, with an occurence of horizontal gaze of 56%, and right-left kappa agreements of 0.39 and 0.45, respectively. MRI performed on 31 patients showed a high DWI signal in 22 patients, with 20/22 positive showed CGAL > 0.35  $\Box$  (Sensitivity = 90%). Eight of nine Negative DWI correlated with CGAL < 0.35 on initial CT  $\Box$  (Specificity = 89%). CGAL correlated with stroke score with r=0.72, p=0.01.

## CONCLUSION

Three-dimensional CED evaluation displays a high sensitivity and specificity for acute stroke, correlating with both vascular territory and stroke severity.

## **CLINICAL RELEVANCE/APPLICATION**

Three-dimensional reconstruction of eye deviation reveals the powerful potential of the Prevost sign, which is may be an ancillary tool in the hands of the radiologist to appreciate cerebrovascular accident vascular territory and severity.

Convolutional Neural Networks Trained on Noisy Annotations Achieve Accurate Detection and Labeling of Vertebrae in Lumbar MR Images

Tuesday, Nov. 29 12:15PM - 12:45PM Room: IN Community, Learning Center Station #4

# Participants

Daniel Forsberg, PhD, Linkoping, Sweden (*Presenter*) Employee, Sectra AB Erik Sjoblom, Linkoping, Sweden (*Abstract Co-Author*) Employee, Sectra AB Jeffrey L. Sunshine, MD, PhD, Pepper Pike, OH (*Abstract Co-Author*) Research support, Siemens AG; Travel support, Siemens AG; Travel support, Koninklijke Philips NV; Travel support, Sectra AB; Travel support, Allscripts Healthcare Solutions, Inc

# CONCLUSION

Accurate detection and labeling of MR images depicting the lumbar spine is possible using DL, even with readily available limited training data. These results demonstrate that allowing DL trained models to provide assistance to radiologists for their review could increase efficiency of anatomic labeling.

## Background

Deep learning (DL) lately has received attention within a large number of disparate application domains, including medical imaging and radiology, and has been shown repeatedly to outperform other approaches for a variety of tasks. However, a challenge for DL is that large amounts of well curated data is typically needed for training. In this work, we investigate whether a small set of clinically annotated spine labels can be used to train convolutional neural networks (CNNs) capable of detection and labeling of vertebrae in lumbar MR images.

#### **Evaluation**

Lumbar MR cases with annotated spine labels were identified and corresponding mid sagittal T1 and T2 images along with labels and locations were extracted from the PACS. The annotations were visually reviewed to ensure a reasonable quality (labels located within the vertebral bodies). The retained data (479 cases) was randomly split into training (60%), validation (20%) and test (20%) data. Two CNNs (one general thoracolumbar vertebra detector and one specific S1 vertebra detector) were set up and trained on image patches from the training data. The validation data was used for network configuration along with optimal selection of hyper parameters. The combined detection output from the two CNNs provided the final detection and labeling output, which was evaluated on the test data.

## Discussion

For the T1 images the detection sensitivity, precision and accuracy was 0.98, 0.99 and 0.97 respectively, with a labelling accuracy of 0.93 (0.98 with +/- 1 label shift). Corresponding results for the T2 images were 0.99, 0.98 and 0.97 for detection and 0.94 (0.99 with +/- 1 label shift) for labeling. Failed detections typically involved missed S1 detections, L5 misclassified as S1 or missed vertebrae that were not fully visible. Interestingly, many pathological cases were successfully detected and labeled.

# IN228-SD-TUA5

Workflow Analysis of Custom-made, Semiautomatic Software Option for MRI Quantification of Abdominal Adipose Tissue

Tuesday, Nov. 29 12:15PM - 12:45PM Room: IN Community, Learning Center Station #5

# Participants

Nikita Garnov, Leipzig, Germany (*Abstract Co-Author*) Nothing to Disclose Alexander Schaudinn, MD, Leipzig, Germany (*Abstract Co-Author*) Nothing to Disclose Nicolas Linder, Leipzig, Germany (*Abstract Co-Author*) Nothing to Disclose Kilian Solty, Leipzig, Germany (*Abstract Co-Author*) Nothing to Disclose Thomas Rakete, Leipzig, Germany (*Abstract Co-Author*) Nothing to Disclose Nora Dipper, Leipzig, Germany (*Abstract Co-Author*) Nothing to Disclose Sophia Michel, Leipzig, Germany (*Abstract Co-Author*) Nothing to Disclose Thomas Karlas, MD, Leipzig, Germany (*Abstract Co-Author*) Nothing to Disclose Matthias Bluher, MD, Leipzig, Germany (*Abstract Co-Author*) Nothing to Disclose Arne Dietrich, 04103, Germany (*Abstract Co-Author*) Nothing to Disclose Stefanie Lehmann, Leipzig, Germany (*Abstract Co-Author*) Nothing to Disclose Andreas Oberbach, Leipzig, Germany (*Abstract Co-Author*) Nothing to Disclose Rima Chakaroun, Leipzig, Germany (*Abstract Co-Author*) Nothing to Disclose Rima Chakaroun, Leipzig, Germany (*Abstract Co-Author*) Nothing to Disclose Rima Chakaroun, Leipzig, Germany (*Abstract Co-Author*) Nothing to Disclose Thomas K. Kahn, MD, Leipzig, Germany (*Abstract Co-Author*) Nothing to Disclose Harald F. Busse, PhD, Leipzig, Germany (*Presenter*) Nothing to Disclose

## CONCLUSION

The custom-made software provides a viable option for fast and reliable supervised segmentation of whole-abdominal MRI data within minutes. Only minimal adjustments – suggesting best automatic preprocessing – were required for SEV patients (35–40 kg/m<sup>2</sup>). Pre-segmented data of SUP patients (>45 kg/m<sup>2</sup>) took longest to interactively correct for with  $t_{TI}$  still considered to be tolerable (<10 min).

# Background

Quantification of visceral and subcutaneous adipose tissue (VAT, SAT) amounts has gained considerable interest in obesity research. Total AT volumes can be quantified by segmenting AT areas in tens of CT or MR images which is typically very time-consuming. Various automatic approaches have therefore been described and tested. This work presents a detailed workflow analysis of a custom-made semiautomatic MRI quantification software for users with different experience and over a wide range of BMI groups.

#### Evaluation

A custom-made software (under Matlab) enables the user to graphically adjust the automatically generated SAT and VAT boundaries and histogram thresholds for water-fat separation. A total of 80 patients were divided into six BMI groups: 10 normal (<26 kg/m<sup>2</sup>), 10 overweight (26–30), 20 obese (>30, OBS), 20 severely obese (>35, SEV), 10 morbidly obese (>40) and 10 "super obese" (>45, SUP). All subjects underwent MRI at 1.5T (35 slices, 10 mm thick, diaphragm to pelvic floor). Data were analyzed by one experienced reader ( $R_E$ , all groups, n=80) and two less experienced ones ( $R_1$  and  $R_2$ , OBS+SEV only, n=40). Automatic segmentation time ( $t_{AS}$ ), manual correction time ( $t_{MC}$ , adjustment of boundaries and thresholds) and total interaction time ( $t_{TI}$ , from reading of pre-segmented images to saving of final data) were recorded.

## Discussion

Mean  $t_{AS}$  was 00:28 min per dataset (0.8 s per slice). For 40 OBS+SEV patients, median  $t_{MC}$  per patient were 02:33 ( $R_E$ ), 03:52 ( $R_1$ ) and 03:06 min ( $R_2$ ). Minimum and maximum group-specific  $t_{MC}$  by  $R_E$  were observed for SEV (00:35 min) and SUP (04:09 min); average time exposure was 02:59 min per patient. Median  $t_{TI}$  was 00:56 for SEV and 09:57 min for SUP. Threshold adjustment and modification of the VAT mask were the least and most time-consuming work step, respectively.

An Investigational Patch-based Convolutional Neural Network Model for the Detection of Clinically Significant Prostate Cancer using Multiparametric MRI

Tuesday, Nov. 29 12:15PM - 12:45PM Room: IN Community, Learning Center Station #6

#### Awards

## **Trainee Research Prize - Medical Student**

#### Participants

Karthik V. Sarma, BSc, Los Angeles, CA (*Presenter*) Nothing to Disclose Xinran Zhong, Los Angeles, CA (*Abstract Co-Author*) Nothing to Disclose King Chung Ho, MSc, los angeles, CA (*Abstract Co-Author*) Nothing to Disclose Daniel J. Margolis, MD, Los Angeles, CA (*Abstract Co-Author*) Nothing to Disclose Steven S. Raman, MD, Santa Monica, CA (*Abstract Co-Author*) Nothing to Disclose Fabien Scalzo, PhD, Los Angeles, CA (*Abstract Co-Author*) Nothing to Disclose Kyunghyun Sung, PhD, Los Angeles, CA (*Abstract Co-Author*) Nothing to Disclose Nelly Tan, MD, Los Angeles, CA (*Abstract Co-Author*) Nothing to Disclose Corey W. Arnold, Los Angeles, CA (*Abstract Co-Author*) Nothing to Disclose

## PURPOSE

Despite prostate cancer being the second leading cause of cancer death in American men, the USPSTF recommends against screening to avoid overdiagnosis and treatment of indolent disease. The use of multiparametric magnetic resonance imaging (mp-MRI) has shown potential to discriminate aggressive from indolent disease. We demonstrate a convolutional neural network (CNN) that can generate a voxel-wise cancer probability map for clinically significant (Gleason score >= 7) prostate cancer.

#### **METHOD AND MATERIALS**

mp-MRI data was collected retrospectively for a set of 22 patients who had undergone radical prostatectomy. Surface mesh annotations were manually created from imaging for prostate and lesion segmentation. The prostate and tumors within were segmented by a genitourinary pathologist on whole mount histopathologic slides and manually mapped to the meshes. Ground truth was generated with any voxel contained within a lesion mesh with an assigned score >= 7 assigned to the positive class and all other prostate voxels assigned to the negative class. A CNN was trained on the resulting dataset with manually registered input channels for T2-weighted MRI, ADC, Kep, and Ktrans maps. 21x21 training patches were created for every prostate voxel with ground truth assigned based on the middle voxel. A four-layer model with two convolutional layers with max-pooling and two linear layers with dropout was used.

## RESULTS

Leave-one-patient-out (i.e. 22-fold) cross-validation was performed, with results averaged across each fold. A softmax classifier was used for assignment to the lesion or normal class using a threshold calculated to give 80% specificity. For evaluation, voxels with a positive probability above the threshold value were assigned to the positive class. Average results were as follows: Accuracy 80%, AUC 0.72, S90 40%.

## CONCLUSION

The patch-based CNN system was able to generate results competitive with voxel-based predictive systems. Future work includes training models with larger datasets, which could allow the use of deeper networks that may improve performance. Future models could also attempt to predict Gleason score directly instead of a dichotomized indicator and correct for motion and distortion.

## **CLINICAL RELEVANCE/APPLICATION**

This investigation into the use of CNNs for detecting clinically significant prostate cancer in mp-MRI demonstrates that deep learning may be useful for prostate CAD.

Evaluation of a Machine Learning Approach to Protocol MRI Examinations: Initial Experience Predicting Use of Contrast by Neuroradiologists in MRI Protocols

Tuesday, Nov. 29 12:15PM - 12:45PM Room: IN Community, Learning Center Station #7

# Participants

Steven A. Rothenberg, MD, Baltimore, MD (Presenter) Co-founder, McCoy Medical Technologies

Jigar B. Patel, MD, Phoenix, AZ (Abstract Co-Author) Nothing to Disclose

Misha H. Herscu, BA, Cambridge, MA (*Abstract Co-Author*) Co-founder, McCoy Medical Technologies Eliot L. Siegel, MD, Baltimore, MD (*Abstract Co-Author*) Board of Directors, Brightfield Technologies; Board of Directors, McCoy; Board of Directors, Carestream Health, Inc; Founder, MedPerception, LLC; Founder, Topoderm; Founder, YYESIT, LLC; Medical Advisory Board, Bayer AG; Medical Advisory Board, Bracco Group; Medical Advisory Board, Carestream Health, Inc; Medical Advisory Board, Fovia, Inc; Medical Advisory Board, McKesson Corporation; Medical Advisory Board, Merge Healthcare Incorporated; Medical

Advisory Board, Microsoft Corporation; Medical Advisory Board, Koninklijke Philips NV; Medical Advisory Board, Toshiba Corporation; Research Grant, Anatomical Travelogue, Inc; Research Grant, Anthro Corp; Research Grant, Barco nv; Research Grant, Dell Inc; Research Grant, Evolved Technologies Corporation; Research Grant, General Electric Company; Research Grant, Herman Miller, Inc; Research Grant, Intel Corporation; Research Grant, MModal IP LLC; Research Grant, McKesson Corporation; Research Grant, RedRick Technologies Inc; Research Grant, Steelcase, Inc; Research Grant, Virtual Radiology; Research Grant, XYBIX Systems, Inc; Research, TeraRecon, Inc; Researcher, Bracco Group; Researcher, Microsoft Corporation; Speakers Bureau, Bayer AG; Speakers Bureau, Siemens AG;

# PURPOSE

This study was designed to determine the effectiveness of a machine learning approach to predict the administration of gadolinium based on indications extracted from report text. The goal was to investigate the potential to provide decision support to help clinicians and mid level practitioners request the most appropriate diagnostic MRI (contrast enhanced versus unenhanced) for any given indication and to improve the efficiency of MRI protocoling by radiologists.

## METHOD AND MATERIALS

One thousand radiology reports of consecutive brain MRI exams and associated CPT codes were collected from the electronic medical record. A Python script extracted the indication and/or patient history from each report. Additional pre-processing steps included: deleting words with presumed irrelevance (male, female, etc.), removing all numbers, removing all punctuation and case information.

The indication and history samples were converted into three different document-term matrices (DTMs) to generate tokens of unique 1-5 word n-grams. The cross-validation used 70% of the data for training and 30% for testing. The 300 indications used for model validation were blindly protocolled by a board certified neuroradiologist.

# RESULTS

Of the five types of machine learning classifiers trained and tested, the best overall performing model was Support Vector Machine with a linear kernel and TF-IDF weighting for the feature space. The sensitivity and specificity of the machine learning model to predict contrast from extracted text strings was 80.7% and 82.5% (P=0.0001) respectively, while a board certified neuroradiologist was 86.0% and 85.4%. The trained algorithm's concordance rate for choosing the correct study was 5.0% worse than a neuroradiologist.

## CONCLUSION

Trained supervised machine learning classification algorithms can predict administration of contrast from reported indications for our patient population fairly well. Further advances in preprocessing, the addition of bias filters, larger data sets, and addition of relevant data from the RIS/EMR (such as renal function) may improve performance.

# **CLINICAL RELEVANCE/APPLICATION**

This approach may streamline order entry workflow and decrease error rates for both radiologists and referring clinicians through locally relevant clinical decision support. Similar classification schema has promising applications ranging from scanner utilization workflow to clinical decision management.

# IN231-SD-TUA8

**Evaluation of an Imaging-centric Context-driven Annotation Engine** 

Tuesday, Nov. 29 12:15PM - 12:45PM Room: IN Community, Learning Center Station #8

#### **Participants**

Lucas Oliveira, PhD, Cambridge, MA (*Presenter*) Employee, Koninklijke Philips NV Pritesh Patel, MD, Chicago, IL (*Abstract Co-Author*) Nothing to Disclose Gabriel Mankovich, BSC, Cambridge, MA (*Abstract Co-Author*) Employee, Koninklijke Philips NV Merlijn Sevenster, PhD, Cambridge, MA (*Abstract Co-Author*) Employee, Koninklijke Philips NV Amir Tahmasebi, PhD, Cambridge, MA (*Abstract Co-Author*) Nothing to Disclose Thomas A. Forsberg, MSc, Cambridge, MA (*Abstract Co-Author*) Nothing to Disclose Thomas A. Forsberg, MSc, Cambridge, MA (*Abstract Co-Author*) Employee, Koninklijke Philips NV Igor Trilisky, MD, Chicago, IL (*Abstract Co-Author*) Nothing to Disclose Robbert C. Van Ommering, PhD, Eindhoven, Netherlands (*Abstract Co-Author*) Employee, Koninklijke Philips NV Aaldert J. Elevelt, MS, Best, Netherlands (*Abstract Co-Author*) Nothing to Disclose Paul J. Chang, MD, Chicago, IL (*Abstract Co-Author*) Co-founder, Stentor/Koninklijke Philips NV; Researcher, Koninklijke Philips NV; Medical Advisory Board, lifeIMAGE Inc; Advisory Board, Bayer AG

# CONCLUSION

We proposed a context-driven annotation engine for radiology reading. Our evaluation demonstrated that the suggestion engine could narrow down appropriate description selection.

## Background

Structured Annotation Image Markup (AIM) is a promising approach to improve the quality of reporting of radiology findings. In order for AIM reporting tools to be adopted in the routine workflow, minimal user interaction is desirable. Previous attempts at facilitated codified reporting involved complex and cumbersome selection mechanisms that were disconnected from the image context. In this study, we evaluate the extent to which image finding annotation can be improved by a RadLex-based suggestion engine incorporating contextual information in the search process driven by a codified database.

## **Evaluation**

We designed a framework to generate a database of codified image finding descriptors from a corpus of 200,000 narrative radiology reports from an academic hospital. The framework encompasses: 1) a RadLex-based concept extraction pipeline; 2) a database for storing and querying the structured results; and 3) a description suggestion engine which uses user-supplied anatomical location and/or finding context to reduce the search space of the query. To evaluate the system, we extracted 158 unique tumor descriptors from a prospective clinical study. These descriptors contained anatomy, finding, and a series of descriptions. 77% of the annotations were covered in the database.Providing no contextual information, the suggestion engine's accuracy was <0.1. When the anatomical context was provided, 12% of the suggestions were relevant; and when both anatomical and finding context, the relevance was 25%.

# Discussion

Our evaluation demonstrated that by providing anatomical and finding context, the proposed suggestion engine could narrow down the appropriate description selection to 1 out of 4. This research can be complemented by anatomical segmentation and finding characterization software to automatically generate contextual cues. Despite large corpus used to build the database, 23% of the evaluation annotations were not represented in it (e.g., "chest wall mass" was included but "chest wall lesion" was not).

# The Scapulothoracic Articulation: Often Imaged, but Rarely Discussed

Tuesday, Nov. 29 12:15PM - 12:45PM Room: MK Community, Learning Center Station #8

#### **Participants**

Sumin S. Lee, MD, Winston-Salem, NC (*Presenter*) Nothing to Disclose J. Michael Holbert, MD, Greensboro, NC (*Abstract Co-Author*) Author, Reed Elsevier Scott D. Wuertzer, MD, MS, Winston-Salem, NC (*Abstract Co-Author*) Nothing to Disclose

# **TEACHING POINTS**

Review the anatomy and biomechanics of the scapulothoracic (ST) articulation Review clinical presentations Present an approach to the imaging findings within congenital, systemic, inflammatory/infectious, neoplastic, traumatic, and surgical categories Present case examples to illustrate approach to ST articulation pathology

# TABLE OF CONTENTS/OUTLINE

Background The ST articulation is important in coordinating movement of the shoulder Although this articulation is imaged on all chest radiographs and CT studies, pathology is often unexpected and may be overlooked in this location Knowledge of the anatomy, biomechanics, clinical presentation, and systematic approach will help radiologists characterize and identify pathologyAnatomy Scapula ST articulationBiomechanics Motion StabilityClinical Presentation ST dissociation ST crepitus Scapular winging and dyskinesisCase Examples Congenital - Sprengel deformity, hemiatrophy Systemic - calcification from dermatomyositis, renal osteodystrophy Inflammatory/infectious - bursitis, abscess, osteomyelitis Neoplastic - elastofibroma dorsi, lipoma, multiple hereditary exostosis, myeloma, metastasis Trauma - fracture, hematoma, subcutaneous emphysema, winging, dissociation Surgical - thoracic wall resection, forequarter amputation

# Multiligamentous Knee Injury: Putting Together the Pieces

Tuesday, Nov. 29 12:15PM - 12:45PM Room: MK Community, Learning Center Station #9

#### **Participants**

Barry G. Hansford, MD, Sandy , UT (*Presenter*) Nothing to Disclose Corrie M. Yablon, MD, Ann Arbor, MI (*Abstract Co-Author*) Nothing to Disclose Christopher J. Hanrahan, MD, PhD, Salt Lake City, UT (*Abstract Co-Author*) Nothing to Disclose

# **TEACHING POINTS**

After reviewing this exhibit, the learner will be able to:1. Discuss the anatomy and function of the major and minor static and dynamic stabilizers of the knee2. Describe the common imaging patterns of multiligamentous knee injuries using a mechanism - based approach3. List pearls for increasing recognition of injuries to specific stabilizing structures4. Appreciate the orthopedic surgeon's perspective on multiligamentous knee reconstructions

# TABLE OF CONTENTS/OUTLINE

Introduction-Anatomy of key posterolateral, posteromedial, anterolateral and anteromedial supporting structures of the knee-Function of key static and dynamic stabilizers of the knee-Case-based, mechanism-specific imaging review of multiligamentous knee trauma (i.e. pivot shift injury, posterior knee dislocation, etc.)-Orthopedist perspective on multiligamentous knee reconstruction including: -How the radiologist adds value -Which structures are repaired and why -Patient population specific surgical approaches (i.e. elite athlete, weekend warrior, etc.)Outcomes of multiligamentous knee reconstructionImaging evaluation of ligamentous reconstructionSummary

# It's Not a Tumor! A Comprehensive Review of Musculoskeletal Masses Often Mistaken for Neoplasm

Tuesday, Nov. 29 12:15PM - 12:45PM Room: MK Community, Learning Center Station #11

## Participants

Jonathan K. Kazam, MD, New York, NY (*Presenter*) Nothing to Disclose Dana Lin, MD, New York, NY (*Abstract Co-Author*) Nothing to Disclose Tony T. Wong, MD, New York, NY (*Abstract Co-Author*) Nothing to Disclose

# **TEACHING POINTS**

Understand general imaging features that can help differentiate between non-neoplastic and neoplastic masses Describe the characteristic imaging features of the most common non-neoplastic masses Develop a differential diagnosis for etiologies of non-neoplastic masses

# TABLE OF CONTENTS/OUTLINE

I. Pre-testII. Post-Traumatic Masses Heterotopic ossification (myositis ossificans) Hemolymphatic collection (Morel-Lavallee lesion) HematomaIII. Iatrogenic and Postsurgical Masses Fat extravasation from augmentation gluteoplasty Vascularized soft tissue graft Calcium gluconate extravasationIV. Cystic Masses Para-meniscal cyst Para-labral cyst Ganglion cyst Synovial cystV. Masses in the Setting of Deposition Disease or Dysplasia Intraosseous migration of calcific tendinosis Tophaceous gout Pyrophosphate arthropathy with pseudomass Giant cell tendon sheath tumor and pigmented villonodular synovitis Tumoral calcinosis MelorheostosisVI. Fibrous/Reactive Masses Elastofibroma Fibromatosis Morton NeuromaVII. Bursae Anatomic bursae Adventitial bursaeVIII. Post-test

# MK269-ED-TUA10

# Imaging findings in Polymyalgia Rheumatica: A Pictorial Essay

Tuesday, Nov. 29 12:15PM - 12:45PM Room: MK Community, Learning Center Station #10

#### **Participants**

Renata V. Leao, Sao Paulo, Brazil (*Presenter*) Nothing to Disclose Luciana C. Zattar-Ramos, MD, Sao Paulo, Brazil (*Abstract Co-Author*) Nothing to Disclose Marcos Felippe P. Correa, Sao Paulo, Brazil (*Abstract Co-Author*) Nothing to Disclose Marcelo Bordalo-Rodrigues, MD,PhD, Sao Paulo, Brazil (*Abstract Co-Author*) Nothing to Disclose Denise T. Amaral, Sao Paulo, Brazil (*Abstract Co-Author*) Nothing to Disclose Rodrigo Y. Fernandes, MD, Sao Paulo, Brazil (*Abstract Co-Author*) Nothing to Disclose Eduardo L. Bizetto, MD, Sao Paulo, Brazil (*Abstract Co-Author*) Nothing to Disclose Ceci Obara Kurimori, MD, Sao Paulo, Brazil (*Abstract Co-Author*) Nothing to Disclose Paulo Victor P. Helito, MD, Sao Paulo, Brazil (*Abstract Co-Author*) Nothing to Disclose Afranio D. Teixeira Neto, MD, Houston, TX (*Abstract Co-Author*) Nothing to Disclose Giovanni G. Cerri, MD, PhD, Sao Paulo, Brazil (*Abstract Co-Author*) Nothing to Disclose Hugo P. Costa, MD, Sao Paulo, Brazil (*Abstract Co-Author*) Nothing to Disclose

## **TEACHING POINTS**

LEARNING OBJECTIVES• This study aims to illustrate the cases of polymyalgia rheumatica (PR) emphasizing the imaging findings that may contribute for the specific diagnosis of this entity.• Illustrate the main image patterns of polymyalgia rheumatica that should make the radiologist think of this pathology: including the classical imaging findings and some possible new findings related to this pathology that we have been observed in our institution.2. Illustrate the main affected sites of this pathology3. Illustrate the typical patterns of PR in different imaging methods, such as ultrasonography, PET-scan and magnetic resonance imaging (MRI)4. Emphasize the differential diagnosis of PR

## **TABLE OF CONTENTS/OUTLINE**

1. Introduction: prevalence PMR and its clinical importance2. Brief diagnostic approach review - clinical setting- laboratory findingsimaging examination approach3. Review of the imaging findings: in ultrasonography, PET-scan and magnetic resonance imaging (MRI)- classical findings already described in literature- some possible new imaging finding that may be related to this pathology 4. Review of imaging findings based on clinical cases5. Review of the main differential diagnosis6. Conclusion

# MK314-SD-TUA1

Association of Weight Change with Progression of Meniscal Degeneration over 48 months: Data from the Osteoarthritis Initiative

Tuesday, Nov. 29 12:15PM - 12:45PM Room: MK Community, Learning Center Station #1

#### Awards

**Student Travel Stipend Award** 

#### Participants

Julio B. Guimaraes, MD, San Francisco, CA (*Presenter*) Nothing to Disclose Alexandra S. Gersing, MD, Munich, Germany (*Abstract Co-Author*) Nothing to Disclose Benedikt J. Schwaiger, MD, San Francisco, CA (*Abstract Co-Author*) Nothing to Disclose Luca Facchetti, San Francisco, CA (*Abstract Co-Author*) Nothing to Disclose Charles E. McCulloch, San Francisco, CA (*Abstract Co-Author*) Nothing to Disclose Michael C. Nevitt, PhD, San Francisco, CA (*Abstract Co-Author*) Nothing to Disclose Thomas M. Link, MD, PhD, San Francisco, CA (*Abstract Co-Author*) Nothing to Disclose Thomas M. Link, MD, PhD, San Francisco, CA (*Abstract Co-Author*) Nothing to Disclose Science+Business Media Deutschland GmbH; Consultant, Springer Science+Business Media Deutschland GmbH; Research Consultant, Pfizer Inc;

### PURPOSE

To investigate the association of different degrees of weight loss and weight gain with the rate of progression of meniscal degeneration over 48 months compared to weight-matched stable weight subjects.

## **METHOD AND MATERIALS**

We selected 487 subjects ( $61.8\pm8.9$  years, 302 women) from the Osteoarthritis Initiative with meniscal intrasubstance degeneration shown as hyperintense signal changes on baseline 3T MR images, but without more severe pathologies such as meniscal tears, who over 48 months lost weight ( $\geq3\%$  weight loss (WL), n=141), gained weight ( $\geq3\%$  weight gain (WG), n=92) or maintained a stable weight (SW; n=254). Subjects were frequency-matched for age, sex, baseline BMI, trauma, knee alignment and Kellgren-Lawrence scores. MRIs of the right knee were assessed for progression of meniscal intrasubstance degeneration to degenerative meniscal tears over 48 months and rates of progression were compared between the stable weight and two weight change groups, using multivariable linear and logistic regression models and generalized estimating equations.

## RESULTS

The odds of meniscal intrasubstance degeneration worsening to meniscal tears in subjects with weight gain over 48 months were significantly higher compared to those of subjects with stable weight for both menisci (OR: 5.1 (95% CI 2.75-9.59), p<0.001) as well as for each meniscus separately (medial meniscus: OR: 7.0 (95% CI 3.72-13.34), p<0.001; lateral meniscus: OR: 2.9 (CI 1.23-6.85), p=0.01). Odds of progression of meniscal intrasubstance degeneration to meniscal tears in the WL group over 48 months were substantially lower compared to the SW group in the medial meniscus (OR: 0.5 (95% CI 0.30-1.10), p=0.09), yet this finding, as well as both menisci combined (OR: 0.6 (95% CI 0.33-1.26), p=0.2) were not statistically significant.

## CONCLUSION

Our findings suggest that subjects with meniscal intrasubstance degeneration that gain weight are at significantly higher risk of developing meniscal degenerative tears. Also, weight loss in these subjects may be protective and decrease the risk of developing meniscal tears.

## **CLINICAL RELEVANCE/APPLICATION**

Our study shows that weight gain in subjects with meniscal intrasubstance degeneration has a significant impact on the development of meniscal degenerative tears.

Assessment of Femoral Trochlear Morphology on Cross Sectional Imaging: Comparing the DeJour Classification and Quantitative Measurements in Patients Later Treated with Deepening Trochleoplasty

Tuesday, Nov. 29 12:15PM - 12:45PM Room: MK Community, Learning Center Station #2

# Participants

Michael G. Fox, MD, Charlottesville, VA (*Presenter*) Stockholder, Pfizer Inc Barrett Luce, MD, Charlottesville, VA (*Abstract Co-Author*) Nothing to Disclose David Diduch, MD, Charlottesville, VA (*Abstract Co-Author*) Consultant, Johnson & Johnson Dustin Boatman, MD, Charlottesville, VA (*Abstract Co-Author*) Nothing to Disclose

## PURPOSE

The purpose of the study was to evaluate interobserver variability in the qualitative application of the DeJour classification for trochlear dysplasia with subsequent correlation to quantitative measurements of femoral trochlear morphology.

# METHOD AND MATERIALS

A retrospective review was performed of CT and MRI knee exams from patients having deepening trochleoplasty surgery. Images were independently assessed by MSK radiologists with 1 and 19 years of experience. Each case was assigned to a Dejour category of trochlear dysplasia with quantitative measurements performed of the sulcus angle, tibial tubercle to trochlear groove distance (TT-TG), trochlear depth, lateral trochlear inclination, trochlear facet symmetry, and patellar lateralization.

# RESULTS

31 knees from 27 patients were included in the study. In 77% (24/31) of the cases, the two readers were in exact agreement using the DeJour classification (kappa 0.69 [95% CI 0.48,0.89]) to qualitatively grade the degree of dysplasia. Of the remaining 7 cases, only 3 showed disagreement between a grading of low-grade (LG=DeJour A) versus high-grade (HG=DeJour B, C, or D) dysplasia. When comparing those considered LG (n=4) and HG (n=24) by both readers, there was agreement in >90% (28/31) of the cases when performing the assessment 3 cm cranial to the tibiofemoral joint. When analyzing the mean measurements of the 24 cases of exact DeJour agreement, sulcus angle (mean LG=153, mean HG=167, p<0.001), trochlear depth (mean LG=4, mean HG=0, p<0.001), lateral trochlear inclination (mean LG=12, mean HG=3, p<0.01), and lateralization of the patella (mean LG=-6, mean HG=-12, p<0.05) were significantly different between LG and HG dysplasia. Trochlear depth and lateral trochlear inclination were also significantly different between categories B and C and B and D (both with p<0.05).

# CONCLUSION

There is good interobserver agreement when qualitatively applying the DeJour classification in grading trochlear dysplasia. The agreement improved when using a simplified LG (DeJour A) versus HG (DeJour B, C, and D) approach. In addition, quantitative measurements of femoral trochlear morphology can be used to differentiate between LG and HG trochlear dysplasia.

## **CLINICAL RELEVANCE/APPLICATION**

Varying degrees of trochlear dysplasia can be reliably differentiated using both qualitiative DeJour classification as well as quantitative measurements of femoral trochlear morphology.

# MK316-SD-TUA3

Ultrasound- versus CT-guidance for Treatment of Sacroiliac Joint Arthritis with Steroid and O2-O3 Mixture Injections: Main Aspects, Advantages and Clinical Response in Young Women

Tuesday, Nov. 29 12:15PM - 12:45PM Room: MK Community, Learning Center Station #3

# Participants

Fernando Smaldone, MD, L'Aquila, Italy (*Presenter*) Nothing to Disclose Simone Quarchioni, Laquila, Italy (*Abstract Co-Author*) Nothing to Disclose Francesco Arrigoni, Coppito, Italy (*Abstract Co-Author*) Nothing to Disclose Silvia Mariani, MD, L'Aquila, Italy (*Abstract Co-Author*) Nothing to Disclose Luigi Zugaro, L'Aquila, Italy (*Abstract Co-Author*) Nothing to Disclose Carlo Masciocchi, MD, L'Aquila, Italy (*Abstract Co-Author*) Nothing to Disclose Antonio Barile, MD, L'Aquila, Italy (*Abstract Co-Author*) Nothing to Disclose

## PURPOSE

To evaluate the efficacy, accuracy and clinical response of US- versus CT-guided sacroiliac joint injections in young women affected by sacroiliac joint (SI) arthritis

# **METHOD AND MATERIALS**

77 young female patients (mean age 38) affected by SI arthritis were treated with anaesthetics, steroid and O2-O3 mixture injections. Thirty-two out of 77 (41.5%) patients (Group A) were treated using US-guided injection and 45 out of 77 (58.4%) (Group B) with CT-guided injection. The patients were randomly assigned to each group. Exclusion criteria were histories of significant allergic reactions to inject solutions, local malignancy, bleeding disorders and diabetes. Symptoms intensity were evaluated with VAS scale before and after 3 and 6 months from treatment. We considered the advantages of both techniques in terms of procedure time, radiation exposure and clinical outcome

## RESULTS

Twenty-four out of 32 (75%) patients (Group A) and thirty-three out of 45 (73%) patients (Group B) showed a significant improvement of symptomatology after 3 and 6 months. We observed a faster execution procedure and also no radiation dose exposure for patients belonging to Group A. We did not observe any major complications in both groups

# CONCLUSION

Us-guided injection is a safe and effective procedure for sacroiliac joint arthritis with same results if compared to CT-guided treatment in terms of improvement of symptoms.

# **CLINICAL RELEVANCE/APPLICATION**

US is preferred in young women in fertile age for its shorter duration times and lack of radiation dose exposure.

The Atrophic Phenotype of Knee Osteoarthritis is not Associated with Faster Progression of Disease: The Multicenter Osteoarthritis (MOST) Study

Tuesday, Nov. 29 12:15PM - 12:45PM Room: MK Community, Learning Center Station #4

# Participants

Michel D. Crema, MD, Boston, MA (*Abstract Co-Author*) Shareholder, Boston Imaging Core Lab, LLC Ali Guermazi, MD, PhD, Boston, MA (*Abstract Co-Author*) President, Boston Imaging Core Lab, LLC Research Consultant, Merck KgaA Research Consultant, Sanofi-Aventis Group Research Consultant, TissueGene, Inc Research Consultant, OrthoTrophic Research Consultant, AstraZeneca PLC David T. Felson, MD, MPH, Boston, MA (*Abstract Co-Author*) Consultant, Zimmer Biomet Holdings, Inc Michael C. Nevitt, PhD, San Francisco, CA (*Abstract Co-Author*) Nothing to Disclose Monica D. Marra, MD, Boston, MA (*Abstract Co-Author*) Shareholder, Boston Imaging Core Lab, LLC Frank W. Roemer, MD, Boston, MA (*Presenter*) Chief Medical Officer, Boston Imaging Core Lab LLC; Research Director, Boston Imaging Core Lab LLC; Shareholder, Boston Imaging Core Lab LLC; ;

# PURPOSE

In tibiofemoral compartments exhibiting fast progression of osteoarthritis (OA), osteophyte formation may lag behind cartilage loss, which might then manifest as an atrophic OA phenotype. The aim of this study was to assess the associations of atrophic tibiofemoral OA with progression of radiographic joint space narrowing (JSN) and magnetic resonance imaging (MRI)-defined progression of cartilage damage.

# METHOD AND MATERIALS

Participants of the Multicenter Osteoarthritis (MOST) Study with available radiographic and 1.0T MRI assessments at baseline and 30 months follow-up (FU), were included. Radiographs were assessed according to the OARSI system for JSN and osteophytes (grades 0-3). Ten tibiofemoral regions were assessed on MRI for cartilage morphology (grades 0-6) and osteophytes (grades 0-7) using the WORMS system. On radiographs, atrophic OA was defined as OARSI grades 1 or 2 for JSN and grade 0 for osteophytes. On MRI, atrophic OA was defined as tibiofemoral cartilage damage grades  $\geq$  3 in at least 2 of 10 subregions with absent or equivocal osteophytes (grades 0 and 1) in all subregions. Progression of JSN and cartilage loss on MRI, was defined as 1) no, 2) slow, and 3) fast progression. Chi-square test and logistic regression with generalized estimated equations were performed to assess the association of atrophic knee OA with any progression, compared to non-atrophic OA knees (reference group).

## RESULTS

A total of 476 knees from 432 participants were included. Using the radiographic definition, 50 (10.5%) had atrophic OA and 426 (89.5%) had non-atrophic OA knees at baseline. Using the MRI definition, there were 16 (3.4%) knees with atrophic OA and 460 (96.6%) with non-atrophic OA. Non-atrophic OA knees more commonly exhibited fast progression of JSN (p=0.002) and fast progression of MRI cartilage damage (p=0.02). Logistic regression showed that the atrophic phenotype of knee OA was modestly protective against progression of JSN and MRI when compared to non-atrophic OA knees.

# CONCLUSION

In this sample of subjects with or at risk for knee OA the atrophic phenotype of knee OA did not predispose to more rapid progression compared to non-atrophic OA. Instead, the atrophic phenotype demonstrated a decreased risk for OA progression.

# **CLINICAL RELEVANCE/APPLICATION**

Our results may potentially impact on subject selection in clinical trials of knee OA, as the atrophic phenotype is not associated with more progression of disease.

## **Honored Educators**

Presenters or authors on this event have been recognized as RSNA Honored Educators for participating in multiple qualifying educational activities. Honored Educators are invested in furthering the profession of radiology by delivering high-quality educational content in their field of study. Learn how you can become an honored educator by visiting the website at: https://www.rsna.org/Honored-Educator-Award/

Ali Guermazi, MD, PhD - 2012 Honored Educator

T2\* Mapping of Peroneal Tendons Using Clinically Relevant Subregions in an Asymptomatic Population

Tuesday, Nov. 29 12:15PM - 12:45PM Room: MK Community, Learning Center Station #5

#### Participants

Katharine Wilson, MS, Vail, CO (Abstract Co-Author) Nothing to Disclose Rachel K. Surowiec, MSc, Vail, CO (Abstract Co-Author) Nothing to Disclose Nicholas S. Johnson, MD, Milwaukee, WI (Abstract Co-Author) Nothing to Disclose Carly Lockard, MS, Vail, CO (Presenter) Nothing to Disclose Thomas Clanton, MD, Vail, CO (Abstract Co-Author) Research funded, Siemens AG Research funded, Smith & Nephew plc Research funded, Arthrex, Inc Research funded, Ossur Charles P. Ho, MD, PhD, Vail, CO (Abstract Co-Author) Research funded, Siemens AG Research funded, Smith & Nephew plc Research funded, Arthrex, Inc Research funded, Ossur HF Scientific Advisory Board, Rotation Medical, Inc PURPOSE

Quantify and analyze T2\* mapping values in clinically relevant subregions of the peroneal brevis and longus tendons in an asymptomatic cohort. This will provide baseline normative values for future comparison with chronic and acute injuries of the tendon and will improve our understanding of the normal variation of these biomarker values within the tendons.

# **METHOD AND MATERIALS**

Unilateral ankle scans with T2\* mapping were acquired of 26 asymptomatic subjects in the prone position with a 3.0 T MRI system (axial plane, 2.5mm slice thickness, 0.54 x 0.54 mm in plane resolution, 4:47 acquisition time). The peroneal brevis and longus tendons were manually segmented and a bony landmark was placed at the most inferior and lateral point of the lateral malleolus. Six subregions, each 1 cm in length, were isolated along the length of the tendon including three subregions proximal to the lateral malleolus and three subregions distal (Table 1). Summary statistics for T2\* values in each subregion were calculated as well as for the whole 6cm length of tendon (i.e. all subregions combined).

## RESULTS

The peroneal brevis and longus tendons exhibited similar mean T2\* values when the 6 cm length of tendon was analyzed as a whole, with  $10.28 \pm 2.37$  ms (mean  $\pm$  standard deviation) found in the brevis tendon and  $10.75 \pm 2.08$  ms in the longus tendon. However, a trend of higher T2\* values in the distal subregions was found. The distal subregions had significantly higher T2\* values than the two most proximal subregions (proximal 2 and 3) of both the brevis and longus tendons (p<0.05). The subregional results are summarized in Table 1.

# CONCLUSION

T2\* mapping values were presented for the peroneal tendons with a focus on clinically relevant subregions. Regions immediately distal to the tip of the lateral malleolus had significantly higher T2\* values than those proximal to the lateral malleolus. This study provides a quantitative methodology and a normative baseline of T2\* mapping values for comparison with clinically compromised peroneal tendon patients (acute and chronic cases) in the future.

## **CLINICAL RELEVANCE/APPLICATION**

Higher T2\* values distal to the lateral malleolus could be clinically relevant to peroneal tendon tears that often initiate near the lateral malleolus, 5th metatarsal, inferior retinaculum and cuboid.

# MK319-SD-TUA6

Efficacy of Ultrasound-guided Needle Tenotomy for the Treatment of Chronic Tendinopathies: Preliminary Results

Tuesday, Nov. 29 12:15PM - 12:45PM Room: MK Community, Learning Center Station #6

# Participants

Federico Bruno, MD, LAquila, Italy (*Presenter*) Nothing to Disclose Fernando Smaldone, MD, L'Aquila, Italy (*Abstract Co-Author*) Nothing to Disclose Alice La Marra, MD, L'Aquila, Italy (*Abstract Co-Author*) Nothing to Disclose Silvia Mariani, MD, L'Aquila, Italy (*Abstract Co-Author*) Nothing to Disclose Francesco Arrigoni, Coppito, Italy (*Abstract Co-Author*) Nothing to Disclose Luigi Zugaro, L'Aquila, Italy (*Abstract Co-Author*) Nothing to Disclose Antonio Barile, MD, L'Aquila, Italy (*Abstract Co-Author*) Nothing to Disclose Carlo Masciocchi, MD, L'Aquila, Italy (*Abstract Co-Author*) Nothing to Disclose

## PURPOSE

To determine the effectiveness of ultrasound-guided percutaneous needle tenotomy in terms of clinical improvement and tendon morphological recovery in patients with chronic tendinopathies.

## **METHOD AND MATERIALS**

30 tendons (10 Achilles, 10 supraspinatus, 10 common extensor elbow) in 24 patients (14 men, 10 women, mean age 32.5 years, range 20-45). The patients underwent MRI and ultrasound examination following referral with clinical diagnosis of tendinosis (mean symptom duration 6 months) that had failed conservative treatment. Pre- and post-procedure (at 6 months follow-up) VAS scores were collected to assess patient clinical response. All patients were treated with sonographically guided percutaneous tenotomy. The procedure was performed twice, 3 weeks apart. All complications were recorded. Follow up ultrasound and MRI examination was performed 6 months after the treatment to evaluate tendon morphology.

## RESULTS

Mean VAS scores were significantly lower at 6th month follow-up  $(2.2 \pm 0.7)$  compared with the baseline  $(5.8 \pm 0.6)$  in 80% of patients. The imaging follow up with sonographic assessment showed a reduction in overall tendon thickness and in the size of the area of tendinosis in 21 tendons (70%). MRI findings confirmed improvement of the tendon morphology and signal intensity in the same cases. 6 tendons showed no improvement (20%), in 3 tendons (10%) degenerative changes evolved.

# CONCLUSION

The results of our study show that sonographically guided percutaneous needle tenotomy as a stand alone procedure is effective in reducing pain in patients with chronic tendinopathy without complications. Our imaging results confirm the effectiveness of the treatment in modifying tendon morphology.

## **CLINICAL RELEVANCE/APPLICATION**

Dry needling shows promise as a cheap, safe and effective treatment, suitable for patients with degenerative tendon disease.

# MK320-SD-TUA7

Comparing CT Derived Measures of Sarcopenia with Serum Biomarkers for Prediction of Survival in Patients with Colorectal Cancer

Tuesday, Nov. 29 12:15PM - 12:45PM Room: MK Community, Learning Center Station #7

# Participants

ChihYing Deng, Tao Yuan, Taiwan (*Presenter*) Nothing to Disclose Jim S. Wu, MD, Boston, MA (*Abstract Co-Author*) Research Grant, Kaneka Corporation Yu-Ching Lin, MD, Tao Yuan, Taiwan (*Abstract Co-Author*) Nothing to Disclose Kun-Yun Yeh, Keelung, Taiwan (*Abstract Co-Author*) Nothing to Disclose Yun-Chung Cheung, MD, Kwei Shan, Taiwan (*Abstract Co-Author*) Nothing to Disclose Yu-Hsiang Juan, MD, Taoyuan, Taiwan (*Abstract Co-Author*) Nothing to Disclose Colm J. McMahon, MBBCh, Boston, MA (*Abstract Co-Author*) Nothing to Disclose

## PURPOSE

Depleted muscle mass (sarcopenia) has been associated with adverse outcome for patients with colorectal cancer. The goal of this study is to compare CT derived measures of sarcopenia with established serum biomarkers for prediction of overall survival.

## **METHOD AND MATERIALS**

Patients with colorectal cancer between were followed for at least 5 years following diagnosis. Baseline CT and CT 1 year after diagnosis were analyzed. Skeletal Muscle Index (SMI) of psoas and paraspinal muscles, and mean Hounsfield Units (HU) were measured at baseline, and 1 year CTs. Interval change in parameters between baseline and 1 year were calculated. Measurements were taken at L4 level. Baseline carcinoembryonic antigen (CEA), Glasgow Prognostic Score (GPS) and neutrophil-lymphocyte ratio were measured. Multivariate Cox proportional hazard regression model was used to evaluate independent predictors of survival. Age, tumor stage and body mass index (BMI) were included in the model.

### RESULTS

99 patients were included, mean (SE) age 65.1 (1.30) years, 36 females. Controlled for age, tumor stage and BMI, 1 year interval decrease in psoas muscle SMI was the strongest predictor of survival, Hazard Ratio (HR) = 26.80, p = 0.008. Baseline paraspinal SMI was also an independent predictor, HR = 0.53, p = 0.024. Neutrophil-lymphocyte ratio was also an independent predictor, HR = 1.16, p = 0.004. CEA, baseline psoas SMI, 1 year decrease in paraspinal SMI, GPS, were not significant independent predictive factors.

# CONCLUSION

The decrease of psoas muscle SMI one year after diagnosis of colorectal cancer is an independent predictor of survival, as are, to a lesser extent, baseline paraspinal SMI and neutrophil-lymphocyte ratio.

## **CLINICAL RELEVANCE/APPLICATION**

The findings of this study highlight the importance of CT derived measures of sarcopenia as imaging biomarkers predictive of clinical outcome for patients with colorectal cancer.

# **Imaging Features of Myeloproliferative Neoplasms**

Tuesday, Nov. 29 12:15PM - 12:45PM Room: MS Community, Learning Center Station #1

#### **Participants**

Ian Murphy, MBBCh, MRCS, Cambridge, United Kingdom (*Presenter*) Nothing to Disclose Emily Mitchell, MD, Cambridge, United Kingdom (*Abstract Co-Author*) Nothing to Disclose Anna Godfrey, MD, PhD, Cambridge, United Kingdom (*Abstract Co-Author*) Nothing to Disclose Edmund M. Godfrey, MBBCh, FRCR, Cambridge, United Kingdom (*Abstract Co-Author*) Nothing to Disclose

# **TEACHING POINTS**

Discuss the clinical and pathological aspects of the heterogeneous group of hematological disorders known as myeloproliferative neoplasms (MPNs).

Recognize typical imaging features suggestive of underlying MPN.

Identify unusual imaging signs that may enable the radiologist to suggest an MPN as a possible underlying cause, particularly splanchnic venous thrombosis.

## **TABLE OF CONTENTS/OUTLINE**

Categorization of Myeloproliferative Neoplasms (MPN)Imaging feature, related to:- Thrombosis- Osseous findings- Solid lesions-Other findingsBrief discussion on treatment, clinical aspects

# Checking In with Checkpoint Inhibition: Imaging Review of PD1 Inhibitor Immune-Related Adverse Events

Tuesday, Nov. 29 12:15PM - 12:45PM Room: MS Community, Learning Center Station #2

**FDA** Discussions may include off-label uses.

#### Awards

**Certificate of Merit** 

## Participants

Matthew Quirk, MD, Los Angeles, CA (*Presenter*) Nothing to Disclose Antonio J. Gutierrez, MD, Los Angeles, CA (*Abstract Co-Author*) Nothing to Disclose Kathleen Ruchalski, MD, Santa Monica, CA (*Abstract Co-Author*) Nothing to Disclose Robert D. Suh, MD, Los Angeles, CA (*Abstract Co-Author*) Nothing to Disclose Dean Wallace, MD, Los Angeles, CA (*Abstract Co-Author*) Nothing to Disclose Pawan Gupta, Los Angeles, CA (*Abstract Co-Author*) Nothing to Disclose Antoni Ribas, Los Angeles, CA (*Abstract Co-Author*) Nothing to Disclose

# **TEACHING POINTS**

1. Discuss the novel role of programmed cell death 1 (PD1) inhibitors in current cancer therapy, and understand their pharmacologic mechanisms.

2. Recognize the imaging manifestations of PD1 inhibitor immune-related adverse events across a variety of organ systems.

3. Case-based approach to PD1 inhibitor immune-related imaging findings.

## TABLE OF CONTENTS/OUTLINE

PD1 inhibition – novel role in cancer therapy Pharmacologic mechanisms of PD1 inhibition FDA-approved use in cancer subtypes and emerging applications Immune-related adverse events and their treatmentImaging manifestations of PD1 inhibitor immune-related adverse events Hypophysitis – enlargement and abnormal MRI signal with clinical hypopituitarism Thyroiditis – heterogeneous enhancement and atrophy with clinical hypothyroidism Organizing Pneumonia – airspace consolidations and ground-glass attenuation ARDS – diffuse ground-glass attenuation and consolidations Pleuritis – progressive diffuse pleural thickening with pathologic correlation Pancreatitis – diffuse hypermetabolism on FDG PET/CT Nephritis – geographic hypoenhancing renal lesions Mesenteritis – soft tissue masses, lymphadenopathy and fat stranding with pathologic correlation Colitis – colonic wall thickening and fat strandingConclusion Consider immune-related adverse events in patients on PD1 therapy

# Lung Scintigraphy in Transplant Patients - A Primer

Tuesday, Nov. 29 12:15PM - 12:45PM Room: S503AB Hardcopy Backboard

### Awards Certificate of Merit

## Participants

Daniella F. Pinho, MD, Dallas, TX (*Presenter*) Nothing to Disclose Amit Banga, Dallas, TX (*Abstract Co-Author*) Nothing to Disclose Fernando Torres, MD, Dallas, TX (*Abstract Co-Author*) Nothing to Disclose Dana Mathews, MD, PhD, Dallas, TX (*Abstract Co-Author*) Nothing to Disclose

## **TEACHING POINTS**

1. To review the indications of lung scintigraphy in patients pre and post single and bilateral lung transplant2. To assess the added value of physiologic information given by lung scintigraphy in the lung transplant setting3. To discuss the impact of scintigraphy findings in the management of lung transplant patients.4. To correlate lung scintigraphy findings with other studies modalities (for example, CTA of the chest) and with lung transplant histology.

# TABLE OF CONTENTS/OUTLINE

- 1. Indications for lung transplant
- 2. Pre-transplant lung scintigraphy a. imaging findings in different diseases

b. quantitative perfusion lung scintigraphy for surgical planning lung scintigraphy a. Early post transplant complications c. Chest CT and histology correlations3. Post transplant I. pulmonary embolism

- II. bronchial stenosis
- III. acute rejection

IV. quantitative scintigraphy for prediction of chronic rejection b. Late post transplant complications I. Subacute/chronic rejection

- II. Pulmonary embolism III. Other complications
  - c. Chest CT and histology correlations4. Summary

### **Honored Educators**

Presenters or authors on this event have been recognized as RSNA Honored Educators for participating in multiple qualifying educational activities. Honored Educators are invested in furthering the profession of radiology by delivering high-quality educational content in their field of study. Learn how you can become an honored educator by visiting the website at: https://www.rsna.org/Honored-Educator-Award/

Daniella F. Pinho, MD - 2015 Honored Educator

## NM218-SD-TUA6

To Evaluate the Relevance of 18F-FDG PET-CT in the Diagnosis of Various Pathologies for the Pyrexia of Unknown Origin

Tuesday, Nov. 29 12:15PM - 12:45PM Room: S503AB Station #6

## Participants

Sikandar M. Shaikh, DMRD, Hyderabad, India (Presenter) Nothing to Disclose

### PURPOSE

This study aims to demonstrate the diagnostic performance of PET-CT in patients with PUO.

### METHOD AND MATERIALS

141 consecutive patients with criteria of PUO (78 male, mean age 52+/-18) were retrospectively evaluated using PET-CT after inconclusive conventional imaging. FDG PET-CT was done after injecting the FDG contrast and scan done after 60 minutes. The varied uptake on FDG was evaluated based on SUV max values. Final diagnosis was based on biopsy, Laboratory tests and imaging follow-up.

### RESULTS

The cause of PUO was identified in cases were diagnosed as 41 infection, 37 malignancy, 41 non-infectious inflammatory diseases and 21 other causes. The patients had PET-CT scan at day 11day on average (+/- 5days) of hospital admission. Results Table: True Positive in 49/141: 16 infection, 16 malignancy, 17 inflammation. False Positive lesions in 9/141, due to reactive nodes confirmed with subsequent CT. True Negative lesions in 41/141, clinically self-limiting conditions with full spontaneous recovery. Such spontaneous recovery took 14 days on average (+/- 18 days) after hospital admission. False Negative lesions in 15/141: 3 infection, 5 malignancy, 6 inflammation, 1 others. PET-CT appears to miss some of the connective tissue diseases, non-FDG-avid malignancy and poorly-FDG-avid malignancy or infection within the organs of normal physiological FDG-uptake such as brain and liver. The PPV, NPV and accuracy of PET-CT were 84%, 73% and 79% respectively. On multivariate analysis, none of the inflammatory markers (white cell counts, ESR and CRP) statistically satisfied as independent predictor of PET-positivity.

## CONCLUSION

Thus 18F-FDG PET-CT correctly diagnosed acause of PUO in 89% of patients. A negative PET-CT with no spontaneous recovery still requires further investigations in order to exclude various causes such as myeloma and FDG avid small gastrointestinal/renal/pancreatic malignancies.

## **CLINICAL RELEVANCE/APPLICATION**

Thus FDG PET-CT helps in evalaution of PUO cases.

## NM219-SD-TUA7

Association of Deauville Visual 5-point Scale and SUV- or MTV-related Parameters in FDG PET after Treatment of Follicular Lymphoma

Tuesday, Nov. 29 12:15PM - 12:45PM Room: S503AB Station #7

## Participants

Mitsuaki Tatsumi, MD, PhD, Suita, Japan (*Presenter*) Nothing to Disclose Kayako Isohashi, Suita, Japan (*Abstract Co-Author*) Nothing to Disclose Hiroki Kato, Suita Osaka, Japan (*Abstract Co-Author*) Nothing to Disclose Noriyuki Tomiyama, MD, PhD, Suita, Japan (*Abstract Co-Author*) Nothing to Disclose Jun Hatazawa, MD, PhD, Osaka, Japan (*Abstract Co-Author*) Nothing to Disclose

# PURPOSE

Deauville visual 5-point scale(D5S) on FDG PET is adopted as a new response assessment method of lymphoma in the Lugano classification published in 2014. The purpose of this study was to clarify the association of D5S and changes of SUV or metabolic tumor volume(MTV) in FDG PET after treatment(Tx) of follicular lymphoma(FL).

# METHOD AND MATERIALS

FDG PET-CT examinations were performed before and after chemotherapy in 45 FL patients. SUVmax and SUVpeak(1cm3 ROI) were obtained in the hottest lesion in each exam. MTV was calculated for the hottest as well as whole-body lesions(SUV threshold 2.5). Changes of these parameters before and after Tx were calculated. PostTx PET images were evaluated using D5S. In this study two patterns of negative definition were tested either with Scores 1 and 2(uptake  $\leq$  mediastinum) or Scores 1,2, and 3(uptake > mediastinum but  $\leq$  liver). D5S and quantitative PET parameters were compared each other and to the recurrence within 2 years. Statistical analysis was performed with a Spearman's rank correlation coefficient and receiver operating characteristic(ROC) curves.

## RESULTS

45 FL pts represented the following D5S after treatment; Score 2 – 30 pts, 3 – 2, 4 – 6, and 5 – 7. D5S exhibited no correlations with preTx SUV- nor MTV-related parameters, but showed strong correlations with postTx SUV- and MTV-related parameters (Rho=0.82-0.88, p<0.001). D5S also showed moderate(Rho=0.47-0.52) and strong(Rho=0.86) correlations with changes of SUV- and MTV-related parameters, respectively. Recurrence within 2 years exhibited strong correlations with postTx SUV-, MTV-, and changes of MTV-related parameters as well as with D5S(Rho=0.59-0.66). ROC analysis revealed negative interpretation with Scores 1-2(area under the curve:0.79, sen.68%, spe.96%, acc.82%) better than Scores 1-3 as negative in predicting recurrence in this study. Although ROC AUC 0.87 of postTx SUVmax was the greatest, it did not differ statistically from the AUC of D5S.

### CONCLUSION

This study demonstrated D5S had correlations with postTx SUV- and MTV-related parameters as well as changes of SUV- and MTV-related parameters after Tx in FL. D5S provided comparable results to those parameters in predicting recurrence of FL.

## **CLINICAL RELEVANCE/APPLICATION**

Deauville visual 5-point scale on FDG PET after treatment was demonstrated to provide comparable results to SUV- and MTVrelated parameters in predicting recurrence of follicular lymphoma.

## Density-threshold for FDG-PET/CT-based N-staging in Lung Cancer Patients

Tuesday, Nov. 29 12:15PM - 12:45PM Room: S503AB Station #8

#### Participants

Paul G. Flechsig, Heidelberg, Germany (Presenter) Nothing to Disclose

Clemens Kratochwil, MD, Heidelberg, Germany (Abstract Co-Author) Nothing to Disclose

Hans-Ulrich Kauczor, MD, Heidelberg, Germany (*Abstract Co-Author*) Research Grant, Siemens AG Research Grant, Bayer AG Speakers Bureau, Boehringer Ingelheim GmbH Speakers Bureau, Siemens AG Speakers Bureau, Novartis AG Speakers Bureau, GlaxoSmithKline plc Speakers Bureau, Almirall SA

Lawrence H. Schwartz, MD, New York, NY (*Abstract Co-Author*) Committee member, Celgene Corporation Committee member, Novartis AG Committee member, ICON plc Committee member, BioClinica, Inc

Uwe Haberkorn, MD, Heidelberg, Germany (Abstract Co-Author) Nothing to Disclose

Frederik L. Giesel, MD, MBA, Heidelberg, Germany (Abstract Co-Author) Patent application for F18-PSMA-1007

### PURPOSE

Mediastinal N staging done by integrated 18F-FDG-PET/CT in lung cancer patients is not always accurate. In order to reduce the need for invasive staging procedures, additional surrogate parameters for the detection of malignant lymph node infiltration would be helpful. The purpose of this study was to evaluate if semi-automated density measurements in mediastinal lymph nodes can improve pre-clinical N-staging, irrespective of the specific lung cancer entity.

### METHOD AND MATERIALS

This retrospective study was approved by the institutional review board. 248 histologically proven lymph nodes in 122 lung cancer patients were investigated. Non-contrast enhanced 18F-FDG-PET/CT was performed before surgery/biopsy. Lymph nodes analyses were performed on the basis of FDG-uptake and volumetric CT histogram analysis for metric lymph node sampling.

## RESULTS

Of the 248 lymph nodes, 118 were benign, 130 malignant. Malignant lymph nodes had a significantly higher median CT density (>30HU) compared to benign lymph nodes (9.3 HU, p < 0.05), irrespective of the histological subtype. The discrimination between different malignant tumour subtypes by means of volumetric density analysis failed. Irrespective of the malignant subtype, a possible cut off value of 20HU may help differentiate between benign and malignant lymph nodes.

### CONCLUSION

Density measurements in unclear mediastinal and hilar lymph nodes with equivocal FDG uptake in PET might serve as a possible surrogate parameter for N-staging in lung cancer patients, irrespective of the specific lung cancer subtype. This could also help to find possible high yield targets in cases where invasive lymph node staging is necessary.

### **CLINICAL RELEVANCE/APPLICATION**

Semi-automated density measurement in lymph nodes in lung cancer patients might create a promising imaging surrogate for Nstaging, irrespective of malignant tumour subtype, which is of clinical relevance in patients with unclear PET findings in PET/CT, prior to invasive lymph node sampling.

# Differential Diagnostic Value of 18F-FDG PET/CT in Osteolytic Lesions

Tuesday, Nov. 29 12:15PM - 12:45PM Room: S503AB Station #9

### **Participants**

Xiaomeng Li, MD, Beijing, China (*Presenter*) Nothing to Disclose Ning Wu, MD, Beijing, China (*Abstract Co-Author*) Nothing to Disclose

## PURPOSE

To investigate the differential diagnostic value of 18F-FDG PET/CT in osteolytic lesions.

## METHOD AND MATERIALS

This retrospective study spanned 8 years and included 344 newly diagnosed patients with osteolytic lesions. They all underwent both FDG PET/CT and biopsy/surgery because of the suspicion of malignancy. Both FDG uptake and morphologic changes such as soft tissue mass formation were compared with pathological results.

## RESULTS

A total of 8896 osteolytic lesions were evaluated. The SUVmax of MM osteolytic lesions is significantly lower than bone metastases  $(1.6\pm0.7 \text{ vs. } 5.5\pm2.7, P=0.000)$ . The best cutoff value of SUVmax in the differentiation of MM and bone metastasis is 2.65 (sensitivity 86.1% and specificity 94.7%, P=0.000). Bone lesions with soft tissue mass have higher SUVmax than pure osteolytic lesions (both P=0.000). SUVmax of bone metastases showed significant correlation with those of primary tumors (r=0.532, P=0.000). Furthermore, the formation of soft tissue mass is more common in bone metastases than in MM (7% vs. 2%).

## CONCLUSION

FDG PET/CT is a valuable tool in the differential diagnosis of osteolytic lesions.

## **CLINICAL RELEVANCE/APPLICATION**

In osteolytic lesions, the best cutoff value of SUVmax in the differentiation of multiple myeloma and bone metastasis is 2.65. For patients with metastatic bone cancer of unknown primary origin, our results can help to detect primary tumors.

## NM222-SD-TUA10

FDG PET/MR Uptake Measurements of Tumor and Normal Structures in Cancer Patients: Same Day Assessment of Reproducibility with PET/CT and PET/MR Test-retest Repeatability

Tuesday, Nov. 29 12:15PM - 12:45PM Room: S503AB Station #10

# Participants

Liran Domachevsky, MD, Tel Aviv, Israel (*Presenter*) Nothing to Disclose Hanna Bernstine, MD, Petah Tikva, Israel (*Abstract Co-Author*) Nothing to Disclose Dorit Stern, Tel Aviv, Israel (*Abstract Co-Author*) Nothing to Disclose Natalia Goldberg, MD, Petah Tiqwa, Israel (*Abstract Co-Author*) Nothing to Disclose Meital Nidam, Tel Aviv, Israel (*Abstract Co-Author*) Nothing to Disclose Dan Stein, Tel Aviv, Israel (*Abstract Co-Author*) Nothing to Disclose Ifat Abadi-Korek, PhD, Tel Aviv, Israel (*Abstract Co-Author*) Nothing to Disclose David Groshar, MD, Tel Aviv, Israel (*Abstract Co-Author*) Nothing to Disclose

### PURPOSE

To determine PET/CT and PET/MR reproducibility and test-retest PET/MR repeatability of measurements of fluorine 18 fluorodeoxyglucose (FDG) uptake in normal structures and in tumor lesions, obtained by PET/CT and by two sequential PET/MR examinations performed on the same day in patients with cancer.

### **METHOD AND MATERIALS**

This prospective observational study was IRB approved and written informed consent was obtained. Between October 2015 and February 2016, consecutive patients performing FDG PET/CT and two sequential non-enhanced whole-body FDG PET/MR were included. Studies order was random. A total of 34 patients with no visible tumor lesion (20 women and 14 men, mean age 54.9±11.2 years) and 33 patients (19 women and 14 men, mean age 53.1±12.1) with visible tumor lesions (a total of 63) were enrolled. Maximal, peak and mean standardized uptake value normalized for body weight (SUV's) and lean body mass (SUL's) were obtained for normal structures (aorta, liver, spleen, vertebra, iliac bone and subcutaneous fat) in PET/CT and PET/MR using a spherical volume of interest (VOI). For lesions an isocontour VOI with a threshold of 40% of maximal SUV/L was placed and SUV/L's and metabolic tumor volume (MTV) were calculated. A sphere VOI was placed in the liver and the tumor to liver ratio (T/L) calculated. Coefficient of variation, intraclass correlation coefficient and repeatability coefficient were used to estimate the measurements reliability.

### RESULTS

There was a high lesional reproducibility and repeatability with an almost perfect agreement of SUV/L's and MTV measured between lesional PET/MR and PET/CT and by two sequential PET/MR. T/L ratio reproducibility and repeatability demonstrated almost perfect agreement despite changes in SUV/L's measurements of the liver. PET/MR measurements of SUV/Lpeak showed to be more consistent compared to SUV/Lmax of lesions. For normal structures, there was only slight-moderate agreement in SUV/L's measured in PET/MR compared with PET/CT. There was substantial-almost perfect agreement in SUV/L's measured in two sequential PET/MR for all normal structures with the exception of the aorta and subcutaneous fat.

## CONCLUSION

PET/MR is reliable with regard to quantification of PET metrics and could be used to assess the metabolic response to treatment of cancerous tumors.

## **CLINICAL RELEVANCE/APPLICATION**

PET/MR is reliable with regard to quantification of PET metrics

**Imaging of Neurovascular Cranial Nerve Compression Syndromes** 

Tuesday, Nov. 29 12:15PM - 12:45PM Room: NR Community, Learning Center Station #9

### Participants

Juan Carlos Monte Gonzalez, MD, Madrid, Spain (*Presenter*) Nothing to Disclose Jose Luis Lerma Gallardo, MD, Madrid, Spain (*Abstract Co-Author*) Nothing to Disclose Manuela M. Jorquera, Madrid, Spain (*Abstract Co-Author*) Nothing to Disclose Natividad Gomez Jr, MD, Madrid, Spain (*Abstract Co-Author*) Nothing to Disclose Juan Arrazola, Madrid, Spain (*Abstract Co-Author*) Nothing to Disclose Miguel Yus Fuertes, MD, Alcala De Menares, Spain (*Abstract Co-Author*) Nothing to Disclose

## **TEACHING POINTS**

To review the cranial nerves (CN) normal anatomy in their cisternal course. To discuss the most frequent neurovascular compression syndromes.

## TABLE OF CONTENTS/OUTLINE

Neurovascular compression syndromes result from contact between a CN and a vessel, that may displace and compress the CN. MR with heavily T2-weigthed 3D and angiographic 3D Time of Flight sequences is the state-of-the-art imaging technique to image this patology, since it provides an optimal anatomic detail of both CN and tiny vascular structures to identify the cause and site of compression. Neurovascular compression syndromes include: Trigeminal and glossopharyngeal neuralgia (CN V and CN IX) Vestibular paroxysms (CN VIII) Eye muscles myokimia (CN III, IV and VI) Hemifacial spasm (CN VII) It has also been proposed as a possible pathogenesis of essential hypertension (CN X) and spasmodic torticollis (CN XI). Since neurovascular contact has also been observed in asymptomatic patients, it should be assessed in the context of a specific clinical presentation. When imaging these contacts, it has to be considered the sensibility of different CN segments to vascular pressure related to the kind of myelin sheath. The excellent anatomical detail may be extremely useful for neurosurgeons in order to predict which patients will benefit from microvascular decompression.

## NR369-SD-TUA1

Using CT Texture Analysis to Predict Treatment Response of HPV-positive Oropharyngeal Squamous Cell Carcinoma

Tuesday, Nov. 29 12:15PM - 12:45PM Room: NR Community, Learning Center Station #1

### Awards

### **Student Travel Stipend Award**

#### Participants

Tamari A. Miller, BA, Chicago, IL (*Presenter*) Nothing to Disclose Anup J. Alexander, MD, Elmhurst, IL (*Abstract Co-Author*) Nothing to Disclose Maryellen L. Giger, PhD, Chicago, IL (*Abstract Co-Author*) Stockholder, Hologic, Inc; Stockholder, Quantitative Insights, Inc; Cofounder, Quantitative Insights, Inc; Royalties, Hologic, Inc; Royalties, General Electric Company; Royalties, MEDIAN Technologies; Royalties, Riverain Technologies, LLC; Royalties, Mitsubishi Corporation; Royalties, Toshiba Corporation; Hui Li, MD, PhD, Chicago, IL (*Abstract Co-Author*) Nothing to Disclose James M. Melotek, MD, Chicago, IL (*Abstract Co-Author*) Nothing to Disclose Daniel J. Haraf, MD, Chicago, IL (*Abstract Co-Author*) Nothing to Disclose Daniel Ginat, MD, Chicago, IL (*Abstract Co-Author*) Nothing to Disclose

## PURPOSE

There is variability in treatment response among patients with HPV-positive oropharyngeal squamous cell carcinomas. There is a clinical need to be able to non-invasively evaluate which HPV-positive tumors will respond positively to induction chemotherapy or display local of distal progression. Texture analysis has emerged as a potentially useful non-invasive imaging biomarker. The goal of this study is to correlate texture features of pretreatment CT with response to therapy and progression-free survival for patients with oropharyngeal HPV-positive oropharyngeal carcinoma treated with Nab-Paclitaxel..

### **METHOD AND MATERIALS**

Texture features of the pre-treatment head and neck CT exams were ascertained retrospectiely for 20 of these patients pending further analysis, including 11 who responded well to induction chemotherapy and nine who responded poorly. The texture analysis was performed on in-house texture analysis software developed at the University of Chicago by Marellyn Giger. The software can analyze images converted DICOM image format as a stand-alone analysis software.

### RESULTS

Figures 1 and 2 show plots for the tumor texture features in terms of response to induction chemotherapy and tumor progression, respectively. The median entropy for patients who responded poorly to induction trended higher (5.7, n=9) than that of those who responded well (4.8, n=11) but is not statistically significant, P=0.42. The median entropy for patients who had no progression trended higher (5.09, n=17) than that of those who showed tumor progression (4.20, n=3), but was not statistically significant, P=0.48. Median energy and homogeneity trended lower for patients who showed no tumor progression after treatment (0.01 and 0.48 respectively, n=17) than for those who displayed progression (0.02 and 0.58 respectively, n=3) without statistical significance, P(energy)=0.62, P(homogeneity)=0.69. Contrast and skewness trended higher patients who responded poorly to induction chemotherapy, P=0.62 and P=0.62 respectively.

## CONCLUSION

Certain texture feaure trends were observed that differed among tumors that had good treatment response versus those taht did not, although further evaluation is warranted.

# **CLINICAL RELEVANCE/APPLICATION**

Texture features may potentially be a useful method for helping to predictresponse to induction chemotherapy and progression-free survival in HPV-positive oropharyngeal squamous cell carcinomas.

## **Honored Educators**

Presenters or authors on this event have been recognized as RSNA Honored Educators for participating in multiple qualifying educational activities. Honored Educators are invested in furthering the profession of radiology by delivering high-quality educational content in their field of study. Learn how you can become an honored educator by visiting the website at: https://www.rsna.org/Honored-Educator-Award/

Daniel Ginat, MD - 2016 Honored Educator

White Matter Lesions and Cardiovascular Risk Factors in Adults

Tuesday, Nov. 29 12:15PM - 12:45PM Room: NR Community, Learning Center Station #2

#### Awards

### **Student Travel Stipend Award**

#### **Participants**

Veska Pandika, MD, Bryn Mawr, PA (*Presenter*) Nothing to Disclose W. Scott Enochs, MD, PhD, Wayne, PA (*Abstract Co-Author*) Nothing to Disclose

### PURPOSE

Diffuse cerebral white matter hyperintense signal changes (WMC) on MR T2 weighted sequences, also known as leukoaraiosis, are nonspecific and a common finding in the general population. These subtle brain lesions have previously been studied with a statistically significant relationship with glucose and cholesterol levels: the severity of these lesions have also been linked with higher blood pressure (BP). We seek to create a practical visual classification system of varying patterns of WMC on MRI and attempt correlation with known markers for small vessel disease risk (hypertension, hyperlipidemia, and diabetes mellitus).

## **METHOD AND MATERIALS**

We retrospectively evaluated 98 MR brain studies of patients meeting our inclusion criteria: patients who had MR brain study performed under routine medical care greater than 45 years old and with BP and lipid panel levels available in our charting system within 1 month of the study date and HbA1c within 3 months. We then systematically noted MR pattern based on location (central, peripheral, diffuse) and severity (on a 0-3 scale) and analyzed our data using multivariate regression analysis.

### RESULTS

Our preliminary results confirm a statistically significant positive association between overall WMC severity with age and HbA1c levels (P<0.05) but without the strong associations with BP or lipid levels reported previously. We further found that a central only pattern is more associated with age and BP, whereas a diffuse pattern is more associated with HbA1c. The peripheral only pattern was found to be significantly less frequent than that of the other two.

### CONCLUSION

We propose a simple and practical classification system for WMC that involves both distribution pattern and severity grading. Using such a system, we found positive associations between pattern and specific modifiable cardiovascular (CV) risk factors. Reporting WMC thusly may guide clinicians in addressing these underlying risk factors in their patients.

## **CLINICAL RELEVANCE/APPLICATION**

Cerebral WMC are common and often reported as nonspecific findings on MR exams. We found a positive association with the severity of these WMC with age and HbA1C, but not with other modifiable CV risk factors. Reporting the pattern of leukoaraiosis in a radiologists' daily practice may guide clinicians in identifying untreated preventable risk factors. A more practical classification would involve both severity grading and overall pattern of WMC.

# **Cerebral Abnormalities in Myotonic Dystrophy Type 1**

Tuesday, Nov. 29 12:15PM - 12:45PM Room: NR Community, Learning Center Station #3

#### **Participants**

Alvaro Gargallo, Tudela, Spain (*Presenter*) Nothing to Disclose Marina Iridoy Zulet, Pamplona, Spain (*Abstract Co-Author*) Nothing to Disclose Raquel Seijas Gomez, Pamplona, Spain (*Abstract Co-Author*) Nothing to Disclose Pablo Lecumberri Villamediana, Pamplona, Spain (*Abstract Co-Author*) Nothing to Disclose Ivonne Jerico Pascual, Pamplona, Spain (*Abstract Co-Author*) Nothing to Disclose Teresa Cabada Giadas, Pamplona, Spain (*Abstract Co-Author*) Nothing to Disclose

# PURPOSE

Our aim was to evaluate the presence of white matter and gray matter abnormalities in myotonic dystrophy type-1 patients, and to investigate its relationship with neurocognitive dysfunction.

## **METHOD AND MATERIALS**

40 myotonic dystrophy type 1 patients and a corresponding healthy control group, were studied with MRI (1.5 Tesla Simenes Avanto). White matter lesions were visually rated according to "age-related white matter change score". The morphometric analysis, with reconstruction and volumetric segmentation, was performed with the Freesurfer software (http://surfer.nmr.mgh.harvard.edu/). Cognitive functioning was assessed in all patients and controls using a comprehensive neuropsychological test battery (CPT-II, TMT-B, BDI, HARS, forward and reverse digits, Spatial location, Bento's test).

## RESULTS

Structural MRI showed significant differences of gray matter volumes in both, cortical and subcortical areas (thalamus, putamen, accumbens and corpus callosum), between patients and control group. White matter lesions were more prevalent and severe in patient's group. Temporal regions were the most frequently and severely affected. Anterior temporal lobe lesions were specifically founded in these patients.Cognitive analysis showed that these patients had a higher susceptibility to interference, and significant deficits of the executive and visuospatial functions compared with control group. Visuospatial functions impairment was significant associated with a volume decrease in corpus callosum, left and right frontal cortex, isthmus cingulated, right occipital lateral and pericalcarinum areas. It was also associated with a higher rate of white matter lesions.

### CONCLUSION

Myotonic distrophy type 1 patient's brain shows white matter and gray matter abnormalities. These findings seem to be related to a progressive neurological impairment.

### **CLINICAL RELEVANCE/APPLICATION**

MRI findings in DM1 patients may shed light into the different pathogenetic mechanisms underlying brain damage in this multisystem disease and contribute to identify new therapeutic targets.

Evaluating the Presence of Reduced Global Cerebral Venous Oxygen Saturation in Patients with Long-term Haemodialysis using Susceptibility Mapping

Tuesday, Nov. 29 12:15PM - 12:45PM Room: NR Community, Learning Center Station #4

## Participants

Chao Chai, MD, Tianjin, China (*Presenter*) Nothing to Disclose Linlin Fan, Tianjin, China (*Abstract Co-Author*) Nothing to Disclose Chao Zuo, Tianjin, China (*Abstract Co-Author*) Nothing to Disclose Lei Liu, Tianjin, China (*Abstract Co-Author*) Nothing to Disclose Jinping Li, Tianjin, China (*Abstract Co-Author*) Nothing to Disclose E. Mark Haacke, PhD, Detroit, MI (*Abstract Co-Author*) Research Grant, Biogen Idec Inc President, Magnetic Resonance Innovations, Inc Wen Shen, Tianjin, China (*Abstract Co-Author*) Nothing to Disclose Shuang Xia, MD, Tianjin, China (*Abstract Co-Author*) Nothing to Disclose

## PURPOSE

To calculate and compare global cerebral venous oxygen saturation using susceptibility mapping (SM) from the straight sinus in patients with haemodialysis and healthy controls to explore clinical risk factors and correlations with neuropsychiatric test.

### **METHOD AND MATERIALS**

86 haemodialysis patients and 64 age-and gender-matched healthy controls were enrolled in this prospective study. SM reconstructed from original phase data of susceptibility weighted imaging (SWI) was used to calculate global cerebral venous oxygen saturation and compare with healthy controls. The global cerebral venous oxygen saturation of healthy controls was compared to that reported in the literature. Stepwise regression analysis and Spearman's correlation were used to explore the correlation between global cerebral venous oxygen saturation, clinical parameters and neuropsychiatric test.

## RESULTS

The global cerebral venous oxygen saturation of healthy individuals was 78.6 $\pm$ 3.0%, consistent with that in the literature. The global cerebral venous oxygen saturation of haemodialysis patients was 73.3 $\pm$ 4.7%, significantly lower than that of healthy individuals (P<0.05). The global cerebral venous oxygen saturation correlated with hemoglobin (r=0.570, P=0.000) and red blood cell (r=0.457, P=0.000). Hemoglobin was the independent predictor of decreased global cerebral venous oxygen saturation by Stepwise regression ( $\beta$ =0.571, P=0.000). There was no significant correlation between decreased global cerebral venous oxygen saturation of patients with haemodialysis and Mini-Mental Statement Examination scores.

## CONCLUSION

Our study suggests that SM is a feasible and reliable means by which to measure global cerebral venous oxygen saturation. In haemodialysis patients, hemoglobin was the independent predictor of decreased global cerebral venous oxygen saturation, which did not cause cognitive impairment.

## **CLINICAL RELEVANCE/APPLICATION**

The decreased global cerebral venous oxygen saturation did occur in patients with haemodialysis, which did not result in the cognitive impairment.

## NR373-SD-TUA5

Diagnosis of Small Posterior Fossa Stroke on Brain CT Scans: Effect of Iterative Reconstruction Designed for Brain CT on the Detection Performance of Radiologists

Tuesday, Nov. 29 12:15PM - 12:45PM Room: NR Community, Learning Center Station #5

## Participants

Taihei Inoue, MD, Kumamoto, Japan (*Presenter*) Nothing to Disclose Takeshi Nakaura, MD, Kumamoto, Japan (*Abstract Co-Author*) Nothing to Disclose Morikatsu Yoshida, Amakusa, Japan (*Abstract Co-Author*) Nothing to Disclose Koichi Yokoyama, Amakusa, Japan (*Abstract Co-Author*) Nothing to Disclose Kenichiro Hirata, Kumamoto, Japan (*Abstract Co-Author*) Nothing to Disclose Masafumi Kidoh, Kumamoto, Japan (*Abstract Co-Author*) Nothing to Disclose Seitaro Oda, MD, Kumamoto, Japan (*Abstract Co-Author*) Nothing to Disclose Kazunori Harada, Amakusa, Japan (*Abstract Co-Author*) Nothing to Disclose Yasuyuki Yamashita, MD, Kumamoto, Japan (*Abstract Co-Author*) Nothing to Disclose

### PURPOSE

The purpose of this study was to evaluate the usefulness of iterative model reconstruction designed for brain CT (IMR-neuro) for the diagnosis of ischemic stroke in the posterior fossa.

### **METHOD AND MATERIALS**

This retrospective study was approved by our institutional review board; patient informed consent was waived. We enrolled 18 patients in the acute and chronic stage of ischemic stroke in the posterior fossa; 18 patients without stroke were the controls. All patients underwent brain CT. We reconstructed axial images with filtered back projection (FBP) and IMR-neuro. The paired t-test was used to compare the CT number [in Hounsfield units (HU)] of the infarcted area, the image noise in the pons, the image contrast, and the contrast to noise ratio (CNR) of the infarcted and the non-infarcted area on scans subjected to IMR-neuro and FBP. The performance of 6 radiologists for the detection of parenchymal hypo-attenuation was analyzed using receiver-operating characteristic (ROC) techniques with the jackknife method.

#### RESULTS

The image noise was significantly lower with IMR-neuro than FBP ( $2.3 \pm 0.5$  vs.  $5.3 \pm 0.9$  HU, p < 0.01). The CNR between the infracted- and the non-infarcted area was significantly greater with IMR-neuro than FBP ( $2.0 \pm 1.4$  vs.  $1.1 \pm 0.5$ , p = 0.02) and the value of the average area under the ROC was significantly higher with IMR-neuro than FBP (0.88 vs. 0.80, p < 0.01).

#### CONCLUSION

IMR-neuro yielded better image quality and improved the observer performance for the detection of parenchymal hypo-attenuation in patients with ischemic stroke.

## **CLINICAL RELEVANCE/APPLICATION**

Compared to FBP, MBIR specialized for brain CT yielded a higher image quality and improved the performance of readers for the detection of parenchymal hypo-attenuation in the posterior fossa.

## Structural Changes in Parkinson's Disease: DTI and VBM Analysis based on 123I-MIBG Uptake

Tuesday, Nov. 29 12:15PM - 12:45PM Room: NR Community, Learning Center Station #6

#### **Participants**

Kazufumi Kikuchi, MD, Fukuoka, Japan (*Presenter*) Nothing to Disclose Akio Hiwatashi, MD, Fukuoka, Japan (*Abstract Co-Author*) Nothing to Disclose Osamu Togao, MD, PhD, Fukuoka, Japan (*Abstract Co-Author*) Nothing to Disclose Koji Yamashita, MD, PhD, Fukuoka, Japan (*Abstract Co-Author*) Nothing to Disclose Ryotaro Kamei, MD, Fukuoka, Japan (*Abstract Co-Author*) Nothing to Disclose Shingo Baba, Fukuoka, Japan (*Abstract Co-Author*) Nothing to Disclose Hiroshi Honda, MD, Fukuoka, Japan (*Abstract Co-Author*) Nothing to Disclose

## PURPOSE

Patients with Parkinson's disease (PD) could show symptoms of sympathetic dysfunction which can be measured on 123I-MIBG myocardial scintigraphy. The purpose of this study was to investigate the changes in brain structures of PD based on both diffusion tensor imaging (DTI) data measured by tract-based spatial statistics (TBSS) and voxel-based morphometry (VBM) depending on MIBG uptake.

### **METHOD AND MATERIALS**

This retrospective study included 24 PD patients, divided into two groups; 12 MIBG-positive and 12-negative cases (10 men and 14 women; age ranged 60-81 years, corrected for gender and age) who underwent DTI at 3T MR scanner and 123I-MIBG scintigraphy. For DTI, motion probing gradients were conducted at 15 directions with b-values of 0 and 800 s/mm2. The heart/mediastinum count (H/M) ratio was calculated on anterior planar 123I-MIBG images obtained 4 hours after injection. The H/M ratio less than 2.00 was considered positive. Fractional anisotropy (FA) and mean diffusivity (MD) with a TBSS were calculated to investigate structural changes between these two groups by performed permutation-based testing with 5,000 permutations and statistical inference by using threshold-free cluster enhancement with a threshold of P < 0.05. VBM was also performed to detect structural difference between these two groups. For VBM analysis, an uncorrected P-value of P < 0.0001 was chosen as the threshold for peak-level statistical significance and all P values were two-tailed.

#### RESULTS

Patients with low H/M ratio showed significantly lower FA in left anterior thalamic radiation, left inferior fronto-occipital fasciculus, left superior longitudinal fasciculus, and left uncinate fasciculus than in those with high H/M ratio (P < 0.05). There were no statistically significant differences in MD in any tracts between patients with high and low H/M ratio (P > 0.05). Patients with low H/M ratio demonstrate a significant reduction of brain volume in right inferior frontal gyrus (P < 0.05).

## CONCLUSION

DTI and VBM could reveal microstructural changes related to degree of MIBG uptake in PD patients.

### **CLINICAL RELEVANCE/APPLICATION**

DTI and VBM could reveal microstructural changes related to degree of MIBG uptake in PD patients. These findings may be a clue for the mechanism of progression of PD.

Clinical Criteria for Computed Tomography in Acute Head Injury

Tuesday, Nov. 29 12:15PM - 12:45PM Room: NR Community, Learning Center Station #7

#### Awards

### **Student Travel Stipend Award**

#### **Participants**

Vincent Leung, MBCHB, Stoke-On-Trent, United Kingdom (*Presenter*) Nothing to Disclose Stephen Sammut, MBChB, Stoke-on-Trent, United Kingdom (*Abstract Co-Author*) Nothing to Disclose Zafar Hashim, MBBS, MRCS, Stoke-on-Trent, United Kingdom (*Abstract Co-Author*) Nothing to Disclose Jooly Joseph, Stoke on Trent, United Kingdom (*Abstract Co-Author*) Nothing to Disclose

#### PURPOSE

The National Institute for Health and Care Excellence (NICE) updated their guidance regarding the clinical criteria for performing CT following head injury in January 2014. We wanted to establish our local adherence to this guidance, any significant change in number of scans performed year-on-year following change in guidance and identify if there were additional risk factors in patients found to have intracranial haemorrhage (ICH).

## **METHOD AND MATERIALS**

A retrospective review was conducted in a UK based University Teaching Hospital of CT heads performed in the emergency department for head injury, during the months of December 2013 and December 2014. 324 scans were performed during these two months (143 in 2013, and 181 in 2014). The mean age was 58.8 years and 58% of patients were male. The clinical criteria were identified through interrogation of the examination request card, as well as the clinical notes.

## RESULTS

In the 2014 group, 164 of 181 (90.6%) patients met the NICE criteria for CT head. There was a 30% increase in examinations yearon-year but despite this there was no change in the rate of haemorrhage (18.9% vs 21.5%, p>0.1).Overall, 59 of 324 scans were positive for ICH, of which 24 had a concurrent fracture. An additional 35 patients had fractures in the imaged range but no ICH. 20% of the patients who met the NICE criteria were found to have ICH compared to only 6.8% in the cohort of patients who did not meet the criteria. 56 of the 59 patients (94.9%) who had ICH met the updated clinical criteria as stated in the NICE guidance. Of the 3 remaining cases of ICH, all patients were over the age of 75 (mean 83 years) and two had a significant mechanism of injury as defined by the guidelines.

## CONCLUSION

Overall our compliance with the NICE guidance was high. There were cases of ICH in patients who did not meet the NICE guidance, which justifies using clinical judgement in selected cases. A potential group of patients who are not identified as at risk by the guidance are the elderly, particularly those with a significant mechanism of injury. No clear reason (e.g. related to change in the guidance) was identified for the 30% increase in number of scans performed year-on-year.

## **CLINICAL RELEVANCE/APPLICATION**

Although the NICE guidance is clinically useful for stratifying patients into high and low risk groups for ICH, there should be a low threshold for imaging the elderly following head injury even if deemed low risk.

## NR376-SD-TUA8

## Vascular Mapping of the Face with 3D Non-contrast Enhanced MR Angiography at 3T-MRI

Tuesday, Nov. 29 12:15PM - 12:45PM Room: NR Community, Learning Center Station #8

#### **Participants**

Etsushi Iida, MD, Ube, Japan (*Presenter*) Nothing to Disclose Matakazu Furukawa, MD, Ube, Japan (*Abstract Co-Author*) Nothing to Disclose Naofumi Matsunaga, MD, PhD, Ube, Japan (*Abstract Co-Author*) Nothing to Disclose

### PURPOSE

Facial reconstruction and transplantation require preoperative vascular mapping of the face. Time-of-flight (TOF) MRA is a common technique for head and neck angiography but saturation effects often lead to signal reduction of the external carotid branches. **NATIVE trueFISP** (Non-contrast Angiography of the Arteries and Veins, true Fast Imaging with Steady-state Precession) is a relatively new MR angiography technique to visualize vascular flow after preparation of the imaging volume with an inversion recovery pulse. The purpose of this study was to evaluate the usefulness of NATIVE trueFISP for vascular mapping of the face.

## METHOD AND MATERIALS

Ten external carotid arteries in five healthy volunteers were visualized with NATIVE trueFISP and three-dimensional TOF-MRA using three-tesla MR unit. Three different inversion times (TI=1300, 1500, 1700ms) were applied for NATIVE trueFISP which affect the extent of inflowing arterial signal and background signal suppression. We evaluated continuity of the whole of the facial arteries, the length and the visibility of the branches including the submental artery, inferior labial artery, superior labial artery and lateral nasal artery as well as the length of the transverse facial arteries. The length of the arteries and their branches was measured by a 3D measuring tool on source images. Friedman's nonparametric test and one-way ANOVA repeated measurement were used for the statistical analysis. A P value of less than 0.05 was considered statistically significant.

## RESULTS

The continuity of the facial artery was better on NATIVE trueFISP, regardless of the inversion times (P < 0.01). Regarding the length of the facial artery, TOF-MRA didn't show a significant difference compared to NATIVE trueFISP with inversion time of 1500ms and 1700ms. NATIVE trueFISP visualized the transverse facial arteries longer than the TOF-MRA (P < 0.01). The transverse facial artery was clearly depicted on NATIVE trueFISP with the inversion time of 1700 ms. The submental artery and inferior labial artery were well visualized on NATIVE trueFISP with the inversion time of 1700 ms.

## CONCLUSION

NATIVE trueFISP is useful to visualize feeding arteries of the face and might be applied to preoperative vascular mapping for a facial reconstruction.

## **CLINICAL RELEVANCE/APPLICATION**

NATIVE trueFISP might be applied to preoperative vascular mapping for a facial reconstruction.

The Safety of Magnetic Resonance Imaging during Pregnancy

Tuesday, Nov. 29 12:15PM - 12:45PM Room: OB Community, Learning Center Station #1

#### **Participants**

Shannon L. St Clair, MD, MPH, New York, NY (*Presenter*) Nothing to Disclose Robert W. Perone, MD, New York, NY (*Abstract Co-Author*) Nothing to Disclose Cory Pfeifer, MD, Phoenix, AZ (*Abstract Co-Author*) Nothing to Disclose Peter S. Assaad, MD, Redlands, CA (*Abstract Co-Author*) Nothing to Disclose Christopher G. Filippi, MD, Grand Isle, VT (*Abstract Co-Author*) Research Consultant, Regeneron Pharmaceuticals, Inc; Research Consultant, Syntactx, LLC

# TEACHING POINTS

MRI is an excellent diagnostic tool which may be utilized to evaluate maternal and/or fetal conditions during pregnancy. There is currently no evidence that MRI causes fetal harm, but a clear consensus on the safety of MRI during pregnancy is also not forthcoming. The proposed risks inherent in MRI are very different from computed tomography. A thorough understanding of these risks allows the radiologists to minimize risk as appropriate to the clinical situation. The current research has failed to show detriment to the fetus using a 1.5 Tesla magnet. More research is warranted to determine the safety profile for 3.0 Tesla magnets and studies with maternal intravenous Gadolinium.

## TABLE OF CONTENTS/OUTLINE

3 main components of MRI including potential hazards & current safety research: Static Magnetic Field Time-Varying Magnetic Gradient Fields Pulse Radio Frequency Fields Fetal Diagnostic Applications Maternal Diagnostic Applications Pregnant MRI Workers: Safety and Recommendations Recommendations: Trimester Magnet Strength Sequences Intravenous contrast Areas for Future Research

First Experience of 18F- FDG PET/ MR Imaging for Whole Body Staging of Women with Gynecologic Malignancies: A Pictorial Essay

Tuesday, Nov. 29 12:15PM - 12:45PM Room: OB Community, Learning Center Station #2

# Participants

Sophie Egels, Paris, France (*Presenter*) Nothing to Disclose Philippe Maksud, Paris, France (*Abstract Co-Author*) Nothing to Disclose Yasmina Badachi, MD, Paris, France (*Abstract Co-Author*) Nothing to Disclose Isabelle Thomassin-Naggara, MD, Paris, France (*Abstract Co-Author*) Speakers Bureau, General Electric Company; Mathilde Wagner, MD, PhD, Paris, France (*Abstract Co-Author*) Consultant Olea Medical Catherine Uzan, Paris, France (*Abstract Co-Author*) Nothing to Disclose Aurelie Kas, Paris, France (*Abstract Co-Author*) Nothing to Disclose Olivier Lucidarme, MD, Paris, France (*Abstract Co-Author*) Consultant, Bracco Group Consultant, F. Hoffmann-La Roche Ltd Consultant, Boehringer Ingelheim GmbH

## **TEACHING POINTS**

Clinical 18F- FDG PET/MRI is becoming a superior alternative to PET/CT in the initial evaluation of women with pelvic malignancies. Indeed it allows a local anatomic evaluation of pelvic cancers with a superior soft tissue contrast, and a functional evaluation combining MRI and PET with less patient radiation compared to PET/CT. But this technique has to be finely tuned to avoid technical problems.The aim of this exhibit is to:1) present Imaging protocols of PET/MRI in gynecologic malignancies used in our institution and the specific technical problems induced by this technology.2) describe the aspects of endometrial, cervical and ovarian cancers in 18F-FDG PET/MRI, and the pitfalls that can be encountered with this technique.

## TABLE OF CONTENTS/OUTLINE

- Patient preparation
- Imaging PET/MRI protocols in the evaluation of endometrial, cervical and advanced ovarian cancers.
- Patterns of endometrial, cervical and advanced ovarian cancers in 18 F-FDG PET/MRI.
- Pitfalls

## PD112-ED-TUA6

Neuroimaging Findings in Children with Organic Acidemias and Aminoacidopathies: A Pattern Recognition Approach

Tuesday, Nov. 29 12:15PM - 12:45PM Room: PD Community, Learning Center Station #6

#### Awards

**Identified for RadioGraphics** 

#### Participants

Nihaal K. Reddy, MBBS, MD, Baltimore, MD (*Presenter*) Nothing to Disclose Sonia F. Calloni, MD, Milan, Italy (*Abstract Co-Author*) Nothing to Disclose Andrea Poretti, MD, Baltimore, MD (*Abstract Co-Author*) Nothing to Disclose Thierry Huisman, MD, Baltimore, MD (*Abstract Co-Author*) Nothing to Disclose Hilary J. Vernon, MD, PhD, Baltimore, MD (*Abstract Co-Author*) Nothing to Disclose Eugen Boltshauser, MD, Zurich, Switzerland (*Abstract Co-Author*) Nothing to Disclose Marjolein H. Dremmen, MD, Rotterdam, Netherlands (*Abstract Co-Author*) Nothing to Disclose

### **TEACHING POINTS**

•To provide a classification of organic acidemias and aminoacidopathies.•To recognize key clinical symptoms/findings that may point out specific organic acidemias and aminoacidopathies•To identify conventional and advanced (e.g. DWI/DTI, MRS) neuroimaging findings of organic acidemias and aminoacidopathies.•To establish a neuroimaging-based pattern recognition approach to help the diagnosis of organic acidemias and aminoacidopathies in children.

## TABLE OF CONTENTS/OUTLINE

•Classification of organic acidemias and aminoacidopathies in children.•Characterization of organic acidemias and aminoacidopathies in children based on 1) age at presentation and 2) clinical features. We will 1) classify the diseases based on neonatal, early infantile, late infantile, and juvenile presentation and 2) highlight specific clinical symptoms/findings that may point out a particular organic acidemia or aminoacidopathy.•Review of neuroimaging findings. We will review/illustrate conventional and advanced (e.g. DWI/DTI, MRS) neuroimaging findings of the diseases.•Neuroimaging-based pattern-recognition approach. We will propose a neuroimaging-based pattern-recognition approach that should help the diagnosis of organic acidemias and aminoacidopathies in children.•Take-home messages.

Low Dose CT-guided 3D-printed Models for the Diagnosis and Management of Double Outlet Right Ventricle

Tuesday, Nov. 29 12:15PM - 12:45PM Room: PD Community, Learning Center Station #7

#### Participants

Li Wei Hu, DIPLENG, MENG, Pudong, China (*Presenter*) Nothing to Disclose Ai-Min Sun, MD, Shanghai, China (*Abstract Co-Author*) Nothing to Disclose Qian Wang, Shanghai, China (*Abstract Co-Author*) Nothing to Disclose Haisheng Qiu, Shanghai, China (*Abstract Co-Author*) Nothing to Disclose Yumin Zhong, MD, Shanghai, China (*Abstract Co-Author*) Nothing to Disclose

## **TEACHING POINTS**

Present low dose cardiac CT protocol for diagnosing DORV Illustrate how to print 3D cardiac models under CT Discuss how to use models to classify DORV Concept of 3D-printing for designing surgical planning

## **TABLE OF CONTENTS/OUTLINE**

1.Low dose cardiac CT for children <10kg Prospective-triggering, 80ms padding 80kVp, 100-150mA2.Build 3D printed cardiac models in DORV Segment cardiac CT DICOM image in region growing Take post-processing procedures and create surface models Export and print the models3.Illustrate DORV in 3D printed models Case 1: with complex congenital heart disease (CHD) of DORV(S,D,D), doubly committed VSD and coarctation of aorta(COA) Case 2:with complex CHD of DORV(S,D,D), remote VSD and atrial septal defect Case 3: with cardiac malformation of DORV(S,D,D), subpulmonary VSD and COA4.Provide individualized surgical planning with anatomical navigation of DORV Case 1: Intraventricular tunnel repair Case 2: Pulmonary artery banding Case 3: Switch operationSummery3D printing technology has applied recently in diagnosis and management of congenital heart disease. The DICOM images of low dose CT cardiac scan can accurately construct 3D printed models. it is helpful for developing surgical procedures according to different types of DORV based on 3D-printed model. Not Every Pediatric Gastric Mass is a Stromal Tumor! A Pictorial Essay of Common and Uncommon Gastric Lesions Found in Pediatric Population

Tuesday, Nov. 29 12:15PM - 12:45PM Room: PD Community, Learning Center Station #8

## Participants

Alexia Dabadie, MD, Vancouver, BC (*Presenter*) Nothing to Disclose Helen R. Nadel, MD, Vancouver, BC (*Abstract Co-Author*) Nothing to Disclose Heather J. Bray, MD, Vancouver, BC (*Abstract Co-Author*) Nothing to Disclose

# **TEACHING POINTS**

To describe and review the radiological features of common and uncommon gastric lesions in children To discuss the combined radiological/nuclear medicine strategy used to investigate a pediatric patient presenting with gastric mass

# TABLE OF CONTENTS/OUTLINE

Review of common and uncommon gastric lesions found in children, using cases examples, with description of their corresponding epidemiological data Imaging description of each case, and correlation with endoscopic, operative and pathological findings when available Discussion of the utility and limitations of imaging modalities for each diagnosis, including US, upper GI, CT scan, MRI and PET-CT Discussion of the radiological strategy that should be offered when dealing with a pediatric gastric mass

Optimal Method of Contrast-enhanced CT for Children with Congenital Heart Disease after Fontan Operation

Tuesday, Nov. 29 12:15PM - 12:45PM Room: PD Community, Learning Center Station #5

#### Participants

Motoo Nakagawa, MD, Nagoya, Japan (*Presenter*) Nothing to Disclose Yoshiyuki Ozawa, MD, PhD, Nagoya, Japan (*Abstract Co-Author*) Nothing to Disclose Yuta Shibamoto, MD, PhD, Nagoya, Japan (*Abstract Co-Author*) Nothing to Disclose

## PURPOSE

Children with congenital heart disease (CHD) after Fontan operation need follow-up with contrast-enhanced CT because complications such as occlusion of conduits and systemic venous to pulmonary venous collaterals (V-V collaterals) can occur. However, CT protocol should be refined not to deliver excessive radiation doses. The purpose of this study is to optimize contrast-enhanced CT protocol for children after Fontan operation.

## METHOD AND MATERIALS

Between Nov. 2013 and Jan. 2016, 23 patients with CHD after Fontan operation (aged 2 to 10 years, median 5 years) were analyzed using dual source CT with ECG-triggered high-pitch spiral acquisition (Flash Spiral Cardio mode). CT scans were performed at 80 kV. The tube current was adjusted using automodulation. A non-iodinated contrast medium (300 mgI/ml, 2 ml/kg, body weight x 0.1 ml/sec) was injected through the dorsum manus vein. Scanning was began at 20 sec after non-iodinated contrast medium injection started and thereafter a delayed phase scan was obtained. Start of the delayed phase was randomly chosen to be 60 sec in 14 cases or 70 sec in 9 cases. We evaluated 1) enhancement of conduits of Fontan operation at delayed phases of 60 or 70 sec and 2) detectability of the V-V collateral in image findings of the early phase (20 sec). For evaluating enhancement of conduits, a region of interest was placed on conduits and CT values of 60- and 70-sec images were measured. We compared these CT values and evaluated whether conduits were enhanced homogeneously or heterogeneously.

## RESULTS

Enhancement of conduits at 60 and 70 sec were  $185\pm46$  H.U. and  $161\pm33$  H.U., respectively. Enhancement of conduits were homogeneous in 12/14 (86%) and 9/9 (100%) for the 60-sec and 70-sec groups, respectively. 2) In the early phase, CT image revealed a V-V collateral in 5/23 (22%) children after Fontan operation. These V-V collaterals were more clearly depicted in the early phase than in the delayed phase.

## CONCLUSION

For contrast-enhanced CT for children after Fontan operation, both of the delayed phases (60 sec and 70 sec) were optimal for evaluation of intra-conduit patency. The early phase is also useful for detecting V-V collaterals in children after Fontan operation.

### **CLINICAL RELEVANCE/APPLICATION**

This study revealed optimal scan delay time for evaluating patency of Fontan conduit and detecting V-V shunt. Therefore, we can prevent excess irradiation for failure of CT scan for children after Fontan operation.

# PH009-EB-TUA

## Characteristic CT Value Changes in Postmortem Brain Analyzed by Statistical Parametric Mapping

Tuesday, Nov. 29 12:15PM - 12:45PM Room: PH Community, Learning Center Hardcopy Backboard

#### Participants

Yuichi Nishiyama, PhD, RT, Izumo, Japan (*Presenter*) Nothing to Disclose Hiroshi Mori, Izumo, Japan (*Abstract Co-Author*) Nothing to Disclose Keiji Tada, Izumo, Japan (*Abstract Co-Author*) Nothing to Disclose Hidekazu Kanayama, Izumo, Japan (*Abstract Co-Author*) Nothing to Disclose Yasushi Yamamoto, Izumo, Japan (*Abstract Co-Author*) Nothing to Disclose Kazunori Kawakami, Tokyo, Japan (*Abstract Co-Author*) Nothing to Disclose Kazunori Kawakami, Tokyo, Japan (*Abstract Co-Author*) Employee, FUJIFILM Holdings Corporation Takashi Katsube, Izumo, Japan (*Abstract Co-Author*) Nothing to Disclose Haruo Takeshita, Izumo, Japan (*Abstract Co-Author*) Nothing to Disclose Hajime Kitagaki, MD, Izumo, Japan (*Abstract Co-Author*) Nothing to Disclose

## Background

Understanding the characteristics of postmortem changes is necessary in the forensic investigation using imaging modalities. Measurement of CT value in manually defined regions of interest is a standard method to examine postmortem changes on brain CT image. However, it requires great effort and time for the entire brain assessment of the CT value changes. The aim of this study was to investigate postmortem changes in the entire brain by voxel-based image analysis with statistical parametric mapping (SPM) technique.

## **Evaluation**

A total of 2073 cases of unenhanced postmortem CT were performed from Jun 2011 to March 2016 at our hospital. This retrospective study included 128 deceased patients (male/female ratio: 72/53, mean age: 72.4 years old) without cerebral abnormality for assessing postmortem changes in the brain. They received postmortem CT within 450 min after death. Their antemortem and postmortem brain CT images were spatially normalized using the CT template image that was constructed from 130 unenhanced brain CT images from living patients (male/female ratio: 67/63, mean age: 69.1 years old). Voxel values of the postmortem CT images were then compared with those of the antemortem CT images using a SPM8 software (Wellcome Trust Centre for Neuroimaging, University College London, UK).

#### Discussion

Cortical gray matter (GM) showed a rapid decrease of CT values within 70 min after death, indicating cytotoxic edema of GM cells. White matter (WM), basal ganglia, and thalamus showed a delayed increase of CT values in later than 120 min after death, which was different from general findings in acute cerebral infarction. The increased CT value in WM may depend on hypoxic circulation in agonal stage. Accumulation of metal substances may partly explain the increased CT value in basal ganglia and thalamus.

## CONCLUSION

SPM technique demonstrated that unclear GM-WM interface on early postmortem brain CT was caused by the rapid decrease of CT value in cortical GM and the delayed increase of CT value in WM. There may be different change between postmortem brain and brain infarction in less than 7 hours.

### FIGURE

mi;1/27i;1/22i;1/2gi;1/2

Reduction of Coronary Motion Artifact in Monochromatic Imaging at Various Energy Levels using a Motion Correction Algorithm in Electrocardiography-gated Single-source Dual-energy Coronary CT with Fast kVp Switching: Phantom Experiment

Tuesday, Nov. 29 12:15PM - 12:45PM Room: PH Community, Learning Center Station #3

### Participants

Rika Fukui, Tokyo, Japan (*Abstract Co-Author*) Nothing to Disclose Haruhiko Machida, MD, Tokyo, Japan (*Abstract Co-Author*) Nothing to Disclose Yuzo Yamamoto, Tokyo, Japan (*Presenter*) Nothing to Disclose Isao Tanaka, Tokyo, Japan (*Abstract Co-Author*) Nothing to Disclose Yun Shen, PhD, Beijing, China (*Abstract Co-Author*) Employee, General Electric Company Researcher, General Electric Company Eiko Ueno, MD, Chiyoda-Ku, Japan (*Abstract Co-Author*) Nothing to Disclose Xiao Zhu Lin, MD, Shanghai, China (*Abstract Co-Author*) Nothing to Disclose

### PURPOSE

To assess in a phantom the reduction in coronary motion artifact in monochromatic imaging (MI) at various energy levels using a motion correction algorithm (MCA) in ECG-gated single-source dual-energy coronary computed tomography with fast kVp switching (DECCT)

### **METHOD AND MATERIALS**

We performed DECCT scan with and without the MCA (SnapShot Freeze; GE Healthcare) of a phantom model of coronary artery branching (PFCP-1; FUYO Corporation) filled with iodine contrast medium and pulsating at 40 to 100 bpm at 10-bpm intervals, reconstructed MI at 50 to 90 keV at 10-keV intervals using an algorithm blending 40% adaptive statistical iterative reconstruction with 60% filtered back projection. Three readers independently graded coronary motion artifact in 9 segments of the coronary models from one (poor) to 5 (excellent) (3 to 5, interpretable), and we compared grades obtained with and without the MCA using Wilcoxon signed-rank test.

## RESULTS

Grades of coronary motion artifact at 70 bpm were  $3.4 \pm 1.4$  without the MCA (and  $4.1 \pm 0.9$  with the MCA) at 50 keV,  $3.4 \pm 1.4$  ( $4.0 \pm 0.9$ ) at 60 keV,  $3.4 \pm 1.5$  ( $4.0 \pm 0.9$ ) at 70 keV,  $3.2 \pm 1.5$  ( $3.1 \pm 1.2$ ) at 80 keV, and  $3.0 \pm 1.3$  ( $2.8 \pm 1.3$ ) at 90 keV. At 50 to 70 keV, the grades were significantly better with the MCA (P < 0.05 for all); its use significantly reduced the artifact in MI at 50 to 70 keV and at 40 to 60 and 80 to 100 bpm (P < 0.05 for all). At 70 bpm, 67% (6 segments) of segments were interpretable at 50 to 90 keV without the MCA, and 100% (9) at 50 to 70 keV and 67% (6) at 80 to 90 keV were interpretable with the MCA.

## CONCLUSION

MI at lower energy levels is useful for reducing coronary motion artifact using the MCA in DECCT.

### **CLINICAL RELEVANCE/APPLICATION**

Use of MI at lower energy levels can reduce coronary motion artifacts with the MCA in DECCT even with low image contrast from reduced contrast medium dose or cardiac function.

Four New Microbubble Formulations and their Subharmonic Response Compared to Three Commercially Available Ultrasound Contrast Agents

Tuesday, Nov. 29 12:15PM - 12:45PM Room: PH Community, Learning Center Station #4

**FDA** Discussions may include off-label uses.

### **Participants**

Amanda Q. Nio, Philadelphia, PA (*Abstract Co-Author*) Nothing to Disclose Cara Esposito, Philadelphia, PA (*Abstract Co-Author*) Nothing to Disclose Jie Chen, MD, Philadelphia, PA (*Abstract Co-Author*) Nothing to Disclose Flemming Forsberg, PhD, Philadelphia, PA (*Abstract Co-Author*) Equipment support, Toshiba Corporation; Research Grant, Toshiba Corporation; Equipment support, Siemens AG; In-kind support, General Electric Company; In-kind support, Lantheus Medical Imaging, Inc Ji-Bin Liu, MD, Philadelphia, PA (*Abstract Co-Author*) Nothing to Disclose Jaydev K. Dave, PhD, MS, Philadelphia, PA (*Presenter*) Nothing to Disclose Jie Zhang, Tianjin, China (*Abstract Co-Author*) Nothing to Disclose Xing Zhong, MD, PhD, Wynnewood, PA (*Abstract Co-Author*) Nothing to Disclose Renfa Liu, Beijing, China (*Abstract Co-Author*) Nothing to Disclose

Jin Rui Wang, MD, Beijing, China (*Abstract Co-Author*) Nothing to Disclose

Zhifei Dai, Beijing, China (Abstract Co-Author) Nothing to Disclose

#### Ziniel Dai, Deijing, Cinina (ADStract CO-Author) Nothing to

## PURPOSE

Characterizing the subharmonic response of contrast microbubbles is useful for subharmonic imaging (SHI), especially because lack of subharmonic signal generation in tissues leads to increased contrast to tissue ratio. The purpose of this work was to evaluate the subharmonic response of four new microbubble formulations relative to three commercially available ultrasound contrast agents.

## **METHOD AND MATERIALS**

The 3 commercial ultrasound contrast agents used in this study were Definity (Lantheus Medical Imaging, MA, USA), Sonazoid (GE Healthcare, Oslo, Norway) and SonoVue (Bracco, Milan, Italy). The 4 new microbubble formulations consisted of different configurations of the phospholipid shells (comprised of polyethylene glycol 4000) with different solid weights per vial (25 and 50 mg), different gas compositions (perfluoropropane or a mixture of perfluoropropane and nitrogen) and different microbubble concentration (1.4 to 3.4 billion microbubbles/ml). Equal concentrations of each contrast agent were tested in vitro using a SonixTablet (Analogic Ultrasound, MA, USA) ultrasound scanner and an SA4-2 transducer at four acoustic pressure levels (25-100%) for four transmit frequencies (2.5-4.0 MHz) and four pulse inversion configurations. The pulse repetition frequency was set at 1000 Hz. Acquisitions were repeated (n = 3; each iteration for 5 s). Subharmonic amplitudes were extracted as the mean signal amplitude in a 0.5 MHz bandwidth around the theoretical subharmonic frequency and averaged over the acquired pulses. Subharmonic enhancement over baseline (no contrast) conditions and the effect of different parameters were compared.

#### RESULTS

The subharmonic enhancement for Sonazoid, Definity and SonoVue was  $10.8 \pm 3.2 \text{ dB}$ ,  $4.8 \pm 3.3 \text{ dB}$  and  $9.7 \pm 3.5 \text{ dB}$ , respectively whereas it ranged from  $8.9 \pm 3.7 \text{ dB}$  to  $11.5 \pm 6.5 \text{ dB}$  for the 4 new microbubble formulations. ANOVA revealed a significant effect of the 3 transmit parameters as well as the interaction terms on the subharmonic amplitude of the agents used in this study (p < 0.05); this effect was dominated by the acoustic pressure parameter.

### CONCLUSION

Subharmonic response of the 4 new microbubbles formulations was similar to the commercial ultrasound contrast agents.

## **CLINICAL RELEVANCE/APPLICATION**

Contrast enhanced ultrasound (CEUS) imaging is expanding and amongst the CEUS modes, subharmonic imaging provides a relatively high contrast to tissue ratio and exclusive view of the vasculature.

## Effective Radiation Dose of Perfusion CT Exams of Ovarian Cancer Patients: A Multi-center Study

Tuesday, Nov. 29 12:15PM - 12:45PM Room: PH Community, Learning Center Station #5

#### **Participants**

Ting-Yim Lee, MSc, PhD, London, ON (*Presenter*) License agreement, General Electric Company Kyle Burgers, BEng, London, ON (*Abstract Co-Author*) Nothing to Disclose Chaan Ng, MD, Houston, TX (*Abstract Co-Author*) Nothing to Disclose Zheng Zhang, PhD, Providence, RI (*Abstract Co-Author*) Nothing to Disclose Robert Coleman, MD, Houston, TX (*Abstract Co-Author*) Nothing to Disclose Robert Mannel, MD, OKlahoma City, OK (*Abstract Co-Author*) Nothing to Disclose Mark A. Rosen, MD, PhD, Philadelphia, PA (*Abstract Co-Author*) Nothing to Disclose Susanna I. Lee, MD, PhD, Boston, MA (*Abstract Co-Author*) Nothing to Disclose

## CONCLUSION

Perfusion CT is a feasible clinical technique in terms of radiation dose for monitoring chemotherapy outcome in ovarian cancer.

### Background

ACRIN-6695/GOG-262 demonstrated that perfusion CT could serve as a quantitative biomarker of patient outcome in ovarian cancer chemotherapy. This study aims to determine the effective dose (ED) of radiation from the perfusion CT examinations on the patient cohort.

#### **Evaluation**

Materials and MethodsFIGO stage III or IV epithelial ovarian cancer patients underwent perfusion CT exams before (T0) and at 3-(T1) and 4-weeks (T2) after chemotherapy initiation. Scanning protocol involved a noncontrast scan for target lesion localization followed by a two-phased dynamic contrast enhanced scan through the target lesion (i.e. 24 images at 2.8 s intervals, then a 8 images at 15 s intervals acquired at 120 kV and 50 mAs). Scanner accreditation required central review of water phantom images. ED estimates were derived from the DLP (dose length product) using a conversion coefficient for an adult abdominopelvic scan at 120kV. Result228 perfusion CT exams were performed on 76 patients at 19 centers on six different scanner types. Dose data was submitted on 225 exams. 174, 36 and 15 exams from vendors 1, 2 and 3 were represented. Average ED (range) and axial coverage (range) for localizer and dynamic contrast were 6.5 (0.9-28.2) mSv and 316 (110-520) mm and 14.5 (4.9-29.9) mSv and 62 (24-120) mm respectively. The average CTDIvol±standard deviation of the dynamic phase were 129.1±11.8 mGy, 108.0±7.0 mGy and 255.3±120.0 mGy for vendors 1, 2 and 3 respectively (p<0.001).

#### Discussion

ED from perfusion CT exams was below the 50mSv recommended but demonstrated seven-fold variability. Most of this is attributable to axial coverage differences. Average ED of the dynamic contrast scan normalized to axial target lesion coverage  $\pm$  standard deviation were 2.2 $\pm$ 0.6 mSv/cm, 1.9 $\pm$ 0.3 mSv/cm and 3.6 $\pm$ 1.8 mSv/cm for vendors 1, 2 and 3 respectively (p<0.001).

#### **Honored Educators**

Presenters or authors on this event have been recognized as RSNA Honored Educators for participating in multiple qualifying educational activities. Honored Educators are invested in furthering the profession of radiology by delivering high-quality educational content in their field of study. Learn how you can become an honored educator by visiting the website at: https://www.rsna.org/Honored-Educator-Award/

Susanna I. Lee, MD, PhD - 2013 Honored Educator

## PH233-SD-TUA6

Application of 80kV Combined with Adaptive Statistical Iterative Reconstruction Technique in Low Doselumber CT Examination

Tuesday, Nov. 29 12:15PM - 12:45PM Room: PH Community, Learning Center Station #6

## Participants

Fei Fu, Tianjin, China (Presenter) Nothing to Disclose

### PURPOSE

To assess radiation dose reduction and image quality for lumber CT examination with 80kV combined with adaptive statistical iterative reconstruction (ASiR) technique, compared to a standard 120 kV protocol.

### **METHOD AND MATERIALS**

60 patients who underwent lumber CT scan were randomly separated into two groups: conventional 120 kV group with tube current of 230mA (n=30) and 80kV low dose group with tube current of 230mA (n=30), 80kV group was reconstructed with FBP and 40%ASiR. Image noise and CT value of the L3 vertebral body center level and erector apinae were measured. Signal-to-noise ratio (SNR) and contrast-to-noise ratio (CNR) for vertebral body were calculated, according the formulas: SNR=CTver/SD and CNR= (CTver-CTmus)/SD. The volumetric CT dose index (CTDIvol) was recorded for each group. Subjective image quality was evaluated by two radiologists with a 5-point scale.

# RESULTS

Compared with the conventional 120 kV protocol, 80kV allowed for an overall average decrease of 72 % in CTDIvol (15.75 $\pm$ 0.08 mGy vs 4.40 $\pm$ 0.49 mGy, p<0.05). The CNR and SNR showed statistical difference between 120kV group, 80kV+FBP group and 80kV+ASiR group (CNR, 1.83 $\pm$ 0.58 vs 1.28 $\pm$ 0.37 vs 2.04 $\pm$ 0.84; SNR, 2.57 $\pm$ 0.58 vs 2.00 $\pm$ 0.46 vs 2.86 $\pm$ 0.90, both p<0.05), respectively. The image quality was rated higher in 80kV+ASiR group than other groups (3.57 $\pm$ 0.85 vs 3.07 $\pm$ 0.83 vs 4.14 $\pm$ 0.66, p< 0.05).

### CONCLUSION

80kV combination with 40%ASiR reduced radiation dose nearly by 72% than standard 120 kV protocol and provide better image quality in lumber CT examination.

## **CLINICAL RELEVANCE/APPLICATION**

80kV combination with 40%ASiR can reduced radiation dose significantly and provide better image quality, recommended in lumber CT examination.

## Quantitative Assessment of Lean Skeletal Muscle Hydration Using Water-Fat MRI

Tuesday, Nov. 29 12:15PM - 12:45PM Room: PH Community, Learning Center Station #7

#### **Participants**

Thobias Romu, Linkoping, Sweden (*Abstract Co-Author*) Stockholder, AMRA AB; Employee, AMRA AB Patrik Tunon, MSc, Linkoping, Sweden (*Abstract Co-Author*) Stockholder, AMRA AB Fredrik Uhlin, RN, Linkoping, Sweden (*Abstract Co-Author*) Nothing to Disclose Micael Gylling, RN, Linkoping, Sweden (*Abstract Co-Author*) Nothing to Disclose Anders Fernstrom, MD,PhD, Linkoping, Sweden (*Abstract Co-Author*) Nothing to Disclose Marten Segelmark, MD,PhD, Linkoping, Sweden (*Abstract Co-Author*) Nothing to Disclose Olof Dahlqvist Leinhard, PhD, Linkoping, Sweden (*Presenter*) Stockholder, AMRA AB; Employee, AMRA AB

### PURPOSE

To investigate if the hydration of lean muscle tissue can be measured using water-fat MRI.

### **METHOD AND MATERIALS**

Water-fat MRI tissue composition can be described by a three compartment model, i.e. water, fat and MR-invisible tissue. The water intensity (*W*) is proportional to the water proton density (PD) and fat (*F*) to the lipid PD. If a compartment's fat content is known and invisible volume is constant, then W and lean tissue volume should be proportional to the hydration. It should thus be possible to determine the hydration level of a lean tissue based on *W*.11 hemodialysis patients were recruited, whole-body T2\* and lipid spectra compensated water-fat MRI images were collected pre/post dialysis. The net fluid drawn (NFD), i.e. machine setting compensated for tubular dead space and ingestion, was logged. Images were acquired on a Philips Ingenia 3T with 10 axial 3D Spoiled GRE stack with alpha=10, TE=1.15, 2.3, 3.35, 4.6 ms, TR 5.8 ms, FOV 340x560 mm2, voxel size 2.5x2.5x4 mm3.Leg and abdominal muscles were segmented automatically (Karlsson, jMRI 2015). *W* and *F* were calibrated using adipose tissue (AT) as an intensity reference (Romu, ISBI 2011), so *F* becomes the AT concentration and *W* is related to the PD of lipids in AT. Based on the average *W* of muscle tissue a hydration ratio H = W/(t\*g) was computed; t=1+(f-fn) compensates for the hydration of AT, *f* is the AT factions (*F*/(*F*+*W*)) of the patient and fn the normal value; g=k\*F+m compensates for fat infiltration, *F* is the average muscle AT concentration, *m* and *k* is beyond the scope of this study, *fn=0.95*, *k=-0.6* and *m=0.65* was used. The lean muscle volume (V) and muscle *H* differences was measured pre/post, and tested by paired T-tests.

### RESULTS

Mean delta-V was -0.38 L (p<0.001), delta-H -0.015 (p=0.015) and NFD was -1.87 L. The correlation delta-V vs NFD was 0.84, and delta-H vs NFD was 0.85.

## CONCLUSION

As hypothesized, both V and H decreased when the hydration was lowered through dialysis. To infer over/under hydration further work is needed. However, H strongly correlates with hydration.

### **CLINICAL RELEVANCE/APPLICATION**

Potentially regional tissue hydration can be of interest in, 1) treatment of renal disease and congestive heart failure, 2) measuring functional muscle volume by eliminating the effect of swelling.

# Development and Clinical Translation of the "Level Check" Algorithm for Decision Support in Spine Surgery

Tuesday, Nov. 29 12:15PM - 12:45PM Room: PH Community, Learning Center Station #8

#### **Participants**

Tharindu De Silva, Baltimore, MD (*Presenter*) Nothing to Disclose Ali Uneri, Baltimore, MD (*Abstract Co-Author*) Nothing to Disclose Michael Ketcha, Baltimore, MD (*Abstract Co-Author*) Nothing to Disclose Sureerat Reaungamornrat, Baltimore, MD (*Abstract Co-Author*) Nothing to Disclose Joseph Goerres, Baltimore, MD (*Abstract Co-Author*) Nothing to Disclose Sebastian Vogt, PhD, Monument, CO (*Abstract Co-Author*) Employee, Siemens AG Gerhard Kleinszig, Salzburg, Austria (*Abstract Co-Author*) Employee, Siemens AG Jean-Paul Wolinsky, Baltimore, MD (*Abstract Co-Author*) Nothing to Disclose Jeffrey H. Siewerdsen, PhD, Baltimore, MD (*Abstract Co-Author*) Research Grant, Siemens AG; Research Grant, Carestream Health, Inc; Advisory Board, Siemens AG; Advisory Board, Carestream Health, Inc; License agreement, Carestream Health,Inc; License agreement, Elekta AB; ; ;

## PURPOSE

A 3D2D image registration framework for automatic labelling of vertebrae on intraoperative radiographs ("LevelCheck") is under development for translation to clinical use for decision support in spine surgery. This work describes key advances that improve robustness, accommodate deformation, and allow CT-to-radiograph or MR-to-radiograph registration.

# METHOD AND MATERIALS

The registration transforms vertebral labels defined in preoperative CT or MR to intraoperative radiographs via gradient-orientation (GO) similarity and CMA-ES optimization. Robustness of GO was evaluated in clinical images with strong content mismatch. For cases involving preoperative MRI, forward projection involves a simple automatic vertebrae segmentation and the performance for both 3D modalities was evaluated in images from 51 patients. To improve accuracy in the presence of spinal deformation, a multistage, locally-rigid, globally-deformable process was implemented in which the registration narrows from N levels to single-level about each vertebrae in parallel. Finally, the clinical utility of the LevelCheck algorithm was evaluated by 3 spine surgeons using a large retrospective study of 398 radiographs from 198 patients.

### RESULTS

GO similarity was shown to outperform other gradient-based metrics, achieving geometric accuracy of  $5.5 \pm 2.6$  mm (median  $\pm$  iqr). Registration based on preoperative MRI also demonstrated robust performance with accuracy =  $4.0 \pm 1.9$  mm and with 100% success rate. In cases demonstrating strong changes in spinal curvature, the multi-stage framework improved accuracy to  $3.0 \pm 3.8$  mm. Assessment of utility in retrospective review by spine surgeons showed that LevelCheck was "helpful" to the decision process in 42.2% of cases (168/398), and improved confidence in 30.6% of cases (122/398). In no case did the algorithm diminish performance (0/398), supporting its potential as a means of independent check for decision support.

## CONCLUSION

The LevelCheck framework has been extended to include more robust similarity metric, operate on preoperative CT or MR, and accommodate spinal deformation. These findings support translation to prospective clinical studies to further evaluate benefits to surgical workflow.

### **CLINICAL RELEVANCE/APPLICATION**

An algorithm for automatic vertebrae labelling in radiographs could provide valuable decision support in target localization and present a potentially useful means against wrong-level spine surgery.

## QS013-EB-TUA

## Reducing the Time to Upload Outside Images into PACS in a Radiology Department

Tuesday, Nov. 29 12:15PM - 12:45PM Room: QS Community, Learning Center Hardcopy Backboard

#### **Participants**

Laurie A. Perry, RN, Cincinnati, OH (*Abstract Co-Author*) Nothing to Disclose Timothy OConnor, MBA, Cincinnati, OH (*Presenter*) Nothing to Disclose Elizabeth Ruemler, Cincinnati, OH (*Abstract Co-Author*) Nothing to Disclose Anthony Lyttle, Cincinnati, OH (*Abstract Co-Author*) Nothing to Disclose Sarah O'Brien, Cincinnati, OH (*Abstract Co-Author*) Nothing to Disclose David Hulefeld, Cincinnati, OH (*Abstract Co-Author*) Nothing to Disclose Keith Mills, Cincinnati, OH (*Abstract Co-Author*) Nothing to Disclose John Holcomb, Cincinnati, OH (*Abstract Co-Author*) Nothing to Disclose Alex Towbin, MD, Cincinnati, OH (*Abstract Co-Author*) Author, Reed Elsevier; Grant, Guerbet SA; Grant, Siemens AG;

## PURPOSE

Patients are referred to our facility from all over the US and the world often bringing with them prior imaging studies. The prior imaging studies help the care team understand the patient's medical and surgical history and may provide a baseline as well as a reference for new imaging to be performed. These outside studies are delivered to our department by patients and their families, referring hospitals and providers primarily on disc media such as CD or DVD. Each year we import more than 35,000 outside studies into our PACS. Our Health Information Management (HIM) department is typically responsible for collecting and uploading this data. This large amount of data has caused problems related to the backlog of disks waiting on upload and consequently, delays in the availability of imported images in the PACS where clinicians and radiologists use the images to care for the patient. In our project we sought to optimize the process of referring study ingestion in order to decrease the amount of time required to get studies into the PACS and available to physicians.

#### **METHODS**

We began our quality improvement project by assembling a multidisciplinary team involving all stakeholders of the disc upload process. We then collected baseline data on uploaded disks on a daily basis initially collecting data on 133 disks representing 1084 imaging studies. Hospital personnel responsible for dropping off discs to the HIM department filled out forms with the following required information: date/time of drop off, the department, the date/time the images were needed in PACS, along with other patient and contact data. As the discs were processed, the HIM staff augmented the data collected on the forms with additional information including: the number of disc media for the set, the completed upload date/time, and the staff member performing the upload. The disc intake forms were collected and verified on a daily basis. Each week new form data was entered into a spreadsheet where calculations produced the percentage of discs meeting their defined SLA and run charts were produced to visualize the data over time. As various process interventions were tried, the run charts allowed the team to see the effect of each those interventions toward the overall goal.

#### RESULTS

The baseline data indicated that 64% of the discs processed were loaded into PACS by the time listed as needed on the forms. Deeper analysis of the data indicated several issues which we addressed through a process of phased interventions.One of the early interventions we adopted was a re-organization of the disc intake process and the creation of defined service level agreements (SLA) for each disc set to be processed. Education of HIM staff on the SLA's allowed them to better organize their outstanding work items and process disks in a more efficient manner based on expected turnaround time. The SLA's also provided better communication to customers (departments and physicians requesting upload) on expected upload timeframes. An additional intervention restructured the physical disc intake area of HIM by relocating personnel to enable more efficient use of human resources. Another intervention implemented during the project was to transfer the task of uploading discs out of the HIM area and into the relevant clinical area. This was successfully implemented in one of our orthopedic clinics. Ortho technologists and medical assistants were trained on the use of the disc upload tool and how to complete the upload forms. This allowed them to collect the discs from the patient and begin upload while the patient was waiting to be seen for their appointment. To date, six different interventions have been tried with several being permanently adopted into the disc upload process. The percentage of discs uploaded within their defined SLA has increased from 64% to 98%. Data continues to be collected in order to track our progress and is used as part of personnel performance measures.

## CONCLUSION

Quality improvement techniques can be used to increase the percent of outside imaging studies uploaded in a timely manner. We believe that the changes we have made improve the satisfaction of our radiologists and hospital clinicians by providing additional clinical information at the time it is needed for patient care.

#### **Honored Educators**

Presenters or authors on this event have been recognized as RSNA Honored Educators for participating in multiple qualifying educational activities. Honored Educators are invested in furthering the profession of radiology by delivering high-quality educational content in their field of study. Learn how you can become an honored educator by visiting the website at: https://www.rsna.org/Honored-Educator-Award/

Alex Towbin, MD - 2014 Honored Educator

## QS014-EB-TUA

## Improving the Patient Experience in Breast Imaging by Using Lean Principles to Reduce Waste and Errors

Tuesday, Nov. 29 12:15PM - 12:45PM Room: QS Community, Learning Center Hardcopy Backboard

#### Awards

### **Quality Storyboard Award**

#### Participants

Lyn Webb, RT, ARRT, Rochester, MN (*Presenter*) Nothing to Disclose Royce Ruter, Rochester, MN (*Abstract Co-Author*) Nothing to Disclose Birgit Klinkhammer, Rochester, MN (*Abstract Co-Author*) Nothing to Disclose Linda M. Chida, BS, RT, Rochester, MN (*Abstract Co-Author*) Nothing to Disclose Ashley Rosier, Rochester, MN (*Abstract Co-Author*) Nothing to Disclose Kathleen R. Brandt, MD, Rochester, MN (*Abstract Co-Author*) Nothing to Disclose Bethanie Flattum, Rochester, MN (*Abstract Co-Author*) Nothing to Disclose Yvonne Biers, Rochester, MN (*Abstract Co-Author*) Nothing to Disclose Kim Reinsvold, Rochester, MN (*Abstract Co-Author*) Nothing to Disclose Laura Tibor, MBA, BEng, Rochester, MN (*Abstract Co-Author*) Nothing to Disclose Amy L. Conners, MD, Rochester, MN (*Abstract Co-Author*) Nothing to Disclose

### PURPOSE

Background: Radiology's Division of Breast Imaging and Intervention started a Lean journey empowering staff to improve patient experience. Since waiting is a significant source of patient dissatisfaction, the team's efforts focused on reducing wait time for screening mammogram patients. 63% of a screening mammogram patient's lead time was waiting/waste.Objectives: Decrease each screening mammogram patient's total lead time from 39 minutes to 29 minutes by implementing a subwaitless practice. Additional goals included reducing hand-offs, eliminating batching, improving communication via visual management, decreasing paperwork stacking errors, and improving patient satisfaction.

### **METHODS**

Methods: A multi-disciplinary team developed a value stream map (VSM) to analyze the screening mammogram practice which averages 150 patients per day. Using Lean principles, potential improvements were tested from August-November 2015. Nine Plan-Do-Study-Act (PDSA) cycles helped create an improved workflow while maintaining superb patient care. The previous workflow involved a Clinical Assistant batching patients from the main lobby to the subwait, having patients use changing booths, sit in subwait chairs, and finally being escorted to the mammogram room by a technologist. The new streamlined workflow uses a technologist to escort an individual patient directly from the lobby to the mammogram room to change and have their exam.

#### RESULTS

Results: Patient surveys and comments indicate remarkable satisfaction with the new workflow. The use of the subwait location was discontinued. We eliminated two hand-offs, reduced batching, minimized paperwork stacking errors, and decreased wait time by over 50%. Four months into implementation, average total screening mammogram lead time decreased from 39 minutes to 24 minutes.

### CONCLUSION

Conclusion: Utilizing Lean methodology in our screening mammogram practice, patient experience has improved while waste and errors were significantly reduced.

# Improving Patient Care by Effective Communication of PICC Line Placement

Tuesday, Nov. 29 12:15PM - 12:45PM Room: QS Community, Learning Center Hardcopy Backboard

### Participants

Ronald L. Eisenberg, MD, JD, Boston, MA (*Presenter*) Nothing to Disclose Benedikt H. Heidinger, MD, Boston, MA (*Abstract Co-Author*) Nothing to Disclose

### PURPOSE

To improve quality and rapidity of interpretations of PICC line placement with minimal disruption of work flow for chest radiologists and venous access nurses.

### **METHODS**

Patients and referring physicians need quick response times to document that PICC lines are positioned properly so that patients can be discharged home, to a nursing home/rehabilitation facility, or admitted to the hospital. At an initial meeting among the chest radiologists, radiology residents, and representative of the PICC team, no one was satisfied with the system in use for communicating this information. The procedure entailed multiple telephone calls - first by the technologist taking the radiograph to the radiologist, indicating that the PICC placement examination had been performed, and second by the radiologist to the PICC nurse describing the position of the tip. Frequently, the PICC nurse was doing another line placement and it was inconvenient to receive the information. This often required that the PICC nurse telephone the radiologist to obtain this information, disrupting the workflow in the radiology department. Three subsequent meetings were held in which a new procedure was developed and refined. There was agreement that the radiologist would immediately dictate and sign an interpretation for all PICC placements within 60 minutes (30 minutes, if possible), while the PICC nurse would consult the dictated reports and receive the information. Residents reading a PICC placement study would immediately consult with the attending radiologist so that a final report could be dictated promptly and signed. To speed up the process, members of the committee decided that a special code be used so that radiologists would recognize that a post-PICC placement examination had been performed and promptly report it. In addition, to meet the need for the PICC nurses to have a uniform method for describing PICC line placement, the radiologists developed a standard protocol which includes a description of the position of the tip of the PICC line (upper, middle, or lower superior vena cava) and precisely how far it is above or below the desired position at the cavoatrial junction.

### RESULTS

Prior to the intervention, there was a daily average of 15 telephone calls (range, 9-20) regarding PICC line placement. After the new process was in use, this number dropped to an average of less than 5 per week. During regular work hours, all PICC placements were reported within the 60-minute time limit. At a follow-up meeting one month after implementation, all stakeholders (PICC nurses, radiology residents, and staff radiologists) reported that they were extremely pleased with the new procedure.

## CONCLUSION

Identifying cases of PICC placements, using a standard reporting protocol, and prioritizing interpretation of these studies resulted in a dramatic decrease in telephone calls that disrupted the workflow of both radiologists and PICC nurses. All parties agreed that the new procedure was a great success and ultimately led to improvements in patient care.

## **Honored Educators**

Presenters or authors on this event have been recognized as RSNA Honored Educators for participating in multiple qualifying educational activities. Honored Educators are invested in furthering the profession of radiology by delivering high-quality educational content in their field of study. Learn how you can become an honored educator by visiting the website at: https://www.rsna.org/Honored-Educator-Award/

Ronald L. Eisenberg, MD, JD - 2012 Honored Educator Ronald L. Eisenberg, MD, JD - 2014 Honored Educator Improving the Identification of Underserved Women at High Risk for Breast Cancer and Increasing the use of Breast MRI Screening in this Population

Tuesday, Nov. 29 12:15PM - 12:45PM Room: QS Community, Learning Center Station #1

## Participants

Heather I. Greenwood, MD, San Francisco, CA (*Presenter*) Nothing to Disclose Louise Truong, San Francisco, CA (*Abstract Co-Author*) Nothing to Disclose Elissa R. Price, MD, San Francisco, CA (*Abstract Co-Author*) Nothing to Disclose

### PURPOSE

Breast cancer risk assessment services and high risk screening breast MRI are underutilized resources at our county hospital. The purpose of this study was to increase the use of these services for our underserved patient population.

#### **METHODS**

We made two interventions to achieve our purposes. First, we no longer required patient's to fill out an additional questionnaire to be identified for referral to genetics. Several of the questions on this form were duplicates of an additional form, the San Francisco Mammography Registration (SFMR) form that each patient at our breast center is asked to fill out upon arrival. The patient therefore had one less form to fill out. Our genetic team tracked three months of data prior to (October 2015 to December 2015) and following this intervention. Second, upon discussion with referring providers we realized that several providers were not familiar with the indications for high risk screening MRI. Therefore, we provided basic teaching sessions for referring providers during which we went over the American Cancer Society's recommendations for which patient's met the criteria of being "high-risk" (>20-25% lifetime risk) for whom screening breast MRI is appropriate. Additionally we sent an e-mail with a document outlining these guidelines to our referring providers. Through our radiology IT system we collected three months of data on how many breast MRIs were performed prior to (October 2015 to December 2015) and after (January 2015 to March 2015) our intervention. We then determined the number of these that were performed for an indication of high-risk screening.

### RESULTS

In the three months prior to our intervention, October 2015 through December 2015, 609 patients filled out the additional form required to determine if they met criteria for genetic risk assessment; of these 50/609 (8%) met criteria to be contacted for an official genetic risk assessment. In the three months following our intervention 2,212 patients filled out the SFMR required form for consideration for genetic assessment; of these 134/2,212 (6%) met the criteria for genetic risk assessment. There was a 2.7 fold increase in the number of patients we identified for genetic risk assessment. In the three months following our intervention 8/16 (50%) of our breast MRIs were performed for an indication of high-risk screening. In the three months following our intervention, 14/25 (56%) of our breast MRIs were performed for-high risk screening.

# CONCLUSION

Breast cancer risk assessment coupled with high risk MR screening are essential resources for patients. These are readily available at our county hospital but underutilized. Simple interventions, including decreasing required paperwork patient's need to fill out and can increase the number of patients identified for formal breast cancer risk assessment. In addition basic teaching sessions for referring providers on which patients to refer for breast cancer screening MRI can increase the amount of patients appropriately identified for this exam. In the future, we will continue with our new method of identifying patient's for genetic risk assessment and continue to offer teaching sessions on high-risk breast MRI screening.

### QS117-ED-TUA2

Improvement in Clinical Decision Support Coverage and Reduction in "Unscored" Examination through a PDSA project

Tuesday, Nov. 29 12:15PM - 12:45PM Room: QS Community, Learning Center Station #2

## Participants

Maitraya K. Patel, MD, Sylmar, CA (*Presenter*) Nothing to Disclose John F. Brunner, MD, Los Angeles, CA (*Abstract Co-Author*) Nothing to Disclose Orest B. Boyko, MD, PhD, Los Angeles, CA (*Abstract Co-Author*) Speakers Bureau, Bracco Group; Speakers Bureau, Guerbet SA Jennifer Sayles, MD, Los Angeles, CA (*Abstract Co-Author*) Nothing to Disclose

## PURPOSE

A clinical decision support (CDS) platform that includes the American College of Radiology Appropriateness criteria was implemented at our institution for RF, CT, US, MR, NM and MG examinations. CDS requires providers answer 1-2 questions when ordering imaging studies, then assigns a score – usually not appropriate (Low, 1-3), may be appropriate (Medium, 4-6), and usually appropriate (High, 7-9). During this implementation, "hard stops" were not included in the decision support process. This resulted in many orders triggering decision support, yet remaining "unscored." A PDSA (Plan-Design-Study-Act) project was initiated analyzing these "unscored" orders and solutions implemented to reduce the number of unscored studies thus improving CDS "coverage."

#### **METHODS**

Exams triggering CDS were scored as follows: High (score 7-9), Medium (Score 4-6), Low (score 1-3). "Recommendation provided" was a category used when recommendations were provided by the software, but the provider chose a procedure that was not scored. "Unscored" examinations were those in which no CDS was able to be provided. "Coverage" was defined as the sum of (High + Medium + Low+ Recommendations provided + Cancelled exams) / Total orders. Unscored exams were a result of three causes -(1) "Custom indications" in which a provider entered an indication not included or selected from the CDS database, (2) "Logic gaps" were clinical indications without rules designed in CDS, commonly due to the fact that some American College of Radiology (ACR) Appropriateness Criteria do not provide recommendations for all variations of a given decision tree logic and (3) "Unanswered questions" due to some clinical indications allowing an optional element to question answering, which if unanswered resulted in no score. Periodic analysis was performed on CDS utilization from 8/7/2015 to 3/31/2016 to improve coverage of the software and reduce unscored exams. Custom indications were targeted by (1) development of an instructional video and reference card to the providers on proper utilization of the software, (2) identification of areas that would benefit from locally created consensus rules based on best-practice, or other available evidence-based guidelines (3) implementation of a user interface change with a "drop down" of the top indications chosen at our institution for the order selected, allowing the provider to simply "pick and click" instead of "type and search" and (4) utilizing provider incentives in locations where a Radiologist approval was required for an examination, particularly in the Emergency Department; if a provider selected exam resulted in a medium or high score, the exam would be automatically approved and the technologist would perform the exam. Logic gaps were targeted by creating decision support rules where ACR recommendations were not all encompassing for a given indication. Unanswered questions were not able to be modified, due to current limitations in the software. Finally, "Recommendations provided" was targeted by identifying procedures in the order catalog not currently mapped in CDS but equivalent to currently mapped exams, thus providing a score when these equivalent procedures were ordered.

### RESULTS

At baseline for the 90-day period prior to 8/7/2015 there were 25.7% "high" orders (n=7864), 3.8% "medium" orders (n=1174), 2.1% "low" orders (n=633), 0.2% canceled orders (n=51), 12% "recommendations provided" orders (n=3690), and 56.2% "unscored" orders (n=17208). Following the interventions, in the 90-day period prior to 3/31/2016, there were 52% "high" orders (n=47177), 9.6% "medium" orders (n=8724), 6.1% "low" orders (n=5580), 0.8% canceled orders (n=716), 9% "recommendations provided" orders (n=8453) and 22.2% "unscored" orders (n=20154). CDS coverage increased from 43.8% in 8/2015 to 77.5% in 3/2016. Order volumes increased during the observation period as additional facilities were brought onto the CDS platform.

## CONCLUSION

Through a PDSA process, we were able to improve coverage of CDS from 43.8% at baseline, to 76.7% at the end of the study period, through a reduction in unscored examinations from 56.2% at baseline to 22.2% at the end of the study period. Doing so improved the number of exams undergoing clinical decision support, providing appropriateness feedback to ordering providers at the time of order selection.

## Radiology Driving Change in Primary Care: The Diagnostic Imaging Appropriateness (DI-APP) Project

Tuesday, Nov. 29 12:15PM - 12:45PM Room: QS Community, Learning Center Station #3

#### **Participants**

Jisla Mathews, Toronto, ON (*Presenter*) Nothing to Disclose Karen Weiser, MBA, Toronto, ON (*Abstract Co-Author*) Nothing to Disclose Ravi Menezes, PhD, Toronto, ON (*Abstract Co-Author*) Nothing to Disclose Jennifer Catton, Toronto, ON (*Abstract Co-Author*) Nothing to Disclose Catherine Wang, BSc, Toronto, ON (*Abstract Co-Author*) Nothing to Disclose Amy W. Lin, MD, London, ON (*Abstract Co-Author*) Nothing to Disclose

# PURPOSE

Inappropriate diagnostic imaging (DI) can be defined as the use of imaging procedures when they have a small chance of affecting patient management. The negative system-level consequences of inappropriate DI referral include increased wait times and costs with no associated benefit for patients. While most referral guidelines aimed to reduce unnecessary imaging are directed at primary care providers (PCPs), few guidelines have been developed with their dedicated involvement. The DI Appropriateness (DI-APP) Project was launched by our imaging department in 2014 as a regional initiative, involving multidisciplinary panels led by PCPs, to develop pathways to guide imaging referral and promote evidence-based care for clinical scenarios that present commonly in primary care. The goals of the project were as follows: Align clinically relevant, evidence-based DI guidelines to develop imaging pathways for clinical scenarios that present commonly to primary care: headache, low back pain, transient ischemic attack (TIA) and knee pain Develop recommendations for implementation and sustainability to ensure tools can be adopted into primary care practice

## METHODS

**Pathway development process:** Four imaging pathways were developed by multidisciplinary panels of over 50 members that included PCPs, radiologists and specialists from urban, suburban and rural practice settings. Panels were led by PCPs to ensure applicability of the pathway format and content to their practice. The pathway development approach combined methodological rigor and current evidence with physicians' expertise. The process was informed by elements of the CAN-IMPLEMENT framework, a streamlined version of the ADAPTE methodology for guideline adaptation. Key steps included: Guideline screening and summarization Assessment of recommendations via online surveys and meetings Consensus building of the final pathway via modified Delphi technique**Development of implementation and sustainability recommendations:**Recommendations for implementation and sustainability of the pathways were developed by a separate panel comprising system leaders with experience in guideline development, clinical change management and/or successful implementation in the primary care setting, as well as a patient representative. Key steps included: Evaluation of impact and effort required for various implementation experiences **Pathway evaluation by PCPs:**PCPs who were not involved in pathway development were surveyed to assess face validity based on review of the pathways. Survey items focused on value and applicability of the pathways to the primary care setting and factors that may influence adoption of the pathways in primary care.

### RESULTS

**Pathway development results:**Using the consensus-based methodology, panel members successfully developed pathways for low back pain, headache, TIA/stroke and knee pain. Strong clinician engagement and multidisciplinary collaboration were key success factors. Clinician engagement via meeting attendance and survey response rates were consistently high, ranging from 70-90%. **Implementation and sustainability recommendations:** The advisory panel comprised close to 15 members. The panel recommended that enabling easy adoption of the pathways via implementation in multiple formats is crucial to making an impact on imaging referral practices. **Results of pathway evaluation by PCPs:** A group of 55 PCPs were surveyed to evaluate the pathways. More than 90% of respondents either agreed or strongly agreed that the pathway recommendations are relevant and applicable to their patient population. Close to 85% of PCPs either agreed or strongly agreed that the pathways could help facilitate communication with patients and 70% felt that the pathways could help change their practice. Survey results related to pathway adoption showed that more than 80% of PCPs supported integration of the pathways into electronic medical records. More than 70% of survey respondents indicated that supporting patient education materials, conversation tools, and endorsement by peers and professional bodies would be helpful. More than 60% of PCPs favored the integration of the pathways into a mobile application.

## CONCLUSION

Using a methodology based on the principles of guideline adaptation and obtaining consensus, four imaging pathways were developed to assist regional PCPs determine the most appropriate use of medical imaging. These pathways are expected to be applicable to the local practice setting and accurately reflect patient presentation in primary care. Based on feedback received from PCPs and the project's implementation and sustainability advisory panel, the next phase of work will focus on developing an IT tool for the pathways to be accessed by physicians at the point of care via smart phones, tablets and computers.

## QS119-ED-TUA4

A Clinical Decision Support Module Significantly Reduces Ambiguity in Reports of Nuclear Medicine Gastric Emptying Studies

Tuesday, Nov. 29 12:15PM - 12:45PM Room: QS Community, Learning Center Station #4

# Participants

Leslie K. Lee, MD, Boston, MA (*Presenter*) Nothing to Disclose David Z. Chow, MD, Cambridge, MA (*Abstract Co-Author*) Nothing to Disclose Edwin L. Palmer III, MD, Boston, MA (*Abstract Co-Author*) Nothing to Disclose James A. Scott, MD, Boston, MA (*Abstract Co-Author*) Nothing to Disclose Yingbing Wang, MD, Boston, MA (*Abstract Co-Author*) Nothing to Disclose

# PURPOSE

Nuclear medicine gastric emptying studies (GES) have accepted standards by which they are performed and reported. We sought to standardize and improve the quality of reporting of these studies at our academic medical center, by increasing the proportion reported as 'normal' or 'abnormal,' via the design and implementation of a clinical decision support (CDS) module to aid study interpretation.

### **METHODS**

We reviewed the reports of all GES from January 1, 2015 to August 14, 2015, prior to the implementation of a CDS module. Reports were characterized as to whether they conveyed a normal, abnormal, or ambiguous result. Studies with non-standard protocol or aborted studies were excluded. The divisional Quality Assurance committee was convened to design a CDS tool for adult GES, following published consensus guidelines. Standard text language was composed based on published guideline cutoff values of gastric emptying at 1, 2 and 4 hours post-ingestion of the standard test meal. A CDS module was designed accordingly; activation of the module at the time of study interpretation prompts the interpreting physician to input 1, 2 and 4-hour emptying values, to trigger the appropriate standard text output which is then inserted into the impression field of the GES report. After a two-week implementation period at the end of August 2015, we reviewed the reports of all GES from September 1, 2015 until March 31, 2016. Chi square test was used to assess the proportion of ambiguous studies pre- and post-CDS implementation.

#### RESULTS

Prior to implementation of the CDS module, the default template text in a GES report read, "Solid phase gastric emptying values as above." A total of 320 reports in the Pre-CDS period were reviewed; 25 non-standard studies were excluded. In the Pre-CDS period, normal, abnormal, and ambiguous reports numbered 0/295 (0%), 1/295 (0.3%), and 294/295 (99.7%), respectively. The CDS module was designed with standard text outputs such as "Gastric emptying study within normal limits," and "Abnormally delayed gastric emptying, as defined by emptying less than 90% at four hours." A total of 308 reports in the Post-CDS period were reviewed; 28 non-standard studies were excluded. In the Post-CDS period, normal, abnormal, and ambiguous reports numbered 196/280 (69.5%), 80/280 (28.4%), and 4/280 (1.4%), respectively. Comparing Pre- and Post-CDS periods, the proportion of ambiguous reports decreased from 99.7% (95% CI 97.9-100%) to 1.4% (95% CI 0.4-3.7%), p<0.001.

## CONCLUSION

A clinical decision support module, designed to aid interpretation of nuclear medicine gastric emptying studies, significantly decreased the rate of ambiguous reports from 99.7% to 1.4%.

A Pilot Study of a Novel Radiation Therapy Support Garment for Patients Undergoing Radiation following Lumpectomy for Breast Cancer

Tuesday, Nov. 29 12:15PM - 12:45PM Room: RO Community, Learning Center Station #5

### **Participants**

Alfred Tinger, MD, Yonkers, NY (Presenter) Nothing to Disclose

#### ABSTRACT

Purpose/Objective(s): It is well established that women with large breast size undergoing lumpectomy and radiation therapy (RT) are at increased risk for side effects due to the larger field size required. Pulmonary, cardiac and hepatic effects from RT can be reduced by limiting radiation exposure to these tissues. Short term morbidities caused by skin folds can lead to interruptions of the RT course, possibly compromising local outcomes. The purpose of this IRB-approved pilot study is to assess whether a novel garment ("Bra") for support of the breast during RT will reduce the exposure of non-target tissues, reduce RT side effects and improve quality of life (QOL). We report on the technical details of the Bra and preliminary results of the first 6 patients enrolled Materials/Methods: The patented Bra was developed and is manufactured by a U.S.-based company. Materials neither absorb radiation nor are they altered by it. It has adjustments in the shoulder, rear and lateral regions. Irritability, sensitivity, cytotoxicity tests, and Radiologic Test Reports have been completed and FDA 510K Clearance has been received. All patients in the study had a self-reported bra size of 36B or larger and were provided the Bra at no charge. All underwent lumpectomy for DCIS or invasive breast cancer and were scheduled for postoperative RT. Treatment plans were devised with and without the Bra and the various parameters were compared using paired t-tests. Physician and patient assessments of comfort, tolerance, QOL, and toxicity were performed throughout the treatment course and at first follow-up.Results: Patients received a mean RT dose of 48.0 Gy (range 45-50.4 Gy). The Bra was well tolerated by all 6 patients, and there were no garment-related adverse events. Based on dosimetric comparisons, the Bra reduced the global maximum field dose by a mean of 122.3 cGy, the global maximum breast dose by 45.7 cGy, and other parameters in a similar fashion (Table), although none of the comparisons reached statistical significance likely due to the small number of patients. Table Comparison of Dosimetric Parameters With vs Without the Bra Without BraWith Bra% Change Global maximum field (cGy)5874.985752.68-2.08 Global maximum breast (cGY)5743.675698.00-.80 V110%18.6310.30-44.77 Lung V5%22.4019.77-11.74 Lung V10%16.6714.64-12.18 Lung V20%13.0711.32-13.39 Heart V5%5.675.00-11.77 Heart V10%4.003.33-16.75 Heart V20%3.132.58-17.57 Lung mean dose (cGy)709.83631.67-11.01 Heart mean dose (cGy)233.67202.83-13.20 Liver mean dose (cGy)251.30240.67-4.23 Conclusion: The Bra resulted in a decrease in RT dose to non-target organs in this pilot study and was well-tolerated by the patients. With more patients and follow up, we will additionally be able to assess morbidity, QOL and cosmesis.

# UR122-ED-TUA7

CT Cystography: When to Do It, How to Do It, and What to Look for When Traumatic Urinary Bladder Injury is Suspected

Tuesday, Nov. 29 12:15PM - 12:45PM Room: GU/UR Community, Learning Center Station #7

# Awards

Cum Laude Identified for RadioGraphics

## Participants

Gayatri Joshi, MD, Atlanta, GA (*Abstract Co-Author*) Nothing to Disclose Eugene Y. Kim, MD, Saint Louis, MO (*Presenter*) Nothing to Disclose Tarek N. Hanna, MD, Atlanta, GA (*Abstract Co-Author*) Nothing to Disclose Christine O. Menias, MD, Chicago, IL (*Abstract Co-Author*) Nothing to Disclose Alexa O. Levey, MD, Atlanta, GA (*Abstract Co-Author*) Nothing to Disclose Cary L. Siegel, MD, Saint Louis, MO (*Abstract Co-Author*) Nothing to Disclose

### **TEACHING POINTS**

Discuss the indications for CT cystogram Review proper technique for CT cystogram Illustrate the spectrum of urinary bladder injury patterns as seen on CT cystography and briefly review commonly associated respective pelvic fracture patterns Demonstrate diagnostic pitfalls in evaluation of suspected urinary bladder injury

## TABLE OF CONTENTS/OUTLINE

This exhibit will review the indications and proper technique for CT cystography in the acute traumatic setting. The commonly used classification schemes of urinary bladder injury based on degree and location of injury will be discussed. Examples of each injury type will be illustrated by CT cystogram with fluoroscopic, radiographic, MRI, and operative correlates, using a case-based approach. Companion cases demonstrating pitfalls in diagnosis will accompany these core cases. Associated traumatic imaging findings, such as pelvic fracture patterns and trajectory of penetrating pelvic injuries, which have a high association with bladder injury will be reviewed. An understanding of the indications, appropriate technique, and spectrum of imaging findings is critical in the evaluation of suspected traumatic urinary bladder injury.

### **Honored Educators**

Presenters or authors on this event have been recognized as RSNA Honored Educators for participating in multiple qualifying educational activities. Honored Educators are invested in furthering the profession of radiology by delivering high-quality educational content in their field of study. Learn how you can become an honored educator by visiting the website at: https://www.rsna.org/Honored-Educator-Award/

Christine O. Menias, MD - 2013 Honored Educator Christine O. Menias, MD - 2014 Honored Educator Christine O. Menias, MD - 2015 Honored Educator Christine O. Menias, MD - 2016 Honored Educator

# CT Guided Cryoablation of Primary and Metastatic Lung Tumors: Low Recurrence and Complication Rates

Tuesday, Nov. 29 12:15PM - 12:45PM Room: VI Community, Learning Center Station #1

### **Participants**

Hussein D. Aoun, MD, Dearborn, MI (*Abstract Co-Author*) Nothing to Disclose
Peter J. Littrup, MD, Providence, RI (*Abstract Co-Author*) Founder, CryoMedix, LLC; Research Grant, Galil Medical Ltd; Research
Grant, Endo International plc; Consultant, Delphinus Medical Technologies, Inc
Hamza M. Beano, MD, Detroit, MI (*Presenter*) Nothing to Disclose
Mohamed M. Jaber, MD, Detroit, MI (*Abstract Co-Author*) Nothing to Disclose
Barbara A. Adam, MSN, Detroit, MI (*Abstract Co-Author*) Nothing to Disclose
Matthew Prus, BS, Detroit, MI (*Abstract Co-Author*) Nothing to Disclose
Mark J. Krycia, BS, Detroit, MI (*Abstract Co-Author*) Nothing to Disclose

### PURPOSE

To assess technical feasibility, efficacy and complication rates of CT guided cryoablation of lung tumors in multiple locations.

## **METHOD AND MATERIALS**

CT fluoroscopic-guided percutaneous cryoablation was performed in 277 procedures on 375 tumors (106 primary, 269 metastatic tumors) in 158 patients. Tumor and ablation volumes, location, abutting vessels >3mm, recurrences, and PFT's were reviewed for all patients. Complications were graded by the National Institutes of Health, Common Terminology of Complications and Adverse Events 4.0 (CTCAE).

# RESULTS

All procedures were performed with conscious sedation. Mean FEV1 and DLCO2 were 80.2 (32-145) and 69.5 (27-110), respectively. Overall tumor and ablation median size was 2.4 cm (0.5 - 12.3 cm) and 4.6 cm (1.7-12.8 cm), respectively. Total major complication rates were only 4.3% (12/277), however major complication rates were significantly lower in tumors  $\leq 3$  cm as opposed to  $\geq 3$ cm, 1.0% (2/194) vs. 12.0% (10/83) (p<0.001) No statistical significance was noted for major complications with central tumors or major vessel proximity. Recurrence rates of 8.3% (31/375) were not significantly affected by tumor size (<3cm or >3cm). Recurrence rates increased for central tumors near major vessels 13.5% (19/141) compared with peripheral tumors 5.1% (12/234) (p<0.005).

## CONCLUSION

CT guided percutaneous cryoablation in the lung provides a low morbidity alternative with superb efficacy. Complication rates are significantly lower for tumors <3cm and total complications were low.

### **CLINICAL RELEVANCE/APPLICATION**

Appropriately delivered thoracic cryoablation is affected by vessel location yet still produces low recurrence and complication rates.

Advantages of the Reduced Expansion Technique of Cisplatin-loaded Superabsorbent Polymer Microspheres for Chemoembolization in Rabbit VX2 Liver Tumors

Tuesday, Nov. 29 12:15PM - 12:45PM Room: VI Community, Learning Center Station #2

# Participants

Takeshi Sato, Kashihara, Japan (*Presenter*) Nothing to Disclose Toshihiro Tanaka, MD, Kashihara, Japan (*Abstract Co-Author*) Nothing to Disclose Hideyuki Nishiofuku, Kashihara, Japan (*Abstract Co-Author*) Nothing to Disclose Yasushi Fukuoka, Kashihara, Japan (*Abstract Co-Author*) Nothing to Disclose Tetsuya Masada, Kashihara, Japan (*Abstract Co-Author*) Nothing to Disclose Kimihiko Kichikawa, MD, Kashihara, Japan (*Abstract Co-Author*) Nothing to Disclose Shota Tatsumoto, Kashihara, Japan (*Abstract Co-Author*) Nothing to Disclose

### PURPOSE

Previously, it was revealed that superabsorbent polymer (SAP) microspheres could absorb and elute cisplatin. Cisplatin-loaded SAP microspheres mixed with nonionic contrast medium expand approximately 4 times larger than those original sizes in the dry stage. However, theoretically, smaller size of microspheres could be ideal for tumors with fine feeding arteries. Recently, it has been newly developed that adding 10 % NaCl could reduce the expansion of SAP by half. The purpose of this study is to evaluate the pharmacological and histological advantages of cisplatin-loaded SAP with the reduced expansion technique in a rabbit VX2 tumor model.

## METHOD AND MATERIALS

Eighteen rabbits with VX2 liver tumors were treated with cisplatin-loaded SAP. In the normal expansion group, 25 mg/vial Hepashpere was preloaded with 25 mg cisplatin dissolved in 5 mL of nonionic contrast medium. In the reduced expansion group, 4 mL of nonionic contrast medium and 1 mL of 10 % NaCl. In both groups, cisplatin-loaded SAP suspension was injected into the left hepatic artery until stasis of hepatic arterial flow was achieved. All rabbits were sacrificed at 1 (n=3), 24 (n=3), and 72 (n=3) hours after administration of cisplatin. The concentrations of platinum in the tumor tissue and the histopathological findings were analyzed.

## RESULTS

The mean diameters of cisplatin-loaded SAP with the normal technique and the reduced expansion technique were 377 and 200  $\mu$ m, respectively. The mean platinum concentrations in VX2 tumor at 1, 24 and 72 hours were 1.57, 3.76 and 0.73  $\mu$ g/g, respectively, in the normal expansion group; and 10.76, 4.85 and 2.79  $\mu$ g/g, respectively, in the reduced expansion group. The tumor platinum concentrations of the reduced expansion group at 1 hour was significantly higher than the concentrations of the normal expansion group (P = .044). Histopathological findings revealed that the microspheres in the reduced expansion group were more frequently observed inside the liver tumors and peripheral liver parenchyma compared with those in the normal expansion group.

# CONCLUSION

Chemoembolization using cisplatin-loaded SAP with the reduced expansion technique has an advantage of achieving a better distribution of microspheres and a higher drug concentration of cisplatin in tumors.

# **CLINICAL RELEVANCE/APPLICATION**

The newly developed reduced expansion technique could be useful for tumors with fine feeding arteries in chemoembolization using cisplatin-loaded SAP.

# VI244-SD-TUA3

### MRI Study of Probucol Therapy on Atherosclerotic Plaque in Watanabe Heritable Hyperlipidemic Rabbits

Tuesday, Nov. 29 12:15PM - 12:45PM Room: VI Community, Learning Center Station #3

#### **Participants**

Chiaki Kaneko, Shiga, Japan (*Abstract Co-Author*) Nothing to Disclose Norihisa Nitta, MD, Kyoto, Japan (*Presenter*) Nothing to Disclose Keiko Tsuchiya, Otsu, Japan (*Abstract Co-Author*) Nothing to Disclose Kiyoshi Murata, MD, Otsu, Japan (*Abstract Co-Author*) Nothing to Disclose Shinichi Ota, MD,PhD, Otsu, Japan (*Abstract Co-Author*) Nothing to Disclose Akinaga Sonoda, MD, PhD, Otsu, Japan (*Abstract Co-Author*) Nothing to Disclose Shobu Watanabe, MD, Otsu, Japan (*Abstract Co-Author*) Nothing to Disclose Ayumi Seko, MD, Otsu, Japan (*Abstract Co-Author*) Nothing to Disclose

## PURPOSE

The purpose of this study was to evaluate the effect of a Probucol on atheroscletotic regression by MRI studies and histopathological studies.

### **METHOD AND MATERIALS**

We divided 14 Watanabe heritable hyperlipidemic (WHHL) rabbits into 2 equal groups (6-7 months). One group was fed on mixed of Probucol, and the other group received normal chow without active drug as control. Five times of MRI (a baseline, 2,4,6,10,months after) and lastly MRI of USPIO were performed. The last MRI study was followed by histologic examination. The black blood sequence, cardiac-gated 2D fast spin echo sequence was used with triple inversion recovery pulses to suppress fat and blood signals was used. The vessel wall area was measured in the wall of the lower thoracic aorta on axial images. Specimens from the same level of the aorta were subjected to RAM-11 immunostaining ,and used for histopathological study. For statistical analysis of the MRI and histopathological findings we used t-test.

## RESULTS

The vessel wall area with Probucol group were larger than compared with control (p < 0.05) in the serial MRI (2,4,6,10,months after.) The significant difference was not seen by the vessel wall area in the first pre MRI.Pathologically, in RAM-11 staining, the positive area of the macrophage was decreasing significantly in the group with probucol (p < 0.05).

## CONCLUSION

In the evaluation of the aorta of WHHL by MRI, the vessel wall thickness was controlled by probucol. Pathologically, reduction of the macrophage in the atherosclerotic plaque was seen.

### **CLINICAL RELEVANCE/APPLICATION**

The evaluation of the atherosclerosis in a rabbit by the MRI can apply to carotid artery plaque diagnosis of the human, and it is useful to evaluation of medical treatment.

## VI245-SD-TUA4

### Local Pulse Wave Velocity Profile in the Murine Abdominal Aorta at 17.6 T MRI

Tuesday, Nov. 29 12:15PM - 12:45PM Room: VI Community, Learning Center Station #4

#### **Participants**

Stefan M. Herz, MD, Wuerzburg, Germany (*Presenter*) Nothing to Disclose Volker Herold, Wurzburg, Germany (*Abstract Co-Author*) Nothing to Disclose Patrick Winter, Wurzburg, Germany (*Abstract Co-Author*) Nothing to Disclose Julian Kunz, MD, Wurzburg, Germany (*Abstract Co-Author*) Nothing to Disclose Tobias Gassenmaier, MD, Wurzburg, Germany (*Abstract Co-Author*) Nothing to Disclose Thorsten A. Bley, MD, Hamburg, Germany (*Abstract Co-Author*) Nothing to Disclose Wolfgang R. Bauer, MD, PHD, Wuerzburg, Germany (*Abstract Co-Author*) Nothing to Disclose

### PURPOSE

The aim of our study was to determine the local pulse wave velocity profile of the murine abdominal aorta in a multi-local setting and its potential to predict atherosclerotic plaque formation. Inflammation in atherosclerosis impairs the vessel wall function and reduces the wall elasticity which can be assessed by measuring the pulse wave velocity (PWV).

### **METHOD AND MATERIALS**

ECG- and respiratory-gated MRI at 17.6 T was used to determine the local PWV profile (10x accelerated K-T BLAST QA method) and to visualize atherosclerotic plaques (multi-slice-multi-spin-echo sequence). 7 ApoE(-/-) and 7 C57Bl/6 wild type (WT) mice were imaged at the age of 19 and 30 weeks. Local PWV was calculated from the change in volume flow and cross sectional area of the abdominal aorta in early systole. Morphological plaque imaging was conducted in early systole to realize a "black blood" effect. Hematoxylin and Eosin staining were used for histological analysis.

### RESULTS

Due to a 10 fold accelerated K-T BLAST method we were able to determine the local PWV profile along 8 subsequent slices. At the age of both 19 and 30 weeks ApoE(-/-) mice showed a significantly elevated local PWV compared to WT controls. In contrast at 30 weeks the maximum wall thickness of ApoE(-/-) mice was significantly elevated indicating the presence of atherosclerotic plaques while at the age of 19 weeks no elevated wall thickness was found. Statistical analysis indicates a positive correlation between local PWV and wall thickness at the age of 30 weeks. In contrast, no significant correlation was found for local PWV of ApoE(-/-) mice at 19 weeks and the corresponding wall thickness at 30 weeks. Results were supported by histological findings.

### CONCLUSION

These results indicate a significant correlation of local PWV and wall thickness when atherosclerotic plaques are present. They support previous studies indicating that an elevated local PWV in early atherosclerosis precedes later plaque development. However, local PWV was not able to predict the exact location of the subsequent plaque formation.

### **CLINICAL RELEVANCE/APPLICATION**

Elevated local PWV precedes subsequent plaque development in murine atherosclerosis and might have the potential as indicator of cardiovascular risk.

Do Immunohistochemistry Features of Thrombus Affect Outcome of Catheter-directed Thrombolysis in Patients with Deep Venous Thrombus?

Tuesday, Nov. 29 12:15PM - 12:45PM Room: VI Community, Learning Center Station #5

## Participants

Eiji Furukoji, Miyazaki-shi, Japan (*Abstract Co-Author*) Nothing to Disclose Masatsugu Kawano, Miyazaki, Japan (*Presenter*) Nothing to Disclose Yoshihito Kadota, Miyazaki, Japan (*Abstract Co-Author*) Nothing to Disclose Norihiro Shinkawa, MD, Miyazaki, Japan (*Abstract Co-Author*) Nothing to Disclose Tatefumi Sakae, MD, Miyazaki, Japan (*Abstract Co-Author*) Nothing to Disclose Toshinori Hirai, MD, PhD, Miyazaki, Japan (*Abstract Co-Author*) Nothing to Disclose

### PURPOSE

If the mechanism of thrombus organization is more clearly understood, the efficacy of catheter-directed thrombolysis (CDT) for venous thromboembolism may increase. We aimed to evaluate the relationship of patient characteristics, treatment effects of CDT, and immunohistochemistry features of thrombus.

#### **METHOD AND MATERIALS**

This study included consecutive 19 patients (11 males, 8 females; age range 20-78 years; mean age 54.6 years) treated with CDT for venous thromboembolism. Venous thrombus developed on the left leg in 14 cases and the right in 5; 10 cases also had pulmonary embolism. The patients had trauma (n = 4), prolonged immobility (n = 3), postoperative state (n = 2) and cancer (n = 2); the remaining 8 patients were idiopathic. The risk factors of the thrombotic diathesis included high homocysteinemia, AT III deficiency, protein C deficiency. After placement of an 8Fr guiding catheter at the popliteal vein, CDT using urokinase and aspiration of venous thrombus were performed in all patients. Experienced pathologists assessed the aspirated thrombi on histology and immunohistochemistry. The patients were followed at least 3 months. We evaluated the relationship between patient characteristics, treatment effects of CDT, and immunohistochemistry features of aspirated venous thrombus. We used the Pearson correlation coefficient to assess the associations.

#### RESULTS

Time from symptom onset to treatment was 5-60 days (mean, 19.3 days). The venous thrombus disappeared in the follow up completely in 3 and partially in 13 cases, and recurred after thrombus reduction in 3 cases. In the histologic examination of aspirated thrombus, the degree of thrombus organization varied according to the period from symptom onset to CDT, and a significant correlation was found between the time from symptom onset and the expression of alpha-smooth muscle actin (myofibroblast and smooth-muscle cells) in thrombus (p < 0.05). The relationship between the expression of alpha-smooth muscle actin and the effect of treatment was not found.

## CONCLUSION

In patients with deep venous thrombus, the time from symptom onset affects the expression of alpha-smooth muscle actin in thrombus. However, it is not determined whether the immunohistochemistry features of thrombus affect treatment outcome.

## **CLINICAL RELEVANCE/APPLICATION**

Although the mechanism of thrombus organization is complex, catheter-directed thrombolysis is useful for treating deep venous thrombus.

# Microwave-Ablation in the Proximity of Surgical Clips: Does it Influence the Ablation Zone?

Tuesday, Nov. 29 12:15PM - 12:45PM Room: VI Community, Learning Center Station #6

#### Awards

### **Student Travel Stipend Award**

### **Participants**

Martin Liebl, MD, Aachen, Germany (*Presenter*) Nothing to Disclose Markus Zimmermann, MD, Aachen, Germany (*Abstract Co-Author*) Nothing to Disclose Maximilian F. Schulze-Hagen, MD, Aachen, Germany (*Abstract Co-Author*) Nothing to Disclose Federico Pedersoli, Aachen, Germany (*Abstract Co-Author*) Nothing to Disclose Philipp Bruners, MD, Aachen, Germany (*Abstract Co-Author*) Nothing to Disclose Christiane K. Kuhl, MD, Bonn, Germany (*Abstract Co-Author*) Nothing to Disclose Peter Isfort, MD, Aachen, Germany (*Abstract Co-Author*) Nothing to Disclose

### PURPOSE

Microwave ablation (MWA) is an established treatment option for patients suffering from hepatic malignancies. If materials with good electric conductivity, like surgical clips, are placed near the microwave antenna, unwanted heating effects may occur due to the induced electric current. We evaluated the possible influences of surgical clips within the ablation zone on the temperature and shape of the ablation volume during MWA.

## METHOD AND MATERIALS

18 microwave ablations were performed in bovine liver tissue with an AMICA-microwave device (Mermaid Medical) using an ablation protocol with application of 60 Watts for 3 minutes. A titanium surgical clip was placed 7,5 mm distant from the microwave probe. Temperature was measured every second at 4 points of interest (POI): at the site of the clip and 7,5 mm distal from the clip, and at the same distances (7,5 and 15 mm) on the opposite side of the probe (without clip). We calculated the mean temperature curve at the 4 POI during the energy application. After the MWA, the liver was dissected to measure the ablation zone and evaluate the shape of the ablation.

## RESULTS

MWA could be successfully performed in all 18 liver specimens. No significant changes of the size and shape of the ablation zone were ascertained. The Temperature at the position of the clip was significantly higher compared to the same distance on the opposite position of the probe without clip at all times during ablation with a maximum difference of 17 degrees at the end of the energy deposition. (p=0,009).

# CONCLUSION

Surgical clips within the target volume result in an significant increase in local temperature but do not lead to changes in shape and volume of the ablation zone.

# **CLINICAL RELEVANCE/APPLICATION**

Heating of surgical clips during MWA is likely to happen, but damage to surrounding structures such as biliodigestive anastomosis or the stomach wall would need direct contact to the clip, as the ablation volume is not influenced by the clip.

# VI248-SD-TUA7

Extravascular Incidental Malignant Findings in Follow-up CT Angiograms in Patients Post Endovascular Aneurysm Repair

Tuesday, Nov. 29 12:15PM - 12:45PM Room: VI Community, Learning Center Station #7

#### Awards

### **Student Travel Stipend Award**

#### **Participants**

Mohammad W. Butt, BMedSc,BMBS, Derby, United Kingdom (*Presenter*) Nothing to Disclose Permesh S. Dhillon, MBBS, Derby, United Kingdom (*Abstract Co-Author*) Nothing to Disclose Peter D. Thurley, MBBS, Nottingham, United Kingdom (*Abstract Co-Author*) Nothing to Disclose Mario De Nunzio, Derby, United Kingdom (*Abstract Co-Author*) Nothing to Disclose Graham Pollock, Derby, United Kingdom (*Abstract Co-Author*) Nothing to Disclose Peter Bungay, FRCR, MBChB, Derby, United Kingdom (*Abstract Co-Author*) Nothing to Disclose Peter Bungay, FRCR, MBChB, Derby, United Kingdom (*Abstract Co-Author*) Consultant, Terumo Corporation Speaker, Terumo Corporation Christopher A. Squirrell, FRCR, Derby, United Kingdom (*Abstract Co-Author*) Nothing to Disclose

James E. Kirk, MBChB, MRCP, Nottingham, United Kingdom (Abstract Co-Author) Nothing to Disclose

## PURPOSE

To evaluate the incidence and clinical relevance of extravascular incidental findings (EVIF), particularly malignancies, in follow-up CT angiograms (CTA) of the abdominal aorta in patients who underwent endovascular aneurysm repair (EVAR) of abdominal aortic aneurysm.

### **METHOD AND MATERIALS**

Retrospective study of 2199 planning and follow-up CTAs of 418 patients who underwent EVAR in a single tertiary centre between 2006 – 2015. CTA reports were scrutinized for EVIFs, which were classified according to clinical relevance, into (I) immediate, (II) potential and (III) no clinical relevance. Clinical follow-up and management were reviewed for significant findings. Follow-up CTAs of patients with incidental malignancies were re-reviewed by 2 consultant radiologists and early missed malignant findings on previous CTAs were identified.

#### RESULTS

In total, 934 EVIFs were noted in 418 patients [31 females (7.4%), 387 males (92.6%); age range 63-93, mean age 78.5 years]. The number of patients with findings in each category were; Category I (114), Category II (166), Category III (304).Incidental malignant findings were reported in 51 patients (12.2%), of which 25 were noted on the initial CTA (6.0%) and 26 on follow-up CTAs (6.2%). Of the 26 patients, 15 had early malignant findings missed or misinterpreted on previous CTAs, while 11 had no significant abnormality even on retrospective review.

## CONCLUSION

A high number of significant EVIFs, particularly incidental malignancies, can be identified in follow-up CTAs of patients who undergo EVAR. Hence, it is prudent to be vigilant in evaluation of abdominal CTAs and necessary clinical follow-up arranged.

# **CLINICAL RELEVANCE/APPLICATION**

Specific 'review areas' when reporting surveillance CTAs can be recommended on the basis of the findings of our study.

## VI280-SD-TUA8

Palliative Treatment of Painful Bone Metastases with MR Imaging-guided Focused Ultrasound Surgery: A Twocentre Study

Tuesday, Nov. 29 12:15PM - 12:45PM Room: VI Community, Learning Center Station #8

# Participants

Alessandro Napoli, MD, Rome, Italy (*Abstract Co-Author*) Nothing to Disclose Andrea Leonardi, Roma, Italy (*Abstract Co-Author*) Nothing to Disclose Fabrizio Andrani, Roma, Italy (*Abstract Co-Author*) Nothing to Disclose Vincenzo Noce, MD, Rome, Italy (*Abstract Co-Author*) Nothing to Disclose Carlo Catalano, MD, Rome, Italy (*Abstract Co-Author*) Nothing to Disclose Alberto Bazzocchi, MD, Bologna, Italy (*Abstract Co-Author*) Nothing to Disclose Hans Peter Erasmus, Rome, Italy (*Presenter*) Nothing to Disclose

### PURPOSE

To evaluate the efficacy of non-invasive high intensity MR guided focused Ultrasound Surgery (MRgFUS) for pain palliation of bone metastasis in patients over a large population.

### **METHOD AND MATERIALS**

This prospective, single arm, two-centre study received IRB approval. 102 patients (female: 38, male: 64, mean age: 62,3) with painful bone metastases were enrolled. 121 non-spinal lesions underwent MRgFUS treatment using ExAblate 2100 system (InSightec). European Organization for Research and Treatment of Cancer QLQ- BM22 was used for clinical assessment additionally to Visual Analog Scale (VAS), at baseline and 1, 3 and 6 months after treatment. All patients underwent CT and MRI before treatment and 3-6 months afterward.

## RESULTS

No treatment-related adverse events were recorded. 48/102 (47%) patients reported complete response to treatment and discontinued medications. 39/102 (38,2%) experienced a pain score reduction >2 points, consistent with partial response. Remaining 15 (14,7%) patients had recurrence after treatment. Statistically significant differences between baseline (6, 95%CI 5-8) and follow-up (2, 95%CI 0-3) VAS values and medication intake were observed (p<0.05). Similarly a significant difference was found for QLQ- BM22 between baseline and follow-up (p<0.05).

# CONCLUSION

MRgFUS can be safely and effectively be adopted for treatment of painful bone metastases.

# **CLINICAL RELEVANCE/APPLICATION**

MRgFUS can be safely and effectively used as totally noninvasive treatment for pain palliation of acoustically accessible bone metastasis

# A Multimodality Exploration of Unilateral Breast Edema: It's Not Just Cancer

Tuesday, Nov. 29 12:45PM - 1:15PM Room: BR Community, Learning Center Station #8

### **Participants**

Suraj Ĥ. Rambhia, MD, New Hyde Park, NY (*Presenter*) Nothing to Disclose Suzanne McElligott, MD, Manhasset, NY (*Abstract Co-Author*) Nothing to Disclose Ekta Gupta, MD, Floral Park, NY (*Abstract Co-Author*) Nothing to Disclose

## **TEACHING POINTS**

1. Breast edema presents as diffuse breast enlargement, skin thickening and increased interstitial markings on imaging.2. Unilateral breast edema (UBE) has a limited differential diagnosis, including mammary, non-mammary, and systemic etiologies, which radiologists should be familiar with in order to accurately diagnose and guide treatment. History and physical exam are important in narrowing the differential.3. UBE should be considered as a rare presentation of congestive heart failure.4. Breast infection/mastitis can mimic the clinical signs and imaging appearance of inflammatory breast cancer.5. In a post lumpectomy surveillance period, when consecutive mammograms demonstrate no change or increasing breast edema, recurrent cancer should be considered.

### **TABLE OF CONTENTS/OUTLINE**

(1) Overview of the pathophysiology and differential diagnosis of unilateral breast edema.(2) Imaging findings related to breast edema on mammography, ultrasound, CT, and breast MRI.(3) Case based approach of pathologies that result in unilateral breast edema with attention to correlation between various imaging modalities.a. Low oncotic pressure states.b. Abscess/infection and inflammation.c. Post-radiation/post postsurgical state and post traumad. Mechanical problems.e. Neoplastic.(4) Diagnostic Workup, Pitfalls, Management and Summary

Prediction the Likelihood of Malignancy According to Morphological Analysis of Phyllodes Tumor in Breast MRI

Tuesday, Nov. 29 12:45PM - 1:15PM Room: BR Community, Learning Center Station #9

### Awards Certificate of Merit

#### **Participants**

Ok Hee Woo, MD, Seoul, Korea, Republic Of (*Presenter*) Nothing to Disclose Gayoung Choi, MD, Seoul, Korea, Republic Of (*Abstract Co-Author*) Nothing to Disclose Hyeseon Shin, Seoul, Korea, Republic Of (*Abstract Co-Author*) Nothing to Disclose Ah Young Park, MD, Ansan, Korea, Republic Of (*Abstract Co-Author*) Nothing to Disclose Sung Eun Song, MD, Seoul, Korea, Republic Of (*Abstract Co-Author*) Nothing to Disclose Kyu Ran Cho, MD, PhD, Seoul, Korea, Republic Of (*Abstract Co-Author*) Nothing to Disclose Bo Kyoung Seo, MD, PhD, Ansan, Korea, Republic Of (*Abstract Co-Author*) Nothing to Disclose

## **TEACHING POINTS**

Phyllodes tumor typically has a rapidly growing breast mass and high incidence of local recurrence and shows malignant potential in 15-40%. However, radiologic differential diagnosis of benign and malignant phyllodes tumors are difficult. In this exhibit, the purpose of to correlate the imaging findings of phyllodes tumor with histologic grades and to suggest imaging clues to distinguish malignant phyllodes tumor from benign in breast MRI.

# TABLE OF CONTENTS/OUTLINE

1. Retrospective review of MR findings according to pathologic subtypes of phyllodes tumor in consensus of 2 radiologists Tumor size Shape (round, oval, irregular) Margin (smooth, irregular, spiculated) Internal haemorrhage or cystic change Smooth or irregular wall Dynamic enhancement pattern (Type I, II, III)2. Statistics Tumor size and histologic grade: Spearman correlation coefficient analysis Tumor shape, margin, internal haemorrhage/cystic change, enhancement pattern and histologic grade: Fisher exact test3. 3. Conclusions The tumour size, shape, margin, and internal enhancement pattern were not correlated with histologic grade in phyllodes tumours Internal haemorrhage or cystic change with irregular wall are suggestive of the malignant phyllodes tumour of the breast

## BR245-SD-TUB1

Strain Elastography and Shear-wave Elastography for the Differentiation of Benign and Malignant Breast Lesions

Tuesday, Nov. 29 12:45PM - 1:15PM Room: BR Community, Learning Center Station #1

### Awards

### **Student Travel Stipend Award**

#### Participants

Nicola Di Leo, MD, Rome, Italy (*Presenter*) Nothing to Disclose Vito Cantisani, MD, Rome, Italy (*Abstract Co-Author*) Speaker, Toshiba Corporation; Speaker, Bracco Group; Speaker, Samsung Electronics Co, Ltd; Emanuele David, Roma, Italy (*Abstract Co-Author*) Nothing to Disclose Giorgio Ascenti, MD, Messina, Italy (*Abstract Co-Author*) Nothing to Disclose Carlo Catalano, MD, Rome, Italy (*Abstract Co-Author*) Nothing to Disclose Ferdinando D'Ambrosio, Rome, Italy (*Abstract Co-Author*) Nothing to Disclose Isabella Guerrisi, Rome, Italy (*Abstract Co-Author*) Nothing to Disclose Francesca Di Pastena, Rome, Italy (*Abstract Co-Author*) Nothing to Disclose Hektor Grazhdani, MD, PhD, Rome, Italy (*Abstract Co-Author*) Nothing to Disclose Alfredo Blandino, Messina, Italy (*Abstract Co-Author*) Nothing to Disclose Silvia Gigli, roma, Italy (*Abstract Co-Author*) Nothing to Disclose Silvia Gigli, roma, Italy (*Abstract Co-Author*) Nothing to Disclose

## PURPOSE

to evaluate the diagnostic performance of strain elastography (SE) and shear-wave elastography (SWE), in combination with Bmode US, in improving BI-RADS classification and differentiating benign and malignant breast lesions by using a qualitative and quantitative assessments.

## **METHOD AND MATERIALS**

in this prospective study we included 145 histopathologically proven breast masses who were evaluated by using baseline US, CDUS, SE and SWE (Toshiba Aplio 500 with a 7-15 MHz wide-band linear transducer). Each lesion was classified according to the BIRADS lexicon, by evaluating the size, the B-mode and color-Doppler features, the SE qualitative (color-coded images) and SE semi-quantitative dynamic features (strain ratio), and SWE through a qualitative (color-coded) and quantitative approach (expressed by m/s and k/Pa). Results were correlated with pathologic findings. The area under the ROC curve was used to evaluate the diagnostic performance of B-mode ultrasound, SE and SWE, and their combination.

### RESULTS

Histologiacl examination revealed 83 benign and 64 malignant breast lesions US, SE and SWE, considered alone, showed respectively a sentitivity (Se) of 92%, 82% and 81% and a specificity (Spe) of 83%, 75% and 79%. SE, as an additional tool to B mode US examination (US+SE) significantly increased the diagnostic performance of breast US (Se: 96%, Spe: 88%, AUC: 0.9 p<0.004), while the addition of SWE (US+SWE), although was a valid tool in selected cases was lower (Se: 93%, Spe: 84%)

### CONCLUSION

our experience suggest that SE and SWE in combination with B-mode US, are valid tool in clinical setting, improving BIRADS category assessment and may help in the differentiation of benign from malignant breast lesions. However SE shows more accuracy than SWE.

#### **CLINICAL RELEVANCE/APPLICATION**

Elastography, with both strain and shear wave, can increase the diagnostic confidence in assigning BIRADS category and discriminating benign from malignant breast lesions

## Lobular Neoplasia of the Breast: A Stronger Statement on an Old Issue

Tuesday, Nov. 29 12:45PM - 1:15PM Room: BR Community, Learning Center Station #2

#### Awards

### **Student Travel Stipend Award**

#### **Participants**

Bryan E. Ashley, MD, Chapel Hill, NC (*Presenter*) Nothing to Disclose Sheryl G. Jordan, MD, Chapel Hill, NC (*Abstract Co-Author*) Nothing to Disclose Thomas J. Lawton, MD, Chapel Hill, NC (*Abstract Co-Author*) Nothing to Disclose

## PURPOSE

The management of pure lobular neoplasia of the breast remains inconsistent. While some institutions excise all cases of atypical lobular hyperplasia and lobular carcinoma in situ, other institutions excise only one or the other. Our institution pursues surgery for both diagnoses and the purpose of this study is to ascertain the advisability of this approach.

### **METHOD AND MATERIALS**

IRB-approved, study retrospectively identified all patients with histologic confirmed diagnosis of pure lobular neoplasia from January 1, 2004 through December 30, 2013 in our CoPath database. Diagnoses of additional high risk lesions were excluded. Remaining cases N=109 were reviewed in multivariate manner. Further, detailed literature review from 1999-2013 identified 48 reports of lobular neoplasia upgrade on surgical excision. Each study was reviewed for the following confounding factors: missing radiologic-pathologic concordance assessment and/or including discordant cases; including another high risk biopsy lesion; assigning associated high risk lesion at excision as upgrade; no histologic review by breast pathologist and no comment on the distance of the upgrade from the original biopsy site.

## RESULTS

109 patients with pure lobular carcinoma in situ or atypical lobular neoplasia were identified, 102 had complete data to include two year followup. Median age 53, range 36-87. Pathology results yielded pure ALH in 54, pure LCIS in 44, and both in 4. We had no instances of immediate upgrades on surgical excision. On additional surveillance, mucinous carcinoma was diagnosed at one year, DCIS at two years, and infiltrating ductal carcinoma at three years in three patients. Of note, 33 patients had a prior or coexistent history of malignancy in the contralateral breast defining them already as high risk patients. Published literature upgrade ranges are 0-61%, average 17% but ten studies with 2% or less. However, identification of one or more confounders previously described eliminates many of the upgrade articles.

### CONCLUSION

Concordant pure lobular neoplasia on core needle biopsy should be assigned BI-RADS@ Assessment Category 3: Probably Benign, as well as Management Recommendations: Short interval 6-month followup surveillance

## **CLINICAL RELEVANCE/APPLICATION**

Lobular neoplasia of the breast is considered a risk lesion for which excision is recommended at many institutions; using appropriate criteria, these patients can avoid unnecessary surgery.

# BR247-SD-TUB3

### Abbreviated Screening Breast MRI: Accuracy and Reliability in a Multiple-Reader Setting

Tuesday, Nov. 29 12:45PM - 1:15PM Room: BR Community, Learning Center Station #3

#### Participants

Cristina I. Campassi, MD, Baltimore, MD (*Presenter*) Nothing to Disclose Paul B. Stoddard, MD, Baltimore, MD (*Abstract Co-Author*) Nothing to Disclose Sonya Khan, MD, Baltimore, MD (*Abstract Co-Author*) Nothing to Disclose Luke J. Robinson, MD,MA, BROOKLYN, NY (*Abstract Co-Author*) Nothing to Disclose Lyn W. Ho, MD, Baltimore, MD (*Abstract Co-Author*) Nothing to Disclose Daniel W. Maver, MD, Laurel, MD (*Abstract Co-Author*) Nothing to Disclose Hannah Nien, MD, Long Branch, NJ (*Abstract Co-Author*) Nothing to Disclose Jason W. Mitchell, MD, Ellicott City, MD (*Abstract Co-Author*) Nothing to Disclose

### PURPOSE

To assess accuracy and reliability of screening breast magnetic resonance imaging (MRI) in a multiple-reader setting for the detection of primary breast malignancy using an abbreviated protocol (AP) consisting of a pre-contrast and single post-contrast T1W sequence.

## **METHOD AND MATERIALS**

HIPAA-compliant, IRB-approved retrospective study of 101 asymptomatic patients who received screening breast MRI; patients were at intermediate to high risk for breast cancer with concurrent negative or benign mammogram. Exams were performed on 3T or 1.5T Siemens scanners and protocolled in accordance with the ACR requirements for breast MRI accreditation. Aegis Sentinelle software was utilized for interpretation. Two experienced fellowship-trained breast radiologists, one breast imaging fellow and one PGY5 radiology resident individually reviewed all cases blinded to the original interpretation, prior studies, and outcome. Readers assigned a BI-RADS assessment category for each of three 'protocols' for every patient: subtracted first post-contrast Maximum Intensity Projection (MIP), pre- and first post-contrast T1W sequences with subtraction and source images (AP), and full protocol (FP). Accuracy was assessed using multiple-reader receiver operating characteristic (ROC) curve analysis, using histologic and clinical follow-up as the reference standard. Reliability was assessed with intraclass correlation coefficients (ICC).

#### RESULTS

On multiple-reader ROC curve analysis, overlapping 95% confidence intervals for mean accuracy were noted: MIP 0.794-0.914, AP 0.773-0.941, FP 0.734-0.964. No significant difference between accuracy of the three protocols was observed as assessed using a random-reader effects model (F = 0.028, p = 0.9725). Among readers, accuracy varied with years of experience (most experienced 0.816-0.942 versus least 0.784-0.874). Nonetheless, when malignancy was present, no cases were missed combining MIP and AP interpretations. A strong degree of reliability between readers for all protocols was also noted (ICC: MIP 0.786; AP 0.781; FP 0.715).

## CONCLUSION

The abbreviated protocol (AP) for screening breast MRI provides similar accuracy and superior inter-reader reliability compared to the full protocol (FP).

# **CLINICAL RELEVANCE/APPLICATION**

An abbreviated protocol for breast MRI may be successfully introduced in screening programs without sacrificing accuracy and with high reliability across readers of varying experience levels. Bilateral Contrast-enhanced Spectral Mammography Compared to Breast Magnetic Resonance Imaging for Presurgical Imaging Evaluation In Newly Diagnosed Breast Cancer

Tuesday, Nov. 29 12:45PM - 1:15PM Room: BR Community, Learning Center Station #4

# Participants

Stephanie A. Lee-Felker, MD, Los Angeles, CA (*Presenter*) Nothing to Disclose Leena Tekchandani, MD, Mineola, NY (*Abstract Co-Author*) Nothing to Disclose Mariam Thomas, MD, Sylmar, CA (*Abstract Co-Author*) Nothing to Disclose Denise M. Andrews-Tang, MD, Sylmar, CA (*Abstract Co-Author*) Nothing to Disclose Antoinette R. Roth, MD, Sylmar, CA (*Abstract Co-Author*) Nothing to Disclose Esha A. Gupta, MD, Los Angeles, CA (*Abstract Co-Author*) Nothing to Disclose James Sayre, PhD, Los Angeles, CA (*Abstract Co-Author*) Nothing to Disclose Guita Rahbar, MD, Beverly Hills, CA (*Abstract Co-Author*) Nothing to Disclose

### PURPOSE

To compare the diagnostic performance of contrast-enhanced spectral mammography (CESM) and breast magnetic resonance imaging (MRI) for presurgical imaging evaluation of extent of disease in newly diagnosed breast cancer, using histology as the gold standard.

## **METHOD AND MATERIALS**

This IRB-approved, HIPAA-compliant, retrospective study included consecutive women with newly diagnosed unilateral breast cancer on core needle biopsy (CNB) who underwent presurgical CESM and MRI, followed by CNB of additional imaging-detected suspicious secondary cancer sites, at a single institution between April 2014 and October 2015. Exclusion criteria included: inflammatory breast cancer (n = 1) and contraindications for intravenous contrast administration (n = 3) or MRI (n = 2). Images were analyzed by 1 of 5 breast radiologists with 2-17 years of experience. Sensitivity (Sn), positive predictive value (PPV), and accuracy were calculated with 95% confidence intervals for both modalities. Specificity (Sp) and negative predictive value (NPV) were also calculated for CESM but not for MRI because the latter did not have true negative lesions. The number of false positive (FP) lesions for each modality was compared using the McNemar exact test. A p value <0.05 was significant.

#### RESULTS

52 women with 86 biopsy-proven breast lesions were included for analysis (mean age 50 years; range, 29-73 years). The performance of CESM was: Sn 98.4% [90.3%-99.9%], Sp 82.6% [59.9%-94.0%], PPV 93.9% [84.4%-98.0%], NPV 95.0% [71.9%-99.7%], and accuracy 94.2% [86.8%-98.0%]. In comparison, the performance of MRI was: Sn 98.4% [90.3%-99.9%], PPV 72.9% [62.9%-82.5%], and accuracy 72.1% [62.2%-82.0%]. Of 8 additional biopsy-proven secondary cancer sites, CESM detected all 8 of 8 (100.0%) and MRI detected 7 of 8 (87.5%).CESM and MRI each had 1 false negative for DCIS in 2 different women.CESM had significantly fewer FPs than MRI (p <0.001): 4 FPs (2 high risk lesions, 1 fibroadenoma, and 1 non-high risk benign lesion) on CESM and 23 FPs (8 high risk lesions, 4 fibroadenomas, and 11 non-high risk benign lesions) on MRI.

# CONCLUSION

In this limited study, CESM was as sensitive and more specific than MRI for detecting breast cancer.

## **CLINICAL RELEVANCE/APPLICATION**

In the appropriate clinical setting, CESM may substitute for breast MRI in presurgical imaging evaluation for extent of disease in newly diagnosed breast cancer.

# Quantitative Heterogeneity Analysis of DCIS Grades and Types on Breast MRI

Tuesday, Nov. 29 12:45PM - 1:15PM Room: BR Community, Learning Center Station #6

#### Awards

### **Student Travel Stipend Award**

### **Participants**

Shinnhuey S. Chou, MD, Boston, MA (*Presenter*) Nothing to Disclose Eva C. Gombos, MD, Boston, MA (*Abstract Co-Author*) Royalties, Reed Elsevier Sona A. Chikarmane, MD, Boston, MA (*Abstract Co-Author*) Nothing to Disclose Catherine S. Giess, MD, Wellesley, MA (*Abstract Co-Author*) Nothing to Disclose David Z. Chow, MD, Cambridge, MA (*Abstract Co-Author*) Nothing to Disclose Jayender Jagadeesan, PHD, Boston, MA (*Abstract Co-Author*) Nothing to Disclose

#### PURPOSE

Determining DCIS imaging biomarkers in the era of precision medicine is increasingly crucial. We aim to develop MRI biomarkers to predict DCIS grades and types.

## METHOD AND MATERIALS

Informed consent was waived in this HIPAA-compliant IRB-approved study. Case inclusion was conducted from a database containing 7332 breast MRI studies from 1/1/2009-12/31/2012. After excluding MRI studies with benign assessments, pathology without DCIS, pathology with invasive disease, and MRI without DCIS visualization, 52 MRI studies with pathology-proven DCIS seen on dynamic contrast-enhanced MRI were reviewed. Regions-of-interest representing DCIS were segmented on the open-source 3D Slicer software by a radiologist using semi-automatic algorithms. Fifty-seven quantitative metrics of each DCIS were obtained, including distribution statistics, shape, morphology, Renyi dimensions, geometrical measure and texture, using the open-source HeterogeneityCAD module in 3D Slicer. Statistical correlation of heterogeneity metrics with DCIS grade and receptor status was performed using the univariate Mann-Whitney test.

#### RESULTS

The 52 studies included 31 (60%) high-grade and 21 (40%) non-high-grade DCIS. Among them, 41 (79%) were ER+ and 11 (21%) were ER-. HER2 amplification results were unavailable in 3 cases and equivocal in 8 cases. Of the 41 cases with known HER2 status, 10 (24%) were HER2+ and 31 (76%) were HER2-. One metric, surface area-to-volume ratio, showed significant difference (p<0.05) between high-grade and non-high-grade DCIS on pre-contrast, first post-contrast, and first post-contrast subtraction images. No metric significantly differentiated ER+ from ER- DCIS. However, multiple metrics showed significant differences between HER2+ and HER2- DCIS (7 on pre-contrast, 7 on first post-contrast, 8 on first post-contrast subtraction, 1 on fourth post-contrast, and 2 on fourth post-contrast subtraction images).

## CONCLUSION

Quantitative MRI heterogeneity analysis of DCIS identified significant metrics in predicting high-grade DCIS and HER2 amplification. Validation of these metrics with larger sample sizes and prospective studies is needed to translate these results into clinical applications.

### **CLINICAL RELEVANCE/APPLICATION**

Quantitative heterogeneity analysis of DCIS identified MRI biomarkers that differentiated high-grade and HER2+ DCIS, providing prognostic significance in the era of precision medicine.

#### **Honored Educators**

Presenters or authors on this event have been recognized as RSNA Honored Educators for participating in multiple qualifying educational activities. Honored Educators are invested in furthering the profession of radiology by delivering high-quality educational content in their field of study. Learn how you can become an honored educator by visiting the website at: https://www.rsna.org/Honored-Educator-Award/

Catherine S. Giess, MD - 2015 Honored Educator

## BR251-SD-TUB7

Comparison of Deep Learning and Conventional CADx Across Two Large Clinical Datasets from FFDM and Breast Ultrasound

Tuesday, Nov. 29 12:45PM - 1:15PM Room: BR Community, Learning Center Station #7

# Participants

Benjamin Q. Huynh, Chicago, IL (*Presenter*) Nothing to Disclose
Karen Drukker, PhD, Chicago, IL (*Abstract Co-Author*) Royalties, Hologic, Inc
Hui Li, MD, PhD, Chicago, IL (*Abstract Co-Author*) Nothing to Disclose
Maryellen L. Giger, PhD, Chicago, IL (*Abstract Co-Author*) Stockholder, Hologic, Inc; Stockholder, Quantitative Insights, Inc; Co-founder, Quantitative Insights, Inc; Royalties, Hologic, Inc; Royalties, General Electric Company; Royalties, MEDIAN Technologies; Royalties, Riverain Technologies, LLC; Royalties, Mitsubishi Corporation; Royalties, Toshiba Corporation;

## PURPOSE

To explore properties of image descriptors extracted from clinical FFDM and breast ultrasound images with deep convolutional neural networks (CNNs) by comparing CNN-extracted features to computer-extracted, human-designed features in the task of distinguishing between benign and malignant lesions.

#### **METHOD AND MATERIALS**

Two large clinical datasets were used: a breast ultrasound dataset containing 1125 breast lesions and 2393 regions of interest (ROIs) containing the lesions, and a full-field digital mammography (FFDM) dataset with 219 breast lesions and 607 ROIs. The ultrasound ROIs had been categorized as benign solid, benign cystic, or malignant; the FFDM ROIs as either benign or malignant. Each region was subjected to two analyses: (i) direct input to a CNN and (ii) input to computer segmentation and feature extraction. Outputs from (i) the CNN and (ii) the human-designed features were input to support vector machine (SVM) classifiers and five-fold cross validation (by lesion) was used to assess performance in the task of distinguishing between benign and malignant breast lesions, with area under the receiver operating characteristic curve (AUC) as performance metric.

## RESULTS

SVMs trained on CNN-output features had similar high-level performances compared to those trained on the computer-extracted human-designed features (AUC = 0.81 vs 0.80 (SE = 0.01) for FFDM, AUC = 0.90 vs 0.90 (SE = 0.01) for ultrasound), but the outputs were only moderately correlated (r = 0.46 for FFDM, r = 0.62 for ultrasound), implying the potential for gains when both are used.

## CONCLUSION

The moderate correlations between the high-performing outputs suggest that CNN-extracted features may complement conventional CADx features, allowing for a benefit of improved performance when combined. Comparison between methods facilitates the interpretation of image properties of CNN-extracted features, which would otherwise be unintuitive.

## **CLINICAL RELEVANCE/APPLICATION**

Deep learning techniques show extreme promise in improving computer-aided diagnosis, and combination with conventional CADx may yield interpretation of otherwise unintuitive outputs.

# CA121-ED-TUB8

## Beyond the Heart: Expanding Applications of 4D-Flow from Head to Toe

Tuesday, Nov. 29 12:45PM - 1:15PM Room: CA Community, Learning Center Station #8

**FDA** Discussions may include off-label uses.

#### Awards

**Identified for RadioGraphics** 

### **Participants**

Horacio Murillo, MD, PhD, Stanford, CA (*Presenter*) Nothing to Disclose John Axerio-Cilies, PhD, San Francisco, CA (*Abstract Co-Author*) Founder, Arterys Inc; Officer, Arterys Inc

## **TEACHING POINTS**

To learn the basics of 4D flow MRI acquisition and developing applications; The quantitative and qualitative advantages of 4D flow MRI wherever hemodynamic measurements are needed for shunts, regurgitation, and flow patterns/stress; To learn about the added value to patient care that radiologists can provide with 4D flow MRI speed and convenience.

# TABLE OF CONTENTS/OUTLINE

PURPOSE

Review the fundamentals of 4D Flow MRI and its developing and expanding applications. Describe 4D Flow MRI applications with illustrative examples from head to toe. Discuss the advantages of 4D Flow MRI over 2D Flow MRI beyond pretty pictures.

#### CONTENT

Fundamentals of 4D Flow MRI.Data postprocessing and storage.Developing and expanding applications illustrative examples:-Comprehensive congenital heart MRI in minutes-Neurovascular imaging-Gastrointestinal arterial and venous imaging-Advantages and challenges of 4D flow MRI-Quantitative hemodynamics-Qualitative flow patterns

#### SUMMARY

The major learning points of this exhibit are (i) to learn the basics of 4D flow MRI acquisition and developing applications; (ii) the quantitative and qualitative advantages of 4D flow MRI for hemodynamic measurements and flow patterns/stress; and, (iii) the added value to patient care that radiologists can provide with 4D flow MRI speed and convenience.

# CA157-ED-TUB9

# The Role of MR Imaging in the Exploration of Myocardial Hypertrophy

Tuesday, Nov. 29 12:45PM - 1:15PM Room: CA Community, Learning Center Station #9

#### **Participants**

Sultan H. Yahya, MBBS, Angers, France (*Presenter*) Nothing to Disclose Djamel Ait Ali Yahia, Angers, France (*Abstract Co-Author*) Nothing to Disclose Serge Willoteaux, MD, Angers, France (*Abstract Co-Author*) Nothing to Disclose Christophe Aube, MD, PhD, Angers, France (*Abstract Co-Author*) Speaker, Bayer AG Support, General Electric Company Antoine Bouvier, Angers, France (*Abstract Co-Author*) Nothing to Disclose Cosmina R. Nedelcu, MD, Angers, France (*Abstract Co-Author*) Nothing to Disclose Filippo Caporilli Razza, MD, Rome, Italy (*Abstract Co-Author*) Nothing to Disclose

## **TEACHING POINTS**

The purpose of the educational exhibit is to:- define the diagnostic criteria of left ventricular hypertrophy - identify the features and classification of the phenotypes of hypertrophic cardiomyopathy (HCM) via MRI and precise the key

sequences needed in the MR exploration of HCM

- explore the different etiologies of HCM and their MR features

- emphasize the prognostic value of MRI in in the clinical outcome of patients suffering from HCM.

# TABLE OF CONTENTS/OUTLINE

compaction AmyloidosisConclusion

Influence of Heart Rate on Coronary CT Angiography Image Quality Using a Third-generation Dual Source Scanner: Defining an Optimal Heart-rate Target for Beta-blocker Administration

Tuesday, Nov. 29 12:45PM - 1:15PM Room: CA Community, Learning Center Station #2

# Participants

Brian Trinh, Chicago, IL (*Presenter*) Nothing to Disclose Lee Goodwin, Chicago, IL (*Abstract Co-Author*) Nothing to Disclose Vahid Yaghmai, MD, Chicago, IL (*Abstract Co-Author*) Nothing to Disclose James C. Carr, MD, Chicago, IL (*Abstract Co-Author*) Research Grant, Astellas Group Research support, Siemens AG Speaker, Siemens AG Advisory Board, Guerbet SA Jeremy D. Collins, MD, Chicago, IL (*Abstract Co-Author*) Nothing to Disclose

## PURPOSE

To evaluate the influence of heart rate (HR) on image quality at coronary CT angiography (CCTA) using a third-generation dual source (3GDS) CT system, before and after the institution of a beta-blocker protocol with a HR threshold of 75 beats per minute (bpm) for prospectively ECG-triggered scans.

## **METHOD AND MATERIALS**

A single-center, retrospective, IRB approved, HIPAA compliant study of 140 consecutive patients with low to intermediate risk for coronary artery disease who underwent CCTA on a 3GDS CT system between 2/1/2015 and 8/31/2015. The first 80 of the 140 consecutive patients composed the derivation cohort and were scanned by ECG-gated prospective triggering or retrospective gating depending on the patients' baseline rhythm without routine administration of beta-blockers. An optimal threshold for beta-blockade was defined using the derivation cohort and applied to the validation cohort. The remaining 60 patients comprised the validation cohort and were scanned with prospective ECG-triggering (pulsing 65-75% R-R) if HR  $\leq$ 75 bpm, or with retrospective gating (pulsing 35-70% R-R) if HR >75 bpm following beta-blocker administration (Table 1). 0.4mg sublingual nitroglycerin was administered to all patients unless contraindicated. Image quality (IQ) was assessed by a single observer and rated on a four-point scale. The body mass index (BMI), HR, and dose length product (DLP) were recorded. Differences between numerical data were assessed using the student's t-test and differences in proportions were assessed with the Chi-squared test.

### RESULTS

In the derivation cohort, patients with HR >75 bpm had significantly lower IQ than those with HR  $\leq$ 75 bpm (p<0.05). The derivation cohort had 6 non-diagnostic studies (7.5%), all of which were from patients with HR >75 bpm while the validation cohort had 1 non-diagnostic study (1.7%, p=0.12) from a patient with HR of 283 bpm. Overall IQ was similar between derivation and validation cohorts (p>0.05). The derivation cohort recorded higher DLP than the validation cohort (p<0.05) (Table 2).

## CONCLUSION

Chronotropic protocols on 3GDS CT systems should endeavor to achieve a target resting HR of  $\leq$ 75 bpm for prospective ECG-gating, reserving retrospective ECG-gating for patients with HR >75 bpm.

## **CLINICAL RELEVANCE/APPLICATION**

A defined target HR for ECG-gated prospectively triggered CCTA on a 3GDS CT system reduced the rate of non-diagnostic scans while simultaneously reducing the radiation dose.

## **Honored Educators**

Presenters or authors on this event have been recognized as RSNA Honored Educators for participating in multiple qualifying educational activities. Honored Educators are invested in furthering the profession of radiology by delivering high-quality educational content in their field of study. Learn how you can become an honored educator by visiting the website at: https://www.rsna.org/Honored-Educator-Award/

Vahid Yaghmai, MD - 2012 Honored Educator Vahid Yaghmai, MD - 2015 Honored Educator Pulmonary Venous Drainage: Anatomical Comparative Study through MDCT between Patients with Atrial Arrhythmias and Subjects with Sinus Rhythm

Tuesday, Nov. 29 12:45PM - 1:15PM Room: CA Community, Learning Center Station #1

## **Participants**

Alfonso Martin Diaz, BMedSc, San Sebastian De Los Reyes, Spain (*Presenter*) Nothing to Disclose Emilio Cuesta-Lopez, MD, Madrid, Spain (*Abstract Co-Author*) Nothing to Disclose Carmelo Palacios Miras, Madrid, Spain (*Abstract Co-Author*) Nothing to Disclose Montserrat Bret, Madrid, Spain (*Abstract Co-Author*) Nothing to Disclose Elena Refoyo, madrid, Spain (*Abstract Co-Author*) Nothing to Disclose Inmaculada Pinilla Fernandez, Madrid, Spain (*Abstract Co-Author*) Nothing to Disclose Maria Fernandez Velilla, Madrid, Spain (*Abstract Co-Author*) Nothing to Disclose Maribel Torres Sanchez, MD, Madrid, Spain (*Abstract Co-Author*) Nothing to Disclose Jose Antonio Blazquez, Madrid, Spain (*Abstract Co-Author*) Nothing to Disclose

## PURPOSE

To determine possible differences in diameter and anatomy of the pulmonary vein (VP) ostium between patients with susceptible radiofrequency ablation for atrial arrhythmias, compared to controls.

## METHOD AND MATERIALS

73 patients: 49% (36) with paroxysmal atrial fibrillation (PAF), 32% (23) with atypical atrial flutter (AAF) and 19% (14) controls. Angio-MDCT study (64 detectors) was performed without cardiac synchronization.

## RESULTS

Craniocaudal (cc) and anteroposterior (ap) diameter (mm) of the pulmonary veins ostium in patients with arrhytmias and controls, respectively:

RSPVcc: 17 and 14,8; Signif. 0,02 RSPVap: 15,7 and 12,8; Signif. 0,008 RIPVcc: 15,4 and 13,2; Signif. 0,04 RIPVap: 14,7 and 12,3; Signif. 0,04 LSPVcc: 17 and 15,8; Signif. 0,04 LSPVap: 15,2 and 12,8; Signif. 0,01 LIPVcc: 15,9 and 13,3; Signif. 0,05 LIPVap: 13,7 and 12,3; Signif. 0,28 PV anatomical variability of both right (r) and left (l) in patients with PAF, AAF, controls and total values, respectively. p=NS 2r+21: 69%(25); 56%(13); 72%(10); 66%(48) 3r+21: 8%(3); 35%(8); 7%(1); 16%(12) 2r+11: 17%(6); 0%; 14%(2); 11%(8) 3r+11: 3%(1); 9%(2); 7%(1); 6%(4) Others: 3%(1); 0%(0); 0%(0); 1%(1) Total: 100% (36); 100% (23); 100% (14); 100% (73)

### CONCLUSION

A larger diameter (both craniocaudal and anteroposterior) of the ostium of the right pulmonary veins (both upper and lower) was observed in patients with atrial arrhythmias (FAP and FTA) susceptible of ablation, compared to controls. A trend to drainage of right PV in middle lobe was observed in patients with FTA.

## **CLINICAL RELEVANCE/APPLICATION**

Our data seem to indicate that patients with AAT and PAF have a higher variability in the anatomy of the pulmonary veins. Future studies should be necessary to analyze whether the same degree of variability in subjects with no history of atrial arrhythmia.

## CA234-SD-TUB4

Predictive Value of Aortic Valve Calcification and Cerebral White Matter Lesion Load on Peri-procedural Acute Cerebrovascular Events in Patients Undergoing Transcatheter Aortic valve Implantation (TAVI)

Tuesday, Nov. 29 12:45PM - 1:15PM Room: CA Community, Learning Center Station #4

#### Awards

### **Student Travel Stipend Award**

#### **Participants**

Jonas Doerner, MD, Cologne, Germany (*Presenter*) Nothing to Disclose Patrick A. Kupczyk, MD, Bonn, Germany (*Abstract Co-Author*) Nothing to Disclose Julian A. Luetkens, MD, Bonn, Germany (*Abstract Co-Author*) Nothing to Disclose Klaus Storm, Bonn, Germany (*Abstract Co-Author*) Nothing to Disclose Tilman Hickethier, MD, Cologne, Germany (*Abstract Co-Author*) Nothing to Disclose Claas P. Naehle, MD, Bonn, Germany (*Abstract Co-Author*) Nothing to Disclose Hans H. Schild, MD, Bonn, Germany (*Abstract Co-Author*) Nothing to Disclose Alexander Ghanem, Bonn, Germany (*Abstract Co-Author*) Nothing to Disclose

## PURPOSE

Cerebral magnetic resonance imaging (MRI) is able to depict and quantify morphological signs of hypo perfusion and vascular embolism. This is of particular interest in patients with symptomatic aortic stenosis, since the evolving valve dysfunction impairs brain perfusion. In addition, subjects who undergo transcatheter aortic valve implantation (TAVI) are prone to suffer clinically silent peri-procedural cerebrovascular events (CVEs). We aimed to investigate the influence of aortic valve calcification on acute periprocedural CVEs and to characterize brain phenotypes by MRI in order to find risk factors associated with acute peri-procedural CVEs.

### **METHOD AND MATERIALS**

A total of 119 patients who were referred to TAVI were investigated for aortic valve calcification using transesophageal echocardiography. Furthermore, subjects were consecutively investigated using MRI with a dedicated scan protocol including: T2-, FLAIR-, and Diffusion-Weighted Imaging (DWI). Prior to TAVI brains were characterized for total brain volume (TBV), white matter lesion load (WML) and lacunar infarction. Post TAVI, brains were investigated for the onset of acute peri-procedural CVEs using DWI.

## RESULTS

Seventy-eight patients (65.5%) revealed acute peri-procedural CVEs on MRI after TAVI procedure with a favor for the left hemisphere (57.5%). The severity of valve degeneration was associated with peri-procedural CVE burden. Further, patients with acute peri-procedural CVEs demonstrated a baseline WML burden twice as high as patients without ((OR) 2.36 (95% CI: 1.09 - 5.15; p=0.037)). In particular, a peri-ventricular WML distribution pattern was associated with procedural events ((OR: 3.27; 95% CI: 1.47 - 7.26; p=0.0038)). In contrast, lacunar infarctions prior TAVI were not related to acute peri-procedural CVEs. In total, three clinically relevant strokes were observed.

### CONCLUSION

Patients undergoing TAVI demonstrated a wide variety of baseline WML burden, as well as different degrees of aortic valve calcification. Since, the degree of aortic calcification and peri-ventricular WML burden was correlated with acute peri-procedural CVEs, future studies are needed to evaluate the value of such parameters for the prediction of clinical outcome.

## **CLINICAL RELEVANCE/APPLICATION**

Echocardiography and cerebral MRI prior to TAVI can help to identify and allocate patients with high procedural risk.

## CA235-SD-TUB5

Coronary Calcium Detectability and Score across Three Generations of Dual-source CT:A Comparative Phantom Study

Tuesday, Nov. 29 12:45PM - 1:15PM Room: CA Community, Learning Center Station #5

# Participants

Marleen Vonder, MSc , Groningen, Netherlands (*Presenter*) Nothing to Disclose Gert Jan Pelgrim, MD, Groningen, Netherlands (*Abstract Co-Author*) Nothing to Disclose Marcel Greuter, PhD, Groningen, Netherlands (*Abstract Co-Author*) Nothing to Disclose Thomas Henzler, MD, Mannheim, Germany (*Abstract Co-Author*) Research support, Siemens AG; Speaker, Siemens AG Rozemarijn Vliegenthart, MD, PhD, Groningen, Netherlands (*Abstract Co-Author*) Nothing to Disclose Matthijs Oudkerk, MD, PhD, Groningen, Netherlands (*Abstract Co-Author*) Nothing to Disclose Jan Willem C. Gratama, MD, Apeldoorn, Netherlands (*Abstract Co-Author*) Nothing to Disclose Sevrin Ezrah Murray Huijsse, MSc, Groningen, Netherlands (*Abstract Co-Author*) Nothing to Disclose

### PURPOSE

Until now, it remains unclear whether follow-up for coronary calcium score should only be performed on equal generations of dualsource CT (DSCT), or whether different generations of DSCT lead to comparable results. The purpose of this study was to compare coronary calcium detection and quantification of three generations of DSCT systems.

### **METHOD AND MATERIALS**

Three successive generations of DSCT systems (SOMATOM Definition, Definition Flash, Force, Siemens, Forchheim, Germany) were used to scan a non-moving anthropomorphic thorax phantom in which two calcium inserts were placed consecutively (QRM, Möhrendorf, Germany). The first insert, containing 100 small calcifications, was used to determine the detectability. The second insert, containing nine larger calcifications, was used to determine the Agatston calcium score. Scan data acquisition was performed at 120 kVp and 90 reference mAs and reconstructed with generation-specific vendor-recommended settings. Measures were determined automatically using a Matlab script. Kruskal-Wallis test and Mann-Whitney U test were used to analyze differences in detectability and Agatston score

#### RESULTS

The median number and range of detected calcifications were 11(8), 11(4) and 12(2) for first, second and third generation DSCT respectively (p>0.143 for all comparisons). The respective median Agatston score and range were 599 (549-695), 635 (616-685) and 638 (607-680) for the insert with large calcifications. Significant differences in distribution of the Agatston score were found between the first and second (p=0.019), as well as the first and third generation DSCT systems (p=0.026).

# CONCLUSION

This comparative phantom study showed a significant difference in distribution of the Agatston score of first generation compared to second and third generation DSCT. Therefore, one should be cautious when comparing a calcium score or risk stratification based on first generation DSCT with a calcium score based on second or third generation DSCT.

# **CLINICAL RELEVANCE/APPLICATION**

Due to lower variability in calcium scores for second and third generation DSCT, the percentage of misclassification of a patient into one of the CVD risk categories is probably lower compared to stratification based on first generation DSCT calcium score.

# CA236-SD-TUB6

## Dynamic CT Perfusion Study on the Optimal Timing of Single-shot Iodine Distribution Scans

Tuesday, Nov. 29 12:45PM - 1:15PM Room: CA Community, Learning Center Station #6

#### **Participants**

Gert Jan Pelgrim, MD, Groningen, Netherlands (*Presenter*) Nothing to Disclose Eliane Nieuwenhuis, BSC, Groningen, Netherlands (*Abstract Co-Author*) Nothing to Disclose Taylor M. Duguay, Charleston, SC (*Abstract Co-Author*) Nothing to Disclose Matthijs Oudkerk, MD, PhD, Groningen, Netherlands (*Abstract Co-Author*) Nothing to Disclose U. Joseph Schoepf, MD, Charleston, SC (*Abstract Co-Author*) Research Grant, Astellas Group; Research Grant, Bayer AG; Research Grant, General Electric Company; Research Grant, Siemens AG; Research support, Bayer AG; Consultant, Guerbet SA; ; ; Rozemarijn Vliegenthart, MD, PhD, Groningen, Netherlands (*Abstract Co-Author*) Nothing to Disclose Rob J. van der Geest, PhD, Leiden, Netherlands (*Abstract Co-Author*) Nothing to Disclose Akos Varga-Szemes, MD, PhD, Charleston, SC (*Abstract Co-Author*) Nothing to Disclose Stephen R. Fuller, Charleston, SC (*Abstract Co-Author*) Nothing to Disclose

## PURPOSE

This study aims to determine the optimal timing of arterial first pass CT myocardial perfusion imaging (MPI) based on dynamic CT MPI acquisitions.

#### **METHOD AND MATERIALS**

Dynamic stress CT MPI (Definition Flash, Siemens, Germany) at 100 kV and 300 mAs and adenosine perfusion MRI (Magnetom Avanto 1.5T, Siemens, Germany) were used to analyse twenty-five symptomatic patients ( $59 \pm 8.4$  years, 14 male). MRI analysis was only used to determine whether segments were ischemic or non-ischemic. For CT, the Hounsfield units (HU) were monitored during the dynamic CT scan for all myocardial segments along with regions of interest (ROIs) in the ascending (AA) and descending aorta (DA). The time difference between peak enhancement in the myocardium and peak AA and peak DA was calculated. In patients with myocardial ischemia, we calculated the time delay to observe a minimal difference of 15 Hounsfield Unit between normal and ischemic segments after a pre-defined baseline enhancement of 150 or 250 HU in the AA or DA.

#### RESULTS

Ischemia on MRI was observed in 10 patients( $56 \pm 9$  years; 8 male). Time delay between maximal HU in the non-ischemic segments and maximum HU in the DA and AA and was 0.0 s [0.0-2.8] and 2.8 s [2.2-4.3], respectively. Differentiation between ischemic and non-ischemic myocardial segments in CT was best during a time window of 8.6  $\pm$  3.8 s, with a mean maximal HU difference of 28.0  $\pm$  14.5 HU. For the AA, time delays were 4.5 s [2.2-5.6] and 2.2 s [0-2.8] for the 150 HU and 250 HU thresholds, respectively. With the DA, time delays were 2.4 s [0.0-4.8] and 0.0 s [-2.2-2.6] for the 150 HU and 250 HU thresholds, respectively.

## CONCLUSION

Differentiation between normal and ischemic myocardium is best accomplished during a time interval of  $8.6 \pm 3.8$  s. In order to scan during this time window, test bolus or bolus tracking in the AA or DA can be used with the time delays identified here.

## **CLINICAL RELEVANCE/APPLICATION**

The time delays provided in this studies can be used to acquire single shot CT MPI. Imaging at the right moment will secure optimal differentiation between ischemic and non-ischemic segments.

## CA237-SD-TUB7

Volume-Outcome Relationships for Transcatheter Aortic Valve Replacement - Risk-Adjusted and Volume Stratified Analysis of Outcomes

Tuesday, Nov. 29 12:45PM - 1:15PM Room: CA Community, Learning Center Station #7

# Participants

Divya Verma, MD, Phoenix, AZ (*Abstract Co-Author*) Nothing to Disclose Yash Pershad, Phoenix, AZ (*Abstract Co-Author*) Nothing to Disclose Ashish Pershad, MD, Phoenix, AZ (*Abstract Co-Author*) Nothing to Disclose Mohamad Lazkani, MD, Phoenix, AZ (*Abstract Co-Author*) Nothing to Disclose Kenith Fang, MD, Phoenix, AZ (*Abstract Co-Author*) Nothing to Disclose George Gellert, Phoenix, AZ (*Abstract Co-Author*) Nothing to Disclose George Gellert, Phoenix, AZ (*Abstract Co-Author*) Nothing to Disclose Gonsultant, Abbott Laboratories; Consultant, Koninklijke Philips NV; Consultant, Siemens AG Michael F. Morris, MD, Phoenix, AZ (*Presenter*) Speakers Bureau, Medtronic plc

## PURPOSE

The relationship between procedural volume and patient outcome has not been extensively studied in patients undergoing transcatheter aortic valve replacement (TAVR). This study sought to evaluate patient outcomes at low, intermediate, and high volume TAVR sites.

## **METHOD AND MATERIALS**

Within a large health system, TAVR is performed at low volume (<40 cases/year), intermediate volume (40-75 cases/year), and high volume sites (>75 cases/year). 181 consecutive patients undergoing TAVR from 1/2014-6/2015 were studied: 21 from a low volume site, 62 from an intermediate volume site, and 98 from a high volume site. All patients had a pre-procedural CT interpreted by the site radiologist. Heart teams independently decided TAVR prosthesis sizing. Patient data was abstracted from the medical record. The primary endpoint was defined as a 30-day composite of all-cause mortality, in-hospital major adverse cardiovascular events, new post-TAVR hemodialysis, post-procedural cerebrovascular accident, new permanent pacemaker implantation, and hospital readmission. Data were analyzed using risk-adjusted multivariate logistic regression and propensity score analysis.

#### RESULTS

The primary endpoint was reached in 38.8% of patients at the high volume site, 50% at the intermediate volume site, and 76.2% at the low volume site (p<0.01). A significant difference in 30-day readmission rate was primarily responsible for differences in the primary endpoint (47.6%, 32.3% and 9.2% respectively; p<0.01). Propensity score and multivariate regression models identified the following independent predictors of the 30-day composite endpoint: larger hospital volume (OR 0.33, p<0.01), Society of Thoracic Surgeons Predicted Risk of Mortality Score  $\geq 12$  (OR 5.72, p<0.01), and female gender (OR 1.99, p=0.04). Bivariate regression analysis identified additional patient characteristics associated with better post-TAVR outcomes at the high volume site compared to intermediate or low volume sites:  $age \geq 80$  yrs, BMI>30, diabetes, hypertension, prior coronary artery disease (CAD), chronic kidney disease (CKD), and NYHA class III/IV heart failure.

# CONCLUSION

Higher risk patients undergoing TAVR have a better 30-day outcome at a high volume site compared to intermediate and low volume sites.

# **CLINICAL RELEVANCE/APPLICATION**

Among patients undergoing TAVR, those with greater clinical complexity may have better outcomes by undergoing their procedure at a high volume TAVR site.

## CA247-SD-TUB3

Role of Magnetic Resonance in the Prediction of Development of Adverse Outcome and Atrial Fibrillation in Hypertrophic Cardiomyopathy

Tuesday, Nov. 29 12:45PM - 1:15PM Room: CA Community, Learning Center Station #3

### **Participants**

Ana Belen Alcolado Jaramillo, MD, PhD, MAJADAHONDA, Spain (*Presenter*) Nothing to Disclose Isabel Zegri, MAJADAHONDA, Spain (*Abstract Co-Author*) Nothing to Disclose Miguel Pastrana, MD, Majadahonda, Spain (*Abstract Co-Author*) Nothing to Disclose Pablo Garcia Pavia, MAJADAHONDA, Spain (*Abstract Co-Author*) Nothing to Disclose

## PURPOSE

The presentation and clinical course of the Hypertrophic cardiomyopathy (HCM) are extremely variable. The identification of patients at risk of unfavorable out-come is one of the most important issues of the disease. We have analyzed the factors that are associated with adverse events and to the development of atrial fibrillation (AF) in magnetic resonance imaging (MRI).

# METHOD AND MATERIALS

352 HCM patients in sinus rhythm who underwent CMR in 5 centers during the period for 2006-2012 were retrospectively evaluated.Left atrial (LA) volume, indexed LA volume, Left Ventricular (LV) function, myocardial thickness, presence and the extent of late gadolinium-enhancement (LGE) were assessed using CMR.We analyzed the MRI findings in relation to cardiovascular events (heart failure requiring hospitalization, appropriate discharge of Implantable Cardioverter-desfibrillator(ICD) /aborted sudden death (SD), cardiovascular death) and relating to the development of AF

### RESULTS

During a follow-up time of 42+/-24 months, 40 patients developed AF and 30 patients presented adverse events (4 cardiovascular death, 3 aborted sudden deaths, 22 heart failure requiring hospitalization, 5 appropriate discharge of ICD).LA volume and indexed LA volume are predictors of adverse events (LAV 150,5+/-53,1ml vs 126.9+/-51,8ml, p<0,001 and LAV ind 80,5+/-30,1ml/mm2 vs 66,5+/-26,6ml/m2, p<0,001).LA volume and Indexed LA volume were significantly higher in HCM patients with AF than in HCM patients without AF (LAV 152,4+/-74,9 vs 126,1+/-48,3ml, p<0,05 and LAV ind 81,4+/-27,3 vs 66,1+/-25,0ml/m2, p<0,05).However, we have not found a statistically significant relation between fibrosis and development of adverse events or atrial fibrillation.

### CONCLUSION

The LA volume and indexed LA volume are markers of adverse events, regardless of the presence of atrial fibrillation and the presence of fibrosis.LA volume and indexed LA volume have prognostic value more sensitive than fibrosis in predicting adverse cardiovascular events among HCM patients.The LA volume and indexed LA volume are predictors of atrial fibrillation more sensitive than the presence of fibrosis.

## **CLINICAL RELEVANCE/APPLICATION**

Our findings could have important implications for the management of these patients. Patients with increased LA volume would benefit from a comprehensive monitoring and more aggressive therapies for diastolic dysfunction even anticoagulation

Added Value of Functional Lung MRI for Improved Patient Care: Current Techniques and Future Perspectives

Tuesday, Nov. 29 12:45PM - 1:15PM Room: CH Community, Learning Center Station #6

#### Awards Certificate of Merit

## Participants

Julius Renne, MD, Hannover, Germany (*Presenter*) Nothing to Disclose Till F. Kaireit, Hannover, Germany (*Abstract Co-Author*) Nothing to Disclose Christian O. Schoenfeld, MD, Hannover, Germany (*Abstract Co-Author*) Nothing to Disclose Christoph P. Czerner, MD, Hannover, Germany (*Abstract Co-Author*) Nothing to Disclose Andreas Voskrebenzev, Hannover, Germany (*Abstract Co-Author*) Nothing to Disclose Marcel Gutberlet, Dipl Phys, Hannover, Germany (*Abstract Co-Author*) Nothing to Disclose Agilo L. Kern, Hannover, Germany (*Abstract Co-Author*) Nothing to Disclose Frank K. Wacker, MD, Hannover, Germany (*Abstract Co-Author*) Research Grant, Siemens AG; Research Grant, Pro Medicus Limited; Research Grant, Delcath Systems, Inc; Jens Vogel-Claussen, MD, Hannover, Germany (*Abstract Co-Author*) Nothing to Disclose

# **TEACHING POINTS**

1. Familiarize the readers with MRI techniques for regional pulmonary function assessment, including proton MRI as well as fluorine and hyperpolarized gas MRI.2. To learn about advantages and drawbacks of functional lung MRI techniques.3. To learn about current clinical applications and promising future clinical applications of functional lung MRI.

### TABLE OF CONTENTS/OUTLINE

1. Brief summary of morphological MRI sequences.2. Pulmonary functional imaging, the technical prerequisites: i. Proton MRIii. Fluorinated gas MRIii. Hyperpolarized gas MRI3. Advantages and drawbacks of each technique, emphasizing on practical aspects in clinical routine as well as in the research environment.4. Overview of recent studies and clinical applications in different disease areas of the introduced techniques.5. Future perspectives.

# CH205-ED-TUB7

Recurrence Patterns Post Treatment for Early Stage Lung Cancer and the Emerging Evidence for Imaging Surveillance: A Pictorial Review

Tuesday, Nov. 29 12:45PM - 1:15PM Room: CH Community, Learning Center Station #7

## Participants

Orla Drumm, MBBCh, MSc, Dublin, Ireland (*Abstract Co-Author*) Nothing to Disclose Eoghan J. McCarthy, MBBCh, Philadelphia, PA (*Abstract Co-Author*) Nothing to Disclose John Kavanagh, FFR(RCSI), FRCR, Dublin, ON (*Abstract Co-Author*) Nothing to Disclose Peter Beddy, MD, FRCR, Dublin, Ireland (*Presenter*) Nothing to Disclose

## **TEACHING POINTS**

Teaching Points1. Identify common sites of disease recurrence post radical treatment for early stage lung cancer2. Learn how to detect lung cancer recurrence - assessment for disease recurrence requires knowledge of the normal post treatment appearance and how this can change over time, especially post SBRT and ablation.3. Illustrate the current guidelines for surveillance post curative treatment of early stage disease and update on the recently published literature on imaging follow up (table 1).

# TABLE OF CONTENTS/OUTLINE

OverviewSurgery remains the gold standard treatment for early stage disease in suitable candidates however Stereotactic Body Radiotherapy (SBRT) and percutaneous ablation are effective alternatives.Recurrence PatternsThe risk of recurrence post treatment for early stage disease ranges from 15-30% depending on the patient cohort and treatment employed. This exhibit will review the common local and distance recurrence patterns for each treatment modality. Tips and TricksThe clinical cases will highlight how to identify recurrent disease and differentiate from post treatment changeEvidence for Imaging Follow-upDiscuss the evidence behind current imaging surveillance guidelines. The review will also focus on new evidence to support PET-CT surveillance for patients treated with SBRT and lung ablation.

# CH260-SD-TUB1

Quantification of Lung Perfusion Blood Volume (lung PBV) by Dual-energy CT in Patients with Chronic Thromboembolic Pulmonary Hypertension (CTEPH) before and after Balloon Pulmonary Angioplasty (BPA): Preliminary Results

Tuesday, Nov. 29 12:45PM - 1:15PM Room: CH Community, Learning Center Station #1

## Participants

Hirofumi Koike, Nagasaki, Japan (*Presenter*) Nothing to Disclose Eijun Sueyoshi, MD, Nagasaki, Japan (*Abstract Co-Author*) Nothing to Disclose Ichiro Sakamoto, Nagasaki, Japan (*Abstract Co-Author*) Nothing to Disclose Masataka Uetani, MD, Nagasaki, Japan (*Abstract Co-Author*) Nothing to Disclose Tomoo Nakata, Nagasaki, Japan (*Abstract Co-Author*) Nothing to Disclose Kouji Maemura, Nagasaki, Japan (*Abstract Co-Author*) Nothing to Disclose

## PURPOSE

Balloon pulmonary angioplasty (BPA) is a treatment option for patients with chronic thromboembolic pulmonary hypertension (CTEPH). Its effect on pulmonary perfusion has not been quantified; we examined the clinical significance of pulmonary blood volume (PBV) using dual-energy computed tomography (DECT) in patients with CTEPH undergoing BPA.

## **METHOD AND MATERIALS**

In this retrospective study of 16 BPAs in eight female patients with CTEPH, we evaluated both-lung (n=16), right- or left-lung (n=32), and three right- or left-segment (upper, middle, and lower) (n=96) PBVs before and after BPA, using DECT. We evaluated the relationships between improvement in lung PBV and pulmonary artery (PA) pressure (PAP), cardiac index (CI), pulmonary vascular resistance (PVR), and 6-min walking distance. We measured PA enhancement (PAenh) on DECT images and calculated lung PBV/PAenh to adjust timing.

### RESULTS

Pre- and post-BPA 6-segment lung PBV/PAenh were  $0.067\pm0.021$  and  $0.077\pm0.019$ , respectively, in the treated segment (p<0.0001). There were significant positive correlations between pre- to post-BPA improvements in both-lung PBV/PAenh and PAP (R=0.69, p=0.005), PVR (R=0.56, p=0.03), and 6-min walking distance (R=0.67, p=0.01).

## CONCLUSION

Improved PBV after BPA, reflecting increased lung perfusion, was positively correlated with PAP, PVR, and 6-min walking distance. Lung PBV may be an indicator of BPA treatment effect.

# **CLINICAL RELEVANCE/APPLICATION**

Lung PBV may be an indicator of BPA treatment effect.

# CH261-SD-TUB2

Type B Intramural Hematoma of the Aorta: Clinical Importance of Minimal Enhancement of the Thrombosed False Lumen on CT

Tuesday, Nov. 29 12:45PM - 1:15PM Room: CH Community, Learning Center Station #2

# Participants

Eijun Sueyoshi, MD, Nagasaki, Japan (*Presenter*) Nothing to Disclose Hiroki Nagayama, Shimabara, Japan (*Abstract Co-Author*) Nothing to Disclose Ichiro Sakamoto, Nagasaki, Japan (*Abstract Co-Author*) Nothing to Disclose Masataka Uetani, MD, Nagasaki, Japan (*Abstract Co-Author*) Nothing to Disclose

## PURPOSE

To investigate the instability, morphology, natural course, and prognostic value of enhancement of the thrombosed false lumen on contrast-enhanced CT scans in patients with type B intramural hematoma of the aorta (IMH).

# METHOD AND MATERIALS

The ethics committee of our hospital approved this study. A total of 65 patients (42 men; mean age: 75 years) with type B IMH were retrospectively evaluated between 2007 and 2014. On initial CT scans, attenuation of the false lumen (AFL) was determined before enhancement and in the early and delayed phases of contrast enhancement. Then enhancement of the false lumen (EFL) was calculated (AFL in the delayed image – AFL in the precontrast image). The Cox proportional hazards model was employed to estimate the risk of IMH-related events, including death or surgical repair.

### RESULTS

The mean AFL for precontrast CT, arterial phase enhanced CT, and delayed phase enhanced CT was  $56.3\pm10.5$ ,  $59.9\pm10.8$ , and  $63.7\pm11.1$  HU, respectively, while the mean EFL was  $7.4\pm9.0$  HU.According to multivariate Cox regression analysis, EFL was the only independent predictor of IMH-related events (n=23) (hazard ratio, 1.008; 95% CI, 1.03 - 1.15; P=0.0044) and IMH-related death/surgical repair (n=10) (hazard ratio, 1.111; 95% CI, 1.017 - 1.213; P=0.0197).

## CONCLUSION

In patients with IMH, EFL is the most powerful predictor of IMH-related events, as well as IMH-related death or surgical repair. Patients with type B IMH who have a high EFL should be followed more carefully by surveillance imaging than patients with a low EFL.

## **CLINICAL RELEVANCE/APPLICATION**

Type B IMH patients with a high enhancement of the false lumen (EFL) should be monitored more carefully by imaging during followup than those with a low EFL.

# CH262-SD-TUB3

### Mycobacterium Tuberculosis Infection in HIV Positive Patients: HRCT Evaluation

Tuesday, Nov. 29 12:45PM - 1:15PM Room: CH Community, Learning Center Station #3

#### Participants

Akash Rajaram, MBBS, MD, Bangalore, India (*Presenter*) Nothing to Disclose Sanjaya Viswamitra, MD, Bengaluru, India (*Abstract Co-Author*) Nothing to Disclose Ashok Adekal, MD, Bangalore, India (*Abstract Co-Author*) Nothing to Disclose SRINATH MG, BANGALORE, India (*Abstract Co-Author*) Nothing to Disclose

## PURPOSE

1. To learn the HRCT findings of pulmonary tuberculosis in HIV positive patients. 2. To correlate the mortality rate and CD4 count with HRCT findings.

## METHOD AND MATERIALS

The study was a hospital based retrospective study. Five hundred cases were reviewed from the past seven years. The HRCT findings from patients diagnosed with pulmonary TB, established by M. tuberculosis detection in bronchoalveolar lavage or sputum/biopsy samples. Two observers independently reviewed HRCT images and decided on the presence and distribution of: (i) miliary nodules, (ii) cavitation (iii) centrilobular tree-in-bud nodules, (iii) ground-glass attenuation and consolidation, (iv) pleural effusion and (v) mediastinal lymphadenopathy.

### RESULTS

500 patients [330 males, 170 females; median age, 48 years (range, 17–69 years)]. The main HRCT pattern was miliary nodules (45%), followed by cavitation (15%), centrilobular tree-in-bud nodules (8%), ground-glass attenuation and consolidation (10%), pleural effusion (10%) and mediastinal lymph node enlargement (12%). The miliary nodules were randomly distributed. In patients with cavitation and centrilobular tree-in-bud nodules, 70% of abnormalities were found in the upper lobes. Pleural effusion was unilateral in 70% of cases. The overall mortality rate was 30%. The mortality rate was increased significantly in patients with miliary nodules (p < 0.05). It was 56% in these patients. The mean CD4 count was lowest in patients with miliary nodules.

# CONCLUSION

The main HRCT finding in HIV positive patients with pulmonary TB was miliary nodules, followed by cavitation. Miliary nodules were associated with a worse prognosis in these patients. The CD4 count was the lowest in patients with miliary nodules.

## **CLINICAL RELEVANCE/APPLICATION**

HRCT findings of pulmonary tuberculosis in HIV positive patients aids to the diagnosis and prognosis of the disease and is recommended in the initial evaluation of high risk population.

## Quantitative Chest CT for Predicting Survival in Patients with Restrictive Allograft Syndrome

Tuesday, Nov. 29 12:45PM - 1:15PM Room: CH Community, Learning Center Station #4

#### **Participants**

Miho Horie, MSc, Toronto, ON (*Presenter*) Research Grant, Toshiba Corporation Pascal Salazar, Minnetonka, MN (*Abstract Co-Author*) Employee, Toshiba Corporation Tomohito Saito, MD, PhD, Toronto, ON (*Abstract Co-Author*) Nothing to Disclose Tereza Martinu, Toronto, ON (*Abstract Co-Author*) Nothing to Disclose Shafique Keshavjee, MD, Toronto, ON (*Abstract Co-Author*) Nothing to Disclose Narinder S. Paul, MD, Toronto, ON (*Abstract Co-Author*) Research Grant, Toshiba Corporation Research Grant, Carestream Health, Inc

## PURPOSE

Chronic lung allograft dysfunction (CLAD) limits long-term survival following lung transplantation (LTx). Restrictive Allograft Syndrome (RAS) is a particularly aggressive sub-type of CLAD and a significant cause of morbidity and mortality. There is no established prognostic indicator for RAS. The purpose of this study was to investigate the utility of quantitative lung density analysis in predicting patient survival at time of RAS diagnosis.

## **METHOD AND MATERIALS**

A retrospective study of patients following bilateral LTx who underwent surveillance with corresponding pulmonary function tests (PFT) and low dose CT (120kV, 50mA, 0.5s) was conducted. 22 patients were diagnosed with RAS (Average of 26 months after LTx) on the basis of abnormal PFT (FEV1<80% and TLC<90% of post-LTx baseline). The CT density of lung parenchyma for each patient was plotted as a histogram and evaluated quantitatively using customized software and a 3D post processing workstation (Vitrea, Vital Images, Minn). The relative contributions of low and high density areas from each lung were determined from the histogram. Nonparametric indices were calculated; including the right tail weight (rqw) and the left tail weight (lqw) of the CT density distribution as well as the ratio: log (rqw0.75/lqw 0.25). A higher tail ratio indicates more high-density regions (e.g. fibrosis) compared with low-density regions (e.g. emphysema). The maximum values for each patient were obtained. The Spearman's correlation coefficient was calculated to evaluate the correlation between the survival post RAS diagnosis and the tail ratio. The area under the Receiver Operating Characteristic curve (AUC) was calculated for prediction of survival times (>1-year versus  $\leq$  1-year).

## RESULTS

The Spearman's correlation coefficient showed a moderate correlation, r = -0.49 (P<0.05) between the survival post RAS diagnosis and the tail ratio. The AUC was 0.73 with a sensitivity of 89% and specificity of 54% when the optimal criterion tail ratio value (0.65) was selected for prediction of 1-year survival.

## CONCLUSION

In patients with RAS, quantitative parameters derived from a lung density histogram may predict the 1-year survival after the clinical diagnosis.

## **CLINICAL RELEVANCE/APPLICATION**

A quantitative metric for RAS patients that helps to determine likelihood of survival 1-year post diagnosis may be useful for patient management.

## CH264-SD-TUB5

Accuracy of Hyperpolarized 129Xe Ventilation MRI in Obstructive Pulmonary Disease: A Retrospective Casecontrol Study

Tuesday, Nov. 29 12:45PM - 1:15PM Room: CH Community, Learning Center Station #5

**FDA** Discussions may include off-label uses.

### Participants

Lukas Ebner, MD, Durham, NC (*Presenter*) Nothing to Disclose Rohan Virgincar, Durham, NC (*Abstract Co-Author*) Nothing to Disclose Andreas Christe, Bern, Switzerland (*Abstract Co-Author*) Nothing to Disclose Achille Mileto, MD, Durham, NC (*Abstract Co-Author*) Nothing to Disclose Joseph G. Mammarappallil, MD, PhD, Durham, NC (*Abstract Co-Author*) Nothing to Disclose Mu He, Durham, NC (*Abstract Co-Author*) Nothing to Disclose H. Page McAdams, MD, Durham, NC (*Abstract Co-Author*) Research Grant, General Electric Company; Consultant, MedQIA Imaging Core Laboratory ; Author, Reed Elsevier; Author, UpToDate, Inc; Research Consultant, F. Hoffmann-La Roche Ltd; Research Consultant, Boehringer-Ingelheim GmbH Bastiaan Driehuys, PhD, Durham, NC (*Abstract Co-Author*) Research support, General Electric Company; Royalties, General Electric Company; Stockholder, Polarean, Inc

Justus E. Roos, MD, Durham, NC (Abstract Co-Author) Nothing to Disclose

### PURPOSE

To determine the diagnostic accuracy of hyperpolarized (HP)129Xe MR imaging in detecting ventilation defects in obstructive lung disease by using a multi-reader based approach.

## **METHOD AND MATERIALS**

This retrospective, HIPAA-compliant study was approved by our IRB; informed consent was obtained prior to enrolment. From 2012 through 2015, 66 subjects (n=38 healthy volunteers [mean age, 41 years]; asthma patients, n=20 [mean age, 44 years]; COPD patients, n=8 [mean age, 67 years]) underwent HP129Xe ventilation MR imaging at 1.5T, following inhalation of 0.5-1 liter of isotopically enriched 129Xe gas (83% 129Xe, polarized to 20% by spin-exchange optical pumping). 129Xe ventilation MR images were reconstructed and assessed by five blinded, independent readers for the presence of ventilation defects using a percentage scoring-system (0-100%). Pre-MR pulmonary function testing (PFT), which was prospectively obtained in all study participants, represented the reference standard for establishing the presence of airway obstruction (diagnostic threshold: FEV1%<0.8; FEV1/FVC<0.70). A linear regression analysis was employed to compare reader-based scores from 129Xe ventilation MR imaging assessment and PFTs. Sensitivity, specificity and diagnostic accuracy of 129Xe ventilation MRI in detecting ventilation defects were estimated using a receiving operating characteristic (ROC) analysis. Inter-rater agreement was assessed by using kappa statistics.

### RESULTS

Reader-based scores of 129Xe ventilation MR images were significantly higher in patients with airway obstruction compared to healthy subjects (P<.0001). 129Xe ventilation MRI showed a moderate correlation with FEV1% (R2=.378), whereas it strongly correlated with FEV1/FVC (R2=.664). Our ROC analyses showed that an optimized threshold of 12% from reader-based scores of 129Xe ventilation MR images yielded a sensitivity of 86%, specificity of 93%, and an overall diagnostic accuracy of 91% for detection of ventilation defects. There was a moderate agreement among the five readers ( $\kappa$ =.44).

### CONCLUSION

HP129Xe ventilation MR imaging can accurately detect ventilation defects in patients with obstructive, pulmonary disease.

# **CLINICAL RELEVANCE/APPLICATION**

HP129Xe MRI is clinically useful in detecting ventilation defects in obstructive, pulmonary disease. Based on our findings, it might also be used for monitoring regional ventilation changes.

## **Honored Educators**

Presenters or authors on this event have been recognized as RSNA Honored Educators for participating in multiple qualifying educational activities. Honored Educators are invested in furthering the profession of radiology by delivering high-quality educational content in their field of study. Learn how you can become an honored educator by visiting the website at: https://www.rsna.org/Honored-Educator-Award/

## H. Page McAdams, MD - 2012 Honored Educator

# ER223-SD-TUB1

### Perisiplenic Hematoma Volume Calculation with a New Formula Confirmed with Semi-Automated Method

Tuesday, Nov. 29 12:45PM - 1:15PM Room: ER Community, Learning Center Station #1

#### Participants

Uygar Teomete, MD, Coral Gables, FL (*Presenter*) Nothing to Disclose Tuncer Ergin, MD, Ankara, Turkey (*Abstract Co-Author*) Nothing to Disclose Ozgur Dandin, MD, Bursa, Turkey (*Abstract Co-Author*) Nothing to Disclose Onur Osman, PhD, Istanbul, Turkey (*Abstract Co-Author*) Nothing to Disclose Ferhat Cuce, MD, PhD, Van, Turkey (*Abstract Co-Author*) Nothing to Disclose Gokalp Tulum, Istanbul, Turkey (*Abstract Co-Author*) Nothing to Disclose Adlan Olsun, Istanbul, Turkey (*Abstract Co-Author*) Nothing to Disclose

### PURPOSE

The correct calculation of intraperitoneal hematoma is vital for the management of patients who have trauma. Our aim is to present a new formula for calculating perisplenic hematoma due to abdominal trauma comparing to the conventional method.

## **METHOD AND MATERIALS**

Data of the patients who had traumatic spleen injuries were evaluated from the database of trauma registry. Randomly selected 25 CT scans from 25 patients with traumatic perisplenic hematomas were studied. We developed a semi-automated system calculating the perisplenic hematoma volumes in trauma patients utilized as the reference standard. By two radiologists, the calculations were performed by using conventional formula, trilinear formula, direct method and semiautomatic computer-aided method. Finally, the results were compared. Total volume (spleen+ hematoma) was provided by using the W1T1L1/2 formula in the conventional method. The spleen volume was obtained as 0.36(W2T2L2)+28. The total volume was provided as total volume minus spleen volume. We proposed trilinear approximation functions as total volume=13.96W1-3.20T1-0.44L1-0.067W1T1-0.13W1L1+0.0417T1L1+9.66x10-4W1T1L1, spleen volume=6.055W2+1.75T2-2.76L2-0.119W2T2-0.0154W2L2+0.0255T2L2+8.82x10-4W2T2L2. The hematoma volume was provided by the subtracting of spleen volume from total volume. With direct method, the hematoma volume was calculated as hematoma volume=3.713W1+5.834W2-0.606T1+0.503T2+1.52L1-4.257L2+0.016W1T1-0.128W2T2 -0.0691W1L1+0.015W2L2+0.006T1L1+0.0326T2L2+5.51 x10-4W1T1L1-4.89x10-4W2T2L2 where W,T, L are width, thickness and length.All co-efficient were obtained by least squares method which minimize the error.

#### RESULTS

The root mean square error of hematoma volume for, the conventional method, trilinear and direct method were 78.54, 67.60 and 24.07 mL, respectively.

# CONCLUSION

The volume of perisplenic hematoma calculation was feasible for all cases. Our new formula created with direct method had high accuracy rate comparing the conventional method. This new formula considered to has an important role in the management of patients who have perisplenic hematoma due to trauma.

## **CLINICAL RELEVANCE/APPLICATION**

The correct and rapid calculation of perisplenic hematoma volume with our new formula and semiautomatic methods will help to clinicians by affecting the management and outcome of the patients who have abdominal trauma.

Perinephric Fat Stranding on Abdominal CT in Adult Emergency Department Patients: What Are The Clinical Implications?

Tuesday, Nov. 29 12:45PM - 1:15PM Room: ER Community, Learning Center Station #2

# Participants

Erin N. Gomez, MD, Columbia, MD (*Abstract Co-Author*) Nothing to Disclose Susan Lin, Baltimore, MD (*Abstract Co-Author*) Nothing to Disclose Elliot K. Fishman, MD, Baltimore, MD (*Abstract Co-Author*) Institutional Grant support, Siemens AG; Institutional Grant support, General Electric Company; Linda Regan, MD, Baltimore, MD (*Abstract Co-Author*) Nothing to Disclose Amit Pahwa, MD, Baltimore, MD (*Abstract Co-Author*) Nothing to Disclose Pamela T. Johnson, MD, Baltimore, MD (*Presenter*) Consultant, National Decision Support Company

## PURPOSE

Perinephric fat stranding (PFS) is a common finding on abdominal CT. Practitioners have voiced uncertainty regarding the clinical significance of patients with PFS on CT and whether it is an indicator of urinary tract infection (UTI). The purpose of this study is to determine the frequency of UTI and define an evidence-based management algorithm for adult emergency department patients with PFS on CT.

## **METHOD AND MATERIALS**

CT reports of adult patients imaged in the ED were retrospectively searched to identify "perinephric stranding" in the dictated report. Medical records of 166 subjects imaged between 2013 and 2015 were reviewed for clinical presentation, laboratory and culture data, CT findings, medical diagnosis and management.Criteria for clinical diagnoses were defined as follows: Uncomplicated cystitis: asymptomatic pyuria UTI: symptomatic pyuria Pyelonephritis: symptomatic pyuria + fever OR flank pain elevated WBC + fever + flank pain Statistical analysis was performed using Microsoft Excel and Stata version 14.

### RESULTS

Preliminary data includes 93 male and 73 female subjects with average age of 53 years (range 20-88 years). The most common additional CT finding reported in subjects with PFS was obstructing stone (72/166, 43%). These subjects were removed from further evaluation. Of the 94 patients without an obstructing stone, 17% (16/94) met criteria for UTI and 12% (11/94) met criteria for pyelonephritis. Of the 91 patients without an obstructing stone who had urinalysis, 70% (64/91) had pyruia, but 52% (47/91) had asymptomatic pyuria. Additional analyses of the imaging and clinical findings for the entire cohort of 300 subjects will be used to generate a management algorithm defining which patients with PFS should be treated for urinary tract infection.

# CONCLUSION

Most adult emergency department patients in this cohort with perinephric stranding on abdominal CT had pyuria, but it was asymptomatic in the majority of cases. Clinical criteria for UTI and pyelonephritis were met in < 30% and should be heavily weighted in management decision making.

## **CLINICAL RELEVANCE/APPLICATION**

Practitioners and radiologists must recognize that perinephric fat stranding, even in patients with pyuria, does not necessarity indicate the presence of a clinically significant urinary tract infection. Evidence based management algorithms are warranted to define which patients require treatment.

### **Honored Educators**

Presenters or authors on this event have been recognized as RSNA Honored Educators for participating in multiple qualifying educational activities. Honored Educators are invested in furthering the profession of radiology by delivering high-quality educational content in their field of study. Learn how you can become an honored educator by visiting the website at: https://www.rsna.org/Honored-Educator-Award/

Pamela T. Johnson, MD - 2016 Honored Educator Elliot K. Fishman, MD - 2012 Honored Educator Elliot K. Fishman, MD - 2014 Honored Educator Elliot K. Fishman, MD - 2016 Honored Educator Non-contrast MDCT for Ureteral Calculi and Alternative Diagnoses: Yield in Adult Women versus in Adult Men

Tuesday, Nov. 29 12:45PM - 1:15PM Room: ER Community, Learning Center Station #3

#### Awards

#### **Student Travel Stipend Award**

#### **Participants**

Parisa Fani, MD, Hamilton, ON (*Presenter*) Nothing to Disclose Michael N. Patlas, MD, FRCPC, Hamilton, ON (*Abstract Co-Author*) Nothing to Disclose Sandra Monteiro, PhD, Hamilton, ON (*Abstract Co-Author*) Nothing to Disclose Douglas S. Katz, MD, Mineola, NY (*Abstract Co-Author*) Nothing to Disclose

#### PURPOSE

To determine the yield of non-contrast CT(NCCT) for the diagnosis of ureteral calculi and alternative diagnoses in adult men versus adult women presenting with suspected renal colic to the emergency department (ED) of a teaching hospital.

#### **METHOD AND MATERIALS**

Our IRB-approved a retrospective review of the non-contrast CT scans of the abdomen and pelvis (APNCCT) performed on adult patients (18 years and older) presenting to a single emergency department with acute flank pain over a 25-month period. Patients with known obstructive ureteral calculi, or with known urinary tract infection, malignancy, or trauma, prior to CT, were all excluded. We compared the prevalence of ureteral calculi and alternative diagnoses between the men and the women, based on review of the images. P values and Confidence Intervals (CI) were determined using the chi-square test.

#### RESULTS

One attending radiologist and one radiology resident randomly selected (using a number generator) and reviewed 400 scans from a total of 1097 APNCCT examinations performed from October 1, 2011, to October 30, 2013, at our institution (representing approximately 1/3 of the examinations). The mean patient age was 55.2 years, with a range of 19 to 90 years. This included 170 women (mean age 56.8 years), and 230 men (mean age 54.2 years). Ureteral calculi were observed in 42.5% of all patients, including in 111 men (48%) and 59 women (34.7%). The prevalence of ureteral calculi in men was significantly higher than in women (p<0.01, Confidence Level of 95%, and CI of 13.3). Alternative diagnoses were demonstrated on APNCCT in 12.5% of patients, including 23 in men (5.7%) and 27 in women (6.7%). Alternative diagnoses in women included ovarian cyst (n=1), ovarian torsion (n=1), and degeneration of a uterine fibroid (n=1).There was no statistically significant difference in the overall prevalence of alternative diagnoses between men and women (p>0.2).

## CONCLUSION

Based on our single-institution retrospective review of a subset of adult patients, the likelihood of a ureteral calculus being present on APNCCT performed for suspected renal colic was significantly higher in men compared with in women.

## **CLINICAL RELEVANCE/APPLICATION**

APNCCT had a lower yield in women presenting to a single teaching hospital's ED with suspected renal colic, compared with in men, although the alternative diagnosis rate was not statistically different.

#### **Honored Educators**

Presenters or authors on this event have been recognized as RSNA Honored Educators for participating in multiple qualifying educational activities. Honored Educators are invested in furthering the profession of radiology by delivering high-quality educational content in their field of study. Learn how you can become an honored educator by visiting the website at: https://www.rsna.org/Honored-Educator-Award/

Douglas S. Katz, MD - 2013 Honored Educator Douglas S. Katz, MD - 2015 Honored Educator

## The Feasibility of Dual Energy Computed Tomography in Cardiac Contusion Imaging

Tuesday, Nov. 29 12:45PM - 1:15PM Room: ER Community, Learning Center Station #5

#### Awards

#### **Student Travel Stipend Award**

#### **Participants**

Recep Sade, MD, Erzurum, Turkey (*Presenter*) Nothing to Disclose Mecit Kantarci, MD, PhD, Erzurum, Turkey (*Abstract Co-Author*) Nothing to Disclose Hayri Ogul, Erzurum, Turkey (*Abstract Co-Author*) Nothing to Disclose Ummugulsum Bayraktutan, Erzurum, Turkey (*Abstract Co-Author*) Nothing to Disclose Mustafa Uzkeser, Erzurum, Turkey (*Abstract Co-Author*) Nothing to Disclose Sahin Aslan, Erzurum, Turkey (*Abstract Co-Author*) Nothing to Disclose Enbiya Aksakal, Erzurum, Turkey (*Abstract Co-Author*) Nothing to Disclose Necip Becit, Erzurum, Turkey (*Abstract Co-Author*) Nothing to Disclose

# PURPOSE

The purpose of this study is the evaluation of the efficiency and feasibility of DECT use in the diagnosis of cardiac contusion with the mildest blunt cardiac injury (BCI)

## **METHOD AND MATERIALS**

From February 2014 to September 2015, a total of 17 consecutive patients (10 men and 7 women; median age 51 years [20-78]) were enrolled in the study. DECT was performed within 48 hours of the trauma and a subsequent control DECT was performed a little less than one year after the first examination. All examinations were analyzed on iodine map images by two experienced radiologists. Interobserver agreement was calculated.

## RESULTS

The contusion areas were amorphous, with considerable variation in their size, shape, and density. Contusions were primarily located in the left ventricle's free wall, the ventricular septum, and the apex, respectively. In 10 patients, contusion areas disappeared upon control examination. In four patients, the contusion areas decreased but were still present in the control examination. The interobserver agreements were almost perfect with respect to the presence of cardiac contusion, the anatomic location of contusions, and the contusion areas (kappa values of 1.0, 1.0, and 0.9, respectively).

#### CONCLUSION

DECT can show cardiac contusion and can be usable and feasible for the diagnosis and follow-up study in BCIs. DECT is a very new, user-independent and valuable imaging technique

## **CLINICAL RELEVANCE/APPLICATION**

DECT can show cardiac contusion and can be usable and feasible for the diagnosis and follow-up study in BCIs.

# GI024-EB-TUB

# Enterocutaneous Fistula: Can Interventional Radiologists Fix Big Leaks?

Tuesday, Nov. 29 12:45PM - 1:15PM Room: GI Community, Learning Center Hardcopy Backboard

#### **Participants**

Nicole A. Keefe, MD, Charlottesville, VA (Presenter) Nothing to Disclose

Ziv J. Haskal, MD, Baltimore, MD (*Abstract Co-Author*) Advisory Board, W. L. Gore & Associates Research Consultant, W. L. Gore & Associates Advisory Board, IC Sciences Corporation Royalties, Cook Group Incorporated Research Support, C. R. Bard, Inc Research Consultant, C. R. Bard, Inc Advisory Board, NovaShunt AG Advisory Board, Endoshape, Inc

# **TEACHING POINTS**

Enterocutaneous fistulae (ECF) can be a chronic, debilitating, high cost condition with a significant impact on quality of life. While surgical and medical approaches may prove successful, these approaches carry operative morbidity, a protracted time course and notable failure rates. Interventional radiologic management comprises mapping, abscess control, and, increasingly, closure techniques. Methods include glues, sealants, collagen, and plugs for both low and high output ECF. Case series have demonstrated success rates ranging from 71-100%. Newer materials, including smooth intestinal submucosa (SIS), may allow treatment of larger, high output, complicated proximal fistulae. This poster reviews indications, fistulography, and an algorithmic approach to catheter-based interventions.

## **TABLE OF CONTENTS/OUTLINE**

- 1. Pathophysiology
- 2. Diagnostic Imaging
- 3. Conventional Treatment
- 4. Indications/Contraindications
- 5. Sample cases
- 6. Outcomes

# GI379-SD-TUB1

Colorectal Carcinoma: Ex Vivo Evaluation with 3-T High-Spatial-Resolution Quantitative T2 Mapping--Correlation with Histopathologic Findings

Tuesday, Nov. 29 12:45PM - 1:15PM Room: GI Community, Learning Center Station #1

## **Participants**

Ichiro Yamada, MD, Tokyo, Japan (*Presenter*) Nothing to Disclose Norio Yoshino, DDS, Bunkyo-ku, Japan (*Abstract Co-Author*) Nothing to Disclose Keigo Hikishima, PhD, MS, Kawasaki, Japan (*Abstract Co-Author*) Nothing to Disclose Naoyuki Miyasaka, MD, Tokyo, Japan (*Abstract Co-Author*) Nothing to Disclose Shinichi Yamauchi, MD, Bunkyo-ku, Japan (*Abstract Co-Author*) Nothing to Disclose Hiroyuki Uetake, MD, Bunkyo-ku, Japan (*Abstract Co-Author*) Nothing to Disclose Masamichi Yasuno, MD, Bunkyo-ku, Japan (*Abstract Co-Author*) Nothing to Disclose Yukihisa Saida, MD, Bunkyo-ku, Japan (*Abstract Co-Author*) Nothing to Disclose Ukihide Tateishi, MD, PhD, Tokyo, Japan (*Abstract Co-Author*) Nothing to Disclose Daisuke Kobayashi, MD, Tokyo, Japan (*Abstract Co-Author*) Nothing to Disclose Yoshinobu Eishi, MD, Tokyo, Japan (*Abstract Co-Author*) Nothing to Disclose

#### PURPOSE

To establish the feasibility of high-spatial-resolution (HSR) quantitative T2 mapping at 3-T MR imaging as a method of diagnosing the depth of mural invasion by colorectal carcinomas.

# METHOD AND MATERIALS

Twenty colorectal specimens each containing a carcinoma were imaged with a 3-T MR system equipped with a 4-channel phasedarray surface coil. HSR quantitative T2 maps were acquired by using a spin-echo sequence: repetition time/echo time (TR/TE), 7650/22.6-361.6 ms (16 echoes); field of view (FOV), 87 x 43.5 mm; section thickness, 2 mm; matrix, 448 x 224; and averages, one. HSR T2-weighted images were also acquired by using a fast spin-echo sequence: TR/TE, 5000/91 ms; FOV, 87 x 43.5 mm; section thickness, 2 mm; matrix, 384 x 192; averages, 10; and turbo factor, 12. Differences between the T2 values (ms) of the tumor tissue and both the colorectal wall layers and fibrosis were measured, and the MR images and the histopathologic findings were then compared.

#### RESULTS

HSR quantitative T2 maps and T2-weighted images acquired at 3 T clearly depicted the normal colorectal wall in all 20 specimens (100%) as consisting of eight layers, each of which had T2 values that differed from its adjacent layers (P < 0.001): epithelium (84.1 ± 7.4 ms), lamina propria mucosae (111.8 ± 5.2 ms), muscularis mucosae (85.5 ± 10.4 ms), submucosa (165.9 ± 20.9 ms), inner circular muscle (95.2 ± 4.7 ms), intermuscular connective tissue (121.2 ± 10.6 ms), outer longitudinal muscle (95.1 ± 5.9 ms), and subserosa-serosa or adventitia (166.4 ± 16.4 ms). HSR quantitative T2 maps made it possible to clearly differentiate between the tumor tissue (104.2 ± 6.4 ms) and fibrosis (73.6 ± 9.4 ms) (P < 0.001). In 19 of the 20 colorectal carcinomas (95%), HSR quantitative T2 maps made it possible to determine the same depth of tumor invasion of the colorectal wall as determined by the histopathologic examination.

# CONCLUSION

3-T HSR quantitative T2 mapping enables clear depiction of the layers of the colorectal wall and clear differentiation of tumor tissue from fibrosis, and it provides excellent diagnostic accuracy of mural invasion by colorectal carcinomas.

## **CLINICAL RELEVANCE/APPLICATION**

By using 3-T HSR quantitative T2 mapping, we may have an effective tool to noninvasively diagnose the depth of mural invasion by colorectal carcinomas.

## GI380-SD-TUB2

Dual-energy CT to Evaluate the Efficacy of Neoadjuvant Chemotherapy in Patients with Stage III/IV Gastric Cancer

Tuesday, Nov. 29 12:45PM - 1:15PM Room: GI Community, Learning Center Station #2

# Participants

Xiaoyuan Gao, MD, Shanghai, China (*Abstract Co-Author*) Nothing to Disclose Huan Zhang, Shanghai, China (*Presenter*) Nothing to Disclose Zilai Pan, MD, Shanghai, China (*Abstract Co-Author*) Nothing to Disclose Lianjun Du, Shanghai, China (*Abstract Co-Author*) Nothing to Disclose Jing Yan, Shanghai, China (*Abstract Co-Author*) Nothing to Disclose Fuhua Yan, MS, Shanghai, China (*Abstract Co-Author*) Nothing to Disclose

## PURPOSE

The study was to prospectively evaluate the different parameters of dual-energy CT in the assessment of efficacy during neoadjuvant chemotherapy for stage III/IV gastric cancer.

# METHOD AND MATERIALS

Thirty patients with stage III/IV gastric cancer were examined with DECT one week before, and three cycles after the start of neoadjuvant chemotherapy. Image data were processed with the prototype software syngo.IPIPE. The percentage decrease of tumor volume (%ΔV), mean iodine-uptake (%ΔMIU-p, %ΔMIU-d), total iodine-uptake (%ΔTIU-p, %ΔTIU-d) in portal-phase and delayed-phase, tumor density in portal-phase (%ΔHU, Choi criteria), maximum transverse diameter (%ΔD, RECIST) and tumor area (%ΔS, WHO criteria) were calculated. After surgery, the correlation between %ΔV, %ΔMIU-p, %ΔMIU-d, %ΔTIU-p, %ΔTIU-d, %ΔHU, %ΔD, %ΔS and histopathologic grades of regression (Becker score) were determined. The best cutoff value to distinguish responder and nonresponder were calculated by ROC analysis. The association between responder, nonresponder and progression-free survival (PFS) time was assessed.

## RESULTS

 $\% \Delta V$ ,  $\% \Delta MIU$ -p and  $\% \Delta TIU$ -p were significant correlation with the pathological reaction(P=0.007, P=0.005, P=0.007, respectively). The correlation of the pathological regression with WHO, RECIST, and Choi criteria were no statistically significant(P=0.878, 0.100, 0.105, respectively).  $\% \Delta V$  cutoff value of -43.34% and  $\% \Delta MIU$ -p cutoff value of -21.51% were acquired and the differences of the PFS time between the responder and non-responder groups were not statistically significant (P=0.303, 0.512, respectively). Using -66.13% as the  $\% \Delta TIU$ -p cutoff level, the differences of the PFS time between the responders and non-responders were statistically significant (P=0.046).

## CONCLUSION

The percentage decrease of volume and iodine-uptake in DECT can be used to assess the response of neoadjuvant chemotherapy in patients with stage III/IV gastric cancer.  $\&\Delta$ TIU-p is hopeful to be a valuable predictive parameter of PFS time for the patients with gastric cancer after neoadjuvant chemotherapy and surgery.

# **CLINICAL RELEVANCE/APPLICATION**

(dealing with gastric cancer)"the volume and iodine-uptake changes in DECT are hopeful to replace WHO, RECIST and Choi criteria to evaluate the effect of neoadjuvant chemotherapy for gastric cancer."

# GI381-SD-TUB3

Protocol Optimization of Magnetic Resonance Colonography for Polyp Detection Using Pig Colonic Phantom: Influence of Magnetic Field Strength, Colonic Distension Technique, and MRI Sequence

Tuesday, Nov. 29 12:45PM - 1:15PM Room: GI Community, Learning Center Station #3

# Participants

Eun-Suk Cho, Seoul, Korea, Republic Of (*Presenter*) Nothing to Disclose Jeong Min Choi, Seoul, Korea, Republic Of (*Abstract Co-Author*) Nothing to Disclose Junyoung Kim, Seoul, Korea, Republic Of (*Abstract Co-Author*) Nothing to Disclose Yun Jung Choi, Seoul, Korea, Republic Of (*Abstract Co-Author*) Nothing to Disclose

## PURPOSE

There is currently no consensus for the optimal techniques of MR colonography (MRC), in respect of magnetic field strength, colonic distension technique and MRI sequences. The aim of this study was to compare the diagnostic performance for polyp detection and image quality of different techniques of MRC using pig colon phantoms and to evaluate the influence of magnetic field strength (1.5 T or 3.0 T), colonic distension technique (bright- or dark-lumen), and MRI sequences.

# METHOD AND MATERIALS

Six pig colon segments (60–92 cm) with 56 artificial colon polyps (0.4–1.6 cm in diameter, fat and sessile in shape) were placed in plastic container containing soybean oil. The colon was distended using room air for dark-lumen MRC and with tap water or a gadolinium-chelate based enema fluid for bright-lumen MRC. Each colon phantom was scanned on both 1.5 T and 3.0 T scanners using the following sequences: two-dimensional (2D) fast imaging with steady-state precession (True-FISP), T2-weighted fat-suppressed (FS) 2D single-shot fast spin echo (SSFSE), and/or T1-weighted FS three-dimensional gradient-echo (3D GRE) sequences. We tried to acquire the highest spatial resolution within a 20-s acquisition time. Two radiologists evaluated the presence of polyps based on a 4-point scale and analyzed image quality with respect to artifacts, colonic wall conspicuity, polyp conspicuity, and polyp contrast using a 5-point scale.

## RESULTS

For polyp detection sensitivity and image quality, MRC obtained at 1.5 T was better than that obtained at 3.0 T, and a bright-lumen technique was superior to a dark-lumen technique. Bright-lumen MRC at 1.5 T was most sensitive for polyp detection (p < 0.001) and gave the highest image quality (p < 0.05) regardless of polyp size and shape. SSFSE and 3D GRE sequences at bright-lumen MRC at 1.5 T had highest sensitivity for polyp detection (83.9% and 83.0%, respectively) and highest image quality.

## CONCLUSION

The most effective sequences of MRC for polyp detection were SSFSE- or 3D GRE-based bright-lumen MRC obtained with a 1.5 T scanner. These sequences had the highest polyp detection rate and the best image quality.

#### **CLINICAL RELEVANCE/APPLICATION**

Single-shot fast spin echo or 3D gradient echo-based bright-lumen MR colonography obtained at 1.5T scanner has higher sensitivity for polyp detection and superior image quality, compared to dark-lumen MRC or MRC obtained at 3.0T scanner.

Experience with Second and Third Generation Iterative Reconstruction (IR) Techniques for Improving Routine Abdomino-pelvic CT in Morbidly Obese Patients

Tuesday, Nov. 29 12:45PM - 1:15PM Room: GI Community, Learning Center Station #4

# Participants

Khalid W. Shaqdan, MD, Boston, MA (*Presenter*) Nothing to Disclose Manuel Patino, MD, Boston, MA (*Abstract Co-Author*) Nothing to Disclose Rodrigo Canellas, MD, Cambridge, MA (*Abstract Co-Author*) Nothing to Disclose Avinash R. Kambadakone, MD, Boston, MA (*Abstract Co-Author*) Nothing to Disclose Debra A. Gervais, MD, Boston, MA (*Abstract Co-Author*) Nothing to Disclose Dushyant V. Sahani, MD, Boston, MA (*Abstract Co-Author*) Research support, General Electric Company; Medical Advisory Board, Allena Pharmaceuticals, Inc

## PURPOSE

To investigate the diagnostic performance of abdomen CT images reconstructed using filtered back projection (FBP) and 2nd (ASiR, SAFIRE) and 3rd generation (ADMIRE) iterative reconstruction (IR) algorithms in morbidly obese patients (BMI 40-55).

## **METHOD AND MATERIALS**

A total of 193 portal phase abdomen-pelvis CT exams (5mm thickness) performed between Feb 2015 to Feb 2016 in 186 morbidly obese patients (mean age=51, mean BMI = 45.6) were reviewed. 76/188 exams were reconstructed using FBP (120 kVp, ATCM 74-550 mA), and 117 exams were processed using IR (ASIR = 32, SAFIRE = 37, ADMIRE = 48) using 100-140 kVp and ATCM. Patients were stratified into three BMI groups (<45, 45-49.9, 50-55) and images were reviewed for image quality (IQ), image noise (IMN), and artifacts. Objective noise and attenuation were also determined. Complex cases were identified as: presence of truncation artifacts, presence of metal artifacts, and arms positioned on abdomen. Size-specific-dose-estimates (SSDE) were compared and statistically analyzed.

# RESULTS

Diagnostic interpretation was rendered in all 193 exams with higher mean IQ score for IR (FBP = 3.4 and IR = 4.1). The mean image noise and CNR was comparable between ADMIRE (IMN = 15.2, CNR = 1.8) and SAFIRE (IMN = 15 and CNR = 2). Trends for all parameters were similar in patients across weight and BMI sub-categories. 94 exams (11 which had >1 complex issue) were categorized as complex due to truncation artifacts in 65 (FBP=31, IR=34), metal artifacts in 26 (FBP = 6, IR = 20), and in 3 exams arms were positioned by waist (IR = 3). Patients with BMI 45-55 were frequently scanned using IR (FBP exams = 32 and IR exams = 60). To correct for patient distribution based on BMI, dose comparisons were made for exams in <45 BMI group (FBP = 44, IR=57), and results showed lower dose for IR (IR = 13.8 mGy, FBP = 15.4).

## CONCLUSION

In morbidly obese patients, despite technical challenges (abdomen girth, metal artifacts, proper positioning), diagnostic quality images could be generated with minimal artifacts and image noise with 2nd and 3rd generation IR when compared to FBP.

## **CLINICAL RELEVANCE/APPLICATION**

As obesity rates continue to rise in the United States, radiologists and technologists face challenges imaging larger patients. For CT, achieving diagnostic imaging studies with minimum noise and artifacts is challenging. This abstract aims to show benefits of IR compared to FBP when imaging morbidly obese patients.

## **Honored Educators**

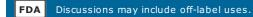
Presenters or authors on this event have been recognized as RSNA Honored Educators for participating in multiple qualifying educational activities. Honored Educators are invested in furthering the profession of radiology by delivering high-quality educational content in their field of study. Learn how you can become an honored educator by visiting the website at: https://www.rsna.org/Honored-Educator-Award/

Debra A. Gervais, MD - 2012 Honored Educator Dushyant V. Sahani, MD - 2012 Honored Educator Dushyant V. Sahani, MD - 2015 Honored Educator Dushyant V. Sahani, MD - 2016 Honored Educator

# GI383-SD-TUB5

Acoustic Radiation Force Impulse - Virtual Touch tissue Quantification ( ARFI - VTQ ) imaging in Acute and Chronic Pancreatitis

Tuesday, Nov. 29 12:45PM - 1:15PM Room: GI Community, Learning Center Station #5



## Awards

# **Student Travel Stipend Award**

#### Participants

Pushkaran Muralitharan, MBBS, DMRD, Chennai, India (*Presenter*) Nothing to Disclose Sudhakar Kattoju, DMRD, MD, Chennai, India (*Abstract Co-Author*) Nothing to Disclose

#### PURPOSE

To determine whether pancreatic parenchyma in acute and chronic pancreatitis exhibit significantly different ARFI-VTQ values as compared to normal pancreatic parenchyma.

## METHOD AND MATERIALS

A prospective observational study was conducted in our institution. Consecutive patients of acute and chronic pancreatitis were included. For standardisation of reference values, controls were also included. Imaging was done with a 4C1 curved array transducer of Siemens Acuson S2000 ultrasound system having virtual touch tissue quantification software. Three ARFI-VTQ values were obtained from head & neck, body and tail of pancreas. Mean ARFI-VTQ of these three regions was calculated and from these the mean for the entire pancreas was obtained. In patients for whom the entire pancreas could not be visualised due to technical factors, at least three ARFI-VTQ values were obtained from a particular segment (head & neck, body or tail) and this mean alone or combined with the mean of less than three ARFI-VTQ values from other segments was used to compute the mean for the entire pancreas.

## RESULTS

Mean ARFI-VTQ values in acute pancreatitis patients  $(1.37\pm0.44 \text{ m/s})$  and chronic pancreatitis patients  $(2.23\pm0.35 \text{ m/s})$  were higher than controls  $(0.93\pm0.13 \text{ m/s})$  with a statistically significant difference.Using mean ARFI-VTQ cut off values of 1.01 m/s & 1.39 m/s, acute and chronic pancreatitis patients could be differentiated from controls by 80% & 100% sensitivity, 73% & 93% specificity, 75% & 93% positive predictive value, 79% & 100% negative predictive value respectively.There was no significant difference in mean ARFI-VTQ values between acute necrotising pancreatitis  $(1.36\pm0.53 \text{ m/s})$  and interstitial oedematous pancreatitis  $(1.37\pm0.39 \text{ m/s})$ .No significant difference in mean ARFI- VTQ values was seen between chronic pancreatitis patients with calcification  $(2.22\pm0.34 \text{ m/s})$  and chronic pancreatitis patients without calcification  $(2.24\pm0.37 \text{ m/s})$ .

#### CONCLUSION

ARFI-VTQ imaging can distinguish acute and chronic pancreatitis from normal parenchyma. ARFI-VTQ cannot differentiate acute necrotising and interstitial oedematous pancreatitis. ARFI-VTQ cannot differentiate chronic pancreatitis patients with and without calcification.

#### **CLINICAL RELEVANCE/APPLICATION**

ARFI-VTQ may detect chronic pancreatitis before calcification and significant atrophy have occurred.

Non-invasive Prediction of Portal Hypertension with MR Elastography and DCE-MRI of the Liver and Spleen

Tuesday, Nov. 29 12:45PM - 1:15PM Room: GI Community, Learning Center Station #6

#### **Participants**

Mathilde Wagner, MD, PhD, Paris, France (*Presenter*) Consultant Olea Medical Stefanie Hectors, PhD, New York, NY (*Abstract Co-Author*) Nothing to Disclose Octavia Bane, PhD, New York, NY (*Abstract Co-Author*) Nothing to Disclose Thomas Schiano, NEW YORK, NY (*Abstract Co-Author*) Nothing to Disclose Aaron M. Fischman, MD, Harrison, NY (*Abstract Co-Author*) Consultan, Surefire Medical, Inc Consultant, Terumo Corporation Speakers Bureau, Koninklijke Philips NV Bachir Taouli, MD, New York, NY (*Abstract Co-Author*) Consultant, MEDIAN Technologies ; Grant, Guerbet SA

## PURPOSE

To assess the diagnostic performance of MR elastography (MRE) and dynamic contrast-enhanced MRI (DCE-MRI) of liver and spleen for non-invasive prediction of portal pressures.

## **METHOD AND MATERIALS**

This ongoing prospective study included 26 patients (M/F 11/15, mean age 50y) with chronic liver disease who underwent hepatic venous pressure gradient (HVPG) measurement. MRI examination (1.5T/3.0T) was performed within 3 months of HVPG and included 2D-GRE-MRE of liver and spleen (n=25) and abdominal DCE-MRI using 3D-FLASH sequence (n=20). Liver (LS) and spleen (SS) stiffness were determined from stiffness maps. DCE-MRI data was analyzed using model-free parameters and pharmacokinetic modeling (dual-input single compartment model for liver and Tofts model for spleen). MRI parameters were correlated with HVPG. ROC and sensitivity/specificity analysis for prediction of HVPG  $\geq$ 5 mm Hg (portal hypertension) and  $\geq$ 10mmHg (significant portal hypertension) were performed for individual and combinations of parameters.

#### RESULTS

Mean HVPG was  $8.0\pm7.5$  mmHg. There were significant positive correlations between HVPG and liver time-to-peak (TTP; r=0.712, P<0.001), liver mean transit time (MTT; r=0.514, P=0.020) and LS (r=0.478, P=0.016), while liver upslope was negatively correlated with HVPG (r=-0.548, P=0.01). ROC analysis provided significant AUCs for HVPG  $\geq$ 5mmHg (LS 0.786/SS 0.752) and for HVPG  $\geq$ 10mmHg (LS 0.833, SS 0.771, liver MTT 0.786, liver TTP 0.857, liver upslope 0.869, spleen TTP 0.845, spleen upslope 0.786). Sensitivity/specificity of LS for detection of HVPG $\geq$ 10mmHg were 67% and 92%, while LS and spleen TTP combined yielded the highest sensitivity/specificity (100%/92%).

## CONCLUSION

These preliminary results suggest that liver and spleen perfusion and stiffness metrics can be combined into a multiparametric analysis to maximize diagnostic performance for the non-invasive prediction of clinically significant portal hypertension.

## **CLINICAL RELEVANCE/APPLICATION**

MRE and DCE-MRI parameters can be used as potential biomarkers of portal hypertension in patients with liver disease.

# GI385-SD-TUB7

Combined Hepatocellular Carcinoma-cholangiocarcinoma: Clinicopathologic Features and Gadoxetic Acidenhanced MRI Findings

Tuesday, Nov. 29 12:45PM - 1:15PM Room: GI Community, Learning Center Station #7

**FDA** Discussions may include off-label uses.

#### Participants

So Hyun Park, MD, Incheon, Korea, Republic Of (*Presenter*) Nothing to Disclose Seung Soo Lee, MD, Seoul, Korea, Republic Of (*Abstract Co-Author*) Nothing to Disclose Cheol Mog Hwang, MD, Daejeon, Korea, Republic Of (*Abstract Co-Author*) Nothing to Disclose Eun Sil Yu, MD, Seoul, Korea, Republic Of (*Abstract Co-Author*) Nothing to Disclose Jae Ho Byun, MD, Seoul, Korea, Republic Of (*Abstract Co-Author*) Nothing to Disclose Yong Moon Shin, Seoul, Korea, Republic Of (*Abstract Co-Author*) Nothing to Disclose Moon-Gyu Lee, MD, Seoul, Korea, Republic Of (*Abstract Co-Author*) Nothing to Disclose

#### PURPOSE

To assess clinicopathologic features and imaging findings of combined hepatocellular carcinoma-cholangiocarcinoma (cHCC-CC) on gadoxetic acid-enhanced MRI according to the latest WHO classification and determine survival outcomes of patients in relation to arterial enhancement of tumors after curative surgery.

#### **METHOD AND MATERIALS**

Our institutional review board approved this study and waived the requirement for informed consent. 82 consecutive patients (64 men, 18 women: mean age, 54.0 years; range, 30-81 years) with surgically-proven cHCC-CC who underwent gadoxetic acidenhanced liver MRI were included in this retrospective study. We assessed clinical characteristics and pathologic findings according to the 2010 WHO classification. We analyzed imaging findings about arterial enhancement, hepatobiliary phase findings and morphologic features in gadoxetic acid-enhanced MR imaging and compared these features with pathologic types. We also studied 60 patients with cHCC-CC of surgical outcome in correlation with arterial enhancement after curative surgery.

#### RESULTS

Of 82 patients liver cirrhosis or chronic hepatitis was presence in 73 (89.0%) patients. 82 cHCC-CCs were classified into the classical type (n = 53) or stem cell type (n = 29) including typical (n=14), intermediate (n=7), cholangiolocellular (n=3), and unclassified (n=5) subtypes. In the arterial phase, global enhancement was the most common enhancement pattern seen in 48 (58.8%) lesions, followed by rim enhancement (n = 21, 25.6%), peripheral enhancement (n = 11, 13.4%), and isointensity (n = 2, 2.4%). In the HBP, all tumors showed hypointensity or target pattern. Target appearance in the HBP was seen in 30 (36.6%) lesions. When MR imaging findings were compared between classical type and stem cell type tumors, none of morphologic and enhancement characteristics showed statistically significant difference ( $p \ge 0.33$ ). Arterial enhancement of cHCC-CC was an independent factors associated with overall survival (p = 0.033).

# CONCLUSION

cHCC-CC had various imaging findings on gadoxetic acid-enhanced MR and histologic diversity. Imaging findings seems to be significant and important to predict tumor composition and prognosis of cHCC-CC. Arterial enhancement cHCC-CC was an independent factor of overall survival.

## **CLINICAL RELEVANCE/APPLICATION**

cHCC-CC shares clinical characteristics with HCC. Arterial enhancement of cHCC-CC is an independent factor associated with overall survival.

Role of Late Enhancement in Magnetic Resonance Imaging of the Prostate: Is There an Added Value in the Reclassification of Intermediate Risk Lesions (PI-RADS 3)?

Tuesday, Nov. 29 12:45PM - 1:15PM Room: GU/UR Community, Learning Center Station #3

#### Awards

## **Student Travel Stipend Award**

#### Participants

Giulia Cristel, MD, Milan, Italy (*Presenter*) Nothing to Disclose Giorgio Brembilla, Milano, Italy (*Abstract Co-Author*) Nothing to Disclose Alessandro Ambrosi, Milan, Italy (*Abstract Co-Author*) Nothing to Disclose Antonio Esposito, MD, Milan, Italy (*Abstract Co-Author*) Nothing to Disclose Alessandro Del Maschio, MD, Milan, Italy (*Abstract Co-Author*) Nothing to Disclose Francesco A. De Cobelli, MD, Milan, Italy (*Abstract Co-Author*) Nothing to Disclose

## PURPOSE

Late-gadolinium enhancement (LGE) is the retention of gadolinium-contrast agent in tissues in delayed magnetic resonance imaging (MRI) sequences and is routinely used in cardiac MRI to reveal areas of increased extracellular space with small cellularity, such as fibrosis. The aim of our study was to assess whether the presence of LGE could improve the characterization of intermediate-risk lesions (PI-RADS 3) in the setting of prostate cancer.

#### **METHOD AND MATERIALS**

Among a total of 687 patients who underwent prostatic MRI (1.5T), we selected 58 intermediate risk lesions classified as PI-RADS 3 with available corresponding histological specimen, obtained through prostatectomy or core needle biopsies. The imaging protocol consisted of multiplanar T2W, diffusion weighted imaging (with different b values: 50, 800, 1400 s/mm2), DCE and delayed axial T1W images. For each lesion the presence or absence of LGE in delayed axial T1W images was retrospectively qualitatively evaluated by the consensus of 2 different radiologists, blinded to the histological report. The association between the presence/absence of LGE and the histological result was then evaluated dividing the patients both basing on the presence/absence of insignificant prostate cancer as for Epstein criteria and basing on Gleason score  $\geq 6$ .

## RESULTS

The histological results of the 58 lesions (15 prostatectomies, 43 biopsies) were as follows: 24 negative (that included no abnormalities, acute or chronic inflammation), 5 prostatic intraepithelial neoplasia, 16 Gleason 6 lesions, 13 Gleason  $\geq$ 7 lesions. Significant prostate cancer (SPC) was found in 18 patients (31%). LGE was observed in 19 (33%) cases overall. 17/19 (89%) patients in which LGE was found presented insignificant prostate cancer and 2 (11%) patients with LGE had SPC, p=0.03. Moreover, 14/19 (74%) patients with LGE had Gleason score <6 and 5/19 (26%) showed Gleason  $\geq$ 6, p=0.02. The presence of LGE determined a risk reduction of having SPC (logOR= -1.77, p=0.02) or Gleason  $\geq$ 6 lesions (logOR= -1.49, p=0.01).

# CONCLUSION

LGE presence in patients with PI-RADS 3 lesions is associated with low probability of SPC. LGE evaluation could enable a downgrading of these intermediate risk lesions.

## **CLINICAL RELEVANCE/APPLICATION**

LGE finding may allow a down-grading of lesions in which the presence of clinically significant cancer is equivocal, leading to a reduction of redundant biopsies or short term follow up.

# A Rapid MRI Protocol for Detection of Prostate Cancer

Tuesday, Nov. 29 12:45PM - 1:15PM Room: GU/UR Community, Learning Center Station #1

#### **Participants**

Shivani Pahwa, MD, Cleveland, OH (*Presenter*) Research support, Siemens AG
William Tabayoyong, Cleveland, OH (*Abstract Co-Author*) Nothing to Disclose
Sara Dastmalchian, MD, Cleveland, OH (*Abstract Co-Author*) Research support, Siemens AG
Yun Jiang, Cleveland, OH (*Abstract Co-Author*) Research support, Siemens AG
Karin A. Herrmann, MD, PhD, Cleveland, OH (*Abstract Co-Author*) Nothing to Disclose
Soham V. Shah, MD, Cleveland, OH (*Abstract Co-Author*) Nothing to Disclose
Robert Abouassaly, Cleveland, OH (*Abstract Co-Author*) Nothing to Disclose
Gregory Maclennan, MD, Cleveland, OH (*Abstract Co-Author*) Nothing to Disclose
Mark A. Griswold, PhD, Cleveland, OH (*Abstract Co-Author*) Research support, Siemens AG Royalties, Siemens AG Royalties, General
Electric Company Royalties, Bruker Corporation Contract, Siemens AG
Raj M. Paspulati, MD, Cleveland, OH (*Abstract Co-Author*) Nothing to Disclose
Vikas Gulani, MD, PhD, Cleveland, OH (*Abstract Co-Author*) Research support, Siemens AG

#### PURPOSE

To evaluate a short, non-contrast, pelvic MRI protocol for detection of prostate cancer

#### METHOD AND MATERIALS

In this IRB approved study, 68 men (age 40-75y) without prior biopsy and with elevated PSA or abnormal digital rectal exam were prospectively enrolled. The non-contrast rapid protocol was: Siemens 3T Verio/Skyra, 3 plane single shot T2w (0.8x0.8x4mm resolution, TR/TE 2000/92ms), axial high resolution T2w TSE (0.6x0.6x3mm, TR/TE 7200/96ms), and DWI (1.2x1.2x3mm, TR7900ms, b= 50, 600, 1000 s/mm2). Lesions were categorized according to PIRADS 2.0 system of classification by an attending radiologist with 16 years' experience in prostate imaging. Lesions diagnosed as PIRADS 3, 4 or 5 were recommended for targeted biopsy. MR was followed by a standard 12 core TRUS biopsy with the urologist initially blind to the MR read. After biopsy, MR data were revealed and suspicious lesions targeted with 2 cores per lesion.

#### RESULTS

Average table time was 15.2 min, and total scan time was 11min9s. 95 lesions were identified in 68 patients (age range: 40-78 yr). On MRI, 14 lesions were identified as PIRADS 5, 18 as PIRADS 4, 21 as PIRADS 3, 33 as PIRADS 2, and 9 lesions were identified as PIRADS 1. Multiple lesions were seen in 19 patients. On pathology, cancer was detected in 32 patients. On MRI-pathology correlation, MRI was found to have a sensitivity of 94%, specificity of 78%, negative predictive value of 93% and positive predictive value of 79% for detection of cancer. Two patients were false negative on MRI – one was a Gleason 3+3 tumor, and the other was a Gleason 3+4 tumor in 5% of the core. MRI was false positive in 8 patients: all were read as PIRADS 3; on pathology, 6 of these were chronic prostatitis and 2 were (HGPIN).

#### CONCLUSION

A fast non-contrast pelvic MRI protocol can detect cancer with a high accuracy in patients with a clinical suspicion of prostate cancer.

## **CLINICAL RELEVANCE/APPLICATION**

A fast, low cost, non-contrast screening MRI protocol with targeted biopsies, could be used as a secondary screening tool for detection of prostate cancer and improve risk stratification.

Diffusion Weighted and Magnetization Transfer Imaging in Testicular Spermatogenic Function Evaluation: Preliminary Results

Tuesday, Nov. 29 12:45PM - 1:15PM Room: GU/UR Community, Learning Center Station #2

# Participants

Huanjun Wang, MD, GuangZhou, China (*Abstract Co-Author*) Nothing to Disclose Jian Guan, MD, Guangzhou, China (*Presenter*) Nothing to Disclose Zhongwei Zhang, MD, PhD, Winston-Salam, NC (*Abstract Co-Author*) Nothing to Disclose Jinhua Lin, Guangzhou, China (*Abstract Co-Author*) Nothing to Disclose Yan Guo, MD, Guangzhou, China (*Abstract Co-Author*) Nothing to Disclose

# PURPOSE

To assess the value of MR functional imaging applied in testicular spermatogenic function evaluation in young males.

## **METHOD AND MATERIALS**

Subjects ranging 20 to 40 years old males were recruited. Two main groups were classified as followed. (1)Group A: Subjects with normal semen analysis additionally were classified as two subgroups as Ay (younger group) and Ao (older group) respectively. In subgroup Ay, 15 males ranging 20-30 years with a mean age of (25.4±3.1) years were contained. And in subgroup Ao, 16 males ranging 31-40 years with a mean age of (35.4±3.3) years were contained. (2)Group B: Subjects were featured as 16 males with a mean age of (28.1±3.7) years and testicular spermatogenesis hypofunction confirmed by percutaneous testis biopsy. All subjects in group A and B underwent a 3.0T MR examination including routine and functional sequences [diffusion weighted imaging (DWI) and magnetization transfer (MT)]. DWI were scanned using EPI sequence (b=0, 900, 4000 s/mm2). ADC map were generated automatically. MT imaging were performed using a three-dimensional gradient-echo MT sequence, scanning slice and slice gap were consistent with DWI. ADC and MTR value were manually measured by a same radiologist according to place region of interest on Matlab software. Testicular ADC and MTR value in group B were compared with group A, subgroup Ay and Ao, respectively (independent- sample t test).

# RESULTS

A total of 62 testes (31 males) were included in group A. Testicular ADC value in group A, subgroup Ay and Ao were  $(459.9\pm31.2)\times10-3$ ,  $(453.4\pm17.9)\times10-3$  and  $(460.8\pm34.3)\times10-3$  mm2/s, respectively. Totally 32 testes (16 males) were included in group B, with a testicular ADC value of  $(496.7\pm37.2)\times10-3$  mm2/s, which was significantly higher than those in group A, subgroup Ay and Ao, respectively (P<0.001). Testicular MTR value in group A, subgroup Ay and Ao were 16.14\pm4.20, 17.88\pm2.00 and 15.09\pm4.28, respectively, each of which was significantly higher than those in group B (14.84\pm2.84) (P<0.001).

# CONCLUSION

Testicular ADC values of young males with testicular spermatogenesis hypofunction were much higher than normal subjects, and MTR values of them were lower. DWI combined with MT imaging can be a new meaningful method for testicular spermatogenic function evaluation.

# **CLINICAL RELEVANCE/APPLICATION**

MR functional imaging can provide us a new selection for noninvasive evaluation of testicular spermatogenic function.

Split-bolus CT-urography after Microwave Ablation of Renal Cell Carcinoma: Feasibility, Image Quality and Dose Reduction

Tuesday, Nov. 29 12:45PM - 1:15PM Room: GU/UR Community, Learning Center Station #4

# Participants

Shane A. Wells, MD, Madison, WI (*Presenter*) Nothing to Disclose
Lori Mankowski Gettle, MD, Hummelstown, PA (*Abstract Co-Author*) Nothing to Disclose
Timothy J. Ziemlewicz, MD, Madison, WI (*Abstract Co-Author*) Consultant, NeuWave Medical, Inc
Ayman M. Mithqal, MD, Charlottesville, VA (*Abstract Co-Author*) Nothing to Disclose
Jason Abel, Madison, WI (*Abstract Co-Author*) Nothing to Disclose
J. Louis Hinshaw, MD, Middleton, WI (*Abstract Co-Author*) Stockholder, NeuWave Medical Inc; Stockholder, Cellectar Biosciences, Inc
Sarah Best, Madison, WI (*Abstract Co-Author*) Nothing to Disclose
Fred T. Lee JR, MD, Madison, WI (*Abstract Co-Author*) Nothing to Disclose
Meghan G. Lubner, MD, Madison, WI (*Abstract Co-Author*) Grant, Koninklijke Philips NV; Grant, Johnson & Johnson;

# PURPOSE

To compare image parameters and radiation dose between single-bolus 2-phase and split-bolus single-phase CT urography following microwave ablation of renal cell carcinoma.

# METHOD AND MATERIALS

21 single-bolus and 21 split-bolus CTU examinations performed immediately following microwave ablation of RCC were retrospectively compared. Four experienced GU radiologists quantified renal enhancement, ablation zone sharpness, urinary tract distention and opacification and rated diagnostic confidence for residual tumor at the index ablation. Imparted radiation dose for the entire procedure and the CECT was recorded and converted to size specific dose estimates (SSDE) using an established formula.

# RESULTS

Patient characteristics were similar (p>0.05). Mean RCC diameter in the split-bolus cohort was larger (3.6 vs 2.9 cm; p=0.04). Tumor complexity and number of applicators used were similar (p>0.05). Ablation zone sharpness and index ablation attenuation were similar (p>0.05). Renal enhancement and excretion, collecting system opacification and distention were superior in the splitbolus cohort (p<0.05). Split-bolus image quality was superior (p<0.003) despite a significant reduction in SSDE (p<0.001).

## CONCLUSION

Performing split-bolus CTU after microwave ablation of RCC is an effective technique to reduce radiation exposure without compromising image quality.

## **CLINICAL RELEVANCE/APPLICATION**

As the indications for thermal ablation continue to expand, utilizing novel strategies to mitigate radiation exposure while preserving image quality after microwave ablation of RCC is imperative.

#### **Honored Educators**

Presenters or authors on this event have been recognized as RSNA Honored Educators for participating in multiple qualifying educational activities. Honored Educators are invested in furthering the profession of radiology by delivering high-quality educational content in their field of study. Learn how you can become an honored educator by visiting the website at: https://www.rsna.org/Honored-Educator-Award/

Meghan G. Lubner, MD - 2014 Honored Educator Meghan G. Lubner, MD - 2015 Honored Educator

Extraprostatic Extension of Prostate Cancer: Detailed Analysis of Specific Criteria on Multiparametric MRI using Radical Prostatectomy as Reference Standard

Tuesday, Nov. 29 12:45PM - 1:15PM Room: GU/UR Community, Learning Center Station #5

# Participants

Rajan T. Gupta, MD, Durham, NC (*Presenter*) Consultant, Bayer AG; Speakers Bureau, Bayer AG; Consultant, Koninklijke Philips NV; Consultant, Halyard Health, Inc; Consultant, Siemens AG Alison F. Brown, BA, Durham, NC (*Abstract Co-Author*) Nothing to Disclose Rachel K. Silverman, MS, Chapel Hill, NC (*Abstract Co-Author*) Nothing to Disclose Kae Jack Tay, MBBS,MMed, Durham, NC (*Abstract Co-Author*) Nothing to Disclose Thomas J. Polascik, MD, Durham, NC (*Abstract Co-Author*) Nothing to Disclose

## PURPOSE

To assess the agreement between staging of prostate cancer (PCa) by multiparametric magnetic resonance imaging (mpMRI) and pathologic staging following radical prostatectomy (RP) as well as the performance of specific criteria on mpMRI in detecting/characterizing extraprostatic extension (EPE).

## **METHOD AND MATERIALS**

In this retrospective, HIPAA-compliant, IRB-approved study, 157 patients underwent 3T mpMRI with endorectal coil (ERC) prior to RP; mpMRI used to assess clinical stage and presence of EPE. EPE was categorized on MRI on 0-3 scale (0 = no EPE; microscopic EPE: 1 = broad based capsular contact without discrete capsular breakthrough, 2 = capsule bulge without discrete capsular breakthrough; extensive EPE: 3 = capsular disruption). Pathologic EPE categorized on 0-2 scale (0 = no EPE, 1 = microscopic EPE, 2 = extensive EPE) based on pathologic findings after RP. Weighted Kappa coefficient was calculated using Cicchetti-Allison weights to assess agreement between mpMRI and pathologic staging. For EPE, sensitivity (SN), specificity (SP), accuracy (ACC), and positive predictive value (PPV) were calculated for mpMRI.

# RESULTS

There is substantial agreement between mpMRI and pathologic staging of PCa (Weighted Kappa Coefficient 0.64, 95% confidence interval: 0.53-0.74). EPE present on pathologic staging in 74/157 patients (47.1%). For EPE detection by mpMRI, SN: 0.86, SP: 0.86, ACC: 0.86, PPV: 0.84. When EPE was scored as 0,1,2, or 3 by mpMRI, ACC is 87.7% (71/81 patients), 76.9% (10/13 patients), 0% (0/6 patients), and 94.4% (51/54 patients), respectively. In 3 patients, there was isolated seminal vesicle involvement without other evidence of EPE (mpMRI correctly classified).

# CONCLUSION

There is substantial agreement of mpMRI staging with pathologic staging of PCa based on weighted Kappa coefficient 0.64 and high SN, SP, PPV and ACC of EPE detection using mpMRI. This helps validate data from prior studies. Subset analysis of patients with EPE reveals parameters that assist in correctly assessing EPE. Specifically, broad based contact (>1 cm in setting of high grade PCa) and capsular disruption are good indicators of EPE; however, presence of a capsular bulge did not accurately predict EPE.

# **CLINICAL RELEVANCE/APPLICATION**

The role of mpMRI in staging PCa and detecting EPE is validated by our study. Also, when specific criteria are utilized to assess the extent of EPE, high diagnostic accuracy by mpMRI is obtained.

Can Virtual Non-Contrast Images Created from Contrast-Enhanced Dual-Energy CT Scans Help to Accurately Differentiate Uric Acid from Non-Uric Acid Urinary Stones?

Tuesday, Nov. 29 12:45PM - 1:15PM Room: GU/UR Community, Learning Center Station #6

# Participants

Juan Montoya, Rochester, MN (*Presenter*) Nothing to Disclose Ahmed Halaweish, PhD, Rochester, MN (*Abstract Co-Author*) Employee, Siemens AG Shuai Leng, PhD, Rochester, MN (*Abstract Co-Author*) Nothing to Disclose Cynthia H. McCollough, PhD, Rochester, MN (*Abstract Co-Author*) Research Grant, Siemens AG

## PURPOSE

Studies have shown that for stone detection, the unenhanced phase of CT urography could potentially be replaced with virtual non-contrast (VNC) images created from contrast-enhanced dual-energy CT (CE-DECT) scans. The purpose of this study was to evaluate whether VNC images created from a CE-DECT dataset could be used to assist in differentiating uric acid (UA) and non-UA stones using the low- and high-energy CE-DECT images.

# METHOD AND MATERIALS

This study included 32 UA and 32 non-UA urinary stones, each from a different patient. Initially, stones were embedded in gelatin to acquire true unenhanced images. Subsequently, the gelatin was replaced with contrast-enhanced gelatin having an iodine concentration consistent with a clinical CT urogram (20 mgI/mL). For each type of gelatin, stones were submerged in 35- and 40- cm wide water phantoms and scanned with multiple tube potential combinations using a 3rd generation dual-source CT system (Somatom FORCE, Siemens) operated in dual-energy mode. VNC images were created using commercial software (Virtual Unenhanced, Syngo VIA, Siemens) and used for stone detection and segmentation. The ratios of CT numbers between the low- and high-energy images, which are a surrogate for stone composition, were then measured in segmented stones using the unenhanced- and CE-DECT images. CT number ratios were compared between UA and NUA stones, and receiver operating characteristic (ROC) curves were constructed. Sensitivity, specificity and area under the ROC curve (AUC) were calculated and used to assess the accuracy of stone type differentiation in CE-DECT using VNC images as masks.

#### RESULTS

For both phantom sizes and all tube potential combinations, CT number ratios derived from CE-DECT images using VNC images for stone detection and segmentation were similar to those derived from true unenhanced scans. 100% sensitivity and specificity were achieved in the detection of UA stones using the CE-DECT images, except when 100-Sn150 kV was used in the 40-cm wide phantom, where one UA stone was misclassified and the AUC fell to 0.99.

## CONCLUSION

Differentiation of UA from non-UA stones can be accurately performed in CE-DECT using VNC images to detect and segment urinary stones.

## **CLINICAL RELEVANCE/APPLICATION**

For modest iodine concentrations, VNC CE-DECT images can be used to detect and segment urinary stones, allowing characterization of stone composition in contrast enhanced exams.

MR Safety Controversies: Basic Concepts to Practical Implementation

Tuesday, Nov. 29 12:45PM - 1:15PM Room: HP Community, Learning Center Station #6

**FDA** Discussions may include off-label uses.

#### **Participants**

Nicole M. Hindman, MD, New York, NY (*Presenter*) Nothing to Disclose Nathan Hyson, BS, New York, NY (*Abstract Co-Author*) Nothing to Disclose Thomas Callahan, BA,ARRT, New York, NY (*Abstract Co-Author*) Nothing to Disclose Graham Wiggins, New York, NY (*Abstract Co-Author*) Nothing to Disclose Danny C. Kim, MD, White Plains, NY (*Abstract Co-Author*) Nothing to Disclose

## **TEACHING POINTS**

1. Learn about the physics principles that guide the practical interpretation of MR Safety 2. Cover current controversies in MR imaging, and present a practical approach to balancing patient safety and best clinical care (eg, gadolinium deposition in the brain, imaging cardiac stents, pregnant patients and peri-operative patients).

## **TABLE OF CONTENTS/OUTLINE**

1. MR Safety History (2001 Westchester seminal incident; ACR safety creation, Zoning, MAUDE database)2. MR Physics principles (Maps of different scanners, magnetic field strength variance, RF heat deposition, antenna principle of increased burns at 3T vs. 1.5T).3. Sample MR Screening workflow4. Current Controversies A. Pacemakers (on and off label scanning) B. Pregnancy C. Cardiac stent scanning 1.5T and 3T. D. Perioperative scanning - 6 weeks time limit, what is data? E. Gadolinium and NSF/Brain deposition

## HP221-SD-TUB1

Bacterial Contamination of CT Equipment: Efficacy of ATP Detection as a Surrogate Marker for Equipment Cleanliness

Tuesday, Nov. 29 12:45PM - 1:15PM Room: HP Community, Learning Center Station #1

# Participants

John C. Childress III, MD, Ann Arbor, MI (*Presenter*) Nothing to Disclose Deb Burch, Ann Arbor, MI (*Abstract Co-Author*) Nothing to Disclose Carol Young, Ann Arbor, MI (*Abstract Co-Author*) Nothing to Disclose Cheryl Kucharski, RT, Ann Arbor, MI (*Abstract Co-Author*) Nothing to Disclose Ella A. Kazerooni, MD, Ann Arbor, MI (*Abstract Co-Author*) Nothing to Disclose Matthew S. Davenport, MD, Cincinnati, OH (*Abstract Co-Author*) Royalties, Wolters Kluwer nv; ;

## PURPOSE

Evaluate the suitability of an adenosine triphosphate (ATP) sanitation monitoring system as a surrogate marker for CT equipment bacterial contamination.

# METHOD AND MATERIALS

The bore, table, and wrap of two tertiary care center inpatient CT scanners were assayed with an ATP detection system and bacterial culture on eight consecutive weekdays. ATP detection swabs were applied to a 6 x 3" area of the bore, table, and wrap of each scanner. Swabs were placed in an ATP detector (AccuPoint ATP Sanitation Monitoring System by Neogen, Lansing, MI). The relative light unit (RLU) value was recorded for each sample. A cutoff value of 350 RLU was considered positive for contamination per manufacturer recommendations. Cotton swabs (Eswab by Copan Diagnostics, Murrieta, CA) were applied synchronously to a 6 x 3" adjacent area of the bore, table, and wrap of each scanner. Swabs from each site were placed into a Staphylococcus enrichment broth and incubated aerobically at 37C for 48 hours. Broths were then applied to Staph aureas Select and Methicillin Resistant Staph aureus (MRSA) Select chromogenic agar culture material. Culture results were recorded as positive or negative at the enrichment broth phase. Results were recorded as MRSA positive or negative at the agar phase. Culture rates were compared with Chi Square tests; RLU values were compared with Mann-Whitney U test.

#### RESULTS

A cutoff value of 350 RLU did not predict a positive generic broth culture (>350 RLU: 36% [4/11];  $\leq$ 350 RLU: 49% [18/37], p=0.5) or a positive SA select culture (>350 RLU: 0% [0/11];  $\leq$ 350 RLU: 19% [7/37], p=0.18). Positive SA select cultures were more likely to be found on the CT wrap (38% [6/16]) than the CT table (0% [0/16], p=0.02) or CT bore (6% [1/16], p=0.08). Similarly, the RLU values were higher on the CT wrap (median 173, mean 632) than the CT table (median 58, mean 100; p=0.06) and CT bore (median 42, mean 208; p=0.16), but those differences were not statistically significant.

## CONCLUSION

There was no relationship between ATP detection and the likelihood of a positive culture. However, both the ATP detection system and the bacterial culture results identified the CT wrap as the most contaminated piece of equipment, providing an opportunity for targeted intervention.

# **CLINICAL RELEVANCE/APPLICATION**

ATP detection is a crude method of evaluating CT equipment cleanliness that is less labor intensive than bacterial culture but is unreliable for the prediction of culture positivity.

#### **Honored Educators**

Presenters or authors on this event have been recognized as RSNA Honored Educators for participating in multiple qualifying educational activities. Honored Educators are invested in furthering the profession of radiology by delivering high-quality educational content in their field of study. Learn how you can become an honored educator by visiting the website at: https://www.rsna.org/Honored-Educator-Award/

Ella A. Kazerooni, MD - 2014 Honored Educator

# HP222-SD-TUB2

# Predictors of High Scores in the American College of Radiology In-Training Exam (DXIT):A National Multicenter Study

Tuesday, Nov. 29 12:45PM - 1:15PM Room: HP Community, Learning Center Station #2

# Participants

Fadi Toonsi, MBBS, FRCPC, Montreal, QC (*Presenter*) Nothing to Disclose Fahad Essbaiheen, MBBS, FRCPC, Ottawa, ON (*Abstract Co-Author*) Nothing to Disclose Jeffrey Chankowsky, MD, Montreal West, QC (*Abstract Co-Author*) Nothing to Disclose

## PURPOSE

Training programs implement various methods to ensure trainees are attaining certain benchmarks during residency. The American Board of Radiology In-Training Exam (DXIT) is one example. We aim to identify predictors of high scores on DXIT, assessing factors identified in clinical fields other than radiology.

# METHOD AND MATERIALS

An internet-based questionnaire was distributed to 263 residents in 11 Canadian radiology training programs inquiring about various study habits. DXIT results and residency levels were collected by a follow-up survey and from consenting residents' programs. Hierarchical multiple linear regression was performed using SPSS.

# RESULTS

80 residents responded. DXIT scores were collected from 63 participants. The average number of hours spent studying per weak was eleven (SD = 8.6). The average number of hours slept per night was 6.75 (SD= .9). The mean DXIT scaled score was 61.61 (SD= 10.8). Controlling for participants' residency training program, our model accounted for 61.9% of the variance of DXIT scores (p < .001). Significant predictors (p < .05) were 1- Being a resident in one of three of the 12 residency training programs. 2- The average number of hours slept per night, and 3- The residency level. The number of hours spent studying per week was not a significant predictor.Holding other variables constant, the residency level was the best predictor of the scaled score. An increase of one year in residency level would increase the score on DXIT by 6.37 points. An increase of one hour of sleep would increase DXIT score performance by 2.38 points.

# CONCLUSION

Our results concur with non-radiology literature on the effect of sleep and residency level on exam performance and could help radiology residents' exam preparation. The detected significant difference among various accredited residency programs and non significance of the number of hours spent studying is unexpected and warrants exploration.

## **CLINICAL RELEVANCE/APPLICATION**

Employing healthy sleeping habits could promote residents' performance in standardized tests. Investigating the reasons behind significantly different scores amongst universities, despite their being equally accredited by a national governing body, could potentially enhance some programs' performance by identifying un-monitored gaps in their training.

## Use of Statistical Analysis in Publications from an Academic Medical Imaging Department: Back to the Basics

Tuesday, Nov. 29 12:45PM - 1:15PM Room: HP Community, Learning Center Station #3

#### **Participants**

Pascal N. Tyrrell, PhD, Toronto, ON (*Presenter*) Nothing to Disclose Alan R. Moody, MD, Toronto, ON (*Abstract Co-Author*) Nothing to Disclose Hao-Yue H. Lan, Toronto, ON (*Abstract Co-Author*) Nothing to Disclose Alana Man, Toronto, ON (*Abstract Co-Author*) Nothing to Disclose

## PURPOSE

To assess what statistical methods are most commonly used in medical imaging research and how they are presented in articles published from a large academic medical imaging department.

#### **METHOD AND MATERIALS**

A cross-sectional survey of abstracts of original articles published in 2013 from a large academic department of medical imaging was conducted. Data collected consisted of article citation, bibliometric indicators, study methodology and statistical analysis. The primary outcome was level of statistical methods performed categorized into four levels: Basic I, Basic II, Intermediate, and Advanced. Descriptive, summary, and parametric statistics were performed.

# RESULTS

Three hundred and twenty-two articles were published in 2013 by 177 faculty (26 full professor, 43 associate professor, 92 assistant professor, and 16 lecturers). The most common study types were retrospective cohort (18%), prospective cohort (22%), review (15%), and case-report (14%). Statistical analyses were performed in 65% of published articles with the majority of Basic I (45%) and Basic II (34%) levels. Relatively few studies required Intermediate or Advanced statistical analyses (19% and 3%, respectively). The median journal impact factor was 2.7 (IQR = 1.7 - 3.7) with American Journal of Neuro Radiology (6%), Pediatric Radiology (4%), and Canadian Association of Radiologists Journal (3%) as the most frequently published journals. The median h-index of the corresponding authors was 10 (IQR = 4 - 22) and only 20% of corresponding authors were faculty from within the department. No association was found between corresponding author h-index and journal impact factor or level of statistics.

## CONCLUSION

These data support the continued need to offer broad training in research methodology, but suggest that a more cost effective and enabling education program would result from better emphasis on basic level statistics. These results should be of interest to academic departments when addressing their own training needs, and help support the development of research methodology curricula in the field of medical imaging.

#### **CLINICAL RELEVANCE/APPLICATION**

Academic departments need to address their own training needs in order to better support the development of research methodology curricula in the field of medical imaging.

Patient Satisfaction in Radiology: Where Should We Improve?

Tuesday, Nov. 29 12:45PM - 1:15PM Room: HP Community, Learning Center Station #4

#### Participants

Johannes Boos, MD, Boston, MA (*Abstract Co-Author*) Nothing to Disclose Jieming Fang, Boston, MA (*Presenter*) Nothing to Disclose Aideen Snell, MSW, Boston, MA (*Abstract Co-Author*) Nothing to Disclose Alexander Brook, PhD, Boston, MA (*Abstract Co-Author*) Nothing to Disclose Ronald L. Eisenberg, MD, JD, Boston, MA (*Abstract Co-Author*) Nothing to Disclose Olga R. Brook, MD, Boston, MA (*Abstract Co-Author*) Research Grant, Toshiba Medical Systems Corporation

# PURPOSE

To analyze radiology department patient satisfaction surveys to detect patterns of less-than-optimal patient experiences and potential areas of improvement.

## **METHOD AND MATERIALS**

Patient satisfaction surveys with less-than-optimal rating from the radiology department submitted during calendar year 2015 were retrospectively analyzed. Surveys were filled out on electronic kiosks at different locations within the department and consisted of questions regarding overall experience, cleanliness and interactions with receptionist, technologist, nurse, doctor. Ratings were given on a 5-point scale (1: poor – 5: excellent), with option for free text comments. Likelihood to recommend to friends and family was regarded as an indicator of satisfaction and our primary evaluation metric. Data were analyzed for the entire department as well as by modality, site where the service was provided, individual survey questions, and free text comments. Statistical analysis was performed using Chi-squared test, Kruskal-Wallis test, and Spearman correlation.

## RESULTS

Out of 6736 surveys, 4938 (73.3%) were completed. Of these, 608 (9.0%) had less-than-optimal "likelihood to recommend" ratings. Frequency of non-completed surveys was significantly higher for kiosks in changing and waiting areas, compared to kiosks next to elevators (856/2365, 36.2% vs. 868/3927, 22.2%; p<.0001). Time of day, day of the week, and location had no significant impact on satisfaction (p=.39, p=.97, p=.25, respectively). The lowest rating per survey showed a strong correlation with overall patient satisfaction (r=.57). There were 1656 ratings across 608 surveys which were the lowest or tied for lowest. Cleanliness (329/1656, 19.9%) and receptionist courtesy (299/1656, 18.1%) received lowest ratings most frequently. There were 278 free text complaints in 608 surveys with wait time (61/278, 21.9%) and inadequate communication with the patient (37/278, 13.3%) being most frequent.

# CONCLUSION

Proper placement of patient satisfaction kiosks is important for survey completion rate. Cleanliness, courtesy of the receptionist, wait time, and patient communication were found to be potential areas of improvement.

## **CLINICAL RELEVANCE/APPLICATION**

Survey kiosks located next to elevators decrease non-completion rate compared to kiosks in waiting/changing areas. Improving cleanliness, courtesy of the receptionist, wait time, and communication appear to have the most positive effect on patient satisfaction.

## **Honored Educators**

Presenters or authors on this event have been recognized as RSNA Honored Educators for participating in multiple qualifying educational activities. Honored Educators are invested in furthering the profession of radiology by delivering high-quality educational content in their field of study. Learn how you can become an honored educator by visiting the website at: https://www.rsna.org/Honored-Educator-Award/

Ronald L. Eisenberg, MD, JD - 2012 Honored Educator Ronald L. Eisenberg, MD, JD - 2014 Honored Educator

# Improving Oncology Patient and Caregiver-Centered Radiology Reporting

Tuesday, Nov. 29 12:45PM - 1:15PM Room: HP Community, Learning Center Station #5

#### Participants

Andy Tang, BS, Seattle, WA (*Abstract Co-Author*) Nothing to Disclose Daniel S. Hippe, MS, Seattle, WA (*Abstract Co-Author*) Research Grant, Koninklijke Philips NV; Research Grant, General Electric Company Ryan O'Malley, MD, Seattle, WA (*Abstract Co-Author*) Nothing to Disclose

Carolyn L. Wang, MD, Seattle, WA (Presenter) Nothing to Disclose

## PURPOSE

To explore optimal mechanisms of delivering radiology results directly to patients through a survey of patients' values in current and new models of reporting.

## **METHOD AND MATERIALS**

A questionnaire was developed in collaboration with oncology patient representatives to evaluate how patients are currently receiving radiology images and reports and to identify gaps between information patients desire to learn from radiology reports and what they currently receive. This questionnaire was administered to all oncologic patients undergoing CT or MRI at a major cancer institute over a 4-month period. Responses were converted to a 5-point Likert scale for quantitative analysis.

## RESULTS

105 questionnaires were completed. 66% of the patients have been offered their written report at least once. 76% of patients who read their written reports graded their understanding of the report as well or completely and 93% found their written report useful. 72% of patients would like to always receive copies of the written report. 76% of patients had been shown their images at least once and 88% of them found it useful. 66% of imaging review was with oncologists, 10% with radiologists. 65% of patients always want to see their images, and 66% in all circumstances. When asked how responders would like to get their imaging results (first choice out of 6 options): 19% preferred a photo diary of significant images along with the written report, 19% the same written report their doctor receives, 19% a simplified written report in non-technical language, and 18% wanted to review images with a radiologist.

# CONCLUSION

A significant portion of oncology patients have received their written radiology reports and reviewed their images at least once and have found it useful. There is also a significant portion of patients who want to receive written reports and view images more frequently. However current data do not yet show consensus on a single best option for the model of delivering radiology images and reports to patients. Speaking directly to the patient may not be the solution for patient-centered reporting. Further work needs to be done to develop individualized reporting which is feasible, effective, and cost effective.

# **CLINICAL RELEVANCE/APPLICATION**

Patients desire more access to both radiology written reports and images but there is currently no consensus amongst the patients as to the best model for delivering this information to patients.

# Application of Computer Algorithm for Detection of Uncertainty in Unstructured Radiology Reports

Tuesday, Nov. 29 12:45PM - 1:15PM Room: IN Community, Learning Center Hardcopy Backboard

#### Participants

Adi Price, MD, San Francisco, CA (*Presenter*) Nothing to Disclose David McCoy, San Francisco, CA (*Abstract Co-Author*) Nothing to Disclose Joseph Mesterhazy, BS, San Francisco, CA (*Abstract Co-Author*) Nothing to Disclose Mark W. Wilson, MD, San Francisco, CA (*Abstract Co-Author*) Nothing to Disclose Bao H. Do, MD, Stanford, CA (*Abstract Co-Author*) Nothing to Disclose Jared A. Narvid, MD, San Francisco, CA (*Abstract Co-Author*) Nothing to Disclose

# CONCLUSION

The (NLP) algorithm tested is an effective tool for automatic detection of uncertainty in large numbers of unstructured radiology reports.

#### FIGURE

#### Background

The radiology report necessarily communicates the certainty or doubtfulness of particular diagnoses. Yet interpretative performance varies significantly among radiologists, affecting clinician satisfaction and patient care. The purpose of this study is to validate a natural language processing (NLP) algorithm to automatically detect uncertainty in unstructured radiology reports. We hypothesize that our algorithm demonstrates test characteristics which would facilitate the accurate detection of uncertainty in large numbers of reports.

# **Evaluation**

Twenty terms and their derivatives indicating uncertainty from prior work were collected to build an uncertainty signal database. Additionally, reports containing disease terms felt to be associated with uncertainty (for example appendicitis) were reviewed for new uncertainty signals. An NLP algorithm running on the Apache/PHP/MySql platform was designed to accept entire unstructured reports as input and detect contextually appropriate use of expressions of uncertainty in the "Impression" section. Three-hundred and forty-five randomly selected diagnostic radiology reports across sub-specialties were independently reviewed by three radiologists and the NLP algorithm for the presence of uncertainty. Performance of the algorithm was evaluated using sensitivity, specificity, accuracy and area under the curve.

#### Discussion

In the adjudicated list 109 (32%) reports contained expressions of uncertainty. Inter-observer agreement regarding uncertainty between the three human reviewers was 0.50, 0.59, and 0.50. For the NLP algorithm, sensitivity, specificity, accuracy and area under the curve was 93% (95% CI: 86%, 97%), 94% (95% CI: 91%, 97%), 94% (95% CI: 89%, 98%) and 0.94 (95% CI: 0.90, 0.97). Errors in detection revealed challenges for the algorithm, such as contextually appropriate recognition of diagnostic versus other types of uncertainty, and navigating typographical or dictation errors.

# Deep-learning-based Electronic Cleansing for Single- and Dual-Energy CT Colonography

Tuesday, Nov. 29 12:45PM - 1:15PM Room: IN Community, Learning Center Custom Application Computer Demonstration

#### Awards

## **Identified for RadioGraphics**

#### Participants

Rie Tachibana, Boston, MA (*Presenter*) Nothing to Disclose Janne J. Nappi, PhD, Boston, MA (*Abstract Co-Author*) Royalties, Hologic, Inc.; Royalties, MEDIAN Technologies; Toru Hironaka, Boston, MA (*Abstract Co-Author*) Nothing to Disclose Se Hyung Kim, Seoul, Korea, Republic Of (*Abstract Co-Author*) Nothing to Disclose Daniele Regge, MD, Torino, Italy (*Abstract Co-Author*) Speakers Bureau, General Electric Company Hiroyuki Yoshida, PhD, Boston, MA (*Abstract Co-Author*) Patent holder, Hologic, Inc; Patent holder, MEDIAN Technologies;

#### **TEACHING POINTS**

Electronic cleansing (EC) is used for subtracting tagged materials in non-cathartic CT colonography (CTC) examinations to improve the detection sensitivity of virtual endoscopic fly-through reading. The teaching points of this exhibit are to (1) introduce how EC works, (2) understand the nuisance and causes of EC artifacts that distract and mislead readers with existing EC schemes, (3) learn about the emerging deep-learning EC (DL-EC) methods, and (4) demonstrate how DL-EC improves image quality in noncathartic single- and dual-energy CTC.

# TABLE OF CONTENTS/OUTLINE

1. Introduction and background: Review the role of EC in CTC and the principles of existing EC schemes.2. EC artifacts: Review the artifacts generated by existing EC schemes, and review the diagnostic pitfalls due to these artifacts.3. Deep-learning EC (DL-EC): Present overview of the emerging DL-based EC methods for single- and dual-energy CTC.4. Image quality improvement by DL-EC: Describe the effect of DL-EC in removing image artifacts, in comparison with existing EC schemes.5. DL-EC in action: Demonstrate DL-EC results in non-cathartic single- and dual-energy CTC cases.

# IN233-SD-TUB1

## Application of 3D Printed Models of Diverse Hip Pathologies to Augment Resident Training

Tuesday, Nov. 29 12:45PM - 1:15PM Room: IN Community, Learning Center Station #1

#### Participants

Leonid Chepelev, MD, PhD, Ottawa, ON (*Presenter*) Nothing to Disclose Adnan M. Sheikh, MD, Ottawa, ON (*Abstract Co-Author*) Nothing to Disclose Taryn Hodgdon, MD, Ottawa, ON (*Abstract Co-Author*) Nothing to Disclose Frank J. Rybicki III, MD, PhD, Ottawa, ON (*Abstract Co-Author*) Nothing to Disclose

# CONCLUSION

The use of 3D printed models in resident education for communication of anatomically complex disease greatly facilitates understanding of disease pathophysiology.

#### Background

Complex hip pathologies require excellent understanding for mastery of accurate diagnosis. Unfortunately, traditional teaching may be limited in addressing complex cases requiring urgent intervention. Specifically, acetabular fractures, pre-arthritic hip deformities (e.g. femoroacetabular impingement and dysplasia), and proximal femoral fractures may pose a challenge to trainees. 3D printing has enabled facile and relatively economic exploration of intricacies of complex anatomy, rapidly granting unanticipated understanding by incorporating multisensory feedback in learning. In this study, we evaluated the potential of 3D printing in resident teaching.

#### **Evaluation**

Following ethics approval, we enrolled 15 patients representing a wide spectrum of hip disease who underwent CT imaging as part of their clinical workup. The pathologies included 5 acetabular fractures, 3 pre-arthritic hip deformities, 4 proximal femoral fractures, and 3 postoperative complications. We processed CT images using Mimics software (Leuven, Belgium) to isolate bones and the involved neurovascular structures. We then fabricated these structures on an Objet260 printer (Stratasys, Eden Prairie MN) and incorporated these models into dedicated teaching workshops. We matched 46 consenting resident physicians into control and exposure groups. Residents were assigned to either receive lectures augmented with 3D model interaction or lectures without it. Resident understanding was then formally tested using practical imaging questions as well as theoretical questions.

# Discussion

3D printed models of hip pathologies facilitate learning as evidenced by significantly higher test scores in the 3D model-augmented teaching group relative to the control group. 3D printed models provide immediate tactile and visual feedback and thus enable rapid, intuitive understanding of disease pathophysiology beyond verbose textual descriptions or traditional image collations. Interaction with 3D printed models may become an important teaching modality in radiology.

#### **Honored Educators**

Presenters or authors on this event have been recognized as RSNA Honored Educators for participating in multiple qualifying educational activities. Honored Educators are invested in furthering the profession of radiology by delivering high-quality educational content in their field of study. Learn how you can become an honored educator by visiting the website at: https://www.rsna.org/Honored-Educator-Award/

Frank J. Rybicki III, MD, PhD - 2016 Honored Educator

# The Key Points of Automated Generation of Radiological Description from Brain MR Images

Tuesday, Nov. 29 12:45PM - 1:15PM Room: IN Community, Learning Center Station #2

#### Participants

Kentaro Akazawa, Baltimore, MD (*Presenter*) Nothing to Disclose Ryo Sakamoto, MD, PhD, Kyoto, Japan (*Abstract Co-Author*) Nothing to Disclose Satoshi Nakajima, MD, Kyoto, Japan (*Abstract Co-Author*) Nothing to Disclose Dan Wu, PhD, Baltimore, MD (*Abstract Co-Author*) Nothing to Disclose Yue Li, PhD, Baltimore, MD (*Abstract Co-Author*) Employee, AnatomyWorks LLC Susumu Mori, PhD, Baltimore, MD (*Abstract Co-Author*) Research Consultant, AnatomyWorks LLC CEO, AnatomyWorks LLC

# CONCLUSION

The key points of automated generation of radiological description from brain MR image might be how to set the threshold after corrected the spatial information reduction, relational tables and the Boolean expression.

#### Background

Our technologies for quantitative brain MR image analyses advanced significantly, supporting numerous MR-based brain research. However, those have been rarely adopted to clinical practice.We describe a method of automated anatomical descriptions (AAD) that summarize clinically important anatomical features from raw MR images like radiologists and clarify the problems to develop tools that would be compatible with daily clinical practices.

#### **Evaluation**

Our approach is based on several technical components. First, recent advancement in the multi-atlas image segmentation methods. Second, the ontology-based multi-granular anatomical analysis can evaluate the brain anatomy at five different segmentation levels. This approach was applied to data from more than 500 normal subjects and the age-dependent normal values were defined for all segmented structures. We applied this approach to 93 patients that were concerned about dementia and AAD about brain atrophy were generated. Three neuroradiologists (3Rs) then independently evaluated the same data and the agreement was observed.332 pairs of sentences between AAD and 3Rs were generated and 189 pairs (56.9%) were same among them. The unmatched pairs were classified based on the causes into no matched structure in 3 subjects, non-necessity to report in 22, the defined formula in 28 and the threshold setting in 90.

#### Discussion

There were several challenges to improve the method. Regarding the spatial information reduction, medial temporal lobe was not in the atlas. The knowledge-based clinical significant filter did not work for limbic and parietal lobe and caudate nucleus. The Boolean expression did not have the definition for amygdala and each single lobe. Radiologists seemed to change the thresholds according to the structures and solitary threshold appeared to be an issue. In this research, the subjects were concerned about dementia and the elements noted above should be changed depending on the given clinical information.

# Multi-label Deep Convolutional Neural Networks for Holistic Interstitial Lung Disease Detection

Tuesday, Nov. 29 12:45PM - 1:15PM Room: IN Community, Learning Center Station #3

FDA Discussions may include off-label uses.

#### **Participants**

Mingchen Gao, PhD, Bethesda, MD (*Presenter*) Nothing to Disclose Ziyue Xu, PhD, Bethesda, MD (*Abstract Co-Author*) Nothing to Disclose Le Lu, PhD, Bethesda, MD (*Abstract Co-Author*) Nothing to Disclose Adam P. Harrison, PhD, Bethesda, MD (*Abstract Co-Author*) Nothing to Disclose Ronald M. Summers, MD, PhD, Bethesda, MD (*Abstract Co-Author*) Royalties, iCAD, Inc; ; Daniel J. Mollura, MD, Bethesda, MD (*Abstract Co-Author*) Nothing to Disclose

# PURPOSE

Computer-aided detection (CAD) of interstitial lung diseases (ILDs) using single CT images is a difficult and important medical imaging problem. The challenges stem from the tremendous variation of disease appearance, location, and configuration. In this work, we describe a new "deep learning" method using convolutional neural networks (CNN) to detect multiple ILDs simultaneously on a CT slice.

## **METHOD AND MATERIALS**

Beyond the basic approaches from most of the previous work, focusing on predicting a single ILD label to manually pre-defined region of interest, we propose a multi-label deep regression model for holistic CT slices. Our method is composed of two main stages. First, an end-to-end convolutional neural network (CNN) network is trained directly on CT slices for ILD detection. The deep CNN regression model learns the deep image features and the final multi-label predictions simultaneously. While CNNs can learn effective image features, their feature learning strategy is not invariant to the spatial locations. To accommodate the large spatial variations of the ILD locations, the second stage of our method aggregates the learned CNN features at different network depths and turns them into location-invariant representations using Fisher Vector (FV) Encoding.

#### RESULTS

The proposed algorithms are evaluated on a publicly available Lung Tissue Research Consortium (LTRC) dataset. The experiments are conducted on 533 CT scans, using five-fold cross-validation. Four most typical ILDs are investigated here, Ground Glass, Reticular, Honeycomb and Emphysema. In total there are 11677 healthy CT slices, 5675, 1410, 119, and 2 slices with one, two, three, or four ILD disease types, respectively. We achieved high area-under-curve (AUC) scores of 0.982, 0.972, 0.893 and 0.993 for each disease, respectively. This is performed without the manual ROI inputs needed by much of the state-of-the-art and is the first solution to detection multiple ILDs simultaneously.

#### CONCLUSION

We present a new ILD detection algorithm using deep-feature learning combined with location-invariant encoding. Our work represents an important step forward in providing clinically effective ILD detection.

## **CLINICAL RELEVANCE/APPLICATION**

The method sheds light to holistically detecting multiple ILDs simultaneously. This method can be readily adapted to other CAD problems that face similarly large spatial and appearance variations.

# Clinical Applications of 3D Portable Document Format (PDF) for Image Visualization

Tuesday, Nov. 29 12:45PM - 1:15PM Room: IN Community, Learning Center Station #4

**FDA** Discussions may include off-label uses.

## Participants

Peter Metherall, PhD, Sheffield, United Kingdom (*Presenter*) Nothing to Disclose Rebecca Denoronha, MBCHB, FRCR, Sheffield, United Kingdom (*Abstract Co-Author*) Nothing to Disclose Keith Chapple, Sheffield, United Kingdom (*Abstract Co-Author*) Nothing to Disclose Nicholas Kelland, Sheffield, United Kingdom (*Abstract Co-Author*) Nothing to Disclose Justin Lee, Sheffield, United Kingdom (*Abstract Co-Author*) Nothing to Disclose Jonathan Sahu, MRCP, Sheffield, United Kingdom (*Abstract Co-Author*) Nothing to Disclose Paul Sutton, Sheffield, United Kingdom (*Abstract Co-Author*) Nothing to Disclose Nikhil Kotnis, FRCR, Sheffield, United Kingdom (*Abstract Co-Author*) Nothing to Disclose Nikhil Kotnis, FRCR, Sheffield, United Kingdom (*Abstract Co-Author*) Nothing to Disclose Jaydip Ray, Sheffield, United Kingdom (*Abstract Co-Author*) Nothing to Disclose Nigel Hoggard, MD, FRCR, Manchester, United Kingdom (*Abstract Co-Author*) Nothing to Disclose Frank Johnson, Sheffield, United Kingdom (*Abstract Co-Author*) Nothing to Disclose Trevor Cleveland, Sheffield, United Kingdom (*Abstract Co-Author*) Nothing to Disclose John M. Himsworth, PhD, Sheffield, United Kingdom (*Abstract Co-Author*) Nothing to Disclose John M. Himsworth, PhD, Sheffield, United Kingdom (*Abstract Co-Author*) Nothing to Disclose Judith Sugden, Sheffield, United Kingdom (*Abstract Co-Author*) Nothing to Disclose

## CONCLUSION

3D PDF offers a simple and interactive method of displaying complex anatomy. Using registration techniques it is possible to easily combine models from multiple modalities and derived information such as thickness analysis. We have shown that Adobe viewer offers a versatile platform for displaying complex medical images.

#### Background

CT and MR volume rendered (VR) images are usually produced in the Radiology Department and saved as an animimation for the referring clinician. Whilst sufficient for some applications, if the observer needs to gain a detailed understanding of the 3D anatomy it is important that they can fully interact with the 3D image. 3D Portable Document Format (PDF) is a relatively new surface rendering method for visualising medical data and is becoming more widely available in imaging software.

## **Evaluation**

Commercial software (3-matic, Materialise) was used to generate 3D PDF for a wide variety of clinical applications and viewed with Adobe Acrobat reader Anaplastology – Cranioplasty Cardiology – Multimodality fusion for endo/epicardial catheter ablation procedures for ventricular tachycardia ENT – Bone conduction implant planning General Surgery – Perianal fistula, abdominal vasculature for hemicolectomy Oncology – CBCT/CT fusion for transarterial chemoembolization Orthopaedic Surgery – Trochlear dysplasia and complex surgical planning Renal – complex renal stones

## Discussion

The Adobe viewer offers a familiar and user friendly interface with sophisticated 3D functionality which can be extended with the JavaScript for Acrobat API. This offers programmatic control of the 3D view enabling a powerful method to customise the PDF. Accurate segmentation is imperative to obtain an authentic representation of the anatomy. Although this can often be time consuming this may be offset by benefits such as improved safety, efficacy and reduced surgical time owing to the improved understanding and confidence of the surgeon. As the models are often easier to understand than cross sectional or VR images they can also be useful for obtaining patient consent. In addition to displaying anatomy, derived data such as thickness analysis can easily be incorporated into the model.

# Automated Segmentation of Liver Metastases with Deep Convolutional Neural Networks

Tuesday, Nov. 29 12:45PM - 1:15PM Room: IN Community, Learning Center Station #5

FDA Discussions may include off-label uses.

#### **Participants**

Eugene Vorontsov, Montreal, QC (Presenter) Intern, Imagia Cybernetics Inc Gabriel Chartrand, BEng, Montreal, QC (Abstract Co-Author) Research intern, Imagia Cybernetics Inc Olina Dagher, Montreal, QC (Abstract Co-Author) Nothing to Disclose Vi Thuy Tran, Montreal, QC (Abstract Co-Author) Nothing to Disclose Mathieu Flamand, Montreal, OC (Abstract Co-Author) Nothing to Disclose Aline Khatchikian, Quebec City, QC (Abstract Co-Author) Nothing to Disclose Amine Smouk, Montreal, QC (Abstract Co-Author) Nothing to Disclose Nicolas Siron, Montreal, QC (Abstract Co-Author) Nothing to Disclose Anne-Catherine Maynard-Paquette, Montreal, QC (Abstract Co-Author) Nothing to Disclose David Roy, Montreal, QC (Abstract Co-Author) Intern, Imagia Cybernetics Inc Nicolas Chapados, Montreal, QC (Abstract Co-Author) Officer, Imagia Cybernetics Inc Simon Turcotte, Montreal, QC (Abstract Co-Author) Nothing to Disclose Real Lapointe, Montreal, QC (Abstract Co-Author) Nothing to Disclose Franck Vandenbroucke-Menu, MD, Montreal, QC (Abstract Co-Author) Nothing to Disclose Bich Nguyen, Montreal, QC (Abstract Co-Author) Nothing to Disclose Christopher Pal, PhD, Montreal, QC (Abstract Co-Author) Nothing to Disclose Samuel Kadoury, Montreal, QC (Abstract Co-Author) Nothing to Disclose An Tang, MD, Montreal, QC (Abstract Co-Author) Advisory Board, Imagia Cybernetics Inc

## PURPOSE

To evaluate the agreement and accuracy of fully automated segmentation of colorectal metastases with deep convolutional neural networks (DCNN), using expert segmentation as the reference standard.

# METHOD AND MATERIALS

Patient consent was waived by the institutional review board for this retrospective study based on a biobank registered by a national tumour repository network. Thirty contrast-enhanced computed tomography (CT) studies from patients with colorectal liver metastases with a total of 60 liver lesions were included. We adopted a supervised feature learning model. A feed-forward DCNN with skip connections was trained using labeled data to perform liver lesion segmentation on contrast-enhanced CT images acquired in the portal venous phase. Segmentation was evaluated on all data using five-fold leave-six-out cross-validation (in each fold, retaining 24 cases for training the model). The segmentation reference standard was based on segmentations of pathology-proven liver metastases. Reference segmentations were prepared by trainees, supervised by trained image analysts and approved by a radiologist. Dice scores and Bland-Altman analysis on tumor volume were calculated for different size thresholds (<20 mm, 20-40 mm, and  $\geq$ 40 mm). Estimates of diagnostic accuracy (area under the receiver operating characteristic [AUC] analysis, sensitivity and specificity) were also computed across the dataset.

#### RESULTS

For size thresholds of <20 mm, 20-40 mm,  $\ge$ 40 mm, and all combined, the Dice scores were respectively 0.72 ± 0.08, 0.74 ± 0.13, 0.84 ± 0.08, and 0.76 ± 0.12 (mean, standard deviation). The Bland-Altman analysis revealed inter-method agreement of 1.8 ± 24.9 mL (95% confidence interval). For pixel-wise detection of liver lesions, the AUC was 0.97; for a threshold of 0.5, the pixel-wise sensitivity and specificity were respectively 0.89 and 0.98.

## CONCLUSION

Deep learning showed high accuracy for automated segmentation of liver metastases. However, preliminary results with this technique provided moderate precision, especially for larger tumors.

# **CLINICAL RELEVANCE/APPLICATION**

Deep learning shows promise for automated tumor segmentation, but larger datasets with a wider spectrum of liver lesions will be needed to refine performance.

# PI-RADS Report Builder: Semi-automated Dictation Support for Structured Reporting

Tuesday, Nov. 29 12:45PM - 1:15PM Room: IN Community, Learning Center Station #6

#### Awards

#### **Student Travel Stipend Award**

#### **Participants**

Steven A. Rothenberg, MD, Baltimore, MD (*Presenter*) Co-founder, McCoy Medical Technologies Paul B. Stoddard, MD, Baltimore, MD (*Abstract Co-Author*) Nothing to Disclose Jason M. Thomas, MD, Baltimore, MD (*Abstract Co-Author*) Nothing to Disclose Jade J. Wong-You-Cheong, MD, Baltimore, MD (*Abstract Co-Author*) Nothing to Disclose Melina Pectasides, MD, Boston, MA (*Abstract Co-Author*) Nothing to Disclose

# PURPOSE

Prostate Imaging Reporting and Data System (PI-RADS) is an algorithmic tool used for multiparametric prostate MRI (mpMRI) that lends itself well to structured reporting. The goal of PI-RADS is to improve methodologic rigor of mpMRI interpretation. However, there is broad resistance to the use of structured reporting in the radiology community stemming from a perceived detriment to efficiency and lack of value added. Our goal was to create a semi-automated PI-RADS report builder (RB) with a user-friendly interface. We hypothesized that this would 1) decrease time to report creation 2) increase reliability of interpretation and 3) increase accuracy.

# METHOD AND MATERIALS

Retrospective, IRB-approved, HIPAA compliant study. PI-RADS (v2) scoring algorithms were scripted into a web-based, userfriendly interface to allow entry of lesion descriptors and automatically provide a PI-RADS score and structured report in return (Figure 1). Readers were blinded to the medical record and original mpMRI interpretation. Time of interpretation with or without RB was evaluated with Wilcoxon signed rank tests on a per reader basis. Reliability was assessed with intraclass correlation coefficients. Accuracy was assessed with receiver operating characteristic curve analysis using a reference standard of MRI/Ultrasound fusion biopsy.

## RESULTS

Time to report creation (in minutes) significantly decreased with the RB (Reader 1: without  $11.6 \pm 2.88$ , with  $7.2 \pm 1.48$ , p = 0.042; Reader 2: without  $16.2 \pm 1.30$ , with  $7.2 \pm 1.30$ , p = 0.039). Rater reliability also greatly improved with implementation of the RB (ICC without RB = 0.455; ICC with RB = 0.974). Per reader analysis of accuracy revealed no significant change in experienced reader performance (AUC with RB = 1.0; without RB = 1.0), but improved novice reader accuracy (AUC with RB = 1.0; without RB = 0.75).

# CONCLUSION

PI-RADS RB can facilitate creation of a structured mpMRI report. Our semi-automated tool increases efficiency and reliability. In more novice readers, RB also improves accuracy. Standardization of interpretation and reporting of mpMRI greatly enhances methodological rigor of mpMRI, encouraging growth in the arena of MRI/Ultrasound fusion biopsy.

# **CLINICAL RELEVANCE/APPLICATION**

PI-RADS report builder is a semi-automated, user-friendly tool that creates a structured mpMRI report, increasing radiologist efficiency, reliability and, potentially, accuracy.

Realizing benefits of an Enterprise Imaging Platform in 27 Months by Standardizing Processes and Tools to Share Images and Information for over 18,000 Daily Clinician Accesses within the Public Healthcare System, Serving more than 8,500,000 Inhabitants

Tuesday, Nov. 29 12:45PM - 1:15PM Room: IN Community, Learning Center Station #7

#### Participants

Juan Lucas Retamar Gentil, Sevilla, Spain (*Presenter*) Nothing to Disclose Manuel Lepe Gonzalez, Huelva, Spain (*Abstract Co-Author*) Nothing to Disclose

# CONCLUSION

The Enterprise Imaging Platform consists of a single instance of diagnostic viewer, centralized VNA in DC storing 30,876,056 historic exams plus replicated secondary DC. Connecting 94 hospitals plus 162 sites producing 9,859,051 of exams per year, and 1,560 ambulatory sites that consumes images and other related patient information. The project was completed in short 15 month from kick off to go-live.. 100% of Radiology and Nuclear Medicine, some Retinography, Endoscopy and ECG exams are already managed within the platform. Other "ologies" are planned. Significant economic benefits by (1) consolidating 9 disparate systems (maintenance contracts), (2) Reducing the number of integrations and optimizing support resources by the utilization of a common platform, (3) Eliminating cost of printing film with an image exchange capability. The project has a calculated payback period of 12.25 months with the annual savings rate of average 65%. The organization has already realized a cost savings of 1.58M€ during the initial 15 months project timeframe.

#### Background

Main objective is to guarantee the same level of care to any patient of the Region no matter where they live. Enable every clinician to treat every case with the right information and tools, no matter where he or she is located. Additional goals are upgrade to state of the art enterprise imaging solution and reduce integrations, maintenance and operating costs.

#### **Evaluation**

The System counts with 9 disparate solutions not integrated at the enterprise level. The result is a workflow that doesn't allow real collaboration amongst the clinicians. Multiple information systems and data silo's causing increasing management costs and resource constraint. Imaging exams are repeated.

## Discussion

Given the scale of the regional deployment, early understanding of workflow and various system integration, clear definition of the project scope and on-going monitoring of the platform performance are all elements to success. Benefits includes flexibility to assign workload to the radiologists regardless of where images were acquired, allowing transparent access to complete patient information and use of all tools needed.

# USPIO-Labeling in Different Macrophage Population: A In Vitro and In Vivo MR Study

Tuesday, Nov. 29 12:45PM - 1:15PM Room: S503AB Station #2

#### **Participants**

Chiara Zini, MD, Rome, Italy (*Presenter*) Nothing to Disclose Maryanna Venneri, Rome, Italy (*Abstract Co-Author*) Nothing to Disclose Damiano Caruso, MD, Rome, Italy (*Abstract Co-Author*) Nothing to Disclose Selenia Miglietta, Roma, Italy (*Abstract Co-Author*) Nothing to Disclose Marco Rengo, MD, Rome, Italy (*Abstract Co-Author*) Nothing to Disclose Natale Porta, Latina, Italy (*Abstract Co-Author*) Nothing to Disclose Andrea Isidori, Rome, Italy (*Abstract Co-Author*) Nothing to Disclose Vincenzo Petrozza, Latina, Italy (*Abstract Co-Author*) Nothing to Disclose Andrea Laghi, MD, Rome, Italy (*Abstract Co-Author*) Nothing to Disclose Andrea Laghi, MD, Rome, Italy (*Abstract Co-Author*) Speaker, Bracco Group Speaker, Bayer AG Speaker, General Electric Company Speaker, Koninklijke Philips NV

#### PURPOSE

Tumor-associated macrophages (TAM) are recruited to the tumor site and programmed by tumor-derived factors in tumorsupportive M2-polarized macrophages, although M1-polarized TAM with anti-tumor activity have been described in several types of cancer.Aim of the present study was to evaluate if ultrasmall superparamagnetic iron oxide (USPIO) magnetic resonance (MR) could be used to depict distinct population of macrophages.

## METHOD AND MATERIALS

Human monocytic cell line THP-1 were differentiated into macrophages using PMA and polarized according to the Tjiu method. A control population of macrophages, was developed from THP-1 cells with PMA (M0 macrophages). M1-polarized, M2-polarized and the M0 were incubated with USPIO research prototype (P904, CheMatech, Guerbet Research)(200 µg Fe/mL) for 36 hours. A M0 without P904 was the control non-treated population. M0, M0+P904, M1+P904 and M2+P904 were analyzed in gel phantoms containing at least 1x106 cells/milliliter with a 3.0T MR scan (Discovery MR750). Optical and electron microscopy was used as gold standard to evaluate the iron uptake.

#### RESULTS

M2+P904 showed a much greater T1 signal compared to the other population (p<0.0001), and the T2\* signal was significantly lower compared to the other groups (p<0.0001); the R\* was significantly higher for the M2+ P904 compared to the other populations (p<0.0001). Hystological analysis demonstrated higher iron content in the M2+P904 as compared to both the M1+904 (p=0.04) and the M0+P904 population (p=0.003). Ultrastructure analysis with a electron microscope demonstrated ubiquitous localization of P904 within the cellular compartments. Those results were confirmed with human macrophages.

## CONCLUSION

Avid and selective USPIO-labeling for M2-like population was demonstrated with a 3.0T clinical scan.

## **CLINICAL RELEVANCE/APPLICATION**

USPIO-RM is able to depict M2 macrophage population. Further studies on same topic would be highly desirable to investigate the possible role of non-invasive diagnosis in inflammation and cancer imaging

The SAPHO Syndrome Revisited with an Emphasis on Spinal Manifestations

Tuesday, Nov. 29 12:45PM - 1:15PM Room: MK Community, Learning Center Station #8

#### Awards Certificate of Merit

#### Participants

Antonio Leone, MD, Rome, Italy (*Presenter*) Nothing to Disclose Victor N. Cassar-Pullicino, MD, Oswestry, United Kingdom (*Abstract Co-Author*) Nothing to Disclose Cesare Colosimo, MD, Rome, Italy (*Abstract Co-Author*) Nothing to Disclose

# **TEACHING POINTS**

The primary aims of this exhibit are:To provide an overview of the radiological appearances of SAPHO syndrome, focusing on the magnetic resonance imaging findings of vertebral involvement.To present relevant clinical and pathological features that assist early diagnosis.To illustrate the differential diagnosis

# TABLE OF CONTENTS/OUTLINE

1)Etiological hypotheses of S.A.P.H.O.2)Clinical features3)Imaging featuresAnterior chest wallAxial skeletonAppendicular skeletonFlat bones4)Diagnosis5)Clinical course6)Treatment

# MK177-ED-TUB9

# Lumps and Bumps: Musculoskeletal Ultrasound of Unknown Palpable Masses

Tuesday, Nov. 29 12:45PM - 1:15PM Room: MK Community, Learning Center Station #9

#### **Participants**

Talentshia Vethanayagamony, MD, Bolingbrook, IL (*Presenter*) Nothing to Disclose Suraj Chandrasekar, MD, MS, Hoffman Estates, IL (*Abstract Co-Author*) Nothing to Disclose Rina Patel, MD, San Francisco, CA (*Abstract Co-Author*) Nothing to Disclose

# **TEACHING POINTS**

1. Provide sonographic imaging features of commonly encountered palpable masses2. To demonstrate that some palpable masses can be definitively diagnosed with ultrasound, while concerning features should prompt further evaluation.

# TABLE OF CONTENTS/OUTLINE

Commonly Encountered Palpable Masses Imaging Features of common lesions 1. Location Specifica. Knee - Baker's cyst; Popliteal aneurysm

b. Lower Extremity - venous thrombosis.

c. Foot - Morton's neuroma; Plantar fibroma2. Neoplasm- imaging features that lead to definitive diagnosis and those that should prompt further evaluation.

- a. Lipoma
- b. Atypical Lipoma
- c. Hemangioma
- d. Nerve Sheath Tumor
- e. Lymphadenopathy
- f. Sarcoma3. Miscellaneousa. Ganglion
- b. Abscess
- c. Hematoma
- d. Morel Lavallee
- e. Sebaceous cyst/Epidermal cyst4. Mimics of Massesa. Tendon tears biceps, planters, quadriceps, achilles.
- b. Bursitis prepatellar bursitis, olecranon bursitis.
- c. Ligament tear UCL tear; stener lesion.

# MK215-ED-TUB10

# Soft Tissue Pathology on Trauma CT Scans: A Frequently Overlooked Entity

Tuesday, Nov. 29 12:45PM - 1:15PM Room: MK Community, Learning Center Station #10

#### **Participants**

Padmaja A. Jonnalagadda, MD, Wynnewood, PA (*Abstract Co-Author*) Nothing to Disclose Stephen E. Ling, MD, Philadelphia, PA (*Abstract Co-Author*) Nothing to Disclose Summer L. Kaplan, MD, MS, Philadelphia, PA (*Abstract Co-Author*) Nothing to Disclose Sarah D. Fenerty, MD, Philadelphia, PA (*Abstract Co-Author*) Nothing to Disclose Sayed Ali, MD, Aston, PA (*Presenter*) Nothing to Disclose

#### **TEACHING POINTS**

1. Soft tissue pathology is frequently encountered while interpreting trauma CT scans, but under-recognized. 2. Failure to recognize these findings affects prognosis and may alter management. 3. Imaging artifacts and normal variants may affect interpretation.

## **TABLE OF CONTENTS/OUTLINE**

Muscular interposition between fracture fragments affecting fracture fixation, and internal derangement including anterior cruciate ligament and meniscal tears/entrapment will be demonstrated. Hematoma, infected hematoma, abscess, emphysema and Morel-Lavallee lesions will be shown. We will demonstrate tendon entrapment and displacement by bone fragments and surgical hardware, tendon tear/laceration and tendon subluxation (posterior tibial/peroneal) from retinacular injuries. Traumatic lipohematoma of the tendon sheath will be shown, and the risk of subsequent tendon rupture will be emphasized. Lipohematoma of the subacromial-subdeltoid bursa in patients with proximal humerus fractures indicates associated rotator cuff tear and will be demonstrated on CT/MRI. Normal variants such as a peroneus quartus tendon simulating peroneal tendon tear will also be illustrated. Finally, artifact from metallic hardware can obscure soft tissue evaluation, and examples of these artifacts and ways to reduce them will be outlined.

# MK276-ED-TUB11

# **Musculoskeletal Abnormalities: A Clue to Systemic Diseases**

Tuesday, Nov. 29 12:45PM - 1:15PM Room: MK Community, Learning Center Station #11

#### **Participants**

Leonor G. Savarese, MD, Ribeirao Preto, Brazil (*Presenter*) Nothing to Disclose Mateus A. Hernandes, MD, Chapel Hill, NC (*Abstract Co-Author*) Nothing to Disclose Marcelo N. Simao, MD, PhD, Ribeirao Preto, Brazil (*Abstract Co-Author*) Nothing to Disclose Douglas J. Racy, MD, Sao Paulo, Brazil (*Abstract Co-Author*) Nothing to Disclose Paulo M. Agnollitto, MD, Ribeirao Preto, Brazil (*Abstract Co-Author*) Nothing to Disclose Marcello H. Nogueira-Barbosa, MD, PhD, Ribeirao Preto, Brazil (*Abstract Co-Author*) Nothing to Disclose Jorge Elias JR, MD, PhD, Ribeirao Preto, Brazil (*Abstract Co-Author*) Nothing to Disclose Valdair F. Muglia, MD, PhD, Ribeirao Preto, Brazil (*Abstract Co-Author*) Nothing to Disclose

# **TEACHING POINTS**

1.To describe the most relevant musculoskeletal imaging findings of systemic diseases.2.To recognize clues that may suggest a systemic cause for musculoskeletal abnormalities.3.To list the main differential diagnosis based on musculoskeletal manifestations and suggest further investigation of a previously unsuspected systemic disease.

## **TABLE OF CONTENTS/OUTLINE**

Many systemic diseases share underlying musculoskeletal (MSK) manifestations, which may respond for the patient's initial symptoms. In this review, we describe systemic conditions that may manifest by MSK abnormalities, grouping by etiology: a-metabolic and deposition diseases (e.g. renal osteodystrophy, amiloidosis, Gaucher's disease); b-inflammatory diseases (e.g. inflammatory bowel disease-associated arthropathy, mastocytosis); c-infectious diseases (e.g. tuberculosis, paracoccidiodomicosis,); d-vascular diseases (e.g. Maffucci syndrome); e-hematologic diseases (e.g. sickle cell disease) and; f-neoplastic diseases (e.g. Erdheim Chester, Gardner's syndrome). All cases were confirmed either by histology or based on clinical history, serologic tests and follow-up. This exhibit will provide a comprehensive imaging review, helping general radiologists to recognize a previously unsuspected systemic disease based on an initial MSK manifestations and suggests further investigation.

Evaluation of the Synovium using Double Inversion Recovery Sequence at the Knee Joint: Comparison with Contrast-enhanced T1-weighted Fat-Saturated Image

Tuesday, Nov. 29 12:45PM - 1:15PM Room: MK Community, Learning Center Station #1

## Participants

Ye Na Son, Seoul, Korea, Republic Of (*Presenter*) Nothing to Disclose Wook Jin, Seoul, Korea, Republic Of (*Abstract Co-Author*) Nothing to Disclose Geon-Ho Jahng, PhD, Seoul, Korea, Republic Of (*Abstract Co-Author*) Nothing to Disclose Jang Gyu Cha, MD, Bucheon, Korea, Republic Of (*Abstract Co-Author*) Nothing to Disclose Seong Jong Yun, Cheongwon-gun, Korea, Republic Of (*Abstract Co-Author*) Nothing to Disclose Yunkyung Shin, Seoul, Korea, Republic Of (*Abstract Co-Author*) Nothing to Disclose So Young Park, Seoul, Korea, Republic Of (*Abstract Co-Author*) Nothing to Disclose Ji Seon Park, MD, PhD, Seoul, Korea, Republic Of (*Abstract Co-Author*) Nothing to Disclose Kyung Nam Ryu, MD, PhD, Seoul, Korea, Republic Of (*Abstract Co-Author*) Nothing to Disclose

#### PURPOSE

To investigate the efficacy of the double inversion recovery (DIR) in evaluation of the synovium at the knee joint without contrast enhancement.

## **METHOD AND MATERIALS**

Institutional review board approval was obtained. 34 knees from 33 patients (M:F = 11:22; mean age, 41.35 years) were included. Two radiologists (R1 and R2) performed independent analysis of paired MR images [DIR image and contrast-enhanced T1-weighted fat-saturated image (CET1FS)] at each five level of the knee joint for four-point visual score and a location with the thickest synovium. If both visual scaling and the location of the thickest synovium were concordant by two reviewers, the maximum synovial thickness on each sequence and each level was measured by consensus between R1 and R2. The synovium-to-effusion signal ratio (SER) and the synovium-to-bone signal ratio (SBR) for DIR and CET1FS images were assessed at each level.

# RESULTS

Inter-observer agreement between R1 and R2 for four-point scale was good ( $\kappa = 0.736$ ). And inter-observer agreements for location of the thickest synovium on DIR and CET1FS were very good ( $\kappa = 0.955$  and 0.954, respectively). Inter-sequential agreements between DIR and CET1FS for location of the thickest synovium were very good (R1,  $\kappa = 0.845$ ; R2,  $\kappa = 0.828$ ). The mean thicknesses of the synovium, mean SERs, and mean SBRs were  $3.62\pm1.75$  mm on DIR and  $3.08\pm1.55$ mm on CET1FS; 4.55 and 2.22; and 14.63 and 4.07, respectively. The synovial thickness on DIR and CET1FS showed a statistically excellent correlation (r=0.872).

# CONCLUSION

DIR sequence for evaluating the synovium at the knee joint showed good correlation with CET1FS sequence. DIR may be a one of useful MR techniques for evaluating the synovium of the knee without contrast enhancement.

# **CLINICAL RELEVANCE/APPLICATION**

The application of DIR sequence makes it possible to differentiate the synovium of the joint without contrast enhancement, and also may be helpful for patients with contrast allergy and for reducing the imaging time.

## MK322-SD-TUB2

Voxel-based Analysis of SUVs and ADCs in a PET/MR System: Initial Experience in the Evaluation of Treatment Effect of Soft-tissue Tumors

Tuesday, Nov. 29 12:45PM - 1:15PM Room: MK Community, Learning Center Station #2

## Participants

Koji Sagiyama, MD, Fukuoka, Japan (*Presenter*) Nothing to Disclose Yuji Watanabe, MD, Kurashiki, Japan (*Abstract Co-Author*) Nothing to Disclose Ryotaro Kamei, MD, Fukuoka, Japan (*Abstract Co-Author*) Nothing to Disclose Sungtak Hong, PhD, Tokyo, Japan (*Abstract Co-Author*) Nothing to Disclose Satoshi Kawanami, MD, Fukuoka, Japan (*Abstract Co-Author*) Nothing to Disclose Hiroshi Honda, MD, Fukuoka, Japan (*Abstract Co-Author*) Nothing to Disclose

## PURPOSE

To investigate the feasibility of the voxel-by-voxel comparisons of SUVs and ADCs in the evaluation of the treatment effect in softtissue tumors.

# METHOD AND MATERIALS

Eight patients with soft-tissue tumors (3 osteosarcomas, 2 pleomorphic sarcomas, 1 synovial sarcoma, 1 MPNST and 1 clear cell sarcoma) were examined with Ingenuity TF PET/MR system (Philips Healthcare) before and after the treatment. Five patients underwent chemotherapy and 3 patients underwent heavy-particle radiotherapy. Zoomed diffusion-weighted image (DWI) (b = 0 and 800), and 18FDG-PET (4.0 MBq/kg FDG) were acquired along with fat-suppressed T2-weighted image (T2WI). Image registration was performed on a workstation (ISP6.0, Philips Healthcare) and post-processing was performed by using Image J software (version 1.43, NIH). The regions of interest (ROIs) were manually drawn on T2WI to include the tumor in all slices. The ROIs were copied and pasted on the ADC maps and PET images. The tumor ROIs were extracted and reconstructed in 4 mm resolution. The ADCs and SUVs within the tumor ROIs were recorded in a voxel-by-voxel manner, and voxel-based SUV/ADCs were calculated. The scatter plots of SUV vs. ADC and SUV/ADC vs. ADC were generated for each tumor. The indicators of SUVpeak, ADCmin, tumor volume, slopes of linear regression of SUV/ADC vs. ADC and correlations between SUVs and ADCs were compared between the pre- and post-treatment.

#### RESULTS

The correlation coefficient between SUV and ADC significantly increased ( $-0.52 \pm 0.14$  vs.  $-0.23 \pm 0.21$ , P < 0.01) and the slope of linear regression of SUV/ADC vs. ADC significantly decreased ( $-3.42 \pm 1.22$  vs.  $-1.82 \pm 1.79$ , P < 0.05) after treatment. In contrast, the conventional indicators of tumor volume, SUVpeak, and ADCmin did not show significant differences between pre- and post-treatment. In a representative case of pleomorphic sarcoma, the treatment effect was clearly demonstrated after heavy-particle radiotherapy (figure).

#### CONCLUSION

Voxel-based analysis of SUVs and ADCs with PET/MR hybrid systems is useful for the evaluation of the treatment effect in softtissue tumors.

### **CLINICAL RELEVANCE/APPLICATION**

Voxel-based analysis of SUV and ADC with PET/MR system provides unique biomarkers such as the SUV-ADC correlation coefficient and the slope of SUV/ADC for the early determination of tumor response.

# MK323-SD-TUB3

Contrast-Enhanced Ultrasound (CEUS) in Diagnosis, Evaluation, and Management of Soft Tissue Sarcoma (STS)

Tuesday, Nov. 29 12:45PM - 1:15PM Room: MK Community, Learning Center Station #3

**FDA** Discussions may include off-label uses.

#### Participants

Mittul Gulati, MD, La Canada Flintridge, CA (*Presenter*) Nothing to Disclose James Hu, MD, Los Angeles, CA (*Abstract Co-Author*) Nothing to Disclose William Tseng, Los Angeles, CA (*Abstract Co-Author*) Nothing to Disclose Darryl Hwang, PhD, Los Angeles, CA (*Abstract Co-Author*) Nothing to Disclose Vinay A. Duddalwar, MD, FRCR, Los Angeles, CA (*Abstract Co-Author*) Nothing to Disclose

## PURPOSE

Contrast enhanced ultrasound (CEUS) was used to assess clinically suspected soft tissue sarcomas (STS). Evaluation included enhancement pattern and quantitative analysis (QA) of enhancement kinetics, as well as comparison to CT/MRI.

#### **METHOD AND MATERIALS**

20 patients with clinically suspected STS underwent CEUS. All underwent subsequent image-guided biopsy. Enhancement pattern: masses were categorized as P1 (non-enhancing), P2 (peripherally enhancing with central necrosis), P3 (heterogeneously enhancing with necrotic foci), or P4 (homogeneously enhancing). QA included evaluation of enhancing tumor, necrotic tumor, and adjacent skeletal muscle (control) parameters including time to peak (TTP) and wash in slope (WIS), with generation of time-intensity curves (TIC). Comparison was made to contrast-enhanced CT/MRI as available. Follow-up CEUS exams were also performed on 3 patients after neoadjuvant chemotherapy (NAC).

## RESULTS

Enhancement pattern: Of the 20 masses, none were non-enhancing (P1) on initial CEUS. 7 (35%) were peripherally enhancing with central necrosis (P2), and 11 (55%) were heterogeneously enhancing with internal necrotic foci (P3). All 18 masses with either P2 or P3 enhancement patterns were biopsy proven STS (100%). 2 masses demonstrated homogenous enhancement (P4); both were biopsy-proven lymphoma. Interestingly, both masses with P4 pattern were clinically suspected to be STS until CEUS and biopsy. QA: All 18 biopsy-proven STS demonstrated a typical enhancement pattern on TIC, with higher PI and steeper WIS of tumor relative to control (skeletal muscle). 3 patients demonstrated a quantifiable increase in tumor necrosis following NAC, from a mean of 21% necrosis on pre-therapy CEUS to 54% necrosis following NAC. CEUS exam results correlated closely with contemporaneous CT/MRI (available in 18 of 20 patients, or 90%).

## CONCLUSION

CEUS enhancement patterns of STS are distinct (P2 or P3), and may differentiate STS from lymphoma, which typically shows homogeneous enhancement (P4); STS also demonstrate a typical TIC on CEUS, with higher PI and steeper WIS than adjacent muscle. Finally, a subgroup of patients undergoing NAC demonstrated an expected, quantifiable increase in tumor necrosis during STS treatment, correlating closely with CT/MRI.

# **CLINICAL RELEVANCE/APPLICATION**

CEUS may aid in initial diagnosis, evaluation, and treatment monitoring of STS.

## MK324-SD-TUB4

Magnetic Resonance Imaging of the Sacroiliac Joints in SpA: The Real Added Value of Intravenous Contrast Media

Tuesday, Nov. 29 12:45PM - 1:15PM Room: MK Community, Learning Center Station #4

# Participants

Francesco Gentili, MD, Siena, Italy (*Presenter*) Nothing to Disclose Francesco G. Mazzei, MD, Siena, Italy (*Abstract Co-Author*) Nothing to Disclose Marta Fabbroni, Siena, Italy (*Abstract Co-Author*) Nothing to Disclose Susanna Guerrini, MD, Siena, Italy (*Abstract Co-Author*) Nothing to Disclose Nevada Cioffi Squitieri, MD, Siena, Italy (*Abstract Co-Author*) Nothing to Disclose Luca Cantarini, Siena, Italy (*Abstract Co-Author*) Nothing to Disclose Bruno Frediani, Siena, Italy (*Abstract Co-Author*) Nothing to Disclose Mauro Galeazzi, Siena, Italy (*Abstract Co-Author*) Nothing to Disclose Luca Volterrani, Siena, Italy (*Abstract Co-Author*) Nothing to Disclose Maria A. Mazzei, MD, Siena, Italy (*Abstract Co-Author*) Nothing to Disclose

#### PURPOSE

Active sacroiliitis based on MRI without intravenous (I.V.) contrast material injection is considered sufficient to diagnose spondyloarthritis (SpA), according to the Assessment of SpondyloArthritis International Society (ASAS) criteria. The aim of this work is to show the real added value of administering I.V. contrast material when evaluating the response to TNF antagonists therapy, on the extension and intensity of bone marrow oedema (BMO) and osteitis/synovitis in the sacroiliac joints (SIJ) on MRI.

#### **METHOD AND MATERIALS**

Thirty patients (16 females, mean age of 51 years, range 29-75 years,) with a diagnosis of SpA and active sacroiliitis at MRI with I.V. contrast material, were considered for a follow up MRI after 6 months of TNF antagonists therapy. Finally, 25 patients completed the study. Disease activity was monitored in 17 patients by a BASDAI questionnaire every 2 weeks and BASFI at baseline and at 6 months. MRI was performed with a 1.5 T MR unit (Signa Twin Speed Hdxt; General Electric Healthcare), before and after I.V. injection of gadobenate dimeglumine (Gd-BOPTA, 0.1mg/kg).

#### RESULTS

Thirteen patients showed reduction/disappearance of both pathological enhancement and BMO but the reduced grade of the first parameter was higher; six patients showed reduction/disappearance of enhancement whereas BMO was unchanged; one patient showed reduction of enhancement in absence of BMO before or after the therapy; five patients did not show a significant variation of MRI findings. We also found a better agreement between BASDAI and MRI post contrast images, when compared to BMO.

## CONCLUSION

The evaluation of enhancement is a clear predictor of response to therapy in SIJ involvement in SpA, better than BMO; hence it should be strongly advised in the MRI of these patients.

# **CLINICAL RELEVANCE/APPLICATION**

This study demonstrates the improved accuracy od MRI with contrast media in the assessment of active sacroiliitis, both at the time of diagnosis and in evaluating the response to anti TNF therapy.

Predicting the Development of Osteoarthritis over 8 Years using Baseline Clinical Data and MR Imaging: A Preliminary Study using Data from the Osteoarthritis Initiative

Tuesday, Nov. 29 12:45PM - 1:15PM Room: MK Community, Learning Center Station #5

## Participants

Gabby B. Joseph, San Francisco, CA (*Presenter*) Nothing to Disclose Charles E. McCulloch, San Francisco, CA (*Abstract Co-Author*) Nothing to Disclose Alexandra S. Gersing, MD, Munich, Germany (*Abstract Co-Author*) Nothing to Disclose Benedikt J. Schwaiger, MD, San Francisco, CA (*Abstract Co-Author*) Nothing to Disclose Ursula R. Heilmeier, MD, Munich, Germany (*Abstract Co-Author*) Nothing to Disclose Michael C. Nevitt, PhD, San Francisco, CA (*Abstract Co-Author*) Nothing to Disclose Thomas M. Link, MD, PhD, San Francisco, CA (*Abstract Co-Author*) Nothing to Disclose Thomas M. Link, MD, PhD, San Francisco, CA (*Abstract Co-Author*) Nesearch Grant, General Electric Company; Research Consultant, General Electric Company; Research Consultant, InSightec, Ltd; Research Grant, InSightec Ltd; Royalties, Springer Science+Business Media Deutschland GmbH; Consultant, Springer Science+Business Media Deutschland GmbH; Research Consultant, Pfizer Inc;

## PURPOSE

The purpose of this study was to determine whether the addition of MR imaging to baseline clinical and demographic data improves the prediction of symptomatic or radiographic osteoarthritis (OA) over 8 years.

## **METHOD AND MATERIALS**

775 subjects with no or mild radiographic OA (Kellgren Lawrence (KL) 0-2) and no or mild symptoms (WOMAC 0-3) in the right knee were selected from the Osteoarthritis Initiative (OAI) database. Compartment-specific baseline 3T MRI readings (WORMS scoring) and cartilage T2 quantification were performed. The outcome was moderate to severe radiographic or symptomatic OA defined by: an incident total knee replacement (TKR) over 8 years, progression to KL 3-4 over 8 years, or progression to a WOMAC pain score of >=5 at 7 or 8 year follow-up. Integrated discrimination Index (IDI, a measure of the prognostic improvement of a model when adding variables) was used to determine whether baseline risk factors (previous injury, family history of TKR), KL score, WORMS max. score (the maximum of all compartments), and cartilage T2 (5 knee compartments) improve the prediction of radiographic or symptomatic OA compared to a base model (age, gender, BMI) using stepwise forward selection.

#### RESULTS

Subjects had a mean age of  $56.1\pm7.1$  years, a mean BMI of  $27.2\pm4.3$  kg/m<sup>2</sup>, and 58.3% were female. 57 subjects (7.4%) developed symptomatic or radiographic OA at follow-up. The IDI showed that baseline KL grade (IDI=0.03, p=0.00009), WORMS max. score (IDI=0.02, p=0.001), and cartilage T2 (medial femur: IDI=0.02, p=0.03; patella: IDI=0.006, p=0.008) significantly improved model performance compared to the base model. The AUC of the base model was 0.59; the AUC of the base+KL model was 0.70 (p=0.01 vs. base model); the AUC of the final model (base+KL+WORMS+T2) was 0.76 (p=0.0003 vs. base model; p=0.05 vs. base+KL), Figure 1.

# CONCLUSION

This study showed that beyond demographic data, X-ray based KL score, and MRI-based WORMS and cartilage T2 aid in the prediction of symptomatic or radiographic OA.

# **CLINICAL RELEVANCE/APPLICATION**

This study demonstrates that the addition of MR imaging data to baseline clinical and demographic data improves the prediction of symptomatic or radiographic osteoarthritis over 8 years.

# MK326-SD-TUB6

#### An Imaging-based Method to Identify Regulators of Muscle Regeneration

Tuesday, Nov. 29 12:45PM - 1:15PM Room: MK Community, Learning Center Station #6

#### **Participants**

Srinath C. Sampath, MD, PhD, San Diego, CA (*Presenter*) Nothing to Disclose Srihari C. Sampath, MD, PhD, San Diego, CA (*Abstract Co-Author*) Nothing to Disclose Andrew Ho, PhD, Palo Alto, CA (*Abstract Co-Author*) Nothing to Disclose Stephane Corbel, PhD, Palo Alto, CA (*Abstract Co-Author*) Nothing to Disclose Christian Schmedt, PhD, San Diego, CA (*Abstract Co-Author*) Nothing to Disclose Helen Blau, PhD, Palo Alto, CA (*Abstract Co-Author*) Nothing to Disclose

## PURPOSE

In order to enable the development of new musculoskeletal therapeutics, we devised and applied a small animal imaging-based strategy to identify secreted proteins (biologics) capable of enhancing stem cell-mediated muscle regeneration.

## METHOD AND MATERIALS

All animal procedures were approved by the Stanford University School of Medicine IACUC. Primary muscle stem cells (MuSC) were isolated from donor mice expressing a *luciferase-GFP* transgene, and were treated *in vitro* with pools of recombinant proteins derived from a library of secreted or transmembrane proteins (563 clones representing 329 genes). Stem cell proliferation was monitored by bioluminescence imaging (BLI) over 6 days *in vitro*, followed by direct intramuscular transplant of treated cells into immunodeficient recipient mice. Stem cell engraftment and proliferation were monitored by BLI *in vivo* at 7, 30 and 60 days post-transplant. Positive pools were deconvolved to individual proteins through iterative rounds of imaging-based re-screening.

#### RESULTS

Bioluminescence imaging allowed quantitative evaluation of the response of stem cells to biologics. Our imaging-based screening strategy succeeded in evaluating complex mixtures of proteins for biological activity *in vivo*, leading to the identification of the IL-6 family cytokine Oncostatin M (OSM) as a potent inducer of muscle stem cell engraftment. Treatment of stem cells with OSM allowed their prolonged culture *in vitro* while maintaining 'stemness' and transplantation potential. Genetic deletion of the OSM receptor in muscle stem cells severely blocked regeneration after muscle injury, demonstrating a critical but previously unknown role for OSM in muscle repair.

#### CONCLUSION

We conclude that *in vivo* imaging techniques can be successfully applied to identify novel, pharmacologically relevant pathways of musculoskeletal regeneration. This imaging-based approach is sensitive, specific, generalizable, and bypasses many traditional inefficiencies of drug discovery by moving pathway and target identification *in vivo*.

#### **CLINICAL RELEVANCE/APPLICATION**

Biologics which activate muscle regeneration may improve the treatment of disorders characterized by stem cell dysfunction, including sarcopenia, cancer cachexia, and congenital muscular dystrophies.

In Need of Reference Values: Shear Wave Elastography (SWE) of Healthy Achilles Tendons: A Comparison Between Professional Athletes and the Non-Athletic General Population

Tuesday, Nov. 29 12:45PM - 1:15PM Room: MK Community, Learning Center Station #7

## Participants

Timm Dirrichs, Aachen, Germany (*Presenter*) Nothing to Disclose Christiane K. Kuhl, MD, Bonn, Germany (*Abstract Co-Author*) Nothing to Disclose Valentin Quack, Aachen, Germany (*Abstract Co-Author*) Nothing to Disclose Simone Schrading, MD, Aachen, Germany (*Abstract Co-Author*) Nothing to Disclose

#### PURPOSE

It has been shown that SWE is a useful tool to evaluate tendon stiffness, e.g. in diagnosing tendinopathies, as diseased tendons are intra-individually softer than healthy ones. But inter-individual reference values between different population groups and ages are still missing. Purpose of this prospective clinical study was to comparatively analyze tendon stiffness in professional athletes and non-athletic persons.

#### **METHOD AND MATERIALS**

Prospective study in 70 asymptomatic healthy participants, 35 (50 %) of them professional athletes with at least 3 training units of running per week and 35 (50 %) normal non-athletic persons, asymptomatic respectively. A consecutive of 140 Achilles tendons underwent standardized multi-modal US consisting of B-mode US (US), power Doppler (PD-US), and SWE, using a high-resolution linear 15 MHz probe (Aixplorer, Supersonic). Semi-quantitative-analysis of SWE-color-charts and quantitative, ROI-based-analysis of tendon elasticity were performed. SWE values of athletes and non-athletes were compared using student's t-test.

#### RESULTS

Mean SWE-value for Achilles tendon was 183.8 kPa ( $\pm$  98 kPa) in athletes and 103.6 kPa ( $\pm$  30.5 kPa) in the non-athletic control group. The difference between athletes and non-athletic participants was statistically significant (p<0.001). No significant changes were found between right and left side intra-individually. At semi-quantitative analysis of SWE-color-charts, athlete-tendons were rated as "soft" in 1/70 (1.4 %), as "intermediate" in 12/70 (17.1 %) and as "rigid" in 57/70 tendons (81.5 %). Non-athlete tendons were rated as "soft" in 25/70 (35.7%), as "intermediate" in 34/70 (48.6%) and as "rigid" in 11/70 (15.7%).

#### CONCLUSION

Tendon stiffness differs significantly between healthy athletes and healthy non-athletes. Athletes exhibit significantly higher SWEvalues in Achilles tendons, that is to say they have stiffer tendons. This might be caused by repeated training effects. SWE is able to measure and display these effects. Inter-individual varieties should be taken into consideration, especially when rating tendonstiffness in symptomatic persons, emphasizing that intra-individual comparison is of particular interest.

# **CLINICAL RELEVANCE/APPLICATION**

SWE appears to be useful to monitor tendon stiffness, especially in athletes or patients with tendinopathies. Knowledge about reference values is crucial in this context.

## MS119-ED-TUB1

Revisiting Taxonomy, Classification, and Cross Sectional Imaging Findings in Lymphatic Disorders-A Road Less Travelled

Tuesday, Nov. 29 12:45PM - 1:15PM Room: MS Community, Learning Center Station #1

## Participants

Ameya J. Baxi, MBBS, DMRD, San Antonio, TX (*Presenter*) Nothing to Disclose Carlos S. Restrepo, MD, San Antonio, TX (*Abstract Co-Author*) Nothing to Disclose Dhanashree Rajderkar, MD, Gainesville, FL (*Abstract Co-Author*) Nothing to Disclose Daniel Vargas, MD, Denver, CO (*Abstract Co-Author*) Nothing to Disclose

#### **TEACHING POINTS**

To define, classify, and discuss taxonomy and etiopathogenesis of various lymphatic disorders (LD)

To review the characteristic multimodality imaging findings of LD

To discuss differential diagnosis and post treatment follow up imaging

# TABLE OF CONTENTS/OUTLINE

LD are rare diverse pathologies of the lymphatic system characterized by isolated or widespread involvement of lung, bone, and other tissues. Due to its rarity, occasional case reports are published & limited radiology literature is available in regards to natural history, etiopathogenesis, classification and radiological manifestations. A more accurate and precise terminology term of LD is a need of time and is proposed. Cross sectional imaging MDCT and MRI provides accurate information on location, behavior, aggressiveness, mass effect & severity of disease. Imaging plays a critical role in the patient management and at times eliminates invasive diagnostic or therapeutic procedures. We excluded diseases like lymphoma, lymphadenopathy & lymphangitis carcinomaosa.Aims/ObjectivesIntroduction

Taxonomy Pathology, imaging and proposed classification of LDCongenital:Lymphangioma Lymphangiectasis Lymphangiomatosis Lymphatic dysplasia syndromeAcquired:Lymphocele Miscellaneous: LymphedemaDifferential diagnosis Review of literature Conclusion Teaching points

# **Honored Educators**

Presenters or authors on this event have been recognized as RSNA Honored Educators for participating in multiple qualifying educational activities. Honored Educators are invested in furthering the profession of radiology by delivering high-quality educational content in their field of study. Learn how you can become an honored educator by visiting the website at: https://www.rsna.org/Honored-Educator-Award/

Carlos S. Restrepo, MD - 2012 Honored Educator Carlos S. Restrepo, MD - 2014 Honored Educator

# Multimodality Imaging in Secondary Hypertension: A Comprehensive Review and Pictorial Essay

Tuesday, Nov. 29 12:45PM - 1:15PM Room: MS Community, Learning Center Station #2

#### Awards Certificate of Merit

#### **Participants**

Hyungwoo Ahn, MD, Seongnam-si, Korea, Republic Of (*Presenter*) Nothing to Disclose Hak Jong Lee, MD, PhD, Seongnam-Si, Korea, Republic Of (*Abstract Co-Author*) Nothing to Disclose Sung Il Hwang, MD, Seongnam-Si, Korea, Republic Of (*Abstract Co-Author*) Nothing to Disclose Yeo Goon Kim, MD, Seoul, Korea, Republic Of (*Abstract Co-Author*) Nothing to Disclose Sang Il Choi, MD, Seongnam-Si, Korea, Republic Of (*Abstract Co-Author*) Nothing to Disclose Eun Ju Chun, MD, PhD, Seongnam-Si, Korea, Republic Of (*Abstract Co-Author*) Nothing to Disclose

# **TEACHING POINTS**

To list various causes of secondary hypertension. To understand the diagnostic algorithm and appropriate imaging modality for evaluation of each cause of secondary hypertension. To identify specific imaging findings for each cause of secondary hypertension using multimodality imaging technique.

## **TABLE OF CONTENTS/OUTLINE**

Overview of clinical and lab-based approach for patients with hypertension. Various etiologies of secondary hypertension according to categorical classification and diagnostic algorithm. Advantages and limitations of multimodality imaging for evaluation of the secondary hypertension: US, CT, MRI, nuclear imaging and invasive angiography. Imaging spectrum of secondary hypertension using multimodality imaging technique. Renal parenchymal disease: polycystic kidney disease, glomerulonephritis Renovascular hypertension: atherosclerosis, fibromuscular dysplasia Endocrine hypertension: primary aldosteronism, Cushing's syndrome, pheochromocytoma, hyper/hypothyroidism, hyperparathyroidism, acromegaly Vascular hypertension: coarctation of aorta, midaortic dysplastic syndrome (congenital, Takayasu's arteritis) Miscellaneous: obstructive sleep apnea Summary table

# NM119-ED-TUB11

Influence of Radionuclide 123 MIBG Scintigraphy with Additional Curie Score in the Management of Pediatric Neuroblastoma

Tuesday, Nov. 29 12:45PM - 1:15PM Room: S503AB Station #11



#### Participants

Anderson B. Collier III, MD, Jackson, MS (*Presenter*) Nothing to Disclose Vani Vijayakumar, MD, Ridgeland, MS (*Abstract Co-Author*) Grant, General Electric Company

#### **TEACHING POINTS**

Explain Curie Score in Pediatric NeuroblastomasShow examples of MIBG study with Curie Scoring

#### **TABLE OF CONTENTS/OUTLINE**

Neuroblastoma (NBL) is the most common extracranial solid tumor of children. Despite improvement in outcomes, high risk patients have an unacceptably low survival. Over 90% of NBLs uptake metaiodobenzylguandine (MIBG) making MIBG scans useful in staging. MIBG is being evaluated for use in stratification. The curie score is a semi-quantitative measure of MIBG uptake at 10 different body sites. This score has been evaluated retrospectively in high risk NBL patients. The curie score after induction is the most predictive of outcome being able to differentiate a group of patients with a score  $\pounds 2$  who have a 44.9% 4-year event free survival (EFS) compared to a group with a score >2 who have a 15.4% 4-year EFS. When the status of the oncogene MYCN is included in this analysis, patients who are MYCN amplified and have a post-induction curie score >2 have a 3-year EFS of 0%. The score is being evaluated prospectively to confirm the results with more recent therapy. References:Yanik, GA. et.al. J Nucl Med 2013;54:541-8.Naranjo A. et.al. Pediatr Blood Cancer 2011;56:1041-5.Ady N. et.al. Eur J Cancer 1995;31A:256-61.Matthay KK. et.al. J Clin Oncol 2003;21:2489-91.Messina JA. et.al. Pediatr Blood Cancer 2006;47:865-74.

## NM223-SD-TUB6

Combination of PET SUV and Heterogeneity for Detecting Malignant Tumor in Case of Incidental Localized FDG Uptake in the Colorectal Region

Tuesday, Nov. 29 12:45PM - 1:15PM Room: S503AB Station #6

## Participants

Katsuya Mitamura, Kita-gun, Japan (*Presenter*) Nothing to Disclose Yuka Yamamoto, MD, PhD, Kagawa, Japan (*Abstract Co-Author*) Nothing to Disclose Takashi Norikane, Kita-gun, Japan (*Abstract Co-Author*) Nothing to Disclose Hanae A. Okuda, MD, Kita-Gun, Japan (*Abstract Co-Author*) Nothing to Disclose Yoshihiro Nishiyama, MD, Kagawa, Japan (*Abstract Co-Author*) Nothing to Disclose

# PURPOSE

The textural analysis using PET images has been proposed as a method to quantify the heterogeneity in several types of tumor. The purpose of this study was to investigate the feasibility of combination of PET parameters using decision-tree analysis to distinguish malignant tumor from benign tumor and physiological uptake in patients with incidental localized FDG uptake in the colorectal region.

#### **METHOD AND MATERIALS**

We conducted a retrospective review of the clinical data of 4983 patients who underwent FDG PET/CT imaging between April 2012 and December 2015 except patients for examination of the colorectal region. The FDG uptake (maximum standardized uptake value [SUVmax]) and FDG heterogeneity (entropy) were derived from FDG PET images. A decision-tree was developed in which the PET imaging investigations were applied sequentially to identify malignant colorectal tumors.

#### RESULTS

In 4983 FDG PET/CT images, 63 foci of localized FDG uptake were observed in the colorectal region in 60 patients. In these patients, 40 foci in 37 patients were examined using colonoscopy. The subsequent decision tree applied entropy as the initial PET parameter for differentiating between physiological uptake and tumor. The SUVmax was assessed second for differentiating between benign tumor and malignant tumor. Thus, the final decision tree comprised 2 decision nodes and 3 terminal nodes, one of which identified malignant tumor. The final diagnosis was malignant tumor in 11, benign tumor in 16, and no lesion (physiological FDG uptake) in 13 foci. The mean value of entropy in tumors was significantly higher than that in physiological uptake (p<0.01). The mean value of SUVmax in malignant tumor was significantly higher than that in benign tumor (p<0.02). The net sensitivity and net specificity for the decision tree were 91% and 76%, respectively. The net sensitivity was better than that for only SUVmax (73%). The net specificity was better than that for only entropy (45%).

## CONCLUSION

A decision-tree analysis using combination of PET parameters might have the potential to distinguish malignant tumor from benign tumor and physiological uptake in patients with incidental localized FDG uptake in the colorectal region.

## **CLINICAL RELEVANCE/APPLICATION**

Combination of PET parameters might have the potential to distinguish malignant tumor from benign tumor and physiological uptake in patients with incidental localized FDG uptake in the colorectal region.

## NM224-SD-TUB7

# Quantification of the Myocardial Perfusion Reserve in Chronic Kidney Disease Patients Using Dynamic SPECT Imaging

Tuesday, Nov. 29 12:45PM - 1:15PM Room: S503AB Station #7

# Participants

Noriko Tsuda, Kumamoto, Japan (*Presenter*) Nothing to Disclose Shinya Shiraishi, Kumamoto, Japan (*Abstract Co-Author*) Nothing to Disclose Fumi Sakamoto, Kumamoto, Japan (*Abstract Co-Author*) Nothing to Disclose Masataka Nakagawa, Kumamoto, Japan (*Abstract Co-Author*) Nothing to Disclose Hideaki Yuki, MD, Kumamoto, Japan (*Abstract Co-Author*) Nothing to Disclose Seiji Tomiguchi, MD, Kumamoto, Japan (*Abstract Co-Author*) Nothing to Disclose Yasuyuki Yamashita, MD, Kumamoto, Japan (*Abstract Co-Author*) Nothing to Disclose

#### PURPOSE

The aim of this retrospective study was to examine the relationship between chronic kidney disease (CKD), myocardial blood flow (MBF) and myocardial perfusion reserve (MPR) when calculated from dynamic 201Tl-chloride (Cl) kinetic analysis using a cadmium zinc telluride (CZT) ultra-fast camera.

# METHOD AND MATERIALS

A total of 263 patients assessed with dipyridamole 201TI-chloride (CI) SPECT-MPI using a CZT ultra-fast camera were enrolled in this study. All cases were assessed for stressK1, restK1 and MPRi evaluations by 2 compartment model analysis. SPECT-MPI clinical results showing ischemia myocardium to be more than 5% (summed stress score (SSS) > 3) were excluded. Patients having a past myocardial infarction and cases with a previous treatment history of percutaneous coronary intervention (PCI) and coronary artery bypass graft (CABG) surgery were also not included in the subjects enrolled.

## RESULTS

The CKD group consisted of 129 patients who had an eGFR below 60, and the control group of 134 patients with an eGFR over 60. As for clinical risk factors, age, BNP and Hb showed significant differences between the two groups. There were no statistically significant differences as to gender, BMI, smoking history, HL, DM, HT, TG, HDL-CHO, LDL-CHO, HbA1c, HR, SBP, DBP, LVEF, ESV and EDV between the two groups. Quantitative indicators for restK1 and MPRi showed statistically significant differences between the two groups (control group vs. CKD group: restK1, 0.191  $\pm$  0.045 vs. 0.211  $\pm$  0.061, P = 0.013; MPRi, 2.17  $\pm$  0.51 vs. 1.93  $\pm$  0.50, P < 0.001). StressK1 rates revealed no statistically significant difference (control group vs. CKD group: stressK1, 0.406  $\pm$  0.100 vs. 0.398  $\pm$  0.120).

## CONCLUSION

In patients with normal myocardial perfusion imaging (SSS  $\leq$  3), the CKD group showed impaired MPRi and increased rest MBF on dynamic 201TI-chloride (CI) kinetic analysis using a cadmium zinc telluride (CZT) ultra-fast camera.

## **CLINICAL RELEVANCE/APPLICATION**

A novel cardiac SPECT technology with solid-state semiconductor detectors is being used for the calculation of MBF and MPR.

Correlation of Intratumor Heterogeneity of 18F-FLT Uptake with Tumor Grade and Proliferation in Patients with Newly Diagnosed Gliomas

Tuesday, Nov. 29 12:45PM - 1:15PM Room: S503AB Station #8

## Participants

Yuka Yamamoto, MD, PhD, Kagawa, Japan (*Presenter*) Nothing to Disclose Katsuya Mitamura, Kita-gun, Japan (*Abstract Co-Author*) Nothing to Disclose Takashi Norikane, Kita-gun, Japan (*Abstract Co-Author*) Nothing to Disclose Tetsuhiro Hatakeyama, Kagawa, Japan (*Abstract Co-Author*) Nothing to Disclose Yoshihiro Nishiyama, MD, Kagawa, Japan (*Abstract Co-Author*) Nothing to Disclose

# PURPOSE

The nucleoside analog 3'-deoxy-3'-18F-fluorothymidine (FLT) has been investigated for evaluating tumor proliferating activity in brain tumors. The textural analysis using PET images has been proposed as a method to quantify the heretogeneity in several types of tumor. The purpose of this study was to evaluate FLT uptake using textural analysis in patients with newly diagnosed gliomas and to correlate the results with tumor grade and proliferative activity.

## **METHOD AND MATERIALS**

FLT PET was investigated in 36 patients with newly diagnosed gliomas. PET emission scanning of the head region with a 15-min acquisition of one bed position was performed at 60 min after FLT injection. The maximum standardized uptake value (SUVmax), tumor-to-contralateral normal brain tissue (T/N) ratio, and metabolic tumor volume (MTV) and textural features (standard deviation, skewness, kurtosis, entropy, and uniformity) were derived from FLT PET images. Tumor grading and proliferative activity as indicated by the Ki-67 index were estimated in tissue specimens.

## RESULTS

There was a significant difference in SUVmax between grades II and IV (p<0.02), in T/N ratio between grades II and IV (p<0.02), in standard deviation between grades II and IV (p<0.03), and in entropy between grades III and IV (p<0.05). Linear regression analysis indicated a significant correlation between Ki-67 index and SUVmax (r=0.40, p<0.03), T/N ratio (r=0.43, p<0.02), MTV (r=0.41, p<0.002), kurtosis (r=0.51, p<0.003), entropy (r=0.73, p<0.001), and uniformity (r=-0.61, p<0.001).

# CONCLUSION

FLT based heterogeneity may be useful in the noninvasive assessment of tumor grade and proliferation in newly diagnosed gliomas.

## **CLINICAL RELEVANCE/APPLICATION**

FLT based heterogeneity may be useful in the noninvasive assessment of tumor grade and proliferation in newly diagnosed gliomas.

## Evaluation of PET/MR (including DWI) for Assessment of Bone Metastases in Oncologic Patients

Tuesday, Nov. 29 12:45PM - 1:15PM Room: S503AB Station #9

#### **Participants**

Chiara Giraudo, MD, Vienna, Austria (*Presenter*) Nothing to Disclose Michael Weber, Vienna, Austria (*Abstract Co-Author*) Nothing to Disclose Daniela Senn, Vienna, Austria (*Abstract Co-Author*) Nothing to Disclose Georgios Karanikas, MD, Vienna, Austria (*Abstract Co-Author*) Nothing to Disclose Markus Hartenbach, MD, Ulm, Germany (*Abstract Co-Author*) Nothing to Disclose Marius E. Mayerhoefer, MD, PhD, Vienna, Austria (*Abstract Co-Author*) Nothing to Disclose

# PURPOSE

To evaluate whether quantitative or qualitative measures derived from PET/MR (including DWI) enable the detection of bone metastases (BM), despite the known underestimation of tracer uptake on PET due to the currently used attenuation correction technique.

#### **METHOD AND MATERIALS**

Patients with histologically proven cancer, who were referred to our tertiary care center for PET/MR between August 2014 and March 2016, were included in this retrospective study. Inclusion criteria were:[18F]-FDG- or [68Ga]-PSMA-PET/MR (fully integrated 3T system) at staging; BM at imaging (hypointense lesion on T1w with high uptake on PET, non-inflammatory); T1w and DWI implemented the protocol. Patients with a history of radio/immuno/chemotherapy were excluded. For each patient with BM (pBM) a control patient (Co), matching the inclusion criteria, but without BM, was included. SUVmax, SUVavg, ADCmin, ADCavg, mean T1w SI were collected from each BM and from 1 healthy bone area (HB) in each pBM (pHB) and Co (cHB). For each BM, the diagnostic confidence (dc) of PET, DWI, T1w, and the DWI image quality of DWI, were assessed on a 10-point scale.One-way-ANOVA and Bonferroni-corrected Games-Howell post-hoc tests were used to assess quantitative differences between BM and HB. Correlation coefficients (Spearman) between SUVs and ADCs and between DWI dc and image quality were calculated.

## RESULTS

Overall, 14 pBM and 14 Co out of 130 PET/MR exams met our inclusion criteria. Primary tumors were lymphoma (n=9), prostate-(n=7), cervix-(n=5), breast-, ovarian-, adrenal gland-, pancreas-, thyroid cancer, HCC and thymoma (1 each).Statistically significant differences for SUVmax, SUVavg, ADCmin, ADCavg, and mean T1w SI emerged between BM (n=56) and HB (14pHB, 14cHB) (p=0.000, respectively). No significant differences occurred between pHB and cHB. No correlation emerged between SUVs and ADCs (pSUVmax vs ADCmin=0.963; pSUVavg vs ADCavg=0.294). Mean Dc ratings were 9.3 (PET), 8.4 (T1) and 7.5 (DWI); mean DWI image quality was 8.46. DWI dc significantly correlated with DWI image quality (r=0.394 p=0.000).

# CONCLUSION

PET/MR with DWI may enable a reliable quantitative differentiation of BM from HB. Moreover, PET showed the highest dc.

## **CLINICAL RELEVANCE/APPLICATION**

Despite the technical limitations associated with MR-AC, PET/MR including DWI demonstrated to be a robust tool for detecting and quantifying bone metastases in oncologic patients.

## Injection to Scan Time Practices in Oncologic FDG PET: A 10-Year Intra and Multi Institutional Review

Tuesday, Nov. 29 12:45PM - 1:15PM Room: S503AB Station #10

#### **Participants**

Katherine Binzel, PhD, Columbus, OH (*Presenter*) Nothing to Disclose David Poon, BS, Columbus, OH (*Abstract Co-Author*) Nothing to Disclose Ajay Siva, Columbus, OH (*Abstract Co-Author*) Nothing to Disclose Jun Zhang, PhD, Columbus, OH (*Abstract Co-Author*) Nothing to Disclose Barbaros S. Erdal, PhD, Columbus, OH (*Abstract Co-Author*) Nothing to Disclose Michael V. Knopp, MD, PhD, Columbus, OH (*Abstract Co-Author*) Nothing to Disclose Chadwick L. Wright, MD, PhD, Lewis Center, OH (*Abstract Co-Author*) Nothing to Disclose Preethi Subramanian, MS, BEng, Columbus, OH (*Abstract Co-Author*) Nothing to Disclose

#### PURPOSE

As injection to scan time variation is the most common deviation from protocol when oncologic PET/CT is used within clinical trials, we set out to investigate the clinical reality within a 10 year window, both intra-institutionally and within multi-institutional trials.

#### **METHOD AND MATERIALS**

We started to record all image acquisition related information since 2005 in a searchable database infrastructure. Our team also manages national clinical trials on behalf of NCI (NCTN) and are thus intensively involved in quality assurance for clinical trials that use PET/CT for staging and response assessment. We developed and analyzed our databases using query tools and pivot tables.

# RESULTS

Variations from the protocol defined imaging time post injection remains the most common protocol violation in FDG PET/CT. Compliance has overall improved within the last decade apparently due to better training, communication and clinical trial expectations. This improvement continued over the years even when local practice is different from protocol specifications with the following trends. One multi-center trial expecting a 50-70 minutes imaging start p.i. had a 99% compliance (n=476), while another with a 60-80 minute target window had only 75%. Within the single institution review of standard clinical imaging, we found also improvement over the years but only 61% of studies fell within 10 minutes of the 75 minute target uptake time. Most institutions do not regularly monitor injection to scan time compliance especially in regard to consistency between baseline and follow up for response assessment.

#### CONCLUSION

Adherence to protocol expectations for FDG PET/CT imaging has improved in regard to imaging time post injection, but remains a constant source of protocol inconsistencies. Multicenter national clinical trials have seen overall the best improvement which is apparently due to better communication, training, trial QC and feedback mechanisms. Outside of clinical trials, variability remains very high and appears to fluctuate over the years. Therefore, clinical services should also use quality assurance and management tools to ensure being aware of local practice changes.

## **CLINICAL RELEVANCE/APPLICATION**

Inconsistency with clinical protocol requirements in regard to imaging time post FDG injection remains a common occurrence. Integrated feedback mechanisms are essential for local and clinical trial adherence.

# High Resolution Study of Temporal Bone Anatomy and Pathology with Flat Panel CT

Tuesday, Nov. 29 12:45PM - 1:15PM Room: NR Community, Learning Center Hardcopy Backboard

#### Participants

Sonia F. Calloni, MD, Milan, Italy (*Presenter*) Nothing to Disclose Clara Sina, MD, Milan, Italy (*Abstract Co-Author*) Nothing to Disclose Elisa Scola, MD, Milan, Italy (*Abstract Co-Author*) Nothing to Disclose Sabrina Avignone, MD, Milan, Italy (*Abstract Co-Author*) Nothing to Disclose Luciano Lombardi, Milan, Italy (*Abstract Co-Author*) Nothing to Disclose Fabio M. Triulzi, Milan, Italy (*Abstract Co-Author*) Nothing to Disclose

# **TEACHING POINTS**

1) To show how Flat panel CT (FPCT) provides CT-like images with high-contrast and high spatial resolution acquired with a C-arm x-ray system using of flat panel image detectors.2) To show how FPCT provides an excellent assessment of ear anatomy, ear pathology, prothesis and choclear implants with better spatial resolution and lower dose compared to multislices CT.

## **TABLE OF CONTENTS/OUTLINE**

FPCT acquisition and reconstruction parameters: a collimated 20-second FPCT of bilateral temporal bone is performed by using Carm x-ray system with flat panel image detectors (80kV, small focus, 240° degree rotation angle, acquisition slice thickenss 0.14 mm). High-resolution secondary reconstructions are created (voxel size 0.07 mm3, 512x512 section matrix).Compared to multisection CT, FPCT offers higher spatial resolution (FPCT cubic voxel size 0.07 mm3 vs 0.6 mm3 CT) and a lower dose (crystalline lens 2.20 vs 60.90 mSv CT – brain 10.66 vs 26.40 mSv CT).The determinant role resides in studying temporal bone anatomy, malformations, fractures and otosclerosis. It creates less streak artifacts improving imaging of the cochlea enabling identification of electrodes of cochlear implants and their possible proximity with the fallopian canal. Due to thin thickness and the sharpen quality of images, FPCT also shows very small prothesis and their right placement. Atypical Neurocutaneous Syndromes: Clinicoradiological Approach to Diagnosis

Tuesday, Nov. 29 12:45PM - 1:15PM Room: NR Community, Learning Center Station #8

#### Awards Magna Cum Laude

#### **Participants**

Felipe Scortegagna Sr, MD, Sao Paulo, Brazil (*Presenter*) Nothing to Disclose Lazaro F. Amaral, MD, Sao Paulo, Brazil (*Abstract Co-Author*) Nothing to Disclose Antonio J. da Rocha, MD, PhD, Sao Paulo, Brazil (*Abstract Co-Author*) Nothing to Disclose Fabricio G. Goncalves, MD, Brasilia, Brazil (*Abstract Co-Author*) Nothing to Disclose Nasjla Saba, Sao Paulo, Brazil (*Abstract Co-Author*) Nothing to Disclose Leonardo F. Freitas, MD, Sao Paulo, Brazil (*Abstract Co-Author*) Nothing to Disclose Victor R. Marussi, MD, Campinas, Brazil (*Abstract Co-Author*) Nothing to Disclose Marcelo R. Natal, MD, Brasilia, Brazil (*Abstract Co-Author*) Nothing to Disclose

## **TEACHING POINTS**

The purpose of this exhibit is: 1.To review the pathophysiology and clinical aspects of rare neurocutaneous syndromes. 2.To describe the typical imaging features of different types of these entities, particularly in brain and spine.3.To show illustrative clinical photograps and also neuroimaging findings in magnetic resonance imaging (MRI) and computed tomography (CT) of confirmed cases from the Radiology and Neurology Divisions of our hospital

# TABLE OF CONTENTS/OUTLINE

IntroductionReview of pathophysiology and clinical findings of rare neurocutaneous syndromesNeuroimaging findings in rare neurocutaneous syndromes, with sample cases of our institution, particularly in brain and spine: -MRI - CT Summary and key points

## NR378-SD-TUB2

Olfactory fMRI Activation Pattern Changes during Difference Concentration Odor Stimulation in Alzheimer's Disease

Tuesday, Nov. 29 12:45PM - 1:15PM Room: NR Community, Learning Center Station #2

# Participants

Jianzhong Yin, MD, Tianjin, China (*Presenter*) Nothing to Disclose Dongxu Ji, Tianjin, China (*Abstract Co-Author*) Nothing to Disclose Hui Zhang, Tianjin, China (*Abstract Co-Author*) Nothing to Disclose Hongyan Ni, PhD, Tianjin, China (*Abstract Co-Author*) Nothing to Disclose Wen Shen, Tianjin, China (*Abstract Co-Author*) Nothing to Disclose

# PURPOSE

The Alzheimer's disease can involve the olfactory system at the early stage. To improve the reliability of the olfactory fMRI, we examined the response of primary olfactory cortex across three different concentrations of odors.

## **METHOD AND MATERIALS**

24 normal controls, 24 MCI, and 22 AD patients were scanned using a 3.0T MR for an olfactory fMRI with three different (0.10%, 0.33%, and 1.00%) concentrations of lavender stimuli. The data was processed to observe the activation of the whole brain and analyze the number of activated voxels in the primary olfactory cortex (POC), especially the activation changes during different concentrations.

## RESULTS

The AD groups showed low activation in multiple brain areas; the total activated voxel numbers in the POC of MCI subjects and AD patients were significantly lower than that of controls (P<0.001, <0.001, respectively). During different concentrations, the POC activation pattern of NC group showed olfactory adaptation, but the AD patients showed not only increased olfactory threshold but also lack of olfactory habituation (X2=28.384, P<0.001).

## CONCLUSION

This finding indicates that the POC activation pattern of olfactory fMRI across different concentrations is reliable in the evaluation of olfactory function changes in the AD patients.

#### **CLINICAL RELEVANCE/APPLICATION**

During olfactory fMRI, the response of POC across different concentrations may show olfactory adaptation in normal controls, but increased olfactory threshold and lack of habituation in AD.

## Disrupted Dynamic Functional Connectivity Variance in First-episode, Drug-naive Major Depressive Disorder

Tuesday, Nov. 29 12:45PM - 1:15PM Room: NR Community, Learning Center Station #3

#### **Participants**

Zhan Feng Sr, Hang Zhou, China (*Presenter*) Nothing to Disclose Hong Yang, MD, Hangzhou, China (*Abstract Co-Author*) Nothing to Disclose Manli Huang, Hangzhou, China (*Abstract Co-Author*) Nothing to Disclose

#### PURPOSE

Previous resting-state FC analysis generally assume that the functional connections remain constant during the whole period of data collection. But more and more memerging experimental observations and theories propose that FC of human brain is constantly changing human brain connectome is most likely to be time dependent and dynamic, and to be related to ongoing rhythmic activity. So we exploratory tracked the variability of the topology of the brain connectome through dynamic FC(d-fc) analysis.

## **METHOD AND MATERIALS**

Twenty-three patients diagnosed based on DSM-IV, twenty matched normal controls were recruited. Twenty-four axial slices covering whole brain were acquired using a 3.0T Philips scanner (TR/TE 2000/35ms, FOV 24 cm, total 200 time points). The result of a Meta-analysis on MDD neuroimaging studies was directly used to set the coordinates of the anterior cingulate cortex: (-6, 30, 12) for voxel wise d-FC analysis. D-FC was computed using a sliding window approach with a window size of 30 TR in steps of 15 TR. Variability of time series of d-FC between the seed node and whole-brain voxel was then determined by DynamicBC software package. Finally two-sample t test was used for analysis of the differences of FC variability mapping between the two groups.

#### RESULTS

Compared to the normal control group, d-FC variability between ACC and cerebral domains (dorsal prefrontal cortex, the right occipital lobe, and posterior cingulate cortex) significantly decreased in untreated first-onset MDD patients.

#### CONCLUSION

Our analysis suggests that patients show reduced d-FC variability in dorsal prefrontal cortex, the right occipital lobe, and posterior cingulate cortex. It has been proved that such brain areas are called zone of instability, namely, their FC in temporal domain is flexible. These results indicated that FC variability of MDD patients is weakened, suggesting problems in functional emerge and dissolve paradigm among visual network, dorsal attention network, and the default network, instead of simple increase or decrease of static FC, which reflects decease in functional diversity and integration capacity of these cerebral domains.

# **CLINICAL RELEVANCE/APPLICATION**

Quantify changes in functional connectivity may provide greater insight into neuropathologic mechanism of the MDD

# Evaluation of Ex-vivo 9.4T MRI in Post-surgical Specimens from Temporal Lobe Epilepsy Patients

Tuesday, Nov. 29 12:45PM - 1:15PM Room: NR Community, Learning Center Station #5

#### **Participants**

Benjamin Kwan, MD, London, ON (*Presenter*) Nothing to Disclose
Fateme Salehi, MD, London, ON (*Abstract Co-Author*) Nothing to Disclose
Ryan Kope, London, ON (*Abstract Co-Author*) Nothing to Disclose
Donald H. Lee, MD, London, ON (*Abstract Co-Author*) Nothing to Disclose
Manas Sharma, MBBS, MD, Toronto, ON (*Abstract Co-Author*) Nothing to Disclose
Robert Hammond, MD, London, ON (*Abstract Co-Author*) Nothing to Disclose
Terry Peters, PhD, London, ON (*Abstract Co-Author*) Research support, Synaptive Medical Inc; Research support, NeoChord, Inc;
Research support, Northern Digital Inc; Research support, Analogic Corporation
Ali R. Khan, PhD, London, ON (*Abstract Co-Author*) Nothing to Disclose

#### PURPOSE

Hippocampal sclerosis (HS) is the most common underlying etiology in adult patients with drug resistant temporal lobe epilepsy. Conventional clinical MRI systems, are not able to reliably differentiate between HS subtypes. However, advances in ultra-high field MRI have led to enhanced spatial resolution, tissue contrast, and sensitivity in structural brain imaging. This study evaluates hippocampal pathology through usage of ultra-high field 9.4T ex vivo imaging of resected surgical specimens in patients who have undergone temporal lobe epilepsy surgery.

## **METHOD AND MATERIALS**

MRI scanning of resected surgical specimens from patients who have undergone temporal lobe epilepsy surgery was performed on a 9.4T small bore Varian MR magnet (Varian, Palo Alto, CA) in a millipede birdcage MP30 coil (Agilent, Santa Clara, CA). Structural images employed a balanced steady-state free precession sequence (TrueFISP, resolution = 0.1 mm isotropic, TR = 7.6 ms, TE = 3.8 ms, flip angle = 30 degrees, FOV =  $38 \times 25.6 \times 19.2 \text{ mm2}$ ). Two neuroradiologists qualitatively reviewed 4 ex-vivo MRIs of resected specimens which were acquired at 9.4T. The specimen MRIs were reviewed while blinded to the histopathology reports for the ability to identify abnormal features in hippocampal subfield structures including atrophy, architectural irregularities and signal abnormality.

## RESULTS

4 patients (1 female; 3 males) were included in the study with an average age at surgery of 33.5 years (range 20-60). Average follow up time was 610 days (range 327–906). Qualitative evaluation by the two neuroradiologists was in complete agreement and was able to detect subfield abnormalities corresponding to histopathological reports. The most common finding was CA subfield atrophy. Dentate gyrus atrophy was present in one specimen and this was qualitatively detected on imaging.

## CONCLUSION

This study presents a technical framework for high resolution qualitative radiological-pathological correlation by neuroradiologists. Preliminary results using ultra-high field 9.4T MRI of resected surgical specimens suggests that improved resolution/SNR allows identification of abnormalities which typically are only seen at histopathology.

#### **CLINICAL RELEVANCE/APPLICATION**

This paper presents a technical framework for radiological-pathological correlation using ex-vivo ultra-high field 9.4T MRI in temporal lobe epilepsy surgical specimens.

## Functional MRI and Diffusion Tensor Imaging for Young Athletes' Sport-related Concussion: A Pilot Study

Tuesday, Nov. 29 12:45PM - 1:15PM Room: NR Community, Learning Center Station #6

#### Participants

Wen-Ching Liu, PHD, Peoria, IL (*Presenter*) Nothing to Disclose Laurence Jiang, MD, Peoria, IL (*Abstract Co-Author*) Nothing to Disclose Dzung Dinh, MD, Peoria, IL (*Abstract Co-Author*) Nothing to Disclose Cristin Rassi, Peoria, IL (*Abstract Co-Author*) Nothing to Disclose Peggy Flannigan, PhD, Peoria, IL (*Abstract Co-Author*) Nothing to Disclose David Ho, DO, Houston, TX (*Abstract Co-Author*) Nothing to Disclose Kyle Mou, Peoria, IL (*Abstract Co-Author*) Nothing to Disclose Michael T. Zagardo, MD, Peoria, IL (*Abstract Co-Author*) Nothing to Disclose

## PURPOSE

The CDC estimates that there are 1.6 -3.8 million concussions each year. Currently, conventional MRI cannot detect any intracranial abnormalities associated with concussive injury. Functional MRI (fMRI) and diffuse tensor imaging (DTI) sequence have been utilized to unveil abnormalities in deep white matter after mild traumatic brain injury (mTBI). To further explore these diagnostic modalities for sport related concussion, we enroll high school and college athletes without and with concussion in a prospective study to see if we can delineate the area of injury sustained from mTBI.

#### **METHOD AND MATERIALS**

A total of 37 male subjects age 16-44 participated in the study. There were 8 athletes without current concussion, 8 within 48 hours of concussion and 21 non-athletes who never had any concussion before. The 8 athletes with concussion were also studied on 2 weeks and 4 weeks later. All the subjects were scanned using a GE 3.0 Tesla High Definition Excite system. The imaging sequences contains 3D anatomical images plus BOLD functional MRI (N-back tasks, mental rhyming task, and rest state), and Diffusion weighted images.Imaging data were analyzed individually and as a group using FMRIB Software Library from Oxford University with associated tools (i.e. FEAT, MELODIC & TBSS) with a threshold of p < 0.05. Group comparisons were also performed with multiple comparison considerations.

#### RESULTS

The DTI data showed both the concussed and normal athlete groups have significantly higher fractional anisotropy (FA) in corpus callosum, internal capsule, and corona radiata when compared with normal control group, but not between the concussed (including 2 and 4 weeks) vs. normal athlete groups. The concussed group (only within 48 hours) showed higher activity in the left caudate and putamen than the normal control when performing a paradigm. The 48 hour-concussed group demonstrated weaker networks in cerebellum and posterior parietal lobe than the normal athlete group.

## CONCLUSION

The alternations in brain networks and white matters caused by sport-related concussions in athletes may remain longer than 4 weeks. The combination of fMRI and DTI in a longitudinal study demonstrated a unique way to unveil brain injury that otherwise not detected by conventional MRI.

## **CLINICAL RELEVANCE/APPLICATION**

The combination of fMRI and DTI in a longitudinal study demonstrated a unique way to unveil brain injury that otherwise not detected by conventional MRI.

# Review of Common Fetal Neural Tube Defects and Central Nervous System (CNS) Anomalies

Tuesday, Nov. 29 12:45PM - 1:15PM Room: OB Community, Learning Center Station #1

#### **Participants**

Sarah R. Ceglar, MD, Los Angeles, CA (*Presenter*) Nothing to Disclose Kristina E. Hoque, MD, PhD, Los Angeles, CA (*Abstract Co-Author*) Nothing to Disclose Daphne K. Walker, MD, Los Angeles, CA (*Abstract Co-Author*) Nothing to Disclose

## **TEACHING POINTS**

The purpose of this exhbit is:(1) Schematic review of CNS embryology and developmental anatomy (2) Imaging and review of common neural tube defects and CNS anomalies (3) Presentation of select cases from our institution

# TABLE OF CONTENTS/OUTLINE

Introduction Schematic review of normal CNS embryology and developmental anatomy Imaging of the fetal CNS Ultrasound (US) First trimester Second trimester screening Maternal Fetal Medicine Neurosonogram Adjunct imaging 3D ultrasound Volumetric analysis of intracranial structures Fetal MRI Virtual autopsy: post mortem fetal brain MRI Review of common neural tube defects and CNS anomalies Head: Chiari II malformation, ventriculomegaly, anencephaly, encephalocele, Dandy-Walker malformation, holoprosencephaly, etc. Spine: spina bifida, vertebral anomalies, etc. Presentation of select cases from our institution Review of in utero interventions: myelomeningocele repair, ventriculoamniotic shunting, etc.

# OB157-ED-TUB2

## Functional MR Imaging in Gynecologic Malignancies: Current Status and Future Perspectives

Tuesday, Nov. 29 12:45PM - 1:15PM Room: OB Community, Learning Center Station #2

#### **Participants**

Sung Bin Park, MD, Seoul, Korea, Republic Of (*Presenter*) Nothing to Disclose Hyun Jeong Park, Seoul, Korea, Republic Of (*Abstract Co-Author*) Nothing to Disclose Eun Sun Lee, MD, PhD, Seoul, Korea, Republic Of (*Abstract Co-Author*) Nothing to Disclose Jong Beum Lee, Seoul, Korea, Republic Of (*Abstract Co-Author*) Nothing to Disclose Byung Ihn Choi, MD, PhD, Seoul, Korea, Republic Of (*Abstract Co-Author*) Nothing to Disclose

# **TEACHING POINTS**

The major teaching points of this exhibit are:1. Functional MR imaging techniques play an important role in detection, characterization, staging, treatment response, and outcome prediction, as well as providing conventional morphologic imaging.2. Familiarity with the characteristics and imaging features of functional MR imaging in gynecologic malignancies will facilitate prompt and accurate diagnosis and treatment.

#### **TABLE OF CONTENTS/OUTLINE**

Functional MR Imaging Techniques - Diffusion weighted imaging (DWI) and ADC: cellularity - Dynamic contrast enhanced MR imaging (DCE-MRI): perfusion, vascularity - Blood oxygen level-dependent (BOLD) MR imaging: Hypoxic status - MR spectroscopy (MRS): metabolismUterine Cervical Cancer - Tumor detection and characterization - Staging - Assessing response and predicting outcomeEndometrial Cancer - Tumor detection and characterization - Staging - Predicting outcomeLeiomyosarcoma: accurate diagnosisOvarian cancer - Tumor detection and characterization - Staging - Predicting outcomeFuture Perspectives - Specialized DWI techniques: IVIM, DTI - BOLD- ASL- MRS- Hybrid imaging technique: Enhanced imaging + DWI

# PD111-ED-TUB6

Childhood Interstitial Lung Disease (chILD): An Illustrated Review of the Classification of the American Thoracic Society

Tuesday, Nov. 29 12:45PM - 1:15PM Room: PD Community, Learning Center Station #6

# Participants

Alexia Dabadie, MD, Vancouver, BC (*Presenter*) Nothing to Disclose Ema Todorovic, Vancouver, BC (*Abstract Co-Author*) Nothing to Disclose Anna Lee, MD, Vancouver, BC (*Abstract Co-Author*) Nothing to Disclose Connie Yang, MD, Vancouver, BC (*Abstract Co-Author*) Nothing to Disclose Helen R. Nadel, MD, Vancouver, BC (*Abstract Co-Author*) Nothing to Disclose Douglas H. Jamieson, MBBCh, Vancouver, BC (*Abstract Co-Author*) Nothing to Disclose Heather J. Bray, MD, Vancouver, BC (*Abstract Co-Author*) Nothing to Disclose

## **TEACHING POINTS**

To review the latest classification of Childhood Interstitial Lung Disease (chILD) provided by the American Thoracic Society and discuss its strengths and weaknesses To illustrate this classification with imaging features of some common or specific diagnoses of chILD and to correlate with pathologic findings on lung biopsy when available To discuss the role of the chest High-Resolution (HR) CT in the diagnostic strategy of chILD

# TABLE OF CONTENTS/OUTLINE

Review the clinical definition and epidemiology of chILD Review the American Thoracic Society classification and discuss its strengths and weaknesses: From a radiological point of view From a clinical point of view From a pathological point of view Review, with illustrative cases, the radiologic manifestations of common and/or specific diagnoses of chILD, with pathological correlation when available Discuss the indications for and technical parameters of chest HRCT in the diagnostic workup of chILD

# PD114-ED-TUB7

## Imaging Signs in the Diagnosis of Acute Appendicitis in Children using Magnetic Resonance Imaging

Tuesday, Nov. 29 12:45PM - 1:15PM Room: PD Community, Learning Center Station #7

#### **Participants**

Larry A. Kramer, MD, Houston, TX (*Presenter*) Nothing to Disclose Steven S. Chua, MD, PhD, Houston, TX (*Abstract Co-Author*) Nothing to Disclose

## **TEACHING POINTS**

MR imaging without oral or intravenous contrast material has rapidly replaced computed tomography at our institution in ultrasound equivocal cases of acute appendicitis in children. Similar to all modalities, early appendicitis can be challenging to diagnose. There are imaging signs that can be employed to improve the likelihood of efficient and accurate interpretation. The teaching objectives of this exhibit are as follows: 1. To identify the appendix as reliably and quickly as possible.2. To recognize subtle changes of early appendicitis.3. To diagnose perforated appendicitis and abdominal/peritoneal abscess.4. To identify other causes of acute abdominal pain in children.5. To learn how to apply DWI in the acute abdomen.

## **TABLE OF CONTENTS/OUTLINE**

Outline:1. Comprehensive description of the rapid free breathing MRI protocol.2. Role of MR imaging in the workup of acute appendicitis.3. Novel descriptors in the evaluation of acute appendicitis that are useful to quickly identify and characterize the appendix (i.e. the spectacle, ring and the dripping candle wax signs).4. Description of MR imaging signs of ruptured appendicitis (i.e. morel mushroom and fecalith signs).5. Application of diffusion weighted imaging in the acute abdomen.6. Examples of other causes of acute abdominal pain in children.

# PD153-ED-TUB8

Multi-slice Computed Tomography Assessment of Tracheobronchial Patterns in Partial Anomalous Left Pulmonary Artery

Tuesday, Nov. 29 12:45PM - 1:15PM Room: PD Community, Learning Center Station #8

# Participants

Shiyu Wang, MD, Shanghai, China (*Presenter*) Nothing to Disclose Li Wei Hu, DIPLENG, MENG, Pudong, China (*Abstract Co-Author*) Nothing to Disclose Haisheng Qiu, Shanghai, China (*Abstract Co-Author*) Nothing to Disclose Yumin Zhong, MD, Shanghai, China (*Abstract Co-Author*) Nothing to Disclose

## **TEACHING POINTS**

Illustrate the definition of partial anomalous left pulmonary artery (PALPA) Demonstrate the relationship between PALPA and tracheobronchial tree Illustrate the pros and cons

## **TABLE OF CONTENTS/OUTLINE**

1. The definition and clinical features of PALPA One of left pulmonary arterial branch arises from the right pulmonary artery Tracheobronchial abnormalities Kabuki syndrome2. The relationship between PALPA and tracheobronchial patterns Formed a pulmonary sling with a long segment trachea stenosis Passed below the tracheal bifurcation and went anterior to left bronchus without causing bronchial compression Went below the level of carina and coursed inferior-anterior to the left bronchus with or without causing bronchial compression3. Three patterns of tracheobronchial tree in PALPA A normal tracheobronchial branch A normal tracheobronchial branch with right tracheal bronchus A bridging bronchus4. The pros and cons of MSCT to assess PALPA and airway Low dose 3D reconstruction Light sedation or no sedation Identify the cardiovascular and tracheal anomalies and lung lesions simultaneouslySummaryPALPA can potentially cause tracheobronchial anomalies. Noninvasive imaging modalities such as MSCT can be helpful for accurate diagnosis and will be helpful for making further management decisions.

# PD225-SD-TUB1

Obstructive Reproductive Tract Anomalies in Pediatric Patients: Different Obstruction Sites by MR Imaging and its Role in Preoperative Evaluation

Tuesday, Nov. 29 12:45PM - 1:15PM Room: PD Community, Learning Center Station #1

#### Awards

#### **Student Travel Stipend Award**

#### Participants

Heng Zhang, MD, Chengdu, China (*Presenter*) Nothing to Disclose Haibo Qu, MD, Chengdu, China (*Abstract Co-Author*) Nothing to Disclose Gang Ning, MD, Chengdu, China (*Abstract Co-Author*) Nothing to Disclose Fenglin Jia, MD, Chengdu, China (*Abstract Co-Author*) Nothing to Disclose Li Bao, Chengdu, China (*Abstract Co-Author*) Nothing to Disclose

# PURPOSE

To outline the anatomic variations of Obstructive reproductive tract anomalies(ORTA) in MR imaging and its role in preoperative evaluation.

# METHOD AND MATERIALS

The MR imaging and treament of seventeen pediatric patients with this condition was reviewed and analyzed.

#### RESULTS

Patients presented in two distinct ways: primary amenorrhea with cyclic pelvic pain, or progressive dysmenorrhea. MR imaging showed hematocolpos, hematocervix, hematometra, and/or hematosalpinx; it also provided detailed information regarding uterine morphology, ipsilateral kidney absence and endometriosis. All the seventeen cases were complete or non-communicating ORTA. Obstruction occurred at different level of genital tract, and surgical treatment was given based on the obstruction sites. There was one case of imperforate hymen who had excision of hymenal tissue; four lower vagina atresia and one agenesis of vagina were treated with vaginoplasty; three Herlyn-Werner-Wunderlich syndrome(HWWS) had their vaginal septum resected, and the one with concurrent postpartum placenta implantation was treated accordingly; there were eight cases of cervical agenesis or cervico-vaginal dysgenesis, seven of which were complicated with uterine anomalies, and all cases had their uterus removed. Among the eight obstructive cervical anomalies, there were four cases of cervical agenesis with obliterated cervical os, and one cervical dysgenesis with a fibrous stroma.

## CONCLUSION

ORTA are usually complex female genital malformations which can not fit into single one category of any present classification. ORTA can occur from hymen to cervix, therefore, the preoperative evaluation with MR imaging is vital to guide proper surgery.

# **CLINICAL RELEVANCE/APPLICATION**

MR imaging, with its advantages, is the imaging modality of choice to assess the obstruction sites and complicated anomalies of ORTA.

# Functional Network Reorganization of Multimodal Integration Regions in Blind Children

Tuesday, Nov. 29 12:45PM - 1:15PM Room: PD Community, Learning Center Station #2

#### **Participants**

Laura Ortiz Teran, MD, PhD, Boston, MA (*Presenter*) Nothing to Disclose Ibai Diez, Boston, MA (*Abstract Co-Author*) Nothing to Disclose Tomas Ortiz, Madrid, Spain (*Abstract Co-Author*) Nothing to Disclose David Perez, Boston, MA (*Abstract Co-Author*) Nothing to Disclose Jose Ignacio Aragon, Majadahonda, Spain (*Abstract Co-Author*) Nothing to Disclose Victor Costumero, Castellon de la Plana, Spain (*Abstract Co-Author*) Nothing to Disclose Georges El Fakhri, PhD, Boston, MA (*Abstract Co-Author*) Nothing to Disclose Alvaro Pascual-Leone, Boston, MA (*Abstract Co-Author*) Nothing to Disclose Jorge Sepulcre, Boston, MA (*Abstract Co-Author*) Nothing to Disclose

#### PURPOSE

Cross-modal neuroplasticity has been proposed as a mechanism by which individuals without sight recruit visual-related cortices to process sensory information from other perceptual modalities. We have previously observed in adults with blindness compared to healthy subjects that multimodal integration regions are prominent sites of neuroplastic reorganization. This study uses network-based functional connectivity analyses to investigate network connectivity differences in blind children compared to controls. We hypothesize that in addition to connectivity differences in visual and other sensory cortices, blind subjects show functional connectivity changes that centralize within multimodal integration regions.

# METHOD AND MATERIALS

We studied 13 children with blindness (N=9 boys) ages between 7-12 years old (mean= $9.6\pm1.3$ ), and 15 sighted controls (N=6 boys) (mean= $10.3\pm1.4$ ). Subjects were scanned on a 3T MRI scanner, acquiring BOLD and high-resolution 3D T1WI. Following pre-preprocessing, whole brain weighted-degree functional connectivity and step-wise connectivity graph theory analyses were applied.

#### RESULTS

In weighted-degree analyses corrected for multiple comparisons, blind children exhibited enhanced connectivity in bilateral ventral premotor, middle cingulate cortex/supplementary motor area and right temporal parietal junction. Several of these connectivity changes positively correlated with age. Using step-wise connectivity analysis, blind children compared to controls demonstrated increased functional streams along certain multimodal integration regions such as the anterior insula and temporoparietal junction bilaterally and right lateral occipital cortex.

# CONCLUSION

Blind children show increased functional connectivity in multimodal integration areas compared to controls, and older children showed greater increases within these regions.

## **CLINICAL RELEVANCE/APPLICATION**

Understanding the changes in neuroplasticity developed by blind children, is critical for future clinical and neuroeducational interventions.

# Altered Spontaneous Brain Activity in early Tourette Syndrome Children: A Resting-state fMRI Study

Tuesday, Nov. 29 12:45PM - 1:15PM Room: PD Community, Learning Center Station #3

#### **Participants**

Yue Liu, Beijing, China (*Presenter*) Nothing to Disclose Jieqiong Wang, Beijing, China (*Abstract Co-Author*) Nothing to Disclose Jishui Zhang, Beijing, China (*Abstract Co-Author*) Nothing to Disclose Huiguang He, Beijing, China (*Abstract Co-Author*) Nothing to Disclose Yun Peng, MD, Beijing, China (*Abstract Co-Author*) Nothing to Disclose

#### PURPOSE

Tourette syndrome (TS) is a childhood-onset chronic disorder characterized by the presence of multiple motor and vocal tics. This study investigated the alterations of spontaneous brain activities in the children with Tourette syndrome (TS) by resting-state functional magnetic resonance imaging (rs-fMRI).

#### **METHOD AND MATERIALS**

We obtained rs-fMRI scans from 29 drug-naïve TS children and 30 demographically matched healthy children. The amplitude of low-frequency fluctuation (ALFF), fractional ALFF (fALFF) and regional homogeneity (ReHo) of rs-fMRI data were calculated to measure spontaneous brain activity. We obtained rs-fMRI scans from 29 drug-naïve TS children and 30 demographically matched healthy children. The amplitude of low-frequency fluctuation (ALFF), fractional ALFF (fALFF) and regional homogeneity (ReHo) of rs-fMRI data were calculated to measure spontaneous brain activity.

## RESULTS

After assessing the between-group differences of ALFF/fALFF and ReHo, we found the significantly decreased ALFF/fALFF in the bilateral paracingulate gyrus, left insular cortex, and the CSTC circuit including right putamen, the thalamus, and the orbito-frontal cortex, of TS patients. Increased fALFF/ReHo was found in the precuneus cortex, the intracalcarine cortex, and the cuneal cortex of patients. We also found decreased ReHo in the cerebellum. Through the further analysis of the relationship between abnormal brain activities and tic severity scores, we found the significantly positive correlation relationship between the ALFF value of the right putamen and severity scores in TS patients.

# CONCLUSION

Our study provides empirical evidence for abnormal spontaneous neuronal activity in TS patients, which may implicate the neurophysiological mechanism in TS children. Moreover, the right putamen can be potentially used as a biomarker of the pathophysiologic pattern of early TS children.

## **CLINICAL RELEVANCE/APPLICATION**

TS is a developmental neuropsychiatric disorder which begins at the age of 6 to 7 years. The study of brain changes is very important for the treatment. Previous study mainly focused on brain structure changes. We try to investigate the alterations of spontaneous brain activities in TS children with resting-state functional MRI.

Computed Tomography Based Small Airway and Emphysema Volume Measurements and Correlation with Pulmonary Function Test in Children with Post-infectious Bronchiolitis Obliterans

Tuesday, Nov. 29 12:45PM - 1:15PM Room: PD Community, Learning Center Station #4

## Participants

Jonghyeon Kim, MD, Seoul, Korea, Republic Of (*Presenter*) Nothing to Disclose Mi-Jung Lee, MD, PhD, Seoul, Korea, Republic Of (*Abstract Co-Author*) Nothing to Disclose Haesung Yoon, MD, Seoul, Korea, Republic Of (*Abstract Co-Author*) Nothing to Disclose Hyun Joo Shin, MD, Seoul, Korea, Republic Of (*Abstract Co-Author*) Nothing to Disclose Myung-Joon Kim, MD, Seoul, Korea, Republic Of (*Abstract Co-Author*) Nothing to Disclose

# PURPOSE

To investigate the utility of computed tomography (CT) based quantitative small airway and emphysema volume measurements for estimating pulmonary function in children with post-infectious bronchiolitis obliterans (PIBO).

## **METHOD AND MATERIALS**

This retrospective study included 18 chest CT scans and pulmonary function tests (PFT) of 13 children diagnosed with PIBO. The quantitative analysis of segmental and subsegmental bronchi was performed on each chest CT scan measuring following parameters; wall thickness (WT), wall area (WA), lumen average diameter (LAD), lumen area (LA), WA/LA ratio, airway average diameter (AAD), and airway area (AA). The emphysema volume (EV), which was defined as the volume of area showing lower attenuation than the mean attenuation of normal and air trapping areas, was also measured in each lobe. The ratio of emphysema volume to total lung volume (emphysema ratio, ER) was then calculated. The PFT values included forced vital capacity (FVC), forced expiratory volume in one second (FEV1) and FEV1/FVC. Comparison analyses between CT based parameters and PFT results were made with Pearson correlation.

#### RESULTS

The patients were aged between 4-17 years with the mean of  $9.9 \pm 4.6$  years. A total of 297 segmental bronchi and 235 subsegmental bronchi were analyzed. Among the measured airway parameters, WA, AAD and AA showed significant negative correlation with FEV1 in bilateral pulmonary lobes. Especially in the left lower lobe (LLL), WA, LAD, LA, AAD, and AA showed strong negative correlation with both FEV1 and FEV1/FVC. The volume measurement showed that both EV and ER had significant negative correlations with FEV1 and FEV1/FVC, especially in LLL. In particular, EV showed stronger correlation than ER in both lungs.

## CONCLUSION

Quantitative small airway measurement and emphysema volume assessment on chest CT can demonstrate lung function in pediatric PIBO patients. Our results suggest the airway and emphysema parameters measured in LLL may represent the severity of disease and functional impairment in these children, in spite of regional inhomogeneity of PIBO.

## **CLINICAL RELEVANCE/APPLICATION**

Quantitative small airway and emphysema volume measurements based on chest CT can estimate the severity of disease regarding pulmonary function in children with post-infectious bronchiolitis obliterans, whose pulmonary function test may be uneasy to perform due to limited compliance.

# PD229-SD-TUB5

Pediatric Liver CT at 70kVp: Preserved Image Quality and Decreased Radiation Dose in Comparison with Standard Scanning at 80-100kVp

Tuesday, Nov. 29 12:45PM - 1:15PM Room: PD Community, Learning Center Station #5

#### Awards

#### **Student Travel Stipend Award**

#### Participants

Bo Ram Kim, MD, Seoul, Korea, Republic Of (*Presenter*) Nothing to Disclose Young Hun Choi, MD, Seoul, Korea, Republic Of (*Abstract Co-Author*) Nothing to Disclose

#### PURPOSE

To assess the image quality and radiation dose of pediatric liver CT acquired at 70kVp during the hepatic arterial phase in comparison with standard scanning at 80-100kVp

#### **METHOD AND MATERIALS**

From April 2015 to September 2015, 19 cases of pediatric liver CT were performed in 15 children (mean age 50.5 months, mean BMI 20.9) with a fixed tube potential of 70kVp and a reference tube current of 700mAs during the hepatic arterial phase (AP) (group A) and the portal venous phase (PP) was obtained with the standard protocol using the automatic tube voltage selection and current modulation (reference tube voltage, 120 kV; reference tube current, 150mAs). 25 cases of liver CT in 18 children (mean age 39.3 months, mean BMI 20.6) where both the AP and PP were obtained with the same standard protocol were included for comparison (group B). For quantitative analysis, noise, signal to noise ratio (SNR) and contrast to noise ratio (CNR) were calculated. Subjective overall image quality, noise, visibility of main hepatic arteries and streaking artifacts were evaluated using a 3- or 5-point scoring system for qualitative comparison. Radiation dose reduction (%) of 70kVp scanning was calculated on the basis of the volume CT dose index (CTDIvol) during the AP divided by the CTDIvol during the PP.

#### RESULTS

Group A showed significantly higher noise and lower SNRs at the paraspinal muscle, liver than group B. Liver-to-muscle and aortato-liver CNRs were similar in both groups (group A vs group B, 1.62 vs 1.61 and 13.86 vs  $13.30 \pm 0.97$ , respectively, all P > 0.05). Scores for overall image quality, visibility of main hepatic arteries and artifacts showed no significant difference between two groups (overall image quality score, 3.78 vs. 4.12; visibility of main hepatic arteries, 4.33 vs. 4.56; artifacts, 1.94 vs. 2.00; all P > 0.05), while subjective noise was significantly more in group A (3.05 vs. 3.92, P=.002). The average percentage radiation dose reduction with 70kVp scanning was 25%.

#### CONCLUSION

Low kilovoltage arterial phase liver CT at 70kvP provided comparable image quality and reduced radiation dose by 25%, compared with the standard protocol at 80-100kVp

#### **CLINICAL RELEVANCE/APPLICATION**

The use of 70kVp in the arterial phase liver CT can be an effective strategy for reducing radiation dose in children, while maintaining image quality.

# PH121-ED-TUB10

Easy Understanding of the Technical Aspects of Computed Diffusion-weighted Image (cDWI) for Radiologists

Tuesday, Nov. 29 12:45PM - 1:15PM Room: PH Community, Learning Center Station #10

#### Awards

## **Identified for RadioGraphics**

#### **Participants**

Toru Higaki, PhD, Hiroshima, Japan (*Presenter*) Nothing to Disclose Yuko Nakamura, MD, Bethesda, MD (*Abstract Co-Author*) Nothing to Disclose Hiroaki Sakane, MD, Hiroshima, Japan (*Abstract Co-Author*) Nothing to Disclose Wataru Fukumoto, Hiroshima, Japan (*Abstract Co-Author*) Nothing to Disclose Yoshimori Kassai, MS, Otawara, Japan (*Abstract Co-Author*) Employee, Toshiba Corporation Kazuo Awai, MD, Hiroshima, Japan (*Abstract Co-Author*) Research Grant, Toshiba Corporation; Research Grant, Hitachi, Ltd; Research Grant, Bayer AG; Research Grant, Eisai Co, Ltd; Medical Advisor, General Electric Company; ; ; ; ;

## **TEACHING POINTS**

Computed diffusion-weighted images (cDWIs) are virtual DWIs calculated from actual DWIs using two arbitrarily selected low bvalues. cDWI is advantageous because images can begenerated on MR scanners that do not allow the acquisition of high bvalue DWIs. cDWI can also reduce the scan time and lower the image noise when DWIs are acquired with routinely-used b-values. We easily demonstrate the technical aspects and applications relating to the cDWIs.

# TABLE OF CONTENTS/OUTLINE

Basic knowledge about diffusion weighted image Principle of computed diffusion weighted image Advantages and limitations of computed diffusion weighted image Clinical applications of computed diffusion weighted image

Influences of Pitch Factors and Rotation Times on Response Characteristics of a Tube Current in Chest CT for Infants under a CT-Auto Exposure Control: Phantom Study

Tuesday, Nov. 29 12:45PM - 1:15PM Room: PH Community, Learning Center Station #1

## Participants

Takuya Akagawa, MSc,RT, Komatsushima, Japan (*Presenter*) Nothing to Disclose Sachiko Goto, PhD, Okayama, Japan (*Abstract Co-Author*) Nothing to Disclose Yoshiharu Azuma, PhD, Okayama, Japan (*Abstract Co-Author*) Nothing to Disclose

#### CONCLUSION

In considering response characteristic of a tube current under CT-AEC, we strongly suggest that scanning speed of CT should be determined according to a rotation time with the pitch factor of 0.656 or 0.844 in chest CT for infants.

#### Background

ICRP publication 87 has reported that CT- Auto Exposure Control (AEC) is the most effective to dose reduction of CT examination, in especially pediatric CT. We know from experience that the effect of dose reduction of CT-AEC may change with scan parameters.We investigated the response characteristics of a tube current by phantoms under the examination that high performance AEC is required such as the infant chest CT and analyzed the influence of scan parameters on the response characteristics.

#### **Evaluation**

Fig. a shows the location of two acrylics phantoms and an interval. The intervals of 5 - 30 cm were employed. The helical scan protocol was used under the CT-AEC system (Aquilion ONE; Toshiba). Fixed the scan parameters were  $32 \times 1.0$  mm beam collimation, 120 kV x-ray tube voltage, 10 - 500 mA of x-ray tube current and setting AEC parameters were slice thickness 3 mm, standard deviation 12.0 HU with CT-AEC system (SureExposure; Toshiba). We changed the rotation time and pitch factor were 1.0/0.75/0.5/0.35 and 0.656/0.844/1.406, respectively. We evaluated the response characteristic of a tube current of the z-axis direction.

#### Discussion

CT-AEC system modulated the tube currents from 10 to 500 mA at the 20 cm-interval (Fig. a). In using the pitch factor of 1.406 CT-AEC system was not able to modulate the tube currents at the rotation time of 0.5 sec/rot (Fig. b). At the pitch factor of 0.844, as rotation time becomes longer the response of a tube currents becomes better (Fig. c). From above results the best combination of the pitch factor/ the rotation time, was 0.844/0.5 (Fig. d). The table speed was 49.6 mm/sec in this combination. If faster table speed was required, a shorter rotation time should be chosen. If the pitch factor of 1.406 is chosen, the patent dose reduction can't be expected.

## PH238-SD-TUB2

Organ Dose Evaluations Based on Monte Carlo Simulation and In-phantom Dosimetry for Interventional Radiology

Tuesday, Nov. 29 12:45PM - 1:15PM Room: PH Community, Learning Center Station #2

# Participants

Keisuke Fujii, Nagoya, Japan (*Presenter*) Nothing to Disclose Keiichi Nomura, MS, Kashiwa, Japan (*Abstract Co-Author*) Nothing to Disclose Yoshihisa Muramatsu, PhD, Kashiwa, Japan (*Abstract Co-Author*) Nothing to Disclose Miki Yoshimura, Tokyo, Japan (*Abstract Co-Author*) Employee, Toshiba Corporation Naotaka Sato, Otawara, Japan (*Abstract Co-Author*) Employee, Toshiba Corporation Masahiko Kusumoto, MD, Chuo, Japan (*Abstract Co-Author*) Nothing to Disclose

#### PURPOSE

The aims of this study were to evaluate organ doses determined using Monte Carlo (MC) simulations for X-ray fluoroscopy and digital subtraction angiography in transcatheter arterial chemoembolization (TACE) procedure for hepatocellular carcinoma (HCC) and to validate the values through comparisons with the doses measured using in-phantom dosimetry.

# METHOD AND MATERIALS

Fluoroscopy and angiography were performed with tube voltage of 70 and 80 kVp, added filtration of 0.5 mm copper and 1.8 mm aluminum, tube current of 47 and 160 mA, exposure time of 10.3 and 3.3 seconds, respectively. X-ray projection angles were posteroanterior (PA) for fluoroscopy, and PA and 30-degree right anterior oblique (RAO 30°) for angiography. The entrance skin doses (ESD) and organ doses were measured using 200 radio-photoluminescence glass dosimeters located at various organ positions on and within an adult anthropomorphic phantom. Dose-area products (DAPs) for fluoroscopy and angiography were also measured. For dose simulations, dose distribution images were obtained by inputting the geometry of a digital angiography system (Infinix; Toshiba Medical Systems, Japan), fluoroscopic and angiographic parameters and CT images of the phantom into MC simulation software (ImpactMC; CT Imaging, Germany). Organ doses for each organ were determined from dose values at the corresponding dose measurement positions on the dose distribution images.

#### RESULTS

Measured ESD and DAP were 8.1 mGy and 3.1 Gy cm2 for fluoroscopy, 71.2 mGy and 28.9 Gy cm2 for PA angiography and 68.4 mGy and 30.0 Gy cm2 for RAO 30° angiography. Relative differences between the simulated and measured doses were 5.1% for fluoroscopy, 4.3% for PA angiography and 1.7% for RAO 30° angiography. The relative differences were 9.2% to 11.3%, 5.1% to 11.0% and 8.9% to 14.0% for liver, stomach and colon within x-ray irradiated region in fluoroscopy, PA and RAO 30° angiography, respectively.

# CONCLUSION

This study showed that the simulated and measured organ doses agreed well. The doses determined using MC simulation will be useful for the evaluation of organ doses and the estimation of radiation risks for individual patients in TACE procedures for HCC.

# **CLINICAL RELEVANCE/APPLICATION**

MC dose simulation will be useful for the real-time dose estimation for individual patients in fluoroscopy and angiography for interventional radiology.

## PH239-SD-TUB3

Comparative Evaluation of Super-Resolution Methods Using Sparse Coding and Deep Convolutional Neural Network for Improving Image Quality of Extended Images in Chest Radiography

Tuesday, Nov. 29 12:45PM - 1:15PM Room: PH Community, Learning Center Station #3

# Participants

Junko Ota, Boston, MA (*Presenter*) Nothing to Disclose Kensuke Umehara, Boston, MA (*Abstract Co-Author*) Nothing to Disclose Naoki Ishimaru, Suita, Japan (*Abstract Co-Author*) Nothing to Disclose Shunsuke Ohno, Suita, Japan (*Abstract Co-Author*) Nothing to Disclose Kentaro Okamoto, Suita, Japan (*Abstract Co-Author*) Nothing to Disclose Takayuki Ishida, PhD, Suita, Japan (*Abstract Co-Author*) Nothing to Disclose Takanori Suzuki, Suita, Japan (*Abstract Co-Author*) Nothing to Disclose Naoki Shirai, Suita, Japan (*Abstract Co-Author*) Nothing to Disclose

#### PURPOSE

Radiologists detect small diagnostic signals such as lung nodule with zooming on a detail, however simple image magnification methods tend to generate over-smoothed images with jagged artifact. The purpose of this study was to improve the image quality of extended images in chest radiography using learning-based Super-Resolution (SR) techniques.

# METHOD AND MATERIALS

One hundred fifty four radiographs (matrix size: 2048x2048, pixel size: 0.175 mm, and 12 bits) with nodules (average diameter±std: 17.24±7.50 mm, diameter range: 5-60 mm) from Japanese Society of Radiological Technology dataset were used for this study. We applied two SR methods, Sparse Coding Super-Resolution (ScSR) and Super-Resolution Convolutional Neural Network (SRCNN). ScSR constructs extended images by embedding optimal patches selected from a dictionary, coupled high and low resolution images represented as downscaled images of high resolution ones. SRCNN constructs using directly learned end-to-end mapping, represented as a deep convolutional neural network that takes the low resolution image as input and outputs as the high resolution one. In our study, we magnified cropped images focused on nodules (matrix size: 320x320) up to 2 times (x2.0) and 4 times (x4.0). We compared the image quality of SR schemes and the traditional enlarging schemes, Nearest Neighbor (NN) and Bilinear (BL) interpolations. Image noise was evaluated quantitatively by measuring peak signal-to-noise ratio (PSNR) and image perceived quality was also evaluated by computing structural similarity (SSIM).

#### RESULTS

In SR schemes (x2.0), the mean±std of PSNR for ScSR and SRCNN were  $41.47 \pm 2.34$  dB and  $41.82 \pm 2.49$  dB respectively, which were higher than those of NN ( $39.87 \pm 2.24$  dB, p<.001 and p<.001 respectively), and BL ( $40.39 \pm 2.32$ , p<.001 and p<.001 respectively) and those of SSIM for ScSR and SRCNN were  $0.944 \pm 0.028$  and  $0.947 \pm 0.029$  respectively, which were higher than those of NN ( $0.924 \pm 0.033$ , p<.001 and p<.001 respectively), and BL ( $0.928 \pm 0.035$ , p<.001 and p<.001 respectively), followed the same trend for 4 times (x4.0).

# CONCLUSION

SR methods significantly outperformed traditional interpolation methods in observing small lung structures in chest radiographs.

## **CLINICAL RELEVANCE/APPLICATION**

SR methods can provide substantial high image quality of enlarged images on chest X-rays, leading to more accurate diagnosis of small lung diseases.

# XACT: A Novel Imaging Modality for Breast in 3D

Tuesday, Nov. 29 12:45PM - 1:15PM Room: PH Community, Learning Center Station #4

#### **Participants**

Shanshan Tang, PhD, Norman, OK (*Presenter*) Nothing to Disclose Yong Chen, Oklahoma City, OK (*Abstract Co-Author*) Nothing to Disclose Liangzhong Xiang, PhD, Norman, OK (*Abstract Co-Author*) Nothing to Disclose

#### PURPOSE

Exposure to radiation increases the lifetime risk of cancer. We have proposed a new imaging paradigm, X-ray induced acoustic computed tomography (XACT). Applying this innovative technology to breast imaging, an X-ray exposure can generate a 3D acoustic image with high spatial resolution, which dramatically reduces the radiation dose, while still maintaining the imaging performance.

## METHOD AND MATERIALS

Theoretical calculations are done to determine the X-ray energy and ultrasound frequency in breast XACT. Taking the unique advantages of XACT, a low energy X-ray(20 Kev) and a high frequency ultrasound (5.5 MHz) can be employed in breast imaging, which offers better imaging contrast for soft tissues and spatial resolution for breast calcification detection. A series of breast CT image along the coronal plane with calcifications in the breast tissue are used as the source image. The skin, adipose tissue, glandular tissue, breast calcification, and chest bone are segmented from each image. X-ray dose deposition in each pixel is calculated based on the tissue type by using GEANT4 Monte Carlo toolkits. The initial pressure rise caused by X-ray energy deposition is calculated and the propagation of XA waves are simulated by MATLAB K-Wave toolkit. Breast XACT images are reconstructed from the recorded time-dependent XA waves by a filtered back-projection algorithm.

## RESULTS

For a breast with 16cm diameter at the chest wall, the effective energy of pulsed X-ray source and the center frequency of ultrasound detector are determined as 20KeV and 5.5MHz. High contrast between the calcification and the background glandular tissue can be acquired from XACT. The spatial resolution for breast calcification detection reaches  $\sim$ 100µm. The location and shape of the calcification can be clearly identified from the XACT image of 3D breast volume.

# CONCLUSION

XACT technique takes the advantages of high X-ray absorption contrast and high ultrasonic resolution. With the proposed innovative technique, one can potentially reduce the radiation dose to patient in 3D breast imaging as compared with current X-ray modalities, while still maintaining the high imaging contrast and spatial resolution.

# **CLINICAL RELEVANCE/APPLICATION**

This technique has the potential for breast cancer screening and imaging with high contrast and spatial resolution.

Initial Study of Dose Reduction and Image Quality in Abdominal CT using Prospective Adaptive Statistical Iterative Reconstruction-V Technique

Tuesday, Nov. 29 12:45PM - 1:15PM Room: PH Community, Learning Center Station #5

## Participants

Jin Wei, Fuzhou, China (*Presenter*) Nothing to Disclose Yunjing Xue, MD, Fuzhou, China (*Abstract Co-Author*) Nothing to Disclose Yuanfeng Liu, Fuzhou, China (*Abstract Co-Author*) Nothing to Disclose Xuhui Chen, Fuzhou, China (*Abstract Co-Author*) Nothing to Disclose Yu Xia, Fuzhou, China (*Abstract Co-Author*) Nothing to Disclose

# PURPOSE

To evaluate the dose reduction and image quality with the application of prospective adaptive statistical iterative reconstruction-V (ASiR-V) in the abdominal CT scan on GE Revolution CT.

## **METHOD AND MATERIALS**

Totally 132 patients with BMI above 20 in our hospital underwent abdominal contrast-enhanced CT scan on GE Revolution CT were randomly divided into four groups using prospective ASiR-V technique (0%, 20%, 40%, 60%). All the scans were used the same parameters as tube voltage of 120kV, automatic mA modulation of 10-500mA and noise index (NI) of 10. To measure the SD value of fat as image noise in three different locations of the abdomen: right branch of portal vein, left renal artery and navel. CT dose index volumes (CTDI vol), dose length product (DLP) were recorded from dose report, and effective dose (ED) was calculated. The image quality was evaluated by two experienced abdominal radiologists blindly and independently with a five-point scale (1 for poor and 5 for excellent). CTDI vol, ED, average image noise and average image score were compared with ANOVA.

### RESULTS

There was statistical difference of CTDI vol and ED between each group. Images of the 60% ASiR-V yielded relatively lowest objective image noise (SD=7.57 $\pm$ 0.71, P=0.02<0.05), significantly lowestCTDI (3.48 $\pm$ 1.08mGy, P=0.00<0.05) and ED(2.72 $\pm$ 0.93mSv, P=0.00<0.05), compared with other groups. However, the subjective image quality of the 60% ASIR-V scores was poorest (2.33 $\pm$ 0.60, P=0.000<0.05) and could not meet the diagnostic requirement while images of other three groups(0%, 20%, 40%ASiR-V) were qualified to make the diagnosis. There was no significantly difference in image noise and subjective image quality between 0%, 20% and 40% ASiR-V, SD values were 8.13 $\pm$ 0.93 VS 8.05 $\pm$ 0.91 vs 7.70 $\pm$ 0.74 (P=0.69>0.05) and image quality scores were 4.79 $\pm$ 0.42 VS 4.67 $\pm$ 0.48 vs 4.27 $\pm$ 0.67 (P=0.37>0.05).

#### CONCLUSION

Images of prospective 60% ASiR-V provided the lowest SD values, CTDI vol and ED in all the groups, but the poorest image quality and could not meet the diagnostic requirement. Images obtained from 40% ASiR-V had the similar objective image noise and subjective image quality with 0%,20% ASiR-V, produced lower radiation dose. 40% ASiR could be recommended on the abdominal CT scan.

## **CLINICAL RELEVANCE/APPLICATION**

Prospective ASiR-V technique is a promising method to reduce radiation dose and maintain relatively good image quality during abdominal CT scan and may represent a new clinical option.

Creation of Realistic Structured Backgrounds using Adipose Compartment Models in a Test Object for Breast Imaging Performance Analysis

Tuesday, Nov. 29 12:45PM - 1:15PM Room: PH Community, Learning Center Station #6

## Participants

Lesley Cockmartin, Leuven, Belgium (*Presenter*) Nothing to Disclose Hilde Bosmans, PhD, Leuven, Belgium (*Abstract Co-Author*) Co-founder, Qaelum NV Research Grant, Siemens AG Kristina Bliznakova, PhD, Varna, Bulgaria (*Abstract Co-Author*) Nothing to Disclose David D. Pokrajac, PhD, Dover, DE (*Abstract Co-Author*) Nothing to Disclose Abdullah-AI-Zubaer Imran, Dover, DE (*Abstract Co-Author*) Nothing to Disclose Nicholas Marshall, Leuven, Belgium (*Abstract Co-Author*) Research Grant, Siemens AG Andrew D. Maidment, PhD, Philadelphia, PA (*Abstract Co-Author*) Research support, Hologic, Inc; Research support, Barco nv; Research support, Analogic Corporation; Spouse, Employee, Real-Time Tomography, LLC; Spouse, Stockholder, Real-Time Tomography, LLC; Scientific Advisory Board, Real-Time Tomography, LLC; Scientific Advisory Board, Gamma Medica, Inc Predrag R. Bakic, PhD, Philadelphia, PA (*Abstract Co-Author*) Research collaboration, Barco nv Research collaboration, Hologic, Inc

# PURPOSE

To create a realistic, structured background for a breast imaging test object based on 3D printed volumes representing adipose compartments.

### **METHOD AND MATERIALS**

In previous work, models of manually segmented breast adipose compartments were generated and characterized from CT images of a mastectomy specimen. Based on this work, a collection of segmented compartments (of average size 12-29 mm) was printed with a stereolithographic 3D printer (FORM 1+, formlabs, Somerville, MA) using formlabs Clear Resin. The printed models were placed in a semi-cylindrical container, 48 mm thick, filled with water. Mammographic and tomosynthesis images were acquired under automatic exposure control. The resulting images were evaluated in terms of power spectra (PS) and other quantitative and qualitative means. The results were compared to PS from 80 patient images, and a previous structured background phantom with various sized acrylic spheres in water.

#### RESULTS

Visual inspection shows that the phantom images demonstrate a strong resemblance to breast structure. Power spectra for mammographic images of the phantom are close to the average patient PS at very low spatial frequencies (<0.2mm-1); the phantom PS is lower than the patient PS at higher spatial frequencies (0.2-0.7mm-1). The power law exponent ( $\beta$ ), a quantitative descriptor of the parenchymal texture, was superior for the compartment-based phantoms vs. sphere-based phantoms;  $\beta$  = 3.8 for the compartments, and 2.8 for the spheres, versus 3.4 for patient mammograms. Modifications of the compartment model aimed at improving the agreement with the patient data may include the use of less dense print material to increase the contrast of the compartments, inclusion of smaller compartments by downscaling the existing models, and refining the compartment segmentation method.

# CONCLUSION

A mixture of printed adipose compartments was developed as a concept for the creation of an anthropomorphic 3D structured background in a test object for breast imaging performance analysis.

### **CLINICAL RELEVANCE/APPLICATION**

We present a new means of creating 3D structured backgrounds aimed at improving the realism of test objects for breast imaging, based on 3D printed adipose compartments segmented from clinical images.

## PH243-SD-TUB7

### An Interaction-free Second Pass Cardiac Motion Compensation Method

Tuesday, Nov. 29 12:45PM - 1:15PM Room: PH Community, Learning Center Station #7

#### **Participants**

Michael Grass, PhD, Hamburg, Germany (*Presenter*) Employee, Koninklijke Philips NV Axel Thran, Hamburg, Germany (*Abstract Co-Author*) Employee, Koninklijke Philips NV Rolf Bippus, Hamburg, Germany (*Abstract Co-Author*) Employee, Koninklijke Philips NV Sven Kabus, PhD, Hamburg, Germany (*Abstract Co-Author*) Employee, Koninklijke Philips NV Rafael Wiemker, PhD, Hamburg, Germany (*Abstract Co-Author*) Employee, Koninklijke Philips NV Mani Vembar, MS, Cleveland, OH (*Abstract Co-Author*) Employee, Koninklijke Philips NV

# PURPOSE

A user interaction-free approach is introduced for motion compensated CT coronary angiography reconstruction. This second pass correction method can be switched on whenever motion artefacts due to strong motion or sub-optimal cardiac phase selection show up in cardiac CT scans. Its fully automatic processing can be applied to prospectively-triggered (Step-and-Shoot) as well as retrospectively gated helical cardiac CT scans to improve the assessment of coronary arteries.

#### **METHOD AND MATERIALS**

A time series of cardiac CT volume images is first reconstructed at different phase points in the cardiac cycle. For helical scans a temporal distance of 5% cardiac cycle has been chosen for the time series. When using Step-and-Shoot data sets partial scan reconstruction is used to generate a sequence of images from an angular range of 360°. Vessel features are enhanced in the reconstructed images by a ray-casting vessel filter. Using elastic image registration, dense motion vector fields are calculated for the different cardiac phases for the whole heart. The resulting motion vector fields are included in the motion compensated reconstruction and interpolated in the time domain to cover the temporal projection range required for reconstruction. The method is applied to clinical datasets with high heart rate (> 70 bpm) acquired with a 256-slice CT scanner (iCT, Philips Healthcare, Cleveland, USA) using both helical and Step-and-Shoot data acquisitions.

# RESULTS

The method achieves motion artifact reduction for both helical and Step-and-Shoot cardiac CT data sets. Improved delineation and segmentation of the coronary arteries is feasible from motion compensated cardiac CT volumes compared to gated reconstructions. The method does not require user interaction.

#### CONCLUSION

User interaction-free motion compensated reconstruction is feasible using vessel filtering and image based registration for motion estimation. Improved image quality can be achieved in CT coronary angiography.

#### **CLINICAL RELEVANCE/APPLICATION**

Motion compensated reconstruction yields reduced artefact levels in helical and step and shoot coronary CT angiography.

## PH244-SD-TUB8

Adaptive Optimization of the Number of OSEM Subsets improves Image Quality and Lesion Detectability in Time-of-Flight FDG PET

Tuesday, Nov. 29 12:45PM - 1:15PM Room: PH Community, Learning Center Station #8

## Participants

Jun Zhang, PhD, Columbus, OH (*Presenter*) Nothing to Disclose Ajay Siva, Columbus, OH (*Abstract Co-Author*) Nothing to Disclose Prayna Bhatia, BS, Columbus, OH (*Abstract Co-Author*) Nothing to Disclose Katherine Binzel, PhD, Columbus, OH (*Abstract Co-Author*) Nothing to Disclose Bin Zhang, PhD, Cleveland, OH (*Abstract Co-Author*) Nothing to Disclose Bin Zhang, PhD, Cleveland, OH (*Abstract Co-Author*) Employee, Koninklijke Philips NV Michael V. Knopp, MD, PhD, Columbus, OH (*Abstract Co-Author*) Nothing to Disclose Chadwick L. Wright, MD, PhD, Lewis Center, OH (*Abstract Co-Author*) Nothing to Disclose Preethi Subramanian, MS, BEng, Columbus, OH (*Abstract Co-Author*) Nothing to Disclose

#### PURPOSE

While OESM iterative reconstruction has been widely utilized as the standard for clinical time-of-flight (TOF) PET image quality and lesion detectability may vary with changing patient size, dose administration, voxel size, and scanner type. In order to harmonize the approach to determine this important recon parameter, we developed an optimization strategy for the number of subsets (#S) to consistently improve image quality and lesion detectability in FDG PET.

### METHOD AND MATERIALS

With the introduction of next generation digital PET, we started with previous default setting of #S=29 despite the fact that the TOF timing resolution improved from 550ps to 325ps. We used 30 wholebody FDG PET cases having a total of 109 lesions for analysis. PET imaging was reconstructed using different voxel volumes 64mm3 (SD), 8mm3 (HD) and 1mm3 (UHD) and with varying #S from 1 to the default 29. Quantitatively, ROIs on liver and lesions were placed with SUV and STDEV measured together with penalty scores being assigned for images based on noise levels. Visually, blinded image reviews were performed with 5-level scores (1-worst to 5-best) determined by professional readers. All results were evaluated and compared including consideration for patient size.

### RESULTS

Using the default 29 subsets let to inadequate image quality when imaging was performed using 325ps TOF (dPET) compared to the previous 550ps TOF cPET. Apparently, the iterative convergence is different which leads to increased apparent noise on images, particular in the liver, decreased image quality and deteriorated lesion detectability. We found, that lower #S substantially resolved these issues and let to improved image quality. The most favorable #S was found to be dependent on several aspects such as BMI and relative count density indicating that an adaptive reconstruction approach should be considered with variable #S. Overall, 15 subsets was found to be most preferable for SD, 13 for HD and 9 for UHD recon.

## CONCLUSION

Adaptive optimization of iteration subsets is essential to capitalize on TOF image quality improvements as the recon remains dependent on relative county density factors (Dose, BMI etc.).

# **CLINICAL RELEVANCE/APPLICATION**

Contrary to current standards, adaptive subset reconstruction approaches are essential to leverage advanced TOF technology to achieve best image quality and quantitative accuracy.

## Assessment of Anal Fistulas with T2 Weighted BLADE Sequence

Tuesday, Nov. 29 12:45PM - 1:15PM Room: PH Community, Learning Center Station #9

#### Participants

Safiye Sanem D. Bulut, Istanbul, Turkey (*Presenter*) Nothing to Disclose Hadi Sasani, MD, Isparta, Turkey (*Abstract Co-Author*) Nothing to Disclose Yasar Bukte, MD, PhD, Istanbul, Turkey (*Abstract Co-Author*) Nothing to Disclose Cem N. Balci, istanbul, Turkey (*Abstract Co-Author*) Nothing to Disclose

## CONCLUSION

Fat sat T2 weighted BLADE and contrast enhanced FSE T1weight sequences' diagnostic quality were equal to each other for the diagnosis of perianal fistule. BLADE was significantly superior to TSE regarding motion artifacts, vasculary flow phenomena, and other artifacts.

## Background

The aim of the present study was to prospectively compare overall image quality, contrast, and diagnostic information of the recently implemented T2-weighted BLADE TSE sequence with fat saturation and contrast enhanced T1-weighted TSE sequence and T2-weighted TSE with fat saturation sequence for perianal fistulas.

## **Evaluation**

Twenty three consecutive patients with the clinical diagnosis of anal fistul.MRI was performed in supine position on a 1.5-T wholebody scanner (Magnetom Avanto; Siemens Healthcare, Erlangen, Germany) using a six-channel phased array body coil. MR images were evaluated separately by two radiologists, and all images were presented in random order to each of the readers and were evaluated on a three-point scale for various criteria defining image quality. Statistical evaluations were performed by using the Wilcoxon and the 2 test; differences with P .05 were regarded as statistically significant. Finally, readers were asked to indicate their preferred sequence (T2weighted BLADE TSE or T2-weighted TSE or contrast enhanced T1-weighted TSE sequence) and the view ( sagittal or coronal or axial ) taking into account the diagnostic performance and overall contrast. If no difference was visible equal ranking was allowed.

#### Discussion

Using the Fat sat T2 weighted BLADE sequence for pelvic imaging proved to be advantageous to reduce various kinds of artifacts. To use Diffusion-weighted imaging as an adjunct to T2-weighted imaging in the diagnosis of anal fistulae, especially for patients who have risk factors for IV contrast agents, increase the radiologist's level of confidence and to add value imaging.

### QS002-EB-TUB

## Application of a Unified Database for Rejected Acquisition Analysis in Radiography

Tuesday, Nov. 29 12:45PM - 1:15PM Room: QS Community, Learning Center Hardcopy Backboard

#### **Participants**

Kevin Little, PhD, Chicago, IL (*Presenter*) Nothing to Disclose Lili Liu, chicago, IL (*Abstract Co-Author*) Nothing to Disclose Kateland Haas, Chicago, IL (*Abstract Co-Author*) Nothing to Disclose Adrian A. Sanchez, PhD, Chicago, IL (*Abstract Co-Author*) Nothing to Disclose Carmen M. Froman, ARRT, MBA, Chicago, IL (*Abstract Co-Author*) Nothing to Disclose Tiffany Kinsey, Chicago, IL (*Abstract Co-Author*) Nothing to Disclose Zheng Feng Lu, PhD, Chicago, IL (*Abstract Co-Author*) Nothing to Disclose Ingrid Reiser, PhD, Chicago, IL (*Abstract Co-Author*) Nothing to Disclose

### PURPOSE

In order to minimize unnecessary radiation exposure to patients and maintain an efficient patient throughput, it is important to monitor the percentage of acquisitions in radiography that are discarded without being sent to radiologists for review ("rejects"). We found that tracking rejected acquisitions was especially important during and after the transition from computed radiography (CR) to digital radiography (DR). At our institution, this transition led to a perceived increase in the number of rejected studies. However, variations in the reporting of acquisition data provided by the 25 CR and DR units (6 models from 3 manufacturers) used in our adult general medical imaging areas made a thorough analysis of reject rates complicated and time-consuming. Each unit provided exposure logs and reject logs in varying formats, and the automated generation of reject rate reports was inconsistent and often unreliable on some units. Since it is crucial to collect acquisitions was developed to allow us to collect acquisition data consistently and reliably across different types of radiography systems. This allowed us to analyze rejects more easily based on factors such as equipment, reject reason, type of examinations, anatomy, and technologist. The conclusions drawn from the reject analysis were used to guide efforts to reduce the reject rate.

#### **METHODS**

Logs containing reject data and information about all system exposures were obtained from each system. The format used by each model to record these data varied, especially in the way that dual-energy, auto-pasted, and reprocessed images were recorded. We developed counting rules for each model to ensure that multiple records for a single acquisition (as in the case of a dual-energy acquisition) were not duplicated. Each manufacturer had different default reasons that could be indicated by a technologist for a rejected acquisition. On some units, it was possible to modify these reasons, but on other units, modification of reject reasons was not possible. We mapped each reject reason into one of five categories: Incorrect Technique, Positioning/Collimation, Artifact/Obstruction, Patient Motion, and Other. We also mapped the widely varying anatomy and view descriptions for each model to unified descriptions. Acquisition and reject data were imported into an SQL database, and these counting and mapping rules were applied. We also developed an interface with RIS to record the technologist for each acquisition record. The results were made available for analysis using a customized, interactive dashboard that was accessible by physicists, radiologists, managers, and lead technologists who meet monthly to plan and assess interventions.

### RESULTS

Initial reject rates in October 2014 were found to be higher than expected (24.5%). The reject rate and number of rejects for each anatomy were used to identify exams that could be targeted for improvement. Reject rates for each technologist were used by the area manager to identify staff in need of additional training. By targeting exams with high reject rates and by providing guidance for technologists with a high individual reject rate, we are able to implement interventions to reduce the reject rate. By March 2016, our overall reject rate was 13%. In general, we found that reject rates were higher for DR (~15%) than they were for CR (~7%). This may be partly due to unfamiliarity with new equipment and partly due to the ease of rapid repeat acquisitions without a processing delay in image readout. This understanding led us to place intervention emphasis on "operational errors". We have implemented technologists' education and training in multiple formats including in-service lectures, peer reviews, individual review with a supervisor, and personal training sessions done by a technical coordinator. A centralized reject analysis program made it possible to identify opportunities for much-needed education and training.

### CONCLUSION

Monitoring the rate of rejected acquisitions in radiography can be a complicated task when multiple manufacturers and models are used in the same department. Vendor tools in general do not allow the aggregation of this information. A centralized database, reject reason categorization, and anatomy/view mapping allows reject data to be fully analyzed using an interactive dashboard and used for process improvement.

## Quality and Safety Scorecard for Outpatient Imaging: Development, Implementation, Results

Tuesday, Nov. 29 12:45PM - 1:15PM Room: QS Community, Learning Center Hardcopy Backboard

#### Participants

Sophia B. Peterman, MD, MPH, Alpharetta, GA (Presenter) Chief Medical Officer, MedQuest Associates, Inc

#### PURPOSE

A multicenter, multistate outpatient imaging company developed a quality and safety component to its overall company scorecard.

#### **METHODS**

Quality and safety metrics were developed to evaluate the quality or safety of an imaging process or outcome. They utilized available variables, which were measurable via computerized data inquiry. Seven quality and safety metrics were added to the 2010 scorecard. In 2015, four additional metrics were included. The five states in the company from 2010-2015 were analyzed. The number of centers each year ranged from 35-44. Every center had a magnetic resonance (MR) scanner. 28-36 centers also had computed tomography (CT) scanners. The centers were either independent diagnostic testing facilities (IDTF) or hospital outpatient departments (HOPD). Monthly and year-to-date metrics were e-mailed each month to the center managers and leadership team. The managers had the ability to query lists of patient exams or instances where a metric benchmark was not met. The company was held accountable to the established metric results. 24-Hour Report Turnaround Time Delivery of a timely report on a consistent basis is important for patient care. No meaningful change in the dictation/transcription software. Guidelines set and reported: exam to dictation (< 8 hours), dictation to transcription (< 6 hours), transcription to signature (< 4 hours). Monthly metric by radiologist was distributed. Glomerular Filtration Rate (GFR) Testing >= 60 Years Old Among the indications for pre-contrast renal screening, age is consistently known. Point-of-care serum creatinine analysis was available in the center. GFR calculator was developed in the Tech Module. In 2011, GFR became a required field for submitting a Tech Module in contrast exam patients >= 60 years. Crash Cart Inventory Medications should be current. Technologists should be familiar with them. The completed inventory with a bar code of the date and center name was scanned each week. An e-mail was automatically sent to the center manager if no scanned inventory by Friday morning. CT and MR Equipment Quality Assurance (QA) MR and CT scanners should have daily and/or weekly QA for quality images. The completed CT and MR QA checklists with bar codes of the date and center name were scanned each week. The CT QA checklist was modified for the new American College of Radiology (ACR) accreditation requirements in 2013. % CT Abdomen With/Without, % CT Chest With/Without and % Brain CT with Sinus CT In many clinical situations, choosing either a with or without CT or either a CT head or CT paranasal sinus results in half the patient radiation dose without loss of clinical information. Followed the Centers for Medicare & Medicaid Services (CMS) Hospital Outpatient Quality Reporting Imaging Efficiency Measures OP-10, OP-11, and OP-14. Benchmarks were based on reported national and state averages. Exam recommendations were discussed with radiologists. Radiologists and marketers worked with ordering physicians to change ordering patterns. Head CT Dose <= 75 mGy and Abdomen CT Dose <= 25 mGy The ACR published reference radiation exposure values for head and abdomen CT. Technologists copied the CT Dose Index--volume (CTDIvolume) from the scanner into a Tech Module field. The Radiologic Technologist Director addressed CT protocol adjustments and equipment service needs. Contrast Reaction Drills Serious contrast reactions are rare. A drill helps team members rehearse and prepare. The completed drill attendance list with a bar code of the date and center name was scanned. Reminders were sent encouraging the first drill before July and the second before December.

### RESULTS

Run charts of each metric's results over time showed the most change in the first one to two years. The improved performance was maintained. The difference between the highest center value and the lowest center value decreased over time. Bar charts of the percent of centers achieving the benchmark of each metric over time showed an increase corresponding to the overall company performance.

# CONCLUSION

The quality and safety scorecard moved outpatient imaging quality and safety of processes and outcomes to a higher, ongoing standard in a multicenter, multistate company. Attention to the CMS Imaging Efficiency measures helped impact the CT ordering behavior of the referral community to reduce patient radiation exposure. On-line CT and MR QA software and intranet availability of scanner protocols are currently being evaluated.

A Continuous Quality Improvement Process to Reduce Excessive CT Radiation Dose Events across a Large, Multi-institutional Academic Center

Tuesday, Nov. 29 12:45PM - 1:15PM Room: QS Community, Learning Center Station #1

## Participants

Matthew E. Zygmont, MD, Decatur, GA (*Abstract Co-Author*) Nothing to Disclose Rebecca Neill, Atlanta, GA (*Abstract Co-Author*) Nothing to Disclose Shalmali Dharmadhikari, PhD, Atlanta, GA (*Presenter*) Nothing to Disclose Phuong-Anh T. Duong, MD, Charlottesville, VA (*Abstract Co-Author*) Nothing to Disclose

### PURPOSE

Many radiology departments have instituted computed tomography (CT) radiation dose tracking systems with the goal of reducing dose. However, relatively few reports exist on how the data is used to continuously monitor and reduce excessive dose events. The purpose of this quality improvement project is to reduce overall CT radiation dose by developing a process to identify excessive CT radiation exposures and continuously refine and optimize CT protocols.

## METHODS

A standardized institutional protocol naming convention was developed and deployed on 26 scanners across 11 inpatient and outpatient sites. Protocols were mapped within the dose tracking software to a specific RPID based on the updated ACR Radlex 2.0 playbook. A master protocol repository containing approximately 150 protocols stored within the dose tracking system (Radimetrics, Bayer Health) was created outlining expected scanner specific technical parameters, reconstructions and special instructions including contrast dose and rate for each unique machine. All CT protocols have been assigned a maximum dose threshold based on national dose benchmarks from the ACR Dose Index Registry. Alerts may be triggered based on Size-Specific Dose Estimate (SSDE) or CT Dose Index volume (CTDIvol) depending on available data in the national registry. The new process for reviewing dose alerts was implemented in July 2015. Dose alerts for specific exams were sent immediately after the event to the lead technologist for the site, the responsible radiologist(s), and a physicist. Because the dose tracking software in use currently does not capture proprietary settings from equipment (e.g. noise index, reference mAs, iterative reconstruction values), the lead technologist makes any necessary changes at the modality to bring protocols into compliance. A root cause analysis is then sent to the physicist. If the exam is in compliance with the master protocol, a review of the master protocol is performed to see if technical parameters require adjustment.

#### RESULTS

Dose alerts were reviewed for a six-month period spanning July 2015 to December 2015. 372 dose alerts were reviewed out of 55,988 total exams yielding an average of 62 alerts per month (0.7% of total exams). Alerts per exam volume at the 11 site locations ranged between 6.62% -0.04%. The higher range value belonged to an orthopedic center CT scanner, which experienced a large number of spine protocols triggering alerts prior to optimization. The lower range value was from an outpatient CT scanner that had been fully optimized against the master protocol repository. Analyzing alerts by type of resolution revealed 69% of alerts were due to the protocol not matching the master protocol book (See Fig. 1A). 17% of dose alerts occurred with exams that matched the master protocol book and required modification to the current master protocol. The technologist was found to have adjusted technique in 4%. The incorrect protocol was selected in 2% of alerts and additional series triggered a dose alert in 1%. The remaining 7% were unresolved or other (e.g. body habitus, hardware, positioning). The average dose of all exams decreased by 0.59 mSv post-intervention (See Fig. 1B) although the total number of alerts did not.

### CONCLUSION

A standardized process for reviewing institutional dose alerts provides a robust mechanism for vetting CT dose outliers. The majority of dose alerts were due to protocols that deviated from the master protocol repository, underscoring the importance of a centrally managed and accessible protocol repository. By implementing a technologist driven review in the initial process, protocol deviation can be quickly brought into compliance and reinforced by the continued iterative process. Rapid response to a dose alert is crucial as the proprietary scanner settings are only available for the outlier examination as long as the examination data remains on the scanner. Although the number of alerts has not yet declined substantially, the overall average effective dose has decreased. Comprehensive dose alert review on a continual cycle allows the CT Quality group to celebrate units that have become champions of dose and are performing at the highest level.

### QS121-ED-TUB2

Reducing MRI Delay Time at a Pediatric Hospital Setting through Improved MRI workflow: A Continuous Improvement Project

Tuesday, Nov. 29 12:45PM - 1:15PM Room: QS Community, Learning Center Station #2

#### Awards

**Identified for RadioGraphics** 

#### Participants

Tushar Chandra, MD, Orlando, FL (*Presenter*) Nothing to Disclose Christopher N. Alsip, RT, ARRT, Cincinnati, OH (*Abstract Co-Author*) Nothing to Disclose Monica Epelman, MD, Orlando, FL (*Abstract Co-Author*) Nothing to Disclose Sarah Kirchner, Orlando, FL (*Abstract Co-Author*) Nothing to Disclose Daniel J. Podberesky, MD, Orlando, FL (*Abstract Co-Author*) Author with royalties, Reed Elsevier; Speakers Bureau, Toshiba Corporation; Travel support, General Electric Company; Travel support, Koninklijke Philips NV; Travel support, Siemens AG ; Consultant, Guerbet SA

## PURPOSE

As a busy tertiary care Pediatric center, our MRI studies were starting on time in only 39% cases and exceeding scheduled appointment length over 40% of the time, causing a delay for patients and families. We focused on all MRI studies on non-sedated children with a scan time of less than 60 minutes for this study. The target was to start 75% cases on time, 50% improvement in adherence to appointment length and improvement in our top box likelihood to recommend Press Ganey scores to > 90% from the baseline 80.5%. We aimed to accomplish these targets in a timeframe of 45 days, while maintaining diagnostic quality. The overall aim was to improve patient, provider and staff satisfaction as the MRI volumes continue to increase.

#### **METHODS**

After identifying the problem and setting up goals, the entire process from the time of arrival of the patient to our institute to the time MRI ends was diligently mapped in a 3-day Focused Improvement Event (FIE). Individual steps were carefully sorted out by role and problems in each step in the process were identified and categorized. We performed root cause analysis to identify cause and effect using tools such as fishbone diagram and the 5-whys to identify various factors causing delay in the workflow. After an elaborate discussion and brainstorming with members of the team involved in the entire process, countermeasures were suggested for each problem and prioritized based upon frequency, impact, and control. Variations in process were identified and their major causes discussed. A new workflow process map and standard work was created to formulate a predictable, stable process with little variation in output. Daily MRI audits were planned and results were reviewed at 15, 30 and 45 days and critically analyzed by the work team to make adjustment to the workflow and refine the process.

#### RESULTS

The new workflow was implemented on 9/1/2015 with the end point at 10/15/2015. In this period of 45 days, there was improvement in starting time of MRI studies from a baseline of 39% to 65% (67% improvement). Additionally, the average delay time of studies starting late decreased from 30 minutes to 18 minutes. Furthermore, the number of MRI studies with adherence to appointment time increased from 59% to 83%. This all reflected in our top notch likelihood to recommend Press Ganey scores for MRI, which increased from 80.5% to 100%.

#### CONCLUSION

MRI workflow can be optimized by following a standard procedure and elimination of variations. This process is sustainable over time and leads to not only cost savings and increased revenue, but also improved consistency and work efficiency. This project emphasizes the value of involving the entire team including the technicians and the support staff in planning and implementation. This goes a long way in improving patient, provider and staff satisfaction.

## Improving Patient Safety by Standardizing the Pre-Procedural Time-Out Process

Tuesday, Nov. 29 12:45PM - 1:15PM Room: QS Community, Learning Center Station #4

#### **Participants**

Pratik Rachh, MD, Atlanta, GA (*Abstract Co-Author*) Nothing to Disclose Deborah G. Walls, MS, Atlanta, GA (*Presenter*) Nothing to Disclose Susan Reich, atlanta, GA (*Abstract Co-Author*) Nothing to Disclose Edwin J. Herrod, Atlanta, GA (*Abstract Co-Author*) Nothing to Disclose Janice M. Newsome, MD, Alexandria, VA (*Abstract Co-Author*) Nothing to Disclose C. Matthew Hawkins, MD, Decatur, GA (*Abstract Co-Author*) Nothing to Disclose

## PURPOSE

There is wide variation in patient identification and pre-procedural time-out (PTO) processes for radiology procedures performed within our department, which is spread across five different hospitals, each with its unique culture and procedural workflow. Variations include: (a) patient identification methods, (b) site-marking processes, (c) personnel present during PTO, and (d) defined roles of technologists, nurses, and physician or Advanced Practice Provider (APP) proceduralists during the PTO process. Collectively, this variability imposes gaps in patient safety. The purpose of this project is the development and implementation of a standardized PTO process, which aims to prevent wrong procedure, wrong site and wrong patient errors in patients undergoing radiology procedures.

### **METHODS**

The initial scope of the project was narrowed to a single hospital and a charter was drafted. A multidisciplinary team of radiologists, technologists, nurses and APPs participated in two, 2-hour, process-mapping facilitated workshops detailing the current time-out process. With guidance from the quality program manager, the team mapped the entire pre-procedural patient identification and procedure readiness process, spanning from arrival in the department until procedure-start time. The team identified areas of inconsistencies and brainstormed countermeasures, and areas of potential improvement. Development of a PTO safety checklist, standardization of processes using the checklist, along with a focused emphasis on a "Just Culture and a Culture of Safety" were identified as essential steps for preventing future errors. Over a six month course the team designed, tested and piloted the PTO checklist and standardized the time-out process. Radiologists (attendings, fellows and residents), technologists, nurses, and APPs were trained in the use of the new safety checklist that is based on the organizations "Pledge", which is an empowerment tool to ensure all members of the interdisciplinary healthcare team feel authorized to speak up for patient safety. Metrics were designed to track progress. This included completion of a paper checklist audit tool, direct observation audits and documentation of the PTO in the patient's electronic medical record (EMR). The new process designated specific roles for the proceduralist, nurse, and technologist to carry out during every PTO. Designating specific roles and responsibilities ensures familiarity and ownership, thus decreasing the likelihood of a safety breach. The proceduralist was designated leader of the PTO, and using the checklist they direct the nurse and technologist through the time-out process. The nurse or technologist then completes the paper audit tool and documents the time-out in the EMR. Minor revisions were made to the PTO checklist after two months of use based on feedback from frontline staff and proceduralists. All procedure charts were reviewed for completion of the PTO in the patient's (EMR). Data collection results including paper audits of the checklist, results from "secret" direct observations of the PTO process, and documentation of the time-out in the EMR were discussed at monthly team meetings. In an effort to increase adherence to the new PTO process, team leads provided immediate feedback during direct observations when there was deviation from the new workflow.

### RESULTS

Baseline direct observations (n=13) in June 2015 indicated zero PTO processes met the new standard. The new PTO workflow and checklist were piloted starting with the week of January 10, 2016. Since then, the average rate of completion of all elements of the checklist as marked on the audit tool (n=602) across three modalities (Interventional Radiology, Computed Tomography and Ultrasound) is 95%. "Secret" direct observations of PTOs in February (n=5) and March 2016 (n=13) indicate 20% and 85% of procedures met the new standards. Average rate of all time-out documentation in the EMR (n=602) is 93% since implementation of the new PTO process.

### CONCLUSION

Workflow process and culture change require focused, multidisciplinary teamwork actively supported by executive leadership. Emphasis on creating a safe environment for our patients led to an honest assessment of the current PTO process and identification of wide variations in practice. Currently, the new standardized PTO process is completed >90% of the time. Next steps include ensuring the gains are sustained, embedding the new process into the culture, integrating PTO training into the onboarding process of new staff and providers, and implementing the new PTO at the remaining four institutions in our department. Outcomes Following Proton Therapy for the Treatment of High-risk Prostate Cancer: Efficacy and Toxicity Results from a Prospective Single Institution Cohort

Tuesday, Nov. 29 12:45PM - 1:15PM Room: RO Community, Learning Center Station #2

#### **Participants**

Seungtaek Choi, MD, Houston, TX (Presenter) Nothing to Disclose

#### ABSTRACT

Purpose/Objective(s): Proton therapy is currently used for the treatment of prostate cancer but reports of outcomes for various risk groups have been limited. We aim to report the outcomes of high-risk prostate cancer patients treated with definitive proton therapy at a single institution.Materials/Methods: This prospective single center cohort aimed at evaluating the acute and late normal tissue sequelae in adult patients treated with proton therapy for various tumor sites. For the purpose of this analysis, only patients with high-risk prostate cancer were considered. High risk was defined according to NCCN guidelines: stage =T3a, Gleason score =8, or prostate specific antigen (PSA) =20 ng/ml. All patients had a negative metastatic work-up. Follow-up was scheduled every 6-12 months for up to 5 years. Biochemical relapse was defined as PSA above nadir + 2 ng/mL. Overall survival (OS), biochemical progression free survival (bPFS), and distant metastasis free survival (DMFS) were analyzed for this cohort. Results are presented as numbers and percentages and survival rates are computed using Kaplan Meier, using the end of radiation therapy as the start date. Results: From 2009 to 2015, 159 high-risk prostate cancer patients were treated with proton beam radiation therapy (stage =T3a: n=31, 19.5%, Gleason score =8: n=135, 84.9%; =20 ng/ml: n=27, 17.0%). 121 pts (76.1%) had an age adjusted Charlson Comorbidity Index of 0 or 1. Patients received a median dose of 78 Cobalt Gray Equivalent (CGE) in 39 fractions over 8 weeks using passively scattered beams in 13 pts (8.2%) and spot scanning in 146 pts (91.8%). The target volume included prostate and seminal vesicles (SV) in 66.7% of the patients and prostate and proximal SV in 32.7%. The pelvic lymph nodes were not treated. Androgen deprivation therapy (ADT) using leuprolide was given to 152 pts (95.6%) for a median duration of 14.4 months (range: 2-44). Some patients are still receiving ADT as of last follow-up, which underestimates the reported duration. The median follow-up was 2.8 years. Three-year OS, bPFS and DMFS rates were 97%, 93% and 97%, respectively. Cumulative acute grade =3 genitourinary (GU) and gastrointestinal (GI) toxicity rates were 2% and 0%, respectively. Three-year cumulative rates of late grade =3 GU and GI toxicity rates were 3% and 1%, respectively.Conclusion: This prospective single institution cohort of highrisk prostate cancer patients treated with proton therapy combined with ADT demonstrates the efficacy and safety of this treatment approach. These results need to be confirmed with longer follow-up and compared with competing treatment options.

## Assessment of Acute Toxicity in Prostate Cancer Patients using Hydrogel Spacer During Proton Therapy

Tuesday, Nov. 29 12:45PM - 1:15PM Room: RO Community, Learning Center Station #3

#### **Participants**

Jesse Conterato, Warrenville, IL (Presenter) Nothing to Disclose

### ABSTRACT

Purpose/Objective(s): Patients undergoing proton beam radiotherapy (PBRT) with hydrogel spacer (HS) should experience low rates of acute toxicity. HS will likely have an impact on the reduction of late gastrointestinal (GI) toxicity by reducing the risk of proctitis. This single institution review evaluates acute toxicity outcomes in prostate cancer (CaP) patients treated with PBRT with HS placement.Materials/Methods: From April 2015 to February 2016, 63 men with CaP had placement of HS and were treated with PBRT. All patients completed PBRT, receiving 79.2 Cobalt Gray Equivalent in 44 fractions. Toxicity was prospectively assessed weekly during PBRT and scored according to CTCAE v4.0 in 12 categories, including Fatigue (F), Urinary Tract Pain (UT), Urinary Frequency (UF), Urinary Retention (UR), Urinary Incontinence (UI), Urinary Urgency (UU), Hematuria (H), Fecal Incontinence (FI), Rectal Hemorrhage (RH), Erectile Dysfunction (ED), Proctitis (PR), and Diarrhea (D). Of the 63 patients receiving HS, PBRT was delivered for low risk (N=15), intermediate risk (N=33) and high risk (N=15) disease. PBRT targets were prostate (P) only (N=14), P plus seminal vesicles (SV) (N=36) and P plus SV with elective inclusion of pelvic lymph nodes (N=13). In this group, median age was 65 (49 - 80), median IPSS score was 5 (0 - 33), and median prostate size was 63.9 cc (35.0 - 253.0 cc). Results: Change From Baseline F UT UF UR UI UU H FI RH ED PR D Number of Patients No Change 36 25 16 14 46 26 58 60 56 50 62 56 1 Grade Increase 25 29 28 27 12 27 5 2 7 12 1 6 2 Grade Increase 2 7 19 22 5 10 0 1 0 1 0 1 3 Grade Increase 0 2 0 0 0 0 0 0 0 0 0 0 2% of patients experienced an increase of 2 grades in FI from baseline. 11% of patients experienced an increase of 1 grade in RH from baseline. 2% of patients experienced an increase of 1 grade in PR from baseline. 2% of patients experienced an increase of 2 grades in D from baseline. 2% of patients experienced an increase of 2 grades in F from baseline. 14% of patients experienced an increase of 2-3 grades in UT from baseline. 30% of patients experienced an increase of 2 grades in UF from baseline. 35% of patients experienced an increase of 2 grades in UR from baseline. 8% of patients experienced an increase of 2 grades in UI from baseline. 16% of patients experienced an increase of 2 grades in UU from baseline. 8% of patients experienced an increase of 1 grade in H from baseline. 2% of patients experienced an increase of 2 grades in ED from baseline. Conclusion: HS placement for CaP patients has acceptably low rates of acute GI and urinary toxicity. Longer follow up is needed to assess effects of HS placement on late toxicity.

Uncommon Malignant Renal Tumors and Atypical Presentation of Common Ones: A Guide to Radiologists

Tuesday, Nov. 29 12:45PM - 1:15PM Room: GU/UR Community, Learning Center Station #7

# Awards

**Certificate of Merit** 

### Participants

Cassia T. Guimaraes, MD, San Francisco, CA (Presenter) Nothing to Disclose

Zhen J. Wang, MD, Hillsborough, CA (Abstract Co-Author) Stockholder, Nextrast, Inc

Ronald J. Zagoria, MD, San Francisco, CA (Abstract Co-Author) Nothing to Disclose

Jeffry P. Simko, MD, PhD, San Francisco, CA (*Abstract Co-Author*) Consultant, Genomic Health, Inc; Consultant, GenomeDx Biosciences Inc; Consultant, 3Scan; Consultant, 3DBiopsy, Inc; Research support, Genomic Health, Inc; Research support, Myriad Genetics, Inc

Karen Lopez, San Francisco, CA (Abstract Co-Author) Nothing to Disclose

Antonio C. Westphalen, MD, Mill Valley, CA (Abstract Co-Author) Scientific Advisory Board, 3DBiopsy LLC; Research Grant, Verily Life Sciences LLC

## **TEACHING POINTS**

The purpose of this exhibit is:1) To describe the imaging features of uncommon malignant neoplasms of the kidney and atypical presentation of common renal cancers.2) To describe a pattern-based approach to the diagnosis of malignant neoplasms of the kidney.3) To describe the role of imaging in management of malignant neoplasms of the kidney.

## TABLE OF CONTENTS/OUTLINE

The prevalence of renal malignant tumors is described. The more common types of renal cancers are briefly reviewed, with emphasis given to the atypical presentations of these neoplasms. In this part we describe imaging and clinical features of uncommon renal malignancies, for example collecting duct carcinoma, renal medullary carcinoma, carcinoma with Xp11 translocation, as well as nephroblastic, neuroendocrine, mesenchymal, hematologic, and metastatic renal tumors. We emphasize the pattern-based interpretation of uncommon renal cancers that aids the radiologist in narrowing the differential diagnoses.

Vascular Closure Devices from Wrist to Groin: A 2016 Update

Tuesday, Nov. 29 12:45PM - 1:15PM Room: VI Community, Learning Center Station #7

#### **Participants**

Diane Szaflarski, MD, Mineola, NY (Presenter) Nothing to Disclose Sameer Mittal, MD, Mineola, NY (Abstract Co-Author) Nothing to Disclose Ahmed Fadl, MD, Mineola, NY (Abstract Co-Author) Nothing to Disclose Achal Shah, Richmond Hill, NY (Abstract Co-Author) Nothing to Disclose Nicholas A. Georgiou, MD, Westbury, NY (Abstract Co-Author) Nothing to Disclose Jason C. Hoffmann, MD, Mineola, NY (Abstract Co-Author) Consultant, Merit Medical Systems, Inc; Speakers Bureau, Merit Medical Systems, Inc

Osama Hussaini, Old Westbury, NY (Abstract Co-Author) Nothing to Disclose

### **TEACHING POINTS**

1. An understanding of the various types of vascular closure devices (VCDs) is essential for the interventional radiologist to utilize the most appropriate device(s) in various clinical settings to optimize patient outcomes and hemostasis.2. Three general categories of VCDs exist: active approximation devices, passive approximation devices, and external compressive devices.

### **TABLE OF CONTENTS/OUTLINE**

- Review the history of vascular closure device (VCD) development and use in Interventional Radiology-Detail the economic costs and benefits of VCD use, and review the relevant literature (including SIR practice guidelines) regarding their use-Thoroughly discuss the three types of device classes; active approximation, passive approximation, and external hemostatic devices-Discuss the differences of each class of device, including thorough review of the most common devices in each class, their cost, how to use, complications, indications, success rates, and strengths and weaknesses-This will include review of femoral and radial devices-Highlight current trends and possible future products that may further improve safety and efficacy of VCDs

## VI249-SD-TUB1

Non-Invasive Treatment for Osteoid Osteoma by MR-Guided Focused Ultrasound (MRgFUS) Ablation: Clinical Outcomes in Five-year Experience

Tuesday, Nov. 29 12:45PM - 1:15PM Room: VI Community, Learning Center Station #1

## Participants

Carola Palla, MD, Rome, Italy (*Abstract Co-Author*) Nothing to Disclose Fabrizio Andrani, Rome, Italy (*Abstract Co-Author*) Nothing to Disclose Michele Anzidei, MD, Rome, Italy (*Abstract Co-Author*) Nothing to Disclose Roberto Scipione, Terracina, Italy (*Abstract Co-Author*) Nothing to Disclose Carlo Catalano, MD, Rome, Italy (*Abstract Co-Author*) Nothing to Disclose Alessandro Napoli, MD, Rome, Italy (*Abstract Co-Author*) Nothing to Disclose Hans Peter Erasmus, Rome, Italy (*Presenter*) Nothing to Disclose

#### PURPOSE

To determinate long-term clinical response and safety of MRgFUS ablative procedure for symptomatic non-vertebral osteoid osteomas

## **METHOD AND MATERIALS**

In this prospective observational study we enrolled patients with clinical and imaging evidence of Osteoid Osteoma, excluding vertebral lesions as considered inaccessible; recurrences after RFA or surgery were included. MrgFUS was performed towards osteoma nidus using InSightec ExAblate system. Primary endpoints for treatment efficacy were pain relief (assessed by visual analogue pain questionnaires, VAS) and reduction of Non-steroidal drugs (NSAISs) intake. As secondary endpoints we considered bone remineralization after treatment assessed by CT imaging and nidus enhancement decrease (performed through Dynamic contrast-enhanced Imaging MR). Imaging follow-up (MR and CT) was established at 1 and 12 months after treatment; VAS evaluation was scheduled at 1 month after MRgFUS, then yearly.

### RESULTS

We recruited 42 patients for MRgFUS ablation (female 9; male, 33; mean age 25,7  $\pm$  1,3); no intra-procedural or peri-procedural adverse events were observed. A mean number of 5  $\pm$  1,3 sonications was necessary to complete the treatment (average administered energy 985  $\pm$  423 J). Three patients underwent treatment as rescue therapy (2 post-RFA, 1 post surgery). At 1-month follow-up 39/42 patients (92,8%) experienced a complete clinical response (VAS score 0 and NSAIDs therapy interruption), with statistically significant difference (p=0.001) between baseline VAS score (7  $\pm$  2) and follow-up (0  $\pm$  2). 3/42 patients were classified as partial responders. 38 out of 39 complete responders maintained their status over 1-year and 2-year follow-up, while one subject reported pain recurrence requiring RFA.

### CONCLUSION

In our 5-year experience, MRgFUS demonstrated as effective non-invasive treatment for osteoid osteoma, with excellent rate of complete response over time

## **CLINICAL RELEVANCE/APPLICATION**

MRgFUS is feasible and safe for osteoid osteoma ablation, guaranteeing immediate and enduring pain relief

## VI250-SD-TUB2

Single-step versus Stepwise Chemoembolization for Unresectable Giant Hepatocellular Carcinoma: Is Singlestep Chemoembolization Harmful?

Tuesday, Nov. 29 12:45PM - 1:15PM Room: VI Community, Learning Center Station #2

## Participants

Yohei Ikebe, Nagasaki, Japan (*Presenter*) Nothing to Disclose Hideki Ishimaru, MD, Nagasaki, Japan (*Abstract Co-Author*) Nothing to Disclose Kazunori Mitarai, Omura, Japan (*Abstract Co-Author*) Nothing to Disclose Satomi Mine, Omura, Japan (*Abstract Co-Author*) Nothing to Disclose Saori Akashi, Nagasaki, Japan (*Abstract Co-Author*) Nothing to Disclose Hideyuki Hayashi, Nagasaki, Japan (*Abstract Co-Author*) Nothing to Disclose Eijun Sueyoshi, MD, Nagasaki, Japan (*Abstract Co-Author*) Nothing to Disclose Ichiro Sakamoto, Nagasaki, Japan (*Abstract Co-Author*) Nothing to Disclose Kazuto Ashizawa, MD, Nagasaki, Japan (*Abstract Co-Author*) Nothing to Disclose Masataka Uetani, MD, Nagasaki, Japan (*Abstract Co-Author*) Nothing to Disclose

#### PURPOSE

Some authors claim that stepwise manner should be chosen in chemoembolization of giant hepatocellular carcinoma (HCC) to avoid complications; however, it has not been confirmed. We aimed to compare the periprocedural toxicity and outcome of single-step and stepwise chemoembolization for unresectable giant HCC.

### **METHOD AND MATERIALS**

Between 2009 and 2015, 27 patients (22 men, 5 women; median age, 72 years; age range, 56-96 years) who underwent singlestep (n=16) or stepwise (n=11) chemoembolization for unresectable HCC more than 8cm in diameter were included. In single-step therapy, detailed evaluation of tumor feeding arteries was performed using rotational DSA, and each feeding artery was embolized tightly and ultraselectively using anticancer-in-oil emulsion followed by gelatin sponge particle. In stepwise therapy one third to half of feeding arteries were embolized in a session. Periprocedural toxicity was graded according to the common terminology criteria for adverse events (CTCAE ver. 4.0). Patient survival from the first TACE session was calculated with Kaplan-Meier analysis.

#### RESULTS

Between the two groups, there were no significant differences in Child-Pugh grade or tumor stage. Chemoembolization did not cause acute tumor lysis syndrome in either group. Grade 3 or 4 toxicity after single-step and stepwise therapy, included abdominal pain (0 and 9%, respectively), elevated aspartate aminotransferase (75 and 73%, respectively) and alanine aminotransferase (44 and 27%, respectively). Stepwise chemoembolization was completed in only 3/11 (27%). The cumulative survival rates of single-step and stepwise therapy were 80 and 60% at 1 year, 67 and 45% at 2 years, and 50 and 0% at 3 years, respectively (log-rank test P=0.32).

### CONCLUSION

This study's results showed non-inferiority of single-step chemoembolization compared with stepwise chemoembolization in periprocedural toxicity and survival. Single step chemoembolization for giant HCCs, in a manner which embolize all feeders tightly and ultraselectively, is not harmful and should not be discouraged.

#### **CLINICAL RELEVANCE/APPLICATION**

Single-step chemoembolization, which induces larger tumor necrosis and prevents early progression, is challenging but preferable option for unresectable giant HCC.

# VI251-SD-TUB3

### Bedside IVC Filters Placed with Digital Radiograph Guidance: A Single Institution's Initial Experience

Tuesday, Nov. 29 12:45PM - 1:15PM Room: VI Community, Learning Center Station #3

#### **Participants**

John A. Walker, MD, San Antonio, TX (*Presenter*) Nothing to Disclose Jorge E. Lopera, MD, San Antonio, TX (*Abstract Co-Author*) Nothing to Disclose Ryan M. Hegg, MD, Rochester, MN (*Abstract Co-Author*) Nothing to Disclose Girish Kumar, MD, Stickney, IL (*Abstract Co-Author*) Nothing to Disclose

## PURPOSE

Acute pulmonary embolism is associated with high mortality, and prophylaxis among high risk patients is the standard of care. Critically ill patients are often among those at highest risk and frequently require mechanical prophylaxis with an IVC filter. Transporting these critically ill patients however can be a logistical challenge and sometime carries significant risk. Therefore bedside filter placement should be considered. Here we review bedside IVC filter placement in the intensive care unit (ICU) using digital radiography (DR).

#### **METHOD AND MATERIALS**

Bedside IVC filters placed in ICU patients as part of a quality improvement project implemented in July 2015 were retrospectively reviewed. Indication for filter placement followed SIR guidelines. The majority of patients had prior CT imaging available for procedure planning. CT images were used to assess cava anatomy and define the lowest renal vein and IVC bifurcation with respect to the spine. Filters were then placed at bedside with DR guidance. In the absence of a prior CT scan, intravascular ultrasound (IVUS) was utilized with DR. DR was used to visualize wire placement, adjust position of the delivery sheath and confirm final deployed filter position.

### RESULTS

A total of 29 IVC filters were placed at beside with DR guidance, two with the aid of IVUS. Seventeen were placed for trauma prophylaxis and 14 for documented deep vein thrombosis and/or pulmonary embolism. Twenty were placed from a right common femoral access and 9 from the left. Average recorded procedural time was 18.6 minutes, ranging from 13-25 minutes. Median number of abdominal radiographs used was 5, ranging from 4-6. 18 Denali, 9 Option and 2 Celect filters were used. All 29 filters were positioned as planned. Two filters were considered significantly tilted, 3 mildly tilted and 24 centered. Eleven patients have received CT since placement with all filters adequately positioned in the infra-renal IVC. Three of the bedside placed filters have been removed to date, all without difficulty.

#### CONCLUSION

Bedside IVC filter placement with DR guidance after pre-planning from prior CT imaging is safe and effective while reducing complicated patient transfers.

## **CLINICAL RELEVANCE/APPLICATION**

Digital radiography provides convenient rapid bedside imaging and when used in conjuction with pre-planning CT provides a platform for delivering bedside IVC filters effectively and safely.

Predictive Factors for Hypertrophy of the Future Liver Remnant after Portal Vein Embolization with Absolute Ethanol

Tuesday, Nov. 29 12:45PM - 1:15PM Room: VI Community, Learning Center Station #4

# Participants

Keitaro Sofue, MD, Kobe, Japan (*Presenter*) Nothing to Disclose Yoshito Takeuchi, MD, Kyoto, Japan (*Abstract Co-Author*) Nothing to Disclose Masakatsu Tsurusaki, MD, PhD, Osaka, Japan (*Abstract Co-Author*) Nothing to Disclose Masato Yamaguchi, MD, PhD, Kobe, Japan (*Abstract Co-Author*) Nothing to Disclose Koji Sugimoto, MD, Kobe, Japan (*Abstract Co-Author*) Nothing to Disclose Kazuro Sugimura, MD, PhD, Kobe, Japan (*Abstract Co-Author*) Nothing to Disclose Philips NV Research Grant, Bayer AG Research Grant, Eisai Co, Ltd Research Grant, DAIICHI SANKYO Group Yasuaki Arai, Tokyo, Japan (*Abstract Co-Author*) Nothing to Disclose

### PURPOSE

To identify predictive factors associated with hypertrophy of the future liver remnant (FLR) after portal vein embolization (PVE) and to clarify the value of PVE with absolute ethanol in patients with negative predictive factors for liver regeneration.

### METHOD AND MATERIALS

A total of 102 patients (68 men and 34 women) who underwent PVE were evaluated. PVE via ipsilateral approach was performed to increase insufficient FLR before major hepatic resection. Outcome of PVE and hepatic resection were evaluated. Changes in FLR and FLR/TFLV ratio were calculated by CT volumetry. Patient demographics including chronic liver disease, diabetes mellitus, and cholestasis, laboratory tests, PVE procedure, and volumetric parameters of the liver before PVE were assessed to identify predictive factors associated with hypertrophy of the FLR using a multiple linear regression analysis with stepwise backward elimination method. Prespecified analysis in the presence/absence of the identified predictive factor was also performed to compare the outcome of PVE and postoperative complication.

## RESULTS

PVE was successful in all patients and complications occurred in seven (6.9%). The mean FLR and FLR/total functional liver volume (TFLV) ratio significantly increased after PVE (P<.0001). FLR and FLR/TFLV ratio before PVE were inversely correlated (P<.0001) to hypertrophy of the FLR, and extent of embolized segments was also a significant factor (P<.02). The change in FLR and FLR/TFLV ratio were significantly smaller in patients who underwent left and right anterior PVE than those underwent right PVE (P<.01). Successful major hepatic resection was achieved in 85 (83.3%) patients. Postoperative complications occurred in 27 (31.8%) and developed more frequently in patients who underwent left trisegmentectomy (61.5%) than in patients who underwent right major hepatectomy (26.4%) (P=.021).

# CONCLUSION

FLR and FLR/TFLV ratio before PVE with absolute ethanol were associated with hypertrophy of the FLR after PVE, and negative predictive factors for liver regeneration did not affect hypertrophy of the FLR. PVE before left trisegmentectomy confined insufficient FLR hypertrophy and resulted in higher rate of postoperative complications.

### **CLINICAL RELEVANCE/APPLICATION**

Chronic liver disease, diabetes mellitus, and cholestasis do not affect hypertrophy of FLR after PVE, and therapeutic strategy for liver trisegmentectomy is needed to achieve better clinical outcome.

## VI253-SD-TUB5

Hemorrhagic Pulmonary Sheath Accompanying Acute Stanford A Aortic Dissection: Prevalence, CT Appearance and Consequences

Tuesday, Nov. 29 12:45PM - 1:15PM Room: VI Community, Learning Center Station #5

## Participants

Qiuxia Xie, Guangzhou, China (*Presenter*) Nothing to Disclose Xuhui Zhou, MD, PhD, Guangzhou, China (*Abstract Co-Author*) Nothing to Disclose Ling Lin, Guangzhou, China (*Abstract Co-Author*) Nothing to Disclose Jifei Wang, Guangzhou, China (*Abstract Co-Author*) Nothing to Disclose

### PURPOSE

To retrospectively investigate the prevalence , computed tomography (CT) appearance and consequences of hemorrhagic pulmonary sheath(HPS) in Stanford A aortic dissection(AD) patients.

### **METHOD AND MATERIALS**

Institutional review board approval and informed consent were not required. One hundred eighty eight consecutive acute Stanford A aortic dissection patients (mean age,59 years; range29-78years; 136 male, 52 female) underwent CT aortic angiography were reviewed. CT images were interpreted by two independent radiologists. Clinical charts were reviewed for outcomes of patients up to 30-days after the initial CT scan. By using Chi-square tests, Fisher exact tests, Wilcoxon rank sum test, CT findings were compared with patient outcome—survival or death.

### RESULTS

Eighteen (9.6%) of the 188 patients had HPS. HPS involved right pulmonary artery in 50% (9 of 18) patients, left pulmonary artery in 11.1% (2 of 18) and both in38.9% (7 of 18) respectively. HPS extending bronchovascular sheaths were indentified in 44.4% (8 of 18) patients, and 6 (75%) of 8 patients with HPS had alveolar opacity around the thickened bronchovascular sheath. During 30days of follow-up in 18 patients with HPS, 61.1% (11 of 18) patients died and 38.9% (7 of 18) patients showed HPS absorption. HPS extending bronchovascular sheaths was more frequent in death group (6 of 11, 54.5%) than survival (2 of 7, 28.6%), but not significantly( $\rho$ =0.3665). Patients in death group were more likely to have involved abdominal visceral arteries by AD (7 of 11, 63.6%) than patients in survival group (0 of 7, 0%)( $\rho$ =0.0103). There were no significant differences in their age, ascending aorta maximum diameter, pleural effusion and hemopericardium.

## CONCLUSION

HPS is not a rare complication in patients with Stanford A aortic dissection, and patients with abdominal visceral arteries involvement by AD have a poor short-term outcome. The impact of HPS extending bronchovascular sheaths on prognosis of patients need further research to confirmed.

#### **CLINICAL RELEVANCE/APPLICATION**

CT appearance of hemorrhagic pulmonary sheath has been reported in several cases of Stanford A aortic dissection. There are no published data about the prevalence and consequences of this complication.

# The Safety and Efficacy of Radiofrequency Ablation with Hydrochloric Acid Infusion in Rabbit Liver Model

Tuesday, Nov. 29 12:45PM - 1:15PM Room: VI Community, Learning Center Station #6

#### **Participants**

Jinhua Huang, Guangzhou, China (*Presenter*) Nothing to Disclose Senmiao Huang, GuangZhou, China (*Abstract Co-Author*) Nothing to Disclose Tianqi Zhang, Guangzhou, China (*Abstract Co-Author*) Nothing to Disclose Ruhai Zou, Guangzhou, China (*Abstract Co-Author*) Nothing to Disclose Yangkui Gu, Guangzhou, China (*Abstract Co-Author*) Nothing to Disclose

## PURPOSE

To evaluate the safety and efficacy of radiofrequency ablation with hydrochloric acid (HCl) infusion using monopolar perfusion electrode in rabbit liver model.

## METHOD AND MATERIALS

Thirty rabbits were randomly divided into five groups and received corresponding infusion for RFA: normal saline infused RFA (NS-RFA) group (n=6); four different concentration (5%, 10%, 15% and 20%) of HCl infused RFA (HCl-RFA) groups, each group contains 6 rabbits (n = 24). Hepatic and renal toxicity, and electrolytes were evaluated by means of blood biochemical analysis for all animals before and 2, 7, 14 days after ablation. Magnetic Resonance Imaging (MRI) and histopathologic examinations were proceeded to evaluate the ablation zone.

#### RESULTS

All animals tolerated the ablation without any deaths. Blood biochemical analysis indicating hepatic and renal toxicity and electrolytes did not differ among the five groups before or after ablation (P > 0.05). MRI showed all RFA lesions were irregular or ellipsoid, and limited in the liver. Longitudinal diameters of the ablation zones were from  $2.20\pm0.15$  cm to  $2.69\pm0.17$  cm in HCl-RFA groups, larger than  $1.68\pm0.14$  cm in NS-RFA group (P<0.05), while transverse diameters were from  $1.92\pm0.2$  cm to  $2.29\pm0.11$  cm in HCl-RFA groups, larger than  $1.47\pm0.19$  cm in NS-RFA group (P<0.05). Histopathologic examinations showed HCl-RFA create more serious necrosis compared with NS-RFA.

### CONCLUSION

HCI-RFA could enlarge the ablation zone obviously compared to NS-RFA with reversible liver function damage without renal toxicity. HCl infusion may be a feasible and safe method to enhance the efficacy of RFA.

# **CLINICAL RELEVANCE/APPLICATION**

HCl infusion may be a safe method to enhance the efficacy of RFA, so it is predictively feasible to treat large Hepatocellular Carcinoma.

# A Practical Approach to the Radiological Diagnosis of Breast Calcifications for Resident

Wednesday, Nov. 30 12:15PM - 12:45PM Room: BR Community, Learning Center Station #8

#### **Participants**

Karina Pesce, Vicente Lopez, Argentina (*Presenter*) Nothing to Disclose Flavia B. Sarquis, MD, Vicente Lopez, Argentina (*Abstract Co-Author*) Nothing to Disclose Silvia Giusti, Vicente Lopez, Argentina (*Abstract Co-Author*) Nothing to Disclose Carlos M. Lamattina, MD, Vicente Lopez, Argentina (*Abstract Co-Author*) Nothing to Disclose Bernardo O. Blejman, MD, Buenos Aires, Argentina (*Abstract Co-Author*) Nothing to Disclose Julio A. San Martino, Vicente Lopez, Argentina (*Abstract Co-Author*) Nothing to Disclose

# **TEACHING POINTS**

To review the various appearances of breast microcalcificationsSuggestions and tips for management of calcificationsInteractive imaging case review

## TABLE OF CONTENTS/OUTLINE

Introduction: Overview of Mammographic microcalcificationsTechnique Mammographic views to evaluate microcalcificationsAnatomyBI-RADS® Lexicon for CalcificationsCauses of pseudocalcificationsManagement of calcificationsBiopsy techniqueCasesTest casesConclusion

Evaluation of Response to Neoadjuvent Chemotherapy on Breast MRI: Illustrative Depiction of Enhancement Pattern Response with Pathologic Correlation

Wednesday, Nov. 30 12:15PM - 12:45PM Room: BR Community, Learning Center Station #9

#### Awards

**Certificate of Merit** 

### Participants

Raman Verma, MD, Ottawa, ON (*Presenter*) Nothing to Disclose Mukta D. Mahajan, MBBS, Vienna, Austria (*Abstract Co-Author*) Nothing to Disclose Zuzana Kos, Ottawa, ON (*Abstract Co-Author*) Nothing to Disclose Jean M. Seely, MD, Ottawa, ON (*Abstract Co-Author*) Nothing to Disclose

## **TEACHING POINTS**

Evaluating treatment response to neoadjuvent chemotherapy is important in determining optimal surgical management. This exhibit will:1) Contrast common patterns of disease presentation and their associated treatment response on breast MRI with final pathologic correlation.2) State and review factors which may contribute to the extent of response following treatment in the context of current literature3) Provide a summary of imaging features post-treatment

# TABLE OF CONTENTS/OUTLINE

MRI is the imaging study of choice when evaluating response to treatment after neoadjuvent chemotherapy (NAC). Pretreatment and post-treatment breast MRI studies will be contrasted, specifically illustrating examples of treatment response on MRI including:1. No response

- 2. Concentric shrinkage without surrounding lesions
- 3. Concentric shrinkage with surrounding lesions
- 4. Shrinkage with residual multinodular lesions
- 5. Diffuse contrast enhancement in whole quadrants
- 6. Nonvisualization of enhancement
- 7. False positive MRI suspected imaging complete response (cIR) without pathologic complete response (pCR)
- 8. False negative MRI residual imaging disease with pCR
- 9. Overestimation of residual disease
- 10. Underestimation of residual disease

A Pilot Study: Radiogenomics of Inflammatory Breast Cancer

Wednesday, Nov. 30 12:15PM - 12:45PM Room: BR Community, Learning Center Station #1

#### **Participants**

Takeo Fujii, MD, MPH, HOUSTON, TX (*Abstract Co-Author*) Nothing to Disclose Ying Wang, PhD, HOUSTON, TX (*Abstract Co-Author*) Nothing to Disclose Arvind Rao, Houston, TX (*Abstract Co-Author*) Nothing to Disclose Bora Lim, MD, HOUSTON, TX (*Abstract Co-Author*) Nothing to Disclose Naoto Ueno, MD, PHD, Houston, TX (*Abstract Co-Author*) Nothing to Disclose H. Carisa Le-Petross, MD, Houston, TX (*Presenter*) Nothing to Disclose

## PURPOSE

Inflammatory breast cancer (IBC) is one of the most aggressive rare breast cancer types with imaging features different from non-IBC such as non-mass enhancement or multicentric small masses, global skin thickening, extensive edema, and diffuse breast enlargement. It is unclear if these imaging features correlate with or can predict genomic characteristics. The objective of this study is to assess for any association between radiographic features and RNA expression in IBC patients.

#### **METHOD AND MATERIALS**

Retrospective analysis was performed of IBC patients who had available gene profile, between 2000 and 2005. Baseline ultrasound (US), mammography (MG), MRI, and CT were reviewed by 1 radiologist. Imaging features collected on target lesions were based on ACR BI-RADs descriptors. 21 patients had available data for analysis. Samples were run on Affymetrix HG-U133A platform with 506,944 probes corresponding to 22,283 genes. Frozen robust multiarray analysis was used to quantify and summarize array data. To test association between imaging features and gene expression, gene-by-gene 1-way ANOVA test was used for categorical variables and gene-by-gene linear model for continuous variables. Beta-uniform mixture models were used to estimate the number of significant genes at different false discovery rates (FDRs).

### RESULTS

Among 21 imaging features, breast density, calcifications, and edema showed a peak of small p-values on histogram (tables 1-3). There are 2, 13 and 106 genes significantly associated with breast density on MG at FDRs of 0.05, 0.1 and 0.2, respectively. One and 5 genes were significantly associated with calcifications at FDRs of 0.25 and 0.3, respectively. There are 22 and 77 genes significantly associated with breast edema on US at FDRs of 0.2 and 0.25, respectively. The rest of the imaging features on all modalities do not show an obvious association with genomic data. Those genes associated with the above three features are various and there is no critical pathways regulating them such as PI3K/Akt/mTOR, MAPK, and TGF- $\beta$  pathways.

## CONCLUSION

Our analysis suggests some associations between gene expression profile and breast density and calcifications on MG, and tissue edema on US. Larger studies are necessary to confirm and identify additional subset of imaging features

### **CLINICAL RELEVANCE/APPLICATION**

Some gene expression profile are associated with breast density, calcifications, and edema on imaging of IBC patients.

Searching an Imaging Biomarker for Tamoxifen Resistance: Correlation between Background Parenchymal Enhancement (BPE) and CYP2D6 Genotype in Patients under Tamoxifen

Wednesday, Nov. 30 12:15PM - 12:45PM Room: BR Community, Learning Center Station #2

## Participants

Annika Keulers, MD, Aachen, Germany (*Abstract Co-Author*) Nothing to Disclose Timm Dirrichs, Aachen, Germany (*Abstract Co-Author*) Nothing to Disclose Kevin Strobel, MD, PhD, Aachen, Germany (*Abstract Co-Author*) Nothing to Disclose Joachim Arnemann, Cologne, Germany (*Abstract Co-Author*) Nothing to Disclose Christiane K. Kuhl, MD, Bonn, Germany (*Presenter*) Nothing to Disclose Simone Schrading, MD, Aachen, Germany (*Abstract Co-Author*) Nothing to Disclose

### PURPOSE

Tamoxifen is a pro-drug metabolized via cytochrome P450 2D6 (CYP2D6) into the active metabolite endoxifen. Mutations in genotyp may lead to less effective CYP2D6 alleles resulting in slow metabolism contributing to tamoxifen resistance, which is an important clinical problem. Tamoxifen is known to substantially reduce the background parenchymal enhancement (BPE) in DCE MRI. We hypothesized that degree of BPE may serve as biomarker to indicate reduced tamoxifen efficacy and investigated the correlation between BPE in women under tamoxifen and changes in CYP2D6 genotype.

## **METHOD AND MATERIALS**

Prospective study performed between 5/2014 and 7/2015 on 100 patients (mean age 53years) with treatment for breast cancer and on regular dose tamoxifen for at least 3months. BPH was classified according to the ACR-categories from MR-ACR1(no BPE) to MR-ACR4(strong BPE). At time of MRI genotypes the following CYP2D6 allels were investigated:CYP2D6\*4, a stop-codon, CYP2D6\*5, leading to deletion, and CYP2D6\*10, resulting in reduced enzymatic function. Degree of BPH was correlated with the respective CYP2D6 genotypes.

### RESULTS

91/100 women exhibited no BPE(MR-ACR1), 8/100 minimal(MR-ACR2) and 1/100 moderate BPE(MR-ACR3). None of the 9 patients with noticeable BPE(MR-ACR2/3) had a pathogenic CYP2D6 genotype: Six had wildtype CYP2D6, the remaining 3 had heterozygous mutations that are not supposed to impact tamoxifen metabolism. Among the 91 women without noticeable BPE(MR-ACR1), 67 had a wildtype genotype and 22 exhibited minor genotype variations with single or combined heterozygous mutations of CYP2D6\*4, \*5 or \*10. A total 2/91 patients without BPE(MR-ACR1) had a pathogenic mutation of CYP2D6. Accordingly there was no correlation between CYP2D6 genotypes and the degree of BPE(r=0.42).

## CONCLUSION

The lack of correlation between BPE and CYP2D6 genotypes can be interpreted as follows: BPE in MRI may not be useful for identifying tamoxifen resistance, or CYP2D6 genotypes are not predictive. Since determination of the CYP2D6 genotype is not established for lack of evidence on correlation between genotypes and patient outcome, lack of correlation between BPE and genotypes may encourage further research on BPE as imaging biomarker for tamoxifen resistance.

## **CLINICAL RELEVANCE/APPLICATION**

The lack of correlation between BPE in DCE-MRI and CYP2D6 genotypes in women under tamoxifen encourages further research on BPE as imaging biomarker for tamoxifen resistance.

Utility of Screening Mammography for Detecting Clinically Occult Malignancy in Autologous Myocutaneous Flap Reconstructed Breasts after Mastectomy

Wednesday, Nov. 30 12:15PM - 12:45PM Room: BR Community, Learning Center Station #3

#### Awards

#### **Student Travel Stipend Award**

#### **Participants**

Julia Savage, MD, Ann Arbor, MI (*Presenter*) Nothing to Disclose Leah W. Carlson, MD, Ann Arbor, MI (*Abstract Co-Author*) Nothing to Disclose Mitra Noroozian, MD, Ann Arbor, MI (*Abstract Co-Author*) Nothing to Disclose Stephanie K. Patterson, MD, Ann Arbor, MI (*Abstract Co-Author*) Nothing to Disclose Deborah O. Jeffries, MD, Ann Arbor, MI (*Abstract Co-Author*) Nothing to Disclose Annette I. Joe, MD, Farmington Hills, MI (*Abstract Co-Author*) Research Consultant, Delphinus Medical Technologies, Inc Colleen H. Neal, MD, Ann Arbor, MI (*Abstract Co-Author*) Nothing to Disclose Lubomir M. Hadjiiski, PhD, Ann Arbor, MI (*Abstract Co-Author*) Nothing to Disclose Mark A. Helvie, MD, Ann Arbor, MI (*Abstract Co-Author*) Institutional Grant, General Electric Company

## PURPOSE

Screening mammography to detect clinically occult malignancy in autologous myocutaneous flap reconstruction (AMF) after mastectomy is controversial. We sought to determine the utility of screening these patients.

## METHOD AND MATERIALS

This IRB-approved, HIPAA-compliant, retrospective, single institution study identified 485 women (mean age 58 years, range 26-88), who had mammography of the AMF from 1/1/2000 - 7/15/2015, and > one year clinical follow-up. Of 617 AMF (132 bilateral), 78% (483/617) followed mastectomy for cancer (CA-AMF) and 22% (134/617) followed prophylactic mastectomy (P-AMF).

#### RESULTS

4,159 screening mammograms (mean 6.7/AMF, median 8.5, range 1-16) were obtained. 3.1% (15/485) of patients developed 18 local-regional malignancies; 10 in-flap (8 invasive breast, 2 lymphoma), 1 in overlying skin, 4 in axillary lymph node, and 3 in chest wall. 83% (15/18) of malignancies occurred in CA-AMF and 17% (3/18) in P-AMF (1 lymphoma and 2 axillary metastases), difference between malignancy in CA-AMF & P-AMF p< 0.001. Excluding in-flap lymphoma and recurrence confined to skin, the in-flap breast cancer recurrence rate in CA-AMF was 1.7% (8/483, CI 0.5%, 2.8%). Screening detected 4/8 non-palpable cancers, 1 was detected by MRI, and 3 were symptomatic interval cancers at time of diagnosis. The in-flap cancer detection rate of screening mammography in CA-AMF was 0.12%. The in-flap cancer detection rate of mammography in CA-AMF was 0.21%. Mean time to AMF malignancy was 7.6 years (median 8, range 0.8-16.2). Median invasive cancer size was 0.8 cm (range 0.6-1.2). Screening CA-AMF and P-AMF resulted in 0.63% (26/4159) FP biopsy recommendations. The PPV3 of screening mammography was 13% (4/30).

#### CONCLUSION

Screening detected some clinically occult breast cancer in CA-AMF, with in-flap breast cancer detection rate of 0.12% and a low false positive biopsy rate. No clinically occult breast cancer was detected in P-AMF.

### **CLINICAL RELEVANCE/APPLICATION**

Screening mammography in CA-AMF detected some clinically occult in-flap breast cancer with low rate of FP biopsy recommendations. No breast cancer was detected from screening P-AMF.

3D Breast Tomosynthesis with Digital Mammography versus Digital Mammography Alone: Comparison of Performance Metrics at Prevalence versus Incidence Screens

Wednesday, Nov. 30 12:15PM - 12:45PM Room: BR Community, Learning Center Station #4

#### Awards

#### **Student Travel Stipend Award**

#### Participants

Kathryn Lowry, MD, Boston, MA (Presenter) Nothing to Disclose

Pragya A. Dang, MD, Boston, MA (Abstract Co-Author) Nothing to Disclose

Natasha K. Stout, PhD, Boston, MA (Abstract Co-Author) Nothing to Disclose

Elkan F. Halpern, PhD, Boston, MA (*Abstract Co-Author*) Research Consultant, Hologic, Inc; Research Consultant, Real Imaging Ltd; Research Consultant, Gamma Medica, Inc; Research Consultant, K2M Group Holdings, Inc

G. Scott Gazelle, MD, PhD, Boston, MA (Abstract Co-Author) Consultant, General Electric Company Consultant, Marval Biosciences Inc

Constance D. Lehman, MD, PhD, Boston, MA (*Abstract Co-Author*) Research Grant, General Electric Company; Medical Advisory Board, General Electric Company

Anne Marie McCarthy, Boston, MA (Abstract Co-Author) Nothing to Disclose

#### PURPOSE

Prior screening trials with digital breast tomosynthesis (DBT) have suggested reduced recall rates and increased cancer detection rates compared with digital mammography (DM) alone. However, most trials have only examined test performance after the first (prevalence) DBT exam, and it is not clear whether these effects are sustained on subsequent exams. The purpose of this study was to compare the performance of DBT at initial and subsequent screens to performance with DM.

### **METHOD AND MATERIALS**

After IRB approval, electronic medical records review identified screening mammograms performed 1/2009-2/2011 before DBT integration (DM), and performed 1/2013-2/2015 after DBT integration. DBT examinations were grouped into initial DBT examinations (DBT1) and DBT examinations with one or two prior DBT exams (DBT2+). Women without documentation of any prior screening mammography were excluded from analysis. Differences in recall rates, cancer detection rates, and biopsy rates were examined using chi square statistics.

### RESULTS

A total of 69,049 screening DM examinations were compared with 12,153 DBT1 screens and 43,267 DBT2+ screens. Recall rates significantly decreased with DBT1 relative to DM (53 versus 62 recalls per 1,000; p<0.001), and DBT2+ remained significantly lower than DM (56 per 1000; p<0.001). Total cancer detection rate significantly increased with DBT1 relative to DM (6.4 versus 4.4 per 1,000; p=0.003), but decreased at DBT2+ exams and was no longer significantly different than DM (4.4 per 1,000; p=0.97). Invasive cancer detection rate similarly increased at DBT1 exam compared to DM (4.4 versus 2.8 per 1,000, p=0.003) but decreased at DBT2+ (3.0 per 1,000; p=0.53). A similar trend was observed with biopsy rates, which increased with DBT1 compared with DM (12.1 versus 9.2 per 1,000; p=0.002) and decreased with DBT2+ exams (10.3 per 1,000; p=0.07).

### CONCLUSION

Cancer detection rates increase with initial DBT examinations relative to DM but return to similar rates as DM at subsequent examinations, suggesting an underlying prevalence screen effect. The benefit of recall reductions observed with initial DBT screening persists on subsequent screens.

#### **CLINICAL RELEVANCE/APPLICATION**

The added value of DBT over time appears to be the benefit of improvements in recall rather than sustained increased cancer detection rates that are found with initial DBT prevalence screens.

Analysis of Stereotactic Biopsies Performed on Calcifications Identified after Recent Completion of Breast Conserving Therapy: Can Biopsy be Obviated?

Wednesday, Nov. 30 12:15PM - 12:45PM Room: BR Community, Learning Center Station #5

## Participants

Palita Hansakul, MD, Houston, TX (*Abstract Co-Author*) Nothing to Disclose Rosalind P. Candelaria, MD, Houston, TX (*Presenter*) Nothing to Disclose H. Carisa Le-Petross, MD, Houston, TX (*Abstract Co-Author*) Nothing to Disclose Monica L. Huang, MD, Houston, TX (*Abstract Co-Author*) Nothing to Disclose Lumarie Santiago, MD, Houston, TX (*Abstract Co-Author*) Nothing to Disclose Beatriz E. Adrada, MD, Houston, TX (*Abstract Co-Author*) Nothing to Disclose

### PURPOSE

To determine the yield of cancer in stereotactic biopsies performed on suspicious calcifications identified within 24 months after breast conserving surgery (BCS)

## METHOD AND MATERIALS

An IRB-approved, single-institution retrospective review was completed on all stereotactic biopsies performed from 2009-2013 in patients with history of breast cancer who underwent breast conserving surgery (BCS) and radiation therapy (RT). Data collected included tumor characteristics, type of surgery and RT, imaging findings and time interval between treatment and calcification detection. Calcifications were characterized using ACR lexicon. Histopathology from biopsy was correlated with clinical and mammographic findings.

#### RESULTS

94 patients met inclusion criteria and had 100 biopsies for suspicious calcifications, with cancer yield of 7% (7/100). The 7 cancer cases were high-grade invasive ductal carcinoma with DCIS (14%, 1/7), high-grade DCIS (57%, 4/7), intermediate-grade DCIS (14%, 1/7) and low-grade DCIS (14%, 1/7); all 7 had clear surgical margins ( $\geq$ 2mm). Whole breast irradiation was performed in 6/7 (86%); partial breast irradiation in 1/7 (14%). Mean times were 15 months from BCS to detection of calcifications and 11 months from RT completion to detection. Although univariate analysis did not identify any variable which showed significant association with histopathology, a few trends emerged. In 5/7 (71%) cancer cases, calcifications were located in the scar or same quadrant of the primary cancer with similar histopathology to the primary; in 2/7 (29%) cases, calcifications were in a different quadrant with different histopathology from the primary. Morphology for the 7 malignant calcifications was amorphous (43%, 3/7), coarse heterogeneous (29%, 2/7) and fine pleomorphic (29%, 2/7), with grouped distribution in all 7. Pathology primarily was post-therapeutic effect in the benign cases (70%; 65/93); no case of benign pathology developed ipsilateral malignancy with two-year followup.

## CONCLUSION

Stereotactic biopsy of suspicious calcifications identified in the ipsilateral breast within 24 months of completing BCS has a cancer yield of 7%, which is above the 2% risk of malignancy allowed for imaging followup (BI-RADS 3).

## **CLINICAL RELEVANCE/APPLICATION**

Although adjuvant RT reduces the risk of ipsilateral recurrence, metachronous malignancy should be suspected in patients presenting with new calcifications during early post-treatment surveillance.

Contrast Enhanced Ultrasound (CEUS) and Gray Scale (GS) Ultrasound Features of Benign and Malignant Axillary Sentinel Lymph Nodes (SLN) in Breast Cancer Patients

Wednesday, Nov. 30 12:15PM - 12:45PM Room: BR Community, Learning Center Station #7

**FDA** Discussions may include off-label uses.

#### Participants

Lumarie Santiago, MD, Houston, TX (*Presenter*) Nothing to Disclose Rosa Hwang, MD, Houston, TX (*Abstract Co-Author*) Nothing to Disclose Elizabeth Mittendorf, MD, Houston, TX (*Abstract Co-Author*) Nothing to Disclose Basak E. Dogan, MD, Houston, TX (*Abstract Co-Author*) Nothing to Disclose

#### PURPOSE

To determine the CEUS and GS morphologic features of benign and malignant axillary sentinel lymph nodes (SLN) identified using microbubble contrast-enhanced ultrasound (CEUS).

#### **METHOD AND MATERIALS**

Twenty-one early stage breast cancer patients were enrolled on a prospective clinical trial evaluating microbubble CEUS of axillary nodes, followed by needle biopsy and I-125 seed placement. CEUS parameters included enhancement pattern (homogeneous versus heterogeneous), enhancement intensity (mild, moderate, significant). The following GS parameters were collected from the CEUS identified node: short axis (SA) size, length-width ratio (L/W), cortical (C) features, hilar (H) features, and C/H ratio. All patients underwent standard of care (SOC) SLN biopsy using Tc99m with or without blue dye, and removal of the localized node. Final histopathology (malignant [M] versus benign [B]), number of M nodes, metastasis size, and the presence or absence of extranodal extension, was correlated with CEUS morphological features.

## RESULTS

CEUS identified a single enhancing node in 20 of 21 (95.2%) cases. All enhancing nodes correlated with a SLN identified surgically; 2 (10%) M and 18 (90%) B. The mean SA size was 0.62 cm (range 0.3-1.1). The L/W was < 2 in 6 of 20 (30%), and >2 in 14/20 (70%) nodes. SLN GS features included homogeneous hilum (14, 70%), heterogeneous hilum (5, 25%) and focal hilum compression (1, 5%). All SLN had <3mm cortical thickness. The GS mean cortex-hilum ratio was 0.51 (0.11-1.0). Heterogeneous CEUS enhancement was noted in 12 (60%) of cases. Enhancement intensity was significant (8, 40%), moderate (5, 25%) and mild (7, 35%). Enhancement of both malignant SLN was mild. SLN enhancement patterns were cortical (1, 5%), thin (7, 35%) or thick paracortex (5, 25%) and diffuse hilar (7, 35%). Enhancement patterns of malignant SLN were diffuse hilar and thin paracortex.

#### CONCLUSION

CEUS contributes additional imaging features of lymph nodes reflecting their underlying architecture. Larger studies are needed to evaluate the ability of CEUS features to differentiate benign from malignant SLN.

### **CLINICAL RELEVANCE/APPLICATION**

CEUS parameters of SLN may complement GS ultrasound features for non-invasive distinction of M versus B nodes.

## BR264-SD-WEA6

### Breast Cancer and the Hyperechoic Rim: The Cutting Edge to a More Accurate T Stage

Wednesday, Nov. 30 12:15PM - 12:45PM Room: BR Community, Learning Center Station #6

#### **Participants**

Dana Ataya, MD, Cleveland, OH (*Presenter*) Nothing to Disclose Alana Donaldson, Cleveland, OH (*Abstract Co-Author*) Nothing to Disclose Jennifer Bullen, MSc, Cleveland, OH (*Abstract Co-Author*) Nothing to Disclose Benjamin Calhoun, Cleveland, OH (*Abstract Co-Author*) Nothing to Disclose Laura Dean, MD, Cleveland, OH (*Abstract Co-Author*) Nothing to Disclose Alice S. Rim, MD, Cleveland, OH (*Abstract Co-Author*) Nothing to Disclose Leah K. Sieck, MD, Shaker Hts, OH (*Abstract Co-Author*) Nothing to Disclose

### PURPOSE

Assessment of primary tumor size is crucial for accurate staging and determination of treatment for breast cancer. A hyperechoic rim can be seen around primary breast carcinomas, but no clear guidelines exist on whether this echogenic halo should be included in the sonographic measurements. The purpose of this study is to clarify the impact of including and excluding the hyperechoic rim on preoperative sonographic tumor size assessments.

### **METHOD AND MATERIALS**

A retrospective review of 115 patients with primary breast cancer was completed. In 39 of 115 (33.9 %) cases, a hyperechoic rim was detected on preoperative ultrasound (US). The maximal sonographic measurements of each mass was obtained, including and excluding the hyperechoic rim. These measurements were compared with the actual histopathological tumor size on excision. Bias was characterized by the mean difference between US measurements and pathologic size and a 95% confidence interval (CI) was provided.

#### RESULTS

Mean pathologic size of the 39 breast cancers demonstrating a hyperechoic rim was 2.1 cm (SD: 0.9, range: 0.3, 4.0). The maximal US measurement without the hyperechoic rim underestimated the pathologic size in 97% (38/39) of cancers, which translated in an underestimation of the tumor size/stage (T1 vs T2) for 10 cancers (25.6% of cases). Underestimation of size was 0.59 cm on average without the hyperechoic rim (95% CI: 0.46, 0.72). This bias was reduced when the hyperechoic rim was included (mean underestimation: 0.05 cm, 95% CI: -0.02, 0.12). Tumor size/staging based on US measurements agreed with pathologic findings in 100% (39/39) of cancers when the hyperechoic rim was included in the measurement.

## CONCLUSION

The hyperechoic rim should be included in the sonographic measurement of tumor size to ensure a more accurate preoperative T stage.

### **CLINICAL RELEVANCE/APPLICATION**

Including the hyperechoic rim in the sonographic measurement of primary breast carcinomas is important in ensuring more accurate preoperative staging.

The Assessment of Aortic Flow Hemodynamics and Wall Shear Stress in Patients with Varying Aortic Valve Morphologies

Wednesday, Nov. 30 12:15PM - 12:45PM Room: CA Community, Learning Center Hardcopy Backboard

## Participants

Ozair A. Rahman, MD, Chicago, IL (*Presenter*) Nothing to Disclose Faysal Altahawi, MD, Chicago, IL (*Abstract Co-Author*) Nothing to Disclose Bradley D. Allen, MD, Chicago, IL (*Abstract Co-Author*) Nothing to Disclose Alex Barker, Chicago, IL (*Abstract Co-Author*) Nothing to Disclose Michael Markl, PhD, Chicago, IL (*Abstract Co-Author*) Institutional research support, Siemens AG; Consultant, Circle Cardiovascular Imaging Inc; Jeremy D. Collins, MD, Chicago, IL (*Abstract Co-Author*) Nothing to Disclose James C. Carr, MD, Chicago, IL (*Abstract Co-Author*) Research Grant, Astellas Group Research support, Siemens AG Speaker, Siemens AG Advisory Board, Guerbet SA Patrick L. McCarthy, MD, Lisle, IL (*Abstract Co-Author*) Nothing to Disclose Kenichiro Suwa, MD, Chicago, IL (*Abstract Co-Author*) Nothing to Disclose

The purpose of this exhibit is to: Review the developmental variants of the aortic valve and associated pathology. Describe the association of aortic valve variants with aortopathy. Describe a potential clinical role of 4D flow imaging as it applies to diagnostic assessment of aortic valve variants and associated disease states. Compare traditional cardiac MRI and 2D phase contrast with 4D flow guantitative and gualitative findings in aortic valve disease variants via a case based approach.

#### TABLE OF CONTENTS/OUTLINE

Table of Contents: Aortic valve variants and associated pathology Diagnostic assessment of the aortic valve morphology and classification schema Role of CT, echocardiography, Cardiac MRI alone, & Cardiac MRI with 4D flow MRI 4D flow MRI Different processing tools in 4D flow imaging Clinically applicable information derived from 4D flow MRI data Recent technical advances in 4D flow MRI Assessment of valvular and aortic flow patterns in patients with malformed aortic valves Qualitative and Quantitative evaluation complex flow hemodynamics Future directions Novel tools available for quantitative analysis of 4D flow MRI data. Potential utility of 4D flow MRI for risk stratifying patients with aortic valve disease

# CA135-ED-WEA8

Fibrous Skeleton of the Heart: Comprehensive Anatomical Overview and Evaluation of Pathologies Using Cardiac CT and MR

Wednesday, Nov. 30 12:15PM - 12:45PM Room: CA Community, Learning Center Station #8

# Awards

Cum Laude Identified for RadioGraphics

#### **Participants**

Farhood Saremi, MD, Los Angeles, CA (*Presenter*) Nothing to Disclose Cameron Hassani, MD, Los Angeles, CA (*Abstract Co-Author*) Nothing to Disclose Diane Spicer, Valrico, FL (*Abstract Co-Author*) Nothing to Disclose Shumpei Mori, Kobe, Japan (*Abstract Co-Author*) Nothing to Disclose Damian Sanchez-Quintana, MD, Badajoz, Spain (*Abstract Co-Author*) Nothing to Disclose Robert Anderson, MD, Newcastle, United Kingdom (*Abstract Co-Author*) Nothing to Disclose

#### **TEACHING POINTS**

The purpose of this exhibit is:1. Review the relevant anatomy of the structures forming the fibrous skeleton of the heart2. Review characteristic imaging findings of common and uncommon diseases involving this region

# TABLE OF CONTENTS/OUTLINE

Normal embryology and anatomy of the fibrous skeleton of the heartDevelopment Imaging characteristics of the septal components of the AV junctionAorto-ventricular membrane concept Arterial valve fibrous elements and differences as shown by imaging with cadaveric correlation Right and left fibrous trigones Membranous septum Tendon of Todaro Tendon of the infundibulum?Difference in anatomic characteristics of the mitral and tricuspid annuluses Relationship to the major vessels and normal conduction pathwaysAbnormalities of the fibrous skeleton of the heartDegenerative changesAging calcification and clinical significanceInfection, para- and peri-valvular fistula and abscess Ischemia and trauma Masses and infiltrative processes Electrophysiology applications Relevant findings related to percutaneous interventions

## **Honored Educators**

Presenters or authors on this event have been recognized as RSNA Honored Educators for participating in multiple qualifying educational activities. Honored Educators are invested in furthering the profession of radiology by delivering high-quality educational content in their field of study. Learn how you can become an honored educator by visiting the website at: https://www.rsna.org/Honored-Educator-Award/

Farhood Saremi, MD - 2015 Honored Educator

# CA154-ED-WEA10

**Congenital Anomalies of the Pulmonary Arteries: An Imaging Overview** 

Wednesday, Nov. 30 12:15PM - 12:45PM Room: CA Community, Learning Center Station #9

#### **Participants**

Jason B. Hobbs, MD, Aurora, CO (*Presenter*) Nothing to Disclose Lorna Browne, MD, FRCR, Aurora, CO (*Abstract Co-Author*) Nothing to Disclose Carlos S. Restrepo, MD, San Antonio, TX (*Abstract Co-Author*) Nothing to Disclose Daniel Ocazionez, MD, Houston, TX (*Abstract Co-Author*) Nothing to Disclose Daniel Vargas, MD, Denver, CO (*Abstract Co-Author*) Nothing to Disclose

## **TEACHING POINTS**

1. Review the clinical and imaging findings in patients with congenital anomalies of the pulmonary arteries. 2. Discuss the role of various imaging modalities in the evaluation of these patients. 3. Describe the imaging findings related to surgical and interventional procedures performed for managing these patients.

## TABLE OF CONTENTS/OUTLINE

Proximal interrruption of the pulmonary artery Pulmonary atresia with VSD Pulmonary atresia with intact septum Absent pulmonary valve Congenital pulmonic stenosis Quadricuspid and bicuspid pulmonary valve Pulmonary sling Pulmonary branch stenosis

# **Honored Educators**

Presenters or authors on this event have been recognized as RSNA Honored Educators for participating in multiple qualifying educational activities. Honored Educators are invested in furthering the profession of radiology by delivering high-quality educational content in their field of study. Learn how you can become an honored educator by visiting the website at: https://www.rsna.org/Honored-Educator-Award/

Carlos S. Restrepo, MD - 2012 Honored Educator Carlos S. Restrepo, MD - 2014 Honored Educator

## CA238-SD-WEA1

The Influence of Iterative Model Reconstruction on Coronary Artery Calcium Scoring - Phantom and Clinical Study

Wednesday, Nov. 30 12:15PM - 12:45PM Room: CA Community, Learning Center Station #1

## Participants

Seitaro Oda, MD, Kumamoto, Japan (*Presenter*) Nothing to Disclose Daisuke Utsunomiya, MD, Kumamoto, Japan (*Abstract Co-Author*) Nothing to Disclose Takeshi Nakaura, MD, Kumamoto, Japan (*Abstract Co-Author*) Nothing to Disclose Yoshinori Funama, PhD, Kumamoto, Japan (*Abstract Co-Author*) Nothing to Disclose Hideaki Yuki, MD, Kumamoto, Japan (*Abstract Co-Author*) Nothing to Disclose Masafumi Kidoh, Kumamoto, Japan (*Abstract Co-Author*) Nothing to Disclose Kenichiro Hirata, Kumamoto, Japan (*Abstract Co-Author*) Nothing to Disclose Narumi Taguchi, Kumamoto, Japan (*Abstract Co-Author*) Nothing to Disclose Hiroko Takaoka, Kumamoto, Japan (*Abstract Co-Author*) Nothing to Disclose Shinichi Tokuyasu, RT, Minato-ku, Japan (*Abstract Co-Author*) Nothing to Disclose Shinichi Yamashita, MD, Kumamoto, Japan (*Abstract Co-Author*) Nothing to Disclose

#### PURPOSE

The purpose of this study was to investigate the influence of iterative model reconstruction (IMR) on coronary artery calcium (CAC) scoring as compared to the filtered back projection (FBP) and hybrid iterative reconstruction (HIR).

#### **METHOD AND MATERIALS**

CAC scan images of 30 consecutive patients (18 men and 12 women; age 70.1±12.2 years) were reconstructed with FBP, HIR, and IMR. Image noise were measured for all reconstructions. Two radiologists independently measured the CAC scores (Agaston score) using semi-automated software. Interobserver agreement was evaluated. Statistical analysis included the Spearman correlation coefficient and Bland-Altman analysis.

## RESULTS

The mean image noise of FBP-, HIR-, and IMR images was  $48.0\pm7.9$  HU,  $29.6\pm4.8$  HU, and  $9.3\pm1.3$  HU, respectively; there was a significant difference among all comparison combinations for the three reconstructions (p<0.01). The CAC score decreased by 4.2 % in HIR and 8.9 % in IMR as compared to FBP. There was no significant difference in the mean CAC score among the three reconstructions. For all three reconstructions the interobserver correlations were excellent [r2=0.96 (FBP), 0.99 (HIR), 0.99 (IMR)]. Interobserver comparisons showed that the best Bland-Altman measure of agreement was with IMR, followed by HIR and FBP.

### CONCLUSION

For the CAC scoring, IMR can reduce the image noise and blooming artifacts, consequently reduces the measured CAC score. IMR can lessen measurement variability and enable stable and reproducible measurement.

#### **CLINICAL RELEVANCE/APPLICATION**

IMR can lessen measurement variability and enable stable and reproducible measurement even in low dose setting. This may beneficial for comparison of CAC scores for follow-up observations.

## CA239-SD-WEA2

Optimal Scan Timing for 320-row Coronary Computed Tomography Angiography (CCTA) Generated by the Time to Peak at the Ascending Aorta Using a Test-bolus Injection

Wednesday, Nov. 30 12:15PM - 12:45PM Room: CA Community, Learning Center Station #2

## Participants

Takashi Shirasaka, BS, Fukuoka, Japan (*Presenter*) Nothing to Disclose Michinobu Nagao, MD, Tokyo, Japan (*Abstract Co-Author*) Nothing to Disclose Satoshi Kawanami, MD, Fukuoka, Japan (*Abstract Co-Author*) Nothing to Disclose Yamato Shimomiya, Tokyo, Japan (*Abstract Co-Author*) Nothing to Disclose Yasuhiko Nakamura, RT, Fukuoka, Japan (*Abstract Co-Author*) Nothing to Disclose Hiroshi Honda, MD, Fukuoka, Japan (*Abstract Co-Author*) Nothing to Disclose Tsukasa Kojima, RT,MSc, Fukuoka, Japan (*Abstract Co-Author*) Nothing to Disclose Yuzo Yamasaki, MD, Fukuoka, Japan (*Abstract Co-Author*) Nothing to Disclose Takeshi Kamitani, MD, Fukuoka, Japan (*Abstract Co-Author*) Nothing to Disclose

#### PURPOSE

The time around the aortic peak enhancement on coronary computed tomography angiography (CCTA) can be predicted by using the test-bolus method. However, the actual scan timing at CCTA requires some adjustment from the peak time obtained by the test bolus, due to the long injection duration of the contrast medium (CM). The actual scan timing with aortic peak attenuation is thus sometimes missed in the CM protocol according to Bae's theory. In the present study we propose a new index using a time-density curve (TDC) of the ascending aorta (AAo) based on test-bolus data, to obtain the optimal scan timing for 320-row CCTA.

### **METHOD AND MATERIALS**

Ninety-four consecutive patients with known or suspected coronary artery disease who underwent 320-row CCTA between August 2015 and March 2016 were enrolled. After a test-bolus injection of 25.9 mgI/kg/s of nonionic CM at a fixed duration of 4.0 s, the actual CCTA scan with 25.9 mgI/kg/s of nonionic CM at a fixed duration of 10.0 s followed by saline flushing was performed. For the initial 64 patients, the scan timing was determined as a 3.0 s delay at the peak time in the TDC of the AAo from the test bolus. For next 30 patients, three delay times (1.0, 3.0, and 5.0 s) were determined by the interval from the CM arrival to peak time (AP time) in the TDC of the AAo. In the actual CCTA, the attenuation for the AAo, descending aorta (DAo), left atrium (LA) and left ventricle (LV) was measured. The patients were divided into LA/LV, AAo, and DAo groups by the site at which the maximum attenuation among the three sites was observed. The AAo group was identified as optimal. The LA/LV and DAo groups were identified as suboptimal. The prevalence of optimal scans was analyzed by chi-squared test.

### RESULTS

Among the initial 64 patients, 41 patients (64%) were classified as belonging to the AAo group. Among the next 30 patients, 27 patients (90%) were in the AAo group. The prevalence of optimal scans was significantly increased in this group of 30 patients (P=0.0068).

## CONCLUSION

Optimal scan timing for 320-row CCTA is achieved by the corrected delay time obtained from the AP time in the time-density curve of the ascending aorta at a test bolus.

## **CLINICAL RELEVANCE/APPLICATION**

The determination of the scan timing generated by the AP time is not influenced by the cardiac output of individual patients. Optimal scan timing can reduce the amount of contrast medium required.

## CA240-SD-WEA3

Evaluation of a High Contrast Injection Protocol in Combination with Low Tube Current for Dose Reduction in Coronary Computed Tomography Angiography: A Randomized, Single Centre, Prospective Study

Wednesday, Nov. 30 12:15PM - 12:45PM Room: CA Community, Learning Center Station #3

## Participants

Yibo Sun, Shanghai, China (*Presenter*) Nothing to Disclose Yanqing Hua, MD, Shanghai, China (*Abstract Co-Author*) Nothing to Disclose Mingpeng Wang, MD, Shanghai, China (*Abstract Co-Author*) Nothing to Disclose Dingbiao Mao, shanghai, China (*Abstract Co-Author*) Nothing to Disclose Kailei Shi, Shanghai, China (*Abstract Co-Author*) Nothing to Disclose Jianhua Guo, Shanghai, China (*Abstract Co-Author*) Nothing to Disclose Xiu Jin, Shanghai, China (*Abstract Co-Author*) Nothing to Disclose

### PURPOSE

To prospectively evaluate the radiation dose reduction potential and image quality of a high contrast injection protocol in combination with a low tube current (mAs) in coronary computed tomography angiography (CCTA).

## METHOD AND MATERIALS

Eighty-one consecutive patients (mean age 62 years; 34 female; BMI 18-31) were included and were randomized assigned into two groups. All CT examinations were performed with the same tube voltage (100 kV), flow rate of contrast medium (CM) (5.0 mL/s) and iodine dose (22.8 g). The protocol entailed an automatic mAs and low concentration CM (300 mgI/mL) for group A (n = 41), whereas effective mAs was reduced by a factor 0.6 in group B (n = 40) which used high concentration CM (400 mgI/mL). Applied radiation dose was assessed (CTDIvol and DLP), overall and per vessel based objective image quality was measured for various regions of interest (enhancement, noise, signal-to-noise ratio [SNR] and contrast-to-noise-ratio [CNR]), and subjective image quality was evaluated with a five-point Likert scale.

### RESULTS

The CT attenuation of coronary arteries in group B were significantly higher (ranges; 507.5-548.1 HU) than those in group A (407.5-444.5 HU), as well as overall image noise ( $20.0 \pm 7.0 \text{ vs.} 16.1 \pm 5.3$ ), respectively ( $P \le 0.0166$ ). The SNR, CNR and subjective image quality of coronary arteries revealed no significant differences between the two groups (29.4-31.7, 21.9-24.7, medium score 5 vs. 29.4-32.4, 24.3-26.5, medium score 5, respectively,  $P \ge 0.695$ ). The mean CTDIvol, DLP and effective radiation dose of group B were both 58% of those of group A ( $13.6 \pm 0.9$ ,  $187.5 \pm 54.4$  and  $2.6 \pm 0.8$  vs.  $23.5 \pm 6.2$ ,  $324.0 \pm 86.2$  and  $4.5 \pm 1.2$ , respectively, P < 0.0001).

## CONCLUSION

The protocol with a high concentrated CM combined with low tube current permits further dose reduction in CCTA and does not compromise image quality.

## **CLINICAL RELEVANCE/APPLICATION**

The protocol with a high concentrated CM combined with low tube current permits further dose reduction in CCTA and does not compromise image quality.

## CA242-SD-WEA5

Segmental Agreement of T2 Mapping and Triple Inversion Recovery Sequences in Assessment of Myocardial Edema

Wednesday, Nov. 30 12:15PM - 12:45PM Room: CA Community, Learning Center Station #5

## Participants

Ahmed E. Kharabish, MD, MSc, Aswan, Egypt (Presenter) Nothing to Disclose

#### PURPOSE

To evaluate the agreement of the T2 mapping and the triple inversion recovery sequences (TRIM) per myocardial segments in patients presenting with acute myocardial infarction.

### **METHOD AND MATERIALS**

Twenty-eight patients presented with acute myocardial infarction underwent primary percutaneous revascularization were sent to cardiac magnetic resonance (CMRI) in order to assess their myocardial salvage index (MSI). All CMRI studies were scanned using the routine protocol of cine, TRIM and late gadolinium enhancement (LGE) in short axis views covering the whole left ventricle (LV). In addition, T2 mapping slices were added in short axis views. Position of the T2 mapping slices were copied from the TRIM in order to copy same orientation and thickness. The LV was divided into apical, mid and basal segments according to visualization of the papillary muscles. Edema mass was assessed separately in each segment using both the TRIM and T2 mapping. Total amount of edema from both sequences was compared as well as the agreement of the amount of edema measured per segment was tested.

#### RESULTS

No statistical significance was found neither in the total amount of edema nor the amount of edema measured per each segment. The non parametric tests due to abnormal distribution of the standard deviation of both sequences, showed no statistically significance difference between the total amount of edema, basal segments' edema, mid segments' edema, and apical segments' edema (0.409, 0.36, 0.106, and 0.84 respectively).

### CONCLUSION

Quantitative T2 mapping reliably measures myocardial edema, and may therefore be clinically more robust in measuring the edema amount in acute myocardial conditions.

## **CLINICAL RELEVANCE/APPLICATION**

T2 mapping overcomes the follwoing TRIM limitations, through providing direct segemntal edema assessment:Edema in culprit coronary disease is measured in comparison to the remote non affected myocardium using the TRIM sequence. Involvement of multi-vessel territory may give false results.Edema may be assessed in inflammatory conditions using TRIM as a signal ratio to skeletal muscle signals. False negative ratio may be obtained due to skeletal muscle involvement.

## CA243-SD-WEA6

Reproducibility of Cardiac Cine MRI for Sequential Assessment of Right Ventricular Volumes and Ejection Fraction: Short-axis vs. Transverse Cine SSFP

Wednesday, Nov. 30 12:15PM - 12:45PM Room: CA Community, Learning Center Station #6

#### Awards

### **Student Travel Stipend Award**

#### **Participants**

Luigia D'Errico, MD, Toronto, ON (*Presenter*) Nothing to Disclose Mariana M. Lamacie, MD, Toronto, ON (*Abstract Co-Author*) Nothing to Disclose Laura Jimenez-Juan, MD, Toronto, ON (*Abstract Co-Author*) Nothing to Disclose Djeven P. Deva, MBBCh, Toronto, ON (*Abstract Co-Author*) Nothing to Disclose Rachel Wald, MD, Toronto, ON (*Abstract Co-Author*) Nothing to Disclose Sebastian Ley, MD, Heidelberg, Germany (*Abstract Co-Author*) Nothing to Disclose Kate Hanneman, MD, FRCPC, Toronto, ON (*Abstract Co-Author*) Nothing to Disclose Dinesh Thavendiranathan, MD, Toronto, ON (*Abstract Co-Author*) Nothing to Disclose Bernd J. Wintersperger, MD, Toronto, ON (*Abstract Co-Author*) Speakers Bureau, Siemens AG; Research support, Siemens AG

## PURPOSE

Inter-study reproducibility is of utmost importance in follow-up of right ventricular (RV) volumes and function. The purpose was therefore to evaluate and compare inter-study reproducibility and intra-/inter-observer variability of right ventricular (RV) volumes and function with short-axis and transverse cardiac MRI cine SSFP.

#### **METHOD AND MATERIALS**

18 volunteers underwent cardiac MRI for RV assessment using cine SFFP (6mm/2mm, 1.4x1.4mm2) obtaining ventricular coverage in both, short-axis and transverse slice orientation. For comparison, free-breathing 2D phase contrast analysis at the main pulmonary artery (MPA) was performed (5mm, 1.6x1.6mm2). Repeat acquisitions were performed after a 5min break with complete repositioning of subjects. Data sets were contoured independently by two blinded observers. Statistical analysis included Student's t-test, Bland-Altman plots, intra-class correlation coefficient (ICC) and 2-way ANOVA, SEM and minimal detectable difference calculations.

## RESULTS

There was no significant difference in HR ( $65.0\pm7.4vs.67.6\pm9.9bpm;P=0.1$ ) or MPA forward flow ( $92.2\pm18.9vs.87.2\pm14.9mL;P=0.1$ ) between studies. EDV and ESV demonstrated a bias of 0.4%[-9.5%,10%] and 2.1%[-12%,16%], respectively for short-axis and a bias of 1.1%[-7.3%,9.4%] and 0.8%[-16%,18%], respectively, for transverse orientation. There was no significant interaction between imaging orientation and inter-study reproducibility (p=0.395-0.824), intra-observer variability (p=0.726-0.862) or inter-observer variability (p=0.447-0.706) by 2-way ANOVA. Inter-observer agreement by ICC was greater for short axis versus transverse orientation for all parameters with overlapping confidence intervals (0.769-0.986 vs. 0.625-0.983, respectively). Minimal detectable differences for short axis and transverse orientations were 10.1mL vs. 11.5mL for EDV, and 4.1 vs. 4.7% for EF, respectively.

### CONCLUSION

Both, short-axis and transverse orientations provide reliable and reproducible measures of RV volumes and function. Therefore, transverse cine SSFP is not required for quantitative RV assessment which could improve workflow by limiting acquisition to short-axis cine SSFP for bi-ventricular analysis.

## **CLINICAL RELEVANCE/APPLICATION**

Our study demonstrates that the short axis orientation is sufficient for quantitative assessment of RV. This would shorten MR acquisition, improving patient comfort and the workflow efficiency.

## CA244-SD-WEA7

Isolated Partial Anomalous Pulmonary Venous Connection: Is it Really a 'Tension' Free Diagnosis? Cardiologist Needs to get Hyper

Wednesday, Nov. 30 12:15PM - 12:45PM Room: CA Community, Learning Center Station #7

## Participants

Madhav Hegde, MD, Bangalore, India (*Presenter*) Nothing to Disclose Ganesh Hegde, MBBS, DMRD, hyderabad, India (*Abstract Co-Author*) Nothing to Disclose

### PURPOSE

To test the hypothesis that isolated PAPVC involving vein draining single lobe of lung parenchyma is not a risk factor for development of pulmonary hypertension. To test the hypothesis that number of pulmonary lobe segments involved in anomalous drainage does not determine the age of manifestation of PAPVC.

### **METHOD AND MATERIALS**

MDCT report database of a large tertiary care centre for cardiovascular diseases was analysed for consecutive cases of PAPVC. 122 cases of PAPVC were identified .However 12 of these patients were excluded from the study.Studies of 110 patients obtained over a period of 4 years were retrospectively analysed.All these patients had undergone detailed clinical evaluation,standard ECG,and a detailed two dimensional and doppler echocardiography before the MDCT angiogram.Retrospective gating with ECG was used whenever deemed fit. Percentage analysis was performed in Microsoft Excel and chi squared test of association was performed using MedCalc software .Categorical variables were analysed using one variable - one way classification chi squared test.

### RESULTS

Among the 110 subjects 54 (49%)had isolated PAPVC.Out of 54,14 patients had pulmonary hypertension, dilated main pulmonary artery. Among these 14, in 4 cases only one pulmonary vein was involved, in 6 cases 2 pulmonary veins were involved. The remaining 4 cases had 3 anomalous pulmonary veins. Among the 110 patients 70 patients(63.6%) are more than 18 years of age. There is significant association between drainage of anomalous veins to SVC and age above 18yrs(Chi squared test p value-.003). Among individuals with isolated PAPVC , in 18 anomalous drainage was to SVC. Among isolated PAPVC cases 38 were of the age more than 18 years. Two were infants. Among the 38 adults who had isolated PAPVC ,14 had pulmonary hypertension. Among all the individuals who had PAPVC ,6 subjects presented in infancy and two of these did not have any associated abnormality. Two individuals developed symptoms at the age of 17 years.

## CONCLUSION

Isolated PAPVC (including anomaly involving single lobe) an independent risk factor for the development of pulmonary hypertension.Number of pulmonary veins involved has a moderate association with the age of manifestation.

## **CLINICAL RELEVANCE/APPLICATION**

PAPVC being an independent risk factor, needs to be ruled out USING MDCT or MRbefore ASD closure is contemplated to prevent the development of pulmonary hypertnesion and if found should be treated.

# Respiratory Tract Infections (RTIs) in Returning Travelers: Imaging Findings and Differential Diagnosis

Wednesday, Nov. 30 12:15PM - 12:45PM Room: CH Community, Learning Center Station #7

#### Awards Certificate of Merit

#### **Participants**

Tomas C. Franquet, MD, Barcelona, Spain (*Presenter*) Nothing to Disclose Kyung S. Lee, MD, PhD, Seoul, Korea, Republic Of (*Abstract Co-Author*) Nothing to Disclose Edson Marchiori, MD, PhD, Rio de Janeiro, Brazil (*Abstract Co-Author*) Nothing to Disclose Kyong R. Peck, Seoul, Korea, Republic Of (*Abstract Co-Author*) Nothing to Disclose Arthur Soares-Sousa Jr, Sao Jose do Rio Preto, Brazil (*Abstract Co-Author*) Nothing to Disclose Takeshi Johkoh, MD, PhD, Itami, Japan (*Abstract Co-Author*) Research Consultant, Bayer AG Research Consultant, F. Hoffman-La Roche Ltd

## **TEACHING POINTS**

Review the spectrum of imaging findings of varied respiratory tract infections (RTIs) in returning travelers Correlate imaging findings with clinical setting and geographic location Provide a structured framework for formulating a differential diagnosis

## TABLE OF CONTENTS/OUTLINE

With increasing international travel, a number of respiratory tract infections (RTIs) have emerged as important health threats among travelers to regions of the world where these infections are endemic. This exhibit will review and illustrate the highresolution CT manifestations of varied travel-related respiratory tract infections (RTIs). **Bacterial infections:** Meliodosis, Legionnaires' disease and leptospirosis**Rickettsial infectionsFungal infections:** Histoplasmosis, Cryptococcosis, Coccidiodomycosis, Paracocidiodomycosis**Viral infections:** Middle East respiratory syndrome (MERS), Dengue), Hantavirus and Pumala virus, Chikungunya virus**Parasites and worms:** Paragonimiasis, Schistosomiasis, Filariasis and ToxocariasisRespiratory tract infections (RTIs) in returning travelers vary with the specific causative microorganism and the patient's immune status. Knowledge on the geographic location and the recognition of specific imaging features on specific RTI allow the formulation of a focused differential diagnosis.

## Mediastinal and Pleural MRI: Practical Approach for Daily Practice

Wednesday, Nov. 30 12:15PM - 12:45PM Room: CH Community, Learning Center Station #8

#### Awards

### **Identified for RadioGraphics**

### Participants

Constantine A. Raptis, MD, Saint Louis, MO (*Presenter*) Nothing to Disclose Sebastian R. McWilliams, MBBCh, Saint Louis, MO (*Abstract Co-Author*) Nothing to Disclose Jordi Broncano, MD, Cordoba, Spain (*Abstract Co-Author*) Nothing to Disclose Daniel B. Green, MD, New York, NY (*Abstract Co-Author*) Nothing to Disclose Sanjeev Bhalla, MD, Saint Louis, MO (*Abstract Co-Author*) Nothing to Disclose

## **TEACHING POINTS**

1. Understand important indications for the use of mediastinal and pleural MRI in daily practice2. Review protocol considerations that can be applied to answer clinical questions3. Recognize key imaging findings that can be encountered on MRI examinations of the mediastinum and pleura

## **TABLE OF CONTENTS/OUTLINE**

1. Protocol designa) Sequence menu for mediastinal and pleural MRIb) Tips on selecting appropriate MRI sequences to answer specific clinical questionsc) Considerations for optimization of mediastinal and pleural MRI sequences2. Indications for mediastinal and pleural MRIa) Thymic hyperplasia vs thymic massb) "Don't touch" mediastinal lesions - cystic and lymphatic lesionsc) Identifying targets for biopsy or surgical resectiond) Determining invasion of mediastinal structures and vesselse) Characterization of pleural masses and effusionsf) Evaluation of diaphragmatic motion3. Key interpretative considerationsa) Understanding the difference between "don't touch" and "need further evaluation" mediastinal lesionsb) Adding value to reports on mediastinal MRI examinations - focusing on clinical questions

### **Honored Educators**

Presenters or authors on this event have been recognized as RSNA Honored Educators for participating in multiple qualifying educational activities. Honored Educators are invested in furthering the profession of radiology by delivering high-quality educational content in their field of study. Learn how you can become an honored educator by visiting the website at: https://www.rsna.org/Honored-Educator-Award/

Sanjeev Bhalla, MD - 2014 Honored Educator Sanjeev Bhalla, MD - 2016 Honored Educator

## CH265-SD-WEA1

Pleural Invasion/adhesion of Subpleural Lung Cancer: Quantitative 4-dimensional CT Analysis Using Dynamic-ventilatory Scanning

Wednesday, Nov. 30 12:15PM - 12:45PM Room: CH Community, Learning Center Station #1

## Participants

Kotaro Sakuma, MD, Fukushima, Japan (*Presenter*) Nothing to Disclose Tsuneo Yamashiro, MD, Nishihara, Japan (*Abstract Co-Author*) Research Grant, Toshiba Corporation Hiroshi Moriya, MD, Fukushima-City, Japan (*Abstract Co-Author*) Nothing to Disclose Sadayuki Murayama, MD, PhD, Nishihara-Cho, Japan (*Abstract Co-Author*) Research Grant, Toshiba Corporation

### PURPOSE

Using 4-dimensional dynamic-ventilatory scanning provided by a 320-row computed tomography (CT) scanner, we aimed to assess pleural invasion and adhesion of peripheral (subpleural) lung cancer quantitatively.

## METHOD AND MATERIALS

Sixteen patients with subpleural lung cancer underwent dynamic-ventilation CT during free breathing. No pleural invasion or adhesion was surgically confirmed in 10 patients subsequently, while the other six patients were judged to have pleural invasion or adhesion. Using research software, we tracked the movements of the cancer center and the adjacent structures every 0.35 seconds and converted the data to 3-dimensional loci. The following quantitative indices were obtained and compared by Mann-Whitney test: the ratio of the total movement distance of each (cancer/adjacent structures), the cross-correlation coefficient between time curves for the movement distances of the cancer and the adjacent structures, and the cosine similarity between the inspiratory and expiratory vectors (from the cancer to the adjacent structures).

### RESULTS

Generally, the movements of the loci of the lung cancer and the adjacent structures were similar in patients with pleural invasion and adhesion, while they were independent in patients without. There were significant differences in all parameters between the two patient groups (movement ratio and cross-correlation coefficient, P < 0.01; cosine similarity, P < 0.05).

### CONCLUSION

Dynamic-ventilation CT can be utilized as a novel imaging approach to preoperative analysis of pleural invasion and adhesion.

#### **CLINICAL RELEVANCE/APPLICATION**

This study is the first to demonstrate a quantitative 4-dimensional analysis of peripheral lung cancer and the potential for an accurate preoperative diagnosis of pleural invasion and adhesion.

Quantitative CT Texture Analysis for the Distinction of Invasive Adenocarcinoma From Adenocarcinoma in Situ or Minimally Invasive Adenocarcinoma

Wednesday, Nov. 30 12:15PM - 12:45PM Room: CH Community, Learning Center Station #2

## Participants

Takuya Yagi, Niigata City, Niigata Prefecture, Japan (*Presenter*) Nothing to Disclose Motohiko Yamazaki, MD, Niigata, Japan (*Abstract Co-Author*) Nothing to Disclose Hiroyuki Ishikawa, MD, Niigata, Japan (*Abstract Co-Author*) Nothing to Disclose Hidefumi Aoyama, MD, PhD, Niigata, Japan (*Abstract Co-Author*) Nothing to Disclose

### PURPOSE

To distinguish invasive adenocarcinoma (IADC) from adenocarcinoma in situ (AIS) or minimally invasive adenocarcinoma (MIA) by quantitative computed tomography (CT) texture analysis.

## METHOD AND MATERIALS

This retrospective study included 54 consecutive patients with 63 pure or part-solid ground-glass nodules (GGNs)  $\leq$ 3 cm that were surgically resected and pathologically diagnosed as AIS, MIA, or IADC between April 2011 and March 2015. Each tumor was manually segmented at 1-mm intervals on axial CT images and assessed using ImageJ, a software program for quantitative analyses. The quantitative CT texture parameters analyzed in each lesion included the whole tumor volume, weight, mean CT value, variance, skewness kurtosis, entropy, uniformity, contrast, and percentile CT numbers. The differences between the IADCs and the AIS-MIAs were evaluated by Mann-Whitney U-test, a logistic regression analysis, and receiver operating characteristic curves.

### RESULTS

The pathologic analysis confirmed 31 IADCs (4 lepidic, 22 papillary, 3 mucinous, 1 papillary/mucinous, and 1 non-classified), 17 AISs, and 15 MIAs. Compared with the AIS-MIA group, the IADCs showed significantly larger mean CT values, variance, entropy, and CT attenuation values at the 10th, 25th, 50th, 75th, 90th, and 95th percentiles (P<0.001 each), but significantly smaller skewness, kurtosis, uniformity, and contrast values (P<0.001 each) on the histogram. The multivariate analysis revealed that the only independent differentiator between the AIS-MIAs and the IADCs was the 90th percentile CT numbers (P<0.001), with excellent accuracy (area under the curve, 0.934). The best cut-off value of the 90th percentile CT numbers was –117 Hounsfield units (sensitivity 87%, specificity 91%)

## CONCLUSION

The 90th percentile CT numbers can accurately distinguish IADCs from AIS-MIAs.

### **CLINICAL RELEVANCE/APPLICATION**

The distinction of IADCs from AIS-MIAs by only visual assessment is difficult. Quantitative analyses can help distinguish them more accurately to identify proper treatments such as sublobar resection.

## CH267-SD-WEA3

### Value of Computed Tomography of the Chest in Patients with Acute Respiratory Distress Syndrome

Wednesday, Nov. 30 12:15PM - 12:45PM Room: CH Community, Learning Center Station #3

#### Participants

Christoph A. Berliner, MD, Hamburg, Germany (*Presenter*) Nothing to Disclose Marcel Simon, Hamburg, Germany (*Abstract Co-Author*) Nothing to Disclose Maria Metschke, Hamburg, Germany (*Abstract Co-Author*) Nothing to Disclose Maria Kalsow, Hamburg, Germany (*Abstract Co-Author*) Nothing to Disclose Hans Klose, MD, Hamburg, Germany (*Abstract Co-Author*) Nothing to Disclose Stefan Kluge, Hamburg, Germany (*Abstract Co-Author*) Nothing to Disclose Gerhard B. Adam, MD, Hamburg, Germany (*Abstract Co-Author*) Nothing to Disclose Azien Lagmani, Hamburg, Germany (*Abstract Co-Author*) Nothing to Disclose

### PURPOSE

The value of computed tomography (CT) of the chest in the management of patients with acute respiratory distress syndrome (ARDS) are ill defined. The aim of this study was to assess the clinical utility of CT scans of the chest in patients with ARDS using the Berlin definition.

### **METHOD AND MATERIALS**

Retrospective study on all patients with ARDS in whom a CT scan of the chest was performed immediately prior to or during intensive care unit stay between 01/2007 and 06/2013.

## RESULTS

During the study period CT scans were performed on 204 patients with ARDS. ARDS was most often due to hospital acquired pneumonia (53.9 %) and community acquired pneumonia (32.8 %). ARDS was classified as severe in 84.3 % and moderate in 15.2 % of cases. The most common pathologies of lung parenchyma were consolidations (94.1 % of cases), ground glass opacities (85.3 %) and interstitial changes (59.3 %). Furthermore, CT scans showed pleural effusions in 80.4 %, mediastinal lymphadenopathy in 66.7 %, signs of right ventricular strain and pulmonary hypertension in 53.9 %, pericardial effusion in 37.3 %, emphysema of the chest wall in 12.3 %, pneumothorax in 11.8 %, emphysema of the mediastinum in 7.4 % and pulmonary embolism in 2.5 % of cases. Results of CT scans lead to changes in management in 26.5 % of cases. Mortality was significantly increased in patients with involvement of lung parenchyma of more than 80 % (p = 0.004). Intrahospital transport from the ICU to the radiology department lead to critical incidents in 17 cases (8.3 %).

### CONCLUSION

Systematic evaluation of thoracic CT scans yielded information useful for making a diagnosis, predicting prognosis and recognizing concomitant disorders requiring therapeutic interventions. In 1 out of 4 cases results of CT scans lead to changes in management.

### **CLINICAL RELEVANCE/APPLICATION**

Critically ill patients with ARDS are less likely to die if CT scan lead to changes in management.

## CH268-SD-WEA4

### Dual Energy CT Pulmonary Angiography with 6 g Iodine - a Propensity Score-Matched Study

Wednesday, Nov. 30 12:15PM - 12:45PM Room: CH Community, Learning Center Station #4

#### **Participants**

Andreas A. Meier, MD, New York, NY (*Presenter*) Nothing to Disclose Kai Higashigaito, Zurich, Switzerland (*Abstract Co-Author*) Nothing to Disclose Katharina Martini, Zurich, Switzerland (*Abstract Co-Author*) Nothing to Disclose Moritz Wurnig, Zurich, Switzerland (*Abstract Co-Author*) Nothing to Disclose Burkhardt Seifert, PhD, Zurich, Switzerland (*Abstract Co-Author*) Nothing to Disclose Dagmar Keller Lang, MD, Zurich, Switzerland (*Abstract Co-Author*) Nothing to Disclose Thomas Frauenfelder, MD, Zurich, Switzerland (*Abstract Co-Author*) Nothing to Disclose Hatem Alkadhi, MD, Zurich, Switzerland (*Abstract Co-Author*) Nothing to Disclose

#### PURPOSE

To evaluate the performance of low contrast media (CM) dose dual-energy computed tomography pulmonary angiography (CTPA) with advanced monoenergetic reconstructions in patients with suspected pulmonary embolism (PE).

### **METHOD AND MATERIALS**

The study had institutional review board approval; all patients gave written informed consent. Forty-one patients (25 men, 16 women, mean age 62.9±14.7 years) undergoing low CM dose (15ml, 6g iodine) dual-energy CTPA with advanced monoenergetic reconstructions were matched via propensity-scoring based on logistic regression analysis with a comparison group of 41 patients (24 men, 17 women, mean age 62.7±13.9 years) undergoing standard CM dose single-energy CTPA (80ml, 24g iodine). Subjective (noise, artifacts) and objective (attenuation, noise, contrast-to-noise ratio (CNR)) image quality was assessed at the level of the pulmonary artery, the right lower lobe pulmonary artery, the right inferior pulmonary vein, the aorta, the brachiocephalic vein, and the subclavian vein by two blinded, independent readers. All patients underwent clinical follow-up after three months for evaluation of adverse events.

## RESULTS

Interrater agreement for subjective image quality at the different levels in both groups ranged from fair to excellent (ICC: 0.46-0.84); agreement for objective image quality was excellent (ICC: 0.83-0.93). There was no significant difference regarding subjective noise (p=0.15-0.72) and artifacts (p=0.16-1) between the low and the standard CM dose group. There was no significant difference regarding CNR between the CM dose groups (p=0.11-0.87). 7/41 (17%) patients in the low and 5/41 (12%) in the standard CM dose group were diagnosed with PE (p=0.32). No patient suffered from subsequent PE or PE-associated death during follow-up.

## CONCLUSION

Dual-energy CTPA with advanced monoenergetic reconstruction is feasible with 15ml CM (6g iodine) and allows for the diagnosis and safe exclusion of PE.

### **CLINICAL RELEVANCE/APPLICATION**

In patients with impaired kidney function, CTPA can be performed with a low volume of CM using dual-energy and advanced monoenergetic image reconstructions with the benefit of reducing the risk of developing contrast-induced nephropathy.

Effects of the Radiation Dose and Type of Reconstruction Algorithms on the Measurement of Small Pulmonary Nodules with Low Dose CT:A Phantom Study

Wednesday, Nov. 30 12:15PM - 12:45PM Room: CH Community, Learning Center Station #5

### Participants

Yeon Joo Jeong, MD, Busan, Korea, Republic Of (*Presenter*) Nothing to Disclose Ji Won Lee, MD, Busan, Korea, Republic Of (*Abstract Co-Author*) Nothing to Disclose Geewon Lee, MD, Seoul, Korea, Republic Of (*Abstract Co-Author*) Nothing to Disclose Min Ki Lee, Pusan, Korea, Republic Of (*Abstract Co-Author*) Nothing to Disclose

### PURPOSE

To quantify the effect of the radiation dose used for the examination and type of reconstruction algorithms on the measurement of simulated lung nodules with low dose CT.

## METHOD AND MATERIALS

Fifteen synthetic nodules of three radiodensities (100, -630, -800 HU) and five sizes (nominal diameters of 12, 10, 8, 5, and 3 mm) were inserted into an anthropomorphic chest phantom and scanned with techniques varying in CTDIvol (from 0.18 mGy to 1.74 mGy). Images were reconstructed by filtered back projection (FBP) and hybrid iterative reconstruction (IR) at 4 different denoising strength levels (30%, 50%, 80%, 100%). Nodule diameter, mass (diameter x density), and volume were measured from the each reconstructed CT images. We calculated and compared the absolute percentage error (APE) of measurements on each data set.

### RESULTS

The APEs of nodule size, mass, and volume at the CTDIvol of 0.18mGy were significantly higher than those at other levels of CTDIvol (p < 0.001). For solid nodules, CTDIvol was 0.18 mGy, while ground glass opacity (GGO) nodules required a slightly higher CTDIvol of 0.33 mGy for lung nodule measurement. The effect of radiation dose was more pronounced for smaller GGO nodules (p < 0.001). No clinically significant difference was observed between FBP and different levels of hybrid IR in the APEs of nodule size, mass and volume.

### CONCLUSION

Lung nodule measurements in ultralow-dose CT with CTDIvol of 0.33mGy by application of any reconstruction algorithms showed a reliable accuracy in a phantom study.

## **CLINICAL RELEVANCE/APPLICATION**

Results of our phantom study supports that lung nodule measurements in ultralow-dose CT can be reliably compared despite different iterative reconstruction algorithms.

## CH270-SD-WEA6

Measurement of Pulmonary Nodule Size with Digital Tomosynthesis, Plain Radiography, and Dual-energy Subtraction Radiography

Wednesday, Nov. 30 12:15PM - 12:45PM Room: CH Community, Learning Center Station #6

### Participants

Eun Young Kim, MD, Suwon , Korea, Republic Of (*Abstract Co-Author*) Nothing to Disclose Joo Sung Sun, MD, Suwon-Si, Korea, Republic Of (*Abstract Co-Author*) Nothing to Disclose Dong Hyun Lee, MD, SUWON, Korea, Republic Of (*Abstract Co-Author*) Nothing to Disclose Taeyang Ha, MD, Suwon, Korea, Republic Of (*Presenter*) Nothing to Disclose Pae Sun Suh, Suwon, Korea, Republic Of (*Abstract Co-Author*) Nothing to Disclose Kyung Joo Park, MD, Suwon, Korea, Republic Of (*Abstract Co-Author*) Nothing to Disclose

### PURPOSE

(1) To evaluate accuracy, intra- and interobserver variability for nodule size manual measurement on DTS, CXR, and DES images (2) investigate factor affecting nodule size measurement

## METHOD AND MATERIALS

Total 120 images comprising four different size (5, 8, 10, 12mm) artificial nodules in four different locations (upper, middle, and lower) and three different depths (anterior, middle, and posterior) were prepared for each set of modality. Four observers independently measured twice the right to left (R-L) and superior to inferior (S-I) diameter of nodules on randomly arranged three sets of image data. Nodule size measurement errors against actual size on CXR, DES and DTS were compared and whether anatomic characteristics (location, depth) of nodule affect measurement variation was assessed. Intra- and inter-observer reproducibility were calculated. Bland-Altman plot and intraclass correlation coefficient (ICC) were used for statistical analysis.

### RESULTS

On DTS, non-measurable nodule was not found. However, average number of non-measurable nodule on CXR and DES were 33 and 37, respectively. Manual measurement using DTS showed higher accuracy and reproducibility than those of using CXR, DES. The overall mean measurement error was 0.25mm (SD:1.03) on CXR, -0.14mm (SD:1.20) on DES and -0.09mm (SD:0.41) on DTS. The mean measurement error on DTS was -0.05mm for R-L diameter and -0.25mm for S-I diameter. In terms of factor affecting size measurement on DTS, measuring R-L diameter was more accurate for nodules located in middle depth than measuring S-I diameter (measurement error -0.02 for R-L and -0.21 for S-I diameter). Inter-observer variability between four observes was 0.87 for CXR, 0.83 for SUB and 0.98 for DT. Intra-observer variability was almost perfect for all imaging modalities (CXR;0.93, SUB;0.93, DT;0.96).

## CONCLUSION

The manual measurement of nodule on DTS showed higher accuracy and less inter-observer variability compared with DES and CXR. However, limited depth resolution and in-plane artefact of DTS could be a limiting factor for nodule size measurement.

### **CLINICAL RELEVANCE/APPLICATION**

DTS seems to be a superior modality for size measurement of pulmonary nodule compared with CXR and DES. Also, understanding the limiting factors for accurate size measurement could maximize effectiveness of nodule follow up with DTS in clinical practice.

**Evaluation of Bone Marrow Edema in Thoracolumbar Spinal Trauma: Early Experience with the Third Generation Dual Source CT Technology in the Acute Setting** 

Wednesday, Nov. 30 12:15PM - 12:45PM Room: ER Community, Learning Center Station #1

### Participants

Sudha R. Muly, MBBS, FRCR, Vancouver, BC (*Presenter*) Nothing to Disclose Patrick D. McLaughlin, FFRRCSI, Vancouver, BC (*Abstract Co-Author*) Speaker, Siemens AG Luck J. Louis, MD, Vancouver, BC (*Abstract Co-Author*) Nothing to Disclose Savvas Nicolaou, MD, Vancouver, BC (*Abstract Co-Author*) Institutional research agreement, Siemens AG

### PURPOSE

Traumatic bone marrow edema results in small but measurable increase in CT attenuation values due to hemorrhage and increased interstitial fluid within the bone marrow cavity. To evaluate the sensitivity and specificity of dual energy CT (DECT) in detecting bone marrow edema (BME) in thoracic and lumbar spine. To identify the pitfalls and common artifacts which limit DECT bone marrow assessment.

## METHOD AND MATERIALS

In this retrospective study, 26 trauma patients who underwent DECT scanning of the thoracic and lumbar using a third generation dual source CT scanner (Definition FORCE, Siemens Health care, Germany) between January and April of 2016 were evaluated. There were 57 vertebral bodies assessed for bone marrow edema. The DECT data (100 kv and 150kvSN) was reconstructed using bone marrow edema algorithm on the syngovia platform VB 10. Visual analysis using color overlay images and quantitative objective analysis was performed using dual energy region of interest on the vertebral bodies to evaluate presence of bone marrow edema

#### RESULTS

Dual energy CT showed a sensitivity of 89% and specificity of 88%. The positive predictive value of was close to 96% and a negative predictive value close to 70%. There were 12 cases, which were indeterminate on grey scale mixed data CT sets simulating a 120 kvp scan and analysis of dual energy CT BME helped differentiate acute versus chronic fractures. Subtle end plate compression fracture may be difficult to evaluate on dual energy due to close proximity of the area of interest to the cortex. Movement and streak artifact cause spurious positive results and that could be alleviated with faster rotation, wider collimation and higher pitch.

## CONCLUSION

Due to its superior quality and the advancements in dual-energy CT technology with materialdecomposition, detection of bone marrow edema helps to identify subtle fractures and to differentiate acute from chronic fractures with high sensitivity and specificity.

### **CLINICAL RELEVANCE/APPLICATION**

We believe that dual-energy CT will serve as a good replacement for detection of bone marrow edema for patients who have a contraindication to MR imaging or when there is no immediate availability MRI due to resource constraints. But more importantly DECT can increase the diagnostic confidence in confirming a spinal fracture as acute when BME is present in the setting of trauma where CT is recognized as the Gold standard for the evaluation of spinal trauma.

Utilization of MRI and CT Imaging for ED Patients with Clinically Suspected Stroke: A Retrospective Institutional Review, Comparing True Negatives to True Positive Stroke Population

Wednesday, Nov. 30 12:15PM - 12:45PM Room: ER Community, Learning Center Station #2

## Participants

Sarika Pamarthy, MBBS, MS, Columbus, OH (*Abstract Co-Author*) Nothing to Disclose
Manav Bhalla, MD, Milwaukee, WI (*Presenter*) Nothing to Disclose
John L. Ulmer, MD, Milwaukee, WI (*Abstract Co-Author*) Stockholder, Prism Clinical Imaging, Inc Medical Advisory Board, General Electric Company
Andrew P. Klein, MD, Pewaukee, WI (*Abstract Co-Author*) Nothing to Disclose
Kieran E. McAvoy, Milwaukee, WI (*Abstract Co-Author*) Nothing to Disclose
Leighton P. Mark, MD, Milwaukee, WI (*Abstract Co-Author*) Nothing to Disclose
Stephen A. Quinet, MD, Milwaukee, WI (*Abstract Co-Author*) Nothing to Disclose
Namrata Bhalla, Brookfield, WI (*Abstract Co-Author*) Nothing to Disclose

### PURPOSE

CT/MRI neurologic stroke (3rd leading cause of death in the US) imaging has immense value in guiding patient management. However, the rate of CT and MRI utilization in patients ultimately found not to have stroke is understandably high in the ED setting, as 'time is brain' and the consequences of misdiagnosing a vascular event are profound. Yet, the judicious utilization of imaging resources in today's healthcare environment is more important than ever. Our study seeks to evaluate the clinical parameters that differentiate stroke negative patients to those who were positive. The information could aid clinical decision-making and optimize stroke imaging algorithms.

### METHOD AND MATERIALS

The EHR of 500 patients who presented with stroke like symptoms, and had CT/MRI performed in a span of 24 hours, were retrospectively reviewed. The predictive values of CT and MRI were obtained by comparing imaging diagnosis with the final clinical diagnosis at discharge. Final diagnosis of stroke negative patients were reviewed, and their clinical profile (age, gender, race and risk factors) were compared with stroke positive patients.

#### RESULTS

Radiologic data analysis revealed 250/500 patients (50%) were 'true negative for stroke based on final clinical discharge diagnoses. The clinical non-stroke diagnoses were as follows: 53/250 with TIA, 19/250 with migraine, 15/250 with seizure, 10/250 with emergent hypertension, 10/250 with behavioral or psychogenic (depression, adjustment disorder, etc.), 9/250 with UTI, and 138 with miscellaneous neurologic or non-neurologic diagnoses. Significant differences in mean age, absence of vascular risk factors and mean NIHSS score were noted between the true negatives and true positives.

## CONCLUSION

Many neurological presentations may mimic stroke clinically, requiring imaging for diagnosis and management. However, imaging resources are limited and are ever shrinking in the current healthcare environment, fostering an emphasis on appropriate utilization. Our data indicates that up to 50% of patients imaged for stroke are ultimately found to have other diagnoses, providing a baseline to test refinements in clinical stroke algorithms that may optimize utilization of neuroimaging in the ED.

## **CLINICAL RELEVANCE/APPLICATION**

Clinical parameters of patients presenting with stroke like symptoms may be used to optimize algorithms that facilitate appropriate utilization of imaging modalities for stroke imaging.

## ER230-SD-WEA3

Spontaneous Visceral Artery Dissection: Clinical and Radiologic Characteristics, Management Strategies and Patients' Outcome

Wednesday, Nov. 30 12:15PM - 12:45PM Room: ER Community, Learning Center Station #3

### **Participants**

Min Yeong Kim, MD, Seoul, Korea, Republic Of (Presenter) Nothing to Disclose

### PURPOSE

To report CT finidngs of spontaneous visceral artery dissection (SVAD) with clinical circumstances. To evaluate treatment strategies correlated with patients' prognosis.

### **METHOD AND MATERIALS**

For 4 years, 18 patients had been diagnosed as SVAD on enhanced abdominal CT scans. The clinical characteristics, comorbidities, risk factors and the treatment with prognosis were evaluated by data from the electronic medical records. Analysis of CT exams included location of SVAD, affected visceral organs, abnormalities of other abdominal arteries. If endovascular intervention was performed, angiographic finidngs were also reviewed.

## RESULTS

Fifteteen patients were men and average age was 49.9 years (range, 29-84). The location of SVAD was superior mesenteric artery (SMA) only in 9, celiac axis (CA) only in 5, both SMA and CA in 2, renal artery (RA) in 2 patients. In one patient, CA dissection developed 20 months after SMA dissection. Most common symptoms were acute abdominal pain in 10 patients, but all two patients with RA dissection complained acute flank pain with segmental infarct in corresponding renal parenchyma. There are no organic ischemia in SMA dissection and only one case of CA dissection resulted in segmental splenic infarct. Only 7 patients had hypertension, no patients had coronary arterial diseases while metabolic diseases were more common: diabetus mellitus (DM) in 5, impaired glucose tolerance (IGT) in 7, dyslipidemia in 8 patients. Smokers were 6 patients and CT finidngs of atherosclerosis were found in 3 patients. No patients underwent for surgical procedures and 4 patient underwent endovascular procedures, one stenting and 3 angioplasty. The others were managed by medical treatment.

### CONCLUSION

Clinical manifestation of SVAD is very similar to other conditions of acute abdomen. Most affected persons are late thirties to ealry fifties males. SMA is most common site of SVAD. The major risk factors are metabolic disease such as DM, IGT and dyslipidemia, however smoking, hypertension or other cardiovascular diseases are not frequent in SVAD. Most SVAD do not result visceral ischemia and are treated by medical management. Although dissection in RA is rarer than in CA or SMA, renal infarct is serious problem and prompt management must be performed.

## **CLINICAL RELEVANCE/APPLICATION**

SVAD is emerging disease entity in acute abdomen. It is important to understand both CT finidngs and clinical characteristics of SVAD for accurate diagnosis and appropriate management.

## ER231-SD-WEA4

Criteria-based Direct Access to Polytrauma Whole-body CT Scans in the Emergency Department, and Impact on Proportion of Normal Scans at a Major Trauma Centre

Wednesday, Nov. 30 12:15PM - 12:45PM Room: ER Community, Learning Center Station #4

#### Awards

### **Student Travel Stipend Award**

#### Participants

James S. Kho, MBBCh, Brighton, United Kingdom (*Presenter*) Nothing to Disclose Ahmed Daghir, MRCP, FRCR, Oxford, United Kingdom (*Abstract Co-Author*) Nothing to Disclose

### PURPOSE

A set of criteria for direct Emergency Department access to polytrauma whole-body CT scans, was introduced to help guide clinical decision making and speed up patient imaging in the Emergency Department. This study aims to determine if use of criteria-based patient selection for polytrauma whole-body CT scans in the Emergency Department is associated with a change in proportion of normal polytrauma whole-body CT scans.

#### **METHOD AND MATERIALS**

Criteria-based direct Emergency Department access to polytrauma whole-body CT scans was introduced over 2013 at our institution, with criteria modified from patient inclusion criteria to the REACT-2 trial. When the criteria are met the patient proceeds directly to CT without prior discussion with a radiologist.

A retrospective sample of 60 polytrauma whole-body CT scans per year was obtained over a fixed 2 month period in 2012, 2014 and 2015. The consultant radiology reports of these CT scans were retrieved from the hospital's radiology information system. Scans were categorised based on the consultant reports as normal (no acute injury or subcutaneous soft tissue injury only), or abnormal (any acute injury other than subcutaneous soft tissue injury). The proportion of normal polytrauma CT scans for 2012 prior to the introduction of the criteria-based patient selection, was compared to 2014 and 2015 post-introduction of the criteria.

#### RESULTS

The proportion of normal polytrauma whole-body CT scans in this major trauma centre, rose from 27% in 2012, to 33% in 2014, to 47% in 2015 (p = 0.02, Z test for equality of proportions). The introduction of criteria-based direct Emergency Department access to polytrauma whole-body CT scans in 2013 thus appears to be associated with a significant rise in proportion of normal scans in our major trauma centre. Our percentage of normal polytrauma whole-body CT scans in 2015 of 47% exceeds published percentages of 27-37% for such scans at other trauma centres in this country.

## CONCLUSION

Introduction of criteria-based direct access of Emergency Department to polytrauma whole-body CT has been associated with a rise in proportion of normal scans at our major trauma centre, from 27% to 47%.

### **CLINICAL RELEVANCE/APPLICATION**

The rising proportion of normal polytrauma CT studies suggests criteria-based direct access to polytrauma whole-body CT in our institution has lowered the threshold for selection of patients that receive these scans.

## Reasonable Utilization of CT Angiogram for Evaluation of Spontaneous Parenchymal Hemorrhage

Wednesday, Nov. 30 12:15PM - 12:45PM Room: ER Community, Learning Center Station #5

#### Awards

### **Student Travel Stipend Award**

#### **Participants**

Li-Hsiang Yen, MD, West Orange, NJ (*Presenter*) Nothing to Disclose Ali F. Jon, MD, Boston, MA (*Abstract Co-Author*) Nothing to Disclose Shira Slasky, MD, Tenafly, NJ (*Abstract Co-Author*) Nothing to Disclose

### PURPOSE

Spontaneous, non-traumatic parenchymal hemorrhage may be caused by a variety of etiologies. CT angiogram (CTA) is a fast and effective modality to diagnose underlying vascular malformations. CTA has limitations due to its high ionizing radiation dose and its cost. Judicious utilization of CTA is necessary to follow the dictum of ALARA. Current guidelines (AHA/ASA 2015) recommend using CTA to evaluate for an underlying structural lesion if there is clinical or radiological suspicion. Risk factors for underlying structural lesions include: age <65 years, female sex, nonsmoker, lobar hemorrhage, intraventricular extension, and absence of hypertension or coagulopathy. Our hypothesis was that many low risk patients with parenchymal hemorrhage in our institution were imaged with CTA unnecessarily.

## METHOD AND MATERIALS

We reviewed our PACS for CT angiograms of the head performed during 2014 and 2015 to identify all patients with intracranial parenchymal hemorrhage. Any abnormality of the cerebral vasculature was subsequently reviewed. Arteriovenous malformation or cerebral aneurysm that may have potentially caused the hematoma were considered positive findings. Other vascular abnormalities such as stenosis were considered negative. Electronic medical records were reviewed for relevant clinical information.

### RESULTS

We identified a total of 74 patients with parenchymal hemorrhage, 36 male and 38 female. 12% of the total patients had positive CTA findings. 20% of these patients were older than 65 years. 10 patients (13.5%) were imaged despite not having any of the risk factors and all had a negative CTA result. The yield of CTA for evaluation of parenchymal hemorrhage was previously reported as 14.6% (AJNR 2009), which is similar to our study.

### CONCLUSION

13.5% of CT angiograms of the head performed for parenchymal hemorrhage were unnecessary as per the AHA/ASA guidelines. Implementation of clinical guidelines into a clinical decision making system may be helpful to reduce unnecessary examinations. We will try to implement the guidelines into our electronic ordering system and follow up on results after implementation.

## **CLINICAL RELEVANCE/APPLICATION**

We have identified a number of unnecessary examination that may be avoided by following the AHA/ASA guideline and will perform a follow-up study to assess the reduction of unnecessary examinations after implementing a check list into our electronic ordering system.

## Fifty Shades of Intraductal Papillary Neoplasm of the Bile Duct

Wednesday, Nov. 30 12:15PM - 12:45PM Room: GI Community, Learning Center Station #9

### Awards Magna Cum Laude

#### **Participants**

Hyo Jung Park, Seoul, Korea, Republic Of (*Abstract Co-Author*) Nothing to Disclose So Yeon Kim, MD, Seoul, Korea, Republic Of (*Presenter*) Nothing to Disclose Hyoung Jung Kim, MD, Seoul, Korea, Republic Of (*Abstract Co-Author*) Nothing to Disclose Seung Soo Lee, MD, Seoul, Korea, Republic Of (*Abstract Co-Author*) Nothing to Disclose Gil-Sun Hong, MD, Seoul, Korea, Republic Of (*Abstract Co-Author*) Nothing to Disclose Seung-Mo Hong, Seoul, Korea, Republic Of (*Abstract Co-Author*) Nothing to Disclose Jae Ho Byun, MD, Seoul, Korea, Republic Of (*Abstract Co-Author*) Nothing to Disclose Moon-Gyu Lee, MD, Seoul, Korea, Republic Of (*Abstract Co-Author*) Nothing to Disclose

## **TEACHING POINTS**

1. To outline the current concept in intraductal papillary neoplasm of the bile duct2. To present various morphologic features of intraductal papillary neoplasm of the bile duct and their mimickers3. To establish radiologic perspectives on multidisciplinary management

## TABLE OF CONTENTS/OUTLINE

1. Introduction of the current concept in intraductal papillary neoplasm of the bile duct (IPNB)(1) Previous names (2) New concept according to the 2010 WHO classification(3) Similarities and differences of intraductal papillary neoplasms involving the pancreaticobiliary system2. Imaging features(1) Factors associated with morphologic features: The presence or absence of mucin hyper secretion, the size and morphology of tumors, tumor location(2) Four morphologic features and their mimickers: Mass with proximal duct dilatation, mass with proximal and distal duct dilatation, disproportional duct dilatation with mass, cystic mass(3) New MRI features: DWI findings, mucus thread sign3. Radiologic perspectives on multidisciplinary management(1) Disease extent evaluation(2) Diagnosis and plans for an optimal treatment

## GI386-SD-WEA1

Contrast Enhancement in Abdominal CT: Comparison of the Different CT Scanners from Different Vendors; Phantom and Clinical Study

Wednesday, Nov. 30 12:15PM - 12:45PM Room: GI Community, Learning Center Station #1

## Participants

Narumi Taguchi, Kumamoto, Japan (*Presenter*) Nothing to Disclose Seitaro Oda, MD, Kumamoto, Japan (*Abstract Co-Author*) Nothing to Disclose Takeshi Nakaura, MD, Kumamoto, Japan (*Abstract Co-Author*) Nothing to Disclose Daisuke Utsunomiya, MD, Kumamoto, Japan (*Abstract Co-Author*) Nothing to Disclose Yoshinori Funama, PhD, Kumamoto, Japan (*Abstract Co-Author*) Nothing to Disclose Masanori Imuta, MD, Kumamoto, Japan (*Abstract Co-Author*) Nothing to Disclose Hideaki Yuki, MD, Kumamoto, Japan (*Abstract Co-Author*) Nothing to Disclose Masafumi Kidoh, Kumamoto, Japan (*Abstract Co-Author*) Nothing to Disclose Kenichiro Hirata, Kumamoto, Japan (*Abstract Co-Author*) Nothing to Disclose Masafumi Kidoh, Kumamoto, Japan (*Abstract Co-Author*) Nothing to Disclose Kenichiro Hirata, Kumamoto, Japan (*Abstract Co-Author*) Nothing to Disclose Masahiro Hatemura, Kumamoto, Japan (*Abstract Co-Author*) Nothing to Disclose Yasuyuki Yamashita, MD, Kumamoto, Japan (*Abstract Co-Author*) Nothing to Disclose

#### PURPOSE

As different CT scanners feature different x-ray spectra and photon energy even at the same kVp settings, contrast enhancement can be different on different CT scanners. This have not been fully validated in clinical settings. We attempted to address this issue in phantom and clinical studies.

### **METHOD AND MATERIALS**

Two different CT scanners were used in this study: scanner A (Brilliance-64; Philips Healthcare) and scanner B (Aquilion ONE, Toshiba). In phantom study, we compared the contrast enhancement between the two scanners under 80-, 100- and 120-kVp. Then, we calculated the effective energies of the two CT scanners by using the half-value layer measurement. In clinical study, 40 patients underwent abdominal scanning with scanner A and other 40 patients were scanned on scanner B at the same scanningand contrast material injection protocol at 120-kVp. The contrast enhancement of their abdominal organs were assessed quantitatively and qualitatively.

#### RESULTS

In phantom study, the contrast enhancement for scanner B was 36.9%, 32.6% and 30.8% higher than scanner A at 80-, 100- and 120-kVp, respectively. The effective energies was higher for scanner A than scanner B (eg, 62.4 keV vs. 54.4 keV for 120-kVp with the large filter). In clinical study, quantitative analysis revealed that scanner B yielded significantly better contrast enhancement of the liver, kidney, portal vein, and inferior vena cava than scanner A. The mean visual scores in regard to contrast enhancement were significantly higher on images obtained by scanner B than scanner A.

## CONCLUSION

There were significant differences in contrast enhancement of the abdominal organs between the two different CT scanners from different vendors even at the same scan- and contrast parameters.

## **CLINICAL RELEVANCE/APPLICATION**

Contrast enhancement of the abdominal organs is slightly different between the two different CT scanners even at the same scan protocols.

### Evaluation of the ACR's Recommendations for Management of Incidental Nodal Findings

Wednesday, Nov. 30 12:15PM - 12:45PM Room: GI Community, Learning Center Station #2

#### Awards

### **Student Travel Stipend Award**

#### **Participants**

Paul Smereka, MD, New York, NY (*Presenter*) Nothing to Disclose Ankur Doshi, MD, New York, NY (*Abstract Co-Author*) Nothing to Disclose Justin M. Ream, MD, Ann Arbor, MI (*Abstract Co-Author*) Nothing to Disclose Andrew B. Rosenkrantz, MD, New York, NY (*Abstract Co-Author*) Nothing to Disclose

#### PURPOSE

The ACR Incidental Findings Committee (ACR-IFC) advises that incidental abdominopelvic lymph nodes (LNs) with certain indeterminate imaging features undergo a 3 month follow-up exam and be deemed benign after 12 month stability. Our aim was to assess the utility of the ACR-IFC's recommendations for identifying and following-up abnormal incidental abdominopelvic LNs.

## METHOD AND MATERIALS

We searched for abdominopelvic CT reports mentioning a LN in the Impression. Among 3,074 results from a 27 month period, 64 LNs met ACR criteria as incidental (no malignancy or lymphoproliferative disorder) and with sufficient follow-up to be classified as benign (biopsy; decrease in size;  $\geq$ 12 month stability) or malignant (biopsy; increased FDG activity and detection of a primary malignancy). Two radiologists independently assessed the LNs for suspicious features by the ACR-IFC criteria. Outcomes were assessed in summary fashion.

## RESULTS

10% (6) of LNs were malignant [lymphoma (n=4), lung cancer (n=1), small bowel adenocarcinoma (n=1)]; 90% (54) benign. 2 of the 6 malignant LNs were stable at initial 3-6 month follow-up prior to eventual diagnosis. 22% (13), 8% (5), 13% (8), and 15% (9) were deemed benign based on decreased size at initial <3 month, 3-5 month, 6-11 month, or  $\geq$ 12 month follow-up, respectively; 23% (14) based on  $\geq$ 12 month stability. Among 5 LNs stable at 3-5 month with additional follow-up, 2 were malignant (lymphoma on biopsy), 2 decreased at 11 month and 23 month follow-up, and 1 was stable at 20 month follow-up. No ACR-IFC feature (round with indistinct hilum; necrosis; hypervascularity; cluster  $\geq$ 3 LNs; cluster  $\geq$ 2 LNs in  $\geq$ 2 stations; size  $\geq$ 1cm in retroperitoneum) was significantly different between benign and malignant LNs (p=0.15-1). Nearly all LNS (97-98%) had  $\geq$ 1 suspicious feature for each reader. Two features (necrosis and hypervascularity) were not identified in any LN; one feature (cluster  $\geq$ 3 LNs) was present in 88%-93% of LNs.

## CONCLUSION

ACR-IFC imaging features did not differentiate benign and malignant LNs. Abnormal LNs rarely decreased at the advised 3 month follow-up exam. When stable at 3 months, LNs were occasionally malignant or decreased on continued follow-up.

## **CLINICAL RELEVANCE/APPLICATION**

The management of incidental abdominopelvic LNs remains a challenge. Further optimization of strategies for both the definition and follow-up of suspicious LNs is warranted.

Hepatopulmonary Shunting on Tc99m-MAA Liver Mapping: Correlation with Dynamic Cross Sectional Imaging and Description of Different Shunting Patterns

Wednesday, Nov. 30 12:15PM - 12:45PM Room: GI Community, Learning Center Station #3

#### Awards

### **Student Travel Stipend Award**

#### Participants

Mohammed S. Bermo, MD, FRCR, Seattle , WA (*Presenter*) Nothing to Disclose Fatemeh Behnia, MD, Seattle, WA (*Abstract Co-Author*) Nothing to Disclose Claudia Zacharias, MD, Seattle, WA (*Abstract Co-Author*) Nothing to Disclose Malak Itani, MD, Seattle, WA (*Abstract Co-Author*) Nothing to Disclose Hubert J. Vesselle, MD, PhD, Seattle, WA (*Abstract Co-Author*) Consultant, MIM Software Inc

#### PURPOSE

Various types of intrahepatic vascular shunting are seen on dynamic CT/MRI, especially in patients with liver tumors. Intrahepatic shunts diverting hepatic arterial blood flow to systemic venous return could potentially increase radiation dose to the lungs after intra-arterial Y90-microsphere treatment. To simulate this therapy, patients undergo an intra-arterial injection of Tc-99m MAA and gamma camera imaging (mapping), which is used to estimate the hepato-pulmonary shunt fraction. We compared findings on pre-therapy dynamic CT/MRI with the calculated shunt fraction from Tc99m-MAA mapping.

#### **METHOD AND MATERIALS**

We reviewed 523 Tc99m-MAA scans in 453 patients (301 males, 152 female) and their correlative cross sectional imaging. Cases with corresponding well-timed dynamic CT/MRI studies performed within 3 months of Tc-99m MAA mapping, and who had not received embolization between the two scans, were enrolled in the comparison of shunt fraction as calculated on Tc99m-MAA study and vascular shunting as identified on dynamic CT/MRI.

### RESULTS

342 studies met these inclusion criteria: CT/MRI showed visible shunting in 63 of the studies. In 271 studies, no shunt was identified by cross sectional imaging. In 8 cases, CT/MRI studies were inconclusive for the presence of vascular shunting. In the first group with visible shunting on dynamic CT/MRI, the mean shunt fraction was 12.9% +/- 10.36% (95% CI 10.29-15.15%). In the second group without visible shunting, the mean shunt fraction was 4.3% +/-3.17% (95% CI 3.93-4.68%). The difference was statistically significant (p value <0.001). Three CT/MRI patterns of hepatic arterial flow shunting that potentially lead to increased hepatopulmonary shunting were identified: 1) Shunting to a hepatic vein. 2) To the portal vein with recanalized Paraumbilical vein. 3) To the portal vein with a TIPS in place.

### CONCLUSION

Mean hepatopulmonary shunt fraction, calculated on Tc99m-MAA liver mapping, is higher when vascular shunting is visible on dynamic CT/MRI. Differences are statistically significant. Three patterns of shunting associated with increased hepatopulmonary shunt fractions are identified.

## **CLINICAL RELEVANCE/APPLICATION**

Our results might help better understand the pathophysiology of hepatopulmonary shunting, and may help predict the patients with high hepatopulmonary shunting based on their dynamic non-invasive imaging.

## GI389-SD-WEA4

Single-source Dual Energy Spectral CT Imaging for Evaluation of Pancreatic Ductal Adenocarcinoma -A Preliminary Study

Wednesday, Nov. 30 12:15PM - 12:45PM Room: GI Community, Learning Center Station #4

## Participants

Huanhuan Xie, Shanghai, China (*Presenter*) Nothing to Disclose Xiao-Zhu Lin, Shanghai, China (*Abstract Co-Author*) Nothing to Disclose

#### PURPOSE

To explore the quantitative parameters and characteristics of pancreatic ductal adenocarcinoma in dual energy spectral CT imaging.

## METHOD AND MATERIALS

From 2013 to 2014, 113 patients were scanned with Gemstone Spectral Imaging (GSI). The ROI files including the monochromatic CT values , the eff-Z, the iodine-water concentration and the corresponding normalized values of the lesion (normalized to pancreatic parenchyma) and of pancreatic parenchyma in AP and PVP. The works were performed three times repeatedly. Paired T-test or Wilcoxon test were used for analyzing the differences between different phases and between PDAC and pancreatic parenchyma, and P <0.05 was considered statistically significant.

## RESULTS

The eff-Z and iodine-water concentration of PDCA in two phases were  $8.14 \pm 0.36$  and  $8.45 \pm 0.39$ ,  $9.38 \pm 5.75$  (100ug/cm3) and  $14.73 \pm 7.00$  (100ug/cm3),  $1034 \pm 12$  (mg/cm3) and  $1034 \pm 14$  (mg/cm3) respectively. The monochromatic CT values, the eff-Z, iodine (water) concentration and normalized monochromatic CT values (rang from 40 keV to 54 keV) of PDCA have significant differences between two phases (P<0.05), and no difference in the water (iodine) concentration. The monochromatic CT values in late arterial phase were lower than in portal venous phase at each energy level. And normalized monochromatic CT values increased with the increase of energy level. The eff-Z, iodine (water) concentration and water (iodine) concentration of pancreatic parenchyma in two phases were  $8.91\pm0.41$  and  $9.24\pm0.39$ ,  $23.67\pm7.89$  (100ug/cm3) and  $30.41\pm8.55$  (100ug/cm3),  $1042\pm14$  (mg/cm3) and  $1041\pm15$  (mg/cm3) respectively. The differences of eff-Z and iodine-water concentration between PDCA and pancreatic parenchyma were significant in both two phases.

## CONCLUSION

The CT spectral HU curves, eff-Z and iodine concentration of PDCA were lower than those of pancreatic parenchyma in both AP and PVP. The CT spectral HU curve, eff-Z, iodine (water) concentration of PDCA in AP were lower than those of in PVP. The differences of CT spectral HU curves were more distinct at lower energy.

### **CLINICAL RELEVANCE/APPLICATION**

The study suggests that combined with multi-parameter of spectral imaging can improve pancreatic ductal adenocarcinoma CT density resolution.

Disappearing or Residual Tiny (<= 5 mm) Colorectal Liver Metastases after Chemotherapy on Gadoxetic Acidenhanced Liver MRI:Is Local Treatment Required?

Wednesday, Nov. 30 12:15PM - 12:45PM Room: GI Community, Learning Center Station #5

## Participants

Kyoung Doo Song, MD, Seoul, Korea, Republic Of (*Presenter*) Nothing to Disclose Seung Soo Kim, MD, Seoul, Korea, Republic Of (*Abstract Co-Author*) Nothing to Disclose

### PURPOSE

To evaluate the follow-up results of disappearing colorectal liver metastases (DLM) or residual tiny ( $\leq$  5 mm) colorectal liver metastases (RTCLM) on gadoxetic acid-enhanced magnetic resonance imaging (MRI) in patients who had colorectal liver metastases (CLM) and received chemotherapy.

### METHOD AND MATERIALS

Our institutional review board approved this retrospective study and informed consent was waived. Among patients who received chemotherapy for CLM and underwent gadoxetic acid-enhanced MRI between 2010 and 2012, 43 patients with 168 DLMs and 48 RTCLMs were included. The cumulative in situ recurrence rate of DLM and progression rate of RTCLM and their predictive factors were evaluated.

## RESULTS

A total of 150 DLMs and 26 RTCLMs were followed up without additional treatment. The median follow-up period was 22.1 months (range, 2.4–73.8 months) for DLMs and 11.9 months (range, 2.4–60.9 months) for RTCLMs. At 1 and 2 years respectively, the cumulative in situ recurrence rates for DLM were 10.9% and 15.7% and the cumulative progression rates for RTCLM were 27.2% and 33.2%. The in situ recurrence rates at 1 and 2 years were both 4.9% for the DLM group that did not show reticular hypointensity of liver parenchyma on hepatobiliary phase.

### CONCLUSION

DLM on gadoxetic acid-enhanced liver MRI indicates a high possibility of true complete response, especially in patients without chemotherapy-induced sinusoidal obstruction syndrome. Thirty seven percent of RTCLMs showed progression at 2 years.

## **CLINICAL RELEVANCE/APPLICATION**

1. Follow-up without local treatment can be considered one of management options for disappearing liver metastasis on gadoxetic acid-enhanced liver MRI.2. Management of residual tiny colorectal liver metastases on gadoxetic acid-enhanced MRI should be determined with consideration of the patient's performance status and the risk of local treatment.

## GI391-SD-WEA6

### Virtual Enteroscopy: A Role for Small Bowel Imaging? A Preliminary and Feasibility Study

Wednesday, Nov. 30 12:15PM - 12:45PM Room: GI Community, Learning Center Station #6

#### **Participants**

David Szapiro, MD, Kirkcaldy, United Kingdom (*Presenter*) Nothing to Disclose Anmol Gangi, Kirkcaldy, United Kingdom (*Abstract Co-Author*) Nothing to Disclose Luc Bidaut, Kirkcaldy, United Kingdom (*Abstract Co-Author*) Nothing to Disclose Thomas Hartley, Kirkcaldy, United Kingdom (*Abstract Co-Author*) Nothing to Disclose Hasnain Jafferbhoy, Kirkcaldy, United Kingdom (*Abstract Co-Author*) Nothing to Disclose Dean D. Maglinte, MD, Indianapolis, IN (*Abstract Co-Author*) Nothing to Disclose

## PURPOSE

CT-based Virtual Enteroscopy (VE) uses warm CO2 as an intraluminal negative contrast agent eliciting bowel wall relaxation responses via thermoreceptors in the gut. VE is a feasible technique for small bowel imaging whenever fluid-filled exams are contraindicated or inconclusive. VE has been applied to subocclusive small bowel diseases, whether from known Crohn's disease or from other causes. When no definite cause for the patient's symptoms was found and capsule endoscopy was discarded as an alternative for diagnosis, VE was considered as an appropriate modality for optimising therapeutic management.

### **METHOD AND MATERIALS**

Patients were prospectively selected after multidisciplinary discussion. Warm CO2 was delivered by a dedicated insufflator (VMX-1020A, Vimap Technologies) using a two-ends insufflation technique via a nasojejunal (NJ) tube and a rectal cannula. Simultaneous CO2 insufflation was then performed at 45 degrees Celsius. Automatic feedback from the insufflator indicated when optimal distention was reached. CT acquisition with IV iodine contrast followed. Image analysis was performed by using virtual endoscopy software. Each exam was then compared to a previous fluid-filled agent exam whenever available.

### RESULTS

Small bowel insufflation with warm CO2 was applied successfully to 12 consecutive patients from July 2015 to March 2016, while 215 fluid-filled exams were performed during the same period. Compared to fluid-filled exams jejunal distention was significantly improved and more homogenous distention of the small bowel was obtained altogether. Patients with subocclusive disease have found VE more comfortable than with fluid-filled exams. In total, additional findings not found on fluid-filled exams included non-described stenosis (n=7), fistula (n=1), jejunal diverticulum (n=1) and tumours (n=2). Questionnaires demonstrated satisfactory patient experience despite NJ tube insertion.

## CONCLUSION

While VE is more technically demanding for imaging patients with subocclusive symptoms, it is feasible and has shown promising results. All patients presenting with subocclusive pathologies showed better tolerance to warm CO2 insufflation than with orally ingested agents.

## **CLINICAL RELEVANCE/APPLICATION**

Subocclusive disorders of the small bowel can be explored by warm CO2 when fluid-filled exams are non diagnostic, or contraindications to more sophisticated or expensive exam like capsule endoscopy are present.

## Evaluation Precision of Liver Surface Nodularity Measurements using a CT Imaging Phantom

Wednesday, Nov. 30 12:15PM - 12:45PM Room: GI Community, Learning Center Station #7

#### Awards

### **Student Travel Stipend Award**

#### **Participants**

Kevin A. Zand, MD, Jackson, MS (*Presenter*) Nothing to Disclose
Tara Lewis, BS,RN, Jackson, MS (*Abstract Co-Author*) Nothing to Disclose
Seth Lirette, MS, Jackson, MS (*Abstract Co-Author*) Nothing to Disclose
Joshua Levy, Salem, NY (*Abstract Co-Author*) Stockholder, The Phantom Laboratory President, The Phantom Laboratory
Stockholder, Image Owl, Inc
Jason Bryan, MS, Cleveland, OH (*Abstract Co-Author*) Nothing to Disclose
Amit Vasanji, PhD,BEng, Cleveland, OH (*Abstract Co-Author*) Officer, ImageIQ, Inc
Michael Griswold, PhD, Jackson, MS (*Abstract Co-Author*) Nothing to Disclose
Andrew D. Smith, MD, PhD, Jackson, MS (*Abstract Co-Author*) Research Grant, Pfizer Inc; President, Radiostics LLC; President, Liver
Nodularity LLC; President, Color Enhanced Detection LLC; President, eMASS LLC; Pending patent, Liver Nodularity LLC; Pending

#### PURPOSE

To evaluate precision of liver surface nodularity measurements using a CT imaging phantom.

### **METHOD AND MATERIALS**

An anthropomorphic CT imaging phantom was constructed with simulated normal/cirrhotic liver and visceral/subcutaneous fat components. Simulated liver surface had regions with no surface nodules (SMOOTH) and with 2 mm radius half spheres (NODULAR). The phantom was scanned multiple times on a GE Lightspeed 16 CT scanner with adjustment of individual imaging parameters (section thickness, kVp, mA, field of view [FOV], and smoothing kernel) and on 22 different CT scanners from 4 manufacturers at 12 imaging centers. Simulated LSN was measured using quantitative software. Repeatability, reproducibility, and inter-reader agreement were evaluated by repeatability coefficient (RC), reproducibility coefficient (RDC), and intra-class correlation (ICC), respectively.

### RESULTS

LSN measurements of SMOOTH and NODULAR simulated liver surface (2.13 and 3.50, respectively) were significantly different (p<0.001) and matched expected values from previously assessed patient exams. Optimal LSN measurements were obtained for section thickness between 1.0-5.0mm, kVp  $\geq$ 200, mAs  $\geq$ 200, and FOV  $\leq$ 40cm. Smoothing kernel had little impact on LSN measurements. LSN measurements from CT images derived from a single scanner showed high repeatability (RC=0.321). LSN measurements had high inter-reader agreement (ICC=0.996; N=5 readers) with a RDC of 0.287. LSN measurements are highly reproducible across multiple CT scanners (N=22) from 4 different manufacturers at 12 different imaging centers using routine imaging protocols (RDC=0.511).

## CONCLUSION

Routine liver CT imaging parameters can be used to measure LSN with high precision, suggesting that the technology is adaptable to multi-institutional clinical studies.

### **CLINICAL RELEVANCE/APPLICATION**

Routine liver CT imaging parameters can be used to measure LSN with high precision, suggesting that the technology is adaptable to multi-institutional clinical studies. Routine liver CT imaging parameters can be used to measure liver surface nodularity with high precision, suggesting that the technology is highly reproducible across multiple different CT scanners from different manufacturers and different imaging centers and therefore adaptable to multi-institutional clinical studies.

## **CT in Occlusive and Non-Occlusive Ischemic Colitis**

Wednesday, Nov. 30 12:15PM - 12:45PM Room: GI Community, Learning Center Station #8

#### **Participants**

Nadia S. Gonzalez, MD, Dresden, Germany (*Presenter*) Nothing to Disclose Verena Plodeck, MD, Dresden, Germany (*Abstract Co-Author*) Nothing to Disclose Jakob Dobroschke, Dresden, Germany (*Abstract Co-Author*) Nothing to Disclose Michael Laniado, MD, Dresden, Germany (*Abstract Co-Author*) Reviewer, Johnson & Johnson

## PURPOSE

To evaluate CT findings of Ischemic Colitis (IC) and to correlate findings with etiology (occlusive versus non-occlusive).

### **METHOD AND MATERIALS**

We retrospectively evaluated 41 patients with IC confirmed by surgery and/or endoscopy. CT and clinical history were reviewed. CT signs of IC (pericolic fat stranding/fluid, colonic wall thickening/thinning, abnormal wall enhancement, dilatation, pneumatosis intestinalis, portomesenteric gas, pneumoperitoneum and/or mesenteric vascular stenosis/occlusion) and its localization were analyzed and correlated with the presence of occlusive IC (OIC) and non-occlusive IC (NOIC).

### RESULTS

There were 29 male and 12 female patients (mean age 70 years). NOIC was the cause of IC in 26 patients (low flow state, s.p. cardiac surgery, aortic wall hematoma and dissection) and OIC in the remaining 15 patients (s.p. infrarenal aortic surgery, cardioembolic and thrombotic event, portal hypertension). All patients showed signs of pericolic fat stranding or fluid. Wall thinning was found in 24 patients (58%) and wall thickening in 14 (34%). Fourteen patients (34%) showed abnormal wall enhancement. Mesenteric vascular abnormalities were found in 31 patients (75.6%). Segmental involvement was more frequent (n=29, mostly right colon) than subtotal involvement of the colon (n=12). A significant correlation was found between NOIC and the presence of wall thinning and colonic dilatation (p=0.002 and p=0.001 respectively). Patients with OIC showed a significant correlation with wall thickening (p=0.002). The presence of intraabdominal gas significantly correlated with NOIC (p=0.005). Right colon involvement was more frequent with NOIC (66%). All patients had cardiovascular comorbidities. Overall mortality was 31% (n=13).

### CONCLUSION

CT allows the detection of signs of IC. NOIC is the more frequent cause of IC compared to OIC. NOIC usually shows wall thinning with dilatation, affecting more frequently the right colon. OIC frequently presents with wall thickening. Knowledge of the full spectrum of potential CT signs and certain risk factors of IC is essential for diagnosis, allowing a prompt and effective treatment.

### **CLINICAL RELEVANCE/APPLICATION**

Ischemic Colitis shows a wide spectrum of CT findings which are often subtle. Knowledge of the etiology (occlusive or non-oclusive) and certain CT signs is essential to make the diagnosis.

Value of Dynamic Contrast-enhanced and Diffusion-weighted-MR Imaging for the Detection of Pathological Complete Response in Locally Advanced Cervical Cancer after Neoadjuvant Therapy

Wednesday, Nov. 30 12:15PM - 12:45PM Room: GU/UR Community, Learning Center Station #2

## Participants

Aurelie Jalaguier-Coudray, MD, Marseille, France (*Abstract Co-Author*) Nothing to Disclose Rim Villard-Mahjoub, Marseille, France (*Abstract Co-Author*) Nothing to Disclose Beatrice Delarbre, Marseille, France (*Abstract Co-Author*) Nothing to Disclose Isabelle Thomassin-Naggara, MD, Paris, France (*Presenter*) Speakers Bureau, General Electric Company;

### PURPOSE

To evaluate the ability of dynamic contrast-enhanced magnetic imaging (DCE-MRI) and diffusion-weighted imaging (DWI) to predict pathological complete response (CR) after preoperative radio-chemotherapy for cervical carcinoma and to predict local recurrence

## **METHOD AND MATERIALS**

Institutional ethics committee approved this retrospective study. The study population comprised 52 patients with locally advanced carcinoma treated first by chemoradiation and who underwent MR imaging between June 2011 and July 2015 before final surgery. Three radiologists, who were blinded to the pathological results and to each other's, retrospectively evaluated conventional, DW-imaging and quantitative and semi-quantitative DCE-MRI to identify a complete response. The reference standard was surgical pathologic findings.

## RESULTS

On DCE-MRI, an initial rise in the signal of cervical lesion that was steeper than that of myometrium was described as time intensity curve (TIC) type B and was significantly associated with a non CR (p=0.0004). DCE-MRI parameters (i.e MS: Max slope enhancement, IAUGC90: initial area under the gadolinium concentration –time curve during the first 90 sec after gadolinium injection and KTRANS) and a low signal on visual ADC were significantly associated with a non CR (respectively, p=0.027, p= 0.041, p=0.037, p=0.032). Patient with ADCMOY  $\leq$  0,0014 m2/s (HR=8,3), low ADC signal (HR=7,3), high DW signal intensity (HR=7,1) and TIC type B (HR = 4,3) were associated with earlier recurrence (p<0.05). There was perfect agreement ( $\kappa$  >0.80) for each parameter between the readers.

## CONCLUSION

DCE-MRI is a feasible and accurate technique to differentiate CR and non-CR and could potentially help oncologists with management decisions. Moreover, DCE-MRI with the help of DWI could help the oncologists to accentuate the follow-up for patients with high risk of local recurrence and therefore to detect more previously these recurrences.

## **CLINICAL RELEVANCE/APPLICATION**

In some centers, cervical carcinoma after neo-adjuvant therapy did not be operated. Thus, MR with the help of Perfusion and Diffusion imaging could separate patients needed a surgery than patients without surgery. Moreover, with the use of time intensity curve, diffusion and ADC, MRI could predict local recurrence.

## GU236-SD-WEA3

### PI-RADS Score 3: Do This Patient Collective Really Need Prompt Biopsy?

Wednesday, Nov. 30 12:15PM - 12:45PM Room: GU/UR Community, Learning Center Station #3

#### Participants

Lars Schimmoeller, MD, Duesseldorf, Germany (*Presenter*) Nothing to Disclose Frederic Dietzel, Dusseldorf, Germany (*Abstract Co-Author*) Nothing to Disclose Tim Ullrich, Duesseldorf, Germany (*Abstract Co-Author*) Nothing to Disclose Michael Quentin, MD, Dusseldorf, Germany (*Abstract Co-Author*) Nothing to Disclose Dirk Blondin, MD, Duesseldorf, Germany (*Abstract Co-Author*) Nothing to Disclose Gerald Antoch, MD, Duesseldorf, Germany (*Abstract Co-Author*) Nothing to Disclose Christian Arsov, MD, Duesseldorf, Germany (*Abstract Co-Author*) Nothing to Disclose Robert Rabenalt, Duesseldorf, Germany (*Abstract Co-Author*) Nothing to Disclose Peter Albers, MD, PhD, Duesseldorf, Germany (*Abstract Co-Author*) Nothing to Disclose

### PURPOSE

This study evaluates diagnostic accuracy in patients with multi-parametric prostate MRI and an overall PI-RADS score of 3.

### **METHOD AND MATERIALS**

One hundred and twenty consecutive patients with a PI-RADS (Version 2) overall score of 3 in the multi-parametric MRI (T2WI, DWI, DCE-MRI) at 3T and subsequent targeted MR-guided biopsy (group A: MRI-guided in-bore biopsy; group B: MR/US fusion-guided plus transrectal ultrasound-guided biopsy) were retrospectively included in this study. Data were analyzed regarding PCa and clinical significant PCa detection. Furthermore several parameters (prostate volume, PSA value, number of previous negative TRUS-GB) were correlated to biopsy positive patients to find a potential predictor of these patients.

### RESULTS

In group A in 35 of 39 (90%) and in group B in 73 of 81 patients (90%) prostate biopsy was negative. Overall in 12 patients biopsy detected PCa (10%), whereas significant PCa was detected in none patient in group A and only in two patients (both Gleason score 4+3=7) in group B (1.6%). PCa in these patients were mostly detected by the additional systematic cores. Prostate volume was tendentially lower, but regarding PSA value, and number of previous negative TRUS-GB there were no significant differences in the biopsy positive compared to the biopsy negative patients.

## CONCLUSION

In patients with a PIRADS overall score of 3 detection of significant PCa is very uncommon, but low-risk PCa can occur. Therefore these patients need follow-up monitoring, but not necessarily prompt biopsy, so far quality of mp-MRI protocol and MRI diagnostic was confirmed.

### **CLINICAL RELEVANCE/APPLICATION**

In patients with a PI-RADS score 3, diagnosis of significant PCa is very uncommon in a high volume center with experienced uroradiologists. Therefore, these patients should be primary radiologically and clinical-urologically followed. The Effect of Prostate-specific Antigen Density on Positive and Negative Predictive Values of Multiparametric Magnetic Resonance Imaging to Detect Gleason Score 7-10 Prostate Cancer in a Repeat Biopsy Setting

Wednesday, Nov. 30 12:15PM - 12:45PM Room: GU/UR Community, Learning Center Station #4

## Participants

Nienke L. Hansen, MD, Aachen, Germany (*Abstract Co-Author*) Nothing to Disclose Tristan Barrett, MBBS, BSc, Guildford, United Kingdom (*Presenter*) Nothing to Disclose Brendan C. Koo, MBBCh, Cambridge, United Kingdom (*Abstract Co-Author*) Nothing to Disclose Anne Warren, Cambridge, United Kingdom (*Abstract Co-Author*) Nothing to Disclose Christof Kastner, Cambridge, United Kingdom (*Abstract Co-Author*) Nothing to Disclose Ola Bratt, Cambridge, United Kingdom (*Abstract Co-Author*) Nothing to Disclose

### PURPOSE

The interaction between prostate-specific antigen density (PSA-D) and multiparametric prostate magnetic resonance imaging (mpMRI) on Gleason score (GS) 7-10 prostate cancer detection is unclear. Purpose of the study was to evaluate the effect of PSA-D on the positive (PPV) and negative (NPV) predictive values of mpMRI to detect GS 7-10 cancer in a repeat biopsy setting.

### **METHOD AND MATERIALS**

Retrospective study of 514 men with previous prostate biopsy showing no or GS 6 cancer. All had mpMRI, graded 1-5 on a Likert scale for cancer suspicion, and subsequent targeted and systematic 24-core image-fusion guided transperineal biopsy in 2013-2015. NPVs of Likert 1-2 and PPVs of Likert 3-5 mpMRIs for detecting GS 7-10 cancer were calculated ( $\pm$ 95% confidence intervals) for PSA-D <0.1, 0.1-0.2,  $\leq$ 0.2 and >0.2 ng/ml/cm3, and compared by Chi square test for linear trend.

### RESULTS

GS 7-10 cancer was detected in 31% of the men. NPV of Likert 1-2 mpMRI was 0.91 ( $\pm$ 0.04) with PSA-D  $\leq$ 0.2 and 0.71 ( $\pm$ 0.16) with >0.2 (p=0.003). For Likert 3 mpMRI, PPV was 0.09 ( $\pm$ 0.06) with PSA-D  $\leq$ 0.2 and 0.44 ( $\pm$ 0.19) with >0.2 (p=0.002). PSA-D also significantly affected the PPV of Likert 4-5 mpMRI lesions: the PPV was 0.47 ( $\pm$ 0.08) with PSA-D  $\leq$ 0.2 and 0.66 ( $\pm$ 0.10) with >0.2 (p=0.0001).

## CONCLUSION

In a repeat biopsy setting, PSA-D  $\leq 0.2$  is associated with low detection of GS 7-10 prostate cancer, not only in men with negative mpMRI, but also in men with equivocal imaging. Surveillance, rather than repeat biopsy, may be appropriate for these men. Conversely, biopsies are indicated in men with high PSA-D, even if an mpMRI shows no suspicious lesion, and in men with an mpMRI suspicious for cancer, even if PSA-D is low.

## **CLINICAL RELEVANCE/APPLICATION**

Men with previous biopsies showing no or Gleason 6 cancer, low PSA density, and negative or equivocal MRI have low risk of aggressive prostate cancer and may not require a repeated biopsy.

## GU239-SD-WEA6

### Assessment of Mixed Stone Chemical Composition using Dual-energy Computed Tomography

Wednesday, Nov. 30 12:15PM - 12:45PM Room: GU/UR Community, Learning Center Station #6

#### **Participants**

Alice Huang, Rochester, MN (*Presenter*) Nothing to Disclose Shuai Leng, PhD, Rochester, MN (*Abstract Co-Author*) Nothing to Disclose Juan Montoya, Rochester, MN (*Abstract Co-Author*) Nothing to Disclose James C. Williams, PhD, Indianapolis, IN (*Abstract Co-Author*) Nothing to Disclose Cynthia H. McCollough, PhD, Rochester, MN (*Abstract Co-Author*) Research Grant, Siemens AG

### PURPOSE

We have demonstrated that the high spatial resolution of 3rd-generation dual-source, dual-energy CT (DECT) allowed accurate estimation of % uric acid (UA) and % non-uric acid (NUA) of mixed stones. A study investigating performance of a range of kV pairs as a function of phantom size found the accuracy of %UA quantification to be optimal across phantom sizes at 90/Sn150 and 100/Sn150 kV. The purpose of this study was to validate our prediction model at 90/150Sn kV with a new stone collection on which the model was not trained.

#### **METHOD AND MATERIALS**

Training data consisted of 22 mixed UA/NUA stones and 2 pure stones, scanned with micro-CT (Skyscan 1172, Bruker) to produce reference values for the percentage of UA and NUA in each stone. Stones were placed in water phantoms and scanned with DECT (Somatom Force, Siemens). Images were processed using in-house software. For each stone, each pixel was classified as UA or NUA by comparing its CT number ratio (CTR) to a size- and kV-specific threshold. Classification thresholds were chosen based on the lowest root-mean-square error (RMSE) at a given size and kV. The test data for this study consisted of 25 mixed UA/NUA stones and 4 pure stones. 35 and 45 cm phantoms were scanned with DECT at 90/Sn150 kV. Micro-CT and image processing was performed as above. Pixel-by-pixel analysis of stone composition was performed with the optimal thresholds identified from the training data. DECT quantification of percent UA was compared to micro-CT percentages using paired t-tests.

## RESULTS

The absolute RMSE across all stones was 15% and 14% UA for the 35 and 45 cm phantoms, respectively. RMSE ranged from -33% to +32% UA across stones and phantom sizes. A small but statistically significant difference was found between the percent UA composition estimated by micro-CT and DECT for both phantom sizes (mean difference in %UA = -8% and -7%, p = 0.01 and 0.01). There was insignificant correlation between stone volume and RMSE in DECT quantification of %UA (p = 0.49).

## CONCLUSION

This validation study demonstrated that DECT at a single kV pair setting across phantom sizes is capable of accurately quantifying the composition of mixed UA/NUA stones reliably across different stone samples.

## **CLINICAL RELEVANCE/APPLICATION**

Accurate and consistent quantification of renal stones, which mostly have mixed composition, is necessary for disease management and treatment selection. DECT can reliably provide this information.

## How to Safely Perform MRI in Patients with Pacemakers/ICDs? - A Primer for Radiologists

Wednesday, Nov. 30 12:15PM - 12:45PM Room: HP Community, Learning Center Station #6

#### Awards Certificate of Merit

#### **Participants**

Fernando U. Kay, MD, Dallas, TX (*Abstract Co-Author*) Nothing to Disclose Verghese George, MBBS, Houston, TX (*Abstract Co-Author*) Nothing to Disclose Prabhakar Rajiah, MD, FRCR, Dallas, TX (*Presenter*) Institutional Research Grant, Koninklijke Philips NV; Speaker, Koninklijke Philips NV

### **TEACHING POINTS**

To review the safety aspects of MRI in patients with devices such as pacemakers/ICDs To review the currently available, FDA approved MR conditional pacemakers/ICDs To present a flow-chart on management of this challenging scenario

### **TABLE OF CONTENTS/OUTLINE**

Introduction Safety issues with devices (**Static magnetic field-** Movement; Activation of reed switch; **Gradient and RF fields**-Heating, tissue damage, interference with device function) Designing changes in MRI-conditional pacemakers/ICD (Reduced ferromagnetic content, modified Reed switch, lead design changes, improved circuitry, shields, programming) Currently available FDA approved MR conditional pacemakers/ICDs (**PM**- Revo & Advisa (Medtronic); Entovis, Evia & Eluna (Biotronik); **ICD**- Evera (Medtronic). Steps for safe MRI- Establish multidisciplinary team; Electrophysiology clearance; Proper selection of patients; Program device to MR mode before the scan; Adequately trained staff in place (radiologist, cardiologist, radiology nurse, electrophysiology nurse, physicist); Scan according to the conditions specified for the device; Continuous monitoring of patient; Maintaining image quality; Checking parameters after scan; Reprogram the device; Follow-up if parameters are changed significantly Management of artifacts during scanning. Specific MR conditions for the different devices MRI in "MR unsafe" devices.

### **Honored Educators**

Presenters or authors on this event have been recognized as RSNA Honored Educators for participating in multiple qualifying educational activities. Honored Educators are invested in furthering the profession of radiology by delivering high-quality educational content in their field of study. Learn how you can become an honored educator by visiting the website at: https://www.rsna.org/Honored-Educator-Award/

Prabhakar Rajiah, MD, FRCR - 2014 Honored Educator

### HP226-SD-WEA1

Practice Ready? Assessing Medical Students' Abilities in Recognizing Important and Emergent Radiological Findings

Wednesday, Nov. 30 12:15PM - 12:45PM Room: HP Community, Learning Center Station #1

### Participants

Andrew J. Lukaszewicz, MD, Pontiac, MI (*Presenter*) Nothing to Disclose Rashpal S. Sandhu, MD, Pontiac, MI (*Abstract Co-Author*) Nothing to Disclose Ryan Kuhnlein, Bloomfield, MI (*Abstract Co-Author*) Nothing to Disclose Melody Dankha, Pontiac, MI (*Abstract Co-Author*) Nothing to Disclose Diyan Raza, Pontiac, MI (*Abstract Co-Author*) Nothing to Disclose Grygori Gerasymchuk, MD, Troy, MI (*Abstract Co-Author*) Nothing to Disclose

### PURPOSE

The purpose of this study was to examine medical students' abilities to recognize important radiological findings on plain film and computed tomography (CT) scans.

## METHOD AND MATERIALS

An online survey invitation was sent to third and fourth-year medical student rotating at our institution. The questionnaire contained ten radiological images, including both positive and negative plain film and CT studies. Students were asked to describe the pertinent finding in each image. Additional information was gathered about each respondent, including year of study, clinical rotations completed, confidence in interpreting radiological imaging, preparation and desired residency specialty.

### RESULTS

Sixty-one (61) completed surveys were received and analyzed. The majority of students were not able to correctly identify important imaging findings, with an overall average of 29% correct responses. The normal chest radiograph was most correctly identified, at 59%; acute pancreatitis on CT had the lowest correct response rate at 3.1%. Having completed an intensive care unit (ICU) rotation was associated with better diagnostic ability (approaching significance, p=0.054). When plain film chest radiographs were analyzed separately, students who completed an ICU rotation were significantly better able to make the correct diagnosis (p<0.01). Neither the completion of any other clinical rotation, nor desired residency specialty, was correlated with improved diagnostic ability. Likewise, students' year of study did not show any significance.

## CONCLUSION

Radiology education is a crucial yet often overlooked aspect of medical education. Although a radiologists' insightful interpretation of complex studies will always play an important role in guiding patient care, every physician should posses the ability to accurately recognize basic and common disease processes. Based on the findings of this study, medical students are not adequately prepared to diagnose important diseases on radiological studies. Therefore, a heavier emphasis should be placed on teaching students how to accurately interpret medical imaging, both during basic sciences and clinical years, to help foster well-rounded physicians.

### **CLINICAL RELEVANCE/APPLICATION**

Medical students must be provided with greater exposure to radiology, in order to ensure that they can adequately interpret basic imaging findings.

## HP228-SD-WEA3

Evidence-Based Surveillance Imaging Schedule after Liver Transplantation for Hepatocellular Carcinoma Recurrence

Wednesday, Nov. 30 12:15PM - 12:45PM Room: HP Community, Learning Center Station #3

## Participants

Dan Liu, PhD, MSc, Hong Kong, Hong Kong (*Abstract Co-Author*) Nothing to Disclose Chi Yan A. Chan, MBBS, Hong Kong, Hong Kong (*Abstract Co-Author*) Nothing to Disclose Daniel Y. Fong, PhD, Hong Kong, Hong Kong (*Abstract Co-Author*) Nothing to Disclose Chung-Mau Lo, MS, Hong Kong, Hong Kong (*Abstract Co-Author*) Nothing to Disclose Pek Lan Khong, MBBS, FRCR, Hong Kong, Hong Kong (*Presenter*) Nothing to Disclose

## PURPOSE

here is presently no evidence-based recommendation for surveillance of recurrent hepatocellular carcinoma (HCC) after liver transplantation (LT). We aim to evaluate and develop evidence-based alternate surveillance imaging schedules for post LT HCC patients.

## METHOD AND MATERIALS

Imaging and pathologic reports for consecutive post-LT patients followed-up by regular surveillance imaging from a single institution's prospective database were evaluated with institutional review board approval. Outcome variable was time to diagnosis of first recurrence post-LT by surveillance imaging. Recurrence-free survival times (RFST) from alternative surveillance schedules were compared with the existing schedule (3-monthly) using a parametric frailty model. Expected delay (EpD) in diagnosis compared to the existing schedule was also computed for the alternate surveillance schedules. A p value of less than 0.05 was considered to indicate a significant difference.

### RESULTS

One hundred twenty five patients (108 men; 59.4 years  $\pm$ 16.6) underwent 1953 CT and 255 MRI scans. RFST was not significantly different in the first five years after LT when the imaging interval was extended from current 3-monthly to 6-monthly (p=0.786, EpD= 55 days). This alternative schedule incurred ten (50.0%) fewer surveillance scans than the 20 in the original schedule, and a corresponding reduction in radiation dose (if involved) and cost during the 5-year follow-up period.

## CONCLUSION

In conclusion, modeled alternative surveillance schedules have the potential to reduce the frequency of scans without compromising surveillance benefits.

### **CLINICAL RELEVANCE/APPLICATION**

Extending imaging surveillance schedules to 6-monthly from 3-monthly offers reduced frequency of scans without compromising surveillance benefits in post-transplant hepatocellular carcinoma patients.

Power to the People: A Multi-institutional United States Survey in Adult and Pediatric Teaching Hospitals on Patient Preferences for Information Before their Radiology Exams

Wednesday, Nov. 30 12:15PM - 12:45PM Room: HP Community, Learning Center Station #4

### Participants

Jay K. Pahade, MD, New Haven, CT (*Presenter*) Consultant, Precision Imaging Metrics, LLC Andrew T. Trout, MD, Cincinnati, OH (*Abstract Co-Author*) Advisory Board, Koninklijke Philips NV; Travel support, Koninklijke Philips NV ; Author, Reed Elsevier; Research Grant, Siemens AG Bin Zhang, PhD, Cincinnati, OH (*Abstract Co-Author*) Nothing to Disclose Victorine V. Muse, MD, Boston, MA (*Abstract Co-Author*) Nothing to Disclose Lisa R. Delaney, MD, Carmel, IN (*Abstract Co-Author*) Nothing to Disclose Pradeep G. Bhambhvani, MD, Birmingham, AL (*Abstract Co-Author*) Nothing to Disclose Evan J. Zucker, MD, Boston, MA (*Abstract Co-Author*) Nothing to Disclose Pari Pandharipande, MD, MPH, Boston, MA (*Abstract Co-Author*) Nothing to Disclose James A. Brink, MD, Boston, MA (*Abstract Co-Author*) Nothing to Disclose Marilyn J. Goske, MD, Cincinnati, OH (*Abstract Co-Author*) Nothing to Disclose

#### PURPOSE

To assess what information patients find useful before their imaging exam, who they want the information from, and how preference varies based on demographics and patient specific variables

### **METHOD AND MATERIALS**

A 24 item survey assessing preferences on receiving information prior to an imaging exam, and which specific information was most valued was distributed at 3 pediatric and 3 adult hospitals across the U.S.. Chi-square or Fisher's exact test (categorical variable) and one way ANOVA or two sample t-test (continuous variable) were used for comparison between groups. Multivariate logistic regression with stepwise selection was used to determine the association between survey responses and demographics.

## RESULTS

1542/1742 (89%) surveys were at least partially completed. Mean respondent age was  $46.2\pm16.8$  years with respondents more frequently female (1025/1506, 68%), Caucasian (1132/1504, 75%) and English speaking (1428/1542, 95%) and 86.5% (1249/1542) having undergone prior imaging. 78% (1117/1438) had received information about their exam (range 64% - 88% across sites), most commonly from the ordering provider (824/1292, 64%). Exam type (p<0.0001) and years of schooling (p=0.0084) predicted whether information was provided and site, race and exam type predicted who provided information (all p<0.0001). The ordering provider was the preferred source of pre-exam information (72.4%, 1005/1388). Half of respondents (52%, 57/1452) had sought exam information themselves, most commonly through the ordering provider (33.6%, 430/1279) and non-radiology websites (31.2%, 399/1279). Respondents assigned the highest importance to information on test preparation (mean Likert 4.2±1.3) and the lowest importance to whether an alternative radiation-free exam could be utilized (mean Likert:  $3.6\pm1.4$ ).

## CONCLUSION

More than 20% of patients are not receiving any information prior to radiologic testing. Ordering providers are providing the majority of information and this is the preferred method of receiving information for patients. Patients are most interested in information related to test preparation and least interested in information related to radiation exposure.

### **CLINICAL RELEVANCE/APPLICATION**

This study provides insight into patient preferences regarding pretest information and should help design, improve and implement a more patient-centric model of healthcare delivery in Radiology.

## HP230-SD-WEA5

Teaching Radiologists Who Perform Image Guided Interventions Effective Communication Skills through Simulation

Wednesday, Nov. 30 12:15PM - 12:45PM Room: HP Community, Learning Center Station #5

## Participants

Carolynn M. DeBenedectis, MD, Worcester, MA (*Presenter*) Nothing to Disclose Max P. Rosen, MD, MPH, Worcester, MA (*Abstract Co-Author*) Stockholder, Everest Scientific Inc; Consultant, PAREXEL International Corporation; Stockholder, Cynvenio Biosystems, Inc; Medical Advisory Board, Cynvenio Biosystems, Inc

#### PURPOSE

Communication for Radiologists (RADS) performing interventional procedures (IR) may be challenging, as often patients do not meet the RAD until the day of the procedure, and procedures are often performed with conscious sedation, making effective communication with the patient essential. The purpose of this project was to create a workshop to teach IR RADS to communicate more effectively with the patients during procedures.

### **METHOD AND MATERIALS**

7 attending RADS (in groups of 2 or 3) participated in 3 workshops at our simulation center. All workshops were conducted with professional actor-patients, who had been trained in simulation. Each workshop involved 4 communication scenarios: 1) Obtain informed consent, 2) Discuss the need to change/cancel a procedure, 3) Deal with a combative patient, and 4) Disclosure and apology for an error. One RAD participated in each simulation while the other 1-2 RADS watched (via video monitors) in the debriefing room. A debriefing/teaching session followed, and then another simulation occurred with a different RAD participating in the next simulation. Pre and post simulation surveys were obtained from each RAD.

#### RESULTS

Prior to and after undergoing the training/simulations, all 7 RADS rated their comfort with the 4 scenarios. 71.4% strongly agreed they felt very comfortable performing informed consent before the workshop vs. 85.7% after (+14.3%). 57.1% strongly agreed they felt very comfortable talking to patients about having to change/cancel a procedure before the workshop vs. 71.4% after (+14.3%). 14.3% strongly agreed they felt very comfortable dealing/communicating with a combative patient before the workshop vs. 57.1% after (+42.8%). 14.3% strongly agreed they felt very comfortable disclosing and apologizing for errors before the workshop vs. 57.1% after (+42.8%).

## CONCLUSION

Communication skills simulation workshops can be an important component of Radiologists' professional development and ongoing training. The participants felt more comfortable in all the scenarios after the workshop with the greatest increase reported in dealing/communicating with combative patients and disclosing and apologizing for errors during IR procedures.

### **CLINICAL RELEVANCE/APPLICATION**

Workshops that teach radiologists' effective communication skills may increase radiologists' comfort communicating with patients during image guided procedures.

## A Web-based System for Patient-Oriented Reports in Musculoskeletal Imaging

Wednesday, Nov. 30 12:15PM - 12:45PM Room: IN Community, Learning Center Custom Application Computer Demonstration

#### **Participants**

Sri Ram T. Sathi, MD, Philadelphia, PA (*Abstract Co-Author*) Nothing to Disclose Tessa S. Cook, MD, PhD, Philadelphia, PA (*Abstract Co-Author*) Nothing to Disclose Charles E. Kahn JR, MD, MS, Philadelphia, PA (*Presenter*) Nothing to Disclose

### CONCLUSION

PORTER can be incorporated into patient portals to annotate and help explain radiology reports without storing or exchanging protected health information. The system has been applied to a wide range of musculoskeletal imaging procedures, and is presented for demonstration.

#### Background

Patients frequently have access to their radiology reports through online patient portals. Although the reports can help patients become better informed and participate more actively in their care, the language of radiology reports remains challenging to understand. The PORTER (Patient-Oriented Radiology Reporter) system applies a lay-language glossary of words and phrases from radiology reports to improve patients' understanding.

## **Evaluation**

From an original prototype system of 314 terms for knee MRI reports, PORTER's vocabulary has been expanded to more than 800 terms to address the most common imaging procedures of the musculoskeletal system. Its glossary includes synonyms, abbreviations, plurals, and adjectival forms. A web service uses a secure HTTP POST transaction; it takes as input the text of the radiology report and the imaging procedure's RadLex Playbook code. The web service generates an HTML document that highlights terms in the report that are defined in PORTER's glossary of musculoskeletal imaging terms. No personally-identifiable information is exchanged. Glossary terms are highlighted; when the reader's mouse hovers over a glossary term, a pop-up balloon provides the lay-language definition, which may be supplemented by a link to a relevant public reference such as Wikipedia. Relevant illustrations, if available, can be displayed in a sidebar. Mechanisms have been incorporated to track user interactions, such as the terms over which the reader hovers or clicks.

## Discussion

PORTER annotates radiology reports with lay-language definitions and illustrations to help improve patients' understanding. The expanded vocabulary allows the system to address a wide range of frequently performed imaging procedures. This interactive exhibit provides a live demonstration of the system.

## **Honored Educators**

Presenters or authors on this event have been recognized as RSNA Honored Educators for participating in multiple qualifying educational activities. Honored Educators are invested in furthering the profession of radiology by delivering high-quality educational content in their field of study. Learn how you can become an honored educator by visiting the website at: https://www.rsna.org/Honored-Educator-Award/

Charles E. Kahn JR, MD, MS - 2012 Honored Educator

# Multi-reader Studies: Encountered Problems and Solutions in Prostate mpMRI

Wednesday, Nov. 30 12:15PM - 12:45PM Room: IN Community, Learning Center Station #7

#### **Participants**

Matthew Greer, BS, Cleveland Heights, OH (Presenter) Nothing to Disclose

Joanna Shih, Bethesda, MD (Abstract Co-Author) Nothing to Disclose

Peter L. Choyke, MD, Rockville, MD (*Abstract Co-Author*) Researcher, Koninklijke Philips NV; Researcher, General Electric Company; Researcher, Siemens AG; Researcher, iCAD, Inc; Researcher, Aspyrian Therapeutics, Inc; Researcher, ImaginAb, Inc; Researcher, Aura Biosciences, Inc

Baris Turkbey, MD, Bethesda, MD (Abstract Co-Author) Nothing to Disclose

### **TEACHING POINTS**

Multi-reader studies are a powerful clinical research tool to assess accuracy and agreement of readers of varying experience across institutions. However, these can be complicated by logistical issues of delivering DICOM images between institutions, collecting reliable data, correlating subjective reads between readers, and analyzing complex data. We have developed a methodology to anonymize DICOMs, collect large amounts of data using readily available Microsoft Access applications, and assess inter-observer agreement for prospectively detected and scored lesions. We will use prostate mpMRI studies as an example of how these principles can be applied to multiple radiological setting.

## TABLE OF CONTENTS/OUTLINE

DICOM Cleaning Tools User-friendly freeware can anonymize patient information (**Figure 1**) Facilitated data accrual to ensure data integrity Paper based reporting tools result in unreported variables (**Figure 2**) Microsoft Access tools can offer solutions to enforce data integrity (**Figure 3** and **Figure 4**) In prospective oncological lesion detection, agreement between readers is best assessed with the index of specific agreement (ISA). Kappa statistics do not adequately assess scoring agreement in prospective lesion detection. ISA provides an appropriate measure for prospective lesion detection (**Figure 5**)

## IN240-SD-WEA1

Validation of Natural Language Processing Tools for Identification of Pulmonary Embolism in Clinica Alemana Between 2013-2014

Wednesday, Nov. 30 12:15PM - 12:45PM Room: IN Community, Learning Center Station #1

#### Awards

### **Student Travel Stipend Award**

#### **Participants**

Esteban E. Hebel, MD, Santiago, Chile (*Presenter*) Nothing to Disclose Guillermo J. Ortiz, MD, Santiago, Chile (*Abstract Co-Author*) Nothing to Disclose Claudio Silva Fuente-Alba, MD, Santiago, Chile (*Abstract Co-Author*) Nothing to Disclose

#### CONCLUSION

Our study proves that the use of NLP has a very high performance for identification of patients with PE.

#### Background

The extensive adoption of picture archiving and communication systems (PACS) has enabled access to a great volume of valuable information for institutional work. Natural language processing (NLP) has proven to be effective in analyzing the content of reports to identify diagnosis and patient characteristics. Unfortunately, very little has been done in Spanish. Such a tool would allow identifying cases of interest among a large volume of non-structured reports. The objective of this study was to develop and evaluate multipurpose NLP software for detection of pulmonary embolism (PE) cases among computed tomography pulmonary angiography (CTPA) reports in our center between 2013-2014.

#### **Evaluation**

In this IRB approved study, all diagnosis were tagged (using SNOMED-CT terminology) in a significant random sample of the 1973 CTPAs performed (n=219), in search of concepts and relevant relationships, such as negations and timing of the diagnosis on each report's conclusion. A classifier was developed that would identify relevant studies for PE and its negations. The classification models were assessed using measures of precision, recall and F-measure. Statistical significance was calculated using a x2 test for dichotomical variables, considering a p-value of 0.05, and estimating 95% confidence intervals when feasible. Out of all the CTPAs, a total of 51.4 percent were performed to women, with a median age of 57.9 years (IQR: 44-72). The tool correctly identified 26 (11.9%) positive studies and 190 negative studies for current PE. It failed to identify one case and miscategorized two cases as positive. The software obtained a F-measure of 0.946, with precision and recall of 92.9% and 96.3% respectively (p<0.001).

#### Discussion

Much of the report information in PACS persists in free-text format, which is a challenge to be used for research, teaching or quality improvement. Although our software was designed to study one condition in particular, it was developed with multipurpose in mind by using SNOMED-CT, in order to use non-structured information from radiology reports in any clinical context.

# IN241-SD-WEA2

# Addressing the Challenges of Patient Problem Lists with Radiology Structured Reporting

Wednesday, Nov. 30 12:15PM - 12:45PM Room: IN Community, Learning Center Station #2

#### Participants

David J. Vining, MD, Houston, TX (*Presenter*) Royalties, Bracco Group; CEO, VisionSR; Stockholder, VisionSR Andreea Pitici, Houston, TX (*Abstract Co-Author*) Employee, COMPUTER PATRISOFT SAC Adrian Prisacariu, Houston, TX (*Abstract Co-Author*) Employee, COMPUTER PATRISOFT SAC Mark Kontak, Houston, TX (*Abstract Co-Author*) Consultant, VisionSR, Inc

# CONCLUSION

Many critical deficiencies exist today with patient problem lists. Radiology structured reporting employing SNOMED-CT coding and filtering by medial priorities and disease timeline analysis can be used to create meaningful and relevant PPLs.

#### Background

The creation of patient problem lists (PPLs) containing current and active diagnoses for each patient in an electronic health record (EHR) was mandated in Meaningful Use Stage 1, and this was followed by Stage 2 which required diagnoses to be coded with SNOMED-CT terminology. Many problems confront the creation of meaningful PPLs including the lack of EHR tools to achieve efficient coding, under-coding (e.g., selecting pneumonia vs. viral pneumonia), incorrect coding, failure to code, over-coding with exceedingly long lists, and not updating lists to include only active diagnoses. A solution to these problems is found in a radiology structured reporting system since image findings form the basis of many PPL diagnoses.

#### **Evaluation**

We develop a structured reporting system that captures key images and voice descriptions of each image finding, tags the images with SNOMED-CT terms, and assembles a multimedia structured report that is organized by anatomical categories or medical priorities. Each diagnosis is prioritized on a 5-point scale to indicate a level of action required by a clinician: 1 Incidental, 2 Important (needs serial monitoring), 3 Indeterminate (needs further evaluation), 4 Urgent, 5 Life-threatening. The system links related serial findings in disease timelines to calculate temporal data for each finding. The list of radiological findings can be filtered to exclude incidental findings and those that have been inactive for a period of time. As a result, dynamic PPLs can be generated to supplement EHR PPLs.

# Discussion

Multimedia structured reporting provides a means to not only create standardized radiology reports but also create lists of radiological diagnoses that can supplement an EHR PPL. The implementation of filtering to exclude incidental findings and inactive problems can help to guide PPLs to support meaningful use and clinical quality measures.

# IN242-SD-WEA3

Segmentation Label Propagation using Deep Convolutional Neural Networks and Dense Conditional Random Field

Wednesday, Nov. 30 12:15PM - 12:45PM Room: IN Community, Learning Center Station #3

FDA Discussions may include off-label uses.

### Participants

Mingchen Gao, PhD, Bethesda, MD (*Presenter*) Nothing to Disclose Ziyue Xu, PhD, Bethesda, MD (*Abstract Co-Author*) Nothing to Disclose Le Lu, PhD, Bethesda, MD (*Abstract Co-Author*) Nothing to Disclose Aaron Wu, Bethesda, MD (*Abstract Co-Author*) Nothing to Disclose Isabella Nogues, BA, Bethesda, MD (*Abstract Co-Author*) Nothing to Disclose Ronald M. Summers, MD, PhD, Bethesda, MD (*Abstract Co-Author*) Royalties, iCAD, Inc; ; Daniel J. Mollura, MD, Bethesda, MD (*Abstract Co-Author*) Nothing to Disclose

#### PURPOSE

Incomplete labeling is a common issue within medical image datasets due to the labor-intensive and expert-driven nature of annotations. In this work, we describe a segmentation-based propagation method that fully annotated datasets based on partial labeling.

### **METHOD AND MATERIALS**

Robust supervised learning within medical image analysis relies upon the availability and accessibility of large-scale annotated datasets. However, many datasets are only partially labeled. For instance, on the publicly available University Hospitals of Geneva (UHG) interstitial lung disease (ILD) dataset, less than 15% of the lung region is labeled, significantly restricting the amount of training data. To address this problem, our method uses the features from the incomplete manual annotations to propagate labels to unlabeled regions. We first employ a deep convolutional neural network (CNN) to predict the label of each unannotated pixel independently. While CNNs are state-of-the-art, they do not consider the correlation between pixels. For this reason, we refine the CNN output using a dense fully-connected conditional random field, incorporating locality and intensity similarity into the label propagation. This produces more coherent and finer annotations.

#### RESULTS

The proposed algorithm was evaluated on the UHG dataset, which contains 120 CT scans with partial ILD annotations. After label propagation, the resulting accuracy reaches 92.8% compared to expert manual annotations. Importantly, our method increases the amount of labeled pixels by 7.8 times. As well, differing from the partial annotations, which only labeled one ILD disease per CT slice, our method is able to label all diseases that occur on the same slice, which is crucial for future slice-wise disease detection. This demonstrates another important facet in how our method can augment partial annotations.

# CONCLUSION

We present a segmentation label propagation method that accurately populates labels from annotated regions to entire datasets. When tested on an IDL dataset, the amount of labeled training data is substantially and accurately expanded. We plan to publicly share this and other expanded datasets, upon publication.

# **CLINICAL RELEVANCE/APPLICATION**

Our method is applicable to any multi-class segmentation problem. Combined with expert annotations, the proposed system could be used to iteratively produce fully-labeled large-scale datasets.

Evaluating Vertebral Bone Strength Prediction by Advanced Characterization of Trabecular Microarchitecture using Scaling Index Computation on Volumetric Quantitative Computed Tomography

Wednesday, Nov. 30 12:15PM - 12:45PM Room: IN Community, Learning Center Station #4

# Participants

Anas Z. Abidin, MS, Rochester, NY (*Presenter*) Nothing to Disclose Adora M. D'Souza, MSc, Rochester, NY (*Abstract Co-Author*) Nothing to Disclose Mahesh B. Nagarajan, PhD, Los Angeles, CA (*Abstract Co-Author*) Nothing to Disclose Thomas Baum, MD, Munich, Germany (*Abstract Co-Author*) Nothing to Disclose Axel Wismueller, MD, PhD, Rochester, NY (*Abstract Co-Author*) Nothing to Disclose

# PURPOSE

To use advanced geometric characterization of the trabecular bone microarchitecture in spinal vertebrae for improved fracture risk assessment.

## **METHOD AND MATERIALS**

Volumetric CT data (0.14 x 0.14 x 0.3 mm^3 resolution) was acquired from 19 spinal vertebrae specimens using a whole-body 256row CT scanner with a dedicated calibration phantom. Each sample consisted of three vertebral segments; the images of the central vertebra were used for analysis. After imaging, the true failure load was measured through a biomechanical test involving uni-axial compression on the middle vertebra of the specimen. A semi-automated method was used to annotate the trabecular compartment within a cylindrical volume of interest (VOI) to exclude cortical bone in each sample, and voxel intensities within the VOI were converted to bone mineral density (BMD). A 3D geometric analysis technique based on local scaling properties (Scaling Index Method, SIM) was used to characterize the microarchitecture of the trabecular bone. The high-dimensional SIM features and the mean BMD of the VOI (which served as a surrogate for the current clinical standard) were used with support vector regression to predict the specimen failure load. The performance was measured by computing the root-mean-square error (RMSE) between the actual and the predicted failure load. A Wilcoxon signed-rank test was used to identify significant differences between RMSE distributions.

### RESULTS

Geometric SIM features outperformed CT-measured mean BMD (RMSE =  $1.11 \pm 0.33$ ) (p < 0.01). The best failure load prediction performance was obtained when SIM-derived features were combined with mean BMD (RMSE =  $0.79 \pm 0.11$ ).

## CONCLUSION

Our results suggest that advanced methods for characterization of the trabecular microarchitecture can significantly improve biomechanical bone strength prediction in spinal vertebrae. We conclude that our method has the potential to improve spinal fracture risk estimation over traditional BMD measurement.

# **CLINICAL RELEVANCE/APPLICATION**

Geometric characterization of trabecular microarchitecture in osteoporotic spinal vertebrae can improve image-based vertebral fracture risk estimation and thus contribute to better therapy management.

## IN245-SD-WEA6

A Novel Tool to Convert MIRC Teaching Files into Interactive Mobile eBooks for Precision Medical Imaging Education

Wednesday, Nov. 30 12:15PM - 12:45PM Room: IN Community, Learning Center Station #6

# Participants

Tsung-Lung Yang, MD, Kaohsiung, Taiwan (*Presenter*) Nothing to Disclose Huay-Ben Pan, MD, Kaohsiung, Taiwan (*Abstract Co-Author*) Nothing to Disclose Wei-Juhn Chen, Kaosiung, Taiwan (*Abstract Co-Author*) Nothing to Disclose

#### CONCLUSION

With this new application, we enhance the merits of MIRC TFS into a precision interaction for medical imaging education and we believe that this innovation could be used to ease the steep learning curve of modern radiology.

#### Background

In order to complement the apprenticeship of medical imaging education from on-the-scene finger-pointing or cursor-pointing to off-sight interactive engagement, we invent a novel tool to marry the beauty of MIRC TFS, giving birth to interactive eBooks compatible with current available platforms.

#### **Evaluation**

A new plug-in application was developed on the existing eBook teaching and knowledge platform for medical education. This plug-in was endowed with the functions to parse the XML files embedded in the MIRC TFS zip files as well as the scalable vector graphics (SVGs) created by authors to annotate the regions of interests of the images. Then this novel application could automatically transcript the annotated information of the SVGs into the events of interaction of lesion identification on mobile apps or HTML5 web pages for readers by using reader's finger tips. And all the associated transaction data from the learning interaction could be collected for teaching analytical purposes.

#### Discussion

The associated data collected during learning or reading include the number of clicks and the time needed to hit the right targets as well as the inter-reader differences for paticular quizzes. For example, a finding of architecture distortion on a right MLO view of tomosynthesis could be rendered as a hot spot of stacked images using our plug-in application then the residents in training could be able to swipe the images to find and depict the lesions using his or her finger tip. While the regions of interest on the right image was hit by the resident, a hurrah sign will popup to show approval, otherwise a disapproval sign will show up.

# MI220-SD-WEA1

Development of a Patient Derived Xenograft Model for Ultrasound Molecular Imaging Applications in Regnal Cell Carcinoma

Wednesday, Nov. 30 12:15PM - 12:45PM Room: S503AB Station #1

FDA Discussions may include off-label uses.

#### Participants

Ingrid Leguerney, Villejuif, France (*Abstract Co-Author*) Nothing to Disclose Alexandre Ingels, MD, Villejuif, France (*Presenter*) Nothing to Disclose Catherine Sebrie, Orsay, France (*Abstract Co-Author*) Nothing to Disclose Laurene Jourdain, Orsay, France (*Abstract Co-Author*) Nothing to Disclose Jean-Jacques Patard, Le Kremlin-Bicetre, France (*Abstract Co-Author*) Nothing to Disclose Nathalie B. Lassau, MD, PhD, Villejuif, France (*Abstract Co-Author*) Speaker, Toshiba Corporation; Speaker, Bracco Group

# PURPOSE

To develop a reliable in vivo model to assess by ultrasound and MRI imaging techniques tumor development and local molecular expressions

# **METHOD AND MATERIALS**

The model used is a patient derived xenograft: a 8 mm tumor core is gathered from a fresh renal cell carcinoma (RCC) at time of surgery. The tissue core is cut in homogenous 300 µm slices with a dedicated device (Krumdieck, Alabama Research & Development). Each slice is engrafted under renal capsula of RAG2-/-Yc-/- immunocompromised mice in order to develop a cohort with the same tumor. The tumor engrafted is routinely followed-up with ultrasound (US) imaging (Aplio, Toshiba and VEVO2100, Visualsonics). Once the tumor is detected, a first 7T MRI (Bruker spectrometer) is performed in order to measure precisely the tumor volume and series of US molecular imaging are performed.US molecular imaging is based on microbubble contrast agents linked with antibodies through (MicroMarker™, Visualsonics). The antibodies selected for our RCC study are VEGFR1 and 2 and FSHR. The targeted signal enhancement is quantified and compared with the untargeted microbubble signal 10 minutes after injection. Imaging is performed. The specific targeted US imaging signal is compared with the MRI specific growth rate (ln(V2/V1)/(t2-t1)) through a Spearman's correlation index to search for a correlation. The targeted US imaging signal at 1 month is compared with the same antibody immunohistochemistry expression from the paraffin embedded graft.

#### RESULTS

At this stage, seven tumors have been gathered and implanted. Tumor volumes measured by MRI on the 1rst cohort of mice (n=7) ranged between 118.39 and 390.40 mm3. We performed a first US molecular imaging session using VEGFR2 targeting versus non-targeted contrast agents. We observed a difference in expression between targeted and non-targeted microbubbles by a factor of about 3.5. Initial analyzes indicate that the expression of VEGFR2 marking is correlated with tumor volume.

### CONCLUSION

The patient derived xenograft is a feasible model for molecular imaging studies. These preliminary results are encouraging to follow up the molecular imaging with the other markers (VEGFR1 and FSHR).

# **CLINICAL RELEVANCE/APPLICATION**

Good pre-clinical models are paramount to better tailored clinical trials in molecular imaging

# MI221-SD-WEA2

Designed Multifunctional Gold Nanocomposites for Targeted Tri-mode CT/ MR/ Optical Imaging of Human Non-small Cell Lung Cancer Cells

Wednesday, Nov. 30 12:15PM - 12:45PM Room: S503AB Station #2

#### Awards

#### **Trainee Research Prize - Medical Student**

#### **Participants**

Jingwen Chen, Shanghai, China (*Presenter*) Nothing to Disclose Qian Chen, Shanghai, China (*Abstract Co-Author*) Nothing to Disclose Gui-Xiang Zhang, MD, Shanghai, China (*Abstract Co-Author*) Nothing to Disclose Xiang-Yang Shi, Shanghai, China (*Abstract Co-Author*) Nothing to Disclose Han Wang, MD, PhD, Shanghai, China (*Abstract Co-Author*) Nothing to Disclose

#### PURPOSE

The high incidence and mortality rate of non-small cell lung cancer (NSCLC) prompts exhaustive efforts to develop new effective methods for its diagnosis at the early-stage to improve the survival rate. We are developing multifuctional gold nanocomposites to use as the nanoprobes for targeted tri-mode CT / MR / optical imaging of human non-small cell cancer cells both in vitro and in vivo.

## METHOD AND MATERIALS

Amine-terminated generation 5 poly(amidoamine) dendrimers were used as a nanoplatform to be covalently modified with Gd chelator, Cy5.5, and FA. Then the multifunctional dendrimers were used as templates to entrap gold nanoparticles, followed by chelating Gd(III) ions and acetylation of the remaining dendrimer terminal amines. The thus-formed multifunctional Au DENPs (in short, Cy5.5-Gd-Au DENPs-FA) were characterized via different techniques, and then were used for both in vitro and in vivo targeted CT/ MR/ NIR optical tri-mode imaging of human NSCLC cells (NCI-H460 cells) and the xenograft tumor model.

#### RESULTS

CT/MR/optical images show that NCI-H460 cells can be detected after incubation with the Cy5.5-Gd-Au DENPs-FA in vitro and the xenograft tumor model can be imaged after intravenous administration of the particles. Combine the inductively coupled plasmaatomic emission spectroscopy (ICP-AES) measurements with the transmission electron microscopy (TEM) data confirm that the Cy5.5-Gd-Au DENPs-FA is able to be uptaken by the treated cells. MTT (3-(4,5-dimethylthiazol-2-yl)-2,5-diphenyltetrazolium bromide) assay show that the Cy5.5-Gd-Au DENPs-FA has a good biocompatibility at the given concentration range.

#### CONCLUSION

The findings of this study suggest that the developed Cy5.5-Gd-Au DENPs-FA may be used as a promising tri-mode nanoprobe for targeted CT/MR/opticl imaging of human NSCLC and other folate receptor (FR) over-expressing cancers.

### **CLINICAL RELEVANCE/APPLICATION**

In consideration of the special structural characteristic, the dendrimer based nanocomposites may be further modified with therapeutic antibodies or small interfering RNA (siRNA) to be expectably developed for the personalized theranostics of cancers at early-stage with the high accuracy and sensitivity.

**Toes: Anatomy, Pathology and Common Surgical Procedures** 

Wednesday, Nov. 30 12:15PM - 12:45PM Room: MK Community, Learning Center Station #7

#### **Participants**

Adam D. Singer, MD, Atlanta, GA (*Presenter*) Nothing to Disclose Jason Bariteau, Atlanta, GA (*Abstract Co-Author*) Nothing to Disclose Yara Younan, MD, Atlanta, GA (*Abstract Co-Author*) Nothing to Disclose Walter A. Carpenter, MD, PhD, Atlanta, GA (*Abstract Co-Author*) Nothing to Disclose Jean Jose, MS, DO, Miami Beach, FL (*Abstract Co-Author*) Nothing to Disclose Ty K. Subhawong, MD, Miami, FL (*Abstract Co-Author*) Nothing to Disclose Monica B. Umpierrez, MD, Atlanta, GA (*Abstract Co-Author*) Nothing to Disclose

## **TEACHING POINTS**

1. The complex anatomy of the toes can make their imaging evaluation challenging2. A thorough knowledge of the toe anatomy helps to understand function and to detect developing pathological states3. In combination with physical examination, good multimodality imaging techniques can assist in diagnosing toe pathology and can help guide treatment4. Toe pathology is common and it is important for the radiologist to be familiar with commonly performed surgeries when interpretting post-operative imaging

#### **TABLE OF CONTENTS/OUTLINE**

1. Osseous and soft tissue toe anatomya. The great toeb. Lesser toes2. Pathophysiology of the toesa. Hallux valgus, varus and rigidusb. Hammer and mallet toesc. Hallux sesamoid injuryd. Turf toee. Bunion and bunionettef. Frieberg infractiong. Neuromah. Metatarsalgia3. Clinical presentation and prevalence of various toe pathology4. Commonly encountered surgical procedures and complications

# A Review of Athletic Pubalgia: Synthesis at the Pubic Symphysis

Wednesday, Nov. 30 12:15PM - 12:45PM Room: MK Community, Learning Center Station #8

#### Awards Certificate of Merit

## Participants

Dana Lin, MD, New York, NY (*Presenter*) Nothing to Disclose Tony T. Wong, MD, New York, NY (*Abstract Co-Author*) Nothing to Disclose Jonathan K. Kazam, MD, New York, NY (*Abstract Co-Author*) Nothing to Disclose

# **TEACHING POINTS**

By the end of this educational exhibit, the participant should be able to: Define the anatomy of the tendinous origins and insertions at the symphysis pubis Describe the underlying biomechanics of injuries surrounding the symphysis pubis Develop a differential diagnosis for etiologies of groin pain in athletes

## TABLE OF CONTENTS/OUTLINE

I. Pre-test

II. Anatomy of the symphysis pubis and normal MR appearance Rectus abdominis Adductor longus Common aponeurosis Surrounding musculature including adductor brevis, obturator externus, obturator internus, pectineus Inguinal canalIII. Predisposing activities, clinical presentation, and physical examination

IV. Optimization of MR technique

V. Imaging findings Muscle strain Tendon tears – acute and chronic Avulsion injuries Bone marrow edema "Secondary cleft" Osteitis pubisVI. Differential diagnosis Visceral etiologies Labral pathology Infection Stress fracture Apophysitis Nerve entrapmentVII. Treatment

VIII. Post-test

# MK283-ED-WEA10

# Mechanisms and Patterns of Elbow Fracture: It is Not Tricky Anymore

Wednesday, Nov. 30 12:15PM - 12:45PM Room: MK Community, Learning Center Station #10

**FDA** Discussions may include off-label uses.

#### **Participants**

Eun Hae Park, Jeon Ju, Korea, Republic Of (*Presenter*) Nothing to Disclose Jung Hee Byun, Jeon Ju, Korea, Republic Of (*Abstract Co-Author*) Nothing to Disclose Jin Hee You, MD, Jeonju, Korea, Republic Of (*Abstract Co-Author*) Nothing to Disclose Gong Yong Jin, MD, PhD, Jeonju, Korea, Republic Of (*Abstract Co-Author*) Nothing to Disclose

# **TEACHING POINTS**

1. Introduce detail mechanism of elbow fracture (supracondylar, lateral condylar, medial epicondylarradial head, coronoid, radial head)2. Introduce cases of tricky elbow fractures : once you know the mechanism, it is not tricky anymore.

## **TABLE OF CONTENTS/OUTLINE**

1. Introduction of elbow joint and reason why radiologist needs to understand the mechanism2. Supracondylar fracture - mechanism, case, complications3. Lateral condylar fracture - mechanism, displacement stage, case, complications4. Medial epicondyle fracture - mechanism, case, complications - importance of ossification center - importance of right positioning when obtaining the radiograph5. radial head and coronoid process fracture - mechanism, case, complications - introduce posterolateral rotatory instability

# MK330-SD-WEA3

The Relationship between Disease Activity and Joint Involvement Evaluated by MRI in Patients with Rheumatoid Arthritis

Wednesday, Nov. 30 12:15PM - 12:45PM Room: MK Community, Learning Center Station #3

# Participants

Ronaldo G. Rondina, MD, Vitoria, Brazil (*Abstract Co-Author*) Nothing to Disclose Ricardo A. Mello, MD, Vitoria, Brazil (*Presenter*) Nothing to Disclose Elton Francisco P. Batista, MD, Vitoria, Brazil (*Abstract Co-Author*) Nothing to Disclose

## PURPOSE

To assess the relationship between disease activity measured by the Disease Activity Score (DAS28) and joint involvement evaluated bymagnetic resonance imaging (MRI) measured by Rheumatoid Arthritis MRI Scoring System (RAMRIS) in the clinicaly dominant foot of pacients with rheumatoid arthritis (RA).

## METHOD AND MATERIALS

We conducted a cross-sectional descriptive study of fifty-five patients diagnosed with RA between February and December 2014. The patients' clinically dominant foot were assessed by MRI and clinical and laboratory data were collected to measure the DAS28.

# RESULTS

The majority of patients classified as in clinical remission showed some inflammatory activity on MRI (67.5% synovitis or bone marrow edema, 53.6% just synovitis and 53.6% just bone marrow edema). The statistical analysis demonstrated no linear relationship between disease activity measured by the Disease Activity Score (DAS28) and RAMRIS even when its variables were analyzed separately.

### CONCLUSION

Despite of clinical remission assessed by DAS28, MRI evaluation can document a state of persistently active disease.

#### **CLINICAL RELEVANCE/APPLICATION**

Demonstrate that MRI can be a useful tool in managing the treatment of patients with RA.

# MK331-SD-WEA4

# Simplified CT Therapy Response Monitoring Criteria in Multiple Myeloma Undergoing Therapy

Wednesday, Nov. 30 12:15PM - 12:45PM Room: MK Community, Learning Center Station #4

#### **Participants**

Georg Bier, MD, Tubingen, Germany (*Presenter*) Nothing to Disclose Christoph Schabel, MD, Tubingen, Germany (*Abstract Co-Author*) Nothing to Disclose Katja Weisel, Tuebingen, Germany (*Abstract Co-Author*) Nothing to Disclose Maximilian M. Schulze, MD, Tuebingen, Germany (*Abstract Co-Author*) Nothing to Disclose Konstantin Nikolaou, MD, Tuebingen, Germany (*Abstract Co-Author*) Speakers Bureau, Siemens AG; Speakers Bureau, Bracco Group; Speakers Bureau, Bayer AG Marius Horger, MD, Tuebingen, Germany (*Abstract Co-Author*) Nothing to Disclose PURPOSE

To test for correlation between the course of size and CT-attenuation values of medullary lesions in the axial skeleton and that of established hematological myeloma-specific parameters for accurate monitoring multiple myeloma during bortezomib- or lenalidomide-based treatment.

#### **METHOD AND MATERIALS**

Reduced-dose whole-body CT examinations of 78 consecutive patients (43 male, 35 female, mean age 63.69±9.2 years) with stage III multiple myeloma were re-evaluated in retrospect. Either one medullary lesion located in the bone marrow cavities of the appendicular skeleton (right/left upper humerus, right/left femur) was defined as "target lesion" by 2 readers in consensus and lenght diameter, transverse diameter, and average CT-attenuation values both at baseline and follow-up were measured. The course of myeloma specific haematological biomarkers (M-gradient, light-chains and B2-microglobulin) was used for validation. Sensitivity and specificity were calculated after ROC-curve analysis. Multivariate analysis including primary component analysis was performed to test for patient-wise covariance and correlation.

# RESULTS

The lesion-based sensitivity/specificity values of lenght diameter vs. transverse diameter vs. CT attenuation were 94.4%/95.7% (AUC=.965) vs. 86.1%/92.2% (AUC=.953) vs. 72.2%/94.0% (AUC=.916) for progressive disease, 70.6%/85.0% (AUC=.89) vs. 77.8%/82.1% (AUC=-828) vs. 44.4%/72.5% (AUC=.625) for stable disease and 78.6%/93.3% (AUC=.965) vs. 73.2%/95.6% (AUC=.917) vs. 71.4%/83.3% (=.853) for therapy response. By measurement of 3 lesions per patient, the therapy response can be described in cumulatively 97.8% of the cases by the lenght diameter, in 97.2% by the transverse diameter and 92.5% by CT attenuation.

# CONCLUSION

The assessment of only 3 myeloma-associated medullary lesions per patient suffices for radiological therapy response assessment. In this regard, the lenght diameter of these lesions serves best followed by the transverse diameter and lesion attenuation.

## **CLINICAL RELEVANCE/APPLICATION**

Assessment of only three medullary multiple myeloma lesions durding treatment seems to be sufficient for correct classification of therapy response, which may serve as a basis for a simplified response criteria system.

MR Imaging and Clinical Findings of Lateral Epicondylitis: Comparison in Patients Treated with and without Arthroscopic Surgery and Factors Associated with Management Plans

Wednesday, Nov. 30 12:15PM - 12:45PM Room: MK Community, Learning Center Station #5

## Participants

Ji Young Jeon, Incheon, Korea, Republic Of (*Presenter*) Nothing to Disclose Min Hee Lee, MD, Seoul, Korea, Republic Of (*Abstract Co-Author*) Nothing to Disclose In Ho Jeon, Seoul, Korea, Republic Of (*Abstract Co-Author*) Nothing to Disclose Hye Won Chung, MD, Seoul, Korea, Republic Of (*Abstract Co-Author*) Nothing to Disclose Sang Hoon Lee, Seoul, Korea, Republic Of (*Abstract Co-Author*) Nothing to Disclose Myung Jin Shin, MD, Seoul, Korea, Republic Of (*Abstract Co-Author*) Nothing to Disclose

### PURPOSE

We compared MR imaging and clinical findings of lateral epicondylitis in patients treated conservatively and with arthroscopic surgery to identify factors associated with management plans.

# METHOD AND MATERIALS

60 patients with lateral epicondylitis who treated conservatively (n = 38) and with arthroscopic surgery (n = 22) were included. Two radiologists reviewed elbow MR images independently as follows: grade of common extensor tendon (CET) abnormality and size of tear which were measured as a maximum length on axial and coronal planes— grade 1, tendinosis or  $\leq$  2mm partial tear (PT); grade 2, 2 mm6 mm or complete tear, presence of increased signal in adjacent muscles, injury of RCL complex, synovitis/effusion, synovial fringe, increased signal of ulnar nerve, radiocapitellar joint space widening, chondral lesions. Clinical data recorded were frequency (intermittent/persistent), duration, NRS (numerical rating scale) of pain, trauma history, range of motion. MR imaging and clinical findings in both groups were compared and analyzed with univariate analysis and multivariable logistic regression models.

#### RESULTS

All MR imaging findings except a chondral lesions, frequency and NRS of pain were significantly different between both groups (p<0.05). Among them, factors with significant association (p<0.01) which were grade of CET abnormality and size of tear on axial and coronal planes, presence of increased signal in muscles, frequency of pain were tested with multivariable models. Grade of CET abnormality on coronal plane (grade 2, OR 343, p = 0.021; grade 3, OR 2922, p = 0.015, respectively), increased signal in muscles (one muscle, OR 156, p = 0.022; multifocal muscles, OR 116, p = 0.019) and persistent pain (OR 68, p = 0.006) were significant factors associated with surgical treatment.

#### CONCLUSION

In patients with lateral epicondylitis, MR imaging, along with pain characteristics, provided features of different severity between conservative and operative managements, and can assist in treatment planning by predicting conditions may require operative management.

#### **CLINICAL RELEVANCE/APPLICATION**

In lateral epicondylitis, grade of CET abnormality on longitudinal plane, increased signal in muscles on MR imaging and persistent pain were associated with conditions may require surgical treatment.

# MK333-SD-WEA6

Joint Space Width Contrast Dispersion Cartilage and Talar Dome Osteochondral Lesion Visibility during MRI Ankle using Finger Coil with Traction

Wednesday, Nov. 30 12:15PM - 12:45PM Room: MK Community, Learning Center Station #6

#### Awards

**Student Travel Stipend Award** 

#### Participants

Eric K. Law, MBChB, FRCR, Hong Kong, China (*Presenter*) Nothing to Disclose Ka Lok Lee, MBChB, Shatin, Hong Kong (*Abstract Co-Author*) Nothing to Disclose James F. Griffith, MD, Shatin, Hong Kong (*Abstract Co-Author*) Nothing to Disclose Alex Ng, Hong Kong, Hong Kong (*Abstract Co-Author*) Nothing to Disclose David Yeung, Shatin, Hong Kong (*Abstract Co-Author*) Nothing to Disclose

#### PURPOSE

To assess the impact of axial traction during MRI of the ankle joint using finger coil to assess talar dome osteochondral lesion on joint space widening, contrast dispersion between cartilage surfaces, cartilage and talar dome osteochondral lesion visibility.

## METHOD AND MATERIALS

Prospective study of 33 patients with MRI ankle using finger coil, with and without axial traction. Two radiologists independently measured ankle joint space widths and semi-quantitatively graded contrast material dispersion between the opposing cartilage surfaces, and articular cartilage and osteochondral visibility allowing these parameters to be compared before and after traction. Patient were instructed to report on pain and complications.

#### RESULTS

The width of talotibial joint spaces (bone-bone distance and cartilage-cartilage distance,  $\Delta$ = 0.47-0.69mm, all p <0.05) was significantly greater in the traction than non traction. The amount of contrast and cartilage visibility of talotibial joint spaces significantly improved after traction (all p<0.05). Traction also significantly improved the visibility of cartilage part of the talar dome osteochondral lesion (p<0.05). No patient asked for termination of examination. There were no cases of neuropraxia.

### CONCLUSION

Traction MRI ankle is safe and technically feasible. This is the first study to evaluate the effect of traction on the MRI of ankle joint using finger coil for assessment of osteochondral lesion. There is beneficial effect of ankle traction on joint space widening, cartilage and talar dome osteochondral lesion visibility.

## **CLINICAL RELEVANCE/APPLICATION**

Better assessment of cartilage using traction in MR ankle is beneficial in detecting potential osteochondral lesion.

# MS120-ED-WEA1

Points and Pitfalls for Interpreting Digital Tomosynthesis Radiographs: What the Radiologist Needs to Know

Wednesday, Nov. 30 12:15PM - 12:45PM Room: MS Community, Learning Center Station #1

#### Participants

Haruhiko Machida, MD, Tokyo, Japan (*Presenter*) Nothing to Disclose Toshiyuki Yuhara, Tokyo, Japan (*Abstract Co-Author*) Nothing to Disclose Mieko Tamura, Tokyo, Japan (*Abstract Co-Author*) Nothing to Disclose Katelyn Nye, Waukesha, WI (*Abstract Co-Author*) Employee, General Electric Company John M. Sabol, PhD, Waukesha, WI (*Abstract Co-Author*) Employee, General Electric Company Takuya Ishikawa, Tokyo, Japan (*Abstract Co-Author*) Nothing to Disclose Eiko Ueno, MD, Chiyoda-Ku, Japan (*Abstract Co-Author*) Nothing to Disclose

### **TEACHING POINTS**

To describe imaging techniques and artifacts in digital tomosynthesis (DT) radiography To illustrate points and pitfalls for interpreting DT radiographs by presenting clinical images To demonstrate various clinical applications of DT radiography

### **TABLE OF CONTENTS/OUTLINE**

Imaging techniques and artifacts in DT DT scan: sweep direction/angle/number of projections 2D images: scout scan/synthesized views Reconstruction: slice interval/sampling factor/FBP/iterative reconstruction/oblique multiplanar reconstruction Artifacts: ripple/ghost/metallic/motion artifacts/limited depth resolution vs. CT Points and pitfalls for interpreting DT Evaluation of scout/synthesized 2D images Recognition of potential DT artifacts Optimization of reconstruction parameters/algorithms CT-like image review Understanding of spatial relationships/continuity in the slice direction Sensitive detection of calcified densities vs. conventional radiographs Understanding of image differences between DT and CT: patient positioning/imaging techniques/spatial and contrast resolution Clinical applications of DT Head & neck: sinonasal/dental disease Chest: pulmonary nodules Orthopedic: fracture detection/postoperative follow-up with metal implants/spine disease/joint space assessment Breast: breast cancer

A Comprehensive Approach to Managing Patient Radiation Exposure in Nuclear Medicine Gamma Camera Imaging: Combining Expert-based Guidelines with Practical and Efficacious Gamma Camera Technique to Lower Radiopharmaceutical Administered Activity

Wednesday, Nov. 30 12:15PM - 12:45PM Room: S503AB Station #11

#### **Participants**

Donna Eckstein, MD, New York, NY (*Abstract Co-Author*) Nothing to Disclose Shivam Shah, MD, North Brunswick, NJ (*Abstract Co-Author*) Nothing to Disclose Murray D. Becker, MD, PhD, New Brunswick, NJ (*Presenter*) Nothing to Disclose

## **TEACHING POINTS**

1. Goal: Obtain Diagnostic Images at The Lowest Patient Radiation Exposure.2. Primary Means of Lowering Patient Radiation Exposure is to Reduce Administered Activity.3. Expert Based Recommendations: Reference Level Surveys, Appropriateness Criteria, and Society Guidelines as a Framework for NM Laboratory Policies and Procedures.4. Understanding How Camera Technique Impacts Image Quality is Crucial to Lowering Patient Radiation Exposure.5. Newer Hardware and Software Techniques Further Lower Patient Radiation Exposure.

#### **TABLE OF CONTENTS/OUTLINE**

Appropriateness Criteria/Society Guidelines Eliminated Unindicated Exams. Examples: Nuc Cardiology; PET/CT Oncology Reference Levels and Achievable Adminstered Activities Review of concepts. The most Recent Data, and How to Use the Surveys Adminstered Activity and Patient Radiation Dose Expected Impact of Radiopharmaceutical Administered Activity on NM Counting Statistics/Image Formation with Example Cases Balancing Adminstered Activity with Imaging Quality Optimizing Gamma Camera Technique Lower Administered Activity Example Cases Optimizing Patient Preparation/Radiopharmaceutical Excretion. New Software and Hardware Example Cases incl. Reconstruction Algorithms/New Detectors

## Quantitative Analysis of Prostate Cancer Invasion by using Successive Whole-body Bone Scans

Wednesday, Nov. 30 12:15PM - 12:45PM Room: S503AB Station #6

#### **Participants**

Junji Shiraishi, Kumamoto, Japan (*Presenter*) Research Grant, FUJIFILM Holdings Corporation; Research Grant, Nihon Medi-Physics Co, Ltd

Shinya Shiraishi, Kumamoto, Japan (*Abstract Co-Author*) Nothing to Disclose Kazunori Kawakami, Tokyo, Japan (*Abstract Co-Author*) Employee, FUJIFILM Holdings Corporation

#### PURPOSE

Whole-body (WB) bone scan scintigram is commonly used to image skeletal pathologic changes due to prostate cancer invasion. Although the temporal changes in successive WB bone scans can be observed, quantitative analysis of prostate cancer invasion is a challenging task for the physicians. In this study, we developed a new method for analyzing prostate cancer invasion quantitatively by using successive WB bone scans.

## METHOD AND MATERIALS

We collected 22 series of successive WB bone scans with skeletal pathologic changes due to prostate cancer invasion. Each scan included at least four pairs of posterior and anterior views obtained simultaneously by using a set of two face-to-face gamma cameras. For each series of WB bone scans, the first exam was considered as the base line, and then, temporal changes between the base line and the other images obtained from the follow-up exams were analyzed quantitatively. Prototype computer software for subtracting two WB bone scans by matching images nonlinearly was developed. In addition, a new interval change index (ICI) was proposed in order to quantify the temporal changes. The ICI was defined as the ratio of the total area of abnormal interval changes and that of WB bone scan image multiplied with weighted factor for six anatomically segmented regions. Clinical utility of the ICI was evaluated by comparing with a difference of two bone scan indices ( $\Delta$ BSI) of which each index was calculated by using commercially available software for one bone scan image.

### RESULTS

As a result, the ICI was highly correlated to  $\Delta$ BSI in 15 of 22 cases (68%). For remaining 7 cases, the ICI was considered as accurate in 4 cases compared with the  $\Delta$ BSI.

# CONCLUSION

Temporal changes on whole-body bone scans due to prostate cancer invasion would be quantitated by using our new software to obtain temporal subtraction images between successive bone scans and to estimate new index of ICI.

# **CLINICAL RELEVANCE/APPLICATION**

Temporal change of successive whole body-bone scans has a potential to demonstrate beneficial/detrimental drug effect for prostate cancer patients, and can be used for prediction of treatment effect.

## **Role of PET Parameters in Multiple Myeloma Response Assessment**

Wednesday, Nov. 30 12:15PM - 12:45PM Room: S503AB Station #7

#### **Participants**

Terry Lim, MD, Atlanta, GA (*Presenter*) Nothing to Disclose Jeffrey Switchenko, PhD, Atlanta, GA (*Abstract Co-Author*) Nothing to Disclose Padma P. Manapragada, MD, atlanta, GA (*Abstract Co-Author*) Nothing to Disclose Chika Obidike, Atlanta, GA (*Abstract Co-Author*) Nothing to Disclose Yan Li, Atlanta, GA (*Abstract Co-Author*) Nothing to Disclose James R. Galt, PhD, Atlanta, GA (*Abstract Co-Author*) Nothing to Disclose Ajay Nooka, MD, atlanta, GA (*Abstract Co-Author*) Nothing to Disclose Ayse T. Karagulle Kendi, MD, Rochester, MN (*Abstract Co-Author*) Nothing to Disclose

### PURPOSE

To assess value of adding Positron Emission Tomography/Computed Tomography (PET/CT) parameters in treatment response of multiple myeloma (MM) patients through progression-free survival (PFS) and overall survival (OS) following 100 day Autologous Stem Cell Transplantation (ASCT). To determine PET/CT parameters most useful as a prognostic indicator.

### **METHOD AND MATERIALS**

MM patients recently admitted to our institution for ASCT were reviewed. Along with hematologic restaging and treatment response; SUVmax, SUVmean, SUVpeak, TLG, MTV, SAM, and NSAM were calculated and compared. Response was categorized into  $\geq$ CR,  $\geq$ VGPR, ORR or other. Statistical quantitative analyses were performed using the Kaplan-Meier method, chi-squared test or Fisher's exact tests, where appropriate. Significance was assessed at the 0.05 level, and the analysis was performed using SAS 9.4.

### RESULTS

Out of 174 patients, 90 (51.7%) had a complete response (CR) or stringent complete response (sCR). Ninety-six (55.5%) were male, the mean age was 60.1 years, and the mean time from diagnosis to BMT was 1.3 years. Eighty-six percent of the patients had a value of 0 for each PET parameter. The hazards ratio (HR) for PFS for PET positive patients defined by SUVmax was 1.3 (95% CI: 1.03-1.63, p=0.027), SUVpeak 1.38 (95% CI: 1.06-1.80, p=0.016), TLG 1.01 (95% CI: 1:00-1.03, p=0.040), SAM 1.02 (95% CI: 1:00-1.04, p=0.018) and NSAM 1.03 (95% CI: 1:00-1.06, p=0.027). Neither SUVmean nor MTV showed statistical significance. Although addition of PET in treatment response and PFS demonstrated qualitative improvement, findings were not statistically significant.

# CONCLUSION

Vast majority (86%) of MM patients studied did not have a PET parameter value. As a whole, PET positivity was significantly associated with PFS at 100th day restaging following ASCT, whereas patient demographics was not. In subset of patients with PET positivity, SUVmax, SUVpeak, TLG, SAM, and NSAM demonstrated statistical significance with PFS. SUVpeak showed the highest association with PFS in PET positive cases. Neither SUVmean nor MTV showed statistical significance. Although addition of PET in treatment response and PFS demonstrated qualitative improvement, findings were not statistically significant.

### **CLINICAL RELEVANCE/APPLICATION**

(dealing with multiple myeloma) "PET positivity was significantly associated with PFS at 100th day restaging following ASCT, with SUVpeak showing highest association in PET positive cases."

# NM230-SD-WEA8

Quantitative Assessment of New Regularized Time-of-Flight (R-TOF), or QClear by GE, Compared to Conventional Time-of-Flight (TOF) and Non-TOF PET Reconstructions in an Oncologic Patient Population

Wednesday, Nov. 30 12:15PM - 12:45PM Room: S503AB Station #8

#### Awards

#### **Student Travel Stipend Award**

#### **Participants**

Charles B. Chism, MD, Houston, TX (*Presenter*) Nothing to Disclose Tinsu Pan, PhD, Waukesha, WI (*Abstract Co-Author*) Nothing to Disclose Gregory C. Ravizzini, MD, Houston, TX (*Abstract Co-Author*) Nothing to Disclose Homer A. Macapinlac, MD, Houston, TX (*Abstract Co-Author*) Nothing to Disclose

# PURPOSE

To assess how the new R-TOF (or QClear by GE) alters the observed and quantitated metabolic activity of 18F-FDG avid lesions of sizes less than 3 cm versus TOF and non-TOF PET reconstructions in an oncologic setting.

#### **METHOD AND MATERIALS**

Data from 30 patients who underwent PET-CT in October 2015 through February 2016 at a large cancer center were evaluated. Patients with a contrast enhanced CT exam were excluded in order to eliminate any potential confounder in SUV measurements. Multiple reconstructions of the PET data were created for each patient, including R-TOF, TOF, and non-TOF, using OSEM of 3 iterations and 24 subsets. Regions of interest were contoured for measureable lesions of less than 3 cm on fused PET-CT, and SUVmax measurements and the lesion size were recorded for a total of 64 lesions. Comparative statistical analysis of SUVmax and lesion size between reconstructions was performed.

### RESULTS

R-TOF had the highest SUVmax for all 64 lesions in our study sample followed by TOF then non-TOF. Paired t-tests were used to determine if there was a statistically significant difference between the SUVmax values of R-TOF and TOF, TOF and non-TOF, and R-TOF and non-TOF reconstructions. The mean difference for all comparisons was different than 0 and statistically significant (two-tail p=9.27E-10, 1.58E-17, 2.42E-13, respectively). Scatter plots of percent increase SUVmax vs. lesion size were made for these same comparisons, and linear trendlines were added. R-TOF vs. TOF, TOF vs. non-TOF, and R-TOF vs. non-TOF all demonstrated negative slopes, with R-TOF vs. non-TOF having the steepest negative slope value (m=-14.9). All r^2 values were low on the order of 0.1.

# CONCLUSION

R-TOF demonstrates greater enhancement of the perceived and quantitated metabolic activity of 18F-FDG avid lesions, with a greater effect for smaller lesions, compared to TOF and non-TOF reconstructions. This may be of clinical utility for detecting metabolic activity within very small lesions (e.g. small lung nodules) of which further investigation is needed.

### **CLINICAL RELEVANCE/APPLICATION**

Physicians employing R-TOF should be aware it enhances the observed and quantitated activity of 18F-FDG avid lesions, especially for smaller foci, versus TOF and non-TOF PET.

# NM231-SD-WEA9

## Correction for Body Mass Index Aids Cardiovascular Risk-stratification with PET Vascular Imaging

Wednesday, Nov. 30 12:15PM - 12:45PM Room: S503AB Station #9

#### Participants

Mark A. Ahlman, MD, Bethesda, MD (*Presenter*) Nothing to Disclose Roberto Maass-Moreno, PhD, Bethesda, MD (*Abstract Co-Author*) Nothing to Disclose David A. Bluemke, MD, PhD, Bethesda, MD (*Abstract Co-Author*) Research support, Siemens AG

### PURPOSE

18-Fluorodeoxyglucose (FDG) vascular imaging may offer the ability to improve individualized cardiovascular risk stratification. Obesity is related to higher cardiovascular risk and the same relationship of obesity to vascular FDG activity may imply higher levels of inflammation. However, higher max voxel intensity is also related to higher image noise, which is caused by photon attenuation with due to greater body size within the field of view, measured by body mass index (BMI).

## METHOD AND MATERIALS

Prospectively, 74 PET/CTs from 37 subjects (41% female) with hyperlipidemia >55 y/o were acquired (~300MBq FDG, 136 min uptake time, iterative reconstruction, 256x256 matrix, 1.5mm slice thickness). The liver and descending aorta were segmented to calculate standard deviation (SD), mean, and max voxel (highest in whole volume) intensity. The %increase of max over mean activity was calculated. Using the generalized estimating equation, the normalized multivariate beta coefficient of BMI related to measurements was reported and corrected for gender, age, and statin dose equivalence (normalized to simvastatin). Where appropriate, the relationship to BMI was also corrected for mean liver and mean blood (inferior/superior vena cava) activity, respectively.

### RESULTS

There is a significant independent positive relationship of BMI to %max SUV increases over mean activity for the liver and aorta as well as the SD within the structures (all P-values <0.01). One unit change in BMI is proportional to approximately 3% liver max SUV (P<0.0001) change in this model.

# CONCLUSION

Independent of gender, age, treatment, and regional background FDG activity, the highest max SUV selected in the liver or aorta is significantly related to higher image noise related to photon attenuation due to higher BMI.

# **CLINICAL RELEVANCE/APPLICATION**

For cardiovascular risk stratification, higher dosing, adaptive image smoothing, and/or longer imaging time for obese individuals may be considered if SUV max values measured in this fashion are used to compare between individuals. Alternatively, correction for BMI or noise levels may be applied in multivariate models or by inference of expected maximum voxel intensity differences. These results likely also apply in oncology FDG imaging where inter-subject comparisons of maximum activity is desired. A Meta-analysis of Test-retest Repeatability of Amyloid PET Imaging with 11C-PIB and 18F-labeled Amyloid Radiotracers in Alzheimer's Disease Patients and Healthy Controls

Wednesday, Nov. 30 12:15PM - 12:45PM Room: S503AB Station #10

## Participants

Sara Sheikhbahaei, MD, MPH, Baltimore, MD (*Presenter*) Nothing to Disclose Nancy A. Obuchowski, PhD, Cleveland, OH (*Abstract Co-Author*) Research Consultant, Siemens AG; Research Consultant, QT Ultrasound Labs; Research Consultant, Elucid Bioimaging Inc Victor L. Villemagne, Baltimore, MD (*Abstract Co-Author*) Nothing to Disclose Rathan M. Subramaniam, MD, PhD, Dallas, TX (*Abstract Co-Author*) Nothing to Disclose

# PURPOSE

In this meta-analysis we aim to determine the repeatability of amyloid PET imaging with 11C-Pittsburgh compound-B (11C-PIB) and 18Fluorine (18F) labeled radiotracers using the available literature.

## **METHOD AND MATERIALS**

Systematic electronic search were performed in PubMed and EMBASE (last updated in Jan 2016) to identify studies addressing the test-retest repeatability of amyloid PET imaging with 11C-PIB and 18F labeled radiotracers in patients with Alzheimer's disease (AD) or healthy controls (HCs). The individual patient data or the mean test-retest variability (TRV%) and the standard deviation of two PET tracer retention measurements were extracted from the eligible studies. The study authors were contacted seeking for more information. The average neocortical SUVr were considered as a measure of amyloid load and the cerebellar cortex as the reference region. The percent repeatability coefficient (RC%) was calculated as an index of absolute reliability. The pooled estimates of mean TRV% with SE and the RC% with bootstrapped 95%CI were generated for summary effect.

#### RESULTS

A total of 7 studies were included in this individual patient data meta-analysis. Four studies evaluated the test-retest variability of 18F labeled amyloid tracers (Florbetapir, AZD4694, Flutematol, Florbetaben). The test-retest amyloid PET studies were performed between 1 to 4 weeks apart. The pooled mean TRV% for average cortical SUVr was 2.77(SE=0.75) in patients with AD (n=26) with a RC% of 10.36% (4.76-14.92). The pooled mean TRV% for average cortical SUVr was 3.12 (SE=1.39) in HCs (n=22) with a RC% of 10.41 (3.33-20.3). Three studies evaluated the test-retest variability of 11C-PIB amyloid imaging. The test-retest amyloid PET studies were performed on same day and up to 60 days apart. The pooled mean TRV% for average cortical SUVr was 4.33 (SE=0.25) for AD (n=12) with a RC% of 15.4% (8.49-20.05). The pooled mean TRV% for average cortical SUVr was 3.61 (SE=0.59) in HCs (n=16) with a RC% of 9.38% (7.55-10.92).

## CONCLUSION

Our results showed no significant differences in RC% of 18F labeled and 11C-PIB amyloid tracers for neocortical SUVr.

## **CLINICAL RELEVANCE/APPLICATION**

The repeatability coefficient of 18F amyloid radiotracers is about 10% for neocortical SUVr in both Alzehimers Disease patients and healthy controls. This effect should be considered when using neocortical SUVr as an outcome measure for assessing anti-amyloid therapy.

# Face of The Unborn: Evaluation of Fetal Facial Anomalies with MRI

Wednesday, Nov. 30 12:15PM - 12:45PM Room: NR Community, Learning Center Station #10

Awards Magna Cum Laude Identified for RadioGraphics

#### **Participants**

Kedar G. Sharbidre, MD, Chicago, IL (*Presenter*) Nothing to Disclose Murali Nagarajan, MD, FRCR, Chicago, IL (*Abstract Co-Author*) Nothing to Disclose Ravi M. Sheth, Chicago, IL (*Abstract Co-Author*) Nothing to Disclose Sudeep H. Bhabad, MD, FRCR, Chicago, IL (*Abstract Co-Author*) Nothing to Disclose Xavier Pombar, MD, Chicago, IL (*Abstract Co-Author*) Nothing to Disclose Sharon E. Byrd, MD, Chicago, IL (*Abstract Co-Author*) Nothing to Disclose

### **TEACHING POINTS**

1. Recognizing normal fetal facial structures on MRI.

2 .Introduction to well established fetal facial anomalies such as facial clefts, anomalies of globes and orbits, anomalies of jaw, malformations of nose and external ears, and facial masses.

3. Ultrasound is the first-line imaging modality. However, MRI helps in better characterization and detection of the associated malformations.

4. Facial anomalies can be associated with characteristic intracranial malformations such as holoprocencephaly, callosal dysgeneis, absent septum pellucidum, etc. They have syndromic associations such as trisomy 13, trisomy 18, Pierre-Robin sequence and hemifacial microsomia.

5. Detection of facial anomalies should prompt search for associated intracranial malformations and genetic counseling.

# TABLE OF CONTENTS/OUTLINE

1. Anatomy and embryology of fetal facial structures.2. Classification of facial anomalies into structural/positional anomalies, facial clefts and facial masses.3. Pictorial review and diagnostic features of facial anomalies.4. Outline of associations with intracranial malformations and genetic syndromes.5. Clinical implications.

## NR387-SD-WEA4

Multi-Spectral Optoacustic Tomography of Supraclavicular Brown/Beige Adipose Tissue in Comparison to Quantitative MRI

Wednesday, Nov. 30 12:15PM - 12:45PM Room: NR Community, Learning Center Station #4

# Participants

Daniela Franz, MD, Munich, Germany (*Presenter*) Nothing to Disclose Gael Diot, Neuherberg, Germany (*Abstract Co-Author*) Nothing to Disclose Dimitrios C. Karampinos, Munich, Germany (*Abstract Co-Author*) Research Grant, Koninklijke Philips NV Reinhard Meier, MD, PhD, Ulm, Germany (*Abstract Co-Author*) Nothing to Disclose Thomas Baum, MD, Munich, Germany (*Abstract Co-Author*) Nothing to Disclose Christian Cordes, Munich, Germany (*Abstract Co-Author*) Nothing to Disclose Vasilis Ntziachristos, PhD, Munich, Germany (*Abstract Co-Author*) Nothing to Disclose Ernst J. Rummeny, MD, Munich, Germany (*Abstract Co-Author*) Nothing to Disclose

### PURPOSE

To evaluate Multi-Spectral Optoacoustic Tomography (MSOT) in comparison with MRI applied to brown/beige adipose tissue (BAT) detection in-vivo, based on fat-to-water ratio analysis.

### METHOD AND MATERIALS

19 adult volunteers (8 male, 11 female, mean age 30.3 years) underwent MSOT and MRI (Philips Ingenia 3T) examinations of the neck. MRI acquisition included a six-echo mDixon-sequence (TR/TE1/DTE 12/1.24/1.0 ms, 1.5 mm isotropic voxel size). PDFF maps were generated online after accounting for known confounding factors including a single T2\* correction. MSOT acquisition wavelength ranged from 700 nm to 970 nm with heavy water coupling. The data was unmixed using linear unmixing techniques in order to identify oxy-, deoxy-hemoglobin, fat and water, and fat-to-water ratio maps were generated. In each volunteer, regions of interest (ROIs) were placed into the PDFF map and the fat-to-water ratio map of the left deep supraclavicular fat depot.

### RESULTS

Fat-to-water ratio of the supraclavicular fat tissue as determined by MSOT ranged from 28 to 74%, with a mean of 49.4%. MR-PDFF ranged from 53 to 90%, with a mean of 77.5%. Correlation analysis of MSOT fat-to-water ratio and PDFF showed a strong correlation (r = 0.59, p=0.008).

# CONCLUSION

MSOT is comparable to MRI with regard to the ability to determine fat-water composition of fatty tissue, thus it is able to detect and characterize areas of more hydrated and less fatty brown/beige adipose tissue.

# **CLINICAL RELEVANCE/APPLICATION**

MSOT is a possible new imaging method for identification and characterization of brown/beige adipose tissue.

## NR388-SD-WEA5

Effects of 2-Repeat Allele of DRD4 Gene on Neural Networks Associated with Prefrontal Cortex in ADHD Children

Wednesday, Nov. 30 12:15PM - 12:45PM Room: NR Community, Learning Center Station #5

# Participants

Andan Qian, Wenzhou, China (*Presenter*) Nothing to Disclose Meihao Wang, Wenzhou, China (*Abstract Co-Author*) Nothing to Disclose

## PURPOSE

The aim of this study is to explore the effects of 2-repeat allele in the DRD4 gene on the functional connectivity of ADHD patients.

#### **METHOD AND MATERIALS**

Using independent component analysis (ICA) and dimension analysis, we analyzed resting-state functional magnetic resonance imaging data obtained from 52 Asian medicine-naive children and adolescence with ADHD(33 2-repeat absent and 19 2-repeat present). All participants were genotyped for the DRD4 48-bp repeat VNTR polymorphism.

#### RESULTS

We found that 2-repeat absent demonstrated declined synchronization in the right middle frontal gyrus(MFG) of the sensorimotor network(SMN) and in the right middle and inferior frontal gyrus(IFG), the right orbital cortex, and the right anterior cingulate cortex of the executive control network (ECN) compared to individuals with 2-repeat present. Within the default-mode network (DMN), 2-repeat absent showed decreased in the left IFG and increased in the right precuneus. Clusters of right MFG and IFG in ECN showed a significant positive correlation between functional connectivity strength and Impulsivity-Hyperactivity, Conners Index of Hyperactivity.

### CONCLUSION

These results provided evidence of DRD4 gene polymorphism, as well as 2-repeat, had effects on ECN, SMN and DMN, especially on prefrontal cortex had been confirmed. On the top of that, DRD4 2-repeat allele, as a plasticity gene, had a less negative effect on brain networks and appeared to be a protective factor of ADHD.

#### **CLINICAL RELEVANCE/APPLICATION**

These findings suggested that the polymorphism in the DRD4 gene affected the functional synchronization in the several brain networks.DRD4 2-repeat, as a plasticity gene, had a small negative effect on brain networks and appeared to be a protective factor of ADHD.

# NR389-SD-WEA6

Observation of Cerebrospinal Fluid Pulsatility in Real Time Magnetic Resonance Imaging by Means of Time Spatial Labeling Inversion Pulse (Time-SLIP) Technique; Validation Study of Pulsatility Traceability with a Phantom Push-Pull Pump

Wednesday, Nov. 30 12:15PM - 12:45PM Room: NR Community, Learning Center Station #6

## Participants

Takahiro Sakai, Tokyo, Japan (*Presenter*) Nothing to Disclose Kohki Yoshikawa, MD, Tokyo, Japan (*Abstract Co-Author*) Nothing to Disclose Shinya Yamada, MD, PhD, Kanagawa, Japan (*Abstract Co-Author*) Nothing to Disclose

#### PURPOSE

Recently, the creditability of a "classic" cerebrospinal fluid (CSF) circulation physiology was seriously brought into question. CSF pulsatility associated with cardiac pulsation and respiration was observed. However, no bulk CSF flow was detected by the real time spatial spin labeling (Time-SLIP) technique in normal physiological brain. In this study, accuracy of traceability of real time Time-SLIP technique was measured using phantom pulsatile flow generated by a mechanical push-pull pump.

# METHOD AND MATERIALS

Different regions of CSF dynamics in the central nervous system (CNS) were observed (foramen of Monro, aqueduct of Sylvius, prepontine cistern, and spinal subarachnoid space) in healthy volunteers using real time 2D steady state free precession Time-SLIP method. Automated tracing software was used to trace CSF pulsatility and analyzed characteristics of waveform and speed range of CSF pulsatility in normal volunteers. The phantom pulsatile flow generated by the handmade mechanical push-pull pump was used for validation of traceability of real time Time-SLIP technique. Accuracy of the real time Time-SLIP technique regarding traceability of CSF pulsatile flow was investigated.

#### RESULTS

CSF pulsation driven by cardiac pulsation and respiration were observed in different regions of CNS. Amplitudes of CSF pulsatility were varied depending on the location of observation even in the same individuals. CSF pulsatility was simulated by handmade mechanical push-pull pump. Accurate measurement and traceability of real time Time-SLIP were verified in the range of normal CSF pulsatile speed.CSF dynamics in volunteers and the phantom experiment will be shown.

#### CONCLUSION

Real time Time-SLIP can be used to trace human CSF dynamics.

## **CLINICAL RELEVANCE/APPLICATION**

Cerebrospinal fluid Dynamics observed by Time-SLIP MRI technique was very much different from what was believed as "classic" CSF circulation theory. These foundament CSF physiogical infrmations may contribute treatment stratgy of CSF related disease such as hydrocephalus ,arachnoid cyst and syringomyelia.

Computer extracted Texture Descriptors on MRI that Distinguish Radiation, Necrosis and Tumor Recurrence Post-Radiotherapy in Primary Neoplasms are Associated with Vascular, Necrotic and Demyelinating changes

Wednesday, Nov. 30 12:15PM - 12:45PM Room: NR Community, Learning Center Station #8

# Participants

Prateek Prasanna, Cleveland, OH (*Abstract Co-Author*) Nothing to Disclose Lisa Rogers, Detroit, MI (*Abstract Co-Author*) Nothing to Disclose Mark A. Cohen, MD, Pepper Pike, OH (*Abstract Co-Author*) Nothing to Disclose Gagandeep Singh, MBBS, Cleveland, OH (*Abstract Co-Author*) Nothing to Disclose Chaitra A. Badve, MD, MBBS, Cleveland, OH (*Abstract Co-Author*) Nothing to Disclose Leo J. Wolansky, MD, Cleveland, OH (*Abstract Co-Author*) Nothing to Disclose Anant Madabhushi, PhD, Piscataway, NJ (*Abstract Co-Author*) Nothing to Disclose Pallavi Tiwari, PhD, Cleveland, OH (*Presenter*) Nothing to Disclose

#### PURPOSE

Radiation therapy in brain neoplasms results in chronic histological changes, sometimes leading to radiation necrosis (RN). While RN has distinct histological characteristics, it mimics the appearance of tumor recurrence (RT) on routine MRI. Previously, we have shown the utility of computer extracted texture descriptors (CETDs), which capture statistics (e.g. entropy, variance) of co-occurrences of gradient orientations, to be highly discriminative of RN and RT on routine MRI. The goal of this work is to investigate the association of these CETDs, with the histologic attributes on the corresponding surgical specimen associated with RT and RN. The hypothesis is that this radio-histologic correlation will provide us with a biological underpinning for improved discrimination of RT from RN on routine MRI.

# METHOD AND MATERIALS

3T MRI studies (Gd-T1w, T2w, FLAIR) and surgical resection specimens were obtained from 20 patients (10 RN, 10 RT) with primary neoplasms, 9-months (or later) post-radiation. Histological traits including vessel-wall thickening, demyelination, and zonal necrosis were graded by an expert neuropathologist who assigned a 'score' between 0 and 4 based on the percentage of each of the observed attribute on the surgical specimens. FLAIR-hyper intensity, necrosis, and enhancing tumor regions were independently delineated on the 3 MRI sequences. 13 CETDs were computed for every region for each protocol. A pair-wise Spearman correlation was performed between every CETD and the pathologic 'score', for each of the 3 histologic traits.

#### RESULTS

Correlation CETDs from enhancing tumor on Gd-T1w were found to be significantly associated (p<0.05) with zonal necrosis, as well as vessel wall thickening. Demyelination was found to be significantly correlated with variance features on hyperintensities of FLAIR. Zonal necrosis, vessel wall thickening, and demyelination are histologically known to be high in RN and contribute to lesion heterogeneity, which may be reflected in CETDs at the radiologic scale.

# CONCLUSION

The CETDs found to be discriminative of RT and RN might be capturing histological changes due to zonal necrosis, vessel wall thickening, and demyelination.

# **CLINICAL RELEVANCE/APPLICATION**

Understanding associations of histologic phenotypes and CETDs will enable developing biologically inspired CETDs that capture cellular differences on routine MRI to distinguish RT and RN.

## NR392-SD-WEA9

Upright Magnetic Resonance Imaging (MRI) of the Lumbar Spine: A Fail Safe Diagnostic Method for Spine Instability

Wednesday, Nov. 30 12:15PM - 12:45PM Room: NR Community, Learning Center Station #9

# Participants

Lucia Patriarca, LAquila, Italy (*Presenter*) Nothing to Disclose Federico Bruno, MD, LAquila, Italy (*Abstract Co-Author*) Nothing to Disclose Simone Quarchioni, Laquila, Italy (*Abstract Co-Author*) Nothing to Disclose Alessandra Splendiani, MD, L'Aquila, Italy (*Abstract Co-Author*) Nothing to Disclose Carlo Masciocchi, MD, L'Aquila, Italy (*Abstract Co-Author*) Nothing to Disclose

# PURPOSE

Definition of spine stability is not clear and interobserver reliability is not always guaranteed. We aimed to evaluate interobserver agreement in the definition of spine instability among spine neuroradiologists with or without experience in recumbent and upright magnetic resonance imaging (MRI)

# METHOD AND MATERIALS

this retrospective study was approved by institutional ethics board. Two expert neuroradiologists and two residents retrospectively evaluated the pre-operative dynamic MRI examinations of patients with vertebral instability. Segmental motion, defined as excessive (more than 3 mm) translational motion from supine to upright, was investigated in 103 subjects (309 segments) using kinetic MRI. Were simultaneously evaluated disc degeneration, facet joint osteoarthritis, and ligament flavum hypertrophy and were assigned a value to each parameter (from grade 0 to grade 5) at each level. The agreement among the neuroradiologists was calculated using the kappa coefficient. All patients had neurosurgical intervention to stabilize the spine

### RESULTS

4 radiologists agreed to participate: two highly experienced (more 20 years) and two less-experienced (4 years experienced). The agreement was nearly perfect for all parameters among experienced aradiologists and was good between experienced and non-experienced neuroradiologists

## CONCLUSION

This study demonstrates that the experience of the evaluator has a low impact on the assessment of spinal instability if correct classification is used. The interobserver agreement confirms the usefulness and safety of kinetic MRI in the correct diagnosis of spinal instability even by less experienced evaluators.

# **CLINICAL RELEVANCE/APPLICATION**

Upright MRI is a safe and simple method in diagnosing spine stability

## OB004-EB-WEA

Finding the Fetus: A Multimodality Overview of the Ectopic Pregnancy Spectrum, Mimickers and Clinical Management

Wednesday, Nov. 30 12:15PM - 12:45PM Room: OB Community, Learning Center Hardcopy Backboard

# Participants

Stephen Herrmann, MD, Galveston, TX (*Presenter*) Nothing to Disclose Eric Bih, MD, Sugar Land, TX (*Abstract Co-Author*) Nothing to Disclose Sara M. Ortiz-Romero, MD, Galveston, TX (*Abstract Co-Author*) Nothing to Disclose Mary S. Guirguis, MD, Houston, TX (*Abstract Co-Author*) Nothing to Disclose Rami Eldaya, MD, Galveston, TX (*Abstract Co-Author*) Nothing to Disclose Devon M. Divito, MD, Galveston, TX (*Abstract Co-Author*) Nothing to Disclose Samuel Gatzert, MD, Galveston, TX (*Abstract Co-Author*) Nothing to Disclose Eduardo J. Matta, MD, Houston, TX (*Abstract Co-Author*) Nothing to Disclose Kimberly S. Kirschner, MD, Galveston, TX (*Abstract Co-Author*) Nothing to Disclose

# **TEACHING POINTS**

-Anatomical review of normal uterine, endometrial and placenta utilizing: cartoons, magnetic resonance imaging (MRI) and ultrasound (US).-Provide a summary table for pathophysiology, diagnostic criteria, imaging findings, and common clinical complications.-Provide radiological imaging of ectopic pregnancies in multiple modalities including MRI, and US.-Presentation of multiple cases of pathology mimicking various ectopic pregnancies and tips to make the correct diagnosis.

# TABLE OF CONTENTS/OUTLINE

We will present a pictorial essay of the imaging features of ectopic pregnancies, using a location-specific approach.

- 1) Patient demographics and clinical presentation of ectopic pregnancies.
- 2) MRI, US and cartoon representation of ectopic pregnancies.
- 3) Ectopic pregnancy mimickers and strategies for when follow up or further imaging should be obtained.
- 4) Important imaging features that must be reported to aid the clinicians to aid in making the appropriate treatment strategy.
- 5) Clinical management of patients with ectopic pregnancies.

# 'How to Sort through This Mess?' Role of MRI in Managing Post-operative Patients with Sling and Mesh

Wednesday, Nov. 30 12:15PM - 12:45PM Room: OB Community, Learning Center Station #1

#### **Participants**

Gitanjali Bajaj, MBBS, Little Rock, AR (*Abstract Co-Author*) Nothing to Disclose Tarun Pandey, MD, FRCR, Little Rock, AR (*Abstract Co-Author*) Nothing to Disclose Kedar Jambhekar, MD, Little Rock, AR (*Abstract Co-Author*) Nothing to Disclose Roopa Ram, MD, Little Rock, AR (*Presenter*) Nothing to Disclose

# **TEACHING POINTS**

1. Discuss various surgical techniques for management of patients with stress urinary incontinence and pelvic organ prolapse, two common conditions in the spectrum of pelvic floor dysfunction

2. Discuss role of imaging in evaluating and managing complicated post operative patients with sling/mesh with emphasis on high resolution pelvic MRI

3. Discuss evolving role of newer techniques such as MR neurography in diagnosing post operative patients with chronic pelvic pain

## TABLE OF CONTENTS/OUTLINE

- 1. Schematics showing various surgical approaches used to treat stress incontinence and pelvic organ prolapse
- 2. MRI appearances of normal and abnormal sling and mesh
- 3. Case based examples to show how MRI changed management of complicated post operative patients.
- 4. MR neurography technique and examples showing nerve entrapment
- 5. Reporting template for mesh and sling

# PD119-ED-WEA6

Pearls and Pitfalls in MRI Diagnosis of Ovarian Torsion in Children

Wednesday, Nov. 30 12:15PM - 12:45PM Room: PD Community, Learning Center Station #6

#### **Participants**

Kimberly Winsor, MD, Tucson, AZ (*Presenter*) Nothing to Disclose S. Pinar Karakas, MD, Oakland, CA (*Abstract Co-Author*) Nothing to Disclose Iva Petkovska, MD, Tucson, AZ (*Abstract Co-Author*) Nothing to Disclose Eugene Duke, MD, Tucson, AZ (*Abstract Co-Author*) Nothing to Disclose Sarah M. Desoky, MD, Tucson, AZ (*Abstract Co-Author*) Nothing to Disclose Diego R. Martin, MD, PhD, Tucson, AZ (*Abstract Co-Author*) Nothing to Disclose Bobby T. Kalb, MD, Tucson, AZ (*Abstract Co-Author*) Nothing to Disclose Unni K. Udayasankar, MD, FRCR, Tucson, AZ (*Abstract Co-Author*) Nothing to Disclose

## **TEACHING POINTS**

Describe the normal MRI appearance of the ovary at different pediatric age groups, with cyclical variations.List the key clinical and MRI features of ovarian torsion and its mimics.Discuss role of MRI in guiding management with particular emphasis on assessing ovarian viability on imaging

#### **TABLE OF CONTENTS/OUTLINE**

A fast pediatric pelvic MRI technique that provides exquisite details of the uterus and adnexa will be described. Illustrate normal MRI appearance of ovaries with emphsis on normal follicles and stroma, and description of arterial/venous anatomy. Describe classic MRI findings in ovarian torsion. MR features that indicate viability of the of the ovary will be emphasized. Common and rare mimics of ovarian torsion in children will be discussed including simple ovarian cysts, hemorrhagic ovarian cysts, endometrioma, ruptured acute appendicitis, ruptured ovarian cysts, and ovarian neoplasms.

# PD154-ED-WEA7

Imaging of the Pediatric Hypothalamic-Pituitary Axis: A Pictorial Review of Developmental, Infiltrative and Tumoral Pathology

Wednesday, Nov. 30 12:15PM - 12:45PM Room: PD Community, Learning Center Station #7

## Awards Cum Laude

# Participants

Jeet Patel, MD, Boston, MA (*Presenter*) Nothing to Disclose V. Michelle Silvera, MD, Boston, MA (*Abstract Co-Author*) Nothing to Disclose

## **TEACHING POINTS**

1. To describe and illustrate imaging findings of congenital and developmental anomalies, infiltrative lesions and tumors of the hypothalamus-pituitary axis in children.

2. To explain the clinical context and indications for imaging of the pediatric hypothalamic-pituitary axis.

## TABLE OF CONTENTS/OUTLINE

- 1. Brief review of key anatomic imaging findings of the normal hypothalamic-pituitary axis in children on MRI.
- 2. Description of routine pituitary MRI protocols and important supplementary sequence considerations.
- 3. Review of clinical indications and context for pituitary imaging referrals from endocrinologists, neurologists, and ophthalmologists.
- 4. Abnormalities of the pediatric hypothalamic-pituitary axis: a. congenital, b. developmental, c. inflammatory, d. tumors.

# PD231-SD-WEA2

External and Intraoral-External Hybrid B0 Field Correction Devices for Decreasing Magnetic Susceptibility Artifacts on Brain MRI Induced by Stainless Steel Orthodontic Appliances

Wednesday, Nov. 30 12:15PM - 12:45PM Room: PD Community, Learning Center Station #2

**FDA** Discussions may include off-label uses.

#### Participants

Zhiyue J. Wang, PhD, Dallas, TX (*Presenter*) Nothing to Disclose Yong Jong Park, Dallas, TX (*Abstract Co-Author*) Nothing to Disclose Michael C. Morriss, MD, Pinehurst, TX (*Abstract Co-Author*) Nothing to Disclose Rami R. Hallac, PhD, Dallas, TX (*Abstract Co-Author*) Nothing to Disclose Ana Nava, Dallas, TX (*Abstract Co-Author*) Nothing to Disclose Rajiv Chopra, PhD, Dallas, TX (*Abstract Co-Author*) Nothing to Disclose Yonatan Chatzinoff, Dallas, TX (*Abstract Co-Author*) Nothing to Disclose Nancy K. Rollins, MD, Dallas, TX (*Abstract Co-Author*) Nothing to Disclose

### PURPOSE

Susceptibility artifacts from orthodontia (braces) can interfere with brain MRI. It has been shown that an intraoral device containing permanent magnets drastically decreased the artifacts. However, variability of magnetic moments of molar and incisor orthodontic brackets in different braces limits the effectiveness of intraoral devices. We investigated the feasibility of external device.

# METHOD AND MATERIALS

The external device used a facemask allowing mounting correction magnets outside the mouth. Separate plastic strips embedding permanent magnets were used for right and left molars and incisors. While an external device is more flexible, intraoral device allows closer proximity between brackets and correction magnets. Hybrid intraoral and external devices may be combined for best results; a variety of plastic strips and intraoral devices with different magnetic moments allow customization for individual patients.Image quality with and without the external device were compared in 4 patients with ferromagnetic braces undergoing MRI for headache/seizure in 2, optic nerve tumor in 1, and thalamic tumor in 1. The device was assembled based on a calibration B0 mapping. The study was IRB approved with informed consent.A 3D printed brain phantom was filled with agar gel and mounted with a dental model for evaluating B0 homogeneity using the hybrid device. Dental models of three sizes (average size, 8.5% smaller or bigger) were bonded with stainless steel orthodontic brackets (0.022, American Orthodontics) and guide-wires (0.016", Class One). We investigated whether a one-size hybrid device kit will work for different arch sizes.

### RESULTS

The external device was well tolerated by all patients and improved the quality of orbital, sub-frontal, and anterior temporal MRI, in particular DWI.In phantom studies, whole brain B0 peak-to-peak and S.D. values (in ppm) were 13.8 and 0.40 (baseline), 28.7 to 32.2 and 3.0 to 3.1 (with braces), and 12.7 to 17.3 and 0.64 to 0.76 (braces and correction device).

#### CONCLUSION

The external field correction device is feasible in clinical studies. A single sized hybrid device can be used for different maxillary/mandibular arch sizes.

#### **CLINICAL RELEVANCE/APPLICATION**

The study may lead to a device kit that enables diagnostic quality MR examinations for patients with difference maxillary/mandibular arch sizes wearing a variety of orthodontic appliances.

# PD232-SD-WEA3

## Essentials of Intrauterine Zika Virus Infection: Pre and Postnatal CNS Findings

Wednesday, Nov. 30 12:15PM - 12:45PM Room: PD Community, Learning Center Station #3

#### **Participants**

Heron Werner, MD, Rio de Janeiro, Brazil (*Presenter*) Nothing to Disclose Bianca Guedes Ribeiro, MD, Rio de Janeiro, Brazil (*Abstract Co-Author*) Nothing to Disclose Luiz Celso H. Da Cruz, MD, Rio De Janeiro, Brazil (*Abstract Co-Author*) Nothing to Disclose Pedro Daltro, MD, Rio De Janeiro, Brazil (*Abstract Co-Author*) Nothing to Disclose Renata A. Nogueira, MD, Rio De Janeiro, Brazil (*Abstract Co-Author*) Nothing to Disclose Tatiana M. Fazecas, MD, Rio de Janeiro, Brazil (*Abstract Co-Author*) Nothing to Disclose Leise Rodrigues, Rio De Janeiro, Brazil (*Abstract Co-Author*) Nothing to Disclose Jorge Lopes, Rio de Janeiro, Brazil (*Abstract Co-Author*) Nothing to Disclose Gerson Ribeiro, Rio de Janeiro, Brazil (*Abstract Co-Author*) Nothing to Disclose Arine S. Pecanha, MD, Rio de Janeiro, Brazil (*Abstract Co-Author*) Nothing to Disclose

#### PURPOSE

Zika virus (ZIKV) owns to the family of flavivirus and as for dengue and chikungunya infections may recognized Ae. Aegypti and Ae. Albopictus mosquitoes as transmission agents. This virus has tropism for the central nervous system (CNS) and has been strongly associated with common findings to congenital infections, with some features which are described in this presentation.

#### **METHOD AND MATERIALS**

We performed a prospective study with seven pregnant patients with ZIKV infection at different gestational ages. They were subjected to ultrasound and fetal MRI.After birth, the newborns performed transfontanellar US, CT and MRI of the head, with posterior 3D reconstructions of the skull.We compared the cases with and without CNS involvement in the patients with intrauterine ZIKV infection. We quantified and illustrated the most frequent findings in the patients who had changes in their CNS.The main findings of CNS abnormalities were reported and several specific findings were displayed on a chart, including microcephaly, and submitted to statistical analysis.

#### RESULTS

From the 7 cases of ZIKV infection, 4 showed brain abnormalities with microcephaly.Multiple calcifications with cortical and mainly subcortical distribution were seen in all of these 4 cases.Significant thinning of the brain parenchyma, which have extensive periventricular areas of hyperintensity on T2 MR-WI were reported in all of the 4 cases. Neuronal migration anomalies were reported in 3 cases.Dysgenesis of the corpus callosum and ventricular enlargement secondary to cortical/subcortical atrophy were also detected in all of these 4 cases.The cerebellum was affected only in 1 case.Brain stem was not affected on these 7 cases.

## CONCLUSION

Microcephaly with almost complete agyria, hydrocephalus, and multifocal dystrophic calcifications in the cortex and subcortical white matter, with associated cortical displacement were the main findings on intrauterine ZIKV infection with CNS involvement.

## **CLINICAL RELEVANCE/APPLICATION**

Brain calcifications detected prenatally was a finding suspicious with a intrauterine infection. Moreover, perinatal imaging by MRI and CT scan enabled diagnosis of pachygyria, corpus callosum dysgenesis, small anterior fontanel with premature closure of cranial sutures. All of these aspects are seen in the majority of the intrauterine ZIKV infection with CNS involvement and it can be considered on diagnosis criteria.

## PD233-SD-WEA4

Vessel wall changes and microbleeding after radiochemotherapy in a cohort of patients with pediatric medulloblastoma

Wednesday, Nov. 30 12:15PM - 12:45PM Room: PD Community, Learning Center Station #4

## Participants

Yasemin Tanyildizi, MD, Mainz, Germany (*Presenter*) Nothing to Disclose Stefanie Keweloh, MD, Mainz, Germany (*Abstract Co-Author*) Nothing to Disclose Arthur Wingerter, Mainz, Germany (*Abstract Co-Author*) Nothing to Disclose Marie Neu, Mainz, Germany (*Abstract Co-Author*) Nothing to Disclose Alexandra Russo, Mainz, Germany (*Abstract Co-Author*) Nothing to Disclose Andrei Tropine, Mainz, Germany (*Abstract Co-Author*) Nothing to Disclose Jorg Faber, Mainz, Germany (*Abstract Co-Author*) Nothing to Disclose Marc A. Brockmann, Mainz, Germany (*Abstract Co-Author*) Nothing to Disclose

#### PURPOSE

Medulloblastoma (MB) is a primitive neuroectodermal tumor, located in the midline of the cerebellum. MB cause 10% of all pediatric brain tumors. The imaging of the whole cerebrospinal axis is required. Treatment is: surgical resection and radio chemotherapy. As improvements in treatment have increased the survival rate, the sequelaes of radio-chemotherapy gains in importance, regarding follow up examinations/preventive treatment. The aim of this study was to image asymptomatic cerebrovascular changes, such as micro bleedings/vessel wall changes with MRI and ultrasound

# METHOD AND MATERIALS

In this prospective study 26 former MB patients were enrolled (range 4.58-53.75 years, mean age 24.2 years). 26 SWI; 22 T1 (CE) weighted vessel-wall images (TE: 14, TR: 1270, TI: 850, 3 Tesla) and time of flight angiographies (TOF); 19 ultrasound images of the common carotid intima-media-thickness (IMT) were analyzed. SWI lesions for both hemispheres,divided into infra/supratentorial,classified in to 3 groups: < 2 mm;  $\ge$  2 mm - 4mm;  $\ge$  4mm. The IMT was classified into: normal vessel wall < 0.045mm; marginal/ abnormal vessel wall:  $\ge$  0.45mm  $\le$  0.50mm/ > 0.5mm. Vessel wall images of the ICA were classified as abnormal if CE was seen in the vessel wall

#### RESULTS

All patients showed SWI lesions (in total 1053 lesions, supratentorial right hemisphere: 461, left: 472; infratentorial right: 69; left: 51) 62% presented with lesions > 4 mm. The right (left) IMT was 0.46 mm  $\pm$  0.04 mm (0.45 mm  $\pm$  0.04 mm). Nine (47.36 %) patients revealed r IMT < 0.045 mm,12 (63.16 %) | IMT< 0.45 mm; 7(36.84 %) showed a r IMT  $\ge$  0.45 mm  $\le$  0.50 mm,5 (26.31%) for the I IMT.3 (15.78 %) showed a r IMT >0.5mm, two (10.52 %) for the IIMT. In 45% of the patients a CE in the right and 59.1 % in the left ICA was found. In total 63.64 % presented vessel wall changes. In the TOF angiography no alteration of the ICA was found.

# CONCLUSION

Cerebrovascular changes after radio chemotherapy gain in importance, as treatment for MB patients is improving and survivors get older. In this study vessel wall changes could be imaged with ultrasound and MRI in > 50 % patients; micro bleedings in even 100 % patients. Further studies are needed to image the progression and determine the time for a preventive treatment regarding vessel stenosis and cavernoma bleeding

#### **CLINICAL RELEVANCE/APPLICATION**

MRI and ultrasound examinations should be used to analyze vessel wall changes in medulloblastoma survivors after radio chemotherapy

# PD234-SD-WEA5

**Recurrence Risk Factors in Cervicofacial Venous Malformation** 

Wednesday, Nov. 30 12:15PM - 12:45PM Room: PD Community, Learning Center Station #5

#### Participants

Mark Le, MD, Detroit, MI (*Presenter*) Nothing to Disclose Karan N. Patel, MD, Detroit, MI (*Abstract Co-Author*) Nothing to Disclose Vasavi Paidpally, MD, Detroit, MI (*Abstract Co-Author*) Nothing to Disclose Hamza M. Beano, MD, Detroit, MI (*Abstract Co-Author*) Nothing to Disclose Haiying Yu, MD, PhD, Detroit, MI (*Abstract Co-Author*) Nothing to Disclose Shane N. Newberger, MD, Detroit, MI (*Abstract Co-Author*) Nothing to Disclose Monte L. Harvill, MD, Franklin, MI (*Abstract Co-Author*) Nothing to Disclose Terrence Metz, MD, Royal Oak, MI (*Abstract Co-Author*) Nothing to Disclose

### PURPOSE

Cervicofacial venous malformation (CVM) is a common vascular anomaly in children. It is composed of abnormally dilated venous components without cellular proliferation. The disease severity varies as well as their treatment options including surgery, laser therapy, and interventional sclerotherapy. There are numerous studies regarding the treatment CVM with absolute ethanol. However, risks factors associated with recurrence have not fully been addressed. The aim of this study was to investigate the therapeutic efficacy, complication, and associated risk factors in recurrence rates of absolute ethanol for the treatment of CVM.

## **METHOD AND MATERIALS**

A total of 30 patients with CVM were treated with absolute ethanol (98%) from December 31, 2005 to January 1, 2014. The treatment outcome and complications were recorded and the therapeutic efficacy was classified as one of two categories: effective treatment without further intervention and ineffective treatment with further intervention(s). The therapeutic efficacy was analyzed from 1-24 months after treatment.

#### RESULTS

24 out of the 30 patients included in the study were females with an average age of 10.5 years-old (range: 2-27). 22 patients had more than one CVM lesion. The technical success was 100% and no major complication was observed. 57% of the patients required more than one treatment session to obtain an effective treatment. The predominant anatomic location of these CVM lesions were in the lips (53%) and cheek (31%). Recurrence was observed in 17 out of 30 patients. Higher rates of recurrence were observed in patients with more than one treated CVM lesion and in patients treated after the age of 7 years-old (RR 2.727 (0.9-16.1), p<0.05; RR 2.727 (0.9-16.1), p<0.05).

## CONCLUSION

Delayed treatment and multiplicity of cervicofacial venous malformations have higher rates of recurrence and decreased therapeutic efficacy after initial treatment with ethanol ablation.

# **CLINICAL RELEVANCE/APPLICATION**

Cervicofacial venous malformations are a common vascular anomaly in pediatric patients. As such, targeted treatment with absolute ethanol is safe with a low complication risk and should be performed at an earlier age especially in patients with multiple lesions to increase therapeutic efficacy and decrease the rate of recurrence.

# DTI in Healthy Children Pre/post Musical Training

Wednesday, Nov. 30 12:15PM - 12:45PM Room: PD Community, Learning Center Station #1

#### **Participants**

Pilar Dies-Suarez, MD, Mexico City, Mexico (*Presenter*) Nothing to Disclose Silvia Hidalgo-Tobon, PhD, Mexico City, Mexico (*Abstract Co-Author*) Nothing to Disclose Benito De Celis IV, Puebla, Mexico (*Abstract Co-Author*) Nothing to Disclose Coral Guerrero, Mexico, Mexico (*Abstract Co-Author*) Nothing to Disclose Eduardo Castro Sierra, mexico, Mexico (*Abstract Co-Author*) Nothing to Disclose

#### PURPOSE

Music modulates structural and functional changes in the brain, which promotes cognitive, motor, sensory, emotional and even social processes. The maturation of tracts and connections between motor, auditory and other modalities areas, allow the development of cognitive functions during the course of life, including musical skills.

#### **METHOD AND MATERIALS**

15 pediatric healthy subjects between 5 and 6 years old were recruited for this study. All subjects were: right handed, and had no antecedents of sensory, perception or neurological disorders. All volunteers had not been trained in the past in any kind of artistic discipline. Volunteers were healthy during the study protocol. Scanning was performed in a 1.5 T Philips-InteraAchieva scanner (Philips)Children received musical training for 9 months.Diffusion tensor imaging(DTI)data wereacquiredusing a SE-EPI sequence. Diffusionweightedgradientswereappliedalong 15 non-collineardirectionswith a b-value=800 s/mm2. High-resolutionimageswereacquiredusing 3DT1.Thediffusion tensor wasfittedwith linear least-squareafter a preprocessingstepcorrectingforheadmovementsandeddycurrentswasapplied by registeringallvolumes. Finally, usingMedINRI, diffusiontensorswerecalculatedtoobtainFractionalAnisotropy (FA) with FA thresholdof 0.2 and Mean Diffusivityvalues.Segmentationofthecerebellum CB wasmanuallydrawnonmidlinesagittal 3D-T1 images.

#### RESULTS

It shows that there was an increase in fiber length of minor forceps, which involves fibers interconnecting the front regions and some axons of the cingulate cortex rostral anterior and medial and ventral prefrontal cortex via the knee and face of the corpus callosum, which could be caused by music instruction and demand required to perform certain activities that are within the training, such as imitate coordinated movements.

#### CONCLUSION

We show the plastic effects that can provide music instruction to extend axons of the fibers, especially in the minor forceps are evident. This may have occurred because of the need to create more connection between the two hemispheres to run more efficiently the tasks required for musical training.

#### **CLINICAL RELEVANCE/APPLICATION**

Musical training might be an option for intervention to treat the disorders mentioned above, because although it is known that music can help patients with autism and ADHD, with the results shown in this paper, could create targeted strategies especially these pathologies.

## PH246-SD-WEA1

Radiation Dose, Contrast Medium Dose, and Image Quality at Low Tube Voltage CT for Right Adrenal Vein Imaging

Wednesday, Nov. 30 12:15PM - 12:45PM Room: PH Community, Learning Center Station #1

## Participants

Kensuke Omura, MD, Sendai, Japan (*Presenter*) Nothing to Disclose Hideki Ota, MD, PhD, Sendai, Japan (*Abstract Co-Author*) Nothing to Disclose Yuhki Takahashi, MD, Sendai, Japan (*Abstract Co-Author*) Nothing to Disclose Tomonori Matsuura, Sendai, Japan (*Abstract Co-Author*) Nothing to Disclose Kazumasa Seiji, MD, PhD, Sendai, Japan (*Abstract Co-Author*) Nothing to Disclose Kei Takase, MD, PhD, Sendai, Japan (*Abstract Co-Author*) Nothing to Disclose

### PURPOSE

Right adrenal vein (RAV) imaging prior to adrenal venous sampling with less radiation and iodine contrast dose is preferred. We aimed to compare radiation dose, contrast medium dose, and image quality for CT imaging of the RAV among conventional, low kV, and low kV with reduced contrast protocols.

#### **METHOD AND MATERIALS**

This institutional-review-board approved prospective study included 90 consecutive patients with primary aldosteronism. Written informed consent was obtained from all patients. Patients were randomized into three groups: contrast dose of 600 mg/kg body weight at conventional 120 kV tube voltage setting (600-120 group), 600 mg/kg at 80 kV (600-80 group), and 360 mg/kg at 80 kV (360-80 group). All patients were imaged with a second generation dual-source MDCT scanner. Images at 120 kV were reconstructed with filtered back projection and those at 80 kV with iterative reconstruction (SAFIRE, strength 3). Slice thickness was 1mm with 1mm interval. RAV visualization was evaluated using a 5-point scale (0-4). A score of  $\geq$  2 was defined as detectable. Estimated effective radiation dose (ED), background noise, signal-to-noise ratio (SNR), and contrast-to-noise ratio (CNR) were calculated. Analysis of variance with Tukey's test for post hoc comparisons was used for continuous variables, and Kruskal Wallis test was used for categorical variables. P < .05 indicated statistical significance.

#### RESULTS

RAV detectabilities were 96% (26/27), 97% (30/31) and 97% (31/32) for 600-120 group, 600-80 group, and 360-80 group, respectively (P = .99). No significant differences in the visualization scores were found among the three groups ( $3.5 \pm 0.8$ ,  $3.6 \pm 0.8$  and  $3.3 \pm 0.9$ , respectively (P = .20). EDs were  $1.9 \pm 0.8$ ,  $1.6 \pm 0.6$  and  $1.3 \pm 0.6$ , respectively. The 360-80 group showed significantly lower ED than 600-120 group (P = .004). Both 80kV groups showed significantly lower background noise than 120kV group. The 600-80 group showed significantly higher SNR and CNR than 600-120 group.

## CONCLUSION

RAV detectability was comparable among the three groups. Low tube voltage CT can reduce radiation and contrast medium dose while keeping image quality and RAV detectability.

## **CLINICAL RELEVANCE/APPLICATION**

Low tube voltage CT can precisely identify the RAV while reducing radiation dose and contrast medium dose in patients with primary aldosteronism.

# A New Automatic Registration Technique for Temporal Subtraction in Successive Hand CR Images

Wednesday, Nov. 30 12:15PM - 12:45PM Room: PH Community, Learning Center Station #2

#### **Participants**

Seiichi Murakami, Kitakyusyu, Japan (*Presenter*) Nothing to Disclose Shota Kajiwara, Kitakyusyu, Japan (*Abstract Co-Author*) Nothing to Disclose Hyoungseop Kim, PhD, Kitakyushu, Japan (*Abstract Co-Author*) Nothing to Disclose Takatoshi Aoki, MD, PhD, Kitakyushu, Japan (*Abstract Co-Author*) Nothing to Disclose

# PURPOSE

Although the radiographic assessment of joint damage is essential in characterizing disease progression and prognosis in rheumatoid arthritis (RA) patients, it is often difficult even for trained radiologists because interval changes are often subtle. The purpose of this study is to develop an automatic registration technique for temporal subtraction images in order to assist radiologists in the detection of interval changes on phalange radiographs.

# METHOD AND MATERIALS

We developed an automatic registration technique with scale-invariant salient region features. First, we performed a segmentation technique for extracting the detailed phalangeal regions using the multiscale gradient vector flow snakes method. Next, the salient regions were detected based on entropy from the image of the phalangeal regions. Then, the optimum deformation value was determined from the relationship between the previous salient region features and current ones. Finally, the interval changes are detected by registration of phalangeal regions based on rigid registration technique. We applied our developed method to 84 bone pairs (current and previous images) of hand CR images. For quantitative assessments, we employed the Jaccard similarity coefficient in the registration area between the previous and the current segmented region. For qualitative assessments, the temporal subtraction images was reviewed by two radiologists using a four-point scale (1=poor: most of outline not registered; 4=excellent: all of outline perfectly registered).

# RESULTS

The Jaccard similarity coefficient of our registration technique was 94% at average. Overall image quality was good to excellent in the observers' qualitative assessment.

# CONCLUSION

We have developed a new computerized scheme to enhance the temporal change based on image registration technique. The novel automatic registration technique for temporal subtraction images has high registration accuracy.

#### **CLINICAL RELEVANCE/APPLICATION**

We have been developing a new temporal subtraction method using the salient region featured image registration technique. This registration technique can reduce computational time and can potentially be used for detection of subtle interval changes caused by arthritis.

# PH248-SD-WEA3

Change in ADC during Cardiac Cycle in Idiopathic Normal Pressure Hydrocephalus Decreases with Shunt Surgery

Wednesday, Nov. 30 12:15PM - 12:45PM Room: PH Community, Learning Center Station #3

# Participants

Ryoko Yamamori, RT,BS, Kanazawa, Japan (*Presenter*) Nothing to Disclose Tosiaki Miyati, PhD, Kanazawa, Japan (*Abstract Co-Author*) Nothing to Disclose Naoki Ohno, PhD, Kanazawa, Japan (*Abstract Co-Author*) Nothing to Disclose Mitsuhito Mase, MD, Nagoya, Japan (*Abstract Co-Author*) Nothing to Disclose Tomoshi Osawa, Nagoya, Japan (*Abstract Co-Author*) Nothing to Disclose Shota Ishida, BS, Kanazawa, Japan (*Abstract Co-Author*) Nothing to Disclose Harumasa Kasai, MSc, Nagoya, Japan (*Abstract Co-Author*) Nothing to Disclose Yuta Shibamoto, MD, PhD, Nagoya, Japan (*Abstract Co-Author*) Nothing to Disclose

#### PURPOSE

We have reported that the apparent diffusion coefficient (ADC) in brain significantly changed during the cardiac cycle, and this change ( $\Delta$ ADC) in the frontal white matter in patients with idiopathic normal pressure hydrocephalus (iNPH) characterized by low intracranial compliance was significantly higher than those in patients with atrophic ventricular dilatation and control subjects. Shunt surgery by which the reduced intracranial compliance can be improved is the most common treatment for iNPH. In this study, we assessed the  $\Delta$ ADC of the white matter in iNPH before and after shunt surgery.

# METHOD AND MATERIALS

With a 1.5-T MR imaging unit (Gyroscan Intera; Philips Medical Systems, Best, The Netherlands), ECG-triggered single-shot diffusion echo-planar imaging (b = 0 and 1000 s/mm2) was used with sensitivity encoding and half-scan techniques to minimize the bulk motion. The imaging parameters were set at TR, two R-R intervals; TE, 70 msec; flip angle, 90 degrees; section thickness, 4 mm; imaging matrix, 64x64; field of view, 256 mm; number of signals averaged, two; the number of cardiac phases, 20; duration and respective times between leading edges of the diffusion gradients, 28.6 and 48.7 msec. Then, we determined the maximum change in ADC ( $\Delta$ ADC) during the cardiac cycle and compared those values of the white matter in patients with iNPH before and after shunt surgery (n = 7, all patients improved symptoms after the shunt procedure, ie., definite iNPH). This study was approved by the institutional review board.

#### RESULTS

 $\Delta$ ADC in the frontal white matter in iNPH after the shunt surgery was significantly lower than that before shunt surgery, indicating that fluctuation of water molecules in the white matter caused by the arterial inflow, ie., volume loading of the brain as the driving force was reduced by increase in the intracranial compliance after the shunt. However, there was no significant difference in ADC values in iNPH before and after shunt surgery.

# CONCLUSION

 $\Delta$ ADC in the frontal white matter in iNPH decreases with the shunt surgery. Determination of  $\Delta$ ADC makes it possible to obtain more detailed information on change in the intracranial condition in iNPH than standard ADC measurement before and after shunt surgery.

# **CLINICAL RELEVANCE/APPLICATION**

ΔADC analysis makes it possible to noninvasively provide detailed information on change in the intracranial condition due to the shunt surgery.

# PH249-SD-WEA4

## Framework for Objective and Fully Automated Image Quality Control of Dedicated Breast CT Systems

Wednesday, Nov. 30 12:15PM - 12:45PM Room: PH Community, Learning Center Station #4

#### **Participants**

Christian Steiding, PhD, Erlangen, Germany (*Presenter*) Employee, CT Imaging GmbH Daniel Kolditz, PhD, Erlangen, Germany (*Abstract Co-Author*) Employee, CT Imaging GmbH Veikko Ruth, MSc, Erlangen, Germany (*Abstract Co-Author*) Nothing to Disclose Ferdinand Lueck, DIPLPHYS, PhD, Erlangen, Germany (*Abstract Co-Author*) Employee, CT Imaging GmbH Willi A. Kalender, PhD, Erlangen, Germany (*Abstract Co-Author*) Founder, CT Imaging GmbH; CEO, CT Imaging GmbH

## PURPOSE

Dedicated breast CT (BCT) represents an emerging 3D imaging modality that has significant potential for breast cancer detection and diagnosis; the first BCT system has recently been granted FDA approval. As for all new tomographic imaging devices, the conformance of system characteristics with specifications needs to be checked on a regular basis, but to date there is no consensus on acceptance and constancy testing for image quality (IQ) in BCT. The aim of this work was to introduce and validate a quality assurance (QA) framework for objective and easy-to-use IQ control of BCT scanners.

#### **METHOD AND MATERIALS**

A cylindrical QA phantom, with a diameter of 14 cm, a height of 10 cm, made of water-equivalent plastic, was chosen. Various test inserts are embedded in this phantom to determine the desired IQ parameters. Noise by means of the standard deviation and the noise power spectrum as well as uniformity are determined in homogeneous phantom compartments located at different axial positions. Special inserts providing defined CT values allow for assessing image contrast and CT value accuracy. For fully volumetric evaluation of high-contrast spatial resolution, the 3D modulation transfer function of a 12 mm PTFE sphere can be calculated. We implemented an automated detection algorithm for the proposed QA phantom to make automatic and easy-to-use tracking of imaging characteristics feasible. Measurement series were carried out on a photon-counting BCT prototype equipped with a tiled cadmium telluride detector with 0.1 mm pixel size.

# RESULTS

Only one scan is required to determine all essential IQ parameters routinely when using the novel QA framework. The interscan variation of repeated measurements was neglectable for all the assessed IQ metrics. Less than 10 s were required for the phantom detection and IQ analysis. The robustness of the proposed QA framework was validated successfully over a period of several months.

# CONCLUSION

The proposed QA framework provides quantitative, robust, and fully automated 3D IQ control and is applicable for arbitrary scan protocols. Our study indicates that the concept is suitable for any acceptance and constancy testing in BCT to come.

# **CLINICAL RELEVANCE/APPLICATION**

The proposed framework ensures accurate and reproducible assessment of the stability of objective IQ aspects in BCT and may thereby help to establish QA standards for this emerging imaging modality.

# PH251-SD-WEA6

Technical and Clinical Factors Affecting Success Rate of a Novel Holistic Deep Learning Method for Pancreas Segmentation on CT Scans

Wednesday, Nov. 30 12:15PM - 12:45PM Room: PH Community, Learning Center Station #6

# Participants

Mohammad Hadi Bagheri, MD, Bethesda, MD (*Presenter*) Nothing to Disclose Holger R. Roth, PhD, Bethesda, MD (*Abstract Co-Author*) Nothing to Disclose William Kovacs, Bethesda, MD (*Abstract Co-Author*) Nothing to Disclose Le Lu, PhD, Bethesda, MD (*Abstract Co-Author*) Nothing to Disclose Jianhua Yao, PhD, Bethesda, MD (*Abstract Co-Author*) Royalties, iCAD, Inc Francine Thomas, BS,RT, Bethesda, MD (*Abstract Co-Author*) Nothing to Disclose Ronald M. Summers, MD, PhD, Bethesda, MD (*Abstract Co-Author*) Royalties, iCAD, Inc; ;

# PURPOSE

Pancreas segmentation on CT scans is an extremely difficult problem due to the pancreas's high deformability and complex surroundings. In order to improve the accuracy of pancreas segmentation, it is important to identify the technical and clinical factors that affect it.

# METHOD AND MATERIALS

A holistic deep convolutional neural network approach for pancreas segmentation in 82 abdominal CT scans from 53 men and 27 women, combining interior and boundary mid-level cues via spatial aggregation segmentation method for the pancreas was evaluated by the Dice similarity coefficient (DSC). Seventeen patients were healthy kidney donors and the remaining 65 patients had neither major abdominal pathologies nor pancreatic lesions. All scans were in the portal-venous phase (~70 seconds after intravenous contrast injection). Mean slice thickness was  $1.2 \pm 0.7$  mm. Using multiple regression analysis (PSPPIRE, Linux Version: 0.7.9), the DSC was compared with CT technical factors (image pixel size, slice thickness, presence or absence of oral contrast), demographic data (age, gender, height, weight, BMI) and CT imaging findings (volume and density of pancreas, visceral and subcutaneous abdominal fat volume and CT attenuation of the structures within 5-mm neighborhood of the pancreas).

#### RESULTS

The overall DSC was 78.0%  $\pm$  8.0. Factors that were statistically significantly correlated with DSC included age (r=0.25, p=0.03), abdominal fat (visceral (r=0.4, p=0), subcutaneous (r=0.25, p=0.02) and total abdominal fat(r=0.38, p<0.01)), standard deviation of CT attenuation within the pancreas (r=0.28, p=0.01), volume of the pancreas (r=0.22, p=0.05) and median and average CT attenuation in the immediate neighborhood of the pancreas (r=-0.41, p<0.01 and r=-0.40, p<0.01 respectively). We found no significant correlation between the DSC and the height, weight, BMI, gender or mean CT attenuation of the pancreas.

## CONCLUSION

Increased abdominal and visceral fat, age and fat within or around the pancreas are major factors associated with better segmentation (higher DSC) of the pancreas. These results provide a clear direction for future research for solutions to this difficult image processing problem.

# **CLINICAL RELEVANCE/APPLICATION**

This pancreatic segmentation method, which achieves the current state-of-the-art performance, is more accurate in elderly patients and those with greater pancreatic and peripancreatic fat.

## QS001-EB-WEA

Reduction of Radiation Dose of Fluoroscopic Gastrointestinal Examinations by Education to Residents and Radiographers

Wednesday, Nov. 30 12:15PM - 12:45PM Room: QS Community, Learning Center Hardcopy Backboard

# Participants

Moon Hyung Choi, MD, Seoul, Korea, Republic Of (*Presenter*) Nothing to Disclose Seung Eun Jung, MD, Seoul, Korea, Republic Of (*Abstract Co-Author*) Nothing to Disclose Jae Young Byun, MD, Seoul, Korea, Republic Of (*Abstract Co-Author*) Nothing to Disclose

# PURPOSE

Optimization of radiologic examinations is an important issue in radiology. Radiation dose has been increased by wide use of x-ray examinations in medicine. Although CT is regarded as an important source of radiation, fluoroscopy should not be ignored as it is used more frequently due to increase in need of minimal invasive procedures using fluoroscopy unit. A unique feature of fluoroscopy is that radiation exposure and examination time depend on a physician who performs examination. Staff in our institution recognized that some residents performed fluoroscopic examinations using proper radiation in proper examination time, but others performed examinations with high radiation exposure for excessively long time. We aim to evaluate the causes of differences in radiation dose and fluoroscopy time in many fluoroscopy examinations. Our goal is to reduce radiation dose by educating residents and radiographers about the well-known methods to reduce radiation exposure in fluoroscopy examinations.

#### **METHODS**

From June 2014 to February 2016, 2,499 fluoroscopy examinations for GI tract were performed using two fluoroscopic units in our institution, a tertiary academic hospital. Examinations were performed by staffs or residents from radiology or other departments. Radiographers assisted all procedures. A GI radiologist reviewed all examinations and evaluated many factors related to examinations. Number of total, spot, captured, cine, captured video, collimated and magnified images, frame rate of cine images, fluoroscopy time and dose area product (DAP) measurement were recorded. Patient information including sex, age, height and weight was collected from electric medical record (EMR). We offered an hour's education to radiology residents and radiographers in April 2015 about how much radiation exposure and how to reduce radiation dose in fluoroscopic examinations. We also changed the protocol of defecography that showed much higher radiation exposure than other examinations. In our institution, end of all fluoroscopic examinations for gastrointestinal tract performed by radiology residents was determined by staff we believed that change of protocols did not impair image quality and diagnostic performance.

#### RESULTS

Fluoroscopic GI examinations consisted of 10 kinds of examinations, including colon study with water soluble contrast media (WSCM) (90 cases), colon study with barium (71 cases), defecography (67 cases), esophagography with WSCM (137 cases), esophagography with barium (297 cases), small bowel series (SBS) with WSCM (212 cases), SBS with barium (29 cases), upper GI series (UGI) with WSCM (327 cases), and UGI with barium (65 cases). Barium swallowing tests (1203 cases) were performed by otolaryngology or rehabilitation medicine residents. Among all GI examinations, 123 cases were for pediatric patients under 16 years old. There was significant difference in radiation dose before and after education (41.449 and 30.22 Gy·cm2) despite there was no difference in fluoroscopy time. Spot and cine images that contributed to increase radiation dose were used less frequently after education than before education (P = 0.001). Instead more captured image or video was used after education (P < 0.001). Although fluoroscopy time in defecography was not reduced significantly after change of the protocol to replace spot images by captured images, DAP measurement was reduced dramatically after change of protocol from 201.595 Gy cm2 to 29.061 Gy cm2 (P < 0.001). In the most common two examinations, esophagography with water soluble contrast and upper GI series (UGIS) with water soluble contrast, there were significant differences in ratio of spot, capture, cine, captured video images to total images among radiologists. DAP measurement was also different among radiologists (P < 0.001). DAP in UGIS examinations by a radiologist who used the most radiation was more than two times of that by a radiologist who used the least radiation (P = 0.001). In barium swallowing test, radiographers collimated images more frequently after education than before (P < 0.001) and DAP was significantly reduced after education from 23.8 Gy cm<sup>2</sup> to 20.4 Gy cm<sup>2</sup> (P < 0.03). Multivariate regression test showed total number of frame in cine images, numbers of total and collimated images and fluoroscopy time were significant factors related to DAP.

## RESULTS

There were 1203 barium swallowing tests and fluoroscopic GI examinations consisted of 9 examinations; colon study with water soluble contrast (n = 90), colon study with barium (n = 71), defecography (n = 67), esophagography with water soluble contrast (n = 137), esophagography with barium (n = 297), small bowel series (SBS) with water soluble contrast (n = 212), SBS with barium (n = 29), upper GI series (UGI) with water soluble contrast (n = 327), and UGI with barium (n = 65). Barium swallowing tests were performed by otolaryngology or rehabilitation medicine residents. Other examinations were performed by 9 radiology residents and one pediatric radiology staff. Among all GI examinations, 123 examinations were for pediatric patients under 16 years old. There was significant difference in radiation dose before and after education (41.449 and 30.22 Gy cm2) despite there was no difference in fluoroscopy time. Spot and cine images that contributed to increase radiation dose were used less frequently after education than before education (P = 0.001). Instead more captured image or video was used after education (P < 0.001). We found that radiation exposure was much higher during defecography that other examinations, we change the protocol to replace spot images by captured images. Although fluoroscopy time was not reduced significantly, DAP measurement was reduced dramatically after change of protocol from 201.595 Gy·cm<sup>2</sup> to 29.061 Gy·cm<sup>2</sup> (P < 0.001). In the most common two examinations, esophagography with water soluble contrast and upper GI series (UGIS) with water soluble contrast, there were significant differences in ratio of spot, capture, cine, captured video images to total images among radiologists. DAP measurement was also different among radiologists (P < 0.001). DAP in UGIS examinations by a radiologist who used the most radiation was more than two times of that by a radiologist who used the least radiation (P = 0.001). In barium swallowing test, radiographers collimated images more frequently after education than before (P < 0.001) and DAP was significantly reduced after education from 23.8 Gy·cm2 to 20.4 Gy·cm2 (P < 0.001) 0.03). Multivariate regression test showed total number of frame in cine images, numbers of total and collimated images and fluoroscopy time were significant factors related to DAP.

# CONCLUSION

We achieved significant decrease of radiation dose by educating physicians or radiographers who operated fluoroscopy unit as the

collimation and capture image were used frequently after education. We also achieved significant reduction of radiation dose by change of the protocol in an examination. We can conclude that awareness of radiation exposure in fluoroscopy examinations and understating of methods to reduce radiation are very important.

## QS016-EB-WEA

# Reducing Patient Time, Staff Time and Cost using the Time-Driven Activity-Based Costing (TDABC) Methodology in MRI

Wednesday, Nov. 30 12:15PM - 12:45PM Room: QS Community, Learning Center Hardcopy Backboard

# Participants

Stacy R. Schultz, BA, Rochester, MN (*Presenter*) Nothing to Disclose Laura Tibor, MBA, BEng, Rochester, MN (*Abstract Co-Author*) Nothing to Disclose Ronald Menaker, MBA, Rochester, MN (*Abstract Co-Author*) Nothing to Disclose Bradley A. Weber, DO, Dayton, OH (*Abstract Co-Author*) Nothing to Disclose Brent Warndahl, ARRT, Rorchester, MN (*Abstract Co-Author*) Nothing to Disclose Jay Ness, Rochester, MN (*Abstract Co-Author*) Nothing to Disclose Elizabeth Wendorff, Rochester, MN (*Abstract Co-Author*) Nothing to Disclose Paula Murphy, RN, Rochester, MN (*Abstract Co-Author*) Nothing to Disclose Phillip M. Young, MD, Rochester, MN (*Abstract Co-Author*) Nothing to Disclose

#### PURPOSE

Share our success in using Time-Driven Activity-Based Costing (TDABD) methodology to better understand and improve our MR Enterography practice. MR Enterography is a complex technique that involved eight different care providers and required a patient to spend an average of three hours in our department. Prior attempts at improving the process had been disappointing.

## METHODS

TDABC is a cost accounting methodology designed to measure the time and cost of providing patient care services. When married to workflow maps, it can help graphically represent the labor, space, machine and supply costs associated with the steps in an imaging workflow. A multidisciplinary team of patient-care personnel (nurses, radiologists, and technologists) and Radiology management staff (managers, finance, and supply chain) was formed. The team mapped the current state, completed multiple observations of process steps, performed manual timings where data could not be gathered electronically, and calculated the associated costs to each element of the workflow process. The team utilized Pareto charts to understand the highest cost and time-consuming activities, brainstormed opportunities for improvement, and assessed the impact of those changes. Multiple Plan-Do-Study-Act (PDSA) cycles were developed to test changes and control charts were utilized to monitor progress. Through a targeted change management plan, which included multiple communication avenues along with education and training of several technologists, the improvements were implemented in less than three months. Staff satisfaction was monitored through the process.

# RESULTS

The TDABC method produced detailed and actionable data-rich workflow maps for current state and potential future states. The most impactful process change consisted of transitioning the steps in preparation and administration of glucagon from the registered nurse to the technologist. Our modifications demonstrated success by reducing non-value added waste and cost by 13%, staff time by 16% and patient process time by 17%. This methodology led to a successful outcome in modifying daily workflow in an area of past challenges and frustration.

#### CONCLUSION

The TDABC methodology led our radiology department to more accurately identify the current state costs of providing an MR Enterography exam and opportunities for improvement. A multidisciplinary team utilizing a structured problem-solving approach was necessary to achieving success. With the success of this initiative, additional TDABC work is being done in other areas within our Radiology practice.

# Benefits of Web-Lectures and Video Based Content on Radiologic Physics Education

Wednesday, Nov. 30 12:15PM - 12:45PM Room: QS Community, Learning Center Station #1

#### **Participants**

Thomas Oshiro, PhD, Los Angeles, CA (*Presenter*) Nothing to Disclose Megan Donaghy, BS, Northridge, CA (*Abstract Co-Author*) Nothing to Disclose Anita Slechta, MS, RT, Canyon Country, CA (*Abstract Co-Author*) Nothing to Disclose Michael F. McNitt-Gray, PhD, Los Angeles, CA (*Abstract Co-Author*) Institutional research agreement, Siemens AG Research support, Siemens AG

## PURPOSE

At many institutions, radiologists and physicists are often asked to provide educational content to staff, faculty and students in addition to clinical responsibilities. Through the development of web-based content, lectures and demonstration videos can be distributed throughout a medical enterprise and can be repurposed for multiple applications and audiences.

#### METHODS

Lectures were produced using a combination of PowerPoint<sup>™</sup> for slideshows, Audacity<sup>™</sup> for audio voiceover and iSpring<sup>™</sup> for conversion of the materials to a video/web format. Produced content included the fundamentals of radiography, fluoroscopy, mammography and ultrasound physics. Over 350 short segments were created (~ 5-7 minutes each in duration). These shorter segments were believed to benefit over longer lectures for maintaining attention and ease of navigation for review.In addition, approximately 70 short quality control videos (ranging in 1-3 minutes in length) were created using digital video cameras and Final Cut Pro<sup>™</sup> editing software. Topics focused on routine technologist and physicist equipment testing procedures.Total content was approximately 3 GB in size. Ultrasound content (140MB) was placed on an internal hospital web-server and HTML links were sent to attendees. In some cases, distribution on the enterprise web servers was not feasible due to bandwidth and security restrictions and therefore materials were dispensed on USB or CD media.Approximately 3000 multiple choice review questions were created using the Moodle<sup>™</sup> learning management system to supplement the content. The system was hosted on an externally accessible website to provide greater access. Short quizzes were created that randomly pulled items from this question bank.

#### RESULTS

Content was assembled based on the audience and need. Approximately 35 hours of radiography and fluoroscopy lectures were integrated into flipped undergraduate radiologic technology (RT) physics courses. 4 hours of mammography and ultrasound content was distributed separately to radiology residents and medical physics graduate students. 20 hours of fluoroscopy-specific content was reassembled for physicians specializing in pain management. A 20 hour radiographic review guide was distributed to RT students in preparation for their national exam. While no official outcomes or surveys were obtained from residents, fellows or medical physics graduate students, the content was generally well received. However, informal canvassing of fellows and residents showed a preference toward in-class training compared to video delivery.RT course final examination scores were tallied between 2001 and 2015 and showed improvements with the flipped RT classes compared to the in-classroom experience. On average, students performed 13% better for the subjects covered in the quality control videos and 8% better for didactic lectures covering radiography and fluoroscopy.The RT program's national certification examination scores (ARRT-R) in physics-related categories showed an average improvement of 0.15 points (0-10 point scale) on the exam. Although this was not a statistically significant improvement it was also combined with a 60% increase in class size. (from 13.8 pre-flip to 22.7 students post-flip)

## CONCLUSION

Creation of web-lectures and video segments requires extensive up-front work but accessibility of screen capture and slide conversion software can make this transition easier. The repurposing of the content to multiple audiences can reduce the additional overhead in teaching especially when courses and content repeat on a year to year basis. As radiological procedures become more widespread throughout an institution, an even greater need for this type of training will exist. In the RT program it was seen that despite an increase in class size the flipped classroom produced an improvement in academic exam performance. This was believed to be from the ability to review content multiple times and at a pace to each student's preference. While it is debatable to use the standardized test scores as a metric of student aptitude, flipping these classes appears to show promise and does not seem to have an adverse effect on national exam scores. With increased class sizes, hands-on quality control experiments can be difficult to manage and coordinate by a single instructor due to limitations on specialized test equipment, radiographic phantoms and x-ray room size. The video segments allowed all students to experience the same "over-the-shoulder" view of the experimental setup. In the evolving radiology department, equipment and technology will change over time. The creation of legacy videos allows students to gain some experience for systems no longer available. In this video library, testing with film processors (e.g: sensitometry, specific gravity) and analog systems (e.g: film/screen contact, mammography spatial resolution) are still reviewable for historical purposes.

#### QS125-ED-WEA2

# Improving the Efficiency of Patient Care in Radiology through an Educational Presentation for Surgical Interns

Wednesday, Nov. 30 12:15PM - 12:45PM Room: QS Community, Learning Center Station #2

# Participants

Aman Khurana, MD, San Diego, CA (*Presenter*) Nothing to Disclose Sreenath Narayan, MD, PhD, Cleveland, OH (*Abstract Co-Author*) Stockholder, Abbott Laboratories Stockholder, Cardinal Health, Inc Stockholder, CareFusion Corporation Stockholder, Cigna Corporation Stockholder, General Electric Company Stockholder, Johnson & Johnson Stockholder, Medtronic plcStockholder, The Procter & Gamble Company Cosette M. Stahl, DO, San Diego, CA (*Abstract Co-Author*) Nothing to Disclose Tudor H. Hughes, MD, San Diego, CA (*Abstract Co-Author*) Nothing to Disclose

## PURPOSE

The purpose of this quality storyboard is to describe our quality improvement project to improve patient care by improving the interdepartmental communication between the radiology and surgical departments (general surgery, neurosurgery, otorhinolaryngology, orthopedics and urology) through an educational presentation that outlined how to request the appropriate study, resources for facilitating interdepartmental communication, and the institutional policies regarding contrast material and associated allergic reaction prophylaxis.

#### **METHODS**

18-19 surgical interns within the first month of their intern year were chosen from the surgical departments (general surgery, neurosurgery, otorhinolaryngology, orthopedics and urology) at our institution, over the course of two years (2014 and 2015). A short 12 question quiz was administered to the surgical interns that covered the three competencies (requesting the appropriate examination, resources for facilitating interdepartmental communication, and institutional policies regarding contrast administration). Some of the questions covered more than a single competency. Then, a short 40 minute educational presentation was provided by the radiology residents covering the three competencies. To address the appropriate examination competency, the presentation covered how to request the appropriate study for common diagnoses, such as small bowel obstruction, acute appendicits, acute diverticulitis, pulmonary embolism, and anastomotic leaks. To address the communication competency, screenshots were shown of the department website, which contained information about how to find numbers for each subspecialty reading room, and how to find pager numbers for the radiologist on call during off hours. Guidance was given on how to write an appropriate history when requesting a study, and why this is important. To address the contrast competency, the presentation showed screenshots of how to access to the institutional contrast policies on the department website, and reviewed the institutional policies for nephrotoxicity and allergy prophylaxis.After the presentation, the short quiz was again given to the surgical interns to assess the performance of the educational presentation in fulfilling the objectives of the presentation. The number of correct answers was tabulated before and after the educational presentation.

## RESULTS

A 12 question quiz was given to the surgical interns prior to the educational presentation. 6 questions addressed the competency of how to request the proper study, 3 questions addressed institutional policies regarding contrast administration and 5 questions addressed how to properly communicate with the radiology department. Some questions addressed multiple competencies. The comparative data before and after the educational presentation for each competency is shown in the figure. For the interdepartmental communication competency, the percentage of correct answers increased from 53.5% to 81.1% after the educational presentation of questions addressing the competency). Similarly, for the appropriate study competency, the increase was from 38.3% to 80.6% and for the contrast policy competency, the numbers rose from 30.6% to 88.3%. In total, the percentage of correct answers more than doubled from 40.8% to 83.3% after the presentation.

#### CONCLUSION

A short educational presentation that covered the competencies of requesting the correct study, communicating with the department of radiology, and the institutional policies for contrast administration was successfully able to convey the intended information, as shown by an improvement in the scores on a quiz administered before and after the presentation. Proficiency of the requesting provider with these competencies may help decrease the number of distracting tasks for radiologist, thereby decreasing the time from acquisition to interpretation of studies (Ratwani, Raj M. et al. A Human Factors Approach to Understanding the Types and Sources of Interruptions in Radiology Reading Rooms. Journal of the American College of Radiology, http://dx.doi.org/10.1016/j.jacr.2016.02.017).

## QS126-ED-WEA3

Developing a Multidisciplinary Prostate MRI Program in a Community-based Health System - Essential Initial Activities and Clinical Outcomes

Wednesday, Nov. 30 12:15PM - 12:45PM Room: QS Community, Learning Center Station #3

# Participants

Crystal Farrell, MD, Grand Rapids, MI (*Presenter*) Nothing to Disclose Sabrina Noyes, Grand Rapids, MI (*Abstract Co-Author*) Nothing to Disclose Joseph Joslin, Belmont, MI (*Abstract Co-Author*) Nothing to Disclose Manish K. Varma, MD, Ada, MI (*Abstract Co-Author*) Nothing to Disclose Andrew K. Moriarity, MD, Grand Rapids, MI (*Abstract Co-Author*) Nothing to Disclose Christopher M. Buchach, MD, Grand Rapids, MI (*Abstract Co-Author*) Nothing to Disclose Leena Mammen, MD, Grand Rapids, MI (*Abstract Co-Author*) Nothing to Disclose Brian R. Lane, MD, Grand Rapids, MI (*Abstract Co-Author*) Nothing to Disclose

#### PURPOSE

There has been considerable recent interest in expanding multi-parametric prostate MRI (mpMRI) services at major medical centers, including both diagnostic and interventional service lines. While there is growing experience and expertise with mpMRI at many academic centers, implementation in community-based health systems has lagged, and literature to support outcomes in this setting are currently lacking. Not surprisingly, results from more "mature" academic programs may not accurately reflect the performance of mpMRI through the "learning curve" of program development. After we began our community prostate mpMRI program in 2010, we found that we initially had a high false positive rate for studies, as many "suspicious lesions" resulted in benign findings at biopsy. This pattern of discordant cases prompted two initiatives aimed at increasing the reliability of mpMRI and improving patient outcomes. The first was to introduce a standardized interpretation and reporting system, which later led to the adoption of the PI-RADSv2 criteria. The second was to begin a monthly multispecialty mpMRI meeting in order to foster more experience in developing a community-based mpMRI program, including the evolution of imaging interpretation and reporting methods and key aspects of our multidisciplinary patient management approach.

## METHODS

Information regarding all mpMRI studies at our institution is maintained in a prospectively-collected database for quality purposes. IRB approval was obtained for a retrospective analysis of all mpMRI performed between program inception (August 2010) and December 2015. Patient demographic information, clinical notes, MRI interpretations, available biopsy/surgical pathology, and individual management pathways were recorded and analyzed. Results were stratified by three distinct radiology reporting periods to observe changes in clinical impact over time, including before and after the implementation of a standardized reporting system in June 2014, and following the adoption of PI-RADSv2 in March 2015. The overall lesion suspicion level on mpMRI was correlated with patient pathology results, management decisions and clinical outcomes. Narrative input from multispecialty team members was compiled and categorized into operations activities, quality and process improvement, and impact on patient-specific management. Thus, outcomes are described both quantitatively with mpMRI and biopsy concordance values, and qualitatively with descriptive analyses of the clinical impact of the multidisciplinary meetings.

# RESULTS

During the initial program development, 537 mpMRI were performed, increasing in volume and number of ordering physicians every year. Overall, majority of cases were performed for previously diagnosed prostate cancer (65%) rather than screening (35%), however, the percentage of PCa screening patients more than quadrupled from 9.5% to 41% over 5 years. Staging information was consistent even early in the program, with relatively constant rates of suspected extraprostatic extension (EPE) (17%), lymph node metastasis (6.9%), and bone or other sites of pelvic metastasis (4.1%) over time. However, when mpMRI reports were examined by successive reporting periods, there was a significant decrease in the number of high suspicious lesions identified by mpMRI, from 61.7% initially, to 55.4% following the implementation of standardized reporting, to 42.2% with PI-RADS v2. This trend corresponded to a significant increase in the positive biopsy rate from 49% and 47% in the initial and standardized reporting periods to 70% using PI-RADSv2 criteria. This increased specificity is likely due to a combination of factors, including improved standardization of interpretation and reporting methods using the PI-RADSv2 system, and multidisciplinary teamwork providing regular feedback and pathologic correlation.Since the institution of regular multispecialty mpMRI meetings in July 2014, 67 patients were reviewed (14%). Of those, 51% had a change in management as a result. Multispecialty participants indicated that timely review of cases, standardized reporting and management processes, radiology-pathology correlation and cross-disciplinary treatment coordination as several benefits of the monthly meetings.This report details over thirty specific patient outcome and clinical activities identified by participants in multispecialty care.

# CONCLUSION

Prostate MRI can be successfully performed in the community healthcare setting. High rates of locoregional staging accuracy can be obtained with radiologic proficiency; however lesion discrimination and pathologic yield improve with reader experience and application of standardized reporting methods. Multidisciplinary meetings are well received by participants and have been shown to improve both patient specific impact and treatment outcomes.

Pre-treatment Multiparametric MRI as a Predictive Marker for Biochemical Recurrence Following External Beam Radiation Therapy for Prostate Cancer

Wednesday, Nov. 30 12:15PM - 12:45PM Room: RO Community, Learning Center Station #1

#### Awards

#### **Student Travel Stipend Award**

#### Participants

Luca F. Valle, BA, Spokane, WA (*Presenter*) Nothing to Disclose Matthew Greer, BS, Cleveland Heights, OH (*Abstract Co-Author*) Nothing to Disclose Andra Krauze, Bethesda, MD (*Abstract Co-Author*) Nothing to Disclose Aradhana Kaushal, MD, Philadelphia, PA (*Abstract Co-Author*) Nothing to Disclose Joanna Shih, Bethesda, MD (*Abstract Co-Author*) Nothing to Disclose Peter L. Choyke, MD, Rockville, MD (*Abstract Co-Author*) Researcher, Koninklijke Philips NV; Researcher, General Electric Company; Researcher, Siemens AG; Researcher, iCAD, Inc; Researcher, Aspyrian Therapeutics, Inc; Researcher, ImaginAb, Inc; Researcher, Aura Biosciences, Inc Baris Turkbey, MD, Bethesda, MD (*Abstract Co-Author*) Nothing to Disclose Deborah Citrin, MD, Bethesda, MD (*Abstract Co-Author*) Nothing to Disclose

#### PURPOSE

The capacity of pretreatment multiparametric MRI (mpMRI) to predict biochemical recurrence (BR) after external beam radiation therapy (EBRT) +/- androgen deprivation therapy (ADT) is largely unexplored. We evaluated if pretreatment mpMRI of the prostate with dynamic contrast enhanced (DCE) imaging and diffusion weighted imaging (DWI) with apparent diffusion coefficient (ADC) maps could predict the risk of BR after EBRT +/- ADT.

#### **METHOD AND MATERIALS**

All patients from our institution with diagnostic mpMRI prior to EBRT were included in this retrospective analysis. BR was defined by Phoenix criteria. mpMRI consisted of endorectal coil T2W imaging, DCE, and DWI with ADC maps. Prostate lesions were identified in each MRI sequence by a prostate-dedicated radiologist. The hazard ratio (HR) of BR associated with mpMRI features was estimated with Cox proportional cause-specific hazard models. mpMRI features were correlated with known clinical predictors of BR using the Kruskal-Wallis rank test. To account for multiple comparisons, p<0.01 defined significance.

#### RESULTS

141 patients (11 low, 43 intermediate, and 87 high risk by D'Amico grouping) were included. At a median follow up of 60 months, BR occurred in fourteen (10%) patients. High pre-treatment PSA and detectable post-EBRT PSA nadir were predictors of BR (HR 1.2, p<0.0001 and HR 4.92, p=0.003, respectively). T2 imaging characteristics including the number of lesions (mean 1.4, range 0-4, p=0.099), size of the dominant prostate lesion (p=0.436), and location of the tumor (p=0.394-0.694) did not predict for BR. DWI and DCE positivity did not predict BR (p=0.868 and p=0.368, respectively). Tumor size did correlate with known predictors of BR, such as increasing Gleason score (p<0.001), T stage (p=0.009), and D'Amico risk grouping (p<0.001).

# CONCLUSION

In this retrospective series, mpMRI findings did not predict for BR after EBRT +/- ADT. Although this is the largest series evaluating these parameters as predictive markers in this setting, it is possible that larger patient numbers or a higher proportion of BR may provide an opportunity to elucidate mpMRI characteristics capable of predicting BR.

## **CLINICAL RELEVANCE/APPLICATION**

While mpMRI is effective in the detection of prostate cancer and in the prediction of BR following radical prostatectomy, it may have shortcomings when predicting the risk of BR after EBRT +/- ADT.

# RO235-SD-WEA2

Image-based Response Assessment of HCC Treated by Stereotactic Body Radiotherapy with Respiratory Tracking

Wednesday, Nov. 30 12:15PM - 12:45PM Room: RO Community, Learning Center Station #2

# Participants

Hajer Jarraya, Lille, France (*Presenter*) Nothing to Disclose Xavier Pauwels, Lille, France (*Abstract Co-Author*) Nothing to Disclose Xavier Mirabel, Lille, France (*Abstract Co-Author*) Nothing to Disclose Jerome Durand Labrunie, lille, France (*Abstract Co-Author*) Nothing to Disclose Wilfrid Kouakam, Lille, France (*Abstract Co-Author*) Nothing to Disclose David Buob, Lille, France (*Abstract Co-Author*) Nothing to Disclose Luc Ceugnart, MD, Lille, France (*Abstract Co-Author*) Nothing to Disclose

# PURPOSE

To describe post therapeutic imaging features of HCC treated by SBRT as an aid in assessing response to treatment. To assess tumor response using RECIST , mRECIST and EASL.

#### **METHOD AND MATERIALS**

Imaging Data and medical records of 50 patients with 60 HCC treated with stereotactic body radiotherapy (SBRT) were reviewed. Tumor size and contrast enhancement of lesions were evaluated up to 6 months after radiation. Contrast Enhanced Ultrasound performed in 5 patients were reviewed.

#### RESULTS

Median age was 70 years (range, 44–86 years). Cirrhosis was mainly due to alcohol consumption and majority of patients had CTP A cirrhosis. Half of the patients had already received treatment for HCC, the majority with chemoembolization (23.7%). Median tumor diameter was 32 mm (11,96). Local control rate according to RECIST, mRECIST and EASL were respectively 98.6%, 98.6%, 98% (Kappa : -0.45)

Contrast Enhanced US performed in 5 cases was unconclusive. Reasons will be be detailed.At MRI, local control was associated with, disappearance, shrinkage of the target and decrease or disappearance of internal enhancement. Progression was associated with size increase and persistence of internal enhancement.Evaluation with m RECIST and EASL are more adequat than RECIST criteria assessed to Localprogression free survival LPFS rates.Histological results were obtained in one case showing a radiohistological correlation between radiological features and liver induced focal inflammatory reaction.

# CONCLUSION

SBRT is an emerging technique for treatment of unresectable liver malignancies, especially HCC. The interpretation of post therapeutic imaging features may be challenging for radiologists. Being familiar with these features may improve patient management and avoid additional treatments.

# **CLINICAL RELEVANCE/APPLICATION**

Stereotactic Body Radiotherapy is an emerging technique in the treatment of liver malugnancies espicially HCC and may be safely used as a bridge treatment before transplantation. Radiologists should be familiar with post therapeutic features the interpretation of which may be challenging, to improve patient management and avoid errors of interpretations that may lead to additional harmful treatments. Response assessment is more adequat with m RECIST or EASL compared to RECIST criteria.

# Prognosis of Patients who Received Palliative Intent Radiotherapy for Bone Metastases in Recent Years

Wednesday, Nov. 30 12:15PM - 12:45PM Room: RO Community, Learning Center Station #4

#### Participants

Yasushi Hamamoto, MD, Toon-City, Japan (*Presenter*) Nothing to Disclose Noriko Nishijima, Toon-City, Japan (*Abstract Co-Author*) Nothing to Disclose Kei Nagasaki, Toon-City, Japan (*Abstract Co-Author*) Nothing to Disclose Hiromitsu Kanzaki, Toon-City, Japan (*Abstract Co-Author*) Nothing to Disclose Toshiharu Manabe, Imabari-City, Japan (*Abstract Co-Author*) Nothing to Disclose Teruhito Mochizuki, MD, Toon, Japan (*Abstract Co-Author*) Nothing to Disclose

# PURPOSE

With the development of systemic cancer therapy, unignorable proportion of patients who receive palliative intent radiotherapy (PIRT) for bone metastases have become to live longer. To consider individualization of PIRT for recent year patients, reinvestigation of survival time after PIRT is necessary. In this study, we examined prognostic factors after PIRT.

# METHOD AND MATERIALS

Between December 2009 and June 2015, 100 patients received the initial PIRT for bone metastases in our institution. Of these, 83 patients (range 50-86 years, median 69 years; male : female = 56:27; performance status (PS) 0-1 : PS 2-4 = 45:38; breast cancer : other cancer = 10:73) were followed up until death (80%) or for more than six months (20%). Clinical records concerning the initial PIRT of these 83 patients were examined. Follow-up time was 0.4 - 36.6 months (median 4.7 months).

# RESULTS

The overall survival rates at 2-years from the initial PIRT were 19% for all 83 patients, 17% for lung cancer, 28% for breast cancer, 18% for digestive tract cancer, 0% for liver/biliary tract/pancreas cancer. On univariate analysis, statistically significant factors for survival were gender (p=0.0491) and PS (PS0-1 vs. PS2-4) (p=0.0007). Age (<75 vs. 75<) and primary sites (breast vs. other cancer) were not statistically significant factors (p=0.8032 and p=0.0544, respectively), On multivariate analysis, both gender and PS were statistically significant factors for survival. The overall survival rates at 2-years from the Initial PIRT were 33% for female (12% for male) and 26% for PS0-1 patients (11% for PS2-4 patients).

# CONCLUSION

Recently, individualized PIRT seemed to be necessary for bone metastases. Based on our series, female and good PS patients seemed to need PIRT with comparatively high total doses and small fraction size.

# **CLINICAL RELEVANCE/APPLICATION**

Female and good performance status seemed to be favorable prognostic factors for patients who received radiotherapy to bone metastases in recent years.

# RO238-SD-WEA5

A Phase I Trial of Ketogenic Diet with Concurrent Chemoradiation (ChemoRT) in Head and Neck Squamous Cell Carcinoma (HNSCC)

Wednesday, Nov. 30 12:15PM - 12:45PM Room: RO Community, Learning Center Station #5

#### **Participants**

Carryn Anderson, MD, Iowa City, IA (Presenter) Nothing to Disclose

#### ABSTRACT

Purpose/Objective(s): Ketogenic diet (KD) combined with chemoRT reduced tumor growth and improved survival in pre-clinical models. We hypothesized stage III-IVb HNSCC patients would be able to remain compliant with KD because of PEG tube requirement during chemoRT. Research supported by NIH U54TR001356 and KetoCal® 4:1 provided by Nutricia Pharmaceuticals.Materials/Methods: This phase I clinical trial enrolled stage III-IVb definitive and post-op HNSCC patients receiving concurrent platinum-based chemoRT. PEG placement was required, but subjects were encouraged to continue KD by mouth. KD recipes and KetoCal® shakes were provided for daily consumption for 5 weeks starting 2 days prior to chemoRT. Fingerstick ketones (FK) were checked Mon-Fri, and serum beta-hydroxybutyrate (BHB), glucose, and uric acid were checked weekly. Lipid panel was checked at week 3. Serum oxidative stress parameters were assessed prior to, during, and after completing KD. Adverse events were graded utilizing CTCAE version 4.0. Results: Median follow-up for all enrolled subjects (n=12) from completion of RT was 4.9 mo (range: 0-16.6). 4/12 subjects successfully completed 5 weeks of KD as prescribed. Successful subjects used scheduled anti-emetics, consumed shakes via PEG tube as opposed to orally and had strong social support. Median days on KD for those who discontinued was 5.5 (range: 2-8). Of the first 4 subjects treated, 2 completed, 1 withdrew due to fatigue (gr. 3), and 1 had a dose limiting toxicity (DLT) (hyperuricemia, grade 4; 12.7 nd/dL; nl ref 2.4-7.0). The protocol was amended to address diet-related hyperuricemia and allow for increased protein intake. Subsequently, 8 eligible subjects enrolled with 2 completing therapy and 2 experiencing DLTs (acute pancreatitis grade 3; hyperuricemia with complicating nausea and vomiting, grade 3). The remaining 4 subjects withdrew due to diet intolerance prior to beginning chemoRT (n=1), and nausea with vomiting (nausea grade 2, vomiting grade 1, n=3). Serious adverse events included hospitalizations for parotiditis (n=1), acute pancreatitis (n=1), neutropenic fever (n=1), and nausea with vomiting (n=1). Both the acute pancreatitis and nausea with vomiting SAEs were considered related to study diet and were deemed DLTs. In those who completed KD, the median days FK were elevated and weeks the BHB levels were above baseline were 24.5 days (range: 19-25) and 5 weeks (range: 4-6), respectively. Median uric acid levels were 4.9 nd/dL (range: 3.4-5.4). Lipids remained normal. Serum oxidative stress markers, as assessed by protein carbonyls, increased linearly with increasing days on KD.Conclusion: While challenging despite PEG availability, KD compliance is possible when combined with concurrent chemoRT for HNSCC. Enrollment continues.

Stereotactic Ablative Radiotherapy (SABR) for Stages I-II Non-Small Cell Lung Cancer (NSCLC): Setting up with Multi-Dampening, First Analysis Has Shown Promising Results

Wednesday, Nov. 30 12:15PM - 12:45PM Room: RO Community, Learning Center Station #6

**FDA** Discussions may include off-label uses.

## Participants

Elena Montero, Seville, Spain (*Presenter*) Nothing to Disclose Maria Rubio, MD, Seville, Spain (*Abstract Co-Author*) Nothing to Disclose Santiago Velazquez, DIPLPHYS, Seville, Spain (*Abstract Co-Author*) Nothing to Disclose Maria Jose Ortiz, PhD,MD, Seville, Spain (*Abstract Co-Author*) Nothing to Disclose

#### ABSTRACT

Purpose/Objective(s): The standard of care for treatment of early-stage non-small cell lung cancer patients is definitive surgery. However, there are patients who refuse surgery or are not surgical candidates. In these patients SABR is an alternative to surgery. Our hypothesis is that multidampening SABR, developed in our hospital, is an efficient method for these patients, well-tolerated and have high rates of local tumor control. Materials/Methods: Between April 2014 and January 2016, a total of 11 patients with 11 primary lung tumors with stage I and II NSCLC [T1, n=3;T2, n=8] were enrolled on prospective study of SABR for lung cancer. All patients had histological confirmation by biopsy or cytological evaluation, the histologies were: 7 adenocarcinoma, 2 squamous cell carcinoma and 1 NSCLC. All patients had ECOG 0-1. The median age was 74 years (67-86). The implementation of SARB in routine requires a careful considering of organ motion, we used stringent customized breathing control that was obtained with our multidampening system. In all cases the technique was guided by CBCT image after CT simulation and calculation. The SABR dose was either 54 Gy in 3 fractions or 50 Gy in 5 fractions, according a risk adapted fractionation scheme of biologically effective dose DBE > 100 Gy, and treatment lasted between one-and-a-half to two weeks. Failure was defined radiographically, chest radiography the first month after treatment, thereafter every 3 months for 2 years and then annually; CT of chest and upper abdomen every 3 months the first year and then every 6 months. PET/CT is obtained at the 6 month in all cases. Results: The median follow-up period was 11 months (range, 3-22). The results in terms of local control after treatment were: 5 patients in partial radiographically response, 2 patientes with stable disease and 2 in complete response. 8 patients had a pre- and post-treatment PET/TC imaging. All patients had a decrease in post-treatment SUV (decrease percentage, 31-90%). 2 exitus at the time of the study, one from secondary head and neck cancer and one form comorbidities. Median disease-free survival was 11 months. The toxicity reported in all patients was less than G2 in CTCAE.4 scale by site. Conclusion: SABR used as a radical treatment for non-operable patients is safe and promising. The SABR with multidampening method is well-tolerated, seems to be an efficient alternative and to have a low risk of complications. Although recommendations exist for CT- and PET/CT-based follow-up after SABR, better metrics are required for early detections of recurrence and distinguishing recurrence from fibrosis.

# Adrenal Cortical Hyperplasia: Diagnostic Workup, Subtypes, Imaging Features and Mimics

Wednesday, Nov. 30 12:15PM - 12:45PM Room: GU/UR Community, Learning Center Station #7

#### Awards Certificate of Merit

#### Participants

Michelle M. Agrons, MD, DVM, Houston, TX (*Abstract Co-Author*) Nothing to Disclose Corey T. Jensen, MD, Houston, TX (*Abstract Co-Author*) Nothing to Disclose Akram M. Shaaban, MBBCh, Salt Lake City, UT (*Abstract Co-Author*) Nothing to Disclose Christine O. Menias, MD, Chicago, IL (*Abstract Co-Author*) Nothing to Disclose Nicolaus A. Wagner-Bartak, MD, Houston, TX (*Abstract Co-Author*) Nothing to Disclose Alicia M. Roman-Colon, MD, Houston, TX (*Abstract Co-Author*) Nothing to Disclose Prakash M. Masand, MD, Houston, TX (*Abstract Co-Author*) Nothing to Disclose Khaled M. Elsayes, MD, Ann Arbor, MI (*Presenter*) Nothing to Disclose

## **TEACHING POINTS**

- Describe the diagnostic workup of adrenal cortical hyperplasia- Discuss the pathological subtypes, pathogenesis, associations and presentation of adrenal cortical hyperplasia- Review the spectrum of imaging features of adrenal cortical hyperplasia- Illustrate most commonly encountered mimics of adrenal cortical hyperplasia-

# TABLE OF CONTENTS/OUTLINE

- Pathology and laboratory workup of adrenal cortical hyperplasia- Subtypes: -ACTH dependent adrenal cortical hyperplasia - ACTH independent macronodular adrenal hyperplasia - Congenital adrenal hyperplasia (CAH) [Classical:Salt losing form of CAH - Simple virilizing form of CAH - Nonclassic or Late-Onset from of CAH]- Imaging workup and utility of various imaging modalities.- Typical Imaging features of adrenal cortical hyperplasia and its associations- Correlation of imaging features with laboratory findings and impact on management- Mimics of adrenal cortical hyperplasia, for example:- Adrenal lipomatous metaplasia - Metastases - Lymphoma

## **Honored Educators**

Presenters or authors on this event have been recognized as RSNA Honored Educators for participating in multiple qualifying educational activities. Honored Educators are invested in furthering the profession of radiology by delivering high-quality educational content in their field of study. Learn how you can become an honored educator by visiting the website at: https://www.rsna.org/Honored-Educator-Award/

Khaled M. Elsayes, MD - 2014 Honored Educator Akram M. Shaaban, MBBCh - 2015 Honored Educator Akram M. Shaaban, MBBCh - 2016 Honored Educator Christine O. Menias, MD - 2013 Honored Educator Christine O. Menias, MD - 2014 Honored Educator Christine O. Menias, MD - 2015 Honored Educator Christine O. Menias, MD - 2016 Honored Educator Developing TACE 2.0:Targeting Hepatocellular Carcinoma Cells through the Unfolded Protein Response, Hypoxia Inducible Factor, and Autophagy Inhibition

Wednesday, Nov. 30 12:15PM - 12:45PM Room: VI Community, Learning Center Station #1

#### Awards

#### **Student Travel Stipend Award**

#### Participants

Mikhail Silk, MD, Philadelphia, PA (*Presenter*) Nothing to Disclose Hillary Nguyen, Philadelphia, PA (*Abstract Co-Author*) Nothing to Disclose Stephen J. Hunt, MD,PhD, Philadelphia, PA (*Abstract Co-Author*) Nothing to Disclose Gregory J. Nadolski II, MD, Philadelphia, PA (*Abstract Co-Author*) Nothing to Disclose Terence P. Gade, MD, PhD, New York, NY (*Abstract Co-Author*) Research Grant, Guerbet SA

#### PURPOSE

There is increasing evidence that hepatocellular carcinoma cells (HCC) mount an adaptive response to transarterial chemoembolization (TACE)-induced ischemia to enable their survival as well as induce resistance to cell cycle specific chemotherapeutic agents (i.e. Doxorubicin). The unfolded protein response (UPR), Hypoxia-Inducible Factor (HIF)-1 Regulatory Pathway, and Autophagy are several response pathways which enable tumor cell survival under ischemia. We hypothesize HCC cells surviving severe TACE-like ischemia are susceptible to inhibition of the UPR, HIF and autophagy pathways and combination of the inhibition of these pathways would lead to synergistic effects.

# **METHOD AND MATERIALS**

Viability assays and cytotoxicity profiles of HepG2, SNU-387, and SNU-449 HCC cell lines were studied under standard (21% O2 with complete medium) and severely ischemic conditions (0.5 or 1% O2, 1% serum, 1 mM glucose) with an inhibitor of the UPR (GSK2606141), a HIF-1 alpha inhibitor (BAY 87-2243) and an inhibitor of autophagy (Hydroxychloroquine). Cytotoxicity measurements were derived from measured dose-response curves using the WST-1 cytotoxicity assay.

#### RESULTS

Each of the three cell lines tested demonstrated decreased cellular viability with incubation of either of the inhibitory agents (EC50 GSK2606141, BAY 87-2243, Hydroxcychloroquine of 75-150µM, 400-500µM, 100-200µM respectively). Ischemia potentiated the cytotoxicity of GSK2606141 and Hydroxychloroquine more than BAY87-2243, however all agents showed increased cytotoxicity under ischemic conditions (EC50 GSK2606141, BAY 87-2243, Hydroxcychloroquine of 25-50µM, 200-400µM, 50-80µM respectively). Combination of the three drugs under TACE-like ischemia lead to a synergistic response showing cell death at concentrations well below any single drug alone.

## CONCLUSION

Inhibition of the UPR, HIF, and autophagy independently lead to a reduction in viability of HCC cells. Combination of the three drugs under TACE-like ischemia lead to a synergistic response and should be considered as potential chemotherapeutics for TACE.

## **CLINICAL RELEVANCE/APPLICATION**

Inhibition of the Unfolded Protein Response, Hypoxia-Inducible Factor, and Autophagy show synergistic reduction in HCC viability under ischemic conditions and should be considered for TACE procedures.

Pulmonary Hemorrhage in Patients Undergoing Percutaneous CT Guided Lung Biopsy: A Retrospective Review of Risk Factors, including Aspirin Usage

Wednesday, Nov. 30 12:15PM - 12:45PM Room: VI Community, Learning Center Station #2

# Participants

Brigid A. Bingham, MD, Houston, TX (*Presenter*) Nothing to Disclose Steven Y. Huang, MD, Houston, TX (*Abstract Co-Author*) Nothing to Disclose Pamela L. Chien, Houston, TX (*Abstract Co-Author*) Nothing to Disclose Joe Ensor, Houston, TX (*Abstract Co-Author*) Consultant, Aetna, Inc Sanjay Gupta, MD, Houston, TX (*Abstract Co-Author*) Nothing to Disclose Michael J. Wallace, MD, Houston, TX (*Abstract Co-Author*) Speaker, Siemens AG Research support, Siemens AG

## PURPOSE

To identify risk factors (RF), including use of aspirin, associated with increased incidence and volume of hemorrhage in patients undergoing percutaneous CT guided lung biopsy.

# METHOD AND MATERIALS

From 09/2013 to 12/2014, 252 patients on aspirin undergoing CT guided lung biopsy at a single institution were included in our retrospective study. Waiver of informed consent by the institutional review board was obtained. Of the 252 study patients, 49 (18.4%) stopped aspirin  $\leq$  4 days prior to biopsy; 203 (80.6%) stopped aspirin  $\geq$  5 days prior to biopsy. The impact of withholding aspirin ( $\leq$  4 days vs.  $\geq$  5 days), age, sex, platelet count (K/µL), INR, GFR (mg/mmol), lesion composition, lesion volume (cm3), location, type of biopsy, and size of vessels transgressed upon incidence and volume of biopsy related hemorrhage was retrospectively evaluated. Hemorrhage was quantified volumetrically from CT images obtained following biopsy.

## RESULTS

Clinical hemoptysis was documented in 13 of 252 procedures (5.2%); all cases were managed conservatively. Pulmonary hemorrhage, as identified by CT, was documented in 174 cases (69.0%). Higher grade hemorrhage (>10cm3) occurred in 70 procedures (27.8%). Univariate analysis identified the following risk factors (RFs) influencing the incidence of hemorrhage: increased distance from lesion to pleura (P<0.0001), largest vessel transgressed (P<0.0001), lesion volume (P<0.0001), and aspirin use within 4 days of biopsy (P=0.0154); multivariate analysis revealed that longer distance from pleura (odds ratio, OR, 1.902) and lesion volume (OR 0.976) were the most important RFs. For volume of hemorrhage, univariate analysis identified longer distance from pleura (P<0.0001), largest vessel transgressed (P<0.0001), lesion volume (P=0.0044), and aspirin use within 4 days of biopsy (P=0.0297) as RFs; multivariate analysis revealed that longer distance from pleura (P<0.0001) were the most important RFs.

# CONCLUSION

In CT guided coaxial needle biopsy, lesion distance from the pleura and lesion volume are the greatest predictors for increased incidence and volume of hemorrhage. Aspirin therapy stopped within 4 days of biopsy is not an independent RF for increased incidence or severity of pulmonary hemorrhage.

# **CLINICAL RELEVANCE/APPLICATION**

Pulmonary hemorrhage following lung biopsy is multi-factorial; aspirin use is not an independent predictor of increased risk.

The Application of Tc99m Tagged Red Blood Cells (TRBC) SPECT/CT Scan for Detection and Localization of Gastrointestinal (GI) Bleeding: Potential for Guiding Subsequent Angiographic Intervention

Wednesday, Nov. 30 12:15PM - 12:45PM Room: VI Community, Learning Center Station #3

# Participants

Shayandokht Taleb, Minneapolis, MN (*Presenter*) Nothing to Disclose Rakhee S. Gawande, MD, Stanford, CA (*Abstract Co-Author*) Nothing to Disclose Jerry W. Froelich, MD, Minneapolis, MN (*Abstract Co-Author*) Researcher, Siemens AG Jafar Golzarian, MD, Minneapolis, MN (*Abstract Co-Author*) Chief Medical Officer, EmboMedics Inc

# PURPOSE

To determine the added value of SPECT/CT scan in conjunction with TRBC planar imaging for detection of GI bleeding and guiding subsequent endovascular intervention.

# METHOD AND MATERIALS

A retrospective review of clinical and imaging records of all patients who underwent SPECT/CT scan in addition to TRBC planar imaging for suspected GI bleeding between 09/2011 and 12/2015, was performed. A single reviewer, blinded to clinical information, evaluated all planar TRBC images separately, and then in conjunction with SPECT/CT scan. The reviewer also determined whether the SPECT/CT scan helped with anatomical localization of bleeding compared to planar images. The imaging interpretations were compared with interventional angiographic and/or endoscopy/colonoscopy results.

# RESULTS

A total of 137 patients were included in this study. The average age at the time of scan was  $54.32 \pm 18.2$  years; and 83 (60.5%) patients were men. The TRBC SPECT/CT scans were interpreted as positive in 58/137 (42%) patients. In only 1 patient, SPECT/CT scan changed the interpretation for GI bleeding from negative to positive compared to planar images. On the other hand, the SPECT/CT helped with anatomical localization in 57/58 patients (98%) compared to planar imaging. Within 1 month of imaging, 19 (14%) patients underwent angiography, 78 (57%) had colonoscopy, 75 (55%) had upper GI endoscopy, and 28 (20%) had capsule endoscopy. The colonoscopy/angiographic studies were positive in 51 (88%) of 58 patients with positive SPECT/CT; whereas, only 8/79 (6%) patients with negative SPECT/CT interpretation had active bleeding in endoscopy/colonoscopy exam. Angiography was able to identify the bleeding vessel in 11/18 (61%) patients, all of whom had positive SPECT/CT interpretation.

## CONCLUSION

The addition of SPECT/CT scan to TRBC planar imaging slightly improved the accuracy for detection of GI bleeding; however, combined imaging substantially helped with precise anatomical localization of the site of GI bleeding, and was able to guide the subsequent angiographic intervention.

## **CLINICAL RELEVANCE/APPLICATION**

The TRBC SPECT/CT scan helps with precise anatomic localization of the site of GI bleeding and can guide angiographic intervention; thus, potentially lowers the procedure duration and patients' radiation exposure.

# Solution for Problematic Antegrade SFA Canulation in Interventions of SFA and BTK Arteries

Wednesday, Nov. 30 12:15PM - 12:45PM Room: VI Community, Learning Center Station #4

#### **Participants**

Johan W. Marsman, MD, PhD, Hilversum, Netherlands (Presenter) Nothing to Disclose

#### PURPOSE

Antegrade canulation of the SFA is frequently hampered by erroneous entering the DFA. Goal of this work is to test a dedicated 'SFA finding' guidewire and compare it with conventinal guidewires, without making use of fluoroscopic or other manipulations.

# METHOD AND MATERIALS

A true to life transparant silicon 3D model of the femoral bifurcation using CT data is used. An experimental guidewire with a double curve is tested and compared with conventional angled-tip and J-tip guidewires. The CFA is punctured at verious distances proximally from the femoral bifurcation. The guidewire is inserted into the needle with the tip end of the double curve, angled-tip or J-tip turned anteriorly. Subsequently, without any manipulation, the guidewire is pushed through the needle into the CFA. Guidewire movements inside the CFA are filmed. For each type of guidewire the number of movements entering the SFA or DFA are scored, for each needle position relatively to the bifurcation.

## RESULTS

Three needle tip positions relatively to the femoral bifurcation were used:1) needle tip at the bifurcation,2) needle tip 1cm proximally to bifurcation.3) needle tip 2cm proximally to bifurcation. In position 1 and 2 the double curved tip entered the SFA in 100%, and the conventional tips in 0%. In position 3 the double curved tip entered the SFA in 100%, and the conventional tips in 25%.

#### CONCLUSION

In a true to life 3D model of the femoral bifurcation a double curved guidewire successfully entered the SFA in 100%, no matter the distance of the needle to the bifurcation. Conventional guidewires entered the SFA only when the needle to bifurcation distance amounted 2cm, and even in that situation only in 25%. When the needle was closer to the bifurcation, the conventional wires enevitably entered the DFA instead of the SFA.

## **CLINICAL RELEVANCE/APPLICATION**

Erroneous entering the DFA instead of the SFA in antegrade canulation of the SFA is a common clinical problem in interventions of the SFA and/or lower leg arteries. In a 3D model a double curved guidewire appears advantageous compared to conventional guidewires. Therefore, a clinical trial with a double curved guidewire is justified.

Utility of 4D-Flow Magnetic Resonance Angiography in Assessment of Patients for Uterine Fibroid Embolization

Wednesday, Nov. 30 12:15PM - 12:45PM Room: VI Community, Learning Center Station #5

#### Awards

#### **Student Travel Stipend Award**

#### **Participants**

Christopher D. Malone, MD, San Diego, CA (Presenter) Nothing to Disclose

Marcus T. Alley, PhD, Stanford, CA (Abstract Co-Author) Research funded, General Electric Company; Research Consultant, Arterys Inc

Shreyas S. Vasanawala, MD, PhD, Stanford, CA (*Abstract Co-Author*) Research collaboration, General Electric Company; Consultant, Arterys Inc; Research Grant, Bayer AG;

Anne C. Roberts, MD, La Jolla, CA (Abstract Co-Author) Nothing to Disclose

Albert Hsiao, MD, PhD, San Diego, CA (Abstract Co-Author) Founder, Arterys, Inc Consultant, Arterys, Inc Research Grant, General Electric Company

# PURPOSE

To assess the utility of 4D Flow MRA in the assessment of patients with uterine fibroids either before or after uterine fibroid embolization (UFE).

## **METHOD AND MATERIALS**

With HIPAA-compliance and IRB-approval we retrospectively reviewed all pelvic MRIs performed with 4D Flow between September 2015 and March 2016. Four patients without fibroids and 12 patients with fibroids were analyzed; 7 had yet to undergo UFE, 2 underwent UFE after MR, and 3 underwent UFE before MR. All fibroid patients were assessed as either right or left dominant based on multiphasic contrast-enhanced MRI. Blood flow (mL/min) within the distal abdominal aorta, bilateral common, external and internal iliac arteries was measured in triplicate using Arterys software. Ratios of ipsilateral internal and external iliac flow (I/E) and the ratio of dominant and nondominant internal iliac flow (I/I) were calculated. Statistical significance was determined using t-tests.

# RESULTS

The I/E ratio was markedly increased in patients with uterine fibroids compared to controls, with flow of the internal iliac artery exceeding that of the external in 4 of 12 patients (0.80+0.38, range 0.24-1.92, vs. 0.47+0.1, p=0.001). I/E ratio was lower in patients who were status post UFE with decrease in fibroid size compared to those pre-procedure (0.57+0.26 vs. 0.87+0.39, p=0.05). Pre-UFE patients whose fibroids showed a definite lateral dominance demonstrated significantly higher I/I ratios compared to control patients (1.86+0.56 vs. 1.14+0.12, p=0.02). In 2 patients who later had UFE, higher amounts of embolic material were used on the dominant side compared to the nondominant.

# CONCLUSION

4D Flow MRA can complement routine MRI sequences in assessment of fibroid burden and response to UFE by enabling measurement of total and fractional iliac blood flow. In addition, flow ratios between dominant and nondominant internal iliac arteries may help to anticipate the amount of embolic needed during UFE.

## **CLINICAL RELEVANCE/APPLICATION**

Quantification of total and fractional iliac blood flow may be a promising biomarker to assess fibroid burden before and after UFE.

Evaluation of Detection Methods for Local Marginal Recurrence after Transcatheterarterial Chemoembolization of Hepatocellular Carcinoma: Comparison between Parenchymal Blood Volume (PBV) Mapping using Cone Beam CT (DynaCT) and Multiphase Dynamic CT

Wednesday, Nov. 30 12:15PM - 12:45PM Room: VI Community, Learning Center Station #6



Discussions may include off-label uses.

# Awards

## **Student Travel Stipend Award**

# Participants

Na Rae Kim, MD, Dajeon metropolitan city, Korea, Republic Of (*Presenter*) Nothing to Disclose Ji-Dae Kim, Dajeon metropolitan city, Korea, Republic Of (*Abstract Co-Author*) Nothing to Disclose

#### PURPOSE

To evaluate the usefulness of parenchymal blood volume (PBV) mapping using cone beam CT (DynaCT) compare to multiphase dynamic CT for detecting local marginal recurrence after transcatheter arterial chemoembolization of hepatocellular carcinoma.

# METHOD AND MATERIALS

This retrospective study was approved by the IRB. From March 2015 to January 2016, we included 20 patients with 28 HCC lesions who previously underwent TACE and considered recurred tumor on follow up CT.We compared with multiphase dynamic CT within 1 month prior to receive TACE and parenchymal blood volume (PBV) mapping using cone beam CT during TACE to detect local marginal recurrence of HCC.We considered presence of viable or recurred tumor by dense accumulation of oil during chemoembolization.

# RESULTS

All patients were successfully completed TACE without complication. The sensitivity, specificity, and predictive value of PBV mapping using cone beam CT (DynaCT) was better than multiphase dynamic CT. In two cases, PBV mapping was able to demonstrate that lesions unidentified at multiphase dynamic CT due to beam hardening artifact, were in fact viable marginal tumor. On the other hand, 5 cases which considered recurrent HCC on multiphase dynamic CT were proven to be negative lesions by observing no uptake of iodizied oil during chemoembolization .And, one case which was unable to distinguish between arterioportal shunt and HCC on multiphase dynamic CT was in fact proven to be arterioportal shunt in PBV mapping.

## CONCLUSION

Multiphase dynamic CT has limitation in interpretation after chemoembolization because of beam hardening artifact from iodized the oil.Otherwise, parenchymal blood volume (PBV) mapping using cone beam CT (DynaCT) is free from beam hardening artifact. In addition, this method applies quantitative assessment of tumor angiogenesis, easy to get images during chemoembolization, and exposure to radiation is less than that of computed tomography (CT).Compared with multiphase dynamic CT, our study shows parenchymal blood volume (PBV) mapping using cone beam CT (DynaCT) is more feasible follow-up modality for detecting local marginal recurrence after transcatheter arterial chemoembolization.

# **CLINICAL RELEVANCE/APPLICATION**

Parenchymal blood volume (PBV) mapping using cone beam CT (DynaCT) is more feasible follow-up modality for detecting local marginal recurrence after transcatheter arterial chemoembolization than CT.

# BR163-ED-WEB8

# Lessons to Learn in Breast Calcifications: How to Avoid Misinterpretations

Wednesday, Nov. 30 12:45PM - 1:15PM Room: BR Community, Learning Center Station #8

#### **Participants**

Giselle G. Mello, PhD, Sao Paulo, Brazil (*Abstract Co-Author*) Nothing to Disclose Luciano F. Chala, MD, Sao Paulo, Brazil (*Abstract Co-Author*) Nothing to Disclose Vera L. Aguillar, MD, Sao Paulo, Brazil (*Abstract Co-Author*) Nothing to Disclose Marcia M. Aracava, MD, Sao Paulo, Brazil (*Presenter*) Nothing to Disclose Carlos Shimizu, MD, Sao Paulo, Brazil (*Abstract Co-Author*) Nothing to Disclose Fernanda F. Guirado, Sao Paulo, Brazil (*Abstract Co-Author*) Nothing to Disclose Bruna M. Thompson, MD, Sao Paulo, Brazil (*Abstract Co-Author*) Nothing to Disclose

# **TEACHING POINTS**

To know the essentials of appropriate assessment of breast calcifications To understand the reasons of common misinterpretations in the evaluation of breast calcifications

To show a pathway to avoid mistakes

# **TABLE OF CONTENTS/OUTLINE**

Classification of breast calcifications according to ACR BI-RADS 5th edition Essentials of the appropriate assessment of breast calcifications: Complete imaging work – up Knowledge of interpretation criteria Comparison to previous examinations when appropriate Limitations of sonography and MRI in the assessment of breast calcifications Case based review showing misinterpretations in the evaluation of breast calcifications and discussing their reasons Pathway to avoid mistakes Conclusions

# Mimics of Highly Suspicious BI-RADS 5 Cancers in the Breast

Wednesday, Nov. 30 12:45PM - 1:15PM Room: BR Community, Learning Center Station #9

#### **Participants**

Cindy S. Lee, MD, San Francisco, CA (*Presenter*) Nothing to Disclose Man Sei M. Yiu, MD, Mill Valley, CA (*Abstract Co-Author*) Nothing to Disclose Sheth Sujay, MD, Chicago, IL (*Abstract Co-Author*) Nothing to Disclose Rita I. Freimanis, MD, Winston-Salem, NC (*Abstract Co-Author*) Nothing to Disclose Iryna Lobach, San Francisco, CA (*Abstract Co-Author*) Nothing to Disclose Edward A. Sickles, MD, San Francisco, CA (*Abstract Co-Author*) Nothing to Disclose Bonnie N. Joe, MD, PhD, San Francisco, CA (*Abstract Co-Author*) Nothing to Disclose

# **TEACHING POINTS**

According to the BI-RADS Atlas, BI-RADS 5 assessment should be reserved for lesions which are highly suggestive of malignancy, with a positive predictive value (PPV) of >95%. However, literature shows PPVs ranging between 74% to 92%, suggesting that the 95% PPV for BI-RADS 5 lesions is not commonly achieved or adhered to in clinical practice. This study was performed to see whether the long-term PPV of BI-RADS 5 lesions at an academic breast center falls within the ACR guideline of >95%. Out of the 22,564 patients who underwent diagnostic breast evaluations between January 2010 and September 2015, 239 patients (1.1%) received a BI-RADS 5 assessment. Only 5 (2.1%) of the BI-RADS 5 lesions were false positive, with benign pathology, giving a PPV of 97.9%. Our results demonstrate that a PPV of >95% for BI-RADS 5 category assessment is achievable in clinical practice. This presentation reviews the imaging features of these benign BI-RADS 5 lesions, as well as lessons learned from our experience.

# TABLE OF CONTENTS/OUTLINE

Definition and clinical significance of BI-RADS 5 lesions, both true and false positive Non-standard use of BI-RADS 5 assessment in the literatureImaging review of 5 false positive cases• Fat necrosis• Phyllodes tumor (2 cases)• Radial sclerosing lesion• FibromatosisLessons learned

# Neoplastic Seeding in the Setting of Percutaneous Image Guided Breast Biopsies

Wednesday, Nov. 30 12:45PM - 1:15PM Room: BR Community, Learning Center Station #6

#### **Participants**

Lumarie Santiago, MD, Houston, TX (*Presenter*) Nothing to Disclose Beatriz E. Adrada, MD, Houston, TX (*Abstract Co-Author*) Nothing to Disclose Monica L. Huang, MD, Houston, TX (*Abstract Co-Author*) Nothing to Disclose Rosalind P. Candelaria, MD, Houston, TX (*Abstract Co-Author*) Nothing to Disclose

# PURPOSE

To describe imaging features, primary tumor features, and biopsy technique in neoplastic seeding (NS) following percutaneous breast biopsies (BX).

#### **METHOD AND MATERIALS**

An IRB-approved retrospective review of patients presenting from January 1, 2009 - January 30, 2016 with new diagnosis of breast cancer, abnormal mammogram or palpable abnormality and subsequent diagnosis of NS along the BX needle tract. All patients underwent diagnostic mammography (FFDM) and whole breast ultrasound (US). Tumor histology, grade, receptor status, size, and TNM staging as well as BX guidance, needle gauge, and number of passes were recorded. The time from BX to NS diagnosis was measured. The imaging features of the primary breast malignancy (PBM) and NS were reviewed.

#### RESULTS

Eight (0.2%) NS cases were identified in 4,010 patients. Mean PBM cancer size was 2.7 cm (range1.6-5.7). US guidance was used in 6 cases (75%). Multiple insertion core needle BX was done in 6 (75%) cases. Single insertion vacuum assisted needle BX was done in 1 case. Sampling information was absent in 1 case. The mean number of passes was 4.25 (range 1-11). The mean time from BX to NS diagnosis was 60.8 days (range 34-165). In 7 (87.5%) cases tumor histology was IDC. A single case of papillary carcinoma was noted. In 6 (75%) cases tumor grade was high (2/3). All (100%) PBM were Her2 negative, 6 (75%) were PR negative and 5 (62.5%) were ER negative. In 7 (87.5%) cases tumors were unifocal. All PBM presented with a mass by FFDM. Associated calcifications were noted in 2 (25%) cases. Corresponding US masses were most frequently irregular (75%), not circumscribed (87.5%) and heterogeneous (50%). Most frequent NS FFDM presentation was focal asymmetry (37.5%) and occult (25%). Most frequent NS US presentation was mass (87.5%) often irregular (62.5%), not circumscribed (75%) and hypoechoic (87.5%)]. NS was most frequently subdermal in location (75%).

#### CONCLUSION

Multiple insertion BX, Her2 negative and high grade tumors may be risk factors for NS after percutaneous BX. PBM and NS have variable FFDM and US features. NS most frequently presented as a mass on US while having variable presentation at FFDM.

#### **CLINICAL RELEVANCE/APPLICATION**

Although rare, NS should be suspected based on its temporal and geographic relationship to the initial biopsy when there is apparent disease progression in HER2 negative and high-grade cancers.

Performance of Pre-operative Breast MRI in Newly Diagnosed Cancer: Comparison of Outcomes Based on Mammographic Modality, Breast Density and Breast Parenchymal Enhancement

Wednesday, Nov. 30 12:45PM - 1:15PM Room: BR Community, Learning Center Station #1

#### Awards

**Student Travel Stipend Award** 

#### Participants

Azadeh Elmi, MD, Philadelphia, PA (*Presenter*) Nothing to Disclose Emily F. Conant, MD, Philadelphia, PA (*Abstract Co-Author*) Consultant, Hologic, Inc; Consultant, Siemens AG Andrew Kozlov, MD, Philadelphia, PA (*Abstract Co-Author*) Nothing to Disclose Elizabeth S. McDonald, MD, Philadelphia, PA (*Abstract Co-Author*) Nothing to Disclose

# PURPOSE

To determine the performance of pre-operative MRI in newly diagnosed breast cancer based on breast density, background parenchymal enhancement (BPE), and mammographic modality, e.g. digital mammography (DM) or digital breast tomosynthesis (DBT).

# METHOD AND MATERIALS

Retrospective IRB approved review was conducted of 401 consecutive MRI exams from women who underwent pre-operative breast MRI at our institution (10/1/2013-7/31/2015) for newly diagnosed, untreated cancer prior to surgery with a prior DM or DBT mammogram within 12 weeks. 13 cases were excluded because the final disposition of pathology of the possible additional disease seen on MRI was unknown. 388 exams were evaluated with prior DM (201 cases) or DBT (187 cases) imaging. MRI performance for detection of mammographically occult additional sites of malignancy was stratified by modality, mammographic density, and BPE. Differences between the groups were compared using two-proportion z-test equal variance. A true positive finding was defined as malignancy (DCIS or invasive disease) in the ipsilateral breast >2cm away from the index lesion or in the contralateral breast.

#### RESULTS

50 additional occult malignancies were prospectively detected in 388 exams (50/388, 12.9%), 37 ipsilateral (37/388, 9.5%) and 13 contralateral (13/388, 3.4%). In patients with DBT exams, MRI detected significantly more cancers in dense than in non-dense breasts (p=0.016, 15/83 (18.1%) vs. 7/104 (6.7%)). In patients with DM exams, there was no significant difference between cancer detection in dense versus non-dense breasts (p=0.79, 16/110 (14.5%) vs. 12/91 (13.2%), respectively). There was no observed difference in cancer detection (p=0.54) or false positive exams (p=0.47) in women who underwent DM versus DBT. Overall, higher BPE was associated with higher false positive rate (p=0.040, 14/113 (12.4%) high BPE vs. 17/275 (6.2%) low BPE ), but no significant difference in true positive exams (p=0.25, 32/275 11.6% low BPE vs. 18/113 15.9% high BPE).

# CONCLUSION

In patients with a prior DBT exam, those with dense breasts are more likely to have additional disease detected on pre-operative MRI. A prior DBT exam was not observed to decrease the likelihood of finding additional disease on MRI.

# **CLINICAL RELEVANCE/APPLICATION**

Additional studies are needed to determine if there is a specific cohort of women who might benefit most from pre-operative MRI.

# BR260-SD-WEB2

Synthesized Mammography (SM) versus Full Field Digital Mammography (FFDM): A Comparison of Lesion Detection by Radiologists

Wednesday, Nov. 30 12:45PM - 1:15PM Room: BR Community, Learning Center Station #2

# Participants

Deanna L. Lane, MD, Houston, TX (*Presenter*) Nothing to Disclose Lumarie Santiago, MD, Houston, TX (*Abstract Co-Author*) Nothing to Disclose Rosalind P. Candelaria, MD, Houston, TX (*Abstract Co-Author*) Nothing to Disclose Marion E. Scoggins, MD, Houston, TX (*Abstract Co-Author*) Nothing to Disclose Gaiane M. Rauch, MD, PhD, Houston, TX (*Abstract Co-Author*) Nothing to Disclose Beatriz E. Adrada, MD, Houston, TX (*Abstract Co-Author*) Nothing to Disclose Monica L. Huang, MD, Houston, TX (*Abstract Co-Author*) Nothing to Disclose William R. Geiser, MS, Houston, TX (*Abstract Co-Author*) Nothing to Disclose Kenneth Hess, PhD, Houston, TX (*Abstract Co-Author*) Nothing to Disclose

## PURPOSE

To compare lesions detected on synthesized mammography (SM) to lesions detected on FFDM

## **METHOD AND MATERIALS**

An IRB-approved retrospective review was performed of patients who underwent both FFDM and SM. Patients were seen over a 6 week period, from the time of SM implementation at our institution 12/15-1/26/16. Screening and diagnostic mammograms were included. Our mammography database identified all patients who underwent FFDM and tomosynthesis. All patients with mammogram BIRADS 0, 3, 4, or 5 reports were included, as well as an equal number of consecutive patients with mammograms read as BIRADS 1 or 2. Patients were excluded if they did not have both FFDM and SM available for review.Six fellowship-trained breast radiologists participated as readers; images were reviewed on a Hologic SecurView workstation. Standardized hanging protocols displayed only FFDM or only SM. Each radiologist performed two reading sessions - one for FFDM and one for SM. FFDM images were reviewed at least one week prior to SM images. Prior films were not utilized for comparison. Radiologists recorded mammographic findings and assigned a BIRADS category to each finding. Mammographic findings and assigned BIRADS category were compared between FFDM and SM.

#### RESULTS

FFDM and SM images were available for review in 147 patients. Radiologists detected significantly more noncalcified masses on FFDM than on SM (71 vs 55 masses, p=0.0015). Eight noncalcified masses were seen on FFDM without correlate on SM; most were small (0.5-1 cm), equal density oval-shaped masses with obscured margins. All were appropriately downgraded at BIRADS assessment from either BIRADS 4/5 or BIRADS 0 (FFDM) to BIRADS 1/2 (SM). We did not find a significantly greater number of calcifications on SM than on FFDM (p=0.68). 76% of radiologists' readings had concordant BIRADS between FFDM and SM; the weighted kappa coefficient was 0.66 with 95% confidence interval (0.59,0.73). SM downgraded BIRADS classification compared to FFDM in 16% of radiologists' readings and upgraded BIRADS classification in 8%.

# CONCLUSION

Significantly more masses were detected by radiologists on FFDM compared to SM. We did not detect significantly more calcifications on SM than on FFDM.

#### **CLINICAL RELEVANCE/APPLICATION**

Some mammographic findings may be better seen on FFDM than on SM, or vice versa. As we implement SM into clinical practice, it is valuable to know which, if any, lesions are visualized more easily on SM versus FFDM.

# BR261-SD-WEB3

#### Inter-observer Agreement between the 4th and 5th Edition BI-RADS Density Scales

Wednesday, Nov. 30 12:45PM - 1:15PM Room: BR Community, Learning Center Station #3

#### **Participants**

Sian E. Iles, MD, Halifax, NS (*Abstract Co-Author*) Nothing to Disclose Kaitlyn Tsuruda, MSc, Halifax, NS (*Abstract Co-Author*) Employee, Densitas Inc Peter Brown, MD, Halifax, NS (*Abstract Co-Author*) Nothing to Disclose Christopher B. Lightfoot, MD, Halifax, NS (*Abstract Co-Author*) Nothing to Disclose Gerald H. Schaller, MD, Sydney, NS (*Abstract Co-Author*) Nothing to Disclose Judy S. Caines, MD, Halifax, NS (*Abstract Co-Author*) Nothing to Disclose Syed Arsalan Raza, MBBS, FRCPC, Toronto, ON (*Abstract Co-Author*) Nothing to Disclose Mohamed Abdolell, MSc, Halifax, NS (*Presenter*) Founder and CEO, Densitas Inc

#### PURPOSE

The emphasis on the masking effect in the 5th edition of the BI-RADS mammographic density scale versus percent density in the 4th edition has the potential to affect which women are notified through breast density notification legislation. This study evaluates the agreement between these two classification scales.

## **METHOD AND MATERIALS**

Six radiologists assessed mammographic breast density on a set of 375 cases using the 4th and 5th editions of the BI-RADS density scale (labeled 1/2/3/4 and A/B/C/D, respectively). Classifications were subsequently categorized into "low" (1/2 or A/B) and "high" (3/4 or A/B) density categories. A consensus assessment was calculated based on the majority assessment and was used to calculate the proportions of each density category for each scale. Between-scale agreement was evaluated based on the consensus assessment using the kappa statistic.

#### RESULTS

The observed proportions of low/high density categories were virtually identical for both the 4th and 5th edition scale (63% vs 62% for the low density categories, p = 0.2). Additionally, 96% of the studies classified as 1/2 were also classified as A/B and 90% of studies classified as 3/4 were also classified as C/D. Agreement between the low-high consensus classifications using the two scales was almost perfect (Kappa = 0.86). 7% of women had a change in density status between the 4th and 5th editions of the density scale.

#### CONCLUSION

When considered on a two-category scale, as is often done for risk assessment, there was not a significant difference in the distribution of density categories across the 4th and 5th editions of the BI-RADS density scales. This, taken into consideration with the high agreement observed between the two scales, suggests that the two scales are nearly interchangeable. However there may be a small group of women living in states with enacted notification legislation for which there could be a change in density notification status as radiologists adopt the 5th edition BI-RADS lexicon.

## **CLINICAL RELEVANCE/APPLICATION**

There is almost perfect agreement between the BI-RADS 4th and 5th edition density scales; the impact on patient pathways due to a change in scale is likely small. For a subset of women a change in scale may alter their density classification and notification status.

# BR262-SD-WEB4

The Impact of the Introduction of a Breast Cancer Screening Programme on a Tertiary Symptomatic Breast Cancer Unit

Wednesday, Nov. 30 12:45PM - 1:15PM Room: BR Community, Learning Center Station #4

# Participants

Brian M. Moloney, MBBCh, Galway, Ireland (*Presenter*) Nothing to Disclose Ronan Waldron, BMBCh, Galway, Ireland (*Abstract Co-Author*) Nothing to Disclose Joseph A. Sheehan, MD, MBA, Galway, Ireland (*Abstract Co-Author*) Nothing to Disclose Carmel Malone, BMBCh,MD, Galway, Ireland (*Abstract Co-Author*) Nothing to Disclose Karl Sweeney, MBBCh,MD, Galway, Ireland (*Abstract Co-Author*) Nothing to Disclose Kevin Barry, MBBCh,MD, Galway, Ireland (*Abstract Co-Author*) Nothing to Disclose Ray McLoughlin, MBBCh, Galway, Ireland (*Abstract Co-Author*) Nothing to Disclose Aideen Larke, Galway, Ireland (*Abstract Co-Author*) Nothing to Disclose Sinead M. Walsh, FFR(RCSI), Galway, Ireland (*Abstract Co-Author*) Nothing to Disclose Anne Marie O' Connell, MBBCh, Galway, Ireland (*Abstract Co-Author*) Nothing to Disclose Rachel Ennis, MBBCh, Galway, Ireland (*Abstract Co-Author*) Nothing to Disclose Peter A. McCarthy, MD, Galway, Ireland (*Abstract Co-Author*) Nothing to Disclose

#### PURPOSE

We aim to assess the impact of the introduction of the National Breast Screening Programme on diagnosis of symptomatic invasive breast cancers in the screening population (50 - 64) compared to those 10 years younger (40 - 49) and 10 years older (65 - 74).

## METHOD AND MATERIALS

All symptomatic invasive breast cancers between January 2008 & January 2014 were reviewed. Patients were categorised by age (40 - 49, 50 - 64, 65 - 74). Tumour size, grade, subtype and lymph node status were determined. Disease progression was also recorded. Nottingham Prognostic Index (NPI) was calculated for all. Benign breast disease and non-invasive cancers were excluded.

#### RESULTS

A total of 956 patients between 40 and 75 had invasive breast cancer identified between January 2008 and January 2014. 403 of these were between the age of 50 – 64 and eligible for breast screening. A progressive reduction in patient numbers was identified in this age group biennially (Jan 08 – Jan 10; 151, Jan 10 – Jan 12: 138, Jan 12 – Jan 14: 114). There was no significant change in tumour grade (p=0.775). Favourable outcomes such as fewer nodal metastasis, a lower NPI, and less aggressive disease progression were recorded in subsequent biennial groups when compared with the initial group. Similar biennial outcomes were identified in the 65 - 74 age group. No significant change was identifiable in the 40 - 49 group.

## CONCLUSION

While the outcome may be multifactorial, the results show that the stage and prognosis of the patient groups exposed to breast cancer screening has improved. It can be deduced that this may be attributable to the introduction of breast cancer screening at a specialist centre.

## **CLINICAL RELEVANCE/APPLICATION**

Breast screening with mammography remains the gold standard and is funded in Ireland for women aged 50 - 64. However, several issues including overdiagnosis, overtreatment, false negative mammography, the presence of mammographically occult and interval cancers has led to much controversy. In the west of Ireland, a symptomatic cancer unit deals with all breast cancers in the public setting and would be expected to be impacted by the National Breast Screening Programme (NBSP), established in 2008.

# BR263-SD-WEB5

Digital Breast Tomosynthesis: The Screening Performance of Synthesized Mammograms in Identifying Calcifications in Routine Practice

Wednesday, Nov. 30 12:45PM - 1:15PM Room: BR Community, Learning Center Station #5

# Participants

Ryan W. Woods, MD, MPH, Baltimore, MD (*Presenter*) Nothing to Disclose Susan C. Harvey, MD, Lutherville, MD (*Abstract Co-Author*) Nothing to Disclose

## PURPOSE

Prior research demonstrated the comparable performance of full field digital mammography (FFDM) to that of digital breast tomosynthesis (DBT) with synthesized "2D" mammograms. However, the characterization of calcifications remains challenging, with some studies demonstrating comparable results between FFDM and DBT, while other have demonstrated the superiority of FFDM. The purpose of our study is to describe the screening performance of DBT with synthesized "2D" mammograms in routine clinical practice.

# METHOD AND MATERIALS

We retrospectively analyzed consecutive screening mammograms performed on 10,006 women between Feb and Oct 2015, during a period in which all DBT exams were performed with synthesized "2D" mammograms (Hologic C-View). We extracted 121 cases recalled for calcifications alone in 118 patients where a complete work up was completed including biopsy if indicated. All calcifications were characterized using BI-RADS descriptors and were given a final assessment. We calculated recall rate, the positive predictive value for screening (PPV1), the positive predictive value recommended for biopsy (PPV2) for calcifications specifically. Finally, we calculated the calcification-specific cancer detection rate (CDR).

#### RESULTS

The recall rate for calcifications was 121/10,006 (1.2%). There were 16 cases in which the calcifications identified on the synthesized view were not present at diagnostic mammography. The calcification-specific PPV1 was 42/121 (34.7%). The calcification-specific PPV2 was 14/42 (33.3%). The calcification-specific cancer detection rate, therefore, for calcifications was 14/10,006 (1.4/1000). Among the diagnosed cancers, 8 were DCIS only, and 6 were invasive.

# CONCLUSION

In our study, the calcification-specific recall rate, PPV1 and PPV2, were similar to published results of FFDM, meaning that DBT with synthesized "2D" mammograms adequately detect calcifications. One area in which the performance of DBT with synthesized "2D" mammograms might be improved is to decrease the rate of recall of artifactual "calcifications" identified on the synthesized view.

# **CLINICAL RELEVANCE/APPLICATION**

Digitial breast tomosynthesis with synthesized "2D" mammograms can be safely used to identify all abnormalities at screening mammography, including calcifications.

Communication of Breast Biopsy Results to Patients: A Survey of Providers' Preferences from an Academic Center with Large Community Network

Wednesday, Nov. 30 12:45PM - 1:15PM Room: BR Community, Learning Center Station #7

# Participants

Suma Chandra, MD, Boston, MA (*Presenter*) Nothing to Disclose Jordana Phillips, MD, Boston, MA (*Abstract Co-Author*) Nothing to Disclose Tejas S. Mehta, MD, MPH, Boston, MA (*Abstract Co-Author*) Nothing to Disclose Vandana M. Dialani, MD, Boston, MA (*Abstract Co-Author*) Nothing to Disclose Valerie J. Fein-Zachary, MD, Boston, MA (*Abstract Co-Author*) Nothing to Disclose

# PURPOSE

In our practice, after breast biopsies are performed, radiologists communicate pathology and management recommendations to the referring clinicians who then notify patients. Our purpose is to assess referring providers' preferences regarding communication of breast biopsy results to inform potential practice change.

# METHOD AND MATERIALS

An online survey using RedCap was circulated to providers who order breast imaging studies in our practice. Questions on demographics, perceptions of the current state, and preferences moving forward were included. Responses were analyzed using the Fisher exact test.

# RESULTS

A total of 154/340 (45%) responded, of which 13/154 (8%) were breast specialists and 141/154 (92%) were not. 81/154 (53%) order greater than 100 mammograms per year. Delivering biopsy results is the responsibility of 142/154 (91%) of the respondents. 115/142 (81%) reported being very or somewhat comfortable with discussing pathologies with their patients. However, when given the option, 72/153 (47%) preferred the Breast Radiology department notify the patient while 81/153 (53%) preferred the current system of personally notifying patients of biopsy results. A majority reported giving benign 108/142 (76%) and malignant 95/142 (67%) results by telephone. The reported strengths and challenges of the current system are listed in Figure 1.Regardless of who communicated the results, a majority 125/153 (82%) prefer the Breast Care Center, with non-specialists having a greater preference for this (p < .01). No difference was found in respondents based on number of exams ordered. A majority 88/125 (70%) preferred to be notified of patient-radiologist communication via documentation in the medical record and email or telephone.

# CONCLUSION

There was near equal preference for referring clinician or radiologist to communicate breast biopsy results to patients, with most preferring radiologists be responsible for follow-up recommendations and management. Implementation of such changes may help streamline care. These results support the role of radiologists beyond consultants, as part of the clinical team.

# **CLINICAL RELEVANCE/APPLICATION**

Many referring providers are interested in radiologists playing a larger role in the clinical team through communication of biopsy results and management recommendations to patients.

# State of the Art: Phase-Contrast MRI Flow Imaging

Wednesday, Nov. 30 12:45PM - 1:15PM Room: CA Community, Learning Center Hardcopy Backboard

#### **Participants**

El-Sayed H. Ibrahim, PhD, MSc, Ann Arbor, MI (*Presenter*) Nothing to Disclose Jadranka Stojanovska, MD, MS, Northville, MI (*Abstract Co-Author*) Nothing to Disclose Elizabeth Lee, MD, Ann Arbor, MI (*Abstract Co-Author*) Nothing to Disclose James O'Connor, Ann Arbor, MI (*Abstract Co-Author*) Nothing to Disclose Suzan Lowe, Ann Arbor, MI (*Abstract Co-Author*) Nothing to Disclose Prachi P. Agarwal, MD, Ann Arbor, MI (*Abstract Co-Author*) Nothing to Disclose

# **TEACHING POINTS**

- 1. Review the principles of phase-contrast (PC) MRI flow imaging, clinical indications, and measured parameters.
- 2. Review and illustrate the sources of common artifacts in PC MRI flow imaging.
- 3. Describe strategies for optimizing image quality and minimizing imaging artifacts.4. Describe the spectrum of PC MRI applications
- in different cardiovascular imaging.5. Describe recent advances, including 4D flow imaging and CSF flow quantification.

#### **TABLE OF CONTENTS/OUTLINE**

Phase-contrast (PC) MRI has been established as a valuable tool for measuring flow with high sensitivity and accuracy. Important hemodynamic parameters, e.g. peak flow/velocity, quantification of regurgitation, blood volume, flow rate, and pulse wave velocity, can be measured from the resulting magnitude and phase images. Herein, we review basics of PC flow imaging, clinical indications, and optimal imaging parameter settings in different applications. We then review cases acquired with imaging artifacts or poor image quality, and describe modifications of the imaging parameters / protocol settings to alleviate these artifacts and improve image quality for optimal measurements' accuracy. We will also describe the clinical applications of PC MRI in cardiovascular imaging and CSF flow as well as recent advances, such as 4D flow imaging.

# CA233-SD-WEB3

Contrast Material Injection Protocols at Coronary CT Angiorapraphy with Short Injection Duration Can Yield Sufficient Arterial Enhancement in Wide Range of Cardiac Output Value: Computer Simulation Study

Wednesday, Nov. 30 12:45PM - 1:15PM Room: CA Community, Learning Center Station #3

# Participants

Toru Higaki, PhD, Hiroshima, Japan (*Presenter*) Nothing to Disclose Takeshi Nakaura, MD, Kumamoto, Japan (*Abstract Co-Author*) Nothing to Disclose Masafumi Kidoh, Kumamoto, Japan (*Abstract Co-Author*) Nothing to Disclose Hideaki Yuki, MD, Kumamoto, Japan (*Abstract Co-Author*) Nothing to Disclose Yasuyuki Yamashita, MD, Kumamoto, Japan (*Abstract Co-Author*) Consultant, DAIICHI SANKYO Group Kazuo Awai, MD, Hiroshima, Japan (*Abstract Co-Author*) Research Grant, Toshiba Corporation; Research Grant, Hitachi, Ltd; Research Grant, Bayer AG; Research Grant, Eisai Co, Ltd; Medical Advisor, General Electric Company; ; ; ; Yuko Nakamura, MD, Bethesda, MD (*Abstract Co-Author*) Nothing to Disclose Fuminari Tatsugami, Hiroshima, Japan (*Abstract Co-Author*) Nothing to Disclose

## PURPOSE

Arterial peak enhancement (APE) on contrast-enhanced CT (CECT) images is thought to be higher and longer in patients with low cardiac output (CO). Under the hypothesis that the relationship between CO and APE is affected by the duration of contrast material (CM) injection we performed computer simulations to investigate the relationship between CO on APE by using protocols with different injection durations.

# METHOD AND MATERIALS

We developed computer simulation software for contrast enhancement of various organs and vessels based on the Bae pharmacokinetics model [Bae et al., Radiology, 98]. We also implemented models for CM transmission within organs, for the diffusion of CM in blood plasma based on the osmotic pressure, and for the pulsatile flow. We confirmed the clinical validity of our software by comparing our computer data with data obtained in 136 patients undergoing test bolus for cardiac CT angiography.We simulated contrast enhancement of the ascending aorta at coronary CT angiography for a subject 166-cm tall and weighing 65 kg. The simulated injection protocols were: CM dose 40 ml, CM iodine concentration 350 mgI/ml, osmotic pressure 590 mOsm/kgH2O, injection duration 8-, 10-, 12-, 14-, 16-, 18-, and 20 sec. The simulated CO range was 0 to 10.0 L/min.We calculated simulated arrival time (sAT) of CM to the aortic aorta, peak enhancement time (sPT) time of the CM, Peak CT number (sPCT#) under different injection duration.

#### RESULTS

In validation study, difference between sST and actual mean AT, sPT and actual mean PT, sPCT# and actual mean CT# were less than standard deviation of each actual parameter. Percent errors between sST and actual mean AT, sPT and actual mean PT, sPCT# and actual mean CT# were 12%, 8.5%, and 2%, respectively.In the simulation study, when the injection duration was 8 or 10 sec, sAPE was larger than 400 HU at CO ranging from 1.0 – 9.0 L/min. On the other hand, the injection duration was 18 or 20 sec, sAPE was larger than 400 HU at CO ranging from 1.0 – 4.1 L/min.

# CONCLUSION

Our software could accurately simulate arterial enhancement. In the simulation of arterial enhancement, shorter injection duration (8, 10 sec) could yield sufficient enhancement (400 HU) at cardiac outputs ranging from 1.0 - 9.0 L/min.

#### **CLINICAL RELEVANCE/APPLICATION**

CM injection durations of 8 or 10 sec can yield sufficient arterial peak enhancement at wide range of patient cardiac output.

# CA245-SD-WEB1

Identification and Assessment of Cardiac Amyloidosis by Myocardial Strain Analysis of Tagged Magnetic Resonance Imaging

Wednesday, Nov. 30 12:45PM - 1:15PM Room: CA Community, Learning Center Station #1

# Participants

Seitaro Oda, MD, Kumamoto, Japan (*Presenter*) Nothing to Disclose Daisuke Utsunomiya, MD, Kumamoto, Japan (*Abstract Co-Author*) Nothing to Disclose Kosuke Morita, Kumamoto, Japan (*Abstract Co-Author*) Nothing to Disclose Takatoshi Matsubara, Kumamoto, Japan (*Abstract Co-Author*) Nothing to Disclose Takeshi Nakaura, MD, Kumamoto, Japan (*Abstract Co-Author*) Nothing to Disclose Hideaki Yuki, MD, Kumamoto, Japan (*Abstract Co-Author*) Nothing to Disclose Kenichiro Hirata, Kumamoto, Japan (*Abstract Co-Author*) Nothing to Disclose Narumi Taguchi, Kumamoto, Japan (*Abstract Co-Author*) Nothing to Disclose Yasuyuki Yamashita, MD, Kumamoto, Japan (*Abstract Co-Author*) Nothing to Disclose

## PURPOSE

Myocardial strain analysis by cardiac magnetic resonance (CMR) facilitate the noninvasive measurement regional myocardial function, and the early identification of contractile dysfunction. This study sought to explore the potential role of myocardial strain analysis by CMR for the identification of cardiac amyloidosis.

## **METHOD AND MATERIALS**

Thirty five systemic amyloidosis patients (23 men and 12 women, age 56.5±16.5 years) underwent 3.0T CMR including tagged MR and late gadolinium enhancement (LGE) imaging. Their circumferential strain (CS) was measured using mid-ventricular short-axis images and compared between LGE-positive- and LGE-negative patients.

#### RESULTS

There were 29 LGE-positive- and 6 LGE-negative patients with systemic amyloidosis. The peak CS was significantly lower in LGE-positive amyloidosis patients compared to LGE-negative patients (-9.4 $\pm$ 2.5 % vs. -12.7 $\pm$ 1.5 %, p<0.01). The CS peak time was significantly prolonged in LGE-positive- than LGE-negative amyloidosis patients (422.7 $\pm$ 121.8 ms vs. 355.6 $\pm$ 43.1 ms, p=0.02). The  $\Delta$  peak time was significantly longer in LGE-positive- than LGE-negative patients (79.2 $\pm$ 49.2 ms vs. 17.2 $\pm$ 26.6 ms, p<0.01).

## CONCLUSION

Myocardial strain analysis by CMR helps to detect LGE-positive cardiac amyloidosis considered to have a poor prognosis without contrast material.

# **CLINICAL RELEVANCE/APPLICATION**

Myocardial strain analysis by CMR may be useful for the identification of cardiac amyloidosis and does not require gadolinium-based contrast material.

# CA246-SD-WEB2

Accuracy of Iodine Density Image Using Single Source Dual-energy CT in the Assessment of Myocardial Infarction

Wednesday, Nov. 30 12:45PM - 1:15PM Room: CA Community, Learning Center Station #2

# Participants

Shinichiro Kitao, Yonago, Japan (*Presenter*) Nothing to Disclose Yasutoshi Ohta, MD, Yonago, Japan (*Abstract Co-Author*) Nothing to Disclose Junichi Kishimoto, Yonago, Japan (*Abstract Co-Author*) Nothing to Disclose Natsuko Mukai, MD, Yonago, Japan (*Abstract Co-Author*) Nothing to Disclose Tomomi Watanabe, MD, Yonago, Japan (*Abstract Co-Author*) Nothing to Disclose Kazuhiro Yamamoto, Yonago, Japan (*Abstract Co-Author*) Nothing to Disclose Toshihide Ogawa, MD, Yonago, Japan (*Abstract Co-Author*) Nothing to Disclose

## PURPOSE

To clarify the usefulness of iodine density image (IDI) using single source dual-energy CT (ssDECT) for qualitative and quantitative analysis in myocardial infarction.

#### **METHOD AND MATERIALS**

Both late iodine enhancement (LIE) and late gadolinium enhancement (LGE) images were obtained in 17 patients with myocardial infarction in the study. LIE image was acquired using rapid-kV switching ssDECT. IDI and virtual monochromatic image (VMI) of 40 to 140keV were used as evaluating image sets. On LIE images, the presence of infarction was evaluated and extent of transmurality was graded using a 5-point scale by two experienced radiologists blinded to other clinical information. The LGE images were used as reference standard. Kappa coefficient for the concordance rate of transmurality was also calculated. Infarct myocardium volume and percentage of infarct myocardium for each patient were measured and compared with those of LGE image using linear regression analysis.

# RESULTS

Myocardial infarction was identified in 89 of 272 segments. Any infarct was identified on 40 to 70keV VMI and IDI. No infarct was identified on 80 to 140keV VMI. The IDI demonstrated the best contrast-to-noise ratio (CNR) of 8.74 $\pm$ 3.79 among the evaluating image sets (P < 0.001). The IDI achieved the best diagnostic performance (sensitivity 84.27%, specificity 100%, positive predictive value 100%, negative predictive value 92.89%, accuracy 94.85%, and area under the curve 0.921). Additionally, the IDI demonstrated the highest concordance rate of transmurality ( $\kappa$ =0.759) among the image sets. Both infarct myocardium volume and percentage of infarct myocardium on IDI showed the best correlation to LGE (r=0.865, 0.902, respectively, P < 0.001) among the image sets.

# CONCLUSION

The IDI using ssDECT is best to visualize infarct myocardium and enables accurate measuring of infarct myocardium.

## **CLINICAL RELEVANCE/APPLICATION**

IDI derived from ssDECT enables to evaluate accurately the transmurality and percentage of infarct myocardium as well as MRI.

# CA248-SD-WEB4

## Diagnostic Value of Quantitative Myocardial T1- and T2- Mapping in Patients with Biopsy Proven Sarcoidosis

Wednesday, Nov. 30 12:45PM - 1:15PM Room: CA Community, Learning Center Station #4

#### **Participants**

Daruis Dabir, Bonn, Germany (*Presenter*) Nothing to Disclose Daniel Kuetting, MD, Bonn, Germany (*Abstract Co-Author*) Nothing to Disclose Julian A. Luetkens, MD, Bonn, Germany (*Abstract Co-Author*) Nothing to Disclose Rami Homsi, Bonn, Germany (*Abstract Co-Author*) Nothing to Disclose Christian F. Marx, MD, Bonn, Germany (*Abstract Co-Author*) Nothing to Disclose Hans H. Schild, MD, Bonn, Germany (*Abstract Co-Author*) Nothing to Disclose Daniel K. Thomas, MD, PhD, Bonn, Germany (*Abstract Co-Author*) Nothing to Disclose

## PURPOSE

Cardiac involvement of sarcoidosis hallmarked by myocardial inflammation and subsequent myocardial fibrosis is a life threatening condition that makes early diagnosis necessary. Native T1- as well as T2-mapping have been proposed as reliable methods to non-invasively assess diffuse myocardial fibrosis and edema respectively. Our aim was to investigate the value of both methods for the assessment of myocardial involvement in sarcoidosis.

# **METHOD AND MATERIALS**

Patients with biopsy proven extracardiac sarcoidosis who previously underwent a CMR examination were invited for a follow up scan. The scan performed on a 1.5T Philips INGENIA scanner comprised a clinically routine CMR-protocol with additional T1-and T2-mapping in midventricular short axis (SA) slice. T1-mapping was performed using Modified Look-Locker Inversion Recovery Imaging (3-3-5 MOLLI). T1-relaxation times were quantified within the septal myocardium (CONSEPT-approach). For T2 mapping an optimized 6-echo gradient spin echo (GraSE) sequence was used measuring T2 relaxation times within the whole SA slice. Cardiac involvement was diagnosed if at least one of the following pathologies occured: pathological relative enhancement,LGE,myocardial edema. According to CMR results patients were divided into 4 groups: group 1: positive findings in both exams, group 2: positive findings only in the initial exam; group 3: sarcoidosis but inconspicuous initial CMR exam, group 4: control group of healthy age matched volunteers.

#### RESULTS

T1 relaxation times were significantly longer in patients with positive CMR findings in both the initial examination and the follow-up scan (group 1) in comparison to all other groups (p<0,05). However no significant difference in T1 relaxation time could be revealed in patients with history of cardiac involvement of sarcoidosis (group 2) as well as patients with sarcoidosis but no CMR findings (group 3; p>0,05). No significant difference in T2 relaxation times could be revealed between all 4 groups (p>0,05, Table1).

# CONCLUSION

Patients with consistent cardiac involvement of sarcoidosis have significantly increased T1 relaxation times as a sign of diffuse cardiac fibrosis whereas no relation between diffuse myocardial edema and cardiac involvement of sarcoidosis could be revealed.

# **CLINICAL RELEVANCE/APPLICATION**

Results indicate that T1-mapping has the potential to serve as an indicator for myocardial involvement of sarcoidosis.

## Value of Repeat Coronary CT Angiography in Patients Presenting with Acute Chest Pain

Wednesday, Nov. 30 12:45PM - 1:15PM Room: CA Community, Learning Center Station #5

#### **Participants**

Jared Nesbitt, MD, Stony Brook, NY (*Presenter*) Nothing to Disclose Christopher Shackles, DO,MPH, Stony Brook, NY (*Abstract Co-Author*) Nothing to Disclose Jie Yang, Stony Brook, NY (*Abstract Co-Author*) Nothing to Disclose Eric J. Feldmann, MD, Smithtown, NY (*Abstract Co-Author*) Nothing to Disclose Donglei Yin, PhD, Stony Brook, NY (*Abstract Co-Author*) Nothing to Disclose Kavitha Yaddanapudi, DMRD, MBBS, Stony Brook, NY (*Abstract Co-Author*) Nothing to Disclose

## PURPOSE

The purpose of this study is to evaluate if repeat coronary CT angiography (CCTA) in patients presenting with acute chest pain to the emergency department (ED) has any added value and shows any significant change from prior study and to identify factors associated with this change.

## **METHOD AND MATERIALS**

We retrospectively evaluated 365 patients who presented to the ED with acute chest pain and underwent repeat CCTA. We excluded patients with obstructive disease (>50%) on initial CCTA from the study. The coronary artery disease (CAD) was graded on a 3 point system, grade 0 is normal, Grade 1 non-obstructive CAD (<50% stenosis) and grade 2 obstructive CAD (>50% stenosis). Significant change between the two studies was defined as change from grade 0 to 1 or 2 and grade 1 to 2. Chi square test was utilized to examine marginal association between known risk factors as diabetes, hypertension, smoking, hyperlipidemia, time interval between the two scans and significant change on repeat CCTA. Multivariable regression analysis was applied to identify significant independent risk factors.

## RESULTS

A total of 47 (12%) patients had a significant interval change in their CAD on repeat CCTA. Of these, 32 (8.77%) grade 0-1, 1 (0.27%) from grade 0 to 2 and 14 (3.8%) grade 1 to 2 on repeat scan. Interval change was strongly associated with diabetes (p=0.039, OR=2.0) and time interval between scan of more than 3 years (p=0.0384 and OR= 2.04). The rest of the risk factors were not significantly associated with interval change. Presence of non-obstructive disease was not significantly associated with a change on subsequent scan.

### CONCLUSION

Significant interval change with repeat CCTA was seen in only 12% of our studies. Repeat coronary CT angiography is more likely to show significant interval change in diabetic patients and if scan duration is more than three years from initial scan.

### **CLINICAL RELEVANCE/APPLICATION**

Acute chest pain accounts for approximately 6 million emergency department visits every year with acute coronary syndrome in 15-20% of these cases. CCTA has an established role in triaging these patients who present with acute chest pain with a clinical concern for acute coronary syndrome. Currently repeat coronary CTA does not figure in the appropriateness guidelines for CCTA. Studies are needed to evaluate what the added value of repeat coronary CTA is in the emergency setting.

## CA250-SD-WEB6

Assessing the Cardiovascular System with Whole-body Na18F PET/CT and Opportunities for New Quantitative Methodologies

Wednesday, Nov. 30 12:45PM - 1:15PM Room: CA Community, Learning Center Station #6

### Awards

### **Student Travel Stipend Award**

#### Participants

Carl I. Odom, MD, Columbus, OH (*Presenter*) Nothing to Disclose Chadwick L. Wright, MD, PhD, Lewis Center, OH (*Abstract Co-Author*) Nothing to Disclose Preethi Subramanian, MS, BEng, Columbus, OH (*Abstract Co-Author*) Nothing to Disclose Katherine Binzel, PhD, Columbus, OH (*Abstract Co-Author*) Nothing to Disclose Subha V. Raman, MD, Columbus, OH (*Abstract Co-Author*) Nothing to Disclose Michael V. Knopp, MD, PhD, Columbus, OH (*Abstract Co-Author*) Nothing to Disclose

### PURPOSE

Sodium fluoride-18 (Na18F) is a positron emitting radionuclide typically used for oncologic imaging of osteoblastic tumor burden but recent studies have demonstrated the potential for 18F as a PET biomarker of vascular microcalcifications (miCalcs) as well as vulnerable atherosclerotic plaque. Since the vast majority of Na18F PET studies are usually performed as whole-body evaluations for osteoblastic lesions, the purpose of this study is to assess the clinical feasibility of performing qualitative and quantitative imaging assessment of cardiovascular 18F activity on whole-body oncologic Na18F PET/CT imaging.

## METHOD AND MATERIALS

In this retrospective study, 20 patients underwent routine Na18F PET/CT for prostate or thyroid cancer. Qualitative assessment for cardiovascular 18F-avidity was performed by a reader panel. Using threshold-based isocontouring, quantitative assessment of vascular 18F activity was performed and provided the total fluoride uptake (TFU) and fluoride volume (FV) for the cardiovascular structures as well as the highest SUVmax (hSUVmax) and average SUVmax values.

#### RESULTS

Although FV for the cardiovascular system varied widely between patients, the average SUVmax values remained relatively consistent. Vascular macrocalcifications (maCalcs) represented less than half of whole body cardiovascular FV. In particular, maCalcs tended to be within the aorta whereas the majority of vascular 18F activity tended to be in lower extremity arteries with no associated vascular maCalcs on CT. Presumably this lower extremity activity represents early vascular miCalcs.

## CONCLUSION

In general, it appears feasible that whole-body Na18F PET/CT can also be used to detect focally or systemically increased 18F uptake in the cardiovascular system. Although this uptake may reflect vulnerable plaque in the acute setting, it can also be used to assess for the presence of early vascular miCalcs. New quantitative 18F PET methodologies will likely enable nuclear medicine physicians to detect occult regions of cardiovascular disease earlier and potentially improve imaging response assessment to new and emerging cardiovascular therapeutic agents.

# **CLINICAL RELEVANCE/APPLICATION**

Whole-body detection and quantification of vulnerable vascular plaques and miCalcs using Na18F PET will enable new methods for non-invasive monitoring of disease stabilization and treatment response.

## CA251-SD-WEB7

Virtual Simulation of the Amplazar Septal Occluder for Atrial Septal Defect in CT: 3-D CT/CT Image Fusion with Different Subjects

Wednesday, Nov. 30 12:45PM - 1:15PM Room: CA Community, Learning Center Station #7

**FDA** Discussions may include off-label uses.

### Participants

Akira Kurata, PhD, Toon, Japan (*Presenter*) Nothing to Disclose Takahiro Yokoi, Toon, Japan (*Abstract Co-Author*) Nothing to Disclose Yuki Tanabe, Toon, Japan (*Abstract Co-Author*) Nothing to Disclose Naoki Fukuyama, Toon, Japan (*Abstract Co-Author*) Nothing to Disclose Adriaan Coenen, MD, Rotterdam, Netherlands (*Abstract Co-Author*) Nothing to Disclose Koen Nieman, MD, PhD, Rotterdam, Netherlands (*Abstract Co-Author*) Nothing to Disclose Ryo Ogawa, MD, Toon, Japan (*Abstract Co-Author*) Nothing to Disclose Emiri Watanabe, Ehime, Japan (*Abstract Co-Author*) Nothing to Disclose Masashi Nakamura, Toon, Japan (*Abstract Co-Author*) Nothing to Disclose Tomoyuki Kido, Toon, Japan (*Abstract Co-Author*) Nothing to Disclose Teruhito Kido, MD, PhD, Toon, Japan (*Abstract Co-Author*) Nothing to Disclose Masao Miyagawa, MD, Toon, Japan (*Abstract Co-Author*) Nothing to Disclose Teruhito Kido, MD, PhD, Toon, Japan (*Abstract Co-Author*) Nothing to Disclose

### PURPOSE

In patients with secundum atrial septal defects (ASD), the trans-catheter closure device (Amplazar septal occludor; ASO) is commonly used in clinical practice. The anatomical location and the size of ASD are carefully evaluated with echocardiography before and during the ASO closure therapy. Cardiac computed tomography (CT) allows for precise measurement of the defect size and the rim around ASD. We developed a simulation system using virtual CT/CT fusion image that obtained different objects. We introduce the simulation system showing its clinical feasibility in patients with ASD.

### **METHOD AND MATERIALS**

We assessed the proof-of-principle cohort study at single centre. Patients (aged  $\geq$ 13 years) with secundum ASD who performed cardiac CT were non-selectively enrolled to the study. Eight different ASO device (size 10, 13, 14, 16, 20, 24, 32, and 38 mm) were independently done with static CT, and the 3-D data was obtained. Two datasets of patient's heart and ASO device were three-dimensionally imposed, and clinically relevant ASO device were virtually deployed.

## RESULTS

A total of 18 patients (median age 55 years, range 13-77) were assigned to the study. For the patients successfully performed with the ASO closure therapy (n=10), the CT/CT fusion image showed that the all-round rim around ASO device that physically deployed remained eligibly as well as transesophageal echocardiography. For the other patients (surgical ASD closure, n=4; wait and see, n=4), the CT/CT fusion image showed that the most clinically relevant ASO device virtually failed to be deployed to the ASD in size or location (Figure 1 shows that the maximum ASO device was undersized but protruding over the left atrial wall).

### CONCLUSION

We propose the virtual simulation for the ASO using CT/CT image fusion with different subjects is technically accurate for guiding the trans-catheter ASO closure and feasible for clinical use in the management of ASD.

## **CLINICAL RELEVANCE/APPLICATION**

Xenogeneic CT/CT image fusion with different subjects allows for precise virtual simulation of trans-catheter intervention in congenital heart disease.

## Progression of Interstitial Lung Disease in Patients Treated with Stereotactic Body Radiation Therapy

Wednesday, Nov. 30 12:45PM - 1:15PM Room: CH Community, Learning Center Station #1

#### **Participants**

Stephen M. Lyen, FRCR, Toronto, ON (*Abstract Co-Author*) Nothing to Disclose Daniel Glick, MD, Toronto, ON (*Abstract Co-Author*) Nothing to Disclose Lisa Le, Toronto, ON (*Abstract Co-Author*) Nothing to Disclose Meredith Giuliani, MBBS, MEd, Toronto, ON (*Abstract Co-Author*) Nothing to Disclose Sonja Kandel, MD, Toronto, ON (*Abstract Co-Author*) Nothing to Disclose Patrik Rogalla, MD, Toronto, ON (*Presenter*) Research Grant, Toshiba Corporation; Speakers Bureau, Bayer AG

# PURPOSE

To determine whether SBRT induces progression of interstitial lung disease (ILD) contralateral to treatment site compared to noncancer ILD patients.

## **METHOD AND MATERIALS**

Patients treated with SBRT from October 2004 to March 2015 were identified from a prospective database. CT scans pre- and 1year post-treatment were reviewed by a thoracic radiologist. The lung contralateral to the side of SBRT was assessed and the extent of total ILD, proportion of reticulation, honeycombing, and ground glass were scored to the nearest 5% at 6 anatomical levels. The coarseness of fibrosis was scored and the ILD pattern classified according to ATS guidelines. A control cohort of ILD patients without lung cancer who had their baseline and 1 year CTs scored according to the same method was used for comparison. The baseline scans were obtained from Apr 2008 to Oct 2014. Our primary outcome measures were change in total disease extent score (TDES) and the presence of >10% increase in ILD extent at any level. Imaging scores and SBRT were subject to uni- and multivariate linear regression analysis and logistic regression analysis.

### RESULTS

607 SBRT patients were assessed and 21 (3.4%) patients were found to have features of ILD on pre-treatment scans (mean age 76  $\pm$  11 years). 25 were patients in the non-cancer ILD cohort (mean age 62  $\pm$  11 years). Average time to follow up scan was 12.7 and 13 months for SBRT and non-cancer patients respectively. In total, there were 13 patients with imaging consistent with usual interstitial pneumonia (UIP), 26 with possible UIP, and 7 inconsistent with UIP. SBRT was a significant predictor of an increase in ILD extent >10% at any level (p<0.05), but not for change in total disease extent score on both univariate and multivariate analysis. UIP was a significant predictor of progression in both primary outcomes (p <0.01). None of the imaging descriptors (ground glass, reticulation, honeycombing), traction bronchiectasis or coarseness score were significant predictors of progression.

# CONCLUSION

SBRT and UIP are significant predictors of a >10% increase in ILD extent at any level. Further long-term studies will be required to determine this effect on morbidity and survival.

## **CLINICAL RELEVANCE/APPLICATION**

Our findings suggest that SBRT could increase the degree of ILD progression compared to non-cancer ILD patients which may have implications on decision making.

## CH272-SD-WEB2

Detection of Lung Carcinoma with Predominant Ground-glass Opacity on CT Using Temporal Subtraction Method: JAFROC Observer Study

Wednesday, Nov. 30 12:45PM - 1:15PM Room: CH Community, Learning Center Station #2

## Participants

Takashi Terasawa, MD, Kitakyushu, Japan (*Presenter*) Nothing to Disclose Takatoshi Aoki, MD, PhD, Kitakyushu, Japan (*Abstract Co-Author*) Nothing to Disclose Seiichi Murakami, Kitakyusyu, Japan (*Abstract Co-Author*) Nothing to Disclose Masami Fujii, MD, Kitakyushu, Japan (*Abstract Co-Author*) Nothing to Disclose Chihiro Chihara, MD, Kitakyushu, Japan (*Abstract Co-Author*) Nothing to Disclose Yukunori Korogi, MD, PhD, Kitakyushu, Japan (*Abstract Co-Author*) Nothing to Disclose Michiko Kobayashi, MD, Kitakyushu, Japan (*Abstract Co-Author*) Nothing to Disclose Yoshiko Hayashida, MD, Fukuoka, Japan (*Abstract Co-Author*) Nothing to Disclose

#### PURPOSE

We have been developing a new temporal subtraction (TS) method in order to significantly reduce misregistration artifacts on the subtraction images in successive thoracic CTs, and have shown that TS can improve the diagnostic accuracy of solid lung nodules less than 2cm. However, the performance of TS for the detection of the lung cancer with predominant ground-glass opacity (LC-pGGO) has not been clarified. The purpose of this study is to evaluate the usefulness of TS for the detection of LC-pGGO with jackknife free-response receiver operating characteristics (JAFROC) observer study.

### **METHOD AND MATERIALS**

Twenty-five pairs of standard-dose CT and their TS images in patients with LC-pGGO and 25 pairs of those in patients without nodule were used for an observer performance study. A total of 31 LC-pGGO lesions, ranging in size from 5 to 22 mm, were identified as the reference standard of actionable lesions (GGO lesions increased in size or demonstrated appearance or growth of the solid component) by two thoracic radiologists. Eight radiologists (four attending radiologists and four radiology residents) participated in this observer study. Ratings and locations of "lesions" determined by the observers were utilized for assessing the statistical significance of differences between radiologists' performances without and with the CT-TS images in JAFROC analysis. The statistical significance of differences in the reviewing time was determined by use of a two-tailed paired Student's t test.

### RESULTS

The average figure-of-merit (FOM) values for all radiologists increased to a statistically significant degree, from 0.861 without the CT-TS images to 0.912 with the images (P<.001). The average sensitivity for detecting the actionable lesions was improved from 73.4 % to 85.9 % at a false-positive rate of 0.15 per case by use of the CT-TS images. The reading time with CT-TS images was not significantly different from that without.

## CONCLUSION

The use of CT-TS would improve the observer performance for the detection of the LC-pGGO without considerably extending the reading time.

## **CLINICAL RELEVANCE/APPLICATION**

A CT temporal subtraction method can sufficiently assist the radiologists' interpretation for the detection of the lung cancer with predominant ground-glass opacity.

# CH273-SD-WEB3

## Lung Perfused Blood Volume (PBV) Value as a Prognosis Factor for Idiopathic Pulmonary Fibrosis (IPF)

Wednesday, Nov. 30 12:45PM - 1:15PM Room: CH Community, Learning Center Station #3

#### **Participants**

Masahiro Kobayashi, MD, Tokyo, Japan (*Presenter*) Nothing to Disclose Nobuyuki Shiraga, MD, Ohta-Ku, Japan (*Abstract Co-Author*) Nothing to Disclose Hideaki Suzuki, MD, PhD, Tokyo, Japan (*Abstract Co-Author*) Nothing to Disclose Keiko Matsumoto, Tokyo, Japan (*Abstract Co-Author*) Nothing to Disclose Keishi Sugino, Tokyo, Japan (*Abstract Co-Author*) Nothing to Disclose Sakae Honma, MD, PhD, Tokyo, Japan (*Abstract Co-Author*) Nothing to Disclose

## PURPOSE

Idiopathic pulmonary fibrosis (IPF) is a chronic and progressive interstitial pneumonia with a poor prognosis, and there are few imaging prognosis factors to predict disease progression. It is difficult to predict clinical course of IPF with conventional CT, because conventional CT provides only morphological information of fibrosis. Lung perfused blood volume images with dual-energy CT is feasible and provides not only morphological information, but also hemodynamic information of the lung. We assume that there may be some relations between prognosis of pulmonary fibrosis and pulmonary hemodynamics, so the purpose of this study was to assess and evaluate lung PBV imaging as a prognosis factor for IPF.

## **METHOD AND MATERIALS**

Institutional review board approval and written informed consent were obtained. Twenty-six patients with IPF (mean age: 74.8 years, range: 60-86 years) underwent pulmonary CTA using dual-energy CT. Lung perfused blood volume images were obtained by three-material decomposition algorithm, and mean lung PBV values were calculated. To evaluate the perfusion decrease in lower lung fields, mean PVB value ratio (lung PBV value of lower lung field/upper lung field) was also calculated on the hypothesis that upper lung fields are relatively stable, less involved by fibrosis. We divided the patients into two groups; progressed group and stable group by checking the fibrosis progression with follow-up CT, and compared lung PVB value ratio between two groups.

## RESULTS

Lung PVB images showed pulmonary perfusion defects in fibrosis areas. The areas where perfusion decrease were not noted adjacent to fibrosis tended to progress fibrosis. In contrast, the areas in which perfusion decrease were noted with slight fibrosis tended to be stable disease. Mean decreased lung PVB ratio in progressed group was significantly higher than that of stable group  $(1.05\pm0.15 \text{ vs } 0.72\pm0.12, \text{ p}<0.01)$ .

### CONCLUSION

Lung PVB shows the difference between progressing fibrosis and stable fibrosis areas, which is difficult with conventional CT. Lung PBV ratio may have the potential to be the new prognosis factor for IPF.

## **CLINICAL RELEVANCE/APPLICATION**

With lung PVB images, calculating lung PVB value ratio has the potential to predict its clinical course of IPF.

## CH274-SD-WEB4

Differential Pulmonary Artery Left Ventricular and Aortic Enhancement as a Predictor of Left Ventricular Systolic Dysfunction

Wednesday, Nov. 30 12:45PM - 1:15PM Room: CH Community, Learning Center Station #4

# Participants

Joel P. Thompson, MD, Rochester, NY (*Presenter*) Nothing to Disclose Timothy M. Baran, PhD, Rochester, NY (*Abstract Co-Author*) Research Consultant, Zenalux Biomedical Inc Abhishek Chaturvedi, MD, Rochester, NY (*Abstract Co-Author*) Nothing to Disclose

### PURPOSE

Decreased cardiac output is linearly correlated with delayed aortic peak enhancement on CT angiography. We sought to determine the prognostic significance of decreased aortic and left ventricular (LV) enhancement on pulmonary CTA (CTPA).

## METHOD AND MATERIALS

CTPA protocols at our institution utilize timing bolus or bolus tracking techniques for IV contrast timing. Both protocols include a minimum 6 second delay to account for CT gantry transit time, allowing for aortic enhancement in normal patients. An IRB-approved retrospective review was performed of adults who received both an echocardiogram and CTPA within 48 hours of each other. LV systolic dysfunction was defined as LV ejection fraction (LVEF) <40% on echocardiogram; control cases being LVEF >50%. Exclusion criteria: central pulmonary emboli & pulmonary hypertension. CTPA contrast attenuation was measured in the main pulmonary artery, LV, and descending thoracic aorta. Subjective enhancement was also graded on a Likert 1-4 scale.

## RESULTS

94 patients met inclusion criteria; 36 cases and 58 controls had similar gender composition, age, BMI, scan protocol, IV contrast volume and injection rate. When timing bolus protocol was used, LVEF <40% was associated with a significantly longer time to peak pulmonary artery attenuation (14.2 sec vs 9.3 sec, p<0.001). At an average IV contrast injection of about 4 cc/sec, decreased aortic to pulmonary artery enhancement ratio (Ao:PA) of 0.3 was associated with reduced LVEF, with a sensitivity of 77% and specificity of 82%. A decreased LV to pulmonary artery enhancement ratio (LV:PA) of 0.3 was also associated with reduced LVEF, with a sensitivity of 58% and a specificity of 96%. Subjective grading of decreased LV and aortic enhancement compared to pulmonary artery enhancement was predictive of LVEF <40% (LV, sensitivity=85%, specificity=96%; Aorta, sensitivity=97%, specificity=78%). Adding LV short axis diameter above 5.6 cm did not improve prediction of LV dysfunction.

## CONCLUSION

Quantitative Ao: PA & LV: PA enhancement ratios below 0.3 and subjective assessment of decreased LV and aortic enhancement compared to the pulmonary artery were associated with LVEF <40%.

# **CLINICAL RELEVANCE/APPLICATION**

Quantitative Ao:PA & LV:PA enhancement ratios below 0.3 and subjective assessment of decreased LV and aortic enhancement compared to the pulmonary artery were associated with LVEF <40%.

## Lung Cancers Detected in Low-Dose CT Lung Cancer Screening Usually Show Exponential Growth

Wednesday, Nov. 30 12:45PM - 1:15PM Room: CH Community, Learning Center Station #5

#### **Participants**

Marjole<sup>in</sup> A. Heuvelmans, MD,PhD, Groningen, Netherlands (*Presenter*) Nothing to Disclose Rozemarijn Vliegenthart, MD, PhD, Groningen, Netherlands (*Abstract Co-Author*) Nothing to Disclose Harry De Koning, Rotterdam, Netherlands (*Abstract Co-Author*) Research Grant, F. Hoffmann-La Roche Ltd Equipment support, Siemens AG Medical Advisory Board, F. Hoffmann-La Roche Ltd Harry Groen, Groningen, Netherlands (*Abstract Co-Author*) Nothing to Disclose Michel J. van Putten, MD, PhD, Enschede, Netherlands (*Abstract Co-Author*) Nothing to Disclose Pim A. De Jong, MD, PhD, Utrecht, Netherlands (*Abstract Co-Author*) Nothing to Disclose Matthijs Oudkerk, MD, PhD, Groningen, Netherlands (*Abstract Co-Author*) Nothing to Disclose

## PURPOSE

Although exponential growth is assumed for lung cancer, there is only limited information on in-vivo quantification of this pattern. Purpose of this study was to evaluate and quantify growth patterns of lung cancers detected in a low-dose computed tomography (CT) lung cancer screening trial, in order to elucidate the development and progression of early lung cancer.

## METHOD AND MATERIALS

Data from a randomized low-dose CT lung cancer screening trial were used. The trial was approved by the Ministry of Health. All participants gave informed consent. Solid lung nodules found at  $\geq$ 3 CT examinations before lung cancer diagnosis were included. Nodule volume was determined semi-automatically by software (LungCARE, Siemens, Erlangen, Germany). Lung cancer volume (V) growth curves were fitted with a single exponential, expressed as V=V1exp(t/ $\tau$ ), with t time from baseline (days), V1 estimated baseline volume (mm3), and  $\tau$  estimated time constant. Overall volume-doubling time (VDT) for the individual lung cancer is given by  $\tau$ \*log(2). The R2 coefficient of determination was used to evaluate goodness of fit.

## RESULTS

Forty-seven lung cancers in 46 participants were included. Forty participants were male (87.0%); mean age was 61.7 (standard deviation,  $\pm$ 6.2) years. Nodules were followed for a median of 770 days (inter-quartile range [IQR]: 383–1102 days) before lung cancer diagnosis. One cancer (2.1%) was diagnosed after six CT examinations, six cancers (12.8%) were diagnosed after five CTs, 14 (29.8%) after four, and 26 cancers (55.3%) after three CTs. Median overall volume-doubling time was 348 days (IQR: 222-492 days). The fit of the exponential function was excellent, with median R2 of 0.98 (IQR: 0.94–0.99).

# CONCLUSION

This study based on CT lung cancer screening provides in-vivo evidence that lung cancers usually evolve at an exponential growth rate. VDT can be used to describe the growth of lung nodules detected at low-dose CT lung cancer screening.

## **CLINICAL RELEVANCE/APPLICATION**

This study shows that lung cancers usually grow exponentially, and provides a biological basis for the use of volume-doubling time for monitoring lung cancer growth rate in CT lung cancer screening.

Role of Massive-Training Artificial Neural Network {MTANN} Algorithm in Radiation Dose Reduction and Image Quality for Sub-milli Sievert Chest CT Examinations: A Preliminary Study

Wednesday, Nov. 30 12:45PM - 1:15PM Room: CH Community, Learning Center Station #6

# Participants

Azadeh Tabari, Boston, MA (*Presenter*) Nothing to Disclose Florian J. Fintelmann, MD, FRCPC, Boston, MA (*Abstract Co-Author*) Consultant, McKesson Corporation Shaunagh McDermott, FFR(RCSI), Boston, MA (*Abstract Co-Author*) Nothing to Disclose Michael S. Gee, MD, PhD, Jamaica Plain, MA (*Abstract Co-Author*) Nothing to Disclose Sarabjeet Singh, MD, Boston, MA (*Abstract Co-Author*) Research Grant, Siemens AG; Research Grant, Toshiba Corporation; Research Grant, General Electric Company; Research Grant, Koninklijke Philips NV

## PURPOSE

To evaluate Massive-Training artificial neural network {MTANN} algorithm and Filter Back Projection (FBP) reconstruction techniques for 27% radiation dose reduction and image quality for chest CT

# METHOD AND MATERIALS

In an IRB approved and HIPAA study, 13 patients (mean age  $63.9 \pm 11$  years, M:F 9:4, weight  $174.8 \pm 38$  lbs) underwent "routine" chest CT with standard and low dose. Patients were scanned on 128 slice MDCT {SOMATOM Definition Flash, & Discovery 750HD}. Only tube current was reduced to achieve low dose, compared to standard dose {120 kV, thickness 3 mm and scan length}. Low dose images were post processed with MTANN, which is a pattern-recognition technique based on the use of an artificial neural network as a filter. Radiation dose parameters, including CTDIvol, Dose Length Product and estimated effective dose was calculated as per ICRP103. Detailed CT image quality, including objective image noise, Hounsfield Unit values and contrast to noise ratio (CNR) were measured in thoracic aorta, pectoral muscles, para-spinal muscles, air outside the thoracic cavity. Standard dose images were considered as the reference standard for image quality and statistical analyses were performed using the t-test

# RESULTS

Standard and low dose chest CT examinations were performed for clinical indications, including metastasis evaluation, pneumonia, pulmonary obstructive disease. Low dose chest CT images were acquired at 81% {CTDIvol  $9.1\pm6/1.8 \pm 0.2 \text{ mGy}$ } lower dose. DLP was  $66 \pm 2 \text{ mGy.cm}$  and  $322.7 \pm 217 \text{ mGy.cm}$ , effective dose 1 mSv and  $4.8 \pm 3.3 \text{ mSv}$ , for low and standard dose, respectively. Image noise was significantly decreased by 27% { $62.3 \pm 19/84.1 \pm 28$ } in low dose MTANN images as compared to low dose FBP{p <0.004}. HU values were similar in low dose MTANN ( $27.5 \pm 23$ ) as compared to standard dose ( $39.2 \pm 10$ ) (p> 0.1). CNR was significantly improved in MTANN compared to standard dose FBP images {p<0.002}

# CONCLUSION

MTANN algorithm reconstructed CT images lowers noise by 27% in 81% low dose images {1.8 mGy} compared to conventional FBP

## **CLINICAL RELEVANCE/APPLICATION**

Low dose chest CT acquired at 1.8 mGy is feasible with MTANN algorithm

# ER233-SD-WEB1

## The role of MD-CECT in the Diagnosis of Necrotizing Fasciitis and Correlation with the LRINEC Score

Wednesday, Nov. 30 12:45PM - 1:15PM Room: ER Community, Learning Center Station #1

#### **Participants**

Marco Di Girolamo, MD, Rome, Italy (*Presenter*) Nothing to Disclose Francesco Carbonetti, MD, Rome-Roma, Italy (*Abstract Co-Author*) Nothing to Disclose Antonio Cremona, Rome, Italy (*Abstract Co-Author*) Nothing to Disclose Daniela Sergi, Rome, Italy (*Abstract Co-Author*) Nothing to Disclose Valentina Caturano, Rome, Italy (*Abstract Co-Author*) Nothing to Disclose Elsa Iannicelli, MD, Rome, Italy (*Abstract Co-Author*) Nothing to Disclose

## PURPOSE

To evaluate the diagnostic efficacy of the CT findings in predicting the diagnosis of Necrotizing Fasciitis (NF).

### **METHOD AND MATERIALS**

In a period of a year 36 pts with a clinical suspicion of NF underwent to CE-MDCT .CT findings studied were : involvement and thickening of the muscular fascia, fluid collections along the deep fascial sheaths , extension of oedema into the intramuscular septa and the muscles, low attenuation areas in the deeper fascial planes suggestive for colliquative necrosis, a non enhancement of the muscular fascia and vascular thrombosis.Radiological findings were compared with the LRINEC score and with the surgical data.

#### RESULTS

CT findings were suggestive for NF in 10 pts , for non-NF in 2 pts and for gas-gangrene in 2 pts .The rest of the pts showed CT finding suggestive for cellulitis (10 pts) , myositis (5 pts) , soft tissue abscess (7 pts).Among the patients with CT findings suggestive for NF, non-NF and gas gangrene , 9 pts showed a non enhancing fascia, subcutaneous gas was present in 12 pts, involvement of the fascia in 12 pts, fluid collections along the deep fascial sheaths in 7 pts ,low attenuation areas in the deeper fascial planes in 3 pts. Surgical examination confirmed the diagnosis of NF in 12 pts who showed at the CE-MDCT a non enhancement of the fascia (9/12), low areas of attenuation (3/12), fluid collections (4/12), presence of subcutaneous gas (10/12) . The LRINEC score in pts with NF was equal or superior to 6 points : 6 pts had a score of 6/8 , 4 pts a score of 7/8 , 2 pts a score of 8/8 . The diagnoses of the other pts (cellulitis 10 pts, myositis 5 pts, musculoskeletal abscess 7 pts) were confirmed.

### CONCLUSION

The presence of a non-enhancing fascia after contrast medium administration, the involvement of the fascia and the presence of subcutaneous gas are the radiological findings mostly related to NF, and could strongly suggest to the radiologist the presence of NF; these findings with an intermediate-high LRINEC should address to a surgical evaluation. CT could discriminate NF from the most common musculoskeletal infections.

### **CLINICAL RELEVANCE/APPLICATION**

NF is a fatal disease if it is not treated, in order to permit a prompt surgical intervention radiological findings correlated with the LRINEC score permit a better evaluation of the pts disease and a prompt surgical intervention in order to avoid the complication of NF.

# Acute Mesenteric Isquemia? Can We Predict It?

Wednesday, Nov. 30 12:45PM - 1:15PM Room: ER Community, Learning Center Station #2

#### **Participants**

Lorena F. Rodriguez-Gijon, MD, Madrid, Spain (*Presenter*) Nothing to Disclose Angel Aguado, Madrid, Spain (*Abstract Co-Author*) Nothing to Disclose Milagros Marti, Madrid, Spain (*Abstract Co-Author*) Nothing to Disclose Aurea Diez Tascon, MD, Madrid, Spain (*Abstract Co-Author*) Nothing to Disclose Maria Jose Simon, Madrid, Spain (*Abstract Co-Author*) Nothing to Disclose Alfonso Martin Diaz, BMedSc, San Sebastian De Los Reyes, Spain (*Abstract Co-Author*) Nothing to Disclose Lucia Fernandez Rodriguez, BMBS, Madrid, Spain (*Abstract Co-Author*) Nothing to Disclose Carolina Martinez Gamarra, MD, Madrid, Spain (*Abstract Co-Author*) Nothing to Disclose Maria Claudia Pulido, Madrid, Spain (*Abstract Co-Author*) Nothing to Disclose

#### PURPOSE

Acute mesenteric ischemia remains a difficult diagnosis to establish on a clinic base, so diagnosis requires advanced imaging techniques, such as CT angiography or invasive techniques. Recent studies suggest that the elevation of the neutrophyl to lymphocyte ratio (NLR) is present in the moment of the acute mesenteric ischemia (AMI) diagnosis. The objective of our work is to study the association between NRL and radiological signs of AMI by all causes.

### **METHOD AND MATERIALS**

A retrospective, case-control study has been performed, within the years 2013-2016 in a third level hospital. 34 cases with AMI diagnosed by TC and confirmed by histology or clinical outcome has been taken. As control group, there were 34 patients diagnosed with a no-AMI disease by TC and confirmed by surgical or histological findings.Study variables were sex, age, NRL, CT diagnosis, pathological diagnosis, cause of AMI and radiological signs described in other reports for AMI.Non parametric test (Mann-Whitney) and chi 2 or Fischer's exact test were performed to analyze the differences between case and control groups. To evaluate the NLR discriminative capacity, ROC curves were used.

#### RESULTS

We observed statistically significant association of NRL with the following radiological signs in patients with AMI: parietal thickening of the ascending colon (p = 0.04), transverse colon (p = 0.04), descending colon (p = 0.029) and sigma (p = 0.03) and with occlusion of the superior mesenteric artery (SMA) (p = 0.03).Including AMI of any cause, the area under the ROC curve (AUC) was 0.6 (CI 95%: 0.46-0.74; p=0.151). In the cases of AMI by SMA occlusion, the AUC was 0.83 (CI 95%: 0.67-0.98; p=0.004). There was no patient with diagnose of SMA occlusion AMI with a NLR <5. (Negative predictive value: 100%). The optimal cut-off by Youden's index was 18.7 (sensitivity 77.8% and specificity of 80%).

## CONCLUSION

In our study, ability NRL to discriminate between cases and controls was low but the area under the curve of NRL to classify AMI by SMA occlusion with respect to other causes was 0.83, so we propose that at high values of NRL, an arterial phase helix should be performed.

## **CLINICAL RELEVANCE/APPLICATION**

The results of our study show an association between NRL and ischemia of arterial origin, so that a high NRL value could consider a predictor factor of arterial origin AMI and an arterial phase helix should be performed in these cases.

# Role of CT in the Definition of Therapeutic Approach in Polytrauma Patients with Kidney Injury

Wednesday, Nov. 30 12:45PM - 1:15PM Room: ER Community, Learning Center Station #3

#### Awards

### **Student Travel Stipend Award**

### **Participants**

Bruno Tuscano, MD, Milano, Italy (*Presenter*) Nothing to Disclose Luca Caschera, MD, Milano, Italy (*Abstract Co-Author*) Nothing to Disclose Ettore Colombo, MD, Milan, Italy (*Abstract Co-Author*) Nothing to Disclose Stefania Cimbanassi, MD, Milan, Italy (*Abstract Co-Author*) Nothing to Disclose Osvaldo Chiara, Milan, Italy (*Abstract Co-Author*) Nothing to Disclose Angelo Vanzulli, MD, Segrate, Italy (*Abstract Co-Author*) Travel support, Bracco Group

### PURPOSE

To evaluate the role of CT in the management of kidney injury, on basis of OIS degree (Organ Injury Scale) and outcome.

### METHOD AND MATERIALS

Retrospective study of 91 polytrauma patients with kidney lesions classified according to the American Association of Trauma Surgery in five degrees of gravity. Patients were admitted to a large metropolitan hospital from 2011 to 2015 (44 OIS 1, 18 OIS 2, 11 OIS 3, 16 OIS 4 and 2 OIS 5). For each case imaging data (CT) and treatment strategy were collected.

## RESULTS

In almost all OIS 1 to 3 degree kidney lesions conservative treatment was chosen, while in lesions of OIS 4 and 5, surgical (n = 2) or minimally invasive (n = 12) procedures were performed. CT revealed urinoma in 12.1% of cases. In 6 cases a ureteral stent was positioned after ascending pyelography which confirmed the injury; in 5, with limited spreading of the contrast agent, a conservative approach was chosen. The CT scan showed in 3 patients (OIS 4) arterial blushing of renal vessels and embolization was performed. In 1 patient (OIS 2) the first CT did not reveal the presence of renal artery branch pseudoaneurysm, identified in the subsequent CT, treated with embolization. In 2 patients (OIS 4) total nephrectomy was done for the impossibility to reconstruct the urinary tract and renal parenchyma. In 2 patients (1 OIS 4, 1 OIS 5) CT documented renal artery occlusion, and both cases were treated with stenting.

## CONCLUSION

CT has provided reliable evaluation of all lesion degrees, allowing in most cases minimally invasive interventions and reducing nephrectomy rates. CT monitoring allowed non operative management in many patients.

### **CLINICAL RELEVANCE/APPLICATION**

Contrast enhanced CT in polytrauma patients with renal injuries reduce total or partial nephrectomy rate in favor of conservative management.

## ER236-SD-WEB4

The Application of Dual-energy Technique to Whole-body CT in Blunt Trauma Patients: Can the Virtualunenhanced CT Images Substitute Unenhanced CT Images?

Wednesday, Nov. 30 12:45PM - 1:15PM Room: ER Community, Learning Center Station #4

## Participants

Yukichi Tanahashi, MD, Tokyo, Japan (*Presenter*) Nothing to Disclose Hiroshi Kondo, MD, Tokyo, Japan (*Abstract Co-Author*) Nothing to Disclose Satoshi Goshima, MD, PhD, Gifu, Japan (*Abstract Co-Author*) Nothing to Disclose Nobuyuki Kawai, MD, Gifu, Japan (*Abstract Co-Author*) Nothing to Disclose Yoshifumi Noda, MD,PhD, Gifu, Japan (*Abstract Co-Author*) Nothing to Disclose Hiroshi Kawada, MD, Gifu, Japan (*Abstract Co-Author*) Nothing to Disclose Toshihisa Kojima, MD, Gifu, Japan (*Abstract Co-Author*) Nothing to Disclose Shigeru Furui, MD, Itabashi-Ku, Japan (*Abstract Co-Author*) Nothing to Disclose Masayuki Matsuo, Gifu, Japan (*Abstract Co-Author*) Nothing to Disclose

### PURPOSE

To evaluate the efficacy of virtual-unenhanced CT for the assessment of blunt trauma patients.

### **METHOD AND MATERIALS**

Eighty-two trauma patients (55 men and 27 women; mean age, 51.6 yrs; range, 12-90 yrs) who underwent whole-body dynamic contrast-enhanced CT with dual-energy technique, following unenhanced CT, constituted study population. The virtualunenhanced CT image was reconstructed. Two observers independently and randomly reviewed images in three image sets; 1st, contrast-enhanced images, 2nd, combined unenhanced and contrast-enhanced images, and 3rd, combined virtual-unenhanced and contrast-enhanced images for the evaluation of traumatic change. The confidence level of traumatic change probability (visceral trauma, bone trauma, and extravasation of contrast media) were scored by 5-point scale for each image sets. Areas under the receiver operating characteristic curve (AUC) for the detection of traumatic change was evaluated. The image quality and radiation exposure were assessed.

#### RESULTS

Diagnosis of 63 visceral injuries in 47 patients and 138 bone fracture in 59 patients were clinically established. No significant difference was found in AUCs for visceral (0.90, 0.90, and 0.90), bone injury (0.87, 0.87 and 0.87), extravasation of contrast media (0.72, 0.72, and 0.72) among three image sets (P = 0.68, 0.50, and 0.51). The artifact and noise were worth in virtual-unenhanced images (P < 0.017). The Diagnostic acceptability of virtual-unenhanced image was substantial for all image. Mean DLP of unenhanced CT, arterial phase and venous phase were 1249.9 mGy\*cm, 742.2 mGy\*cm, and 1246.0mGy\*cm, respectively.

## CONCLUSION

Combined virtual-unenhanced and contrast-enhanced images showed comparable diagnostic performance of trauma with contrastenhanced images alone and combined unenhanced and contrast-enhanced images.

## **CLINICAL RELEVANCE/APPLICATION**

Our result showed unenhanced CT can be omitted in trauma patients and substituted by virtual-unenhanced CT reconstructed from dual-energy CT as needed, resulting in the decrease of radiation exposure.

# Pattern of Head Injuries in the Elderly

Wednesday, Nov. 30 12:45PM - 1:15PM Room: ER Community, Learning Center Station #5

#### Awards

### **Student Travel Stipend Award**

#### **Participants**

Kenedy A. Foryoung, MD, Hamden, DC (*Presenter*) Nothing to Disclose Felix T. Nautsch, MS, BA, New Haven, CT (*Abstract Co-Author*) Nothing to Disclose Xiao Wu, New Haven, CT (*Abstract Co-Author*) Nothing to Disclose Ajay Malhotra, MD, Stamford, CT (*Abstract Co-Author*) Nothing to Disclose Diego B. Nunez JR, MD, MPH, Boston, MA (*Abstract Co-Author*) Nothing to Disclose

## PURPOSE

Head and cervical spine computed tomography (CT) are the workhorse modalities for the evaluation of neurologic trauma in the emergency setting. Knowledge of typical injury patterns and typical injury mechanisms as they occur in different age groups may help improve performance by guiding search patterns, key ancillary data given to the radiologist and possibly reformatting algorithms.

## METHOD AND MATERIALS

CT studies of the brain and brain and cervical spine of adults performed in the Emergency Department between 2/15/2014 and 2/15/2015 were retrieved from the electronic medical records. For all studies with critical findings, the images, reports and associated medical record were manually reviewed. Histories of trauma or possible trauma with findings of traumatic injuries by CT were included. The data was separated by Age into two groups aged above 65 and 18-64. We grouped fractures and hemorrhages by type and anatomic location. Collateral information such as anticoagulation status and additional history were manually retrieved.

## RESULTS

A total of 384 studies with patients above the age of 65 and 518 studies with patients aged between 18 and 65 with critical results were identified for manual review. Following preliminary manual review approximately 70% met inclusion criteria by history and findings in both age groups. 85% of the group aged above 65 suffered a traumatic fall and 37% were on anti-coagulation. The most common traumatic bleed above the age of 65 was an acute subdural bleed, which occurred 35% of the time. The predominant cranial area of fracture was the face in 30% of all studies above 65. High velocity mechanisms of injury in the elderly were present in only 6% of the cases. Diffuse axonal injuries, parenchymal hemorrhage and arterial epidural collections were rare. While epidural and subarachnoid hemorrhage remained a relatively rare finding in the younger age group, the preponderance of subdural hemorrhages decreased to 23%. Similarly, high velocity injury mechanisms occurred about 10% of the time and a second predominant mechanism of injury, assault, occurred 12% of the time.

### CONCLUSION

The elderly suffer specific injury patterns closely associated with their typical mechanisms of injury and anti-coagulation state.

## **CLINICAL RELEVANCE/APPLICATION**

Injury patterns after blunt trauma might be different in the elderly patients relative to younger population.

# GI165-ED-WEB8

Evaluation of Abdominal and Pelvic Manifestations of Graft versus Host Disease (GvHD) after Hematopoietic Stem Cell Transplantation

Wednesday, Nov. 30 12:45PM - 1:15PM Room: GI Community, Learning Center Station #8

#### Awards

**Certificate of Merit** 

#### Participants

Kinan Alhalabi, Scottsdale, AZ (*Presenter*) Nothing to Disclose Christine O. Menias, MD, Chicago, IL (*Abstract Co-Author*) Nothing to Disclose Meghan G. Lubner, MD, Madison, WI (*Abstract Co-Author*) Grant, Koninklijke Philips NV; Grant, Johnson & Johnson; Venkata S. Katabathina, MD, San Antonio, TX (*Abstract Co-Author*) Nothing to Disclose Khaled M. Elsayes, MD, Ann Arbor, MI (*Abstract Co-Author*) Nothing to Disclose Amy K. Hara, MD, Scottsdale, AZ (*Abstract Co-Author*) Royalties, General Electric Company; Perry J. Pickhardt, MD, Madison, WI (*Abstract Co-Author*) Co-founder, VirtuoCTC, LLC; Stockholder, Cellectar Biosciences, Inc; Stockholder, SHINE Medical Technologies, Inc; Research Grant, Koninklijke Philips NV

### **TEACHING POINTS**

- 1. Describe the pathology behind Graft-versus-Host-Disease.
- 2. Review the most important radiologic findings of the disease in the abdomen and pelvis.
- 3. Highlight the contribution of radiology in the management of the disease.

## **TABLE OF CONTENTS/OUTLINE**

Graft versus Host disease is a frequent complication of bone marrow and liver transplantation. Grafted T cells proliferate in the immunocompromised host and attack host cells with 'foreign" proteins, leading to severe organ dysfunction. T cells can attack any organ in the body, but the GI tract, skin, liver, eyes, mucous membranes are the main affected organs. GvHD can present within 100 days after transplantation (acute phase), or after 100 days (chronic phase). It usually presents with a maculopapular rash, jaundice, diarrhea, and hepatosplenomegaly. Radiology plays a significant role in diagnosing GvHD, showing the extent of the disease, and in guiding the management. Radiologic findings depend on the organs involved. When the GI tract is affected, the bowel is described as having a 'ribbon" appearance with fold thickening. Immunosuppressant drugs have reduced the incidence of the disease, although it does still frequently occur.

### **Honored Educators**

Presenters or authors on this event have been recognized as RSNA Honored Educators for participating in multiple qualifying educational activities. Honored Educators are invested in furthering the profession of radiology by delivering high-quality educational content in their field of study. Learn how you can become an honored educator by visiting the website at: https://www.rsna.org/Honored-Educator-Award/

Meghan G. Lubner, MD - 2014 Honored Educator Meghan G. Lubner, MD - 2015 Honored Educator Christine O. Menias, MD - 2013 Honored Educator Christine O. Menias, MD - 2014 Honored Educator Christine O. Menias, MD - 2015 Honored Educator Christine O. Menias, MD - 2016 Honored Educator Venkata S. Katabathina, MD - 2012 Honored Educator Amy K. Hara, MD - 2015 Honored Educator Khaled M. Elsayes, MD - 2014 Honored Educator Perry J. Pickhardt, MD - 2014 Honored Educator

## GI174-ED-WEB9

Old Friends, New Foes: Hepatic Vascular Tumors on Gadoxetic Acid-enhanced MRI & Diffusion-weighted Images

Wednesday, Nov. 30 12:45PM - 1:15PM Room: GI Community, Learning Center Station #9

# Participants

Bohyun Kim, MD, Suwon, Korea, Republic Of (*Presenter*) Nothing to Disclose So Yeon Kim, MD, Seoul, Korea, Republic Of (*Abstract Co-Author*) Nothing to Disclose Jei Hee Lee, MD, Suwon, Korea, Republic Of (*Abstract Co-Author*) Nothing to Disclose Kyoung Won Kim, Seoul, Korea, Republic Of (*Abstract Co-Author*) Nothing to Disclose Seung Soo Lee, MD, Seoul, Korea, Republic Of (*Abstract Co-Author*) Nothing to Disclose Jin Roh, Seoul, Korea, Republic Of (*Abstract Co-Author*) Nothing to Disclose Moon-Gyu Lee, MD, Seoul, Korea, Republic Of (*Abstract Co-Author*) Nothing to Disclose

## **TEACHING POINTS**

To describe the causes why hepatic vascular tumors can look so different on gadoxetic acid-enhanced MRI compared to conventional ECF contrast agent-enhanced MRI. To outline the imaging spectrum of hepatic vascular tumors on gadoxetic acid-enhanced MRI and describe imaging pearls and pitfalls in comparison with features on MRI using ECF contrast agents To present imaging pearls and pitfalls of common hepatic vascular tumors on diffusion-weighted images with an emphasis on the speed of enhancement.

## TABLE OF CONTENTS/OUTLINE

1. Introduction to vascular tumors of the liver

(1) Spectrum of benign, borderline, and malignant entities

(2) Why can hepatic vascular tumors look so different on gadoxetic acid-enhanced MRI compared to conventional ECF contrast agent-enhanced MRI?2. Cavernous hemangioma

(1) Pearls and pitfalls

(2) Special considerations

- i. Speed of intratumoral enhancement: effects on DWI
- ii. Sclerosing hemangioma: a great mimicker 3. Epithelioid hemangioendothelioma
- (1) Pearls and pitfalls4. Primary hepatic angiosarcoma

(1) Pearls and pitfalls5. Summary for key features in gadoxetic acid-enhanced MR and diffusion-weighted images

## GI396-SD-WEB3

Different Curative Effect of Preoperative Chemoradiotherapy in Subgroups with Different Proportion of Mucous Lake of Rectal Cancer

Wednesday, Nov. 30 12:45PM - 1:15PM Room: GI Community, Learning Center Station #3

# Participants

Wuteng Cao, Guangzhou, China (*Presenter*) Nothing to Disclose Zhiyang Zhou, PhD, Guangzhou, China (*Abstract Co-Author*) Nothing to Disclose Fangqian Li, guangzhou, China (*Abstract Co-Author*) Nothing to Disclose Yanbang Lian, Zhengzhou, China (*Abstract Co-Author*) Nothing to Disclose Dan Liang, Guangzhou, China (*Abstract Co-Author*) Nothing to Disclose Xinhua Wang, Guangzhou, China (*Abstract Co-Author*) Nothing to Disclose Dechao Liu, Guangzhou, China (*Abstract Co-Author*) Nothing to Disclose

### PURPOSE

There was a certain proportion of rectal carcinoma with different proportions of mucus lake. The purpose is to compare curative effects after CRT in subgroups with different proportion of mucous lake.

## **METHOD AND MATERIALS**

323 patients with rectal cancer were underwent rectal MRI examinition including T2-weighted and T1-weighted FSE sequences before CRT. High signal area of mucous lake in T2 imaging was manually draw up and the proportion of mucous lake was calculated automatically in GE AW4.5 post-processing workstation, according which the cases were divided into the following subgroups: conventional carcinoma without any mucous lake (Group AC); cases containing the proportion of 1-25% (Group1), 26-50% (Group2), 51-75% (Group3), 76-100% (Group4) mucous lake compared with the whole tumor area. Cases of Group3 and Group4 were known as MC. Compare TN stage of rectal cancer using MRI before CRT with pathologic TN stage of the specimen after surgical removal. The TN downstaging and degree of tumor regression after CRT were evaluated in different subgroups above.

# RESULTS

The five subgroups with different proportions of mucous lake had statistical differences in T downstaging rate (P = 0.002). The downstage rate of Group3 was significantly lower than that of Group1 AC (6/26 vs 128/214, P < 0.001). The downstage rate of Group 4 was higher than that of group 3 (5/7 vs. 6/26). There were no significant statistical differences of N downstaging rate in the five subgroups (84.6% vs. 79.5%, 76.9%, 66.7%, 76.9%, p = 0.081). The downstage degree of Group3 was significantly lower than that of the conventional AC (P < 0.001), and that of Group1 (P < 0.001). Compare tumor completely response (CR) and there were overall statistical differences in subgroups (CR rate, respectively, 22.4% for AC, 19.1% for group1, 20.7% for group2, 0% for group3, 42.9% for group4. P = 0.017). The CR rate of Group 3 was obviously lower than other groups, but Group4 obviously higher than that of other groups.

# CONCLUSION

T downstaging rate after CRT in MC( with 51-75% mucous lake) was poor than that of conventional adenocarcinoma without any mucous lake and adenocarcinoma with a small quantity of mucous lake( < 50%). However, the curative effect index in MC cases(with mucous lake > 75%) was better than that of cases with 51-75% mucous lake after CRT.

# **CLINICAL RELEVANCE/APPLICATION**

Cases with mucous lake of more than 75% proportion may be more sensitive to neoadjuvant therapy.

# GI397-SD-WEB4

Diffusion Weighted Magnetic Resonance Imaging of Pancreatic Ductal Adenocarcinoma: Correlation with Metastatic Disease Potential

Wednesday, Nov. 30 12:45PM - 1:15PM Room: GI Community, Learning Center Station #4

#### Awards

### **Student Travel Stipend Award**

#### **Participants**

Trevor Morrison, MD, Boston, MA (*Presenter*) Nothing to Disclose Alejandro Garces-Descovich, Boston, MA (*Abstract Co-Author*) Nothing to Disclose Arthur Moser, Boston, MA (*Abstract Co-Author*) Nothing to Disclose Koenraad J. Mortele, MD, Boston, MA (*Abstract Co-Author*) Nothing to Disclose

# PURPOSE

To analyze the possible relationship between the apparent diffusion coefficient (ADC) of pancreatic ductal adenocarcinoma (PDAC), at the time of initial staging, and the presence or development of metastatic disease.

#### **METHOD AND MATERIALS**

IRB approval with waiver of informed consent was obtained for this HIPPA compliant retrospective study. A total of 75 consecutive patients with histopathologically proven PDAC who underwent DWI-MRI between January 2012 and December 2014 were evaluated; 24/75 patients were excluded because PDAC was not seen on MRI (n=14) or due to the patient being on neo-adjuvant therapy already (n=10). Outcome data for the remaining 51 patients (28 male with average age 65.8, 23 female with average age 66.7) was obtained from the online medical record (mean follow-up 720 days). The overall correlation between the ADC value and the presence or development of metastatic disease was assessed using Student's T-test.

### RESULTS

Of 51 patients, 22 (43%) either had metastatic disease at the time of the MRI (n=12) or went on to develop metastatic disease (n=10). Metastasis were observed primarily in liver (n=19), but also in omentum (peritoneum) (n=1), lung and liver (n=1) and bone (n=1). Patients with metastatic disease had a significantly lower mean pre-treatment ADC value (1,271 mm2/s) than those who did not (1,472 mm2/s) (p<0.01). No significant difference between ADC values of those who had metastatic disease at the time of the MRI (1,232 mm2/s) compared to those who developed metastasis at a later date (1,316 mm2/s) (p=0.2) was identified.

### CONCLUSION

Pre-treatment ADC values of PDAC are significantly lower in patients who have or will develop metastatic disease.

### **CLINICAL RELEVANCE/APPLICATION**

An MRI biomarker that determines which patients with PDAC have or go on to develop metastasis would have great impact on clinical management. While more investigation is needed, our results suggest that DWI-MRI can be of value in determining which patients with PDAC will develop metastatic disease.

Follow-up of Multicentric HCC according to the mRECIST Criteria: Role of 320-Row CT with Semi-automatic 3D Analysis Software for Evaluating the Response to Systemic Therapy

Wednesday, Nov. 30 12:45PM - 1:15PM Room: GI Community, Learning Center Station #5

# Participants

Marco Moschetta, MD, Bari, Italy (*Abstract Co-Author*) Nothing to Disclose Michele Telegrafo, MD, Bari, Italy (*Presenter*) Nothing to Disclose Amato Antonio Stabile Ianora, Bari, Italy (*Abstract Co-Author*) Nothing to Disclose Giuseppe Angelelli, Bari, Italy (*Abstract Co-Author*) Nothing to Disclose

### PURPOSE

To evaluate the role of 320-row CT with 3D Analysis software in the follow-up of multicentric hepatocellular carcinoma (HCC) treated with systemic therapy according to the mRECIST criteria.

# METHOD AND MATERIALS

In the period between December 2012 and June 2015 38 patients with multicentric HCC undergoing systemic therapy were assessed twice a year by MDCT before and after injection of contrast medium with three-phasic technique. Two blinded radiologists evaluated multi-planar images (MPR) images classifying the response to therapy in PR (partial response), PD (progressive disease), SD (stable disease) and CR (complete response) by using the mRECIST criteria. 30 days later, the same two blinded radiologists evaluated the same target lesions applying the 3D semi-automatic analysis software. The differences between the two evaluating systems were assessed using the analysis of variance (ANOVA test). The inter-observer agreement for both the evaluating systems was calculated using Cohen's kappa statistics.

### RESULTS

In 10/38 cases (26%) PR was found; in 6/38 (16%) PD; in 22/38 (58%) SD. The analysis of variance did not detect statistically significant differences between the two systems of measurement (p>0.05). The inter-observer agreement (k) was 0.62 for the measurements in MPR and 0.86 for the measurements performed by using the 3D Analysis Software, with a significantly higher value for the proposed semi-automatic software (p<0.05).

### CONCLUSION

The semi-automatic 3D Analysis Software represents a reliable method for evaluating the HCC response to therapy according to the mRECIST criteria and could be proposed in the clinical practice.

# **CLINICAL RELEVANCE/APPLICATION**

The proposed semi-automatic 3D Analysis Software represents a fast, reliable and accurate technique for evaluating the HCC response to therapy according to the mRECIST criteria and could be proposed in the clinical practice.

## GI399-SD-WEB6

Two-Dimensional US Elastography for Focal Lesions in Liver Phantoms: Influencing Factors for Stiffness Measurement of Small Lesions

Wednesday, Nov. 30 12:45PM - 1:15PM Room: GI Community, Learning Center Station #6

## Participants

Jeong Ah Hwang, Seoul, Korea, Republic Of (*Presenter*) Nothing to Disclose Woo Kyoung Jeong, MD, Seoul, Korea, Republic Of (*Abstract Co-Author*) Nothing to Disclose Kyoung Doo Song, MD, Seoul, Korea, Republic Of (*Abstract Co-Author*) Nothing to Disclose Tae Wook Kang, MD, Seoul, Korea, Republic Of (*Abstract Co-Author*) Nothing to Disclose Hyo Keun Lim, MD, Seoul, Korea, Republic Of (*Abstract Co-Author*) Nothing to Disclose Ji Eun Lee, MD, Seoul, Korea, Republic Of (*Abstract Co-Author*) Nothing to Disclose

### PURPOSE

US elastography (USE) has been investigated for the purpose of estimating liver fibrosis, but 2-dimensional (2-D) USE can depict a focal lesion with different elasticity with a color map. The purpose of this study is to determine accuracy and influencing factors of stiffness value of focal lesions in the phantoms using 2-D USE.

#### **METHOD AND MATERIALS**

Using two customized phantoms with different elasticity (4±1 kilopascal [kPa], mimicking normal liver; 15±2 kPa, mimicking liver cirrhosis [LC]) which have 9 spherical hypoechoic inclusions with same elasticity (23±3 kPa), different size (20mm, 15mm and 10mm in a raw) and different depth (3cm, 5cm and 7cm). Two radiologist investigated stiffness of inclusion bodies and background for each inclusions using in the region of interest (ROI). Mean stiffness and standard deviation (SD) in ROI were acquired, and the shape of inclusion was also assessed with a qualitative 5-graded scoring system about target visualization on color map. As possible influencing factors, the type of background phantom, depth of inclusions, size of inclusions, and observers were considered. We compared by Kruskal-Wallis test, and performed multiple regression tests to detect significant influencing factors about 2-D USE.

# RESULTS

Measured mean stiffness value was significantly higher in LC phantom (10.50 kPa in normal, 13.81 kPa in LC; p=0.013), inclusions in 7cm of depth (10.94 kPa in 3cm, 11.20 kPa in 5cm and 15.59 kPa in 7cm; p=0.001). In multiple regression analysis in mean stiffness, there was significant difference of mean stiffness in type of phantom, depth and size of inclusions. Mean SD in ROI was also significantly larger in 7cm of depth (0.86 kPa in 3cm, 1.23 kPa in 5cm and 3.94 kPa in 7cm; p=0.001). In multiple regression analysis for SD in ROI, there were significant differences in type of phantom and depth of inclusions. Morphologic score was significantly different only in aspect of the size of inclusion bodies (p<0.001). Background stiffness was not different according to depth or observers (p=0.491 and 0.522, respectively).

## CONCLUSION

2-D USE for focal lesion evaluation could be influenced by different background stiffness, deep position of the lesion, and small size of lesion.

## **CLINICAL RELEVANCE/APPLICATION**

Background liver stiffness, depth and size of the target lesion should be considered for focal hepatic lesion evaluation using 2-D USE.

Agreement of Six- and Composite Three-echo Magnitude PDFF-Estimation MRI Sequences in a Multi-center Clinical Trial

Wednesday, Nov. 30 12:45PM - 1:15PM Room: GI Community, Learning Center Station #7

# Participants

Michael S. Middleton, MD, PhD, San Diego, CA (*Presenter*) Consultant, Allergan plc Institutional research contract, Bayer AG Institutional research contract, sanofi-aventis Group Institutional research contract, Isis Pharmaceuticals, Inc Institutional research contract, Johnson & Johnson Institutional research contract, Synageva BioPharma Corporation Institutional research contract, Takeda Pharmaceutical Company Limited Stockholder, General Electric Company Stockholder, Pfizer Inc Institutional research contract, Pfizer Inc

Mary Kosinski, PhD, Nashville, TN (Abstract Co-Author) Employee, NuSirt Biopharma, Inc

Omar Flores, PhD, MBA, Nashville, TN (Abstract Co-Author) Employee, NuSirt Biopharma, Inc

Michael Zemel, PhD, Nashville, TN (Abstract Co-Author) Employee, NuSirt Biopharma, Inc

Claude B. Sirlin, MD, San Diego, CA (Abstract Co-Author) Research Grant, General Electric Company; Research Grant, Siemens AG; Research Grant, Guerbet SA; ;

## PURPOSE

Most MR scanners can acquire 6-echo and/or composite 3-echo magnitude MRI sequences to estimate proton density fat fraction (PDFF). PDFF estimated from the first 3 echos of a 6-echo sequence is nearly equivalent to that estimated from all 6-echos. However, to pool data in clinical trials, we need to show that PDFF derived from 6-echo sequences is essentially equivalent to that derived from separately-acquired composite 3-echo sequences. Hence, the purpose of this study was to calculate the agreement of baseline 6- and composite 3-echo sequences using regression and Bland-Altman analysis in a multi-center clinical trial.

## METHOD AND MATERIALS

Anonymized baseline MRIs were analyzed to estimate PDFF for 64 subjects from 7 sites in an ongoing multi-center clinical trial. A multi-echo (ME) magnitude spoiled gradient-recalled-echo (6-echos) MRI sequence, and a pair of double-echo sequences were acquired for each subject. A composite 3-echo dataset was created from the double-double-echo (DDE) sequences. Two additional composite three-echo datasets (one from 1st, 2nd, an 4th echoes; one from first 3 echoes) were created directly from the ME sequence. Three co-localized regions of interest were placed in the right lobe of the liver for all sequences. PDFF was calculated for each dataset using a custom MatLab algorithm. Regression and Bland-Altman analysis was performed to evaluate agreement between PDFF derived from the three composite DDE datasets, and the ME sequence.

### RESULTS

ME sequence-derived PDFF ranged from 2.11 to 35.07%. PDFFs from separately- acquired ME and composite DDE sequences showed strong agreement (slope near 1, intercept near 0), but were slightly different (mean difference 0.46%; difference range - 2.01 to 1.96%; p < 0.0001). Agreement was even stronger for the composite DDE sequences derived directly from the ME sequence, with best agreement for the composite DDE sequence derived from the first 3 echos of the ME sequence (mean difference 0.14%; difference range - 0.86 to 0.69%).

# CONCLUSION

PDFFs derived from ME sequences showed strong agreement with those derived from separately-acquired and derived composite DDE sequences, with small differences that are likely to be considered negligible in clinical trials.

## **CLINICAL RELEVANCE/APPLICATION**

Our data support that PDFFs from 6-echo and separately-acquired composite 3-echo magnitude MRI sequences may be pooled, given their strong agreement in a multi-center clinical trial.

## GU240-SD-WEB1

Validation of PI-RADS v2 for Detection of Prostate Cancer Using US/MRI Fusion Guided Prostate Biopsy as Reference Standard

Wednesday, Nov. 30 12:45PM - 1:15PM Room: GU/UR Community, Learning Center Station #1

## Participants

Jinxing Yu, MD, Richmond, VA (*Presenter*) Nothing to Disclose Ann S. Fulcher, MD, Midlothian, VA (*Abstract Co-Author*) Nothing to Disclose Sarah G. Winks, MD, Richmond, VA (*Abstract Co-Author*) Nothing to Disclose William C. Behl, MS, Richmond, VA (*Abstract Co-Author*) Nothing to Disclose Mary A. Turner, MD, Richmond, VA (*Abstract Co-Author*) Nothing to Disclose Michael Brooks, Richmond, VA (*Abstract Co-Author*) Nothing to Disclose Anna L. Ware, Richmond, VA (*Abstract Co-Author*) Nothing to Disclose Baruch Grob, Richmond, VA (*Abstract Co-Author*) Nothing to Disclose Lance Hampton, Richmond, VA (*Abstract Co-Author*) Nothing to Disclose

### PURPOSE

Purpose: To evaluate the diagnostic performance and inter-reader reliability of the Prostate Imaging Reporting and Data System (PI-RADS) version 2 at multi-parametric MRI (mp-MRI) for the diagnosis of prostate cancer using US/MRI fusion guided prostate biopsy as the reference standard.

## METHOD AND MATERIALS

Materials and Methods: From August 2014 to April 2016, a total of 117 consecutive men with elevated PSA and regions classified as PI-RADS  $\geq$  3 at mp-MRI based on PI-RADS v2 by a single experienced reader underwent confirmatory US/MRI fusion guided biopsies of the regions. The results of the histopathologic analyses, including Gleason scores from the target biopsies, were recorded and used as the reference standard. All lesions were retrospectively evaluated according to PI-RADS v2 by an experienced reader blinded to the biopsy results. The weighted kappa method was used to calculate inter-reader reliability between the original reader (pre biopsy) and the second reader (post biopsy).

#### RESULTS

Results: US/MRI fusion guided prostate biopsies of 149 lesions in 117 patients were performed and revealed 126 malignant lesions (85% tumor detection rate). In PI-RADS 5 (n=72), 4 (n=49) and 3 (n=28) lesions, the detection rates of prostate cancer were 100%, 82% and 50%, respectively. Prostate cancer Gleason score  $\geq$ 7 was noted in 93%, 92% and 78% of PI-RADS 5, 4 and 3 lesions, respectively. Inter-reader agreement on PI-RADS v2 between the original reader and the second reader was moderate (K = 0.67).

# CONCLUSION

Conclusions: A tumor detection rate of 85% amongst prostate lesions deemed suspicious for malignancy at mp-MRI using PI-RADS v2 was demonstrated. Among them, 100% of PI-RADS 5 lesions were proven to be prostate cancer. Our results support PI-RADS v2 as a reliable and replicable reporting system for detection of prostate cancer.

## **CLINICAL RELEVANCE/APPLICATION**

PI-RADS v2 is a reliable and replicable system that simplifies and enhances the characterization of prostate lesions at mp-MRI, thus optimizing the MR detection of prostate cancer.

# Contrast-Enhanced Transrectal Ultrasound for Prostate Cancer Detection: Impact of Race

Wednesday, Nov. 30 12:45PM - 1:15PM Room: GU/UR Community, Learning Center Station #2

**FDA** Discussions may include off-label uses.

### Participants

Ethan J. Halpern, MD, Philadelphia, PA (Presenter) Nothing to Disclose

Flemming Forsberg, PhD, Philadelphia, PA (*Abstract Co-Author*) Equipment support, Toshiba Corporation; Research Grant, Toshiba Corporation; Equipment support, Siemens AG; In-kind support, General Electric Company; In-kind support, Lantheus Medical Imaging, Inc

Leonard G. Gomella, MD, Philadelphia, PA (*Abstract Co-Author*) Consultant, Johnson & Johnson Consultant, Dendreon Corporation Consultant, Astellas Group Consultant, Bayer AG

Edouard J. Trabulsi, MD, Philadelphia, PA (*Abstract Co-Author*) Consultant, Intuitive Surgical, Inc Stockholder, Intuitive Surgical, Inc Consultant, Amgen Inc Speaker, Amgen Inc Consultant, Johnson & Johnson Speaker, Johnson & Johnson

### PURPOSE

Clinical trials have demonstrated improved detection of larger volume and higher grade "clinically significant" prostate cancer (PCa) with contrast-enhanced transrectal ultrasound (CE-TRUS). As PCa tends to be a more aggressive disease among African American patients, this study evaluated the impact of race upon PCa detection with CE-TRUS.

# METHOD AND MATERIALS

A retrospective review was performed of demographics, ultrasound imaging and pathology results from 272 consecutive participants in an NIH funded clinical trial who underwent conventional 12-core systematic prostate biopsy as well as CE-TRUS-guided biopsy with up to 6 additional targeted biopsy cores using the microbubble agent Definity<sup>TM</sup> (Lantheus Medical Imaging).

## RESULTS

The study population consisted of 210 Caucasian, 54 African American, 2 Asian and 4 Hispanic males. PCa was detected in 87 (41%) of Caucasian and 29 (54%) of African American males. Among patients with a positive biopsy, PCa was present in multiple systematic cores in 41/87 (47%) of Caucasian and 17/29 (59%) of African American males, and high grade PCa (Gleason score  $\geq$  7) was present in 30/87 (34%) of Caucasian and 11/29 (38%) of African American males. The frequency of high grade PCa detected by systematic biopsy was similar in both populations (7/54 vs. 27/210, both 13%). The overall frequency of PCa detection with CE-TRUS was similar for Caucasian (57/210=27%) and African American males (14/54=26%). However, the frequency of high grade PCa detected by targeted biopsy with CEUS was greater among African American patients (9/54 = 17%) as compared with Caucasian patients (21/210 = 10%), p=0.06.

## CONCLUSION

Although the frequency of detection for high grade (Gleason score  $\geq$  7) PCa with a systematic 12-core biopsy was similar in Caucasian and African American subjects at 13%, and the overall frequency of PCa detection with a targeted CE-TRUS biopsy approach was similar in Caucasian and African American subjects (26-27%), high grade PCa was detected more frequently in our African American study subjects (17% vs 10%) using a limited targeted CE-TRUS biopsy approach

## **CLINICAL RELEVANCE/APPLICATION**

CEUS targeted biopsy improves the detection of high grade PCa with fewer biopsy cores as compared with systematic biopsy, especially among the high risk African American population. A targeted CE-TRUS approach may be more specifically selective for higher grade "clinically significant disease" in the African American population.

Reduced Contrast Media Volume and Radiation Dose Employing a Patient-tailored Approach during Renal CTA: Effects on Image Quality and Reader Confidence

Wednesday, Nov. 30 12:45PM - 1:15PM Room: GU/UR Community, Learning Center Station #3

# Participants

Charbel Saade, PhD, MS, Beirut, Lebanon (*Presenter*) Research Grant, General Electric Company Racha Kerek, Beirut, Lebanon (*Abstract Co-Author*) Nothing to Disclose Bassam El-Achkar, MD, Beirut, Lebanon (*Abstract Co-Author*) Nothing to Disclose Maurice Chehade D. Haddad, MD, Beirut, Lebanon (*Abstract Co-Author*) Nothing to Disclose Alain S. Abi-Ghanem, Beirut, Lebanon (*Abstract Co-Author*) Nothing to Disclose Fadi M. El-Merhi, MD, New York, NY (*Abstract Co-Author*) Nothing to Disclose

### PURPOSE

The aim of our study was to investigate the opacification of renal vasculature, by a patient-tailored contrast administration protocol during renal CTA.

# METHOD AND MATERIALS

This hybrid retrospective (protocol A) and continuous prospective (protocol B) study was institutional review board approved. In 201 consecutive patients, renal CTA was performed with one of two protocols: protocol A, 100 mL of contrast material injected intravenously; and protocol B, employing the patient-tailored contrast media protocol. Each protocol employed a contrast material and saline flow rate of 4.5 mL/sec. Attenuation profiles and contrast-to-noise ratio (CNR) of the renal arteries and veins was measured. Effective dose was calculated. Data were compared with the independent sample t test. Receiver operating characteristic (ROC) and visual grading characteristic analyses were performed.

## RESULTS

Arterial opacification in the abdominal aorta (mean  $\pm$  standard deviation : protocol A = 290.35  $\pm$  105.82 Protocol B= 269.47  $\pm$  58.74), main proximal and distal renal arteries in both kidneys and protocols demonstrated no statistical significance (p>0.05) except for the left kidney in the distal segments in protocol B (p<0.046). In the venous circulation, the IVC demonstrated significant reduction in protocol B (59.39 HU  $\pm$  19.39) compared to A (87.74 HU  $\pm$  34.06) (p<0.001). The mean CNR for protocol B (14.75 HU  $\pm$  5.76) was significantly higher than that for protocol A (22.68 HU  $\pm$  13.72; P<.0001). Effective dose was significantly reduced in protocol B (2.46  $\pm$  0.74 mSv) compared to A (3.07  $\pm$  0.68 mSv) (p<0.001). ROC analysis demonstrated significantly higher area under the ROC curve for protocol B (P < .0001), with interreader agreement increasing from moderate to excellent in renal arterial visualization.

## CONCLUSION

Significant improvement in renal vasculature is achieved with a patient-tailored contrast media injection protocol.

## **CLINICAL RELEVANCE/APPLICATION**

Renal CT angiography (CTA) is increasingly being used to guide management of renovascular diseases. However, little has been reported about the safety of intravenous contrast administration associated with these studies in the acute population, including the volume of contrast media and radiation dose effects.

Utility of a Novel Continuously Acquired Radial Golden-Angle Compressed Sensing Sequence for Detecting Local Recurrence of Prostate Cancer Following Radical Prostatectomy

Wednesday, Nov. 30 12:45PM - 1:15PM Room: GU/UR Community, Learning Center Station #4

# Participants

Anunita Khasgiwala, MD, New York, NY (*Presenter*) Nothing to Disclose Ankur Doshi, MD, New York, NY (*Abstract Co-Author*) Nothing to Disclose Justin M. Ream, MD, Ann Arbor, MI (*Abstract Co-Author*) Nothing to Disclose Samir S. Taneja, MD, New York, NY (*Abstract Co-Author*) Consultant, Eigen; Consultant, GTx, Inc ; Consultant, Bayer AG; Consultant, HealthTronics, Inc; Speaker, Johnson & Johnson; Investigator, STEBA Biotech NV; Royalties, Reed Elsevier Herbert Lepor, MD, New York, NY (*Abstract Co-Author*) Nothing to Disclose Andrew B. Rosenkrantz, MD, New York, NY (*Abstract Co-Author*) Nothing to Disclose

### PURPOSE

A novel continuously acquired Golden-angle Radial Acquisition with Sparse Parallel reconstruction using compressed sensing (termed "GRASP") offers motion robustness as well as simultaneous high spatial and high temporal resolution. The aim of this study was to compare GRASP with a standard dynamic contrast-enhanced (DCE) MR sequence in terms of image quality and diagnostic performance for detecting local recurrence (LR) after radical prostatectomy (RP) for prostate cancer.

### **METHOD AND MATERIALS**

A departmental database was searched for prostate MRI reports containing the phrase "radical prostatectomy". Identified cases were then included when: MRI performed for suspected LR after RP with PSA $\geq$ 0.2; no prior therapy; and review of all follow-up clinical, laboratory, and pathologic data allowed classification of the patient as positive (e.g., PSA reduction after pelvic radiation) or negative (e.g., spontaneous PSA normalization) for LR. The final cohort included 16 patients with standard DCE (13 with LR) and 17 patients with GRASP (14 with LR). Exams were performed at 3T using phased-array coil. Standard DCE had a voxel size of 3.0x1.9x1.9 mm and a temporal resolution of 5.5 sec. GRASP had a voxel size of 1.0x1.1x1.1 cm and was retrospectively reconstructed using the k-t SPARSE-SENSE method at 2.3 sec resolution. Two radiologists evaluated solely the DCE sequences in separate sessions for measures of image quality (1-5 scale) and LR (positive vs. negative).

#### RESULTS

GRASP achieved higher scores than standard DCE from both readers (all  $p \le 0.02$ ) for anatomic clarity (R1: 4.6±0.7 vs. 2.9±0.6; R2: 4.8±0.4 vs. 3.3±0.6), sharpness (3.9±0.9 vs. 2.5±0.7; 4.7±0.5 vs. 2.7±0.5), confidence in interpretation (4.0±0.9 vs. 3.1±0.8; 4.0±0.9 vs. 3.1±1.1) and conspicuity of detected lesions (4.7±0.5 vs. 3.4±1.1; 4.6±0.5 vs. 3.6±0.9). For detecting LR, GRASP also achieved for both readers higher sensitivity (69% vs. 46%; 77% vs. 54%), specificity (75% vs. 67%; 100% vs. 67%), and accuracy (71% vs. 50%; 82% vs. 56%).

## CONCLUSION

Compared with standard DCE, GRASP acquisition technique achieved substantially better image quality and diagnostic performance for detecting local recurrence in patients with elevated PSA after prostatectomy.

## **CLINICAL RELEVANCE/APPLICATION**

A novel DCE method that provides motion robustness, high spatial resolution, and high temporal resolution facilitates the role of MRI in evaluating patients with suspected local recurrence after RP.

# Spectral Analysis of Renal Tumors: Evaluation of a CT Radiomic Technique

Wednesday, Nov. 30 12:45PM - 1:15PM Room: GU/UR Community, Learning Center Station #6

#### Participants

Bino Varghese, Los Angeles, CA (*Presenter*) Nothing to Disclose Darryl Hwang, PhD, Los Angeles, CA (*Abstract Co-Author*) Nothing to Disclose Steven Cen, PhD, Los Angeles, CA (*Abstract Co-Author*) Nothing to Disclose Bhushan Desai, MBBS, MS, Los Angeles, CA (*Abstract Co-Author*) Nothing to Disclose Felix Y. Yap, MD, Los Angeles, CA (*Abstract Co-Author*) Nothing to Disclose Vinay A. Duddalwar, MD, FRCR, Los Angeles, CA (*Abstract Co-Author*) Nothing to Disclose Passant Mohamed, MBBS, Los Angeles, CA (*Abstract Co-Author*) Nothing to Disclose

## PURPOSE

Spectral analysis has been used to quantify the shape and spatial patterns of a variety of lesions in the lung, brain, breasts, prostrate etc. The aim of this study was to evaluate the feasibility of spectral analysis to differentiate malignant from benign renal tumors as well as differentiate the varying subtypes of renal cell carcinomas (RCCs) using contrast-enhanced computed tomography (CECT) images of renal masses

## **METHOD AND MATERIALS**

CECT images from 140 patients with renal masses were included. The dataset included, angiomyolipomas (AML) n = 17; chromophobe RCC n = 10; clear RCC (cRCC) n = 68; oncocytoma (ONCO) n = 26 and papillary RCC (pRCC) n = 19. Tumor grades were also analyzed for the cRCC and pRCC datasets spanning 1(n=3), 2(n=54), 3(n=32) and 4(n=4). The lesions were manually segmented in the nephrographic phase and , the axial image that provided the largest tumor diameter, along with its 2 adjacent image was selected for further analysis. Two dimensional Fast Fourier Transform (FFT) was used to analyze the greyscale images of the segmented tumors using Matlab (Mathworks, Natick,MA) software. Here, complexity index, defined as the sum of the amplitude of all harmonics was measured . ANOVA test followed by post hoc comparisons with bonferroni correction was used to compare the complexity across tumor types and grade levels. Complexity was reported using million as the unit

#### RESULTS

Across all groups, the spectral amplitudes decreased with the increase in spectral frequency. The highest complexity index was recorded for ONCO ( $365.12 \pm 12.28$ ), followed by chromophobe and cRCC with  $349.86 \pm 19.8$  and  $349.31\pm7.59$ , respectively. The lowest complexity index was recorded for pRCC ( $242.62\pm14.37$ ) (Figure 1). The difference in complexity indices between ONCO and AML, and, ONCO and pRCC were significant (p < 0.01). The complexity index increased with increase in tumor grade and significant (p < 0.01) differences were reported between grade 1 and all the other levels (Figure 1).

# CONCLUSION

The complexity index is a promising metric to differentiate between the various types and grades of renal tumors. In combination with various other radiomics features, spectral analysis could offer another quantitative technique to help analyze renal masses

## **CLINICAL RELEVANCE/APPLICATION**

Spectral analysis offers an additional radiomic technique to differentiate renal tumors types and will help improve patient-specific care-management options.

# HP143-ED-WEB6

Contrast Induced Nephropathy in the Light of Residual Renal Function: Stepping Out of the Darkness and into the Renal Realm

Wednesday, Nov. 30 12:45PM - 1:15PM Room: HP Community, Learning Center Station #6

# Participants

Justin White, DO, Little Rock, AR (*Presenter*) Nothing to Disclose Narendra B. Gutta, MBBS, MD, Little Rock, AR (*Abstract Co-Author*) Nothing to Disclose John C. Faircloth, DO, Sherwood, AR (*Abstract Co-Author*) Nothing to Disclose Kedar Jambhekar, MD, Little Rock, AR (*Abstract Co-Author*) Nothing to Disclose

## **TEACHING POINTS**

Describe Residual Renal Function (RRF) and it's importance. Review contrast induced nephropathy with emphasis on morbidity and mortality in dialysis patients. Present recent literature surrounding CIN, RRF, and hypoalbuminemia in dialysis patients.

## TABLE OF CONTENTS/OUTLINE

Present data demonstrating residual renal function as key independent risk factor for survival in long term dialysis patients. Review contrast induced nephropathy morbidity and mortality in general and dialysis subset. Discuss studies on rates of contrast induced nephropathy in setting of low serum albumin. Present recent data concerning contrast effect on residual renal function. Propose criteria for managing contrast administration to dialysis patients.

Appropriate Use of CT Pulmonary Angiography - An Analysis of Ordering D-Dimers in the Emergency Department and the Potential for Improvement

Wednesday, Nov. 30 12:45PM - 1:15PM Room: HP Community, Learning Center Station #1

#### **Participants**

Amit Chacko, MBBS, Brisbane, Australia (Presenter) Nothing to Disclose

#### PURPOSE

The symptoms and signs of a pulmonary embolism (PE) are extremely varied and thus a clinical diagnosis of PE can be unreliable. A robust way to stratify a patient's risk of PE is to use one of the validated clinical decision tools such as the Wells score. 1 Using these tools, a patient can be stratified into a low, moderate or high pretest probability of PE. The addition of a d-dimer test provides a pathway to determine if a patient requires imaging to exclude a PE. 2 The d-dimer is a breakdown product of crosslinked fibrin and occurs coincident with activation of the coagulation cascade. The d-dimer level may be elevated in the presence of a clot that embolises to the lungs causing a pulmonary embolism (PE). The d-dimer level should be used in patients with a low to moderate pretest probability for PE. 3

# METHOD AND MATERIALS

A retrospective audit was performed of patients who underwent CT Pulmonary Angiography (CTPA) for suspected PE from the emergency department in January 2016. IMPAX search parameters: Study Dates = 01/01/2016-01/03/2016.Study Description = "CT Pulm"Request = ED Clinician and/or location ED. Using these studies a more detailed review of the available documentation including d-dimer result, a recent chest x-ray, vital signs and clinical history were used to produce a retrospective Wells PE probability score.

### RESULTS

The first 100 CTPAs performed were analyzed. 13% of the patients had a positive CTPA for PE. 98% of patients were of low to moderate pretest probability for PE. 15% of these patients had a d-dimer requested prior. 12 (92%) of the patients who had a confirmed PE were of low or moderate pretest probability. It was noted, one patient with low pretest probability of PE, who had a negative d-dimer, still continued to have a CTPA which was also negative.

### CONCLUSION

The positive CTPA rate for PE was 13% - less than the rate recommended by the Royal College of Radiologists of 15.4-37.4%. 4 Only 15% of the low and moderate pretest probability patients had a d-dimer requested. If the d-dimer test was utilized appropriately, it could have conceivably avoided up to 71% of the CTPAs.

# **CLINICAL RELEVANCE/APPLICATION**

Education sessions and emphasis on the diagnostic imaging pathway would save cost, reduce exposure of patients to ionizing radiation, the risk of contrast complications and would improve patient turn over in the emergency department.

# HP232-SD-WEB2

### Diagnostic Errors in Urgent Radiology Reports: The Impact of Time of Day and Teleradiology

Wednesday, Nov. 30 12:45PM - 1:15PM Room: HP Community, Learning Center Station #2

#### **Participants**

Antoni Malet-Munte, MD, Sabadell, Spain (*Presenter*) Nothing to Disclose Jordi M. Puig-Domingo, MD, L'ametlla Del Valle, Spain (*Abstract Co-Author*) Nothing to Disclose Marta Andreu, MD, Sabadell, Spain (*Abstract Co-Author*) Nothing to Disclose Joan Carles Oliva Sr, BS,MS, Sabadell, Spain (*Abstract Co-Author*) Nothing to Disclose Eva Ballesteros Gomiz, MD, Mollet del Valles, Spain (*Abstract Co-Author*) Nothing to Disclose Marta Sola, MD, Sabadell, Spain (*Abstract Co-Author*) Nothing to Disclose Xavier Gallardo, MD, Sabadell, Spain (*Abstract Co-Author*) Nothing to Disclose Francesc Novell Teixido, MD, Sabadell, Spain (*Abstract Co-Author*) Nothing to Disclose Damian Gil, Sabadell, Spain (*Abstract Co-Author*) Nothing to Disclose Joseph M. Mata, MD, PhD, Sabadell, Spain (*Abstract Co-Author*) Nothing to Disclose Eva Castaner, MD, Sabadell, Spain (*Abstract Co-Author*) Nothing to Disclose

## PURPOSE

To determine the impact of the time of day and of teleradiology on the rate of errors in reports of urgent abdominal and/or chest CT studies by residents on call.

### **METHOD AND MATERIALS**

Our imaging department covers calls for our university hospital with 500 acute beds and 500 nursing home beds and, by teleradiology, calls for 13 public hospitals with 2,100 acute beds serving a population of 1.8 million.We reviewed 2,016 prospectively registered reports of urgent abdominal and chest CT studies done between 7/10/2014 and 5/15/2015 at our hospital or the hospitals served by teleradiology that were reported by third- or fourth-year residents on call and then reviewed by subspecialists.Discrepancies with reports by abdominal or thoracic radiologists reviewing the studies later were considered errors. We classified errors in function of whether they could potentially change the urgent management of the patient and cause an adverse event. We also analyzed the difficulty of the findings, the reasons for errors (due to erroneous perception, interpretation, or transmission), and the type of error (false-positives vs. false-negatives).

#### RESULTS

The overall rate of discrepancies that could potentially lead to changes in the urgent management was 3.8%. The rate was higher in the early hours than at other times (8.1% vs. 3.3%, p=0.001). The rate of discrepancies did not differ between studies done onsite and those reported by teleradiology.

# CONCLUSION

The risk of errors that can potentially change the urgent management is higher in the early morning than in the rest of the call period, so only studies that cannot wait until the morning should be done in this period. Teleradiology did not affect the rate of errors.

# **CLINICAL RELEVANCE/APPLICATION**

Radiology reports are crucial for clinical decisions, so it is essential to know what factors can increase diagnostic errors.

## HP233-SD-WEB3

Medical Student Perception of Diagnostic Radiology after Implementation of an Evening Emergency Radiology Rotation

Wednesday, Nov. 30 12:45PM - 1:15PM Room: HP Community, Learning Center Station #3

#### Awards

### **Student Travel Stipend Award**

#### Participants

Anuj K. Rajput, MD, Stony Brook, NY (*Presenter*) Nothing to Disclose Don N. Nguyen, MD, Pittsburgh, PA (*Abstract Co-Author*) Nothing to Disclose Toshie Ahluwalia, MD, Melville, NY (*Abstract Co-Author*) Nothing to Disclose Michael Goodman, BA, Stony Brook, NY (*Abstract Co-Author*) Nothing to Disclose Rayeed Islam, BS, Antigua Guatemala, Antigua And Barbuda (*Abstract Co-Author*) Nothing to Disclose Jared Nesbitt, MD, Stony Brook, NY (*Abstract Co-Author*) Nothing to Disclose Dharmesh Tank, MD, Stony Brook, NY (*Abstract Co-Author*) Nothing to Disclose Robert Matthews, MD, Stony Brook, NY (*Abstract Co-Author*) Nothing to Disclose

### PURPOSE

Our purpose is to assess if there is a change in medical students' current perception of diagnostic radiology after the implementation of an evening emergency radiology rotation.

### **METHOD AND MATERIALS**

A questionnaire was given to 80 rotating medical students after a 2-week diagnostic radiology rotation during a 10-month interval. The rotation included time spent in all the specialities with the addition of a new evening ER rotation. The rotation consisted of spending time after hours with a senior resident and an on-call attending during a typical evening ER shift.

#### RESULTS

Exit responses of the students demonstrated a mean 10% increase in the interest in radiology after the rotation. Perceptions of diagnostic radiology had an average change of 33%. A mean of 2 hours was considered an optimal amount of time spent on a night ER rotation. Majority of students felt there was an insufficient amount of time spent reviewing studies during the ER rotation, however, the number of studies seen was considered to be sufficient in volume.

## CONCLUSION

Medical student perception of diagnostic radiology after the implementation of an evening ER rotation has not changed substantially. They demonstrate awareness of the increased workload and expectations of the night ER radiologist, however, appear to be more interested in radiology after this experience.

# **CLINICAL RELEVANCE/APPLICATION**

Implementation of an evening ER radiology rotation during medical school does not substantially change students perception of radiology in lieu of our changing health care climate, which has fostered increase diagnostic imaging and faster turnaround time with accurate interpretation.

## HP235-SD-WEB5

Propensity Score Analysis of Lung Cancer Risk in Endemic Area with High Prevalence of Nonsmoking-related Lung Cancer

Wednesday, Nov. 30 12:45PM - 1:15PM Room: HP Community, Learning Center Station #5

## Participants

Hsiu Fu Wu, Kaohsiung City, Taiwan (*Presenter*) Nothing to Disclose Fu-Zong Wu, MD, DSc, Kaohsiung, Taiwan (*Abstract Co-Author*) Nothing to Disclose Ming-Ting Wu, MD, Kaohsiung, Taiwan (*Abstract Co-Author*) Nothing to Disclose Chiung Chen Chuo, Kaohsiung City, Taiwan (*Abstract Co-Author*) Nothing to Disclose Wei-Chun Huang, Kaohsiung, Taiwan (*Abstract Co-Author*) Nothing to Disclose Pei-Ling Tang, Kaohsiung City, Taiwan (*Abstract Co-Author*) Nothing to Disclose

### PURPOSE

Lung cancer has been the leading cause of cancer-related mortality worldwide among both men and women in recent years. Smoking is the major risk factor for lung cancer, but an increase in the incidence of nonsmoking-related lung cancer in recent years. The purpose of the present study was to investigate multiple potential risk factors for nonsmoking-related lung cancer among Asian Ethnic Groups.

## METHOD AND MATERIALS

We retrospectively review the medical record of 1974 asymptomatic healthy subjects (40~80 year old) who voluntarily underwent lowldose chest CT (1083 male, 891 female) from August 2013 to March 2015. Clinical information and nodule characteristics were recorded according to ACR lung-RADS classification. Results of subsequent followlup and outcome were also recorded. A propensity score-mated cohort analysis using the retrospective was applied to adjust for potential bias and to create two comparable groups according to family history of lung cancer.

#### RESULTS

For our primary analysis, we matched 392 pairs of subjects with family history of lung cancer and subjects without history. Logistic regression showed that female gender and a family history of lung cancer were the two most important predictor of lung cancer in endemic area with high prevalence of nonsmoking-related lung cancer (odds ratio of 11.146, P value = 0.021; odds ratio of 2.831, P value = 0.05, respectively). In addition, the number of nodules was higher in subjects with family history of lung cancer in comparison with subjects without family history of lung cancer.

## CONCLUSION

In conclusion, Risklbased prediction model based on the family history of lung cancer and female gender can potentially improve efficiency of lung cancer screening programs in Taiwan.

### **CLINICAL RELEVANCE/APPLICATION**

Risklbased prediction model based on the family history of lung cancer and female gender can potentially improve efficiency of lung cancer screening programs in Taiwan.

## IN011-EB-WEB

Effect of Standardized Template Dictation on Assignment of ACR BI-RADS Categories 1 and 2 for Screening Mammography

Wednesday, Nov. 30 12:45PM - 1:15PM Room: IN Community, Learning Center Hardcopy Backboard

# Participants

Aaron Dunn, DO, Philadelphia, PA (*Presenter*) Nothing to Disclose Brian S. Englander, MD, Philadelphia, PA (*Abstract Co-Author*) Nothing to Disclose

### CONCLUSION

With the introduction of standardized templates for breast imaging, there was a change in the use of ACR BI-RADS Categories. Use of template based electronic health records resulted in a decrease in inclusion of benign, inconsequential findings. Screening mammography was determined to be normal, rather than benign, with less extraneous data. Future opportunities exist to consider whether there is any change in the use of other Categories, assessments, or density assignments.

### Background

Normal and benign findings are not always clearly distinguished during interpretation and dictation of screening mammography and assignment of ACR BI-RADS Categories. Multiple variables contribute to the use of 1 or 2 Categories.

### **Evaluation**

Use of ACR BI-RADS Categories was evaluated during a 1-year period preceding implementation of an electronic health record and a 1-year period following implementation. Prior to implementations, reports were dictated with Nuance PowerScribe 360 with no required report structure or language. With the introduction of EPIC for direct reporting of mammography, interpreting radiologists were required to assign an ACR BI-RADS Category with a template report; there was no default Category. Between 1 April 2014 and 31 March 2015, 12,920 screening mammograms were interpreted by 4 experienced radiologists. 11,773 BI-RADS Categories 1 and 2 were assigned; 2,408 studies were assigned Category 1, and 9,365 were assigned Category 2.Between 1 April 2015 through 31 March 2016, 12,665 screening mammograms were interpreted by 4 experienced radiologists. 11,379 BI-RADS Categories 1 and 2 were assigned; 4,783 studies were assigned Category 1, and 6,596 were assigned Category 2. During the 2-year period, there was no change in staffing, equipment, or any other variable.

#### Discussion

There is a statistically significant decrease in the number of patients who were assigned BI-RADS Category 2 (6,598 compared with 9,365), with a statistically significant increase in the number of patients who were assigned BI-RADS Category 1 (4,783 compared with 2,408). Statistical significance was measured with a p-value <0.0001. The increased use of Category 1 was seen for all four radiologists.

Sunburst: Open Source Radiologist Timeline Dashboard for Summarizing Prior Imaging Reports Using NLP and UMLS

Wednesday, Nov. 30 12:45PM - 1:15PM Room: IN Community, Learning Center Custom Application Computer Demonstration

# Participants

Shubham Shukla, New York, NY (*Abstract Co-Author*) Nothing to Disclose
Liana Greer, New York, NY (*Presenter*) Nothing to Disclose
Evan Lustbader, MD, New York, NY (*Abstract Co-Author*) Nothing to Disclose
Jai Chaudhary, MENG, New York, NY (*Abstract Co-Author*) Nothing to Disclose
Praveen Gupta, New York, NY (*Abstract Co-Author*) Nothing to Disclose
George L. Shih, MD, MS, New York, NY (*Abstract Co-Author*) Consultant, Image Safely, Inc; Stockholder, Image Safely, Inc;

## CONCLUSION

Sunburst has the potential to be a key tool radiologist workflow for imaging interpretation. The textual analysis and visual findings display powered by Sunburst provide a complementary application to the PACS image based system in the interpretation and contextualization of new radiographic findings. We hope to continue developing Sunburst to include machine learning algorithms to start to predict disease progression and other imaging findings to further enhance workflow and provide additional triage.

## FIGURE

http://abstract.rsna.org/uploads/2016/16013601/16013601\_nh3p.jpg

#### Background

Imaging interpretation for disease progression requires appropriate understanding of prior imaging context, which is typically done by manually examining prior exam reports and images which can be time-consuming and tedious. Patient timeline tools already exist to provide some of this context, but still require radiologists to review the same data. We present Sunburst (http://sunburst.trove.nyc), an open source radiologist assistant dashboard summary, that allows direct visualization of relevant finding trends over time (http://src.sunburst.trove.nyc).

### **Evaluation**

Sunburst leverages natural language processing (NLP) techniques, the Unified Medical Language System (UMLS) ontology, and Metamap, to analyze the important findings in the relevant radiology reports (eg, 3 prior exams of the same modality). The app contextually analyzes the report impression text and extracts key phrases into either 'presence' or 'absence' categories (eg, presence of adrenal nodules, or absence of hepatic lesions). Sunburst then provides a summary dashboard where clinicians can easily see all key findings, their trends by date, and the actual sentence in the report from which the key finding was extracted.

### Discussion

Our radiologist assistant app allows radiologists to quickly assimilate the most relevant information from prior imaging exams, to orient them for the new uninterpreted exam. While direct review of the prior images may still be necessary, our initial impression is that this tool will significantly enhance our radiologist workflow, especially as we're able to provide the UMLS relationships between the diseases and their related imaging manifestations.

# IN028-EC-WEB

GlioView: An Application that Visualizes Variability in Brain Tumor Segmentation to Inform the Clinical Assessment of Change

Wednesday, Nov. 30 12:45PM - 1:15PM Room: IN Community, Learning Center Custom Application Computer Demonstration

FDA Discussions may include off-label uses.

### Participants

Edgar A. Rios Piedra, MSc , Los Angeles, CA (*Presenter*) Nothing to Disclose Rick K. Taira, PhD, Los Angeles, CA (*Abstract Co-Author*) Nothing to Disclose Suzie M. El-Saden, MD, Los Angeles, CA (*Abstract Co-Author*) Nothing to Disclose Benjamin M. Ellingson, MS, PhD, Los Angeles, CA (*Abstract Co-Author*) Research Consultant, MedQIA Imaging Core Laboratory Research Consultant, F. Hoffmann-La Roche Ltd Research Consultant, Tocagen Inc Research Consultant, Boston Scientific Corporation Research Consultant, Amgen Inc Research Grant, Siemens AG Research Grant, F. Hoffmann-La Roche Ltd Alex A. Bui, PhD, Los Angeles, CA (*Abstract Co-Author*) Nothing to Disclose William Hsu, PhD, Los Angeles, CA (*Abstract Co-Author*) Nothing to Disclose

# CONCLUSION

GlioView automates tumor segmentation and assessment of tumor volumetric change, while providing an estimate of uncertainty in these measurements. In this way, GlioView provides clinicians with an increased level of confidence for interpreting imaging data and improve clinical decision-making.

#### FIGURE

http://abstract.rsna.org/uploads/2016/16006734/16006734\_1dnb.jpg

#### Background

Radiological characterization of high-grade primary brain tumors plays a vital role in diagnosing, treating, and evaluating treatment response. Accurate measurement of tumor burden can be a challenging, labor intensive, and time consuming task for neuroradiologists. Additionally, measurements may have high variability due to rater interpretation and the heterogeneous nature of high-grade gliomas. Currently, there is a significant need for a radiology workstation that can quickly segment brain tumors, including measures of segmentation uncertainty, and provide the radiologist with clear visualization of changes that occur during clinical follow-up.

### **Evaluation**

To address this need, we created an application that: 1) performs automated volumetric segmentation and analysis of brain tumor MR images for each tumor component; 2) visualizes the results and error bounds in tumor segmentation; and 3) captures change and variability over time that arises on subsequent examinations.Segmentation error was estimated by iterative measurements of the tumor boundary using a novel and accurate knowledge-based approach that was incorporated into an automated pipeline that includes image preprocessing and tumor segmentation for all time points for a patient.This process was built into a graphical user interface (GlioView) that lets the user run the automated pipeline and select different visualization options. Results are visualized as color-coded overlays on top of the original images alongside the volume variability estimates.

## Discussion

Measurement of segmentation uncertainty is important for the evaluation of tumor changes over time. GlioView provides an intuitive interface for image analysis and provides an estimate of tumor extent, which can be used for RANO evaluation. The addition of error bounds alongside volumetric measurements provides a more objective approach for interpreting over time change.

# IN246-SD-WEB1

You've Got Mail: A Pilot Study on Notifying Referring Physicians About Missed Patient Follow-Up Directly in the Electronic Medical Record

Wednesday, Nov. 30 12:45PM - 1:15PM Room: IN Community, Learning Center Station #1

## Participants

Tessa S. Cook, MD, PhD, Philadelphia, PA (*Presenter*) Nothing to Disclose Darco Lalevic, Philadelphia, PA (*Abstract Co-Author*) Nothing to Disclose Charles E. Kahn JR, MD, MS, Philadelphia, PA (*Abstract Co-Author*) Nothing to Disclose Christopher Pizzurro, Philadelphia, PA (*Abstract Co-Author*) Nothing to Disclose Mitchell D. Schnall, MD, PhD, Philadelphia, PA (*Abstract Co-Author*) Nothing to Disclose Hanna M. Zafar, MD, Philadelphia, PA (*Abstract Co-Author*) Nothing to Disclose

## CONCLUSION

Referring physicians are willing to provide feedback about their patients who have no documented follow-up in the EMR after an abdominal imaging exam. In this small pilot, there was a preference for notifications to be sent both by e-mail as well as electronically within the EMR. Future development of the system will take this preference into account in order to better care for our patients and serve our referring colleagues.

### Background

When patients miss follow-up issued based on imaging examinations, the reasons are multifactorial. In addition, it can be difficult to ascertain whether a study is clinically indicated by reviewing the patient's chart. To begin to close the loop for patients awaiting follow-up in our health system, we piloted a system to send interactive notifications to referring physicians directly within the electronic medical record (EMR), to determine if follow-up is clinically indicated.

### **Evaluation**

In collaboration with our corporate information technology team, we developed a method to send messages to providers' inboxes within our health system's EMR. We sent messages to 9 providers caring for 11 patients with imaging finding of possible cancer detected on abdominal CT, MR or US exam performed between 8/1/2013 and 9/30/2013, with no completed follow-up and no chart documentation as to why follow-up was not clinically indicated. Messages redirected providers to a radiology recommendation-tracking engine that allowed them to review the original report and offer structured feedback as to whether follow-up was clinically indicated.

### Discussion

Of the 9 physicians, 3 accessed the engine via the messages sent into the EMR; 1 viewed the message but did not access the engine; 1 was unable to view the EMR message; and 4 did not access the EMR messages. Of the latter 6 physicians, 3 were successfully contacted by phone. 5/9 physicians indicated that they were not the correct providers to contact, but 2/9 were able to identify the physicians presently caring for the patient. Follow-up was no longer clinically indicated for 2 patients (one had already completed follow-up elsewhere; the other was deceased). Imaging follow-up remained clinically indicated and will be ordered for 3 patients.

## **Honored Educators**

Presenters or authors on this event have been recognized as RSNA Honored Educators for participating in multiple qualifying educational activities. Honored Educators are invested in furthering the profession of radiology by delivering high-quality educational content in their field of study. Learn how you can become an honored educator by visiting the website at: https://www.rsna.org/Honored-Educator-Award/

Charles E. Kahn JR, MD, MS - 2012 Honored Educator Mitchell D. Schnall, MD, PhD - 2013 Honored Educator

# Improving Reading of T2 MRIs through Deep Learning

Wednesday, Nov. 30 12:45PM - 1:15PM Room: IN Community, Learning Center Station #2

#### Participants

Kevin Mader, DPhil,MSc, Zuerich, Switzerland (*Presenter*) Employee, 4Quant Ltd; Shareholder, 4Quant Ltd Bram Stieltjes, MD, Basel, Switzerland (*Abstract Co-Author*) Nothing to Disclose Elmar M. Merkle, MD, Basel, Switzerland (*Abstract Co-Author*) Speakers Bureau, Siemens AG; Research Grant, Bayer AG; Research Grant, Guerbet SA; Research Grant, Bracco Group Kangqiang Peng, BSC, Guangzhou, China (*Abstract Co-Author*) Officer, 4Quant Ltd; Shareholder, 4Quant Ltd

### CONCLUSION

We show a possible direction for automating the process of finding new relevant imaging biomarkers for disease using a relatively uncommon disease in a heterogeneous patient group.

### Background

Radiological guidelines are currently painstakingly developed by manually aggregating the experience of many prominent physicians from ideally multiple medical centers. For rare diseases the challenge of not only identifying but properly interpreting the stage and progression in standard biologically nonspecific measurements like MRI, Ultrasound, and CT is formidable. Nasopharyngeal Cancer while rare in most of the world is unusually common in Southern China. It is a serious form of head and neck cancer which can be difficult to find and even more difficult to make meaningful prognosis. Determining the aggressiveness of a specific tumor is essential for selecting the proper treatment and ultimately improving the patient's chances at survival.

### **Evaluation**

Using a clinical study with over 200 patient datasets, we trained a neural network to identify both the standard TNM staging as well as the 12 month outcome variable. We used a deep network with over 20 layers and thousands of free parameters to perform the training. To compensate for so many degrees of freedom we augmented the dataset with transformed versions of the original images simulating differently sized as well as poorly positioned patients. We optimized the classifications by using a cross-entropy error. The loss ultimately was below 0.5 for the entire feature vector on both training and validation datasets after 500 epochs of training and 12 hours of computational time. Rather than taking the output diagnosis, we focused on determining to which regions and structures the network paid attention using several outcome-based approaches.

### Discussion

Once the network was trained, computing the regions of interest for a new patient can be done in fractions of a second. From a large 3D volume the relevant features can then be more closely examined. Additionally another byproduct of the network are a collection of patterns and structures validated across hundreds of patients.

# **Coregistration of Liver Cone-Beam CT and CT Datasets**

Wednesday, Nov. 30 12:45PM - 1:15PM Room: IN Community, Learning Center Station #3

#### **Participants**

Marco Solbiati, Busto Arsizio, Italy (*Presenter*) Nothing to Disclose Luigi Solbiati, MD, Rozzano, Italy (*Abstract Co-Author*) Nothing to Disclose Tiziana Ierace, MD, Busto Arsizio, Italy (*Abstract Co-Author*) Nothing to Disclose Alessandro Rotilio, Milano, Italy (*Abstract Co-Author*) Shareholder, RAW Srl Katia Passera, MEng, BUSTO ARSIZIO, Italy (*Abstract Co-Author*) Nothing to Disclose

### CONCLUSION

This method is very promising and could change current workflow of mini-invasive cancer treatments leading to lower risks for patients and operators

#### Background

Interventional rooms for minimally invasive treatments of neoplastic lesions are increasingly equipped with cone-beam CT scanners (CBCT) for the guidance of procedures and the immediate assessment of the results achieved.Accordingly, the need for precise and fast registration of pre-treatment contrast-enhanced CT (CE-CT) and post-treatment contrast-enhanced CBCT (CE-CBCT) datasets is increasingly felt. For thermal ablations incomplete treatments occur in 5-15% of cases and are visualized on follow-up CE-CT studies.In the figure below, a case in which post-treatment CE-CT shows incomplete ablation requiring subsequent re-treatment.

# **Evaluation**

CT and CBCT datasets differ with respect to many parameters, such as FOV, voxel spacing, image quality and liver parenchyma deformations due to respiratory movements. These issues make registration very challenging.Our method consists of different steps: (i) liver and lesion segmentation on pre-treatment CE-CT (ii) registration of CE-CBCT with CECT, performed starting with initial rigid registration, to coarsely realign the two volumes, followed by non-linear registration to correct local deformations (iii) overlap of lesion contours on registered CBCT.In 10 patients with 15 hepatic neoplastic lesions undergone thermal ablation with microwaves (MWA) under ultrasound guidance, datasets of pre-treatment CE-CT and post-treatment CE-CBCT and 24-hr follow-up CE-CT were studied using this method.In 3/10 patients, registration of post-treatment CE-CBCT with pre-treatment CE-CT allowed to identify untreated, still viable portions in 5/15 neoplasms that were immediately targeted and re-treated with MWA under US guidance. On post-retreatment follow-up CE-CT all lesions were completely ablated

### Discussion

Our results show that registration permits to identify untreated areas during the same interventional session, thus decreasing for patients risks and discomfort of retreatments and for operators the difficulties created by new treatments of the same lesions. In addition, management costs significantly decrease

Comparing Wearable Display Technologies: What Are Their Relative Advantages and Disadvantages to the Diagnostic and Interventional Radiologist?

Wednesday, Nov. 30 12:45PM - 1:15PM Room: IN Community, Learning Center Station #4

#### Awards

### **Student Travel Stipend Award**

#### Participants

Vikash Gupta, MD, Baltimore, MD (*Presenter*) Nothing to Disclose Alaa Beydoun, MD, Baltimore, MD (*Abstract Co-Author*) Nothing to Disclose Tammam Beydoun, DO, Phoenix, AZ (*Abstract Co-Author*) Nothing to Disclose Eliot L. Siegel, MD, Baltimore, MD (*Abstract Co-Author*) Board of Directors, Brightfield Technologies; Board of Directors, McCoy; Board of Directors, Carestream Health, Inc; Founder, MedPerception, LLC; Founder, Topoderm; Founder, YYESIT, LLC; Medical Advisory Board, Bayer AG; Medical Advisory Board, Bracco Group; Medical Advisory Board, Carestream Health, Inc; Medical Advisory Board, Fovia, Inc; Medical Advisory Board, McKesson Corporation; Medical Advisory Board, Merge Healthcare Incorporated; Medical Advisory Board, Microsoft Corporation; Medical Advisory Board, Koninklijke Philips NV; Medical Advisory Board, Toshiba Corporation; Research Grant, Anatomical Travelogue, Inc; Research Grant, Anthro Corp; Research Grant, Barco nv; Research Grant, Dell Inc; Research Grant, Intel Corporation; Research Grant, MModal IP LLC; Research Grant, McKesson Corporation; Research Grant, Intel Corporation; Research Grant, Virtual Radiology; Research Grant, XYBIX Systems, Inc; Research, TeraRecon, Inc; Researcher, Bracco Group; Researcher, Microsoft Corporation; Speakers Bureau, Bayer AG; Speakers Bureau, Siemens AG;

### CONCLUSION

The emergence of visual overlay devices creates an exciting era for medicine and allows for significant advancement in radiology. Google Glass and Microsoft HoloLens each have a unique set of advantages and disadvantages. Understanding these technical capabilities and how they relate to applications in radiology will be paramount for future research and clinical implementations.

#### Background

Wearable visual overlay devices are a new and emerging technology with tremendous potential in many disciplines, including radiology. Currently, there is little information about how these devices compare, particularly in the medical setting. This project aims to:1. Compare the technical features and limitations of two wearable devices (Google Glass and Microsoft HoloLens) and how they can be utilized in diagnostic and interventional radiology.2. Demonstrate the benefits and drawbacks of these devices in contrast to traditional display methods.

#### **Evaluation**

Each device is evaluated for how well it can:-Capture and playback procedures-Display imaging or clinical data in a clear, nonobtrusive manner-Co-register imaging during interventional procedures-Facilitate collaboration with other physiciansUsing phantom devices for the abovementioned use cases, the following metrics are assessed:-Operator efficiency-Operator opinion-Rate of technical errorEach device is reviewed regarding ease of implementation including:-Cost and expected lifecycle-Integration with existing imaging hardware-Ease of use/onboarding

### Discussion

Microsoft HoloLens and Google Glass provide similar but unique capabilities. Google Glass offers a reliable solution for recording procedures from a 1st person perspective and displaying ancillary data during cases in a non-obstructive format. Google Glass has a lower barrier to implementation as a recording and teaching device. Microsoft HoloLens provides these capabilities but can also overlay co-registered data on the real world with appropriate depth perception. From a display standpoint, the HoloLens provides superior hardware. The effect of these devices on efficiency and error rate will be better elucidated as operators gain more experience.

Accuracy of the of N0 Nodal Staging of the High-risk Prostatic Carcinoma based on18F-fluorocholine-PET/MRI, Comparison with Surgical Findings

Wednesday, Nov. 30 12:45PM - 1:15PM Room: S503AB Station #1

### Participants

Jiri Ferda, MD, PhD, Plzen, Czech Republic (*Presenter*) Nothing to Disclose Eva Ferdova, MD, Plzen, Czech Republic (*Abstract Co-Author*) Nothing to Disclose Jan Baxa, MD, PhD, Plzen, Czech Republic (*Abstract Co-Author*) Nothing to Disclose Milan Hora, Plzen, Czech Republic (*Abstract Co-Author*) Nothing to Disclose Ondrej Hes, MD, PhD, Plzen, Czech Republic (*Abstract Co-Author*) Nothing to Disclose

# PURPOSE

To evaluate the possibilities of pelvic nodal-staging assessment of the high-risk prostatic carcinoma using 18F-fluorocholine-PET/MRI and to compare findings with surgery.

### **METHOD AND MATERIALS**

25 men (mean age 66,8 years, range 59 - 78) with by biopsy confirmed prostatic carcinoma with Gleason score 8 and more were examined before surgery using 18F-fluorocholine-PET/MRI and with finding of no positive node (N0 N-stage based on PET/MRI) were recommended to radical prostatectomy. All examination were delayed 15 min after intravenous application of 18F-fluorocholine in the dose 1,25 MBq per kilogram of body weight. The imaging included T2 STIR, DWI and dynamic gadolinium enhanced GRE T1 imaging, the PET acquisition last 15 min. All examinations were completed with whole trunk PET/MRI acquisition. The TNM staging was evaluated. In all men, the radical surgery was performed including pelvic lymph node resection. The comparison of the histopathological results were compared with those obtained by PET/MRI according nodal staging and according local T-staging.

### RESULTS

25 surgeries were performed. There were found 22 true negative findings, and three false negative findings including one micrometastase. The negative predictive value of pelvic lymph node metastase reached 88,0 %(22/25) excluding micrometastase, NPV rised to 92,0% (23/25). One deviation between T2 or T3 size was noted after histopathological evaluation, one case was evaluated as T3B by PET/MRI, after histopathological evaluation the stage was set as T2C; in one case, the T2b based on PET/MRI was evaluated as T2C, no other deviation was noted nor between T2 or T3 subcathegories, nor in T3A subcathegory. It results in 92% (23/25) accuracy in local staging.

### CONCLUSION

The 18F-fluorocholine PET/MRI derived pelvic lymph N-staging N0 and T-stage in prostatic carcinoma reaches sufficien results and provides sufficient information in the treatment decisions.

### **CLINICAL RELEVANCE/APPLICATION**

In prostatic carcinoma, the negative pelvic nodal staging and T-staging using 18F-fluorocholine PET/MRI exhibits sufficient clinical value in the decisions to perform radical prostate surgery.

# MI223-SD-WEB2

Molecular Imaging of Metastasis From Pancreatic Cancer in Patient-Derived Xenograft Models Using uPAR-Targeted Multifunctional Nanoparticles

Wednesday, Nov. 30 12:45PM - 1:15PM Room: S503AB Station #2



# Participants

Kai Cao, MD, PhD, ShangHai, China (Presenter) Nothing to Disclose

### PURPOSE

Lymphatic metastasis is an important prognostic factor regarding long-term survival rate of pancreatic cancer (PC) patients. Pretreatment knowledge of lymph node status is extremely helpful for planning treatment and prognosis. However, to date, no imaging method has been demonstrated to be effective for detecting lymphatic metastasis in PC. Molecular imaging probes based on upconversion nanoparticles with unique optical and magnetic properties have provided great hope for early tumor detection. Herein we report highly sensitive detection of lymphatic spread using core@shell structured NaGdF4:Yb,Er@NaGdF4 upconversion nanoparticles coated with polyethylene glycol (PEG).

### **METHOD AND MATERIALS**

The orthotopic patient-derived xenograft model, which can better retained the human pancreatic cancer morphology and genetic stability, was built upon engraftment of pancreatic cancer specimens in nude mice and the tumor development was carefully monitored through histopathological and immunohistochemical analyses to reveal the pathophysiological processes and molecular features of the cancer microenvironment. A PC-speific probe was constructed through "click" reaction between the maleimide moiety of PEG ligand and the thiol group from conjugating amino-terminal fragment of the receptor binding domain of human urokinase plasminogen activator(uPA), whose receptor(uPAR) is highly expressed in the pancreatic cancer.

# RESULTS

Upon 980nm laser excitation, the primary tumor and adjacent lymphatic metastasis site were clearly differentiated owing to the ultralow background of the upconversion luminescence after the uPAR-specific probe was delivered through tail vein injection into tumor-bearing nude mice. Target specificity of nanoparticles is further confirmed by a clinical MRI scanner at a field strength of 3 Tesla.

### CONCLUSION

Our results revealed that the probe could be useful for not only tiny tumor lesion diagnosis but also for lymphatic metastasis detections, indicating potential clinical applications in the early pancreatic cancer diagnosis and lymph node status evaluation.

### **CLINICAL RELEVANCE/APPLICATION**

We believe that the current studies provide a highly effective and potential approach for pancreatic cancer surgical navigation.

# Acute Trauma of the Knee Ligaments: Following the Contusion Pattern

Wednesday, Nov. 30 12:45PM - 1:15PM Room: MK Community, Learning Center Hardcopy Backboard

**FDA** Discussions may include off-label uses.

#### **Participants**

Wilmer O. Aponte Barrios, MD, Bogota, Colombia (*Presenter*) Nothing to Disclose Maria L. Brun, Bogota, Colombia (*Abstract Co-Author*) Nothing to Disclose Emmanuel Salinas Sr, MD, Bogota, Colombia (*Abstract Co-Author*) Nothing to Disclose Karen Cifuentes Gaitan, Bogota, Colombia (*Abstract Co-Author*) Nothing to Disclose Oscar M. Rivero Rapalino, MD, Bogota, Colombia (*Abstract Co-Author*) Nothing to Disclose Rafael Gomez, MD, Bogota, Colombia (*Abstract Co-Author*) Nothing to Disclose

# **TEACHING POINTS**

1. To review the anatomy of the knee ligaments throughout illustrations and figures.2. To describe and schematize the contusion patterns in acute trauma of the knee.3. To discuss representative cases of traumatic lesions of the knee ligaments on MRI and the contusion patterns associated.

# TABLE OF CONTENTS/OUTLINE

1. Anatomy of the knee ligaments.a. ACL (anterior cruciate ligament).b. PCL (posterior cruciate ligament)c. Medial collateral Complex.d. Lateral collateral complex (Arcuate).e. Patellofemoral retinaculum.2. Contusion patterns.a. Pivot shift.b. Clip injury.c. Dashboard.d. Hyperextension.e. Patellofemoral dislocation.3. Representative cases in magnetic resonance ligament injury.a. ACL.b. PCL.c. Medial collateral Complex.d. Lateral complex.d. Lateral complex (Arcuate).e. Patellofemoral retinaculum.

# MK135-ED-WEB10

Dissecting the Sacroiliac Joint: Beyond Pain and Arthropathy - A Detailed Look at the Anatomy, Physiology, and Biokinetics

Wednesday, Nov. 30 12:45PM - 1:15PM Room: MK Community, Learning Center Station #9

# Participants

David C. Gimarc, MD, Denver, CO (*Presenter*) Nothing to Disclose Mary Kristen Jesse, MD, Denver, CO (*Abstract Co-Author*) Nothing to Disclose

# **TEACHING POINTS**

The sacroiliac joint is a unique articulation that provides an important window to numerous disease processes and age-related changes. After viewing this presentation, readers will have a better understanding of the exact anatomy of the joint including the unique osseous characteristics, cartilage composition, and fibromuscular stabilizing structures. This more-specific knowledge will then be applied to the physiology and movement of the joint with respect to biokinetics and demographic factors, with the goal of better understanding disease processes such as arthropathy.

# TABLE OF CONTENTS/OUTLINE

SI Joint overview Osseous details - 3D included Ligamentous and muscular structures Articulating Cartilage - hyaline and fibrocartilage Synovium and Capsule Variations in anatomy Demographic differences: gender, age Joint shape types (1-3) Accessory SI Joint Imaging modality variations: Radiographs, CT, MRI Physiology Biokinetics: axial loading Motion: Nutation and Counternutation Disease Process Examples Degenerative - OA Inflammatory - Psoriatic, Rheumatoid, IBD-related, Seronegative, Reactive Infectious 18F-Fluorodeoxyglucose (FDG) Positron Emission Tomography (PET)-Computed Tomography (CT) Appearance of Benign Musculoskeletal Lesions

Wednesday, Nov. 30 12:45PM - 1:15PM Room: MK Community, Learning Center Station #7

#### Awards

**Identified for RadioGraphics** 

#### Participants

Marit Asadoorian, MD, Glendale, CA (*Abstract Co-Author*) Nothing to Disclose George R. Matcuk Jr, MD, Los Angeles, CA (*Abstract Co-Author*) Nothing to Disclose Aaron Schein, MD, Los Angeles, CA (*Abstract Co-Author*) Nothing to Disclose Anderanik Tomasian, MD, Saint Louis, MO (*Abstract Co-Author*) Nothing to Disclose Dakshesh B. Patel, MD, Porter Ranch, CA (*Presenter*) Nothing to Disclose Eric A. White, MD, Santa Monica, CA (*Abstract Co-Author*) Nothing to Disclose

# **TEACHING POINTS**

Benign musculoskeletal lesions are frequently encountered on FDG PET-CT, often with FDG avidity, and may lead the radiologist to favor a malignant lesion. Some benign lesions encountered on FDG PET-CT have typical imaging findings, and do not require imaging follow up or biopsy. In addition, brown fat and arthritis are frequently metabolically active. Moreover, attenuation correction artifacts may simulate metabolic activity. The aim of this exhibit is to review imaging features of commonly encountered musculoskeletal lesions on FDG PET-CT. An understanding of these imaging features can help improve diagnostic accuracy and prevent unnecessary biopsy or surgery.

### **TABLE OF CONTENTS/OUTLINE**

Review the FDG PET-CT appearance of benign musculoskeletal lesions, including fibrous dysplasia, aneurysmal bone cyst,
 Paget disease, benign cartilaginous neoplasms, osteonecrosis, osteomyelitis, bone island, heterotopic ossification/myositis
 ossificans, and other lesions.
 Discuss the limitations of FDG PET in the evaluation of osseous lesions.
 Create an awareness
 that benign musculoskeletal lesions are frequently FDG avid.
 Review the FDG appearance of musculoskeletal findings that may
 simulate neoplasm including arthritis and brown fat.
 Discuss attenuation correction artifacts and other technical
 considerations.

# MK227-ED-WEB8

**Role of MRI in the Postoperative Assessment of Meniscus** 

Wednesday, Nov. 30 12:45PM - 1:15PM Room: MK Community, Learning Center Station #8

#### **Participants**

Takeshi Wada, MD, Tokyo, Japan (*Presenter*) Nothing to Disclose Taiki Nozaki, MD, Orange, CA (*Abstract Co-Author*) Nothing to Disclose Saya Horiuchi, MD, Tokyo, Japan (*Abstract Co-Author*) Nothing to Disclose Jay Starkey, MD, Tokyo, Japan (*Abstract Co-Author*) Nothing to Disclose Midori Enokido, Tokyo, Japan (*Abstract Co-Author*) Nothing to Disclose Tomoki Kyosaka, MD, Tokyo, Japan (*Abstract Co-Author*) Nothing to Disclose Takahisa Kurosaki, MD, Tokyo, Japan (*Abstract Co-Author*) Nothing to Disclose Masaki Matsusako, MD, PhD, Tokyo, Japan (*Abstract Co-Author*) Nothing to Disclose Yasuyuki Kurihara, MD, Tokyo, Japan (*Abstract Co-Author*) Nothing to Disclose

#### **TEACHING POINTS**

The purpose of this exhibit is To demonstrate indications and techniques used in meniscal surgeries to understand the normal MRI findings of the postoperative meniscus. To teach MRI findings of major complications of the postoperative meniscus. To show new treatments for meniscal tears, including arthroscopic centralization of extruded meniscus for restoring the load bearing function of the lateral meniscus.

### TABLE OF CONTENTS/OUTLINE

1. Anatomy of meniscus as relates to meniscal surgery, especially the vascular supply of the meniscus.

- 2. Normal MRI findings of the postoperative meniscus.
- -Post partial meniscectomy, post meniscal repair.

3. MRI findings of complications of postoperative meniscus.

-Residual meniscal tear, recurrent meniscal tear, subchondral insufficiency fracture of knee after arthroscopic meniscectomy and development of osteoarthritis as a chronic complication.

4. Arthroscopic centralization: indication, procedure details, post-operative MRI findings and prognosis.

# MK335-SD-WEB2

### Prevalence and Significance of Radiographic Sacrolliitis in a Large Inflammatory Bowel Disease Population

Wednesday, Nov. 30 12:45PM - 1:15PM Room: MK Community, Learning Center Station #2

#### Participants

Garrett L. Dejesus, MD, Los Angeles, CA (*Presenter*) Nothing to Disclose Angelica Nangit, MD, Los Angeles, CA (*Abstract Co-Author*) Nothing to Disclose Daphne Scaramangas-Plumley, MD, Los Angeles, CA (*Abstract Co-Author*) Nothing to Disclose Xiaofei Yan, MS, Los Angeles, CA (*Abstract Co-Author*) Nothing to Disclose Dalin Li, PhD, Los Angeles, CA (*Abstract Co-Author*) Nothing to Disclose Thomas J. Learch, MD, Los Angeles, CA (*Abstract Co-Author*) Nothing to Disclose Dermot Mcgovern, MD, Los Angeles, CA (*Abstract Co-Author*) Nothing to Disclose Micheal H. Weisman, MD, Los Angeles, CA (*Abstract Co-Author*) Nothing to Disclose

### PURPOSE

To determine the computed tomographic prevalence of sacroiliitis (SI) in a large inflammatory bowel disease (IBD) population and identify risk factors associated with the development of SI.

### **METHOD AND MATERIALS**

1,247 consecutive patients from our IBD clinic, 350 with ulcerative colitis (UC), and 897 with Crohn's disease (CD) were investigated as long as they had a pre-existing computed tomography (CT) of the abdomen and pelvis for symptoms unrelated to SI joint pain (GE Lightspeed 64-slice VCT scanner, 2.5-5mm slice acquisition, KVp 100-140, automated mA-s). These CTs were re-interpreted for evidence of sacroiliac joint disease. Each sacroiliac joint was graded based on the modified New York Criteria. Each patient was classified as having no disease, suspected disease or definite disease. Gender, age, type of IBD, HLA-B27 status, and IBD serologies (ASCA, antiCBir1,anti-OMPc, ANCA) were also analyzed.

### RESULTS

Prevalence of definite and suspected SI was found in 16.1% and 19.4% in CD and UC, respectively. The prevalence of definite SI was 8.7% and 8.1% in CD and UC, respectively. In patients with SI (definite and suspicious), 57% were male and 43% were female. When looking only at the definite group, there were 68 % males and 32% females (p=0.002). Of significance,16% of patients in the definite SI group were positive for HLA-B27 (OR 4.36, p=0.006). In the suspicious group, 8% of patients were positive for HLAB27. Definite SI was associated with: anti-Cbir1 (p=0.002) in CD, and ASCA (p=0.05) in UC.

### CONCLUSION

In this study, we observed an overall SI prevalence of 17% in our IBD cohort. Historically, UC and CD occur evenly between genders. However, when gender and SI in IBD were compared, there were more males in the definite group. Significant associations with clinically relevant subsets of IBD defined by serological markers were observed. The findings suggest that SI and spondylitis in the IBD population are different pathologic entities, with unique genetic risks, compared with the pure ankylosing spondylitis population.

# **CLINICAL RELEVANCE/APPLICATION**

Radiographic interpretation of the true prevalence has allowed further insight into the pathogenesis of the association between IBD and ankylosing spondylitis. Early identification and treatment of these musculoskeletal manifestations can potentially improve quality of life and prevent debility.

# MK336-SD-WEB3

Recurrences Evaluation in Soft Tissue Extravisceral Tumors: The Contrast Enhanced Ultrasound in Comparison with Magnetic Resonance Imaging

Wednesday, Nov. 30 12:45PM - 1:15PM Room: MK Community, Learning Center Station #3

# Participants

Giuseppe Russo, Genoa, Italy (*Abstract Co-Author*) Nothing to Disclose Simona Pozza, MD, Torino, Italy (*Abstract Co-Author*) Nothing to Disclose Guido Regis, MD, Torino, Italy (*Abstract Co-Author*) Nothing to Disclose Raimondo Piana, Turin, Italy (*Abstract Co-Author*) Nothing to Disclose Alessandra Linari, MD, Turin, Italy (*Abstract Co-Author*) Nothing to Disclose Armanda De Marchi, MD, Torino, Italy (*Presenter*) Nothing to Disclose Michele Boffano, MD, Torino, Italy (*Abstract Co-Author*) Nothing to Disclose Alda Borre, MD, Torino, Italy (*Abstract Co-Author*) Nothing to Disclose

### PURPOSE

The aim of this study is to evaluate the diagnostic performance of Contrast Enhanced Ultrasound (CEUS) compared with Magnetic Resonance Imaging (MRI), in the soft tissue malignant tumors recurrences identification, considering the histological diagnosis as reference standard.

### METHOD AND MATERIALS

An analysis of patients treated for extravisceral malignant soft tissue tumors in a national reference center between January 2012 and December 2015 was performed.Forty patients were identified (men/women 22:18; age range 22-94 years) with following inclusions criteria: age over 18; pathologic report of soft tissue malignant tumors at diagnosis; complete follow-up with CEUS and MRI. We excluded those patients with CEUS or MRI not assessable and the absence of a definitive histologic report at biopsy or at resected surgical specimen. We have calculated sensitivity, specificity, positive predictive value (PPV), negative predictive value (NPV), likelihood ratio for positive value (LH+), likelihood ratio for negative values (LH-), and CEUS and MRI diagnostic accuracy.

# RESULTS

The sensitivity and specificity of CEUS are respectively 1 and 0,67 with VPP=0,97; VPN=1; LH+=3; LH-=0 and diagnostic accuracy=0,98.MRI shows sensitivity=0,97; specificity= 0,67; VPP=0,97; VPN=0,67; LH+=2,9; LH-=0,04 and diagnostic accuracy=0,95.

### CONCLUSION

The CEUS diagnostic accuracy is significantly high, and is superior to MRI in locoregional recurrences detection in patients in followup to extravisceral soft tissue malignant tumors. Negativity at CEUS significantly excludes the absence of local recurrences.

### **CLINICAL RELEVANCE/APPLICATION**

The European Society of Oncology (ESMO) clinical practice guidelines published in 2014 found that there are a few published data to indicate the optimal routine follow-up. The use of MRI to detect local recurrences it has not been demonstrated that is beneficial or cost effective compared clinical assessment of the primary site. There are actually no data concerning the role of CEUS in local recurrences detection compared with MRI. Considering the CEUS feasibility and cost effectiveness, the purpose of this study is to evaluate the diagnostic performance of CEUS to propose its application in soft tissue malignant tumors follow-up.

# MK337-SD-WEB4

Posterior Decentering of the Humeral Head on Shoulder MR Arthrography: Significant Association with Posterior Synovial Proliferation

Wednesday, Nov. 30 12:45PM - 1:15PM Room: MK Community, Learning Center Station #4

#### Awards

### **Student Travel Stipend Award**

#### Participants

Gabin Yun, MD, Seongnam-si, Korea, Republic Of (*Presenter*) Nothing to Disclose Joong Mo Ahn, MD, PhD, Pittsburgh, PA (*Abstract Co-Author*) Nothing to Disclose Yusuhn Kang, MD, Seoul, Korea, Republic Of (*Abstract Co-Author*) Nothing to Disclose Joon Woo Lee, MD, PhD, Sungnamsi, Korea, Republic Of (*Abstract Co-Author*) Nothing to Disclose Eugene Lee, Seongnam-Si, Korea, Republic Of (*Abstract Co-Author*) Nothing to Disclose Heung Sik Kang, Gyeonggi-Do, Korea, Republic Of (*Abstract Co-Author*) Nothing to Disclose Joo Han Oh, MD, Seongnam, Korea, Republic Of (*Abstract Co-Author*) Nothing to Disclose

#### PURPOSE

To retrospectively evaluate MR imaging findings associated with posterior decentering of the humeral head on shoulder MR arthrography.

# METHOD AND MATERIALS

A total of 255 shoulder MR arthrograms (MRAs) were obtained during a 10-month period. MRAs in patients with posterior decentering of the humeral head (n = 27) were reviewed and compared with those of randomly selected control group without posterior decentering (n = 54). MRA was evaluated for posterior factors (glenohumeral joint space narrowing, posterior synovial proliferation), fatty degeneration of rotator cuff, anterior factors (subcoraroid bursa effusion, rotator interval tear), posterior labral abnormality, by two experienced observers who reached in concensus. The Fisher exact test, linear by linear association was used for comparison of categorical data, and multivariate stepwise logistic regression analysis, pooled kappa coefficient was performed.

### RESULTS

Posterior decentering of the humeral head was found in 27 (14%) patients. At univariate analysis, posterior synovial proliferation (29.6% [8/27] in posterior decentering group vs 7.4% [4/54] in control group; p = .008), fatty infiltration of supraspinatus, infraspinatus and teres minor (linear by linear association 8.090, 6.797 and 5.608, respectively; p = .004, .009 and .018, respectively), rotator interval tear (55.6% [15/27] vs 31.5% [17/54]; p < .037) were more frequently found in posterior decentering group with a statistical significance. At multivariate analysis, only the posterior synovial proliferation was significantly associated with posterior decentering of the humeral head (Odds ratio, 5.263; 95% CI, 1.418 – 19.532).

### CONCLUSION

Posterior decentering of the humeral head is most significantly associated with posterior synovial proliferation. In addition, rotator cuff interval abnormality as well as rotator cuff atrophy is associated with posterior decentering to a lesser extent.

### **CLINICAL RELEVANCE/APPLICATION**

Awareness of the association of the posterior decentering of the humeral head with the described MR findings above will facilitate an effective interpretation of shoulder MRA.

Soft Tissue Sarcoma Response to Two Cycles of Neoadjuvant Chemotherapy: A Multi-reader Analysis of MRI Findings and Agreement with RECIST Criteria and Change in SUVmax

Wednesday, Nov. 30 12:45PM - 1:15PM Room: MK Community, Learning Center Station #6

# Participants

Jennifer L. Favinger, MD, Seattle, WA (*Abstract Co-Author*) Nothing to Disclose Daniel S. Hippe, MS, Seattle, WA (*Abstract Co-Author*) Research Grant, Koninklijke Philips NV; Research Grant, General Electric Company Saeed Elojeimy, MD, PhD, Seattle, WA (*Abstract Co-Author*) Nothing to Disclose

Eira S. Roth, MD, Pittsburgh, PA (*Abstract Co-Author*) Nothing to Disclose Antoinette Lindberg, Seattle, WA (*Abstract Co-Author*) Nothing to Disclose Darin J. Davidson, Seattle, WA (*Abstract Co-Author*) Nothing to Disclose Alice S. Ha, MD, Seattle, WA (*Presenter*) Grant, General Electric Company

### PURPOSE

When soft tissue sarcomas (STS) are treated with neoadjuvant chemotherapy (NC), the number of cycles of NC is usually dependent on the tumor's initial response. Popular methods to assess tumor response include RECIST criteria which relies solely on tumor size, and maximum SUV reduction in PET which requires an expensive and high radiation test. We hypothesized that contrast-enhanced MRI may offer a good alternative by providing additional information beyond tumor size.

### **METHOD AND MATERIALS**

Following IRB approval, a retrospective review identified patients with STS who underwent both PET and MRI before and after two cycles of NC. Five readers independently examined the MR exams for: changes in size, T2 or T1 signal, necrosis and degree of enhancement. Readers then made a subjective binary assessment of tumor response to therapy. Each reader repeated the anonymized randomized reading at least 2 weeks apart. 18 F-FDG PET exams were interpreted by a single nuclear medicine specialist. The maximum standardized uptake values (SUVmax) for pre and post-chemotherapy exams were compared with greater than 35% reduction defined as "response" for this study. Intra- and inter-reader agreement was assessed using Cohen's kappa and Light's kappa, respectively.

### RESULTS

Twenty cases were identified, of which 9 (45%) were responders and 11 were non-responders by SUVmax. Using all MRI criteria, 43% were classified as responders based on MRI findings and 1.5% as responders by RECIST criteria alone (30% decrease in longest dimension). Using PET as the reference, the sensitivity and specificity of the MRI diagnosis for response using all findings was 50% and 63%, respectively. There was fair to moderate intra- (kappa = 0.37) and inter-reader agreement (kappa = 0.48) for the MRI diagnosis of response. None of the individual MRI findings were significantly different between the PET responders and non-responders.

# CONCLUSION

By our assessment, there is poor correlation between tumor response by RECIST criteria versus PET SUVmax. In addition, varying MR features did not help in diagnosing tumor response. Imaging of tumor response remains a challenging area that requires further research.

# **CLINICAL RELEVANCE/APPLICATION**

Accurate assessment of post treatment response on imaging is crucial in soft tissue sarcoma treatment.

# Cancer Immunotherapy and Pseudoprogression: Spectrum of Imaging Findings

Wednesday, Nov. 30 12:45PM - 1:15PM Room: MS Community, Learning Center Hardcopy Backboard

#### Awards

### **Identified for RadioGraphics**

#### **Participants**

Gary X. Wang, MD, PhD, Boston, MA (*Presenter*) Nothing to Disclose Vikram Kurra, MD, Cambridge, MA (*Abstract Co-Author*) Nothing to Disclose Justin F. Gainor, MD, Boston, MA (*Abstract Co-Author*) Nothing to Disclose Ryan J. Sullivan, MD, Boston, MA (*Abstract Co-Author*) Nothing to Disclose Keith Flaherty, MD, Boston, MA (*Abstract Co-Author*) Nothing to Disclose Susanna I. Lee, MD, PhD, Boston, MA (*Abstract Co-Author*) Nothing to Disclose Florian J. Fintelmann, MD, FRCPC, Boston, MA (*Abstract Co-Author*) Consultant, McKesson Corporation

# **TEACHING POINTS**

Immunomodulatory antibodies are fast-evolving cancer immunotherapeutic agents recently approved for advanced melanoma, lung and renal cell cancer, and multiple myeloma Immunotherapy differs from conventional chemotherapy in action mechanism, treatment response patterns, and treatment-related toxicity Treatment response may be assessed by the Immune-Related Response Criteria (irRC) or the Response Evaluation Criteria in Solid Tumors (RECIST 1.1) Some patients undergoing immunotherapy can transiently develop new or enlarging lesions in any organ system as part of the treatment response, termed pseudoprogression Pseudoprogression should be differentiated from true progression as the former indicates treatment response Immunotherapy can stimulate the immune system to cause autoimmune reactions, called immune-related adverse events (irAE) irAE can affect many organ systems, some with specific imaging findings

### **TABLE OF CONTENTS/OUTLINE**

General principles of immunomodulatory cancer immunotherapy Comparison of imaging response criteria Response Evaluation Criteria in Solid Tumors (RECIST 1.1) Immune-Related Response Criteria (irRC) Multi-modality multi-organ system imaging findings of atypical tumor response during immunotherapy aka pseudoprogression Multi-modality multi-organ system imaging findings of immune-related adverse events

# **Honored Educators**

Presenters or authors on this event have been recognized as RSNA Honored Educators for participating in multiple qualifying educational activities. Honored Educators are invested in furthering the profession of radiology by delivering high-quality educational content in their field of study. Learn how you can become an honored educator by visiting the website at: https://www.rsna.org/Honored-Educator-Award/

Susanna I. Lee, MD, PhD - 2013 Honored Educator

# NM126-ED-WEB11

Prostate Specific Membrane Antigen (PSMA) PET/CT and PET/MRI: Clinical Utility in Prostate Cancer and Other Malignancies, Normal Patterns, Pearls and Pitfalls in Interpretation

Wednesday, Nov. 30 12:45PM - 1:15PM Room: S503AB Station #11



Awards Cum Laude Identified for RadioGraphics

#### **Participants**

Michael S. Hofman, MBBS, East Melbourne, Australia (*Presenter*) Nothing to Disclose Rodney Hicks, MBBS, East Melbourne, Australia (*Abstract Co-Author*) Nothing to Disclose Tobias Maurer, Munich, Germany (*Abstract Co-Author*) Nothing to Disclose Matthias J. Eiber, MD, Muenchen, Germany (*Abstract Co-Author*) Nothing to Disclose

# **TEACHING POINTS**

1. PSMA PET represents a new modality for imaging prostate cancer with superior sensitivity and specificity compared to conventional imaging, and frequent ability to identify <10mm micro-metastatic disease.2. Despite the terminology "prostate specific", PSMA is a folate hydrolase cell surface glycoprotein expressed in a range of normal tissues and other benign and malignant pathologic processes.3. Causes of interpretative pitfalls include uptake in physiologic sites such as coeliac, stellate or sacral ganglia, uptake in benign entities such as osteoblastic reaction in degenerative disease or fractures, and benign neoplasms.4. The role of PSMA PET continues to evolve as high PSMA cell surface expression is also seen in some other malignancies, such as renal cell and thyroid carcinoma.

### **TABLE OF CONTENTS/OUTLINE**

Ga-68 PSMA PET/CT and PET/MRI is a rapidly evolving modality for imaging prostate cancer. The purpose of this exhibit is:1. To review clinical applications in prostate cancer including primary staging biochemical recurrence, and restaging following systemic therapy.2. Describe advantages compared to conventional imaging including CT, bone scintigraphy, Choline PET and MRI.3. Discuss the pearls and pitfalls in the interpretation of this new modality.4. Describe potential applications of PSMA PET in other diseases.

Retrospective Review of Intracranial Meningioma on C11-Choline PET/CT and Contrast Enhanced MRI

Wednesday, Nov. 30 12:45PM - 1:15PM Room: S503AB Station #6

FDA Discussions may include off-label uses.

#### Awards

**Student Travel Stipend Award** 

### **Participants**

Kevin K. Casper, MD, Rochester, MN (*Presenter*) Nothing to Disclose
Christopher H. Hunt, MD, Rochester, MN (*Abstract Co-Author*) Nothing to Disclose
Andrew C. Homb, MD, Louisville, KY (*Abstract Co-Author*) Nothing to Disclose
Val J. Lowe, MD, Rochester, MN (*Abstract Co-Author*) Research Grant, General Electric Company Research Grant, Siemens AG
Research Grant, Eli Lilly and Company Advisory Board, Bayer AG
Brad Kemp, PhD, Rochester, MN (*Abstract Co-Author*) Nothing to Disclose
Derek R. Johnson, MD, Rochester, MN (*Abstract Co-Author*) Consultant, F. Hoffmann-La Roche Ltd
Ajit H. Goenka, MD, Rochester, MN (*Abstract Co-Author*) Nothing to Disclose
Geoffrey B. Johnson, MD, PhD, Rochester, MN (*Abstract Co-Author*) Nothing to Disclose

#### PURPOSE

The aim of the study is to evaluate the feasibility of using C11-Choline PET/CT to identify intracranial tumors such as meningiomas in a large population.

### **METHOD AND MATERIALS**

A retrospective chart review was performed of 2933 consecutive male patients having undergone C11-choline PET/CT according to standard protocol for prostate cancer between 9/2005 and 2/2016. Standard protocol extends from the skull base through the proximal thighs. All scans were reconstructed with standard 3D OSEM. Patients with possible intracranial tumors noted in their medical record were included. These included incidentally discovered intracranial lesions on choline PET/CT and other imaging. Diagnoses were confirmed with pathology or comparison to contrast enhanced MRI of the head and at least 6 months of follow-up imaging showing stability or slow growth. Maximum standardized uptake values (SUV) of each lesion were compared with background uptake. Data was collected using the electronic medical record, GE Advantage Workstations, GE Picture Archiving Communication System (PACS), and OsiriX 64 bit DICOM Viewing and Storage software. Collected data was analyzed using JMP statistical software using the student's t-test for continuous variables and the chi-square test for categorical variables.

#### RESULTS

All identified presumed and confirmed meningiomas were choline-avid on all scans well above background activity. Eleven patients demonstrated thirteen meningiomas present on twenty-eight C-11 Choline PET/CT scans. Standardized uptake value maximum in these meningiomas averaged 2.8 +/- 1.3 (SD) with C11-Choline dose of 18.6 +/- 0.9 mCi, and uptake time of 4.6 min +/- 1.0 min. Background activity in nearby brain, CSF and bone was very low. All other intracranial tumors detected were much less choline avid or non-choline avid, including three presumed pituitary adenomas and a schwannoma.

### CONCLUSION

Thirteen intracranial meningiomas confirmed by pathology or follow-up imaging demonstrated clear avidity on C11-Choline PET/CT and represent the largest such series to date.

### **CLINICAL RELEVANCE/APPLICATION**

C11-Choline PET/CT may be a useful modality for the detection and evaluation of metabolically active intracranial meningiomas. Further prospective work is needed to evaluate the role of choline C11-PET/CT for evaluation after local or systemic therapy.

### **Honored Educators**

Presenters or authors on this event have been recognized as RSNA Honored Educators for participating in multiple qualifying educational activities. Honored Educators are invested in furthering the profession of radiology by delivering high-quality educational content in their field of study. Learn how you can become an honored educator by visiting the website at: https://www.rsna.org/Honored-Educator-Award/

Geoffrey B. Johnson, MD, PhD - 2015 Honored Educator

Optimum FDG PET/CT Volumetric Parameters in Patients with Locally Advanced Non-Small Cell Lung Cancer: Results from ACRIN 6668/RTOG 0235 Trial

Wednesday, Nov. 30 12:45PM - 1:15PM Room: S503AB Station #7

#### Awards

### **Student Travel Stipend Award**

#### **Participants**

Ali Salavati, MD, MPH, Philadelphia, PA (*Presenter*) Nothing to Disclose Fenghai Duan, PhD, Providence, RI (*Abstract Co-Author*) Nothing to Disclose Bradley S. Snyder, MS, Providence, RI (*Abstract Co-Author*) Nothing to Disclose Bo Wei, Providence, RI (*Abstract Co-Author*) Nothing to Disclose Sina Houshmand, MD, Philadelphia, PA (*Abstract Co-Author*) Nothing to Disclose Benjapa Khiewvan, MD, Philadelphia, PA (*Abstract Co-Author*) Nothing to Disclose Adam Opanowski, Philadelphia, PA (*Abstract Co-Author*) Nothing to Disclose Barry A. Siegel, MD, Saint Louis, MO (*Abstract Co-Author*) Consultant, Merrimack Pharmaceuticals, Inc Consultant, Siemens AG Advisory Board, General Electric Company Stockholder, Radiology Corporation of America Spouse, Speaker, Siemens AG Mitchell Machtay, MD, Cleveland, OH (*Abstract Co-Author*) Research funded, AbbVie Inc; Research funded, Stemnion, Inc; Research funded, Celgene Corporation Abass Alavi, MD, Philadelphia, PA (*Abstract Co-Author*) Nothing to Disclose

### PURPOSE

In recent years, many studies have demonstrated the value of volumetric FDG-PET/CT parameters as independent prognostic factors in patients with NSCLC. We aimed to determine the optimal cut-off points for pretreatment volumetric FDG-PET/CT parameters and examine the discriminatory ability of these parameters over time in predicting overall survival(OS) among patients enrolled in ACRIN 6668/RTOG 0235.

# METHOD AND MATERIALS

Patients with inoperable stage IIB/III NSCLC and evaluable FDG-PET/CT scans were included. Pretreatment FDG-PET/CT scans were quantified using semiautomatic adaptive contrast-oriented thresholding and local background partial volume effect correction algorithms. For each patient, the following whole-body FDG-PET/CT indices were measured:metabolic tumor volume(MTV), total lesion glycolysis(TLG), SUVmax, SUVmean, partial volume corrected TLG(pvcTLG) and pvcSUVmean. The association between each index and patient outcome was assessed using Cox proportional hazards regression.Optimal cut-off points were estimated using recursive binary partitioning in a conditional inference framework. Finally, the discriminatory ability of each index was examined using time-dependent receiver operating characteristic(ROC) curves and corresponding area under the curve(AUC(t)).

### RESULTS

196 patients were included. Pretreatment MTV, TLG and pvcTLG were independently prognostic of OS, while SUVmax,SUVmean and pvcSUVmean were not prognostic.Optimal cut-off points were 175.0, 270.9, and 35.5 cc for TLG, pvcTLG, and MTV, respectively. In time-dependent ROC analysis, AUC(t) for MTV and TLG was uniformly higher than that of the SUV measures over all time points.The discriminatory ability of pvc and non-pvc counterparts appeared to be similar.

### CONCLUSION

Pretreatment whole-body volumetric FDG-PET/CT parameters, MTV, TLG and pvcTLG, are strongly prognostic for OS, and have uniformly better discriminatory ability over time than corresponding SUV measures. After validation in future studies, it is possible that the suggested optimal cut-off points could be incorporated in routine clinical practice for more accurate prognostication and metabolic staging of patients with locally advanced NSCLC.

# **CLINICAL RELEVANCE/APPLICATION**

Defining optimal cut-off points for volumetric FDG-PET/CT parameters, proven independent prognostic factors in patients with locally advanced NSCLC, would further the utilization of these biomarkers in routine clinical practice.

# NM235-SD-WEB8

### Microsphere Localization Using PET/MRI Following Y-90 Radioembolization

Wednesday, Nov. 30 12:45PM - 1:15PM Room: S503AB Station #8

#### **Participants**

Sarah Mohajeri Moghaddam, MD, MPH, Rochester, NY (*Presenter*) Nothing to Disclose Zachary M. Nuffer, MD, Rochester, NY (*Abstract Co-Author*) Nothing to Disclose Alan W. Katz, MD, Rochester, NY (*Abstract Co-Author*) Nothing to Disclose Ashwani K. Sharma, MD, Rochester, NY (*Abstract Co-Author*) Nothing to Disclose

### PURPOSE

To evaluate:1) Feasibility to Y-90 PET/MRI (Positron Emission Tomography/Magnetic Resonance Imaging)2) Technical success of Y-90 radioembolization 3) Presence of extrahepatic microsphere deposition using Y-90 PET/MRI

### **METHOD AND MATERIALS**

The decay of Y-90 microspheres can be visualized by PET due to a small decay branch that results in electron-positron pair production. Y-90 PET imaging has been performed using PET/CT, but is only beginning to be reported using PET/MRI. As part of an ongoing study, we evaluated the deposition pattern of Y-90 microspheres on post-radioembolization PET/MRI exams. At the time of submission of this abstract, 3 exams have been evaluated. Deposition patterns were classified as either 1) targeted tumor hepatic vascular territory only, 2) targeted and nontargeted hepatic vascular territories, or 3) hepatic and extrahepatic vascular territories. All exams were performed on a Siemens 3T PET/MRI system.

#### RESULTS

All 3 Y-90 PET/MRI exams are of acceptable image quality and demonstrate microsphere deposition in the target vascular territory only. Refer to Figure 1 for example images.

### CONCLUSION

Y-90 PET/CT is superior to Y-90 bremsstrahlung SPECT/CT for the assessment of target and non-target activity. While this is an ongoing study, our initial results suggest that Y-90 PET/MRI is feasible and can be used to evaluate for the technical success of Y-90 radioembolization and the presence of extrahepatic microsphere deposition. We would need further studies to compare Y-90 PET/MR with Y-90 PET/CT.

#### **CLINICAL RELEVANCE/APPLICATION**

Not only can post-treatment Y-90 PET/MRI be used evaluate the technical success of Y-90 embolization, it can also provide doseresponse information for developing future treatment-planning models.

# Normal Aging and Patterns of Regional Brain FDG Uptake

Wednesday, Nov. 30 12:45PM - 1:15PM Room: S503AB Station #9

#### **Participants**

Sara Pourhassan Shamchi, MD, Philadelphia, PA (*Presenter*) Nothing to Disclose Sahra Emamzadehfard, MD, MPH, Philadelphia, PA (*Abstract Co-Author*) Nothing to Disclose Koosha Paydary, MD, MPH, Philadelphia, PA (*Abstract Co-Author*) Nothing to Disclose Thomas J. Werner, Philadelphia, PA (*Abstract Co-Author*) Nothing to Disclose Poul Flemming Hoeilund Carlsen, Odense, Denmark (*Abstract Co-Author*) Nothing to Disclose Abass Alavi, MD, Philadelphia, PA (*Abstract Co-Author*) Nothing to Disclose

# PURPOSE

Brain structure and function changes as a result of normal aging. Modern in vivo functional imaging modalities such as 18F-FDG PET provide a powerful tool to study and measure these alterations. However, in order to correctly diagnose pathologic states, it is highly important to recognize the normal age-related changes. The goal of current study is to evaluate the age-related changes in regional brain 18F-FDG uptake in normal healthy population.

#### **METHOD AND MATERIALS**

This study is part of the Cardiovascular Molecular Calcification Assessed by 18F-NaF/18F-FDG PET/CT (CAMONA). CAMONA was approved by the Danish National Committee on Health Research Ethics registered at ClinicalTrials.gov (NCT01724749), and conducted in accordance with the Declaration of Helsinki. 40 normal healthy subjects were prospectively recruited in group A (Age: 22-32 years) and B (Age: 56-66 years) and underwent 18F-FDG PET/CT. Static PET images were obtained 180 minutes following 18F-FDG injection. Supratentorial and cerebellar FDG uptake was measured by manual placement of regions of interest and SUV mean values were calculated using OsirixMD software.

### RESULTS

The mean age of the patients in group A was  $26.1\pm3.4$  versus  $62\pm3.9$  for group B. There were 10 females (50%) in group A compared to 12 females in group B (60%) without significant difference (p=0.37). Mean SUV of cerebellum was  $6.84\pm1.25$  for the young subjects (group A) verus  $6.04\pm0.99$  among older individuals (group B)(p=0.03). Mean SUV of supratentorial brain was  $9.34\pm2.37$  for the young subjects (group A) compared to  $7.20\pm0.98$  among older participants (group B)(p<0.001). More interestingly, Mean SUV of supratentorial brain was significantly higher among female healthy volunteers in both groups (p= 0.040 and 0.034, respectively).

# CONCLUSION

These results demonstrate an overall decrease in Brain 18F-FDG uptake with aging, which is more accentuated in supratentorial areas.

### **CLINICAL RELEVANCE/APPLICATION**

These results may help to better understand the normal age-related changes of Brain function and FDG uptake, and to avoid interpretting them as pathologic findings.

# NM237-SD-WEB10

Adaptive Protocols with New High Sensitivity PET/CT Scanner for Clinical Routine with Innovative Radiotracers

Wednesday, Nov. 30 12:45PM - 1:15PM Room: S503AB Station #10

# Participants

Erwan Gabiache, MD, MSc, TOULOUSE, France (*Presenter*) Nothing to Disclose Delphine Vallot, Toulouse, France (*Abstract Co-Author*) Nothing to Disclose Severine Brillouet, Toulouse, France (*Abstract Co-Author*) Nothing to Disclose Mathilde Bauriaud, Toulouse, France (*Abstract Co-Author*) Nothing to Disclose Lawrence Dierickx, Toulouse, France (*Abstract Co-Author*) Nothing to Disclose Frederic Courbon, MD,PhD, Toulouse, France (*Abstract Co-Author*) Research Grant, General Electric Company Slimane Zerdoud, Toulouse, France (*Abstract Co-Author*) Nothing to Disclose Olivier Caselles, PhD, Toulouse, France (*Abstract Co-Author*) Grant, General Electric Company

### PURPOSE

To take benefit of a new generation high sensitivity BGO non-TOF PET/CT system and reduce injected doses, we use new BMI based 18-FDG prescription rules. For new fluoro and non-fluoro tracers, maximum dose may be limited by availability or price. Considering new 68Ga DOTANOC, the short half-life (68 min) leads to new patient worflow constraints. The aim of this study is to adapt both our prescription rules and acquisition parameters to these radiotracers new constraints.

# **METHOD AND MATERIALS**

In this study 18F-CHOLINE,18F-DOPA and generic 68Ga radiolabeled tracers are considered.Due to organizational and delivery constraints, 97 18F-CHOLINE exams were scheduled by sessions of 6 to 7 male patients. As the maximum available dose per session is limited and to maintain the patient exam rate, the prescription rule is based on a low weight based posology adapted to our PET-CT, with a maximum patient dose of 300 MBq.18F-DOPA is more expensive and of very low availability, we used a constant standard dose of 100 MBq and a weight adapted time per step (2 min baseline). Results relative to 15 patients are presented here.These first experiences were used to define the best prescription rules for 68Ga DOTANOC, integrating the specific constraints of maximum available dose per elution with our 1.85 GBq 68Ge generator, and the fast physical decrease of 68Ga.

### RESULTS

Thanks to low weight posology, dose was kept under maximum allowed for 18F-CHOLINE (260 MBq at maximum). Mean activity was 156.6MBq for an average BMI of 27.5.For 18F-DOPA, time per step was ranging from 90s to 180s for average posology of 1.54MBq/kg and BMI of 23.5.For 68Ga-DOTANOC a mixed protocol based on weight based posology and time per step modulation is used. As the expected available activity per synthesis run and per patient is in the range 100-200 MBq (based on two patients per run), we decided to use a 2 MBq/kg weight prescription and modulate the duration of each based to compensate physical decay with a 2 min baseline for the step centered on the abbdomen.

# CONCLUSION

In this study we demonstrated the usefullness of both weight based prescription and time per step modulation for new generation of 68Ga radiotracers, taking advantage of the high sensitivity of our PET/CT scanner.

# **CLINICAL RELEVANCE/APPLICATION**

This kind of approach will be more and more prevalent in the future with new 68Ga radiolabeled tracers.

### NR199-ED-WEB9

Pocket Guide for DWI and DTI Derived Biomarkers in CNS: Pathophysiological Basis and Clinical Meaning from ADC to Kurtosis

Wednesday, Nov. 30 12:45PM - 1:15PM Room: NR Community, Learning Center Station #9

# Awards

# Cum Laude

#### Participants

Teodoro Martin, MD, Jaen, Spain (*Presenter*) Nothing to Disclose Jose P. Martinez Barbero, MD, PhD, Granada, Spain (*Abstract Co-Author*) Nothing to Disclose Antonio Luna SR, MD, Jaen, Spain (*Abstract Co-Author*) Nothing to Disclose

### **TEACHING POINTS**

1.Review the physical basis of DWI and DTI studies in central nervous system (CNS).2.Describe from an educational point of view, the main signal intensity analysis models: Monocompartmental and Bicompartmental (Intravoxel incoherent motion-IVIM and Kurtosis).3.Perform a pocket guide to enumerate and explain, through different clinical scenarios, the physical origin, biological meaning and practical clinical usefulness of the main biomarkers derived from these models.

### TABLE OF CONTENTS/OUTLINE

Physical basis and technical adjustments for DWI and DTI acquisition and analysis in Introduction2. 1. CNS.a. Monocompartmental analysis.b. Bicompartmental analysis -IVIM model -Kurtosis model3. Pocket guide for DWI and DTI biomarkers derived a. Apparent Diffusion Coefficient (ADC) b. Eigenvalues and Mean Diffusivity (MD). Fractional Anisotropy (FA) d. Axial Diffusivity (AD) e. Radial Diffusivity (RD) f. Diffusion coefficient (D) с. Pseudo-diffusion coefficient (D\*) h. Perfusion fraction (f) i. Mean kurtosis (MK) j. Diffusional kurtosis (DK) g.

# Neuroradiological Findings Related to Zika Epidemic: Experience from a Brazilian University Hospital

Wednesday, Nov. 30 12:45PM - 1:15PM Room: NR Community, Learning Center Station #2

#### Awards

### **Student Travel Stipend Award**

#### Participants

Emerson d. Casagrande, MD, Niteroi, Brazil (*Presenter*) Nothing to Disclose Cristina A. Fontes, MD, Niteroi, Brazil (*Abstract Co-Author*) Nothing to Disclose Alair Augusto S. Santos, MD, Niteroi, Brazil (*Abstract Co-Author*) Nothing to Disclose Victor M. Bussed, Niteroi, Brazil (*Abstract Co-Author*) Nothing to Disclose Daniel G. Neves, MD, Rio de Janeiro, Brazil (*Abstract Co-Author*) Nothing to Disclose Alessandro S. Melo, MD, PHD, Niteroi, Brazil (*Abstract Co-Author*) Nothing to Disclose Edson Marchiori, MD, PhD, Rio de Janeiro, Brazil (*Abstract Co-Author*) Nothing to Disclose Pamela Santos, Niteroi, Brazil (*Abstract Co-Author*) Nothing to Disclose

# PURPOSE

Present the imaging aspects in the three target groups affected by Zika virus infection, as follows: adults who developed acute neurological syndrome, newborns with vertical infection with neurological disorders and pregnant women who presented suggestive exantematic fever syndrome by Zika.

# METHOD AND MATERIALS

Since January 2016 we received patients with exanthematic fever suggesting Zika to perform imaging exams, and we divided these patients, as described. Neural axis MRI were performed in adult patients with acute neurological syndrome after exantematic fever suggestive of Zika infection. Newborns with microcephaly whose mothers had exantematic fever underwent brain MRI, some also with US and CT, and histopathological study of the placenta. Fetal MRI was performed in pregnant women who had have exantematic fever. There is a limited ability for laboratory confirmation of Zika in the locations affected by the epidemic, so that exantematic fever was considered as a marker for infection. Patients were scanned with a 1,5T MRI, and in adults using a protocol with pre and post contrast acquisitions.

#### RESULTS

Most adult patients presented with symptoms of Guillain-Barré syndrome and variants, a few patients presented encephalomyelitis. The most common finding was lumbar root enhancement followed by lumbar dorsal ganglia enhancement and facial nerve enhancement. Other findings included brain stem lesions with high T2/FLAIR signal, spinal cord lesions with high T2/FLAIR signal, and trigeminal nerve enhancement. We found good correlation of symptoms and imaging findings. In newborns MRI and fetal MRI showed anatomical changes in the brain parenchyma and orbital injuries.

### CONCLUSION

MRI was used in clinical investigation of adult patients, excluding other common diseases in this age group, helping in the differential diagnosis, given the limited availability of specific serologic tests for Zika in Brazil. We observed acute neurological syndromes related to Zika, such as Guillain-Barré syndrome and Miller Fisher variant, Bickerstaff syndrome, and encephalomyelitis. In newborns and fetuses anatomical changes can be related to gestational age which pregnant had the exantematic fever.

### **CLINICAL RELEVANCE/APPLICATION**

MRI is a sensitive tool for demonstrating signs of Guillain-Barré syndrome and encephalomyelites associated with Zika virus. In newborns and fetuses, MRI helped us understand the injuries that occur in the developing brain, as other TORCH.

# NR395-SD-WEB3

### Enlarged Perivascular Spaces in Brain are Associated with Disease Activity in Systemic Lupus Erythematosus

Wednesday, Nov. 30 12:45PM - 1:15PM Room: NR Community, Learning Center Station #3

#### **Participants**

Mari Miyata, MD, Kitakyushu, Japan (*Presenter*) Nothing to Disclose Shingo Kakeda, MD, Kitakyushu, Japan (*Abstract Co-Author*) Nothing to Disclose Kazuyoshi Saito, Kitakyushu, Japan (*Abstract Co-Author*) Nothing to Disclose Yoshiya Tanaka, MD, Kitakyushu, Japan (*Abstract Co-Author*) Nothing to Disclose Yukunori Korogi, MD, PhD, Kitakyushu, Japan (*Abstract Co-Author*) Nothing to Disclose

#### PURPOSE

Recently, a few papers have reported the relationship between the EPVS and inflammatory processes within the brain. The purpose of this study was to determine whether MR findings including the EPVS were associated with disease activity and neuropsychiatric symptoms in the systemic lupus erythematosus (SLE).

#### **METHOD AND MATERIALS**

We retrospectively recruited 92 SLE patients (36 SLE with and 56 without neuropsychiatric symptoms) who had no pathologies on conventional MRI except for brain atrophy and white matter hyperintensity (WMH) on T2WI. The disease activity was assessed using the British Isles Lupus Assessment Group (BILAG) index and Systemic Lupus Erythematosus Disease Activity Index (SLEDAI). By consensus reading, two neuroradiologists, who were blinded to the clinical data, evaluated T1WI, T2WI, FLAIR images. The imaging characteristics included centrum semiovale EPVS (CS-EPVS) and basal ganglia EPVS (BG-EPVS) (from Grade 0=none to Grade 4=>40) on T2WI, WMH (Fazekas grade 0, 1, 2, and 3), and cerebral atrophy (from Grade 0=non to Grade 3=severe). For clinical (vascular risk factors: hypertension, hyperlipidemia, diabetes, obesity, and smoking) and imaging characteristics, we used univariate and multivariate logistic regression analyses to determine the variables associated with the disease activity. Regarding these characteristics, we also compared the SLE patients with and without neuropsychiatric symptoms.

### RESULTS

On univariate analyses, the disease activity indices (BILAG index: p=0.001 and SLEDAI: p=0.002) were associated with CS-EPVS, but no association with the clinical data and other imaging characteristics (BILAG index and SLEDAI: BG-EPVS, p=0.817 and 0.963; WMH, p=0.864 and 0.901; and cerebral atrophy, p=0.814 and 0. 637, respectively). High CS-EPVS were associated with the presence of the neuropsychiatric symptoms (OR 3.60; 95% CI 1.47–8.84; p=0.005).

### CONCLUSION

In the SLE patients, the CS-EPVS are specifically associated with the disease activity and the neuropsychiatric symptoms, which suggests a potential role of the perivascular spaces in the neuroinflammatory processes of the SLE patients.

### **CLINICAL RELEVANCE/APPLICATION**

Assessments of enlarged perivascular spaces in the centrum semiovale on conventional T2WI may be a simple and objective way to know the disease activity in the neuropsychiatric SLE patients, for which there have been no useful diagnostic biomarkers.

# NR397-SD-WEB5

### Management for Small Thyroid Nodules: A Comparative Study Applying Six Guidelines for Thyroid Nodules

Wednesday, Nov. 30 12:45PM - 1:15PM Room: NR Community, Learning Center Station #5

#### **Participants**

Jung Hyun Yoon, MD, Seoul, Korea, Republic Of (*Presenter*) Nothing to Disclose Kyunghwa Han, PhD, Seoul, Korea, Republic Of (*Abstract Co-Author*) Nothing to Disclose Eun-Kyung Kim, Seoul, Korea, Republic Of (*Abstract Co-Author*) Nothing to Disclose Hee Jung Moon, MD, Seoul, Korea, Republic Of (*Abstract Co-Author*) Nothing to Disclose Jin Young Kwak, MD, Seoul, Korea, Republic Of (*Abstract Co-Author*) Nothing to Disclose

# PURPOSE

To evaluate and compare the diagnostic performances of six guidelines for thyroid nodules in predicting the outcomes of small thyroid cancer and in differential diagnosis of small thyroid nodules.

# METHOD AND MATERIALS

From March 2007 to February 2010, 4,696 thyroid nodules in 4,585 patients measuring 1-2cm that were diagnosed as benign or malignancy based on surgery or US-FNA were included. US examinations of the thyroid nodules were retrospectively reviewed, and categorized according to the categories of six guidelines for thyroid nodules reported in literature. Medical records of the patients were reviewed for cytopathology results and patient outcome during follow-up. Multivariate regression analysis was used to analyze predictors for distant metastasis and recurrence/persistence in patients with small thyroid cancer. Diagnostic performances of each guideline were calculated and compared.

### RESULTS

Of the 4,696 thyroid nodules, 3,652 (77.8%) were benign and 1,044 (22.2%) were malignancy. Eight-hundred seventy-three patients diagnosed as small thyroid cancer were followed, of which 12 had distant metastasis and 66 had recurrences/persistence of disease. Positive findings of the guidelines did not show significant association to distant metastasis or recurrence/persistence of disease (all P>0.05). Sensitivity and NPV was highest in TIRADS-Kwak, 98.8% and 98.6%, respectively, while specificity, PPV, and accuracy was highest in Kim criteria, 83.1%, 59.6%, and 84.0%, respectively (P<0.001).

### CONCLUSION

Positive features of the six guidelines for thyroid nodules were not associated with patient outcomes in small thyroid cancer. With its high specificity and accuracy, the Kim criteria may be an effective guideline to use in management of small thyroid nodules.

# **CLINICAL RELEVANCE/APPLICATION**

Positive features of the six guidelines for thyroid nodules were not associated with patient outcomes in small thyroid cancer. With its high specificity and accuracy, the Kim criteria may be an effective guideline to use in management of small thyroid nodules.

# NR398-SD-WEB6

Abnormal Functional Connectivity Strength in Default Mode Network in First-Episode, Drug-naive Major Depressive Disorder

Wednesday, Nov. 30 12:45PM - 1:15PM Room: NR Community, Learning Center Station #6

# Participants

Hong Yang, MD, Hangzhou, China (*Presenter*) Nothing to Disclose Zhan Feng Sr, Hang Zhou, China (*Abstract Co-Author*) Nothing to Disclose Shunliang Xu, Hangzhou, China (*Abstract Co-Author*) Nothing to Disclose Manli Huang, Hangzhou, China (*Abstract Co-Author*) Nothing to Disclose

### PURPOSE

Converging findings suggested default mode network(DMN) as a potentially valuable biomarker for major depressive disorder(MDD). Using functional connectivity strength(FCS), a new method for rest-state fMRI(rfMRI), the aim of current study is to explore the abnormal FCS of rest-state in DMN in first-episode, drug-naive MDD, which may be helpful to elucidate the patho-physiology and possible etiology of MDD.

# METHOD AND MATERIALS

Twenty-two patients (aged 31.1±1.5 years) diagnosed based on DSM-IV, twenty matched normal controls were recruited. Twenty-two axial slices covering whole brain were acquired using a 3.0T MR scanner(TR/TE 2000/35 ms, flip angle 90°, matrix  $64 \times 64$ , FOV 24cm, thickness/gap 5/1mm, total 200 volumes) in rest state. DPARSF and SPM8 toolkits were used for rfMRI data pre-processing, including slice timing, head-motion correction, spatial normalization and smooth.Pearson's correlation coefficients were computed between the time series of all pairs of gray matter voxels (threshold of r = 0.5), then transforming into a whole-brain functional connectivity strength matrix for each individual. Two-sample t test was used for analysis of the differences of FCS mapping between the two groups and results were corrected using Monte-Carlo simulation. The correlation between abnormal FCS and clinical variables were investigated in patients.

### RESULTS

Compared to the normal control group, patients showed lower FCS than healthy subjects in the medial prefrontal cortex(MPC), inferior parietal lobule and the posterior cingulate cortex/precuneus(PCC/PCU), the core regions within DMN. The FCS in patients was significantly increased in the right dorsolateral prefrontal cortex and parietal Lobe compared with controls. In post-hoc correlation analysis, the significant value wasn't showed between abnormal FCS values in the demonstrating clusters and behavioral variables in patients.

#### CONCLUSION

Abnormal FCS regions in DMN were found in patients. Reduced FCS in MPC might partly contribute to the emotional and cognitive symptom in MDD. Reduced FCS in PCC/PCU might related to the memory impairment in MDD. Our results prove"DMN" as a potentially valuable biomarker for MDD. HAMD is a comprehensive rating scale, involving many aspects in clinic. A simple FCS value can't reflect all these.

# **CLINICAL RELEVANCE/APPLICATION**

Our findings confirm dysfunction DMN as a potentially valuable biomarker for MDD. It is helpful to predict who will respond to a given treatment.

# NR399-SD-WEB7

Evaluating the Efficacy of Anti-oxidants in Chronic Spinal Cord Injury Treatment: Utility of Tractography as a Tool to Assess Recovery

Wednesday, Nov. 30 12:45PM - 1:15PM Room: NR Community, Learning Center Station #7

**FDA** Discussions may include off-label uses.

#### Participants

Sayna Leylachian, BSC, Richmond Hill, ON (*Abstract Co-Author*) Nothing to Disclose Arun Mensinkai, MD, Hamilton, ON (*Abstract Co-Author*) Nothing to Disclose Parisa Fani, MD, Hamilton, ON (*Presenter*) Nothing to Disclose Sandra Giles, RT, Ancaster, ON (*Abstract Co-Author*) Nothing to Disclose Pankaj E. Bansal, MD, Hamilton, ON (*Abstract Co-Author*) Nothing to Disclose S. Hossein Hosseini, MD,FRCPC, Hamilton, ON (*Abstract Co-Author*) Nothing to Disclose Sunil Kumar Suguru Laxman, MD, Oakville, ON (*Abstract Co-Author*) Nothing to Disclose Shanker Nesathurai, MD, MPH, ancaster, ON (*Abstract Co-Author*) Advisor, Sunbeam Products, Inc; Consultant, Seiden Health Management Inc

# PURPOSE

There are no effective treatments for limb weakness associated with chronic spinal cord injury. This pilot study is the first to administer the anti-oxidants Vitamin E and Selenium to individuals who have experienced SCI. Vitamin E and Selenium are free radical scavengers that may have a significant effect on malfunctioning neuronal pathways in the spinal cord. The aim of this study is to investigate the effects of anti-oxidants on tract regeneration in patients with SCI using standard MRI sequences and diffusion tensor imaging (DTI). We hypothesize that there will be an increase in the FA and decrease in ADC values, indicating axonal tract regeneration in response to therapy.

#### **METHOD AND MATERIALS**

Four adults with SCI (>12 mths) and two controls underwent T2-weighted and diffusion tensor imaging using a 1.5-T MR scanner. After obtaining fiber-tracking maps, FA and ADC values were measured and analyzed in the SCI patients and normal healthy controls. Identical imaging protocol will be performed 1 year post therapy and the FA and ADC values will be compared.

#### RESULTS

Despite heterogeneity in SCI lesion severity and location, diffusion characteristics proximal and at the level of the chronic lesion were significantly elevated compared with those of uninjured controls. Furthermore, fractional anisotropy was significantly lower proximal to and at the chronic lesion compared to controls and appears dependent on the completeness of the injury.

### CONCLUSION

Diffusion tensor imaging is a valuable biometric to assess the extent of spinal cord injury by FA, which is reduced in patients of chronic spinal cord injury, suggesting Wallerian degeneration. Furthermore we suspect that antioxidant therapy will show initial promise in the treatment of SCI with improvement in FA values indicating axonal regeneration.

### **CLINICAL RELEVANCE/APPLICATION**

Using a more accurate biometric such as Diffusion Tensor Imaging will help provide more detail on post injury changes in the spinal tracts. This will provide a better tool in assessment of hypothesized treatment efficacy in patients with spinal cord injury and life long debilitation for the first time.

MR Fingerprinting of the Brain: Preliminary Results of a Reproducibility Study on Simultaneous Multiparametric Tissue Quantification

Wednesday, Nov. 30 12:45PM - 1:15PM Room: NR Community, Learning Center Station #8

# Participants

Lale Umutlu, MD, Essen, Germany (*Presenter*) Consultant, Bayer AG Florian M. Meise, Erlangen, Germany (*Abstract Co-Author*) Employee, Siemens AG Mathias Nittka, PhD, Erlangen, Germany (*Abstract Co-Author*) Employee, Siemens AG Josef Pfeuffer, PhD, Erlangen, Germany (*Abstract Co-Author*) Nothing to Disclose Felix Nensa, MD, Essen, Germany (*Abstract Co-Author*) Nothing to Disclose Harald H. Quick, PhD, Essen, Germany (*Abstract Co-Author*) Nothing to Disclose Mark A. Griswold, PhD, Cleveland, OH (*Abstract Co-Author*) Research support, Siemens AG Royalties, Siemens AG Royalties, General Electric Company Royalties, Bruker Corporation Contract, Siemens AG Vikas Gulani, MD,PhD, Cleveland, OH (*Abstract Co-Author*) Siemens Healthcare Marcel Gratz, Essen, Germany (*Abstract Co-Author*) Nothing to Disclose

#### PURPOSE

In-vivo relaxometry is considered to be a highly desirable and valuable, yet up to current status also time-consuming quantitative imaging technique. Magnetic resonance fingerprinting (MRF) has been demonstrated to enable simultaneous multiparametric tissue characterization based on fast, non-invasive quantification of multiple tissue properties (e.g. T1, T2 values; Ma et al; Nature 2013). The aim of this trial was to evaluate the reproducibility of MRF of the brain in 10 healthy volunteers at 1.5 and 3 Tesla MRI.

# METHOD AND MATERIALS

10 healthy subjects were examined on 1.5T and 3T MR scanners (MAGNETOM Aera and Skyra; both Siemens Healthcare GmbH, Erlangen, Germany) utilizing a 20-channel head-coil and a prototype implementation of the MRF technique with an acquisition time of 50 sec/ slice, resulting in a total AT for 3 slices of 2 min 30 sec (Jiang et al., Magnetic Resonance in Medicine 2015). For quantitative image analysis region-of-interest analyses (ROI) of the following anatomic regions were performed in each subject in 1.5 and 3T MRI: (1) superior frontal white matter (SFWM), (2) frontal WM, (3) parietal WM, (4) putamen, (5) Nucleus caudate, (6) splenium, (7) centrum semiovale, (8) gray matter, (9) cerebellum, (10) pons.

#### RESULTS

MRF was feasible in all examined subjects. Mean values of the assessed anatomic regions showed a reasonable interindividual range with adequate standard deviation, comparable to previous publications. T1 and T2 mean (stdev) values of the putamen accounted to T1(ms)=(1,135 ± 48) / (893 ± 53) and T2(ms)=(35.4 ± 2.9) / (49.9 ± 5.8) for 3T/1.5T. T1 and T2 values of the nucleus caudate were T1(ms)=(1,205 ± 53) / (963 ± 72) and T2(ms)=(36.1 ± 3.6) / (59.9 ± 2.6) for 3T/1.5T.

# CONCLUSION

MRF is a unique quantitative MR imaging technique that enables a simultaneous, robust, rapid and reproducible in vivo quantification of different brain tissue properties in both clinical field strengths.

# **CLINICAL RELEVANCE/APPLICATION**

Based on its simultaneous, rapid and reproducible relaxation parameter mapping, MRF may help to further characterize neoplastic and inflammatory tissue without the application of contrast agent.

# Fetal GI Tract Atresias - From Esophagus to Anus

Wednesday, Nov. 30 12:45PM - 1:15PM Room: OB Community, Learning Center Station #1

### Awards Cum Laude

#### **Participants**

Thomas Gibson, MD, Portland, OR (*Presenter*) Nothing to Disclose Kyle Jensen, MD, Portland, OR (*Abstract Co-Author*) Nothing to Disclose Neda Jafarian, MD, Portland, OR (*Abstract Co-Author*) Nothing to Disclose Roya Sohaey, MD, Portland, OR (*Abstract Co-Author*) Nothing to Disclose Karen Y. Oh, MD, Portland, OR (*Abstract Co-Author*) Nothing to Disclose

# **TEACHING POINTS**

1. Gastrointestinal (GI) tract anomalies can be difficult to diagnose in utero, with detection rate around 34%. 2. Accurate diagnosis can herald unsuspected syndromic or chromosomal abnormalities, which affects pregnancy counseling, expectations, and outcomes.3. Embryologic GI tract development is one key to understanding each site of atresia.4. Ultrasound is the standard for obstetric imaging and can provide clues to the site of atresia.5. Fetal MR can be a helpful adjunct modality to facilitate diagnosis.

# TABLE OF CONTENTS/OUTLINE

- 1. Embryologic development of the GI tract
- 2. Imaging findings seen with esophageal, duodenal, jejunal, ileal, colonic, and anal atresias
- 3. Presentation of antenatal cases with postnatal imaging correlation and outcomes
- 4. Summary of key differentiating imaging features

# OB167-ED-WEB2

Algorithmic Approach to Evaluation of Sonographically Indeterminate Adnexal Masses Using Multi-Parametric MRI

Wednesday, Nov. 30 12:45PM - 1:15PM Room: OB Community, Learning Center Station #2

# Awards Cum Laude

# Participants

Fuki Shitano, MD,PhD, New York, NY (*Presenter*) Nothing to Disclose
Stephanie Nougaret, MD, Montpellier, France (*Abstract Co-Author*) Nothing to Disclose
Shinya Fujii, MD, Yonago, Japan (*Abstract Co-Author*) Nothing to Disclose
Christine O. Menias, MD, Chicago, IL (*Abstract Co-Author*) Nothing to Disclose
Hebert Alberto Vargas, MD, New York, NY (*Abstract Co-Author*) Nothing to Disclose
Hedvig Hricak, MD, PhD, New York, NY (*Abstract Co-Author*) Nothing to Disclose
Evis Sala, MD, PhD, New York, NY (*Abstract Co-Author*) Nothing to Disclose
Yuliya Lakhman, MD, New York, NY (*Abstract Co-Author*) Nothing to Disclose

# **TEACHING POINTS**

Evaluation of sonographically indeterminate adnexal masses is a common indication for MRI. Majority of indeterminate masses are benign and their definitive characterization avoids unnecessary surgery or imaging follow-up which minimizes healthcare costs and patients' anxiety. Small proportion of indeterminate adnexal masses is malignant and their prompt evaluation with MRI ensures timely diagnosis and management.We present a step-by-step schema for the characterization of adnexal masses with multi-parametric MRI. This approach relies on clinical data and MRI features: signal intensity and morphology on conventional T1-weighted and T2weighted imaging (T1WI, T2WI), diffusion and enhancement characteristics on multi-parametric imaging.**Teaching Points:** Highlight tailored MRI protocol for the evaluation of adnexal masses Demonstrate a step-by-step approach for the characterization of adnexal masses using clinical information and multi-parametric MRI

# **TABLE OF CONTENTS/OUTLINE**

Tailored MRI protocol Detection and normal appearance of the ovaries Identification of mass origin Signal characteristics and morphology on T1WI and T2WI T1 hyperintense masses T2 solid masses T2 complex cystic or cystic-solid masses Value of multiparametric MRI Diffusion-weighted imaging Dynamic contrast-enhanced imaging

### **Honored Educators**

Presenters or authors on this event have been recognized as RSNA Honored Educators for participating in multiple qualifying educational activities. Honored Educators are invested in furthering the profession of radiology by delivering high-quality educational content in their field of study. Learn how you can become an honored educator by visiting the website at: https://www.rsna.org/Honored-Educator-Award/

Stephanie Nougaret, MD - 2013 Honored Educator Christine O. Menias, MD - 2013 Honored Educator Christine O. Menias, MD - 2014 Honored Educator Christine O. Menias, MD - 2015 Honored Educator Christine O. Menias, MD - 2016 Honored Educator Evis Sala, MD, PhD - 2013 Honored Educator

# PD009-EB-WEB

Color Doppler Assessment of the Cerebrospinal Fluid Flux as a Prognostic Tool for Obstructive Hydrocephalus in Intraventricular Hemorrhage Papile Grades III and IV

Wednesday, Nov. 30 12:45PM - 1:15PM Room: PD Community, Learning Center Hardcopy Backboard

# Participants

Debora Tomazoni, MD, Sao Paulo, Brazil (*Presenter*) Nothing to Disclose Eduardo K. Fonseca, MD, Sao Paulo, Brazil (*Abstract Co-Author*) Nothing to Disclose Suheyla P. Ribeiro, MD, Sao Paulo, Brazil (*Abstract Co-Author*) Nothing to Disclose Dair Enge JR, MD, Sao Paulo, Brazil (*Abstract Co-Author*) Nothing to Disclose Mauricio Yamanari, Sao Paulo, Brazil (*Abstract Co-Author*) Nothing to Disclose Miguel J. Neto, Sao Paulo, Brazil (*Abstract Co-Author*) Nothing to Disclose Marcelo B. Funari, MD, Ribeirao Pires, Brazil (*Abstract Co-Author*) Nothing to Disclose Yoshino T. Sameshima, MD, Sao Paulo, Brazil (*Abstract Co-Author*) Nothing to Disclose

### **TEACHING POINTS**

We describe a series of 7 cases of non-invasive technique of usage of color Doppler in the assessment of CSF flow as predictive factor for the onset of hydrocephalus in neonates with grades III and IV intraventricular hemorrhage. At the end of this presentation, the viewer will be able to explain the normal anatomy of the CSF flux related structures; to apply the Papile classification; to use the color Doppler assessment of the CSF flux as a prognostic tool in germinal matrix hemorrhage grades III and IV understanding its limitations.

# TABLE OF CONTENTS/OUTLINE

A. Central nervous system anatomy B. Pathophysiology of germinal matrix hemorrhage C. Color Doppler assessment of cerebrospinal fluid flux through transfortanellar ultrasonography: technique and limitations D. Example cases E. Take-home messages

# PD171-ED-WEB6

# Imaging Patterns of Liver Lesions in Children with Emphasis on Ultrasound

Wednesday, Nov. 30 12:45PM - 1:15PM Room: PD Community, Learning Center Station #6

#### Awards Certificate of Merit

#### **Participants**

Tassia R. Yamanari, MD, Sao Paulo, Brazil (*Presenter*) Nothing to Disclose Natally d. Horvat, MD, Sao Paulo, Brazil (*Abstract Co-Author*) Nothing to Disclose Antonio S. Marcelino, MD, Sao Paulo, Brazil (*Abstract Co-Author*) Nothing to Disclose Sandro Rangel Santos, Sao Paulo, Brazil (*Abstract Co-Author*) Nothing to Disclose Publio C. Viana, MD, Sao Paulo, Brazil (*Abstract Co-Author*) Nothing to Disclose Paulo Chapchap, MD, Sao Paulo, Brazil (*Abstract Co-Author*) Nothing to Disclose Claudia D. Leite, MD, PhD, Sao Paulo, Brazil (*Abstract Co-Author*) Nothing to Disclose Claudia D. Leite, MD, PhD, Sao Paulo, Brazil (*Abstract Co-Author*) Nothing to Disclose Gilda Porta, Sao Paulo, Brazil (*Abstract Co-Author*) Nothing to Disclose Eduardo Antunes da Fonseca, Sao Paulo, Brazil (*Abstract Co-Author*) Nothing to Disclose Joao Seda-Neto, Sao Paulo, Brazil (*Abstract Co-Author*) Nothing to Disclose Katia Leite, Sao Paulo, Brazil (*Abstract Co-Author*) Nothing to Disclose

### **TEACHING POINTS**

This presentation aims to exhibit the spectrum of ultrasound imaging findings of benign and malignant pediatric focal liver lesions, with computed tomography or magnetic resonance correlation. The knowledge of the US imaging findings in the detection, characterization and follow-up of liver lesions has a higher relevance in the pediatric population due to the absence of radiation exposure.

# TABLE OF CONTENTS/OUTLINE

1. Overview of the classification of focal liver lesions in children2. Review of US findings of benign and malignant pediatric focal liver lesions, some of which unique to the pediatric population, such as hemangioendotheliomas and mesenchymal hamartoma, hepatoblastoma, undifferentiated (embryonal) sarcoma, angiosarcoma and others more common in adults including hemangiomas, focal nodular hyperplasia, nodular regenerative hyperplasia and hepatocellular adenoma, fibrolamellar hepatocellular carcinoma, lymphoma. CT and MR images will be shown for correlation.

# PD230-SD-WEB1

Combination of Magnetic Resonance Imaging and Virtual Reality Systems to Generate Immersive Fetal 3D Visualizations

Wednesday, Nov. 30 12:45PM - 1:15PM Room: PD Community, Learning Center Station #1

# Participants

Heron Werner, MD, Rio de Janeiro, Brazil (*Abstract Co-Author*) Nothing to Disclose Bianca Guedes Ribeiro, MD, Rio de Janeiro, Brazil (*Presenter*) Nothing to Disclose Jorge Lopes, Rio de Janeiro, Brazil (*Abstract Co-Author*) Nothing to Disclose Gerson Ribeiro, Rio de Janeiro, Brazil (*Abstract Co-Author*) Nothing to Disclose Pedro Daltro, MD, Rio De Janeiro, Brazil (*Abstract Co-Author*) Nothing to Disclose Tatiana M. Fazecas, MD, Rio de Janeiro, Brazil (*Abstract Co-Author*) Nothing to Disclose Renata A. Nogueira, MD, Rio De Janeiro, Brazil (*Abstract Co-Author*) Nothing to Disclose Leise Rodrigues, Rio De Janeiro, Brazil (*Abstract Co-Author*) Nothing to Disclose

#### PURPOSE

Advances in image-scanning technology have led to vast improvements in medicine, especially in the diagnosis of fetal anomalies. In general, three main technologies are used to obtain images within the uterus during pregnancy i.e. Ultrasound (US), Magnetic Resonance Imaging (MRI) and Computed Tomography (CT). MRI offers high-resolution fetal images with excellent contrast that allow visualization of internal tissues. When US yields unexpected results, MRI is generally used, because it provides additional information about fetal abnormalities and conditions for which US cannot provide high-quality images.

# METHOD AND MATERIALS

The construction process of the 3D accurate virtual model starts with the 3D modeling volume built through the MRI slices sequentially mounted, followed by the segmentation process where the Physician selects the important body parts to be analyzed that will be then reconstructed in 3D. Having the accurate 3D model (womb, umbilical, cord, placenta and fetus) the final stage is the programming of the virtual device (Oculus Rift 2), including the heartbeat sounds of the fetus to improve the immersive sensation. The navigation through internal paths can be pre-defined by the physician responsible for the patient in order to highlight the main subjects to be studied by the fetal medicine team as well for parents understanding.

#### RESULTS

Virtual reality fetal 3D models based on MRI were successfully generated. They were remarkably similar to the postnatal appearance of the newborn baby, especially in cases with pathology, increasing the possibilities of digital tools to help fetal medicine researches.

# CONCLUSION

The use of MRI may improve our understanding of fetal anatomical characteristics, and can be used for educational purposes and as a method for parents to visualize their unborn baby. The images can be segmented and applied on virtual reality immersive technologies.

# **CLINICAL RELEVANCE/APPLICATION**

We have demonstrated that MRI data can be used to create a 3D model, including of the respiratory tract in a normal fetus. We believe that this technique could become a useful tool for the assessment of fetal airway patency and for other possible applications.

# PD236-SD-WEB2

# MRI Characteristics of RELA-fused versus Other Pediatric Supratentorial Ependymomas

Wednesday, Nov. 30 12:45PM - 1:15PM Room: PD Community, Learning Center Station #2

#### **Participants**

Johannes Nowak, MD, Wurzburg, Germany (*Presenter*) Nothing to Disclose Torsten Pietsch, Bonn, Germany (*Abstract Co-Author*) Nothing to Disclose Monika Warmuth-Metz, Wurzburg, Germany (*Abstract Co-Author*) Nothing to Disclose

### PURPOSE

Recently identified molecular entities of supratentorial ependymoma (ST-EPN) have shown potential for improved risk stratification and treatment. C11orf95-RELA fusion transcripts occur in more than 70% of pediatric ST-EPN and define a novel entity according to the upcoming WHO classification of brain tumors. In addition, CDKN2A deletions had been shown to correlate with poor prognosis. Imaging features of RELA-fused ependymomas have not yet been analyzed in comparison to other ST-EPN. In this study, we describe and compare MR imaging characteristics of pediatric ST-EPN.

### METHOD AND MATERIALS

A cohort of 57 ST-EPN was obtained from our multi-center neuroimaging database. All cases were centrally reviewed for neuropathology including mRNA analysis for RELA fusions, immunohistochemistry for p65RelA and genome-wide copy analysis by molecular inversion profiling. We analyzed the preoperative MR imaging according to 26 epidemiologic and imaging criteria. Paired comparison was performed for each category between i) RELA-fused/other ST-EPN, ii) ST-EPN with/without CDKN2A deletion, and iii) RELA-fused ST-EPN with/without CDKN2A deletion.

### RESULTS

Highly-cellular hemispheric tumors with cystic and necrotic portions were distributed over all analyzed ST-EPN subgroups. Analysis revealed significant differences between RELA-fused and other ST-EPN with respect to peritumoral edema, cysts, T1 signal, tumor homogeneity and contrast enhancement parameters. Interestingly, diagnosis of tumors with CDKN2A deletion occured at a significantly higher age in our cohort, as well as with different MR morphology regarding intratumoral hemorrhage and diffusion restriction. Within the group of RELA-fused ST-EPN, we found significant differences in terms of age at diagnosis and intratumoral hemorrhage, dependent on CDKN2A deletion status.

# CONCLUSION

We identified imaging parameters that significantly differ between RELA-fused versus other pediatric ST-EPN. In addition, CDKN2A deletion may further influence signal characteristics of ST-EPN. However, a prediction of genetic markers by means of MRI might not be feasible in the individual case.

#### **CLINICAL RELEVANCE/APPLICATION**

This is the first study that describes detailed MR morphology of ST-EPN according to distinct molecular features. Further studies are needed in order to analyze potential differences between ST-EPN entities and to re-evaluate the role of MR imaging in ST-EPN diagnostics and therapy monitoring.

# PD237-SD-WEB3

Abnormal Topological Organization of Structural Networks Revealed by Probabilistic Diffusion Tractography in Tourette Syndrome Children

Wednesday, Nov. 30 12:45PM - 1:15PM Room: PD Community, Learning Center Station #3

# Participants

Yue Liu, Beijing, China (*Presenter*) Nothing to Disclose Hongwei Wen, Beijing, China (*Abstract Co-Author*) Nothing to Disclose Jishui Zhang, Beijing, China (*Abstract Co-Author*) Nothing to Disclose Huiguang He, PhD, Beijing, China (*Abstract Co-Author*) Nothing to Disclose Yun Peng, MD, Beijing, China (*Abstract Co-Author*) Nothing to Disclose

# PURPOSE

Tourette syndrome (TS) is a childhood-onset neurobehavioral disorder characterized by the presence of multiple motor and vocal tics. We integrated the diffusion MRI tractography method and graph theoretical analysis to reveal abnormal topological organization of whole-brain structural networks in TS children.

# METHOD AND MATERIALS

We obtained diffusion tensor imaging (DTI) scans from 44 drug-naïve TS children (age: 8.98±3.11 years, range: 3–16 years; 11 female) and 48 age and sex matched healthy children. Following DTI acquisition, we used the FMRIB's Diffusion Toolbox (FDT2.0) within FSL v4.1 (http://www.fmrib.ox.ac.uk/fsl) for DTI processing.

# RESULTS

Both TS and healthy children showed small-world properties of the white matter (WM) networks, characterized by high local clustering and short path length. Furthermore, TS children exhibited significant decreased nodal efficiency in inferior frontal gyrus, left parietal gyrus and hippocampus. Also, TS children exhibited decreased network connectivity in the occipital gyrus, superior parietal gyrus, cuneus, precuneus and lingual gyrus. Compared with healthy children, we found that, the most pronounced reduction network efficiency in TS, mainly were located in the sensorimotor, visual, default-mode, and language systems. We found that the connection strength of the right superior occipital gyrus linking the right superior parietal gyrus, the left middle occipital gyrus linking the left Superior parietal gyrus, were significantly positively correlated with the tic severity score (YGTSS) in the TS patients.

# CONCLUSION

Thus, our results suggest a disrupted integrity in the large-scale brain systems in TS and provide structural insights into the brain networks of TS children. Our result also suggest that the topology-based brain network analysis can provide potential biomarkers for early-stage TS diagnosis, as well as the monitoring of the disease progression and the treatment effects for TS children.

### **CLINICAL RELEVANCE/APPLICATION**

TS is a developmental neuropsychiatric disorder which begins at the age of 6 to 7 years. The study of brain changes is very important for the treatment. Previous study mainly focused on brain volume structure changes. We try to investigate the alterations of structural networks in TS children with DTI.

# PD238-SD-WEB4

Metastatic Pattern of Rhabdomyosarcoma in Children and Adolescent: Timing, Location, and Associated Factors

Wednesday, Nov. 30 12:45PM - 1:15PM Room: PD Community, Learning Center Station #4

# Participants

Jeong Rye Kim, MD, Seoul, Korea, Republic Of (*Presenter*) Nothing to Disclose Hee Mang Yoon, MD, Seoul, Korea, Republic Of (*Abstract Co-Author*) Nothing to Disclose Jin Seong Lee, MD, Seoul, Korea, Republic Of (*Abstract Co-Author*) Nothing to Disclose Young Ah Cho, Seoul, Korea, Republic Of (*Abstract Co-Author*) Nothing to Disclose Ah Young Jung, MD, Seoul, Korea, Republic Of (*Abstract Co-Author*) Nothing to Disclose

# PURPOSE

Rhabdomyosarcoma(RMS) is most common soft tissue sarcoma in children. The anatomic site of primary tumor, size, resectability, presence of metastases, regional lymph node (LN) involvement, and residual tumor after surgery are known as important prognostic factors. Therefore, careful imaging evaluation of not only the primary tumor but potential disease sites is mandatory for management of pediatric RMS. We investigated metastatic patterns of pediatric RMS including timing, location and associated factors.

# METHOD AND MATERIALS

We performed a computerized search of our hospital's data-base from 2000 to 2016 using codes for RMS and the demographic code for <20 years of age. We selected subjects who were histologically confirmed to have RMS. Clinical characteristics, imaging features of the primary tumor and distant metastasis at initial presentation and during follow-up were evaluated.

#### RESULTS

Nineteen of 69 patients had metastases at initial presentation and seven of 50 patients with localized disease at initial presentation had metastases during follow-up. Median time to first metastases was 14 months. Nine of 26 patients went on to develop metastases twice during follow-up and median time to secondary metastases was 9 months. The most common site of metastasis was bone (n=14), followed by lung (n=12) and LN (n=9). Bone (n=5) and lung (n=5) were the most common metastatic sites in patients with RMS originated from head and neck. In patients with trunk-origin RMSs, bone(n=8) was most commonly involved. LN metastases were more frequently observed in extremity-origin RMSs than in RMSs from other sites (p=0.002). On univariate analysis, age, histologic subtype, initial location of tumor, and involvement of regional LN at initial presentation were significant factors associated with development of distant metastasis.

#### CONCLUSION

RMS can metastasize variable sites throughout the body. The bone, lung and LN were the most frequent sites for metastasis. Extremity-origin RMSs tended to show predilection to metastasize to LN compared to RMSs originated from other sites. Age, histologic subtype, initial location of tumor, and regional LNs involvement at initial presentation were significantly associated with development of distant metastases.

# **CLINICAL RELEVANCE/APPLICATION**

By being familiar with metastatic patterns of RMSs, radiologists can play a crucial role in the multidisciplinary team for management of pediatric patients with RMSs.

Ultrasound-Guided Percutaneous Renal Biopsy Performed by Interventional Radiology in a Pediatric Population: Comparing Complication Rates between the BioPince® Full-Core Biopsy Device with Quick-Core® Coaxial Biopsy Needle Set Cutting Cannula

Wednesday, Nov. 30 12:45PM - 1:15PM Room: PD Community, Learning Center Station #5

# Participants

Heather Cleveland, BS, Houston, TX (*Presenter*) Nothing to Disclose Shireen Hayatghaibi, MA, MPH, Houston, TX (*Abstract Co-Author*) Nothing to Disclose Caleb Fortune, Houston, TX (*Abstract Co-Author*) Nothing to Disclose Daniel J. Ashton, MD, Houston, TX (*Abstract Co-Author*) Nothing to Disclose

# PURPOSE

To compare ultrasound-guided percutaneous renal biopsy (UGPRB) complication rates between the BioPince® Full-Core Biopsy Device and Quick-Core® Coaxial Biopsy Needle Set Cutting Cannula in a pediatric cohort.

### **METHOD AND MATERIALS**

215 non-targeted UGPRB performed by Interventional Radiology in a tertiary care pediatric facility between 01/01/2013 and 12/31/2015 (age range: 0-21, mean: 11.7) were identified retrospectively using EMR. Pertinent patient and procedure information was entered into a Research Electronic Data Capture. Patients were followed up to 30 days post procedure. Complications were categorized according to Society of Interventional Radiology (SIR) complications criteria by a fellowship trained Pediatric Interventional Radiologist and then compared with needle size and type using Fisher's exact test in Minitab. Both biopsy needles price was also compared.

### RESULTS

135 biopsies performed using a 16 gauge (G) or 18G BioPince®. 80 biopsies performed using a 16G or 18G Quick-Core®. 93 (43.26%) performed using a coaxial system. 36 complications detected (16.67%) in 215 renal biopsies. 30 (13.95%) small perinephric hematomas or hematuria complications categorized as SIR A (minor), 1 (.47%) subcapsular hematoma 15mm thick as SIR B (minor), 4 (1.86%) where blood products were given post procedure as SIR C (major) and 1 (.47%) psuedoaneurysm as SIR D (major). No significant difference in complications among needle sizes, 16G (8.37%) and 18G (5.58%) groups (p=0.27). No significant difference in the complications among needle types, 27 performed with BioPince® and 9 with Quick-Core® (p=0.074). A statistically significant difference observed in complications when comparing using a coaxial system verses only using the biopsy device. 9 (9.7%) complications with the use of a coaxial system and 27 (22%) complications without using a coaxial system (p=0.016). Both biopsy needle types were comparable in price.Median number of samples per biopsy was 2 with BioPince® and 3 with Quick-Core®. The mean hemoglobin value for the patients with complications was 12 (range: 8.1 – 16.9). The mean platelet count was 316.8 (minimum: 97).

# CONCLUSION

In a cohort of pediatric patients undergoing UGPRB, the use of a coaxial system decreased the rate of minor complications regardless of the needle type or size.

### **CLINICAL RELEVANCE/APPLICATION**

UGPRB is safe in pediatrics with regardless of needle size.

# Correlation of MRI Derived Parameters and Classical Anthropometry in the Evaluation of Obesity

Wednesday, Nov. 30 12:45PM - 1:15PM Room: PH Community, Learning Center Station #1

#### Awards

### Student Travel Stipend Award

### **Participants**

Nicolas Linder, Leipzig, Germany (*Presenter*) Nothing to Disclose Alexander Schaudinn, MD, Leipzig, Germany (*Abstract Co-Author*) Nothing to Disclose Nikita Garnov, Leipzig, Germany (*Abstract Co-Author*) Nothing to Disclose Thomas Karlas, MD, Leipzig, Germany (*Abstract Co-Author*) Nothing to Disclose Matthias Bluher, MD, Leipzig, Germany (*Abstract Co-Author*) Nothing to Disclose Stefanie Lehmann, Leipzig, Germany (*Abstract Co-Author*) Nothing to Disclose Andreas Oberbach, Leipzig, Germany (*Abstract Co-Author*) Nothing to Disclose Rima Chakaroun, Leipzig, Germany (*Abstract Co-Author*) Nothing to Disclose Rima Chakaroun, Leipzig, Germany (*Abstract Co-Author*) Nothing to Disclose Arne Dietrich, 04103, Germany (*Abstract Co-Author*) Nothing to Disclose Thomas K. Kahn, MD, Leipzig, Germany (*Abstract Co-Author*) Nothing to Disclose Harald F. Busse, PhD, Leipzig, Germany (*Abstract Co-Author*) Nothing to Disclose

#### PURPOSE

The purpose of this study was to evaluate the relationship between common anthropometric measures and MRI-derived adipose tissue volumes in the evaluation of obesity.

### **METHOD AND MATERIALS**

Obese patients of a local obesity research center were MRI examined after IRB approval and data were analyzed retrospectively. Anthropometric parameters consisted of patient weight, BMI and WHR (waist-to-hip ratio). Patients were classified into grades of obesity according to the WHO definition (I°: BMI 30-35 kg/m<sup>2</sup>, II°: 35-40, III°: > 40). MRI data included the segmented volumes of the visceral and subcutaneous adipose tissue (V-VAT and V-SAT) as well as segmented adipose tissue areas at an optimum (BMIdependent) axial reference position (A-VAT and A-SAT). Patients were analyzed according to their class of obesity using a linear regression and calculating the coefficient of determination R<sup>2</sup>. V-VAT was set as the gold standard for evaluation of abdominal obesity.

### RESULTS

261 patients were included in the analysis. 94, 86 and 81 patients were classified as I°, II° and III° obese, respectively. VAT and SAT could be quantified for 261 and 173 patients, respectively. Average weight, BMI, WHR and V-VAT were 160.5 (range 27.7-172.0) kg, 37.7 (30.0-60.3) kg/m<sup>2</sup>, 0.92 (0.70-1.17) and 4.43 (0.91-12.4) cm<sup>3</sup>. A-VAT showed a good correlation with V-VAT both overall ( $R^2 = 0.89$ ) as well as within each obesity class (I°: 0.92, II°: 0.88, III°: 0.84). A-SAT showed good correlation with V-SAT (0.78) with slight variation between individual BMI classes (I°: 0.61, II°: 0.79, III°: 0.60). Correlation of weight, BMI and WHR with volumes of adipose tissue was generally poor, both for V-VAT (0.23, 0.08, 0.35) and for V-SAT (0.20, 0.44 and 0.03).

### CONCLUSION

This comparison confirms the poor performance of common anthropometric measures and the good performance of simplified MRIderived adipose tissue measures for the evaluation of whole-abdominal VAT and SAT volumes.

### **CLINICAL RELEVANCE/APPLICATION**

Simplified, MRI-derived measures of adipose tissue outperform traditional anthropometry in the evaluation of whole-abdominal VAT and SAT volumes and should be evaluated further.

Feasibility of Ultralow Tube Voltage Low Radiation Dose Protocol for Coronary Stent Imaging Using Highdefinition256-Detector Row Gemstone CT: A Phantom Study

Wednesday, Nov. 30 12:45PM - 1:15PM Room: PH Community, Learning Center Station #2

# Participants

Yi-Luan Huang, MD, Kaohsiung, Taiwan (*Presenter*) Nothing to Disclose Ming-Ting Wu, MD, Kaohsiung, Taiwan (*Abstract Co-Author*) Nothing to Disclose Chiung Chen Chuo, Kaohsiung City, Taiwan (*Abstract Co-Author*) Nothing to Disclose Chen Shying Chen, Kaohsiung, Taiwan (*Abstract Co-Author*) Nothing to Disclose

## PURPOSE

To evaluate the feasibility of a low radiation dose protocol at a 256-detector row CT using ultralow tube voltage (70- and 80-kVp) high-definition (HD) imaging to evaluate the in-stent and peri-stent stenosis in a coronary-stent phantom.

# METHOD AND MATERIALS

A coronary-stent phantom (3-mm diameter) with in-stent and peri-stent 70% concentric luminal narrowing made of acrylic resin were filled with iodinated contrast agent and fixed in a water-filled tank. The phantom was scanned on a 256-detector row CT (Revolution CT, GE Healthcare) with ECG-triggered axial cardiac mode at 65 bpm. Different tube voltages (70, 80, 100, 120, and 140-kVp) and tube currents (50mA~580mA) adjusted by CTDI values were applied. CTDI had three groups: low (~1.15 mGy), intermediate (~2.70 mGy), and high (~3.95 mGy). High resolution mode was turned on and off during data acquisition for comparison. Iterative reconstruction was not used. Images were reconstructed with different convolution algorithms: standard, HD-standard, and HD-detail. All images were analyzed at appropriate window settings (AW Server 2.0). The visibility of the peri-stent and in-stent lumen were graded by Likert 5 scale: 1 (not evaluable) to 5 (excellent). A high-CTDI protocol (120-kVp/545-mA) served as reference.

### RESULTS

With standard convolution algorithm, it is hardly to evaluate the in-stent lumens in all 3 CTDI protocols. In high-CTDI group, HDstandard (score:  $3.83\pm0.72$ ) and HD-detail (score:  $3.58\pm0.9$ ) both improved the evaluation of in-stent stenosis as compared to standard algorithm (scores:  $1.42\pm0.66$ ) (P <0.001, P =0.02, respectively).In intermediate CTDI group, the 80-kVp protocol provided higher quality of in-stent lumen than the high (120-/140-) kVp protocol (score:  $5.0\pm0$  vs.  $2.34\pm0.58$ , P=0.102). In low-CTDI group, ultra-low (70-/80-) kVp HD images (score:  $4.34\pm0.28$ ) were superior to high-kVp HD images (score 2.5) for visualization of in-stent lumen. HD-detail images (score:  $3.08\pm1.16$ ) were not superior to HD-standard images (score:  $3.50\pm0.90$ ). Although with higher blooming artifact of the stent, the 70/80-kVp low-CTDI protocol was not inferior to the reference for in-stent lumen while saving of 80% CTDI.

# CONCLUSION

With clinical relevant CTDI, 70/80-kVp CT with HD-standard algorithm is feasible for evaluation of metallic stent.

### **CLINICAL RELEVANCE/APPLICATION**

70/80-kVp CT with HD-standard algorithm is feasible for evaluation of metallic stent.

# PH255-SD-WEB4

Cone Beam CT Radiation Exposure Reduction by Reconstructing Undersampled Data with Prior Knowledge and Symmetry Considerations

Wednesday, Nov. 30 12:45PM - 1:15PM Room: PH Community, Learning Center Station #4

# Participants

Khanlian Chung, Mannheim, Germany (*Presenter*) Nothing to Disclose Lothar R. Schad, PhD, Mannheim, Germany (*Abstract Co-Author*) Nothing to Disclose Frank G. Zoellner, Mannheim, Germany (*Abstract Co-Author*) Nothing to Disclose

#### PURPOSE

Modern cone beam CT allows for dynamic perfusion imaging however it comes with a high patient dose. We propose an iterative reconstruction (IR) algorithm using undersampling and prior knowledge to reduce dose while keeping image quality.

# METHOD AND MATERIALS

IRs typically face the trade-off between fewer projections (equal less information) and higher computational demands, in particular computer memory and reconstruction time. In our algorithm, we implemented cylindrically shaped voxels for image reconstruction, which are ordered in a special pattern. This design takes both, scan trajectory and cone beam geometry symmetries of interventional cone beam CTs, into account. Different projections can be treated as rotations of a reference projection. This reduces the computational demands (computing time and memory capacity) by the magnitude of the number of projections.Furthermore, the algorithm incorporates high quality prior images (e.g. from diagnostic scans) and updates only diverging voxels in the prior image. Typically, only few voxels are updated and therefore, the image quality of the reconstruction is enhanced.To validate the algorithm, a cubic box filled with a sphere was scanned with 397 projections and reconstructed by a commercial cone beam CT. This image was used as reference. Undersampled datasets with 50 projections and size of 240\*182 pixels were generated and, afterwards, reconstructed by our algorithm. To provide prior knowledge, the box was scanned a second time without a sphere.

# RESULTS

The reconstructed undersampled CTs with cylindrically shaped voxel scheme displayed all structure properly. Using a prior image to enhance the reconstruction, the edges became clearer. For example the perforations of the phantom increased about 40 % in contrast.Our approach allows a dose reduction of more than 85 % because instead of 397 only 50 projections are needed.

### CONCLUSION

The presented approach allows reconstructing CT images with a fraction of the number of projections usually needed with only minor quality losses. This was achieved by utilizing prior knowledge and symmetry considerations.

# **CLINICAL RELEVANCE/APPLICATION**

It is intended to use our knowledge- and symmetry- based algorithm in interventional cone beam CT applications (e.g. 3D perfusion imaging) to reduce radiation exposure.

# PH256-SD-WEB5

Comparison of Mass Detection for Digital Breast Tomosynthesis (DBT) with and without Transfer Learning of Deep-learning Convolution Neural Network (DLCNN) from Digitized Screen-film Mammography (SFM) and Digital Mammography (DM)

Wednesday, Nov. 30 12:45PM - 1:15PM Room: PH Community, Learning Center Station #5

# Participants

Ravi K. Samala, PhD, Ann Arbor, MI (*Presenter*) Nothing to Disclose Heang-Ping Chan, PhD, Ann Arbor, MI (*Abstract Co-Author*) Institutional research collaboration, General Electric Company Lubomir M. Hadjiiski, PhD, Ann Arbor, MI (*Abstract Co-Author*) Nothing to Disclose Jun Wei, PhD, Ann Arbor, MI (*Abstract Co-Author*) Nothing to Disclose Kenny H. Cha, MSc, Ann Arbor, MI (*Abstract Co-Author*) Nothing to Disclose Mark A. Helvie, MD, Ann Arbor, MI (*Abstract Co-Author*) Institutional Grant, General Electric Company

# PURPOSE

Transfer learning is expected to be an efficient method for training DLCNN when the available training sample size is small. We compare the performance of DLCNN trained using mass candidates from DBT versus using transfer learning by training first with SFM and DM for false positive (FP) reduction in a mass CADe system for DBT.

### **METHOD AND MATERIALS**

In the CADe system prescreening stage, mass candidates are identified with a combination of first- and second-order features from gradient field convergence map and eigenvalues from Hessian analysis. The candidate regions-of-interest (ROI) are extracted for FP reduction using DLCNN. For training of the DLCNN, heterogeneous mass candidates from SFM, DM and DBT are collected. The training set includes 2200 lesions from 856 SFM and DM cases and 192 lesions from 153 DBT cases. The independent test set consists of 94 views from 47 breasts with 90 lesions, of which 31 are malignant and 59 benign.128x128-pixel ROIs are extracted from the images/slices. To augment the training patterns, each ROI in DM or SFM is rotated and flipped to generate eight patterns. For DBT, five slices are extracted. Over 60,000 SFM, DM and DBT ROIs were available for DLCNN training. The DLCNN structure consists of four convolution layers connected by max-pooling and normalization layers for the first two convolution layers. For transfer learning, the network was first trained with the SFM and DM ROIs, then the first two convolution layers were frozen and the last two convolution layers were allowed to train based on the DBT ROIs (over 18000 ROIs). Without transfer learning, the DLCNN was trained until a stable AUC was achieved.

### RESULTS

The AUC with and without transfer learning reached  $0.94\pm0.01$  and  $0.97\pm0.01$ , respectively. For the independent test set, viewbased sensitivities of 79% and 86% were achieved at 3.8 and 3.9 FPs/view with and without transfer learning, respectively. Similarly, the case-based sensitivity of 85% was achieved at 2.0 and 1.9 FPs/view, respectively.

#### CONCLUSION

Training of the DLCNN on DBT ROIs alone without transfer learning resulted in better learning of the mass patterns for DBT.

### **CLINICAL RELEVANCE/APPLICATION**

An effective CADe systems for mass detection in DBT may be a useful second reader or a component of an efficient visualization tool to improve workflow of DBT interpretation.

# Closing the Loop: A Radiology Follow-up Recommendation Tracking System

Wednesday, Nov. 30 12:45PM - 1:15PM Room: QS Community, Learning Center Hardcopy Backboard

#### **Participants**

Ben C. Wandtke, MD, Rochester, NY (*Presenter*) Nothing to Disclose Sarah Gallagher, RN, Canandiagua, NY (*Abstract Co-Author*) Nothing to Disclose

### PURPOSE

Only 50% of radiologists recommendations for follow-up imaging result in a completed examination. Documented causes of noncompliance with obtaining follow-up imaging studies include inconsistent communication (between radiologists, emergency department providers, subspecialists, and primary care providers) and imperfect tracking systems in primary care providers' offices. Recommendations are most commonly used in the setting of an incidental finding which has potential to develop into a malignancy or other serious medical condition such as an aneurysm. Failure to obtain timely recommended follow-up imaging studies may result in delay in diagnosis of malignancy with an associated increase in morbidity and medical legal liability. Four patients were identified at our institution through our quality assurance program over a 4 year period in which failure to obtain a recommended follow-up study led to delay in diagnosis and presentation with untreatable end stage metastatic malignancy. We have developed a three stage radiology recommendations, identifying the rationale for why recommendations are not obtained, and reducing the rate of patients for whom recommended follow-up "falls through the cracks".

### METHODS

Radiology follow-up recommendations were entered into our tracking system by the radiologist at the time of interpretation over a 13 month period. One month following the recommendation due date, our radiology information system is queried to determine if the recommended study has been performed. If it has not, our Stage 1 intervention, resending the report to the office of the patient's primary care provider, is performed. One month later, if the exam has still not been performed, our Stage 2 intervention, a radiology staff to primary care provider office staff phone call, is performed. The following month, if the exam has still not been performed, our Stage 3 intervention, a radiologist to primary care provider phone call, is performed. At any stage of the process, if information is provided that explains why the recommended study has consciously not been performed, this is documented and the case closed. All interactions were recorded in a Microsoft Access database developed specifically for this project.

#### RESULTS

Over a 13 month period, 757 recommendations were entered into our tracking system and 564 were closed due to the recommended study being performed or a rationale for non-compliance provided. Recommended imaging tests were obtained in 53.2% (300/564) of cases without the aid of our tracking system. 10% (30/300) of initially completed exams were performed at other facilities and not identified until tracking interventions were performed. An additional 2.5% of exams (14) were performed >1 month prior to the recommendation due date. 62% (9/14) of these exams did not answer the clinical question and resulted in another recommendation.15.8% (89/564) of recommendations closed resulted in exam completion following one of 3 stages of intervention. The rate of exam completion following each of the three stages of intervention was 16%, 13%, and 26% respectively. A clinical rationale for why the recommended study was not performed was identified in 21.8% of cases (123/564). The most common rationale provided was referral to a specialist such as an oncologist or surgeon. We were unable to close the loop on just 6.7% of patients (38/564). Of patients lost to follow-up, 19 did not have a primary care provider and did not reply to a letter explaining the overdue recommendation. Additionally, 14 were non-compliant with their primary care provider's attempts to schedule the exam.

### CONCLUSION

Current processes to manage radiology follow-up recommendations are inadequate with approximately half of all recommended imaging tests never being obtained. Our three stage radiology recommendation tracking system was shown to 1) increase the rate of recommended study exam completion by 16%, 2) identify the clinical rationale for non-compliance in 22% of patients, and 3) reduce the rate of patients who were lost to follow-up to fewer than 7%. Increasing the recommended study completion rate 1) improves patient care by potentially identifying malignancy at an early stage, 2) reduces medical legal liability for the radiologist, primary care provider, hospital, and insurer, and 3) increases fee for service revenue.Our radiology recommendation tracking system was designed to be a collaborative effort to assist local primary care providers in managing the large volume of clinical information they receive daily. The concept of our radiology department demonstrating accountability for the outcomes of the patients that we image has been viewed favorably by local primary care providers and has provided an opportunity to both add measureable value to our health system and increase the presence of our radiology department in the community.

# QS008-EB-WEB

## The Impact of QC in Multicenter Clinical Trials-The IROC Experience for NCTN Focusing on MRI

Wednesday, Nov. 30 12:45PM - 1:15PM Room: QS Community, Learning Center Hardcopy Backboard

#### **Participants**

Preethi Subramanian, MS, BEng, Columbus, OH (*Presenter*) Nothing to Disclose Shivangi Vora, BS, MS, Columbus, OH (*Abstract Co-Author*) Nothing to Disclose Tim Sbory, BS, Columbus, OH (*Abstract Co-Author*) Nothing to Disclose Prayna Bhatia, BS, Columbus, OH (*Abstract Co-Author*) Nothing to Disclose Marc J. Gollub, MD, New York, NY (*Abstract Co-Author*) Nothing to Disclose Michael V. Knopp, MD, PhD, Columbus, OH (*Abstract Co-Author*) Nothing to Disclose Ajay Siva, Columbus, OH (*Abstract Co-Author*) Nothing to Disclose Jun Zhang, PhD, Columbus, OH (*Abstract Co-Author*) Nothing to Disclose

# PURPOSE

When MRI is used as the preferred imaging modality in oncologic multi-center clinical trials, imaging based on the Standard of Care at the participating institutions is frequently recommended. Developing neuroimaging standards / best practices as well as the increased use and need of quantification techniques necessitate consistent image acquisitions especially for response assessment to therapies. Phantom based device quality assessments while important for instrumentation do not ensure quality image acquisition due to inter-operator, intra-institutional protocol variability and patient induced artefacts. As our team serves as IROC for the NCI-NCTN, we have embarked upon developing an imaging based MR quality assurance methodology that can also be used for local quality management.

# METHODS

Based on blinded imaging review assessments by independent readers and protocol specifications as defined by the imaging committee, we have identified key parameters for most commonly used MRI sequences. These were then used to develop a semiautomatic parameter-level quantification. A heat-mapping spectrum was developed with three categories: Green: Desired range of parameters for optimal response assessment and quantification; Yellow: Acquisitions outside the desired range, but still acceptable in order to be more "inclusive" to meet accrual targets, and Red: Significant variations that risk making the imaging exam unusable thereby either needing reacquisition or potentially resulting in exclusion of this case from study analysis.MRIs submitted for two multi-centered clinical trials are demonstrated in this approach, with more than 200 examinations from over 60 different institutions.

#### RESULTS

We were able to demonstrate that such a heat-mapping approach can be readily implemented and semi-automatically performed, once DICOM tag criteria are established. Using the color-coded tag system, a mosaic of the exam, case, institution and overall clinical trial can be generated and readily visualized. "Hot spotting" can then quickly identify deviation and trends. In the two trials that we identified for this quality storyboard, 59% of baseline MRI analyzed at the time of this abstract were rated in the Red category, while 64% of the follow-up exams were inconsistent when compared to baseline. Apart from exclusion of sequences (3%), the main parameters that caused these MRI exams into the Red color tag were Slice Gap (37% for Trial 1 and 28% for Trial 2) and inconsistent acquisitions (28% for Trial 1 and 20% for Trial 2). MR exams mapped to the Yellow tag occurred commonly under two scenarios: 1) Slice Thickness within expectations, however Slice Gap not (33%) or 2) Slice Gap as expected, but Slice Thickness not (66%). Highlighting just some of the acquisition deviations from the expectations indicates that we have to reeducate primarily the MR technologist and protocoling clinicians and demonstrate that these variations are at a minimum burdensome to efficient response assessment and increasingly jeopardize the effective use of software tools to analyze and quantify MRI.From prior experiences on other methodologies such as PET, we know that awareness of these issues and feedback to encourage improvements are effective tools to improve image quality performance.

# CONCLUSION

The variability of MRI acquisition parameters is currently severely underappreciated. A semi-automated QC processing can be implemented that can effectively and efficiently identify and visualize deviation from the expected MR acquisition parameter. We found that within national multi-center trials most frequently Standard of Care imaging according to local guidelines is recommended most likely due to lack of awareness in regard to the observed variability. Consistency of MR acquisition parameters is essential for robust and effective response assessment and indispensable for quantification or automated image assessment tools. As established, the parameter level analysis helps to identify trends at the exam, patient, site and clinical trial level. We found that visualizing this level of variability is essential to alter the way MR imaging is performed. The implementation of real-time feedback loops, as currently practiced by IROC, is likely to better educate sites and their MRI technologists. With rapidly increasing use of therapy altering, "adaptive" clinical trials robust image quality is indispensable.

Interpretation of Coronary CTA: Agreement of On-Call Radiology Residents and Cardiothoracic Radiology Faculty

Wednesday, Nov. 30 12:45PM - 1:15PM Room: QS Community, Learning Center Station #1

# Participants

Kimberly G. Kallianos, MD, San Francisco, CA (*Presenter*) Nothing to Disclose David M. Naeger, MD, San Francisco, CA (*Abstract Co-Author*) Nothing to Disclose Brett M. Elicker, MD, San Francisco, CA (*Abstract Co-Author*) Nothing to Disclose Michael D. Hope, MD, San Francisco, CA (*Abstract Co-Author*) Nothing to Disclose Travis S. Henry, MD, San Francisco, CA (*Abstract Co-Author*) Nothing to Disclose Travis S. Henry, MD, San Francisco, CA (*Abstract Co-Author*) Research Consultant, Enlitic Inc; Spouse, Employee, F. Hoffmann-La Roche Ltd Javier Villanueva-Meyer, MD, San Francisco, CA (*Abstract Co-Author*) Nothing to Disclose Abigail V. Berniker, MD, San Francisco, CA (*Abstract Co-Author*) Nothing to Disclose Nicholas S. Burris, MD, San Francisco, CA (*Abstract Co-Author*) Nothing to Disclose

Douglas Avadikian, San Francisco, CA (Abstract Co-Author) Nothing to Disclose

Karen G. Ordovas, MD, San Francisco, CA (Abstract Co-Author) Nothing to Disclose

### PURPOSE

We recently implemented availability of 24-hour coronary computed tomography angiography (CCTA) interpretation in the emergency department (ED), with cardiothoracic radiology faculty available to review CCTA studies at all hours. We aimed to evaluate the feasibility of on-call radiology resident interpretation of CCTA through creation of a dedicated CCTA curriculum for residents and subsequent assessment of agreement between on-call radiology residents and cardiothoracic radiology faculty interpretations.

## METHODS

A curriculum on performance/interpretation of CCTA was created including both lectures and small group sessions. Three 45-minute lectures on core concepts as well as two case-based lectures reviewing 15 CCTA cases were given by cardiothoracic radiology faculty. Faculty-led small group sessions allowed for review of 20 additional CCTA examinations at the PACS workstation, for a total exposure to 50 CCTA cases with faculty-guided review. Only senior radiology residents were responsible for CCTA interpretation oncall, all of which had also completed a required one-month cardiac radiology rotation including exposure to CCTA examinations. A dedicated resident workflow was created to outline the role of the on-call resident at each stage of the CCTA scan protocol. Resident Duties for CCTA from the Emergency Department:STEP 1: Protocol the study. Medication ordering is managed by ED. STEP 2: Check calcium score. Do not proceed with CCTA if calcium score >400 as unlikely to exclude significant stenosis. STEP 3: Interpret the case, including axial images and 3D reformations. If 3D reformations are not available, ask technologist who performed the scan to contact the 3D lab.STEP 4: Enter preliminary interpretation category and discuss with ED. CCTAs were classified by the on-call resident into 5 preliminary categories: 1) normal; 2) coronary stenosis <50%; 3) coronary stenosis >50%; 4) calcium score >400; or 5) non-diagnostic. On-call radiology residents entered the preliminary CCTA score into an online module. Following preliminary scoring, the resident contacted an on-call cardiothoracic radiology faculty member who would interpret the case. We collected 6 months of preliminary resident scores and final faculty interpretation from July 2015 to January 2016. Agreement between the on-call resident and faculty CCTA score was tabulated. Historical data on resident interpretation was not available, as previously on-call residents did not routinely and irreversibly record preliminary interpretations before contacting a faculty member. Feedback on success of the program and areas of concern was obtained from the on-call residents anonymously through the chief radiology residents.

### RESULTS

32 CCTAs were performed in the ED during our 6-month evaluation period. Category 1 (normal) was assigned most commonly (14/32, 43.8%). Categories 2, 3, 4, and 5 were assigned in 7/32, 4/32, 7/32, and 0/32 of CCTAs respectively. There was complete agreement between the on-call resident preliminary category and faculty category in 32/32 cases. Chief residents indicated that the ongoing primary concern of on-call residents throughout the time period was not the interpretation of the studies but rather comfort and familiarly with the workflow including coordination with nursing, technologists, and the 3D lab staff.

# CONCLUSION

On-call radiology resident categorization of CCTA examinations performed in the ED displayed excellent agreement with cardiothoracic radiology faculty interpretation. These results suggest that on-call radiology resident interpretation of CCTA using a simplified scoring system is feasible following dedicated CCTA training. Utilization of on-call resident interpretation may allow institutions to increase after-hour availability of CCTA. In the future, further data collection and a larger sample size will be needed to assess for long-term stability of resident-faculty agreement. Creation of a dedicated on-call resident workflow may be helpful in order to address the learning curve and comfort of residents with the performance of on-call CCTA. Additional feedback from on-call residents will allow assessment of the success of the CCTA curriculum and whether residents develop increased familiarity with the workflow over time.

### **Honored Educators**

Presenters or authors on this event have been recognized as RSNA Honored Educators for participating in multiple qualifying educational activities. Honored Educators are invested in furthering the profession of radiology by delivering high-quality educational content in their field of study. Learn how you can become an honored educator by visiting the website at: https://www.rsna.org/Honored-Educator-Award/

Travis S. Henry, MD - 2016 Honored Educator

Trends in the Utilization of Adjuvant Vaginal Brachytherapy in the Treatment of Women with Stage I and II Endometrial Cancer: Results of an Updated Period Analysis of SEER Data

Wednesday, Nov. 30 12:45PM - 1:15PM Room: RO Community, Learning Center Station #1

### Awards

### **Student Travel Stipend Award**

#### Participants

Ankit Modh, MD, Detroit, MI (Presenter) Nothing to Disclose

# ABSTRACT

Purpose/Objective(s): Adjuvant vaginal brachytherapy (VB) is a well-established and effective radiation treatment (RT) modality in women with early stage endometrial carcinoma (EC). We sought to evaluate and update the trends in utilization of VB versus other RT modalities (pelvic external beam RT (EBRT) or the combination of VB and pelvic EBRT using the National Cancer Institute's Surveillance, Epidemiology, and End Results (SEER) database.Materials/Methods: The SEER database was queried for adult females with histologically confirmed FIGO (1988) stage I-II endometrial cancer diagnosed from 1995-2012 who underwent hysterectomy and adjuvant radiation therapy. Patients with multiple primary malignancies, those who received radiation treatment prior to surgery or those who did not have any adjuvant RT were excluded. Chi-squared tests were used to assess differences by radiation modality (VB, EBRT, and VB+EBRT) and various demographic and clinical variables.Results: We identified 15,201 patients who met our inclusion criteria. There was an overall increase in the use of VB observed from 17.1% in 1995-2000 compared to 57.1% in 2007-2012 (p p p p p p pConclusion: There continues to be a trend for the increased use of VB in the adjuvant setting for patients with FIGO stage I-II EC. This trend was observed across patient or treatment factors analyzed.

Acute Toxicities using Intensity Modulates Radiation Therapy for Adjuvant and Definitive Salvage Treatment of Endometrial Cancer: A Single Institution

Wednesday, Nov. 30 12:45PM - 1:15PM Room: RO Community, Learning Center Station #2

# Participants

Phoebe Chidley, MBBS, Heidelberg, Australia (*Presenter*) Nothing to Disclose Carminia Lapuz, MBBS, FRANZCR, Melbourne, Australia (*Abstract Co-Author*) Nothing to Disclose Adeline Lim, FRANZCR, Heidelberg, Australia (*Abstract Co-Author*) Speaker, Teva Pharmaceutical Industries Ltd

### ABSTRACT

Purpose/Objective(s): Intensity modulated radiation therapy (IMRT) can be used to reduce dose to organs at risk (OARs) whilst maintaining target coverage, theoretically reducing treatment-related morbidity and allowing dose escalation. IMRT is dosimetrically advantageous compared with conventional external beam radiotherapy (EBRT) in the treatment of endometrial cancers as there can be large volumes of OARs within conventional pelvic fields, increasing potential toxicities and limiting dose escalation in recurrent disease. The aim of this study is to evaluate the acute toxicities of adjuvant and definitive salvage EBRT for primary or recurrent endometrial cancer confined to the pelvis using IMRT Materials/Methods: Patients treated with pelvic EBRT for adjuvant or definitive salvage therapy of endometrial cancer between April 2013 to January 2016 were identified from our center's database. All patients were treated using 7 to 9 field IMRT to a dose of 45 - 50.4 Gy to the pelvis in the adjuvant setting and 54 - 59.4 Gy using a simultaneous integrated boost to recurrent disease, with or without chemotherapy. Target and OARs contouring was based on published guidelines. Daily cone beam imaging was used for image guidance. Acute toxicity data was collected according to Common Terminology Criteria for Adverse Events v4.0 weekly. Descriptive statistics was used for analysis. Results: 20 patients were included in this study. Median age was 66.5 years (range: 51-90 years). Stage 1, 2, 3 and recurrent disease was seen in 4, 4, 6 and 6 patients respectively. Concurrent chemotherapy with cisplatin was given in 5 patients. Grade 1 acute genitourinary toxicities was seen in 65% and grade 2 in 15% of patients, predominantly reported as urinary frequency. Grade 1 acute bowel toxicities were seen in 65% of patients and grade 2 in 20%, mainly in the form of diarrhea and bowel frequency. 14 patients experienced grade 1-2 nausea. Grade 1-2 fatigue was seen in 11 patients. There were no cases of acute toxicities greater than grade 2. Conclusion: Pelvic EBRT with doses up to 59.4 Gy for endometrial cancers using IMRT is well tolerated and is associated with low grade acute genitourinary and gastrointestinal toxicities only. This is consistent with published studies, however, longer follow-up is required to assess late toxicities and tumor control. The results of larger prospective studies are awaited to assess whether IMRT results in reduction in acute and long term toxicities and better tumor outcomes compared with conventional EBRT.

# RO242-SD-WEB3

PET Response Assessment in Patients with Hodgkin Lymphoma Receiving Brentuximab: A Single Institution Experience

Wednesday, Nov. 30 12:45PM - 1:15PM Room: RO Community, Learning Center Station #3

### **Participants**

Genevieve Maquilan, MD, Dallas, TX (Presenter) Nothing to Disclose

#### ABSTRACT

Purpose/Objective(s): Brentuximab is increasingly being used for treating CD30-positive Hodgkin lymphoma (HL). Anecdotal reports of high false-positive rates on post-brentuximab imaging with positron emission tomography (PET), including a 75% rate in a phase II study of early stage non-bulky HL (NCT01534078), have caused concern about interpretation of results and guidance of further therapy, including consolidative radiotherapy. This study provides a formal description of the findings on PET on interim scans or after completion of treatment with brentuximab at a single institution.Materials/Methods: Patients with HL who received treatment with brentuximab as part of initial therapy or salvage treatment from 2011 - 2015 were included. Persistence or newly avid sites of Deauville =4 on post-treatment PETs were judged as positive findings.Results: 13 patients were evaluated. Seven patients received brentuximab as part of initial therapy, 4 patients received it as salvage therapy, and 4 received it as consolidative therapy after transplant, with 2 of those latter patients having received brentuximab previously. Six patients had not yet completed the intended course of brentuximab-based treatment and were only evaluated for their interim scans. Four out of the 13 patients (30.8%) had an increase in fluorodeoxyglucose (FDG) avidity of sites of known disease, and 3 out of the 13 patients (23.1%) had appearance of new FDG-avid sites of disease on PET, obtained as either an interim study or after the completion of treatment. Three patients (23.1%) completed therapy and had either an increase in avidity in sites of known disease or development of new sites on the post-treatment PET (Deauville =4). Of these, 2 patients proceeded to a subsequent chemotherapy regimen for progression, with only one patient having biopsy confirmation of active disease. The third patient, treated with brentuximab as part of initial definitive therapy for stage IIAEX disease, underwent mediastinoscopy dissection of newly FDG-avid sites, which was negative. Repeat PET showed resolution of these new sites of uptake one month after dissection with only residual uptake in an initially involved bulky site, and thus he proceeded to standard consolidative radiotherapy.Conclusion: Positive PET findings after the completion of treatment with brentuximab were biopsied in the absence of clear clinical progression, with demonstration of one apparent false positive case that changed therapy. Our single institution findings raise caution in regards to presuming a high false-positive rate on post-treatment PET, and, if feasible, biopsy should be considered.

## Prognostic Potential of CBCT for Tracking Tumor Regression in Stage II-III Non-Small Cell Lung Cancer

Wednesday, Nov. 30 12:45PM - 1:15PM Room: RO Community, Learning Center Station #6

#### Participants

Kylie Kang, BS, Cleveland, OH (Presenter) Nothing to Disclose

### ABSTRACT

Purpose/Objective(s): During external beam radiation therapy (EBRT) of lung cancer, cone beam computed tomography (CBCT) is routinely performed for image guidance. This study was conducted in order to determine the prognostic potential of CBCT for evaluating treatment outcome in terms of GTV reduction and to determine the difference of tumor reduction based on different histology. Materials/Methods: Forty-one NSCLC patients treated with definitive radiotherapy at one institution who received daily CBCT were randomly selected. Patients received mean EBRT of 60.7 Gy (range: 50-71.4 Gy) at 1.8 or 2 Gy per fraction. Initial mean gross tumor volume (GTV) was 197.3 cc (range: 3.4-1815.0 cc). Six sets of CBCT at an interval of one week were chosen, starting from the first fraction of treatment. The CBCTs were transferred to MIM Software (v.6.0) and single physician manually contoured the GTV on each slice. The change in GTV was recorded. Patient's clinical information was obtained from the institution electronic medical record. All statistical analysis was conducted on MedCalc (v.16.2). Univariate survival analysis was done using the Kaplan-Meier method with log-rank test. Median overall GTV reduction was used as a cutoff value (DGTVDGTV=45%). A univariate regression analysis was done to explore the correlation between histology and GTV reduction. A pResults: A consistent regression of GTVs was observed in 29 patients, while 12 patients experienced an increase of GTV at some point during their EBRT. Maximum reductions occurred during week 1 and 2 week of radiation, with mean % reductions of 13.5% and 12.6%, respectively. There was an overall GTV % reduction between weeks 1 to 6 in all 41 patients (median: 45%). The recurrence free survival (RFS) in our stratified group with DGTVDGTV=45% was 24.3 months (SE: 4.6) (p= 0.61). Overall survival (OS) for the group of patients with DGTVDGTV=45% (p= 0.21). There was a 6.6% greater overall GTV reduction in adenocarcinoma versus SCC on univariate regression analysis (p = 0.31). There was no statistical significance between histology and RFS (p = 0.84) or OS (p = 0.06). Conclusion: Large regression of GTV over the course of EBRT for stage II-III NSCLC patients was observed, however, no correlation was found with clinical outcome (RFS, OS). There was slightly higher GTV reduction in adenocarcinoma as compared to SCC, but no statistical significance. A future study with larger sample size involving multivariable analysis is

warranted.VariablesMean/Median/CountSD/Range/%Median Age (y)6244-80Gender (#) Female/Male27/1465.9%/34.1Week 1 GTV (cc) Mean197.33.4-1815 Median68.93.4-1815Follow-Up (months) Median12.41.9-61.3

Portal Vein Embolization: "Who, What, Where, When, Why, and How"

Wednesday, Nov. 30 12:45PM - 1:15PM Room: VI Community, Learning Center Station #8

### Awards Cum Laude

#### **Participants**

Daniel B. Gans, MD, Cleveland, OH (*Presenter*) Nothing to Disclose Jon Davidson, MD, Cleveland, OH (*Abstract Co-Author*) Nothing to Disclose Eric D. McLoney, MD, Chapel Hill, NC (*Abstract Co-Author*) Nothing to Disclose Sidhartha Tavri, MBBS, Boston, MA (*Abstract Co-Author*) Nothing to Disclose Christopher M. Sutter, MD, Cleveland, OH (*Abstract Co-Author*) Nothing to Disclose Indravadan J. Patel, MD, Cleveland, OH (*Abstract Co-Author*) Nothing to Disclose

### **TEACHING POINTS**

To review the patient selection, pathophysiology, indications/contraindications, technique, outcomes, and imaging involved in portal vein embolization.

# TABLE OF CONTENTS/OUTLINE

"What" Brief review of percutaneous, endovascular, and surgical therapies for primary hepatic malignancies Liver regeneration pathophysiology "Why" Justification of procedure prior to liver resection "Where" Anatomy and diagnostic imaging Preprocedural imaging and procedural planning "When" Timeline of liver regeneration prior to resection "Who" Patient selection Indications/contrainidcations "How" How to perform procedure Technical considerations Outcomes Success rates Complications

# Monitoring of Liver MW Ablation in an Ex-vivo Bovine Model with Point Shear Waves Elastography (pSWE)

Wednesday, Nov. 30 12:45PM - 1:15PM Room: VI Community, Learning Center Station #1

#### Participants

Laura Crocetti, MD, Pisa, Italy (*Presenter*) Nothing to Disclose Francesca Calcagni, Pisa, Italy (*Abstract Co-Author*) Nothing to Disclose Giulia Gherarducci, Pisa, Italy (*Abstract Co-Author*) Nothing to Disclose Francesco P. Tarantino, Pisa, Italy (*Abstract Co-Author*) Nothing to Disclose Nevio Tosoratti, PhD, MA, Roma, Italy (*Abstract Co-Author*) Employee, HS Hospital Service SpA Claudio Amabile, Aprilia (LT), Italy (*Abstract Co-Author*) Employee, HS Hospital Service SpA Simone Cassarino, Aprilia (LT), Italy (*Abstract Co-Author*) Employee, HS Hospital Service SpA Roberto Cioni, MD, Pisa, Italy (*Abstract Co-Author*) Nothing to Disclose Davide Caramella, MD, Pisa, Italy (*Abstract Co-Author*) Nothing to Disclose

### PURPOSE

To determine the reliability of point shear wave elastography (pSWE) to delineate, in ex-vivo bovine liver tissue, the boundaries of ablation zone produced by microwave ablation (MWA).

# **METHOD AND MATERIALS**

Cuboidal specimens of at least 5 cm side were obtained from ex-vivo bovine liver and ablated by a commercial MWA system (HS AMICA®, H.S. Hospital Service SpA). B-mode imaging and shear wave velocity (SWV) were acquired simultaneously (Virtual Touch<sup>™</sup> Tissue Quantification, Siemens Healthcare). Based on our previous experimental work, MWA was performed at 60 W until a SWV of 3m/sec was reached in a Region Of Interest (ROI) that was placed 1.5 cm radially from the antenna feed point. Afterwards, SWV was measured in several ROIs at established distances ranging from 10 mm to 40 mm from the antenna feed, acquiring 10 SWV determinations for each ROI. Finally, the specimens were cut along the antenna to obtain a gross-pathologic measurement of the coagulation necrosis boundary. An average SWV contour map was created, superimposing the pathology picture of the liver necrosis with the B-mode ultrasound images of ROIs' positions. The best SWV threshold for discriminating ablated from non-ablated tissue was identified by maximizing the predictive accuracy.

#### RESULTS

In all the experiments, the gross-pathology evaluation confirmed that the necrosis boundary was at approximately 1.5 cm from the antenna feed. The highest accuracy (0.86) of the pSWE-SWV contour maps was obtained with a threshold of 2.5 m/s, based on the 22 independent determinations of SWV available up to date. This finding is in good agreement with the results of our previous study, where we showed a steep and irreversible increase of the SWV when the tissue temperature exceeds 60°C. Reducing the number of SWV determinations in each ROI didn't change the threshold value for best accuracy.

# CONCLUSION

pSWE can provide an elasticity threshold predictive of the presence of coagulation necrosis during and after MW ablation in ex-vivo liver model. An accurately determined elasticity threshold might help monitoring the boundaries of ablation zones in vivo.

# **CLINICAL RELEVANCE/APPLICATION**

Initial results demonstrate clinical promise of elastosonography in thermal ablation procedures as a mean to provide accurate, noninvasive, real-time determinations of the ablation boundary. Prevalence of Malignancy and Invasive Cancer in Analysis of 350 Ground-Glass Nodules 20mm or Smaller Obtained with CT-Guided Core Needle Biopsy

Wednesday, Nov. 30 12:45PM - 1:15PM Room: VI Community, Learning Center Station #2

# Participants

Minako Azuma, Miyazaki, Japan (*Presenter*) Nothing to Disclose Hiroshi Nakada, MD, PhD, Miyazaki-city, Japan (*Abstract Co-Author*) Nothing to Disclose Mei Shimomura, Miyazaki, Japan (*Abstract Co-Author*) Nothing to Disclose Youhei Hattori, Miyazaki, Japan (*Abstract Co-Author*) Nothing to Disclose Koichi Kawanaka, MD, Kumamoto, Japan (*Abstract Co-Author*) Nothing to Disclose Yasuyuki Yamashita, MD, Kumamoto, Japan (*Abstract Co-Author*) Consultant, DAIICHI SANKYO Group Toshinori Hirai, MD, PhD, Miyazaki, Japan (*Abstract Co-Author*) Nothing to Disclose

### PURPOSE

CT-guided core-needle lung biopsy is useful for evaluating pathology of ground-glass nodule (GGN). The aim of this study was to determine the prevalence of malignancy and invasive cancer for GGNs 20mm or smaller using CT-guided core needle biopsy.

### **METHOD AND MATERIALS**

We included 350 GGNs of 333 consecutive patients (204 women, 129 men; age range, 28-86 years; mean age, 67 years) from April 2011 to October 2015, with pulmonary GGN 20 mm or smaller suspected malignancy on CT images. All underwent percutaneous CT-guided core needle lung biopsy; 18G core biopsy needle and co-axial introducer needle were used. The type of GGNs was divided into two categories: pure or part solid type. Specimens were examined for both histology and microbiology. An experienced pathologist assessed the presence of malignancy and the invasiveness of cancer. The differences between the pure and part solid GGN groups were assessed with the chi-square test.

### RESULTS

The success rate of CT-guided lung biopsy was 348 of 350 (99.4%) lesions. The prevalence of malignant tumor was 77.7% for GGNs 10 mm or smaller and 86.0% for GGNs from 11 to 20 mm. For pure GGNs, the prevalence of invasive cancer was 15.4% for lesions 10 mm or smaller and 24.5% for 11 to 20 mm. With regard to part solid GGNs, the prevalence of invasive cancer was 42.3% for lesions 10mm or smaller and 38.9% for 11 to 20 mm. Regardless of lesion size, the prevalence of invasive cancer was significantly higher for part solid GGNs than pure GGNs (p < 0.05).

## CONCLUSION

Of GGNs 20mm or smaller, approximately 80% exhibits malignancy and the prevalence of invasive cancer is about 20%.

# **CLINICAL RELEVANCE/APPLICATION**

For GGNs 20 mm or smaller, CT-guided core needle biopsy is useful for the diagnosis and the prevalence of invasive cancer may be higher than expectation.

# VI266-SD-WEB5

Implementation of a Magnetic-free Pulsating Flow Phantom: Comparison of Five 2D Phase-contrast Processing Systems

Wednesday, Nov. 30 12:45PM - 1:15PM Room: VI Community, Learning Center Station #5

# Participants

Karine Warin-Fresse, Nantes, France (*Presenter*) Nothing to Disclose Pauline Fourquet, Nantes cedex 1, France (*Abstract Co-Author*) Nothing to Disclose Patrice Guerin, MD,PhD, Nantes cedex 1, France (*Abstract Co-Author*) Nothing to Disclose Beatrice Guyomarc'h Delassalle, nantes cedex 1, France (*Abstract Co-Author*) Nothing to Disclose Thomas Senage, MD, Nantes cedex 1, France (*Abstract Co-Author*) Nothing to Disclose Marc Sirol, MD, PhD, Paris, France (*Abstract Co-Author*) Nothing to Disclose Jean-Nicolas Dacher, MD, Rouen, France (*Abstract Co-Author*) Consultant, General Electric Company

### PURPOSE

MRI is a non invasive and functional imaging technique. The 2D phase contrast (2D PC) sequence allows flow quantification. The first aim of the study was to design and build a magnetic free pulsating flow phantom. Second one was to compare, 5 different 2D PC solutions: Argus® (Siemens), Syngo® (Siemens), CVI® (Circle), Medis® and Terarecon®. The reference values were provided by the flow meter included in the device.

### **METHOD AND MATERIALS**

Pulsating flow was generated by an artificial heart to obtain controlled values. Output and volumes were measured by 2D PC ranging 1.6 - 7 l/mn and on the following vessel diameters; 1.7cm, 2 cm and 3.5 cm. Each measure was performed three times with different velocity encoding from 100cm/s to 500 cm/s. Finally, all 285 measures were processed independently with each software.

### RESULTS

Percentage changes between software results and control value were Argus  $12,4\% \pm 14,8$ , Syngo  $9,9\% \pm 10,4$ , CVI $15,5\% \pm 11,3$ , Medis  $15,8\% \pm 15.5$ , terarecon  $13.3\% \pm 14.2$ . The Friedman test showed a significant difference (p<0,001) between the 5 solutions and control values. Medis overestimated the mean outflow and antegrade volume (Wilcoxon test p=0,001).

### CONCLUSION

This study showed a significant difference between 5 commercially available solutions in the evaluation of mean outflow and an overestimation of the mean outflow by Medis® comparatively to control values.

# **CLINICAL RELEVANCE/APPLICATION**

MRI is a reliable tool for the assessment of pulsatil flow.

# VI267-SD-WEB6

Clinical Significance of Stent Abutment in Gastroduodenal Stent Placement for Gastric Outlet Obstructions: Experience in 318 Patients

Wednesday, Nov. 30 12:45PM - 1:15PM Room: VI Community, Learning Center Station #6

# Participants

Jung-Hoon Park, PhD, Seoul, Korea, Republic Of (*Abstract Co-Author*) Nothing to Disclose Guk Bae Kim, Seoul, Korea, Republic Of (*Abstract Co-Author*) Nothing to Disclose Ho-Young Song, MD, Seoul, Korea, Republic Of (*Abstract Co-Author*) Nothing to Disclose Namkug Kim, PhD, Seoul, Korea, Republic Of (*Abstract Co-Author*) Stockholder, Coreline Soft, Inc Jiaywei Tsauo, Seoul, Korea, Republic Of (*Abstract Co-Author*) Nothing to Disclose Min Tae Kim, Seoul, Korea, Republic Of (*Presenter*) Nothing to Disclose

## PURPOSE

To evaluate the clinical significance of stent abutment after gastroduodenal stent placement in 318 patients with gastric outlet obstruction (GOO) due to unresectable gastric cancer.

# METHOD AND MATERIALS

A retrospective study was performed in a single, tertiary-referral, university hospital to identify the incidence and clinical significance for stent abutment in patients who underwent placement of a self-expandable metallic stent (SEMS). Stent abutment was defined as abutment of the distal end of the stent to the duodenal wall and/or superior duodenal flexure. Outcomes analyzed included technical and clinical success, complications, re-intervention, stent patency, and survival.

### RESULTS

A total of 318 patients met our inclusion criteria, including 107 patients in stent abutment (SA) group and 211 patients in non-stent abutment (NSA) group. Stent abutment occurred partially (n = 64, 59.8%) and completely (n = 43, 40.2%). The technical, clinical outcomes and survival were similar in the two groups. Complication and re-intervention rates were higher in the SA than in the NSA group (P = 0.001 and P = 0.008, respectively). Food impaction rate was higher in the SA than in the NSA group (P < 0.001) and was associated with complete SA (P = 0.007). Stent patency rate was lower in the SA than in the NSA group (P = 0.003).

### CONCLUSION

Stent abutment was associated with increased food impaction, resulting in higher stent malfunction and shorter stent patency compared with non-stent abutment. The novel concept of stent abutment may be useful in improving the stent patency and avoiding food impaction.

# **CLINICAL RELEVANCE/APPLICATION**

Stent abutment was associated with frequent food impaction resulting in a shortening of stent patency and an increase of overall complication and re-intervention rates.

Outcomes of a New Very Small Diameter Drug Eluting Embolic Beads for Transarterial Chemoembolization in Unresectable Hepatocellular Carcinoma: A Single Center Experience

Wednesday, Nov. 30 12:45PM - 1:15PM Room: VI Community, Learning Center Station #7

**FDA** Discussions may include off-label uses.

## Participants

Ahmed K. Abdel Aal, MD, PhD, Birmingham, AL (*Presenter*) Consultant, St. Jude Medical, Inc; Consultant, Baxter International Inc; Consultant, C. R. Bard, Inc; Consultant, Boston Scientific Corporation; Consultant, W. L. Gore & Associates, Inc; Bradford Jackson, Birmingham, AL (*Abstract Co-Author*) Nothing to Disclose
George R. Newman, MD, Birmingham, AL (*Abstract Co-Author*) Nothing to Disclose
Christopher G. Baalmann, MD, Birmingham, AL (*Abstract Co-Author*) Nothing to Disclose
Keith Pettibon, MD, Birmingham, AL (*Abstract Co-Author*) Nothing to Disclose
Annie L. Harris, MD, Birmingham, AL (*Abstract Co-Author*) Nothing to Disclose
Anand R. Patel, MD, Birmingham, AL (*Abstract Co-Author*) Nothing to Disclose
Zachary A. Lambertsen, MD, Birmingham, AL (*Abstract Co-Author*) Nothing to Disclose
Sherif M. Moawad, MBBCh, MSc, Birmingham, AL (*Abstract Co-Author*) Nothing to Disclose
Maro M. Hanaoka, MD, Sao Paulo, Brazil (*Abstract Co-Author*) Nothing to Disclose
Maro M. Hanaoka, MBBCh, Little Rock, AR (*Abstract Co-Author*) Nothing to Disclose
Souheil Saddekni, MD, Birmingham, AL (*Abstract Co-Author*) Nothing to Disclose

## PURPOSE

The purpose of the study is to evaluate the tumor response rate and survival outcomes of a transarterial chemoembolization (TACE) of unresectable hepatocellular carcinoma (HCC) using 75 microns Oncozene (Boston Scientific, MA, USA) drug-eluting beads (DEB).

# METHOD AND MATERIALS

We retrospectively reviewed the medical records and radiologic studies of 67 patients who had their first TACE for HCC between November 2013 and December 2015 using 75 microns Oncozene DEB. The primary endpoint of the study was tumor response rate which was categorized according to the modified Response Evaluation Criteria in Solid Tumors (mRECIST) and the toxicity profile of the DEB using Common Terminology Criteria for Adverse Events (CTCAE) version 3.0. The secondary endpoint was patient survival.

# RESULTS

The study included 52 males and 15 females with a mean age of 63.8 years. HCV was seen in 58% of the patients. Overall tumor response on follow up CT and/or MRI done 4-6 weeks after TACE was 24% complete response, 78% objective response and 88% disease control. Complete response, objective response and disease control were 27%, 75% and 88% respectively in Child-Pugh A patients, and 26%, 79% and 91% respectively in Barcelona Clinic Liver Cancer (BCLC) stages A and B patients. Grades 3 toxicity was seen in 9% of the patients. There was no grade 4 toxicity recorded. The 6 and 12 month survival were 98% (95% CI: 89.4-99.9%, p<0.0001) and 90% (95% CI: 68.3-98.8%, p<0.001) respectively.

### CONCLUSION

The present study shows very good tumor response rate to TACE using 75 microns Oncozene DEB, with very low toxicity profile. Short-term survival outcomes appear to be promising with 98% and 90% survival at 6 and 12 months respectively.

### **CLINICAL RELEVANCE/APPLICATION**

The present study shows that TACE using 75 microns Oncozene DEB is effective with very good radiologic response and short-term survival outcomes, and safe with very low toxicity profile, for treatment of nonresectable HCC.

# Additional Tumors in Breast Cancer: What Have We Learnt?

Thursday, Dec. 1 12:15PM - 12:45PM Room: BR Community, Learning Center Station #6

#### **Participants**

Meylin Caballeros, MD, Pamplona, Spain (*Presenter*) Nothing to Disclose Jose Miguel Madrid, MD, Pamplona, Spain (*Abstract Co-Author*) Nothing to Disclose Arlette Elizalde, Pamplona, Spain (*Abstract Co-Author*) Nothing to Disclose Natalia Rodriguez-Spiteri, Pamplona, Spain (*Abstract Co-Author*) Nothing to Disclose Paula Martinez-Miravete, MD, Pamplona, Spain (*Abstract Co-Author*) Nothing to Disclose Luis Pina, MD, PhD, San Sebastian, Spain (*Abstract Co-Author*) Nothing to Disclose

# TEACHING POINTS

The purpose of this exhibit is: To review the radiological features of cancers only detected by US and/or DBT. To review the pathological features of cancers only detected by US and/or DBT.

# TABLE OF CONTENTS/OUTLINE

Introduction: How do we do: Additional US+DBT in all dense breasts Technical principles of DBT and US: why do they detect not suspected cancers in mammography? Features of tumors detected by additional DBTa) Radiological features: DBT was more sensitive to detect spiculated masses and distortions DBT did not detect as many BI-RADS 3 lesions as US DBT needed at least a small amount of peritumoral fat tissueb) Pathological features: All additional tumors were invasive DBT detected less Her2 and Triple Negative tumors than US 4. Features of tumors detected by USa) Radiological features: US was more sensitive to detect masses One of the main problems of US was the high detection rate of BI-RADS 3 lesions US sensitivity was independent to the amount of peritumoral fatb) Pathological features: Most of the additional cancers were invasive with only a few pure DCIS US detected both Luminal as well as Her2/TN cancers 5. Conclusion The highest diagnostic accuracy was achieved by using additional DBT+US Almost all the additional cancers were invasive

# BR266-SD-THA1

Patterns of Eye Movements in Breast Tomosynthesis and Full Field Digital Mammography: An Eye Tracking Study

Thursday, Dec. 1 12:15PM - 12:45PM Room: BR Community, Learning Center Station #1

# Participants

Avi M. Aizenman, Cambridge, MA (*Abstract Co-Author*) Nothing to Disclose Trafton Drew, PhD, Salt Lake City, UT (*Abstract Co-Author*) Nothing to Disclose Dianne Georgian-Smith, MD, Boston, MA (*Abstract Co-Author*) Nothing to Disclose Jeremy M. Wolfe, PhD, Cambridge, MA (*Presenter*) Research collaboration, IBM Corporation;

## PURPOSE

Digital breast tomosynthesis (DBT) is a promising yet relatively new imaging modality. Understanding how eye movements differ from reading DBT to full-field digital mammography (FFDM) can inform best practices for reading DBT. We use eye tracking to quantify and compare the basic pattern of eye movements adopted by radiologists searching DBT to FFDM.

## **METHOD AND MATERIALS**

11 radiologists (Os) read 9 DBT and 8 FFDM images in one projection (either DBT or FFDM). 4 cases in each modality contained positive findings that had led to further testing in clinic. Os had on average 6 years of experience reading FFDM and .62 years reading DBT. Os in the study were asked to mark any asymmetries that were possibly a clinically significant mass or questionable areas of architectural distortion warranting further diagnostic work-up. XY eye position was tracked at 1000 Hz, and was corregistered with slice/depth plane as radiologists scrolled through the DBT images producing a 3D scanpath. Os were given 2 minutes to localize any suspicious findings.

### RESULTS

DBT was overall associated with significantly fewer false positives per case compared to FFDM (t(10)=2.65, p<.05), and significantly longer search durations (75s) than for FFDM (43s) (t(10) = 5.661, p<.001). No significant differences were found for detection. DBT also led to significantly longer fixations (the eye focusing at a particular XY location) than FFDM t(10) = 7.1, p<.0001). In DBT, Os viewed on average 3.8 image slices during fixation, which may explain the longer fixation duration. For DBT, 10/11 of the Os described using a purposeful strategy in which their eyes remain relatively stationary in XY while they "drilled" through depth. Eyetracking revealed that Os often made large scanning movements while drilling, deviating from their described search strategy.

### CONCLUSION

Improvement in performance for DBT comes at a cost in time per case. Eye tracking data shows how radiologists are spending that time, as well as suggesting radiologists are deviating from introspected search strategies. Techniques for increasing speed without sacrificing accuracy can be tested against these baseline data.

# **CLINICAL RELEVANCE/APPLICATION**

Best clinical practices for reading DBT are currently unclear. The current study provides baseline metrics for assessing the effectiveness of different search strategies in DBT.

# BR268-SD-THA3

### Quantification of Breast Cancer Heterogeneity for Identifying Molecular Subtypes on MRI: Preliminary Study

Thursday, Dec. 1 12:15PM - 12:45PM Room: BR Community, Learning Center Station #3

#### **Participants**

Haeji Rue, Iksan, Korea, Republic Of (*Presenter*) Nothing to Disclose Hye-Won Kim, MD, Iksan, Korea, Republic Of (*Abstract Co-Author*) Nothing to Disclose Jong Hyun Ryu, Iksan, Korea, Republic Of (*Abstract Co-Author*) Nothing to Disclose Kwon-Ha Yoon, MD, PhD, Iksan, Korea, Republic Of (*Abstract Co-Author*) Nothing to Disclose

# PURPOSE

Molecular subtype in breast cancer is important for planning further treatment and predicting prognosis. Correlation between molecular subtype of breast cancer and heterogeneity of breast cancer on T1WI, T2WI, diffusion-weighted image, post-contrast subtraction image was evaluated.

## **METHOD AND MATERIALS**

A total of 88 breast cancer lesions (28- luminal A, 27- luminal B, 17- triple negative, 16 - human epidermal growth factor receptor 2(HER-2)) in 88 patients who had biopsy proven invasive carcinoma between July 2014 and December 2015 were enrolled in this study. We measured degree of cancer heterogeneity on T1, T2, fat suppressed T2, diffusion-weighted image and 1minute subtraction image by using MATLAB(matrix laboratory)-based software which calculate a coefficient of variation (CV) map of each pixel in free hand region of interest. The two-sample T-test and one way ANOVA with bonferroni post tests were used for evaluating the relation between degree of heterogeneity (CV value) and tumor molecular subtype. The diagnostic performance of CV value on each sequence of MRI was evaluated using a receiver operating characteristic (ROC) curve.

### RESULTS

Decreased CV values on DWI (b value-300) were observed in luminal A compared with luminal B and increased CV values on DWI (b value-300) were observed in luminal B compared with triple negative (p<.05). There were also significant differences in CV value on subtraction image between luminal A and each of luminal B, Triple negative, HER-2. With Bonferroni correction, CV values on subtraction image between luminal A and triple negative, luminal A and HER-2 were only significantly different. ROC curves of CV value on each sequences of MRI were not significantly different for identifying each molecular subtype of breast cancer.

# CONCLUSION

The quantification of intratumoral heterogeneity values on MRI was different between molecular subtypes.

# **CLINICAL RELEVANCE/APPLICATION**

Intratumoral heterogeneity values on MRI with CV map can help to identify molecular subtype of breast cancer.

HER2-positive Breast Cancer: Correlation between DCE-MRI Spatial Features, Temporal Kinetics, and Predictors of Tumor Progression and Recurrence

Thursday, Dec. 1 12:15PM - 12:45PM Room: BR Community, Learning Center Station #5

# Participants

Laura Heacock, MD, MS, New York, NY (*Presenter*) Nothing to Disclose Yiming Gao, MD, New York, NY (*Abstract Co-Author*) Nothing to Disclose Alana A. Lewin, MD, New York, NY (*Abstract Co-Author*) Nothing to Disclose Neeti Bagadiya, MD, New York, NY (*Abstract Co-Author*) Nothing to Disclose Samantha L. Heller, MD, PhD, New York, NY (*Abstract Co-Author*) Nothing to Disclose James S. Babb, PhD, New York, NY (*Abstract Co-Author*) Nothing to Disclose Amy N. Melsaether, MD, New York, NY (*Abstract Co-Author*) Nothing to Disclose Linda Moy, MD, New York, NY (*Abstract Co-Author*) Nothing to Disclose

#### PURPOSE

To evaluate the magnetic resonance imaging features of human epidermal growth factor receptor 2-positive (HER2+) tumors compared with those of estrogen receptor/progesterone receptor-positive (ER/PR+) and triple negative breast cancers (TNBC), with an emphasis on early temporal kinetic features of use in an abbreviated breast MRI protocol (AB-MRI).

#### **METHOD AND MATERIALS**

An institutional review board-approved study evaluated the DCE-MRI imaging findings in 135 women with pathology-proven HER2+ (22%, 31/135), ER/PR+/HER2- (57%, 77/135) and TNBC (21%, 28/135) invasive cancers imaged at 3.0T with a 7-channel breast coil. MR spatial features evaluated included shape, margins, internal enhancement and size. Initial enhancement ratio (% enhancement over baseline on the first post-contrast images), background parenchymal enhancement (BPE) and peritumoral BPE were assessed. If PET/CT was performed, pre-treatment SUVmax was recorded. Final pathology, tumor markers, ki-67, and positive axillary nodes were examined. Statistics included Fisher's exact tests, Mann-Whitney U tests and Spearman's rho.

# RESULTS

HER2+ cancers were more likely to be irregular (83.8%, 26/31) masses (100%, 31/31) with washout kinetic curves (80.6%, 25/31) and positive nodes (47%, 14/31), but were not statistically different from other tumor types (p=0.417). HER2 tumors were larger (mean=4.4 cm [1.2-9.1 cm]) than ER/PR+ tumors (p<0.001) but not TNBC (p=0.957). For all cancers, IER and ki-67 positively correlated (r=0.28, p=0.002). SUVmax also positively correlated with ki-67 (r=0.454, p=0.026) but was not different between tumor types. Mean IER was higher for HER2+ than ER/PR+ tumors (p=0.026) but not significantly different from TNBC (p=0.34). For HER2+ tumors alone, IER positively correlated with BPE (r=0.532, p=0.003) and peritumoral BPE (0.539, p=0.003), but there was no correlation between IER, grade, SUVmax, or axillary node status.

## CONCLUSION

HER2+ tumors cannot be reliably distinguished from TNBC based on spatial morphology alone. IER, a measure of tumor wash-in, correlated with ki-67, a marker of tumor aggression, as did SUVmax. IER could be easily incorporated into AB-MRI using conventional DCE-MRI.

## **CLINICAL RELEVANCE/APPLICATION**

DCE-MRI lesion morphology alone is not predictive of HER-2+ tumors. IER, an early kinetic marker easily measured in an abbreviated breast MRI (AB-MRI) screening protocol, may predict HER2+ aggressiveness.

**T1** Mapping of Myocardial Fibrosis in Patients with Non-ischemic Heart Failure: Comparison with Late Gadolinium Enhancement

Thursday, Dec. 1 12:15PM - 12:45PM Room: CA Community, Learning Center Station #1

# Participants

Fumi Yamada, MD, Tokyo, Japan (*Presenter*) Nothing to Disclose Yasuo Amano, MD, Tokyo, Japan (*Abstract Co-Author*) Nothing to Disclose Masaki Tachi, MD, PhD, Tokyo, Japan (*Abstract Co-Author*) Nothing to Disclose Shogo Imai, MD, Tokyo, Japan (*Abstract Co-Author*) Nothing to Disclose Shinichiro Kumita, MD, Tokyo, Japan (*Abstract Co-Author*) Nothing to Disclose

# PURPOSE

LGE (late gadolinium enhancement) imaging is able to detect myocardial fibrosis associated with various cardiac diseases. However, gadolinium-based contrast agents cannot be used for patients with end-stage chronic kidney disease associated with heart failure (HF). T1 mapping is another cardiovascular magnetic resonance (CMR) technique for myocardial tissue characterization without contrast. We sought to determine native T1 value to identify myocardial fibrosis in patients with non-ischemic HF.

#### **METHOD AND MATERIALS**

CMR was performed in 45 patients with non-ischemic HF and 15 healthy controls. Native T1 mapping using modified Look-Locker inversion recovery (3-(3)-5 sequence) was performed in all subjects, and LGE imaging was performed in all of the patients. Basal and mid-ventricular short axis slices were divided into 4 segments, and T1 value was measured in each segment. Myocardial LGE was defined on both visual assessment and quantitative assessment (2SD threshold above remote myocardium). The T1 values of septal LGE were compared with those of the septal segments without LGE, the minimal T1 value of each patient, and T1 values of the normal myocardium.

### RESULTS

LGE was present in 14 of the 45patients (31.1%) and 16 basal or mid-ventricular septal segments (17.8%). T1 values were higher in septal segments with LGE than in those without (1377.78±65.91ms vs. 1305.28±70.56; p=0.01) and those of the normal myocardium (1209.07±56.40; p<0.01). When compared with the minimal T1 value + its SD, the sensitivity for the presence of LGE was 87.5%, specificity was 70.3%, positive predictive value (PPV) was 39.0%, negative predictive value (NPV) was 96.0%, and accuracy was 73.3%. When setting T1 value above 1350 ms for identifying LGE, the sensitivity was 75.0%, specificity was 74.0%, PPV was 38.5%, NPV was 93.2%, and accuracy was 73.3%. When combining the minimum T1 value + its SD and T1 value > 1350 ms, the sensitivity was 75.0%, specificity was 86.5%, PPV was 54.6%, NPV was 94.1%, and accuracy was 84%.

### CONCLUSION

Native T1 mapping can be used for assessment of myocardial fibrosis in non-ischemic HF, especially when comparing with minimal T1 value in each patient.

### **CLINICAL RELEVANCE/APPLICATION**

T1 mapping without contrast can be used for detection of myocardial fibrosis in patients with non-ischemic heart failure by comparing septal T1 value to minimal T1 value in each patient.

# Evaluation of the Role of Aging on Calcification in the Aortic Wall Using NaF PET/CT

Thursday, Dec. 1 12:15PM - 12:45PM Room: CA Community, Learning Center Station #2

#### Awards

### **Student Travel Stipend Award**

#### **Participants**

Sahra Emamzadehfard, MD, MPH, Philadelphia, PA (*Presenter*) Nothing to Disclose Koosha Paydary, MD, MPH, Philadelphia, PA (*Abstract Co-Author*) Nothing to Disclose Sara Pourhassan Shamchi, MD, Philadelphia, PA (*Abstract Co-Author*) Nothing to Disclose Saeid Gholami, MD, Philadelphia, PA (*Abstract Co-Author*) Nothing to Disclose Sina Houshmand, MD, Philadelphia, PA (*Abstract Co-Author*) Nothing to Disclose Thomas J. Werner, Philadelphia, PA (*Abstract Co-Author*) Nothing to Disclose Poul Flemming Hoeilund-Carlsen, Odense, Denmark (*Abstract Co-Author*) Nothing to Disclose Abass Alavi, MD, Philadelphia, PA (*Abstract Co-Author*) Nothing to Disclose

# PURPOSE

We conducted this study in order to assess the difference in thoracic aortic wall calcification between two groups of young (20 to 30 years old) and older (60 to 75 years old) healthy subjects using NaF-PET/CT.

# **METHOD AND MATERIALS**

We evaluated 20 healthy subjects in the 20-30 years old age group and 20 healthy subjects in the 60-75 years old age group. The subjects underwent 90-min NaF PET/CT under similar conditions. A whole vessel analysis was performed in axial section for each of the analyzed vascular districts including ascending aorta (AA), aortic arch (AR) and descending thoracic (DA) aorta using a standard workstation. The maximum and mean Standardized Uptake Values (SUV) of NaF within the Regions of Interest (ROI) which were drawn around the aorta by an experienced physician, were calculated to obtain SUVmax and SUVmean for each slice, respectively. The SUVmax and SUVmean were normalized to blood NaF activity obtained from Superior Vena Cava (SVC) and blood-normalized whole artery uptake known as the arterial target-to-background ratio (TBR) was calculated. The TBRmax and TBRmean were assessed using the independent sample T test between the two groups.

#### RESULTS

According to our results, the only significant difference was observed in the arch region between the two groups: TBRmax 1.31 in old vs. 1.16 in young subjects respectively; p value= 0.008. In other regions, TBRmax was slightly higher in the young subjects, though the difference was not statistically significant. With regard to TBRmean, the two groups of study were not significantly different except for the descending thoracic aorta that showed significant difference. TBRmean was higher in young subjects compared to old subjects (TBRmean 2.37 in young vs. 1.83 in old subjects respectively; P value= 0.04).

### CONCLUSION

In this study, we observed a significantly higher NaF uptake in the arch of aorta in subjects of old age groups in comparison to young subjects. This finding may highlight the fact that active process of cholesterol plaque calcification continues in older ages, which may be related to the turbulent blood flow in the arch region as compared to other regions of the aorta.

# **CLINICAL RELEVANCE/APPLICATION**

Ongoing process of thoracic aortic wall calcification with increasing age can be detected and monitored using the NaF-PET/CT.

# CA254-SD-THA3

High-pitch, Double-spiral CTA with Low Radiation Exposure for Assessment of Early Postoperative Patency of Coronary Artery Bypass Grafts

Thursday, Dec. 1 12:15PM - 12:45PM Room: CA Community, Learning Center Station #3

# Participants

Shinsuke Shimoyama, MD, Kobe, Japan (*Presenter*) Nothing to Disclose Tatsuya Nishii, MD, PhD, Kobe, Japan (*Abstract Co-Author*) Nothing to Disclose Yoshiaki Watanabe, MD, Kobe, Japan (*Abstract Co-Author*) Nothing to Disclose Atsushi K. Kono, MD, PhD, Kobe, Japan (*Abstract Co-Author*) Nothing to Disclose Noriyuki Negi, RT, Kobe, Japan (*Abstract Co-Author*) Nothing to Disclose Shumpei Mori, Kobe, Japan (*Abstract Co-Author*) Nothing to Disclose Satoru Takahashi, MD, Suita, Japan (*Abstract Co-Author*) Nothing to Disclose Kazuro Sugimura, MD, PhD, Kobe, Japan (*Abstract Co-Author*) Research Grant, Toshiba Corporation Research Grant, Koninklijke Philips NV Research Grant, Bayer AG Research Grant, Eisai Co, Ltd Research Grant, DAIICHI SANKYO Group

### PURPOSE

This study aimed to evaluate high-pitch, double-spiral acquisition (HPDS) using third-generation dual-source CT (3rd DSCT) compared with the conventional single-spiral (SS) mode for assessing coronary artery bypass graft (CABG) patency regarding image quality and radiation dose.

## **METHOD AND MATERIALS**

Sixty-four consecutive patients who had undergone ECG-gated CT angiography (CTA) for assessment of graft-patency after CABG using 3rd DSCT were retrospectively reviewed. We included 39 patients (median, 75 years; 15 females; 26 with HPDS) who had CTA for checking early graft patency within 4 weeks after CABG surgery. In HPDS (pitch, 3.2; temporal resolution, 66 ms), when the heart rate was higher than 75 bpm, a scan was targeted to the systolic phase instead of diastolic phase. Heart rate and effective radiation dose were recorded. For patient-based analyses, the signal-to-noise ratio (SNR) in the ascending aorta (SNRA) was measured. For graft-based analyses, the SNR of each graft (SNRG) and subjective 5-point Likert scales (0=poor, and 4=excellent) of motion and metal artifacts of each graft were evaluated. Differences between the two modes were assessed by Welch's test and the Cochran-Armitage test.

### RESULTS

The effective dose was significantly lower in HPDS compared with the conventional SS mode ( $24.1\pm8.0$  vs.  $1.8\pm0.6$  mSv, P<0.01). The median heart rate in HPDS (72bpm, range 60 to 107bpm) was not significantly different from that of the SS mode. Mean SNRA was also not significantly different ( $20.1\pm3.9$  in HPDS vs.  $20.1\pm3.9$  in SS). For graft-based analyses, 54 GABGs (25 arterial grafts, 50 patent grafts) were analyzed. Mean SNRG ( $16.2\pm4.1$  in HPDS vs.  $14.2\pm5.7$  in SS) and subjective image scores were not significantly different, with a sufficiently high score (median, 4 for each) for diagnosis in the two modes.

## CONCLUSION

HPDS with 3rd DSCT significantly reduces the radiation dose compared with the conventional SS mode without obscuring image quality for assessing patency of CABG.

# **CLINICAL RELEVANCE/APPLICATION**

Even with a high heart rate, HPDS with 3rd DSCT can be used as a routine method for assessing early postoperative CABG patency with low radiation exposure without obscuring image quality.

Correlation Between Left Ventricular Insertion Points Delayed Enhancement And Right Ventricular Dilation with Cardiac Magnetic Resonance in Patients with Congenital Heart Disease

Thursday, Dec. 1 12:15PM - 12:45PM Room: CA Community, Learning Center Station #4

# Participants

Francesco Secchi, MD, Milano, Italy (*Presenter*) Nothing to Disclose Paola Maria Cannao, MD, San Donato Milanese, Italy (*Abstract Co-Author*) Nothing to Disclose Marco Scarabello, Milan, Italy (*Abstract Co-Author*) Nothing to Disclose Marcello Petrini, Milano, Italy (*Abstract Co-Author*) Nothing to Disclose Francesco Sardanelli, MD, San Donato Milanese, Italy (*Abstract Co-Author*) Speakers Bureau, Bracco Group Research Grant, Bracco Group Speakers Bureau, Bayer AG Research Grant, Bayer AG Research Grant, IMS International Medical Scientific

### PURPOSE

The purpose of our study was the quantitative evaluation of left ventricular (LV) delayed enhancement (DE) in relation to right ventricular (RV) function with cardiac magnetic resonance (CMR) in congenital heart disease.

# METHOD AND MATERIALS

Fifty-one consecutive patients (age mean±standard deviation 30.6±15 years) with congenital heart disease (17 had Tetralogy of Fallot, 8 had pulmonary insufficiency and 6 had RV dilation as main diagnosis) were studied. CMR was performed on a 1.5 T scanner to evaluate ventricular function and mass. Inversion recovery gradient-echo sequences were used 10 minutes after the IV injection of gadobenate dimeglumine 0.1 mmol/kg to produce DE images. Medis Qmass software (version 7.6) was used to quantitatively assess LV DE using 2 standard deviation(sd), 6 sd and automatic scar threshold methods to obtain the percentage, volume and mass of contrast-enhanced myocardial tissue.

## RESULTS

The mean RV end-diastolic volume (EDV) was  $140\pm47$  ml and the mean contrast-enhanced LV myocardial volume was  $3.8\pm2.8$  ml using 6sd method. All DE was localize on inferior and/or superior ventricular insertion points. A significant correlation between LV DE and EDV was found using 6sd method (Rho = 0.477 P<.001).

### CONCLUSION

The amount of contrast-enhanced LV myocardial tissue was significantly correlated with right ventricular end-diastolic volume in patients with congenital heart disease.

## **CLINICAL RELEVANCE/APPLICATION**

LV insertion points delayed enhancement could be a clinical indicator of right ventricular dysfunction and a prognostic tool in patients with congenital heart diseases.

# Added (Lab) Value: Serum Markers and Lung Disease

Thursday, Dec. 1 12:15PM - 12:45PM Room: CH Community, Learning Center Station #8

#### Awards Cum Laude

#### **Participants**

Demetrios A. Raptis, MD, Saint Louis, MO (*Abstract Co-Author*) Nothing to Disclose Travis S. Henry, MD, San Francisco, CA (*Abstract Co-Author*) Research Consultant, Enlitic Inc; Spouse, Employee, F. Hoffmann-La Roche Ltd Sanjeev Bhalla, MD, Saint Louis, MO (*Abstract Co-Author*) Nothing to Disclose

Andrew B. Wallace, MD, Saint Louis, MO (*Presenter*) Nothing to Disclose

# **TEACHING POINTS**

With the increased role of cross-sectional imaging in diagnosing pulmonary and cardiothoracic disease processes, an understanding of serologic markers and their corresponding imaging characteristics can help narrow the differential and make an accurate diagnosis. This exhibit aims to: 1. Provide a case based, pictorial review of the key imaging features of cardiothoracic disease processes and their corresponding serologic markers. 2. Develop an understanding of the imaging features, corresponding serologic markers, and clinical presentation of the following entities to help make an accurate diagnosis.

## **TABLE OF CONTENTS/OUTLINE**

A. Autoimmune disease markers a. Connective tissue diseases b. Other autoimmune diseasesB. Acute phase proteinsC. Elevated white blood cell count a. Pneumonia b. Other cardiothoracic infectious processesD. Red blood cell aplasia a. ThymomaE. Eosinophilic lung disease a. Simple pulmonary eosinophilia b. Chronic eosinophilic pneumonia (increased IgE, ESR) c. Churg-Strauss F. Other markers of infection, including fungal a. Aspergillus b. Mucormycosis G. IgG4 a. IgG4 related lung disease b. IgG4 related thoracic lymphadenopathy

### **Honored Educators**

Presenters or authors on this event have been recognized as RSNA Honored Educators for participating in multiple qualifying educational activities. Honored Educators are invested in furthering the profession of radiology by delivering high-quality educational content in their field of study. Learn how you can become an honored educator by visiting the website at: https://www.rsna.org/Honored-Educator-Award/

Travis S. Henry, MD - 2016 Honored Educator Sanjeev Bhalla, MD - 2014 Honored Educator Sanjeev Bhalla, MD - 2016 Honored Educator

# Thoracic Metastases: A Practical Approach to Typical and Atypical Radiological Patterns

Thursday, Dec. 1 12:15PM - 12:45PM Room: CH Community, Learning Center Station #7

#### **Participants**

Tassia R. Yamanari, MD, Sao Paulo, Brazil (*Presenter*) Nothing to Disclose Hye J. Lee, MD, Sao Paulo, Brazil (*Abstract Co-Author*) Nothing to Disclose Ricardo V. Auad, MD, Sao Paulo, Brazil (*Abstract Co-Author*) Nothing to Disclose Marcio V. Sawamura, MD, Sao Paulo, Brazil (*Abstract Co-Author*) Nothing to Disclose Valter R. Dos Santos Junior, MD, Sao Paulo, Brazil (*Abstract Co-Author*) Nothing to Disclose Thais C. Lima, Sao Paulo, Brazil (*Abstract Co-Author*) Nothing to Disclose Claudia D. Leite, MD, PhD, Sao Paulo, Brazil (*Abstract Co-Author*) Research Grant, General Electric Company Chang k. Chi, MD, Sao Paulo, Brazil (*Abstract Co-Author*) Nothing to Disclose Guilherme H. Bachion, MD, Sao Paulo, Brazil (*Abstract Co-Author*) Nothing to Disclose Giovanni G. Cerri, MD, PhD, Sao Paulo, Brazil (*Abstract Co-Author*) Nothing to Disclose

### **TEACHING POINTS**

Thoracic structures commonly are involved in patients with metastatic neoplasms. Knowledge of the variety of imaging patterns of thoracic metastases and understanding of the mechanisms of spread of metastatic tumors is essential for correct diagnosis. Our exhibit will emphasize the recognition of the primary malignancy based on the specific patterns of thoracic metastases.

### **TABLE OF CONTENTS/OUTLINE**

1. Overview of the mechanisms of spread of metastatic tumors: direct extension, hematogeneous spread, lymphatic spread, within the pleural space and endobronchial spread.

2. Illustrate the imaging spectrum of typical and atypical patterns of thoracic metastasis, including: airways (endobronchial metastases), lung (multiple nodules, cavitations, calcifications, solitary nodule, halo sign, consolidation / ground-glass opacity), interstitial and lymphatic (carcinomatous lymphangitis), mediastinal lymph nodes involvement, vascular (tumor emboli), pleura and chest wall.

3. Recognize the most common primary malignancies that correlate with each imaging pattern of thoracic metastases.

## CH278-SD-THA2

Lymphoid Interstitial Pneumonias (LIP) based on Recent Diagnostic Criteria; CT-Pathologic Correlation in 10 Patients

Thursday, Dec. 1 12:15PM - 12:45PM Room: CH Community, Learning Center Station #2

# Participants

Takeshi Johkoh, MD, PhD, Itami, Japan (*Presenter*) Research Consultant, Bayer AG Research Consultant, F. Hoffman-La Roche Ltd Tomonori Tanaka, MD, Toyama, Japan (*Abstract Co-Author*) Nothing to Disclose Kiminori Fujimoto, MD, PhD, Kurume, Japan (*Abstract Co-Author*) Nothing to Disclose Kazuya Ichikado, MD, PhD, Kumamoto, Japan (*Abstract Co-Author*) Nothing to Disclose Junya Fukuoka, Nagasaki City, Japan (*Abstract Co-Author*) Nothing to Disclose Noriyuki Tomiyama, MD, PhD, Suita, Japan (*Abstract Co-Author*) Nothing to Disclose

### PURPOSE

Although LIP was originally rare diseases, it has been a much more rare entity after revision of diagnostic criteria with ATS-ERS 02 and 13 consensus classification of idiopathic interstitial pneumonias (IIPs). The objective of the present study was to precisely correlate CT findings of LIP based on recent diagnostic criteria with the pathologic ones

### **METHOD AND MATERIALS**

Based on the definition of both ATS/ERS02 and 13 consensus classifications of IIPs, 10 cases diagnosed as LIP (4 female, 6 male, mean age; 52 years old) with surgical lung biopsy were enrolled in the study, 1 to 3 specimens in each case were obtained and total 23 specimens were collected. CT findings corresponding to the 23 specimens were precisely correlated with pathologic ones

## RESULTS

CT showed lower lobe predominance, ground-glass opacities (GGO), and cyst in all cases, thickening of interlobular septa in 5, centrilobular nodules and pleural thickening in 4, respectively, and thickening of bronchovascuar bundels in 2.. Regarding corresponding areas to 23 surgical biopsy sites. CT demonstrated GGO in all 23 cases, centrilobular nodules and thickening of interlobular septa in 3, respectively, and pleural thickening and cysts in2, respectively, Pathologically, GGO correlated with the infiltration of lymphoid cells to alveolar septa and centrilobular nodules corresponded to either the infiltration of lymphoid cells to alveolar septa and centrilobular walls (Fig 1). Thickening of interlobular septa and pleura on CT corresponded to the lymphoid infiltration and lymphoid follicles in interlobular septa and pleural. Cysts pathologically correlated with destruction and elastolysis of alveolar septa surrounding aggregated lymphoid cells (Fig 2)

### CONCLUSION

The common CT finding of LIP is ground-glass opacity due to pathologically the infiltration of lymphoid cells to alveolar septa. Cyst formation is related to elastolysis of alveolar septa.

### **CLINICAL RELEVANCE/APPLICATION**

The common CT finding of LIP is ground-glass opacity and cysts. Ground-glass opacity pathologically corresponds to the infiltration of lymphoid cells to alveolar septa. Cyst formation is related to elastolysis of alveolar septa.

# Classification of Stage 1 Lung Adenocarcinoma Outcomes on CT: Volumetric and Texture Analysis

Thursday, Dec. 1 12:15PM - 12:45PM Room: CH Community, Learning Center Station #3

#### Awards

### **Student Travel Stipend Award**

#### **Participants**

Antonio Pires, MD, NEW YORK, NY (*Presenter*) Nothing to Disclose Bowen Niu, New York, NY (*Abstract Co-Author*) Nothing to Disclose Henry Rusinek, PhD, New York, NY (*Abstract Co-Author*) Nothing to Disclose Harvey I. Pass, MD, New York, NY (*Abstract Co-Author*) Nothing to Disclose Jane P. Ko, MD, New York, NY (*Abstract Co-Author*) Speaker, Siemens AG

# PURPOSE

To determine the ability of semiautomated CT segmentation with texture and volumetric analysis to differentiate stage 1 lung adenocarcinomas (AdCas) with differing clinical outcomes.

## **METHOD AND MATERIALS**

IASLC classified Stage 1 surgically-resected AdCas in 45 patients with at least 3-yr follow up and preoperative noncontrast CTs (1 x 0.8 mm) were studied. IRB exemption was obtained. Average follow up was 3.8 +/- 1.8 yr including 5 of 45 lung-cancer related deaths at mean 2.5 +/- 1.8 yr. In 17 of 45 cases, disease progression, defined as local spread or distant metastasis, occurred at mean 2.6 +/- 1.4 yr). In 3 patients with multiple nodules, the largest nodule was analyzed.3D nodule masks were created using a previously-validated (including phantom validation) segmentation algorithm that estimates nodule volume, mass, and fraction of solid component. The largest nodule slice underwent 2nd order texture analysis of run length and signal co-occurrence. To minimize overfitting, texture features were averaged over directional vectors. Two model types were constructed: 1) linear discriminant analysis (LDA) 2) logistic regression. Models were fitted to combination of 2nd order texture features and 3D segmentation metrics.

### RESULTS

Using LDA classifier, 98% (44/45) of survival outcomes were classified correctly with only 1 case misclassified. Disease progression was correctly classified in 91% (41/45), sensitivity = 88% (15/17).Binomial logistic regression predicted survival in 100% (45/45). It was less accurate for disease progression with accuracy = 80% (36/45) and sensitivity = 71%.Up to 24 unique texture features contributed to classification, including entropy, contrast, and inverse difference moment (homogeneity). For example, entropy is a good measure of inherent structure in an image. Average entropy was 0.95 +/- 0.49 in cases of death and 0.64 +/- 0.30 in cases of survival, indicating decreased CT structural features in lung AdCas with worse prognosis .

# CONCLUSION

Texture and volumetric analysis can potentially differentiate Stage I lung adenocarcinomas with varying clinical outcomes and may improve prognostic stratification of patients.

# **CLINICAL RELEVANCE/APPLICATION**

Outcomes in stage 1 lung adenocarcinoma are difficult to predict based on visual assessment of morphologic features at CT. Texture and volumetric analysis can serve as indicators for clinical behavior and can potentially aid in patient management.

Lung Cancer Screening in a Socioeconomically Disadvantaged Population

Thursday, Dec. 1 12:15PM - 12:45PM Room: CH Community, Learning Center Station #4

#### Awards

### **Student Travel Stipend Award**

### Participants

Phillip Guichet, BA, Los Angeles, CA (*Presenter*) Nothing to Disclose Steven Cen, PhD, Los Angeles, CA (*Abstract Co-Author*) Nothing to Disclose Zul Surani, BS, Los Angeles, CA (*Abstract Co-Author*) Nothing to Disclose Beringia Liu, MPH, Los Angeles, CA (*Abstract Co-Author*) Nothing to Disclose Cameron Hassani, MD, Los Angeles, CA (*Abstract Co-Author*) Nothing to Disclose Leah M. Lin, MD, Los Angeles, CA (*Abstract Co-Author*) Nothing to Disclose Farhood Saremi, MD, Los Angeles, CA (*Abstract Co-Author*) Nothing to Disclose Bonnie Garon, MD, Los Angeles, CA (*Abstract Co-Author*) Nothing to Disclose Ana Maliglig, MD, MPH, Los Angeles, CA (*Abstract Co-Author*) Nothing to Disclose Alison Wilcox, MD, Los Angeles, CA (*Abstract Co-Author*) Nothing to Disclose Alison Wilcox, MD, Los Angeles, CA (*Abstract Co-Author*) Nothing to Disclose

### PURPOSE

To describe preliminary results of our clinical low-dose CT (LDCT) lung cancer screening program targeting a socioeconomically disadvantaged and high-risk population different from that studied in the National Lung Screening Trial (NLST).

### **METHOD AND MATERIALS**

All patients met USPSTF and/or NCCN eligibility criteria for lung cancer screening. A dedicated screening coordinator enrolled eligible patients, scheduled their screening exams, and organized their transportation to and from the medical center. A 2-year grant from a 501(c)(3) tax-exempt public charity covered all expenses, including the creation of an online database.

### RESULTS

505 patients were referred to the program from 7/21/2015 through 3/20/2016. 31 patients declined screening, and 68 were unable to be contacted. Of 209 patients who agreed to participate, 154 met eligibility criteria for lung cancer screening. 112 patients underwent their baseline LDCT during this time period.72 males (64%) and 40 females (36%) received baseline LDCT, with a mean age of 59 years (range 50-76) and median BMI of 27.0. The median pack-years was 40 (range 20-191), and 85% (95) of patients were current smokers. The ethnic makeup of the population was 84% (95) black, 7% (8) white, 7% (8) Hispanic/Latino, and 1% (1) Asian. 66% (74) of patients had no more than a high school education. 38% (43) of patients reported occupational exposure to one or more lung carcinogens.84% (95) of patients received a Lung-RADS score of 1 (32) or 2 (63), 8% (9) received a score of 3, 4% (4) a score of 4A, and 4% a score of 4B (3) or 4X (1). 2 patients (1.8%) have been diagnosed with lung cancer to date. 35% (40) of patients had potentially significant incidental findings including interstitial lung disease (7), severe emphysema (7), aortic aneurysm (1), moderate-severe coronary calcifications (13), extrapulmonary masses (12), severe hepatic steatosis (1), and advanced metastatic disease of extrathoracic origin (1).

# CONCLUSION

Lung cancer screening with LDCT in a socioeconomically disadvantaged population is feasible yet may yield different rates of cancer diagnosis than screening in more affluent communities. More follow-up time is required to determine whether the reduction in lung cancer mortality demonstrated in the NLST applies to this population.

# **CLINICAL RELEVANCE/APPLICATION**

Socioeconomically disadvantaged and high-risk communities may experience differential benefits from LDCT lung cancer screening.

# **Honored Educators**

Presenters or authors on this event have been recognized as RSNA Honored Educators for participating in multiple qualifying educational activities. Honored Educators are invested in furthering the profession of radiology by delivering high-quality educational content in their field of study. Learn how you can become an honored educator by visiting the website at: https://www.rsna.org/Honored-Educator-Award/

Farhood Saremi, MD - 2015 Honored Educator

Utilization Trends of Noncardiac Thoracic Imaging among Radiologists and Other Physicians

Thursday, Dec. 1 12:15PM - 12:45PM Room: CH Community, Learning Center Station #5

#### Participants

Sarah I. Kamel, MD, Philadelphia, PA (*Presenter*) Nothing to Disclose David C. Levin, MD, Philadelphia, PA (*Abstract Co-Author*) Consultant, HealthHelp, LLC; Board of Directors, Outpatient Imaging Affiliates, LLC Laurence Parker, PhD, Philadelphia, PA (*Abstract Co-Author*) Nothing to Disclose Vijay M. Rao, MD, Philadelphia, PA (*Abstract Co-Author*) Nothing to Disclose

#### PURPOSE

To analyze recent trends in the utilization of the various noncardiac thoracic imaging modalities in the Medicare population.

#### **METHOD AND MATERIALS**

The Medicare part B databases for 2002 through 2014 were reviewed. All CPT codes pertaining to noninvasive imaging of the thorax were selected and grouped into seven categories: x-ray, CT, CTA, nuclear scans (noncardiac), MR, MRA and ultrasound. Yearly utilization rates per 1,000 Medicare beneficiaries were calculated. Medicare physician specialty codes were used to determine how many studies were performed by radiologists versus self-referring nonradiologist physicians. Trends over the 12 year period were studied.

# RESULTS

The total utilization rate of all chest imaging peaked at 1090 per 1000 in 2005, then progressively declined to 913 by 2014 (-16%). Among studies performed by radiologists, total thoracic imaging peaked at 969 per 1000 in 2005, then declined to 828 (-14%) by 2014. The chest CT rate rose sharply, peaked at 94 in 2007, then declined to 88 (-6%) by 2014. The CTA utilization rate has risen significantly since 2002, increasing 38% in the last four years alone to a rate of 23 studies per 1,000 in 2014. Utilization rates of nuclear chest imaging, such as VQ scans have decreased steadily by 36% since 2002. Chest x-ray rates reached a peak of 969 in 2005 but then declined by 15% to 828 in 2014. MR, MRA and Ultrasound of the chest were infrequently performed with a rate of 1 to 2 studies per 1,000 without significant changes in rate over time. Total utilization rate of chest imaging among nonradiologists peaked in 2003 with a rate of 92 studies per 1,000 Medicare beneficiaries; this has since declined 48% to 48 per 1000 in 2014. Nonradiologists' use of chest imaging is confined almost entirely to plain x-ray.

### CONCLUSION

Noncardiac thoracic imaging is strongly dominated by radiologists. Trends show increasing utilization of CT and CTA with a decline in x-ray and nuclear imaging. Overall, there has been a substantial decline in utilization rates of chest imaging in recent years; this is due in part to the relatively low level of self-referral.

### **CLINICAL RELEVANCE/APPLICATION**

N/A

# CT Patterns and Serial CT Changes in Lung Cancer Patients Post Stereotactic Body Radiotherapy (SBRT)

Thursday, Dec. 1 12:15PM - 12:45PM Room: CH Community, Learning Center Station #6

#### Participants

Usman Tarique, BSc, Toronto, ON (*Abstract Co-Author*) Nothing to Disclose Laura Jimenez-Juan, MD, Toronto, ON (*Abstract Co-Author*) Nothing to Disclose Patrick C. Cheung, Toronto, ON (*Abstract Co-Author*) Nothing to Disclose Rahim Moineddin, Toronto, ON (*Abstract Co-Author*) Nothing to Disclose Anastasia Oikonomou, MD, PhD, Toronto, ON (*Presenter*) Nothing to Disclose

### PURPOSE

To evaluate the different CT patterns of post SBRT changes in lung cancer patients and to identify specific time points of serial CT changes.

## **METHOD AND MATERIALS**

184 lung cancers in 170 patients (87 female, median age 74 yrs) were evaluated on sequential chest CTs within a period of 29 months (3-72). The frequencies of pre and post-treatment CT patterns were evaluated. Time points of initiation of each pattern from end of treatment and duration were assessed. Time points until size of primary lesion or surrounding CT pattern continued to increase without evidence of local recurrence were assessed. Time points until stabilization, local recurrence, development of metastasis or rib fractures were evaluated.

#### RESULTS

The most frequent pre-treatment patterns were solid nodule (62%) and solid mass (15%). Post-treatment CT patterns could overlap in the same patient and were nodule-like (68%), consolidation with GGO (48%), modified conventional (46%), peribronchial/patchy consolidation (43%), patchy GGO (27%), diffuse consolidation (27%), "orbit-sign" (14%), mass-like (10%), scar-like (5%) and diffuse GGO (4%). Patchy GGO began in 4 months (range:1-14) and lasted up to 16 months. Peribronchial/patchy consolidation (2-35) and consolidation with GGO (1-29) began in 5 months and lasted up to 26 and 41 months respectively. Diffuse GGO began in 7 (3-19) and lasted up to 4 months. Diffuse consolidation (3-38) and orbit sign (3-34) began in 8 months and lasted up to 5 and 18 months respectively. Modified conventional pattern began in 13 months (1-49). Primary lesion (18/184) or surrounding CT pattern (92/184) continued to increase in size 9 (3-32) or 14 months (2-59) respectively after the end of treatment. Time to stabilization in 77 lesions was 23 months (6-59). Local recurrence, metastasis or rib fractures occurred in 17 (7-38), 17 (3-66) or 18 months (7-68) respectively after the end of treatment.

### CONCLUSION

There is a specific timing in sequence of appearance and variable periods of duration of the different CT patterns post-SBRT treatment.

# **CLINICAL RELEVANCE/APPLICATION**

Understanding the different post-SBRT CT patterns expected, the time points of appearance as well as the range of duration is crucial in differentiating local recurrence from radiation changes.

## CH283-SD-THA1

Detection of Ground-glass Opacity Lesions using Breath-hold Black-blood Magnetic Resonance Imaging of the Lungs

Thursday, Dec. 1 12:15PM - 12:45PM Room: CH Community, Learning Center Station #1

# Participants

Ryotaro Kamei, MD, Fukuoka, Japan (*Presenter*) Nothing to Disclose Yuji Watanabe, MD, Kurashiki, Japan (*Abstract Co-Author*) Nothing to Disclose Koji Sagiyama, MD, Fukuoka, Japan (*Abstract Co-Author*) Nothing to Disclose Satoshi Kawanami, MD, Fukuoka, Japan (*Abstract Co-Author*) Nothing to Disclose Hiroshi Honda, MD, Fukuoka, Japan (*Abstract Co-Author*) Nothing to Disclose

# PURPOSE

To investigate the feasibility and usefulness of breath-hold black-blood T2-weighted (BBT2W) turbo spin echo magnetic resonance imaging (TSE MRI) of the lungs in the detection of focal ground-glass opacity (GGO) lesions.

# METHOD AND MATERIALS

We included 44 consecutive patients who underwent high-resolution computed tomography (HRCT) and MRI of the whole lungs between August 2014 and March 2016. MRI scans were acquired using a 3.0-T MR of Ingenuity TF PET/MR instrument (Philips Healthcare). BBT2W imaging was performed using the variable refocusing flip-angle technique under breath-hold with peripheral pulse unit (PPU) gating. Breath-hold T1-weighted imaging (T1WI) with a 3D modified Dixon sequence was also performed to obtain information on the vascular anatomy.Diagnostic HRCT images were used as the reference standards. The location, number, size, and characterization (pure or mixed) of the GGO lesions were recorded. Two radiologists blinded to the HRCT findings performed consensus interpretation of the MR images. For the focal GGOs, lesion-based detection rates were calculated and compared between BBT2WI and T1WI scans. Statistical analyses were performed using the McNemar test. Correlation analysis and the Bland-Altman plot was used for lesion size comparison between the HRCT and MRI scans.

### RESULTS

HRCT revealed 24 GGO lesions in 12 patients. Upon interpretation of the MRI scans, lesion-based detection rates of focal GGOs were 79.2% (19/24) for BBT2WI and 54.2% (13/24) for T1WI. T1WI detected only 1 of 10 pure GGOs and 12 of 14 mixed GGOs, while BBT2WI detected 5 of 10 pure GGOs and all the mixed GGOs. The GGO size on BBT2WI had a strong correlation with that of HRCT (r = 0.9425, p < 0.0001), and the mean difference was small (0.7095 mm). Although there was a significant correlation between the sizes detected on T1WI and HRCT (r = 0.6868, p = 0.0118), the GGOs tended to appear smaller on T1WI than on HRCT, with a mean difference of 6.694 mm.

# CONCLUSION

Breath-hold black-blood T2-weighted MRI of the lungs with PPU gating is feasible and could provide acceptable diagnostic quality for detecting GGO lesions.

### **CLINICAL RELEVANCE/APPLICATION**

Breath-hold black-blood lung MRI using PPU gating is feasible with acceptable diagnostic accuracy and could be useful for the long-term follow-up of GGOs without any irradiation.

# ER238-SD-THA1

### Clinical Relevance of Consecutive CT Scans for the Evaluation and Monitoring of Geriatric Pelvic Fractures

Thursday, Dec. 1 12:15PM - 12:45PM Room: ER Community, Learning Center Station #1

#### **Participants**

Christoph Weber, MD, Hamburg, Germany (*Presenter*) Nothing to Disclose Peter Bannas, MD, Hamburg, Germany (*Abstract Co-Author*) Nothing to Disclose Wolfgang Lehmann, MD, Hamburg, Germany (*Abstract Co-Author*) Nothing to Disclose Thies H. Schroeder, MD, Hamburg, Germany (*Abstract Co-Author*) Nothing to Disclose

## PURPOSE

To evaluate consecutive computed tomography (CT) imaging in fragility fractures of the pelvis (FFP) in geriatric patients and to prove its effect on the indication for surgical stabilisation treatment.

# **METHOD AND MATERIALS**

60 CT Scans of 29 consecutive patients >75y (mean age 83,8±7,8y, 27f/2m) with a history of low impact energy trauma and confirmed pelvic fracture, who had received CT for fracture evaluation and at least one consecutive CT for follow up during the following month after pain adapted ambulation, were evaluated. Pelvic fractures were classified according to the system established by Rommens/Hofmann for fragility fractures of the pelvis. The Barthel ADL index was used as a measure of physical disability after admittance.

# RESULTS

Follow up CT was acquired  $14\pm4,6$  days after initial CT. Isolated fractures of the anterior pelvic ring (FFP Type Ia,b) were initially detected in 13,8% (n=4) of patients. Combined fractures of the anterior and posterior pelvic ring with moderate instability (FFP Type IIa,b,c) accounted for 65,5% (n=19), higher (FFP Type IIIa,b,c) for 3,4% (n=1) and highest instability (FFP Type IVa,b,c) for 17,2% (n=5). 10 patients (34,5%) deteriorated in fracture classification during follow up (3 patients within one category, 4 patients deteriorated by one category, and 3 patients by two categories). There was no significant difference in age or physical disability between patients that showed fracture deterioration and those that did not.

# CONCLUSION

Aggravation of fractures in over a third of patients may indicate that a more aggressive, surgical approach is needed in the management of FFP in the elderly. A progressive surgical approach for FFP IIb+ fractures of the anterior and posterior pelvic ring may prevent aggravation, e.g.by sacro-iliacal screw osteosynthesis.

# **CLINICAL RELEVANCE/APPLICATION**

Conventional Radiography is insufficient in detecting fragility fractures of the pelvis in geriatric patients. CT is mandatory for the initial grading with FFP-Classification and to indicate and plan surgical stabilisation therapy, e.g.by sacro-iliacal screw osteosynthesis.

Mild Traumatic Brain Injury (MTBI): Screening Computerized Tomography(CT)?Utility of Clinical Guidelines in a Tertiary Referral Hospital in Spain

Thursday, Dec. 1 12:15PM - 12:45PM Room: ER Community, Learning Center Station #2

# Participants

Susana Manso Garcia, DDS, valladolid, Spain (*Presenter*) Nothing to Disclose Maria J. Velasco-Marcos Sr, MD, PhD, Valladolid, Spain (*Abstract Co-Author*) Nothing to Disclose Santiago Marzoa Ruiz, Valladolid, Spain (*Abstract Co-Author*) Nothing to Disclose Marta Moya de la Calle, Valladolid, Spain (*Abstract Co-Author*) Nothing to Disclose Arnold Antonio Montes Tome, Valladolid, Spain (*Abstract Co-Author*) Nothing to Disclose

# PURPOSE

To analyze two available prognostic tools sus as the Canadian standard(CT) and New Orleans(NO), both internationally accepted, in order to avoid unnecessary TC. To asses their applicability to decision making in the diagnosis of MTBI.

### **METHOD AND MATERIALS**

Cross-sectional study in Emergency department of a tertiary hospital in patients with diagnosis of MTBI.SPSS20.0 computer program was used to analyze the variables: demographic,clinical,classification,diagnostic management,complementary test,results and CT and NO criteria.CT was performed to 308 out of 1329 patients with MTBI(23,17%).The data from these 308 patients who were submitted to CT as additional proof were analyzed,showing that 47,4% of the applications did meet NO criteria for CT and 73,4%met CT criteria

# RESULTS

The results to CT were normal in 83,4% cases. Amog those in which CT showed pathology,74,5% met CT criteria an 58,8% NO criteria, statistically significant(ES). Among the pathological CT,56,9% patients suffered loss of consciousness and 37,6% were hospitalized. In 58,8% of cases with a pathologic Ct a dangerous mechanic of injury was found as a cause(ES).

# CONCLUSION

Most of the CT requested in patients with MTBI were no pathological. The CT criteria shows greater sensitivity and specify than NO criteria. We haven, t found a relationship between pathological CT and loss of consciousness, however in this groupp a dangerous mechanism of injury is often found a cause.

# **CLINICAL RELEVANCE/APPLICATION**

The use of clinical guidelines in MTBI avoid unnecessary CT and radiation.CT criteria is better predictor of Clinically Important CT Findings in our study.

# ER240-SD-THA3

Does Criteria-based Direct Access to Polytrauma Whole-body CT in the Emergency Department lead to Overscanning? Could Plain Radiography have a Role in Selection of Patients for CT? Exploring a Delicate Interplay between Specificity and Sensitivity

Thursday, Dec. 1 12:15PM - 12:45PM Room: ER Community, Learning Center Station #3

#### Participants

Oliver Duxbury, MBBCh, BSc, Brighton, United Kingdom (*Abstract Co-Author*) Nothing to Disclose Nikola Tomanovic, MBBS, Brighton, United Kingdom (*Presenter*) Nothing to Disclose Ahmed Daghir, MRCP, FRCR, Oxford, United Kingdom (*Abstract Co-Author*) Nothing to Disclose

### PURPOSE

A set of criteria for direct Emergency Department access to polytrauma whole-body CT scans were introduced in 2013 to help guide clinical decision making and speed up patient imaging in the Emergency Department. This study looks at the use of plain radiographs (XR) prior to CT acquisition and the proportion of "normal" scans, before and after the criteria implementation.

# METHOD AND MATERIALS

A retrospective sample of 60 polytrauma whole-body CT scans, performed over a 2 month period, at a major trauma centre was analysed in 2012, 2014 and 2015. We compare the proportion of patients undergoing XR of the chest or pelvis prior to whole body CT, as well as the proportions of XR and CT studies reported as negative for acute injury, before (2012) and after (2014 and 2015) introduction of these criteria.

### RESULTS

The proportion of negative polytrauma whole-body CT scans rose from 27% in 2012, to 33% in 2014, to 47% in 2015.Over the same time period, the proportion of patients undergoing chest XR has decreased from 73% in 2012 to 37% in 2014 and 0% in 2015 and the number undergoing pelvic XR from 60% in 2012 to 25% in 2014 and 2% in 2015.Of the 73% undergoing XR in 2012, 20% of patients had negative XR and CT, 51% had positive XR and CT and 29% had a negative XR but positive CT. 27% of patients had no XR, with 57% having positive and 43% negative CT.Of the 37% undergoing XR in 2014, 33% had negative XR and CT, 38% had positive XR and CT and 28% had a negative XR but positive CT. 63% did not have XR, of which 48% had positive and 52% negative CT.

# CONCLUSION

Our results show how a criteria-based direct Emergency Department access to CT protocol leads to a gradual increase in the numbers of negative CT scans but a dramatic decrease in the use of plain radiographs prior to CT. This suggests a lower threshold for selection of patients who receive whole-body CT.It is not clear from our data, that using plain radiographs to aid clinical judgement for patient selection would increase specificity sufficiently to lead to better outcomes. Further work is needed to better classify the positive CT findings not seen on XR.

# **CLINICAL RELEVANCE/APPLICATION**

Current data implies that faster access to CT removes the need for plain radiographs to direct urgent intervention for lifethreatening injuries. However, further work is required to ascertain if plain radiographs have a role in patient selection for CT in certain patient subsets.

# Abdominal Masses with Central Scar: No Organ Left Behind

Thursday, Dec. 1 12:15PM - 12:45PM Room: GI Community, Learning Center Station #9

#### **Participants**

Amina Saghir, MBBS, Shrewsbury, MA (*Abstract Co-Author*) Nothing to Disclose Daniel Kowal, MD, Sturbridge, MA (*Presenter*) Nothing to Disclose

### **TEACHING POINTS**

To present abdominal mass lesions associated with a central scar (CS). To emphasize that while CS is important to recognize, it is not always pathognomonic for diagnosis, but is often useful as a supplemental diagnostic feature.

### **TABLE OF CONTENTS/OUTLINE**

Numerous abdominal masses contain a CS which may guide a differential diagnosis. A clear understanding of imaging characteristics of not only the scar, but of the mass itself is imperative to avoid pitfalls and mimics. Focal nodular hyperplasia, fibrolamellar hepatocellular carcinoma, giant hemangioma, and metastases are hepatic masses that may be associated with CS. MRI signal characteristics, enhancement patterns, hepatocyte-specific gadolinium-based contrast agents, and presence of calcification aid to differentiate hepatic masses. Pancreatic serous cystadenoma is a benign lesion with a CS which may be calcified. Sclerosing angiomatoid nodular transformation is a rare splenic lesion often associated with a CS which is T2 hyperintense and hypoenhancing on MRI. Splenic pseudotumor is also a rare benign entity with a central stellate scar. CS is seen in 50% of cases of benign renal oncocytoma, but renal cell carcinoma may also exhibit a scar. CS in an abdominal mass is important to recognize, but its presence or absence should not preclude the diagnosis of certain abdominal tumors.

Collateral Damage: Unintended Consequences of Oncologic Therapy in the Chest, Abdomen, and Pelvis

Thursday, Dec. 1 12:15PM - 12:45PM Room: GI Community, Learning Center Station #7

Awards Certificate of Merit Identified for RadioGraphics

#### **Participants**

Julie C. Bulman, MD, Dallas, TX (*Abstract Co-Author*) Nothing to Disclose
Gaurav Khatri, MD, Dallas, TX (*Presenter*) Nothing to Disclose
Lori M. Watumull, MD, Dallas, TX (*Abstract Co-Author*) Research Grant, Toshiba Corporation
Yull Arriaga, Dallas, TX (*Abstract Co-Author*) Nothing to Disclose
John R. Leyendecker, MD, Dallas, TX (*Abstract Co-Author*) Nothing to Disclose

### **TEACHING POINTS**

Radiologists must differentiate effects of various oncologic therapies to help direct management and improve patient outcomes. GI complications from oncologic therapies include inflammation, pneumatosis, fistulae, perforation, graft-versus-host disease (GVHD). Unintended liver abnormalities from oncologic therapy include steatosis, hepatitis, fibrosis, vascular changes. Pancreaticobiliary, GU, vascular, and other systemic complications may manifest on imaging.

## **TABLE OF CONTENTS/OUTLINE**

Chemotherapy- cytotoxic, molecular, immunotherapy GI - inflammation, pneumatosis, necrosis, perforation, fistula, bleed Liver -Steatosis, pseudocirrhosis, autoimmune hepatitis, Hepatic Veno-Occlusive Disease (HVOD) Pancreaticobiliary - Pancreatitis, cholangitis, strictures Genitourinary - Nephrotoxicity, cystitis Vascular – Arterial/venous thrombosis, atherosclerosis Other organs, pseudoprogression, radiation recall Local/regional Rx (ablation, trans-arterial chemoembolization, radiation therapy) GI - Gastritis, radiation enteritis Liver - Radiation injury, fibrosis Biliary - Cholangitis, stricture, biloma, gallbladder injury GU - renal, bladder, fistula Other - infection, dehiscence Bone Marrow Transplant Liver - HVOD, portal hypertension GI - inflammation, pneumatosis, fistula Systemic - PTLD, GVHD HIV below the Belt: Infections, Tumors and Everything in Between

Thursday, Dec. 1 12:15PM - 12:45PM Room: GI Community, Learning Center Station #8

### Awards Certificate of Merit

#### **Participants**

Cecil Patel, MD, Los Angeles, CA (*Presenter*) Nothing to Disclose Cecilia M. Jude, MD, Los Angeles, CA (*Abstract Co-Author*) Author, UpToDate, Inc Maitraya K. Patel, MD, Sylmar, CA (*Abstract Co-Author*) Nothing to Disclose Jacqueline Tang, Sylmar, CA (*Abstract Co-Author*) Nothing to Disclose Michael J. Nguyen, MD, Santa Barbara, CA (*Abstract Co-Author*) Nothing to Disclose Anokh Pahwa, MD, Los Angeles, CA (*Abstract Co-Author*) Nothing to Disclose Shaden F. Mohammad, MD, Sylmar, CA (*Abstract Co-Author*) Nothing to Disclose

## **TEACHING POINTS**

Because HIV can remain undiagnosed or untreated, abdominal manifestations of HIV-associated diseases may be a main presenting feature. Familiarity with these diseases can lead to correct diagnosis and treatment. The purpose of this exhibit is to: Review the pathophysiology and clinical presentations of HIV-associated infections and neoplasms in the abdomen and pelvis. Illustrate the characteristic imaging features of these entities, including treatment related abnormalities. Integrate clinical and radiographic findings to guide appropriate management.

# TABLE OF CONTENTS/OUTLINE

HIV-related infections and neoplasms can have a variety of manifestations and involve multiple organ systems. Treatment response may mimic worsening of an underlying disease. Opportunistic infections Bacterial Mycobacteria Clostridium difficile Typhlitis: grampositive organisms Bartonella henselae Fungal Candida Histoplasma capsulatum Viral Cytomegalovirus Herpes simplex virus 3 Protozoal infections: Cryptosporidium Pneumocystis jirovecii AIDS-related neoplasia Kaposi sarcoma Non-Hodgkin's lymphoma HIVrelated organ manifestations Treatment related Immune reconstitution inflammatory syndrome (IRIS) Preclinical Spectral Detector CT Scanner Derived Iodine-Based Spectral Images reveal Improved Image Quality Metrics Compared to Conventional CT

Thursday, Dec. 1 12:15PM - 12:45PM Room: GI Community, Learning Center Station #3

**FDA** Discussions may include off-label uses.

### Participants

Suhny Abbara, MD, Dallas, TX (*Presenter*) Author, Reed Elsevier; Editor, Reed Elsevier; Institutional research agreement, Koninklijke Philips NV; Institutional research agreement, Siemens AG Lakshmi Ananthakrishnan, MD, Dallas, TX (*Abstract Co-Author*) Nothing to Disclose William A. Moore, MD, Dallas, TX (*Abstract Co-Author*) Nothing to Disclose Luna Fahoum, Andover, MA (*Abstract Co-Author*) Employee, Koninklijke Philips NV Zimam Romman, MSc, Haifa, Israel (*Abstract Co-Author*) Employee, Koninklijke Philips NV Julia R. Fielding, MD, Dallas, TX (*Abstract Co-Author*) Nothing to Disclose Xinhui Duan, PhD, Dallas, TX (*Abstract Co-Author*) Nothing to Disclose

### PURPOSE

Several types of Iodine-based spectral derived images (SDIs) can be reconstructed from a preclinical prototype Spectral Detector CT (SDCT) scanner (IQon, Philips Healthcare) at no additional radiation dose. The potential incremental value over conventional filtered back projection (FBP) images alone has not been evaluated to date. We aim to determine image quality parameters and potential incremental value of iodine-based SDIs obtained from a SDCT scanner.

# METHOD AND MATERIALS

This prospective IRB approved study consists of 562 individual CT DICOM dataset reconstructed from 73 unique SBIs in 53 patients (some had multiple contrast phases). Reconstructions included conventional CT, and the following spectral derived images: Iodine-No-Water and quantitative Iodine-Density image datasets.Image quality and lesion detectability was evaluated on Likert scales (much worse, worse, similar, moderately better, much better) for 1) iodine enhancement 2) hypodense lesion/structure detection, 3) hyper dense lesion/structure detection.Diagnostic reader confidence was evaluated on a 4 point scale (low, moderate, good, high). Comparative statistics were performed.

## RESULTS

Iodine enhancement seen in Iodine-No-Water scored 'moderately better'  $(3.9\pm0.9, n=31)$  and 'similar' to 'moderately better' on Iodine-Density SDIs  $(3.6\pm1.0, n=35)$  compared to FBP.Detection of hyper dense structures on Iodine-No-Water and Iodine-Density images was 'similar' to 'moderately better'  $(3.5\pm1.1, n=31 \text{ and } 2.9\pm1.5, n=34)$ .Compared to conventional images, no added value was found in the detection of hypo dense structures (Iodine-No-Water 2.2±1.2, n=30, Iodine-Density 2.0±1.3, n=34).Diagnostic confidence rating averages scored 'good' to 'high' for iodine enhancement on the Iodine-no-Water images  $(3.1\pm0.8)$  and 'moderate' to 'good' on the Iodine-Density images. Hyper dense structure detection was 'moderate' to 'good' on the Iodine-No-Water images.

### CONCLUSION

Iodine-based spectral derived images can be obtained from a novel detection based spectral CT scanner. This study shows that these SDIs improved high attenuation structure detectability due to improved contrast enhancement compared to conventional FBP images.

### **CLINICAL RELEVANCE/APPLICATION**

Iodine-based spectral derived images from a novel detection based spectral CT scanner have favourable image quality parameters and incremental value for lesion detectability compared to conventional CT images alone.

#### **Honored Educators**

Presenters or authors on this event have been recognized as RSNA Honored Educators for participating in multiple qualifying educational activities. Honored Educators are invested in furthering the profession of radiology by delivering high-quality educational content in their field of study. Learn how you can become an honored educator by visiting the website at: https://www.rsna.org/Honored-Educator-Award/

Suhny Abbara, MD - 2014 Honored Educator

The Prognostic Value of Gadoxetic-acid Enhanced MRI in Prediction of Patients' Survival Following Liver Transplantation for Hepatocellular Carcinoma

Thursday, Dec. 1 12:15PM - 12:45PM Room: GI Community, Learning Center Station #4

# Participants

Ah Yeong Kim, MD, Daejeon, Korea, Republic Of (*Abstract Co-Author*) Nothing to Disclose Woo Kyoung Jeong, MD, Seoul, Korea, Republic Of (*Presenter*) Nothing to Disclose Tae Wook Kang, MD, Seoul, Korea, Republic Of (*Abstract Co-Author*) Nothing to Disclose

#### PURPOSE

Given the limited availability of donor organs for liver transplantation (LT) and recent attempt to expand the Milan criteria, careful patient selection is mandatory to reduce tumor recurrence and maximize the effectiveness. We hypothesized that preoperative magnetic resonance imaging (MRI) can provide prognostic power in prediction of tumor recurrence and survival rate in patient with LT for hepatocellular carcinoma (HCC).

### **METHOD AND MATERIALS**

HCC patients (n=65) with preoperative gadoxetic-acid enhanced MRI underwent LT between Jan. 2009 to Jun. 2012. MRI parameters including signal intensity of the tumor, enhancement pattern and diffusivity were evaluated retrospectively by two radiologists. Overall and disease-free survival rates were analyzed. Uni- and multivariate analyses with MRI parameters, serum alpha-fetoprotein (AFP), and pathologic findings were performed for prediction of overall survival and HCC recurrence. And relationship between selected variables in imaging and pathologic findings was evaluated.

### RESULTS

The 3-year overall and recurrence-free survival rate were 76.7% and 70.4%, respectively. In multivariate analyses, only peritumoral hypointensity on hepatobiliary phase (HBP) (hazard ratio [HR], 8.77; p<0.001) on MRI and intrahepatic metastasis (HR, 2.89; p=0.03) on pathology were significant predictable factor for overall survival. And both the presence of satellite nodule (HR, 5.56; p=0.006) and peritumoral hypointensity on HBP (HR, 11.90; p<0.001) on MRI and histologic grade (HR, 4.98; p =0.006) and absence of fibrous capsule (HR, 3.03; p=0.018) on pathology were significant risk of tumor recurrence. AFP was an independent prognostic factor for both overall survival (HR, 1.26; p=0.025) and tumor recurrence (HR, 1.47; p<0.001). Among the significant predictive variables on preoperative MRI, peritumoral hypointensity on HBP was correlated to the tumor grade on pathologic finding (p=0.015). And presence of satellite nodule on preoperative MRI was correlated to the intrahepatic metastasis on pathology (p<0.001).

### CONCLUSION

Peritumoral hypointensity on HBP on preoperative MRI was significant predictable factor for overall survival and tumor recurrence after LT for HCC, and correlated to the tumor grade on pathologic finding.

### **CLINICAL RELEVANCE/APPLICATION**

Prediction of tumor recurrence and survival after LT for HCC can be attempted using preoperative MRI, and this might be helpful in selection of best candidate for LT.

# GI405-SD-THA5

### Dynamic Enhancement Pattern of Insulinomas on Volume Perfusion CT

Thursday, Dec. 1 12:15PM - 12:45PM Room: GI Community, Learning Center Station #5

#### Participants

Liang Zhu, MD, Beijing, China (*Presenter*) Nothing to Disclose Huadan Xue, MD, Beijing, China (*Abstract Co-Author*) Nothing to Disclose Wei Liu, Beijing, China (*Abstract Co-Author*) Nothing to Disclose Hao Sun, MD, Beijing, China (*Abstract Co-Author*) Nothing to Disclose

## PURPOSE

To assess the enhancement pattern of insulinomas on volume perfusion CT (VPCT), and to select phases for optimal tumorparenchyma contrast.

### **METHOD AND MATERIALS**

From August 2014 to December 2015, consecutive patients who underwent VPCT of the pancreas (80kV) with clinically suspected insulinomas were identified. Patients who received surgery and had pathological diagnosis of insulinomas were included, and patients with known multiple endocrine syndrome were excluded. Two experienced radiologists retrospectively evaluated tumor enhancement patterns on VPCT and analyzed the time-attenuation curve of the tumor and pancreatic parenchyma in consensus. The tumors were identified on CT with reference to surgical reports. Tumor-parenchyma contrast at each time point was measured and phases for optimal tumor-parenchyma contrast were selected.

#### RESULTS

Sixty-three patients were included,with 63 tumors.Five tumors were isoattenuating (tumor-parenchyma contrast <20HU in all 25 dynamic phases), 19 tumors had transient hyperenhancement (tumor-parenchyma contrast >20HU, duration < 10s), and 39 tumors had persistent hyperenhancement. Optimal tumor-parenchyma contrast was observed 9 s after abdominal aorta arriving at threshold of 200HU (AAT), with mean tumor-parenchyma attenuation difference of 77.6±57.2HU. At 9 s after AAT, 14 tumors were isoattenuating, including 5 tumors with intrinsic low contrast and 9 tumors with missed transient hyperenhancement. Complementary phases could be 12 s after AAT (detects another 4 tumors), 4 s after AAT and 1s after AAT (both detect another 3 tumors).

# CONCLUSION

VPCT enables detection of insulinomas even if the hyperenhancement is transient. Optimal tumor-parenchyma contrast occurs 9 s after AAT. Tumors that are inconspicous on single- or biphasic contrast enhanced CT are mainly due to missed transient hyperenhancement.

# **CLINICAL RELEVANCE/APPLICATION**

By analyzing dynamic enhancement of insulinomas, a single opitmal phase was selected, which yeilded the maximum tumorparenchyma contrast and facilitates detection of insulinomas with low radiation dose. It was also found that transient hyperenhancement was the main reason that some insulinomas were inconspicuous on single- or biphasic enhanced CT.VPCT could detect insulinomas even if the hyperenhancement was transient. 3D Dynamic Contrast-Enhanced Ultrasound of Liver Metastases from Gastrointestinal Tumors: First-in-Human Assessment of Feasibility and Reproducibility

Thursday, Dec. 1 12:15PM - 12:45PM Room: GI Community, Learning Center Station #6

**FDA** Discussions may include off-label uses.

### Participants

Ahmed El Kaffas, PhD, Palo Alto, CA (*Presenter*) Co-founder, Oncoustics Rosa Maria Silveira Sigrist, MD, Palo Alto, CA (*Abstract Co-Author*) Nothing to Disclose George Fisher, MD, PhD, Stanford, CA (*Abstract Co-Author*) Nothing to Disclose Sunitha Bachawal, PhD, Stanford, CA (*Abstract Co-Author*) Nothing to Disclose Joy Liau, MD, PhD, Palo Alto, CA (*Abstract Co-Author*) Nothing to Disclose Alexander Karanany, Palo Alto, CA (*Abstract Co-Author*) Nothing to Disclose Jarrett Rosenberg, PhD, Stanford, CA (*Abstract Co-Author*) Nothing to Disclose Huaijun Wang, MD, PhD, Stanford, CA (*Abstract Co-Author*) Nothing to Disclose Dimitre Hristov, PhD, Stanford, CA (*Abstract Co-Author*) Nothing to Disclose Dimitre Hristov, PhD, Stanford, CA (*Abstract Co-Author*) Nothing to Disclose Dimitre Hristov, PhD, Stanford, CA (*Abstract Co-Author*) Research Grant, Koninklijke Philips NV Partner, SoniTrack Systems, Inc Juergen K. Willmann, MD, Stanford, CA (*Abstract Co-Author*) Research Grant, Bracco Group; Research Grant, Siemens AG; Research Grant, Bracco Group; Research Grant, Koninklijke Philips NV; Research Grant, General Electric Company; Advisory Board, Lantheus Medical Imaging, Inc; Advisory Board, Bracco Group

#### PURPOSE

Dynamic contrast enhanced ultrasound (DCE-US) is a low-cost tool proposed for identifying early responders to cancer therapy. To date, sampling errors resulting from 2D imaging have restricted DCE-US when used to assess highly heterogeneous tumors. The purpose of this study was to perform a first-in-human clinical assessment of 3D DCE-US feasibility and reproducibility, and as a way to overcome sampling errors.

# METHOD AND MATERIALS

Patients with liver metastases from gastrointestinal cancers were imaged with a Philips EPIQ7 coupled to an X6-1 matrix transducer. A total of 16 scan sessions were carried out over 10 patients. Pairs of repeated bolus and disruption-replenishment images were acquired within each scan session to determine reproducibility of parameters. Bolus consisted of intravenous injection of 0.2 ml Definity microbubbles followed by saline. Disruption-replenishment was carried out by infusing 0.9 ml of Definity microbubbles in 35.1 ml of saline over 8 min. Volumes-of-interest (VOI) and regions-or-interest (ROI) were segmented in each image to extract timeintensity curves (TICs). Parameters were quantified for the whole VOI and 4 sub-ROIs. Bolus parameters were: time-to-peak (TP), peak enhancement (PE), area-under-the-curve (AUC), mean-transit-time (MTT). Disruption-replenishment parameters were: relative blood volume (rBV), relative blood flow (rBF) and regional mean flow velocity (rMFV).

#### RESULTS

A large coefficient of variation (CV) was for ROIs from the same volume confirming potential sampling errors. The TP and MTT had the lowest CV while the rBF, rBV and rMFV parameters had the largest plane-to-plane variations with CVs up to 54%. Measurements made in 3D were consistently different than measurements made in 2D with an average percent difference of 60%. Reproducibility, evaluated by the concordance correlation coefficient (CCC) between repeated measurements, was good (0.80) to excellent (0.95). The TP and MTT were the least reproducible with CCCs lesser than 0.80.

### CONCLUSION

This first in human study confirms 2D DCE-US sampling errors and demonstrates that 3D DCE-US imaging with a matrix array transducer is feasible and reproducible in the clinic.

# **CLINICAL RELEVANCE/APPLICATION**

DCE-US is inexpensive, exempt from radiation exposure and available at the bedside. Eliminating sampling errors through 3D imaging further potentiates its role as a clinical tool to identify early response to cancer therapy.

Apparent Diffusion Coefficient for Prediction of Parametrial Invasion in Cervical Cancer: A Critical Evaluation Based on Stratification to a Likert scale using T2-weighted Imaging

Thursday, Dec. 1 12:15PM - 12:45PM Room: GU/UR Community, Learning Center Station #1

## Participants

Sungmin Woo, MD, Seoul, Korea, Republic Of (*Presenter*) Nothing to Disclose Sang Youn Kim, MD, Seoul, Korea, Republic Of (*Abstract Co-Author*) Nothing to Disclose Jeong Yeon Cho, MD, Seoul, Korea, Republic Of (*Abstract Co-Author*) Nothing to Disclose Seung Hyup Kim, MD, Seoul, Korea, Republic Of (*Abstract Co-Author*) Nothing to Disclose

### PURPOSE

A few recent studies suggest that apparent diffusion coefficient (ADC) is significantly lower in cervical cancer with parametrial invasion (PMI). However, as ADC itself does not directly provide morphological information but is rather functional in nature, caution may be needed when making an association between ADC and PMI. Therefore, we re-evaluated ADC for determining PMI in patients with cervical cancer, by stratifying them into subgroups based on a Likert scale using T2-weighted imaging (T2WI).

# METHOD AND MATERIALS

In this retrospective study, 87 patients with FIGO stages IA2-IIB cervical cancer who underwent MRI followed by radical hysterectomy were included. The likelihood of PMI was assessed on T2WI using a 6-point Likert scale (0, MRI-invisible; 1, no PMI; 2, probably no PMI; 3, possible PMI; 4, probable PMI; 5, definite PMI) and ADC was measured. MRI findings were compared between patients with and without PMI using the linear-by-linear association and Mann-Whitney U test with subgroup analysis for each score group. The differences in ADC according to the Likert scale was assessed using Kruskal-Wallis test.

### RESULTS

19 (21.8%) patients were identified to have PMI on pathology. The prevalence of PMI demonstrated a significant association with Likert scale (P<0.001). Mean ADC differed according to Likert scale (P<0.001). However, only tumors with a Likert score of 0 showed significantly greater the ADC values than others (P<0.001), while no significant difference was observed among patients with Likert scores of 1-5 (P=0.070-0.889). Patients with PMI had significantly lower ADC ( $0.854 \times 10-3 \text{ mm2/s}$ ) than those without PMI ( $1.033\pm0.324 \times 10-3 \text{ mm2/s}$ , P=0.034). However, no significant differences were seen on subgroup analysis for each score group (P=0.180-0.857).

# CONCLUSION

A Likert scale based on T2WI and ADCs were significantly associated PMI. However, the apparent association seen between ADC and PMI in the whole population may in fact be due to the contribution of MRI-invisible tumors.

# **CLINICAL RELEVANCE/APPLICATION**

Assessment of radiological PMI using T2WI will help stratify patients with cervical cancer to receive proper management and help the clinician in predicting postoperative outcomes and counselling the patient. However, caution is needed when using ADC for determining PMI, as the apparent association seen between them may be due to the contribution of MRI-invisible tumors rather than reflect their true relationship.

# Perfusion and Metabolic Imaging of Acute Kidney Injury

Thursday, Dec. 1 12:15PM - 12:45PM Room: GU/UR Community, Learning Center Station #2

#### **Participants**

Celine Baligand, PhD, San Francisco, CA (*Abstract Co-Author*) Nothing to Disclose David Lovett, San Francisco, CA (*Abstract Co-Author*) Nothing to Disclose Jeremy W. Gordon, PhD, San francisco, CA (*Abstract Co-Author*) Nothing to Disclose Joy Walker, San Francisco, CA (*Abstract Co-Author*) Nothing to Disclose David M. Wilson, MD, PhD, San Francisco, CA (*Abstract Co-Author*) Nothing to Disclose Christopher Owens, San franciscon, CA (*Abstract Co-Author*) Nothing to Disclose John Kurhanewicz, PhD, San Francisco, CA (*Abstract Co-Author*) Nothing to Disclose Zhen J. Wang, MD, Hillsborough, CA (*Presenter*) Stockholder, Nextrast, Inc

### PURPOSE

Acute kidney injury (AKI) is a common problem in hospitalized patients, and leads to chronic kidney disease (CDK) and poor prognosis. Perfusion and metabolic alterations have been suggested to play a key role in the development and progression of AKI. We aim to assess whether arterial spin labeling (ASL) and hyperpolarized (HP) 13C MRI can detect perfusion and metabolic changes in a murine model of AKI.

### METHOD AND MATERIALS

Multiparametric MRI exams were performed in 4-5month old mice (n=7) prior to and 7 days after unilateral moderate ischemia reperfusion (I/R) injury (40min ischemia). Renal perfusion was assessed using ASL-MRI. Redox capacity was assessed after IV injection of HP 13C dehydroascorbate (DHA), which is reduced to Vitamin C (VitC) through a glutathione dependent process. The rate of DHA reduction to VitC, as measured by VitC/(VitC+DHA), reflects cellular redox capacity. Relative glycolytic and oxidative metabolism was assessed after injection of HP 13C-pyruvate. The relative ratios of the metabolites lactate (Lac), alanine (Ala), and bicarbonate (Bic) reflect a balance between the glycolytic pathway (pyruvate conversion to lactate) and the oxidative pathway (entry into the Kreb cycle).

#### RESULTS

7 days after I/R injury, renal perfusion dropped from  $463\pm70$  to  $257\pm60$  mL/min/100g in the AKI kidneys (p=0.001) and remained unchanged in the contralateral kidney. The VitC/(VitC+DHA) ratios were also significantly decreased in AKI kidneys, from 0.24±0.04 at baseline to 0.16±0.03 on day 7 (p=0.001), consistent with impaired redox capacity. Additionally, Lac/(Lac+Ala+Bic) ratios in the injured kidneys increased from 0.76±0.09 to 0.88±0.07 (p=0.03), suggesting a shift towards the glycolytic pathway, and/or away from the oxidative pathway.

# CONCLUSION

ASL and HP 13C MRI can detect alterations in perfusion, redox capacity and pyruvate metabolism in a murine model of AKI. Studies are ongoing to assess longitudinal imaging changes during the evolution of AKI to CKD with pathology and tissue biochemical correlates. Notably, ASL and HP pyruvate MR have been applied to patients, and are readily translatable for the clinical evaluation of kidney injury.

### **CLINICAL RELEVANCE/APPLICATION**

Commonly used serum markers such as creatinine are not sensitive for AKI detection. Perfusion and metabolic imaging may provide early biomarkers of kidney injury, and response to novel treatment.

# **External Validation of ADNEX MR SCORING System**

Thursday, Dec. 1 12:15PM - 12:45PM Room: GU/UR Community, Learning Center Station #3

#### Participants

Kohei Sasaguri, MD, Saga, Japan (*Presenter*) Nothing to Disclose Ken Yamaguchi, MD, Saga, Japan (*Abstract Co-Author*) Nothing to Disclose Takahiko Nakazono, MD, PhD, Saga, Japan (*Abstract Co-Author*) Nothing to Disclose Hiroyuki Irie, MD, PhD, Saga, Japan (*Abstract Co-Author*) Nothing to Disclose

## PURPOSE

To evaluate the usefulness of a published MR imaging scoring system for characterization of adnexal masses (ADNEX MR SCORING system)

#### **METHOD AND MATERIALS**

The study population comprised 305 women with 360 adnexal masses who underwent pelvic MRI between January 2007 and December 2014 and then surgery for the masses. MR images of the patients were retrospectively reviewed by two radiologists who were blinded to pathological diagnosis. The adnexal masses were scored into 5 categories (1: no mass, 2: benign mass, 3: probably benign mass, 4: indeterminate mass, 5: probably malignant mass) according to the ADNEX MR SCORING system by consensus of the reviewers. The reference standard was surgical pathologic diagnosis: 268(74.4%), 25(6.9%) and 67(18.6%) of the 360 adnexal masses were benign, borderline malignant and malignant, respectively. Diagnostic performance of the scoring system for the differentiation of benign and malignant adnexal masses was evaluated by ROC analysis. Score 4 or greater was judged as malignant (including borderline malignancy) according to the original research.

#### RESULTS

Prevalence of malignancy in masses with the Score 2,3,4 and 5 were 1.5% (3/197), 19.2%(14/73), 77.3%(34/44) and 89.1%(41/46), respectively. The diagnostic performance of the scoring system was excellent with AUC (area under the ROC curve) of 0.936. The sensitivity, specificity and accuracy for the diagnosis of malignancy was 81.5%(75/92), 94.4% (253/268) and 91.1% (328/360). Among the 17 masses misclassified into benign, 8 masses were misclassified because of lack of measurable solid component; 7 of the 8 masses were mucinous borderline tumors. Other 9 masses were misclassified because of showing atypical enhancement pattern for malignant tumors. Histological diagnosis of the 15 cases misclassified into malignancy were variable including mature cystic teratoma with enhancing solid portion (n=4), struma ovarii (n=2), thecoma (n=2) and uterine subserosal myoma (n=2).

## CONCLUSION

ADNEX MR SCORING system was highly accurate in the differentiation of benign and malignant adnexal masses, although less accurate for borderline tumors.

### **CLINICAL RELEVANCE/APPLICATION**

The ADNEX MR SCORING system can help radiologists to differentiate benign from malignant when reporting MR imaging of patients with adnexal masses.

The Learning Curve in Prostate MRI Interpretation: Self-Directed Learning versus Continual Reader Feedback

Thursday, Dec. 1 12:15PM - 12:45PM Room: GU/UR Community, Learning Center Station #4

#### **Participants**

Andrew B. Rosenkrantz, MD, New York, NY (*Abstract Co-Author*) Nothing to Disclose Molly Somberg, MD, New York, NY (*Abstract Co-Author*) Nothing to Disclose Paul Smereka, MD, New York, NY (*Abstract Co-Author*) Nothing to Disclose Vinay Prabhu, MD, New York, NY (*Abstract Co-Author*) Nothing to Disclose Anunita Khasgiwala, MD, New York, NY (*Presenter*) Nothing to Disclose David H. Hoffman, MD, New York, NY (*Abstract Co-Author*) Nothing to Disclose Abimbola Ayoola, MD, New York, NY (*Abstract Co-Author*) Nothing to Disclose James S. Babb, PhD, New York, NY (*Abstract Co-Author*) Nothing to Disclose Neil Mendhiratta, Bethesda, MD (*Abstract Co-Author*) Nothing to Disclose Fang-Ming Deng, MD, PhD, New York, NY (*Abstract Co-Author*) Nothing to Disclose Samir S. Taneja, MD, New York, NY (*Abstract Co-Author*) Nothing to Disclose Samir S. Taneja, MD, New York, NY (*Abstract Co-Author*) Nothing to Disclose

#### PURPOSE

To evaluate the roles of self-directed learning and continual feedback in the learning curve (LC) for prostate MRI interpretation.

### **METHOD AND MATERIALS**

We identified men with prior MRI-US fusion targeted biopsy in whom the MRI could be classified as positive (n=52; single PI-RADS $\geq$ 3 lesion showing Gleason $\geq$ 7 tumor) or negative (n=72; PI-RADS $\leq$ 2 and negative fusion/systematic biopsy) for detectable tumor. The exams were divided into four batches with similar mixes of positive and negative cases. Six 2nd-year radiology residents without prior prostate MRI experience reviewed exams to localize tumors. Three of the six readers received feedback after each exam showing the preceding case's solution. A LC was plotted of reader accuracy over time. Logistic regression for correlated data and mixed-model ANOVA were performed.

#### RESULTS

The LC was similar for readers with only self-directed learning and those also receiving continual feedback, exhibiting rapid improvement in accuracy across the first 40 cases reviewed, after which improvement slowed. At multivariate analysis, accuracy was associated with the number of cases reviewed (p<0.01), but not wth the presence of feedback (p=0.75). Accuracy improved from 58% in batch 1 to 71%-75% in batches 2-4 without feedback and from 58% to 72%-77% 4 with feedback (both p<.0.05), with no difference in extent of improvement between groups (p=0.8). Specificity improved from 54% to 69%-82% without feedback (both p<0.05), with no difference in extent of improvement between groups (p=0.8). Specificity improved from 54% to 69%-82% without feedback and from 56% to 74%-82% with feedback (both p<0.05), with no difference in extent of improvement (p=0.9). Overall sensitivity improved from 59%-62% in batches 1-2 to 77%-72% in batches 3-4 with feedback (p=0.05), though did not improve without feedback (p=0.6). Sensitivity for TZ tumor showed a larger change (p=0.02) from batches 1-2 to 3-4 with feedback (27%-33% to 44%-67%) vs. without feedback (44%-78% to 44\%-56\%). Sensitivity for PZ tumor did not improve in either group (p>0.3). Reader confidence increased significantly only with feedback (p<0.01).

#### CONCLUSION

A LC in prostate MRI interpretation was largely due to self-directed learning. Additional continual feedback did not improve overall accuracy, though slightly helped TZ tumor detection and improved reader confidence.

### **CLINICAL RELEVANCE/APPLICATION**

Caution is warranted regarding clinical prostate MRI interpretation by novice radiologists. Insights into the self-directed LC and incremental role of feedback may help guide training efforts.

# Value of Magnetic Resonance Imaging in the Prenatal Diagnosis of the Degree of Placental Invasion

Thursday, Dec. 1 12:15PM - 12:45PM Room: GU/UR Community, Learning Center Station #5

#### **Participants**

Chenyu Yan, MD, Zhengzhou, China (*Presenter*) Nothing to Disclose Chengqun Chen, Zhengzhou, China (*Abstract Co-Author*) Nothing to Disclose Xuemei Gao, zhengzhou, China (*Abstract Co-Author*) Nothing to Disclose Jingliang Cheng, MD,PhD, Zhengzhou, China (*Abstract Co-Author*) Nothing to Disclose

## PURPOSE

The purpose of this study was to evaluate the role of magnetic resonance imaging (MRI) in the prenatal diagnosis of abnormal placentation in women with placenta previa and to assess the ability of MR imaging features to define the degree of placenta invasion.

## METHOD AND MATERIALS

A retrospective review including a total of 178 patients (range 26.3 to 39.7 gestation weeks) with placenta previa between January 2015 and December 2015. All patients underwent prenatal MRI examination with a 1.5 T scanner, including half-Fourier Acquisition Single-Shot Turbo Spin-Echo (HASTE), true fast imaging with steady-state precession (TrueFISP) and Diffusion Weighted Image (DWI) sequence. The MRI features used were dark intraplacental bands and abnormal vascularity, uterine bulging, disruption of the uteroplacental zone and placental thickened and deformity. Based on the presence of four MR imaging features associated with placenta previa, the radiologic impression of the extent of placental invasion was graded on a 5-point scale. The scores of MR imaging features were compared with the post-operative data, which were grouped into normal, placenta accreta, placenta increta and placenta percreta.

### RESULTS

A total of 27 (15.2%) patients were confirmed no placenta invasion at operation. The surgical findings confirmed placenta accreta in 46 (20.5%) patients, placenta increta in 52 (29.2%) patients, and placenta percreta in 53 (29.8%) patients. The score of MR imaging features was positively correlated with the degree of placenta invasion (P < 0.01). The differences in MR imaging features score by extent of placental invasion (normal versus placenta accreta, placenta accreta versus increta and placenta increta versus percreta) were all significant (P < 0.01). Compared to other features, uterine bulging indicated placenta increta or percreta specifically. Low b value (b=0) DWI could demonstrated dark intraplacental bands and abnormal vascularity better than other sequences.

### CONCLUSION

MRI is able to detect abnormal placentation in patients with placenta accreta reliably The score of MR imaging features can be used to predict the degree of placenta invasion in patients with placenta previa with acceptable diagnostic accuracy.

### **CLINICAL RELEVANCE/APPLICATION**

The score of MR imaging features can be used to predict the degree of placenta invasion in patients with placenta previa with acceptable diagnostic accuracy.

## GU251-SD-THA6

Impact of Renal Function on Gadolinium Retention Following Administration of Gadolinium-based Contrast Agents in a Mouse Model

Thursday, Dec. 1 12:15PM - 12:45PM Room: GU/UR Community, Learning Center Station #6

# Participants

Achmad A. Kartamihardja, MD, Maebashi, Japan (*Presenter*) Nothing to Disclose Takahito Nakajima, MD, Maebashi, Japan (*Abstract Co-Author*) Nothing to Disclose Satomi Kameo, PhD, Maebashi, Japan (*Abstract Co-Author*) Nothing to Disclose Hiroshi Koyama, MD,PhD, Maebashi, Japan (*Abstract Co-Author*) Nothing to Disclose Yoshito Tsushima, MD, Maebashi, Japan (*Abstract Co-Author*) Institutional Research Grant, Bayer AG ; Institutional Research Grant, DAIICHI SANKYO Group; Institutional Research Grant, Eisai Co, Ltd; Institutional Research Grant, Nihon Medi-Physics Co, Ltd; Institutional Research Grant, FUJIFILM Holdings Corporation ; Institutional Research Grant, Fuji Pharma Co, Ltd; Institutional Research Grant, Siemens AG ; Institutional Research Grant, OncoTherapy Science, Inc; Institutional Research Grant, Becton, Dickinson and Company; Speaker, Bayer AG ; Speaker, DAIICHI SANKYO Group; Speaker, Eisai Co, Ltd; Speaker, Fuji Pharma Co, Ltd; Speaker, Guerbet SA; .;

### PURPOSE

To investigate the effect of renal failure on gadolinium (Gd) retention in various organs after Gd-based contrast agent (GBCA) injection.

### **METHOD AND MATERIALS**

Following local animal care and review committee approval, 18 normal mice and 18 with renal failure were divided into three treatment groups (Gd-DTPA-BMA, 5 mmol/kg; Gd-DOTA, 5 mmol/kg; GdCl3, 0.02 mmol/kg). Each agent was intravenously administered on weekdays for 4 weeks. All groups were divided into two sub-groups based on sample collection time; days 3 (3D) and days 45 (45D) after the last injection. Saline (5 mL/kg) was injected to different groups as control. Gd concentrations were quantified by mass spectrometry analysis.

# RESULTS

GdCl3 analysis on the 45D was not obtained due to the limitation of sample number. In the Gd-DTPA-BMA group, impaired renal function increased 3D Gd retention in the liver, bone, spleen, skin, and kidney (p < 0.01) but did not affect 45D Gd retention. Although Gd retention in the Gd-DTA group was generally low, impaired renal function increased only 45D hepatic Gd retention. Hepatic and splenic Gd retentions were significantly higher than other organs' Gd retention in the GdCl3 group (p < 0.01). Gd retention in the brain was less affected by renal function, regardless of the Gd compound used.

# CONCLUSION

The tendency of Gd retention varied according to the agent, regardless of renal function. Although renal impairment increased 3D Gd retention after Gd-DTPA-BMA administration, 45D Gd retention for GBCAs was almost unaffected by renal function, suggesting that the chemical structures of retained Gd may not be consistent and some Gd is slowly eliminated after initially being retained.

## **CLINICAL RELEVANCE/APPLICATION**

Gd retention in the Gd-DOTA group was generally low even when administered in a high dose, hence it might be safer particularly for renal impaired patients.

# **Pitfalls of Contrast Reaction Management: How to Avoid Them?**

Thursday, Dec. 1 12:15PM - 12:45PM Room: HP Community, Learning Center Custom Application Computer Demonstration

#### **Participants**

Alexi Otrakji, MD, Boston, MA (*Presenter*) Nothing to Disclose Iris M. Otani, MD, San Diego, CA (*Abstract Co-Author*) Nothing to Disclose Hillary R. Kelly, MD, Boston, MA (*Abstract Co-Author*) Nothing to Disclose Garry Choy, MD, MS, Boston, MA (*Abstract Co-Author*) Nothing to Disclose Sanjay Saini, MD, Boston, MA (*Abstract Co-Author*) Nothing to Disclose Gloria M. Salazar, MD, Boston, MA (*Abstract Co-Author*) Nothing to Disclose Swati Goyal, Boston, MA (*Abstract Co-Author*) Nothing to Disclose

## **TEACHING POINTS**

Diagnostic errors in management of anaphylaxis secondary to contrast media administration can lead to life-threatening patient safety events. Effective management for such events depends on recurrent training of staff with didactic educational tools. Given the incidence of errors reported in the literature and our institutional experience with simulation training program, we structured this exhibit to highlight the following points: The most common mistakes in contrast reactions management. The correct methods of contrast reactions management. Best practices to avoid these mistakes.

# TABLE OF CONTENTS/OUTLINE

This exhibit will take the participants to a multiple choice questions course and video based tour through the most common errors of contrast reactions treatment reported in the literature and in our institution, in addition to the correct management. We will use interactive software (RadIQ) to go through all of the following pitfalls: Failure to administrate the indicated medicine in anaphylaxis. Failure to administrate epinephrine correctly: the way of using auto-injector, injection period, and the place of injection. Failure to administrate the correct dose of epinephrine: using of pediatric versus adult auto injector, wrong concentration intravenously or intramuscularly. Additional help Delay to institute epinephrine

Cost Effectiveness Analysis of Monitoring Strategies in the First Year after Cardiac Transplantation

Thursday, Dec. 1 12:15PM - 12:45PM Room: HP Community, Learning Center Station #1

#### Awards

### **Student Travel Stipend Award**

#### **Participants**

Matthew A. Pilecki, BA, Chicago, IL (*Presenter*) Nothing to Disclose Asad A. Usman, BSc, Chicago, IL (*Abstract Co-Author*) Nothing to Disclose Gordon Hazen, PhD, Evanston, IL (*Abstract Co-Author*) Nothing to Disclose Amir Ali Rahsepar, MD, Chicago, IL (*Abstract Co-Author*) Nothing to Disclose Julie A. Blaisdell, Chicago, IL (*Abstract Co-Author*) Nothing to Disclose Jane Wilcox, MD, Chicago, IL (*Abstract Co-Author*) Nothing to Disclose David Dranove, PhD, Evanston, IL (*Abstract Co-Author*) Nothing to Disclose Jeremy D. Collins, MD, Chicago, IL (*Abstract Co-Author*) Nothing to Disclose Michael Markl, PhD, Chicago, IL (*Abstract Co-Author*) Institutional research support, Siemens AG; Consultant, Circle Cardiovascular Imaging Inc;

James C. Carr, MD, Chicago, IL (*Abstract Co-Author*) Research Grant, Astellas Group Research support, Siemens AG Speaker, Siemens AG Advisory Board, Guerbet SA

### PURPOSE

Development of acute allograft rejection is the primary cause of morbidity in the first year post cardiac transplantation. Endomyocardial biopsy (EMB) combined with echocardiography and cardiac catheterization is considered the gold standard for surveillance of rejection. EMB, however, remains invasive, expensive, carries risk of injury, and is uncomfortable for the patient. Validation of alternative monitoring algorithms combining clinical effectiveness with lower cost and decreased invasiveness remains a strategic priority for physicians and healthcare systems.

### **METHOD AND MATERIALS**

We developed a Markov model using cost, utility of states, sensitivity and specificity of test parameters to assess the comparative effectiveness of various monitoring strategies. We modeled the efficacy based on the utility spent in each Markov state based on reports from the literature. Cost for procedures was estimated based on Medicare reimbursement and validated against institutional data.

### RESULTS

Approximately 37% of recipients will experience at least 1 episode of ACR in the first postoperative year. Approximately 80% to 85% of these rejection episodes respond to the initial treatment regimen. There are very few instances of acute transplant rejection leading to re-transplantation in the first year and most occur in the first month post operatively. At a 16 node level of monitoring, all monitoring strategies analyzed were similarly efficacious at 292 QALD. The average cost of invasive monitoring per patient per year is estimated to be \$231,795 vs \$67,287 for CMR. A mixed strategy of early EMB with subsequent CMR costs \$114,573.

# CONCLUSION

Continued development and improvement of CMR in rejection surveillance for transplant patients indicates it represents a cost effective alternative to the current gold standard. Further research into combined strategies will determine not only comparative effectiveness but the possibility of improving utility of life post-transplant in the first year. Further dedicated randomized controlled trials will be able to elucidate the effectiveness of MR techniques. In the setting of increasing health care costs, a potential reduction of over \$117,000 per patient and \$146,000/QALY can result in significant value for society.

# **CLINICAL RELEVANCE/APPLICATION**

New mixed surveillance modalities utilizing CMR represent promising alternatives to invasive monitoring strategies for cardiac rejection in the first year after transplantation.

# Why are Medical Students Not Choosing Radiology?

Thursday, Dec. 1 12:15PM - 12:45PM Room: HP Community, Learning Center Station #2

#### Awards

### **Student Travel Stipend Award**

#### **Participants**

Luke J. Robinson, MD,MA, BROOKLYN, NY (*Presenter*) Nothing to Disclose Patrick J. Hammill, MD, Brooklyn, NY (*Abstract Co-Author*) Nothing to Disclose Tianyuan Liu, BA, BROOKLYN, NY (*Abstract Co-Author*) Nothing to Disclose Faraz Ahmed, Albertson, NY (*Abstract Co-Author*) Nothing to Disclose

#### PURPOSE

Recent publications demonstrate an alarming drop in the number of US Allopathic Medical Students (USM) applying for Radiology residency. This may be due to perceived weakness of the job market and lack of job security. Are students fearful that teleradiology—the ability to obtain images in one location, transmit them over a distance, and view them remotely, has decreased the need for radiologists in the hospital setting? Are female USM increasingly unlikely to pursue Radiology training? The aim of this study is to survey USM to determine their reasons for not applying to Radiology.

### **METHOD AND MATERIALS**

An IRB-waived prospective cohort cross-sectional study was performed at a single US Allopathic Medical School. 281 USM (response rate 40%) completed the survey. Data was obtained including: demographics, radiology course experience, considered applying to radiology, perception of Radiology Residency, general perception of Radiology, perception of outsourcing, amount of patient interaction relative to ideal job, perceived lifestyle, and fear of radiation. Some basic knowledge of radiation and contrast-agents was assessed. 1-5 Likert scale was used whenever feasible.

### RESULTS

146 (52%) of respondents were male, 135 (48%) were female. Preliminary results indicate 25/146 (17%) of males were considering/strongly considering radiology; compared to 4/135 (3%) in females. 118/281 (42%) of respondents were Asian, 17/118 (14%) of Asians were considering/strongly considering radiology compared to 12/163 (7%) of non-Asians. 42% of USM agree/strongly agree (A/SG) radiologists are not directly part of patient care, while only 10% disagree/strongly disagree (D/SG). 41% of USM A/SG teleradiologists have decreased the need for radiologists in the hospital setting while only 20% D/SG disagree. USM note there is not enough patient contact in radiology compared to ideal job (69% A/SG vs 11% D/SG).

## CONCLUSION

Initial data suggest USM see Radiologists not directly part of patient care and can be outsourced due to teleradiology. USM feel radiologists spend too little time with patients compared to the ideal job. Female USM are particularly unlikely to consider Radiology.

### **CLINICAL RELEVANCE/APPLICATION**

USM are increasingly not choosing Radiology due to: fear of outsourcing and decreased patient interaction; female USM are particularly unlikely to pursue Radiology.

Longitudinal Evaluation of a Lecture Series Based on the American College of Radiology Appropriateness Criteria for Emergency Medicine Providers (A 1 Year Follow-up)

Thursday, Dec. 1 12:15PM - 12:45PM Room: HP Community, Learning Center Station #3

#### Awards

### **Student Travel Stipend Award**

#### Participants

Jeff J. Farrell, MD, Cleveland, OH (*Presenter*) Nothing to Disclose Christos Kosmas, MD, Cleveland, OH (*Abstract Co-Author*) Nothing to Disclose Peter C. Young, MD, Cleveland, OH (*Abstract Co-Author*) Nothing to Disclose

#### PURPOSE

In the near future, the United States health care system will transition from a fee-for-service system to a value base system. Implementing evidence-based guidelines and decision support tools will be essential to the field of radiology. The American College of Radiology has developed the American College of Radiology-Appropriateness Criteria (ACR-AC) as well as ACR Select to help provide evidence based guidelines to ordering providers for imaging ordering advice. Despite the ACR efforts, literature states that medical students, residents, and ordering providers are unaware of the ACR-AC or underutilize it. For the 2015-2016 academic year, our institution continued for a second year a lecture series based on the ACR-AC for emergency medicine providers. The purpose of this study was to assess the long term effectiveness of our ACR-AC lecture based series to educate emergency medicine residents. Specifically, we followed the emergency medicine (EM) resident class of 2016 and 2017 to assess their performance on the pre-test results from the ACR-AC lectures from the academic years of 2014-2015 to 2014-2016 to identify long term effectiveness of our lecture based series. In addition, our group evaluated the pre and post-test performance of the emergency residency class of 2016, 2017, and 2018 for the academic year of 2015-2016.

#### RESULTS

The pre-test and post-test scores of the EM resident class of 2016 (current PGY-3) and 2017 (Current PGY 2) for the academic years of 2014-2015 and 2015-2016 for the same four lectures were analyzed. The pre-test score for the academic year of 2014-2015 was 47% and 53% correct for the class of 2017 and 2016 respectively. The pre-test score for the academic year of 2015-2016 was 88% and 88% for the class of 2017 and 2016, respectively. A sample of the means two-tailed t-test was used to determine if there was a significant difference. The respective pre-test scores for the class of 2018, 2017, and 2016 pre and post test scores were analyzed. The percentage correct for the pre-test quizzes for the class of 2018, 2017, and 2016 were 52%, 88%, and 88 %, respectively. A two tailed t-test sample of the means was used to compare the pre and post test data to determine if a significant difference exists. The p-value for the class of 2018 was P-value <0.05. The class of 2017 and of 2018 were not significantly different with a p-value > 0.05.

# CONCLUSION

The class of 2016 and 2017 EM residents at our institution demonstrated significantly improved pre-test scores for the 2015-2016 academic year which suggests that the ACR-AC lectures based series is effective for long term education of non-radiology residents on the ACR-AC. In addition, the class of 2018 which had no previous exposure to the lectures in the academic year of 2014-2015 demonstrated significant improvement on their post-test quiz following the lectures on the ACR-AC for the 2015-2016 academic year. Implementing a continuing lecture series based on the ACR-AC provides an effective long term means of educating non-radiology physicians on the ACR appropriateness criteria. In addition, new residents not exposed to ACR-AC still lack knowledge on the ACR-AC based on the results of class of 2018 pre-test scores. Such a lecture series is an effective tool to educate the next generation of EM providers on the ACR-AC.

### **METHODS**

During the 2014-2015 academic year, 10 lectures based on the ACR-AC appropriateness criteria were given to EM residents at our institution. The lectures were approximately 20 minutes long with about 10 minutes for questions. All lectures also included information regarding relative radiation dose for the imaging examinations relevant to each topic. Before each lecture, the residents were given a quiz with three questions based on clinical scenarios on the topic of the lecture. The same quiz was given after the lecture. So far for the academic year of 2015-2016, the ACR-AC topics repeated were Small bowel obstruction, Right Lower Quadrant Pain-Rule out Appendicitis, Chest pain- pulmonary embolus, and Aortic Dissection. The remainder of the lectures will be given at later dates before the end of the academic year. There was a total of 7 residents in each EM resident class. The PGY-1, PGY-2, and PGY-3 emergency residency classes participated in each lecture. Thus far, the results of pre-tests from the 2014-2105 and 2015-2016 academic year swere analyzed with a two-tailed paired t-test sample for the means for the class of 2016 and 2017. In addition, the pre-test and post-test results for the 2015-2016 academic year from the four lectures were analyzed from the EM resident class of 2018, 2017, and 2016 with a two-tailed paired t-test sample of means tests.

#### PDF UPLOAD

http://abstract.rsna.org/uploads/2016/16005846/16005846\_z5e8.pdf

**RECIST 1.1** Criteria and Quantitative CT Image Features to Predict Pathologic Response to Immunotherapy in Melanoma: Preliminary Findings

Thursday, Dec. 1 12:15PM - 12:45PM Room: IN Community, Learning Center Station #1

# Participants

Brett W. Carter, MD, Houston, TX (*Presenter*) Editor, Reed Elsevier; Priya R. Bhosale, MD, Bellaire, TX (*Abstract Co-Author*) Nothing to Disclose Mohamed G. Elbanan, MD, Houston, TX (*Abstract Co-Author*) Nothing to Disclose Alper Duran, MD, Houston, TX (*Abstract Co-Author*) Nothing to Disclose Sujaya Rao, Houston, TX (*Abstract Co-Author*) Nothing to Disclose Ebru UNLU, Houston, TX (*Abstract Co-Author*) Nothing to Disclose Jia Sun, Houston, TX (*Abstract Co-Author*) Nothing to Disclose Wei Wei, Houston, TX (*Abstract Co-Author*) Nothing to Disclose David Fuentes, houston, TX (*Abstract Co-Author*) Nothing to Disclose Wei T. Yang, MD, Houston, TX (*Abstract Co-Author*) Nothing to Disclose

### PURPOSE

To determine whether RECIST 1.1 criteria and quantitative CT image features can predict pathologic response to immunotherapy in patients with advanced melanoma.

## **METHOD AND MATERIALS**

Eleven patients (4 female, 7 male; average age 59, age range 45-78) with advanced melanoma (stages III and IV) and biopsyproven metastatic lymph nodes treated with neoadjuvant immunotherapy (nivolumab and ipilimumab) prior to complete surgical resection were included. Surgical specimens were assessed for residual viable tumor (gold standard). RECIST 1.1 measurements were performed on contrast enhanced CT (CECT) scans at two time points (prior to therapy and before surgical resection) for all patients by both radiologists and melanoma medical oncologists. Interobserver agreement and the ability of RECIST 1.1 to predict pathologic response were analyzed. Quantitative image features were extracted from lymph nodes on pre-therapy CECT scans. Histogram, gradient, co-occurrence, gray tone difference, and filtration-based techniques were used for texture feature extraction using the Imaging Biomarker Explorer (IBEX) software platform. One-way analysis of variance (ANOVA) was used to correlate texture features with viable tumor, mutation status, RECIST 1.1 response, and clinical stage.

### RESULTS

At surgical resection, 5 patients had residual viable tumor and 6 had no detectable tumor. For RECIST 1.1 measurements, interobserver agreement was excellent with kappa = 0.84 (95% CI: 0.54 – 1.00). For the ability of RECIST 1.1 to predict pathologic response: accuracy, 64%; sensitivity, 100%; specificity, 33%; positive predictive value, 56%; and negative predictive value, 100%. Despite the limitations of small sample size, several texture features were identified as significant in predicting pathologic response, including contrast, entropy, busyness, and correlation, and patients with complete pathologic response (pCR) showed differences in these features.

# CONCLUSION

This study showed that RECIST 1.1 measurements were at times unreliable in predicting pathologic response in a group of melanoma patients treated with neoadjuvant immunotherapy and that quantitative image feature extracted from CECT were significant for predicting pathologic response. Verification of these texture features in larger studies is necessary.

### **CLINICAL RELEVANCE/APPLICATION**

In the prediction of pathologic response, RECIST 1.1 criteria can at times be unreliable and quantitative CT image features may add value.

#### **Honored Educators**

Presenters or authors on this event have been recognized as RSNA Honored Educators for participating in multiple qualifying educational activities. Honored Educators are invested in furthering the profession of radiology by delivering high-quality educational content in their field of study. Learn how you can become an honored educator by visiting the website at: https://www.rsna.org/Honored-Educator-Award/

Brett W. Carter, MD - 2015 Honored Educator Priya R. Bhosale, MD - 2012 Honored Educator The Quantitative Image Feature Pipeline (QIFP) for Discovery, Validation, and Translation of Cancer Imaging Biomarkers

Thursday, Dec. 1 12:15PM - 12:45PM Room: IN Community, Learning Center Station #2

### **Participants**

Sandy Napel, PhD, Stanford, CA (*Presenter*) Medical Advisory Board, Fovia, Inc; Consultant, Carestream Health, Inc; Scientific Advisor, EchoPixel, Inc; Scientific Advisor, RADLogics, Inc Sebastian Echegaray, MS, Stanford, CA (*Abstract Co-Author*) Nothing to Disclose Dev Gude, Stanford, CA (*Abstract Co-Author*) Nothing to Disclose Olivier Gevaert, PhD, Stanford, CA (*Abstract Co-Author*) Nothing to Disclose

Daniel L. Rubin, MD, MS, Stanford, CA (Abstract Co-Author) Nothing to Disclose

### PURPOSE

To create a publicly available resource for computing image features (radiomics) from regions of interest in 2D and 3D images of cancer patients, and for creating and validating diagnostic and prognostic image biomarkers, and predictors of tumor molecular phenotype.

#### **METHOD AND MATERIALS**

Cancer researchers are actively exploring the association of radiomics in medical images with clinical data (e.g., survival, response, specific gene mutations, tumor -omics) with the ultimate goal of building predictive models. The QIFP is a standards- and cloud-based system that will allow researchers to compute quantitative features from their own or publicly available image and clinical data, or from data that are shared to the QIFP by other users, to create integrative databases including radiomics and clinical data, and to build and evaluate predictive models for survival, response, and tumor molecular phenotype.

# RESULTS

The QIFP as implemented currently computes 3D features (e.g., tumor size, shape, edge sharpness, and pixel value statistics including image textures) from regions in an image series defined by DICOM Segmentation Objects (DSOs). Although these algorithms were developed in Matlab, we deployed them as shareable Docker executable-containers, linked them with a flexible workflow language, and made them available on a server that allows users to work with their own images or with existing images that are resident on the server or on a public resource, such as TCIA, and to compute radiomics features from regions defined by DSOs. Users can download and use these features in radiomics research. Future phases will include a built-in machine learning method for predictive model building, the ability for users to upload and share their own feature-generating and machine learning software in executable Docker containers, and a web-services interface allowing access to the QIFP from within their own platforms.

# CONCLUSION

The QIFP, which enables data and software tool sharing for radiomics research, has the potential to greatly accelerate the development and validation image biomarkers that could be readily translated for use in diagnosis, prognostication, and accelerating the completion of clinical trials.

## **CLINICAL RELEVANCE/APPLICATION**

The QIFP will allow the research community to share standard image feature computation algorithms, data sets, and the resulting predictive models which can then become part of the radiology workflow.

### **Honored Educators**

Presenters or authors on this event have been recognized as RSNA Honored Educators for participating in multiple qualifying educational activities. Honored Educators are invested in furthering the profession of radiology by delivering high-quality educational content in their field of study. Learn how you can become an honored educator by visiting the website at: https://www.rsna.org/Honored-Educator-Award/

Daniel L. Rubin, MD, MS - 2012 Honored Educator Daniel L. Rubin, MD, MS - 2013 Honored Educator

## IN252-SD-THA3

Radiomic Analysis of Salivary Glands for the Prediction of Weight Loss in Irradiated Head and Neck Cancer Patients

Thursday, Dec. 1 12:15PM - 12:45PM Room: IN Community, Learning Center Station #3

# Participants

Minoru Nakatsugawa, PhD, Baltimore, MD (Presenter) Employee, Toshiba Corporation; Research support, Toshiba Corporation; Zhi Cheng, MD, MPH, Baltimore, MD (Abstract Co-Author) Research Grant, Toshiba Corporation Keith Goatman, PhD, Edinburgh, United Kingdom (Abstract Co-Author) Nothing to Disclose Junghoon Lee, PhD, Baltimore, MD (Abstract Co-Author) Nothing to Disclose Adam Robinson, Baltimore, MD (Abstract Co-Author) Nothing to Disclose Ana P. Kiess, MD, PhD, Baltimore, MD (Abstract Co-Author) Nothing to Disclose Xuan Hui, MD, Baltimore, MD (Abstract Co-Author) Nothing to Disclose Scott Robertson, Baltimore, MD (Abstract Co-Author) Nothing to Disclose Michael Bowers, Baltimore, MD (Abstract Co-Author) Nothing to Disclose Amanda Choflet, MS, RN, Baltimore, MD (Abstract Co-Author) Nothing to Disclose Kazuki Utsunomiya, Otawara, Japan (Abstract Co-Author) Employee, Toshiba Corporation Shinya Sugiyama, Otawara, Tochigi, Japan (Abstract Co-Author) Employee, Toshiba Corporation John Wong, PhD, Baltimore, MD (Abstract Co-Author) Research Grant, Elekta AB Research Grant, Xstrahl Ltd Research Grant, Toshiba Corporation Co-founder, JPLC Associates LLC Royalty, Elekta AB Consultant, Xstrahl Ltd Todd R. McNutt, PhD, Baltimore, MD (Abstract Co-Author) Research collaboration, Koninklijke Philips NV Research collaboration, Toshiba Corporation Research collaboration, Elekta AB Harry Quon, MD, Baltimore, MD (Abstract Co-Author) Nothing to Disclose

# PURPOSE

The quality of life of irradiated head and neck cancer (HNC) patients is significantly limited by toxicities leading to weight loss. Our recent analysis identified that radiation (RT)-induced weight loss was influenced by age and dose to parotid glands based on recursive partition models. We hypothesize that these factors reflect the importance of baseline salivary gland function and that high-throughput image analysis, known as radiomics, can quantify baseline function to further refine our model.

#### **METHOD AND MATERIALS**

Clinical and dosimetric data were systematically captured in our analytic database. Computed tomography (CT) images used for RTplanning were extracted from the picture archiving and communicating system. 79 HNC patients treated with intensity-modulated radiotherapy (IMRT) from 2009 to 2015 with imaging and non-imaging datasets were identified. Imaging data included 5,000 features of intensity, volumetry, shape and textures calculated for each of the ipsilateral/contralateral parotid and submandibular glands. Non-imaging data included dose volume histogram, tumor diagnostics and patient demographics. Weight loss (≥5kg) at 3 months post-RT was predicted by the logistic regression with the LASSO algorithm. Three models were developed with 1)all features, 2)non-imaging only and 3)imaging features only.

### RESULTS

Combining imaging and non-imaging features significantly improved the weight loss prediction (p<0.001). The AUC/PPV of the three models was 1) 0.78/0.69, 2) 0.63/0.34, and 3) 0.64/0.42. The predictors were dose to combined parotid glands (D100), and the shape and textures of ipsilateral parotid and submandibular glands (fractal dimension, grey-level run-length and grey-level co-occurrence matrix). Selected texture predictors combined with age showed a significant trend (p<0.05).

### CONCLUSION

Our preliminary results demonstrate that baseline imaging features of salivary glands is potentially quantifiable and can predict RTinduced weight loss when combined with non-imaging features. To our knowledge, this represents a potentially novel observation and role for radiomics in the study of normal parotid function as it relates to predicting radiation-induced xerostomia.

# **CLINICAL RELEVANCE/APPLICATION**

Pre-radiotherapy radiomic analysis of salivary glands can measure baseline function and improve the RT-induced weight loss prediction which can support decisions for RT-planning and toxicity management.

# IN253-SD-THA4

### First Dynamic Study of Image Analyses from DCE-US to Evaluate of the Tumor Vascular Heterogeneity

Thursday, Dec. 1 12:15PM - 12:45PM Room: IN Community, Learning Center Station #4

#### Participants

Baya Benatsou, Villejuif, France (*Presenter*) Nothing to Disclose Mohamed Amine Benadjaoud, Villejuif, France (*Abstract Co-Author*) Nothing to Disclose Serge Koscielny, Villejuif, France (*Abstract Co-Author*) Nothing to Disclose Nathalie B. Lassau, MD, PhD, Villejuif, France (*Abstract Co-Author*) Speaker, Toshiba Corporation; Speaker, Bracco Group Stephanie Pitre-Champagnat, Villejuif, France (*Abstract Co-Author*) Nothing to Disclose

#### PURPOSE

Until there, evaluation of therapeutic response is only based on the perfusion curve averaged over the whole tumor, and does not take into account of its vascular heterogeneity. In this context, the aim of this study is to identify predictive parameters of therapeutic response using both texture and Functional Data Analysis (FDA) of DCE-US images. The originality of our approach is based on a dynamic study of image analysis at different time points of the time-intensity curve (TIC).

### **METHOD AND MATERIALS**

This retrospective study was performed on 62 patients with Hepatocellular carcinoma (CHC) treated by Sorafenib (NEXAVAR) included the DCE-US STIC multicentric studyDCE-US evaluations were available at: baseline; day: 7; 15; 30 and 60. For each examination, raw linear data were acquired during 3 minutes after injection of contrast agent. A region of interest (ROI), including total tumor surrounding the lesion, was defined. Ten frames have been extracted from video format at 10 specific time points of the TIC. Each image has been processed by homemade software on the total tumoral segment using thresholding with mathematical morphology, the vascular tumor signal intensity was extracted and the signal intensity outside tumor was removed. The resulting images were analyzed by three complementary approaches:i) a texture analysis based on the gray-level-spatial-dependence matrix, ii) a FDA study of the intensity histogram over the 10 images of each evaluation, iii) the ratio of low-vascularization surface on the whole tumor surface after Markovian segmentation. Finally, 14 parameters were extracted.

### RESULTS

In 62 patients, 56 male and 6 female were included. Median age was 64 years old. After the validation of image processing, we extracted a total of 2270 images from the 227 DCE-US examinations. The analysis is on progress and results will be presented.

### CONCLUSION

This first dynamic study of image analysis combined texture processing and FDA to evaluate the tumor vascular heterogeneity in order to determine predictive parameters of therapeutic response.

#### **CLINICAL RELEVANCE/APPLICATION**

First dynamic study of image analysis combined texture processing and FDA to evaluate the tumor vascular heterogeneity

## Reproducibility of CT Texture Parameters by Leveraging Publically Available Patient Imaging Datasets

Thursday, Dec. 1 12:15PM - 12:45PM Room: IN Community, Learning Center Station #6

#### Participants

Shih-Hsin Chen, London, United Kingdom (Abstract Co-Author) Nothing to Disclose Balaji Ganeshan, PhD, London, United Kingdom (Presenter) CEO, TexRAD Ltd; Director, Feedback plc; Director, Stone Checker Software Ltd; Director, Prostate Checker Ltd Francesco Fraioli, MD, London, United Kingdom (Abstract Co-Author) Nothing to Disclose

## PURPOSE

Heterogeneity is a key component of malignancy and computed tomography texture analysis (CTTA) is one possible way to quantify it non-invasively. This study aims to use a test-retest methodology to assess the reproducibility of the filtration-histogram technique of CTTA.

### **METHOD AND MATERIALS**

The RIDER Lung CT dataset without the injection of contrast media (source The Cancer Imaging Archive - TCIA, sponsored by the Cancer Imaging Program, DCTD/NCI/NIH) was used for this purpose. For each patient, two readers drew the regions of interest (ROI) on the slice with the largest cross-section of the tumor. One operator analyzed the image data twice with a one-week interval between the two analyses. Filtration-histogram based CTTA was undertaken using TexRAD commercial research software (TexRAD Ltd, www.texrad.com - part of Feedback Plc, Cambridge, UK). The agreement of the texture parameters from CTTA analysis of repeated scans, for the same operator (intra-operator) and between the two operators (inter-operator) was assessed by intra-class correlation coefficients (ICC) and further visualized using Bland-Altman plots.

### RESULTS

Our results showed that most of the filtration-histogram based CT texture parameters are generally reproducible with high ICC for the different permutations. The best ICC for the different texture quantifiers for intra-operator, inter-operator and repeated scan are as follows: Mean (0.968, 0.909, 0.787), SD (0.973, 0.960, 0.838), Entropy (0.998, 0.994, 0.993), Skewness (0.925, 0.862, 0.782), Kurtosis (0.942, 0.885, 0.689) and MPP (0.958, 0.942, 0.882). Bland-Altman plots further provided the average differences between the operators and limits of agreement for the different texture metrics, which are further useful in a clinical setting.

# CONCLUSION

The filtration-histogram technique of CTTA is reproducible. This study using a test-retest methodology forms a vital part in the qualification process of CTTA as a potential imaging biomarker and its translation into clinic.

### **CLINICAL RELEVANCE/APPLICATION**

The reproducibility of the filtration-histogram technique of CTTA suggests its potential application in routine clinical and multicenter setting.

Pharmacokinetic Analysis and Extravasation Study of a Novel Nanobubble Ultrasound Contrast Agent

Thursday, Dec. 1 12:15PM - 12:45PM Room: S503AB Station #1

#### Awards

#### **Trainee Research Prize - Resident**

#### **Participants**

Hanping Wu, MD, Cleveland, OH (*Presenter*) Nothing to Disclose Reshani Perera, Cleveland, OH (*Abstract Co-Author*) Nothing to Disclose Agata A. Exner, PhD, Cleveland, OH (*Abstract Co-Author*) Nothing to Disclose

### PURPOSE

Our group recently presented a simple strategy using the nonionic surfactant, Pluronic, as a size control excipient to produce nanobubbles in the 100 nm range which exhibited stability and echogenicity on par with clinically available microbubbles. The objective of the current study was to evaluate biodistribution and extravasation of the Pluronic-stabilized lipid nanobubbles compared to microbubbles in two experimental tumor models in mice.

### **METHOD AND MATERIALS**

Standard microbubbles or Pluronic L10 lipid-stabilized perfluoropropane nanobubbles were bolus injected into mice bearing either an orthotropic mouse breast cancer (BC4T1) or subcutaneous mouse ovarian cancer (OVCAR-3) through tail vein. The mean echopower value in the liver, kidney and tumor as function of time was acquired and the peak enhancement and decay slope were calculated for each tissue. To quantify extravasation, fluorescently-labeled nanobubbles and microbubbles were intravenously injected into mice bearing the same tumors. Three hours later, 0.1 ml fluorescein labeled tomato lectin (1mg/ml) was i.v. injected into mice to label the vessels. The mice were then perfused with PBS, the tumor tissue was harvested and imaged to measure bubble signal in tissue.

### RESULTS

The mean diameter of nanobubble and microbubble was 123.0 nm  $\pm$  24.9 and 685.0 nm  $\pm$  129.5, respectively. No significant differences were observed in peak enhancement between the nanobubble and microbubble groups in the three tested regions (tumor, liver and kidney). The decay rates of nanobubbles in all 3 ROIs were slower than those of microbubbles, and significant differences were noted in tumor of both models (0.79 dB/min  $\pm$  0.40 vs 1.13 dB/min  $\pm$  0.24 in BC4T1 tumor, and 1.66 dB/min  $\pm$  0.76 vs 2.64 dB/min  $\pm$  0.46 in OVCAR-3 tumor, respectively). Nanobubbles were also retained in tumor tissue to a higher extent compared to microbubbles in both tumor models.

# CONCLUSION

Pluronic-stabilized nanobubbles show equivalent peak enhancement and slower washout in tumors compared to microbubbles. Histological analysis demonstrates enhanced nanobubble extravasation and enhanced retention within tumor tissue. This study demonstrates potential augmented utility of these agents in ultrasound molecular imaging and drug delivery beyond the tumor vasculature.

# **CLINICAL RELEVANCE/APPLICATION**

Pluronic-stabilized nanobubbles can offer more robust properties in areas of molecular imaging and drug delivery.

# MK130-ED-THA7

# Metal Artefact Reduction Using Standard Sequences in MRI: Our Experience with Hip Prostheses

Thursday, Dec. 1 12:15PM - 12:45PM Room: MK Community, Learning Center Station #7

**FDA** Discussions may include off-label uses.

#### **Participants**

Jaime Isern, MD, Barcelona, Spain (*Presenter*) Nothing to Disclose Ferran Pifarre, Barcelona, Spain (*Abstract Co-Author*) Nothing to Disclose Alexandra Banguero, Barcelona, Spain (*Abstract Co-Author*) Nothing to Disclose Nuria Mayolas Sr, MD, Barcelona, Spain (*Abstract Co-Author*) Nothing to Disclose Cristobal Segura, Barcelona, Spain (*Abstract Co-Author*) Nothing to Disclose inmaculada ormazabal, barcelona, Spain (*Abstract Co-Author*) Nothing to Disclose

## **TEACHING POINTS**

1. To expose the method of reducing metal artifacts with standard sequences in 1.5 MRI.2. To describe the utility of each sequence: T1 SE, DP y T2 TSE y STIR.3. To assess the importance of intravenous contrast administration for an appropriate diagnosis of complications.4. To demonstrate the difficulty of reducing artifacts dependent on the type of prosthesis.5. To show the expected range of normal and pathological findings following hip arthroplasty.

### **TABLE OF CONTENTS/OUTLINE**

MR Imaging around Metal Hip Prostheses.- Method to reduce metal artifacts with standard sequences.Pathological findings following hip arthroplasty. - Type of prosthesis variability. - Importance of intravenous contrast administration.

# Why do Nerves Bright on DWI and Other FAQ about Functional MR-Neurography for Beginners

Thursday, Dec. 1 12:15PM - 12:45PM Room: MK Community, Learning Center Station #8

### Awards Certificate of Merit

#### **Participants**

Teodoro Martin, MD, Jaen, Spain (*Presenter*) Nothing to Disclose Antonio Luna SR, MD, Jaen, Spain (*Abstract Co-Author*) Nothing to Disclose Marta Gomez Cabrera, MD, Cadiz, Spain (*Abstract Co-Author*) Nothing to Disclose

## **TEACHING POINTS**

Describe the physiological aspects of functional MR-Neurography (MR-N) studies from peripheral nerve structure and basic DWI sequence design to more complex MRI-N DTI based techniques. Explain, using a similar frequently asked questions (FAQ) guide, the main concepts to understand, perform and approach to a functional MR-N study. Show the utility of functional MR-Neurography in different clinical scenarios.

### **TABLE OF CONTENTS/OUTLINE**

Introduction Physical basis of DWI and DTI focused in peripheral nerve evaluation. FAQ guide about functional MR-N for beginners. a. Why do nerves bright on DWI? b. How it influences the structure of the nerves for a DTI based What is the biological meaning of ADC, FA or other derived parameters? Can they be considered as neural approach? с. biomarkers? d. 1.5T or 3T magnet? e. DWI or DTI approach? f. When do I have to perform a g. Is necessary to integrate functional MR-N in routine protocols? 4.Clinical applications of functional MR-N a. Brachial functional MR-N study? h. How it should be a. Brachial and lumbosacral plexus read a functional MR-N study? evaluation. b. Carpal tunnel syndrome. c. Sciatic nerve assessment. d. Tumor and tumorlike conditions. e. Other neuropathies.

Pain in the Neck: Postoperative Appearance of the Cervical Spine

Thursday, Dec. 1 12:15PM - 12:45PM Room: MK Community, Learning Center Station #9

**FDA** Discussions may include off-label uses.

#### **Participants**

Philip K. Wong, MD, Atlanta, GA (*Presenter*) Nothing to Disclose Matthew L. Uriell, MD, Atlanta, GA (*Abstract Co-Author*) Nothing to Disclose Steven Prescuitti, MD, Atlanta, GA (*Abstract Co-Author*) Nothing to Disclose Douglas D. Robertson, MD, PhD, Decatur, GA (*Abstract Co-Author*) Nothing to Disclose Monica B. Umpierrez, MD, Atlanta, GA (*Abstract Co-Author*) Nothing to Disclose Walter A. Carpenter, MD, PhD, Atlanta, GA (*Abstract Co-Author*) Nothing to Disclose Adam D. Singer, MD, Atlanta, GA (*Abstract Co-Author*) Nothing to Disclose

### **TEACHING POINTS**

Teaching Points:1. Radiologists should be familiar with the various surgical techniques when interpreting post-operative imaging of the cervical spine.2. Factors such as number of stenotic levels, sagittal alignment of the spine, degree of existing motion, and medical comorbidities impact the optimal surgical approach.3. Postoperative complications can be divided into early and late complications.4. Early instrumentation-related complication such as instrument malpositioning can lead to major neurovascular and soft tissue related injuries.5. Long term sequelae of fusion surgery often affects the adjacent nonfused levels.6. Infection can even manifest in the late post-operative period.

# TABLE OF CONTENTS/OUTLINE

1. Overview of cervical spine anatomy on different imaging modalities.2. Review common indications for cervical spine surgery in the non-traumatic setting.3. Discuss and illustrate imaging features of common cervical spinal surgical techniques and hardware in the non-traumatic setting.4. Present examples of postoperative complications and their imaging appearance.

## MK340-SD-THA1

The Relationship between MRI and Histology in a Porcine Model of Intervertebral Disc Degeneration: A 24 week in Vivo Study

Thursday, Dec. 1 12:15PM - 12:45PM Room: MK Community, Learning Center Station #1

## Participants

Jianming Hua, MD, Hangzhou, China (Presenter) Nothing to Disclose

#### PURPOSE

To investigate a slowly progressive, reproducible porcine model of disc degeneration, and the relationship between MRI and histology in the long-term progression of disc degeneration.

### **METHOD AND MATERIALS**

The L4/L5 and L5/L6 intervertebral discs of lumber spine in miniature pigs with a weight of 10-15kg were punctured after anterior surgery, using 20-gauge sterile needles, 0.75 cm depth from annulus fibrosus to the middle of nucleus pulposus, controlled by the handmade stopper. Degeneration of the lumber discs was analyzed before surgery and at 4, 8, 12, and 24 weeks post-surgery by in vivo MRI and histological analysis.

## RESULTS

Based on the histological grading system, the discs of two groups were all categorized as normal, moderately degenerated, and severely degenerated, and the histologic score of puncture discs was significantly correlated with the time post-stab. Meanwhile, MRI measurements showed a progressive decrease in T2 signal intensity and MRI index starting at 4 weeks post-puncture. Furthermore, the degenerated discs did not recover spontaneously, shown by decrease in T2 signal intensity and MRI index and histological analysis. The apparent relativity was found between the content of sulfated glycosaminoglycan and MRI measurements.

### CONCLUSION

This study demonstrates that needle puncture into a lumber disc in the miniature pig induces a slow and progressive disc degeneration process without spontaneous recovery in 24 weeks. The apparent correlation was found among histological score, content of sulfated glycosaminoglycan and MRI measurements. In conclusion, MRI is a convenient, less invasive, and reproducible option to assess the progression of disc degeneration.

### **CLINICAL RELEVANCE/APPLICATION**

To investigate a porcine model and the relationship between MRI and histology in the long-term progression for further in vivo sutdy of disc degeneration.

The MR Quantitative Research of the Vertebral Microvascular Permeability in Alloxan-induced Diabetic Rabbits

Thursday, Dec. 1 12:15PM - 12:45PM Room: MK Community, Learning Center Station #2

#### **Participants**

hu lei, wuhan, China (*Presenter*) Nothing to Disclose Yunfei Zha, Wuhan, China (*Abstract Co-Author*) Nothing to Disclose Jiao Wang, Wuhan, China (*Abstract Co-Author*) Nothing to Disclose Liang Li, Wuhan, China (*Abstract Co-Author*) Nothing to Disclose Dong Xing, MD, Wuhan, China (*Abstract Co-Author*) Nothing to Disclose Wei Gong, MMed, Wu Han, China (*Abstract Co-Author*) Nothing to Disclose

# PURPOSE

To estimate the variation of the vertebral microvascular permeability in alloxan-induced diabetic rabbits using DCE-MRI.

## METHOD AND MATERIALS

Twelve young New Zealand White rabbits were randomly assigned to alloxan-induced diabetic group (n=6) and control group (n=6). All rabbits underwent sagittal magnetic resonance imaging (DCE-MRI) of lumbar on a 3.0T scanner (GE Discovery 750 Plus) with an 8 channel knee coil at fixed time points (0, 4, 8, 12, 16 week). The contrast agent with a concentration of 0.2 mmol/kg was injected after one pre-contrast frame was acquired. L7 was chosen to measure DCE-MRI parameters. The Extended Tofts model was used to estimate the quantitative parameters including Ktrans, kep, ve, and vp. The AIF was determined from a circular ROI in the center of abdominal aorta at the plane of L7. At the week 16, all rabbits were sacrificed, after which L7 sampling, HE staining and immunoperoxidase CD31 labeling. To count microvessel density (MVD), a quantitative estimation was performed. Repetitive measure analysis of variance (ANOVA) was applied in analyzing DCE-MRI parameters at different time points. Pearson correlations of DCE-MRI parameters with MVD were analyzed, respectively. All of the thresholds of statistical significance were set at *P*< 0.05.

### RESULTS

HE staining and immunohistochemistry showed that in comparison to the control group, the amount of the fat cell in diabetic group increased while the bone marrow cells and microvessel reduced. The Ktrans and kep increased while ve and vp decreased in the diabetic group. Only the alloxan-induced diabetic group had statistically significant differences in DCE parameters at each time point (Ktrans: F=63.694, P<0.05; kep: F=5.04, P<0.05; vp: F=4.403,P<0.05; vp: F=9.751, P<0.05).MVD showed negative correlation with Ktrans and kep and positive correlation with ve and vp (Ktrans: r=-0.901, P<0.05; kep:r=-0.731, P<0.05; vp: r=0.741, P<0.05; vp: r=0.593, P<0.05).

### CONCLUSION

The results of this study demonstrated diabetes mellitus could cause the variation of the vertebral microvascular permeabilit.

#### **CLINICAL RELEVANCE/APPLICATION**

DCE-MRI can evaluate quantitatively the variation trends of thevertebral microvascular permeability in alloxan-induced diabetic rabbits.

# Knee Arthroplasty in Knees with Early Osteoarthritis - MRI-Based Analysis from the Osteoarthritis Initiative

Thursday, Dec. 1 12:15PM - 12:45PM Room: MK Community, Learning Center Station #4

#### **Participants**

Frank W. Roemer, MD, Boston, MA (*Presenter*) Chief Medical Officer, Boston Imaging Core Lab LLC; Research Director, Boston Imaging Core Lab LLC; Shareholder, Boston Imaging Core Lab LLC; ;

Kent C. Kwoh, MD, Pittsburgh, PA (*Abstract Co-Author*) Advisory Panel, Pfizer Inc Data Safety Monitoring Board, Novartis AG Tomoko Fujii, Pittsburgh, PA (*Abstract Co-Author*) Nothing to Disclose

Michael Hannon, Oakland, PA (Abstract Co-Author) Nothing to Disclose

Robert Boudreau, PhD, Pittsburgh, PA (Abstract Co-Author) Nothing to Disclose

Ali Guermazi, MD, PhD, Boston, MA (*Abstract Co-Author*) President, Boston Imaging Core Lab, LLC Research Consultant, Merck KgaA Research Consultant, Sanofi-Aventis Group Research Consultant, TissueGene, Inc Research Consultant, OrthoTrophic Research Consultant, AstraZeneca PLC

#### PURPOSE

Knee replacement (KR) is commonly considered the therapy of choice in advanced osteoarthritis (OA) with severe symptoms. However, the proportion of knees that underwent KR from the 12 month visit through the 48 month visit in the Osteoarthritis Initiative (OAI) with no or only mild radiographic disease at baseline (BL) is high ( $\sim$ 30%).Aims are to assess 1.) whether structural damage seen on MRI that is potentially associated with pain differed at BL and the time point prior to reported KR ("T0") between those with mild OA and those with severe OA and 2.) whether change in pain levels from BL to T0 differed between those with mild OA vs. severe OA.

# METHOD AND MATERIALS

Participants who underwent KR were drawn from the OAI, a longitudinal observational study that includes 4,796 participants with or at risk of knee OA. MRIs were assessed for bone marrow lesions (BMLs), Hoffa-synovitis, and effusion-synovitis at BL and TO. Logistic regression was used to compare number of subregions affected by any BMLs per compartment, and presence of any Hoffa-synovitis and effusion-synovitis at BL and TO between knees with mild and advanced ROA at BL. Logistic regression was applied to assess the association of mild OA with change in pain from BL to TO using the severe OA group as the referent.

#### RESULTS

Of 181 knees that underwent KR during the 4 years of observation, 130 knees had severe OA while 51 knees had mild OA at BL. Compared to those with severe OA at BL, mild OA knees that later underwent KR were more strongly associated with presence of BMLs in two or more subregions in the PFJ (crude OR 7.92 95%CI [3.45,18.16]) but not the TFJ. Similar findings were observed for the time point prior KR, with mild OA being associated with two or more subregions with BMLs in the PFJ (crude OR 9.44 95%CI [4.00, 22.28]) but not in the TFJ.Mild OA knees showed an increased odds for change from "no pain" to "pain presence" from BL to T0 (aOR 5.48, 95%CI [1.25, 24.00]) for "pain within the last 12 months".

### CONCLUSION

BMLs in the PFJ were more often seen among knees that had mild OA at baseline.Worsening pain status seems to contribute to KR during a time frame of 4 years particularly in knees with mild OA at BL.

### **CLINICAL RELEVANCE/APPLICATION**

The findings support the role of structural damage in the PFJ in the decision for KR. Worsening pain is an important predictor of KR despite only mild structural radiographic changes.

#### **Honored Educators**

Presenters or authors on this event have been recognized as RSNA Honored Educators for participating in multiple qualifying educational activities. Honored Educators are invested in furthering the profession of radiology by delivering high-quality educational content in their field of study. Learn how you can become an honored educator by visiting the website at: https://www.rsna.org/Honored-Educator-Award/

Ali Guermazi, MD, PhD - 2012 Honored Educator

### MK344-SD-THA5

Effect of Autologous Stem Cell Transplant on Bone Mineral Density and Bone Strength in Patients with Multiple Myeloma

Thursday, Dec. 1 12:15PM - 12:45PM Room: MK Community, Learning Center Station #5

# Participants

Miyuki Takasu, MD, Hiroshima, Japan (*Presenter*) Nothing to Disclose Chikako Fujioka, RT, Hiroshima, Japan (*Abstract Co-Author*) Nothing to Disclose Koumei Takauchi, Hiroshima, Japan (*Abstract Co-Author*) Nothing to Disclose Yasutaka Baba, MD, Hiroshima, Japan (*Abstract Co-Author*) Nothing to Disclose Yoko Kaichi, Hiroshima, Japan (*Abstract Co-Author*) Nothing to Disclose Kazuo Awai, MD, Hiroshima, Japan (*Abstract Co-Author*) Nothing to Disclose Kazuo Awai, MD, Hiroshima, Japan (*Abstract Co-Author*) Research Grant, Toshiba Corporation; Research Grant, Hitachi, Ltd; Research Grant, Bayer AG; Research Grant, Eisai Co, Ltd; Medical Advisor, General Electric Company; ; ; ; ; Masao Kiguchi, RT, Hiroshima, Japan (*Abstract Co-Author*) Nothing to Disclose Chihiro Tani, MD, Hiroshima, Japan (*Abstract Co-Author*) Nothing to Disclose

### PURPOSE

An increase in effective therapies including autologous stem cell transplantation (ASCT) for patients with multiple myeloma (MM) has led to an improvements in overall survival. Osteoporosis and osteoporotic fractures are long-term complications of allogeneic SCT. This study evaluated the overall bone quality and bone strength after ASCT in MM patients using multidetector computed tomography (CT).

# METHOD AND MATERIALS

Spinal microarchitecture was examined by 64-detector CT and quantitative data (SUVmax) of 18F-fluorodeoxyglucose uptake of PET/CT were obtained in 72 MM patients who were classified into the following 3 groups: patients with newly diagnosed MM (control, n = 18); patients who received bortezomib-based regimen (BD, n = 35); and patients who underwent ASCT with bortezomib-based regimen (n = 19). Using a 3-dimensional image analysis system and finite element modeling (FEM), the bone mineral content per tissue volume (tissue BMD), trabecular parameters, failure load, and SUVmax of the third lumbar vertebrae without any focal lesion were calculated. The trabecular parameters and SUVmax were compared among the three groups using the Kruskal-Wallis test.

### RESULTS

No significant differences were seen in trabecular indices, failure load, or SUVmax among the 3 groups. Tissue BMD was significantly higher in the BD group than in the control group (P < 0.05).

### CONCLUSION

Multidetector CT demonstrated that bone strength and bone mass were not significantly reduced in patients who underwent ASCT compared with the BD group. Patients after chemotherapy with BD showed significantly higher BMD than in control patients.

### **CLINICAL RELEVANCE/APPLICATION**

Myeloma patients who had underwent ASCT were not found to have less BMD compared to patients after standard chemotherapy. Osteoporosis does not appear to be a long-term complications of ASCT.

The Effect of Sonication Duration on Ablation Size in MR Guided Focused Ultrasound (MRgFUS) Ablation of Bone

Thursday, Dec. 1 12:15PM - 12:45PM Room: MK Community, Learning Center Station #6

# Participants

Matthew D. Bucknor, MD, San Francisco, CA (*Presenter*) Nothing to Disclose Eugene Ozhinsky, San Francisco, CA (*Abstract Co-Author*) Nothing to Disclose Rutwik Shah, San Francisco, CA (*Abstract Co-Author*) Nothing to Disclose Roland Krug, PhD, San Francisco, CA (*Abstract Co-Author*) Nothing to Disclose Viola Rieke, PhD, San Francisco, CA (*Abstract Co-Author*) Nothing to Disclose

# PURPOSE

One challenge in MRgFUS ablation of bone tumors is extending the depth of ablation beyond the cortical surface, which rapidly attenuates sound. Anecdotally, providers will lower ultrasound frequency or increase sonication duration, in order to achieve better penetration. The purpose of this study was to evaluate the effect of longer versus shorter sonication durations on the size of the post-ablation appearance in a swine model of MR guided focused ultrasound ablation of bone, for a given total energy.

### **METHOD AND MATERIALS**

Experimental procedures received approval from the institutional committee on animal research. MRgFUS was used to create two ablation foci (distal and proximal) in the left femoral diaphysis of 6 pigs. The spacing of sonications was equivalent between the two foci. Both targets were subjected to six sonications with 400 J of energy each: the distal targets were dosed with 20 W for 20 seconds (standard time) and the proximal targets were dosed with 10 W for 40 seconds (long duration). The hypoenhanced ablation zone was then measured on post-contrast MRI sequences in three dimensions.

## RESULTS

MRgFUS created focal hypoenhanced lesions at the distal and proximal targets. Interestingly, the use of the conventional 20 second duration sonication resulted in the largest depth of the transverse intramedullary hypoenhanced zone and the craniocaudal dimension of the ablations, which on average measured 7.3 mm and 26.7 mm, respectively. By comparison, the mean ablation measurements for the 40 second long duration sonication group were 4.5 mm and 21.0 mm: these differences reached statistical significance (paired t-test, p = 0.026 and 0.006). There was no significant difference in the anteroposterior measurements between the two groups.

### CONCLUSION

While different techniques can and should be used to maximize the size of the ablation zone in MRgFUS of bone lesions, these results suggest that increasing the sonication duration, while concomitantly decreasing the acoustic power to maintain a given total energy, is not an effective technique and may be counterproductive.

### **CLINICAL RELEVANCE/APPLICATION**

These results can be used to help clinicians perform more complete MRgFUS ablations of bone lesions. They suggest that in order to maximize bone ablation size, if sonication duration is extended, then acoustic power should be either maintained, or decreased only partially, for a net increase in the total amount of energy delivered.

Beyond Colorectal Carcinoma: Imaging Spectrum of Lynch Syndrome

Thursday, Dec. 1 12:15PM - 12:45PM Room: MS Community, Learning Center Station #1

Awards Certificate of Merit Identified for RadioGraphics

#### **Participants**

Anas A. Saeed Bamashmos, MBChB, Houston, TX (*Abstract Co-Author*) Nothing to Disclose Chaitra M. Muthalgiri, MBBS, Houston, TX (*Abstract Co-Author*) Nothing to Disclose Veronica L. Cox, MD, Palo Alto, CA (*Abstract Co-Author*) Nothing to Disclose Shiva Gupta, MD, Houston, TX (*Abstract Co-Author*) Nothing to Disclose Sireesha Yedururi, MBBS, Sugarland, TX (*Abstract Co-Author*) Nothing to Disclose Naveen Garg, MD, Houston, TX (*Abstract Co-Author*) Consultant, Document Storage Systems, Inc CEO, Garglet LLC Hyunseon C. Kang, MD, PhD, Houston, TX (*Presenter*) Nothing to Disclose

# **TEACHING POINTS**

Understand the genetics of Lynch syndrome and associated tumor biology Review the diagnostic criteria for Lynch syndrome, and characteristics that differentiate it from other hereditary colorectal cancer syndromes Illustrate the imaging features of cancers associated with Lynch syndrome Discuss management of patients with Lynch syndrome

# TABLE OF CONTENTS/OUTLINE

Introduction to Hereditary Colorectal Cancer Syndromes Genetics and Pathology of Lynch Syndrome and Associated Tumor Biology Cancers Associated with Lynch syndrome - Colon, Endometrium, Ovary, Stomach, Small Bowel, Urinary Tract, Biliary Tree, Pancreas, Others Imaging Features of Cancers that Suggest an Association with Lynch Syndrome Management of Patients with Lynch Syndrome Screening/Surveillance Treatment - Surgical Resection, Chemotherapy, Immunotherapy

# NM134-ED-THA11

Clinical FDG and Amyloid Brain PET in the Investigation of Cognitive Impairment: How, When & Why?

# Awards

Cum Laude

# Participants

Sairah Khan, FRCR, London, United Kingdom (*Presenter*) Nothing to Disclose Kathryn L. Wallitt, MBBS, London, United Kingdom (*Abstract Co-Author*) Nothing to Disclose Sameer Khan, MBBS, London, United Kingdom (*Abstract Co-Author*) Nothing to Disclose Kuldip S. Nijran, PhD, London, United Kingdom (*Abstract Co-Author*) Nothing to Disclose Tara D. Barwick, MBChB, London, United Kingdom (*Abstract Co-Author*) Nothing to Disclose Zarni Win, MRCP, FRCR, London, United Kingdom (*Abstract Co-Author*) Nothing to Disclose Gemma Dawe, London, United Kingdom (*Abstract Co-Author*) Nothing to Disclose Paresh Malhotra, London, United Kingdom (*Abstract Co-Author*) Nothing to Disclose Richard Perry, London, United Kingdom (*Abstract Co-Author*) Nothing to Disclose

### **TEACHING POINTS**

1. Understand the role of FDG & amyloid PET/CT in investigating cognitive impairment (CI). In particular, distinguishing between the causes of dementia. 2. Indications for amyloid PET/CT; when it should be performed over FDG brain imaging. 3. Describe the mechanism of action of FDG & amyloid tracers in the investigation of CI & review the differences in patient preparation & image acquisition. 4. Assess the imaging characteristics of positive or negative amyloid PET/CT in Alzheimer's disease (AD). 5. Review characteristic patterns of altered metabolism seen on FDG PET for specific types of dementia, namely fronto-temporal dementia (FTD), AD & dementia with Lewy bodies (DLB). 6. Review pitfalls in image interpretation.

## **TABLE OF CONTENTS/OUTLINE**

• Overview of the causes of CI & importance of accurate diagnosis & characterization • Indications for amyloid & FDG PET/CT; imaging algorithm for investigating CI • Amyloid and FDG PET/CT - Mechanism of action - Patient preparation & imaging protocol • Imaging characteristics of amyloid PET/CT in AD - examples of typical features; subtypes of positive & negative examinations • Characteristic patterns of altered metabolism on FDG PET/CT - examples of FTD, AD & LBD • Pitfalls in image interpretation examples of atrophy & motion artefact \*\*Please note, this exhibit is no longer a CME presentation.\*\* Prostate Specific Membrane Antigen (PSMA) PET/CT Imaging Improves Staging Accuracy and Management in Prostate Cancer Patients at Time of Initial Diagnosis or Biochemical Failure

Thursday, Dec. 1 12:15PM - 12:45PM Room: S503AB Station #7

# Participants

Tima Davidson, MD, Ramat Gan, Israel (*Presenter*) Nothing to Disclose Uri Amit, ramat gan, Israel (*Abstract Co-Author*) Nothing to Disclose Akram Saad, Ramatgan, Israel (*Abstract Co-Author*) Nothing to Disclose Jeffrey Goldstein, Ramat Gan, Israel (*Abstract Co-Author*) Nothing to Disclose Maia Hahiashvili, Ramat Gan, Israel (*Abstract Co-Author*) Nothing to Disclose Elinor Goshen, MD, Ramat Gan, Israel (*Abstract Co-Author*) Nothing to Disclose Yakov Oksman, Ramat Gan, Israel (*Abstract Co-Author*) Nothing to Disclose Raanan Berger, MD, PhD, Ramat Gan, Israel (*Abstract Co-Author*) Nothing to Disclose Bar Chikman, Zrifin, Israel (*Abstract Co-Author*) Nothing to Disclose Zvi Symon, MD, Tel Hashomer, Israel (*Abstract Co-Author*) Nothing to Disclose Simona Ben-Haim, MD, DSc, Ramat Gan, Israel (*Abstract Co-Author*) Nothing to Disclose Simona Sense, Stockholder, Molecular Dynamics

## PURPOSE

68Gallium- Prostatic Specific Membrane Antigen (PSMA) PET/CT has been recently introduced for the assessment of patients with prostate cancer and few studies have reported its value in disease management. We report our initial experience with PSMA PET/CT imaging.

### **METHOD AND MATERIALS**

Ninety patients, mean age 70.5 years (range 50-90), were referred for PSMA PET/CT for staging (n=11), biochemical failure (n=53) or evaluation of known metastatic disease (n=26). Mean Gleason score: 7.6 (range 6-10) and mean PSA: 10.3ng/ml (range 0.04-129). The initial pre-scan therapy plan and revised post-scan recommendations were documented according to National Comprehensive Cancer Network (NCCN) guidelines.

#### RESULTS

PSMA-PET/CT was positive in 68/90 pts. (75.5%); SUV max 10.7+8.8. Local recurrence was observed in the prostate or prostate fossa in 21 pts and 5 pts respectively (28.9%); lymph nodes (n=34, 37.8%), or distant metastasis (n= 35, 38.9%). PSMA PET/CT changed clinical management at time of initial staging in 7/11 (63.6 %) patients, at time of biochemical failure in 36/53 (67.9 %) patients and in only 2/25 (8 %) of patients with known metastatic disease. Changes in management included: Androgen Deprivation Therapy (ADT) to local therapy (n=21), ADT to observation (n=11), local therapy to ADT (n=7), local therapy to observation (n=1), observation to ADT (n=1), and change in radiation therapy plan (n=11).

# CONCLUSION

PSMA PET/CT had an impact on clinical management in 66% of prostate cancer patients referred for staging or initial biochemical failure but had little benefit when used for management of known metastatic disease.

# **CLINICAL RELEVANCE/APPLICATION**

PSMA-PET-CT may be useful in initial staging and treatment planning for patients with intermediate and high risk prostate cancer.

The Calue of Adding Delayed Scans of the Abdomen and Pelvis in the Screening FDG-PET/CT: A Retrospective Cohort Study on Total of 17395 Examinees

Thursday, Dec. 1 12:15PM - 12:45PM Room: S503AB Station #8

#### Awards

### **Student Travel Stipend Award**

#### Participants

Shotaro Naganawa, MD, Tokyo, Japan (*Presenter*) Nothing to Disclose Takeharu Yoshikawa, MD, Bunkyo-ku, Japan (*Abstract Co-Author*) Nothing to Disclose Eriko Maeda, MD, Tokyo, Japan (*Abstract Co-Author*) Nothing to Disclose Koichiro Yasaka, MD, Tokyo, Japan (*Abstract Co-Author*) Nothing to Disclose Naoto Hayashi, MD, Bunkyo-ku, Japan (*Abstract Co-Author*) Nothing to Disclose

### PURPOSE

To investigate how the results of screening were improved by adding delayed scan in FDG-PET/CT.

### **METHOD AND MATERIALS**

Total of 17395 results of screening (average age 58.3 y, range 40-92 y) were reviewed. Whole-body early PET/CT scan were performed, and tentative result was made by two radiologists. Then delayed PET/CT scan was performed after 2 hours, and reevaluated for any necessary changes. All changed records of the results were reviewed, and classified into false positive in the early PET/CT and newly detected findings in the delayed PET/CT, including benign and suspected malignancy. As for the malignancy suspected findings, pathologies were further reviewed.

### RESULTS

In the delayed PET/CT scan 273 records were changed, 38 were changed to false positive, 235 were newly detected lesion. Of the newly detected lesions, 94 were probable benign lesions, 141 were suspected malignancy. Of the suspected malignancy, 10 were actually pathologically malignant (Colorectal cancer: 7, Prostate cancer: 2, Pancreas cancer: 1), 95 were false positive and remaining 36 were not followed up.

### CONCLUSION

With adding delayed PET/CT scan in screening, pathologically malignant lesions could be newly detected, but are rarely found.

# **CLINICAL RELEVANCE/APPLICATION**

Low cancer detection rate in delayed PET/CT scan should be weighed against the extra dose exposure.

Can We Explain the Etiology of Negative Technetium-99m Sestamibi Scans in Patients with the Clinical Diagnosis of Primary Hyperparathyroidism?

Thursday, Dec. 1 12:15PM - 12:45PM Room: S503AB Station #9

# Participants

Amany Aziz, MBBCh, Maywood, IL (*Presenter*) Nothing to Disclose Beverly Gonzalez, PhD, Maywood, IL (*Abstract Co-Author*) Nothing to Disclose Steve James, Maywood, IL (*Abstract Co-Author*) Nothing to Disclose Steven A. De Jong, Maywood, IL (*Abstract Co-Author*) Nothing to Disclose Robert H. Wagner, MD, Maywood, IL (*Abstract Co-Author*) Nothing to Disclose Medhat S. Gabriel, MD, Maywood, IL (*Abstract Co-Author*) Nothing to Disclose Davide Bova, MD, Maywood, IL (*Abstract Co-Author*) Nothing to Disclose Bital Savir-Baruch, MD, Maywood, IL (*Abstract Co-Author*) Nothing to Disclose

#### PURPOSE

Patients with primary hyperparathyroidism (PHPT) are diagnosed clinically by overproduction of PTH. Approximately 80% are single adenomas, 10% hyperplasia, 10% multiple adenomas, and, rarely, parathyroid carcinoma. Histologically, adenomas and hyperplasia may demonstrate similar hypercellular appearance. Application of an intraoperative PTH (IOPTH) level algorithm of >50% decrease and normalized PTH level <65 pg/mL increases cure rate. Preoperative parathyroid adenoma localization using technetium-99m Sestamibi scans (MIBI) is essential to minimize operative time. At our institution we often see patients with a long term clinical diagnosis of PHPT, yet the MIBI scan is negative. Our objective was to retrospectively investigate the etiology of our negative MIBI scans.

### **METHOD AND MATERIALS**

101 patients with a clinical diagnosis of PHPT who underwent a MIBI scan with subsequent parathyroid surgery were included. The results of the MIBI scans was correlated with levels of PTH, vitamin D, calcium, BMI, preoperative and IOPTH levels, number of glands resected, and trend of IOPTH decrease.

#### RESULTS

99/101 patients had  $\geq 1$  gland resected; 13/99 patients had adenoma, 74/99 hypercellular, 9/99 cellular, 2/99 normal, and 1/99 carcinoma. 90/101 patients also had thyroid US. No patient with a negative MIBI had a positive US (38/90). Among 63/90 positive MIBI scans, only 43 had positive US. No optimal PTH level was found to correlate with scan performance. Negative MIBI scans were associated with resection of a higher number of glands to achieve a normal level of IOPTH with mean (±SD) of 2.34 glands (±1.02) compared with 1.81 (±1.04) for positive scans, p=0.01. Trends of IOPTH decrease for the number of glands removed was significant when 3 glands were excised and the scan was negative, p=0.02. No correlations between the MIBI results and levels of calcium, vitamin D, or BMI were found, p>0.05.

# CONCLUSION

Patients with the clinical diagnosis of PHPT who demonstrate a negative MIBI scan will likely undergo resection of two or more parathyroid glands to achieve normal levels of PTH. This may be partly explained by lack of preoperative localization or underlying hypercellular etiology.

# **CLINICAL RELEVANCE/APPLICATION**

We suspect that the clinical identification of adenoma may be overestimated and hyperplasia underestimated. The findings on the MIBI scan may help predict the length of surgery and the pathological results.

Integrated FDG-PET/CT vs Conventional Radiological Examination: Utility for Evaluation of TNM Stage and Limited vs Extensive Stage Systems in Patients with Small Cell Lung Cancer

Thursday, Dec. 1 12:15PM - 12:45PM Room: S503AB Station #10

# Participants

Yuji Kishida, MD, Kobe, Japan (*Presenter*) Nothing to Disclose Yoshiharu Ohno, MD, PhD, Kobe, Japan (*Abstract Co-Author*) Research Grant, Toshiba Corporation; Research Grant, Koninklijke Philips NV; Research Grant, Bayer AG; Research Grant, DAIICHI SANKYO Group; Research Grant, Eisai Co, Ltd; Research Grant, Fuji Pharma Co, Ltd; Research Grant, FUJIFILM RI Pharma Co, Ltd; Research Grant, Guerbet SA; Shinichiro Seki, Kobe, Japan (*Abstract Co-Author*) Nothing to Disclose Takeshi Yoshikawa, MD, Kobe, Japan (*Abstract Co-Author*) Research Grant, Toshiba Corporation Ho Yun Lee, MD, Seoul, Korea, Republic Of (*Abstract Co-Author*) Nothing to Disclose Mark O. Wielpuetz, Heidelberg, Germany (*Abstract Co-Author*) Speakers Bureau, Berlin-Chemie AG; Research Consultant, Boehringer Ingelheim Erina Suehiro, RT, Kobe, Japan (*Abstract Co-Author*) Nothing to Disclose Wakiko Tani, RT, Kobe, Japan (*Abstract Co-Author*) Nothing to Disclose Katsusuke Kyotani, RT, Kobe, Japan (*Abstract Co-Author*) Nothing to Disclose Katsusuke Kyotani, RT, Kobe, Japan (*Abstract Co-Author*) Nothing to Disclose Katsusuke Kyotani, RT, Kobe, Japan (*Abstract Co-Author*) Nothing to Disclose Katsusuke Kyotani, RT, Kobe, Japan (*Abstract Co-Author*) Nothing to Disclose Katsusuke Kyotani, RT, Kobe, Japan (*Abstract Co-Author*) Nothing to Disclose Katsusuke Kyotani, RT, Kobe, Japan (*Abstract Co-Author*) Nothing to Disclose Kazuro Sugimura, MD, PhD, Kobe, Japan (*Abstract Co-Author*) Nothing to Disclose Kazuro Sugimura, MD, PhD, Kobe, Japan (*Abstract Co-Author*) Nothing to Disclose Kazuro Sugimura, MD, PhD, Kobe, Japan (*Abstract Co-Author*) Nothing to Disclose Kazuro Sugimura, MD, PhD, Kobe, Japan (*Abstract Co-Author*) Research Grant, Toshiba Corporation Research Grant, Koninklijke Philips NV Research Grant, Bayer AG Research Grant, Eisai Co, Ltd Research Grant, DAIICHI SANKYO Group

#### PURPOSE

To directly compare the capability for evaluation of TNM and limited vs. extensive stage systems between integrated FDG-PET/CT with contrast-enhanced (CE-) brain MRI and conventional radiological examination in patients with small cell carcinoma (SCLC).

### **METHOD AND MATERIALS**

Fifty consecutive pathologically diagnosed SCLC patients (44 men, 6 women; mean age 69 years) underwent integrated PET/CT, conventional radiological examinations including CE-brain MRI, whole-body CE-CT and bone scintigraphy, and follow-up examination. According to results of all radiological examinations as well as medical records, each patient was evaluated by two stage systems. To determine the capability of each method for assessing these two stage systems in all patients, all PET/CT data were independently evaluated by two radiologist who had more than 10 year experiences as board certified PET physicians. In addition, all conventional examination data were evaluated by other two radiologists. Then, final evaluation results on each method were made by consensus of two readers. Interobserver agreements of all assessments on both methods were assessed by kappa statistics followed by  $\chi^2$  test. Agreements of each factor and clinical stage in both stage systems between each method and final diagnosis were also evaluated by kappa statistics followed by  $\chi^2$  test. Finally, diagnostic accuracies were statistically compared between both methods by McNemar's test.

#### RESULTS

Inter-observer agreements of all assessments were determined as significantly substantial or almost perfect on PET/CT (0.80

#### CONCLUSION

FDG-PET/CT has better potential than conventional radiological examination for evaluation of TNM stage and limited vs. extensive stage systems in patients with SCLC.

### **CLINICAL RELEVANCE/APPLICATION**

FDG-PET/CT has better potential than conventional radiological examination for evaluation of TNM stage and limited vs. extensive stage systems in patients with SCLC.

# Case Series: 3D Image Analysis in Traumatic Brain Injury

Thursday, Dec. 1 12:15PM - 12:45PM Room: NR Community, Learning Center Station #1

#### **Participants**

Lisa H. Merck, MD, MPH, Providence, RI (*Abstract Co-Author*) Nothing to Disclose David Wright, MD, Atlanta, GA (*Abstract Co-Author*) Nothing to Disclose Owen Leary, Providence, RI (*Presenter*) Nothing to Disclose Michael Lunney, MPH, Atlanta, GA (*Abstract Co-Author*) Nothing to Disclose Scott Collins, RT, Providence, RI (*Abstract Co-Author*) Nothing to Disclose Jason W. Allen, MD, PhD, Atlanta, GA (*Abstract Co-Author*) Nothing to Disclose Sharon Yeatts, PhD, Charleston, NC (*Abstract Co-Author*) Consultant, F. Hoffmann-La Roche Ltd Derek Merck, PhD, Providence, RI (*Abstract Co-Author*) Nothing to Disclose

# PURPOSE

This case series compares imaging results from 3DA to results compiled via the standard ABC/2 method.

# **METHOD AND MATERIALS**

A convenience sample of 31 scans from the ProTECTIII multicenter clinical trial were retrospectively reviewed for analysis. 3DA of the largest intracranial hyperdense lesion was completed by a trained research assistant for each CT on an iMAC desktop. DICOM data were first resampled to a 1.5 mm slice thickness and symmetrized using Aquarius (TeraRecon inc, 2012). Then, regions of interest were traced via 3D Slicer v4.5 (2015) and compiled into a single volumetric region of interest. ABC/2 calculations were independently completed for each CT by the ProTECTIII trial's central neuroradiologist on a Macintosh workstation, using the volume of the largest intracranial hyperdense lesion. The agreement between these two approaches was assessed via Altman-Bland. This study was IRB approved.

## RESULTS

The differences (ABC/2 subtracted from 3D segmentation) are predominantly negative, indicating that the volume calculated via 3DA is smaller than that calculated by ABC/2. After log transformation, there is not a significant association between the measurement difference and the size of the measurement (Pearson correlation coefficient 0.04, pvalue 0.81), indicating that 3DA consistently yielded lower measured volumes of traumatic hemorrhage when compared to the ABC/2 method, across both large and small brain lesions. The estimated relative bias between the two measurements (on the log scale) is -0.51 (SD 0.74; pvalue 0.0006; 95% CI -0.78, -0.24).

# CONCLUSION

There is sufficient evidence to conclude that a systematic difference exists in the results from these two techniques. 3DA consistently yielded lower volumes of measured traumatic lesion when compared to the ABC/2 method. Ongoing study of the total trial dataset (n=3,078) will quantify change in bleed over time per patient using these methodologies. 3DA may offer more precise calculations of traumatic hemorrhage, these data are significant to patient treatment and prognosis.

# **CLINICAL RELEVANCE/APPLICATION**

Traumatic brain injury (TBI) is a major cause of death and disability in the U.S. Time to treatment is often directly related to patient outcome. New techniques in semi-automated 3D illustration (3DA) may be used to rapidly quantify intracranial pathology on computed tomography (CT).

Flow Sensitive Black Blood (FSBB) Imaging is More Sensitive than Gradient-Recalled Echo (GRE) T2\* MRI for the Detection of Microbleeds in Diffuse Axonal Injury

Thursday, Dec. 1 12:15PM - 12:45PM Room: NR Community, Learning Center Station #2

#### Awards

#### **Student Travel Stipend Award**

#### **Participants**

Pavel Rodriguez, MD, San Antonio, TX (*Presenter*) Nothing to Disclose Wilson Altmeyer, MD, San Antonio, TX (*Abstract Co-Author*) Nothing to Disclose Maria P. Valencia, MD, San Antonio, TX (*Abstract Co-Author*) Nothing to Disclose Carlos Bazan III, MD, San Antonio, TX (*Abstract Co-Author*) Nothing to Disclose Thomas J. Prihoda, PhD, San Antonio, TX (*Abstract Co-Author*) Nothing to Disclose

#### PURPOSE

Flow sensitive black blood (FSBB) imaging is a form of susceptibility weighted imaging (SWI) that generates slow flowing vessel contrast and T2\* decay using motion probing gradients. We assess the sensitivity of flow sensitive black blood (FSBB) imaging against conventional gradient recalled echo (GRE) T2\* MRI for the detection of intraparenchamal microbleeds (MBs) in diffuse axonal injury (DAI), a form of traumatic brain injury (TBI). The number of MBs was also correlated with DAI grade and clinical outcomes.

# METHOD AND MATERIALS

Retrospective analysis of DAI-TBI (n=10; mean age, 41±3.8) and non-TBI controls (n=12; mean age 48±6.0) in SPSS 22 (IBM). Three neuroradiologists interpreted FSBB and GRE sequences acquired in the same session in each subject. Images were scored for intra-parenchymal microbleeds (1-10mm) using a modified microbleed anatomical rating scale (MARS), and raters were blinded to the clinical information. The sequences were separately scored at least 2 weeks apart in each subject. Pearson correlation was performed between the Glasgow Comma Scale (GCS) score change (discharge - admission) and number of MBs. Three deceased subjects (GCS 3 at admission) were classified as no change. The non-TBI controls helped to test whether the visualization of veins and iron containing structures in the FSBB could result in false positive microbleeds. All subjects were scanned in the same Toshiba 3T MRI scanner, and analyzed using same slice thickness, slice spacing, and similar field of view and matrix size.

# RESULTS

The raters identified 1362 total MBs on FSBB and 929 MBs on GRE (p < 0.001) in the DAI-TBI subjects. The intraclass correlation for the total number of microbleeds in DAI ranged from 0.686 to 0.864 in FSBB, and 0.711 to 0.831 in GRE. There was also a 186-405% increase in the number of brainstem MBs detected in FSBB. There was a negative correlation between change in GCS score and number of MBs in the brainstem (r = -0.58, p = 0.03) for FSBB vs. GRE (r = -0.14, p >> 0.05). There was no difference in the detection of MBs in the non-TBI controls (p >> 0.05).

# CONCLUSION

FSBB is a reliable SWI-type sequence that is more sensitive than GRE in the detection of microbleeds in DAI. The improved detection of microbleeds by FSBB in the brainstem (i.e. high grade DAI) significantly correlated with negative clinical outcomes.

# **CLINICAL RELEVANCE/APPLICATION**

FSBB can improve the grading of DAI severity which helps predict patient otucomes.

Cerebral Computed Tomography Angiography (CCTA) in a 160mm Coverage Axial Scan Mode Using a Low Tube Voltage (70-kVp) Protocol: Objective and Subjective Comparisons with the 120-kVp CCTA

Thursday, Dec. 1 12:15PM - 12:45PM Room: NR Community, Learning Center Station #4

# Participants

Yun-Pei Lin, Kaohsiung City, Taiwan (*Presenter*) Nothing to Disclose Yu Yen, Kaohsiung City, Taiwan (*Abstract Co-Author*) Nothing to Disclose Ping-Hong Lai, Kaohsiung, Taiwan (*Abstract Co-Author*) Nothing to Disclose Tien-Hui Hsieh, Kaohsiung City, Taiwan (*Abstract Co-Author*) Nothing to Disclose Tseng-Jui Hsu, Kaohsiung City, Taiwan (*Abstract Co-Author*) Nothing to Disclose Ying Guo, Guangzhou, China (*Abstract Co-Author*) Nothing to Disclose

# PURPOSE

To assess the image quality by using a 70-kVp protocol in a 160mm axial scan mode in comparison with a 120-kVp protocol for the CCTA, and to investigate a probable reduction in the volume of contrast medium (CM) in the 70-kVp protocol.

# METHOD AND MATERIALS

Forty-one volunteers were enrolled in this prospective study and randomly assigned to one of the three groups: group A: 120 kVp, 170 mAs, and 60 mL of CM; group D: 70 kVp, 350 mAs, and 60 mL of CM; group C: 70 kVp, 350 mAs, and 45 mL of CM. All of these three groups were scanned in a 160mm axial scan mode in a 256-slice CT machine (Revolution, GE Healthcare) with the slice thickness of 0.625 mm, and the radiation dose was controlled as close as to each other (13.22 to 13.42 mGy of volume CT dose index [CTDIvol]. Objective image quality (Hounsfield units, signal-to-noise ratio [SNR], and contrast-to-noise ratio [CNR] of cerebral arteries) and subjective image quality were compared in these three groups. The objective and subjective data was analyzed by Mann-Whitney U tests. Two experienced neuroradiologists independently evaluated the subjective image quality, and inter-observer reliability was calculated by kappa (k) analysis. For all statistical analyses, P value < 0.05 was considered significant.

# RESULTS

In objective image quality, both of group B and C had significantly higher arterial attenuation, SNR, and CNR than group A (all P<0.001). The image quality of group B and C were significantly better than group A in terms of subjective evaluation (all P<0.05). The arterial attenuation, SNR, and CNR between group B and C did not reach statistical significance, and there was no significant difference between group B and group C with respect to subjective image quality. The inter-observer reliability was substantial (k=0.721).

#### CONCLUSION

The arterial enhancement, SNR, and CNR can be improved by using 70-kVp protocol, and better subjective image quality can be provided. Moreover, the lesser amount of CM could be used in the 70-kVp protocol without interference of imaging quality.

# **CLINICAL RELEVANCE/APPLICATION**

Using 70 kVp for CCTA in a 256-slice CT can provide better image quality compared with a 120-kVp protocol, and can afford to lower CM usage with preservation of overall image quality.

# Endometriosis: Helping the Surgeon through MRI

Thursday, Dec. 1 12:15PM - 12:45PM Room: OB Community, Learning Center Hardcopy Backboard

#### **Participants**

Daniela B. Grammatico, Buenos Aires, Argentina (*Presenter*) Nothing to Disclose Lorena Coto Solari, MD, Caba, Argentina (*Abstract Co-Author*) Nothing to Disclose Evelina V. Hernandez, Buenos Aires, Argentina (*Abstract Co-Author*) Nothing to Disclose Maria Gavina, Buenos Aires, Argentina (*Abstract Co-Author*) Nothing to Disclose Maria L. Rico, MD, Tigre, Argentina (*Abstract Co-Author*) Nothing to Disclose Juan C. Mazzucco, MD, Buenos Aires, Argentina (*Abstract Co-Author*) Nothing to Disclose

# TEACHING POINTS

To describe the MRI findings of endometriosis and the relations with adjacent organs required by the surgeon for surgical planningTo explain the utility of high-resolution MRI in the diagnosis of this pathologyTo correlate with a graphic summary the MRI images with the intraoperative findingsobtained in the surgical procedure

# **TABLE OF CONTENTS/OUTLINE**

Describe the pathology Types of affection:ovarian, peritoneal and deep endometriosis Frequent findings: Endometriomas Deep endometriosis: gastrointestinal organs involved, urinary organs involved Review of MRI imaging findings Details lesions in order to perform an adequate surgical strategy Correlation of MRI images with findings during surgery Intraoperative images Conclusion

Saline Infused Sonohysterography-Technique and Spectrum of Disease

Thursday, Dec. 1 12:15PM - 12:45PM Room: OB Community, Learning Center Station #1

#### Awards Certificate of Merit

#### **Participants**

B. Dustin Pooler, MD, Madison, WI (*Abstract Co-Author*) Nothing to Disclose Lori Mankowski Gettle, MD, Hummelstown, PA (*Abstract Co-Author*) Nothing to Disclose Jessica B. Robbins, MD, Madison, WI (*Abstract Co-Author*) Nothing to Disclose Vincenzo K. Wong, Houston, TX (*Presenter*) Nothing to Disclose

#### **TEACHING POINTS**

Review technique for performing saline infused sonohysterography Review normal anatomy on saline infused sonohysterography Identify common pathology encountered with saline infused sonohysterography Discuss pitfalls of saline infused sonohysterography

# TABLE OF CONTENTS/OUTLINE

Saline infused sonohysterography technique Normal saline infused sonohysterography anatomy Pathology encountered with saline infused hysterosonography Endometrial hyperplasia Intrauterine adhesions Tamoxifen changes Endometrial carcinoma Endometrial polyp Submucosal leiomyoma Retained products of conception Pitfalls of saline infused sonohysterography

# Utility of Contrast Enhanced Ultrasound for Assessment of Pediatric Focal Liver Lesions

Thursday, Dec. 1 12:15PM - 12:45PM Room: PD Community, Learning Center Station #7

**FDA** Discussions may include off-label uses.

Awards Certificate of Merit Identified for RadioGraphics

#### **Participants**

Sudha A. Anupindi, MD, Philadelphia, PA (*Presenter*) Nothing to Disclose Susan J. Back, MD, Penn Valley, PA (*Abstract Co-Author*) Nothing to Disclose Aikaterini Ntoulia, MD, PhD, Philadelphia, PA (*Abstract Co-Author*) Nothing to Disclose Laura Poznick, BA, Philadelphia, PA (*Abstract Co-Author*) Nothing to Disclose Trudy Morgan, BA, Philadelphia, PA (*Abstract Co-Author*) Nothing to Disclose David M. Biko, MD, Philadelphia, PA (*Abstract Co-Author*) Nothing to Disclose Kassa Darge, MD, PhD, Philadelphia, PA (*Abstract Co-Author*) Nothing to Disclose

#### **TEACHING POINTS**

Focal liver lesions are discovered incidentally while imaging children or during directed abdominal imaging for pain, abnormal liver function, trauma and tumor surveillance. Traditionally children are assessed using ultrasound which is complemented by contrast enhanced MRI. More recently there is impetus to perform contrast enhanced US (CEUS), particularly as these microbubble agents are now available in the United States and recently FDA approved for use in assessing liver lesions in children (Lumason®- a second generation US contrast). CEUS allows assessment of organ and lesion perfusion and can equate MRI and CT in detection and characterization of these lesions, obviating the need for invasive procedures. CEUS has the added benefits of no radiation or sedation, safe and easy to use, and decreased time to diagnosis.Purpose of this exhibit:Familiarize radiologists with the technique of CEUS for assessing focal liver lesionsDescribe the practical points and advantages of using CEUS as a problem solving imaging modality.Illustrate examples from CEUS applications for the liver.

# TABLE OF CONTENTS/OUTLINE

1. Introduction to CEUS 2. Technique 3. Review of applications of CEUS for the liver4. Summary5. Illustration of various cases

# **Honored Educators**

Presenters or authors on this event have been recognized as RSNA Honored Educators for participating in multiple qualifying educational activities. Honored Educators are invested in furthering the profession of radiology by delivering high-quality educational content in their field of study. Learn how you can become an honored educator by visiting the website at: https://www.rsna.org/Honored-Educator-Award/

Kassa Darge, MD, PhD - 2016 Honored Educator

Pearls and Pitfalls in Diagnosing Pediatric Urinary Bladder Masses

Thursday, Dec. 1 12:15PM - 12:45PM Room: PD Community, Learning Center Station #8

#### Awards

# **Identified for RadioGraphics**

#### **Participants**

Susan C. Shelmerdine, MBBS, FRCR, Toronto, ON (*Presenter*) Nothing to Disclose Armando Lorenzo, Toronto, ON (*Abstract Co-Author*) Nothing to Disclose Abha Gupta, Toronto, ON (*Abstract Co-Author*) Nothing to Disclose Govind B. Chavhan, MD, Toronto, ON (*Abstract Co-Author*) Nothing to Disclose

#### **TEACHING POINTS**

1. Review the differential diagnoses of pediatric urinary bladder masses via a multimodality approach using examples from ultrasound, MRI, CT and fluoroscopy. 2. Presentation and discussion of pathological correlations of common bladder masses.

# **TABLE OF CONTENTS/OUTLINE**

Examples of patients presenting to our institution with a variety of bladder pathologies will be demonstrated in a pictorial review format. The cases will include pathological correlation where available and diagnoses will include, but not limited to rhabdomyosarcoma, inflammatory myofibroblastic tumor, paraganglioma, papillary urothelial neoplasm of low malignant potential (PUNLMP) and eosinophilic cystitis. This will be followed by a review of our ultrasound and MRI imaging protocols for investigation of bladder lesions. We will also include examples of pitfalls in diagnoses including examples of misinterpretation of bladder debris as a mass, adnexal lesions and uterine impressions appearing as lesions on the bladder wall. Familiarity with the differential diagnoses can help prevent potential pitfalls in diagnosis and improve confidence in suggestion of follow-up techniques. Congenital deformities of the urogenital system will not be covered.

# PD241-SD-THA2

Wrist MRI in Children: Effect on Clinical Diagnosis and Management

Thursday, Dec. 1 12:15PM - 12:45PM Room: PD Community, Learning Center Station #2

#### **Participants**

Kevin W. Taylor, MD, Hershey, PA (*Presenter*) Nothing to Disclose Michael M. Moore, MD, Hershey, PA (*Abstract Co-Author*) Nothing to Disclose James M. Brian, MD, Hummelstown, PA (*Abstract Co-Author*) Nothing to Disclose Sosamma T. Methratta, MD, Hummelstown, PA (*Abstract Co-Author*) Nothing to Disclose Stephanie A. Bernard, MD, Hershey, PA (*Abstract Co-Author*) Nothing to Disclose

#### PURPOSE

The clinical utility of wrist MRI has been extensively validated in adults as well as specific pediatric rheumatologic diseases. However, corresponding comprehensive evaluation in children remains lacking. With significantly increased emphasis on cost reduction and value added by imaging, determining the impact of wrist MRI in children on diagnosis and management is necessary.

#### **METHOD AND MATERIALS**

In an IRB approved retrospective study, patients over a four year period were evaluated. Radiological reports and clinic notes were reviewed prior to and after the MRI. Patient demographics, MRI diagnoses, and effect on clinical diagnoses and management were determined. These patients were divided into 4 groups: 1) change in both diagnosis and management, 2) change in diagnosis only, 3) change in management only and 4) no change in diagnosis or management. Statistical analysis of 95% confidence intervals was performed.

### RESULTS

101 patients (69 female) with a mean age of 13.4 years (range 1-17) were included. A total of 176 separate MRI diagnoses were obtained. Ganglion cyst was the most commonly reported diagnosis in 22 cases, followed by contusion in 19 cases and fracture in 10 cases. Post-traumatic tenosynovitis, TFCC tear and scapholunate ligament tear were each diagnosed in 7 cases. Nineteen reports were normal. MRI changed both diagnosis and management in 41% (CI: 31-51%), diagnosis only in 5% (CI: 2-12%), management only in 46% (CI: 36-56%) and no change in either in 9% (CI: 4-17%). Overall, wrist MRI changed the management in 86% of cases (CI: 77-92%) and changed the diagnosis in 46% of cases (CI: 36-56%).

## CONCLUSION

MRI of the wrist in children changes the clinical diagnosis in a substantial proportion and alters management in the vast majority of cases. MRI of the wrist in the pediatric patient is a study of excellent clinical utility.

# **CLINICAL RELEVANCE/APPLICATION**

MRI of the wrist in children changes the clinical diagnosis in a substantial proportion and alters management in the vast majority of cases. MRI of the wrist in the pediatric patient is a study of excellent clinical utility.

Assessment of Pediatric Musculoskeletal Tumors and Treatment Response on Diffusion Weighted MRI

Thursday, Dec. 1 12:15PM - 12:45PM Room: PD Community, Learning Center Station #3

#### Awards

#### **Student Travel Stipend Award**

#### **Participants**

Chul Y. Chung, MD, Pittsburgh, PA (*Presenter*) Nothing to Disclose Andrew J. Degnan, MD, MPhil, Pittsburgh, PA (*Abstract Co-Author*) Nothing to Disclose Amisha J. Shah, MD, Pittsburgh, PA (*Abstract Co-Author*) Nothing to Disclose

# PURPOSE

Assessment of malignant bone and soft tissue tumors treatment response to chemotherapy is vital prior to planning surgical resection to ensure adequate reduction in tumor extent. The objective of this study is to evaluate whether apparent diffusion coefficient (ADC) measurements derived from diffusion-weighted imaging provide information regarding tumor response to chemotherapy.

# **METHOD AND MATERIALS**

Eleven cases of bone and soft tissue sarcomas with magnetic resonance (MR) imaging including diffusion-weighted images (DWI) were retrospectively reviewed following IRB approval. Six cases (three osteosarcomas and three Ewing sarcomas) were performed prior to initiation of chemotherapy, and five cases (two osteosarcomas, two Ewing sarcomas and one chondrosarcoma) were performed following chemotherapy. Minimum, average, and maximum values of ADC of each tumor were obtained and compared between the pre-treatment and post-chemotherapy groups using the nonparametric Mann Whitney U test.

# RESULTS

Treated sarcomas demonstrated significantly greater average, minimum and maximum ADC values compared to untreated tumors (ADC average: 2.16 vs.  $1.2 \times 10-3$  mm2/s, p = 0.004; minimum 1.27 vs.  $0.47 \times 10-3$  mm2/s, p = 0.030; maximum 3.14 vs. 2.23  $\times 10-3$  mm2/s, p = 0.004). No significant gender, age, or volume differences between the groups were observed.

# CONCLUSION

Sarcomas treated with chemotherapy demonstrated greater minimum, average, and maximum ADC values, implying increased cellular diffusivity after therapy presumably due to tumor necrosis compared with greater cellularity of untreated sarcomas with lower ADC values. ADC values may be useful for evaluating chemotherapeutic response of malignant sarcomas.

# **CLINICAL RELEVANCE/APPLICATION**

ADC measurements of malignant sarcomas obtained using diffusion-weighted imaging showed significantly increased values following chemotherapy and may be useful for assessing treatment response.

# PD244-SD-THA5

Relationship between Tube Voltage at Scout View Scanning and Automatic Tube Current Modulation during Helical Scanning: A Phantom Study

Thursday, Dec. 1 12:15PM - 12:45PM Room: PD Community, Learning Center Station #5

# Participants

Takanori Masuda, Hiroshima, Japan (*Presenter*) Nothing to Disclose Yoshinori Funama, PhD, Kumamoto, Japan (*Abstract Co-Author*) Nothing to Disclose Masao Kiguchi, RT, Hiroshima, Japan (*Abstract Co-Author*) Nothing to Disclose Naoyuki Imada, Hiroshima, Japan (*Abstract Co-Author*) Nothing to Disclose Takayuki Oku, Hiroshima, Japan (*Abstract Co-Author*) Nothing to Disclose Kazuo Awai, MD, Hiroshima, Japan (*Abstract Co-Author*) Nothing to Disclose Kazuo Awai, MD, Hiroshima, Japan (*Abstract Co-Author*) Research Grant, Toshiba Corporation; Research Grant, Hitachi, Ltd; Research Grant, Bayer AG; Research Grant, Eisai Co, Ltd; Medical Advisor, General Electric Company; ; ; ; Tomoyasu Satou, Hiroshima, Japan (*Abstract Co-Author*) Nothing to Disclose Yoriaki Matsumoto, HIROSHIMA, Japan (*Abstract Co-Author*) Nothing to Disclose

## PURPOSE

Currently the most common dose reduction techniques at CT are automatic tube current modulation (ATCM) and low tube voltage techniques. In general, the same tube voltage is used during scout view- and helical scanning. Optimal ATCM may not be achieved when the tube voltage differs during helical- and scout view scanning. The purpose of this study was to investigate the relationship between the tube voltage at scout view- and the ATCM during helical scanning.

# **METHOD AND MATERIALS**

We performed helical scans of a phantom representing new born and 5-year-old anthropomorphic phantoms (ATOM phantom e) using a 64-detector CT scanner (VCT, GE; rotation time 0.4 s, helical pitch 1.375). The tube voltage at scout view scanning was 120 kV; during helical scanning it was 80-, 100-, 120-, and 140 kV. The tube current during helical scanning was set based on a preset noise index (NI) of 12. We performed each scan 5 times. We measured the image noise (standard deviation [SD] of the CT number) in the phantoms and analyzed the relationship between the preset NI and the image noise on helical scans acquired with 4 tube voltages.

#### RESULTS

The mean image noise of the 5-year-old phantom was  $13.7\pm2.4$  (SD),  $12.9\pm2.1$ , and  $12.3\pm1.6$  at 80-, 100-, and 120 kVp, respectively. For the new born phantom it was  $9.9\pm0.9$ ,  $9.1\pm0.8$ , and  $8.7\pm0.8$ , respectively. The SD value at 80 kVp was significantly lower at 80- than that at 120 kVp (p<0.01).

# CONCLUSION

The use of different tube voltages during scout view- and helical scanning resulted in suboptimal low tube voltage protocols. Difference of SD value is larger at 80kVp of the 5-year-old 20-cm phantom than at 80kVp of new born phantom.

#### **CLINICAL RELEVANCE/APPLICATION**

As an optimal SD value may not be obtained when different tube voltages are applied during scout view- and helical scanning, we recommend that the same tube voltage be applied during scout view- and helical scanning.

Impact of CT Topogram kV Choice on Radiation Dose in Pediatric Studies with Automatic Dose Modulation

Thursday, Dec. 1 12:15PM - 12:45PM Room: PD Community, Learning Center Station #6

#### Participants

Kirsten Elleray, Doha, Qatar (*Abstract Co-Author*) Nothing to Disclose Hayley Kourofsky, Doha, Qatar (*Abstract Co-Author*) Nothing to Disclose Jennifer Fenwick, Doha, Qatar (*Abstract Co-Author*) Nothing to Disclose Ioannis Delakis, PhD, MSc, Doha, Qatar (*Presenter*) Nothing to Disclose

# PURPOSE

Automatic exposure control technology (mA/kV modulation) has been widely adopted as a tool of minimizing the radiation dose of CT examinations. This technology has also turned localizer radiographs (topograms) into important tools of determining the dose distribution and image quality of the diagnostic scan series. The purpose of our work was to investigate the impact of topogram kV choice on total dose for pediatric CT examinations with automatic exposure control.

# METHOD AND MATERIALS

CT scans were performed with a Siemens SOMATOM Definition Flash system (Siemens Medical Solutions, Germany) on pediatric and small adult/teenager anthropomorphic whole body phantoms (Kyoto Kaguko, Japan). The kV of the topogram was varied between 70-140kV, keeping mA constant at 35 as per default settings. Topograms were followed by pediatric diagnostic scan series (chest/abdomen) with automatic exposure control (kV and mA) and scanning parameters routinely used in our institution. Imaging was repeated by changing the automatic exposure setting (adaptation strength) of the diagnostic scan series to different levels (very weak/average/very strong modulation).

#### RESULTS

The dose of the diagnostic scan series remained effectively constant for topogram kV values equal to or greater than 100kV. For topogram kV values below 100kV, the dose of the diagnostic scan series increased, indicating that the automatic exposure control was not as efficient. However, the decrease in topogram dose at values lower than 100kV, could counter the dose increase in the diagnostic scan series of the exam, keeping the total examination dose approximately constant. Thus, the dose distribution changed when topogram kV values lower than 100kV were used, resulting in higher effective mA in the diagnostic scan series with a potential benefit to diagnostic image quality. The effect of topogram kV on total dose and dose distribution also showed a dependency on adaptation strength and anatomical area imaged.

### CONCLUSION

Our work demonstrated that the topogram kV choice plays an important role in determining the dose of pediatric CT examinations using automatic exposure control. Further work should be pursued by the CT community and vendors to optimize CT topograms in conjunction with diagnostic exam series.

# **CLINICAL RELEVANCE/APPLICATION**

Low topogram kV values are recommended for pediatric CT examinations using automatic exposure control.

Direct Measurement of Breast Surface Dose during Coronary CT Angiography and Effectiveness of Lower Tube Voltage and Cranial Breast Displacement to Reduce Breast Radiation Exposure

Thursday, Dec. 1 12:15PM - 12:45PM Room: PH Community, Learning Center Station #2

# Participants

Min Kyoung Lee, MD, Incheon, Korea, Republic Of (*Presenter*) Nothing to Disclose Yon Mi Sung, MD, Incheon, Korea, Republic Of (*Abstract Co-Author*) Nothing to Disclose Yoon Kyung Kim, MD, Incheon, Korea, Republic Of (*Abstract Co-Author*) Nothing to Disclose Jeong Ho Kim, MD, Incheon, Korea, Republic Of (*Abstract Co-Author*) Nothing to Disclose Hye-Young Choi, MD, PhD, Incheon, Korea, Republic Of (*Abstract Co-Author*) Nothing to Disclose

# PURPOSE

Special consideration is brought up for women regarding safety issue of radiation exposure to the breasts with coronary CT angiography (CTA). The purpose of this study was to measure the surface radiation dose received by the adult female breast during coronary CTA and to evaluate the effectiveness of lower tube voltage and cranial breast displacement to reduce breast radiation exposure.

# **METHOD AND MATERIALS**

The subjects were 276 women (mean age,  $57.8 \pm 10.2$  years) who underwent coronary CTA between March 2014 and June 2015. Patients were divided into four different protocol groups by tube voltages of 120 or 100 kVp and use of cranial breast displacement; group A with no cranial displacement at 120 kVp (n=69), group B with no cranial displacement at 100 kVp (n=69), group C with cranial displacement at 120 kVp (n=69), group D with cranial displacement at 100 kVp (n=69). Direct measurement of breast surface dose was done on each breast quadrant in all patients with optically-stimulated luminescence dosimeters. The degree of breast displacement was evaluated by volume assessment of fibroglandular tissue in both breasts on reconstructed full field-of-view images.

# RESULTS

The breast surface dose was significantly lower in groups B and D (p<0.001; group A, 35.9 ± 16.6 mGy; group B, 22.1 ± 10.0 mGy; group C, 39.2 ± 17.3 mGy, group D, 23.1 ± 8.3 mGy). The greatest dose reduction was observed in the right upper inner quadrant (43.0%) followed by in the left upper inner quadrant (42.6%). No significant difference in the breast surface dose was seen with same tube voltages but different use of cranial breast displacement (p=0.262, group A vs group C; p=0.523, group B vs group D). The total volume of the fibroglandular tissue of the breasts within the scan range was significantly lower in groups C and D (group A, 56.7 ± 37.6 cm3; group B, 51.7 ± 39.0 cm3; group C, 46.6 ± 57.0 cm3; group D, 38.7 ± 30.5 cm3).

# CONCLUSION

Lower tube voltage was effective to reduce breast surface dose during coronary CTA. Significant reduction of the fibroglandular tissue of the breasts within the scan range of coronary CTA was obtained using cranial breast displacement with no significant change in breast surface dose.

# **CLINICAL RELEVANCE/APPLICATION**

Both lower tube voltage and cranial displacement of the breasts can be applied during coronary CTA that may have the most benefit from this technique to avoid radiation risk in the radiosensitive female breasts.

# Factors of Volume Estimation Uncertainty for Low-contrast Liver Lesions in CT: A Phantom Study

Thursday, Dec. 1 12:15PM - 12:45PM Room: PH Community, Learning Center Station #3

#### **Participants**

Benjamin P. Berman, PhD, Silver Spring, MD (*Presenter*) Nothing to Disclose
Qin Li, Silver Spring, MD (*Abstract Co-Author*) Nothing to Disclose
Yongguang Liang, Royal Oak, MI (*Abstract Co-Author*) Nothing to Disclose
Marios A. Gavrielides, PhD, Silver Spring, MD (*Abstract Co-Author*) Nothing to Disclose
Binsheng Zhao, DSc, New York, NY (*Abstract Co-Author*) License agreement, Varian Medical Systems, Inc; License agreement, Keosys SAS; License agreement, Hinacom Software and Technology, Ltd; License agreement, ImBio, LLC; Research funded, ImBio, LLC; License agreement, AG Mednet, Inc
Nicholas Petrick, PhD, Silver Spring, MD (*Abstract Co-Author*) Nothing to Disclose

# PURPOSE

QIBA guidelines for the use of volumetric CT as an imaging biomarker are based primarily on lung nodule assessment; however, lesion-to-background contrast is far lower in liver CT. In this work, we aim to evaluate the performance of liver lesion volumetry with CT using a range of imaging parameters through a phantom study.

# **METHOD AND MATERIALS**

An anthropomorphic abdominal phantom was designed, featuring two substitutable inserts: one modeling the arterial phase (parenchyma 80 HU), and the other modeling the portal-venous phase (parenchyma 110 HU) of contrast enhancement; each includes 19 lesions of various sizes (6-40 mm), shapes, and lesion-to-parenchyma contrasts (10-65 HU, homogenous or mixed-density). The phantom was scanned by 2 commercial CT scanners with multiple imaging protocols (4 slice thicknesses, 3 doses, 2 reconstruction kernels), resulting in 320 datasets. Volume was estimated for all lesions using a model-based algorithm, which incorporated properties of the imaging systems. Statistical analyses were applied to determine the accuracy and precision of the measurements.

# RESULTS

The lesions  $\leq 10$  mm could not be measured and were excluded from analysis. For the lesions >10 mm, the measurements showed low biases (-2% to 1%) and the variances increased with lower dose. Lesion size, contrast, CT dose, and slice thickness were significant factors based on ANOVA; reconstruction kernel and scanner system were not. Lesions with relatively large size and high contrast (size  $\geq 30$ mm, contrast  $\geq 20$ HU; or 20-30mm,  $\geq 35$  HU) showed good reproducibility (reproducibility coefficients (RDC) 7%, 12%, 16% for CTDIvol of 19.0, 7.6, 3.8 mGy, respectively). For the other lesions, the RDC corresponding to those three doses were 16%, 22% and 45%.

# CONCLUSION

Findings in our study showed that volume estimation for liver lesions was strongly dependent on their size, and contrast, as well as the CT dose. These factors differ from similar analyses of lung nodules, where contrast and dose had less impact.

# **CLINICAL RELEVANCE/APPLICATION**

QIBA guidelines for the CT tumor volume biomarker may benefit from being specifically tailored to different contrasts and/or different estimation tasks (lung vs. liver).

# Measuring Head Movement in 3D During CT-Perfusion Analysis - A Pilot Study

Thursday, Dec. 1 12:15PM - 12:45PM Room: PH Community, Learning Center Station #5

#### Participants

Mette C. Marklund, MD, PhD, Roskilde, Denmark (*Presenter*) Nothing to Disclose Anders O. Baandrup, BSC, Roskilde, Denmark (*Abstract Co-Author*) Nothing to Disclose Troels Wienecke, MD,PhD, Roskilde, Denmark (*Abstract Co-Author*) Nothing to Disclose Carsten Thomsen, Copenhagen, Denmark (*Abstract Co-Author*) Nothing to Disclose

# CONCLUSION

A robust, very accurate and low tech marker can be used for measuring head movement in the X-, Y and Z-direction and rotation during a CTP.

#### Background

The purpose of this pilot study is to test a simple, non-anatomical dependent method to calculate head motion in the X-, Y- and Zdimensions and rotation. Most CT-scanners have inbuilt options for movement correction based on landmarks. Some of the algorithms operate in 3D others in 2D. Only very few studies have examined, how much the patient actually moves during a CT perfusion (CTP) study since no external, non-anatomic dependent marker for objective measurement in all 3 dimensions exists.

# **Evaluation**

To determine the motion in patients instructed to lying still, we developed a marker designed to be placed on the patients forehead. The marker was drawn in Autocad® and 3D printed. It contains 4 air filled cones in 2 planes pointing in 2 directions in each plane. It was tested in a phantom set-up with a micrometer (Mitutoyo 164-163 Digimatic Micrometer) enabling the marker moving as little as 0.001 mm. Raw data were calculated by an external radiologist with no knowledge on the applied movement parameters. By applying an advanced mathematical algorithm, measuring the size and elliptical deformation of the black holes during the scan, a very accurate value ( $\delta$ ) for movement in the X-, Y- and Z-direction could be calculated. The marker was placed on the forehead of 5 consecutive patients suspected for Ischemic Stroke (IS) undergoing CTP. The patients were all well-cooperating. Movement parameters (fig. 4) are given for our most restless patient nr. 3:  $\delta(X)$ : -3.6 to 4.4 mm,  $\delta(Y)$ : -1.3 to 1.9 mm, $\delta(Z)$ : -1.4 to 2.0 mm and rotation -2.0 to 3.2 degrees.

# Discussion

Movement artifacts lower the signal/noise ratio and increase the risk of diagnostically insufficient images. Even though the movement errors can be reduced by post processing, the S/N-ratio will remain lower than if the patient had not moved at all. Determining the extent of true motion is fundamental for setting up future projects aiming to optimize head stabilization and developing advanced post processing algorithms.

# PH263-SD-THA6

# Breast Density Estimation from 3D High Spectral and Spatial resolution (HiSS) MRI

Thursday, Dec. 1 12:15PM - 12:45PM Room: PH Community, Learning Center Station #6

#### **Participants**

Hui Li, MD, PhD, Chicago, IL (*Presenter*) Nothing to Disclose
Milica Medved, PhD, Chicago, IL (*Abstract Co-Author*) Nothing to Disclose
William Weiss, BS, Chicago, IL (*Abstract Co-Author*) Nothing to Disclose
Hiroyuki Abe, MD, Chicago, IL (*Abstract Co-Author*) Nothing to Disclose
Gregory S. Karczmar, PhD, Chicago, IL (*Abstract Co-Author*) Nothing to Disclose
Maryellen L. Giger, PhD, Chicago, IL (*Abstract Co-Author*) Stockholder, Hologic, Inc; Stockholder, Quantitative Insights, Inc; Co-founder, Quantitative Insights, Inc; Royalties, Hologic, Inc; Royalties, General Electric Company; Royalties, MEDIAN Technologies; Royalties, Riverain Technologies, LLC; Royalties, Mitsubishi Corporation; Royalties, Toshiba Corporation;

# PURPOSE

We aim to investigate a new 3D breast density estimation method using High Spectral and Spatial resolution (HiSS) MR imaging, combined with a novel semi-automated breast density measurement technique, in order to improve measurements of breast density for cancer risk assessment.

# **METHOD AND MATERIALS**

22 patients (ages 23-71 years) were recruited with informed consent under an IRB approved protocol and in compliance with HIPAA for high risk breast cancer screening at our institution. All patients received a standard-of-care digital X-ray mammogram and MR scans on a 1.5T Philips Achieva MR scanner, as well as HiSS scans (2D high resolution EPSI-based sequence, 0.8x0.8x3 mm3 inplane resolution, 23.9 Hz spectral resolution) during the clinical MR scans. HiSS water signal images were generated by integrating the water resonance obtained from the HiSS dataset in each voxel. There are several steps involved in breast density estimation based on HiSS images, including breast mask generating, breast skin removal, and breast percentage density calculation. The inter- and intra-user variability of HiSS-based density estimation was assessed using correlation analysis and limits of agreement. The correlation analysis was also performed between HiSS-based density estimation and BI-RADS ratings by radiologists.

#### RESULTS

A correlation coefficient of 0.91 (p<0.0001) was obtained between left and right breast percent density estimation based on HiSS images. The interclass correlation coefficient (ICC) of 0.99 (p<0.0001) was observed for reliability assessment of inter-user variability of HiSS-based breast percent density estimation. The limits of agreement for HiSS-based percent density were [-0.8 1.4] between two readers, and [-0.2 0.4] for the same reader. The moderate correlation coefficient of 0.55 (p=0.0076) was observed between HiSS-based breast density estimation and radiologists' BI-RADS density rating.

# CONCLUSION

An objective breast density estimation method using HiSS spectral data was developed. The high reproducibility with low-inter and low-intra user variability suggest that such HiSS-based density metric may be beneficial to breast cancer risk assessment and monitoring response to therapy.

# **CLINICAL RELEVANCE/APPLICATION**

Accurately and objectively measuring breast density using HiSS spectral data may aid clinicians in assessment of breast cancer risk and monitoring of response to therapy in cancer patients.

# Use of Template Reporting to Improve Brain MRI Report Quality in the Setting of Multiple Sclerosis

Thursday, Dec. 1 12:15PM - 12:45PM Room: QS Community, Learning Center Hardcopy Backboard

#### **Participants**

Elliot Dickerson, MD, Ann Arbor, MI (*Presenter*) Nothing to Disclose Benjamin Segal, Ann Arbor, MI (*Abstract Co-Author*) Nothing to Disclose Matthew S. Davenport, MD, Cincinnati, OH (*Abstract Co-Author*) Royalties, Wolters Kluwer nv; ; Bradley R. Foerster, MD, Baltimore, MD (*Abstract Co-Author*) Nothing to Disclose Faiz I. Syed, MD, MS, Chicago, IL (*Abstract Co-Author*) Nothing to Disclose

# PURPOSE

Templated radiology reports may provide a more comprehensive and easily understood means of conveying information for complex clinical entities where diagnosis and management depends heavily on radiologic findings such as multiple sclerosis (MS). We report radiologist and neurologist assessments of report quality for studies performed in the year prior to and following the introduction of an optional MS template for brain MRIs.

#### **METHODS**

This was a HIPAA-compliant health system quality improvement project with an IRB waiver. All relevant MRI brain reports in patients imaged for MS in the year prior to and the year following the introduction of a brain MRI MS template report were assessed for the explicit presence or absence of 12 MS-relevant imaging findings such as enhancing lesions and T2 FLAIR hyperintensities. Utilization of the template report after implementation was monitored and encouraged. At the conclusion of the study period, mean numbers of relevant elements included in each report with and without the use of the MS template were compared with Student's t-test.As many of the neurologists at our institution were integral to the development and implementation of the template, two neurologists recruited to this project from a separate institution with extensive experience in MS practice were blinded to the primary purpose of the study and presented in random order with 10 template and 10 non-template reports. The neurologists independently assessed each report using 5-point Likert scales along four domains: understandability, detail, usefulness for patient management, overall quality.

#### RESULTS

A total of 156 reports were analyzed; 93 were constructed after the MS template was introduced. Of these, 71.0% (66/93) used the optional template. Template reports contained significantly more of the 12 key findings than reports without the template (mean: 11.1 vs. 5.8 findings per report, p<0.0001). Neurologists rated template reports as more detailed (mean 3.48 for template reports vs. 2.32 for non-template reports, p=0.036) and of higher overall quality (mean 3.47 for template reports vs. 2.74 for non-template reports, p=0.025) than non-template reports. Scores for report understandability and usefulness for patient management trended higher for template reports without reaching statistically significance (understandability: mean 3.43 for template reports versus 2.89 for non-template reports, p=0.10; usefulness for patient management: mean 3.58 for template reports vs. 3.11 for non-template reports, p=0.09).

# CONCLUSION

Brain MRI for MS reports using a dedicated MS reporting template contained discussion of a higher number of MS relevant findings. MS template reports were graded as more detailed and of higher overall quality than non-template reports.

# QS018-EB-THA

# The Impact of QC in Multicenter Clinical Trials-The IROC Experience for NCTN Focusing on PET

Thursday, Dec. 1 12:15PM - 12:45PM Room: QS Community, Learning Center Hardcopy Backboard

#### Participants

David Poon, BS, Columbus, OH (*Presenter*) Nothing to Disclose Preethi Subramanian, MS, BEng, Columbus, OH (*Abstract Co-Author*) Nothing to Disclose Richard Jacko, BS, Columbus, OH (*Abstract Co-Author*) Nothing to Disclose Prayna Bhatia, BS, Columbus, OH (*Abstract Co-Author*) Nothing to Disclose Tim Sbory, BS, Columbus, OH (*Abstract Co-Author*) Nothing to Disclose Michael V. Knopp, MD, PhD, Columbus, OH (*Abstract Co-Author*) Nothing to Disclose Shivangi Vora, BS, MS, Columbus, OH (*Abstract Co-Author*) Nothing to Disclose Ajay Siva, Columbus, OH (*Abstract Co-Author*) Nothing to Disclose Talha Saif, Columbus, OH (*Abstract Co-Author*) Nothing to Disclose Jun Zhang, PhD, Columbus, OH (*Abstract Co-Author*) Nothing to Disclose

#### PURPOSE

A major aspect of Quality control in current generation multi-center clinical trials that use PET/CT imaging for patient response assessment is to insure the quality of individual imaging examination. Therefore participating sites need to be capable to perform the imaging expected by the protocols and the quality of every subject need to meet expectations in order to ensure accurate and evaluable imaging. To meet these PET/CT protocol requirements, the quality check standards and workflow at IROC for multiinstitutional NCI National Clinical Trial Network (NCTN) clinical PET imaging trials will be introduced. Additionally, the effectiveness of the workflow on data compliance and trial goals will be discussed.

# METHODS

Our QA center evaluates every received imaging study in an overall standard but protocol-specific approach to assess protocol compliance, image quality and correct scheduling. Upon receipt of the imaging data and relevant case documentation, a 15-point quality evaluation of the data set is performed. The quality analysis takes into account the following: the timing of the PET/CT scan per protocol schedule; the PET emission uptake time; the consistency of this uptake time from baseline to restaging PET/CT scans; the completeness of the imaging data; the protocol defined acceptable imaging format of the imaging data; the consistency of the PET/CT Scanner across restaging scans, including arm positioning and PET scan direction; the Injection site; any De-identification performed; the Image resolution; completeness of Case Report Form/Documentation; patient fasting; glucose levels; and FDG Dosage. Major deficiencies are indicated in a quality check report, conveyed to enrolling institutions' study coordinators or local investigators if major protocol deficiencies are indicated. To evaluate trial impact, a year-by year map of PET/CT studies was created, identifying compliance vs noncompliance over several key points: Uptake time, Uptake time consistency, and PET/CT scanner consistency. Additionally, a weighted scoring system for these individual aspects (hereby referred to as a heat map) was implemented internally with input from the protocol deviations. The PET/CT scheduling, uptake time/uptake time consistency, data formatting, and PET/CT scanner consistency were weighted more heavily over the other evaluation points.

## RESULTS

Over the course of the observed study, out of a total of 477 PET/CT studies evaluated, 65% were found to be fully compliant, with no protocol deviations noted. 35% were found to contain at least one or more deviations from the protocol per the multi-point quality evaluation. Over the first year of the study, 60 % of the studies received were deemed not fully compliant per above. During the second year, this rate dropped to 33% and year 3 had a 22% rate of not fully compliant. However, when these PET/CT studies were evaluated using the internal weighted scoring system, it was found that 92% were found to have been imaged within the protocol tolerances. 5.5% were found to contain protocol deficiencies that did not impact the overall evaluability of the PET/CT scans. 2.5% were found to contain major protocol deviations.

# CONCLUSION

Quality assurance approaches that employ multi-point inspection of individual imaging studies are able to have a positive impact on the quality of data collected within clinical trials. The feedback loop with submission of individual QC reports to institutions creates a dialogue between the QA center and imaging personnel of the enrolling facilities that help to avoid future protocol deviations and overall leads to improved quality of the clinical trials. As more institutions become interested in enrolling patients to clinical trials where quality imaging is essential for therapy assessment and disease staging, a continuing relationship with QA centers and sites can help to ensure that the highest quality of data can be achieved.

## QS128-ED-THA6

Performance Monitoring for Radiographers: Developing Key Performance Indicators that Drive Quality Improvement

Thursday, Dec. 1 12:15PM - 12:45PM Room: QS Community, Learning Center Station #4

#### Awards

**Quality Storyboard Award** 

#### Participants

Siok Mei Ng, Singapore, Singapore (*Presenter*) Nothing to Disclose Michael Ong, Singapore, Singapore (*Abstract Co-Author*) Nothing to Disclose Mei Chyi Kok, BSc, Singapore, Singapore (*Abstract Co-Author*) Nothing to Disclose Swee Ling Koh, SINGAPORE, Singapore (*Abstract Co-Author*) Nothing to Disclose

# PURPOSE

The purpose of this project was to develop meaningful, all-rounded KPIs for radiographers to enable objective performance monitoring and quality improvement to complement the existing subjective competency assessment of radiographers.

#### **METHODS**

Literature review was performed from scholarly articles but there was limited yield. International audit criteria like standards set by the Joint Commission International only provided broad categories. The development of KPIs started with hospital wide general KPIs such as Clinical Competency and Core competencies. The Radiographer specific KPIs (over and above departmental KPIs) were reviewed yearly and evolved: 2011 & 2012: 5 KPIs set (Clinical competency, Workflow Competency, Core Competencies, Portfolio/responsibilities, Others) and radiographers graded on a scale of 1-5 for each KPI2013 & 2014: Using the Institute of Medicine's (IOM) 6 domains of quality as a framework, 3 KPIs were set (2 patient safety indicators, 1 workflow competency which was subdivided into 3 areas), with individual compliance rates. 2015: 9 KPIs set (2 patient safety indicators, 2 general x-ray indicators, 1 modality indicator, 3 PACS-RIS workflow indicator, 2 training indicators) The 2015 KPIs were developed to better measure the IOM's domains of quality: Safety (2 patient Identification Documentation compliance rate, Hand hygiene compliance rate, Reject rates), Effectiveness (General X-ray & Modality Image quality), Efficiency (Recall rates), Patient-Centered (Compliment:Complaint Ratio), Timely (Turn around times) and Equitable. Indicators to meet hospital priorities were Training hours, and meeting attendance rate. The above indicators were specific to radiographers and are over and above the departmental wide targets for financial health, safety (adverse events), quality improvement projects, and research. In 2016, two more "Safety' indicators added were LMP documentation and medication documentation compliance rates. An performance target was set for each indicator based on national targets, hospital targets, and stretch targets derived from baseline data.Different teams from departmental level audit teams (for infection control and documentation audits) to modality audit teams (reject rates, image quality audit) performed data collection, analysis and quality improvement projects. The annual workload of the department is approximately 323,000 and the sample size for most audits is between 3-5%. 40 Senior Radiographers performed the image quality audits. The audits that had 100% sampling rate were reject rates, RIS-PACS errors, recall rates. Individual scores were tabulated for 2 patient ID Documentation compliance rate, Reject rates, Image quality, recall rates, PACS-RIS errors, Training hours and meeting attendance. Other KPIs were measured by modality. The senior radiographers who performed the audits did so during the low patient load periods of the workday. Monitoring data was shared regularly at radiographer meetings, through e-mail, and during the open appraisal exercise for performance feedback and development plans.

# RESULTS

Over the period of 5 years from 2011 to 2015, despite incremental increases in workload, the monitoring data was used to drive quality improvement and a description of improvements over the 5 years is as follows (reporting departmental mean):Hand hygiene compliance rate: 57% (2011) to 79% (2015)2 Patient ID documentation compliance rate: 59% (2011) to 97% (2015). This initiative has reduced Sentinel Events of wrong patient scanned to zero for the last 3 years. This category of Sentinel event is reportable to the local Ministry of Health within 2 days.Reject rates: 7% (2014) to 6% (2015). In 2014, the department began to replace all end of life CR x-ray equipment with DR units and it was observed that with DR, reject rates were higher than the CR reject rates. The CR reject rates failed to include images that were unassigned at the CR terminal, and therefore, was artificially low.Compliment to complaint ratio: 1:1 (2011) to 3:1(2015)Total annual PACS Errors – Unspecified Images: 13/radiographer (2014) to 10/radiographer (2015)Total annual PACS Errors: 5/radiographer (2013) to 4/radiographer (2015)

# CONCLUSION

Performance measurement and monitoring increases the productivity of manpower during low patient load periods of the day and is a tool for evaluation of the progress of a department toward improved outcomes in patient care and reduction in waste. These measures creates a wave of reflection in action, enables quality improvement and quantitatively measures progress towards organizational and professional goals. Objectivity in performance appraisal increases radiographers' satisfaction and provides tangible goals to strive towards. Body Size-Based Optimization of Computed Tomography Protocols: Assessment of the Scientific Literature for Quality Improvement, Dissemination and Knowledge Translation

Thursday, Dec. 1 12:15PM - 12:45PM Room: QS Community, Learning Center Station #1

# Participants

Erin T. Wong, MD, Toronto, ON (*Presenter*) Nothing to Disclose Iris Li, BSC, Toronto, ON (*Abstract Co-Author*) Nothing to Disclose Marie K. MacGregor, MPH, Toronto, ON (*Abstract Co-Author*) Nothing to Disclose Yingming Amy Chen, MD, Toronto, ON (*Abstract Co-Author*) Nothing to Disclose Lianne Concepcion, BSC, Toronto, ON (*Abstract Co-Author*) Nothing to Disclose Timothy R. Dowdell, MD, Toronto, ON (*Abstract Co-Author*) Nothing to Disclose Bruce G. Gray, MD, Toronto, ON (*Abstract Co-Author*) Nothing to Disclose

# PURPOSE

To assess the scientific literature on optimization of computed tomography (CT) protocols based on body size and to evaluate the content and quality of this literature for the purpose of dissemination and translation into clinical practice.

#### **METHODS**

Systematic search of scientific literature databases for studies on the implementation of body size (habitus)-based computed tomography protocols for radiation dose optimization. Inclusion criteria: English language, published between years 2005-2015, human subjects, adult patients, use of body-size specific diagnostic protocols with radiation dose and image quality outcomes. Three researchers (EW, IL and KM) evaluated title, abstracts and full text documents to determine if the study met the inclusion criteria. Three radiologists (EW, AC and BGG) further reviewed the full text documents to determine if they were Quality Improvement (QI) studies defined as "systematic, data-guided activities designed to bring about immediate, positive changes in the delivery of health care in particular settings." Differences in studies to include were resolved by consensus. Data was abstracted from included studies to assess the body of the literature based on protocol and scanner type, software enhancements, radiation dose reduction methods, and qualitative or quantitative image quality assessment. Criteria from the Standards for QUality Improvement Reporting Excellence (SQUIRE 2.0) and a Guide to Effective Quality Improvement Reporting by Larson et al 2014 were used to create a "yes"/"no" checklist to evaluate the quality of papers deemed to be QI studies.

#### RESULTS

There were 79/1976 articles that met the inclusion criteria, however, 5 studies met the definition of a QI study. The most frequent protocol evaluated was for cardiac CT angiography (45/79, 56%); this was followed by abdominal CT (9/79, 11%), chest CT (6/79, 8%), CT for pulmonary angiography (5/79, 6%), abdominopelvic CT (4/79, 5%) and lumbar spine CT (2/79, 3%). Methods of optimization included adjustment to tube voltage or tube current based on a weight metric (65/79, 81%); 25/79 articles (32%) used this method along with some form of iterative reconstruction. Body Mass Index (BMI) was the most common weight-based metric (36/79, 45%), 14 used weight categories (14/79, 18%) and 10 studies used body circumference or diameter (10/79, 13%). The predominant dose metrics were CTDIvol in mGy (24/79, 30%), effective dose in mSv (23/79, 29%) and Dose Length Product (DLP) (13/79, 16%). There were 15 studies without an image quality assessment (15/79, 19%), including 2 QI studies.There were 67 "yes"/"no" questions on QI reporting criteria when the SQUIRE 2.0 and Larson et al (2014) checklists were combined and categorized as: clarity of purpose, appropriate methodology, level of detail, feasibility of the intervention, and reporting of contextual factors such as costs, workflow, training, or unintended impacts. Only 1 study (1/5, 20%) scored positively for all questions (67/67, 100%) and only 2 others (2/5, 40%) scored close to 50% (33/67). Most studies dield to describe how the intervention was embedded in the workflow, how data was captured and analyzed during the intervention period (for prospective studies) and any mention of the costs or the impact of local contextual elements including education, training and institutional policy.

# CONCLUSION

There has been considerable attention paid to the need for optimization of radiation exposure for CT to lower patient and population exposure. One of the most effective ways to eliminate unnecessary exposure to smaller sized patients is to use the equipment features and software designed for dose reduction. We found very few studies that provided practical guidance to easily translate these interventions into clinical practice. Further, the majority of the available studies and the majority of the QI studies focus on cardiac CT angiography when, in fact, these interventions should be applicable to nearly all body diagnostic protocols. The fact that there are few QI studies may be related to a bias in the literature toward publication of "scientific" or hypothesis driven studies versus "quality improvement" studies, suggesting that more needs to be done to encourage robust reporting of QI studies, especially in this important area of patient safety for radiology.

Implementing a Process for Establishing and Sharing Standardized Imaging Protocols to Improve Cross-Enterprise Workflow and Quality

Thursday, Dec. 1 12:15PM - 12:45PM Room: QS Community, Learning Center Station #2

# Participants

Viswanathan Venkataraman, MS, MENG, Dallas, TX (*Presenter*) Nothing to Disclose Travis Browning, MD, Dallas, TX (*Abstract Co-Author*) Advisor, McKesson Corporation Ivan Pedrosa, MD, Dallas, TX (*Abstract Co-Author*) Nothing to Disclose Suhny Abbara, MD, Dallas, TX (*Abstract Co-Author*) Author, Reed Elsevier; Editor, Reed Elsevier; Institutional research agreement, Koninklijke Philips NV; Institutional research agreement, Siemens AG David T. Fetzer, MD, Dallas, TX (*Abstract Co-Author*) Nothing to Disclose Seth Toomay, MD, Dallas, TX (*Abstract Co-Author*) Nothing to Disclose Ronald M. Peshock, MD, Dallas, TX (*Abstract Co-Author*) Nothing to Disclose

# PURPOSE

Value-based imaging requires the delivery of high-quality, consistent and appropriate imaging at an acceptable cost. Challenges include developing standardized imaging protocols, ensuring consistent application by technologists, and monitoring quality control, particularly for large enterprises. Our radiology practice covers three separate health care systems, each with its own equipment, administration, and technical support. Given the complex nature, a patient could undergo differing imaging protocols based more upon the imaging location rather than the nature of the indication. Moreover, each site maintained protocols in a mix of paper and limited access electronic forms, making it difficult for radiology staff to cross cover the systems due to lack of knowledge of local protocols.Our imaging enterprise includes a university hospital and clinic system, a large county hospital and health care system, and a pediatric hospital and health system. Exams across the three systems are interpreted by one large radiology group with expertise in various subspecialties. Our goals were as follows: (1) standardize imaging protocols; (2) adapt the imaging protocols to specific modalities and available equipment; and (3) disseminate this knowledge across all of the sites of care.

#### **METHODS**

Our approach involved three components: (1) facilitation of imaging protocol definition across subspecialty radiologist teams; (2) creation of a database which linked the clinical imaging protocols to the scanner / machine specific acquisition protocols; and (3) delivery of the protocol library to all users regardless of location. Focus initiated with CT, MR, Ultrasound and Nuclear Medicine protocols.A single individual with an background as a technologist and manager, designated the "Protocol Czar," was tasked with reviewing existing protocols and creating radiologist and technologist workgroups to develop standardized protocols. These were reviewed and approved by the radiologist responsible for modality and subspecialty areas. During the process, overlapping protocols were combined, duplicative/outdated protocols were eliminated, and new protocols were developed to fill clinical care gaps. The second step involved creation of a database linking clinical imaging protocols (which includes contrast details and imaging exported to PACS) to machine-specific acquisition protocols (containing the machine specific acquisition parameters). This was implemented in Microsoft Access and included details on tech/nursing workflows, contrast administration, imaging phases, radiation dose, and electronic orders. To facilitate sharing the information and protocols across multiple sites, the protocol library was implemented on a SharePoint site and made available at all institutions. At launch, all systems used this library as the "source of truth" for protocols. Modality-specific operation committees were developed to institute change management controls for ongoing protocol maintenance and to lay the foundation for quality assurance practice for utilization and adherence to established protocols. These committees included representation from the radiologist professional group, administrative and technologist members from the health care systems, and medical physics; this collaborative approach facilitated institutional buy-in that aided implementation. Furthermore, a process was implemented to maintain competencies among technical staff that takes into account the periodical optimization of protocols.

#### RESULTS

Analysis of our existing protocols confirmed the inconsistent protocol approach across the different institutions. For example, our initial analysis identified 84 protocols in Ultrasound with multiple versions across the healthcare systems. The US standardization team was able to reduce the number of US protocols from 84 to 52.After performing the analysis and standardization process there were a total of 606 protocols spanning CT, MR, US and NM. These were then published to all facilities using a SharePoint and utilization was tracked over a 3 month period. Over this period the protocols were accessed 11,207 times with the highest use being complicated protocols (such as "MR Brachial Plexus") and newer protocols (such as "CT Urography").Since standardization, the average number of changes to our protocols occurred at a rate of two per month per modality.A process is being looked into for the data on protocol adherence and callbacks for furthering improvement in quality.

# CONCLUSION

We have instituted an approach for the development, implementation, and delivery of standardized imaging protocols in multiple complex, geographically-distributed healthcare systems. Key elements included (1) the presence of strong modality-specific operating committees for forming consensus on imaging protocols, (2) a "protocol czar" to manage the process, (3) electronic publishing of the protocols to facilitate ease of access and use and (4) a mechanism monitoring compliance.

#### **Honored Educators**

Presenters or authors on this event have been recognized as RSNA Honored Educators for participating in multiple qualifying educational activities. Honored Educators are invested in furthering the profession of radiology by delivering high-quality educational content in their field of study. Learn how you can become an honored educator by visiting the website at: https://www.rsna.org/Honored-Educator-Award/

Suhny Abbara, MD - 2014 Honored Educator

# QS132-ED-THA3

Improving "A Day in the Life" of Radiology Administrative Associates

Thursday, Dec. 1 12:15PM - 12:45PM Room: QS Community, Learning Center Station #3

#### **Participants**

Susie Spielman, Stanford, CA (*Presenter*) Nothing to Disclose Tracy Burk, Stanford, CA (*Abstract Co-Author*) Nothing to Disclose Barbara Bonini, Stanford, CA (*Abstract Co-Author*) Nothing to Disclose Sergio Sousa, Stanford, CA (*Abstract Co-Author*) Nothing to Disclose Jake Mickelsen, BS, Stanford, CA (*Abstract Co-Author*) Nothing to Disclose Susan Kopiwoda, MS, MPH, Stanford, CA (*Abstract Co-Author*) Nothing to Disclose Yun-Ting Yeh, Stanford, CA (*Abstract Co-Author*) Nothing to Disclose Stephanie Go, MD, Stanford, CA (*Abstract Co-Author*) Nothing to Disclose

# PURPOSE

Stanford Radiology experienced significant changes, with the arrival of a new Chair in 2012, followed by many new faculty hires from 2012 to 2015. Administration was unprepared to support this growth and as a result experienced significant turnover in staff. In fact, the Radiological Science Lab, one of our largest research divisions, lost their entire roster of veteran AA's. As a result, the faculty were not well supported, distracting them from their primary goals of patient care, teaching and research, and the new staff felt disconnected and frustrated. The distribution of the Department staff in 21 disparate locations further complicated matters. AA's were constantly searching for information, wasting time creating their own systems and there was limited sharing of knowledge. Our goal was to improve AA satisfaction and engagement with Department resources over the 5 months of our project, June to Oct 2016. The ultimate success of the project would reflect improved efficiency of our operations and a productive and rewarding work culture.

## **METHODS**

We assembled a multidisciplinary team of Radiology business leaders, administrative associates, a resident and a QI coach. We used standard quality improvement tools but faced a challenge in finding a meaningful metric for monitoring our progress in a project that was not quantitative in nature. We decided the survey our population of approximately 40 AA's on a weekly basis by asking them the following question: In performing your job over the last week, how helpful were the currently available Department tools/resources? Ratings were from 1-10 (not at all helpful to extremely helpful). Our baseline score was 5, so we set a target rating of 8 by the end of the project. To analyze our current state, we queried our target on what they would like to see improved in their daily work life. We performed one on one interviews with current staff and reached out to AA's that had left Stanford to Google and eBay to understand what resources they found helpful at their new jobs. We performed root-cause analysis, using a fishbone diagram to visualize factors contributing to AA frustration. We then identified key drivers, which were 1) the need for a central hub of information, 2) lack of structure for engaging colleagues, 3) lack of awareness of Department news/information, 4) struggles with existing technology, and 5) feeling overloaded. We focused on the top three key drivers and specific interventions were as follows: 1) create a central location for accessing tools and resources for AA's, 2) develop a structure for engaging individual AA's as Gurus, 3) develop a consistent communication structure for current and new resources. We developed a weekly tip emailed to all administrators to help share helpful information quickly throughout the Department. We also developed a website we called RadHub which contained all information needed for an AA to perform their jobs. Much of this information already existed but was extremely difficult to find. We were able to consolidate everything in one simple location in a format that allowed for easy updates. To support this website we initiated a Guru program which is essentially a peer support network and onboarding team. We identified experts throughout the Department and they are listed on our website as contacts for help in everything from reimbursements to conference room scheduling. Finally, we initiated a monthly Huddle. We replaced our top down staff meetings with much more collaborative huddles which were fast, direct and allowed for improved engagement. These huddles have increased communication throughout the Department and serve as an important tool for identifying problems and initiating improvements.

#### RESULTS

The interventions were implemented over a 5 month period where we continued to survey our staff and track results on our run chart. The engagement results continued to climb from a baseline of 5 to a 7, and response from staff is extremely positive, relecting the culture change we hoped to achieve. We have consistent use of RadHub and attendance at our huddles has remained high. These changes took a great deal of effort to launch, so we are continuing to further develop the website and our QI team has remained in tact to ensure the huddles retain their structure and effectiveness. Our target of 8 was met in our last survey.

# CONCLUSION

The engagement and efficiency of the department administration is essential to the success of our faculty. By implementing specific interventions to improve our internal communications and access to tools and resources, we successfully reconnected our staff and increased overall satisfaction. We have seen a decrease in staff turnover and positive improvements to the culture of administration in our department. We were surprised to find that the huddle concept could work well for a large, geographically dispersed group. The project also demonstrated that QI concepts could effectively be applied to administration.

# The Impact of Volume of Bone Marrow Irradiated in Head and Neck Cancer on Hematologic Toxicity

Thursday, Dec. 1 12:15PM - 12:45PM Room: RO Community, Learning Center Station #2

#### **Participants**

Jay C. Shiao, BS, Houston, TX (*Abstract Co-Author*) Nothing to Disclose Abdallah S. Mohamed, MD, MSc, Houston, TX (*Abstract Co-Author*) Nothing to Disclose Aasheesh Kanwar, Houston, TX (*Abstract Co-Author*) Nothing to Disclose Andrew Wong, BS, Houston, TX (*Abstract Co-Author*) Nothing to Disclose David I. Rosenthal, Houston, TX (*Abstract Co-Author*) Advisory Board, Bristol-Myers Squibb Company Advisory Board, Merck KGaA Research support, Merck KGaA Brandon Gunn, MD, Galveston, TX (*Abstract Co-Author*) Nothing to Disclose Adam S. Garden, MD, Houston, TX (*Abstract Co-Author*) Nothing to Disclose Merrill Kies, Houston, TX (*Abstract Co-Author*) Nothing to Disclose Clifton D. Fuller, MD, PhD, Houston, TX (*Presenter*) Nothing to Disclose

#### PURPOSE

We aim to determine the effect of the volume of bone marrow irradiated in the head and neck on the hematologic toxicity after single modality radiation treatment.

# METHOD AND MATERIALS

Head and neck cancer patients receiving definitive IMRT alone in one institution was reviewed from 2000 to 2012. Serial hematocrit (Hct), hemoglobin (Hgb), total lymphocyte count (TLC), total neutrophil count (TNC), total monocyte count (TMC), platelets (Plt), and total white blood cell (WBC)) were recorded for pre (latest CBC w/ DIFF before treatment), during (4-6 weeks after start of treatment), and after treatment (0-2, 2-6, 6-12, >12 month after IMRT). CTCAEv.4 criteria was used to determine Hct, Hgb, TLC, TNC, TMC toxicity endpoints. Grade 2-3 toxicity was considered moderate and Grade 4 was considered severe. Radiation treatment plans were restored and isodose lines were regenerated followed by the segmentation of bony structures receiving 1 Gy, 2 Gy, 6 Gy, 10 Gy dose thresholds. Recursive partitioning analysis (RPA) was used to identify bony dose-volume thresholds associated with moderate and severe hematologic toxicity during and after IMRT.

#### RESULTS

Of the 430 patients reviewed, 63 patients head and neck cancer patients were evaluated during and after IMRT; median age was 58 years old (14 – 78), 47 (74.6%) were male, 52 (82.5%) were Caucasian, 39 (61%) were treated for oropharyngeal cancer. Median radiation dose was 66 Gy (14.4-72) in 30 fractions (4-40). 48 patients (76.2%) had stage III-IV cancer. 48 (76.2%) patients suffered moderate to severe lymphopenia. 3 (4.8%) suffered moderate anemia and 3 (4.8%) suffered leukopenia. No patients suffered a decrease in TNC nor Plt. RPA identified whole bone V6 (volume receiving 6 Gy)  $\geq$  541.5 cc to be significantly associated with moderate to severe lymphopenia during IMRT (RPA logworth p<0.002; cumulative ROC AUC 0.7379; chi-square p<0.01). Baseline TLC was normal, dropped 67.5% during treatment, and did not return to baseline after 12 months.

# CONCLUSION

Our findings strongly suggest that treatment related lymphopenia is a common enduring side effect of radiation treatment in head and neck cancer patients. Higher bony V6 was associated with the development of moderate and severe lymphopoenia during the course of treatment.

# **CLINICAL RELEVANCE/APPLICATION**

Dose-volume association of irradiated bone marrow and moderate to severe lymphopenia suggest immune preservation is important in IMRT to the head and neck.

The Sydney Swallow Questionnaire (SSQ) as a Predictor of Clinical Outcomes in Patients Undergoing Radiation Therapy for Head and Neck Cancer

Thursday, Dec. 1 12:15PM - 12:45PM Room: RO Community, Learning Center Station #3

#### Awards

#### **Student Travel Stipend Award**

#### Participants

Luke C. Peng, MD, MSc, Baltimore, MD (Presenter) Nothing to Disclose Zhi Cheng, MD, MPH, Baltimore, MD (Abstract Co-Author) Research Grant, Toshiba Corporation Xuan Hui, MD, Baltimore, MD (Abstract Co-Author) Nothing to Disclose Scott Robertson, Baltimore, MD (Abstract Co-Author) Nothing to Disclose Joseph A. Moore, PhD, Baltimore, MD (Abstract Co-Author) Nothing to Disclose Michael Bowers, Baltimore, MD (Abstract Co-Author) Nothing to Disclose Brandi Page, Baltimore, MD (Abstract Co-Author) Nothing to Disclose Ana P. Kiess, MD, PhD, Baltimore, MD (Abstract Co-Author) Nothing to Disclose Jolyne O'Hare, Kogarah, Australia (Abstract Co-Author) Nothing to Disclose Peter Graham, Kogarah, Australia (Abstract Co-Author) Nothing to Disclose Julia Maclean, Kogarah, Australia (Abstract Co-Author) Nothing to Disclose Michal szcesniak, Kogarah, Australia (Abstract Co-Author) Nothing to Disclose Ian Cook, Kogarah, Australia (Abstract Co-Author) Nothing to Disclose Todd R. McNutt, PhD, Baltimore, MD (Abstract Co-Author) Research collaboration, Koninklijke Philips NV Research collaboration, Toshiba Corporation Research collaboration, Elekta AB Harry Quon, MD, Baltimore, MD (Abstract Co-Author) Nothing to Disclose

# ABSTRACT

Purpose/Objective(s): The Sydney Swallow Questionnaire (SSQ) is a validated quantitative tool for the evaluation of swallowing function in the head and neck cancer (HNC) patient. We hypothesized that the SSQ may predict for clinical outcomes such as weight loss and changes in Functional Oral Intake Scale (FOIS) during a course of radiotherapy to guide management decisions.Materials/Methods: Measures of patient clinical status including SSQ score, weight, feeding tube status, and FOIS were captured at all clinical visits from February 2015 to December 2015 for patients who underwent radiotherapy for head and neck cancer at our institution. Statistical correlations between the SSQ score, its change, and weight loss or FOIS level were evaluated by the Pearson product-moment correlation coefficient. Results: Ninety-three patients who underwent treatment had SSQ scores captured throughout radiation treatment. Median weight change rate during radiation treatment was -0.44 kg per week [interquartile range (IQR), -0.85 to -0.03] and median absolute weight change over treatment course was -2.87 kg [IQR, -6.29 to +0.55]. A negative correlation was found between magnitude of SSQ score increase for each patient and average FOIS (r = 0.479; p). There was also a weak but statistically significant correlation between SSQ score change and max percentage weight loss (r = 0.208; p = 0.0496). For 10 patients who eventually used a PEG tube for nutrition, a strong correlation was found between maximum percentage weight loss and magnitude of SSQ score increase (r = 0.796; p = 0.006). Conclusion: Magnitude of increase in SSQ score was negatively correlated with FOIS confirming that a worsening swallow function leads to compensatory change in functional intake such as switching to softer diet or using a feeding tube. Such adaptations seem to be a partial but incomplete compensation for swallow dysfunction given the weak but significant correlation between SSQ score change and percentage weight loss. SSQ score may be one important predictive factor for identifying patients at increased risk for substantial weight loss, but it likely lacks sufficient explanatory power to predict for such patients independently.

# Contrast Enhanced Ultrasound (CEUS) for the Characterization of Intra-Scrotal Lesions

Thursday, Dec. 1 12:15PM - 12:45PM Room: GU/UR Community, Learning Center Station #7

**FDA** Discussions may include off-label uses.

#### **Participants**

Noah A. Brauner, MD, Los Angeles, CA (Presenter) Nothing to Disclose

Hisham A. Tchelepi, MD, Los Angeles, CA (Abstract Co-Author) Research Grant, General Electric Company; Research Grant, Roper Industries, Inc

# **TEACHING POINTS**

Intra-scrotal lesions are primarily imaged using trans-scrotal ultrasonography (US). Although excellent at detecting intrascrotal lesions, conventional ultrasonography can have difficulty in differentiating benign and malignant entities. The aim of this educational exhibit is to briefly review the relevant scrotal/testicular anatomy, discuss the biophysical properties and safety profile of ultrasound contrast agents (UCAs) and highlight the utility of contrast enhanced ultrasound (CEUS) examinations for the characterization of a spectrum of intrascrotal pathology. We will also briefly discuss the implications of this improved diagnostic certainty on tailoring clinical management.

# TABLE OF CONTENTS/OUTLINE

Testicular and scrotal anatomy UCAs: biophysical properties and safety profile CEUS of the testicles: How it's done CEUS and conventional US appearance of infection CEUS and conventional US appearance of neoplasm CEUS and conventional US appearance of scrotal trauma Implications for management: preventing unnecessary orchiectomy

# VI269-SD-THA4

Radiologic Evidence of Short-term Response of Neuroendocrine Tumor Hepatic Metastasis to 90YRadioembolization

Thursday, Dec. 1 12:15PM - 12:45PM Room: VI Community, Learning Center Station #4

#### Awards

#### **Student Travel Stipend Award**

#### Participants

Haiying Yu, MD, PhD, Detroit, MI (*Presenter*) Nothing to Disclose Shahida M. Danier, MD, Grosse Pointe Shores, MI (*Abstract Co-Author*) Nothing to Disclose Jasmine Koo, MD, Detroit, MI (*Abstract Co-Author*) Nothing to Disclose Vistasp J. Daruwalla, MD, Chicago, IL (*Abstract Co-Author*) Nothing to Disclose Hamza M. Beano, MD, Detroit, MI (*Abstract Co-Author*) Nothing to Disclose Karan N. Patel, MD, Detroit, MI (*Abstract Co-Author*) Nothing to Disclose Mark Le, MD, Detroit, MI (*Abstract Co-Author*) Nothing to Disclose Hiren Rangunwala, MD, Detroit, MI (*Abstract Co-Author*) Nothing to Disclose Robert Wlodarski, MD, Detroit, MI (*Abstract Co-Author*) Nothing to Disclose Monte L. Harvill, MD, Franklin, MI (*Abstract Co-Author*) Nothing to Disclose Roger Kakos, MD, Detroit, MI (*Abstract Co-Author*) Nothing to Disclose Jeffrey J. Critchfield, MD, Royal Oak, MI (*Abstract Co-Author*) Nothing to Disclose

#### PURPOSE

Yttrium-90 (90Y) radioembolization (RE) is a promising approach to treat the liver metastatic neuroendocrine tumor (mNET). However the radiological measurement of RE effectiveness is inconstant, especially at the short duration. We propose to find the optimal radiologic criterion to evaluate the early mNET response to 90Y RE by comparing the correlations of biochemical maker and different radiologic criteria.

# METHOD AND MATERIALS

This is a single-center retrospective study of patients with liver mNET treated with 90Y TheraSphere® between 2008 and 2015. The Chromogranin A (CgA), a biological marker with high sensitivity and specificity for NET burden, was obtained. The change of imaging tumor size was calculated according to Response Evaluation Criteria In Solid Tumors (RECIST) and Modified RECIST (mRECIST) respectively (Fig. 1). Correlation of change of CgA and tumor size at post- to pre-treatment were analyzed.

# RESULTS

17 patients were recruited in the study with follow-up duration of 3 - 4 months. The median change in CgA was -48.32%. According to RECIST and mRECIST respectively, the complete response, partial response, stable disease and progressive disease were found in 0 vs. 0, 3 vs. 10, 11 vs. 7 and 3 vs. 0 patients. The correlation coefficient between the change in CgA level and tumor size was 0.117 (p=0.446) vs 0.397 (p=0.026) (RECIST vs. mRECIST) (Fig. 2).RE induces the intra-tumor necrosis. Measuring the shrinkage of tumor by RECIST neglects the distinction of necrotic and viable portion. Only the viable portion is corresponding to tumor metabolism and biological marker. The positive correlation between the changes of CgA and mRECIST-assessed mNET response indicates that mRECIST accurately reflects the tumor burden.

#### CONCLUSION

The radiologic measurements such as mRECIST are optimal imaging criteria to assess the early mNET response to 90Y RE since they can distinguish the intra-tumor necrosis and residual viable tumor.

# **CLINICAL RELEVANCE/APPLICATION**

The combination of mRECIST and CgA may reflect the early therapeutic effectiveness of 90Y RE which will help physician promptly adjust the treatment regimen and improve prognostication of liver mNET.

Evaluation of Efficacy and Safety of Arterial Embolization with Amplatzer Vascular Plug II using "Compressing Method": Experimental Study in Swine

Thursday, Dec. 1 12:15PM - 12:45PM Room: VI Community, Learning Center Station #1

# Participants

Mika Kodani, Yonago, Japan (*Presenter*) Nothing to Disclose Yasufumi Ouchi, Yonago, Japan (*Abstract Co-Author*) Nothing to Disclose Shinsaku Yata, MD, Yonago, Japan (*Abstract Co-Author*) Nothing to Disclose Toshihide Ogawa, MD, Yonago, Japan (*Abstract Co-Author*) Nothing to Disclose

# PURPOSE

The purpose of this study was to evaluate efficacy and safety of arterial embolization with Amplatzer Vascular Plug II (AVP II) using "compressing method" in animal model.

# METHOD AND MATERIALS

In seven swine, 14 internal iliac arteries (IIA) were embolized with AVP II in two ways: seven left IIAs with compressing method (Group A) and seven right IIAs with conventional method (Group B). Aortography was performed just after AVP II placement and then every 30 seconds until cessation of arterial inflow. Long-axis length of AVPII and recanalization were evaluated after embolization. An arterial blood pressure of both the aorta (Pa) and the distal of the IIA (Pd) were also continuously recorded. We analyzed the arterial blood pressure gradient (BPG) between Pa and Pd, and calculated the inclination of straight line on BPG. Arterial damage was assessed by intravascular ultrasound (IVUS) and pathologically.

# RESULTS

The procedure was successfully performed without arterial damage in both groups with IVUS. There was no histological difference in the intimal damage between both groups. The mean AVP II length in Group A / in Group B ratio was smaller than 0.5. The mean complete occlusion time was 34.3s (range, 30-60s) in Group A, 132.9s (range, 30-300s) in Group B (p-values=0.019). The mean BPG inclination of Group A ( $4.1 \times 10-2$ ) was larger than Group B ( $1.0 \times 10-2$ ) (p-values=0.016). Recanalization was not observed in both groups.

# CONCLUSION

AVPII embolization using "compressing method" is effective and can be performed without pathological damage.

# **CLINICAL RELEVANCE/APPLICATION**

Arterial embolization with AVPII using compressing method is useful to perform short segment arterial embolization.

# VI272-SD-THA3

Renal Cryoablation: Patterns and Chronology of Late Local Recurrence - Implications for Post-Treatment Surveillance

Thursday, Dec. 1 12:15PM - 12:45PM Room: VI Community, Learning Center Station #3

#### Awards

#### **Student Travel Stipend Award**

#### **Participants**

Nirav Patel, MBBS, FRCR, Southampton, United Kingdom (*Presenter*) Nothing to Disclose Alexander King, Southampton, United Kingdom (*Abstract Co-Author*) Nothing to Disclose David J. Breen, MD, Southampton, United Kingdom (*Abstract Co-Author*) Nothing to Disclose

#### PURPOSE

Percutaneous cryoablation is an increasingly utilised treatment for small renal masses and an accepted alternative to nephronsparing surgery. There are however as yet no agreed or evidence-based post-treatment imaging protocols. Imaging is directed towards identifying subtotal treatment (STT) on the initial post-treatment study and late local recurrence (LLR) on later studies. We have evaluated our large single centre experience, identifying the pattern and chronology of LLR, and seek to determine whether this has implications for oncologically appropriate imaging follow-up.

# **METHOD AND MATERIALS**

All percutaneous cryoablation cases from May 2007 to March 2016 at a single teaching hospital were analysed for LLR. Our standard local practice has adapted to an intravenous contrast enhanced CT at 1 month, 1, 3 and 5 years post-cryoablation, although intervening CT may be performed if any suspicious appearances. The time (months) between cryoablation procedure and recurrence was noted as was time to any subsequent intervention.

### RESULTS

427 tumours were treated in 379 patients. 12 LLR cases (3.0%) were present out of 404 tumours with post-treatment CT. This is a supra-regional service and as such some remote patients were lost to imaging follow-up. The mean time to LLR was 36.7 months (range 5-76 months) with 2 tumours presenting <1 year, 4 tumours from 1-3 years and 6 tumours >3 years. 6 tumours had a repeat ablation within 2-6 months of LLR with remaining undergoing surveillance. LLR is usually seen as an enhancing nodule on late arterial phase CT at the margin of the ablation zone whilst primary residual disease (STT) is seen as an enhancing crescentic margin.

# CONCLUSION

In the setting of primary treatment for 'curable' RCC primary, residual (STT) and locally recurrent (LLR) disease are separate entities occurring at different phases post-treatment. LLR is uncommon at 3% and often occurs at 3-5 years post-treatment when it is eminently amenable to secondary treatment. As such our experience suggests that post-treatment surveillance could be considereably curtailed to 1, 3 and 5 years and this would permit the straightforward and oncologically appropriate treatment by delayed ablation where necessary.

# **CLINICAL RELEVANCE/APPLICATION**

Percutaneous cryoablation is an alternative treatment modality of small renal masses and strict imaging follow-up will help identify a recognised complication of late local recurrence.

# VI273-SD-THA5

The Evaluation of Interventionalists Exposure Doses to the Eye Lens Measured with Small Dosimeters on Radiation Protection Glasses

Thursday, Dec. 1 12:15PM - 12:45PM Room: VI Community, Learning Center Station #5

# Participants

Yukichi Tanahashi, MD, Tokyo, Japan (*Presenter*) Nothing to Disclose Hiroshi Kondo, MD, Tokyo, Japan (*Abstract Co-Author*) Nothing to Disclose Masayoshi Yamamoto, MD, Tokorozawa, Japan (*Abstract Co-Author*) Nothing to Disclose Takahiro Yamamoto, Tokyo, Japan (*Abstract Co-Author*) Nothing to Disclose Marie Osawa, Tokyo, Japan (*Abstract Co-Author*) Nothing to Disclose Junichi Kotoku, Tokyo, Japan (*Abstract Co-Author*) Nothing to Disclose Ikuo Kobayashi, Ibaraki, Japan (*Abstract Co-Author*) Nothing to Disclose Shigeru Furui, MD, Itabashi-Ku, Japan (*Abstract Co-Author*) Nothing to Disclose

## PURPOSE

To measure interventionalists' exposure doses to the eye lens during procedures and identify the monitoring value easily assessable on a routine basis.

# METHOD AND MATERIALS

From October 2012 to Jan 2016, 5 radiologists and 3 neurosurgeons conducted interventional procedures wearing 2 optically stimulated luminescence dosimeters (nanoDotTM, Landauer, IL), square-shaped with one side measuring 1cm, on the outside and inside surfaces at the exterior part of the left lens of radiation protection glasses. Dosimetry was performed once a month. The monthly dose equivalents (H3mm) on the outside surface (Do) were compared to those on the inside surface (Di), total fluoroscopy times (FT), total patient's skin dose (PSD), total dose-area-products (DAP), and monthly dose equivalents (H70µm) measured with a personal dosimeter worn outside and above the radiation protection apron at the neck (Dn).

# RESULTS

The monthly Do, Di, FT, DP, DAP, and Dn ranged from 0.03 to 3.33mSv (mean, 0.71mSv  $\pm 0.60$ ), 0.01 to 1.39mSv (mean, 0.33mSv  $\pm 0.28$ ), 110 to 1,184 minutes (mean, 470 minutes  $\pm 206$ ), 1.68 to 47.27 Gy (mean, 12.19 Gy  $\pm 9.50$ ), 20.17 to 4036.67 Gy cm2 (mean, 267.46 Gy cm2  $\pm 473.33$ ), and 0 to 5.0 mSv (mean, 0.60 mSv  $\pm 0.72$ ), respectively. Linear regression equations obtained were Di = 0.418 x Do + 0.031 (R2, 0.85), Do = 2.0 x 10-3 x FT - 0.157 (R2, 0.41), Do = 4.20 x 10-5 x PSD + 0.20 (R2, 0.44), Do = 5.21 x 10-7 x DAP + 0.57 (R2, 0.17), and Do = 0.57 x Dn + 0.364 (R2, 0.45).

#### CONCLUSION

The interventionalist's dose to the eye lens can exceed the equivalent dose limit (20mSv in a year, averaged over periods of 5 years, with no single year exceeding 50mSv) recommended by the International Commission on Radiological Protection 2011, particularly when radiation protection glasses. Dn and PSD are useful value to estimate the interventionalist's dose to the eye lens.

# **CLINICAL RELEVANCE/APPLICATION**

Our result showed interventionalist's dose to the eye may exceed the recommended dose by ICRP 2011. Understanding radiationinduced cataract and the appropriate personal monitoring are crucial. 1H NMR Based Metabolic Signatures to Predict Early Response to Transarterial Chemoembolization for Patients with Hepatocellular Carcinoma

Th

Participants Zhihui Chang, BMedSc, MMed, Shenyang, China (*Presenter*) Nothing to Disclose Jiahe Zheng, Shenyang, China (*Abstract Co-Author*) Nothing to Disclose Zhaoyu Liu, MD, Shenyang, China (*Abstract Co-Author*) Nothing to Disclose Qiyong Guo, MD, Shenyang, China (*Abstract Co-Author*) Nothing to Disclose

#### PURPOSE

We used proton nuclear magnetic resonance (1H NMR) to profile the serum metabolome in patients with hepatocellular carcinoma (HCC) and determine whether a disease signature may exist that is strong enough tc METHOD AND MATERIALS

Metabolic profiling of blood serum was analysised in 100 patients with HCC before TACE and 3 days after TACE and compared with 100 healthy control subjects. The correlations between Metabolic signatures and si

# term tumor imaging response were analyzed. Imaging follow-up was performed one to three months after TACE. Response to treatment was grouped according to RECIST (Response Evaluation Criteria in Solid Tumors). Statistical analysis used paired t test and Fisher exact te

#### RESULTS

1H NMR metabolomic profiling could discriminate patients with HCC from healthy subjects with a cross validated accuracy of 100% 100 patients with HCCs had follow up imaging at mean 39 days post TACE. Accordin responders. Where as no significant change was observed in responders (P<0.001).

#### CONCLUSION

Both pre- and post treatment blood serum levels of choline compounds have potential to predict response to TACE for Patients with HCC.

#### **CLINICAL RELEVANCE/APPLICATION**

Metabolomic profiling is a promising approach to predict early response to TACE for patients with HCC and is recommended for early estimation of the efficacy of TACE in HCC patients.

How Fast Can you Go? Novel Techniques for Breast MRI Acquisition

Thursday, Dec. 1 12:45PM - 1:15PM Room: BR Community, Learning Center Hardcopy Backboard

#### **Participants**

Deepa Sheth, MD, Chicago, IL (*Presenter*) Nothing to Disclose Naoko Mori, MD, PhD, Sendai, Japan (*Abstract Co-Author*) Nothing to Disclose Keiko Tsuchiya, Otsu, Japan (*Abstract Co-Author*) Nothing to Disclose Gregory S. Karczmar, PhD, Chicago, IL (*Abstract Co-Author*) Nothing to Disclose Hiroyuki Abe, MD, Chicago, IL (*Abstract Co-Author*) Nothing to Disclose Federico Pineda, PhD, Chicago, IL (*Abstract Co-Author*) Nothing to Disclose

# TEACHING POINTS

(1) Review the basic acquisition protocol of conventional dynamic contrast enhanced MRI (DCE-MRI)(2) Describe acquisition protocols for three novel breast MRI techniques: abbreviated MRI accelerated MRI true fast technique (ultrafast) view sharing technique (TWIST) (3) Illustrate the various differences between the techniques with regards to technical aspects, image acquisition and image interpretation

#### **TABLE OF CONTENTS/OUTLINE**

(1) Review of the basic acquisition protocol for three novel breast MRI techniques: abbreviated MRI accelerated MRI true fast technique (ultrafast) view sharing technique (TWIST) (2) Demonstration of exemplary cases illustrating each techniques' unique acquisition(3) Discussion of the similarities and differences between the various techniques with regards to technical aspects, image acquisition and image interpretation

# BR271-SD-THB1

Negative Predictive Value of Mammography and Sonography in the Evaluation of a Focal Area of Clinical Concern in the Fatty Breast

Thursday, Dec. 1 12:45PM - 1:15PM Room: BR Community, Learning Center Station #1

#### Awards

**Student Travel Stipend Award** 

#### Participants

Eric M. Blaschke, MD, Boston, MA (*Presenter*) Nothing to Disclose Michelle C. Specht, MD, Boston, MA (*Abstract Co-Author*) Nothing to Disclose Sophie M. Cowan, MD, Boston, MA (*Abstract Co-Author*) Nothing to Disclose Barbara L. Smith, MD, PhD, Boston, MA (*Abstract Co-Author*) Nothing to Disclose Kevin S. Hughes, MD, Boston, MA (*Abstract Co-Author*) Nothing to Disclose Constance D. Lehman, MD, PhD, Boston, MA (*Abstract Co-Author*) Nothing to Disclose Barbara L. Electric Company; Medical Advisory Board, General Electric Company

Michele Gadd, MD, Boston, MA (Abstract Co-Author) Nothing to Disclose

#### PURPOSE

The American College of Radiology (ACR) Appropriateness Criteria support the option of mammography alone in women with only fatty breast tissue at the site of clinical concern, although there is scarce literature to support this recommendation. We assess the performance of mammography and ultrasound in patients with fatty breasts presenting with an area of clinical concern.

# METHOD AND MATERIALS

This IRB approved study included 1,028 consecutive cases in 876 women with fatty breast density who presented with an area of clinical concern and underwent combined mammography and sonography between 3/2006 and 3/2015. Outcomes were determined by imaging, biopsy, or any pathology in our hospital tumor registry within a minimum of 12 months follow up. Performance measures were defined according to the ACR BI-RADS Atlas, Fifth Edition.

#### RESULTS

Of the 876 women (mean age 56.2, range 24-92), 775 (88.5%) were assessed as BI-RADS 1 or 2, 61 (7.0%) as BI-RADS 3, and 40 (4.6%) as BI-RADS 4 or 5 by mammography and ultrasound combined. 20 cancers were diagnosed, for a cancer detection rate of 22.8 per 1000 women. Performance metrics of mammography were: sensitivity 90%, specificity 98.8%, negative predictive value 99.8%. Of the two breast cancers not seen with mammography, one case was a parasternal mass in a patient with prior mastectomy and reconstruction for DCIS and the second was an infiltrating lobular carcinoma in a focal region of density in an otherwise fatty breast found by ultrasound in a 73 year old BRCA positive patient. Performance metrics of combined mammography and ultrasound were: sensitivity 100%, specificity 98.0%, NPV 100%.

#### CONCLUSION

No breast cancers were missed by mammography in patients with fatty breast tissue at the site of clinical concern. These findings support the current ACR Appropriateness Criteria allowing the option of mammography alone in this specific clinical setting.

# **CLINICAL RELEVANCE/APPLICATION**

The high negative predictive value of mammography supports the judicious, rather than routine, use of ultrasound in patients with fatty breast density presenting with areas of clinical concerns.

Perfusion Parameters at Dynamic Contrast-enhanced Breast MR Imaging are Associated with Disease-Specific Survival in Patients with Triple-Negative Breast Cancer

Thursday, Dec. 1 12:45PM - 1:15PM Room: BR Community, Learning Center Station #3

# Participants

Vivian Y. Park, MD, Seoul, Korea, Republic Of (*Presenter*) Nothing to Disclose Eun-Kyung Kim, Seoul, Korea, Republic Of (*Abstract Co-Author*) Nothing to Disclose Min Jung Kim, MD, Seoul, Korea, Republic Of (*Abstract Co-Author*) Nothing to Disclose Jung Hyun Yoon, MD, Seoul, Korea, Republic Of (*Abstract Co-Author*) Nothing to Disclose Hee Jung Moon, MD, Seoul, Korea, Republic Of (*Abstract Co-Author*) Nothing to Disclose

# PURPOSE

The aim of this study is to investigate the association between perfusion parameters in pretreatment MR imaging and survival outcome (disease-free survival [DFS], disease-specific survival [DSS]) in patients with triple negative breast cancer (TNBC).

# **METHOD AND MATERIALS**

Sixty-one patients (median age, 50 years; range, 27-77 years) with TNBC (median size on MR imaging, 255 mm; range, 11-142 mm) who underwent pretreatment MR imaging between November 2010 and August 2012 were included. We analyzed clinical-pathologic variables and MR imaging parameters (including SER, peak enhancement, Ktrans, kep, ve). Calculation of perfusion parameters was performed with dedicated post-processing software, using a semi-automated segmentation method. Cox proportional hazards models were used to determine associations between survival outcome and 1) variables obtainable before treatment (age, menopausal status, MR imaging features, preoperative diagnosis of lymph node metastasis,) and 2) post-treatment clinical-pathologic variables

# RESULTS

The median follow-up time was 46.1 months (range, 6.3- 58.4 months). Eleven of 61 (18.0%) patients had events and seven (11.4%) died from breast cancer. Among pretreatment variables, a larger tumor size on MR images (hazard ratio [HR]=1.024, P=.003) was associated with worse DFS at univariate analysis. In multivariate pretreatment models for DSS, a higher ve value (HR=1.658, P=.038), higher peak enhancement (HR=1.843, P=.018) and a larger tumor size on MR images (HR=1.060, P=.001) were associated with worse DSS. In multivariate post-treatment models, a larger pathologic tumor size (HR for DFS, 1.074 [P=.005]; HR for DSS, 1.050 [P=.042]) and metastasis in surgically resected axillary lymph nodes (HR for DFS, 5.789 [P=.017]; HR for DSS, 23.717 [P =.002]) were associated with worse survival outcome.

#### CONCLUSION

A higher ve value, peak enhancement and larger tumor size of the primary tumor at pretreatment MR imaging were independent predictors of worse DSS in TNBC patients.

# **CLINICAL RELEVANCE/APPLICATION**

For patients with triple-negative breast cancer, a ve value, peak enhancement, and tumor size on pretreatment MR imaging may be incorporated into pretreatment prediction models that can aid in tailoring clinical trial populations and treatment.

# Contrast Enhanced Mammography as a Promising Method of Differentiating Breast Lesions

Thursday, Dec. 1 12:45PM - 1:15PM Room: BR Community, Learning Center Station #4

#### **Participants**

Shayandokht Taleb, Minneapolis, MN (*Presenter*) Nothing to Disclose Bryan Donald, MD, St Paul, MN (*Abstract Co-Author*) Nothing to Disclose Noelle E. Hoven, MD, Minneapolis, MN (*Abstract Co-Author*) Nothing to Disclose Tim H. Emory, MD, Saint Paul, MN (*Abstract Co-Author*) Nothing to Disclose Jessica E. Kuehn-Hajder, MD, Minneapolis, MN (*Abstract Co-Author*) Nothing to Disclose

#### PURPOSE

To determine the accuracy of contrast-enhanced digital mammography(CEDM) in differentiating malignant versus benign breast lesions.

# **METHOD AND MATERIALS**

We retrospectively reviewed the medical and imaging records of all patients who had CEDM at our center from Dec 2012 to Sep 2015 and subsequently underwent imaging guided core needle biopsy. During this time, CEDM was used both for high-risk screening and for staging and characterization pre-biopsy for BI-RADS 4b, 4c and 5 lesions. A single reader reviewed all images and compared the interpretation with final clinical report. In case of discrepancy in interpretation of images, a second reader reviewed all images to reach consensus. The data on calcifications and enhancement were recorded. Histopathology of specimen biopsy was also reviewed and considered as gold standard to classify the lesions as malignant or nonmalignant.

# RESULTS

In a 3-year period, 164 women with mean age of 52 (range: 25-79) underwent CEDM at our center and had imaging guided core needle biopsies performed. Biopsy was recommended based on diagnostic mammography/ultrasound workup of symptoms, abnormal physical exam or screening callback. The results demonstrated that enhancement on CEDM was significantly associated with malignancy (P<0.001). Enhancement on CEDM had 95.3% sensitivity, 50.0% specificity, 85.3 % negative predictive value, and 77.7% positive predictive value for detection of malignant lesions. The receiver operating characteristic (ROC) analysis showed an area under the curve of 0.726(P<0.001). When cases with suspicious calcifications and/or abnormal enhancement were combined, sensitivity was 100%, specificity was 29.3%, negative predictive value was 100% and positive predictive value was 72.1% for detection of malignant lesions. Thus, all cases that did not have either suspicious calcifications or abnormal enhancement were found to be benign.

# CONCLUSION

In a population with highly suspicious lesions, enhancement on CEDM is sensitive for malignancy/atypia. And, when combined with suspicious calcifications, a negative predictive value of 100% suggests that it is possible to downgrade a lesion to probably benign. We hope that as we increase the study population size this finding will be confirmed.

# **CLINICAL RELEVANCE/APPLICATION**

Contrast enhanced mammography appears to add significant sensitivity to other suspicious mammographic findings in differentiation of malignancy/atypia versus benign lesions.

MRI to Predict Nipple-areola Complex (NAC) Involvement: An Automatic Method to Compute the 3D Distance between the NAC and Tumor

Thursday, Dec. 1 12:45PM - 1:15PM Room: BR Community, Learning Center Station #5

# Participants

Valentina Giannini, PhD, Candiolo, Italy (*Presenter*) Nothing to Disclose Emanuele Tabone, Candiolo, Italy (*Abstract Co-Author*) Nothing to Disclose Valeria Doronzio, Candiolo, Italy (*Abstract Co-Author*) Nothing to Disclose Francesca Maria Sambataro, Candiolo, Italy (*Abstract Co-Author*) Nothing to Disclose Daniele Regge, MD, Torino, Italy (*Abstract Co-Author*) Speakers Bureau, General Electric Company Laura Martincich, MD, Candiolo, Italy (*Abstract Co-Author*) Speaker, Bracco Group Consultant, Bayer AG

# PURPOSE

To describe and test an innovative and automatic method able to compute the 3D tumor-NAC distance, by automatically segmenting both the tumor and the NAC, and to assess its role in predicting NAC involvement.

# METHOD AND MATERIALS

99 patients scheduled to NAC sparing mastectomy underwent MR examination at 1.5T, including at least the sagittal T2w and DCE MR imaging. The method developed to compute the 3D tumor-NAC distance consists of different steps. First, the NAC is segmented on the T2w sagittal image, by using a region growing algorithm in which the seeds and the thresholds are automatically found and set based on patients characteristics. Then, the tumor is segmented on the Maximum Intensity Projection over Time image, by extracting contrast-enhanced regions using a normalization technique based on the contrast-uptake of mammary vessels. Finally, the 3D distance is computed between the base of the NAC and the nearest margin of the lesion. Manually axial and sagittal 2D measurements were also evaluated and compared with the 3D distance. NAC involvement was defined by the presence of invasive ductal/lobular carcinoma and/or ductal carcinoma in situ/ductal intraepithelial neoplasia.

# RESULTS

Overall, the tumor-NAC distance was computed on a dataset of 95/99 patients, since 3 patients were discarded because their lesions were not segmented (sensitivity=97%), and one was removed because its inversed nipple was not detected by the system (sensitivity=99%). Among them, 25 had NAC involvement (26.3%). Area under the ROC curve (AUC) was equal to 0.830 (95% CI: 0.749-0.911) for the automatic distance, 0.676 (95% CI: 0.557-0.796) for the manual axial distance, 0.664 (95% V CI: 0.542-0.786) for the manual sagittal distance, and 0.664 (95%CI: 0.542-0.783) for the minimum manual distance. The best performances were obtained by the automatic distance at the cut-off point of 21 mm, where sensitivity, specificity, positive predictive value and negative predictive value were 72%, 80%, 56% and 89%, respectively.

# CONCLUSION

The proposed automatic method outperformed the results obtained with the manual 2D measurements in assessing the NAC involvement.

# **CLINICAL RELEVANCE/APPLICATION**

This method could be integrated in the clinical practice to reduce the reading time, the inter-observer variability and to provide reliable information for surgical planning and intraoperative management of candidate patients to the NAC sparing mastectomy.

Ascending Aorta Size in Patients with Aortic Stenosis Undergoing Transcatheter Aortic Valve Replacement: Debunking the Theory of Post-stenotic Dilation

Thursday, Dec. 1 12:45PM - 1:15PM Room: CA Community, Learning Center Station #1

# Participants

Anthony Ronco, Vacaville, CA (*Presenter*) Nothing to Disclose Sumudu N. Dissanayake, MD, Los Angeles, CA (*Abstract Co-Author*) Nothing to Disclose Luis A. Del Carpio B, MD, Los Angeles, CA (*Abstract Co-Author*) Nothing to Disclose Alison Wilcox, MD, Los Angeles, CA (*Abstract Co-Author*) Speaker, Toshiba Corporation Farhood Saremi, MD, Los Angeles, CA (*Abstract Co-Author*) Nothing to Disclose Christopher Lee, MD, Los Angeles, CA (*Abstract Co-Author*) Nothing to Disclose

# PURPOSE

Previous studies have hypothesized that aortic valve stenosis leads to dilation of the ascending aorta secondary to a post-stenotic dilation phenomenon. The purpose of this study is to dispute this theory with a retrospective review of patients with clinically significant aortic stenosis undergoing preoperative CT angiography (CTA) for transcatheter aortic valve replacement (TAVR).

#### **METHOD AND MATERIALS**

120 patients (mean age  $80.2 \pm 8.4$  years) undergoing preoperative CTA for TAVR between August 2014 and January 2016 were reviewed. All scans were performed on a 320-slice CT with retrospective gating. Maximum ascending aorta diameter and area were measured using centerline technique on a 3-D workstation. Spearman correlations were used to test relationships between ascending aorta size and preoperative echocardiographic measurements of aortic valve area, peak velocity, and peak gradient.

## RESULTS

Maximum ascending aorta median diameter was 3.5 cm (interquartile range [IQR] 3.3 - 3.8 cm) and median area was 900 mm2 (IQR 803 - 1120 mm2). 19 of 120 (15.8%) patients had an ascending aorta diameter over 4 cm and 3 of 120 (2.5%) had a diameter over 4.5 cm. On echocardiography, median aortic valve area was 0.7 cm, median aortic valve peak velocity was 3.9 m/s, and median aortic valve peak gradient was 61.3 mmHg. There were no significant correlations between maximum ascending aorta diameter and echocardiographic measurements of aortic valve area (R=0.16, p=0.08), peak velocity (R=-0.04, p=0.69), and peak pressure gradient (R=0.06, p=0.49). There were also no significant correlations between maximum ascending aorta area and the same echocardiographic measurements.

# CONCLUSION

The ascending aorta was normal in size in the vast majority of patients undergoing evaluation for TAVR despite clinically significant aortic stenosis. There was no significant correlation between ascending aorta size and echocardiographic markers of aortic stenosis.

# **CLINICAL RELEVANCE/APPLICATION**

Contrary to previous theories, aortic valve stenosis does not result in post-stenotic dilation of the ascending aorta.

Signal Density Spectrum of Myocardial Perfusion Defects using Virtual Monochromatic Imaging Derived from Dual Energy Computed Tomography

Thursday, Dec. 1 12:45PM - 1:15PM Room: CA Community, Learning Center Station #2

# Participants

Patricia M. Carrascosa, MD, Buenos Aires, Argentina (*Presenter*) Research Consultant, General Electric Company Macarena De Zan, Vicente Lopez, Argentina (*Abstract Co-Author*) Nothing to Disclose Carlos Capunay, MD, Buenos Aires, Argentina (*Abstract Co-Author*) Nothing to Disclose Roxana Campisi, Vicente Lopez, Argentina (*Abstract Co-Author*) Nothing to Disclose Gaston Rodriguez Granillo, Vicente Lopez, Argentina (*Abstract Co-Author*) Nothing to Disclose Alejandro Deviggiano, MD, Vicente Lopez, Argentina (*Abstract Co-Author*) Nothing to Disclose

### PURPOSE

Virtual monochromatic imaging derived from dual energy imaging has shown the ability to attenuate beam hardening artifacts (BHA). The energy thresholds for the discrimination between normal myocardial perfusion and BHA have been previously established. Nonetheless, the signal density (SD) spectrum of perfusion defects remains poorly understood. Accordingly, we sought to explore the differences in the SD spectrum of myocardial segments with normal perfusion, compared to those with fixed and reversible perfusion defects using dual energy CTP (DE-CTP).

# **METHOD AND MATERIALS**

The present prospective study involved patients with known or suspected CAD clinically referred for myocardial perfusion imaging by SPECT. All patients underwent dipyridamole stress DE-CTP, as well as rest DE-CTP. Rapid switching between low and high tube potentials (80-140 kV) from a single source, allowed the generation of monochromatic image reconstructions with 10 keV increments from 40 to 140 keV.

#### RESULTS

Thirty-six patients were included in the study. The mean age was  $62.1\pm11.4$  years. Ten patients (28 %) had no evidence of myocardial perfusion defects by DE-CTP, 6 (17 %) had  $\geq 1$  segment with fixed perfusion defects, 7 (19 %) had  $\geq 1$  segment with reversible perfusion defects, and 13 (36 %) patients had evidence of both fixed and reversible perfusion defects. The mean effective radiation dose associated to DE-CTP (stress +rest) was  $8.3\pm1.9$  mSv, compared to  $9.8\pm3.4$  mSv with SPECT (p=0.004). The sensitivity, specificity, PPV and NPV of DE-CTP for the identification of perfusion defects was 84 %, 94 %, 77 %, and 96 %. The largest SD differences between segments with normal perfusion and those with perfusion defects were observed among low energy levels (sensitivity of 96 % and specificity of 98 % using a cut-off value  $\leq 153$  HU at 40 keV), progressively declining at the highest energy levels [area under the ROC curve of 40 keV= 0.98 vs.80 keV= 0.94 vs. 140 keV= 0.73 (p<0.001 for all comparisons).

# CONCLUSION

In this study, virtual monochromatic imaging derived from DE-CTP allowed accurate discrimination of perfusion defects, being the lowest energy level (40 keV) the one with the highest diagnostic performance for the detection of perfusion defects.

# **CLINICAL RELEVANCE/APPLICATION**

Dual energy CT cardiac perfusion allowed accurate discrimination of perfusion defects due to its ability to attenuate beam hardening artifacts that can simulate myocardial pathology.

# CA259-SD-THB3

Quantification of Myocardial Susceptibility as an Imaging Biomarker of Cardiac Diseases: Initial Experience in Cardiac Amyloidosis

Thursday, Dec. 1 12:45PM - 1:15PM Room: CA Community, Learning Center Station #3

# Participants

Seitaro Oda, MD, Kumamoto, Japan (*Presenter*) Nothing to Disclose Takeshi Nakaura, MD, Kumamoto, Japan (*Abstract Co-Author*) Nothing to Disclose Tetsuya Yoneda, PhD, Kumamoto, Japan (*Abstract Co-Author*) Nothing to Disclose Daisuke Utsunomiya, MD, Kumamoto, Japan (*Abstract Co-Author*) Nothing to Disclose Hideaki Yuki, MD, Kumamoto, Japan (*Abstract Co-Author*) Nothing to Disclose Masafumi Kidoh, Kumamoto, Japan (*Abstract Co-Author*) Nothing to Disclose Kenichiro Hirata, Kumamoto, Japan (*Abstract Co-Author*) Nothing to Disclose Narumi Taguchi, Kumamoto, Japan (*Abstract Co-Author*) Nothing to Disclose Yasuyuki Yamashita, MD, Kumamoto, Japan (*Abstract Co-Author*) Nothing to Disclose

### PURPOSE

Magnetic susceptibility is a physical tissue property that varies in healthy tissue and may also change with pathologic conditions. We evaluated whether quantification of myocardial susceptibility by cardiac magnetic resonance (CMR) is useful for detection of cardiac involvement in amyloidosis.

### **METHOD AND MATERIALS**

Sixteen cardiac amyloidosis patients underwent 3.0T CMR including magnetic phase imaging with multi-echo spoiled gradient echo sequence. Their myocardial susceptibility was quantified by magnetic phase analysis; measurement of phase values for each echo time, then the phase shift slope was obtained by the method of least squares. Those were compared with 15 healthy volunteers. The diagnostic performance of myocardial susceptibility imaging was also assessed using receiver operating characteristic curve (ROC) analysis.

# RESULTS

There was significant difference in the myocardial susceptibility (magnetic phase shift in myocardium) between cardiac amyloidosis patients and healthy volunteers. The ROC analysis demonstrated that the area under curve of 0.858 for the slope of the myocardial phase shift, and 0.908 when using a logistic regression model.

## CONCLUSION

The quantification of myocardial susceptibility by CMR is capable of identifying cardiac involvement in amyloidosis.

### **CLINICAL RELEVANCE/APPLICATION**

The quantification of myocardial susceptibility by CMR offers new insights into cardiac diseases. It may be able to identify cardiac involvement in patient with amyloidosis.

# Relative Value of Cardiac MRI and FDG-PET in the Initial Diagnosis of Cardiac Sarcoidosis

Thursday, Dec. 1 12:45PM - 1:15PM Room: CA Community, Learning Center Station #4

#### Participants

Richard A. Coulden, MD, Edmonton, AB (*Presenter*) Nothing to Disclose Andrew M. Crean, MD, Toronto, ON (*Abstract Co-Author*) Research support, sanofi-aventis Group Emer P. Sonnex, MPhil, Edmonton, AB (*Abstract Co-Author*) Nothing to Disclose Jonathan T. Abele, MD, Edmonton, AB (*Abstract Co-Author*) Nothing to Disclose

# PURPOSE

Sarcoidosis is a multisystem disorder with cardiac involvement in 25%. Diagnosis of cardiac sarcoidosis is difficult, with FDG-PET and cardiac MR (CMR) proving most reliable. We compare FDG-PET and CMR with late gadolinium enhancement (LGE) in patients with suspected cardiac sarcoidosis.

### METHOD AND MATERIALS

89 patients with suspected cardiac sarcoidosis were investigated with FDG-PET and CMR within 2 weeks (82 same day). Patients undergoing FDG-PET followed a 24 hour low-carbohydrate diet and overnight fast. CMR included SSFP assessment of left ventricular (LV) function and LGE. Images were reviewed by 2 readers blinded to the results of the other examination. FDG-PET was considered positive if any segment (17 segment model) had an SUVmax>3.6. CMR was considered positive if any segment showed 'sarcoid-type' LGE. Patients with biopsy proven sarcoid or lung CT changes consistent with sarcoid were classified according to modified Japanese Ministry of Health & Welfare guidelines as JMHW +ve or -ve (Ohira. Eur J Nucl Med Mol Imaging 2016:43:259).

## RESULTS

82 patients had biopsy proven or lung CT evidence of sarcoid. Of these, 13 met JMHW criteria and all showed myocardial FDG uptake. 10 also showed LGE on CMR. In 69 JMHW -ve patients, 20 showed myocardial FDG uptake with 8 also showing LGE. 5 patients had LGE with no myocardial FDG uptake and 44 showed neither FDG uptake nor LGE. In 7 patients with unexplained arrhythmia but no pathology or lung CT changes of sarcoid, 1 showed myocardial FDG uptake with LGE and 3 showed LGE alone. 3 showed neither FDG uptake nor LGE. 19 patients had LV impairment, 8 were JMHW +ve (62%) and 8 JMHW -ve (12%). Patients with arrhythmia but without known sarcoid were also more likely to have LV impairment (33%).

# CONCLUSION

FDG-PET detects cardiac sarcoid in all JMHW +ve patients with LGE in 77%. In JMHW -ve patients, both techniques can be positive, either together or independently. In those who only show LGE, there is often no extracardiac FDG uptake to indicate active sarcoid elsewhere. In the heart, FDG appears to show active sarcoid whereas LGE shows more advanced disease that has gone on to scar. The presence of LGE is often associated with LV impairment.

#### **CLINICAL RELEVANCE/APPLICATION**

Current literature suggests FDG-PET and CMR are equivalent in detecting cardiac sarcoidosis. This is not our experience. FDG-PET and CMR are complimentary and should be used together whenever possible.

Quantification of the Cardiac Ventricular Functional Parameters: A Comparative Study between Computed Tomography and Cardiac Magnetic Resonance Imaging

Thursday, Dec. 1 12:45PM - 1:15PM Room: CA Community, Learning Center Station #5

### **Participants**

Jae Wook Lee, MD, Seoul, Korea, Republic Of (*Presenter*) Nothing to Disclose Dong Hyun Yang, MD, Seoul, Korea, Republic Of (*Abstract Co-Author*) Nothing to Disclose Joon-Won Kang, MD, Seoul, Korea, Republic Of (*Abstract Co-Author*) Nothing to Disclose Tae-Hwan Lim, MD, PhD, Seoul, Korea, Republic Of (*Abstract Co-Author*) Nothing to Disclose Hongseok Ko, MD, Munich, Germany (*Abstract Co-Author*) Nothing to Disclose

# PURPOSE

To compare the ventricular functional parameters measured with computed tomography (CT) and cardiac magnetic resonance (CMR) imaging.

### **METHOD AND MATERIALS**

We retrospectively reviewed one-hundred seventeen individuals (62 male, 55 female, age range, 21-80 years; median age 58 years) with cardiac disease who underwent both CT and CMR within 30 days of interval (mean 3.5 days). Volumetric analysis was performed on commercialized software products syngo.via (Siemens Healthcare Global) using contiguous multiphase CT data and cvi42 (Circle Cardiovascular Imaging) using short-axis cine CMR. Pearson correlation and Bland-Altman analyses were performed. The intra- and interobserver variability were calculated on the randomly selected patient (n=29) by means of intraclass correlation coefficient (ICC).

### RESULTS

Functional parameters of left ventricle (LV) were well-correlated between CT and CMR (r=0.79 to 0.95). On the Bland-Altman analysis, CT tended to underestimate LV end-diastolic volume (EDV) and LV end-systolic volume (ESV) (LV EDV=- $9.6 \pm 15.6\%$ , LV ESV=- $29.9 \pm 33.7\%$ ), and overestimate ejection fraction (EF) and myocardial mass (LV EF= $14.2 \pm 23.4\%$ , LV mass= $11.5 \pm 14.4\%$ ) than CMR. Functional parameters of right ventricle (RV) were well-correlated between CT and CMR (r=0.76 to 0.90), except for moderate correlation of EF (r=0.66). RV EDV and RV ESV were overestimated by CT on the Bland-Altman Analysis (RV EDV= $11.0 \pm 19.3\%$ , RV ESV= $6.6 \pm 28.4\%$ ). CT showed high reproducibility on both LV and RV functional parameters (intraobserver ICC; LV=0.98 to 1.00, RV=0.81 to 0.95, interobserver ICC; LV=0.97 to 0.99, RV=0.82 to 0.96) and CMR showed high reproducibility on LV functional parameters and moderate reproducibility on RV functional parameters (intraobserver ICC; LV=0.97 to 0.99, RV=0.55 to 0.81, interobserver ICC; LV=0.92 to 0.99, RV=0.59 to 0.89).

# CONCLUSION

Functional parameters measured from CT and CMR generally showed good correlation, but also manifest some difference; CT tended to underestimate LV EDV and LV ESV compared to CMR, whereas overestimate LV myocardial mass, RV EDV and RV ESV. LV functional parameters were highly reproducible on both CT and CMR, whereas RV functional parameters were only highly producible on CT.

# **CLINICAL RELEVANCE/APPLICATION**

Either CT or CMR can be used reliably when measuring cardiac ventricular functional parameters.

# CH173-ED-THB7

Four-dimensional Chest CT with Free Breathing: The use of Dynamic-ventilatory Scanning for Various Thoracic Diseases

Thursday, Dec. 1 12:45PM - 1:15PM Room: CH Community, Learning Center Station #7

# Participants

Tsuneo Yamashiro, MD, Nishihara, Japan (*Presenter*) Research Grant, Toshiba Corporation Hiroshi Moriya, MD, Fukushima-City, Japan (*Abstract Co-Author*) Nothing to Disclose Yukihiro Nagatani, MD, Otsu, Japan (*Abstract Co-Author*) Nothing to Disclose Osamu Honda, MD, PhD, Suita, Japan (*Abstract Co-Author*) Nothing to Disclose Atsuko Fujikawa, MD, PhD, Kawasaki, Japan (*Abstract Co-Author*) Nothing to Disclose Sadayuki Murayama, MD, PhD, Nishihara-Cho, Japan (*Abstract Co-Author*) Research Grant, Toshiba Corporation

### **TEACHING POINTS**

Dynamic-ventilatory scanning is a novel fluoroscopic method of chest CT, which can be acquired by 320- or 256-row scanners (Aquilion ONE by Toshiba and Revolution CT by GE) and can visualize respiratory movement of the thorax with a wide length (160 mm). Compared with conventional CT, the various respiratory motions of thoracic structures can be solely visualized using dynamic-ventilation CT, which is useful to understand pathophysiology in the airways and lung. In this exhibit, we aim (1) to introduce some recommended methods for scanning and reconstruction, (2) to summarize the current achievements for various chest diseases, and (3) to introduce our perspective for the future use of dynamic-ventilation CT.

### **TABLE OF CONTENTS/OUTLINE**

**1.** *Methodology* Scanning: time length, radiation exposure, control of breathingPost-processing: time resolution, data volume, additional interpolation2. *Interpretation*Viewing: currently available viewers and workstationsReading: 4D-movie vs automatic tracking on 2D-image3. *Clinical applications and current achievements* Airways: tracheal stenosis, tracheobronchomalacia, asthma, COPDAround tumors: preoperative analysis of pleural invasion or adhesionInside the lung: heterogeneity of motion in COPD and transplanted lung4. *Future use*Automated analysis for the airway, lung, and pleura

## A Wolf in Sheep's Clothing - Lung Cancers with Benign Features on CT

Thursday, Dec. 1 12:45PM - 1:15PM Room: CH Community, Learning Center Station #8

#### **Participants**

Maria D. Martin, MD, Madison, WI (Presenter) Nothing to Disclose

Cristopher A. Meyer, MD, Madison, WI (*Abstract Co-Author*) Stockholder, Cellectar Biosciences, Inc Investor, NeuWave, Inc Lynn S. Broderick, MD, Madison, WI (*Abstract Co-Author*) Nothing to Disclose Jeffrey P. Kanne, MD, Madison, WI (*Abstract Co-Author*) Research Consultant, PAREXEL International Corporation; Advisory Board, F. Hoffmann-La Roche Ltd

#### **TEACHING POINTS**

Certain lung cancer morphologies can be confused with non-malignant conditions Illustrate and compare ambiguous imaging findings in cases of biopsy proven lung cancers Discuss how data in this era of lung cancer screening and volumetric CT provides insight into the many manifestations of lung cancer Describe strategies to avoid misclassifying lung cancers as benign lesions

## **TABLE OF CONTENTS/OUTLINE**

Examples of lung cancers with morphologic characteristics more typical of benign processes (in parenthesis) Cavity/Cyst will progressive wall thickening (inflammation) Consolidation (pneumonia) Linear opacity (atelectasis) Filling defect in cavities (aspergilloma) Pseudocentral calcification (granuloma) Fat attenuation lesion (hamartoma) Tree-in bud opacity (bronchopneumonia) Distal mucocele (bronchial atresia)Each case will be analyzed, and strategies to avoid misdiagnosis will be discussed

#### **Honored Educators**

Presenters or authors on this event have been recognized as RSNA Honored Educators for participating in multiple qualifying educational activities. Honored Educators are invested in furthering the profession of radiology by delivering high-quality educational content in their field of study. Learn how you can become an honored educator by visiting the website at: https://www.rsna.org/Honored-Educator-Award/

Jeffrey P. Kanne, MD - 2012 Honored Educator Jeffrey P. Kanne, MD - 2013 Honored Educator

Dual-Energy Chest Radiograph: Can Bone-selective Images Increase Radiologists' Detection of Bone Metastasis?"

Thursday, Dec. 1 12:45PM - 1:15PM Room: CH Community, Learning Center Station #1

# Participants

Marcelo K. Benveniste, MD, Houston, TX (*Presenter*) Nothing to Disclose Sonia L. Betancourt Cuellar, MD, Houston, TX (*Abstract Co-Author*) Nothing to Disclose Girish S. Shroff, MD, Houston, TX (*Abstract Co-Author*) Nothing to Disclose Patricia M. de Groot, MD, Houston, TX (*Abstract Co-Author*) Nothing to Disclose Jia Sun, Houston, TX (*Abstract Co-Author*) Nothing to Disclose Jeremy J. Erasmus, MD, Houston, TX (*Abstract Co-Author*) Nothing to Disclose Myrna C. Godoy, MD, PhD, Houston, TX (*Abstract Co-Author*) Research Grant, Siemens AG

# PURPOSE

Evaluate if the use of dual-energy (DE) subtraction images increases radiologist's detection of bone metastasis on chest radiographs.

## METHOD AND MATERIALS

100 consecutive chest radiographs performed in patients with metastatic bone lesions identified on same-day chest CT were retrospectively selected, including 50 patients with lytic and 50 patients with sclerotic bone metastases. 100 consecutive chest radiographs without metastatic bone lesions confirmed on same-day chest CT were included as control group. The selected 200 cases were presented to 3 board-certified chest radiologists in two manners: 1) posteroanterior (PA) and lateral images only (conventional X-ray) and 2) PA, lateral, PA with bone subtraction and PA bone selective images (DE X-ray), resulting in a total of 400 randomized de-identified chest radiograph datasets for review. Readers were blinded for any clinical or prior imaging information, including the same-day CT scan. They recorded the presence, type (sclerotic and lytic) and location (spine, rib, clavicle, scapula, sternum and humerus) of metastatic involvement. Accuracy, sensitivity, specificity, positive predictive value (PPV), and negative predictive value (NPV) were calculated to evaluate the yield of conventional X-ray versus DE X-ray for diagnosis of metastatic bone lesions. Comparison was performed using McNemar's test. All tests were two-sided and p-values of 0.05 or less were considered statistically significant. The study was approved by institutional review board.

#### RESULTS

Readers had significantly higher sensitivity, NPV and accuracy (52%, 68% and 76%, respectively) for detection of bone metastases using DE X-ray versus conventional X-ray (respectively, 26%, 59% and 63%; McNemar's Test P-value < 0.0001). The sensitivity for detection of both lytic and sclerotic bone metastasis was higher with DE X-ray (46% and 58%, respectively) versus conventional imaging (19% and 40%, respectively). The specificity and PPV was 100% for both methods.

# CONCLUSION

The addition of dual-energy selective bone images to conventional chest radiograph improves the diagnostic yield for detection of sclerotic and lytic bone metastases.

# **CLINICAL RELEVANCE/APPLICATION**

Dual-energy chest radiograph subtraction technique is a noninvasive, reliable, and reproducible imaging tool that helps in the assessment of bone metastasis.

### **Honored Educators**

Presenters or authors on this event have been recognized as RSNA Honored Educators for participating in multiple qualifying educational activities. Honored Educators are invested in furthering the profession of radiology by delivering high-quality educational content in their field of study. Learn how you can become an honored educator by visiting the website at: https://www.rsna.org/Honored-Educator-Award/

Sonia L. Betancourt Cuellar, MD - 2014 Honored Educator Jeremy J. Erasmus, MD - 2015 Honored Educator

Breath-Hold Black-Blood T2-weighted Lung Magnetic Resonance Imaging: Optimization of Blood-Flow Signal Suppression using Peripheral Pulse Unit Gating

Thursday, Dec. 1 12:45PM - 1:15PM Room: CH Community, Learning Center Station #2

# Participants

Ryotaro Kamei, MD, Fukuoka, Japan (*Presenter*) Nothing to Disclose Yuji Watanabe, MD, Kurashiki, Japan (*Abstract Co-Author*) Nothing to Disclose Koji Sagiyama, MD, Fukuoka, Japan (*Abstract Co-Author*) Nothing to Disclose Satoshi Kawanami, MD, Fukuoka, Japan (*Abstract Co-Author*) Nothing to Disclose Hiroshi Honda, MD, Fukuoka, Japan (*Abstract Co-Author*) Nothing to Disclose

# PURPOSE

To investigate the feasibility of breath-hold black-blood T2-weighted imaging (BB-T2WI) of the lungs using peripheral pulse unit (PPU) gating for obtaining high quality black-blood images of the lungs.

### **METHOD AND MATERIALS**

Eight male volunteers (28–58 years old) underwent magnetic resonance imaging (MRI) of the lungs with the 3.0-Tesla MR part of an Ingenuity TF PET/MR instrument (Phlips Healthcare). Breath-hold BB-T2WI was performed using the variable refocusing flip-angle (VRFA) technique in combination with PPU gating, during which the electrocardiogram and blood flow rates of the pulmonary artery and vein were monitored. For PPU gating, the trigger delay times were set as follows: (1) random (without gating), (2) shortest (166 ms), (3) longest (374–616 ms, depending on the participants' heart rate), and (4) intermediate (the average of (2) and (3)). T2WI scans without BB were also obtained, and used as references.The uniformity and degree of vascular suppression were assessed visually using a 5-point scale. The vascular signal suppression rate was assessed objectively by extracting the vessel area and measuring the areas with signal intensities >5 fold the standard deviation of the signal intensities of the interlobar fissure. Vascular signal suppression rates were compared between the 4 groups, with reference to non-BB prepared images. All statistical analyses were performed using repeated measures ANOVA and the Friedman test.

# RESULTS

In all the volunteers, the longest trigger delay constantly corresponded to the mid-systolic phase, whereas the shortest and the intermediate delays corresponded to the diastolic phase. The inter-slice uniformity and degree of vascular suppression were significantly higher in the longest trigger delay group than in the shortest and the intermediate trigger delay groups (p < 0.05). The longest trigger delay group showed a markedly better vascular signal suppression rate (76%/77%) compared to the random (59%/58%), shortest (46%/45%), and intermediate (48%/50%) trigger delay groups (right/left lung, p < 0.05).

### CONCLUSION

Black-blood lung MRI with PPU gating is feasible, and the longest trigger delay corresponding to the mid-systolic phase could provide high quality black-blood images of the lungs.

# **CLINICAL RELEVANCE/APPLICATION**

Breath-hold black-blood lung MRI with PPU gating is feasible and could provide high quality black-blood images that could increase the detection of lung nodular lesions.

# CH285-SD-THB3

Evaluation of Tumor Invasiveness of Thymic Epithelial Tumors using Magnetic Resonance Imaging: Correlation with the World Health Organization Histologic Classification System Updated in 2015 and Masaoka-Koga Staging System

Thursday, Dec. 1 12:45PM - 1:15PM Room: CH Community, Learning Center Station #3

FDA C

Discussions may include off-label uses.

### Participants

Asako Kuhara, Kurume, Japan (*Presenter*) Nothing to Disclose Kiminori Fujimoto, MD, PhD, Kurume, Japan (*Abstract Co-Author*) Nothing to Disclose Akiko Sumi, MD, Kurume, Japan (*Abstract Co-Author*) Nothing to Disclose Tomohiro Ebata, Kurume, Japan (*Abstract Co-Author*) Nothing to Disclose Shuji Nagata, MD, Kurume, Japan (*Abstract Co-Author*) Nothing to Disclose Toshi Abe, MD, Kurume, Japan (*Abstract Co-Author*) Nothing to Disclose

#### PURPOSE

To assess magnetic resonance (MR) imaging features with histological assessment and invasiveness of thymic epithelial tumors (TETs) based on the World Health Organization (WHO) histological classification updated in 2015 and to determine the useful finding in differentiating invasive tumors from non-invasive tumors.

#### **METHOD AND MATERIALS**

A total of 126 patients with a TET (94 thymomas and 32 thymic carcinomas) underwent MR imaging before surgery were retrospectively reviewed. There were 57 non-invasive tumors and 69 invasive tumors. Histological subtype of the TET was determined according to the WHO classification. MR imaging features were classified into 10 findings and 3 dynamic contrast-enhanced patterns and were assessed independently by two radiologists without knowledge of any clinical or histologic findings. These MR features were correlated with the histological subtypes and the useful findings for predicting the tumor invasiveness were assessed.

#### RESULTS

There was statistically significant relationship between WHO histological classification and tumor invasiveness (P < .001). All tumors were re-classified into three subtypes: 55 low-risk thymomas (types A, AB, and B1), 39 high-risk thymomas (types B2 and B3), and 32 thymic carcinomas.On MR imaging, thymic carcinomas were more likely to have irregular contour than other subtypes (P < .01). Low-risk thymomas were more likely to have low-intensity rim than other subtypes (P < .01). Signal intensity and Gd-DTPA enhancement of thymic carcinomas were more heterogenous than other subtypes (P < .005). With dynamic contrast-enhanced pattern, type B3 thymomas and thymic carcinomas were more likely to have a gradually signal increase pattern; other subtypes showed a rapidly increase with early peak pattern (P < .05). On diffusion-weighted imaging, the apparent diffusion coefficient (ADC) values of type B3 and carcinomas were statistically significant lower than those of other subtypes (P < .05).

# CONCLUSION

MR imaging characteristics of TETs correlate with the subtypes according to 2015 histological WHO classification; it was shown to reflect the tumor invasiveness; and it may be helpful in the prediction of prognosis.

### **CLINICAL RELEVANCE/APPLICATION**

Characteristic MR features of high-risk thymic tumors were irregular contour, invisible capsule, heterogenous signal intensities, heterogeous contrast-enhancement pattern, and lower ADC values.

Automatic Lung-RADS Classification of CT Lung Screening Reports with a Natural Language Understanding System

Thursday, Dec. 1 12:45PM - 1:15PM Room: CH Community, Learning Center Station #4

# Participants

Sebastian Beyer, MD, Burlington, MA (*Presenter*) Nothing to Disclose Brady J. McKee, MD, Burlington, MA (*Abstract Co-Author*) Spouse, Advisory Board, Medtronic plc Gilan El Saadawi, Pittsburgh, PA (*Abstract Co-Author*) Director, MModal IP LLC Andrea B. McKee, MD, Burlington, MA (*Abstract Co-Author*) Advisory Board, Medtronic plc; Speaker, Medtronic plc; ; Shawn M. Regis, PhD, Burlington, MA (*Abstract Co-Author*) Consultant, Medtronic plc Sebastian Flacke, MD, Burlington, MA (*Abstract Co-Author*) Consultant, BTG International Ltd Consultant, Surefire Medical, Inc Consultant, Koninklijke Philips BV Consultant, XACT Robotics Christoph Wald, MD, PhD, Burlington, MA (*Abstract Co-Author*) Radiology Advisory Committee, Koninklijke Philips NV

# PURPOSE

The aim was to train a natural language understanding (NLU) algorithm to capture all imaging characteristics of lung nodules reported in a structured CT report and suggest the applicable Lung-RADS (LR) category.

### **METHOD AND MATERIALS**

Our study included structured, clinical reports of clinical CT lung screening exams performed from August 2014 to August 2015 at an ACR certified Lung Screening Center. All patients screened were at high-risk for lung cancer according to the NCCN Guidelines. All exams were interpreted by 1 of 3 radiologists credentialed to read CT lung screening exams using ACR Lung-RADS. Training and test sets consisted of consecutive exams. A UIMA platform supporting a pipeline of iterative NLP tasks was used to map the information in the exam findings to the appropriate LR category or indicate that the identified descriptive image data was insufficient to determine the LR category. SNOWMED clinical findings concepts, extended by RadLex where appropriate, constituted the lexicon. Lung screening exams were divided into two groups: Three training sets (500, 120, and 383 reports each) and one final evaluation set (498 reports). NLU algorithm results were compared with the gold standard of LR category assigned by the radiologist.

#### RESULTS

The sensitivity and specificity of the NLU algorithm for correctly assigning LR categories for suspicious nodules (LR 3 or 4) were both 95.5 %. Misclassifications resulted from the failure to identify exams as follow-up and the failure to completely characterize part-solid nodules. The sensitivity and specificity to identify LR 2 among LR 1 and 2 nodules were 98.7 % and 99.7 %, respectively. The sensitivity and specificity to identify LR 4 among LR 3 and 4 nodules were 89.5 % and 94.4 %, respectively. Mismatches could also be noted if features such as inflammation or enlarged lymph nodes were present for which currently no LR guidelines exist.

## CONCLUSION

An NLU system to suggest the appropriate ACR LungRADS category is very sensitive and specific if underlying standardized reporting is used. As lung screening becomes more widely adopted, such a system may provide useful "look-over-the-shoulder" type assistance to novice interpreters of lung screening exams.

# **CLINICAL RELEVANCE/APPLICATION**

As lung screening becomes more widely adopted, automated assistance with assigning ACR LungRADS category may prove useful to assist novice interpreters and as a quality assurance and standardization tool.

## CH287-SD-THB5

Iterative Metal Artifact Reduction in Postsurgical Thoracic CT: Evaluation of Three Different Metal Artefact Reduction Algorithms

Thursday, Dec. 1 12:45PM - 1:15PM Room: CH Community, Learning Center Station #5

# Participants

Joel Aissa, Duesseldorf, Germany (*Presenter*) Nothing to Disclose Johannes Boos, MD, Boston, MA (*Abstract Co-Author*) Nothing to Disclose Patric Kroepil, MD, Duesseldorf, Germany (*Abstract Co-Author*) Nothing to Disclose Rotem S. Lanzman, MD, Duesseldorf, Germany (*Abstract Co-Author*) Nothing to Disclose Gerald Antoch, MD, Duesseldorf, Germany (*Abstract Co-Author*) Nothing to Disclose Christoph K. Thomas, MD, Dusseldorf, Germany (*Abstract Co-Author*) Nothing to Disclose

### PURPOSE

The purpose of this study was to evaluate the impact of three novel iterativemetal artifact reduction (MAR) algorithms on image quality and artifact strength in chest CT of patients with thoracic metallic implants.

# METHOD AND MATERIALS

We evaluated 27 postsurgical patients who had undergone CT between March and May 2015 in clinical routine. Thoracic implants (n=38) included sternal steel wiring (n=25), left ventricular assist devices (n=3), port systems (n=3), pacemakers (n=3) and overlying devices (n=4). Images were retrospectively reconstructed on a workstation with standard weighted filtered back projection (WFBP) and additionally with three iterative MAR algorithms [iMAR 2D: "Cardiac"-algorithm (algo1), "Pacemaker"- algorithm (algo2) and "ThoracicCoils"-algorithm (algo3)]. Subjective image quality was assessed for each implant using a 5 point scale (1: severe artifacts, non-diagnostic - 5: excellent image quality, no artifacts). The objective artifact strength was determined by ROI measurements of image noise insertion next located to the implants.

#### RESULTS

All reconstructions showed diagnostic image quality. Mean overall scores for the iMAR algorithms were  $3.8\pm0.1$  for algo1,  $4.3\pm0.8$  for algo2 and  $4.2\pm0.7$  for algo3. All iMAR algorithms showed a significantly better overall image quality compared to WFBP reconstructions (p<0.01). Concerning mild artifacts, these were strongest for WFBP (near field:  $3.6\pm0.5$ , far field  $4.5\pm0.6$ ) and iMAR algo1 (near field:  $3.8\pm0.5$ , far field  $4.7\pm0.5$ ). We found significantly lower moderate to low artifacts for the algo2 and algo3 reconstructions (near field:  $4.5\pm0.5$ , far field  $4.9\pm0.2$  and near field:  $4.5\pm0.5$ , far field  $4.9\pm0.3$ , p<0.01). Concerning strong artifacts we found no significant difference between the iMAR algorithms. Artifact strength was significantly lower for the algo1 ( $58.9\pm36.1$ ), algo2 ( $52.7\pm43.9$  HU) and algo3 ( $51.9\pm44.1$  HU), compared with standard technique (p<0.01).

### CONCLUSION

Our results showed a significant reduction of metal artifacts and a significant increase in overall image quality for three different iMAR algorithms compared to WFBP in chest CT of patients with metallic implants. The "Pacemaker" and "ThoracicCoils" algorithm were best for mild artifacts while the "Cardiac" algorithm was superior for severe artifacts.

## **CLINICAL RELEVANCE/APPLICATION**

Our results indicate that a selection of iMAR algorithms adjusted to patients' metal implants and artifact severity can help to improve image quality in chest CT.

# Role of Delayed Enhanced Phase in the Intra-Thoracic Staging of Lung Cancer

Thursday, Dec. 1 12:45PM - 1:15PM Room: CH Community, Learning Center Station #6

#### Participants

Paola Franchi, Rome, Italy (*Presenter*) Nothing to Disclose Anna Rita Larici, MD, Rome, Italy (*Abstract Co-Author*) Nothing to Disclose Annemilia del Ciello, MD, Rome, Italy (*Abstract Co-Author*) Nothing to Disclose Giuseppe Cicchetti, Rome, Italy (*Abstract Co-Author*) Nothing to Disclose Davide Coviello, Rome, Italy (*Abstract Co-Author*) Nothing to Disclose Lorenzo Bonomo, MD, Rome, Italy (*Abstract Co-Author*) Nothing to Disclose

# PURPOSE

To investigate the role of a delayed enhanced phase (DEP) in the intra-thoracic staging of lung cancer on Computed Tomography (CT)To evaluate the additional information provided by DEP when compared to the arterial phase (AP) alone

# METHOD AND MATERIALS

150 CT exams of patients with lung cancer at first staging were retrospectively reviewed by two chest radiologists in consesus. All patients were studied after contrast material (CM) injection (concentration: 300–370mgI/mL; flow rate: 3 to 4mL/s) with a standard AP (35-40 seconds after contrast material injection), and with a DEP (50-60 seconds after contrast material injection). Image assessment was performed by the two radiologists in two different reading sessions: AP (session A) and AP+DEP (session B).Parameters analysed in both sessions were: tumor dimensions, invasion of local anatomical structures, venous involvement, and lymph node involvement. The radiologists reported a CT TNM stage in both sessions. During reading sessions, the readers assigned a confidence level for each parameter evaluated.Subsequently, it was studied the occurrence of evaluation change and a statistical analysis with chi-square ( $\chi$ 2) test on the confidence level was performed.

### RESULTS

Between the two reading sessions, evaluation differences were observed in all parameters examined.DEP added information also on dimensions of primary tumor, especially for central ones enabling distinction between pathological tissue and parenchymal atelectasis.The readers changed their CT TNM stage in 10% of T evaluation and in 35% of N evaluation.Confidence level significantly increased in the assessment of each parameter and in the overall evaluation (p<0.05).

# CONCLUSION

-In lung cancer CT staging, a DEP of the chest after the AP could change patient's clinical stage. -DEP dramatically increases the radiologists' confidence level on the evaluation of intra-thoracic extension of lung cancer.

### **CLINICAL RELEVANCE/APPLICATION**

-DEP could change lung cancer TNM staging, thus further diagnostic and treatment plans.-The higher confidence level could be particularly useful for "non-thoracic" radiologists.

# ER242-SD-THB1

Radiology Resident Interpretations of Diffusion-weighted MR Imaging in the Emergency Department: Is the Diagnostic Performance Influenced by Level of Residency Training?

Thursday, Dec. 1 12:45PM - 1:15PM Room: ER Community, Learning Center Station #1

# Participants

Hye Jin Baek, Changwon, Korea, Republic Of (*Abstract Co-Author*) Nothing to Disclose Seung Jin Kim, MD, Basan, Korea, Republic Of (*Presenter*) Nothing to Disclose Kyungsoo Bae, MD, Changwon, Korea, Republic Of (*Abstract Co-Author*) Nothing to Disclose Kyung Nyeo Jeon, MD, Changwon, Korea, Republic Of (*Abstract Co-Author*) Nothing to Disclose Dae Seob Choi, BA, Jinju, Korea, Republic Of (*Abstract Co-Author*) Nothing to Disclose Soo Buem Cho, Jinju, Korea, Republic Of (*Abstract Co-Author*) Nothing to Disclose Bo Hwa Choi, Changwon, Korea, Republic Of (*Abstract Co-Author*) Nothing to Disclose Jin Il Moon, MD, Busan, Korea, Republic Of (*Abstract Co-Author*) Nothing to Disclose Hwa Seon Shin, Jinju, Korea, Republic Of (*Abstract Co-Author*) Nothing to Disclose Hyun Kyung Jung, Busan, Korea, Republic Of (*Abstract Co-Author*) Nothing to Disclose

### PURPOSE

To determine the diagnostic performance of radiology residents interpretations for diffusion-weighted MR imaging (DWI) in the emergency department at different levels of residency training.

### **METHOD AND MATERIALS**

A total 160 patients who underwent DWI with acute neurologic symptoms were included in this retrospective study with institutional review board approval. Four radiology residents with different training years and one attending neuroradiologist independently assessed the results of DWI. Discordancies between the results of residents and attending neuroradiologist were classified as followings; false-positive (FP) and false-negative (FN). We also evaluated a diagnostic performance of four residents according to the reference standard. All data was analyzed by using Fisher's exact test, kappa statistics, and ROC analysis.

# RESULTS

Overall, the agreement rate was 84.8% with 15.2% of overall discrepancy rate. All of discrepancies were insignificant. There were 83 FN results. The most common misses were acute focal infarction (n=13), extraparenchymal hemorrhages (n=18), small vessel disease (n=34), diffuse axonal injury (n=7), solitary mass (n=6), osmotic demyelination syndrome (n=2), and postictal change (n=3). There were 14 FP results including hemorrhage and acute infarction. The 4-year resident showed the highest diagnostic performance (Az value: 0.906; 95% CI: 0.850, 0.947; 87.5% of sensitivity; and 93.8% of specificity). The level of training had a significant influence (P < 0.05) on their interpretations. Kappa statistics showed good agreement of results between residents and attending neuroradiologists.

# CONCLUSION

The level of resident training had a significant effect on their diagnostic performance, and there was a good interobserver agreement between the results of residents and attending neuroradiologists. Therefore, radiology residents could safely make the initial interpretation of DWI which underwent in ER, and formal reporting may wait until a suitable experienced radiologist is available.

# **CLINICAL RELEVANCE/APPLICATION**

Under on-call duty system, radiology residents can make the initial interpretation of emergent DWI safely , and formal reporting may wait until a suitable experienced radiologist is available.

### ER243-SD-THB2

#### Fractures of the Foot Sesamoids: 5-year Imaging Efficacy Analysis of an Underdiagnosed Acute Injury

Thursday, Dec. 1 12:45PM - 1:15PM Room: ER Community, Learning Center Station #2

#### **Participants**

Mohammad Mansouri, MD, MPH, Boston, MA (*Presenter*) Nothing to Disclose Renata R. Almeida, boston, MA (*Abstract Co-Author*) Nothing to Disclose Michael H. Lev, MD, Boston, MA (*Abstract Co-Author*) Consulant, General Electric Company; Institutional Research Support, General Electric Company; Stockholder, General Electric Company; Consultant, MedyMatch Technology, Ltd; Consultant, Takeda Pharmaceutical Company Limited; Consultant, D-Pharm Ltd Ajay K. Singh, MD, Boston, MA (*Abstract Co-Author*) Nothing to Disclose Efren J. Flores, MD, Boston, MA (*Abstract Co-Author*) Nothing to Disclose

## PURPOSE

Sesamoid fractures of the foot are uncommon but often missed in the first radiology exam. Missing them can cause pain, nonunion, malunion and avascular necrosis. We aim to analyze sesamoid fractures of our large academic medical center and to investigate sensitivity of imaging modalities in detecting sesamoid fractures.

#### **METHOD AND MATERIALS**

This is a HIPAA compliant, IRB approved, retrospective study. The PACS system of our institution was searched for patients with sesamoid fracture of the foot between 2010 and 2014. Medical records of these cases were investigated for variables.

### RESULTS

Total of 20 patients (13 females, 7 males) were collected with mean age of 37.5 years. 80% of fractures were due to stress fracture or blunt trauma. In 10% of cases (2/20), tight shoes were used at the time of starting the pain. Sesamoid fractures were missed in 55% (11/20) of patients in the first radiology exam; 36.4% of the missed fractures (4/11) were considered as bipartite at first. Fifty percent of patients (10/20) were diagnosed with fibular sesamoid fracture, 45% (9/20) with tibial and 5% (1/20) with fifth sesamoid fracture. MRI had the highest sensitivity (100%; 9/9), followed by weight-bearing film (66.7%; 4/6), and radiography (60%; 9/15). MRI had significantly higher sensitivity comparing radiography (p=0.02). Rate of sesamoid fractures in foot exams was 0.014% (15/104,962) in radiography, 0.268% (6/2242) in weight-bearing film, 0.032% (1/3164) in foot CT, 0.124% (9/7262) in foot MRI and 0.026% (31/117,630) in total foot exams. This represents a ratio of 1 sesamoid fracture for every: 6997 radiographs, 374 weight-bearing films, 3164 foot CTs, 807 foot MRIs and 3795 in total foot exams. 90% of patients (18/20) were treated conservatively, and 10% (2/20) were treated surgically.

## CONCLUSION

Sesamoid fractures occur at a rate of 0.026% in total foot exams, are usually due to stress fracture or blunt trauma and are most commonly treated conservatively. This study showed radiography has a sensitivity of 60.0% in diagnosing sesamoid fractures. MRI has significantly higher sensitivity and is the next step in evaluating patients with normal radiographs.

### **CLINICAL RELEVANCE/APPLICATION**

Radiography has a low sensitivity in diagnosing sesamoid fractures and MRI is the next step in evaluating patients with normal radiographs.

# ER244-SD-THB3

### Quantitate Analysis of Initial Non-Contrast Computed Tomography in Acute Ischemic Stoke

Thursday, Dec. 1 12:45PM - 1:15PM Room: ER Community, Learning Center Station #3

#### **Participants**

Wilson Altmeyer, MD, San Antonio, TX (*Abstract Co-Author*) Nothing to Disclose Mamie Gao, San Antonio, TX (*Abstract Co-Author*) Nothing to Disclose Junfei Li, San Antonio, TX (*Abstract Co-Author*) Nothing to Disclose Geoffrey D. Clarke, PhD, San Antonio, TX (*Abstract Co-Author*) Nothing to Disclose Feng Gao, MD, San Antonio, TX (*Presenter*) Nothing to Disclose

#### PURPOSE

Non-Contrast Computed Tomography (NCCT) is the imaging modality of choice for acute stroke because of its easy access, efficiency, and cost effectiveness in excluding hemorrhage. However, according to earlier reports, approximately 39% cases show no early signs of infarction on NCCT. The purpose of this study is to retrospectively compare the initial NCCT with the follow up MRI results in patients with acute ischemic infarction and use CT density quantification to detect subtle infarctions that would have been missed by routine qualitative evaluation by radiologist.

#### **METHOD AND MATERIALS**

We retrospectively reviewed 16 patients (20 foci) who presented to the emergency department with acute stroke symptoms, obtained both NCCT and MRI scans. CT Hounsfield Units (HU) of both the infarctions, as defined by the MRI examination, and contralateral normal brain were quantified and compared. The sizes of the infarctions also had been recorded.

# RESULTS

MRI confirmed 20 different foci (3.9mm – 46.3mm) of infarction within the 16 patients with suspected stroke. 15 out of the 20 infarctions were not visualized on NCCT. The CT density of the 15 occult infarctions (16.23 to 29.53 HU) showed an average of 4.34 HU lower than the contralateral normal area (20.86 to 33.21 HU). 12 out of the 15 infarctions had an average difference more than 5.27 HU while the other 3 differed less than 0.61 HU.

# CONCLUSION

Earlier phantom studies indicates that 2 HU hypo-attenuation can be detected by using appropriate parameter settings. By comparing the CT numbers of the ischemic region with the contralateral normal brain, it has been found that 12 out of the 15 negative NCCT results (80%) could have been correctly reported as positive. Therefore, systematic quantification of the initial NCCT may aid in the CT diagnosis rate of acute ischemic stroke. The results of this study may serve as a base to establish a threshold for automatic detecting software development. The method of this study, which quantifies the infarction by measuring CT numbers, may also be used for further research to predict the prognosis of a stroke.

#### **CLINICAL RELEVANCE/APPLICATION**

(dealing with acute ischemic stroke by CT density quantification) "CT numbers have been used to quantify CT scans of acute ischemic stroke patients and the results showed significant improvement in diagnostic rate."

# Added Value of CT in Characterizing Lisfranc Injuries

Thursday, Dec. 1 12:45PM - 1:15PM Room: ER Community, Learning Center Station #4

#### Awards

#### **Student Travel Stipend Award**

#### **Participants**

Brandon Roller, MD, PhD, Winston Salem, NC (*Presenter*) Consultant, Bone Solutions, Inc Pat W. Whitworth III, MD, Boston, MA (*Abstract Co-Author*) Nothing to Disclose Thomas Kelsey, Winston-Salem, NC (*Abstract Co-Author*) Nothing to Disclose Anna N. Miller, MD, Winston Salem, NC (*Abstract Co-Author*) Nothing to Disclose Scott D. Wuertzer, MD, MS, Winston-Salem, NC (*Abstract Co-Author*) Nothing to Disclose Leon Lenchik, MD, Winston-Salem, NC (*Abstract Co-Author*) Nothing to Disclose Maha Torabi, MD, Winston Salem, NC (*Abstract Co-Author*) Nothing to Disclose

### PURPOSE

To determine the added value of computed tomography (CT) compared to conventional radiography (CR) for the diagnosis of fractures associated with Lisfranc injuries.

## **METHOD AND MATERIALS**

A review of CT reports that specifically assessed the Lisfranc joint over the past 6 years was conducted. Only patients with foot radiographs prior to CT were included. Patients with diabetes or neuropathic arthropathy were excluded. CR and CT diagnoses were reviewed for the presence of the following fractures: medial, intermediate, and lateral cuneiforms; first, second, third, fourth, and fifth metatarsal bases; cuboid. The rate of fractures and malalignment on CR and CT were compared. The number of patients that had operative fixation of the Lisfranc injury was determined.

### RESULTS

148 patients were included (5 patients had bilateral CTs). There were 79 men (3 bilateral) and 69 women (2 bilateral); mean age, 49 years; age range, 19-92 years. 65/153 (42%) showed Lisfranc malalignment on CR. 82/153 (54%) showed Lisfranc malalignment on CT. 139/153 (91%) had fractures on CT. Compared to CT, CR diagnosed 17% (16/96) of medial cuneiform, 11% (5/47) of intermediate cuneiform, 7% (5/73) of lateral cuneiform, 45% (26/58) of first metatarsal base, 41% (44/107) of second metatarsal base, 31% (26/85) of third metatarsal base, 39% (31/79) of fourth metatarsal base, 44% (14/32) of fifth metatarsal base, and 34% (23/68) of cuboid fractures. CR missed identifying a fracture 90% (125/139) of the time. 57/153 patients had operative fixations. 9/57 (16%) of the patients who required surgery were CR negative but CT positive for Lisfranc malalignment.

#### CONCLUSION

Compared to conventional radiography, CT provides a more accurate characterization of fractures associated with Lisfranc injuries.

### **CLINICAL RELEVANCE/APPLICATION**

CT provides an accurate characterization of fractures associated with Lisfranc injuries, which impacts patient management.

# GI113-ED-THB9

The Ever-Changing Landscape of Medical Devices Found in the Abdomen and Pelvis: What the Radiologist Can Tell the Clinician

Thursday, Dec. 1 12:45PM - 1:15PM Room: GI Community, Learning Center Station #9

# Participants

Everett Gu, MD, Ann Arbor, MI (*Presenter*) Nothing to Disclose Ashish P. Wasnik, MD, Ann Arbor, MI (*Abstract Co-Author*) Nothing to Disclose Ravi K. Kaza, MD, Ann Arbor, MI (*Abstract Co-Author*) Nothing to Disclose Mahmoud M. Al-Hawary, MD, Ann Arbor, MI (*Abstract Co-Author*) Nothing to Disclose

# **TEACHING POINTS**

While viewing this exhibit, participants will: Review common medical devices and gain exposure to newer or more uncommon medical devices found in the abdomen and pelvis. Appreciate the physical appearance of a spectrum of medical devices as portrayed in photographs, and be comfortable recognizing these devices on plain radiographs and CT. Understand how to properly evaluate various medical devices, including appropriate positioning and potential complications.

# TABLE OF CONTENTS/OUTLINE

Introduction explaining the importance of identifying and evaluating medical devices Overview of various medical devices found in the abdomen and pelvis, grouped into five major categories: Gastrointestinal (e.g. Sengstaken-Blakemore tubes, esophageal stents, over-the-scope clips) Hepatobiliary (e.g. cholecystostomy tubes, biliary stents, cystogastrostomy stents) Genitourinary (e.g. vaginal pessaries, tubal ligation clips, artificial urinary sphincters) Vascular (e.g. endografts, endovascular cooling catheters) Body wall (e.g. spinal cord stimulators, baclofen pumps) Dedicated slides for each medical device, which will focus on the purpose of the device, appropriate placement, and potential complications, supplemented with photographs and radiology images Summary emphasizing the role of radiology in evaluating medical devices

# GI278-ED-THB7

# Computed Tomography (CT) Imaging of Abdominal Hernias Following Mesh Repairs

Thursday, Dec. 1 12:45PM - 1:15PM Room: GI Community, Learning Center Station #7

#### **Participants**

Eugene Bivins JR, BS, Washington, D.C., DC (*Presenter*) Nothing to Disclose Kovosh Dastan, MSc, Ashburn, VA (*Abstract Co-Author*) Nothing to Disclose Sarah Mohamedaly, MPH, Washington, D.C., DC (*Abstract Co-Author*) Nothing to Disclose Adrian Godoy Vazquez, BS, Washington, DC (*Abstract Co-Author*) Nothing to Disclose Andre J. Duerinckx, MD, PhD, Washington, DC (*Abstract Co-Author*) Nothing to Disclose Bonnie C. Davis, MD, Washington, DC (*Abstract Co-Author*) Nothing to Disclose Dahn Truong, BS, Washington, DC (*Abstract Co-Author*) Nothing to Disclose Belen Tesfaye, MD, Washington, DC (*Abstract Co-Author*) Nothing to Disclose Daniel Tran, MD, Washington, DC (*Abstract Co-Author*) Nothing to Disclose

# **TEACHING POINTS**

At the end of this presentation, participants will be able to: Identify normal findings on CT images after abdominal hernia repairs Understand the importance of CT imaging in the identification of mesh displacement, mesh migration, abscess formation, pseudoabscess formaion, and other complications Better detect and manage complications following hernia repairs in the early post-mesh repair period

## TABLE OF CONTENTS/OUTLINE

Review the use of mesh repairs following abdominal hernias and the normal post-op imaging appearance Describe the types of complications that may ensue as a result of hernia repairs and review CT findings of such complications State the relevance of monitoring patients in the early post-mesh repair period and early detection of complications

## GI298-ED-THB8

Hepatic Lesions that Mimic Metastasis on Radiological Imaging during Chemotherapy for Gastrointestinal Malignancy: Recent Updates

Thursday, Dec. 1 12:45PM - 1:15PM Room: GI Community, Learning Center Station #8

#### Awards

**Certificate of Merit** 

#### **Participants**

Yeo Eun Han, Seoul, Korea, Republic Of (*Presenter*) Nothing to Disclose Beom Jin Park, MD, Seoul, Korea, Republic Of (*Abstract Co-Author*) Nothing to Disclose Min-Ju Kim, MD, Seoul, Korea, Republic Of (*Abstract Co-Author*) Nothing to Disclose Deuk Jae Sung, MD, Seoul, Korea, Republic Of (*Abstract Co-Author*) Nothing to Disclose Na Yeon Han, Seoul, Korea, Republic Of (*Abstract Co-Author*) Nothing to Disclose Ki Choon Sim, Seoul, Korea, Republic Of (*Abstract Co-Author*) Nothing to Disclose Sung Bum Cho, Seoul, Korea, Republic Of (*Abstract Co-Author*) Nothing to Disclose

### **TEACHING POINTS**

For multidisciplinary teams involved in cancer care, the precise imaging validation of a newly detected hepatic nodule has become crucial to achieve optimal treatment during chemotherapy for malignancies. Hepatic incidentaloma arising from chemotherapy-induced parenchymal injury, tumor-associated eosinophilic abscess, and fungal infection should be considered a mimicker of metastasis in patients with gastrointestinal malignancy. We have reviewed widely used causative chemo-agents, the updated concept of chemotherapy-induced hepatopathies, and other hepatic pseudometastasis focusing on their pathological and radiological findings for accurate diagnosis.

## **TABLE OF CONTENTS/OUTLINE**

A. The concept of imitator of hepatic metastasis during chemotherapyB. Chemotherapy-induced focal hepatopathy *Chemotherapy for gastrointestinal malignancy Chemotherapy-induced focal sinusoidal injury* Pathophysiology / Clinical issues/ Imaging Features *Chemotherapy-induced focal steatosis/steatohepatitis* Pathophysiology / Clinical issues/ Imaging featuresC. Tumor-associated eosinophilic abscess in the liver Compromised immunity-associated fungal abscess in the liver Take-home message Diagnostic Performance of Surveillance US and Influencing Factors on US Visibility of HCCs: A Prospective Study in Patients with Cirrhosis at High Risk of HCC

Thursday, Dec. 1 12:45PM - 1:15PM Room: GI Community, Learning Center Station #1

**FDA** Discussions may include off-label uses.

### Participants

So Hyun Park, MD, Incheon, Korea, Republic Of (*Presenter*) Nothing to Disclose Hyung Jin Won, MD, Seoul, Korea, Republic Of (*Abstract Co-Author*) Nothing to Disclose So Yeon Kim, MD, Seoul, Korea, Republic Of (*Abstract Co-Author*) Nothing to Disclose Jae Ho Byun, MD, Seoul, Korea, Republic Of (*Abstract Co-Author*) Nothing to Disclose So Jung Lee, Seoul, Korea, Republic Of (*Abstract Co-Author*) Nothing to Disclose Seong Ho Park, MD, Seoul, Korea, Republic Of (*Abstract Co-Author*) Nothing to Disclose Seong Ho Park, MD, Seoul, Korea, Republic Of (*Abstract Co-Author*) Research Grant, DONGKOOK Pharmaceutical Co, Ltd Jihyun An, Seoul, Korea, Republic Of (*Abstract Co-Author*) Nothing to Disclose Young-Suk Lim, Seoul, Korea, Republic Of (*Abstract Co-Author*) Nothing to Disclose

### PURPOSE

To investigate diagnostic performance, the characteristics of nodules detected on surveillance US and influencing factors on US visibility of HCCs in patients with cirrhosis at high risk of HCC.

#### **METHOD AND MATERIALS**

A prospective surveillance study included 407 consecutive patients with an estimated annual risk of HCC >5% who underwent one to three, biannual surveillance US examinations combined with US elastography between November 2011 and August 2014. The findings of lesions detected on US were recorded in a predefined standardized way using a four-point scale indicating the likelihood of HCC, i.e. suspicious, equivocal, probably benign or definitely benign/negative, corresponding to categories 4, 3, 2, and 1, respectively. The confirmation of HCC was based on the results of a histologic examination and/or typical CT images of HCC. The detection rate of HCC and the false-positive rate were calculated. The characteristics of category 4 nodules detected on US were determined using the simultaneous or follow-up gadoxetic acid-enhanced MRI and CT. We investigated clinical factors, including the Child-Pugh class and body mass index as well as imaging characteristics such as liver stiffness, US image quality, tumor location, and tumor size, all of which possibly influenced the US visibility of HCCs.

### RESULTS

Among the 43 patients with HCCs found during 1100 US screening sessions, the detection rate of HCC was 27.9% (12/43) and the false positive rate was 5.6% (59/1057). Among the 71 category 4 lesions, 12 were HCC, 27 were not matched with any lesions seen on MRI or CT, 20 were confirmed as cirrhosis-related nodules, four were exophytic hepatic parenchyma, four were hemangiomas, three were complicated cysts, and one was abnormal vasculature. Among the clinical and imaging characteristics, a subcapsular location was the only significant factor related to the failure to detect HCC on US (P=0.019). Among 20 HCCs in subcapsular locations, US detected only two HCCs.

### CONCLUSION

In patients with cirrhosis at high risk of HCC, surveillance US did not show satisfactory diagnostic performance. The subcapsular location of HCC can be the cause of the suboptimal detection rate.

### **CLINICAL RELEVANCE/APPLICATION**

US is a suboptimal surveillance tool for HCC in patients with cirrhosis at high risk of HCC. The subcapsular area of the liver is where strict scrutiny should be applied when US is performed in these patients.

# GI408-SD-THB2

## Diagnostic Accuracy of Colonic Lesions in Ultra-low Dose CT Colonography: Is Diagnosis in Sub-mSv Possible?

Thursday, Dec. 1 12:45PM - 1:15PM Room: GI Community, Learning Center Station #2

#### **Participants**

Takaaki Yasuda, RT, Nagasaki, Japan (*Presenter*) Nothing to Disclose Tetsuro Honda, MD, Nagasaki, Japan (*Abstract Co-Author*) Nothing to Disclose Takahiro Yasaka, Nagasaki, Japan (*Abstract Co-Author*) Nothing to Disclose Kenichi Utano, MD, Aizuwakamatu-shi, Japan (*Abstract Co-Author*) Nothing to Disclose Takashi Kato, MD, Sapporo, Japan (*Abstract Co-Author*) Nothing to Disclose

#### PURPOSE

To evaluate the diagnostic accuracy of ultra-low dose CT Colonography (CTC).

#### **METHOD AND MATERIALS**

Two hundred patients, (98 male and 102 female, average age 67.5 years), who were scheduled for total colonoscopy (TCS), underwent ultra-low dose CTC. These patients were scanned in prone and supine positions by the 80-slices MDCT with the scanning conditions set to 120 kV, SD45-50, and an adaptive iterative reconstruction algorithm was applied. The targeted size of lesions, which were pathologically diagnosed as adenoma and adenocarcinoma, were 10 mm or larger. A radiologist (R) and a gastroenterologist (G), who had extensive experience of reading CTC images and did not know the endoscopy results, performed the reading independently. By using TCS as a gold standard, the Sensitivity, Specificity, PPV and NPV were calculated.

#### RESULTS

DLP (mGy/cm) was 21.31 (0.32 mSv) for supine and 21.27 (0.32 mSv) for prone (converted using an effective dose conversion coefficient of 0.015).

The CTC per-lesion sensitivity R 73% / G 71% and PPV R 79% / G 94% for lesions larger than 10 mm (n = 45). None of the flat lesions was identified in CTC, but the accuracy for elevated lesions excluding flat lesions was sensitivity R 87% / G 84% and PPV R 85% / G 94%. For the per-patient, sensitivity, specificity, PPV and NPV were R 74% / G 74%, R 96% / G 99%, R 83% / G 94% and R 94% / G 94%, respectively.

### CONCLUSION

Detecting elevated lesions in ultra-low dose CTC is possible with a good diagnostic accuracy; however, detecting flat lesions in ultra-low dose CTC is not possible due to the poor accuracy. It is considered as a limitation.

# **CLINICAL RELEVANCE/APPLICATION**

We have reduced the radiation dose as much as possible by utilizing scanning technology clinically available today. Accuracy for detecting elevated lesions was good at sub-mSv CT scan, and the results of this study will provide an indicator for the most suitable ways to achieve dose reduction in the future.

# Radiology-pathology Box: A Tool for MRI Guidance of Ex Vivo Histopathologic Analysis

Thursday, Dec. 1 12:45PM - 1:15PM Room: GI Community, Learning Center Station #3

#### **Participants**

Tilman B. Schubert, MD, Madison, WI (*Presenter*) Nothing to Disclose Sonja Kinner, MD, Madison, WI (*Abstract Co-Author*) Nothing to Disclose Elisabetta A. Nocerino, Milano, Italy (*Abstract Co-Author*) Nothing to Disclose Shannon Hynes, MS, Madison, WI (*Abstract Co-Author*) Nothing to Disclose Christopher L. Brace, PhD, Madison, WI (*Abstract Co-Author*) Shareholder, NeuWave Medical Inc Consultant, NeuWave Medical Inc Shareholder, Symple Surgical Inc Consultant, Symple Surgical Inc Timothy Colgan, PhD, Madison, WI (*Abstract Co-Author*) Nothing to Disclose Emily Winslow, MD, Madison, WI (*Abstract Co-Author*) Nothing to Disclose Scott B. Reeder, MD, PhD, Madison, WI (*Abstract Co-Author*) Institutional research support, General Electric Company Institutional research support, Bracco Group

#### PURPOSE

Ex vivo pathologic analysis and lesion identification in resected specimen is demanding due to tissue deformation and altered orientation. Small lesion in particular can therefore be missed during tissue sectioning potentially impacting the staging of malignancies. As delineation of resection margins and tumor burden is of utmost importance, we aimed to develop an MRI compatible localization device and test its feasibility for localizing small lesions in explanted liver tissue.

# METHOD AND MATERIALS

An MR-compatible localization device was entirely constructed from Plexiglas consisting of two stationary and one removable MRvisible grid, creating a 3D matrix (Figure). Laser-edged grid lines and labels filled with silicone gel for MR visibility in three dimensions. Alginate is used to fix and stabilize tissue during imaging and cutting. Slicing of the specimen within the box is enabled in a guided fashion through prefabricated grooves corresponding to the grid lines of the device (y-direction). To test the device, five specimen of swine liver with a random number of lesions created by thermoablation (lesion size: 5-15 mm) were imaged on a 3T MR scanner. The MR protocol consisted of a high-resolution T1 SPGRE-sequence (0.5x0.5x0.4mm3). Two readers independently evaluated lesion coordinates and size, which was then correlated with results from cutting.

#### RESULTS

Imaging with the device was feasible and all images were of high diagnostic quality. All 38 lesions were detected in the expected localization with the exception of one lesion incorrectly localized by one of the two readers. Inter-reader agreement of lesion localization was excellent (0.92). Size (5-12mm) was correct within +/-2mm, in 34/35 lesions.

# CONCLUSION

The MR-visible device proved feasible for detection and localization of liver lesions, and has potential to play an important role in lesion identification and in radiologic-pathologic evaluation. Assuming that a comparably high sensitivity can be achieved in clinical trials, this device may enable image-guided pathologic analysis . In addition, this tool might give further insight into radiologic-pathologic pathologic correlation of lesions if in vivo-, ex vivo MR data and histopathology is available.

### **CLINICAL RELEVANCE/APPLICATION**

This tool enables ex vivo lesion detection and localization in resected specimen. This might lead to focused histopathologic analysis which has the potential to impact tumor staging and grading.

## GI410-SD-THB4

Value of Advanced Virtual Monoenergetic Images with Third-generation Dual-Energy CT in Detecting Early Gastric Cancer

Thursday, Dec. 1 12:45PM - 1:15PM Room: GI Community, Learning Center Station #4

## Participants

Wei Liu, Beijing, China (*Presenter*) Nothing to Disclose Jingjuan Liu, MD, Beijing, China (*Abstract Co-Author*) Nothing to Disclose Huadan Xue, MD, Beijing, China (*Abstract Co-Author*) Nothing to Disclose Zheng Yu Jin, MD, Beijing, China (*Abstract Co-Author*) Nothing to Disclose

### PURPOSE

To evaluate the impact of advanced monoenergetic dual-energy computed tomography (DECT) datasets on detection rate and contrast-to-noise ratio (CNR) of early gastric cancer (EGC) on the third generation DECT.

# METHOD AND MATERIALS

20 patients suspected of EGC were prospectively enrolled in this study. Arterial phase (AP) and portal phase (PP) imaging were acquired in dual-energy mode (80/Sn150KV) using third-generation DECT (SOMATOM Force, Siemens Healthcare, Germany). Monoenergetic images (MEIs) (range 40-100keV) were calculated from the 80 and Sn150KV image data using monoenergetic software (Dual energy Mono+, syngo via, Siemens). Differences in detection rates of EGC and CNR numbers were compared between different MEIs from 40 to 100 keV and conventionally reconstructed polyenergetic images (PEIs) at 120 kVp. Histopathologic analysis of resected gastric specimens was used as reference standard. Radiation metrics were compared with those obtained in the second-general DECT (Definition Flash, Siemens Healthcare, Germany) from published reports.

#### RESULTS

MEIs at 40keV and 50keV showed the highest detection rates (60.0% and 60.0% respectively) for EGC, which showed no significant difference with PEIs(35%)(P=0.205). For EGC lesions of less than 2cm, an increase in the detection rates was observed from MEIs at 40keV and 50keV(53.8%,7/13 and 53.8%,7/13) as compared to PEIs(23.1%,3/13), though no statistical significance was found (P=0.226). MEIs at 40keV and 50keV revealed statistical higher CNR-AP and CNR-PP compared to PEIs (all P<0.05). The CTDIvol of the AP and PP were  $4.28 \pm 0.92$  mGy and  $4.67 \pm 0.95$  mGy respectively, which was about 35% of the radiation dose when using routine second-generation DECT (100/Sn140KV) from literatures.

# CONCLUSION

Virtual 40keV and 50keV monoenergetic images calculated using the Mono+ algorithm significantly increase the CNR of EGC, which was helpful to enhance the EGC detection rate. Third-generation DECT could potentially allow for radiation dose reduction in EGC detection as compared to the second-general DECT.

#### **CLINICAL RELEVANCE/APPLICATION**

The third-generation DECT with Mono+ technique could improve the detection rate of early gastric cancer and result in substantial radiation dose reduction for patients.

MRI/US Fusion for Assessment of the Postpartum Uterus - Does it Allow Standardized Measurement of Anterior and Posterior Uterine Wall Thickness after Cesarean Section and Vaginal Delivery?

Thursday, Dec. 1 12:45PM - 1:15PM Room: GU/UR Community, Learning Center Station #1

# Participants

Thomas Fischer, MD, Berlin, Germany (*Presenter*) Speaker, Toshiba Corporation; Advisory Board, Toshiba Corporation Kristina Bolton, Berlin, Germany (*Abstract Co-Author*) Nothing to Disclose Anke Thomas, MD, Berlin, Germany (*Abstract Co-Author*) Nothing to Disclose

#### PURPOSE

To prospectively evaluate the lower uterine segment after vaginal delivery and the Cesarean scar at 6 weeks using transabdominal (TAUS) and transvaginal ultrasound (TVUS) and magnetic resonance imaging (MRI)/US image fusion to evaluate whether image fusion allows standardized and reproducible localization of the scar and uterine wall thickness measurement compared with high-resolution MRI.

# METHOD AND MATERIALS

Six weeks after delivery, plain pelvic MRI (premedication with 40 mg intramsuclar butylscopolamine, HR T2-weighted TSE sequence in sagittal orientation; 1.5T, Siemens, Erlangen, Germany) was performed in 30 women (10 each after primary Cesarean section (PCS), secondary Cesarean section (SCS), and vaginal delivery (VD)). The MRI DICOM datasets were transferred into the ultrasound system (Aplio 500, Toshiba Medical Systems, Otawara, Japan), followed by TAUS (5MHz) and TVUS (10 MHz) using smart fusion with MRI for navigation. The lower uterine segment was examined in a comparable view in real time. Vascularization was determined as percentage area using power Doppler US. Anterior and posterior uterine wall thickness (AW, PW) was measured using TAUS and TVUS with and without MRI fusion and MRI alone.

### RESULTS

TVUS with image fusion was successfully applied for uterine assessment at the end of the puerperium. TAUS failed to identify the scar region in 3 women. All techniques investigated were similar in evaluation of the AW and PW following VD. Comparison of the AW or scar region after PCS and SCS in terms of the difference relative to the PW showed that only MRI and MRI/TVUS fusion revealed significant differences (MRI: PCS=4.3mm; SCS=4.2mm; VD=0.8mm; p=0,034, TVUS-fusion: PCS=2.0mm; SCS=3.3mm; VD=0mm; p=0.010). The degree of vascularization measured by power Doppler US was lower after PCS and SCS (PCS 13.1±9.4 %/area, SCS 17.0±8.2 %/area) than after VD (VD 34.6±8.5 %/area, p=0.0017).

#### CONCLUSION

MRI/US image fusion can be performed in a reproducible manner for examination of the postpartum uterus. MRI/TVUS fusion allows standardized localization of the scar region and yields measurements comparable to MRI. Vascularization is reduced in the scar region.

# **CLINICAL RELEVANCE/APPLICATION**

MRI/US Fusion of the postpartum uterus allows standardized measurement of uterine wall thickness after Cesarean Section and Vaginal Delivery.

Voiding MR-Cystourethrography: A Diagnostic Imaging Technique for the Evaluation of Male Lower Urinary Tract in Normal Volunteers and in Patients with Bladder Outlet Obstruction

Thursday, Dec. 1 12:45PM - 1:15PM Room: GU/UR Community, Learning Center Station #2

# Participants

Marco Di Girolamo, MD, Rome, Italy (*Presenter*) Nothing to Disclose Simone Mariani, Rome, Italy (*Abstract Co-Author*) Nothing to Disclose Francesco Carbonetti, MD, Rome-Roma, Italy (*Abstract Co-Author*) Nothing to Disclose Ines Casazza, Rome, Italy (*Abstract Co-Author*) Nothing to Disclose Andrea Grossi, Rome, Italy (*Abstract Co-Author*) Nothing to Disclose Vincenzo David, MD, Rome, Italy (*Abstract Co-Author*) Nothing to Disclose

### PURPOSE

To evaluate the diagnostic accuracy of a new diagnostic imaging technique called voiding MR-cystourethrography that allows the visualization of the male urethra.

# METHOD AND MATERIALS

10 normal volunteers and 86 male patients with bladder outlet obstruction (evaluated with urine-flow velocity recording) underwent voiding MR-cystourethrography performed with a 1.5T superconductive magnet with the patient placed in supine position. The filling of the urinary bladder was obtainded by the i.v administration 20 mg of furosemide followed by <sup>3</sup>/<sub>4</sub> of the normal dose of a paramagnetic contrast agent (Magnevist, Bayer Pharma, Germany). When the bladder was filled of contrast-material-enhanced urine, the patient was asked to urinate. An appropriate urisheath was placed at the tip of the penis in order to collect urine urine and the patient had to advise when miction started. During the micturition T1-weighted spoiled 3D gradient-echo acquisitions on sagittal plane were performed. 3D row images were post-processed with MIP algorithm. 25 pts performed conventional cystourethrography in the month preceding MRI.

# RESULTS

Homogeneous opacification of the bladder lumen was always obtained. 10 patients were unable to perform the MR examination. In all the volunteers and in all the patients studied (76 pts) we obtained a perfect evaluation of the male urethra with voiding MRcystourethrography. The visualization of the urethra with MIP reconstructed images was considered comparable to that obtained with conventional cystourethrography. We detected 24 bladder neck obstructions, 36 urethral strictures (32 single and 4 double strictures), 10 cases following TURP and TUIP procedures, 2 urethral papillomatosis and 4 BPH. The number, site and length of urethral strictures were accurately determined by MRI. The analysis of 3D sagittal scans allowed a better evaluation of the morphology of the urethral strictures in comparison with conventional cystourethrography.

# CONCLUSION

Voiding MR-cystourethrography demonstrates the morfology of the bladder neck and urethra during micturition and can substitute standard retrograde and micturating cystourethrogram. This novel technique avoids radiation exposure to the gonads and urinary catheterization.

### **CLINICAL RELEVANCE/APPLICATION**

Voiding MR-cystourethrography demonstrates the morfology of the bladder neck and urethra during the micturition and can substitute standard cystourethrogram in bladder outlet obstruction.

Diagnostic Performance of Quantitative CT Texture Analysis for Differentiating Lipid-poor Adrenal Cortical Adenoma from Pheochromocytoma

Thursday, Dec. 1 12:45PM - 1:15PM Room: GU/UR Community, Learning Center Station #3

## Participants

Bing Shi, Beijing, China (*Presenter*) Nothing to Disclose Gu Mu Yang Zhang, MD, Beijing, China (*Abstract Co-Author*) Nothing to Disclose Hao Sun, MD, Beijing, China (*Abstract Co-Author*) Nothing to Disclose Huadan Xue, MD, Beijing, China (*Abstract Co-Author*) Nothing to Disclose Zheng Yu Jin, MD, Beijing, China (*Abstract Co-Author*) Nothing to Disclose

# PURPOSE

To evaluate diagnostic performance of using CT texture analysis (CTTA) to differentiate lipid-poor adrenal cortical adenoma (lp-ACA) from pheochromocytoma.

### **METHOD AND MATERIALS**

In this retrospective study, patients with surgically removed ACA and pheochromocytoma were identified from the pathology database. Patients were excluded for absence of preoperative multiphasic CT images or if the adrenal lesion was primarily cystic. Patients with ACA were further excluded if there was visible fat in the lesion on non-enhanced CT. As a result, 66 lp-ACA and 98 pheochromocytoma lesions were identified for analysis. CTTA was performed on the largest cross-sectional area for each lesion on non-enhanced and enhanced CT images by using TexRAD software, with quantification of texture parameters including mean gray-level intensity (Mean), standard deviation (SD), entropy, mean of positive pixels (MPP), skewness and kurtosis for fine to coarse textures (filters 0-6, respectively). Receiver operating characteristic (ROC) analysis was performed and the area under the ROC curve (AUC) was calculated for texture parameters that were significantly different for the objectives. Sensitivity (Se), specificity (Sp), positive predictive value (NPV) and accuracy were calculated by using the cut-off value of texture parameter with the highest AUC.

### RESULTS

Compared to pheochromocytoma, Ip-ACA had significantly lower mean at all texture scales, and lower entropy(filter 0), lower MPP (filter 0) and higher skewness (filter 0,2) at fine texture scales on non-enhanced CT images (P<0.001). On enhanced CT images, there was predominantly at the medium and coarse texture scales for most of the quantifiers (mean, SD, entropy and MPP) (P<0.001) as mean and MPP at fine texture scales (filter 0). Specifically, these texture-quantifiers followed a significant trend where mean, SD, entropy and MPP were lower in Ip-ACA in comparison to pheochromocytoma. A mean<34.5 at fine texture scale on non-enhanced CT identified Ip-ACA from pheochromocytoma with the highest AUC of 0.87±0.03 (Se=72.4%, Sp=87.5%, PPV=83.3%, NPV=78.6%, accuracy=80.5%, P=0.000).

### CONCLUSION

CTTA could be used to accurately differentiate Ip-ACA from pheochromocytoma.

### **CLINICAL RELEVANCE/APPLICATION**

CTTA could be used as a non-invasive tool to complement adrenal CT washout calculations for differentiating lp-ACA from pheochromocytoma on regular multiphasic CT images.

## Utility of Diffusion-Weighted MR Imaging in the Diagnosis of Morbidly Adherent Placenta

Thursday, Dec. 1 12:45PM - 1:15PM Room: GU/UR Community, Learning Center Station #4

#### **Participants**

Anna Ellermeier, MD, Seattle, WA (*Abstract Co-Author*) Nothing to Disclose Tom Winter, Salt Lake Cty, UT (*Abstract Co-Author*) Nothing to Disclose Susanna I. Lee, MD, PhD, Boston, MA (*Abstract Co-Author*) Nothing to Disclose Daniel S. Hippe, MS, Seattle, WA (*Abstract Co-Author*) Research Grant, Koninklijke Philips NV; Research Grant, General Electric Company

Manjiri K. Dighe, MD, Seattle, WA (Presenter) Research Grant, General Electric Company

### PURPOSE

Rising incidence and potential for catastrophic surgical outcomes underscore the need for sensitive prenatal diagnosis of morbidly adherent placenta (MAP). As such, ambiguous US findings often necessitate MRI. By better defining the border between placenta and myometrium, we hypothesized that diffusion-weighted imaging (DWI) may be a useful adjunct to traditional prenatal MRI.

### **METHOD AND MATERIALS**

Following IRB approval, 2 radiologists blinded to history and pathology retrospectively reviewed MR images (1.5T) from singleton pregnancies with and without pathologically-proven MAP. T2W only and T2W+DWI images were reviewed in separate sessions 2 weeks apart to avoid recall bias, with normal and MAP randomized within and between sessions. Reviewers completed questionnaires regarding placenta/uterus features, MAP presence and diagnostic confidence. MR findings were compared to pathology results with Chi-squared tests, interreader agreement was evaluated with Cohen's kappa and diagnostic accuracy was compared with the sign test.

### RESULTS

In total, 17 patients (mean gest 27w4d) were reviewed (indications: suspected MAP 14/17, fetal anomaly 2/17, abd pain 1/17). Typical MR criteria were reported more frequently with pathologic MAP: loss of retroplacental T2 dark zone (T2W, p=0.008) and dark/thick interplacental bands (T2W+DWI, p=0.032). Compared with T2W only, addition of DWI significantly increased interreader agreement (p=0.045) and tended to increase sensitivity (69% vs. 94%, p=0.25) but decrease specificity (56% vs. 39%, p=0.5) for MAP. Although readers reported increased diagnostic confidence with DWI in 65%, explicit confidence ratings (p=0.7) and diagnostic accuracy (p>0.99) did not change.

### CONCLUSION

MAP is a potentially life-threatening condition that requires increased clinical and radiographic sensitivity to optimize management. Small sample size (due to low incidence), inexperience with DWI interpretation in pregnancy, and poor resolution of DWI are limitations of our study. Trends toward increased sensitivity and improved interreader agreement suggest that DWI may complement traditional MRI evaluation of MAP but more experience and sequence improvement are necessary to improve diagnostic accuracy.

### **CLINICAL RELEVANCE/APPLICATION**

DWI in conjunction with traditional prenatal MRI may aid in evaluation of MAP, a potentially life-threatening condition that requires extensive surgical planning and patient counseling.

## **Honored Educators**

Presenters or authors on this event have been recognized as RSNA Honored Educators for participating in multiple qualifying educational activities. Honored Educators are invested in furthering the profession of radiology by delivering high-quality educational content in their field of study. Learn how you can become an honored educator by visiting the website at: https://www.rsna.org/Honored-Educator-Award/

Susanna I. Lee, MD, PhD - 2013 Honored Educator

Bilaterally Sustained Nephrograms Following the Parenteral Administration of Iodinated Contrast Material Administration Are a Potential Biomarker for Acute Kidney Injury, Dialysis, and Death

Thursday, Dec. 1 12:45PM - 1:15PM Room: GU/UR Community, Learning Center Station #5

## Participants

Jennifer S. McDonald, PhD, Rochester, MN (*Abstract Co-Author*) Research Grant, General Electric Company Robert J. McDonald, MD, PhD, Rochester, MN (*Presenter*) Nothing to Disclose Erik Steckler, MD, BS, Tampa, FL (*Abstract Co-Author*) Nothing to Disclose Richard W. Katzberg, MD, Charleston, SC (*Abstract Co-Author*) Research Grant, Siemens AG; David F. Kallmes, MD, Rochester, MN (*Abstract Co-Author*) Research support, Terumo Corporation Research support, Medtronic plc Research support, Sequent Medical, Inc Research support, Benvenue Medical, Inc Research support, General Electric Company Consultant, General Electric Company Consultant, Medtronic plcConsultant, Johnson & Johnson Eric E. Williamson, MD, Rochester, MN (*Abstract Co-Author*) Research Grant, General Electric Company Nelson Leung, MD, Rochester, MN (*Abstract Co-Author*) Nothing to Disclose

### PURPOSE

To determine whether persistent bilateral global CT nephrograms are associated with acute kidney injury (AKI), dialysis, and death in patients following parenteral administration of iodinated contrast material.

# METHOD AND MATERIALS

This retrospective study was HIPAA compliant and approved by our institutional review board. All patients who received 1) either a contrast-enhanced CT exam or cardiac catheterization with the low-osmolar, nonionic monomer iohexol 350 mgI/mL between 2000-2014 and 2) an unenhanced abdominal CT exam in the subsequent 18-30 hours were identified. Patients who lacked sufficient preand post-procedure creatinine results, or who received additional contrast material within 14 before to 3 days after the contrastenhanced exam were excluded. Nephrograms were identified by radiologist review. The incidence of AKI (AKIN Stages 1-3), dialysis, and death were compared between patients with bilateral global nephrograms and those without using Pearson's chi-squared test.

# RESULTS

A total of 128 patients met all inclusion criteria. The baseline eGFR subgroups were 77 (60%) > 60 mL/min/1.73 m2; 44 (34%) 30-59 mL/min/1.73 m2; and 7 (5.5%) < 30 mL/min/1.73 m2 patients. The overall incidence of persistent global nephrograms was 20% (n=25), with a similar incidence following cardiac catheterization (20%, 13/65) and contrast-enhanced CT (19%, 12/63). Nephrogram patients had significantly higher rates of AKI (Stage 1: 64% (16/25) vs. 19% (20/103), OR = 7.38 (95% CI 2.85-19.1, p<.0001), dialysis (24% (6/25) vs. 2.9% (3/103), OR = 10.5 (2.40-45.8), p=.0002), and death (24% (6/25) vs. 1.9% (2/103), OR = 15.9 (2.99-85.0), p<.0001) compared to non-nephrogram patients.

# CONCLUSION

The observation of persistent bilateral global nephrograms on unenhanced CT suggests a risk of greater adverse clinical outcomes of AKI, dialysis, and death in this selected patient population when compared to patients whose kidneys fully eliminate the contrast material.

### **CLINICAL RELEVANCE/APPLICATION**

Patients who develop a persistent nephrogram following contrast administration are at higher risk of AKI and should warrant greater clinical surveillance.

### GU257-SD-THB6

### Accuracy and Agreement of Nine Readers on PI-RADSv2 for Prostate Cancer mpMRI

Thursday, Dec. 1 12:45PM - 1:15PM Room: GU/UR Community, Learning Center Station #6

#### **Participants**

Matthew Greer, BS, Cleveland Heights, OH (Presenter) Nothing to Disclose Joanna Shih, Bethesda, MD (Abstract Co-Author) Nothing to Disclose Nathan S. Lay, PhD, Bethesda, MD (Abstract Co-Author) Nothing to Disclose Tristan Barrett, MBBS, BSc, Guildford, United Kingdom (Abstract Co-Author) Nothing to Disclose Leonardo K. Bittencourt, MD, PhD, Rio De Janeiro, Brazil (Abstract Co-Author) Nothing to Disclose Samuel Borofsky, MD, Washington, DC (Abstract Co-Author) Nothing to Disclose Ismail M. Kabakus, MD, PhD, Ankara, Turkey (Abstract Co-Author) Nothing to Disclose Yan Mee Law, MBBS, Singapore, Singapore (Abstract Co-Author) Nothing to Disclose Jamie Marko, MD, Bethesda, MD (Abstract Co-Author) Nothing to Disclose Haytham M. Shebel, MD, Mansoura, Egypt (Abstract Co-Author) Nothing to Disclose Francesca Mertan, BS, Bethesda, MD (Abstract Co-Author) Nothing to Disclose Maria Merino, MD, Bethesda, MD (Abstract Co-Author) Nothing to Disclose Peter Pinto, Bethesda, MD (Abstract Co-Author) Nothing to Disclose Peter L. Choyke, MD, Rockville, MD (Abstract Co-Author) Researcher, Koninklijke Philips NV; Researcher, General Electric Company; Researcher, Siemens AG; Researcher, iCAD, Inc; Researcher, Aspyrian Therapeutics, Inc; Researcher, ImaginAb, Inc; Researcher, Aura Biosciences, Inc Ronald M. Summers, MD, PhD, Bethesda, MD (Abstract Co-Author) Royalties, iCAD, Inc; ; Baris Turkbey, MD, Bethesda, MD (Abstract Co-Author) Nothing to Disclose

Dalis Turkbey, MD, Dechesua, MD (Abstract Co-Author) Nothing to

### PURPOSE

PIRADSv2 was recently proposed to standardize the acquisition and interpretation of mpMRI. We conducted a multi-reader study to evaluate the accuracy and agreement of PIRADSv2. We used a controlled study with whole mount prostatectomy specimens as the ground truth.

### **METHOD AND MATERIALS**

9 radiologists from 8 institutions and 6 countries participated: 3 high, 3 moderate, and 3 low experience with prostate MRI. Patients were consecutive treatment-naïve patients who had ERC 3T mpMRI (T2W, ADC, b2000, and DCE). 163 patients were evaluated: n=110 cases who underwent radical prostatectomy after MRI; n=53 controls with no detected lesions MRI and no positive biopsy. Readers were blinded to all outcomes. Up to 3 lesions were prospectively detected and scored with PIRADSv2 on mpMRI. Lesions were correlated between readers and to patient specific 3D-printed mold whole mount prostatectomy. The index lesion was defined as the highest grade or, if equivalent, the highest volume lesion. Average sensitivity, specificity, and positive predictive value (PPV) were calculated per-patient and per-lesion with PIRADSv2 defined as positive. Index of specific agreement (ISA) was calculated as the pairwise proportion of agreement between all readers.

### RESULTS

Average PSA density was 0.29 ng/ml2 vs 0.09 ng/ml2 for cases and controls. On lesion based analysis the average sensitivity and PPV for detecting index lesions were 77.6% and 88.7%. The sensitivity and PPV for all lesions was 49.7% and 76.1%. For index lesions Gleason 3+4 or above the sensitivity and PPV was 80.9% and 88.7%. On patient level analysis the average sensitivity and specificity were 91.5% and 71.2%, respectively. Highly experienced readers reached a specificity of 91.0% vs 51.3% for moderately experienced. ISA was 56.9% for detecting lesions, 65.9% between highly experienced readers vs 57.7% between high and moderate experience. ISA was 75.5% for true positives, 35.3% for the exact PIRADSv2 score, 62.7% for PIRADS>3, and 53.2% for PIRADS=5.

### CONCLUSION

Multiple readers demonstrate good sensitivity for detecting high grade index lesions with PIRADSv2 in a controlled study, but specificity was experience dependent. Readers demonstrate high agreement for true positive lesions and low agreement for overall score.

### **CLINICAL RELEVANCE/APPLICATION**

By using PIRADSv2 readers with varying experience can reproducibly detect high-grade index lesions. Agreement differs on precise scoring of PIRADSv2.

**Interactive Tool to Teach Management of Contrast Media Reactions** 

Thursday, Dec. 1 12:45PM - 1:15PM Room: HP Community, Learning Center Custom Application Computer Demonstration

#### **Participants**

Alexi Otrakji, MD, Boston, MA (*Presenter*) Nothing to Disclose Iris M. Otani, MD, San Diego, CA (*Abstract Co-Author*) Nothing to Disclose Hillary R. Kelly, MD, Boston, MA (*Abstract Co-Author*) Nothing to Disclose Garry Choy, MD, MS, Boston, MA (*Abstract Co-Author*) Nothing to Disclose Sanjay Saini, MD, Boston, MA (*Abstract Co-Author*) Nothing to Disclose Gloria M. Salazar, MD, Boston, MA (*Abstract Co-Author*) Nothing to Disclose Swati Goyal, Boston, MA (*Abstract Co-Author*) Nothing to Disclose

## **TEACHING POINTS**

The symptoms of contrast reaction fluctuate from mild to severe (anaphylactic) reactions. In addition, the symptoms of contrast reaction are classified to allergic like and physiologic reactions. Recognizing these symptoms and their severity is the cornerstone of the proper clinical management. Learning the symptoms and management of contrast reactions through video-based course that simulate the real environment of imaging exam room could be more efficient than conventional lectures. After review of video interactive cases participants will be familiar to: Recognize contrast reaction symptoms severity Understand the different reactions pathway (allergic vs physiologic) Treat contrast reactions.

# TABLE OF CONTENTS/OUTLINE

Interactive software (RadIQ) will be used to allow the participants practice through many clinical scenarios of contrast reactions based on American College of Radiology manual. Multiple choice questions evaluate the knowledge and gaps as well. Clinical scenarios include: Mild allergic-like symptoms: Hives, Itching, sneezing Moderate allergic- like symptoms: Bronchospasm Severe allergic –like reactions: laryngeal edema Anaphylaxis: Hypotension, tachycardia Physiologic reaction: Hypotension with bradycardia Medical Students' Perceptions Regarding the Use of Patient Photographs Integrated with Medical Imaging Studies

Thursday, Dec. 1 12:45PM - 1:15PM Room: HP Community, Learning Center Station #1

# Participants

Diane Siegel, BA, Atlanta, GA (*Presenter*) Nothing to Disclose Ariadne DeSimone, MD,MPH, Atlanta, GA (*Abstract Co-Author*) Nothing to Disclose Carson A. Wick, MS,PhD, Atlanta, GA (*Abstract Co-Author*) Nothing to Disclose Srini Tridandapani, MD, PhD, Atlanta, GA (*Abstract Co-Author*) Co-founder, CameRad Technologies, LLC Kimberly E. Applegate, MD, MS, Zionsville, IN (*Abstract Co-Author*) Nothing to Disclose

# PURPOSE

Integrating patient facial photos with medical imaging may increase detection of misidentified studies, without concomitant increase in interpretation time. We wished to study medical students' perception of this technology.

### **METHOD AND MATERIALS**

607 students were emailed an IRB-approved, SurveyMonkey survey on the use of patient photos in medical imaging in 2015. Associations between students' level of training, radiology exposure, and their perceptions of the technology were studied via multi-linear regression.

### RESULTS

223/607 (37%) students responded (mean age 25; 41% male). 96% support the technology if it increases detection of identification errors. 46% predicted more accurate interpretation of images. 65% predicted more accurate interpretation of lines and tubes. 88% predicted more accurate detection of misidentification. 51% predicted more accurate evaluation of patient health status. 62% predicted no difference in image interpretation time. 81% indicated that the use of patients' photos would result in fewer identification errors. Perceived benefits of the technology include: humanization of bias in interpretation and improved interpretation due to additional clinical context. Student concerns include: introduction of bias in interpretation due to patient appearance, confidentiality, and need for consent. Respondents who left a comment about the use of patient photos were less likely to support use of photos if they reduced errors (P<.001). Students who reported witnessing a wrong-patient error were more likely to comment positively on the technology (P<.01). Students advanced in their degree program, they were less likely to consider patient photographs to be of benefit in terms of accuracy, interpretation time and reducing misidentification errors (P<.01).

### CONCLUSION

The vast majority of medical students support use of patient photos in imaging to detect identification errors. Their comments suggest photos may humanize and improve image interpretation, but express concern about bias and patient confidentiality. Students not completing a radiology elective and with fewer years in training were more positive.

### **CLINICAL RELEVANCE/APPLICATION**

While the vast majority of medical students support implementation of innovative safety technology, they provide rich feedback regarding advantages and potential pitfalls.

Comparison of Temporal Variations in Ultrasound Training in Two Novice Groups of Medical Students

Thursday, Dec. 1 12:45PM - 1:15PM Room: HP Community, Learning Center Station #2

#### Awards

## **Student Travel Stipend Award**

#### **Participants**

Anthony P. Trace, MD,PhD, Richmond, VA (*Presenter*) Nothing to Disclose Craig W. Goodmurphy, PhD, MSc, Norfolk, VA (*Abstract Co-Author*) Nothing to Disclose Carrie Elzie, PhD, Norfolk, VA (*Abstract Co-Author*) Nothing to Disclose Sarah C. Shaves, MD, Virginia Beach, VA (*Abstract Co-Author*) Nothing to Disclose

### PURPOSE

Point of care ultrasound continues to expand across many medical specialties over the past decade. As a result, more medical schools are beginning to incorporate ultrasound training into their curricula. Training varies significantly from institution to institution with key differences in the temporal placement of training within the curricula. This research project aimed to determine if the placement and timing of ultrasound training impacted skill acquisition comparing two ultrasound novice groups: 1st year medical students and 4th year medical students.

### **METHOD AND MATERIALS**

While the curricular content was identical for each novice group, the length of training varied from 16 weeks for the first year medical students and 4 weeks for the fourth year medical students. Each group was given a pre-test at the beginning of the course, a pair-matched post-test upon completion that focused on knowledge of ultrasound, physics and appropriateness of ultrasound studies, as well as a course evaluation.

## RESULTS

While some variation occurred in the scores on the pre-test, similar results were achieved on the post-test.

#### CONCLUSION

Data suggests that the same level of proficiency can be achieved regardless if the curriculum is spread out or concentrated and is independent of year of training within medical school. Details of the curriculum will also be presented along with recommendations for implementation of ultrasound training.

#### **CLINICAL RELEVANCE/APPLICATION**

This work has implications for the medical educator and those interested in point of care ultrasound.

# HP241-SD-THB3

## Virtual Exploration of Egyptian Mummies using 256-Slice and Spectral CT: Preliminary Experience

Thursday, Dec. 1 12:45PM - 1:15PM Room: HP Community, Learning Center Station #3

#### Participants

Etienne Danse, MD, PhD, Brussels, Belgium (*Presenter*) Nothing to Disclose Jean-Philippe Hastir, Brussels, Belgium (*Abstract Co-Author*) Nothing to Disclose Emmanuel E. Coche, MD, Brussels, Belgium (*Abstract Co-Author*) Nothing to Disclose Alain Vlassenbroek, PhD, Brussels, Belgium (*Abstract Co-Author*) Employee, Koninklijke Philips NV Luc Delvaux, Brussels, Belgium (*Abstract Co-Author*) Nothing to Disclose Caroline Tilleux, Louvain La Neuve, Belgium (*Abstract Co-Author*) Nothing to Disclose

# PURPOSE

**Background :** Since the discovery of William Roentgen, imaging was used for the investigation of egyptian mummies. The advent of computed tomography was revolutionary but until now, the technical background was relatively scarse and sparse because of different generations of CT scanners used for this purpose. **Objective** : to report our experience in the exploration of human, animal mummies and art objects from old Egypt collection from the Cinquantenary Museum using the state-of-the art CT technology and define the contribution of 256-slice and spectral CT in this field.

### **METHOD AND MATERIALS**

Hospital hygiene and safety precautions were taken before the imaging investigation of 27 mummies ( 6 humans, 12 animals, 7 human body fragments and 2 art objects, coming from the Old Egypt collection of the Cinquantenary Museum ). All the examinations were performed with a 256-slice CT scan (iCT, Philips Healthcare, Eindhoven, The Netherlands) using the following parameters : at 80 and 140 kv consecutively, slice thickness 128 X 0.625mm, 0,9 mm slice reconstruction, overlap of 0,45 mm, matrix 768 X 768 . For two human mummies, examinations were performed on a dual-layer CT (IQON, Philips Healthcare, Eindhoven, The Netherlands) using the same parameters except for the kv (120 kV). Post-processing was performed on a dedicated MX View workstation (MX view, Philips Healthcare, Eindhoven, The Netherlands) by a CT technologist

### RESULTS

Using 256-slice CT scan, the following items were analysed :1/ for the human bodies and human parts:- analysis of the head , chest and abdomen residues- analysis of the way of evisceration (brain and body)- bone and ligaments (bone integrity, diseases and traumatisms)- estimation of age and sex- identification of mumies damages and presence of parasites2/ for animals- identification of the type of animal3/ art objects:- estimation of the composition4/ in all the cases, analysis of the composition and configuration of the wrapped enveloppes.Using Spectral CT, the HU attenuation of the different tissue composition of the selected human, animal and objects were compared to the data of single energy CT.

# CONCLUSION

256-slice CT scan is helpful for a better understanding of egyptian mummies. The tissue composition analysis is improved by using spectral CT[C1]

## **CLINICAL RELEVANCE/APPLICATION**

The most recent CT techniques are relevant for archeologic non destructive investigations

# IN129-ED-THB7

# Cancer and Phenomics Toolkit (CAPTk): A Software Suite for Computational Oncology and Radiomics

Thursday, Dec. 1 12:45PM - 1:15PM Room: IN Community, Learning Center Station #7

FDA Discussions may include off-label uses.

#### **Participants**

Sarthak Pati, Philadelphia, PA (*Presenter*) Nothing to Disclose Saima Rathore, Philadelphia, PA (*Abstract Co-Author*) Nothing to Disclose Ratheesh Kalarot, Philadelphia, PA (*Abstract Co-Author*) Nothing to Disclose Patmaa Sridharan, Philadelphia, PA (*Abstract Co-Author*) Nothing to Disclose Mark Bergman, Philadelphia, PA (*Abstract Co-Author*) Nothing to Disclose Taki Shinohara, PhD, Philadelphia, PA (*Abstract Co-Author*) Nothing to Disclose Paul Yushkevich, PhD, Philadelphia, PA (*Abstract Co-Author*) Nothing to Disclose Ragini Verma, Philadelphia, PA (*Abstract Co-Author*) Nothing to Disclose Despina Kontos, PhD, Philadelphia, PA (*Abstract Co-Author*) Nothing to Disclose Christos Davatzikos, PhD, Philadelphia, PA (*Abstract Co-Author*) Nothing to Disclose

### CONCLUSION

CAPTk provides a bridge for quick translation between academic research and clinical application, thereby enabling translation of cutting-edge research into clinically practical tools quickly and efficiently.

# FIGURE

http://abstract.rsna.org/uploads/2016/16014589/16014589\_uw28.jpg

### Background

Availability of highly sophisticated methods that help us gain a comprehensive understanding of the underlying mechanisms of cancer, reveal substantive insight into the biological basis of disease susceptibility, treatment response, and identification of new drug targets, has skyrocketed. Translating such academic research into clinical practice is one of the biggest challenges, due to their complexity. We present CAPTk as a tool that facilitates translation of such algorithms from medical imaging research to the clinic. It replicates basic functionality of radiological workstations (accepts MRI data in DICOM & NIFTI formats with manual annotations). It is distributed under a completely free BSD-style license and is designed to be computationally efficient.

# **Evaluation**

CAPTk has been designed for advanced image analysis pertaining to oncological conditions in the brain, breast and lung. It provides a springboard for using a number of algorithms, including but not limited to image registration, thresholding, bias correction, quantitative image analysis applications for predicting the status of Epidermal Growth Factor Receptor variant III in glioblastoma (GBM), semi-automatic mask generation of anatomical structures, evaluation of the peritumoral spatial heterogeneity in GBM, as well as analysis of normal tissues for predicting risk of future cancer. Utilizing industrially validated & open source tools (ITK, VTK, Qt), CAPTk encapsulates the core principles of good software design (usability, stability, scalability), supports all major deployment platforms and provides interfaces to help developers integrate C++ & Python applications utilizing a common interface.

#### Discussion

Users will see an easy-to-use graphical interface to access cutting-edge methods, along with image annotations (drawing points, tumor radius, masks), and developers can easily add applications to CAPTk while having access to the interactive & visualization routines. Examples will be showcased during the demonstration.

Integration of Mammographic, Ultrasound, and Clinical Metrics for Characterization of Breast Lesions using Novel Informatics Modeling with Comparison to OncotypeDX

Thursday, Dec. 1 12:45PM - 1:15PM Room: IN Community, Learning Center Station #1

### Participants

Philip A. Di Carlo, MD, Baltimore, MD (*Presenter*) Nothing to Disclose Vishwa Parekh, MS, Baltimore, MD (*Abstract Co-Author*) Nothing to Disclose Susan C. Harvey, MD, Lutherville, MD (*Abstract Co-Author*) Nothing to Disclose Christopher Umbricht, MD,PhD, Baltimore, MD (*Abstract Co-Author*) Nothing to Disclose Antonio C. Wolff, MD, Baltimore, MD (*Abstract Co-Author*) Research Grant, F. Hoffmann-La Roche Ltd Michael A. Jacobs, PhD, Baltimore, MD (*Abstract Co-Author*) Research Grant, Siemens AG

### PURPOSE

Mammography, ultrasound(US) and MRI are imaging modalities used for breast cancer detection. The BIRADS lexicon provides a set of descriptors that facilitates consistent structure for assessment and reporting of breast lesions. To predict recurrence, oncologists use OncotypeDX, which stratifies patients into three risk groups: low, medium, and high. We hypothesize that there is a relationship between imaging features defined by BIRADS and the genetic profile of cancers. To test this, we developed a machinelearning non-linear dimension reduction(NLDR) algorithm with embedded informatics. Using these techniques, we compare BIRADS descriptors to the OncotypeDX for recurrence prediction.

## **METHOD AND MATERIALS**

Patients(n=48) who underwent diagnostic breast imaging, were ER+, with available OncotypeDX were tested with the algorithm. The clinical and BIRADS parameters for mammography included breast density, asymmetry, microcalcifications(morphology, distribution), mass(size, shape, margins, density) and architectural distortion. Ultrasound parameters included mass presence, size, echogenicity, shape, margins, vascularity, and orientation. These parameters were assigned numerical values to reflect relative suspicion of each descriptor. There were 24 patients with low(0-17), 13 with intermediate(18-31), and seven with high risk(>31) scores from OncotypeDX. Our NLDR and informatics algorithm computes the multidimensional metrics and embeds these results into a two-dimensional heatmap for clinical decision support. Area under the Curve(AUC) and student's t-tests were calculated.

#### RESULTS

The top predictors were mammographic beast density, and mass margins and US directional size. These predictors resulted in a significant AUC( $0.86\pm0.07$ ). The mammographic tumor sizes in high risk groups were larger( $1.9\pm0.58$ cm) compared to the low-risk group( $1.38\pm0.58$ cm) with similar results for US measurements in the radial( $2.7\pm1.2$ cm vs. $1.2\pm0.8$ cm), AP ( $1.8\pm0.76$ cm vs.  $0.98\pm0.61$ cm) and antiradial ( $2.1\pm1.3$ cm vs. $1.0\pm0.58$ cm) dimensions. We created a visualization informatics heat map detailing the contribution of each parameter.

# CONCLUSION

The most important imaging parameters determined from the informatics model were mammographic breast density, and mass margins and US size.

# **CLINICAL RELEVANCE/APPLICATION**

NLDR Informatics modeling of clinical and imaging descriptors will provide the foundation for an advanced clinical decision support system for precision medicine

Novel Algorithm for Pulmonary Nodule Malignancy Prediction

Thursday, Dec. 1 12:45PM - 1:15PM Room: IN Community, Learning Center Station #2

#### Awards

#### **Student Travel Stipend Award**

#### **Participants**

Stephen P. Power, MBBCh, MRCPI, Cork, Ireland (*Presenter*) Nothing to Disclose Pietro Nardelli, MD, Cork, Ireland (*Abstract Co-Author*) Nothing to Disclose Jaspar Pahl, Cork, Ireland (*Abstract Co-Author*) Nothing to Disclose Sean E. McSweeney, MD, Cork, Ireland (*Abstract Co-Author*) Nothing to Disclose Kevin N. O Regan, MD, Cork, Ireland (*Abstract Co-Author*) Nothing to Disclose Padraig Cantillon-Murphy, PhD, Cork, Ireland (*Abstract Co-Author*) Nothing to Disclose

### CONCLUSION

Our work describes a novel algorithm which predicts malignancy in solitary pulmonary nodules with more accurary than previously published methods.

### Background

Pulmonary nodules are detected on between 20-50% of thoracic CT studies, many of them as incidental findings. The follow-up of these nodules places a significant burden on healthcare services considering only a small percentage of these nodules will eventually prove to be malignant in aetiology (1-12%). Computer aided detection systems can help to assist the radiologist in the identification and classification/malignancy prediction of pulmonary nodules.

## **Evaluation**

We describe a novel system for semi-automatic estimation of malignancy of pulmonary nodules, with the aim of minimizing user interaction in this computer-aided identification and classification of nodules. The algorithm automatically extracts size, location, edge smoothness, growth rate, cavity wall thickness and calcification of the analysed nodule and uses these features, combined with clinical details to calculate the probability of malignancy. The algorithm works as a modular structure which consists of four sequential steps: Segmentation of lung regions to exclude unwanted structures and to identify a nodule's location. Analysis of identified nodules to extract characteristics such as size, shape, wall thickness and the presence of calcification. Segmentation of lung lobar fissure and lobes. Nodule diagnosis with estimation of likelihood of malignancy (%)The algorithm was tested on a combination of CT images available online (open-source) and from CT studies at our local institution (n =175 nodules). Estimates of malignancy was provided by reviewing radiologists and compared with the estimation produced from the algorithm.

#### Discussion

This work presents a novel method to predict malignancy in solitary pulmonary nodules, providing automatic extraction of a nodule's radiological characteristics. A comparison with four seperate radiologists' subjective assessment showed that the implemented algorithm is comparable to radiologists' performance. The ability of the algorithm to predict malignancy is higher than the previously published methods.

# Big Data in Radiology: A COPD Case Study

Thursday, Dec. 1 12:45PM - 1:15PM Room: IN Community, Learning Center Station #3

#### **Participants**

Thomas J. Re, MD,MS, Basel, Switzerland (*Presenter*) Nothing to Disclose Kevin Mader, DPhil,MSc, Zuerich, Switzerland (*Abstract Co-Author*) Employee, 4Quant Ltd; Shareholder, 4Quant Ltd Jens Bremerich, MD, Basel, Switzerland (*Abstract Co-Author*) Nothing to Disclose Flavio Trolese, Zurich, Switzerland (*Abstract Co-Author*) Officer, 4Quant Ltd Michael Moor, BSC, Basel, Switzerland (*Abstract Co-Author*) Nothing to Disclose Bram Stieltjes, MD, Basel, Switzerland (*Abstract Co-Author*) Nothing to Disclose

## CONCLUSION

The described pipeline, utilizing fully automatic PACS study retrieval and post-processing lays the groundwork for future big-data analysis of COPD imaging quantities from large radiology archives.

#### Background

Chronic Obstructive Pulmonary Disease (COPD) affects millions of people worldwide. Chest CT studies are often used to assess severity and progress of this disease and this has created a large pool of disease related imaging data. We suggest that a Big Data approach to the analysis of this data could provide new insight and understanding of COPD. This work describes our development and verification of a fully automatic pipeline for identifying, retrieving and analysing COPD CT data from a PACS, a prerequisite to its Big Data analysis.

### **Evaluation**

A ground truth reference was created using a test sample of 45 COPD CT studies using a traditional semi-automatic process choosing Percentile Density 15 (PD15) and Low Attenuation Area -950 (LAA-950) as the quantities of interest. A radiologist identified/retrieved the CT studies' data one at a time via a standard PACS client, then used a semi-automatic software for segmenting lung and calculating PD/LAA values. This process required ~90hrs total radiologist time (2hr/exam). For the fully automatic pipeline, software was developed to query the PACS, identify and retrieve the CT studies of interest and perform PD/LAA calculations (RIQAE, 4Quant Ltd, Zurich, Switzerland). Once implemented, this fully automatic pipeline required under 1hr of radiologist time to prepare and under 1hr total PACS/computing time to generate the results for the 45 CT studies. Average differences in calculated quantities (PD15/LAA-950) between the two techniques was not significant (mean= 0.10%; SD=0.14%; max difference=0.61%; p-value=0.91). Subsequently, a larger cohort of 200 subjects was analyzed automatically in <3hrs.

#### Discussion

A fully automatic pipeline is a prerequisite for a Big-Data approach, as even semi-automatic process, requiring radiologist's interaction, is impractical for assessing thousands of exams. In this work, we show that it is possible to automate both the data search and query and post-processing with negligible effects on final quantitative results.

Implementation and Clinical Evaluation of 3D Visual Representation and Index of Imaging Diagnostic Records for Radiological Imaging Practices

Thursday, Dec. 1 12:45PM - 1:15PM Room: IN Community, Learning Center Station #4

## Participants

Jianguo Zhang, PhD, Shanghai, China (*Presenter*) Shareholder, AXON Medical Technologies Corp; Shareholder, Simed Medical Information Tech Inc

Liehang Shi, Shanghai, China (*Abstract Co-Author*) Nothing to Disclose Tonghui Ling, Shanghai, China (*Abstract Co-Author*) Nothing to Disclose Yanqing Hua, MD, Shanghai, China (*Abstract Co-Author*) Nothing to Disclose Jianyong Sun, Shanghai, China (*Abstract Co-Author*) Nothing to Disclose Yuanyuan Yang, MBBS, Shanghai, China (*Abstract Co-Author*) Nothing to Disclose Mingqing Wang, Shanghai, China (*Abstract Co-Author*) Nothing to Disclose

### CONCLUSION

A new 3DVRI system was introduced into imaging diagnostic practices. Two evaluation results proved that doctors can much more easily and efficiently understand patient historical status by use of 3DVRI system than over use of PACS/RIS.

### Background

Imaging diagnostic records (IDR) in large hospitals has become the main component of medical big data and brings huge values to healthcare services, but also introduces challenges to healthcare professionals as there may be too many imaging studiess for each patient for a doctor to review in a limited time slot. We had developed an innovation method 3D visually to represent and index IDR by using 3D anatomic model and presented it in RSNA Scientific Presentation 2011. In this presentation, we give an engineering implementation of this method and its evaluation, and comparison of the evaluation results with that by use of a clinical RIS-integrated PACS.

## **Evaluation**

The implementation was to build 3D Visual Representation and Index (3DVRI) system including components of NLP for Chinese, Visual Index Creator (VIC), and 3D Visual Rendering Engine. The 3DVRI system has three major functions such as 3D anatomic representation of medical status of patient, quantitative description of lesions, and original data display of related DICOM studies and reports. Two evaluation scenarios were performed: the first one was to train more than 20 radiologists to play 3DVRI system to understand patients' medical status individually and answer eight questions listed in a sheet; the second was to arrange five radiologists to manipulate the 3DVRI system to find historic lesions , brief description of lesions and trend of disease development, et al., by use of the 3 major functions provided by 3DVRI system and compare the results with that by use of a clinical RIS/PACS on same 20 patients with variety of imaging studies.

### Discussion

All participants in first evaluation answered questions very positively and wanted this system to assist them in reviewing the historic studies of patients. The result of second evaluation proved that 3DVRI has great advantage over the use of RIS/PACS in understanding patient's past lesion development and medical treatment conditions

## IN261-SD-THB5

An Image Retrieval System for Diagnosis Support of Idiopathic Interstitial Pneumonia using a Deep Convolutional Neural Network

Thursday, Dec. 1 12:45PM - 1:15PM Room: IN Community, Learning Center Station #5

## Participants

Felix Nensa, MD, Essen, Germany (*Abstract Co-Author*) Nothing to Disclose Sandra Maier, Essen, Germany (*Abstract Co-Author*) Nothing to Disclose Shu Liao, Chapel Hill, NC (*Abstract Co-Author*) Employee, Siemens AG Xiang Zhou, Malvern, PA (*Abstract Co-Author*) Employee, Siemens AG Yiqiang Zhan, Malvern, PA (*Abstract Co-Author*) Employee, Siemens AG Hilmar Kuehl, MD, PhD, Essen, Germany (*Abstract Co-Author*) Nothing to Disclose Michael Forsting, MD, Essen, Germany (*Abstract Co-Author*) Nothing to Disclose Lale Umutlu, MD, Essen, Germany (*Presenter*) Consultant, Bayer AG

#### PURPOSE

Differential diagnosis of idiopathic interstitial pneumonia (IIP) presents a significant challenge in thoracic CT. Using a deep-learning convolutional neural network (CNN) we sought to evaluate whether computer assisted similar image retrieval can improve the diagnostic accuracy of a non-expert radiologist in the differentiation between usual interstitial pneumonia (UIP) and other IIP (non-UIP).

### **METHOD AND MATERIALS**

A prototype CNN-based algorithm 1) automatically extracts salient disease patches within the lung; 2) compares such patches with patches from other patients in a database; and 3) consolidates the matching results at the patient level to retrieve similar lung studies from that database. The CNN was trained with a small database consisting of 250 CT studies in patients with IIP (50 UIP, 50 non-UIP) and additional control cases of emphysema (n=50), pulmonary sarcoidosis (n=50) and normals (n=50). A radiologist without special training in IIP performed blinded diagnosis in 50 cases of UIP and 50 cases of non-UIP that were not included in the databases. In a second read the reader was supported by the CNN, for each case presenting its top 5 similar cases (including disease labels) from the database. Consent diagnosis by a panel of certified IIP experts in a specialized center served as the standard of reference.

### RESULTS

The human reader yielded diagnostic accuracy 72% (kappa=0.44) for the discrimination of UIP and non-UIP against the reference standard. In the CNN supported read the human reader improved to a diagnostic accuracy of 77% (kappa=0.54). None of the emphysema, pulmonary sarcoidosis or normal cases were falsely presented as top matches by the CNN.

## CONCLUSION

IIP reading using a prototype deep-CNN yielded moderate improvement of a non-expert reader in the differentiation of UIP and non-UIP. Technical improvements of the CNN itself as well as the human-machine interaction are expected to provide significantly increased diagnostic accuracy.

## **CLINICAL RELEVANCE/APPLICATION**

Recent advancements in machine learning are poised to support radiologists in clinical routine work and may be particularly helpful in domains otherwise requiring rare specialist knowledge.

# Electronic Consensus Peer Review: Bringing Peer Review to the 21st Century

Thursday, Dec. 1 12:45PM - 1:15PM Room: IN Community, Learning Center Station #6

#### Participants

Avez Rizvi, MD, Doha, Qatar (*Abstract Co-Author*) Nothing to Disclose Zafar Iqbal, MS, Doha, Qatar (*Presenter*) Nothing to Disclose Deepak Kaura, MD, Doha, Qatar (*Abstract Co-Author*) Nothing to Disclose

## CONCLUSION

Consensus peer review is not a novel concept as Alkasab et al. demonstrated in 2014. However, it's widespread use is still not ubiquitous. We hope that by showing another, more simplistic version of the consensus peer review application, further adoption can be enhanced.

#### Background

Peer review processes have evolved considerably from the paper format of yesteryear. The American College of Radiology released RADPEER<sup>™</sup> to address the drawbacks of sorting and collecting a completely paper-based peer review process. However, the need to login remotely and fill out a form based, website limited adoption. Even newer integrated e-Radpeer options were developed inhouse at places like Staten Island University Hospital, which addressed both the storage/sorting issues as well as adoption (SIIM Annual Meeting 2011). Nevertheless, *quality* peer review has always been an issue.

#### **Evaluation**

We have successfully tested RCPR in beta mode with a few dozen cases and anticipate several hundreds of cases in the near future.

#### Discussion

One-to-one peer reviews are fraught with biases and variations on interpretive subjectivity, whereas, consensus 360 peer reviews are far more objective as agreement on interpretation is reached by a range of experts within the field (Alkasab, et al). Our solution is novel in its simplicity and ease of implementation. In order to address subjectivity in traditional peer review, yet still maintain the functionality of an integrated e-peer review application, we built a Radiology Consensus Peer Review (RCPR) application. The application has the ability to "check-in" the radiologists currently in the session. Only cases from radiologists participating in the session will be reviewed via generated worklist. The application anonymizes the radiologist and only shows the body of the report and the impression. The report of the previously interpreted exam is scored by the reviewers using an ACR standardized four-point rating scale. At the end of the consensus, an autogenerated email is sent to the respective radiology faculty member if a discrepancy is found. The email is also sent to the department chair and head of quality and safety. This ensures both anonymity and quality control.

## Characterization of Sentinel Lymph Nodes Using Targeted Ultrasound Contrast Agents

Thursday, Dec. 1 12:45PM - 1:15PM Room: S503AB Station #1

#### Awards

#### **Trainee Research Prize - Fellow**

#### **Participants**

Kibo Nam, PhD, Philadelphia, PA (Presenter) Nothing to Disclose

Maria Stanczak, MS, Philadelphia, PA (Abstract Co-Author) Nothing to Disclose

Flemming Forsberg, PhD, Philadelphia, PA (*Abstract Co-Author*) Equipment support, Toshiba Corporation; Research Grant, Toshiba Corporation; Equipment support, Siemens AG; In-kind support, General Electric Company; In-kind support, Lantheus Medical Imaging, Inc

Ji-Bin Liu, MD, Philadelphia, PA (Abstract Co-Author) Nothing to Disclose

John R. Eisenbrey, PhD, Philadelphia, PA (*Abstract Co-Author*) Support, General Electric Company; Support, Lantheus Medical Imaging, Inc

Andrej Lyshchik, MD, PhD, Philadelphia, PA (Abstract Co-Author) Nothing to Disclose

### PURPOSE

The purpose of this study is to evaluate the ability of molecular ultrasound to detect metastatic involvement in the sentinel lymph nodes (SLNs) of melanoma.

### **METHOD AND MATERIALS**

To date, 8 swine (3-7 kg; Sinclair Bio-Resources, Columbia, MO) with naturally occurring melanoma have been studied. Contrast enhanced ultrasound on a S3000 scanner with a 9L4 probe (Siemens Medical Solutions, Mountain View, CA) was used for imaging. Dual-targeted microbubbles were created from Targestar SA bubbles (Targeson, San Diego, CA) labeled with P-selection and  $\alphaV\beta3$ integrin in a 1:1 ratio. IgG labeled Targestar SA was used as control. A two stage imaging approach was used to first identify and then characterize SLN. First, 0.25 ml of Sonazoid (GE Healthcare, Oslo, Norway) was injected around the tumor and SLNs were identified. Next, dual-targeted and control microbubbles were injected IV with a 30 min interval between injections. Agents were allowed to circulate for 4 min to enable binding. Sets of image clips were then collected before and after a high-power destruction sequence. The mean intensity difference in pre- and post- destruction images was calculated as a relative bubble retention measure in the nodes. Non-SLNs were also imaged by dual-targeted and control bubbles as benign controls. All imaged nodes were dissected and histologically examined.

### RESULTS

Sixteen SLNs and 14 non-SLNs were analyzed. Ten SLNs showed metastatic involvement greater than 5%. All non-SLNs were benign. The mean intensity of the dual-targeted bubbles was significantly higher than that of IgG control bubbles in the metastatic SLNs ( $19.23 \pm 23.95$  AU vs.  $0.20 \pm 0.26$  AU; p=0.03). Benign nodes did not show significant difference in the mean intensity of the dual-targeted and control bubbles ( $0.85 \pm 1.81$  AU vs.  $0.03 \pm 0.26$  AU; p=0.93). Additionally, the mean intensity of dual-targeted bubbles for metastatic nodes was significantly different from that of benign nodes (p=0.002), while control bubbles did not differentiate between metastatic and benign nodes (p=0.91).

## CONCLUSION

The results indicated that dual-targeted microbubbles labeled with P-selectin and  $\alpha V\beta$ 3-integrin can help to characterize metastatic involvement in SLNs.

# **CLINICAL RELEVANCE/APPLICATION**

It may be possible to noninvasively characterize metastatic involvement in SLNs using molecular ultrasound.

# Acetabular Labral Tears: When to Call it

Thursday, Dec. 1 12:45PM - 1:15PM Room: MK Community, Learning Center Station #8

### Participants

Darya P. Shlapak, MD, Temple, TX (*Presenter*) Nothing to Disclose Ricardo D. Garza-Gongora, MD, Temple, TX (*Abstract Co-Author*) Nothing to Disclose Linda M. Parman, MD, Temple, TX (*Abstract Co-Author*) Nothing to Disclose Connie C. So, MD, Temple, TX (*Abstract Co-Author*) Nothing to Disclose

# **TEACHING POINTS**

### The purpose of this exhibit:

1. To review acetabular labrum histology, anatomy and morphology as well as anatomic variants that can be misdiagnosed as tears on Magnetic Resonance Arthrography (MRA) of the hip.

2. To learn acetabular labral tears etiologies, arthroscopic (Lage) and MRA classifications (Czerny and Blankenbaker).

3. To discuss conservative and surgical management of acetabular labral tears as well as MRA evaluation of postoperative acetabular labrum.

# TABLE OF CONTENTS/OUTLINE

- 1. Acetabular labrum overview:
  - -Histology
- -Anatomy
- -Morphology
- -Signal variability
- -Clock face and Quadrant orientation
- 2. MRA criteria for acetabular labral tears.
- 3. Types of acetabular labral tears:
- -Fraying
- -Intrasubstance
- -Partial thickness
- -Complex tear
- -Full thickness through labrum
- -Full thickness-detachment from bone
- 4. MRA classification of acetabular labral tears.
- 5. Arthroscopic classification of acetabular labral tears.
- 6. Etiologies of acetabular labral tears:
- -Femoroacetabular impingement
- -Hip dysplasia
- -Iliopsoas Impingement
- -Trauma
- -Degeneration
- -Hip hypermobility
- 7. Pitfalls in acetabular labrum imaging. Anatomic variants that can mimic tears:
- -Sublabral sulci
- -Transverse ligament sulci
- -Perilabral sulcus
- -Anterosuperior cleft
- 8. MRA evaluation of postoperative acetabular labrum for new tears/retears.

# Tendon Pathology on MRI: Pulling it all Together

Thursday, Dec. 1 12:45PM - 1:15PM Room: MK Community, Learning Center Station #9

### Awards Cum Laude

### **Participants**

Katryana M. Hanley-Knutson, MD, Winston Salem, NC (*Presenter*) Nothing to Disclose Pavani Thotakura, MD, Winston Salem, NC (*Abstract Co-Author*) Nothing to Disclose Scott D. Wuertzer, MD, MS, Winston-Salem, NC (*Abstract Co-Author*) Nothing to Disclose

### **TEACHING POINTS**

Teaching Points Review the normal anatomy, biomechanics, and MRI appearance of tendons Present an approach to tendon pathology based on signal characteristics, size, shape, and location Use this approach to review case examples of typical tendon pathology

## TABLE OF CONTENTS/OUTLINE

Normal Tendons Anatomy Biomechanics MRI Appearance Signal characteristics Size, shape, and location Normal causes of increased signal intensity Magic-angle phenomenon Entheses MRI of Tendon Pathology Tendon degeneration Tendon tears Causes of tendon tears Partial Complete Tendon avulsions Tenosynovitis Causes of tenosynovitis Stenosing tenosynovitis Inflammatory/Infiltrative Process Terminology - paratendinitis, paratenonitis Calcific tendinosis Other - xanthoma, gout, rheumatoid Tumor - giant cell tumor of tendon sheath Abnormal tendon location and/or movement Subluxation/Dislocation Entrapment Intersection syndrome

## MK346-SD-THB1

Quantification of Fat Contents in Vertebral Marrow using Modified DIXON Sequence to Differentiate Benign from Malignant Processes

Thursday, Dec. 1 12:45PM - 1:15PM Room: MK Community, Learning Center Station #1

## Participants

Hye Jin Yoo, MD, Seoul, Korea, Republic Of (*Presenter*) Nothing to Disclose Donghyun Kim, MD, Seoul, Korea, Republic Of (*Abstract Co-Author*) Nothing to Disclose Sung Hwan Hong, MD, Seoul, Korea, Republic Of (*Abstract Co-Author*) Nothing to Disclose Ja-Young Choi, MD, San Diego, CA (*Abstract Co-Author*) Nothing to Disclose Hee-Dong Chae, MD, Seoul, Korea, Republic Of (*Abstract Co-Author*) Nothing to Disclose Bo Mi Chung, MD, Seoul, Korea, Republic Of (*Abstract Co-Author*) Nothing to Disclose

### PURPOSE

To determine whether fat-signal fraction (FF) map using modified DIXON (mDIXON) sequence could help differentiate benign from malignant bone lesions.

# METHOD AND MATERIALS

Spine MRI of 134 consecutive patients were studied by using 3.0 T MR scanner with standard T1-weighted (T1WI) and 3D gradient-echo sequence with flexible echoes and T2\* correction (mDIXON) sequences. Control group consisted of 51 normal vertebrae. Benign group consisted of 40 benign focal bone lesions including endplate degenerations, Schmorl nodes, focal red-marrow depositions, and benign fractures. Malignant group consisted of 29 spinal malignancies. Three parameters were measured on T1WI and automatically reconstructed FF map images by two radiologists independently: T1 signal intensity (SI), T1 SI of normal disc (SId), and FF. The Lesion-to Disc ratio (LDR) was calculated by dividing SI of the lesion to SId. The FF ratio was obtained by dividing FF of the lesion to FF of the normal marrow. The mean values of parameters were compared among the groups. Diagnostic performance of the parameters was analyzed by ROC analysis. A binary logistic regression method was used to determine the best predictors of differential diagnosis between malignancy and benign focal lesions.

# RESULTS

FF (2.8%) and FF ratio (0.082) of malignancy were lower than other benign focal lesions (P<0.001, both). There was no difference of LDR between malignancy (0.87) and Schmorl node (0.87, P = 0.795), or benign fracture (0.90, P = 0.866). The areas under ROC curves of FF and FF ratio were 93% and 87%, which were higher than that of other parameters for differentiation between malignancy and benign lesions (P <0.001). In binary logistic regression analysis, FF remained significant variable that could be used to independently differentiate benign from malignant lesions, with odds ratio of 1.9.

## CONCLUSION

FF and FF ratio obtained from automatically reconstructed FF map using mDIXON sequence could be used to allow distinction between benign and malignant causes of focal bone marrow abnormalities.

### **CLINICAL RELEVANCE/APPLICATION**

mDIXON sequence allows evaluation of fat content within focal bone marrow abnormality with time-effective fashion. FF measured on automatically reconstructed FF map could be used in routine clinical use.

## MK347-SD-THB2

Magnetic Resonance Imaging for the Diagnosis of Knee Pathology: A Comparison of Academic and Community Centers

Thursday, Dec. 1 12:45PM - 1:15PM Room: MK Community, Learning Center Station #2

## Participants

Kevin Sun, Providence, RI (*Presenter*) Nothing to Disclose Grayson L. Baird, PhD, Providence, RI (*Abstract Co-Author*) Nothing to Disclose Eric Borrelli, Wakefield, RI (*Abstract Co-Author*) Nothing to Disclose Micheal Hulstyn, MD, Providence, RI (*Abstract Co-Author*) Nothing to Disclose Peter T. Evangelista, MD, Providence, RI (*Abstract Co-Author*) Consultant, BioMimetic Therapuetics, Inc Stephen Klinge, Providence, RI (*Abstract Co-Author*) Nothing to Disclose

### PURPOSE

Determining the best use of magnetic resonance imaging (MRI) for the evaluation of intra-articular knee pathology requires understanding of factors determining its effectiveness. Factors impacting diagnostic quality may include subspecialty expertise of the radiologist. Academic radiologists (AR) tend to be musculoskeletal fellowship trained and read in their specialty. The converse tends to be true for community radiologists (CR). The goal of this study was to examine the diagnostic MRI sensitivity and specificity of AR and CR for various intra-articular knee pathologies.

### **METHOD AND MATERIALS**

Over a six year period of April 2008 to May 2014, the records of 535 consecutive patients who underwent diagnostic arthroscopy for intra-articular knee pathology were retrospectively reviewed. MRI reports were generated by either AR at a single institution with subspecialty expertise in MSK radiology or by general CR. Diagnostic parameters, including sensitivity and specificity, were determined for MRI reports utilizing a standard comparative grading scale and arthroscopic findings as the gold standard. Only MRI's performed at 1.5T or less were included to eliminate field strength bias at academic centers.

## RESULTS

64.2% (343) of the MRIs were performed at the academic institution while 35.8% (192) were done in the community. For the diagnosis of anterior cruciate ligament (ACL) rupture, AR had better sensitivity compared to CR (91% vs 81% p=0.0072), as well as higher specificity (99% vs 94%), though this difference only approached significance (P=0.054). AR achieved slightly higher sensitivity (89% vs 84%) and specificity (86% vs 75%) than CR for medial meniscus, though these differences only approached significance, p=.0987 and p=.0678, respectively.

#### CONCLUSION

The utilization of radiologists with subspecialty expertise in MSK radiology was associated with better MRI diagnosis of ACL and medial meniscal pathology. The preoperative MRI diagnosis of cartilage injury demonstrated similar outcomes for both academic and community radiologists.

## **CLINICAL RELEVANCE/APPLICATION**

Academic radiology centers have improved diagnostic sensitivity and specificity compared to community radiology centers when diagnosing ACL injuries with MRI.

# Acute PCL Injuries: Mechanism and Associated Injuries

Thursday, Dec. 1 12:45PM - 1:15PM Room: MK Community, Learning Center Station #3

#### Awards

### **Student Travel Stipend Award**

#### **Participants**

Mark A. Anderson, MD, Boston, MA (*Presenter*) Nothing to Disclose Frank J. Simeone, MD, Boston, MA (*Abstract Co-Author*) Nothing to Disclose Connie Y. Chang, MD, Boston, MA (*Abstract Co-Author*) Nothing to Disclose

## PURPOSE

To evaluate the mechanism of acute posterior cruciate ligament (PCL) injuries and associated soft tissue injuries in the knee.

### **METHOD AND MATERIALS**

Our study was HIPAA compliant and IRB-approved. We performed a retrospective review of 75 acute PCL injuries with knee MRIs at our institution ( $36 \pm 16$  (range 15-74) years, 20 F, 55 M). All cases were reviewed by two independent musculoskeletal radiologists. Specifically, PCL, anterior cruciate ligament (ACL), medial and lateral menisci, extensor mechanism, medial and lateral collateral ligament, posteriolateral corner, posterior joint capsule, popliteus, biceps femoris, gastrocnemius muscles, semimembranosus/posterior oblique ligament, patellar retinacula, osseous contusions/fractures, and acute cartilage defects were evaluated. The mechanism of injury was determined based on the pattern of soft tissue and osseous injury. Interobserver agreement on incidence of injury to each structure was assessed by calculating a Kappa coefficient ( $\kappa$ ) for each structure.

### RESULTS

 $\kappa$  ranged from 0.85 to 1.0, showing almost perfect agreement for all structures. The most common concurrently injured structures were: posterior capsule (66/75, 88%), ACL (47/75, 63%), and posterolateral corner (46/75, 61%). Posterolateral corner injuries occurred most commonly where the mechanism of injury was dislocation (11/12, 92%) and varus hyperextension (11/13, 85%). Medial (31/75, 41%) and lateral (36/75, 48%) collateral ligament tears occurred with similar frequency. Medial meniscal injuries (26/75, 35%) were more common than lateral meniscal injuries (8/75, 11%). Thigh and leg muscle injuries were common, ranging from 28-37%. Of note, semimembranosus injuries occurred in 31% (23/75), particularly in dislocations (8/12, 67%). Tibial and femoral fractures or contusions occurred in 73% (55/75) and 68% (51/75) of cases. The mechanisms of injury of the PCL cases were hyperextension only (21/75, 28%), valgus hyperextension (14/75, 21%), pivot shift (13/75, 17%), varus hyperextension (13/75, 17%), and dislocation (12/75, 16%).

## CONCLUSION

Concomitant ligament and muscle injuries with PCL injury are common, particularly of the posterior capsule, ACL, and posterolateral corner.

### **CLINICAL RELEVANCE/APPLICATION**

High suspicion for ACL tear, posterior capsule tear, and posterolateral corner injury should be maintained if an acute PCL tear is identified, especially as the presence of these injuries could affect management.

Morphometric and Volumetric Evaluation of Posterior Cruciate Ligament and Femoral Intercondylar Notch in Subjects with Suspected Anterior Cruciate Ligament Tears: A Comparative Flexed-Knee MRI Study

Thursday, Dec. 1 12:45PM - 1:15PM Room: MK Community, Learning Center Station #4

## Participants

Atul K. Taneja, MD, Sao Paulo, Brazil (*Presenter*) Nothing to Disclose Frederico C. Miranda, MD, Sao Paulo, Brazil (*Abstract Co-Author*) Nothing to Disclose Marcelo P. Prado, MD, Sao Paulo, Brazil (*Abstract Co-Author*) Nothing to Disclose Marco K. Demange, Sao Paulo, Brazil (*Abstract Co-Author*) Nothing to Disclose Laercio A. Rosemberg, MD, Sao Paulo, Brazil (*Abstract Co-Author*) Nothing to Disclose Durval D. Santos, MD, Sorocaba, Brazil (*Abstract Co-Author*) Nothing to Disclose Ronaldo H. Baroni, MD, Sao Paulo, Brazil (*Abstract Co-Author*) Nothing to Disclose

### PURPOSE

To determine the effect of posterior cruciate ligament (PCL) and femoral intercondylar notch (IN) dimensions in anterior cruciate ligament (ACL) tears.

## METHOD AND MATERIALS

We conducted a prospective, IRB-approved, case-controlled MRI study including subjects between 14-50 years with non-contact knee injuries and suspected ACL tear. Exclusion criteria were previous surgery, findings of PCL tear, arthritis, tumors, infections or inflammatory conditions. All participants underwent a flexed-knee 3D-sequence, aiming to uniformly straighten PCL. MR images were reviewed independently by two musculoskeletal radiologists, and assessed for the following measurements: bi-condylar length; IN angle, depth, width and cross-sectional area; PCL width, thickness and cross-sectional area. Volumetry of IN and PCL was computed after manual segmentation. Subjects were divided into cases and controls (ACL tear vs. normal) and statistical analyses evaluated for inter-observer agreement, differences between groups and odds-ratio. Significance was considered for P<0.05.

## RESULTS

The study comprised 64 subjects (30 cases vs. 34 controls), being the majority male with left knee injured. There was no significant difference between groups regarding age, weight, height or BMI. Agreement between readers ranged from strong to almost perfect (ICC=0.72-0.99). Subjects with ACL tear presented lower IN width (mean, 18.31 vs. 19.56 mm, P=0.03; OR=0.80), lower IN minus PCL widths (6.44 vs. 7.78 mm, P=0.01; OR=0.67), higher PCL/IN widths proportion (64.9% vs 60.5%, P=0.03; OR=1.08), higher PCL thickness (6.00 vs. 5.36 mm, P=0.04; OR=1.54), lower IN depth minus PCL thickness (19.74 vs. 21.48 mm, P=0.01; OR=0.77), and higher PCL thickness/IN depth proportion (23.3% vs 20.2%, P=0.03; OR=1.15). Moreover, higher PCL volumes (1.14 vs. 1.00 cm3, P=0.01; OR=12.18) and PCL/IN volumes proportion (25.3% vs 21.3%, P<0.001; OR=1.25) were also found in tear group.

### CONCLUSION

Our study shows that subjects with ACL tears present larger PCL dimensions and decreased IN width when compared to subjects without tears. These findings, either isolated or combined, might be considered as risk factors for ACL tears.

### **CLINICAL RELEVANCE/APPLICATION**

Prospective case-controlled MRI study with morphometric and volumetric evaluation demontrastes that posterior cruciate ligament and femoral intercondylar notch dimensions act as risk factors for anterior cruciate ligament tears, either isolated or combined.

### Analysis of Nondiagnostic Image-guided Needle Biopsies of Musculoskeletal Lesions

Thursday, Dec. 1 12:45PM - 1:15PM Room: MK Community, Learning Center Station #5

#### **Participants**

Vijaya K. Kosaraju, Solon, OH (*Presenter*) Nothing to Disclose Michael J. Kessler, MD, Shaker Heights, OH (*Abstract Co-Author*) Nothing to Disclose Salim E. Abboud, MD, Cleveland, OH (*Abstract Co-Author*) Nothing to Disclose Rayan Abboud, Cleveland, OH (*Abstract Co-Author*) Nothing to Disclose Peter C. Young, MD, Cleveland, OH (*Abstract Co-Author*) Nothing to Disclose Mark R. Robbin, MD, Cleveland Hts, OH (*Abstract Co-Author*) Nothing to Disclose Christos Kosmas, MD, Cleveland, OH (*Abstract Co-Author*) Nothing to Disclose

## PURPOSE

The diagnostic yield of repeat image-guided biopsy for initially non-diagnostic biopsy of musculoskeletal lesions has not been well evaluated in the scientific literature. This study assesses the diagnostic yield of repeat percutaneous CT-guided biopsy (CTB) of musculoskeletal lesions in the setting of initially non-diagnostic CTB, and evaluates factors that impact the success rate of repeat CTB.

### **METHOD AND MATERIALS**

This study received IRB approval. A retrospective review of patients who underwent one or more repeat percutaneous CTB of MSK lesions over a 10-year period was performed utilizing PACS search. Thirty two patients were further analyzed. A successful repeat CTB was defined as a repeat CTB that yielded pathologic diagnosis following an initially non-diagnostic CTB. Pre-procedural diagnostic images, intra-procedural images, procedure notes, and pathology reports were reviewed. Core samples size, number of samples, patient positioning, and targeting of the lesion based on imaging review were analyzed to assess impact on success of repeat CTB.

## RESULTS

Repeat CTB was successful in 22/32 patients. Most common results on repeat CTB were tumor (benign or malignant) in 55% of cases (12/22) and osteomyelitis in 14% of cases[RN1] (3/22). 41% of the successful repeat biopsies utilized more core samples (9/22), and 27% utilized larger cores (6/22).

### CONCLUSION

Increase in number of diagnostic core samples had highest impact in success rate of repeat biopsies of initially non-diagnostic biopsies of percutaneous CTB of musculoskeletal lesions. This was followed by larger core sample size.

### **CLINICAL RELEVANCE/APPLICATION**

Knowledge of factors that contribute to higher success rate in repeat biopsy following initially non-diagnostic sampling of MSK lesions may improve diagnostic yield.

## MK351-SD-THB6

Contrast Enhancement Patterns in Soft Tissue Tumors: Diagnostic Utility and Comparison between Ultrasound and MRI

Thursday, Dec. 1 12:45PM - 1:15PM Room: MK Community, Learning Center Station #6

## Participants

Leonhard Gruber, Innsbruck, Austria (*Presenter*) Nothing to Disclose Hannes Gruber, MD, PhD, Innsbruck, Austria (*Abstract Co-Author*) Nothing to Disclose Anna Luger, Innsbruck, Austria (*Abstract Co-Author*) Nothing to Disclose Bernhard Glodny, MD, Innsbruck, Austria (*Abstract Co-Author*) Nothing to Disclose Patrizia Moser, Innsbruck, Austria (*Abstract Co-Author*) Nothing to Disclose Benjamin Henninger, MD, Innsbruck, Austria (*Abstract Co-Author*) Nothing to Disclose Alexander Loizides, MD, Innsbruck, Austria (*Abstract Co-Author*) Nothing to Disclose

### PURPOSE

To compare ultrasound (US) and MRI contrast-enhancement (CE) patterns in the diagnosis of soft tissue masses and to evaluate their respective diagnostic utility.

### **METHOD AND MATERIALS**

255 patients with a histologically verified soft tissue mass (STM) were included in this retrospective study; 75.3% had undergone CE US, 82.7% CE MRI and 58.0% both prior to histological confirmation, Interrater and interest correlations were calculated and diagnostic properties of each of the four predefined CE patterns were assessed through Fisher's exact test (sensitivity, specificity, positive [PPV] and negative predictive value [NPV], likelihood ratios [LR]). Finally, a logistic regression analysis was performed to determine the correlation final diagnosis and CE pattern, lesion size, age and gender. Furthermore, the influence of size on the occurrence of inhomogeneous CE patterns in malignancies was determined.

#### RESULTS

Homogeneous CE patterns both in US and MRI were highly specific for benign lesions, while inhomogeneous CE was moderately specific for malignancy. A combination of CE patterns predicted malignancy with 88.3%/88.7% sensitivity, 66.7%/59.7% specificity, 73.4%/68.2% correct classification rates, 54.6%/47.8% PPV, 92.6%/92.7% NPV, 2.65/2.20 positive LR and 0.18/0.19 negative LR for CEUS and CE MRI, respectively. Cases with at least one modality demonstrating homogeneous CE were also predominantly benign/intermediate. An increase in lesion size correlated with a higher likelihood of inhomogeneous CE in malignancies.

## CONCLUSION

CE patterns offer important clues on the differentiation of a newly diagnosed STM. CEUS and CE MRI may reveal complementary tissue characteristics and should therefore both be routinely used as an adjunct.

### **CLINICAL RELEVANCE/APPLICATION**

Incorporation of complementary US and MRI contrast-enhanced examinations into a diagnostic algorithm can improve diagnostic performance in soft tissue tumors.

## MS142-ED-THB1

BRCA and Beyond: Comprehensive Image-Rich Review of Hereditary Breast and Gynecologic Cancer Syndromes

Thursday, Dec. 1 12:45PM - 1:15PM Room: MS Community, Learning Center Station #1

#### Awards

**Identified for RadioGraphics** 

#### Participants

Stephanie N. Histed, MD, Los Angeles, CA (*Presenter*) Nothing to Disclose Nina Woldenberg, MD, Los Angeles, CA (*Abstract Co-Author*) Nothing to Disclose Rinat Masamed, MD, Los Angeles, CA (*Abstract Co-Author*) Nothing to Disclose Melissa M. Joines, MD, Los Angeles, CA (*Abstract Co-Author*) Nothing to Disclose Antoinette R. Roth, MD, Sylmar, CA (*Abstract Co-Author*) Nothing to Disclose Maitraya K. Patel, MD, Sylmar, CA (*Abstract Co-Author*) Nothing to Disclose

### **TEACHING POINTS**

Radiologists play a central role in guiding high-risk patients with hereditary breast and gynecologic cancers including patient identification, screening, diagnosis and staging. Familiarity with the associated genetic mutations, pathophysiology, incidence, specific cancer risks and image-based screening guidelines is needed for collaborative high level care of this high-risk patient population. Several hereditary cancer syndromes are associated with increased risk of breast, ovarian, endometrial and cervical cancer as well as other non-breast and gynecologic cancers. Multimodal image based screening may be indicated for these patients. Analyzing the presentation of these high-risk patients appropriately will guide diagnosis and management.

## TABLE OF CONTENTS/OUTLINE

Image-rich comprehensive review of hereditary breast and gynecologic cancer syndromes, including hereditary breast and ovarian cancer associated with BRCA1/BRCA2 and Lynch syndrome, and less common syndromes including Peutz-Jegher, Gorlin, Li-Fraumeni and Cowden. Associated genetic mutations, pathophysiology, incidence, specific cancer risks and image-based screening guidelines. Discussion of the subtypes of breast, ovarian, endometrial and cervical cancer as well as non-breast and gynecologic cancers in each syndrome.

# Before the Force Awakens: Role of 11C-DTBZ in Early Stage Detection of Parkinson's Disease

Thursday, Dec. 1 12:45PM - 1:15PM Room: S503AB Hardcopy Backboard

#### **Participants**

Yean P. Silva Hidalgo, MD, Mexico, Mexico (*Presenter*) Nothing to Disclose Luis A. Ruiz Elizondo, MD, Mexico City, Mexico (*Abstract Co-Author*) Nothing to Disclose Mary C. Herrera-Zarza, MD, Mexico City, Mexico (*Abstract Co-Author*) Nothing to Disclose Gisela Estrada, MD, Mexico City, Mexico (*Abstract Co-Author*) Nothing to Disclose Cesar N. Cristancho Rojas, MD, Mexico City, Mexico (*Abstract Co-Author*) Nothing to Disclose Rafael Curiel Reyes, MD, Morelia, Mexico (*Abstract Co-Author*) Nothing to Disclose Ana M. Lopez, MD, Mexico City, Mexico (*Abstract Co-Author*) Nothing to Disclose Jose L. Criales, MD, Mexico City, Mexico (*Abstract Co-Author*) Nothing to Disclose

## **TEACHING POINTS**

Parkinson disease (PD) is the second most frecuent neurodegenerative disorder after Alzheimer in the elderly population, in recent years imaging has taken a greater role in diagnosis and management. PD is characterized pathologically by loss of dopamine neurons in the substantia nigra pars compacta.11C-9-fluoropropyl-(+)-dihydrotetrabenzazine (11C-DTBZ) is a PET radiotracer of the dopaminergic system that has affinity for VMAT2 (vesicular monoamine transporter 2). VMAT2 is a specific presynaptic protein involved in the transportation of monoamines from the cytosol into the terminal nerves, directly proportional to the neuronal integrity of the dopaminergic system, 95% is concentrated in the striatal regions, one of the main physiological uptake zones, therefore a decreased uptake at this level is highly suggestive of Parkinson's disease. THE AIM OF THIS EXHIBIT: Review the pathophysiology of Parkinson disease Describe the molecular basis and mechanism of action of 11C-DTBZ.Describe the of 11C-DTBZ normal uptake and illustrative cases.

## TABLE OF CONTENTS/OUTLINE

Introduction.Parkinson disease analysis.11C-DTBZ molecular basis.Illustrative pathologic cases.Conclusion.

# Detection of Primary and Metastatic Lesions of Urinary Tract Tumors by 18F-FLT PET/CT

Thursday, Dec. 1 12:45PM - 1:15PM Room: S503AB Station #6

#### **Participants**

Katsuhiko Kato, MD, PhD, Nagoya, Japan (*Presenter*) Nothing to Disclose Yumiko Koshiba, Nagoya-shi, Japan (*Abstract Co-Author*) Nothing to Disclose Shinji Abe, RT, Nagoya, Japan (*Abstract Co-Author*) Nothing to Disclose Masayuki Honda, RT, Nagoya, Japan (*Abstract Co-Author*) Nothing to Disclose Keita Knimoto, RT, Nagoya, Japan (*Abstract Co-Author*) Nothing to Disclose Tetsuro Odagawa, Nagoya, Japan (*Abstract Co-Author*) Nothing to Disclose Atsushi Murai, Nagoya, Japan (*Abstract Co-Author*) Nothing to Disclose Shinji Naganawa, MD, Nagoya, Japan (*Abstract Co-Author*) Nothing to Disclose

## PURPOSE

The aim of this study is to investigate the efficacy of 18F-FLT PET/CT for detection of primary and metastatic lesions of urinary tract tumors.

# METHOD AND MATERIALS

Twenty-two (16 men, 6 women) patients were examined by <sup>18</sup>F-FLT PET/CT (Siemens Biograph 16). All the patients received surgical operation or biopsy and the tumor was diagnosed histopathologically.

## RESULTS

In 22 patients examined by <sup>18</sup>F-FLT PET/CT, 13 were confirmed histopathologically to be urothelial cell carcinoma, 6 renal cell carcinoma, 2 retroperitoneal liposarcoma, and 1 bladder carcinoma. Five patients had lung metastases, 2 had lymph node metastases, and 1 had gallbladder cancer synchronously. In 7 of the 13 patients with urothelial carcinoma and 1 with bladder carcinoma, the primary tumor could not be detected due to retention of urine in the ureter and urinary excretion of <sup>18</sup>F-FLT. In the other 6 patient with urothelial call carcinoma, 2 with retroperitoneal liposarcoma, and 1 with renal cell carcinoma, the primary tumor could be detected due to lack of urinary excretion of <sup>18</sup>F-FLT by renal insufficiency. 18F-FLT uptake in the tumor site expressed as SUVmax in <sup>18</sup>F-FLT PET was 2.17-28.99 (mean±S.D. 8.51±11.50) in urothelial cancer, 1.65 in renal cell carcinoma, and 9.35 and 4.24 (6.8±3.61) in retroperitoneal liposarcoma. Lung metastases after nephrectomy for renal cell carcinoma in 5 patients could be detected (SUVmax: 3.24-6.44 (4.45±1.13)). Lymph node metastases in 5 patients also could be detected (SUVmax:2.16-6.35 (4.45±1.73)).

## CONCLUSION

Usually, <sup>18</sup>F-FLT PET/CT is not suitable for detection of the primary lesions of urinary tract tumors because of its urinary excretion, whereas their metastatic lesions can be detected by <sup>18</sup>F-FLT PET/CT. Nevertheless, in patients whose urinary excretion of <sup>18</sup>F-FLT is disturbed by renal failures, <sup>18</sup>F-FLT PET/CT is useful for detection of the primary lesions of urinary tract tumors.

# **CLINICAL RELEVANCE/APPLICATION**

<sup>18</sup>F-FLT PET/CT is not suitable for detection of the primary lesions of urinary tract tumors because of its urinary excretion, whereas their metastatic lesions can be detected by <sup>18</sup>F-FLT PET/CT.

Intratumoral Heterogeneity Measured by FDG PET and MRI is Associated with Tumor Stroma-ratio and Clinical Outcome in Head and Neck Cancer

Thursday, Dec. 1 12:45PM - 1:15PM Room: S503AB Station #7

**FDA** Discussions may include off-label uses.

### Participants

Su Jin Lee, Suwon, Korea, Republic Of (*Presenter*) Nothing to Disclose Jin Wook Choi, MD, Suwon, Korea, Republic Of (*Abstract Co-Author*) Nothing to Disclose Dakeun Lee, Suwon, Korea, Republic Of (*Abstract Co-Author*) Nothing to Disclose Seung-Hyup Hyun, Seoul, Korea, Republic Of (*Abstract Co-Author*) Nothing to Disclose Miran Han, MD, Suwon, Korea, Republic Of (*Abstract Co-Author*) Nothing to Disclose

## PURPOSE

We evaluated the association between tumor-stroma ratio and intratumoral heterogeneity measured by fluorodeoxyglucose (FDG) positron emission tomography (PET) and magnetic resonance imaging (MRI) with diffusion-weighted imaging (DWI), and further investigated the prognostic significance of these imaging biomarkers in head and neck cancer.

## **METHOD AND MATERIALS**

We evaluated 44 patients who underwent pretreatment FDG PET and MRI. First-order and higher-order textural features of primary tumor were extracted by PET texture analysis. On MRI, the mean, standard deviation, minimum, maximum, skewness and kurtosis of the ADC values were calculated for the first-order texture analysis. The difference between minimum and maximum ADC values (ADCdiff) was calculated. The relationships between tumor-stroma ratio and imaging parameters were evaluated. To assess and compare the predictive performance of imaging parameters, time-dependent receiver operating characteristics (ROC) curves for censored survival data and areas under the ROC curve (AUC) were used. The associations between imaging parameters and recurrent free survival (RFS) were assessed using Cox proportional hazard regression models.

## RESULTS

Low-intensity short-run emphasis (r = -0.382), coarseness (r = -0.382), strength (r = -0.390), low-intensity zone emphasis (r = -0.380), and low-intensity short-zone emphasis (r = -0.411) on PET and ADC (r = 0.434), ADCdiff (r = 0.534) on MRI were significantly correlated with stroma proportion. The best imaging biomarker for 2 year-RFS prediction was coarseness on PET (AUC = 0.741) and ADCdiff on MRI (AUC = 0.779). After adjusting for age, clinical tumor stage and clinical node stage, the multivariate analysis showed that coarseness (HR = 10.549, 95% CI = 2.544-43.748, P = 0.001) and ADCdiff (HR = 3.274, 95% CI = 1.016-10.551, P = 0.047) were independent prognostic factors for RFS.

## CONCLUSION

Heterogeneity parameters derived from FDG PET and MRI are significantly associated with tumor-stroma ratio, a surrogate marker for tumor microenvironment. In addition, these imaging biomarkers may help to facilitate the risk stratification for tumor recurrence in head and neck cancer.

# **CLINICAL RELEVANCE/APPLICATION**

Intratumoral heterogeneity parameters derived from FDG PET and MRI may help to facilitate the risk stratification for tumor recurrence in head and neck cancer.

Quantitation of Cancer Treatment Response by FDG PET/CT: Multi-Center Assessment of Variability

Thursday, Dec. 1 12:45PM - 1:15PM Room: S503AB Station #8

#### Participants

Joo Hyun O, MD, Baltimore, MD (*Presenter*) Nothing to Disclose Brandon Luber, Baltimore, MD (*Abstract Co-Author*) Nothing to Disclose Hao Wang, Baltimore, MD (*Abstract Co-Author*) Nothing to Disclose Jeffrey P. Leal, BA, Baltimore, MD (*Abstract Co-Author*) Nothing to Disclose Richard L. Wahl, MD, Saint Louis, MO (*Abstract Co-Author*) Consultant, Nihon Medi-Physics Co, Ltd;

### PURPOSE

Our aim was to study the variability of quantitative PET parameters used in assessments of treatment response across multiple sites and readers when assessing identical digital images.

## METHOD AND MATERIALS

Paired pre- and post-treatment FDG PET/CT images of 30 oncologic patients were distributed to 22 readers across 15 US and international sites. One reader was aware of the full medical history (readreference), while the 21 other readers were unaware. The readers selected the single "hottest tumor" from each study, and made standard uptake value (SUV) measurements from this target lesion and the liver. Descriptive statistics, percent changes in the measurements, and their agreements were obtained.

### RESULTS

The intra-class correlation coefficient (ICC) for the percent change in maximum SUV ( $\Delta$ SUVmax) of the hottest tumor was 0.894 (95% CI 0.813, 0.941) and the individual equivalence coefficient (IEC) was 1.931 (95%CI 0.568, 6.449) when all reads were included (n=638). Including only the measurements agreeing with the readreference on target selection (n=486), the ICC for the  $\Delta$ SUVmax was 0.944 (95%CI 0.0.841, 0.989), and the IEC was -0.688 (95%CI -1.810, -0.092). For percent change in mean SUV from the liver corrected for lean body mass, the ICC was 0.751 (95%CI 0.631, 0.810), and the IEC was 7.799 (95%CI 3.417, 18.493).

## CONCLUSION

The quantitative tumor SUV changes measured across multiple sites and readers show very high correlation, suggesting that FDG PET/CT studies may be implemented in a more general manner for treatment response assessment. Ensuring selection of the same target among readers is necessary.

## **CLINICAL RELEVANCE/APPLICATION**

FDG PET quantitation of changes in tumor SUVmax and liver mean SULmean from multiple sites have high, though not perfect, degrees of agreement.

Differences in reader selection of target lesions contribute to variability of quantitative measurements from identical image data sets

### **Honored Educators**

Presenters or authors on this event have been recognized as RSNA Honored Educators for participating in multiple qualifying educational activities. Honored Educators are invested in furthering the profession of radiology by delivering high-quality educational content in their field of study. Learn how you can become an honored educator by visiting the website at: https://www.rsna.org/Honored-Educator-Award/

Richard L. Wahl, MD - 2013 Honored Educator

# The Value of 18F FDG-PET/CT in Patients with Mycosis Fungoides

Thursday, Dec. 1 12:45PM - 1:15PM Room: S503AB Station #9

#### **Participants**

Mehdi Taghipour, MD, BOSTON, MA (*Presenter*) Nothing to Disclose Rick Wray, MD, Baltimore, MD (*Abstract Co-Author*) Nothing to Disclose Esther Mena, MD, Bethesda, MD (*Abstract Co-Author*) Nothing to Disclose Sara Sheikhbahaei, MD, MPH, Baltimore, MD (*Abstract Co-Author*) Nothing to Disclose Lilja B. Solnes, MD, MBA, Baltimore, MD (*Abstract Co-Author*) Nothing to Disclose Rathan M. Subramaniam, MD, PhD, Dallas, TX (*Abstract Co-Author*) Nothing to Disclose

# PURPOSE

The purpose of this study is to evaluate the utility of FDG-PET/CT in detecting tumor sites and degree of FDG avidity associated with clinical and pathologic features of mycosis fungoides.

## METHOD AND MATERIALS

This is an IRB-approved retrospective study including 39 patients with pathologic confirmed mycosis fungoides, who underwent 18F FDG-PET/CT examination for initial disease staging or disease relapse. The physical examination findings of the skin lesions and related pathologic findings were recorded using patients' electronic medical records. The FDG-PET/CT scans were evaluated by a board certified nuclear medicine physician using SUVmax and the Lugano classification score for each scan.

#### RESULTS

Out of the total of 39 patients included in the study, more than half of the patients had patches or plaques (24/39, 61.5%), eight patients had maculopapular rashes (20.5%), and the remaining seven patients (18%) had nodular lesions or eczematous rashes. Twenty patients (51.3%) demonstrated FDG avid lesions on the PET/CT scan. Lugano classification showed score 1 in 20 patients, score 2 in 1 patient, score 3 in 5 patients, score 4 in 8 patients, and score 5 in 5 patients The average SUVmax for the FDG-avid lesions was 3.38 (range 0.8-8.7). Extracutaneous sites with FDG-avid lymph node involvement were present in 25.6% of the cases (10/39).

## CONCLUSION

Our findings suggest that 18F-FDG PET/CT scan demonstrates FDG avid cutaneous and extracutaneous lymphomatous involvement in a majority of patients, which may be beneficial in diagnosis, biopsy localization, staging and potential therapy assessment.

# **CLINICAL RELEVANCE/APPLICATION**

FDG-PET/CT is useful in the staging and management of patients with mycosis fungoides.

## NM247-SD-THB10

Performance of 18F-FDG PET/CT in the Diagnosis of Solitary Pulmonary Nodules with Different CT Attenuation Patterns

Thursday, Dec. 1 12:45PM - 1:15PM Room: S503AB Station #10

## Participants

Haiping Liu, BSD, MS, Guangzhou, China (*Abstract Co-Author*) Nothing to Disclose Ping Chen, MD, Guangzhou, China (*Abstract Co-Author*) Nothing to Disclose Peng Hou, guangzhou, China (*Abstract Co-Author*) Nothing to Disclose Jingwu Chen, Guangzhou, China (*Abstract Co-Author*) Nothing to Disclose Huaifu Deng, MD, Guangzhou, China (*Abstract Co-Author*) Nothing to Disclose Yulei Jiang, PhD, Chicago, IL (*Abstract Co-Author*) Nothing to Disclose Yonglin Pu, MD, PhD, Chicago, IL (*Presenter*) Nothing to Disclose

### PURPOSE

The solitary pulmonary nodules (SPNs) are often evaluated with 18F-FDG PET/CT. We determined the diagnostic performance of 18F-FDG PET/CT for differential diagnosis SPNs with different CT attenuation patterns.

# METHOD AND MATERIALS

This study was approved by the institutional review board. 1406 patients with SPNs undergone 18F-FDG PET/CT scan from January 2006 to June 2015 were included in this study. The attenuation patterns of the SPNs were assessed retrospectively and independently by two radiologists from CT images. Differences in interpretations were resolved by consensus. Maximal standardized uptake value (SUVmax) of SPNs was evaluated on the PET/CT. The reference standard for the diagnosis of the SPNs was pathology and CT follow-up. Receiver operating characteristic (ROC) curve was used to evaluate diagnostic performance of the PET/CT in the differential diagnosis of SPNs with three different attenuation patterns.

#### RESULTS

Of the total of 1406 patients with SPNs, there were 792 males with mean (SD) age of 60.0 (11.7) years, and 614 females with mean (SD) age of 57.9 (11.8) years. There were 955 solid nodules [552 malignant and 403 benign nodules, mean (SD) nodule size = 18.5 (7.6) mm], 261 part-solid nodules [247 malignant and 14 benign nodules, mean (SD) nodule size = 21.5 (6.5) mm] and 190 pure ground-glass nodules (GGOs) [94 malignant and 96 benign nodules, mean (SD) nodule size = 9.8 (5.7) mm]. In 1187 patients, the diagnosis of the SPNs was made based pathology, and in 219 patients the diagnosis of the SPNs was made based on CT follow-up. The optimal cut-off value of the SUVmax for the differential diagnosis of malignant and benign nodules was 2.78 for solid SPNs, 1.06 for part-solid SPNs and 0.55 for GGOs, respectively. The area under the ROC curve (AUC) of SUVmax of the SPNs was 0.885 (95% CI, 0.863-0.904, P<0.0001), 0.930 (95% CI, 0.892-0.958, P<0.0001) and 0.569 (95% CI, 0.495-0.640, P = 0.103) for the differential diagnosis of malignant and benign solid SPNs, part-solid SPNs and GGOs, respectively.

## CONCLUSION

18F-FDG PET/CT shows excellent diagnostic performance for differentiating malignant from benign solid and part-solid SPNs, but poor diagnostic performance for GGOs.

### **CLINICAL RELEVANCE/APPLICATION**

Solid and part-solid SPNs on CT can be further evaluated with 18F-FDG PET/CT. However, 18F-FDG PET/CT is not useful for evaluating GGO SPNs seen on CT.

# NR407-SD-THB1

### Safety of Protected Carotid Artery Stenting based on Unstable Findings of Carotid Plaque MR Imaging

Thursday, Dec. 1 12:45PM - 1:15PM Room: NR Community, Learning Center Station #1

#### **Participants**

Jae Yeong Jeong, Jeonju-Si, Korea, Republic Of (*Abstract Co-Author*) Nothing to Disclose Hyo-Sung Kwak, MD, PhD, Jeonju, Korea, Republic Of (*Abstract Co-Author*) Nothing to Disclose Gyung-Ho Chung, MD, PhD, Chonbuk, Korea, Republic Of (*Abstract Co-Author*) Nothing to Disclose Bo Ram Kim, Jeonju, Korea, Republic Of (*Presenter*) Nothing to Disclose

## PURPOSE

Intraplaque hemorrhage (IPH), thin/ruptured fibrous cap, or ulcer were well-known findings of unstable plaque on carotid MR imaging. The aim of this study was to determine the safety of carotid artery stenting (CAS) using an emboli protection device based on unstable findings of carotid plaque MR imaging in patients with severe carotid artery stenosis.

## METHOD AND MATERIALS

This prospective study assessed 102 consecutive patients with severe carotid stenosis. These patients underwent preprocedural carotid MR imaging included routine brain MR imaging and postprocedural diffusion-weighted imaging (DWI) after CAS. Unstable plaque on carotid MR imaging was defined as IPH, thin/ruptured fibrous cap, and ulcer. We then analyzed the incidence of postprocedural ipsilateral ischemic events on DWI and primary outcomes within 30 days of CAS.

### RESULTS

50 patients (49.0%) had IPH, 85 patients (83.3%) had thin/ruptured fibrous cap, or 43 patients (42.2%) had ulcer on carotid plaque MR imaging. IPH was more common in the symptomatic groups than in the asymptomatic groups (58.7% vs 41.1%, p = .12). Overall, the rate of DWI positive finding after CAS was 17%. The rate of 30-day stroke, myocardial infarction, or death was 3.9%. There was no significant difference in the primary outcome and DWI positive findings after CAS between the symptomatic and asymptomatic groups. The primary outcome of CAS based on unstable plaque, such as IPH, thin/ruptured fibrous cap, or ulcer was no significant difference.

# CONCLUSION

The results of this study indicate that protected CAS seems to be safe regardless of unstable plaque findings on carotid MR imaging.

## **CLINICAL RELEVANCE/APPLICATION**

The protected carotid artery stenting is a safe procedure to patients with severe carotid stenosis, regardless of the existence of unstable plaque findings on carotid MR imaging.

Impact of Needle Type on Incidence of Postdural Puncture Headaches Requiring an Epidural Blood Patch Following Fluoroscopy-guided Lumbar Puncture

Thursday, Dec. 1 12:45PM - 1:15PM Room: NR Community, Learning Center Station #2

## Participants

Miguel A. Flores, MD, Orlando, FL (*Presenter*) Nothing to Disclose Haley P. Letter, MD, Orlando, FL (*Abstract Co-Author*) Nothing to Disclose Edward Derrick, MD, Orlando, FL (*Abstract Co-Author*) Nothing to Disclose Michele N. Edison, MD, Orlando, FL (*Abstract Co-Author*) Nothing to Disclose Bo Liu, MD, Maitland, FL (*Abstract Co-Author*) Nothing to Disclose Gary J. Felsberg, MD, Lake Mary, FL (*Abstract Co-Author*) Nothing to Disclose Steven A. Messina, MD, Columbia, MD (*Abstract Co-Author*) Nothing to Disclose

### PURPOSE

A decrease in the incidence of postdural puncture headaches (PDPH) following lumbar puncture (LP) with an atraumatic spinal needle (i.e. Whitacre) versus a traumatic spinal needle (i.e. Quincke) has been adequately documented in the literature. This study aims to use epidural blood patch (EBP) as an objective endpoint in the evaluation of PDPH incidence following fluoroscopic-guided LPs using atraumatic and traumatic spinal needles within a single institution.

### METHOD AND MATERIALS

Retrospective identification of single institution LPs between January 2009 and October 2015. Subsequently, LPs which resulted in an EBP were identified. There were 4,607 LPs within the initial data set, 123 punctures of which resulted in an EBP. Lumbar punctures requiring multiple attempts (17) and for the purpose of lumbar drain placement (337) were excluded. Additionally, lumbar punctures with missing reports in PACS (12) and those with unclear needle type documentation (204) were excluded. Of the 123 LPs identified which necessitated an EBP, 14 were excluded secondary to multiple attempts and unclear needle type documentation. There were 3,819 fluoroscopy-guided lumbar punctures which were analyzed using chi-squared tests.

### RESULTS

A total of 3,819 LPs were in included for analysis: 1769 with a 22G Whitacre, 611 with a 22G Quincke, and 1439 with a 20G Quincke. Incidence of EBP following LP with a 22G Whitacre was 1.02% (18/1769), 22G Quincke was 3.93% (24/611), and 20G Quincke was 4.66% (67/1439). There was a statistically significant difference between the incidence of EBP following fluoroscopy-guided LP with a 22G Whitacre versus 22G Quincke and 22G Whitacre versus 20G Quincke (p<0.001).

#### CONCLUSION

The use of an atraumatic spinal needle during fluoroscopy-guided lumbar puncture resulted in significantly fewer epidural blood patches when compared to a traumatic spinal needle of equal gauge. To the author's knowledge, this analysis is derived from the largest single-institution sample size in published literature.

### **CLINICAL RELEVANCE/APPLICATION**

The use of an atraumatic spinal needle significantly reduces the incidence of epidural blood patches to patients when compared to 22G and 20G Quincke, beveled edge needles. If both needle types are available, and a beveled edge (traumatic needle) is not specifically needed, the atraumatic needle should be chosen. This one change will likely improve patient satisfaction and reduce the departmental complication rate.

## NR409-SD-THB3

### Fetal Asphyxia Evaluation and Quantification with Magnetic Resonance Spectroscopy at 4.7 T in Rats

Thursday, Dec. 1 12:45PM - 1:15PM Room: NR Community, Learning Center Station #3

#### **Participants**

Olivier Ami, MD, PhD, Clermont Ferrand, France (*Presenter*) Nothing to Disclose Guy Bielicki, ST GENES CHAMPANELLE, France (*Abstract Co-Author*) Nothing to Disclose Lucie Cassagnes, MD, Clermont-Ferrand, France (*Abstract Co-Author*) Nothing to Disclose Gerard Mage, MD, PhD, Clermont Ferrand, France (*Abstract Co-Author*) Nothing to Disclose Louis B. Boyer, MD, Clermont-Ferrand, France (*Abstract Co-Author*) Nothing to Disclose

#### PURPOSE

The aim of this study was to evaluate the interest of NMR to monitor fetal response to hypoxia in rats fetuses. We used gradient echo parametric image to quantify the dependence of the signal intensity (SI) at blood oxygen level dependent (BOLD) magnetic resonance imaging of fetal rats brains on maternal oxygen saturation. Lactates were estimated using localised 1H spectrometry, and pH was estimated using localised phosphorous spectrometry in fetal brain.

## **METHOD AND MATERIALS**

21 gravid rats ranging from 17 to 21 days of gestation were studied under isoflurane anesthesia. Hypoxia was obtained using a mix of O2 (15%) and N2 (85%). NMR was performed with a 4.7 T system (Bruker). A T2\*weighted single shot Multi-Gradient-Echo sequence (MGE) was used, and BOLD SI during hypoxia was expressed as normalized BOLD SI (a % of the mean control values) : normalized BOLD SI = (SIh / SIn) \* 100, where SIh is the SI during hypoxia and SIn is the SI during the normoxia period. Lactate was estimated using 1H PRESS sequence (TE 130ms, TR 2000ms) and undercurve area at 1,33 ppm spike. The phosphorus signal was acquired using 31P PRESS sequence (TE 8,8ms, TR 2000ms) and the pH was estimated from the chemical shift of phosphate inorganic (Pi) referenced to the phosphocreatine (Pcr): according to the following formula:pH = 6,73 + log (Pi-3,37) / (5,66 -Pi).

## RESULTS

Mean maternal hemoglobin oxygen saturation was 97% in the control period. During hypoxia, it was reduced to 63%, while fetal normalized BOLD SI decreased to 64 % (95% CI : 44%, 85%). A significant decrease in BOLD SI (p = 0,0076, t-test) was seen in all included animals. Lactate signal was merged with noise line in normoxic conditions, and detectable spike appeared within the few minutes following the beginning of hypoxia. Rate raised with the duration of hypoxia to a maximum of 7 times normoxic value (p = 0,0055). Mean Fetal pH was 7,32 in normoxic rat fetuses, and a decrease to 6,9 was seen after hypoxia.

### CONCLUSION

Fetal oxymetry and lactate estimation in brain of rats fetuses with 1H NMR were suitable and valuable tools to detect hypoxia. pH estimation was feasible but required a long acquisition time to be acceptable in routin.

### **CLINICAL RELEVANCE/APPLICATION**

NMR is a valuable tool with BOLD imaging and multinucleus spectroscopy to evaluate fetal response to hypoxia in a fetal rat model of asphyxia.

Could Quasistatic Ultrasound Elastography (USE) Increase US Accuracy for Parotid Gland Lesions? Preliminary Results of Elasticity Contrast Index (ECI) Index Evaluation

Thursday, Dec. 1 12:45PM - 1:15PM Room: NR Community, Learning Center Station #5

# Participants

Emanuele David, Roma, Italy (Presenter) Nothing to Disclose

Vito Cantisani, MD, Rome, Italy (Abstract Co-Author) Speaker, Toshiba Corporation; Speaker, Bracco Group; Speaker, Samsung Electronics Co, Ltd;

Alfredo Blandino, Messina, Italy (*Abstract Co-Author*) Nothing to Disclose Giorgio Ascenti, MD, Messina, Italy (*Abstract Co-Author*) Nothing to Disclose Carlo Catalano, MD, Rome, Italy (*Abstract Co-Author*) Nothing to Disclose Ferdinando D'Ambrosio, Rome, Italy (*Abstract Co-Author*) Nothing to Disclose Nicola Di Leo, MD, Rome, Italy (*Abstract Co-Author*) Nothing to Disclose Federica Flammia, Roma, Italy (*Abstract Co-Author*) Nothing to Disclose Francesco Flammia, Rome, Italy (*Abstract Co-Author*) Nothing to Disclose Antonello Rubini, MD, Roma, Italy (*Abstract Co-Author*) Nothing to Disclose

#### PURPOSE

The aim of the study was to examine whether the combination of conventional ultrasound imaging with ultrasound elastography might improve the evaluation of parotid gland tumors and to determine a cut-off elasticity value that would be ideal for differentiation between benign and malignant lesions

### **METHOD AND MATERIALS**

126 consecutive patients with parotid gland tumors, treated surgically at a single tertiary center were enrolled. Ultrasound evaluation consisted of B-mode ultrasound, color Doppler ultrasound and by quasistatis ultrasound elastography (USE). For each lesion the following criteria were considered: echogenity, margins, vascularization and capsulation to determine benign or malignant lesion. Sonoelastography was conducted by Elastoscan software and an elasticity contrast index (ECI) was obtained in all lesions.

#### RESULTS

ROC analysis demonstrated that an ECI >3.5 was the ideal cut-off point for diagnosis of malignancy. Using conventional parameters, the observer suggested a malignant lesion in 40 cases and benign in 86 cases. ECI>3.5 alone was the most accurate parameter (accuracy: 90.5%) when considered with other subjective criteria, with a sensitivity of 93.7% and a specificity of 89.4%.

## CONCLUSION

Our results showed that USE with ECI index measurement improves the specificity of US in order to discriminate preoperatively benign from malignant lesions, with the exception that a pleomorphic adenoma is stiffer and may cause confusion.

## **CLINICAL RELEVANCE/APPLICATION**

According to our results USE should be used as an additional tool to conventional US evaluation of salivary gland lesions. The difference in elastographic score was statistically significant between benign and malignant tumours, but the difference between pleomorphic adenomas and malignant tumours was not statistically significant.USE can certainly improve the specificity of US in order to discriminate preoperatively benign from malignant lesions with the exception of the pleomorphic adenoma.

Transvaginal Ultrasound (TV US) Guided Procedures: A Review

Thursday, Dec. 1 12:45PM - 1:15PM Room: OB Community, Learning Center Station #1

# Awards

**Certificate of Merit** 

### Participants

Mollie A. Rashid, MD, Los Angeles, CA (*Presenter*) Nothing to Disclose Hisham A. Tchelepi, MD, Los Angeles, CA (*Abstract Co-Author*) Research Grant, General Electric Company; Research Grant, Roper Industries, Inc

Daphne K. Walker, MD, Los Angeles, CA (Abstract Co-Author) Nothing to Disclose

### **TEACHING POINTS**

To review principles and techniques for ultrasound guided procedures using a transvaginal approach To discuss indications and applications for TV US guided procedures To illustrate case examples with pathologic correlation To discuss potential benefits and disadvantages

## TABLE OF CONTENTS/OUTLINE

History and background Principles Literature review Indications and Applications Patient Selection Types of procedures Biopsies Drainages Limitations of alternative methods Our technique for performing TV US guided procedures Schematic presentation Tips and pearls Case examples from our institution with pathologic correlation, including, but not limited to: Ovarian masses, including malignant tumors Abscess drainage, with and without catheter placement Post-procedural management and potential complications Additional applications and future directions of TV US procedures The New 2014 World Health Organization (WHO) Classification of Ovarian Cancer: A Primer for Radiologists

Thursday, Dec. 1 12:45PM - 1:15PM Room: OB Community, Learning Center Station #2

### Awards Magna Cum Laude

#### **Participants**

Farhan S. Amanullah, MD, Houston, TX (*Presenter*) Nothing to Disclose Varaha Tammisetti, MD, Houston, TX (*Abstract Co-Author*) Nothing to Disclose Philip T. Valente, MD, San Antonio, TX (*Abstract Co-Author*) Nothing to Disclose Christine O. Menias, MD, Chicago, IL (*Abstract Co-Author*) Nothing to Disclose Srinivasa R. Prasad, MD, Houston, TX (*Abstract Co-Author*) Nothing to Disclose Venkata S. Katabathina, MD, San Antonio, TX (*Abstract Co-Author*) Nothing to Disclose

### **TEACHING POINTS**

Familiarize audience with 2014 WHO classification & FIGO staging of ovarian malignanciesReview current research that focus on origin & pathogenesis of different subtypes of ovarian cancerDescribe cross-sectional imaging findings of existing and new borderline ovarian tumors & carcinomasDiscuss potential implications for risk evaluation, screening, and prophylactic treatment for ovarian cancer

## TABLE OF CONTENTS/OUTLINE

2014 FIGO staging of ovarian cancer Serous tumors: borderline tumor (BOT), low-grade carcinoma & high grade carcinoma; primary fallopian tube & peritoneal carcinoma Mucinous: BOT & carcinoma Endometrioid: endometriotic cyst, BOT & carcinoma Clear cell: BOT & carcinoma Brenner tumors: Benign & malignant Seromucinous tumors: New entity; cystadenoma/BOT/carcinomas Cross-sectional imaging spectrum & Future imaging techniques Clinical & management implicationsRecent findings on origin, pathogenesis & prognosis of different ovarian subtypes are taken into account while designing this new classification schemata and is mainly based on histopathologic findings and show important impact on prognosis & treatment. Fallopian tubal epithelium is proven to be the site of origin of most of high-grade serous carcinomas. Based on this, novel imaging techniques, prophylactic treatments & screening methods are being investigated to reduce mortality.

## **Honored Educators**

Presenters or authors on this event have been recognized as RSNA Honored Educators for participating in multiple qualifying educational activities. Honored Educators are invested in furthering the profession of radiology by delivering high-quality educational content in their field of study. Learn how you can become an honored educator by visiting the website at: https://www.rsna.org/Honored-Educator-Award/

Venkata S. Katabathina, MD - 2012 Honored Educator Christine O. Menias, MD - 2013 Honored Educator Christine O. Menias, MD - 2014 Honored Educator Christine O. Menias, MD - 2015 Honored Educator Christine O. Menias, MD - 2016 Honored Educator Srinivasa R. Prasad, MD - 2012 Honored Educator

# **Imaging of Cranial Nerve Pathologies in Pediatric Population**

Thursday, Dec. 1 12:45PM - 1:15PM Room: PD Community, Learning Center Station #7

### Participants

Vijay S. Pande, MD, Memphis, TN (*Presenter*) Nothing to Disclose Asim F. Choudhri, MD, Memphis, TN (*Abstract Co-Author*) Nothing to Disclose

## **TEACHING POINTS**

1) Imaging plays a pivotal role in evaluation of cranial nerves especially in pediatric age group when cllinical examination is often difficult or inconculsive.2) A wide variety of etiologies affect cranial nerves in pediatric population ranging from congenital hypoplasia to involvement in infective, inflammatory and neoplastic etiologies.3) Early indentification and appropriate treatment of cranial nerve deficits in children is of paramount importance for proper neuro-pschycological development.

## TABLE OF CONTENTS/OUTLINE

1) Brief review of imaging anatomic features and pathways of cranial nerves.2) Disscuss various MR sequences and there utility in evaluation of cranial nerves.3) Imaging role in syndromic and non-syndromic congenital abnormalties of cranial nerves.4) Imaging of neoplastic and non-neoplastic cranial nerve pathologies in pediatric age group.

### **Honored Educators**

Presenters or authors on this event have been recognized as RSNA Honored Educators for participating in multiple qualifying educational activities. Honored Educators are invested in furthering the profession of radiology by delivering high-quality educational content in their field of study. Learn how you can become an honored educator by visiting the website at: https://www.rsna.org/Honored-Educator-Award/

Asim F. Choudhri, MD - 2016 Honored Educator

'Wait! It's not Appendicitis?' Alternate MRI Diagnoses in Children with Right Lower Quadrant Abdominal Pain

Thursday, Dec. 1 12:45PM - 1:15PM Room: PD Community, Learning Center Station #8

### Participants

Haramit Hansra, MD, Tucson, AZ (*Presenter*) Nothing to Disclose Sarah M. Desoky, MD, Tucson, AZ (*Abstract Co-Author*) Nothing to Disclose Dorothy L. Gilbertson-Dahdal, MD, Tucson, AZ (*Abstract Co-Author*) Nothing to Disclose Bobby T. Kalb, MD, Tucson, AZ (*Abstract Co-Author*) Nothing to Disclose Diego R. Martin, MD, PhD, Tucson, AZ (*Abstract Co-Author*) Nothing to Disclose Unni K. Udayasankar, MD, FRCR, Tucson, AZ (*Abstract Co-Author*) Nothing to Disclose

# TEACHING POINTS

1. Right lower quadrant pain is a common presenting symptom in the pediatric emergency department, which can be caused by myriad pathology.

2. The role of MRI is to characterize the underlying cause whether it be acute appendicitis or an alternative diagnosis.

3.Ultrasound is the current initial modality of choice in children with suspected acute appendicitis, however advances in MRI technology and speed allow for a more detailed evaluation.

4. Magnetic resonance imaging enhances prognostic outcomes without the use of ionizing radiation.

# TABLE OF CONTENTS/OUTLINE

A fast non enahnced appendicitis MRI protocol will be discussed. Normal appendiceal MRI signal characteristics will be illustrated. The growing role of MRI use in the pediatric population will be described. A number of MRI cases that were ordered for acute appendicitis, but rather depicted alternative diagnoses will be examined. These cases include ovarian pathologies (torsion, complicated cysts, tumors and endometriomas), pyelonephritis, urinary calculi, acute enteritis/colitis, acute hepato-biliary pathologies, and Meckel's diverticulitis, among others. Experience from a large data base of appendicitis MRI performed at a tertiary care children's hospital will be shared. The Stability and Reliability of Subjective Semi-quantitative Grade Method and Objective Quantification Method for Evaluating Leg Muscle Fatty Infiltration in Dystrophinopathy

Thursday, Dec. 1 12:45PM - 1:15PM Room: PD Community, Learning Center Station #1

## Participants

Jing Du, MD, Beijing, China (*Presenter*) Nothing to Disclose Jiangxi Xiao, Beijing, China (*Abstract Co-Author*) Nothing to Disclose Ying Zhu, MD, Beijing, China (*Abstract Co-Author*) Nothing to Disclose

### PURPOSE

To analyze the intra-observer and inter-observer agreement of the subjective semi-quantitative grade score method and the objective fat quantification method in the evaluation of leg muscle fatty infiltration in dystrophinopathy.

## **METHOD AND MATERIALS**

One hundred and ninety-four boys with genetically confirmed dystrophinopathy were recruited. The axial T1-weighted images and IDEAL-IQ images were obtained. The axial T1-weighted images were visually evaluated by three observers for two times with an interval of one week. The muscle FF were measured by three observers twice based on the IDEAL-IQ images. The observers were blinded to the clinical diagnosis. The weighted kappa analysis was used to analyze the intra- and inter-observer agreement. The intra-class correlation coefficient (ICC) was calculated to assess the agreement of the objective muscle FF measured by three observers. The Bland-Altman map was used to show the intra- and inter-observer agreement. The Spearman correlation was used to compare the result of the subjective and the objective methods. Boxplot diagram was showed to visualize the differences between them.

#### RESULTS

The intra-observer agreement values for the 18 leg muscles were 0.73-0.92 (P<0.05), 0.41-0.84 (P<0.05) and 0.34-0.80 (P<0.05), respectively. The intra-observer agreement of the experienced radiologist was the highest. The inter-observer agreement values for all the muscles were 0.42-0.84 (P<0.05), 0.17-0.67 (P<0.05) and 0.21-0.58 (P<0.05), respectively. The ICC values of the intra-observer were 0.9914-0.9990, 0.9901-0.9992 and 0.9861-0.9996, respectively. The ICC values of the inter-observer were 0.9801-0.9985, 0.9936-0.9993 and 0.9837-0.9989, respectively. Significant positive correlation was found between subjective method and objective method for different muscles with the correlation coefficients varied from 0.73 to 0.92 (P<0.05). The fat infiltration level evaluated by the subjective semi-quantitative method was higher than FF measured by the objective method.

## CONCLUSION

The reliability of the subjective method was correlated with observers' experience in neuromuscular disorder. The results of the objective method were more reliable in evaluating leg muscle fatty infiltration level than the subjective method which tend to overestimate the fatty infiltration level.

## **CLINICAL RELEVANCE/APPLICATION**

To find a better method to measure the muscle fatty infiltration level on MRI.

# PD247-SD-THB2

Comparative Outcomes of N-butyl Cyanoacrylate and Onyx Embolization in Intracranial Arteriovenous Malformations of Pediatric Patients

Thursday, Dec. 1 12:45PM - 1:15PM Room: PD Community, Learning Center Station #2

#### Awards

### **Student Travel Stipend Award**

#### **Participants**

Mark Le, MD, Detroit, MI (*Presenter*) Nothing to Disclose Karan N. Patel, MD, Detroit, MI (*Abstract Co-Author*) Nothing to Disclose Vasavi Paidpally, MD, Detroit, MI (*Abstract Co-Author*) Nothing to Disclose Hamza M. Beano, MD, Detroit, MI (*Abstract Co-Author*) Nothing to Disclose Jasmine Koo, MD, Detroit, MI (*Abstract Co-Author*) Nothing to Disclose Monte L. Harvill, MD, Franklin, MI (*Abstract Co-Author*) Nothing to Disclose Terrence Metz, MD, Royal Oak, MI (*Abstract Co-Author*) Nothing to Disclose

#### PURPOSE

Staged preoperative embolization followed by surgical resection or gamma knife radiation may be used to manage intracranial arteriovenous malformations (AVMs) in pediatric patients. The two commonly used liquid embolic agents are N-butyl cyanoacrylate (nBCA) and Onyx. We sought to compare the outcomes of nBCA versus Onyx in pediatric intracranial AVM.

## METHOD AND MATERIALS

All pediatric intracranial AVMs embolized with nBCA and Onyx at our institution from December 31, 2005 to January 1, 2014 were included in this study. Patients were stratified into two treatment groups: nBCA and Onyx. Chorts were compared by age, sex, BMI, Spetzler-Martin grade, and intra- and post-embolization complication prior to surgical resection or gamma knife radiation. Additionally, pre- and post- laboratory values were analyzed. Efficacy of the final treatment outcome was determined by post-procedural MRI.

### RESULTS

10 out of the 21 patients were females with an average age of 11.7 years (range: 4-17). A total of 27 embolizations were performed (nBCA, 10 patients, 16 procedures; Onyx, 11 patients, 11 procedures). There were no significant differences in patient demographics and Spetzler-Martin grade. No major intra- and post-embolization complication prior to surgical resection or gamma knife radiation was observed. No significant differences in the pre- and post-laboratory values were noted for the following: hemoglobin, white blood cell, platelets, INR, PT, PTT, BUN, and Cr. Nineteen patients (90%) underwent surgical resection or gamma knife radiation to achieve complete AVM resection. No significant differences in complication rates were observed among the cohorts.

### CONCLUSION

Staged preoperative embolization with nBCA or Onyx followed by surgical resection or gamma knife radiation showed no significant differences in the outcome of pediatric intracranial AVMs.

# **CLINICAL RELEVANCE/APPLICATION**

Preoperative embolization of intracranial arteriovenous malformations has been showed to improve the outcome of surgical resection or gamma knife radiation. Two commonly used liquid embolic agents are nBCA and Onyx. There are limited studies comparing the outcomes and complication rates of these two embolic agents. Therefore, our study adds additional knowledge to the ultilization of nBCA and Onyx for treatment of pediatric intracranial AVM.

# Adult PICC Device Provides Safe, Durable, Reliable Central Venous Access in Children

Thursday, Dec. 1 12:45PM - 1:15PM Room: PD Community, Learning Center Station #3

#### Awards

### **Student Travel Stipend Award**

### **Participants**

Brooke Lawson, MD, Dundee, United Kingdom (*Presenter*) Nothing to Disclose Nicholas W. Dobbs, MBBS, FRCR, Nottingham, United Kingdom (*Abstract Co-Author*) Nothing to Disclose Ian A. Zealley, MD, Dundee, United Kingdom (*Abstract Co-Author*) Nothing to Disclose

### PURPOSE

Conventional tunnelled central venous catheters (TCVCs) are larger than peripherally inserted central venous catheters (PICCs). Conventional TCVCs are used in pediatric patients which are associated with relatively high complication rates in smaller children (<1yr or <10kg). Our unit has developed a technique employing PICCs as TCVCs in small children. We set out to determine the success, safety and durability of this technique and to identify the rate of delayed complications. We describe the six-year experience in our unit.

## **METHOD AND MATERIALS**

Institutional research approval was obtained and data gathered retrospectively. Electronic and paper medical records were reviewed for consecutive paediatric patients who had a PICC inserted as a TCVC over a 6-year period (September 2009 through July 2015). Data recorded included patient demographics, setting for PICC as TCVC insertion, use of ultrasound and fluoroscopy, PICC device type, delayed complications, date of and reason for removal, and laboratory-confirmed catheter related infections. Data was entered into an Excel spreadsheet and analysed using excel statistical tools.

### RESULTS

Twenty-one PICCs were inserted as TCVCs in 19 children, all aged less than 10 years. Median patient age at time of insertion was 3.25 years (range 1.4 months - 9.6 years, five patients < 1year or <10kg). The total number of catheter-days was 853. Mean catheter life was 41 days. General anaesthesia and local anaesthesia was used for all placements (100%). Eighteen (86%) procedures were carried out under ultrasound and fluoroscopic guidance, and ultrasound only in 3 cases (14%). All insertions were successful with no immediate complications recorded. Non-elective removal was required in 1 case (5%) for suspected catheter-related infection. Dislodgement occurred in one case (5%). Nineteen of the 21 TCVCs (90%) lasted for the total intended duration of use.

## CONCLUSION

Using a PICC as a TCVC in smaller children appears to be a safe and durable technique with an acceptable complication profile.

## **CLINICAL RELEVANCE/APPLICATION**

Using a PICC device as a TCVC in children is a safe and durable option and avoids the higher complication rates associated with conventional TCVC devices in smaller children.

## **Honored Educators**

Presenters or authors on this event have been recognized as RSNA Honored Educators for participating in multiple qualifying educational activities. Honored Educators are invested in furthering the profession of radiology by delivering high-quality educational content in their field of study. Learn how you can become an honored educator by visiting the website at: https://www.rsna.org/Honored-Educator-Award/

Ian A. Zealley, MD - 2016 Honored Educator

## PD249-SD-THB4

The Value of MRI in Evaluating the Efficacy and Complications of Intra-arterial Chemotherapy for the Treatment of Retinoblastoma

Thursday, Dec. 1 12:45PM - 1:15PM Room: PD Community, Learning Center Station #4

## Participants

Shuxian /. Chen JR, MMed, Shanghai City, China (*Presenter*) Nothing to Disclose Yu Hua Li, MD, Shanghai, China (*Abstract Co-Author*) Nothing to Disclose

### PURPOSE

To evaluate the value of MRI and ADC in assessing the efficacy and complications with the treatment of intra-arterial chemotherapy (IAC) for retinoblastoma (RB).

## METHOD AND MATERIALS

Sixty patients with unilateral RB given primary treatment of IAC(average 3 cycles ), were selected from 202 patients with RB in our hospital. MRI and DWI were performed with the same protocols before and after (in three months) the treatment of IAC. Comparison with the parameters, including tumor size, ADC value and enhancement pattern before and after IAC.All patients (median age, 22.5 months; group D(50,83.3%), group E (10,16.7%))were followed up for more than 6 months.

### RESULTS

Of all 60 eyes, tumor size obviously diminished, with the mean maximum diameter changing from  $1.55\pm0.26$ cm to  $0.66\pm0.36$ cm(p<0.001) and mean thickness changing from  $1.41\pm0.34$ cm to  $0.39\pm0.34$ cm(p<0.001); the mean ADC value increased significantly from  $0.94\pm0.24\times10-3$ mm2/s to  $2.24\pm0.40\times10-3$ mm2/s(p<0.001); the degree of enhancement of tumor changed from moderate enhancement to non-enhancement (n=55, 92.7%) or slight enhancement (n=5, 8.3%). Six (10%) affected eyes with enhancement of postlaminar optic nerve were not enhanced after treatment.Tumor control was achieved in 59 eyes (98.3%), but 1 eye was found recurrence in ninth month follow-up.The main complications in MRI findings before and after treatment included affected eyeball volume reduction(15% to 66.7%), retinal detachment with subretinal fluid (16.7% to 56.7%), subretinal hemorrhage(5% to 13.3%), vitreous hemorrhage(1.7% to 6.7%), vitreous opacity(3.3% to 5%), cataract lens (0 to 6.7%), extraocular muscle inflammation (0 to 8.3%), choroidal vascular ischemia (0 to 15%), vascular proliferation(0 to 15%) and extraocular invation or metastasis (0).

## CONCLUSION

MRI could well assess the activity of tumor of RB before and after treatment of IAC, and detect the associated complications of IAC. MRI could also monitor the risk factor of abnormal enhancement of postlaminar optic nerve avoiding unnecessary enucleation. IAC is an effective treatment for RB. At the same time IAC will cause some complications for affected eyeballs.

### **CLINICAL RELEVANCE/APPLICATION**

MRI could well assess the activity of tumor of RB before and after treatment of IAC, and detect the associated complications of IAC.

Reducing Radiation Dose and Contrast Dose with Low Tube Voltage Prospective ECG-triggering and Adaptive Statistic Iterative Reconstruction for Infants with Complex Congenital Heart Disease

Thursday, Dec. 1 12:45PM - 1:15PM Room: PD Community, Learning Center Station #5

## Participants

Shiyu Wang, MD, Shanghai, China (*Presenter*) Nothing to Disclose Li Wei Hu, DIPLENG, MENG, Pudong, China (*Abstract Co-Author*) Nothing to Disclose Haisheng Qiu, Shanghai, China (*Abstract Co-Author*) Nothing to Disclose Yumin Zhong, MD, Shanghai, China (*Abstract Co-Author*) Nothing to Disclose

### PURPOSE

To demonstrate the clinical values of using low tube voltage, prospective ECG-triggering cardiac CT scan with adaptive statistic iterative reconstruction (ASIR) to reduce both radiation dose and contrast dose in examining infants with complex congenital heart disease.

## **METHOD AND MATERIALS**

45 consecutive infant patients (20 male, 25 female, mean age: 8.20±4.37m, weight: 5-10kg, mean weight: 7.36±1.83kg) with complex congenital heart disease underwent prospective ECG-triggered low dose cardiac CT on a 64-slice high definition CT scanner. The tube voltage was 80kVp and tube current was 120mA and contrast agent was Visipaque (270mg I/mL, GE Healthcare). Cardiac CT images were reconstructed with 70% of ASIR. The quantitative CT image quality was assessed by measuring the image noise in erector spinae and aorta and the contrast-to-noise ratio (CNR) in aorta. The qualitative image analysis was performed on a 5-point grading scale by two independent reviewers and interobserver variability was calculated. The results of 26 CT examinations were also compared with the available surgical results for diagnostic accuracy evaluation.

### RESULTS

The effective dose was  $0.60\pm0.07$ mSv for the patient population. The iodine load was  $3.98\pm0.75$ gI. Image noise in erector spinae was  $12.28\pm1.23$ HU and CNR in aorta was  $28.99\pm9.50$ . All images were acceptable for diagnosis with an average subjective image quality score of 4.76 with very good agreement between the reviewers (Kappa=0.75). Comparing to the surgery results in 26 cases, prospective ECG-triggered cardiac CT with ASIR was 96% accurate in the diagnosis for extracardiac defects and 92% accurate for intracardiac defects.

## CONCLUSION

Prospective ECG-triggered cardiac CT using 80kVp, low-concentration iodinated contrast agent (270mgI/mL) and 70%ASIR reconstruction provides excellent image quality and accurate diagnosis for complex congenital heart disease in infants with reduced contrast dose, sub-mSv radiation dose.

#### **CLINICAL RELEVANCE/APPLICATION**

Prospective ECG-triggered cardiac CT with 70%ASIR and low-concentration iodinated contrast may be used to scan infants with complex congenital heart disease to reduce radiation and contrast doses.

Gadolinium Deposition in Globus Pallidus and Dentate Nucleus on Unenhanced T1-weighted Image in the Children is Dependent on the Type of Contrast Agent

Thursday, Dec. 1 12:45PM - 1:15PM Room: PD Community, Learning Center Station #6

## Participants

Young Jin Ryu, MD, Seoul, Korea, Republic Of (*Presenter*) Nothing to Disclose Young Hun Choi, MD, Seoul, Korea, Republic Of (*Abstract Co-Author*) Nothing to Disclose Jung-Eun Cheon, MD, Seoul, Korea, Republic Of (*Abstract Co-Author*) Nothing to Disclose Woo Sun Kim, MD, Seoul, Korea, Republic Of (*Abstract Co-Author*) Nothing to Disclose In-One Kim, MD, Seoul, Korea, Republic Of (*Abstract Co-Author*) Nothing to Disclose Ji-Eun Park, Seoul, Korea, Republic Of (*Abstract Co-Author*) Nothing to Disclose Yu Jin Kim, MD, Seoul, Korea, Republic Of (*Abstract Co-Author*) Nothing to Disclose

### PURPOSE

To identify changes in signal intensity (SI) ratios of the dentate nucleus (DN) and the lobus pallidus (GP) to those of other structures on unenhanced T1-weighted MR images in children and compare between linear or macrocyclic gadolinium-based contrast agents (GBCAs).

### **METHOD AND MATERIALS**

By reviewing 31422 cases of MR examination performed in a tertiary children's hospital between 2006 and 2014, 18 children (mean age  $9.2 \pm 3.6$ , age range 2-14 year) who underwent at least four consecutive MR examinations with the exclusive use of linear GBCA (gadodiamide, group A, n = 8) or macrocyclic GBCA (gadoterate meglumine, group B, n = 10) were found. DN-to-pons SI ratio was calculated by dividing the mean signal intensity of the DN by the mean SI of the pons. GP-to-thalamus SI ratio was calculated by dividing the mean signal intensity of the GP by the mean SI of the thalamus. Differences in DN-to-pons and GP-to-thalamus SI ratios between the first and last MR imaging examinations were calculated. One-sample test and Mann-Whitney test were used to evaluate the difference in SI ratios for both groups.

# RESULTS

In group A, the SI ratio increased significantly between the first and last MR examinations (mean difference in SI ratio, DN-to-pons,  $0.0486 \pm 0.0471$ , P = .022; GP-to-thalamus,  $0.0967 \pm 0.0877$ , P = .017). In group B, the DN-to-pons SI ratio showed no significant difference between the first and last MR exminations (-0.0070 ± 0.0243, P = .384), while the GP-to-thalamus SI ratio decreased (-0.0383 ± 0.0365, P = .009). Differences in SI ratios were significantly larger in group A than in group B (DN-to-pons, P = .002; GP-to-thalamus P = .003). The interval between the first and the last MR examinations and number of MR scans did not differ between both groups (P = .083, .068).

## CONCLUSION

The signal intensities of the DN and GP on unhanced T1-weighted images significantly increased after serial administration of linear GBGA gadodiamide but not by the macrocyclic GBCA gadoterate meglumine in children.

# **CLINICAL RELEVANCE/APPLICATION**

Even though the clinical implication of hyperintensity of DN and GP has not been known, the macrocyclic GBCAs should be applied carefully in the children as well as adult.

# **Computed Diffusion-Weighted Image for Abdominal MRI**

Thursday, Dec. 1 12:45PM - 1:15PM Room: PH Community, Learning Center Station #1

#### **Participants**

Takeshi Yoshikawa, MD, Kobe, Japan (*Presenter*) Research Grant, Toshiba Corporation Yoshiharu Ohno, MD, PhD, Kobe, Japan (*Abstract Co-Author*) Research Grant, Toshiba Corporation; Research Grant, Koninklijke Philips NV; Research Grant, Bayer AG; Research Grant, DAIICHI SANKYO Group; Research Grant, Eisai Co, Ltd; Research Grant, Fuji Pharma Co, Ltd; Research Grant, FUJIFILM RI Pharma Co, Ltd; Research Grant, Guerbet SA; Katsusuke Kyotani, RT, Kobe, Japan (*Abstract Co-Author*) Nothing to Disclose Yoshimori Kassai, MS, Otawara, Japan (*Abstract Co-Author*) Employee, Toshiba Corporation Hisanobu Koyama, MD, PhD, Kobe, Japan (*Abstract Co-Author*) Nothing to Disclose Kouya Nishiyama, Kobe, Japan (*Abstract Co-Author*) Nothing to Disclose Shinichiro Seki, Kobe, Japan (*Abstract Co-Author*) Nothing to Disclose Kazuro Sugimura, MD, PhD, Kobe, Japan (*Abstract Co-Author*) Research Grant, Toshiba Corporation Research Grant, Koninklijke Philips NV Research Grant, Bayer AG Research Grant, Eisai Co, Ltd Research Grant, DAIICHI SANKYO Group

## PURPOSE

To assess capability of computed diffusion-weighted image (cDWI) in evaluation of abdominal diseases

## METHOD AND MATERIALS

102 patients (52 men and 50 women, mean: 67.3years), who were suspected to have hepato-biliary-pancreatic malignancy and underwent 3T-MRI, were retrospectively analyzed. DWIs were obtained with SE-EPI (b: 0 and 1000, DWI0 and DWI1000). cDWI images at b values of 200, 400, 600, 800, 1200, 1400, 1600, 1800, and 2000 were reconstructed (cDWI200-2000). 65 malignant lesions and 68 benign lesions were confirmed. Lesions with a diameter of >10 mm were chosen for quantitative analysis. Signal-to-noise ratio of each organ (SNR=SI*organ*/SD*organ*) and lesion contrasts (*CM*=SI*lesion*-SI*organ*/SI*lesion*+SI*organ*) were compared among the images. Two readers assessed image quality, i.e. organ signal and contour, suppression of vessels and ducts, and signal inhomogeneity and noise on images, and recorded b values with best quality and with complete gallbladder signal suppression for each patient, and assessed lesion conspicuity using a 5-point scale on DWI1000 and cDWIs. Malignant lesion detection for each patient and accuracies of lesion characterization were separately assessed using a 5-point scale on DWI0+1000 and +cDWIs sets. Consensuses were made and compared. ROC analysis was used for detections and accuracies.

## RESULTS

SNRs were significantly highest on cDWI800 in the liver and on cDWI600 in the pancreas and spleen (Ps<0.0001). Malignant lesions contrasts were significantly increased (0.026) and benign ones were significantly decreased (<0.0001) in proportion to increase of b value. Image quality was best on cDWI800 followed by DWI1000 (mean:  $835 \pm 176$ ). Gallbladder signal was completely suppressed on cDWI1200 or higher (mean:  $1777 \pm 266$ ). Conspicuity of malignant lesion was significantly highest (0.005) and that of benign lesion was significantly lowest (<0.0001) on cDWI2000. Malignant lesion detection was significantly higher (Az: 0.728 vs 0.798, 0.033) and accuracy of lesion characterization was significantly higher (Az: 0.662 vs 0.904, <0.0001) on +cDWIs set.

## CONCLUSION

Computed DWI can improve image quality, lesion contrast, detection, and characterization, and is a useful post-processing tool for abdominal MRI.

### **CLINICAL RELEVANCE/APPLICATION**

Computed DWI can improve image quality, lesion contrast, detection, and characterization, and is a useful post-processing tool for abdominal MRI.

Importance of US Coupling Gel on Photoacoustic Signal Attenuation

Thursday, Dec. 1 12:45PM - 1:15PM Room: PH Community, Learning Center Station #2

#### Awards

### **Student Travel Stipend Award**

### Participants

Caitlin Finley, Wynnewood, PA (Presenter) Nothing to Disclose Maria Stanczak, MS, Philadelphia, PA (Abstract Co-Author) Nothing to Disclose Flemming Forsberg, PhD, Philadelphia, PA (Abstract Co-Author) Equipment support, Toshiba Corporation; Research Grant, Toshiba Corporation; Equipment support, Siemens AG; In-kind support, General Electric Company; In-kind support, Lantheus Medical Imaging, Inc Ji-Bin Liu, MD, Philadelphia, PA (Abstract Co-Author) Nothing to Disclose Shunxin Zhang, Beijing, China (Abstract Co-Author) Nothing to Disclose Yanhong Wang, Beijing, China (Abstract Co-Author) Nothing to Disclose

Ping Wang, MD, Nanchong, China (Abstract Co-Author) Nothing to Disclose

John R. Eisenbrey, PhD, Philadelphia, PA (Abstract Co-Author) Support, General Electric Company; Support, Lantheus Medical Imaging, Inc

### PURPOSE

To determine the attenuating effects of various ultrasound (US) coupling gels on photoacoustic signals using a commercial imaging system.

## **METHOD AND MATERIALS**

Photoacoustic signals from 3 tissue phantoms were acquired using the Vevo LAZR system with a LZ250 probe (Visualsonics, Toronto, Canada). Two agar phantoms were dyed with methylene blue or IR820 dye (Sigma-Aldrich). A third phantom was made with no dye. Phantoms were scanned from 680 to 970 nm at a gain of 45 dB and a depth of 8 mm with four different types of acoustic coupling gel: a clear medium viscosity gel (NEXT Medical Products, Branchburg, NJ, USA), a clear high viscosity gel (NEXT Medical Products, Branchburg, NJ, USA), a blue medium viscosity gel (Owens & Minor, Mechanicsville, VA, USA), and a white, medium viscosity opaque US lotion (Parker Laboratories, Inc., Fairfield, NJ, USA). The clear phantom's spectra were subtracted from the spectra of the methylene blue and IR820 phantoms in order to eliminate any photoacoustic signal from the agar. The photoacoustic signal intensities across different coupling gels and phantoms were compared using ANOVA tests.

## RESULTS

The photoacoustic signal from both phantoms showed a dependence on the type of coupling gel used. The average maximum signal intensities in the methylene blue phantom using the white, blue, clear high viscosity, and clear medium viscosity gels were 0.28±0.01, 0.42±0.17, 0.56±0.16, and 0.76±0.20 linear arbitrary units (au), respectively (p=0.03). While variations in intensities were observed between clear and blue gels, these differences were not found to be statistically significant (p=0.12). For the IR820 phantom, the average maximum intensities of the signal due to the white, blue, clear high viscosity, and clear medium viscosity gels were 0.38±0.04, 2.31±0.22, 2.25±0.43, and 2.30±0.23 au, respectively (p<0.001). However, unlike the methylene blue phantom, no differences were observed between clear and blue coupling gels (p=0.9). In both phantoms, no significant differences were observed in peak absorbance wavelengths between the blue and either clear coupling gel groups (p>0.49).

## CONCLUSION

The selection of acoustic coupling gels can lead to the attenuation of photoacoustic signal and should be kept constant during serial imaging studies.

# **CLINICAL RELEVANCE/APPLICATION**

Unlike US imaging, the choice of coupling gel may potentially alter photoacoustic signals and should be kept constant for longitudinal studies.

# The Vertical Positioning on Abdomen and Thorax CT Studies and the Influence to Dose

Thursday, Dec. 1 12:45PM - 1:15PM Room: PH Community, Learning Center Station #3

#### Participants

Hannele M. Niiniviita, MSc, Turku, Finland (*Presenter*) Nothing to Disclose Jukka Jarvinen, Turku, Finland (*Abstract Co-Author*) Nothing to Disclose Heli Maattanen, Turku, Finland (*Abstract Co-Author*) Nothing to Disclose Jarmo Kulmala, DPhil, Turku, Finland (*Abstract Co-Author*) Nothing to Disclose Jani Saunavaara, Turku, Finland (*Abstract Co-Author*) Nothing to Disclose

### PURPOSE

To assess patient positioning in abdomen and thorax studies and its effect on doses.

### **METHOD AND MATERIALS**

DoseWatch (commercial software, GE, Milwauke, USA) was used to collect radiation dose as computed tomography dose index (CTDIvol), body mass index (BMI) and patient positioning as a difference from isocenter on abdomen and thorax studies. The data was collected at six departments from November 2015 to April 2016. The patients were divided by their BMI into four groups (BMI <20, 20-25, 25-30 and >30 kg/m<sup>2</sup>) and mean doses and mean vertical shifts were calculated. Differences in patient positioning at different BMIs and at different departments were assessed. The doses of each BMI group were also compared to the mean doses of patients scanned in isocenter (vertical shift between -3 and 3 mm). The data of 610 thorax and 1545 abdomen studies were collected.

## RESULTS

BMI values ranged from 14.7 to 62.5 kg/m<sup>2</sup> and delta vertical shifts from -45 to 96 mm and from -64 to 70 mm in thorax and abdomen studies, respectively. Vertical shift was BMI dependent as patients with BMI over 25 were centered lower than patients with lower BMI. Patients with BMI over 25 were centered lower than the isocenter in abdomen scans, but on average patients from all BMI groups were centered higher than the isocenter in thorax scans (figure 1 a). When comparing mean doses of all patients to mean doses of patients positioned at isocenter in abdomen studies, the doses were 15.3 % and 4.9 % lower for BMI groups <20 kg/m<sup>2</sup> and 20-25 kg/m<sup>2</sup>, respectively. On the other hand, they were 0.8 % and 8.4 % higher for BMI groups 25-30 kg/m<sup>2</sup> and >30 kg/m<sup>2</sup> (figure 1 b). However, the doses remained the same despite of vertical shift on thorax scans. At department level, the results were similar to overall results.

### CONCLUSION

Vertical shift in both abdomen and thorax CT scans was BMI dependent as smaller patients were positioned higher with respect to the isocenter than larger patients. The miscentering affected patient doses in abdomen imaging.

### **CLINICAL RELEVANCE/APPLICATION**

The patient centering is BMI dependent, where smaller patients are positioned higher.

# PH268-SD-THB5

### Quantitative Evaluation of Coronary Artery Diameter: Effect of CT Scan Modes and Heart Rate

Thursday, Dec. 1 12:45PM - 1:15PM Room: PH Community, Learning Center Station #5

#### **Participants**

Jeong Hoon Hwang, Seoul, Korea, Republic Of (*Presenter*) Nothing to Disclose Moon C. Kim, RT, Seoul, Korea, Republic Of (*Abstract Co-Author*) Nothing to Disclose Yoon C. Nam, RT, Seoul, Korea, Republic Of (*Abstract Co-Author*) Nothing to Disclose Jin Seok Park, Seoul, Korea, Republic Of (*Abstract Co-Author*) Nothing to Disclose Jun-Su Kim, RT, Seoul, Korea, Republic Of (*Abstract Co-Author*) Nothing to Disclose

### CONCLUSION

In high heart rate patients, it demonstrates that scanning at 45% phase of helical (systole) is the best suitable and using high pitch spiral scan mode is unsuitable. In low heart rate patients, it demonstrates that scanning at 75% phase of helical (diastole) is the best suitable for the measurement of exact coronary artery size. If using proper scan mode by heart rate, it could be helpful to accurate diagnosis for cardiovascular patients.

### Background

To evaluate the coronary lumen area and roundness for coronary CT angiography with the change of scan mode and heart rate which are significant factors affecting motion artifact and diagnostic accuracy.

#### **Evaluation**

All CT scans were performed on SOMATOM Definition Flash (Siemens, hereafter, S) with a cardiac motion simulating phantom (MOCOMO, Fuyo Corp, JP) attached 400HU solid phantom of 3 and 4mm diameter. The phantom was scanned at 0(static) for reference and heart rate (HR) simulated of 50-100 beat/min with sequence, helical, high pitch scan mode and reconstructed at 45% and 75% phase (sequence, helical) and 60% start phase (high pitch) of the R\_R cycle. The mean area and roundness of scanned images were analyzed by using Image J software. Statistical analysis was performed to T-test and ANOVA by using SPSS software (version 18.0, IBM corp).

### Discussion

As increased heart rate, the error value of the mean area of 3mm and 4mm phantom were the smallest about 4.9% and 2.9% in helical mode 45 %, and followed sequence mode 45%, helical mode 75%, sequence mode 75%, high pitch mode in ascending order. The error value of the mean roundness of 3mm and 4mm phantom were the smallest about 2.1% and 2.1% in helical mode 45%, and there was no significant difference among the other scan modes. For the comparison of scan modes in 3mm phantom and heart rate 50bpm(suitable phase for high pitch mode), the error value of the mean area was the smallest about 9.2% in helical mode 75% and followed sequence mode 75%, high pitch spiral scan mode. The error value of the mean roundness was the smallest about 3.4% in sequence mode 75% and followed helical mode 75%, high pitch spiral scan mode(P<.05 for all).

## QS133-ED-THB1

## Managing Radiology Information System Downtimes- A Comprehensive Approach

Thursday, Dec. 1 12:45PM - 1:15PM Room: QS Community, Learning Center Station #1

#### Participants

Paul Cornacchione, BSC, Toronto, ON (*Abstract Co-Author*) Nothing to Disclose Catherine Wang, BSc, Toronto, ON (*Abstract Co-Author*) Nothing to Disclose Tanya Spiegelberg, Toronto, ON (*Abstract Co-Author*) Nothing to Disclose Barbara Mesic, Toronto, ON (*Abstract Co-Author*) Nothing to Disclose Daniel Toubassy, BSC, Toronto, ON (*Presenter*) Nothing to Disclose Leon Goonaratne, Toronto, ON (*Abstract Co-Author*) Nothing to Disclose Shaun Dias, Toronto, ON (*Abstract Co-Author*) Nothing to Disclose

## PURPOSE

Most imaging services are now reliant on electronic tools to deliver key diagnostic information required to manage care and these tools require regular updates and maintenance. The launching of new features brings with it the need to manage periods of downtime. Challenges encountered with downtime include disparate planning, communication breakdowns, use of electronic alternatives and gaps in frontline roles and responsibilities. Management of these downtimes require collaborative planning to ensure minimal impact to patient care. The focus of downtime planning is less about IT and more about managing clinical services and reducing risk to patients. The purpose of the initiative was to develop a standardized downtime planning process to ensure timely and safe delivery of imaging services while the RIS was offline. Through multiple iterations, a final program was developed that includes: Integrated planning between Imaging IT and Clinical:Communications Plan

Standardized Job Action SheetsHospital wide communications of downtime, processes, roles and responsibilities Development of workflows to ensure timely delivery of imaging service

Development of worknows to ensure timely delivery of inaging service

Effective communication of the diagnostic interpretationEfficient recovery of downtime information

Provision of a finalized electronic report to the EMR

## METHODS

A lean workshop event was held with the department to identify the interdependencies between IT, clinical services and hospital IT. The event also aimed to develop proper processes that included:Governance and Accountability

Standardized ProcessesPlanning and Communication

Technologist Workflow

Radiologist Workflow

Recovery from DowntimeContingency Planning for Roll BackFigure 1A outlines the product of the workshop. In addition to the process developed, every step or action had an accompanying "Job Action Sheet" that outlined exactly what was to be performed in that action.

### RESULTS

Standardized communication processes were developed to ensure that key hospital departments were aware of the downtime and its impact. Various workflows were piloted through different downtimes, some more reliant on electronic alternatives, while others relied on human resources and paper. Workflows were not only important in the delivery of care; they had a tremendous effect on the recovery post downtime. Medico-legal requirements dictated that the department keep proper records of the downtime and in order to provide electronic interpretation of the results when the system was back up, processes were developed to ensure recovery of the documentation occurred in a timely manner.Contingency planning became vital in order to minimize impact to patients. These plans included:Risk identification and management

Stakeholder engagement in the roll-back decision

Additional staff roles and responsibilities for extended downtimesA key factor to decision making in the event of a critical issue involved weighing the impact of the issue to the clinical service against the likelihood of issue resolution. Overall, the department managed 3 downtimes where CT, general radiography and ultrasound were operational. The attached figure 1B outlines the following performance metrics: Average: Number of studies completed during the downtimes (Volumes) Turnaround time from study requested to study completed (Exam TAT)

Turnaround time from study completed to images interpreted (Report TAT)Percentage change between normal and downtime operationsThe performance data shows a decrease in the average exam TAT during a downtime with an increase in average report TAT over the same period. The expedited turnaround for exams is believed to be the result of comprehensive leadership communication and pressure to provide quality care. Report turnaround times were directly impacted by the recovery process. Complex recovery cases require more rigorous and lengthy recovery which causes delays in making the case available to the radiologist for interpretation. Although the impact of paper tools appears to improve patient access, leadership focus and communication about the downtime and performance may have been a contributing factor. The department took an average of 4hrs and 6 min to recover from the respective downtimes. Recovery included electronic documentation entry and uploading of all paper documents into the patient's file.

## CONCLUSION

The development of an integrated planning process improved communication increased collaboration. Standardized work plans ensured all necessary steps were taken prior to the downtime and enabled a smooth transition for the clinical team as they moved from an electronic to a paper environment. Job action sheets were effective in supporting staff with their roles throughout the downtime. When questions were raised, the Job Action Sheets provided clear direction. Downtime was executed with little to no errors and with performance metrics comparable to normal after-hours operations.

### QS134-ED-THB2

Improving Curriculum and Patient Care: Areas of Weakness Identified Through Competency Based Assessment

Thursday, Dec. 1 12:45PM - 1:15PM Room: QS Community, Learning Center Station #2

# Participants

Linda Lanier, MD, Gainesville, FL (*Abstract Co-Author*) Nothing to Disclose Chris L. Sistrom, MD, Gainesville, FL (*Abstract Co-Author*) Research Consultant, National Decision Support Company Robbie Slater, MD, Hahira, GA (*Abstract Co-Author*) Nothing to Disclose Ilona M. Schmalfuss, MD, Gainesville, FL (*Abstract Co-Author*) Nothing to Disclose Anthony A. Mancuso, MD, Gainesville, FL (*Abstract Co-Author*) Nothing to Disclose Nupur Verma, MD, Gainesville, FL (*Presenter*) Nothing to Disclose

## PURPOSE

The "Emergent/Critical Care Imaging Simulation" is a web-based, case-presentation testing method, designed in collaboration with the American College of Radiology (ACR) to assist academic faculty in the ACGME-mandated task of objectively assessing and documenting a resident's competency, specifically in emergent imaging, prior to independent Entrustable Professional Activity (EPA). An important goal of the Simulation is to provide feedback regarding areas of weakness to both individual users and to training programs in order to enhance and improve resident education. The purpose of this presentation is to share the specific areas of weakness that have been identified through this process that are widely distributed across institutions and that are independent of R level training.

## METHODS

212 residents from 16 institutions participated in two Simulations in 2014 and 2015 in which a total of 129 cases/topics were presented. (SIM 2: n= 94, 63/R1, 31/R2 and SIM 3: n= 118, 85/R1, 33/R2). Case content included all modalities, all body systems and all ages. Normal and abnormal cases were presented reflecting varying degrees of acuity. The The testing simulated an 8 hour 'ED shift' in standard PACS workflow format. Original clinical history was provided and full DICOM image sets were linked to each patient. Resident users reviewed each case and provided a "report" by submitting a free text response as well as an assessment of acuity for each case. User responses were evaluated by four faculty graders, who compared them to a predetermined item-specific grading key for each item, and scored them using a 0-10 scale. All cases had been previously tagged into one of three categories; Neuroradiology, body, and musculoskeletal (MSK) imaging. Average scores and score distribution were evaluated for each item. Performance with regard to modality, category, resident training level, and specific topics were evaluated. Of specific interest were topics in which a high percentage of residents earned a very low score, 0-3 out of 10 possible points.

## RESULTS

Faculty grader reliability was excellent (n=4, reliability = 97%). Resident performance was affected by modality with plain x-ray images resulting in significantly lower scores (p=0.0642) compared to cross sectional images with a mean score of 6.291 for plain films, (6.604 - US, 7.413 - CT and 7.974 - MRI). Of the subspecialty categories, scores were significantly lower for Neuroradiology (mean score = 5.711, p=.0001) when compared to body and MSK imaging. There were 8 specific topics in which a high percentage of respondents earned low scores (0-3 points)[Table 1]. With regard to training level (R level), there were in general higher scores correspondent to increased training levels, however, these specific topics had low scores independent of R level. In addition, these specific topics had similar miss rates across all participating institutions. This would suggest true knowledge gaps or more generalized deficits in training.

### CONCLUSION

The "Emergency/Critical Care Imaging Simulation" is an objective assessment tool useful in identifying areas of individual weakness prior to EPA assignment. It is also valuable in identifying more generalized knowledge gaps that extend across institutions and across R levels. Our results would suggest a greater need for training in emergent Neuroradiology imaging, an increased emphasis on training in plain x-ray interpretation, and focused instruction on the identified specific low performance topics as listed in Table 1.

Clinical Characteristics, Prognosis and Outcome of Elderly Nasopharyngeal Carcinoma Patients in the United States: A Population-Based Study

Thursday, Dec. 1 12:45PM - 1:15PM Room: RO Community, Learning Center Station #1

## Participants

Ying Huang, Houston, TX (*Abstract Co-Author*) Nothing to Disclose

E. Brian Butler, MD, Houston, TX (Presenter) Nothing to Disclose

# ABSTRACT

Purpose/Objective(s): Because of age and co-morbid conditions, most elderly nasopharyngeal carcinoma (NPC) patients were excluded from randomized clinical trials. Survival of elderly NPC patients in the United States was not explored before. This study was to evaluate clinical characteristics, prognosis and outcome of elderly (=65 years old) NPC patients in the United States.Materials/Methods: We searched the Surveillance, Epidemiology, and End results (SEER) database for patients with NPC who were diagnosed from 2004 to 2012. We analyzed the clinical characteristics, prognosis and outcomes of elderly (=65 years old) patients. The overall survival (OS) and cancer-specific survival (CSS) rates were calculated by Kaplan-Meier method, and compared by log-rank test. Prognostic factors were analyzed by Cox regression model.Results: Our search criteria retrieved 3911 NPC patients. Among them, 904 (23.1%) patients were elderly patients (=65 years old). The 1-, 3-, and 5-year CSS rates were 80%, 67.7%, and 60.1% respectively. The 1-, 3-, and 5-year OS rates were 65%, 45.2% and 34.1% respectively. Their clinical characteristics and outcomes were compared with those of younger patients (P=0.459, P=0.462).Conclusion: Elderly NPC patients (=65 years old) have worse survival than younger patients. Important prognostic factors include clinical stage and receiving radiotherapy. Radiotherapy is an effective curative treatment for elderly NPC patients. Radiotherapy needs to be considered in the treatment of elderly patients (=65 year old) with nasopharyngeal carcinoma.

# VI018-EB-THB

Review of Budd-Chiari Syndrome Including the Pathophysiology, Clinical Presentation, and Management Focusing on Interventional Treatment Options

Thursday, Dec. 1 12:45PM - 1:15PM Room: VI Community, Learning Center Hardcopy Backboard

**FDA** Discussions may include off-label uses.

## Participants

Alex F. Munoz, MD,MS, Lexington, KY (*Presenter*) Nothing to Disclose Steven J. Krohmer, MD, Lexington, KY (*Abstract Co-Author*) Speaker, Medtronic plc

# **TEACHING POINTS**

Budd-Chiari Syndrome (BCS) is a rare condition characterized by hepatic venous outflow tract obstruction, which can occur at any level between the small hepatic veins and the junction of the inferior vena cava and the right atrium. The complex pathophysiology of BCS gives rise to multiple etiologies with various clinical presentations. Treatment options include medical management, endovascular interventions and surgery, with transplant as the last option. The purpose of this exhibit is:1. To review the pathophysiology and various clinical presentations of BCS.2. To explain the different treatment options of BCS including medical management, interventional and surgical treatments.3. To outline the different endovascular interventional treatment options including pre-procedural, procedural and post-procedural imaging.

## TABLE OF CONTENTS/OUTLINE

IntroductionPathophysiologyClinical PresentationDiagnostic ImagingMedical ManagementEndovascular Interventions and SurgeryConclusion

## VI271-SD-THB2

Comparison of Contrast Enhancement on CT Angiograms of the Lower Extremity of Dialysis and Non-dialysis Patients

Thursday, Dec. 1 12:45PM - 1:15PM Room: VI Community, Learning Center Station #2

# Participants

Takanori Masuda, Hiroshima, Japan (*Presenter*) Nothing to Disclose Yoshinori Funama, PhD, Kumamoto, Japan (*Abstract Co-Author*) Nothing to Disclose Naoyuki Imada, Hiroshima, Japan (*Abstract Co-Author*) Nothing to Disclose Tomoyasu Satou, Hiroshima, Japan (*Abstract Co-Author*) Nothing to Disclose Takayuki Oku, Hiroshima, Japan (*Abstract Co-Author*) Nothing to Disclose Kazuo Awai, MD, Hiroshima, Japan (*Abstract Co-Author*) Nothing to Disclose Kazuo Awai, MD, Hiroshima, Japan (*Abstract Co-Author*) Research Grant, Toshiba Corporation; Research Grant, Hitachi, Ltd; Research Grant, Bayer AG; Research Grant, Eisai Co, Ltd; Medical Advisor, General Electric Company; ; ; ;

### PURPOSE

Patients with peripheral artery disease (PAD) often present with chronic renal insufficiency (CRI). On CT angiograms of the extremities (e-CTA), PAD patients undergoing dialysis due to CRI show volume overload of the extracellular fluid and arterial contrast enhancement may be impaired. We compared arterial enhancement on lower e-CTA of patients who did and did not undergo dialysis.

# METHOD AND MATERIALS

Between January 2014 and December 2015, 340 patients with PAD underwent lower e-CTA. Group A (n=177) did not undergo dialysis; their mean body weight (BW) was  $56.8\pm12.5 \text{ kg}$  (SD). Group B-1 (n=81, mean BW  $56.3\pm11.5 \text{ kg}$ ) underwent e-CTA just before dialysis. Group B-2 (n=82, mean BW  $54.1\pm11.1 \text{ kg}$ ) underwent e-CTA just after dialysis. Helical scans of the arteries of the lower extremities were performed on a 64-detector CT scanner (VCT, GE, tube voltage 100 kVp, tube current 200-700 mA, detector configuration  $32 \times 1.25 \text{ mm}$ , rotation time 0.4s/r, helical pitch 0.516). The contrast medium (85.0 mL, Omnipaque-300; Daiichi-Sankyo, Tokyo, Japan) was intravenously administered at an injection rate of 3.0 mL/sec; this was followed by 20.0 mL of saline solution delivered at the same injection rate. We compared contrast enhancement at the patella level in all patients using Steel-Dwass multiple comparison analysis.

#### RESULTS

The median CT number and the range for the popliteal artery at the patella level were 421.5 HU (range 210.6-658.1 HU) in group A, 358.7 HU (range 191.4-588.3 HU) in group B-1, and 422.2 HU (range 283.2-617.6 HU) in group B-2. The CT number was statistically lower in group B-1 than group A (p<0.01) and group B-2 (p<0.01). There was no significant difference between group A and B-2 (p=0.99).

# CONCLUSION

Contrast enhancement was significantly lower in patients who underwent e-CTA just before dialysis than in patients without dialysis and patients who were scanned just after dialysis.

## **CLINICAL RELEVANCE/APPLICATION**

In patients with PAD undergoing dialysis, e-CTA should be performed just after dialysis to obtain a sufficient CT number of the arteries.

Tips for Optimal Use and Imaging of Radiopaque Embolization Microspheres

Thursday, Dec. 1 12:45PM - 1:15PM Room: VI Community, Learning Center Station #4

#### **Participants**

Elliot B. Levy, MD, Bethesda, MD (Presenter) Nothing to Disclose Venkatesh P. Krishnasamy, MD, Delaware, OH (Abstract Co-Author) Nothing to Disclose Andrew Lewis, PhD, Camberley, United Kingdom (Abstract Co-Author) Employee, BTG International Ltd Sean Willis, PhD, Camberley, United Kingdom (Abstract Co-Author) Employee, BTG International Ltd Chelsea Macfarlane, PhD, Camberley, United Kingdom (Abstract Co-Author) Employee, BTG International Ltd Bradford J. Wood, MD, Bethesda, MD (Abstract Co-Author) Researcher, Koninklijke Philips NV; Researcher, Celsion Corporation; Researcher, BTG International Ltd; Researcher, W. L. Gore & Associates, Inc ; Researcher, Cook Group Incorporated; Patent agreement, VitalDyne, Inc; Intellectual property, Koninklijke Philips NV; Intellectual property, BTG International Ltd; ; ; ; Victoria L. Anderson, MS, Bethesda, MD (Abstract Co-Author) Nothing to Disclose Imramsjah M. van der Bom, Andover, MA (Abstract Co-Author) Employee, Koninklijke Philips NV Alessandro G. Radaelli, PHD, MS, Best, Netherlands (Abstract Co-Author) Employee, Koninklijke Philips NV Karun V. Sharma, MD, PhD, Mc Lean, VA (Abstract Co-Author) Nothing to Disclose Elizabeth C. Jones, MD, Bethesda, MD (Abstract Co-Author) Nothing to Disclose Ayele Negussie, PhD, Bethesda, MD (Abstract Co-Author) Nothing to Disclose Andrew Mikhail, PhD, Bethesda, MD (Abstract Co-Author) Nothing to Disclose William F. Pritchard JR, MD, PhD, Bethesda, MD (Abstract Co-Author) Nothing to Disclose Jean-Francois H. Geschwind, MD, Westport, CT (Abstract Co-Author) Consultant, BTG International Ltd; Consultant, Bayer AG; Consultant, Guerbet SA; Consultant, Sterigenics International LLC; Consultant, Koninklijke Philips NV; Consultant, Jennerex Biotherapeutics, Inc; Grant, BTG International Ltd; Grant, Bayer AG; Grant, Koninklijke Philips NV; Grant, Sterigenics International LLC; Grant, Threshold Pharmaceuticals, Inc; Grant, Guerbet SA; Founder and CEO, PreScience Labs, LLC Govindarajan Narayanan, MD, Miami, FL (Abstract Co-Author) Consultant, BTG International Ltd; Consultant, AngioDynamics, Inc; Consultant, Medtronic plc; Consultant, Guerbet SA Riccardo A. Lencioni, MD, Pisa, Italy (Abstract Co-Author) Research Consultant, BTG International Ltd; Research Consultant, Guerbet SA; Research Consultant, Bayer AG

### PURPOSE

To describe procedural and post-procedural technical and imaging tips for optimal delivery and follow up of a novel commercial radiopaque image-able microsphere for hepatic embolization.

### **METHOD AND MATERIALS**

20 patients with primary or metastatic liver neoplasms (hepatocellular carcinoma, carcinoid, neuroendocrine, GIST, or adrenocortical carcinoma) underwent transarterial embolization with 1-2ml (sedimented volume) 70-150 µm and/or 100-300 um LC Bead LUMI microspheres. Embolization was slow and selective, with a near-complete flow stasis endpoint. Intra-procedural imaging included fluoroscopy, digital single shot radiographs, conventional CBCT, and custom dual phase CBCT (Oncoblue, Philips, Best, The Netherlands). Tumor segmentation, registration, fusion, and 3D roadmap navigation planning software with feeder detection was used in specific cases both during the procedure and at follow up. Imaging follow up included immediate post-embolization CBCT, 10 min delay CBCT, 48 hr CT, and up to 3 month CT.

#### RESULTS

Optimal bead suspension and handling was achieved with Visipaque 320 non-ionic contrast injected horizontally through  $\geq 2.4$ Fr microcatheters. Microspheres were seen on all modalities at all time points with conspicuity varying among the modalities but not over the short term follow up. Thick slab maximum intensity projection (MIP) optimally showed the microsphere distribution. Intraprocedural fusion of non-enhanced post procedural CBCT with either pre procedural or post-procedural enhanced CBCT demonstrated patent vessels without microspheres and tumor with fewer microspheres presumed to be at risk for under-treatment. Fusion imaging altered treatment plans in 3 of the initial 5 patients at one center (added phrenic embolization or microwave ablation). CT at 1 and 2 months demonstrated microspheres in the expected location with slight alterations related to involution of treated tumors.

### CONCLUSION

Intra-procedural CBCT and digital single shot radiography can visualize and localize radiopaque microsphere delivery. Navigation, treatment planning, and fusion platforms may be integrated with the imageable microsphere embolization procedure. Microsphere location and conspicuity on CT is relatively constant out to 3 months post embolization.

#### **CLINICAL RELEVANCE/APPLICATION**

Embolization with imageable radiopaque beads permits intra-procedural visualization of embolic distribution and identification of potentially under-treated tumor.

A Clinical Trial of Radiation Dose Reduction during Transarterial Chemoembolization(TACE) with Drug-eluting bead(DEB) for Hepatocellular Carcinoma

Thursday, Dec. 1 12:45PM - 1:15PM Room: VI Community, Learning Center Station #1

## Participants

Masakazu Hirakawa, MD, Beppu, Japan (*Presenter*) Nothing to Disclose Yoshiki Asayama, MD, Fukuoka, Japan (*Abstract Co-Author*) Nothing to Disclose Kousei Ishigami, MD, Iowa City, IA (*Abstract Co-Author*) Nothing to Disclose Yasuhiro Ushijima, MD, Fukuoka, Japan (*Abstract Co-Author*) Nothing to Disclose Akihiro Nishie, MD, Fukuoka, Japan (*Abstract Co-Author*) Nothing to Disclose Hiroshi Honda, MD, Fukuoka, Japan (*Abstract Co-Author*) Nothing to Disclose

### PURPOSE

This study aimed to evaluate patient radiation dose reduction, during transarterial chemoembolization (TACE) with drug-eluting bead (DEB) for hepatocellular carcinoma (HCC) while maintaining treatment effect (TE), adverse events(AE) and the image quality (IQ), using a new our clinical trial of radiation dose reduction.

#### **METHOD AND MATERIALS**

Fifty eight HCC cases treated with DEB-TACE were included in this study. Forty five patients (30 men, 15 women; mean age, 71.6 years) were treated under normal mode(the normal group), and 17 patients (10 men, 7 women; mean age, 69.6 years) were treated under radiation reduction mode using reduction filter, lower frame rate and etc (the reduction group). Dose area product (DAP), air kerma (AK) and radiation time of each digital fluoroscopy (DF) were compared between the two groups. IQ of digital subtraction angiography (DSA) and digital angiography (DA) during infusion of DEB was assessed by two blinded and independent readers on a four-rank scale.

#### RESULTS

There were no significant differences in patient's characteristics and tumor burden between the groups. The overall adverse events relating DEB-TACE did not significantly differ between the groups. Fluoroscopy time were equivalent between the groups. Compared to the normal group, in the reduction group, AK and DAP could be significantly reduced by 64.2% (2.63 Gy vs. 1.64 Gy, p<0.05) and 67.4% (483 mGy cm<sup>2</sup> vs. 328 mGy cm<sup>2</sup>, p<0.05), respectively. TE, AEs and IQ were rated comparable between the groups.

## CONCLUSION

Our simple trial of radiation dose reduction during DEB-TACE for HCC could reduce to almost 60% level recorded in the normal mode without negative impact on treatment effect, image quality and severe adverse events.

# **CLINICAL RELEVANCE/APPLICATION**

Simple clinical trial of radiation dose reduction, radiation dose during DEB-TACE could be reduced significantly without negative impact on treatment effect, image quality and severe adverse events.

Significant radiation reduction might be especially important in patients being treated repeatedly with DEB-TACE and also important for the in-room medical staff.

Significant Patient Radiation Exposure Reduction during Complex Liver Interventional Radiology Procedures Using a New Generation Angiography Imaging Room

Thursday, Dec. 1 12:45PM - 1:15PM Room: VI Community, Learning Center Station #5

## Participants

Charles Martin III, MD, Pepper Pike, OH (Presenter) Nothing to Disclose

### PURPOSE

To evaluate patient radiation exposure levels during complex liver interventional radiology (IR) procedures performed with recent angiography equipment & image processing tools.

### **METHOD AND MATERIALS**

An IRB approved retrospective study of all TIPS and liver embolization procedures performed in our new angiography suite (Discovery IGS740, GE Healthcare, Chalfont St Giles, UK) was conducted.

For each case, dedicated imaging protocols were used with the following tools: Cone Beam CT, automated vessel identification software, preoperative CT and CBCT 3D roadmapping, multimodality image fusion, digital magnification. Dose Area Product (DAP), Air Kerma (AK) and Fluoroscopy time (FT) were recorded and compared with historical data and published SIR reference levels. Results are expressed as median (interquartile range Q3-Q1).

# RESULTS

From February 2015 to March 2016, 117 complex liver IR cases were performed in the new room, as follows: 12 TIPS, 55 Hepatic Arterial Embolization(HAE), 23 Y90 mappings (Y90m) and 27 radioembolizations (Y90). Operators were the same in the new and historical cohort, and BMI were equivalent (mean 28.5 vs 28.6 kg/m2, p=0.87). DAP (Gy.cm2) were as follows: TIPS 215.6 (351.6-66.5), HAE 147.3 (221.8-83.3), Y90m 133.6 (195-88.1), Y90 75.3 (161.5-41.8). AK (Gy) were as follows: TIPS 0.65 (1.11-0.26), HAE 0.96 (1.33-0.62), Y90m 0.48 (0.8-0.21), Y90 0.35 (0.98-0.18).AK levels were significantly lower in the new room vs. historical data (54% p=0.027 for TIPS, 43% p=0.037 for HAE, 68% p=0.022 for Y90m and 57% p=0.037 for Y90) and vs. published data (62% p<.05 for TIPS, 25% p<.05 for HAE).No significant difference in DAP for TIPS was observed with historical or published data. HAE DAP was significantly lower in the new room when compared to published data (41% p<.05)

## CONCLUSION

Using the latest angiography technology and available image processing tools enables to significantly reduce the radiation dose exposure to patient, thus to medical staff, during complex liver interventional radiology procedures.

# **CLINICAL RELEVANCE/APPLICATION**

Through our demonstration of these acquisition metrics, future users can modify their respective dose parameters to minimize patient operator radiation dose during complex interventional procedures.